University of Nottingham

UK | CHINA | MALAYSIA

Preparation of Potent and Selective $\alpha_v\beta_6$ Integrin Inhibitors for the Treatment of Idiopathic Pulmonary Fibrosis

and

Synthetic Approaches Towards the Total Synthesis of Mescengricin

Henry Duncan Robinson

Thesis submitted to the University of Nottingham for the degree of Doctor of Philosophy

March 2021

Acknowledgements

First and foremost, I would like to express my appreciation and gratitude to my supervisors Professor Chris Moody, Mr Tom McInally, Dr Simon Macdonald, Dr Andrew Nortcliffe and Mr Ashley Hancock for giving me the opportunity to work on this challenging and rewarding research project. It has been an absolute pleasure and a privilege to work with each of you; your continuous advice and support throughout my PhD has been invaluable and I will forever be grateful for the role you have played in my development as a researcher.

For making me feel so welcome during my research placement at GSK in Stevenage, I wish to thank Heather Barnett, Pawel Slade and the rest of the array team, those working in my bay of the SmartLab and the Sefton Road gang; those months were amongst the most important and rewarding of my entire project and it is because of your support that I was able to achieve what I did. Particular thanks must be paid to James Rowedder for running the integrin assays described throughout this thesis.

Many thanks to the stores and technical services staff within the School of Chemistry at Nottingham; Mandy, Eric, John and Jim (stores), Mick and Ben (MS), Kev and Shaz (NMR), Stephen (X-ray) and Tom (department tech.), without whom, much of the work and analysis that constitute this thesis would have been impossible. Special thanks must go to Mandy for maintaining the smooth running of the lab and for keeping all of us on track over the years!

For all things molecular modelling, I would like to thank Steve Oatley; your work and assistance has added so much to my project and towards my general understanding of the project as a whole, so thank you!

In the first year of my PhD, Professor Hon Lam and his research group were kind enough to provide me with lab space and so I would like to thank them for making me feel so welcome

during that time. I wish also to thank the Moody group for their advice and support during group meetings and for providing me with lab space when I needed it!

To the GSK group, I wish to thank all of the MSci students who worked in A36 throughout my project, and Roger, Katie, Jozef, Andy N and Andy J for supporting and assisting me, and for providing cake and good conversation! Jozef, I've thoroughly enjoyed our time working together and I wish you all the success in the world towards your PhD and for all of your future endeavours!

I'd particularly like to thank both Andy N and Andy J for all of your guidance over the years; not only for imparting your knowledge and experience to me, and for pushing me to become the best researcher I can possibly be, but you've also both helped me through some pretty tough moments and for that I can only say, from the bottom of my heart, thank you.

I would like to pay special thanks to my friends and family; it has been quite a journey to get to this point and each and every one of you has been vital in helping me to arrive here. Mum and Dad, words can never express how grateful I am for everything that you have done for me over the past 27 years; you've given me every opportunity to achieve my goals and supported me every step of the way. LUHTP.

Lastly, I want to thank Char; you've been my rock and I couldn't have managed this without you. Thanks for all the chilli and I think you are nice. Bye friend.

Contents

Abbreviations

acac	Acetoacetate
ADMIDAS	Adjacent to metal-ion-dependent adhesion site
AEs	Adverse effects
Ala	Alanine
Arg	Arginine
Asp	Aspartic acid
ATP	Adenosine triphosphate
ATR	Attenuated total reflectance
AUC	Area under the curve
BEI	Binding efficiency index
Bn	Benzyl
Boc	*tert*-Butoxycarbonyl
BPin	Boronic acid pinacol ester
CBZCl	Benzyl chloroformate
Cl_{int}	Intrinsic clearance
C_{max}	Maximum serum concentration after dosing
cod	Cyclooctadiene
COVID-19	Coronavirus disease - 2019
CPME	Cyclopentyl methyl ether
c-Pr	Cyclopropyl
d.e.	Diastereomeric excess
Da	Daltons
DBU	1,8-Diazabicyclo[5.4.0]undec-7-ene
1,2-DCE	1,2-Dichloroethane
DEAD	Diethyl azodicarboxylate
DIC	*N*,*N*'-Diisopropylcarbodiimide
DMAc	Dimethylacetamide
DMAP	4-Dimethylaminopyridine
DMF	Dimethylformamide
DMPK	Drug metabolism and pharmacokinetics
DMSO	Dimethyl sulfoxide
dppf	1,1'-*Bis*(diphenylphosphino)ferrocene
dtbpf	1,1'-*Bis*(di-*tert*-butylphosphino)ferrocene
dtbpy	4,4'-Di-*tert*-butyl-2-2'-dipyridyl
e.e.	Enantiomeric excess
EC_{50}	Half maximal effective concentration
ECM	Extracellular matrix
EDC	1-Ethyl-3-(3-dimethylaminopropyl)carbodiimide
Et	Ethyl
FDA	U.S. food and drug administration
FGF	Fibroblast growth factors
GSK	GlaxoSmithKline
GST	Glutathione *S*-transferase
h	Hours
HATU	1-[*Bis*(dimethylamino)methylene]-1*H*-1,2,3-triazolo[4,5-*b*]pyridinium 3-oxide hexafluorophosphate
HEPES	4-(2-hydroxyethyl)-1-piperazineethanesulfonic acid
HIV	Human immunodeficiency virus

HLB	Hydrophilic-lipophilic balance
HMDS	Hexamethyldisilazane
HOBt	Hydroxybenzotriazole
HPLC	High performance liquid
HSP47	Heat shock protein 47
HSQC	Heteronuclear single quantum correlation
HSV-1	Herpes simplex virus
HTP	High throughput permeability
HWE	Horner-Wadsworth-Emmons
IF	Interstitial fluid
IPF	Idiopathic pulmonary fibrosis
i-Pr	*iso*-Propyl
IR	Infrared
IV	Intravenous
kDa	Kilodalton
LAP	Latency associated peptide
LCMS	Liquid chromatography-mass spectrometry
LE	Ligand efficiency
LiPE	Lipophilic efficiency
LLC	Large latent complex
LSF	Late-stage functionalisation
LSP	Lipophilicity to selectivity parameter
Lys	Lysine
M	Molar
mAb	Monoclonal antibody
mAbs	Monoclonal antibodies
MAO	Monoamine oxidase
mCPBA	*meta*-Chloroperoxybenzoic acid
MDAP	Mass directed auto purification
MDCK	Madin-Darby canine kidney
MDR1	Multidrug resistance gene-1
Me	Methyl
MHz	Megahertz
MIDAS	Metal-ion-dependent adhesion site
Min	Minutes
MRT	Mean residence time
MS	Molecular sieves
MSci	Masters student
MW	Molecular weight
NADPH	Nicotinamide adenine dinucleotide phosphate
NBS	*N*-Bromosuccinimide
NCEs	New chemical entities
NIS	*N*-Iodosuccinimide
nM	Nanomolar
NMDA	*N*-Methyl-D-aspartic acid
NMP	*N*-Methyl-2-pyrrolidone
NMR	Nuclear magnetic resonance
n-Pr	*n*-Propyl
Ns	Nosyl
PAMPA	Parallel artificial membrane permeation assay
PDGF	Platelet-derived growth factor
Ph	Phenyl

pIC_{50}	The negative log of the half maximal inhibitory concentration
PO	*Per os* – oral administration
PPB	Plasma protein binding
ppm	Parts per million
PyBroP	Bromotripyrrolidinophosphonium hexafluorophosphate
R^2	Coefficient of determination
rac	Racemate
RED	Rapid equilibrium dialysis
RGD	L-Arginine – Glycine – L-Aspartic acid tripeptide
rt	Room temperature
SAR	Structure activity relationship
SDL	Specificity determining loop
SM	Starting material
SPAV3	Human $\alpha_v\beta_3$ immobilized on scintillation proximity beads
SSc	Systemic sclerosis
T3P	Propylphosphonic anhydride
TABO	1,3,3-trimethyl-6-azabicyclo[3.2.1]octane
TBDPS	*tert*-Butyldiphenylsilyl
TBME	Methyl *tert*-butyl ether
TBSCl	*tert*-Butyldimethylsilyl chloride
t-Bu	*tert*-Butyl
TFA	Trifluoroacetic acid
TGF	Transforming growth factor
THF	Tetrahydrofuran
THN	Tetrahydronaphthyridine
Thr	Threonine
T_{max}	The time at which C_{max} is observed
TMP	2,2,6,6-Tetramethylpiperidine
TMSCl	Trimethylsilyl chloride
Tyr	Tyrosine
UIP	Usual interstitial pneumonitis
UoN	University of Nottingham
USA	United states of America
UV	Ultraviolet
V_{dss}	Volume of distribution at steady state
VEGF	Vascular endothelial growth factor
WT	Wild type
XPhos	2-Dicyclohexylphosphino-2',4',6'-triisopropylbiphenyl
ΔG	Gibbs free energy

Abstract

Idiopathic pulmonary fibrosis (IPF) is a terminal illness characterised by excessive build-up of scar tissue within the lungs. Despite a relatively high incidence amongst the population, there are no currently available treatments that prolong the estimated lifespan of an affected individual beyond approximately six years.

Previous work has determined that inhibition of the $\alpha_v\beta_6$ integrin may yield positive results with regards to halting the progression of the disease and so much work has been focussed upon the development of selective $\alpha_v\beta_6$ integrin inhibitors.

The work described in this thesis details the development of such inhibitors; first the preparation of potent and selective 3-monosubstituted β-3-aryl-amino acid derived analogues, of which a number performed well in additional drug metabolism and pharmacokinetics (DMPK) studies indicating potential oral bioavailability, followed by the combination of the most favourable structural features to yield a series of 3,5-disubstituted integrin inhibitor analogues. These latter analogues exhibited improved selectivity profiles and encouraging drug-like features and were viewed as a promising point from which to further progress the series, potentially resulting in the development of a clinical candidate.

Following the halting of the integrin assays used to assess these inhibitor analogues, the total synthesis of mescengricin, a naturally occurring α-carboline containing molecule, was attempted, with the subsequent results from that work being detailed.

Licensed material

Parts of the discussion within this thesis are adapted with permission from:

- John Wiley and Sons. Late-Stage Functionalization by Chan–Lam Amination: Rapid Access to Potent and Selective Integrin Inhibitors: Henry Robinson, Steven A. Oatley, James E. Rowedder, Pawel Slade, Dr. Simon J. F. Macdonald, Dr Stephen P. Argent, Prof. Dr. Jonathan D. Hirst, Thomas McInally, Prof. Dr. Christopher J. Moody, *Chem. Eur. J.* **2020**, 26, 34, 7678-7684
- Iridium-catalysed C-H borylation of β-aryl-aminopropionic acids: H. Robinson, J. Stillibrand, K. Simelis, S. J. Macdonald, A. Nortcliffe, *Org. Biomol. Chem.* **2020**, *18*, 6696–6701 - Published by The Royal Society of Chemistry.

Acknowledgement of MSci student work and contribution

Throughout this thesis, the work of a number of University of Nottingham MSci students is referenced to aid in the discussion of SAR where relevant.

These students are Sarah Armstrong, Harry Bird, Scott Bryers, Edmund J. P. Hogarth, Thomas C. Keenan, May-Li MacKinnon, Esther O. I. Makinde, Christopher Merrett, Makenzie J. Millward, Craig Pike, Nicholas C. Rose, Kimberley R. Saunders-Coombs, Klemensas Simelis, Jay S. Tromans, Jordan Waters.[1–15]

I would like to thank them for their contribution to this project and wish them luck for all of their future endeavours.

Chapter 1

Idiopathic pulmonary fibrosis, integrins and project design

1.1 Medicines

Naturally occurring compounds have been used to treat ailments since the beginning of recorded history.[16] Without modern methods to elucidate the root causes of efficacy, it has only in recent times become established that these materials contain biologically active compounds that provide a therapeutic benefit. Subsequently, natural products have been a significant source of inspiration for drug discovery projects, with many themselves being approved for commercial use (Figure 1).[16–18]

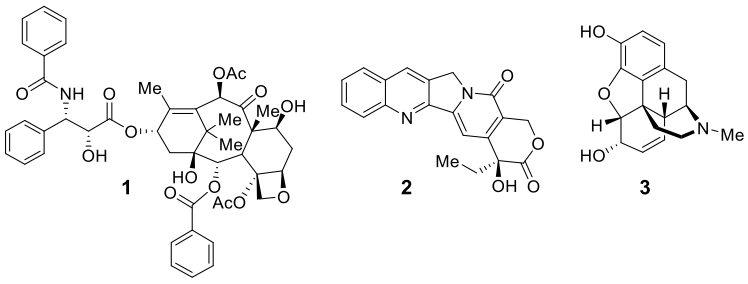

Figure 1. Three medications derived from natural sources: taxol (**1**), camptothecin (**2**) and morphine (**3**).

Farnsworth *et al.* estimated that as of 1985, 119 distinct therapeutic agents considered as important drugs in use in one or more countries, were derived in some form from plant sources and that of these, 74% were discovered after efforts to isolate the active substance responsible for the use of the original plant in traditional medicine.[19] In an analysis published by Craggs *et al.*, it is stated that of the newly approved drugs reported between 1983 and 1994, 78% of all antibacterial agents and 61% of all anticancer drugs (excluding biologics) were derived from natural sources or modelled on a natural product;[20] biologics refer to products that are derived from or contain components of living organisms.

In the modern drug discovery process, medications are now typically developed using a combination of computer modelling, with biological mechanistic elucidation and

experimental trial and error, with natural products steadily playing a smaller role in project initiation each year; approval of biologics has risen sharply over the past two decades, accounting for approximately 16% of the 302 drugs approved between 2009-2017 compared to only 7% of the 209 drugs approved between 2000-2008.[21] Despite the slow decline in interest, natural products ultimately remain an important resource and component of the drug discovery process, due to their ability to inform previously unknown biological mechanisms *via* rich structural diversity.[16,18]

The work herein described will explore two aspects of the drug discovery process: the lead optimisation of L-Arginine – Glycine – L-Aspartic acid (RGD) mimetics, a naturally occurring binding sequence, for the selective inhibition of the $\alpha_v\beta_6$ integrin with the aim of treating idiopathic pulmonary fibrosis (IPF) and the total synthesis of the α-carboline mescengricin (**5**, Figure 2).

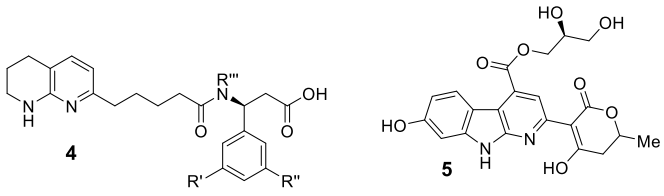

Figure 2. The core structure of the RGD mimetic integrin inhibitor series described herein (**4**) and mescengricin (**5**).

1.2 IPF

IPF is a chronic interstitial lung disease, characterised by excessive scarring of the interstitium. The interstitium is a general term used to describe the network of connecting and supporting tissues that surround vital internal structures within the body, such as the lungs and the circulatory system, beneath structural barriers such as cell walls;[22–24] this complex organ is comprised of two main features: the interstitial fluid (IF) and the

extracellular matrix (ECM). Amongst other roles, IF oversees the transportation of nutrients and waste products from blood capillaries to cells and *vice versa*, proteins and signalling molecules.[22,23] The ECM is a three-dimensional network of tissues such as collagen and elastin that facilitates the exchanges of these entities, whilst also providing structural support to surrounding cells.[23]

The incidence of IPF is estimated to be 4.6 per 100,000 and 6.8 per 100,000 in the UK and the USA respectively, with >5,000 and >14,000 people diagnosed each year, respectively;[25–27] IPF is fatal, with median survival rates of between two and four years.[27,28]

Currently there are two approved treatments for the disease: pirfenidone (**6**) and nintedanib (**7**, Figure 3); both reduce the rate of lung function decline, although neither fully halts disease progression and various side effects are attributed to their use, leading to poor patient compliance.[29]

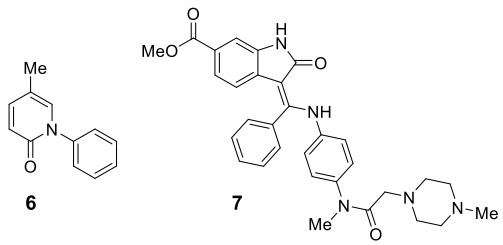

Figure 3. Pirfenidone (**6**) and nintedanib (**7**), the two currently available approved therapeutics for the treatment of IPF.

Pirfenidone (**6**) exhibits anti-inflammatory, antioxidant and antifibrotic properties, however the mechanism of action is currently unknown.[30] *In vivo* experiments have shown that pirfenidone (**6**) reduces the amount of heat shock protein 47 (HSP47) present in fibrotic lesions, which in turn prevents transforming growth factor-β1 (TGF-β1) stimulated collagen synthesis.[30] HSP47 is a collagen-binding protein that directly participates in the production and secretion of procollagens.[31] Thus, by reducing the concentration of this protein within

cells, the rate at which collagen synthesis, and by extension IPF, progresses, is slowed dramatically. Pirfenidone (**6**) is administered orally, requiring up to multigram quantities each day, a contributing factor to the aforementioned incompliance;[32] treatment with pirfenidone (**6**) is not without risk and common side effects include increased skin sensitivity, nausea, respiratory tract infections and joint pain.[32]

Conversely, the mechanism of action for nintedinab (**7**) is well known. Nintedinab (**7**) is a tyrosine kinase inhibitor of the PDGF, FGF and VEGF receptors, that binds at the ATP binding pocket, ultimately leading to reduced proliferation and survival of fibroblasts, which in turn leads to reduced rate of collagen synthesis.[33] Like pirfenidone (**6**), nintedanib (**7**) is orally administered but requires a significantly smaller daily dosage; treatment does however present adverse effects similar to pirfenidone by way of fairly serious side effects such as diarrhoea, nausea, liver complications and hypertension.[33]

These are clearly not sustainable or efficient treatments and as such, many pharmaceutical companies have focussed on the development of therapies that treat the symptoms of IPF without significantly compromising the health of the individual. A strongly recommended alternative and less invasive treatment is long-term oxygen therapy in which an afflicted individual has access to an oxygen tank to treat the symptoms of shortness of breath and hypoxemia;[34] this is a palliative measure and is not curative. The current most effective and strongly recommended treatment for IPF is lung transplantation but due to the low availability of suitable donor organs and the typically high age of patients, this is not a particularly viable solution.[34] Additionally, despite an observed improvement in quality of life for patients post-transplant, the mean survival rate amongst transplantees is reported to be six years;[35] whilst greater than the mean survival time of those suffering with IPF who do not receive a transplant, lung transplantation is clearly not a suitable or sustainable long term solution for this disease.

1.3 Role of integrins

In recent years there has been considerable attention paid towards the role that integrins, specifically the α_v subfamily, play in the progression of fibrotic diseases. Integrins are heterodimeric receptor proteins that are responsible for mediating cell-cell and cell-ECM interactions.[36] Each heterodimer consists of an α- and a β- subunit, bound together *via* non-covalent interactions. In mammals there are a total of eighteen α subunits and eight β-subunits that can bind to one another to form a total of 24 individual integrin heterodimers (Figure 4).[37]

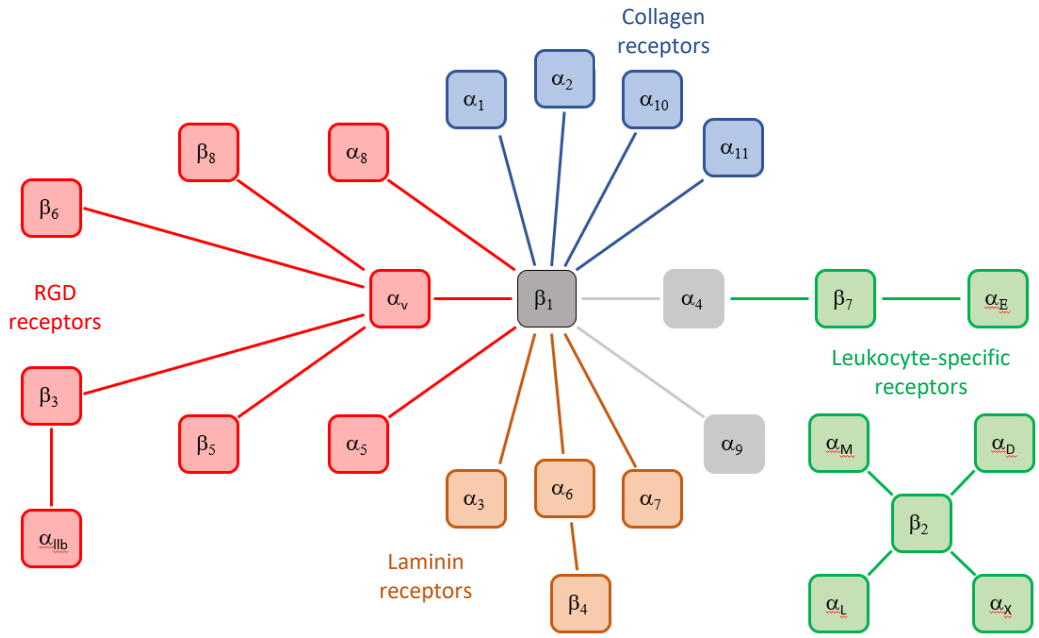

Figure 4. A diagram depicting the various integrin heterodimers that may be constructed with each α and β subunit.

Several integrins, including the α_v subfamily, are known to bind with the cytokine transforming growth factor β (TGF-β).[38,39]

TGF-β is a large pro-fibrotic cytokine and a key regulator of fibrosis within the body;[40] as such, it is hoped that chemical manipulation of this entity and the biological processes it

mediates will aid in the development of effective treatments for fibrotic diseases.[41] TGF-β exists as three distinct isoforms (TGF-β1, -β2 and -β3); TGF-β1 is the most prevalent isoform with -β2 and -β3 occurring in a more limited range of cells and tissues, and whilst all three are typically expressed within fibrotic tissue, TGF-β1 is the primary driver of fibrosis progression.[42] Each of these cytokines is synthesised as a small latent peptide that is non-covalently bound to a much larger peptide, coined the latency associated peptide (LAP).[41,43] Addition of a third protein, the latent TGF-β binding protein, to this heterodimeric complex, forms what is known as the large latent complex (LLC). In this form, the cytokines are inert and must be activated before they can perform their intended functions;[44] activation is achieved *via* release of TGF-β from the LLC by either physical or enzymatic processes.

The RGD tripeptide (**8**) has been shown to play a key role in the mechanism of interaction between integrins and their ligands. The α_v subfamily of integrins for instance, in particular $\alpha_v\beta_3$, -β_5, -β_6 and -β_8, are known to bind to the RGD sequence that is present in the LAP of TGF-β1 and TGF-β3, and thus these entities have the potential to activate latent TGF-β (Figure 5).[44]

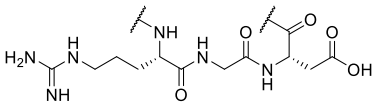

8

Figure 5. The RGD tripeptide **8**.

In this case, TGF-β activation results from recognition and subsequent binding of the RGD tripeptide in the LAP with the relevant α_v integrin, accompanied by subsequent liberation of TGF-β from the LLC. The activated TGF-β proceeds to interact with a cell receptor, triggering a series of complex signalling pathways that ultimately results in fibrosis (Figure 6).

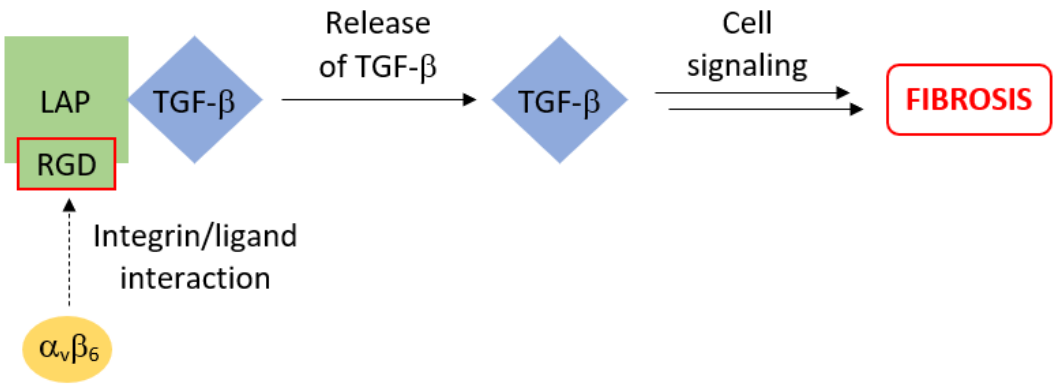

Figure 6. A depiction of the process that leads to TGF release from the LLC upon interaction with $\alpha_v\beta_6$ and how this ultimately causes fibrosis.

The activation of transforming growth factors by the $\alpha_v\beta_3$, -β_5 and -β_8 integrins has been studied rigorously, with their role in the initiation and progression of several diseases now being well understood; $\alpha_v\beta_3$ and -β_5 have been implicated in angiogenesis, with myriad investigations subsequently being performed to evaluate $\alpha_v\beta_3$ as a potential target for anticancer treatments.[45,46] Inhibition of $\alpha_v\beta_5$ has additionally been investigated as a strategy for protecting against acute kidney injury resulting from ischemia-reperfusion injury, a common in-hospital event following surgical procedures, whilst inhibition of $\alpha_v\beta_8$ has shown promise as a method for inducing anti-tumour immunity and is thus of interest in the field of cancer immunotherapy.[47,48] Dodagatta-Marri *et al*. demonstrate the growth suppression or in some cases complete regression in syngeneic models of squamous cell carcinoma (CCK168), mammary cancer (EMT-6), colon cancer (CT26), and prostate cancer (TRAMPC2) upon treatment with an anti-$\alpha_v\beta_8$ monoclonal antibody.[48] Whilst these integrins play a critical role in biological development, from binding ECM ligands such as vitronectin, fibrinogen and osteopontin, to facilitating cerebral vascular development, they do not appear to affect the development of pulmonary fibrosis to the same degree as $\alpha_v\beta_6$.[43,49–53]

In recent years, several studies have detailed the role that $\alpha_v\beta_6$ plays in the activation of TGF-β1;[43,54,55] *in vivo* experiments that simulate inhibition of the $\alpha_v\beta_6$ integrin using monoclonal antibodies have in fact resulted in effective prevention of TGF-β activation.[43,54] Individuals suffering from IPF exhibit increased expression of the $\alpha_v\beta_6$ integrin within their lung tissue, compared to the lung tissue of healthy individuals in which very little $\alpha_v\beta_6$ is present; thus, $\alpha_v\beta_6$ likely triggers the activation of latent TGF-β1 to a greater extent than the other α_v integrins, leading to the progression of fibrosis (Figure 7).

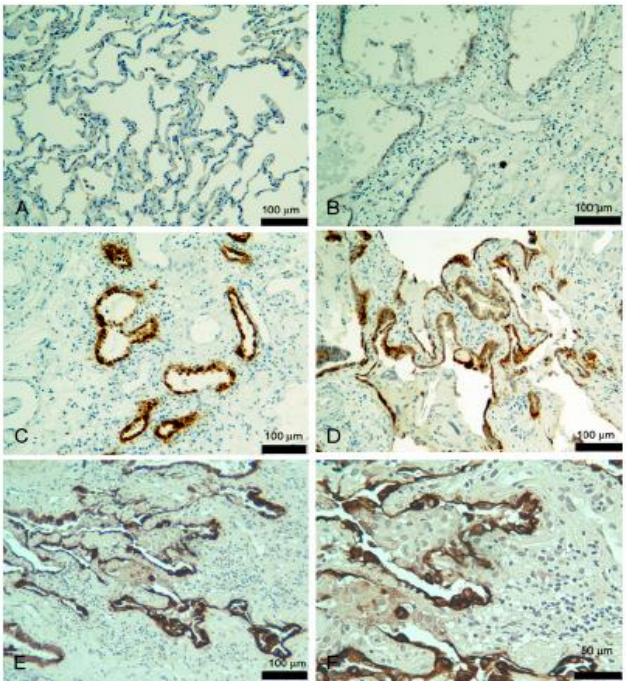

Figure 7. Immunohistochemical staining of pulmonary tissues for $\alpha_v\beta_6$ integrin expression; brown staining indicates cells expressing the $\alpha_v\beta_6$ integrin. Image A depicts healthy pulmonary tissue with no expression of the $\alpha_v\beta_6$ integrin. The significantly increased expression of $\alpha_v\beta_6$ within the pulmonary tissue of IPF patients is observed in images E and F.[56] Reprinted with permission of the American Thoracic Society. Copyright © 2021 American Thoracic Society. All rights reserved. Gerald S. Horan, Susan Wood, Victor Ona, Dan Jun Li, Matvey E. Lukashev, Paul H. Weinreb, Kenneth J. Simon, Kyungmin Hahm, Normand E. Allaire, Nicola J. Rinaldi, Jaya Goyal, Carol A. Feghali-Bostwick, Eric L. Matteson, Carl O'Hara, Robert Lafyatis, Gerald S. Davis, Xiaozhu Huang, Dean Sheppard, and Shelia M. Violette, 2008, Partial Inhibition of Integrin $\alpha_v\beta_6$ Prevents Pulmonary Fibrosis without Exacerbating Inflammation, American Journal of Respiratory and Critical Care Medicine, vol. 177, p. 56-65. The American Journal of Respiratory and Critical Care Medicine is an official journal of the American Thoracic Society.

As a result of the increased expression of $\alpha_v\beta_6$ in IPF patient lung tissue, it is hoped that inhibition of this integrin will result in halting the progression of the disease, leading to the

development of medications that will provide to patients a therapeutic alternative far superior to any that are currently available. Selective inhibition of $\alpha_v\beta_6$ over $\alpha_v\beta_3$ is a particularly attractive target due to the reported inference that $\alpha_v\beta_3$ inhibition results in the intensification of sepsis and acute lung injury associated vascular endothelial leak in mice.[57]

Each integrin inhibition-based treatment that is either in development or commercially available can be separated into three broad categories: monoclonal antibodies (mAbs), peptide inhibitors and small molecule inhibitors.[58]

1.3.1 Monoclonal antibodies

The development of antigen-specific mAbs was first recorded by Köhler and Milstein in 1975;[59] since that time, mAbs have found use in a significant number of applications throughout the field of immunology, from treatment of cancers, to the therapy of septicaemia and even more recently as a potential treatment to disrupt the progression of early COVID-19 infection.[60,61] Whilst superb potential treatments for a variety of diseases due to the exquisite target specificity that can be exhibited by mAbs, there are a number of alternative uses for these entities within the pharmaceutical industry;[59,60,62] specifically, for the development of tools that further the understanding of integrin inhibition, monoclonal antibodies are a rich source of insight to the structure and mechanisms of integrin function.[62–64] There are three subtypes of anti-integrin mAb that regulate integrin function: stimulatory or activation specific, non-functional and inhibitory.[63] The first type encourages an increase of ligand-binding affinity by discouraging ligand dissociation, essentially shifting the equilibrium towards a state of high-affinity binding. This class of mAb can thus find use in a variety of situations where increasing integrin-dependent adhesion is beneficial; an example of this is demonstrated by Schwartz *et al.* who report a substantial improvement in the response to chemotherapy and thus, a strongly reduced growth rate, of M21 melanoma

cells within mice, when treated with a combination of the chemotheraprutic drug 1-β-D-arabinofuranosylcytosine (araC) with reagents that stimulate integrin signalling (either the snake venom disintegrin contortrostatin or the anti-β1 integrin antibody TS2/16).[65] The second type proceed without altering the functionality of the integrin and thus are an important source of controls within studies investigating integrin regulation and function. The third and final type promote stabilisation of a low affinity binding state; this is thought to happen *via* two different processes. In one, ligand binding is prevented by steric interference and thus, by competitive binding of the mAb to the integrin. The other sees mAbs behaving as allosteric inhibitors; that is, binding to the integrin not at the expected binding site, but instead at a position that forces the integrin to adopt a conformation that discourages binding.[58,66] It is this third type of inhibitory mAbs that form the basis of much of the mAb integrin inhibition work in recent years. For these reasons, mAbs can be used as therapies in the treatment of diseases in which integrins are implicated in the mechanism of disease progression. Work performed by Weinreb *et al*. resulted in the generation of the mAb 6.8G6 that showed good levels of potency and selectivity for the $\alpha_v\beta_6$ integrin with a high level of affinity.[67] The mAb BG00011 (formerly known as STX-100), initially developed by Stromedix but now represented by Biogen, recently underwent a Phase 2 clinical study (NCT ID: NCT03573505) in order to evaluate its safety and tolerability upon subcutaneous administration in patients suffering from IPF; unfortunately, the study was halted early due to safety concerns.

1.3.2 Peptide inhibitors

Within the venom of various snake species are found a family of small non-enzymatic proteins known as disintegrins; these are a class of cysteine rich proteins that exhibit an ability to bind to and inhibit the activity of specific integrins.[46,68] Disintegrins can be separated into three classes based on their multi-domain structures; the largest of these

classes contain a RGD tripeptide.[68] As such, there has been a significant amount of work focussed on utilising these proteins as start points for drug development projects, specifically for anticancer and antithrombotic purposes. The disintegrin leberagin-C, isolated from the venom of the Tunisian snake *Macrovipera lebetina transmediterranea*, specifically interacts with the $\alpha_v\beta_3$ integrin and to a lesser extent the $\alpha_5\beta_1$ and $\alpha_v\beta_6$ integrins *via* the RGD motif.[69] Whilst these compounds have displayed encouraging levels of multi-integrin inhibition, they exhibit a number of features that hinder their progression towards becoming effective treatments and ultimately approved medications. Disintegrins are large entities (between 47-84 residues in size) and as a consequence will often elicit a significant immune response from the body. As naturally occurring compounds, they are often metabolised by enzymatic processes at a faster rate than would be desired for pharmaceutically viable medications. However, as mentioned previously, whilst materials such as these may not themselves progress to the clinic as drug candidates, they can often provide invaluable information that assists with future drug optimisation; for example, by mimicking the RGD structure found in certain disintegrins, far smaller compounds are able to elicit a similar inhibitory effect, without the accompanying immunoresponse or enzymatic degradation.

Another peptide inhibitor that has drawn significant interest since its initial discovery in 1995 and subsequent reporting in 1999 is the cyclic peptide *c*(RGDf(NMe)V), dubbed cilengitide (**9**, Figure 8).[70,71]

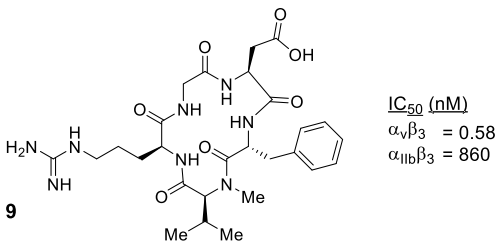

Figure 8. The structure of cilengitide (**9**) with potency values, as reported by Dechantsreiter *et al*.[71]

Developed *via* novel spatial screening methods by Kessler *et al*. as a potential $\alpha_v\beta_3$ integrin inhibitor, this peptide exhibited subnanomolar potency against the $\alpha_v\beta_3$ integrin and nanomolar activity against the $\alpha_v\beta_5$ and $\alpha_5\beta_1$ integrins.[70,71] Cilengitide (**9**) has since been entered into multiple clinical trials for the treatment of various tumours; whilst well tolerated in multigram doses, the progression of the peptide through clinical trials has been hampered by issues relating to low efficacy.[58,72] Whilst there is a changing trend in drug development that favours biopharmaceuticals over small molecules, development of small molecules remains an essential sector of the pharmaceutical industry. As such, there has in recent years been a shift in focus towards the development of small molecule integrin inhibitors for the treatment of IPF.

1.3.3 Small molecule integrin inhibitors

In recent years, several $\alpha_v\beta_6$ selective small-molecule integrin inhibitors have undergone clinical evaluation, with none yet passing phase II trials.[73]

A Phase I trial to evaluate the safety and tolerability of the Indalo Therapeutics drug candidate IDL-2965 (structure not reported) was recently terminated due to development challenges associated with the COVID-19 pandemic (NCT ID: NCT03949530).

A recently published patent by Pliant therapeutics lists a number of potent $\alpha_v\beta_6/\alpha_v\beta_1$ integrin inhibitors, the most promising of which (**10**) is shown in Figure 9.

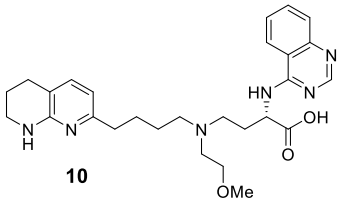

10

Figure 9. The structure of the most promising $\alpha_v\beta_6/\alpha_v\beta_1$ integrin inhibitor from within the recently disclosed Pliant therapeutics patent.[74]

Recruitment is currently underway for a Phase II trial to evaluate the efficacy and safety of the Pliant Therapeutics candidate PLN-74809 (structure not disclosed) in patients with IPF (NCT ID: NCT04396756).[74] This candidate is additionally being evaluated for use in patients with primary sclerosing cholangitis and suspected liver fibrosis, and acute respiratory distress syndrome associated with at least severe COVID-19 (NCT ID: NCT04480840 and NCT04565249).

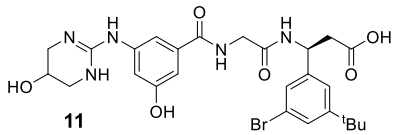

11

Figure 10. The pan α_v integrin inhibitor CWHM 12 (**11**).

Another potential candidate is the pan-α_v inhibitor CWHM 12 (**11**, Figure 10). Whilst **11** has not yet undergone any form of clinical evaluation, preclinical studies demonstrate that **11** is able to affect a reduction of liver and lung fibrosis in mice where fibrotic disease has already been established. Additional studies of **11** indicate that perhaps pan-inhibition of the α_v subfamily of integrins may be the most effective method of maximising efficacy to obtain the desired antifibrotic effect, although this is yet to be widely accepted.[75,76] The benefits of at least dual integrin antagonism have been explored previously, with studies indicating that $\alpha_v\beta_5$ integrin inhibition can protect against adverse effects (AEs) commonly associated with $\alpha_v\beta_3$ integrin inhibition;[57,77] the lack of serious AEs reported during numerous clinical studies of the dual $\alpha_v\beta_3/\alpha_v\beta_5$ inhibitor cilengitide supports this hypothesis.

Recently, the GlaxoSmithKline (GSK) candidate GSK3008348 (**12**) has been evaluated clinically (NCT ID: NCT02612051), and inhibition of the $\alpha_v\beta_6$ integrin with **12** did not cause any adverse effects in healthy volunteers when dosed with 3-3000 µg (Figure 11);[76,78] further Phase I clinical evaluation of **12** (NCT ID: NCT03069989) has since been halted at GSK. Inhibitor **12** and structurally similar compounds are RGD mimetics.

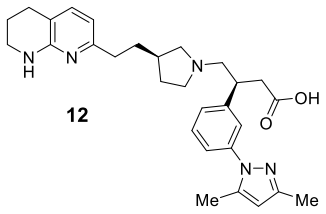

Figure 11. GSK clinical candidate GSK3008348 (**12**).

The University of Nottingham (UoN) series originates from the Merck $\alpha_v\beta_3$ antagonist **13** (Figure 12);[79] as the $\alpha_v\beta_3$ and $\alpha_v\beta_6$ integrin binding sites are structurally similar, there is potential for $\alpha_v\beta_3$ integrin inhibitors to additionally demonstrate significant antagonism towards $\alpha_v\beta_6$.

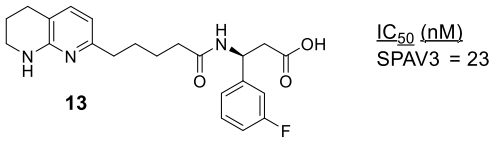

Figure 12. The Merck $\alpha_v\beta_3$ antagonist **13** from which the UoN series originates; potency was evaluated by inhibition of the *in vitro* binding of a high affinity radioligand to human $\alpha_v\beta_3$ immobilized on scintillation proximity beads (SPAV3).[79]

The antagonist **13** binds at the interface between the α and β subunits of the $\alpha_v\beta_6$ integrin, preventing interaction of the integrin with the RGD tripeptide in the LAP, which would otherwise result in TGF-β activation.

Figure 13 depicts the crystal structure of the $\alpha_v\beta_6$ integrin docked with a pro-TGF-β3 peptide.[80]

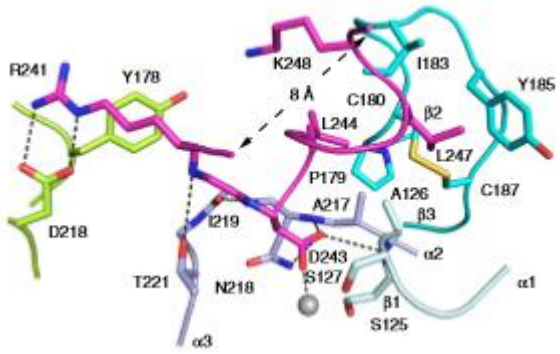

Figure 13. Crystal structure depicting ligand binding of $\alpha_v\beta_6$ to pro-TGF-β3 peptide.[80] Reprinted by permission from Springer Nature: Springer Nature, Nature structural & molecular biology, Structural determinants of integrin β-subunit specificity for latent TGF-β, Xianchi Dong, Nathan E. Hudson, Chafen Lu, Timothy A. Springer, 2014, vol. 21, p. 1091-1096, Copyright © 2014.

The interactions between arginine R241 in the peptide with aspartic acid D218 in the integrin, and aspartic acid D243 in the peptide with the metal-ion-dependent adhesion site (MIDAS) S127 are clearly visible; these interactions are critical for the development of effective $\alpha_v\beta_6$ integrin inhibition.[76]

One of the major modifications that distinguishes the UoN, Merck and related series of compounds from the RGD sequence is the replacement of the guanidine motif with the tetrahydronaphthyridine (THN) moiety (Figure 14). Not only does this increase the lipophilicity of compounds within the series, but it importantly also affects a reduction of pK_aH (~13 relating to the guanidinium, to ~7.5 for the protonated THN), ultimately improving passive permeability and thus oral absorption.[76]

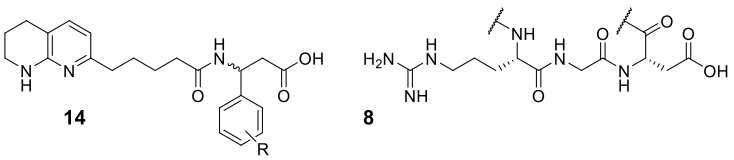

Figure 14. Comparison of the general core structure of the RGD mimetic series of integrin inhibitors (**14**) described in this thesis with the RGD tripeptide (**8**) that is present in TGF-β; the THN motif replaces the arginine residue, whilst the β-amino acid component replaces the aspartic acid residue, both of which are required for correct binding to the α_v integrins.

In these and similar RGD inhibitors, it is often found that the presence of an aryl group in the specificity determining loop (SDL) in the β-subunit of α_v integrins often facilitates increased potency, whilst subtle structural alterations to key sections of the molecule, such as the aryl component or the central linker, can result in significant changes to the selectivity profile of the inhibitor.[76,81]

1.4 Discussion of reported SAR for the UoN series of integrin inhibitors and future project design

Previous work reported by Adams *et al*. primarily focussed upon evaluating the effect of modulating the aryl moiety, resulting in the preparation and subsequent screening of a number of analogues of **14** against the α_v integrins in a cell adhesion assay.[82] These cell adhesion assays assess potency against the α_v integrins, measuring the ability of compounds to inhibit the binding of the integrin expressed on the surface of cells to the endogenous peptide ligand.[83] The upper limit of the assay for $\alpha_v\beta_6$ is pIC_{50} 8.6 – 8.7, and a difference of more than 0.4 log units in compound potency against each α_v integrin is regarded as significant. The protocol regarding how these cell adhesion assays are prepared and performed is described in the experimental section of this thesis.

Within the work described by Adams *et al.*, a diverse selection of aryl-substituents is reported, ensuring thorough investigation of motifs varying in size, position on the ring and electronic properties (Table 1).[82]

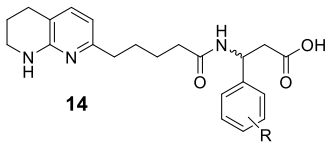

14

Compound no.	R	Chirality	pIC_{50} $\alpha_v\beta_6$	pIC_{50} $\alpha_v\beta_3$	pIC_{50} $\alpha_v\beta_5$	pIC_{50} $\alpha_v\beta_8$	$ChromlogD_{7.4}$
15	H	(*rac*)	5.7	7.0	7.1	6.1	1.56
16	2-OMe	(*rac*)	<5.0	6.3	6.3	<5.0	1.83
17	3-OMe	(*rac*)	6.5	7.4	7.2	6.3	1.66
18	4-OMe	(*rac*)	6.3	7.6	7.3	6.3	1.64
19	3,4-Cl_2	(*rac*)	6.7	7.3	7.0	6.7	2.62
20	3-CF_3-4-Cl	(*rac*)	7.0	6.5	6.9	6.6	3.10
21	3-OCF_3	(*rac*)	6.7	6.4	7.1	6.6	3.11
22	4-OCF_3	(*rac*)	6.2	6.8	6.3	6.1	2.85
23	3-Cl	(*rac*)	6.6	7.1	7.6	6.3	2.30
24	3,5-Cl_2	(*rac*)	6.6	6.4	6.7	6.6	2.93
25	3-CF_3	(*rac*)	7.0	6.7	7.4	6.8	2.73
(*S*)-25	3-CF_3	(*S*)	7.1	7.0	7.2	6.9	2.72
(*R*)-25	3-CF_3	(*R*)	5.2	<5	5.7	<5	2.61

Table 1. Potency and lipophilicity data corresponding to select compounds from the UoN structure-activity relationship (SAR) as reported by Adams *et al*.[82] Error in the cell adhesion assays = 0.3.

The unsubstituted analogue **15** demonstrates that the UoN series inherently exhibits potency towards the $\alpha_v\beta_3$ integrin, with **15** exhibiting greater than 10-fold selectivity over $\alpha_v\beta_6$; the compounds reported by Adams *et al.* exhibit an average selectivity for $\alpha_v\beta_3$ over $\alpha_v\beta_6$ of 0.51 log units with moderate correlation (R^2 = 0.39, Figure 15).

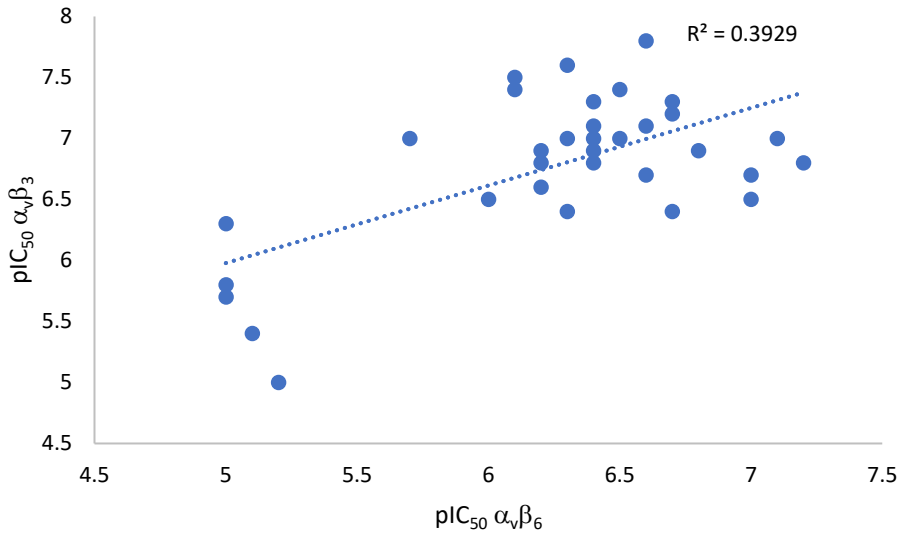

Figure 15. Plot of pIC_{50} against $\alpha_v\beta_6$ *vs* pIC_{50} against $\alpha_v\beta_3$, with R^2 correlation data, for the compounds reported by Adams *et al*.

These compounds additionally exhibit moderate correlation in terms of potency between $\alpha_v\beta_6$ and $\alpha_v\beta_8$ (R^2 = 0.86, average selectivity of 0.19 for $\alpha_v\beta_6$ over $\alpha_v\beta_8$) and between $\alpha_v\beta_3$ and $\alpha_v\beta_5$ (R^2 = 0.52, average selectivity of 0.10 for $\alpha_v\beta_5$ over $\alpha_v\beta_3$, Figure 16); this observation agrees with correlations described in the literature.[76]

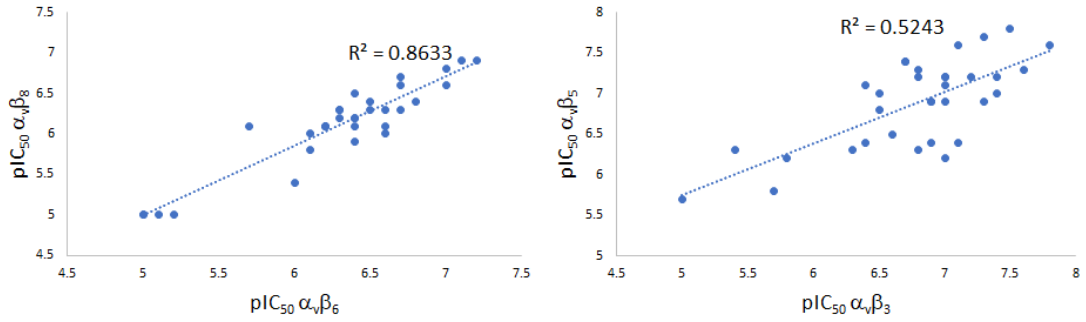

Figure 16. Plots of pIC_{50} against $\alpha_v\beta_6$ *vs* pIC_{50} against $\alpha_v\beta_8$ and pIC_{50} against $\alpha_v\beta_3$ *vs* pIC_{50} against $\alpha_v\beta_5$, with R^2 correlation data, for the compounds reported by Adams *et al*.

Comparison of each series of *ortho*, *meta* and *para* monosubstituted analogues demonstrates that *ortho*-substitution does not typically improve pIC_{50} against $\alpha_v\beta_6$, whereas

meta and *para*-substitution consistently imbues between a 10 and 20-fold increase, *meta*-analogues proving to be slightly more efficacious.

This suggests that the SDL within the binding pocket of the $\alpha_v\beta_6$ integrin contains at least one area of space surrounding the phenyl ring that can comfortably accommodate both *meta* and *para* substituents; this hypothesis is further validated by the 3,4-substituted analogues **19** and **20** that exhibit pIC_{50} against $\alpha_v\beta_6$ values that are similar in magnitude to their equivalent *meta*-substituted analogues (**23** and **25**).

Table 1 shows that 3 and 4-monosubstitution does not generally elicit a reduction of pIC_{50} against $\alpha_v\beta_3$, the exception to this being **21**. Consequently, *para*-substitution was discounted from further developmental work, due to *para* substituents facilitating a smaller increase of pIC_{50} against $\alpha_v\beta_6$ than their *meta* equivalents, in some cases even affecting an increase of pIC_{50} against $\alpha_v\beta_3$ (**18**). Thus, *meta*-substitution became the sole focus of further optimisation of the UoN series towards selective $\alpha_v\beta_6$ inhibition.

Any significant improvement of selectivity for $\alpha_v\beta_6$ over $\alpha_v\beta_8$ would likely require an entirely separate developmental strategy due to their strong, positive correlation (Figure 16) and so for the reason previously discussed, throughout this thesis, $\alpha_v\beta_3$ will be regarded and referred to as the primary target in terms of improving the selectivity profile of these integrin inhibitors for $\alpha_v\beta_6$; the positive correlation and lack of selectivity between $\alpha_v\beta_3$ and $\alpha_v\beta_5$ imply that improving selectivity for $\alpha_v\beta_6$ over $\alpha_v\beta_3$ will also result in improved selectivity over $\alpha_v\beta_5$.

Whilst pIC_{50} against $\alpha_v\beta_1$ is measured for these integrin inhibitors, although with reduced frequency than the other α_v integrins, it is often found that structural changes relating to aryl-substitution has little to no effect on the efficacy of these analogues, with the vast majority of UoN integrin inhibitors exhibiting potency values against $\alpha_v\beta_1$ of approximately

6-6.5 despite significant changes of potency against other integrins. This presumably results from structural differences between the SDLs within the binding sites of the $\alpha_v\beta_1$ integrin and the other α_v integrins. As such, unless a statistically significant result is obtained, in this thesis pIC_{50} against $\alpha_v\beta_1$ will be reported where available but will otherwise not be accompanied by detailed discussion regarding SAR.

The infrequent reduction of pIC_{50} against $\alpha_v\beta_3$ observed upon 3-monosubstitution of the phenyl component, despite improvement of pIC_{50} against $\alpha_v\beta_6$, leads to the conclusion that the environments surrounding this moiety within the $\alpha_v\beta_3$ and $\alpha_v\beta_6$ integrin binding pockets are similar in shape in terms of available chemical space, in turn suggesting that improving selectivity for the $\alpha_v\beta_6$ integrin over $\alpha_v\beta_3$ may be difficult to achieve simply *via* 3-monosubstitution of these analogues. The solution to this challenge may result from modification of the phenyl component of the molecule in such a way that augments the propensity for the inhibitor to bind in the $\alpha_v\beta_6$ integrin pocket, whilst simultaneously providing sufficient steric or electronic hinderance to reduce the affinity with which it binds to the $\alpha_v\beta_3$ integrin. Containing large, bulky *meta*-substitution patterns, **21** and **24** support this hypothesis; whilst **23** does not exhibit any selectivity for $\alpha_v\beta_6$, upon 3,5-disubstitution, **24** experiences an approximate 5-fold reduction of pIC_{50} against $\alpha_v\beta_3$, whilst still exhibiting the same pIC_{50} against $\alpha_v\beta_6$ as its *mono*-substituted parent analogue **23**. Similarly, **21** exhibits a pIC_{50} against $\alpha_v\beta_3$ that is 0.6 log units less than that exhibited by **15**, compared to **25** containing the smaller trifluoromethyl substituent that exhibits approximately the same level of pIC_{50} against $\alpha_v\beta_3$ as **15**.

Combining these results further suggests that, regarding the relative shape of each the $\alpha_v\beta_3$ and $\alpha_v\beta_6$ integrin binding pockets, $\alpha_v\beta_6$ contains either one or two moderate to large spaces that comfortably allow for 3,5-disubstitution with larger substituents without disrupting binding affinity, whilst the $\alpha_v\beta_3$ binding site perhaps only contains space enough for one

single, moderately sized substituent; a visual representation of this hypothesis is provided in Figure 17.

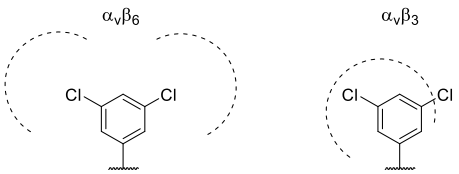

Figure 17. Proposed shape of the binding pocket surrounding the phenyl component in the $\alpha_v\beta_6$ integrin and $\alpha_v\beta_3$ integrin (left and right respectively). The dotted lines indicate the proposed arbitrary boundaries of the relevant integrin binding site surrounding the phenyl component of the integrin inhibitor.

Thus, to compliment the proposed further optimisation of the UoN 3-monosubstituted series, an additional series of work was planned that would facilitate an exploration of the pharmacokinetic potential of 3,5-disubstituted integrin inhibitors.

1.4.1 The relationship between ChromLogD and permeability within the UoN series of integrin inhibitors

LogD, the distribution coefficient, is a measure of the effective lipophilicity of a compound at a given pH, whereas LogP, the partition coefficient, is a measure of the intrinsic lipophilicity of a compound in the absence of ionisation. LogP is measured by calculation of compound concentration in each layer of an octanol/aqueous buffer mixture after equilibration, however LogD considers the concentration of unionised compound in the aqueous layer and as such is a more accurate measure of lipophilicity for the purposes of a medicinal drug development project; this is particularly relevant within the UoN series, due to the presence of ionisable groups at physiological pH within the core integrin inhibitor structure. In this project we use ChromLogD (measured at pH 7.4) which is LogD obtained chromatographically *via* comparison to a series of standard compounds evaluated by reverse phase HPLC, whilst

high throughput permeability (HTP) was determined by the Parallel Artificial Membrane Permeation Assay (PAMPA).[84–86] All ChromLogD and HTP values presented in this thesis were measured by researchers at GSK.

The ideal range of ChromLogD for biologically active compounds is between approximately 1-3; compounds with a value below this range would have particularly poor rates of absorption and would be expected to remain in the blood, whilst solubility and metabolism/toxicity issues may be a concern at higher levels of ChromLogD.[87,88]

Specifically, in the context of the UoN series, we have found that inhibitor analogues exhibiting a ChromLogD less than 2 typically do not have permeability values greater than 100 (measured in nm/s at pH 7.4, Figure 18); often in fact they will be less than 50. We classify permeability values less than 50 as poor, between 50 and 100 as moderate, above 100 as good and above 200 as excellent.

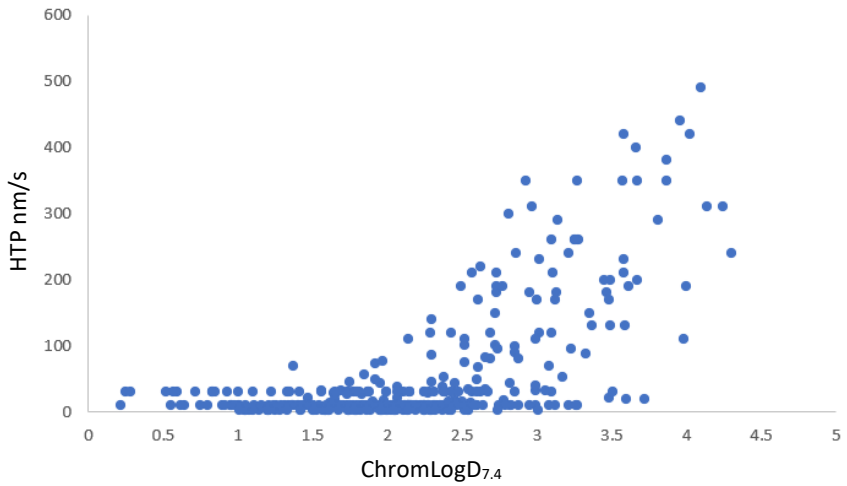

Figure 18. ChromLogD *vs* permeability for the SAR of the UoN series of integrin inhibitors.

Improved permeability values are more frequent between ChromLogD 1.75-2.5, but poor permeability is still a more commonly encountered issue. Achieving permeability values greater than 100 only seems possible when ChromLogD is greater than 2.5, an expected outcome due to the well-established correlation between increasing lipophilicity and

improved absorption/permeability.[88] Thus, to maximise the likelihood of developing potent and selective integrin inhibitors exhibiting excellent permeability values, there is a fairly narrow range of ChromLogD that target compounds must exhibit in order to remain permeable without suffering from the issues commonly associated with excessive lipophilicity.

1.4.2 Importance of the enantiomeric profile of UoN integrin inhibitors

Whilst each of these characteristics are vital considerations in terms of compound design, perhaps the single most important physical characteristic of the molecule to ensure is its enantiomeric profile. Adams *et al*. demonstrate a near 100-fold difference in potency against each integrin between the (*S*) and (*R*) enantiomers (**(*S*)-25** and **(*R*)-25**, respectively) of the trifluoromethyl-substituted inhibitor **25**, favouring the (*S*)-analogue **(*S*)-25** (Figure 19); both **(*S*)-25** and **(*R*)-25** were prepared using enantiopure β-amino acid precursors purchased from commercial sources. Thus, to maximise potency, target compounds were prepared as the single (*S*)-enantiomer or in a small number of cases, as the racemate; the racemic analogues within this series would logically exhibit as little as half the potency of the active (*S*)-analogue, equating to an approximate difference of 0.3 log units. The accepted error of the integrin assay used to evaluate inhibitors in this project is 0.4.

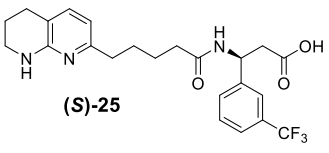

(*S*)-25

Figure 19. The lead compound (**(*S*)-25**) reported in the literature from the UoN series.[82]

1.5 Target compound design

Following the publication of Adams *et al*., a significant quantity of work performed by subsequent cohorts of UoN MSci students has resulted in the exploration of several key areas

of unreported SAR; this allowed us to focus upon more specific regions of unexplored SAR during the following target compound design stage. Much of this work will be used to supplement discussion throughout this thesis.[1,2,11–15,3–10]

1.5.1 Discussion of the GSK series of integrin inhibitors

$\alpha_v\beta_6$ integrin inhibition has undergone substantial investigation at GSK; there are a number of patents and publications available that detail a variety of inhibitor analogues for both inhaled and oral treatments, exhibiting both high levels of potency and selectivity;[89–91] two key compounds from the inhaled series and oral series are **12** and **26**, respectively (Figure 20).

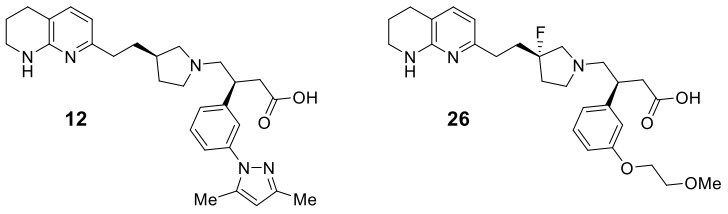

Figure 20. The lead inhaled (**12**) and oral (**26**) compounds resulting from work performed by GSK.

This series of compounds is similar to the UoN series described in this thesis, differing by the presence of the pyrrolidine motif in place of the amide and the positioning of the nitrogen within the alkyl chain. In the oral series, a fluorine atom is present β to the pyrrolidine-amine in order to draw electron density away from the nitrogen, subsequently decreasing its basicity, thus improving the permeability and oral free fraction exhibited by analogues within the series.

Despite containing a different linker functionality to the UoN series as described by Adams *et al*., the SAR developed during optimisation of the phenyl component in the GSK series has

some correlation with the UoN series; comparison of **12** and **26** with their UoN analogues **27** and **28** is shown in Table 2.

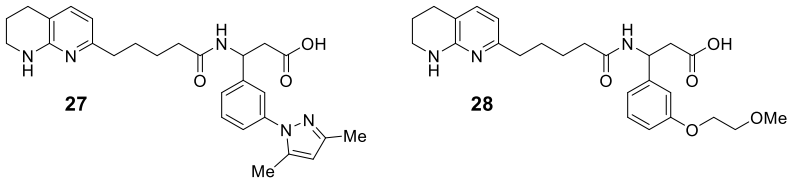

Compound no.	pIC_{50} $\alpha_v\beta_6$	pIC_{50} $\alpha_v\beta_3$	pIC_{50} $\alpha_v\beta_5$	pIC_{50} $\alpha_v\beta_8$	$ChromLogD_{7.4}$
12	8.4	6.0	6.9	7.7	2.82
27	7.3	5.9	6.4	7.2	2.27
26	7.9	7.4	7.4	7.5	-
28	6.9	7.4	6.5	6.0	1.89

Table 2. The biological data corresponding to the lead GSK compounds **12** and **26** and the UoN series compounds **27** and **28**. Error in the cell adhesion assays = 0.3.

As depicted in Table 2, compounds **27** and **28** exhibit a near 10-fold reduction of pIC_{50} against $\alpha_v\beta_6$ compared to their equivalent analogues **12** and **26**, whilst the pIC_{50} against $\alpha_v\beta_3$ remains the same across the two series; these are two of several analogous compound matches exhibiting this same trend. This is particularly useful information for the purposes of future target design, as the reported GSK SAR can be used to filter out unnecessary target compounds or even subseries of compounds by determining whether the potency against $\alpha_v\beta_6$ exhibited by the relevant GSK series analogue would translate to a pIC_{50} against $\alpha_v\beta_6$ above a specific threshold within the UoN series. It is important to note that in these comparisons, compounds within the GSK series are enantiopure, whilst compounds from the UoN series are typically racemic; thus, enantiopure analogues of UoN compounds would be expected to exhibit greater pIC_{50} against $\alpha_v\beta_6$ and each of the other integrins than suggested by utilisation of the method described above.

The GSK series as reported by Procopiou *et al*. exhibits good correlation in terms of potency between $\alpha_v\beta_6$ and $\alpha_v\beta_8$ ($R^2 = 0.74$), and likewise, moderate correlation between $\alpha_v\beta_3$ and $\alpha_v\beta_5$

(R^2 = 0.56, Figure 21);[92] gratifyingly, this matches with correlations relating to the integrin inhibitors reported by Adams *et al*. (Section 1.4), and so we had increased confidence that application of the GSK SAR to our own series was indeed a viable strategy for future target design.

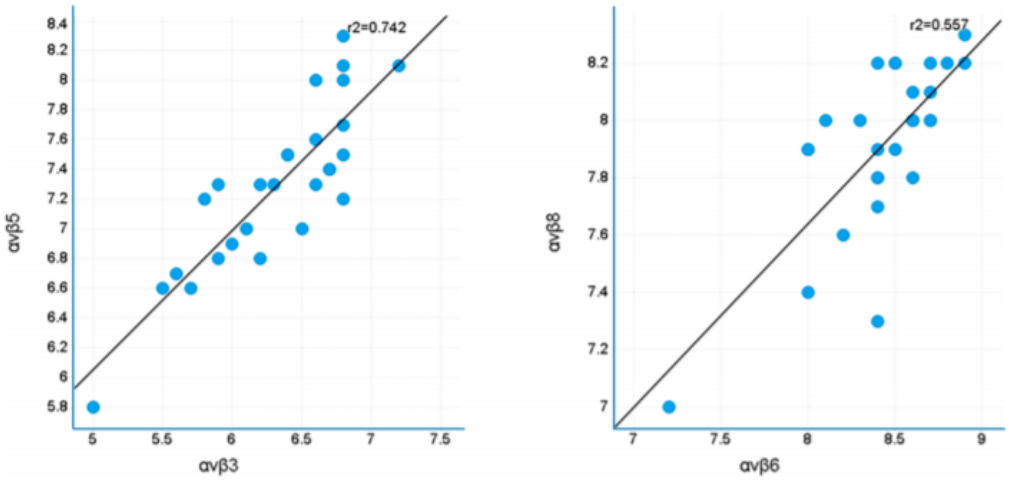

Figure 21. Comparison of pIC_{50} against $\alpha_v\beta_6$ and $\alpha_v\beta_8$, and pIC_{50} against $\alpha_v\beta_3$ and $\alpha_v\beta_6$ with R^2 correlation values as reported by Procopiou.[92] Reprinted with permission from Panayiotis A. Procopiou, Niall A. Anderson, John Barrett, Tim N. Barrett, Matthew H. J. Crawford, Brendan J. Fallon, Ashley P. Hancock, Joelle Le, Seble Lemma, Richard P. Marshall, Josie Morrell, John M. Pritchard, James E. Rowedder, Paula Saklatvala, Robert J. Slack, Steven L. Sollis, Colin J. Suckling, Lee R. Thorp, Giovanni Vitulli, and Simon J. F. Macdonald, *J. Med. Chem.*, 2018, vol. 61, issue 18, p. 8417–8443. Copyright 2018 American Chemical Society.

Subsequent target design has thus been greatly inspired by the GSK SAR, supplementing the work already performed and reported by Adams *et al*. Consequently, further investigation led to the development of an ether subseries and a heterocycle subseries, containing compounds such as **28** and **27**, as well as similar derivatives.

1.5.2 Discussion of SAR regarding the UoN series of integrin inhibitors

1.5.2.1 Ether substituted integrin inhibitor analogues

This subseries primarily focused on the generation of various ether-substituted integrin inhibitor analogues, prepared *via* alkylation of phenolic species, or from commercially available pre-functionalised aldehydes; the preparation of the requisite β-3-aryl-amino acid functionality utilised in this and subsequent series described in this chapter was achieved using the Rodionow reaction, methodology that will be discussed in detail in Section 2.2.1.

The ether subseries proved to be largely successful in terms of progressing towards a clinical drug candidate.

Compared to that of **15**, the ether substituents affect a largely similar increase of pIC_{50} against $\alpha_v\beta_6$ to one another, rendering the majority of these inhibitor analogues indistinguishable from each other (Table 3).

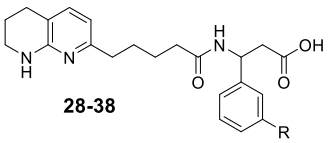

28-38

Compound no.	R	pIC_{50} $\alpha_v\beta_6$	pIC_{50} $\alpha_v\beta_3$	pIC_{50} $\alpha_v\beta_5$	pIC_{50} $\alpha_v\beta_8$	pIC_{50} $\alpha_v\beta_1$	$ChromLogD_{7.4}$	HTP nm/s
28	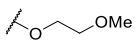	6.9	7.4	6.5	6.0	5.7	1.89	<10
29		6.5	6.7	6.9	6.7	-	3.33	88
30	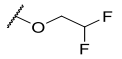	7.5	7.1	7.0	6.7	6.2	2.60	49
31	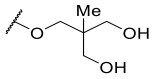	7.5	7.4	7.6	6.5	5.9	1.43	<10
32		7.1	7.0	6.5	6.6	6.3	2.69	80
33	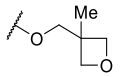	6.7	7.2	7.1	6.7	6.2	2.37	<10
34		6.0	5.9	5.6	5.3	5.4	2.40	-
35	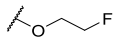	7.0	7.1	7.4	6.5	6.1	2.03	<10
36		7.2	7.0	7.1	7.0	6.3	2.88	80
37	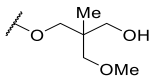	7.2	6.9	7.5	6.7	6.4	2.38	<30
38		6.9	6.7	6.9	7.0	5.6	2.47	46

Table 3. A selection of 3-monosubstituted 'ether-based' integrin inhibitors from the UoN SAR.[1,5,9,14,15] Error in the cell adhesion assays = 0.3.

This subseries of analogues exhibits an average pIC_{50} against $\alpha_v\beta_6$ of 6.8, with a level of average selectivity for $\alpha_v\beta_3$ over $\alpha_v\beta_6$ that is within the error of the assay at 0.18 (R^2 = 0.24); this is an improvement upon that exhibited by the analogues reported by Adams *et al*., with an average pIC_{50} against $\alpha_v\beta_6$ of 6.3, and average selectivity for $\alpha_v\beta_3$ over $\alpha_v\beta_6$ of 0.51 (R^2 = 0.39). These integrin inhibitors otherwise exhibit similar correlations in terms of potency between $\alpha_v\beta_6$ and $\alpha_v\beta_8$ (R^2 = 0.28), and between $\alpha_v\beta_3$ and $\alpha_v\beta_5$ (R^2 = 0.48), with similar levels of average selectivity compared to those described in Section 1.4. Poor permeability (<100

nm/s) however is a common feature of these analogues despite a fairly wide range of ChromLogD; this is perhaps a result of the phenolic oxygen lone pairs shrouding the lipophilic profile of the phenyl group, coupled with the high polarity of the constituent atoms within the majority of the substituents.

Despite the general poor $\alpha_v\beta_6$ potency of the subseries, there are two stand-out compounds, the 2,2-difluoroethyl ether analogue **30** and the diol **31** (Figure 22). Introduction of the diol substituent results in a significant increase of pIC_{50} against $\alpha_v\beta_6$ and a minor improvement of pIC_{50} against $\alpha_v\beta_3$, $\alpha_v\beta_5$ and $\alpha_v\beta_8$ compared to **15**, whilst inclusion of the 2,2-difluoroethyl ether motif results exclusively in a significant improvement of pIC_{50} against $\alpha_v\beta_6$ compared to **15**. Thus **30** exhibits minor selectivity for $\alpha_v\beta_6$ over $\alpha_v\beta_3$ and $\alpha_v\beta_5$; both **30** and **31** demonstrate near 10-fold selectivity for $\alpha_v\beta_6$ over $\alpha_v\beta_8$, an unexpected result.

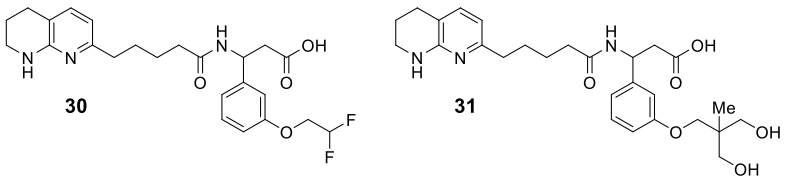

Figure 22. The difluoro analogue **30** and diol analogue **31**.

Due to the highly polar and thus impermeable nature of **31**, despite good potency against $\alpha_v\beta_6$, **31** was discounted as a potential lead compound for further optimisation and as such only **30** was identified as a suitable candidate for further developmental work; the single (*S*)-enantiomer of **30** was subsequently prepared (**(*S*)-30**, Table 4).

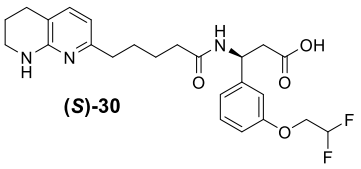

(*S*)-30

Compound no.	pIC_{50} $\alpha_v\beta_6$	pIC_{50} $\alpha_v\beta_3$	pIC_{50} $\alpha_v\beta_5$	pIC_{50} $\alpha_v\beta_8$	pIC_{50} $\alpha_v\beta_1$	$ChromLogD_{7.4}$	HTP nm/s
(*S*)-30	7.9	7.2	7.4	7.4	6.4	2.48	37
30	7.5	7.1	7.0	6.7	6.2	2.60	49

Table 4. Potency and other physical characteristic data for the (*S*)-enantiomer **(*S*)-30**, accompanied by the relevant data pertaining to that of the racemate **30** for comparison. Error in the cell adhesion assays = 0.3.

1.5.2.2 Heterocycle substituted integrin inhibitor analogues

The heterocycle subseries primarily focused on the generation of *C*-linked analogues, prepared *via* Suzuki-Miyaura couplings using commercially available heterocyclic boronate reagents, with a select number of *N*-linked analogues prepared from commercially available pre-functionalised aldehydes; the selected heterocycles were all five-membered rings and were thus analogous to the 3,5-dimethylpyrazole present in **12**.

The data for this subseries is presented in Table 5.

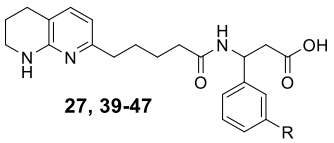

27, 39-47

Compound no.	R	pIC_{50} $\alpha_v\beta_6$	pIC_{50} $\alpha_v\beta_3$	pIC_{50} $\alpha_v\beta_5$	pIC_{50} $\alpha_v\beta_8$	pIC_{50} $\alpha_v\beta_1$	$ChromLogD_{7.4}$	HTP nm/s
27	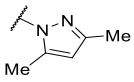	7.3	5.9	6.4	7.2	6.3	2.27	29
39		7.4	6.1	7.0	6.7	6.5	1.05	<3
40		7.0	6.3	6.5	6.5	-	1.64	28
41		6.5	6.5	6.6	6.3	-	1.67	8.9
42		6.7	6.5	6.7	6.3	-	1.21	<10
43		7.2	6.5	6.8	7.1	6.3	1.98	18
44		7.1	6.9	7.3	6.9	6.3	1.20	<3
45		7.1	6.7	7.3	7.3	6.8	2.52	75
46		6.8	7.0	7.0	7.2	6.5	1.74	<3
47	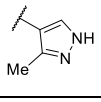	6.7	6.7	6.9	5.0	6.2	1.58	<3

Table 5. A selection of *C*-linked and *N*-linked integrin inhibitor analogues from the UoN SAR.[4,7,8,13] Error in the cell adhesion assays = 0.3.

Focussing solely upon the *C*-linked heterocyclic analogues **41**-**47**, this subseries exhibits an average pIC_{50} against $\alpha_v\beta_6$ of 6.9, with a level of average selectivity for $\alpha_v\beta_6$ over $\alpha_v\beta_3$ that is within the error of the assay at 0.19 (R^2 = 0.04). This is an improvement upon that exhibited by the analogues reported by Adams *et al*. and is perhaps even an improvement upon the

ether subseries described in Section 1.5.2.1; 0.19 log units of selectivity is well within the accepted assay error of 0.4, however where the ether subseries exhibits an average selectivity of 0.17 in favour of $\alpha_v\beta_3$ over $\alpha_v\beta_6$, a total difference of 0.36 on average and a shift to favouring the $\alpha_v\beta_6$ integrin over $\alpha_v\beta_3$ is perhaps a significant result. With the exception of **47**, these analogues do not typically demonstrate particularly noteworthy levels of selectivity for $\alpha_v\beta_6$ over $\alpha_v\beta_8$ (R^2 = 0.38), nor between $\alpha_v\beta_3$ and $\alpha_v\beta_5$ (R^2 = 0.48), and thus follow the expected correlations reported elsewhere.[76] These *C*-linked compounds are on the whole relatively poor, with uninspiring potency and selectivity profiles, coupled with particularly low ChromLogD and poor permeability characteristics.

The three *N*-linked analogues **27**, **39** and **40** on the other hand each exhibit moderate levels of pIC_{50} against $\alpha_v\beta_6$ and on average, greater than 10-fold selectivity against the $\alpha_v\beta_3$ integrin; the 3,5-dimethylpyrazole substituted analogue **27** in particular stands out, with near 30-fold selectivity against $\alpha_v\beta_3$ and 10-fold selectivity against $\alpha_v\beta_5$, with potency against each having been reduced compared to **15**.

There is a trend amongst these *C*- and *N*-linked heterocycle-substituted analogues that demonstrates a general reduction of inhibitor permeability as heteroatoms within the heterocycle are moved to a more 'external' position (Figure 23).

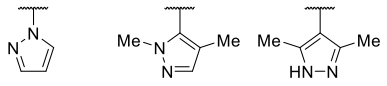

Compound number =	**40**	**43**	**46**
HTP nm/s =	28	18	3

Figure 23. Three integrin inhibitor analogues that well demonstrate the trend observed in *C*-linked and *N*-linked heterocyclic substituted species, where permeability is reduced as heteroatoms are moved to a more external position on the heterocyclic substituent.

It has been hypothesised that an increased hydrogen-bond donor/acceptor count within RGD integrin inhibitors hinders passive absorption and thus permeability, particularly when coupled with high polarity, and so it is likely that the observed reduction of permeability is a result of inclusion of more electron-rich nitrogens within the heterocycle and even secondary amine-like nitrogens, combined with the lone pairs within the heterocycle being moved to a more exposed position.[76] Presumably without the shielding effect provided by the lipophilic carbon component of the heterocycle, the molecule subsequently manifests as a highly polar entity for the purposes of passing through a medium, be it a cell membrane or chromatographic column, rendering it largely impermeable.

Permeability is a vital consideration of drug design, determining whether a compound will permeate the cell membrane, subsequently affecting the desired change to the biological target. Whilst some *C*-linked analogues do display very modest levels of permeability (**43** and **45**), the majority do not. As a result, *C*-linked monosubstituted analogues were discounted as potential future targets and instead, regarding the further development of the heterocycle subseries, methodology was sought that would allow a substantial number of *N*-linked analogues to be prepared, ideally from a single late-stage intermediate.

1.5.2.3 Ligand efficiency and alkyl substituted integrin inhibitor analogues

In drug development, ligand efficiency (LE) is an useful metric that allows comparison between analogues in such a way that the net efficacy of structural features within each molecule may be evaluated;[93,94] it is a calculable quantity that can be defined as the Gibbs free energy (ΔG) of binding per heavy atom over the number of non-hydrogen (or, heavy) atoms within the molecule (Equation 1).[93,94]

$$LE = (\Delta G)/N = (-RT\ln K_d)/N$$

Equation 1. Calculation of LE, where ΔG is the Gibbs free energy and N is the total number of non-hydrogen atoms in the molecule.[93,94]

There is an alternative method of calculating LE that is better suited to the data typically possessed by a medicinal chemist, where LE is determined using the measured pIC_{50} of a compound against a specific target (Equation 2).[95]

$$LE = 1.4(pIC_{50})/N$$

Equation 2. Alternate calculation of LE, where a particular potency value measured as pIC_{50} is used and N is the total number of non-hydrogen atoms in the molecule.[95]

A simple way of demonstrating the application of LE in the context of this project would be to compare the trifluoromethyl and dimethylpyrazole substituted analogues **25** and **27**, compounds differing only by the substituent present on the phenyl ring (Figure 24).

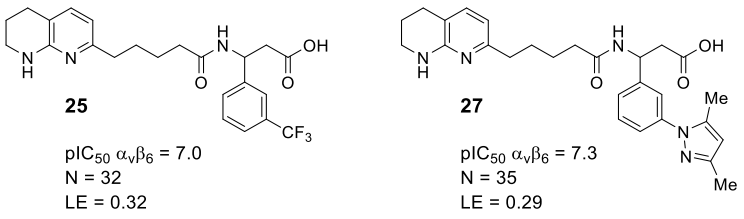

Figure 24. The inhibitor analogues **25** and **27**, accompanied by potency, N and subsequently LE values.

The trifluoromethyl analogue **25** exhibits a pIC_{50} against $\alpha_v\beta_6$ of 7.0, contains a total of 32 non-hydrogen atoms, and thus has LE = 0.32, whereas **27** exhibits a pIC_{50} against $\alpha_v\beta_6$ of 7.3, contains a total of 35 non-hydrogen atoms, and thus has LE = 0.29. Comparing these two compounds *via* this single metric indicates that **25** is the more ligand efficient of the pair and as such it would be reasonable to suggest that the trifluoromethyl group is preferable to the

3,5-dimethylpyrazole group as an aryl-substituent. However, it must be noted that LE does not consider parameters such as lipophilicity, selectivity, permeability etc. and thus should not be relied upon exclusively to influence the course of a drug development project; instead, combination of all available data is often essential for successful and efficient progression.

One disadvantage of LE as a metric is its inability to consider the contribution of larger heteroatoms to the potency of a molecule; Abad-Zapatero and Metz recognised this limitation and subsequently developed the binding efficiency index (BEI), an alternative ligand efficiency metric, where the molecular weight of the compound in question is utilised instead of the total number of non-hydrogen atoms (Equation 3).[96]

$$BEI = pIC_{50}/MW$$

Equation 3. Calculation of BEI as reported by Abad-Zapatero and Metz, where molecular weight (MW) is measured in kDa.[96]

A study of 60 lead/drug compound pairs by Perola indicated that the median BEI value for both lead and drug compounds is 18.4, with BEI values between 15-20 being exhibited by the greatest number of compounds (Figure 25);[97] in this study, ligand efficiency as presented in Figure 25 is referring to the BEI value of compounds.

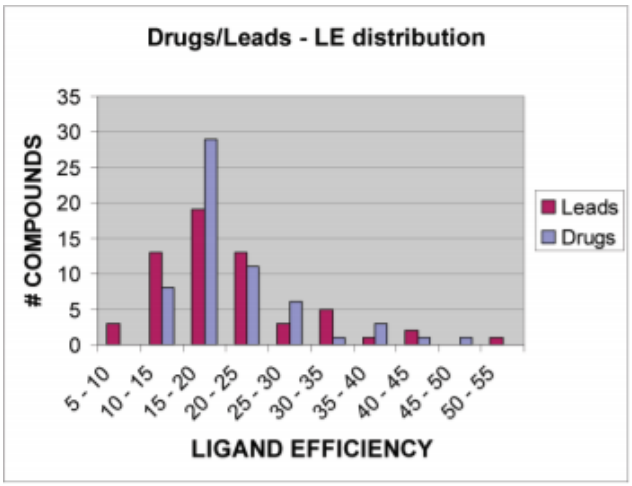

Figure 25. A histogram of BEI values corresponding to 60 pairs of lead and drug compounds, as reported by Perola.[97] Adapted with permission from Emanuele Perola, Journal of Medicinal Chemistry, 2010, vol. 53, p. 2986-2997. Copyright 2010 American Chemical Society.

This trend is approximately correlated by the BEI values corresponding to the UoN series of integrin inhibitors, with BEI values between 13-16 being exhibited by the greatest number of compounds (Figure 26); however, unlike the data depicted in Figure 25, there are no compounds exhibiting BEI values greater than 20 within the UoN series of integrin inhibitors.

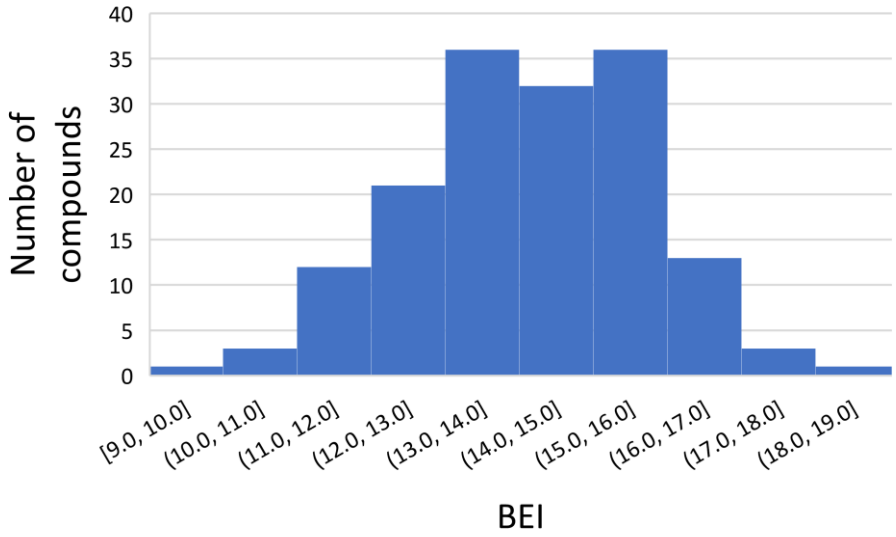

Figure 26. A histogram of BEI values corresponding to every compound within the UoN series of integrin inhibitors whose preparation is not described in this thesis.

Figure 26 reveals a lack of compounds exhibiting BEI values greater than 16 within the UoN SAR, and so it was proposed that small, alkyl substituted analogues be targeted for preparation; this decision was partly based upon the potency profile of the GSK-developed inhibitor **48**, which exhibits a similar level of potency against $\alpha_v\beta_6$ as the GSK clinical candidate **12** and thus a greater BEI value due to its lower MW (Table 6).[92]

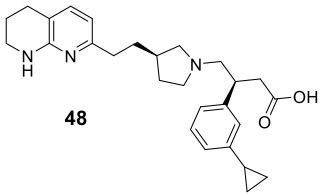

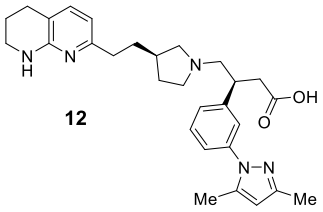

Compound no.	pIC_{50} $\alpha_v\beta_6$	pIC_{50} $\alpha_v\beta_3$	pIC_{50} $\alpha_v\beta_5$	pIC_{50} $\alpha_v\beta_8$	pIC_{50} $\alpha_v\beta_1$	$ChromLogD_{7.4}$	BEI
48	8.4	6.8	8.1	8.2	6.8	3.34	19.4
12	8.4	6.0	6.9	7.8	7.3	2.82	17.2

Table 6. The GSK-developed cyclopropyl analogue **48**, developed in tandem with the clinical candidate **12**; the integrin assay data for **48** is presented with the data for **12** for comparison. Error in the cell adhesion assays = 0.3.

As previously discussed, integrin inhibitor analogues from within the GSK series typically exhibit pIC_{50} against $\alpha_v\beta_6$ values that are approximately one log unit higher than that of the equivalent UoN series compound due to interaction between the protonated pyrrolidine nitrogen and threonine residue; thus, it was hoped that the cyclopropyl analogue **49** and the isopropyl analogue **50** would exhibit potency values against $\alpha_v\beta_6$ between 7.0-7.5, subsequently exhibiting BEI values of approximately 17 (Figure 27).

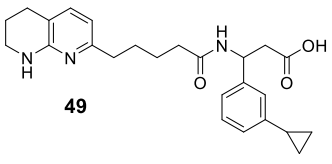

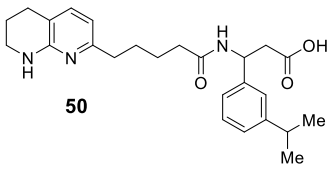

Figure 27. The proposed c-Pr and *i*-Pr analogues **49** and **50** respectively.

Thus, **49** and **50** were targeted for synthesis, as they were regarded as potential improvements upon the lead compound reported by Adams *et al*., compound **25**, both in terms of potency and BEI.

1.5.2.4 *N*-Alkylated integrin inhibitor analogues

Due to the significant increase in potency against $\alpha_v\beta_6$ that is observed following replacement of the central amide with the pyrrolidine motif within the GSK series (Figure 28), this led to speculation that modification of the central β-nitrogen within the UoN series may result in a similar improvement of pIC_{50} against $\alpha_v\beta_6$.

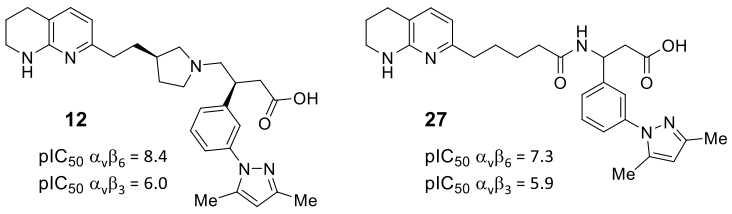

Figure 28. Comparison between **12** and **27**, demonstrating the effect imbued by replacement of the central amide with the pyrrolidine motif found in the UoN series of integrin inhibitors.

The observed increase of pIC_{50} against $\alpha_v\beta_6$ is thought to be attributable to a hydrogen-bonding interaction between the pyrrolidine nitrogen in its protonated form and a threonine residue (Thr238) in close proximity.[92] Within $\alpha_v\beta_3$, Thr238 is replaced by a smaller and non-polar alanine residue (Ala218), thus **12** does not exhibit a similarly increased potency against $\alpha_v\beta_3$ compared to **27**. Additionally, as it is thought that the pyrrolidine structure in **12** and the GSK series as a whole forces the amine into a specific spatial orientation within the SDL of the $\alpha_v\beta_6$ integrin binding site, it was hoped that a similar effect would be induced by the *N*-alkyl substituents in the proposed *N*-alkylated inhibitor targets.

Thus, it was decided that the UoN series was to be modified in such a way as to allow a rudimentary investigation of the chemical space surrounding the amide position within the

$\alpha_v\beta_6$ integrin binding site; this would be achieved *via* preparation of a small number of *N*-alkylated analogues of the trifluoromethyl substituted inhibitor **25** (Figure 29).

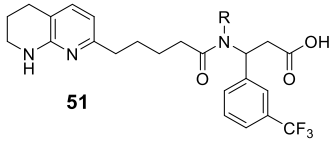

51

Figure 29. General structure of the proposed *N*-alkylated analogues (**51**) where R = simple alkyl substituents such as methyl, and motifs with the capacity to form hydrogen-bonds, such as ethers and alcohols.

As an established pan-α_v inhibitor exhibiting an approximate pIC_{50} against the four α_v integrins of interest of 7, **25** was deemed a suitable substrate for this work; any significant changes in potency or selectivity resulting from the planned structural modifications would become immediately clear and obvious given that up to a 100-fold improvement or deterioration of potency against each integrin would be tolerated before assay inaccuracy would become a concern.

1.5.2.5 3,5-Disubstituted integrin inhibitor analogues

Whilst limited, there is precedent to suggest that the UoN and similar series of integrin inhibitors can exhibit an improved selectivity profile for the $\alpha_v\beta_6$ integrin over $\alpha_v\beta_3$ upon 3,5-disubstitution of the aryl component.[82,92] Development of a 3,5-disubstituted subseries to expand the reported SAR and provide further validation to this hypothesis led to the preparation of a number of 3,5-*bis*-*C*-linked heterocycle substituted analogues and other similar 3,5-disubstituted analogues that demonstrate this hypothesis exceptionally well (Table 7).

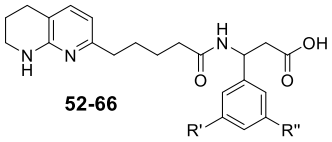

52-66

Compound no.	R’	R’’	pIC$_{50}$ $\alpha_v\beta_6$	pIC$_{50}$ $\alpha_v\beta_3$	pIC$_{50}$ $\alpha_v\beta_5$	pIC$_{50}$ $\alpha_v\beta_8$	pIC$_{50}$ $\alpha_v\beta_1$	ChromLogD$_{7.4}$	HTP nm/s
52	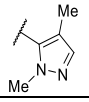	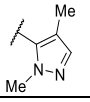	7.0	5.0	5.4	7.2	5.8	2.19	<3
53			7.2	6.2	5.8	7.5	6.3	2.04	<3
54	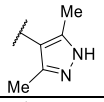	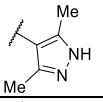	6.8	5.2	5.0	-	6.4	1.42	<3
55	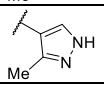	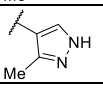	7.0	6.5	6.3	7.2	6.4	1.20	<3
56	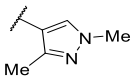	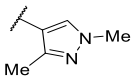	6.9	5.7	5.6	5.0	6.0	1.99	<3
57	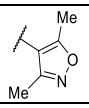	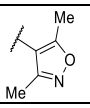	6.9	5.5	5.9	7.3	6.1	3.08	70
58	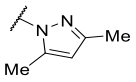	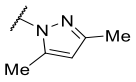	7.4	5.2	5.5	7.0	5.4	3.07	26
59			7.3	6.8	-	-	6.4	3.57	350
60		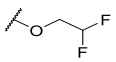	7.5	6.9	7.2	7.5	6.4	3.13	180
61			7.2	6.6	5.9	7.4	6.2	2.66	83
62		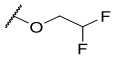	7.1	6.3	7.0	7.1	6.0	3.47	180
63	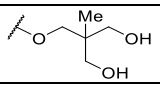		7.5	6.4	6.8	5.0	6.4	2.60	<30
64	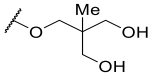	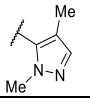	7.5	6.2	6.7	-	6.7	1.86	<3
65	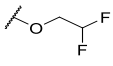	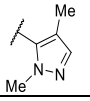	7.2	6.1	6.4	7.3	6.5	3.01	<3
66	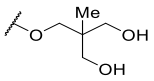	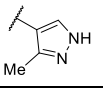	7.2	5.5	7.0	-	6.5	1.21	<3

Table 7. A selection of 3,5-disubstituted integrin inhibitor analogues and the relevant biological data from the UoN SAR.[2,7,9,11,13] Error in the cell adhesion assays = 0.3.

Immediately it can be seen that upon 3,5-disubstitution, the selectivity profile of these analogues for $\alpha_v\beta_6$ against $\alpha_v\beta_3$ and $\alpha_v\beta_5$ is improved significantly; the average selectivity for $\alpha_v\beta_6$ over $\alpha_v\beta_3$ is in fact 0.8 log units, far greater than both the ether subseries and *C*-linked heterocycle-substituted subseries discussed previously. There is no correlation in terms of potency between $\alpha_v\beta_6$ and $\alpha_v\beta_3$ ($R^2 = 0.03$), validating our hypothesis discussed in Section 1.4 postulating that 3,5-disubstitution does not affect binding affinity of the inhibitor within the $\alpha_v\beta_6$ integrin to any significant degree, but instead results in improved selectivity for $\alpha_v\beta_6$ over $\alpha_v\beta_3$ and by extension $\alpha_v\beta_5$, due to increased steric and electronic disruption within the latter mentioned integrin binding sites, leading to reduced binding affinity. Paying particular attention to the *bis*-*C*-linked heterocycle-substituted analogues **52**-**57**, it seems that with an average selectivity for $\alpha_v\beta_6$ over $\alpha_v\beta_3$ of 1.3 log units, we are correct in suggesting that the improved selectivity observed upon 3,5-disubstitution is augmented upon substitution with particularly large, bulky moieties, compared to 3,5-disubstitution with smaller groups (e.g. **52** *vs* **24**); it must be noted however, that 3,5-disubstitution within the UoN series does not guarantee an improvement of selectivity, but simply provides increased confidence during the target-design process that significant levels of selectivity are potentially obtainable.

It is also important to note that there is no beneficial combination effect regarding increasing potency against $\alpha_v\beta_6$ upon addition of a secondary *meta*-substituent and thus 3,5-disubstituted integrin inhibitors typically exhibit the potency of the most efficacious 3-monosubstituted parent compound (Table 8).

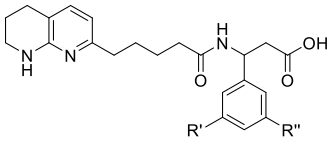

Compound no.	R’	R’’	pIC_{50} $\alpha_v\beta_6$	pIC_{50} $\alpha_v\beta_3$	BEI
31	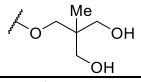	H	7.5	7.4	15.0
47	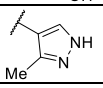	H	6.7	6.7	14.5
66	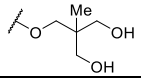	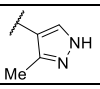	7.2	5.5	12.4

Table 8. Demonstration of the often-observed reduction of pIC_{50} against $\alpha_v\beta_3$ upon 3,5-disubstitution within the UoN series of integrin inhibitors; compound **66** additionally demonstrates that there is typically no improvement of pIC_{50} against $\alpha_v\beta_6$ upon 3,5-disubstitution, with **66** instead simply exhibiting the potency of the most efficacious parent monosubstituted analogue (**31**). Error in the cell adhesion assays = 0.3.

Whilst 3,5-disubstitution is clearly an effective method for improving the selectivity profiles of these integrin inhibitors, as potency against $\alpha_v\beta_6$ is not typically improved upon disubstitution, 3,5-disusbstituted analogues often exhibit reduced ligand efficiencies compared to their 3-monosubstituted parent compounds; the inhibitors **31**, **47** and **66** demonstrate this well.

There is moderate correlation in terms of potency between $\alpha_v\beta_3$ and $\alpha_v\beta_5$ ($R^2 = 0.52$), with a level of selectivity for $\alpha_v\beta_5$ over $\alpha_v\beta_3$ that is within the error of the assay, thus indicating that, as previously hypothesised, these two integrins share many structural similarities in terms of their binding sites.

As is typically the case with all previous subseries of UoN series integrin inhibitors, there is a level of selectivity for $\alpha_v\beta_6$ over $\alpha_v\beta_8$ that is within the error of the assay. There are however two stand-out compounds (**56** and **63**) that exhibit 100-fold and 300-fold selectivity for $\alpha_v\beta_6$

over $\alpha_v\beta_8$, respectively; the cause of this unexpected selectivity is not clear, and so development of additional SAR and perhaps even the use of computer modelling will be required to provide clarity on the origins of this promising pharmacokinetic characteristic. Despite this, it is highly encouraging for the purposes of future target design that excellent levels of selectivity for $\alpha_v\beta_6$ against not only $\alpha_v\beta_3$ and $\alpha_v\beta_5$, but also $\alpha_v\beta_8$, are potentially obtainable upon 3,5-disubstitution.

Despite exhibiting excellent selectivity profiles, the poor permeability characteristics coupled with the high molecular weights relating to the *bis*-heterocycle-substituted analogues **52**-**58**, disqualified them and similar potential target compounds from further development as lead-like analogues.

With this in mind, further optimisation of this UoN 3,5-disubstituted subseries of integrin inhibitors was planned that would see the combination of the most promising drug-like substituents from within the UoN series SAR after development of the proposed 3-monosubstituted subseries, including any advantageous structural functionalities resulting from the intended *N*-alkylation work (Figure 30).

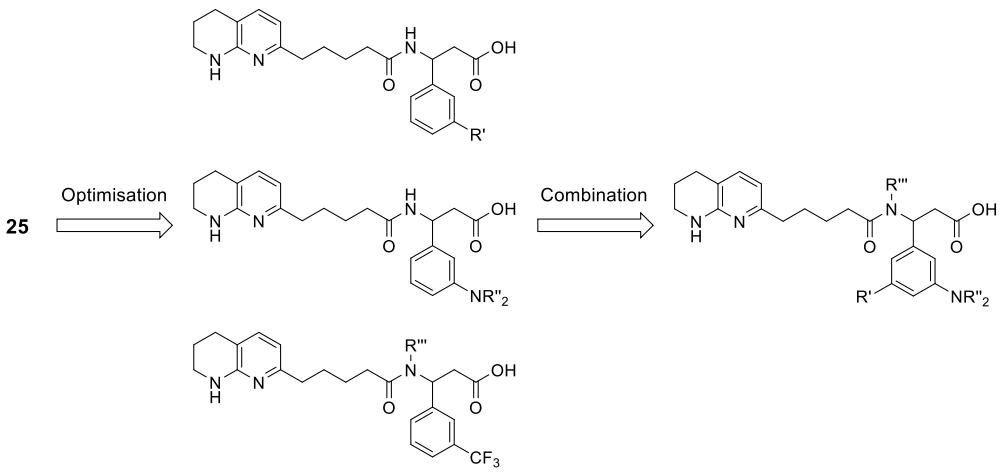

Figure 30. Depiction of the intended outcome of this project: further optimisation of the 3-monosubstituted UoN series, followed by combination of efficacious structural motifs in a series of 3,5-disubstituted analogues.

The work described herein was implemented in a two-stage process; (1) exploration and development of three subseries of 3-monosubstituted UoN series integrin inhibitors and (2) the combination of the most promising structural features from these subseries as determined by the SAR, to facilitate the generation of a series of potent and selective 3,5-disubstituted integrin inhibitors.

Chapter 2

Preparation and biological evaluation of 3-monosubstituted β-3-aryl-amino acid $\alpha_v\beta_6$ integrin inhibitor analogues

This chapter describes in detail the development of three subseries of the UoN series of integrin inhibitors, building specifically upon work reported by Adams *et al.*, Procopiou *et al.* and unpublished work originating from the UoN group.[82,92] Leading into this work, we had three specific goals in mind: (1) to explore the efficacy of *N*-linked heterocycle motifs within the UoN series, hopefully resulting in the development of potent and selective analogues; (2) the further optimisation of small alkyl motifs to build upon the precedent set by the trifluoromethyl-substituted pan-inhibitor compound **25**, and (3) the development of *N*-alkylated compounds in an attempt to generate further understanding of a relatively unexplored area of chemical space within the $\alpha_v\beta_6$ integrin binding site.

2.1 Preparation of the tetrahydronaphthyridine (THN) fragment 82

To install each of the previously discussed motifs to the core integrin inhibitor structure with minimal synthetic difficulties, preparation of these compounds required a modular approach, allowing for target-specific chemical manipulation at each appropriate juncture, whilst largely operating within a single established synthetic procedure.

A retrosynthetic analysis of the core integrin inhibitor structure reveals two primary fragments: the THN pentanoic acid (**67**) and a β-3-aryl-amino ester (Scheme 1).

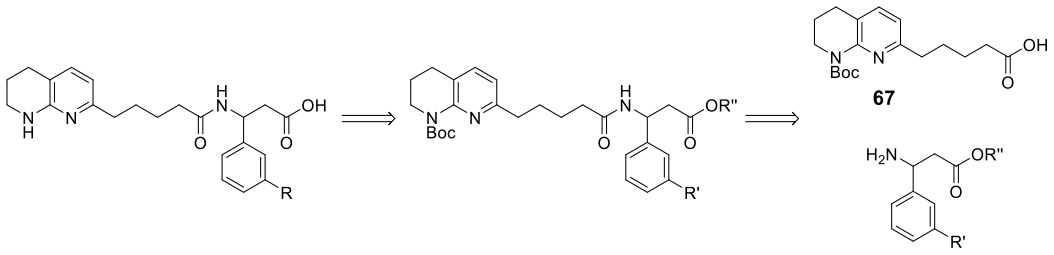

Scheme 1. Initial retrosynthetic analysis of the integrin inhibitor analogue core structure to reveal the two key component fragments **67** and a β-3-aryl-amino ester.

The acid **67** is itself derived from the THN ester **70**, the preparation of which is described in the literature;[79] compound **70** is prepared *via* methyl esterification of the commercially available acid **68**, a Friedländer reaction between the subsequent ester with 2-amino-3-pyridinecarboxaldehyde (**72**) and finally a selective reduction of the naphthyridine moiety in **69** to give the THN ester **70** (Scheme 2).

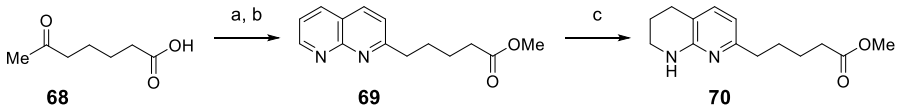

Scheme 2. Preparation of the THN ester **70** as reported in literature.[79] *Reagents and conditions*: a) methanol, conc. H_2SO_4, 1,2-DCE; b) 2-amino-3-pyridinecarboxaldehyde, proline, ethanol; c) PtO_2, H_2 (1 atm), ethanol, 34% (over 3 steps).

A 3:1 mixture of **69** and **71** respectively are generated during the Friedländer reaction described in Scheme 2 (Figure 31); separation of the regioisomers is reportedly more straightforward after selective reduction of the naphthyridine moiety.[79]

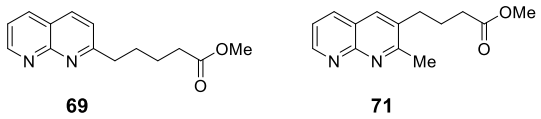

Figure 31. The regioisomers **69** and **71**, generated from the Friedländer reaction depicted in Scheme 2.

Generation of regioisomers is a significant challenge that is commonly encountered during Friedländer reactions where unactivated, unsymmetrical ketone substrates are utilised (Scheme 3).

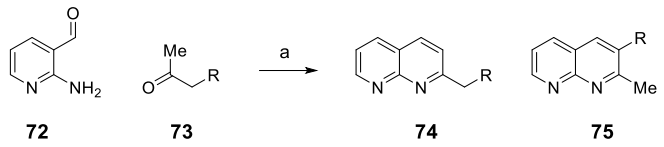

72 **73** **74** **75**

Scheme 3. Typical Friedländer reaction as described by Dormer *et al.* between 2-amino-3-pyridinecarboxaldehyde (**72**) and unsymmetrical methyl ketone derivatives.[98] *Reagents and conditions*: ***base***, conc. H_2SO_4 (5 mol%), ethanol, rt, 23 h.

Dormer *et al.* describe an optimisation of the Friedländer reaction with the specific aim of developing methodology allowing for selective generation of 2-substituted products over 2,3-disubstituted products (Scheme 3);[98] under traditional Friedländer conditions between 2-amino-3-pyridinecarboxaldehyde (**72**) and unsymmetrical methyl ketone derivatives (**73**), using KOH as the base of choice, an approximate 2:1 ratio in favour of **75** is generated. After an initial screening of various bases and acids (both organic and inorganic) under the assumption that formation of an enamine intermediate would likely encourage increased formation of the 2-substituted product, it was discovered that use of pyrrolidine in the presence of H_2SO_4 (5 mol%), with 2-pentanone (**76**) as the requisite ketone substrate provided an 86:14 ratio in favour of the 2-substituted product (**80**) with almost total consumption of starting materials. A small increase of reaction rate is observed upon addition of acid; thus, it is presumed to encourage the formation of imine and enamine intermediates. Furthermore, with additional optimisation, pyrrolidine derivatives, specifically 1,3,3-trimethyl-6-azabicyclo[3.2.1]octane (TABO), provided up to 96% regioselectivity with near total conversion of starting material. The improvement of regioselectivity exhibited by this reaction upon use of these larger bases is likely due to an increase of the steric bulk of the enamine intermediate present during the reaction; this results in the conformation of reagents required during the formation of the minor regioisomer to be more sterically demanding than without use of large bases, thus leading to the reaction increasingly favouring formation of the major regioisomer.

The exact mechanism of the Friedländer reaction is subject to debate, however it is feasible that pyrrolidine causes the reaction to proceed in a manner similar to that depicted in Scheme 4.

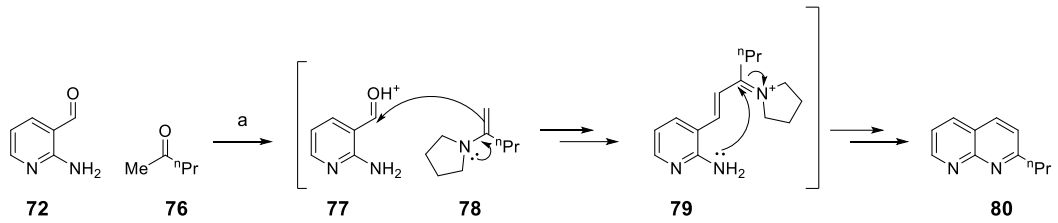

Scheme 4. A plausible mechanism of the Friedländer reaction, showing the effect of pyrrolidine catalysis in the reaction between 2-amino-3-pyridinecarboxaldehyde (**72**) and 2-pentanone (**76**).[98] *Reagents and conditions*: a) pyrrolidine, conc. H_2SO_4 (5 mol%), ethanol, rt, 23 h, 85%.

Use of proline gave a similar regioisomeric profile to that of pyrrolidine, however conversion of starting material was found to be considerably slower (97% *vs* 5% after 23 h), although increased reaction time improved the yield significantly.[98] Presumably the health implications related to the use of pyrrolidine resulted in the use of proline by Coleman *et al*. during the synthesis of **70**.[79]

Reduction of the naphthyridine **69** to give the THN ester **70** proceeds selectively (Scheme 2), with no observed over reduction or reduction of the 2-mono-substituted pyridine ring; this is likely due to the increased steric hindrance experienced by the 2-substituted pyridine ring compared to the unsubstituted ring.

Subsequent *N*-Boc protection of **70** gives the THN ester **81** (Scheme 5).

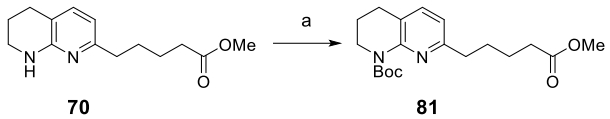

Scheme 5. *N*-Boc protection of **70** to give the THN ester **81**.[99] *Reagents and conditions*: a) di-*tert*-butyl dicarbonate, 1,4-dioxane, 80 °C, 16 h, 53%.

A sufficient quantity of the THN ester **81** was provided by GSK for use in of all the synthesis described in the following chapters; the THN ester **81** was subsequently saponified with $LiOH.H_2O$ in THF/water to give the THN carboxylate **82** (Scheme 6).

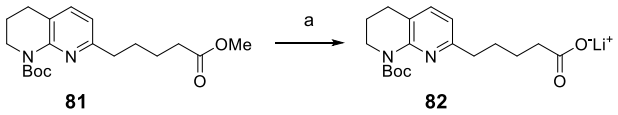

Scheme 6. Saponification of the ester **81** with $LiOH.H_2O$. *Reagents and conditions*: a) $LiOH.H_2O$, THF/water (4:1), rt, 4 h, quant.

With the THN carboxylate **82** in hand, we sought a method of generating the requisite β-3-aryl-amino esters.

2.2 Preparation of β-amino ester derivatives

2.2.1 Reported methodology for β-amino acid derivatives

As illustrated in Scheme 1, the second key fragment of the UoN series of integrin inhibitors is the β-3-aryl-amino ester. Many methodologies for the preparation of such substrates are reported in the literature, with a number described herein.

The primary method of generating the requisite β-3-aryl-amino esters as used by Adams *et al.* is based on a modification of the Rodionow reaction, a notoriously capricious reaction that provides racemic products.[82,100–102] First reported in 1929 by Rodionow and Postovskaja, the methodology facilitates the formation of β-3-aryl-amino acids from condensation of

aromatic aldehydes with alcoholic ammonia and various malonate derivatives;[100] the modification of this protocol utilised by Adams *et al*. was reported in 2002 by Tan and Weaver.[102] This methodology gave the β-3-aryl-amino acid upon condensation of the relevant benzaldehyde with ammonium acetate and malonic acid under reflux (Scheme 7). The electronic properties of the benzaldehyde substrate significantly affect the yield of the reaction. It was found that *para*-substitution with electron-donating groups provided slight improvement in yield compared to that of the unsubstituted benzaldehyde (**88** *vs* **84**), whereas *para*-substitution with electron-withdrawing motifs dramatically decreased the observed yield (**89** *vs* **84**). Whilst there does appear to be a small benefit to *para*-substitution with electron-donating motifs, substitution at any other point of the aryl ring causes the yield to change in a wildly unpredictable manner, a characteristic that renders this methodology incompatible for use in chemistry where consistent and predictable yields are generally desirable. Substantial generation of the cinnamate elimination product (**83**) is often responsible for the observed inconsistencies in yields.[102]

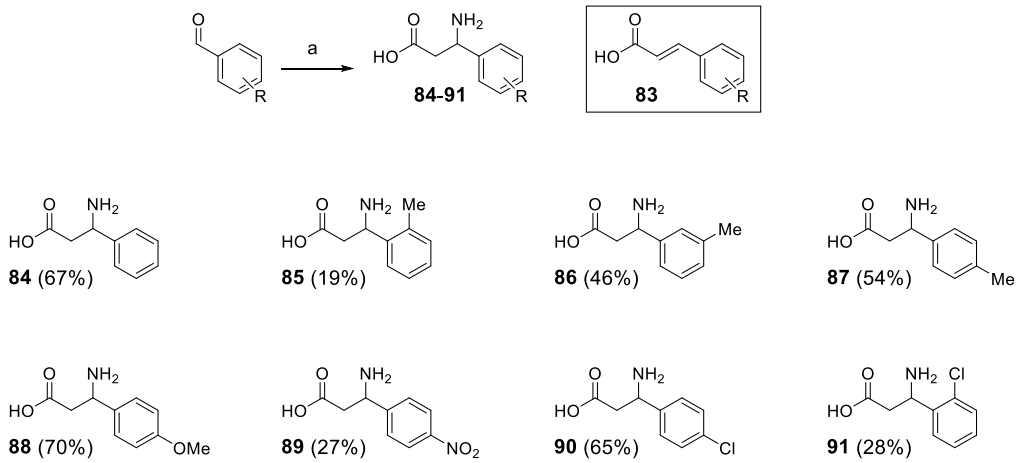

Scheme 7. The modification of the Rodionow reaction as reported by Tan and Weaver to generate racemic β-3-aryl-amino acids, accompanied by a selection of examples demonstrating well the general trends reported in this work.[102] *Reagents and conditions*: a) ammonium acetate, malonic acid, ethanol, reflux, 6-16 h, **22 examples: 16-70%**.

Use of this methodology by Adams *et al*., followed by esterification of the resulting acids using thionyl chloride and ethanol, generated the β-3-aryl-amino esters used to prepare the reported integrin inhibitors (Scheme 8).[82]

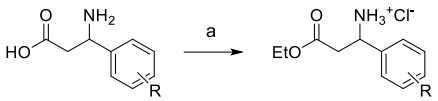

Scheme 8. Esterification of the racemic β-3-aryl-amino acid to give the integrin inhibitor precursor substrates as reported by Adams *et al*.[82] *Reagents and conditions*: a) $SOCl_2$, ethanol, -15 °C then reflux, 16 h.

Adams *et al.* demonstrate that inhibition of the $\alpha_v\beta_6$ integrin within the UoN series is exhibited exclusively by the (*S*)-enantiomer of these integrin inhibitors, and thus the Rodionow reaction is clearly not suitable for use where enantioselectivity is required.[82] Therefore robust methodology allowing for high-yielding, enantioselective generation of the (*S*)-enantiomer was sought.

The use of *tert*-butanesulfinamide to synthesise chiral amines was first described by Ellman in 1997.[103] *tert*-Butanesulfinamide behaves as both a suitable chiral auxiliary and an effective protecting group for the subsequent amine; sulfinamide behaves as an ammonia equivalent, reacting with carbonyls to form stable, chiral sulfinimines (Scheme 9).

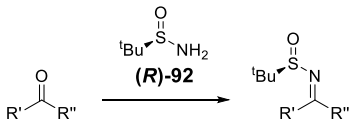

Scheme 9. Preparation of (*R*)-*N*-sulfinimines from carbonyl substrates using (*R*)-*tert*-butanesulfinamide (**(*R*)-92**).

Enantiopure sulfinimines exhibit stereoselective electrophilic reactivity that is significantly enhanced by the electron withdrawing properties of the *N*-sulfinyl motif, compared to that

of a carbonyl group.[104,105] Sulfinimines are additionally often found to be stable to hydrolysis and thus can be produced on scale and isolated chromatographically;[104] these characteristics are particularly advantageous for their use in sensitive organometallic-related reactions. Their high reactivity enables exceptionally reliable reaction with organometallic reagents *via* 1,2 addition, leading to a wide range of chiral amine derived products. Racemisation of the newly formed stereocentre is prevented by the stabilisation afforded by the enantiopure *N*-sulfinyl group and so excellent stereoselectivity is achieved, affording products exhibiting high enantiomeric purity.[103,104]

There are numerous examples of *N*-sulfinimines precursors being used in the preparation of α and β amino esters: α-amino acids have been synthesised *via* an asymmetric Strecker synthesis using enantiopure sulfinimines and diethylaluminium cyanide (Scheme 10).[106]

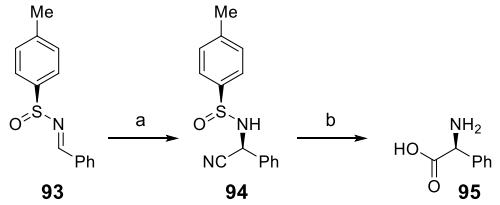

93 **94** **95**

Scheme 10. The α-amino acid **95** is synthesised *via* an asymmetric Strecker synthesis from **93**.[106] *Reagents and conditions*: a) 1M Et_2AlCN in toluene, *i*-PrOH, THF, -78 °C, Ar, 10 min, d.e >95%., 79%; b) 6M $HCl_{(aq)}$, reflux, 6 h, e.e. >95%, 78%.

β-3-Aryl-amino esters have been synthesised *via* ester enolate 1,2 nucleophilic additions to *N*-sulfinyl aldimines; the d.e. values obtained from such addition reactions are reported to be as high as 98% when performed using NaHMDS (Scheme 11).[107]

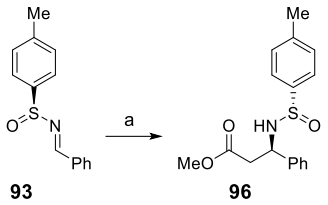

93 96

Scheme 11. The β-3-aryl-amino ester **96** is synthesised from **93** via an ester enolate.[107] *Reagents and conditions*: a) CH_3CO_2Me, NaHMDS, diethyl ether, d.e. >98%, 84%.

An alternative methodology, the Reformatsky reaction, is traditionally used in the preparation of secondary and tertiary alcohols upon reaction of aldehydes or ketones with organozinc Reformatsky reagents; however, this same methodology can also be applied to reactive imine derivatives to generate enantiopure β-amino esters.

The first reported examples of a Reformatsky reaction being used to generate β-amino esters is described by Staas *et al* (Scheme 12).[108] The reaction results in the formation of α,α-difluoro β-amino esters from the ethyl bromodifluoroacetate derived Reformatsky reagent **98** and the appropriate sulfinimine (Scheme 12); the Reformatsky reagent itself is prepared *in situ* by reaction between the bromo ester **97** and zinc powder.

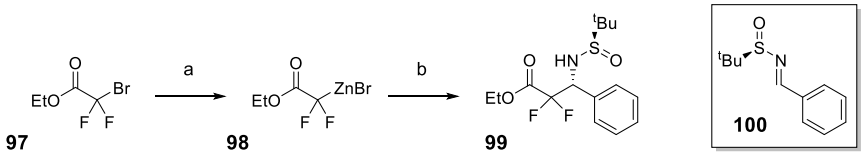

97 98 99

Scheme 12. Sulfinamide **99** is synthesised via an asymmetric Reformatsky reaction between **98** and **100**.[108] *Reagents and conditions*: a) zinc powder, THF, 30 °C; b) **100**, THF, rt, 18 h, d.e. 80%, 82%.

The d.e. values obtained from asymmetric Reformatsky reactions have been reported to be in excess of 99%.[104]

Robak *et al.* describe the general mechanism of the Reformatsky reaction, hypothesising that the reaction proceeds *via* a six membered cyclic transition state, allowing the chirality of the newly generated centre to be determined.[104] Scheme 13 depicts this transition state, showing reaction of the Reformatsky reagent **102** with both the (*R*)-sulfinimine **(*R*)-101** and the (*S*)-sulfinimine **(*S*)-101**, leading to generation of the (*S*) and (*R*) stereocentres, respectively (**(*S*,*R*)-103** and **(*R*,*S*)-103**).

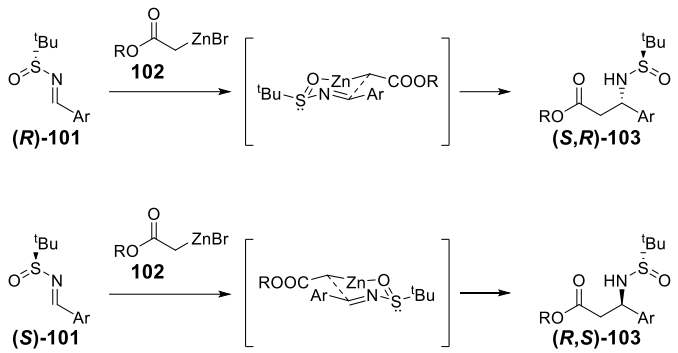

Scheme 13. The (*R*)-sulfinimine **(*R*)-101** generates the (*S*)-stereocentre upon reaction with Reformatsky reagent **102**; likewise, reaction with (*S*)-sulfinimine **(*S*)-101** gives the (*R*)-stereocentre.

The reagents align to form a chair transition state such that each substituent is in an equatorial position minimising the steric interaction between reagents, thus lowering the energy of the intermediate and leading to the formation of the relevant major diastereoisomer.

Removal of the sulfinyl protecting group is achieved upon treatment with HCl in diethyl ether (Scheme 14).

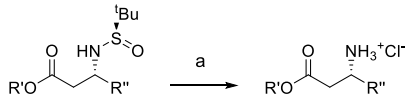

Scheme 14. Removal of the sulfinyl protecting group with HCl in diethyl ether, giving the β-amino ester hydrochloride. *Reagents and conditions*: a) 2M HCl in diethyl ether, rt, 30 min.

Application of this methodology for the purposes of generating integrin inhibitor precursors was largely successful.

2.2.2 Application of reported methodology towards the preparation of β-amino ester derivatives

During initial experimentation with 3-bromobenzaldehyde (**104**), we developed a chromatography-free procedure that generated the desired hydrochloride **107** in yield and enantiomeric purity comparable to a preparation in which the intermediates **105** and **106** were purified at each stage, thus avoiding the large, challenging chromatographic purification methods that can be required when preparing material on scale in excess of 15 g (Scheme 15).

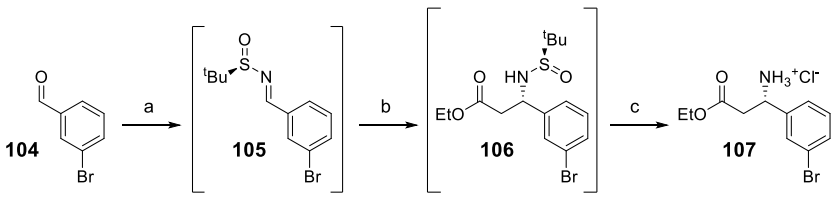

Scheme 15. Enantioselective and chromatography-free preparation of the hydrochloride **107**. *Reagents and conditions*: a) (*R*)-*tert*-butanesulfinamide, Ti(O*i*-Pr)$_4$, THF, rt, 18 h; b) i) zinc powder, TMSCl, ethyl bromo acetate, THF, reflux, N_2, 1 h; ii) **105**, 0 °C to rt, 16 h; c) 4M HCl in 1,4-dioxane, diethyl ether, rt, 20 min, 72% over three steps.

Whilst possible to generate the Reformatsky reagent separately, to avoid potentially hazardous handling of a sensitive reagent, the organozinc reagent was instead generated *in situ*.

Numerous β-3-aryl-amino esters were prepared, both enantiopure and racemic, derived from various benzaldehydes, and containing either ethyl or *tert*-butyl ester motifs, depending on requirements (Table 9).

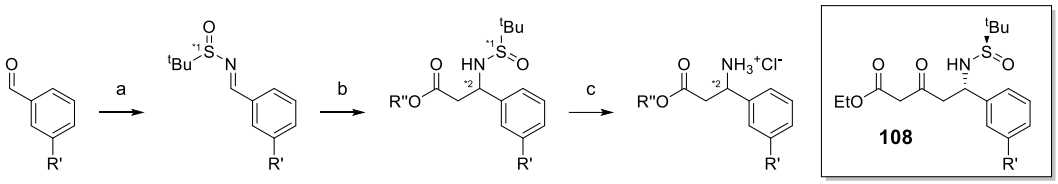

R'	R''	*1	*2	Yield a/%	Yield b/%	Yield c/%
Br	Et	(*R*)	(*S*)	- (**105**)	- (**106**)	72 over 3 steps (**107**)
Br	*t*-Bu	(*R*)	(*S*)	- (**105**)	- (**109**)	66 over 3 steps (**110**)
I	*t*-Bu	(*rac*)	(*rac*)	87 (**111**)	80 (**112**)	98 (**113**)*
CF_3	*t*-Bu	(*rac*)	(*rac*)	86 (**114**)	75 (**115**)	99 (**116**)
CF_3	Et	(*R*)	(*S*)	- (**(*R*)-114**)	- (**117**)	66 over 3 steps (**118**)

Table 9. Preparation of β-3-aryl-amino ester hydrochlorides; compound numbers corresponding to products are given in parentheses. *Reagents and conditions*: a) (*R*)-*tert*-butyl-sulfinamide, Ti(O*i*-Pr)$_4$, THF, rt; b) i) zinc powder, TMSCl, ethyl bromoacetate, THF, reflux, N_2; ii) ***sulfinimine***, 0 °C; c) 4M HCl in 1,4-dioxane, diethyl ether, rt.

*__113__ was isolated as the free base and not the hydrochloride salt.

The general preparation of the hydrochloride substrates and all requisite intermediates is described thus: titanium tetra-*iso*propoxide mediated condensation of *tert*-butyl sulfinamide with the relevant benzaldehyde gave the aryl-sulfinimine (step a); subsequent Reformatsky reaction gave the sulfinamide β-3-aryl-amino ester (step b).[104] The Reformatsky reagent required in step b was formed *in situ* via treatment of either ethyl or *tert*-butyl bromoacetate with TMSCl activated zinc powder, generating the organozinc enolate. The pre-prepared aryl-

sulfinimine was subsequently added to the reaction mixture following cooling to 0 °C in order to minimise formation of the double addition product **108**; this species is generated upon insufficient cooling of the Reformatsky reaction during addition of the organozinc species, specifically when using the less hindered ethyl ester derived species, to the aryl-sulfinimine.[109] Removal of the *N*-sulfinyl protecting group under acidic conditions causes precipitation of the subsequent β-3-aryl-amino ester hydrochloride (step c); this in turn allows separation of the hydrochloride in high purity from the impurities generated during the synthetic process.

HPLC analysis of the (*S*)-*N*-Boc protected analogue of **107** (**(*S*)-119**, preparation depicted in Scheme 16) and the (*rac*)-equivalent **119** (obtained from commercial sources) revealed an e.e. in excess of 97%, whilst NMR and LCMS analysis of the crude reaction mixture in the formation of **106** did not indicate any significant presence of the diastereomer (HPLC traces for **119** and **(*S*)-119** are available in Section 5.3); this is once again in accord with previously reported work, in which the d.e. of the Reformatsky reaction in the context of β-3-aryl-amino ester formation is said to be >99:1.[104]

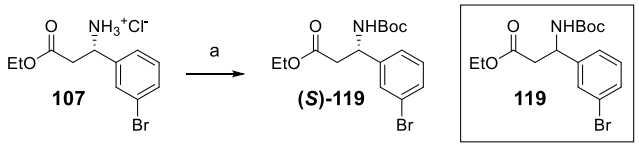

Scheme 16. Preparation of the (*S*)-analogue **(*S*)-119** *via N*-Boc protection of the hydrochloride salt **107**; shown also is the (*rac*)-analogue **119**, obtained from commercial sources. *Reagents and conditions*: a) di-*tert*-butyl dicarbonate, Et_3N, THF, 0 °C to rt, 65 h, 94%.

The (*S*)-stereochemistry of the newly formed stereocentre of the bromo-ester analogue **106** was confirmed by X-ray crystallography (Figure 32), and is in accord with that expected from the work reported by Ellman *et al*.[104]

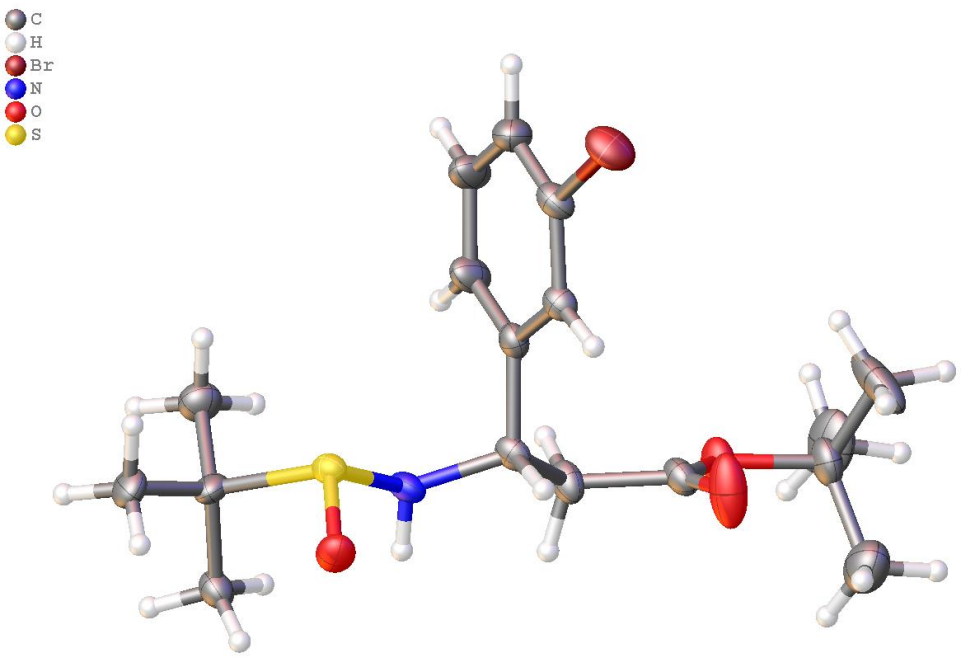

Figure 32. X-Ray crystal structure of *tert*-butyl (*S*)-3-(3-bromophenyl)-3-(((*R*)-*tert*-butylsulfinyl)amino)propanoate (**106**). Ellipsoid view (50% volume) of residue A from the crystal structure of **106** (one of four residues A-D in the asymmetric unit of the P21 cell with similar conformations). The minor disorder component with an inverted phenyl ring has been omitted for clarity (this is an alternate conformation where the bromo-substituent is present on the opposite side of the phenyl ring, relative to the conformation shown above). Atom colours: carbon - grey; hydrogen - white; nitrogen - blue; oxygen - red; sulphur - yellow; bromine - brown. Crystallography method described in Section 5.2.

Having identified a suitable method for the preparation of the β-3-aryl-amino acid portion of these RGD-based integrin inhibitors, we next sought to develop a method from which large quantities of high-quality SAR could be generated rapidly.

2.3 Preparation of *N*-linked, 3-monosubstituted integrin inhibitor analogues

Late-stage functionalisation (LSF) is a powerful tool in medicinal chemistry that enables the rapid generation of highly diverse drug-like molecules from single, complex intermediates. This method of synthesis reduces the overall step count for individual target compounds, thus improving time and cost efficiency whilst also maximising diversity of chemical space exploration in lead optimisation to develop large quantities of high-quality SAR. The most frequently used reactions within medicinal chemistry are amide bond formations, Suzuki-Miyaura couplings, Buchwald-Hartwig couplings and S_NAr reactions;[110] whilst effective tools for introducing diversity, they are often unsuitable for LSF due to forcing reaction conditions such as high temperatures, strong bases, expensive catalysts and complex ligands. On the other hand, installation of a variety of structural motifs at a late stage *via* C-H activation is a preferred and attractive tactic, although notwithstanding recent advances, there are few viable methods available.[111] Despite the fact that nitrogen-containing heterocycles are amongst the most prevalent cyclic structural features in small drug molecules, there are few examples of mild and robust aromatic C-N bond formation methods;[111] this is particularly relevant in the context of this project in which we planned for the generation of a wide range of C-N linked heterocycle substituted integrin inhibitor analogues. Therefore, methodology that is tolerant of a range of functional groups, whilst facilitating the installation of these pharmaceutically valuable structural features at a late stage would be a welcome addition to the medicinal chemist's inventory.[112]

First reported in 1997, the Chan-Lam reaction that formally involves the coupling of two nucleophilic species, typically an aryl boronate species and amine, has been characterised as capricious, with the more commonplace Buchwald-Hartwig and Ullmann nucleophile-electrophile couplings subsequently gaining prominence in drug discovery for the purposes

of C-N bond formation.[110,113–118] However, as previously discussed, due to limited substrate scope and harsh reaction conditions, neither of these are a particularly viable methodology for LSF.

In 2017, the mechanism of the Chan-Lam reaction, specifically in its capacity as a method for amination, was elegantly elucidated by Vantourout *et al*.[119] The substrate scope, including both alkyl and aryl amines, and the improved reliability of the reaction following reaction mechanism elucidation and subsequent reaction optimisation, including its late stage use in the synthesis of imatinib (**132**), thereby marked it as a potential methodology for LSF (Scheme 17).[119]

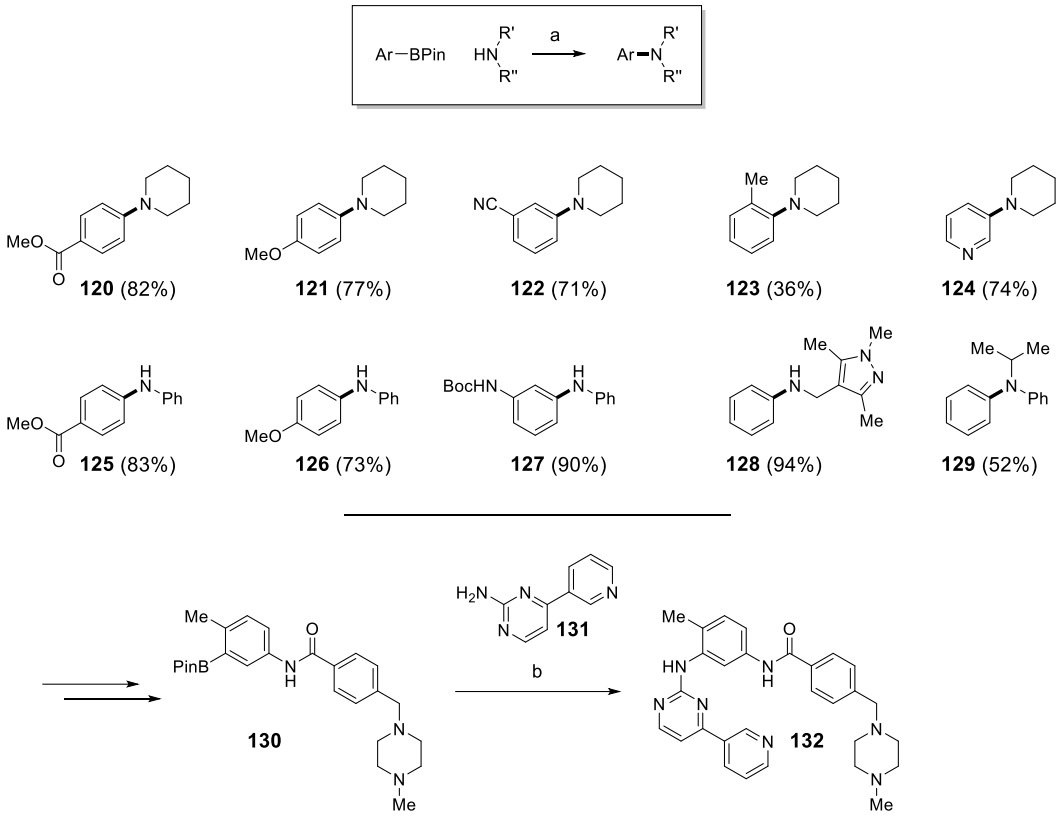

Scheme 17. The general Chan-Lam amination reaction conditions as reported by Vantourout *et al.*; depicted also are a selection of substrate examples clearly demonstrating that these conditions are suitable for a variety of functionalities.[119] The Chan-Lam amination reaction used in the synthesis of imatinib (**132**).[119] *Reagents and conditions*: a) $B(OH)_3$, $Cu(OAc)_2$ (20 mol%), acetonitrile, 4 Å MS, 80 °C, O_2, 24 h, **50 examples: 36-94%**; b) 4-(pyridin-3-yl)pyrimidin-2-amine, $B(OH)_3$, $Cu(OAc)_2$ (20 mol%), acetonitrile/*t*-BuOH (3:1), 4 Å MS, 80 °C, O_2, 24 h, 67%.

Prior to this project, the published SAR relating to heterocyclic substituted RGD inhibitors in this, and related series was limited; the majority of examples containing unsubstituted heterocycles or heterocycles exhibiting a range of substituents that do not represent single point changes for the purposes of SAR analysis. There were however instances where compounds containing more complex substituents appeared to exhibit selectivity for $\alpha_v\beta_6$ over $\alpha_v\beta_3$, albeit with moderately reduced pIC_{50} against $\alpha_v\beta_6$. Thus, in order to implement a

thorough initial exploration of the chemical space within the SDL in the $\alpha_v\beta_6$ and $\alpha_v\beta_3$ integrin binding sites, an array of compounds that would facilitate comparison between one another by single point changes was designed.[76] A range of 58 highly diverse heteroaromatic (19 pyrazoles, 15 imidazoles, 8 triazoles) and 16 cyclic secondary amines was selected (Figure 33); substituents within the amines themselves were intentionally kept simple due to the limited available SAR and therefore included small alkyl groups, halides and polar and non-polar hydrogen bond donors.

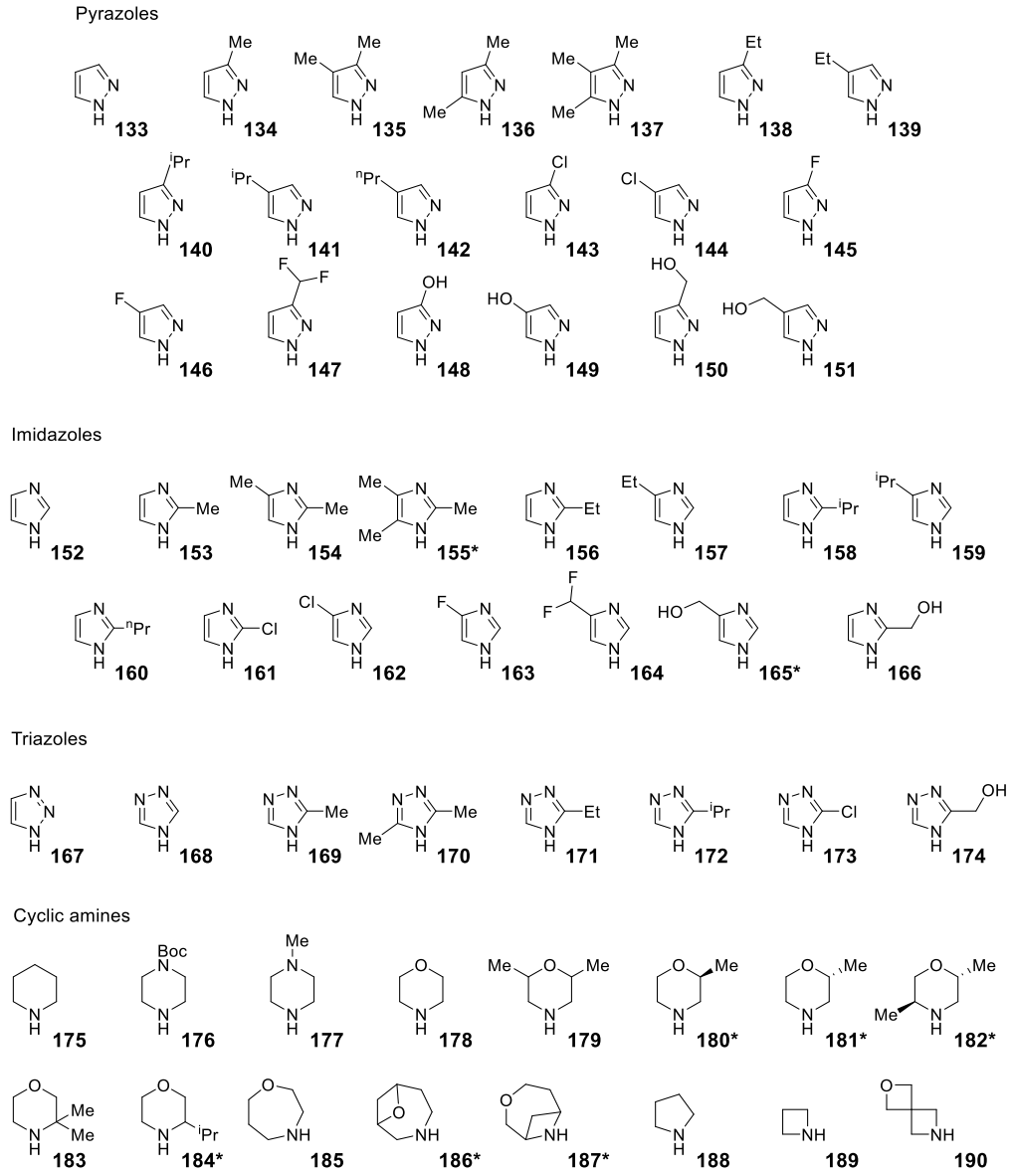

Figure 33. Structures of pyrazoles, imidazoles, triazoles and cyclic secondary amines used in the Chan-Lam amination reactions. Monomers used as the hydrochloride salt are highlighted with an asterisk (*).

The preparation of the requisite boronate intermediate **192** is depicted in Scheme 18.

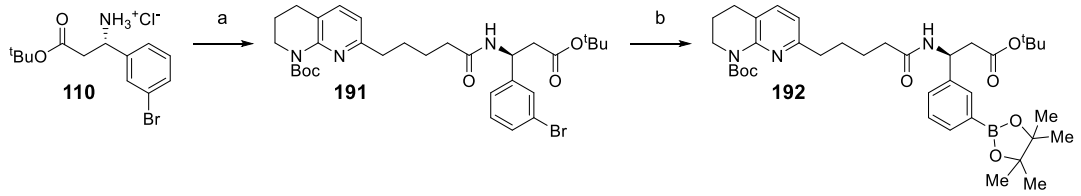

Scheme 18. Preparation of the key boronate intermediate **192**. *Reagents and conditions*: a) **82**, T3P (50% in ethyl acetate), *i*-Pr_2NEt, acetonitrile, 0 °C to rt, 18 h, 86%; b) B_2Pin_2, KOAc, $Pd(dppf)Cl_2{\cdot}CH_2Cl_2$ (10 mol%), 1,4-dioxane, 80 °C, N_2, 16 h, 90 %.

The amide **191** was formed *via* T3P mediated coupling of **110** with the THN carboxylate **82**; the *tert*-butyl ester was utilised as it would allow for a single global deprotection step after the Chan-Lam amination to generate the final integrin inhibitor analogues. The key boronate intermediate **192** was then prepared in excellent yield *via* Miyaura-borylation of **191**.

The *N*-linked heterocyclic analogues were prepared in a high throughput array format; reactions were performed in parallel in 4.00 mL vials in a 6 x 4 block that was placed upon a hotplate (see Section 5.6, General Preparation A and B), and subsequently utilised mass-directed auto purification (MDAP) to facilitate the rapid generation of compounds in order to develop high quality SAR. The inhibitor analogues were prepared *via* Chan-Lam amination between the boronate **192** and the amines depicted in Figure 33 on a 0.100 mmol scale, followed by global deprotection of the *tert*-butyl ester and *N*-Boc functionalities using TFA and subsequent isolation *via* MDAP (Scheme 19).

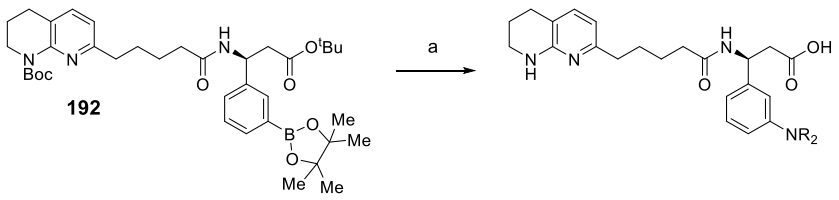

Scheme 19. Preparation of *N*-linked inhibitor analogues from the boronate **192** *via* the Chan-Lam amination reaction. *Reagents and conditions*: a) i) ***amine***, $B(OH)_3$, $Cu(OAc)_2$ (1.00 eq.), acetonitrile, 4 Å MS, 70 °C, 40 h; ii) TFA/CH_2Cl_2 (1:1), rt, 4 h.

From the array of 58 amine coupling partners (Figure 33), 39 samples of sufficient purity (>85% by LCMS) for biological evaluation were isolated *via* MDAP (Table 10, MDAP method for compound isolation described in Section 5.6), including the minor regioisomer products from reaction with 3-methyl- (**134**), 3,4- dimethyl- (**135**) and 3-fluoro-pyrazoles (**145**), compounds **194**, **196** and **206**, respectively.

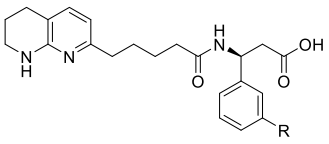

Entry	Amine	R	Compound no.	Isolated yield/%
1			**(*S*)-40**	7
2	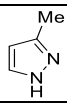	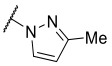	**193**	10
3			**194**	4
4	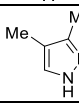	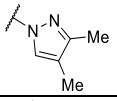	**195**	15
5	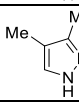	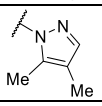	**196**	7
6	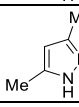	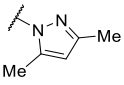	**(*S*)-27**	21
7	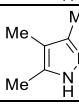	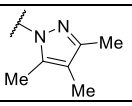	**197**	40
8	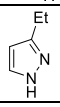	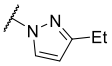	**198**	17
9	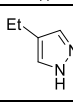	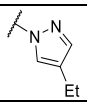	**199**	4
10		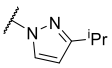	**200**	44
11	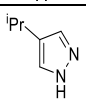	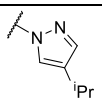	**201**	37
12	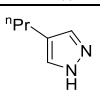	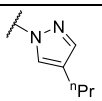	**202**	33
13	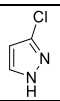	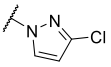	**203**	13
14	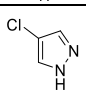	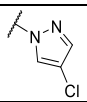	**204**	Not isolated
15	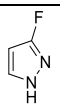	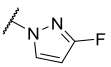	**205**	13

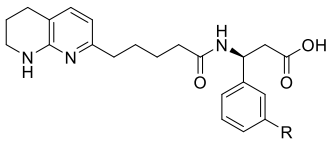

Entry	Amine	R	Compound no.	Isolated yield/%
16	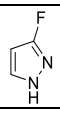		**206**	4
17		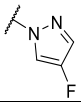	**207**	4
18	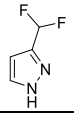	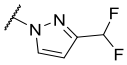	**208**	4
19	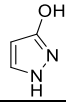	Product not detected	-	-
20		Product not detected	-	-
21	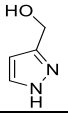	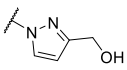	**209**	7
22	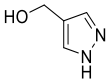	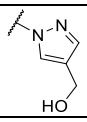	**210**	5
23			**(*S*)-39**	6
24	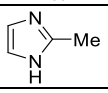		**211**	21
25	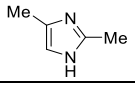	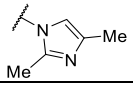	**212**	14
26	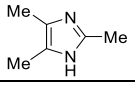	Product not detected	-	-
27			**213**	10
28		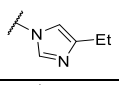	**214**	30
29			**215**	4
30		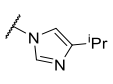	**216**	35

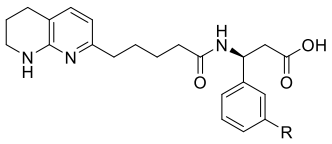

Entry	Amine	R	Compound no.	Isolated yield/%
31			**217**	11
32			**218**	Not isolated
33		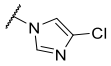	**219**	15
34		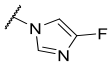	**220**	11
35	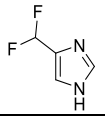	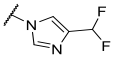	**221**	12
36	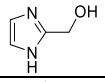	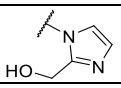	**222**	Not isolated
37	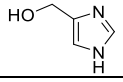	Product not detected	-	-
38		Product not detected	-	-
39		Product not detected	-	-
40	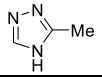	Product not detected	-	-
41	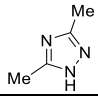	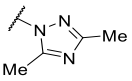	**223**	22
42		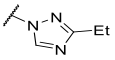	**224**	5
43		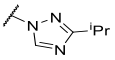	**225**	15
44		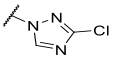	**226**	Not isolated
45	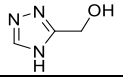	Product not detected	-	-

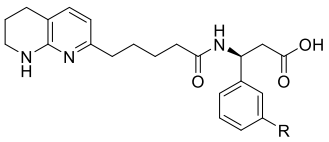

Entry	Amine	R	Compound no.	Isolated yield/%
46			**227**	15
47			**228**	22
48	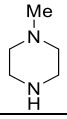	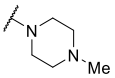	**229**	Not isolated
49			**230**	Not isolated
50	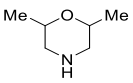	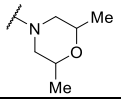	**231**	29
51		Product not detected	-	-
52		Product not detected	-	-
53	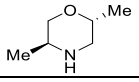	Product not detected	-	-
54		Product not detected	-	-
55		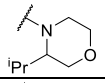	**232**	Not isolated
56		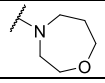	**233**	5
57		Product not detected	-	-
58		Product not detected	-	-
59			**234**	4
60			**235**	Not isolated
61		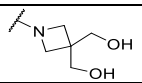	**236**	16

Table 10. Each of the amines used in the array of Chan-Lam amination reactions for the preparation of the *N*-linked integrin inhibitor analogues; shown also are the products of the reactions and the isolated yields of the products after MDAP.

Due to the high UV threshold used by the MDAP method to maximise the likelihood of obtaining a compound sample with high purity, isolated yields were often poor (<20%). The yields of the Chan-Lam amination were improved (45-52%) when the reaction was carried out on larger scale in batch format, albeit on the β-3-aryl-*N*-Boc-amino ester **275** as described in Section 2.7.1, for the coupling of 3-*iso*-propyl- and 3-chloropyrazoles and piperidine (**140**, **143** and **175**). Where two or more regioisomeric products could be formed upon reaction of **192** with unsymmetrical heterocycles, we found that generally, the major regioisomer resulted from Chan-Lam amination at the least sterically hindered nitrogen. In most cases, the major regioisomer was successfully separated from the minor regioisomer, although some analogues were isolated as mixtures; regioisomeric ratios are detailed in the experimental where appropriate (Section 5.6).

Regioisomers were distinguishable by HSQC NMR as demonstrated in Figure 34.

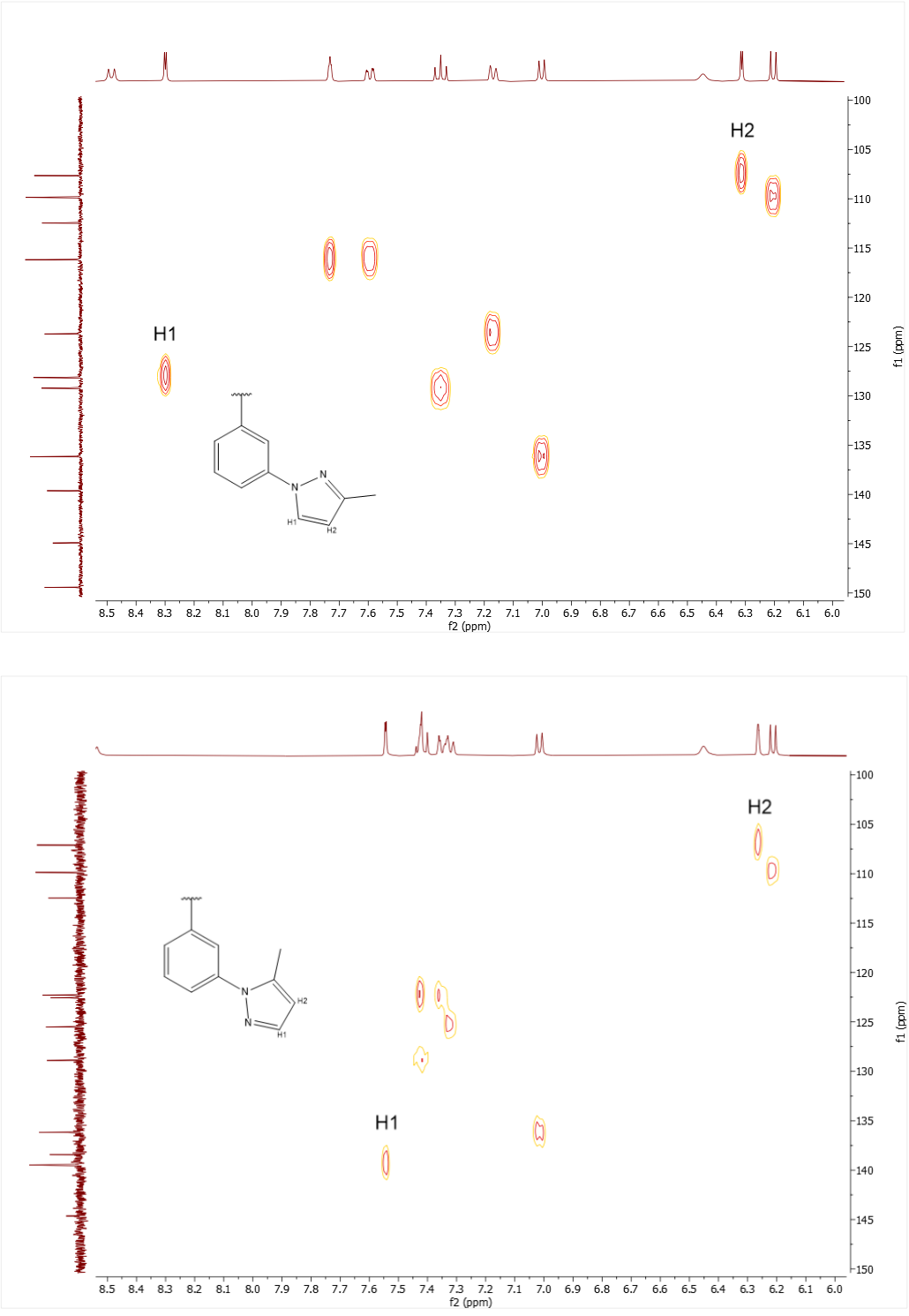

Figure 34. HSQC NMR spectra of the regioisomeric pair **193** (top) and **194** (bottom); the key aromatic portion of the spectra has been enhanced, with the relevant part of the molecule shown. Carbon-proton correlations for both pyrazole C-H moieties are labelled accordingly in each spectrum; the key correlation used to distinguish each regioisomer is listed as H1.

ChemDraw predicts the carbon at position H1 in **193** to have a shift in the region of 130 ppm and for the carbon at position H1 in **194** to have a shift in the region of 140 ppm; the H1 correlation observed for each compound supports this prediction and therefore each regioisomer may be identified with confidence. This process was used to distinguish or identify regioisomers in all other examples where regioisomers were present.

The spiro amine **190** was noted to yield the diol **236** and not the amino oxetane **237** based on LCMS analysis, with HSQC NMR analysis confirming that the oxetane and not the azetidine had ring-opened (Figure 35); the ring opening of oxetanes with use of TFA has been well reported.[120–122]

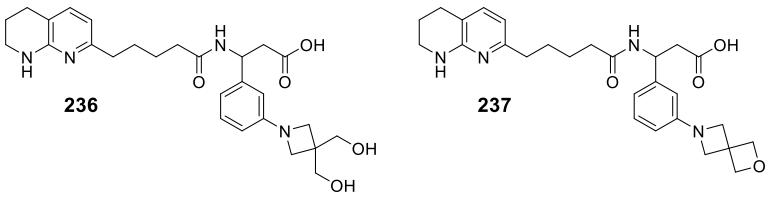

Figure 35. The product of the Chan-Lam amination reaction depicted in Scheme 19 between **192** and the spiro amino **190** (Entry 61), to give the diol **236** and not the oxetane **237**.

Despite being detected via LCMS, the isolation of eight analogues *via* MDAP was unsuccessful (Table 10); the Chan-Lam amination did not proceed with 14 of the selected monomers. Monomers that failed to react were often structurally similar; these were monomers containing a heteroatom that was β to the reactive N-H, the majority of triazoles and most monomers that contained an unprotected hydroxyl group. It is thought that the reduced Lewis basicity of the β-heteroatom and triazole monomers was the cause of their failure to react, as this is known to be an important factor within the Chan-Lam reaction.[119] Alcohols are a suitable nucleophilic coupling partner within the Chan-Lam amination and thus the monomers containing hydroxyl groups likely failed due to a competing reaction between the N-H and O-H functionalities, ultimately leading to a reduced reaction rate and subsequent

increase in the rate of protodeborylation and phenol formation by oxidation.[119] Nevertheless, the range of heteroaromatic coupling partners available for use in the Chan-Lam amination reaction has been extended considerably.

2.4 Preparation of alkyl-substituted inhibitor analogues

2.4.1 Initial installation of isopropyl and cyclopropyl motifs *via* Suzuki-Miyaura coupling reactions

The cyclopropyl and isopropyl analogues **49** and **50** were prepared using the precursor substrate **239**, itself prepared from a previously purchased achiral intermediate **238** (Scheme 20).

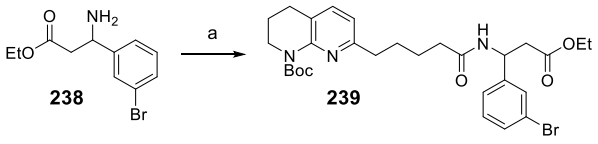

Scheme 20. Preparation of the amide **239** *via* T3P mediated coupling between the β-aminoester **238** and the THN carboxylate **82**. *Reagents and conditions*: a) **82**, T3P (50% in ethyl acetate), *i*-Pr_2NEt, acetonitrile, 0 °C to rt, 19 h, 82%.

The precursor **239** was generated *via* T3P mediated coupling between **238** and **82** and subsequently used to form **241** and **242** upon Suzuki-Miyaura coupling with *iso*propenyl boronic acid pinacol ester and cyclopropyl boronic acid pinacol ester, respectively, using $Pd(dppf)Cl_2.CH_2Cl_2$ as catalyst (Scheme 21).

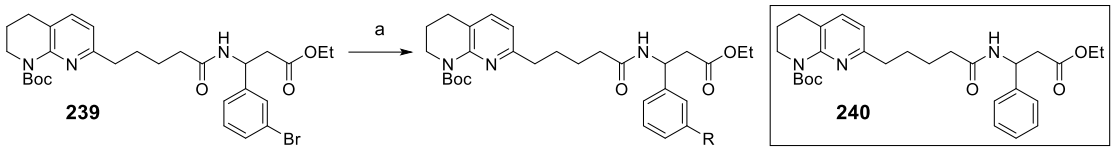

Scheme 21. Preparation of analogues **241** and **242** *via* Suzuki-Miyaura coupling reaction. *Reagents and conditions*: a) *iso*propenyl boronic acid pinacol ester **OR** cyclopropyl boronic acid pinacol ester, K_2CO_3, Pd(dppf)Cl_2.CH_2Cl_2 (20 mol%), 1,4-dioxane, 75 °C, N_2, 16 h, yield: R = *iso*propenyl - 80% (**241**), R = c-Pr - 40% (**242**).

LCMS analysis of both reaction mixtures revealed the presence of a species with the mass of **240**, the result of a protodehalogenation side-reaction. The separation of this by-product from **241** and **242** proved to be particularly challenging using traditional chromatographic methods and so the yields reported in Scheme 21 are not accurate due to reduced purity and multiple purification attempts.

The *iso*propenyl analogue **241** was reduced using methodology reported by Patil and Sasson to give **243**;[123] the reduction is performed under aqueous conditions in water in the presence of iron and Pd/C at a temperature of 100 °C (Scheme 22).

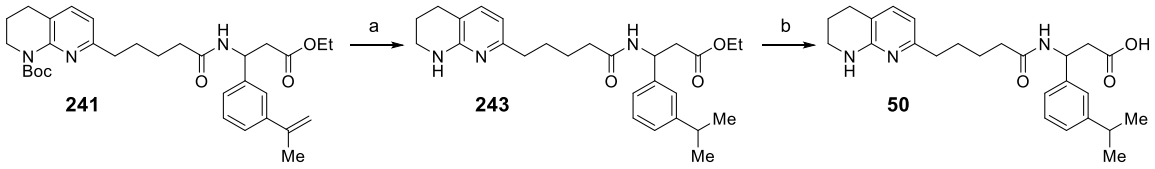

Scheme 22. Preparation of the *iso*-propyl substituted integrin inhibitor **50**. *Reagents and conditions*: a) water, iron powder (325 mesh), Pd/C (10 wt%), 100 °C, N_2, 25 h, 12%; b) 1M $LiOH_{(aq)}$, THF, rt, 68%.[123]

The *N*-Boc protecting group within **241** and similar compounds is particularly labile at temperatures exceeding 80 °C and was thus cleaved during the reduction. Once again, a poor

yield was obtained as **240** remained practically inseparable from **243** during chromatographic purification.

An alternative chromatographic approach was attempted in which the crude material was purified using aminopropyl modified silica gel, a moderately polar, silica-based bonded phase with a weakly basic surface that can be used as an alternative method of separation for acidic and basic analytes. A marginally improved purification of **243** was achieved, and so upon combining fractions exhibiting purity greater than 95% by LCMS, a 12% yield was obtained. The ester **243** was subsequently saponified using 1M $LiOH_{(aq)}$ in THF and the lithium carboxylate converted to the carboxylic acid **50** using Waters OASIS® hydrophilic-lipophilic balance (HLB) resin.

OASIS® HLB is an all-purpose, strongly hydrophilic, reversed-phase, water-wettable polymer used to convert salts of bases and acids to their respective unionised or zwitterionic form. The respective compound is dissolved in water and loaded onto the column, then eluted with water until the pH of the solvent exiting the column is neutral, signifying that the inorganic salts have been removed. The unionised or zwitterionic organic compound is then removed from the column *via* elution with an increasing gradient of aqueous methanol.

The cyclopropyl analogue **242** was treated with TFA and then the crude material purified using an aminopropyl modified silica based chromatographic method to give the ester **244** which was subsequently saponified using 1M $LiOH_{(aq)}$ before conversion to the carboxylic acid **49** using Waters OASIS® HLB resin (Scheme 23).

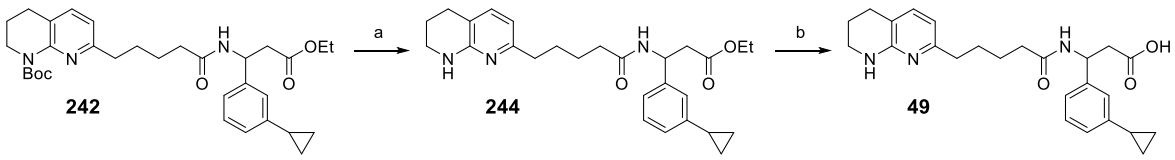

242 **244** **49**

Scheme 23. Preparation of the cyclopropyl substituted integrin inhibitor **49**. *Reagents and conditions*: a) TFA, CH_2Cl_2, rt, 21 h, 20%; b) 1M $LiOH_{(aq)}$, THF, rt, 16 h, 58%.

The 3-cyclopropyl moiety would ultimately become an important structural feature within the UoN series of integrin inhibitors and so a more robust methodology for its installation was sought.

2.4.2 Further investigation towards developing methodology for the installation of the cyclopropyl substituent

Due to the moderately forcing conditions described in Scheme 21, a significant amount of ester hydrolysis was observed in both reactions. This issue is commonly encountered during palladium catalysed coupling reactions in which ethyl esters are present, and thus the *tert*-butyl ester **245** was identified as a suitable alternative substrate for investigative work. The ester **245** was prepared from an amide coupling of the THN carboxylate **82** with the amine **113**, itself prepared *via* the Reformatsky route previously described in Section 2.2.2 (Scheme 24). Due to the increased reactivity exhibited by aryl iodides compared to aryl bromides and chlorides during palladium catalysed cross-coupling reactions, it was hoped that better success would be experienced upon switching to use of both the more stable *tert*-butyl ester and the more reactive iodo-substrate.

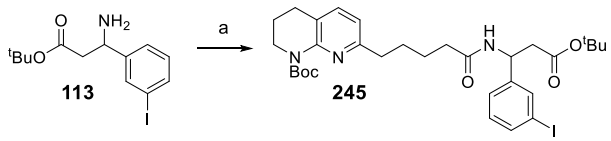

Scheme 24. Preparation of the iodo intermediate **245**. *Reagents and conditions*: a) **82**, T3P (50% in ethyl acetate), *i*-Pr_2NEt, acetonitrile, 0 °C to rt, 16 h, 85%.

Work performed previously by UoN MSci students indicated that for Suzuki-Miyaura coupling reactions in which the protodehalogenation side reaction is prominent, use of the palladium catalyst SK-CCO1-A (**246**) in aqueous solution (ethanol/water) with KOAc often resulted in

reduced generation of the protodehalogenation by-product and increased generation of desired product (Figure 36); the use of this catalyst is described by Schnyder *et al*.[124]

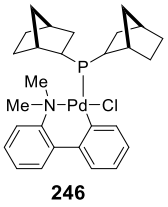

246

Figure 36. The palladium catalyst SK-CCO1-A (**246**).

The reaction was performed as depicted in Scheme 25, however upon purification, the majority of **245** had been converted to the protodehalogenation by-product **248**, with minimal generation of **247**; no yield for **248** was determined.

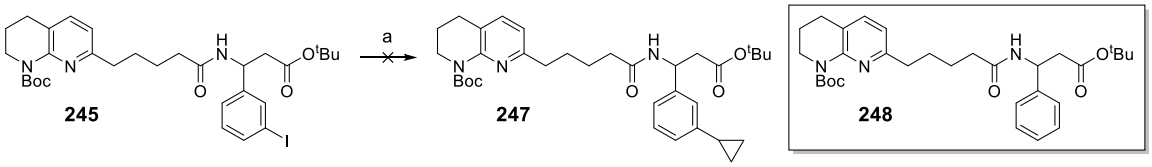

Scheme 25. Attempted synthesis of the cyclopropyl analogue **247** using the palladium catalyst **246**. *Reagents and conditions*: a) cyclopropyl pinacol borane, KOAc, **246**, ethanol/water (4:1), 80 °C, N_2, 16 h.

The difficulty of separating the protodehalogenation by-product from **241** and **242** is likely enhanced by the presence of the THN motif. Despite distinctly different calculated LogP values for the products **241** and **242**, and the by-product **240** (6.64 and 6.15 *vs* 5.21 respectively), the basicity and size of the THN group presumably overwhelms any effect of aryl substitution on the lipophilic profile of the molecule in the context of chromatographic methods, thus altering their Rf values to be largely the same.

To avoid any challenging future purification, installation of the cyclopropyl group at an earlier stage of the synthetic procedure was attempted, before introduction of the THN functionality (Scheme 26).

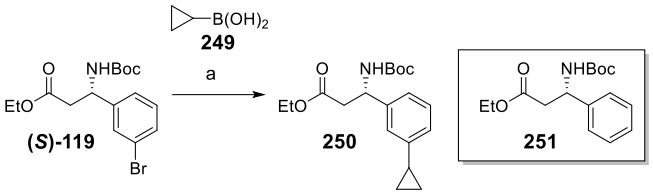

Scheme 26. Preparation of the cyclopropyl analogue **250** with the boronic acid **249** and Pd(dtbpf)Cl_2 from the (*S*)-intermediate **(*S*)-119**. *Reagents and conditions*: a) **249**, $K_3PO_4.H_2O$, Pd(dtbpf)Cl_2 (5 mol%), 1,4-dioxane/water (2:1), 50 °C, N_2, 16 h, 40%.

Despite observing a surprisingly small quantity of ester hydrolysis, little success was experienced using Pd(dtbpf)Cl_2, with significant generation of the by-product **251**; however, more encouraging results were obtained using a modification of methodology reported by Molander and Gominsky, developed specifically for the installation of cyclopropyl motifs to aryl chlorides (Scheme 27).[125]

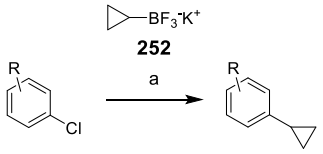

Scheme 27. Methodology reported by Molander-Gominsky for the installation of the cyclopropyl group to aryl chlorides.[125] *Reagents and conditions*: K_2CO_3, $Pd(OAc)_2$ (3 mol%), XPhos (6 mol%), CPME/water (10:1), 100 °C, 24 h, **8 examples: 75-96%**.

In this methodology, use of the Molander's salt **252** rather than the more traditional boronic acid or ester is a key feature, due to increased reactivity and improved stability.[126] A catalyst-ligand system of $Pd(OAc)_2$ and XPhos is used, with K_2CO_3 as base in a biphasic mixture of CPME and water, heated at 100 °C, often resulting with excellent yields of material.

For our own use, we utilised XPhos Pd G2 in place of $Pd(OAc)_2$ and XPhos, with no majorly apparent reduction of yield (based upon those yields reported by Molander and Gominsky).[125] The requisite potassium trifluoroborate salt **252** was prepared in good yield

following methodology reported by Lennox and Lloyd-Jones in which the boronic acid **249** is treated with potassium fluoride and L-(+)-tartaric acid in a mixture of THF, acetonitrile and water (Scheme 28).[126]

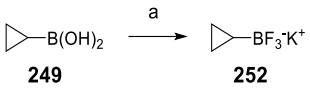

Scheme 28. Preparation of the cyclopropyl potassium trifluoroborate salt **252** utilising reported methodology.[126] *Reagents and conditions*: a) 10M $KF_{(aq)}$, 1.37M L-(+)-tartaric acid in THF, acetonitrile, rt, 10 min, 78%.

Application of this methodology to our own substrates, the *tert*-butyl ester **253** and the ethyl ester **(*S*)-119**, yielded positive results (Scheme 29); **253** was prepared *via N*-Boc protection of **110** in excellent yield.

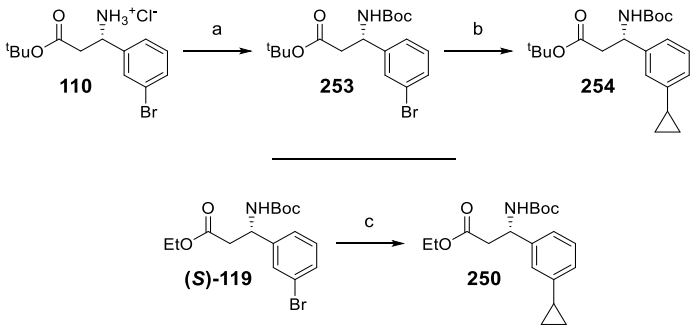

Scheme 29. Preparation of cyclopropyl substituted analogues **254** and **250**. Reagents *and conditions*: a) di-*tert*-butyl dicarbonate, Et_3N, THF, 0 °C to rt, 16 h, 97%; b) **252**, K_2CO_3, XPhos Pd G2 (3 mol%), CPME/water (10:1), 100 °C, Ar, 24 h, 78%; c) **252**, K_2CO_3, XPhos Pd G2 (3 mol%), CPME/water (10:1), 100 °C, Ar, 24 h, 73%

After a period of reaction optimisation, the ester **254** was repeatedly generated on scale, with yields consistently obtained above 75% and with no observable generation of the protodehalogenated by-product. Additionally, despite previous issues regarding the

hydrolysis of ethyl esters under forcing Suzuki-Miyaura conditions, the ethyl ester **250** was generated in good yield with no observable amount of hydrolysis taking place.

With a suitable method for the installation of this important structural feature, we moved our focus towards the development and exploration of SAR surrounding the central amide of this series of integrin inhibitors.

2.5 Preparation of *N*-alkylated inhibitor analogues

2.5.1 Investigation towards *N*-alkylation of the THN amide 258

As discussed in Section 1.5.2.4, within the SDL of the $\alpha_v\beta_6$ integrin binding pocket surrounding the central amide-nitrogen of the UoN series of integrin inhibitors, there is potential for the formation of favourable hydrogen-bonding interactions to encourage a higher affinity ligand binging state with the $\alpha_v\beta_6$ integrin; this effect is well demonstrated by the GSK analogue **12** (Figure 37).[92]

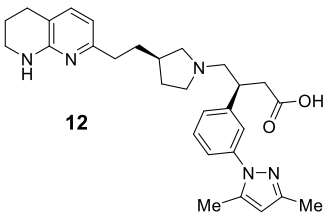

12

Figure 37. The GSK clinical candidate **12**.

It was hypothesised that substitution of the amide-nitrogen with specific alkyl motifs could potentially reveal previously unreported ligand-residue interactions within the integrin binding environment, subsequently allowing the design of highly specific integrin inhibitor targets that exhibit greatly improved potency against, and selectivity for the $\alpha_v\beta_6$ integrin.

As an established and moderately potent pan-integrin inhibitor, the 3-trifluoromethyl substituted analogue **25** was identified as an appropriate standard for comparison with the

proposed *N*-alkylated analogues and thus the target inhibitors were substituted with this group.

At pH 7.4, the pyrrolidine nitrogen within **12** is protonated and is thought to form a hydrogen bonding interaction with a proximal threonine residue (Thr238).[92] To confirm the importance of this proposed interaction between the threonine residue in the binding site and the amide N-H within the UoN series, the first *N*-alkylated analogue to be synthesised was the *N*-methyl amide **255** (Figure 38).

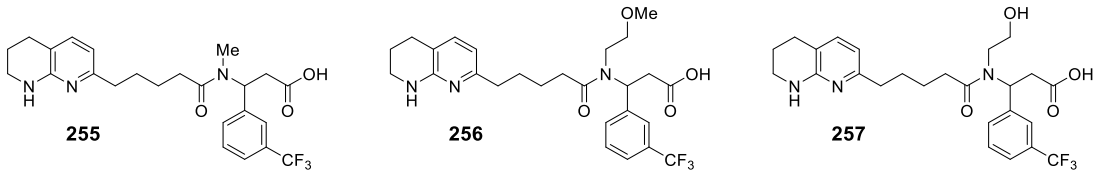

Figure 38. The *N*-alkylated target compounds **255**, **256** and **257**.

As the tertiary amide in **255** would not be expected to be protonated at pH 7.4, **255** would be far less likely to form a beneficial hydrogen bonding interaction with the threonine residue and would thus be expected to exhibit a reduced pIC_{50} against $\alpha_v\beta_6$ due to a lower binding affinity with the integrin binding site.

Two additional *N*-alkylated compounds were proposed to supplement the SAR provided by **255**: the methoxyethyl ether **256** and the hydroxyethyl ether **257** (Figure 38). It was hoped that these polar motifs would compensate for the loss of the amide N-H by forming favourable ligand-residue hydrogen-bonding interactions within the $\alpha_v\beta_6$ integrin binding site.

As with all previous targets in this project, the proposed *N*-alkylations would ideally be performed on a late-stage intermediate and so initial attempts used the THN ester **258** (Scheme 30).

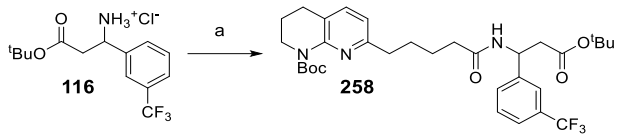

Scheme 30. Preparation of the *N*-alkyl precursor intermediate **258**. *Reagents and conditions*: a) **82**, T3P (50% in ethyl acetate), *i*-Pr_2NEt, acetonitrile, 0 °C to rt, 16 h, 77%.

The intermediate **258** was prepared *via* a T3P mediated amide coupling between the carboxylate **82** and the hydrochloride **116**; the preparation of **116** is described previously in Section 2.2.2.

The amide **258** was deprotonated with sodium hydride and treated with iodomethane to give the *N*-methyl amide **259** in poor yield (Scheme 31).

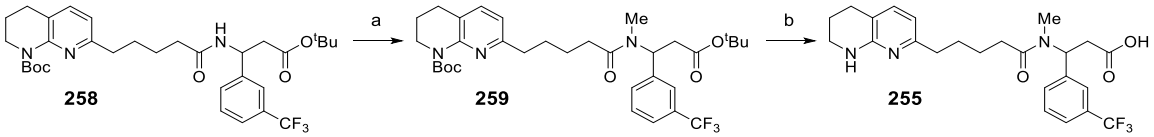

Scheme 31. Preparation of the *N*-methylated integrin inhibitor **255**. *Reagents and conditions*: a) i) sodium hydride, DMF, 0 °C, N_2; ii) iodomethane, 16 h, 33%; b) TFA, CH_2Cl_2, rt, 17 h, 95%.

The *N*-methyl analogue **259** was *N*-Boc deprotected and the ester cleaved in one single step using TFA to give the integrin inhibitor **255**.

Following this encouraging first result, the reaction was repeated using 2-bromoethyl methyl ether as the electrophile (Scheme 32).

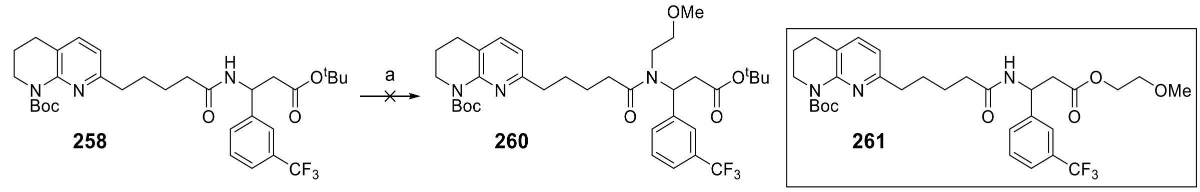

Scheme 32. Attempted *N*-alkylation of **258** using sodium hydride and 2-bromo ethyl methyl ether to generate **260**. *Reagents and conditions*: a) i) sodium hydride, DMF, 0 °C; ii) 2-bromoethyl methyl ether.

LCMS analysis of the crude reaction mixture indicated full consumption of **258**, however mass spectrometry suggested the formation of an entity with the mass of **260** minus a *tert*-butyl group, implying that hydrolysis of **260** had occurred; the retention time of the peak exhibiting this mass did not indicate that a significantly more polar species had been generated (as would be expected with the generation of a carboxylic acid) and so it appeared that the reaction had been successful. The reaction was purified, yet upon NMR analysis, the positions of the R-CH_2CH_2OMe signals in ^1H NMR revealed that the product of the reaction was in fact the ester **261** and not the desired *N*-alkylated analogue **260** (Scheme 32).

tert-Butyl esters are typically cleaved under aqueous acidic conditions and are usually moderately stable to basic environments; however, Filali *et al.* report that reaction systems of powdered KOH in THF and sodium hydride in DMF are able to affect this deprotection.[127] It is thought that in 'wet' DMF, sub-stoichiometric quantities of water allow the formation of non-aggregated anhydrous NaOH upon reaction with sodium hydride; this NaOH is subsequently able to cause the hydrolysis of *tert*-butyl esters.[127] It is likely that this is the cause of the generation of the ester **261**, as the newly formed carboxylic acid analogue of **258** is deprotonated by the remaining sodium hydride within the reaction mixture and subsequently reacts with the alkyl bromide, forming the ester **261**.

This reaction procedure was subsequently abandoned in favour of developing more effective methodology for the generation of *N*-alkylated analogues.

2.5.2 Attempted *N*-alkylation of the sulfinamide 115

A new route was designed in which the sulfinamide **115** was used as the reaction substrate. As an intermediate in the established procedure to synthesise integrin inhibitor analogues, no additional steps would be required to prepare the substrate for alkylation and subsequently, once alkylated, no further steps would be required to process the material through to its pharmacologically active form than stipulated by the established protocol (Scheme 33). As such, this was a particularly attractive alternative to the initially proposed route.

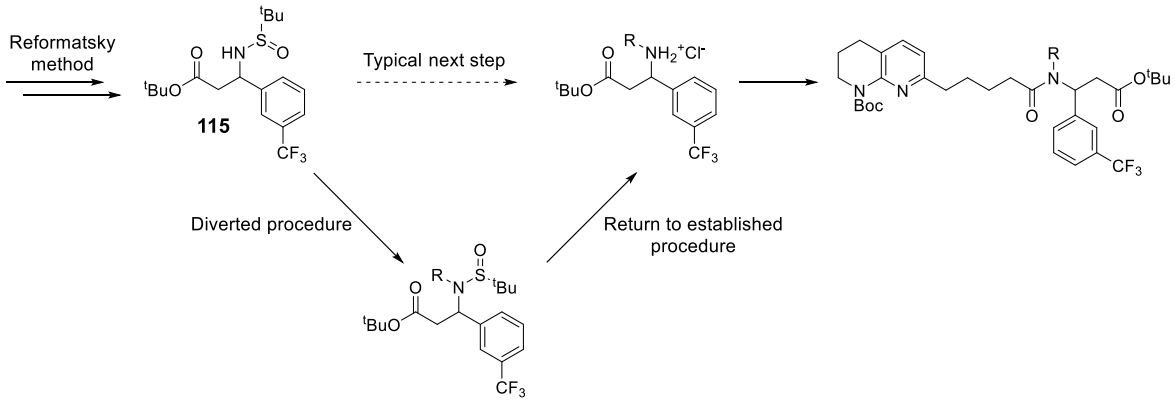

Scheme 33. A depiction of how the proposed alkylation route differs from the established procedure.

The first attempted alkylation of **115** was performed during the Reformatsky reaction itself. It was thought that perhaps the reaction-intermediate **262** would react with the alkylating agent in lieu of a proton, thus forming **263** and so iodomethane was added to the reaction mixture before the typical aqueous quench (Scheme 34).

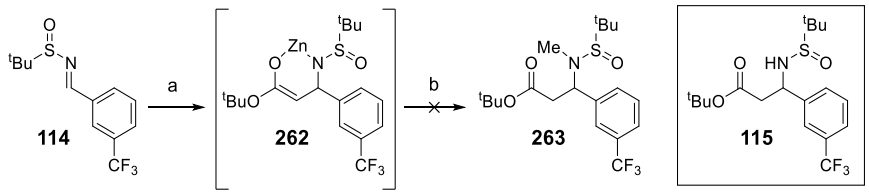

Scheme 34. Attempted generation of the *N*-alkylated analogue **263** by quenching the intermediate **262** with iodomethane. *Reagents and conditions*: a) i) *tert*-butyl bromoacetate, zinc powder, TMSCl, THF, reflux, N_2; ii) **114**, 0 °C, 16 h; b) iodomethane, rt, N_2.

Unfortunately, this was unsuccessful and the Reformatsky reaction proceeded as normal, generating **115.**

Attempting more traditional alkylation methods, the sulfinamide **115** was subjected to conditions as described in Scheme 35.

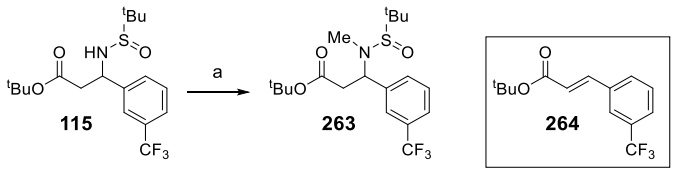

Scheme 35. General conditions used to attempt the synthesis of the *N*-alkylated analogue **263**. *Reagents and conditions*: a) i) ***base***, DMF, 0 °C, N_2; ii) iodomethane, 0 °C, N_2.

The approximate pK_a of the sulfinamide N-H, as calculated by ChemAxon, is 15 and so a variety of appropriately basic reagents were screened, the results of which are presented in Table 11.

Base	Result
Sodium hydride	Mixture of **263** and **264**
LiHMDS	Mixture of **263** and **264**
KOH	Mixture of **263** and **264**
DBU	No change
Cs_2CO_3	Mixture of **263** and **264**
K_2CO_3	No change

Table 11. Each of the bases used and the outcome of the subsequent reaction (based on LCMS analysis) as depicted in Scheme 35.

LCMS analysis of each reaction mixture revealed that any reagent basic enough to initiate the formation of the product **263**, also led to generation of the cinnamate **264** in an approximate 1:1 ratio. This may be due to competitive deprotonation of the amine and the methylene position α to the ester (unlikely due to the significant difference in pK_a between these two positions as predicted by MarvinSketch), or perhaps due to a scenario in which the amine is exclusively deprotonated, with the subsequent nucleophile then proceeding to either attack the electrophilic alkylating reagent or deprotonate α to the ester *via* intermolecular processes, resulting in either *N*-alkylation to give **263** or elimination of the sulfinamide motif and formation of **264** respectively (Scheme 36).

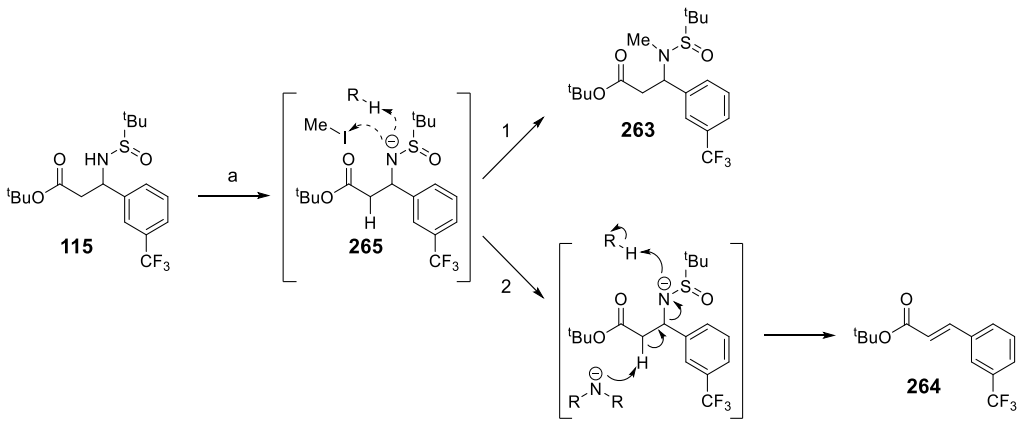

Scheme 36. Proposed scenario in which **263** and **264** are each derived from the single deprotonated intermediate **265**. *Reagents and conditions*: a) ***base***, DMF, 0 °C, N_2; ii) iodomethane.

The conversion of **115** to **263** within these reactions, as determined by LCMS and NMR spectroscopic analysis, was too low to justify further development and so alternative methods of *N*-alkylation were sought.

2.5.3 Preparation and subsequent *N*-alkylation of the nosylate 266

To determine which mechanism was responsible for the formation of the cinnamate **264**, the pK_a of the 2-amino N-H was decreased further; this was achieved upon *N*-nosyl protection of

116 using nosyl chloride and *i*-Pr_2NEt in CH_2Cl_2 (Scheme 37). It was hoped that decreasing the pK_a of the amine N-H with the electron-withdrawing nosyl group, further separating the pK_a from that of the methylene position, would allow for more selective deprotonation using a base that did not facilitate any reaction with **115** and ultimately, *N*-alkylation in good yield.

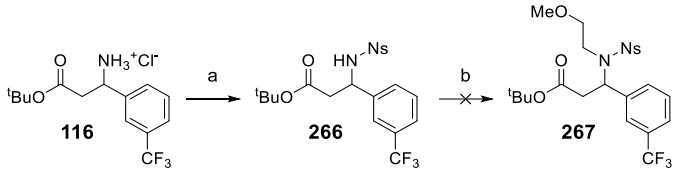

Scheme 37. *N*-Nosyl protection of the β-3-aryl-amino ester **116**, followed by attempted *N*-alkylation of **266** using K_2CO_3 and 2-bromo-ethyl methyl ether to give **267**. *Reagents and conditions*: a) NsCl, *i*-Pr_2NEt, CH_2Cl_2, 0 °C to rt, 16 h, 94%; b) 2-bromo ethyl methyl ether, K_2CO_3, DMF, 90 °C, N_2.

The *N*-nosyl ester **266** was subjected to alkylation conditions, but unfortunately the reaction appeared to proceed in a similar manner to that of the sulfinamide alkylation work described in Section 2.5.2, suggesting that the mechanism of elimination is indeed due to intermolecular processes as depicted in Scheme 36. Thus, traditional methods of alkylation relying on base-deprotonation were discounted, and alternative methods were considered.

One such method of *N*-alkylation that utilises *N*-nosyl protected β-amino esters is described by Kurosawa *et al.* in the total synthesis of (−)-ephedradine A;[128] in this work a Fukuyama-Mitsunobu *N*-alkylation reaction between the *N*-nosylated amine **268** and 3-((*tert*-butyldimethylsilyl)oxy)-propanol is detailed, yielding **269** (Scheme 38).

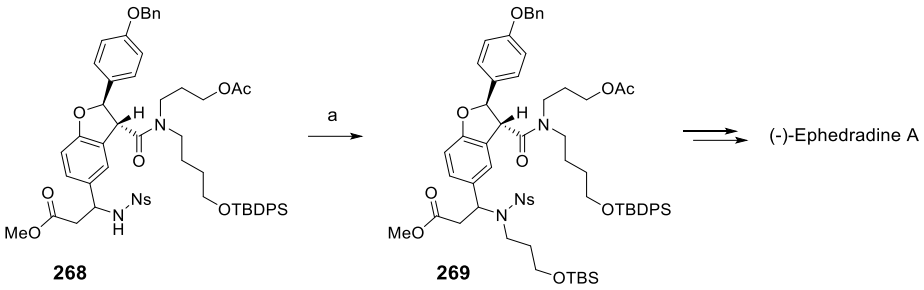

Scheme 38. A Fukuyama-Mitsunobu *N*-alkylation reaction performed in the total synthesis of (-)-Ephedradine A.[128] *Reagents and conditions*: a) 3-((*tert*-butyldimethylsilyl)oxy)-propanol, triphenyl phosphine, DEAD, toluene, 60 °C, 1 h, 95%.

Consequently, two Fukuyama-Mitsunobu reaction were attempted with **266**, using 2-methoxyethanol and 2-((*tert*-butyldimethylsilyl)oxy)-ethanol using triphenylphosphine and DEAD in toluene (Scheme 39).

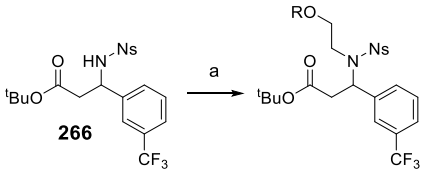

Scheme 39. Fukuyama Mitsunobu *N*-alkylation reaction performed with **266** to generate **267** and **270**. *Reagents and conditions*: a) 2-methoxy ethanol **OR** 2-((*tert*-butyldimethylsilyl)oxy)-ethanol, triphenylphosphine, DEAD, toluene, 60 °C, 1 h, yield: R = Me - 80% (**267**), R = TBS - 57% (**270**).

LCMS of the crude reaction mixtures suggested an approximate 1:1 mixture of the cinnamate by-product **264** and what was assumed to be the products **267** and **270**. However, NMR spectroscopy revealed a total absence of the cinnamate and so the reactions were purified *via* column chromatography, yielding **267** and **270** in 80% and 57% yield, respectively.

The misleading LCMS profile of the reaction mixture suggests that UV based analytical methods are unsuitable for these reactions due to the large extinction coefficient of the cinnamate (**264**) chromophore, resulting in a significant overestimation of its yield.

The 1-position of the nosyl functionality is particularly susceptible to nucleophilic aromatic substitution, thus thiols are able to effectively cleave these groups from amines, resulting in *N*-nosyl deprotection.[129] Consequently, both **267** and **270** were deprotected using thiophenol and submitted to amide coupling conditions with **82** using T3P (Scheme 40); according to standard procedure, the compounds were *N*-Boc deprotected and the esters cleaved with TFA to give the integrin inhibitors **256** and **257**.

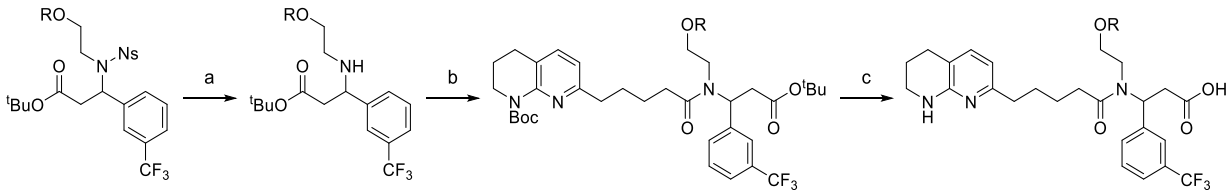

Scheme 40. General scheme depicting the generation of the integrin inhibitors **256** and **257** from **267** and **270**. *Reagents and conditions*: a) **267** OR **270**, PhSH, K_2CO_3, acetonitrile, rt, N_2, yield: R = Me - 80% (**271**), R = TBS - 90% (**272**); b) **82**, HATU, *i*-Pr_2NEt, DMF, 0 °C to rt, N_2, yield: R = Me - 27% (**273**), R = TBS - 29% (**274**); c) TFA/CH_2Cl_2 (10:1), rt, yield: R = Me - quant. (**256**), R = H - quant. (**257**).

2.6 Discussion of newly generated SAR from the 3-monosubstituted integrin inhibitors

Effective analysis of physicochemical data to generate good quality SAR is arguably the most important role of a medicinal chemist for rapid and thorough investigation, and ultimately the advancement of a drug development programme.

Discussion of the data generated by screening the integrin inhibitor analogues described previously will be separated into sections, based upon the subseries from which the compounds originate.

2.6.1 SAR relating to *N*-linked 3-monosubstituted integrin inhibitors

Within this section shall be presented the biological data generated from the Chan-Lam amination array work described in Section 2.3, followed by a detailed discussion of the newly generated SAR and its implications towards further developmental work (Table 12).

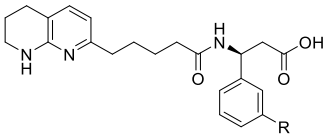

Compound no.	R	pIC_{50} $\alpha_v\beta_6$	pIC_{50} $\alpha_v\beta_3$	pIC_{50} $\alpha_v\beta_5$	pIC_{50} $\alpha_v\beta_8$	pIC_{50} $\alpha_v\beta_1$	$ChromLogD_{7.4}$	HTP nm/s
(*S*)-40		7.8	7.4	6.9	7.0	6.0	1.83	22
193	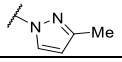	7.8	7.1	7.0	7.2	-	2.31	15
194		7.6	7.3	6.9	7.5	-	2.17	13
195	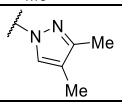	6.9	6.5	6.7	-	-	2.79	30
196	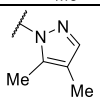	7.3	7.0	6.1	-	-	2.65	17
(*S*)-27	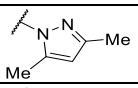	7.9	6.8	6.9	7.5	6.7	2.33	19.5
197	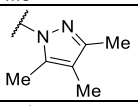	7.5	7.3	6.5	7.1	6.1	2.75	<3
198	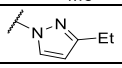	7.7	7.3	6.8	6.9	6.3	2.66	68
199	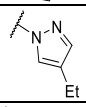	7.5	7.1	7.0	7.0	5.9	2.78	84
200	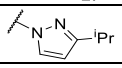	7.7	7.1	7.1	6.8	6.5	3.22	120
201	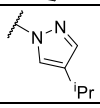	7.7	7.1	7.2	7.1	5.9	3.29	55
202	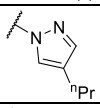	7.2	7.3	6.9	7.1	5.9	3.36	100
203	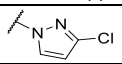	8.0	6.8	7.2	7.2	6.3	2.61	86

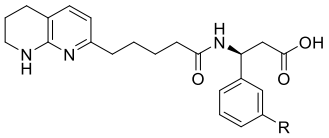

Compound no.	R	pIC_{50} $\alpha_v\beta_6$	pIC_{50} $\alpha_v\beta_3$	pIC_{50} $\alpha_v\beta_5$	pIC_{50} $\alpha_v\beta_8$	pIC_{50} $\alpha_v\beta_1$	$ChromLogD_{7.4}$	HTP nm/s
205	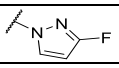	8.0	7.4	7.2	7.1	6.1	2.37	82
206		7.5	7.2	7.0	7.3	6.2	2.09	54
207		7.8	7.5	7.3	7.1	5.9	2.29	71
208	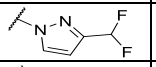	8.0	7.8	6.9	7.0	7.1	2.78	<3
209	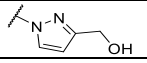	7.5	7.4	6.7	6.9	6.0	1.16	3
210	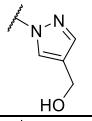	7.4	7.3	7.0	6.9	5.6	1.10	3
(*S*)-39		7.9	7.2	6.7	7.0	6.2	1.23	3
211		7.3	6.8	7.2	6.8	6.0	1.26	3
212	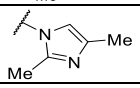	7.7	6.8	6.5	-	-	1.71	<3
213		8.1	7.4	6.8	6.9	6.8	1.59	<3
214	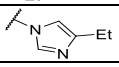	7.7	7.4	7.1	6.8	6.1	1.92	3
215		7.9	7.4	7.1	7.2	6.9	1.75	3
216	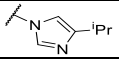	7.1	7.4	6.6	6.9	6.6	2.43	<3

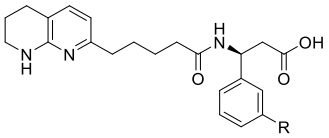

Compound no.	R	pIC_{50} $\alpha_v\beta_6$	pIC_{50} $\alpha_v\beta_3$	pIC_{50} $\alpha_v\beta_5$	pIC_{50} $\alpha_v\beta_8$	pIC_{50} $\alpha_v\beta_1$	$ChromLogD_{7.4}$	HTP nm/s
217	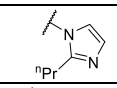	7.7	7.7	6.8	6.9	6.9	1.91	<3
219	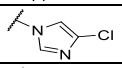	7.8	6.8	7.3	6.9	5.8	1.92	3
220	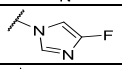	8.1	7.7	7.2	6.8	6.6	1.82	<3
221	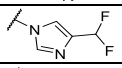	7.6	6.8	6.9	6.7	6.1	1.88	3
223	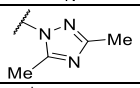	7.6	7.3	6.8	7.0	6.3	1.27	<3
224	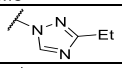	7.4	7.5	6.7	6.8	6.2	1.7	3
225	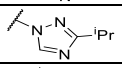	7.4	7.3	7.2	6.9	6.5	2.18	3
227		7.7	7.6	7.1	7.1	6.4	2.85	73
228	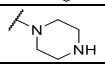	7.3	7.7	7.0	6.8	6.0	0.72	3
231	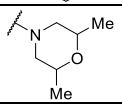	6.7	7.3	7.2	6.7	6.3	2.39	33
233	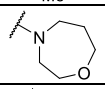	6.7	7.7	7.0	6.7	6.5	1.98	3
234		7.3	7.6	6.7	6.8	6.4	2.84	88
236	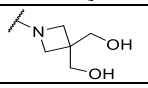	6.5	7.7	7.1	6.6	5.8	-	-

Table 12. Integrin assay potency data and other physical properties for the *N*-linked heterocycle substituted integrin inhibitor analogues prepared *via* Chan-Lam amination. Error in the cell adhesion assays = 0.3.

Analogous pyrazole and imidazole 3-monosubstituted inhibitors, for example the parent heterocycles and their mono-chloro derivatives (**(*S*)-40** and **203** *vs* **(*S*)-39** and **219**), typically display similar levels of potency towards $\alpha_v\beta_6$ and selectivity over $\alpha_v\beta_3$. However, the permeability values exhibited by the pyrazole containing analogues are generally far greater than that of the imidazole containing analogues; no imidazole containing analogue exhibits a permeability greater than 3 nm/s, whereas the pyrazole containing analogues exhibit up to 120 nm/s. This is likely due to the increased basicity of imidazoles (pK_aH of imidazole = 7.0) compared to pyrazoles (pK_aH of pyrazole = 2.5), leading to more basic and polar compounds that are considerably less permeable. This hypothesis is supported by the observation that each pyrazole containing analogue exhibits a ChromLogD value that is at least 0.6 log units greater than the corresponding imidazole containing analogue.

An immediate observation from the data shows that 3-monosubstitution of the unsubstituted inhibitor **15** with either pyrazole (**(*S*)-40**) or imidazole (**(*S*)-39**) provides the initial improvement to the potency against the $\alpha_v\beta_6$ integrin (approximately 2 log units). However, no form of additional substitution on the heterocycle itself provides any further improvement to this potency and simply serves as a tool to reduce the potency towards the $\alpha_v\beta_3$ integrin, ultimately improving the selectivity profile (up to 1.2 log units). This suggests that the heterocycle itself is entirely responsible for the improved binding within the $\alpha_v\beta_6$ pocket, whilst additional substitution on the heterocycle acts as a form of disruption to the binding of the compound within the $\alpha_v\beta_3$ pocket, thus allowing optimisation of each of these two important properties in relative isolation to one another.

Within the pyrazole series, comparison of **193**, **196** and **(*S*)-27** with the parent pyrazole inhibitor **(*S*)-40** suggests that substitution at the 3 position of the pyrazole substituent can facilitate an improvement in selectivity for the $\alpha_v\beta_6$ integrin over the $\alpha_v\beta_3$ integrin *via* reduction of potency against $\alpha_v\beta_3$, with 4 and 5 substitution providing no obvious advantage

on either the observed potency or selectivity; the imidazole analogues **(*S*)-39**, **211** and **212** suggest that substitution at the 4 position of the imidazole substituent provides a similar effect.

As discussed previously, there does not appear to be a predictable correlation between substituent size and selectivity. The data presented in Table 12 suggests that by substituting at the 3 or 4 position in pyrazoles and imidazoles respectively with large, bulky substituents, the likelihood of a net improvement in selectivity is increased. However, this is not always the case, as seen with **208** and **216**, hence the inherent difficulty with predicting the most optimal substitution patterns of these compounds.

As demonstrated in Section 1.4 and 1.5, the UoN series of 3-monosubstituted integrin inhibitors typically exhibit approximate equipotency against the $\alpha_v\beta_6$ and $\alpha_v\beta_8$ integrins, and the $\alpha_v\beta_3$ and $\alpha_v\beta_5$ integrins, with moderate correlation in either case; additionally, with a small number of exceptions, these analogues often exhibit moderate to negligible levels of selectivity for $\alpha_v\beta_3$ and $\alpha_v\beta_5$ over $\alpha_v\beta_6$. However, Table 12 reveals that upon 3-monosubstitution with *N*-linked heterocycles, specifically aromatic substituents, these integrin inhibitor analogues instead exhibit minor to moderate average selectivity for the $\alpha_v\beta_6$ integrin over the $\alpha_v\beta_3$, $\alpha_v\beta_5$ and even $\alpha_v\beta_8$ integrins (0.42, 0.72 and 0.69 log units, respectively) with little to no correlation in all cases (Figure 39). This perhaps indicates that these substituents are interacting with the SDLs within the α_v integrin binding pockets in such a manner that even minor structural or electronic differences between the integrins can be exploited, resulting in the unusual average selectivity profiles and correlations exhibited by this subseries.

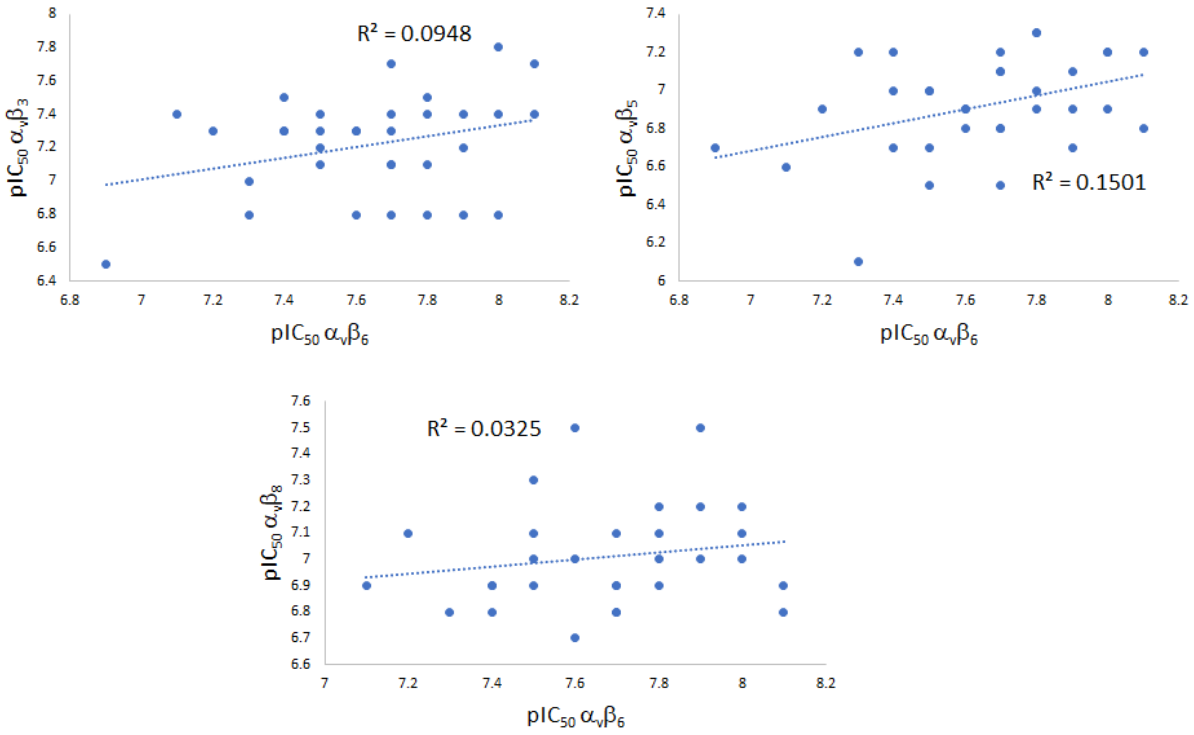

Figure 39. Plots of pIC_{50} against $\alpha_v\beta_6$ *vs* pIC_{50} against $\alpha_v\beta_3$, pIC_{50} against $\alpha_v\beta_6$ *vs* pIC_{50} against $\alpha_v\beta_5$ and pIC_{50} against $\alpha_v\beta_6$ *vs* pIC_{50} against $\alpha_v\beta_8$, with R^2 correlation values, for the aromatic *N*-linked heterocycle substituted analogues depicted in Table 12.

The improved selectivity for $\alpha_v\beta_6$ over $\alpha_v\beta_8$ is especially exciting for the prospect of future development of the UoN series, as selectivity over $\alpha_v\beta_8$ was not originally targeted as a project outcome due to the equipotency with moderate correlation typically exhibited by these RGD mimetic integrin inhibitors towards $\alpha_v\beta_6$ and $\alpha_v\beta_8$ (Section 1.4 and 1.5).[76] One might surmise that this is a result of substitution with a large, planar heterocyclic group, subsequently causing steric disruption within the $\alpha_v\beta_8$ binding site, but as this level of selectivity is not exhibited by the 3-monosubstituted and 3,5-disubstituted *C*-linked heterocyclic analogues depicted in Table 5 and Table 7 (Section 1.5.2.2 and 1.5.2.5), this is unlikely to be the case. It is possible that the cause of this selectivity for $\alpha_v\beta_6$ over $\alpha_v\beta_8$ is the same as that described above regarding specific substitution within heterocycles subsequently affording selectivity for $\alpha_v\beta_6$ over $\alpha_v\beta_3$, but that argument is immediately

undermined by the 10-fold selectivity for $\alpha_v\beta_6$ over $\alpha_v\beta_8$ exhibited by the unsubstituted pyrazole and imidazole analogues **(*S*)-40** and **(*S*)-39**. As such, the reasoning behind this result remains unexplainable without additional SAR and the assistance of computer modelling.

Another interesting observation was the complete lack of correlation in terms of potency between the $\alpha_v\beta_3$ and $\alpha_v\beta_5$ integrins (Figure 40), something that has otherwise been observed throughout the UoN series (Section 1.4 and 1.5).

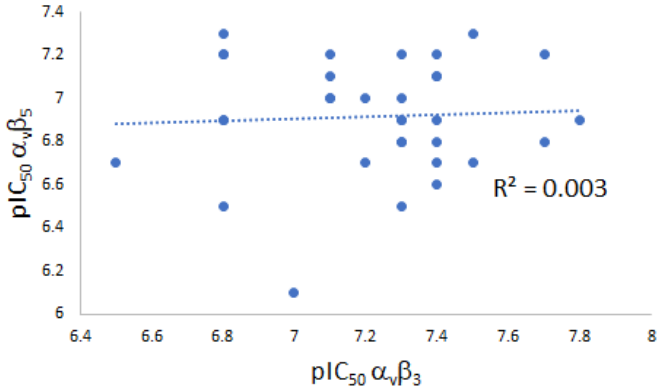

Figure 40. A plot of pIC_{50} against $\alpha_v\beta_3$ *vs* pIC_{50} against $\alpha_v\beta_5$, with the R^2 correlation value, for the aromatic *N*-linked heterocycle substituted analogues depicted in Table 12.

This perhaps indicates that these *N*-linked heterocyclic substituents interact with the $\alpha_v\beta_3$ and $\alpha_v\beta_5$ integrin binding sites differently, even inferring the presence of a previously unspecified ligand-integrin binding site interaction.

With the exception of the piperidine analogue **227** which appears to be an equipotent $\alpha_v\beta_3$ and $\alpha_v\beta_6$ inhibitor, the aliphatic amine analogues **227**-**236** are generally less potent towards the $\alpha_v\beta_6$ integrin, exhibiting a moderate level of average selectivity for $\alpha_v\beta_3$ over $\alpha_v\beta_6$, $\alpha_v\beta_8$ and $\alpha_v\beta_5$. The homo-morpholine inhibitor **233** in fact shows 10-fold selectivity against the $\alpha_v\beta_6$ integrin and good potency against the $\alpha_v\beta_3$ integrin; this is perhaps a result of a hydrogen-bonding interaction between the oxygen atom within the ring and an adjacent residue within either the $\alpha_v\beta_3$ or $\alpha_v\beta_6$ binding sites. It must be noted that there is a

particularly small sample size for these aliphatic *N*-linked analogues and so all assumptions regarding SAR trends must be treated with a level of scepticism.

The triazole substituted analogues **223**-**225** appear to be pan $\alpha_v\beta_6/\alpha_v\beta_3$ inhibitors that exhibit minimal permeability, likely for the same reason as the poor permeability exhibited by the imidazole substituted analogues; however, with this small sample size, no further discussion may be given regarding the SAR of triazole substituted inhibitor analogues.

It would appear that whilst the $\alpha_v\beta_6$ and $\alpha_v\beta_8$ integrins, and $\alpha_v\beta_3$ and $\alpha_v\beta_5$ integrins have typically been thought to share many similarities in terms of binding site structure, hence the often observed equipotency with moderate correlation, the work undertaken to install *N*-linked heterocyclic motifs has revealed previously unknown structural differences that, with the assistance of high-quality computer modelling, may in future be exploited to allow the generation of integrin inhibitors that exhibit excellent selectivity against each of the other α_v-based integrin.

In terms of molecular efficiency, we can see that the unsubstituted pyrazole analogue **(*S*)-40** has a BEI value of 17.4 and is subsequently one of the more ligand efficient inhibitor analogues from the UoN series (Table 13).

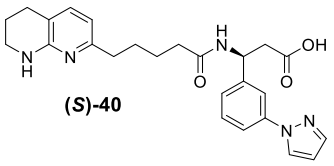

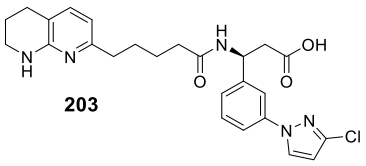

Compound no.	pIC_{50} $\alpha_v\beta_6$	pIC_{50} $\alpha_v\beta_3$	MW	BEI
(*S*)-40	7.8	7.4	447	17.4
203	8.0	6.8	481	16.6

Table 13. Comparison of two of the more potent compounds from Table 12, demonstrating the consequence of improving selectivity upon ligand efficiency. Error in the cell adhesion assays = 0.3.

However, pyrazole **(*S*)-40** does not exhibit selectivity over $\alpha_v\beta_3$ and so is discounted as one of the more lead-like analogues depicted in Table 12. The 3-(3-1*H*-chloropyrazole) substituted inhibitor **203** exhibits a similar potency against $\alpha_v\beta_6$ as **(*S*)-40**, whilst also exhibiting greater than 10-fold selectivity over $\alpha_v\beta_3$ and thus **203** is a more attractive candidate for further development. The ligand efficiencies of these two compounds are comparable despite the almost 10-fold difference in selectivity between them, thus highlighting a common observation of the UoN series, in that improving selectivity does not correlate with a simultaneous improvement of ligand efficiency; in fact, ligand efficiency is often poor within the UoN series due to the high molecular weight of the requisite RGD mimetic structure. As such, whilst 3-monosubstitution with *N*-linked heterocycles has facilitated the preparation of potent and selective integrin inhibitors that are far more drug-like than those previously described in the UoN series, additional work must be undertaken if the preservation of these promising potency and selectivity profiles is to be achieved at greater ligand efficiencies.

As one of the most selective compounds, the 3-(3-1*H*-chloropyrazole) substituted inhibitor **203** was docked into the $\alpha_v\beta_6$ and $\alpha_v\beta_3$ crystal structures (4UM9 and 1L5G, respectively) to generate binding poses that would help to rationalise the observed selectivity (Figure 41).

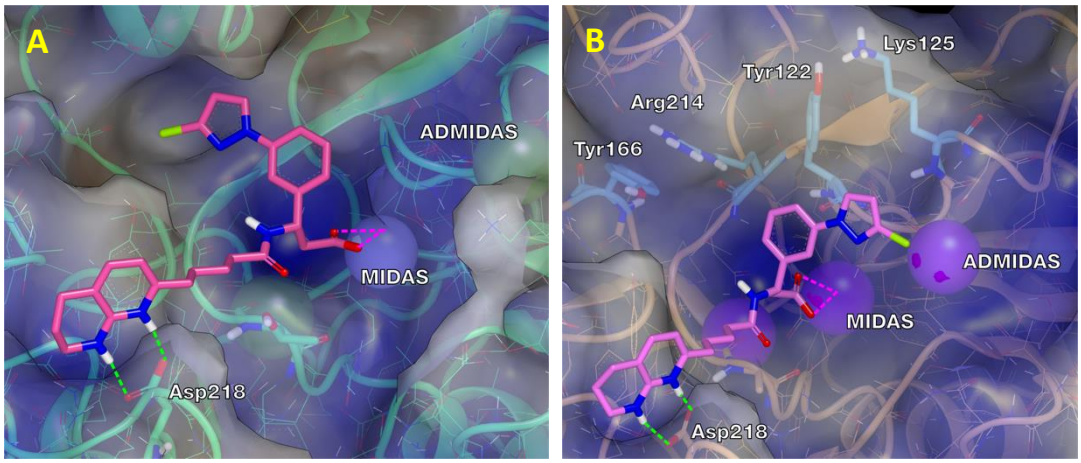

Figure 41. Modelled images of the 3-(3-1*H*-chloropyrazole) substituted inhibitor **203** docked within the $\alpha_v\beta_6$ integrin (A) and the $\alpha_v\beta_3$ integrin (B); key residue interactions vital for the correct orientation of the molecule within the integrins are highlighted with green and pink dotted lines. The Metal-Ion-Dependent Adhesion Site (MIDAS), Adjacent to Metal-Ion-Dependent Adhesion Site (ADMIDAS) and any other key residues within the binding sites are also highlighted. The experimental methods for these docking procedures are described in section 5.5. These molecular dockings and the subsequent generation of images were performed by Steven Oatley.

Figure 41A shows that the SDL in the $\alpha_v\beta_6$ binding site is relatively open and able to accommodate the chloropyrazole substituent. In contrast, Figure 41B shows that there are four amino acid residues within the $\alpha_v\beta_3$ integrin SDL that close off this pocket, preventing **203** from binding in the same conformation as observed within the $\alpha_v\beta_6$ binding site; Tyr166 and Arg214 are particularly influential. These residues limit the size of the pocket, thus forcing the heterocyclic substituent into a more solvent exposed position, which ultimately reduces overall binding affinity. Additionally, in this more solvent exposed position, the ADMIDAS manganese ion in the crystal structure of $\alpha_v\beta_3$ clashes with the chlorine atom in the pyrazole motif, further reducing binding affinity. In combination, these factors lead to the improved selectivity for $\alpha_v\beta_6$ over $\alpha_v\beta_3$ that is observed in several of the analogues that

contain a 3-substituted pyrazole or 4-substituted imidazole (e.g., **(*S*)-27**, **203**, **212**, **219** and **221**).

2.6.2 SAR relating to 3-alkyl-monosubstituted integrin inhibitor analogues

The data for **49** and **50** are presented in Table 14.

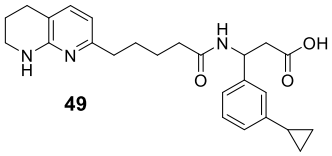

49

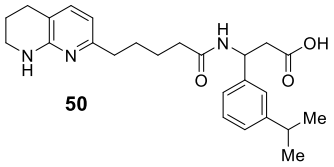

50

Compound no.	pIC_{50} $\alpha_v\beta_6$	pIC_{50} $\alpha_v\beta_3$	pIC_{50} $\alpha_v\beta_5$	pIC_{50} $\alpha_v\beta_8$	pIC_{50} $\alpha_v\beta_1$	$ChromLogD_{7.4}$	HTP nm/s	BEI
49	7.4	7.2	7.0	6.6	6.3	2.69	120	17.6
50	7.1	7.1	6.7	6.6	6.3	3.35	150	16.8

Table 14. Biological data relating to the alkyl-substituted integrin inhibitor analogues **49** and **50**. Error in the cell adhesion assays = 0.3.

Both compounds exhibit largely similar pan potency profiles and have similar permeability characteristics. Gratifyingly, the potency and BEI values for **49** and **50** are not dissimilar from those predicted in Section 1.5.2.3, further legitimising our hypothesis that (*rac*)-analogues in this UoN series of integrin inhibitors exhibit potency values approximately 10-fold less than that of their equivalent GSK-derived analogue.

With **49** exhibiting better selectivity for $\alpha_v\beta_6$ over $\alpha_v\beta_8$ compared to **50** and as **50** exhibits a ChromlogD value more than half a log unit greater than that of **49**, the cyclopropyl substituent may be distinguished from the isopropyl substituent as the more favourable of the two. A ChromLogD value of 2.69 is situated within the optimal range of 1-3 and specifically for this series, grants additional flexibility for further optimisation work as

addition of polar groups will be tolerated to a greater degree without potentially experiencing permeability issues.

The physiochemical profile of the cyclopropyl analogue **49** is similar to that of the *meta*-trifluoromethyl analogue **25**, perhaps exhibiting slightly increased pIC_{50} against $\alpha_v\beta_6$ and pIC_{50} against $\alpha_v\beta_3$, and decreased pIC_{50} against $\alpha_v\beta_5$. However, the cyclopropyl group has a mass that is only 60% that of a trifluoromethyl group and as such is significantly more ligand efficient.

The pan-inhibitory nature of these small, alkyl substituted analogues further legitimises the hypothesis introduced in Section 2.6.1 that *meta*-substitution merely allows the formation of a high affinity binding state with the $\alpha_v\beta_6$ integrin; it does not inherently improve selectivity against the $\alpha_v\beta_3$ integrin as this outcome is only made possible by further steric manipulation of the substituent, as exhibited by **203**.

As the most encouraging alkyl-substituted analogue, the enantiopure (*S*)-analogue **321** was subsequently prepared by UoN MSci students (assay data presented in Table 15).

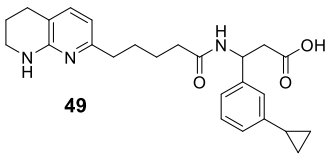

49

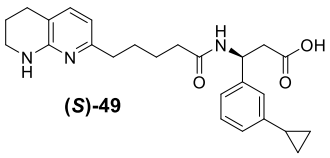

(*S*)-49

Compound no.	pIC_{50} $\alpha_v\beta_6$	pIC_{50} $\alpha_v\beta_3$	pIC_{50} $\alpha_v\beta_5$	pIC_{50} $\alpha_v\beta_8$	pIC_{50} $\alpha_v\beta_1$	$ChromLogD_{7.4}$	HTP nm/s
49	7.4	7.2	7.0	6.6	6.3	2.69	120
(*S*)-49	7.6	7.3	7.4	7.2	6.4	2.70	150

Table 15. Biological data relating to the (*rac*)- and (*S*)-cyclopropyl-substituted integrin inhibitor analogues **49** and **(*S*)-49**. Error in the cell adhesion assays = 0.3.

Comparison of **(*S*)-49** with analogues such as **203** shows that in terms of maximising potency against $\alpha_v\beta_6$ whilst keeping ligand efficiency in mind, the cyclopropyl motif seems an optimal choice for further developmental work. It is only by virtue of the selectivity imbued by specific

structural motifs on the heterocycles themselves that **(*S*)-49** is discounted as a 'lead-candidate' from future mono-substituted optimisation work.

2.6.3 SAR relating to *N*-alkylated 3-trifluoromethyl-monosubstituted integrin inhibitors

The pK_aH of the pyrrolidine nitrogen within the GSK series described previously in Section 1.5.1 is ~10 and so is protonated at pH 7.4. As a consequence, the quaternary amine behaves as a hydrogen bond donor and can form a favourable hydrogen bonding interaction with a proximal threonine residue (Thr238). Upon *N*-methylation, the pK_aH of the tertiary amide would be expected to be approximately 0 (predicted by ChemAxon) and thus would not be protonated at pH 7.4, minimising the likelihood any potential interaction with Thr238.

The data for the *N*-alkylated analogues **255**, **256** and **257**, as well as the standard compound **25** is presented in Table 16.

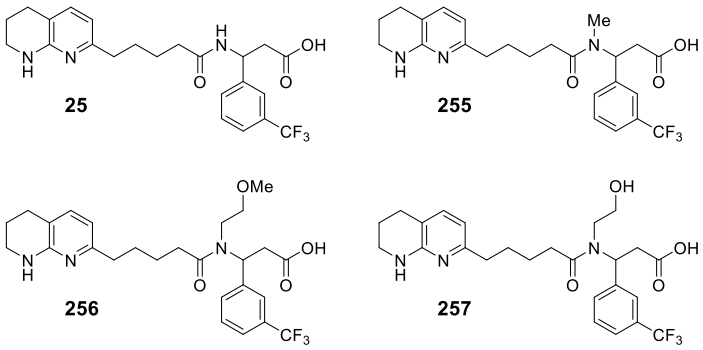

Compound no.	pIC_{50} $\alpha_v\beta_6$	pIC_{50} $\alpha_v\beta_3$	pIC_{50} $\alpha_v\beta_5$	pIC_{50} $\alpha_v\beta_8$	pIC_{50} $\alpha_v\beta_1$	$ChromLogD_{7.4}$	HTP nm/s
25	7.0	6.7	7.4	6.8	-	2.73	180
255	<5	7.1	7.2	6.7	6.5	3.66	400
256	<6	5.4	5.7	5.8	6.1	4.02	390
257	<6	5.8	5.6	5.3	6.0	3.33	200

Table 16. Biological data relating to the three *N*-alkylated integrin inhibitor analogues **255**, **256** and **257**, as well as data for the standard analogue **25**. Error in the cell adhesion assays = 0.3.

As expected, *N*-methylation of the amide **255** resulted in a total loss of activity against the $\alpha_v\beta_6$ integrin, exhibiting the importance of the N-H/threonine interaction. Somewhat surprising was the minor improvement of potency against $\alpha_v\beta_3$, suggesting perhaps that a hydrophobic pocket resides close to the amide in the $\alpha_v\beta_3$ binding site, or perhaps even that the environment surrounding this section of the inhibitor in the SDL of $\alpha_v\beta_6$ is far more constrained than in $\alpha_v\beta_3$.

However, contrary to the proposal that more complex alkylation of the amide nitrogen would infer an improvement of potency towards the $\alpha_v\beta_6$ integrin, each of the *N*-alkylated analogues **256** and **257** exhibit vastly inferior potency profiles across each of the integrin assays. With the structure of the potent Pliant therapeutics analogue **10** available, it is particularly interesting that the methyl ethyl ether analogue **256** does not exhibit any level of potency against any of the α_v integrins; this demonstrates the importance of the N-H/threonine interaction within the SDL of the $\alpha_v\beta_6$ integrin and perhaps also indicates that the central nitrogen in the UoN series of integrin inhibitors is not positioned optimally (Figure 42).

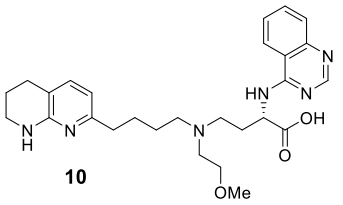

10

Figure 42. The Pliant therapeutics integrin inhibitor analogue **10**.

The loss of potency against $\alpha_v\beta_3$ that is exhibited upon introduction of these more complex motifs to the UoN series of integrin inhibitors suggests that the proposed lipophilic pocket within the $\alpha_v\beta_3$ binding site is relatively small and that ultimately, large *N*-alkyl substituents at this position simply generate high levels of steric disruption within each integrin binding site that are sufficient to minimise binding affinity.

The Thr238 residue in the $\alpha_v\beta_6$ integrin binding site is likely the only residue in the immediate vicinity of the amide that is available for hydrogen-bonding interaction without disrupting the ligand/integrin binding conformation, and as such, optimising hydrogen bonding interaction with this residue must be of the highest priority in order to further improve potency against $\alpha_v\beta_6$ and selectivity over $\alpha_v\beta_3$ where possible.

2.7 Further DMPK studies

2.7.1 Initial Microsomes and MDCK study

Once the initial screening of analogues has been performed in a drug discovery project, if promising potency/selectivity profiles and physical characteristics have been obtained, often the next stage of the project will involve the further evaluation of the most drug-like compounds in the form of DMPK studies. Thus, the 3-(3-chloro-1*H*-pyrazole) substituted analogue **203**, the 3-(3-*iso*propyl-1*H*-pyrazole) substituted derivative **200** and the piperidine substituted analogue **227** were selected for DMPK analysis; the analogue **203** was identified as the most lead-like compound from those presented in Table 12, with high potency and over 10-fold selectivity for $\alpha_v\beta_6$ over $\alpha_v\beta_3$, together with good permeability, **200** exhibited the greatest level of permeability of the analogues presented in Table 12, whilst **227** exhibited the greatest level of potency towards $\alpha_v\beta_6$ of the aliphatic heterocycle substituted analogues.

Thus, compounds **200**, **203** and **227** were resynthesised on a larger scale from the ethyl ester **(*S*)-119**, *via* the boronate **275** and with installation of the heterocycles *via* Chan-Lam amination before introduction of the THN functionality (Scheme 41). The Chan-Lam amination was performed at this stage in order to avoid the challenging separation of regioisomers that had previously been observed during amination of **192** where the THN motif was present (Section 2.3).[130]

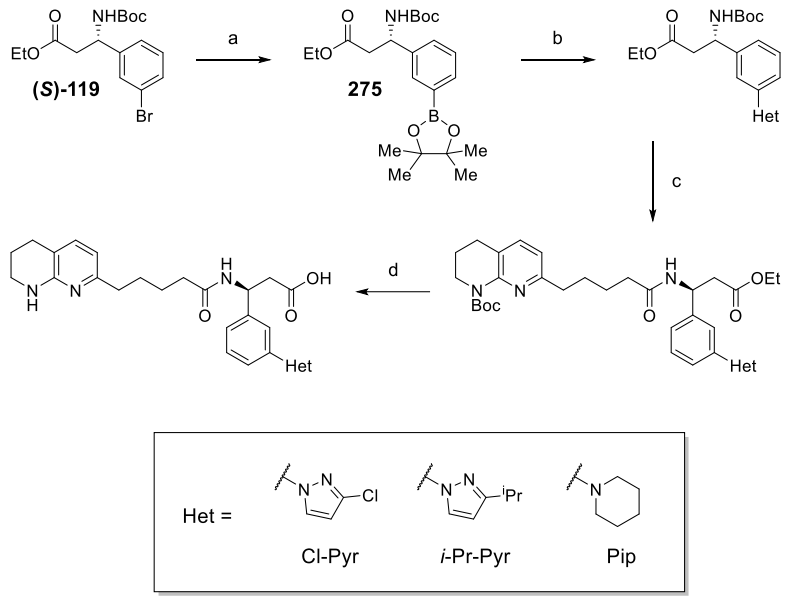

Scheme 41. General synthesis of the three inhibitor analogues **200**, **203** and **227**. *Reagents and conditions*: a) B_2Pin_2, KOAc, $Pd(dppf)Cl_2.CH_2Cl_2$ (10 mol%), 1,4-dioxane, 80 °C, N_2, 16 h, 65%; b) ***amine****, $B(OH)_3$, $Cu(OAc)_2$ (1.00 eq.), acetonitrile, 3 Å M.S., 70 °C, 18 h, yield: **276** (Het = Cl-Pyr) = 50%, **277** (Het = *i*-Pr-Pyr) = 56%, **278** (Het = Pip) = 45%; c) i) 4M HCl in dioxane, diethyl ether, rt, 3 h; ii) **82**, T3P (50% in ethyl acetate), *i*-Pr_2NEt, acetonitrile, 0 °C to rt, 16 h, yield: **279** (Het = Cl-Pyr) = 36%, **280** (Het = *i*-Pr-Pyr) = 41%, **281** (Het = Pip) = 44%; d) i) TFA, CH_2Cl_2, rt, 7 h; ii) 1M $LiOH_{(aq)}$, THF, rt, 18 h; iii) OASIS®, yield: **203** (Het = Cl-Pyr) = 95%, **200** (Het = *i*-Pr-Pyr) = 97%, **227** (Het = Pip) = quant.

*For: **276**, amine = **143**; **277**, amine = **140**; **278**, amine = **175**

The three Chan-Lam amination reactions were performed on 0.95 mmol scale, giving the products **276**, **277** and **278** in moderate yield ranging from 45-56%; on this larger scale, the minor 3-(5-isopropyl-1*H*-pyrazole) regioisomer **282** was isolated separately to the major regioisomer and the resulting combined yield was 77% (Figure 43).

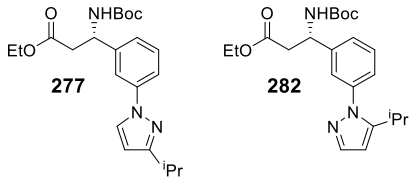

Figure 43. The major and minor regioisomers (**277** and **282** respectively) generated during Chan-Lam amination between 3-*iso*-propyl-1*H*-pyrazole and the boronate **275**.

The Chan-Lam amination products **276**, **277** and **278** were *N*-Boc deprotected and immediately subjected to amide coupling with **82** using T3P to give **279**, **280** and **281**. Following this, the compounds were subsequently *N*-Boc deprotected and the esters saponified to give the desired analogues **203**, **200** and **227**.

All DMPK work described in this thesis was performed by Sygnature Discovery.

Initial *in vitro* DMPK studies reveal that these compounds exhibit acceptable permeability and metabolic stability that complements their measured potency and selectivity profiles, further enhancing their potential as drug-like lead compounds (Table 17 and Table 18).

	MDCK			
		Basal to Apical	Apical to Basal	Corrected efflux ratio
Number	**Cells**	**P_{app} (10^{-6} cm/s)**	**P_{app} (10^{-6} cm/s)**	
203	MDR1	10.2	0.6	23.3
	WT	3.0	4.4	
200	MDR1	15.1	0.6	26.0
	WT	5.6	5.8	
227	MDR1	19.9	3.2	8.2
	WT	7.4	9.7	

Table 17. Madin-Darby canine kidney (MDCK) data regarding MDCK cells transfected with the multidrug resistance gene-1 (MDR1) or simply the wild-type (WT) MDCK cells, for the integrin inhibitor analogues **203**, **200** and **227**. This work was performed by Sygnature Discovery.

The MDCK wildtype/MDR1 assay was performed using PrediPort™-WT/MDR1 Kit from ReadyCell S.L. (Barcelona, Spain). Drug transport was assessed in both directions (apical to basolateral (A-B) and basolateral to apical (B-A)) across the cell monolayer. The buffer used for the assay did not include HEPES, so as to minimise the inhibitory effect on uptake transporters.[131] Test compound concentrations were quantified using a calibration curve following analysis by LC-MS/MS, and the apparent permeability coefficient (P_{app}) and efflux ratio of the compound across the monolayer were calculated. MDCK cells are used to determine both the passive permeability and the efflux ratios of compounds. The passive permeability of compounds into the cell *via* the cell membrane is reported as a measure of A to B permeability in WT cells; MDCK cells in which the MDR1 is not present. The corrected efflux ratio, used as an indicator of active efflux, is a comparison between the efflux ratios (B to A/A to B) relating to the MDR1-MDCK cells and the WT-MDCK cells. This ratio additionally provides an indication as to whether compounds are P-glycoprotein 1 (P-gp) substrates; the data is consistent with **203** and **200** being P-gp substrates, but **227** much less so.

	In vitro metabolic clearance							
	Human liver microsomes				Mouse liver microsomes			
	NADPH+		NADPH-		NADPH+		NADPH-	
C. no.	**$t_{½}$ (min)**	**Cl_{int} (mL/min/mg)**	**$t_{½}$ (min)**	**Cl_{int} (mL/min/mg)**	**$t_{½}$ (min)**	**Cl_{int} (mL/min/mg)**	**$t_{½}$ (min)**	**Cl_{int} (mL/min/mg)**
203	36	39	>480	<1	131	11	>480	<1
200	12	119	291	6	182	5	>480	<1
227	>480	<1	>480	<1	57	24	>480	<1

Table 18. Data relating to *in vitro* clearance of the three 3-monosubstituted integrin inhibitor analogues **203**, **200** and **227** in both human and mouse liver microsomes; C. no. = Compound number. This work was performed by Sygnature Discovery.

The *in vitro* microsomal metabolic stability assay utilised the Phase I cofactor NADPH and indicates the rate of Phase I metabolism for compounds in both human and mouse liver microsomes as a measure of half-life ($t_{½}$); the intrinsic clearance (Cl_{int}) of compounds is monitored in the presence and absence of cofactor (labelled NADPH+ and NADPH- respectively). The assay included two replicates of each compound and were validated by the inclusion of up to 3 species-specific control compounds (human microsomes – verapamil, diltiazem and chlorpromazine; mouse microsomes – verapamil, diphenhydramine and benzydamine).

The piperidine substituted analogue **227** was identified as the most promising of the three analogues, exhibiting a moderate passive permeability (P_{app} = 9.7) and an efflux ratio of 8.2, and stability to Phase 1 metabolism in human liver microsomes, with a half-life of greater than 8 h; the parameters for what Sygnature Discovery consider to be low, moderate or high clearance data values in human and mouse microsomes is depicted in Table 19.

Species	**Microsomal Cl_{int} (μL/min/mg)**		
	Low	**Moderate**	**High**
Human	<10.5	10.5 - 57	>57
Mouse	<10	10 - 54	>54

Table 19. Microsomal data parameters as stated by Sygnature Discovery.

The additional data for **227** suggested that it, and similar 3-monosubstituted integrin inhibitor analogues, may exhibit oral bioavailability.

2.7.2 Additional hepatocytes and *in vivo* DMPK studies of 227

As a result of the promising initial MDCK and *in vitro* microsomal data relating to the piperidine analogue **227**, further DMPK studies were ordered. A follow-up *in vitro* study in mouse hepatocytes and *in vivo* study in mouse was performed, the results of which are displayed in Table 20 and Figure 44.

Compound no.	*In vitro* metabolic clearance				Caco-2	PPB
	Mouse Hepatocytes				Efflux ratio	Mean % binding
	Cells+		Buffer control			
	$t_{½}$ (min)	Cl_{int} (µL/min/x10^6 cells)	$t_{½}$ (min)	Cl_{int} (µL/min/x10^6 cells)		
227	269	6	202	9	1.2	98.3

Table 20. Data regarding *in vitro* clearance of the 3-piperidine-monosubstituted integrin inhibitor analogue **227** within mouse hepatocytes, followed by Caco-2 permeability and plasma protein binding (PPB) data. This work was performed by Sygnature Discovery.

The hepatocyte stability assay monitored the intrinsic clearance of **227** in the presence and absence of hepatocytes (labelled Cells+ and Buffer control, respectively). The assay included two replicates of **227** and was validated by the inclusion of four species-specific positive control compounds (verapamil, 7-hydroxycoumarin, diltiazem and propranolol). Data output consists of $t_{½}$ and Cl_{int} measurements. Caco-2 Permeability was evaluated using the CacoReady™ Kit from ReadyCell S.L. (Barcelona, Spain), drug transport was assessed in both directions (A-B and B-A) across the cell monolayer. The buffer used for the assay did not include HEPES, so as to minimise the inhibitory effect on uptake transporters.[131] Plasma Protein Binding was evaluated using the rapid equilibrium dialysis (RED) device to measure

the percentage binding of **227** to mouse plasma proteins. The analogue **227** and positive controls (diazepam and antipyrine) were incubated in 100% plasma and dialysed against buffer in a RED device for 4 hours at 37 °C in a 5% CO_2 incubator, with continuous shaking at 200 rpm. Samples were matrix matched and analysed by LC-MS/MS against a 6-point standard curve prepared with 100 % plasma.

Compound **227** exhibits moderate clearance in mouse hepatocytes, compensating for the otherwise relatively high plasma binding; the Caco-2 data suggests that **227** exhibits good permeability, correlating with the moderate permeability it demonstrated in the MDCK permeability assay (Table 17).

The data relating to the *in vivo* study of **227** is presented in Table 21 and Figure 44.

Compound no.	**227**	**227**
Animal Species	Mouse (CD1)	Mouse (CD1)
Gender	Male	Male
Matrix	Blood	Blood
Dose (mg/kg)	1.0 mg/kg	10.0 mg/kg
Route	IV	PO
Vehicle	0.86% HCL+ 99.14% dH_2O	0.43% HCL + 99.57% dH_2O
PK Parameter		
C_{max} (ng/mL)	N/A	2878.9
T_{max} (h)	N/A	0.25
Cl (mL/min/kg)	21.07	N/A
V_{dss} (L/kg)	0.7752	N/A
$t_{½}$ (h)	0.8055	N/A
AUC_{0-t} (ng/mL*h)	785.95	2365.7
AUC_{0-inf} (ng/mL*h)	795.51	2400.6
MRT (h)	0.6255	1.0985
Bioavailability (%F)	N/A	30.13

Table 21. Data relating to an *in vivo* study of the 3-piperidine-monosubstituted integrin inhibitor analogue **227** in mouse, comparing both intravenous (IV) at 1.0 mg/kg and per oral (PO) at 10 mg/kg administration. This work was performed by Sygnature Discovery.

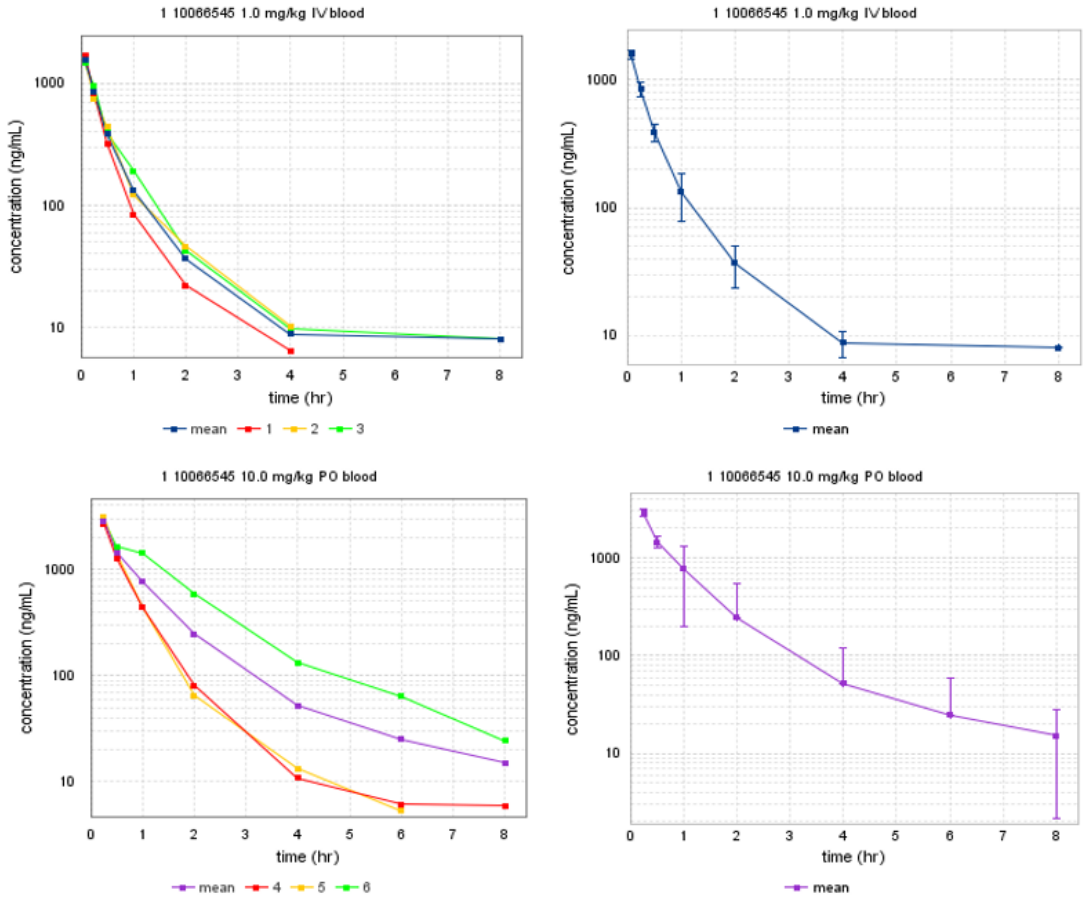

Figure 44. Graphical depictions relating to the calculation of AUC for both the IV and PO administrations: one experiment performed in three separate animals (depicted in the left-hand images) were used to calculate the mean (depicted in the right-hand images) which was in turn used to calculate the AUC. This work was performed by Sygnature Discovery.

This DMPK study suggests that compound **227** is predominantly cleared *via* Phase 1 metabolism, as the scaled up hepatic clearance (from microsomes and hepatocytes *in vitro* data) are comparable to one another; the *in vivo* clearance is also comparable to the scaled *in vitro* clearance. It is worth noting that the volume of distribution (V_{dss}) is low, suggesting that **227** remains predominantly in the systemic circulation; volume of distribution represents the theoretical volume required to contain the total quantity of an administered drug at the concentration that it occurs in the blood plasma, thus indicating the propensity for the drug to either remain in the plasma or redistribute to other tissues in the

body. The low bioavailability exhibited by **227** may result from rapid clearance, solubility or efflux related issues; bioavailability indicates the fraction of an administered drug that reaches the systemic circulation and so with an efflux ratio of 8.2, it is possible that **227** is simply not able to absorb completely before being readily effluxed back into the intestinal tract and excreted out of the body.

The data obtained from this DMPK study validates the UoN series of integrin inhibitors as a series worthy of further development. Demonstrating moderate metabolic stability and permeability, both *in vitro* and *in vivo*, this series of 3-monosubstituted analogues is clearly capable of exhibiting promising drug-like characteristics that, with additional optimisation, could foreseeably result in the development of a candidate suitable for clinical evaluation.

With this newly generated SAR relating to 3-monosubstitution of these RGD integrin inhibitors, we sought to further improve the physicochemical profiles of our most lead-like compounds by combining the most promising aryl-substituents in a series of 3,5-disubstituted integrin inhibitor analogues.

Chapter 3

Preparation and biological evaluation of 3,5-disubstituted β-3-aryl-amino acid $\alpha_v\beta_6$ integrin inhibitor analogues

3.1 Discussion of general SAR relating to 3,5-disubstitution of RGD mimetic integrin inhibitors and target compound design

3,5-disubstitution of the phenyl component within the GSK and UoN series often imbues improved selectivity for the $\alpha_v\beta_6$ integrin against $\alpha_v\beta_3$ and $\alpha_v\beta_5$, compared to 3-monosubstitution (Table 22). The magnitude of this increase is somewhat inconsistent across individual cases, ranging from significant (**52**) to negligible change (**287**), to total loss of activity against all integrins (**286**).

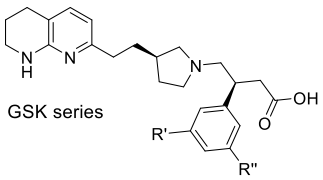

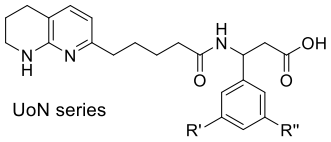

Series	C. no.	R'	R''	pIC_{50} $\alpha_v\beta_6$	pIC_{50} $\alpha_v\beta_3$	pIC_{50} $\alpha_v\beta_5$	pIC_{50} $\alpha_v\beta_8$	pIC_{50} $\alpha_v\beta_1$	$ChromLogD_{7.4}$	HTP nm/s
GSK	**48**		H	8.4	6.8	8.1	8.2	6.8	3.34	-
GSK	**283**		H	8.4	6.2	7.3	7.8	6.6	2.27	-
GSK	**12**	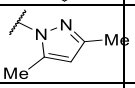	H	8.4	6.0	6.9	7.8	7.3	2.82	-
GSK	**284**			8.4	5.7	6.7	7.8	7.2	3.07	-
GSK	**285**	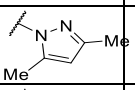		8.1	5.5	5.7	8.0	7.0	2.73	-
UoN	**(*S*)-27**	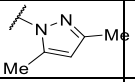	H	7.3	5.9	6.4	7.2	6.3	2.27	29
UoN	**58**	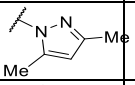	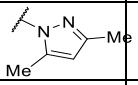	7.4	5.2	5.5	7.0	5.4	3.07	26
UoN	**25**		H	7.0	6.7	7.4	6.8	-	2.73	180
UoN	**286**			<5	<5	<5	5.4	-	3.87	350
UoN	**43**		H	7.2	6.5	6.8	7.1	6.3	1.98	18
UoN	**52**	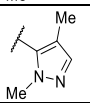	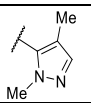	7.0	5.0	5.4	7.2	5.8	2.19	<3
UoN	**45**	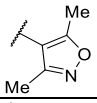	H	7.1	6.7	7.3	7.3	6.8	2.52	75
UoN	**31**	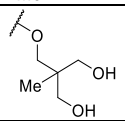	H	7.5	7.4	7.6	6.5	5.9	1.43	<10
UoN	**287**	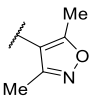	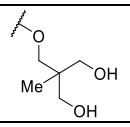	7.4	7.0	7.2	7.4	6.8	2.06	<3

Table 22. Physicochemical data for a selection of integrin inhibitor analogues from both the GSK and UoN series, exhibiting the effect of 3,5-disubstitution compared to the parent 3-monosubstituted compound/s; C. no. = Compound number.[1–5,8,9,11,14,15] Error in the cell adhesion assays = 0.3.

Thus, to elucidate the mechanisms from which selectivity for the $\alpha_v\beta_6$ integrin over $\alpha_v\beta_3$ and $\alpha_v\beta_5$ is imbued, the 3,5-disubstituted subseries of UoN series integrin inhibitors ultimately required further investigation.

Despite the excellent levels of selectivity for the $\alpha_v\beta_6$ integrin over the $\alpha_v\beta_3$ and $\alpha_v\beta_5$ integrins exhibited by compounds **52**, **58** and other similar compounds in the UoN SAR, 3,5-disubstitution with two heterocyclic motifs typically decreases the permeability exhibited by these integrin inhibitors to far below that which is desired in the context of drug design. High molecular mass beyond that which is recommended based on Lipinski's Rule of 5 is additionally a concern and a common characteristic of these *bis*-heterocycle substituted analogues;[132] however, the notion that good bioavailability for oral compounds should have a molecular mass below 500 Da has recently been challenged.[133] An examination of all oral new chemical entities (NCEs) approved by the FDA between 1900-2017, found that between 1900-1997, the mean molecular weight (MW) of oral NCEs was 322.0, with a 90th percentile value of 470.3; in contrast, between 1998-2007, the mean MW of oral NCEs had increased to 360.1, with a 90th percentile value of 525.5, and then furthermore, between 2008-2017, the mean MW of oral NCEs was 436.5, with a 90th percentile value of 607.3.[133]

With this in mind, a series of 3,5-disubstituted analogues combining the most efficacious *N*-linked heterocycles with the more potent and ligand efficient alkyl substituents from the UoN SAR was designed in an effort to improve the drug-likeness of this 3,5-disubstituted series (Figure 45).[82,130]

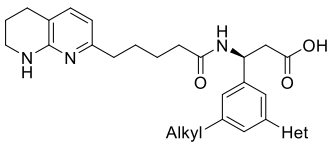

Figure 45. The structure of the proposed 3,5-disubstituted integrin inhibitor analogues, combining the most efficacious alkyl and heterocyclic substituents with one another.

The ultimate aim of this next project was the generation of potent and selective 3,5-disubstituted integrin inhibitors exhibiting similar levels of selectivity for the $\alpha_v\beta_6$ integrin over $\alpha_v\beta_3$ and $\alpha_v\beta_5$ as **58**, ideally with permeability characteristics more appropriate for that of a drug-like lead compound.

Four heterocycles and three alkyl substituents were selected from the UoN SAR based on the favourable physical properties, potency and selectivity values exhibited by their corresponding (*S*)-inhibitor analogues (Table 23): 5-isopropyl pyrazole, 3,5-dimethyl pyrazole, 5-chloro pyrazole, piperidine, trifluoromethyl, cyclopropyl and 2,2-difluoroethyl ether.

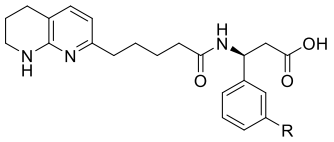

Compound no.	R	pIC_{50} $\alpha_v\beta_6$	pIC_{50} $\alpha_v\beta_3$	pIC_{50} $\alpha_v\beta_5$	pIC_{50} $\alpha_v\beta_8$	pIC_{50} $\alpha_v\beta_1$	$ChromLogD_{7.4}$	HTP nm/s
200	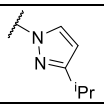	7.7	7.1	7.1	6.8	6.5	3.22	120
(*S*)-27	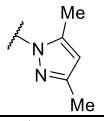	7.9	6.8	6.9	7.5	6.7	2.33	19.5
203	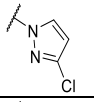	8.0	6.8	7.2	7.2	6.3	2.61	86
227		7.7	7.6	7.1	7.1	6.4	2.85	73
(*S*)-25		7.1	7.0	7.2	6.9	-	2.72	100
(*S*)-49		7.6	7.3	7.4	7.2	6.4	2.70	150
(*S*)-30	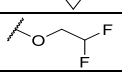	7.9	7.2	7.4	7.4	6.4	2.48	37

Table 23. Physicochemical data of the four *N*-linked heterocycle-substituted and the three alkyl-substituted integrin inhibitor analogues selected for further 3,5-disubstitution investigatory work. Error in the cell adhesion assays = 0.3.

Combination of the heterocycles with the alkyl groups listed in Table 23 generated the 3,5-disubstituted integrin inhibitor targets depicted in Figure 46.

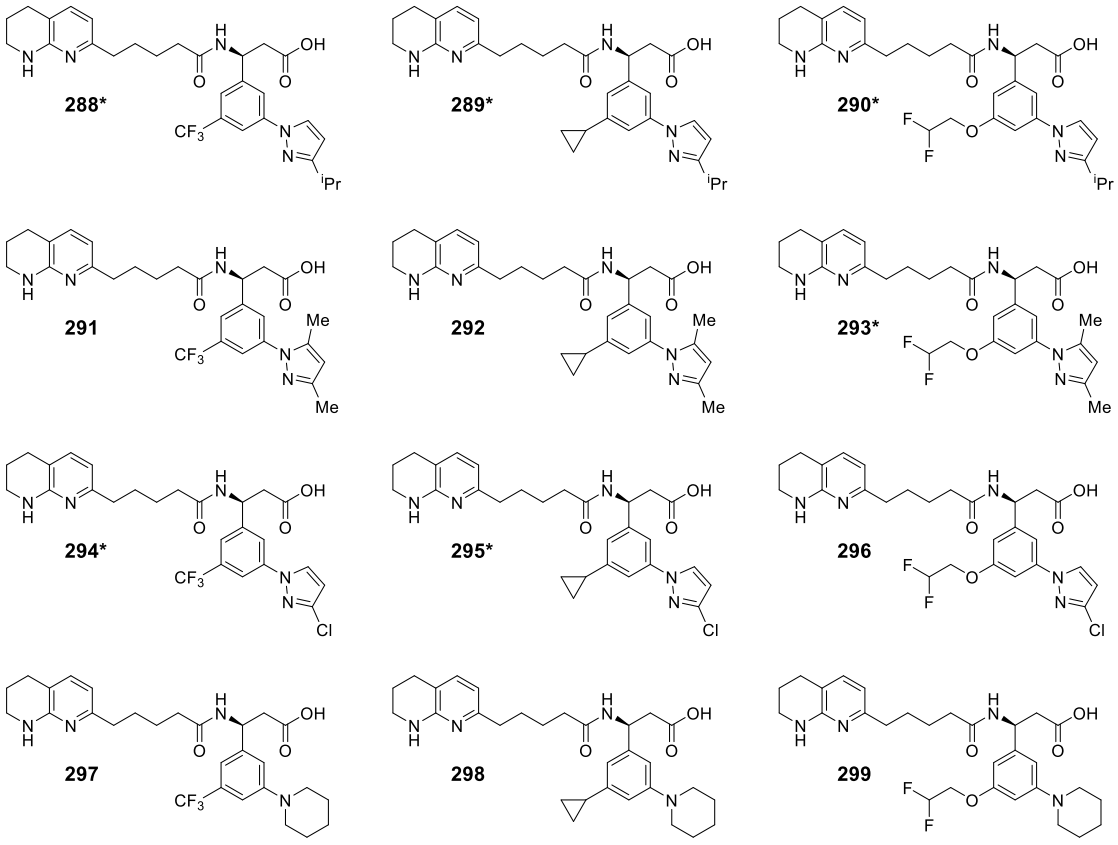

Figure 46. The 12 proposed target 3,5-disubstituted integrin inhibitor analogues generated upon combination of the four heterocycles with the three alkyl substituents listed in Table 23; analogues prepared by the author are highlighted with an asterisk (*).

Due to time constraints, 6 target compounds and their requisite precursor intermediates were prepared by UoN MSci students; these compounds are highlighted in Figure 46.

3.2 Methodology development for the generation of 3,5-disubstituted integrin inhibitor precursors

Due to the non-symmetric aryl components within the target compounds depicted in Figure 46, a highly selective and reliable method of introducing the desired substituents was required.

Ideally, the 12 target compounds would be prepared from a single intermediate in an array-like fashion; 3,5-*bis*-halo-substituted substrates initially appeared to be the most suitable candidate for such a task (Scheme 42).

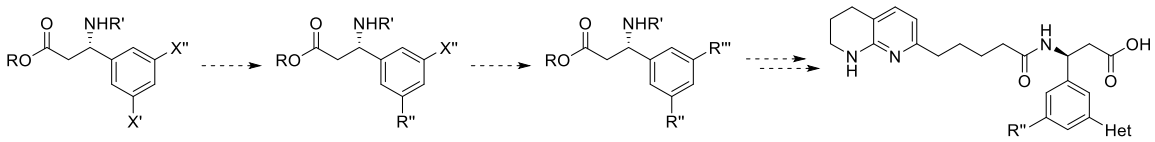

Scheme 42. An approximate synthetic strategy for the preparation of 3,5-disubstituted integrin inhibitor analogues from a single 3,5-*bis*-halo-substituted substrate. X = halo substituent.

As discussed previously, a method of introducing *N*-linked heterocyclic motifs has been developed and tested thoroughly within the UoN series *via* the Chan-Lam amination reaction.[130] This methodology requires the pinacol borane group, most commonly introduced *via* a Miyaura borylation reaction, which in turn requires a halo-substituted precursor (Scheme 43).

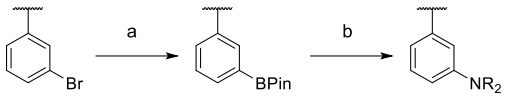

Scheme 43. The synthetic procedure generating *N*-linked heterocyclic-substituted analogues from aryl-bromides, *via* the pinacol boronate species, as reported by Robinson *et al*.[130] *Reagents and conditions*: a) B_2Pin_2, KOAc, $Pd(dppf)Cl_2{\cdot}CH_2Cl_2$ (10 mol%), 1,4-dioxane, 80 °C, N_2, 16 h; b) ***amine***, $B(OH)_3$, $Cu(OAc)_2$ (1.00 eq.), acetonitrile, 4 Å MS, 70 °C, 40 h.

Installation of the secondary target alkyl substituents presented an additional level of complexity to the synthetic route, due to the likely manner in which they would be introduced. Each of the desired substituents could ultimately be derived from a single aryl halide intermediate (Scheme 44): cyclopropyl from the Suzuki-Miyaura coupling previously described (Section 2.4.2), difluoroethoxy *via* alkylation of a phenol, which itself may be introduced *via* a number of different methodologies using aryl boronates or aryl halides (these often involve the use of aqueous base and elevated temperatures) and trifluoromethyl from reaction of an aryl boronate or aryl halide species with various commercially available reagents.

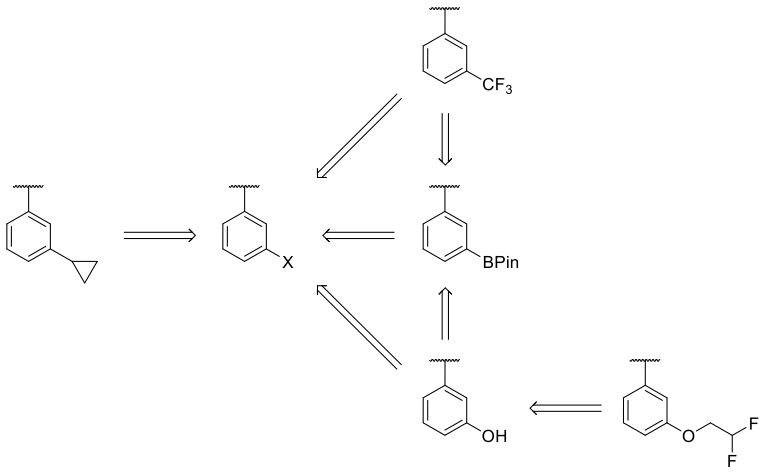

Scheme 44. A general overview of how the three desired substitution patterns can each be derived from one single aryl-halide intermediate.

Whilst appropriate for their intended purpose, each of these methodologies would require a period of reaction optimisation due to the higher levels of complexity and functionalisation present in the 3,5-disubstituted intermediate. This may in turn reveal various synthetic challenges and chemoselectivity issues that would dramatically increase the time taken to prepare each individual target inhibitor, something not particularly conducive to an efficient and productive lead-optimisation drug development program.

Therefore, to avoid these potential issues becoming a reality, it was decided that the target integrin inhibitors would instead be prepared from three 3-monosubstituted intermediates in which the desired alkyl substituted has been previously introduced. As each of the heterocycles selected for these 3,5-disubstituted integrin inhibitor targets are introduced *via* a Chan-Lam aryl amination with a boronate species in our previously reported work, methodology facilitating the regioselective installation of a pinacol borane substituent *via* C-H functionalisation of a pre-functionalised intermediate was sought (Scheme 45).[130]

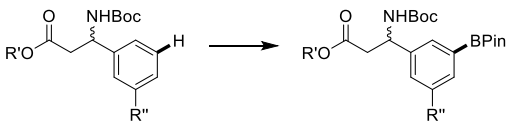

Scheme 45. The desired regioselective C-H functionalisation of the *N*-Boc β-3-aryl-amino ester intermediate, introducing the required pinacol borane substituent to give the 3,5-disubstituted product.

Whilst seemingly complex, the benefits of such C-H functionalisation chemistry include avoiding the use and/or wastage of large quantities of expensive and precious intermediates, also decreasing the total quantity of separate methodologies required and the likelihood of encountering challenging synthetic obstacles in the pursuit of each individual target molecule. Methodology that is able to meet each of these requirements, whilst facilitating the rapid generation of specific and complex pharmacological targets at the lead-

optimisation stage of a drug-development programme would be a powerful synthetic tool indeed.

3.2.1 Iridium catalysed C-H activated borylation

Work reported by Hartwig *et al.*, and Smith *et al*. provides a versatile and powerful methodology for iridium-catalysed aromatic C–H borylation that is particularly valuable given the ever increasing synthetic versatility of boronate groups.[134–138] Encouraged by previous examples of C–H borylation on simple amino acid derivatives, we sought to apply this methodology to our own β-3-aryl-amino ester substrates to facilitate the generation of the target 3,5-disubstituted integrin inhibitors depicted in Figure 46.[139,140]

A series of 3-monosubstituted *N*-Boc β-3-aryl-amino ester derivatives were prepared by the Rodionow and Reformatsky methods described in Section 2.2.1 and 2.2.2. The conditions required to perform the desired borylation on our β-3-aryl-amino ester substrates were optimised previously by UoN MSci students; a screen of reported ligands and solvents ultimately resulted in methoxy(cyclooctadiene)iridium(I) dimer ($[Ir(OMe)(cod)]_2$) being chosen as the catalyst with *bis*(pinacolato)diboron (B_2pin_2) as the boron source, 4-4'-di-*tert*-butyl-2,2'-bipyridine (dtbpy) as the accompanying ligand and TBME as the solvent.[141]

With use of traditional heating methods, these borylation reactions were determined by LCMS analysis to have proceeded to complete conversion of starting material to product when performed at 80 °C over 24 h; shorter reaction times yielded reduced conversions. However, complete conversion could be achieved at 80 °C in 3 h with the addition of microwave irradiation.

Under these conditions a range of β-3-aryl-amino esters were converted into the corresponding boronate species (Figure 47); in this first iteration of substrates, compounds

310, **312**, **316**, **317** and **321** were prepared by the author, all other species were prepared by UoN MSci students.

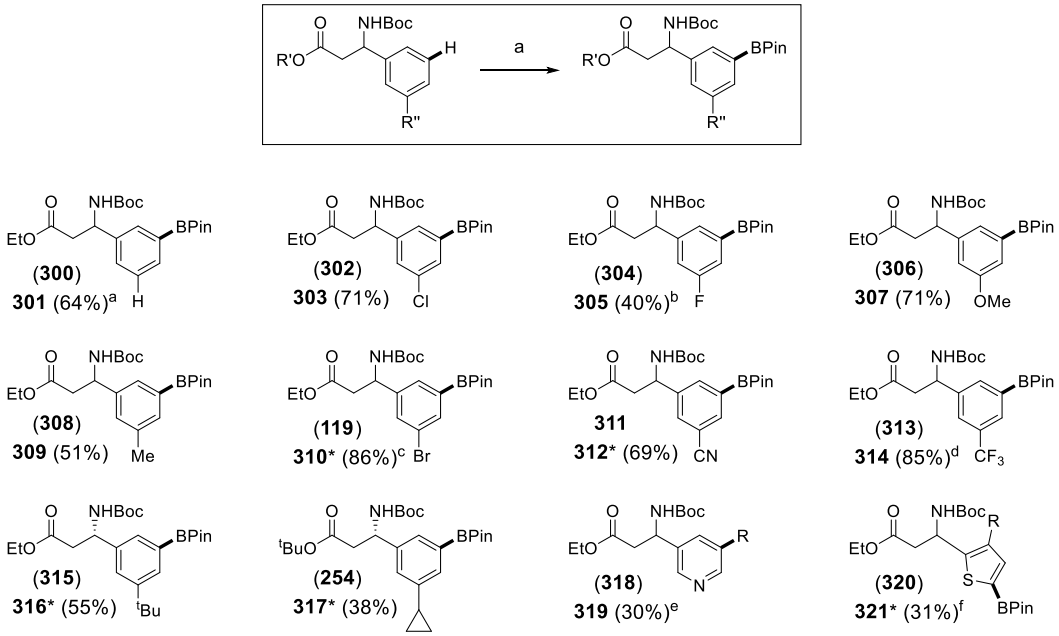

Figure 47. The substrate scope of this reported methodology relating to iridium catalysed C-H activated borylation of β-3-aryl-amino esters.[142] The compound numbers relating to starting substrates is given in parentheses. Compounds prepared by the author are identified with an asterisk (*); the preparation of the starting substrates **311**, **315** and **320** is described in the experimental section of this thesis. *Reagents and conditions*: a) B_2Pin_2, $[Ir(OMe)(cod)]_2$ (2.5 mol%), dtbpy (5 mol%), TBME, 80 °C, Ar, 3 h, μW. [a]1:1:3 mixture of regioisomers (3-monosubstituted:4-monosubstituted:3,5-disubstituted); [b]2:1 mixture of regioisomers (3,5-disubstituted:3,4-disubstituted); [c]2.00 g, 5.40 mmol scale; [d]2.00 g, 6.50 mmol scale; [e]borylated product (R = Bpin) unstable to column chromatography; yield over two steps following Suzuki-Miyaura coupling with *p*-nitroiodobenzene to yield product **319** (R = *p*-nitrophenyl). *Reagents and conditions:* 1-iodo-4-nitrobenzene, K_3PO_4, $Pd(dppf)Cl_2.CH_2Cl_2$ (10 mol%), DME/H_2O (10:1), 70 °C, N_2, 18 h; [f]reaction conducted at 80 °C exclusively generated the 3,5-disubstituted product (R = BPin, not isolated), reaction conducted at room temperature yielded the 5-monosubstituted product (R = H, isolated).

Borylation of this first set of substrates was largely successful, with the boronate product being isolated in every case with between 30-86% yield.

The regioselective outcome of these reactions are primarily controlled by the steric profiles of any aryl substituents present and thus, as predicted, in most cases the 3,5-disubstituted product was generated predominantly if not exclusively, in accordance with the reported directing regiochemistry of iridium-catalysed borylation reactions.[143]

The borylated products were generally found to be stable and could be purified by column chromatography; additionally, the 3-bromo and 3-trifluoromethyl derivatives (**310** and **314**, respectively) were successfully prepared on multigram scale with improved isolated yields, a particularly pleasing outcome for the purposes of any future large-scale array-type chemistry. It should be noted however, that due to the low polarity solvent gradients required to purify the boronate products, contamination with excess B_2Pin_2 was often a likelihood due to its tendency to smear throughout silica-based chromatography apparatus and so to avoid this outcome, extended column chromatography would often be necessary, resulting in minor to moderate loss of material.

Following this initial success, we further demonstrated the versatility of these boronate species and this methodology as a whole, by submitting the boronate products to reactions typically used in the synthesis of biologically active molecules (Figure 48). In each example, the 3-monosubstituted β-3-aryl-amino ester substrate was borylated under the previously described conditions and then functionalised further without purification of the boronate species beyond an aqueous workup; NMR of the crude boronate products revealed a relatively low level of impurities and as such they were deemed suitable for use without further purification, thus avoiding material wastage.

Compounds **323**, **324**, **326**, **331** and **332** were prepared by the author, all other species were prepared previously by UoN MSci students.

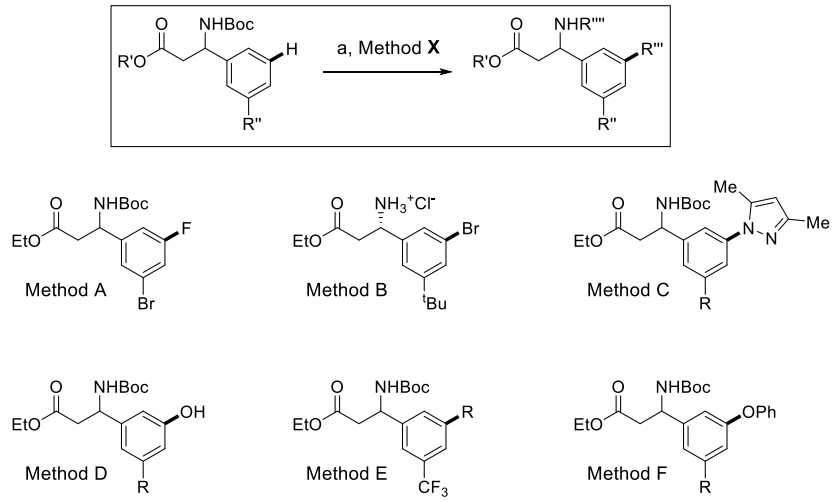

Figure 48. Telescoped functionalisation of β-3-aryl-amino ester substrates *via* the relevant boronate intermediate; quoted yields relate to the combined yield of the borylation and subsequent functionalisation steps. Compounds prepared by the author are identified with an asterisk (*). Starting 3-monosubstituted substrate compound numbers are given in parentheses before product compound numbers. *Reagents and conditions*: a) B_2Pin_2, $[Ir(OMe)(cod)]_2$ (2.5 mol%), dtbpy (5 mol%), TBME, 80 °C, Ar, 3 h, μW; Method A) i) AgOTf, NaOH, methanol, 0 °C, 30 min; ii) Selectfluor®, 3 Å MS, acetone, rt, 3 h, yield: (**119**) **322** - 59%; Method B) i) $CuBr_2$, methanol/water (2:1), 70 °C, 16 h; ii) 4M HCl in 1,4-dioxane, diethyl ether, rt, yield: (**315**) **323*** = 39%; Method C) 3,5-dimethylpyrazole, $B(OH)_3$, $Cu(OAc)_2$ (1.00 eq.), 4 Å molecular sieves, 80 °C, 16 h, yield: R = Br, (**119**) **324*** = 74%; R = CF_3, (**313**) **325** = 68%; Method D) Oxone®, acetone, rt, 45 min, yield: R = Br, (**119**) **326*** = 52%; R = Cl, (**302**) **327** = 77%; R = F, (**304**) **328** = 33%; R = CF_3, (**313**) **329** = 92%; Method E) 1-iodo-4-nitrobenzene, K_3PO_4, $Pd(dppf)\cdot CH_2Cl_2$, 1,2-DME/water, 70 °C, 4.5 h, yield: R = *p*-nitrophenyl, (**313**) **330** = 93%; Method F) phenol, $B(OH)_3$, $CuOAc_2$ (10 mol%), 4 Å molecular sieves, 70 °C, 16 h, yield: R = Br, (**119**) **331*** = 36%; R = CF_3, (**313**) **332*** = 34%.

Bromination of the intermediate boronate of **315** with $CuBr_2$ generated the 3-bromo-5-*tert*-butyl derivative **323**, a 3,5-disubstitution moiety that is featured in recently reported integrin inhibitors.[144,145] Thus, we converted this substrate through to the dipeptide **333** by amide

coupling with *N*-Boc-glycine, followed by *N*-Boc deprotection and amide coupling with 3-guanidinobenzoic acid (**334**), before final ester saponification provided the integrin inhibitor **335** (Scheme 46).

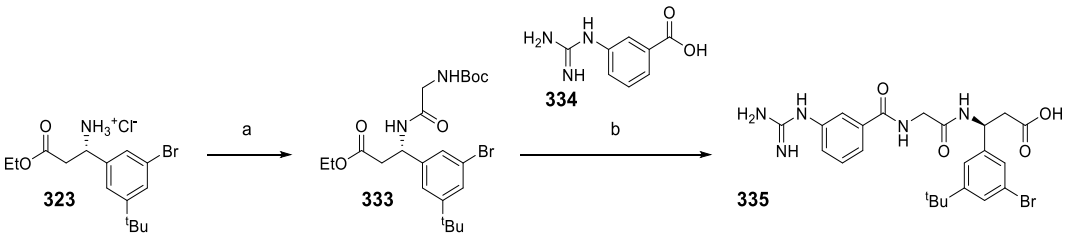

Scheme 46. Synthesis of the reported integrin inhibitor **335** *via* the dipeptide substrate **333**. The preparation of the requisite 3-guanidinobenzoic acid (**334**) is described in the experimental. *Reagents and conditions*: a) *N*-Boc-glycine, HATU, *i*-Pr_2NEt, acetonitrile, 0 °C to rt, 16 h, 50%; b) i) 4M HCl in 1,4-dioxane, 5 h; ii) **334**, diisopropylcarbodiimide, HOBt, CH_2Cl_2/DMF (1:1), rt, 64 h; iii) 1M $LiOH_{(aq)}$, THF, rt, 64 h, 52%.

Reported synthetic procedures for this and similar analogues often require a bespoke aldehyde synthesis for each individual target compound, whereas this telescoped C–H borylation/functionalisation strategy allows for a more straightforward and sustainable synthesis by functionalisation of a common and affordable intermediate, demonstrating the power of this methodology.

Additionally, and more relevantly for the purposes of generating the 3,5-disubstituted integrin inhibitors depicted in Figure 46**,** we demonstrated that this telescoped sequence provided the 3,5-dimethyl pyrazole disubstituted products **324** and **325** *via* Chan-Lam amination in good yield. Forgoing the purification of the intermediate boronate **310** gave the product **324** in a yield comparable to that obtained from the corresponding multi-step synthesis, demonstrating well the benefits of telescoping this process (Scheme 47).[142]

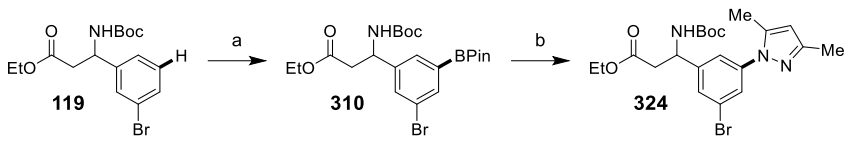

Scheme 47. Synthetic sequence demonstrating how 3-monosubstituted β-3-aryl-amino esters may be regioselectively borylated and subsequently functionalised *via* Chan-Lam amination, giving asymmetric 3,5-disubstituted analogues in good yield. Total yield of steps a and b when **310** **is** purified = 69%; total yield of steps a and b when **310** **is not** purified = 74%. *Reagents and conditions*: a) B_2Pin_2, $[Ir(OMe)(cod)]_2$ (2.5 mol%), dtbpy (5 mol%), TBME, 80 °C, 3 h, μW; b) 3,5-dimethyl pyrazole, $B(OH)_3$, $Cu(OAc)_2$ (1.00 eq.), acetonitrile, 3 Å MS, 70 °C, 40 h.

The increased polarity of the 3,5-disubstituted analogue **324** was sufficient to allow for a far more straightforward separation of the product from all impurities relating to the borylation and Chan-Lam reactions; this contrasts to the typically challenging purification of the boronate species in which co-elution with excess B_2Pin_2 is common, leading to reduced purities and material loss.

In order to determine whether this methodology would be suitable for use in this project where integrin inhibitor analogues exhibiting high enantiopurity are desired, we subjected the enantiopure substrate **(*S*)-119** to C–H borylation followed by oxidation. Gratifyingly, the phenol **(*S*)-326** was obtained, exhibiting a 97% e.e., indicating that no racemisation occurs in the borylation process (Scheme 48, HPLC traces are available in Section 5.4). A more detailed account of this work is reported by Robinson *et al*.[142]

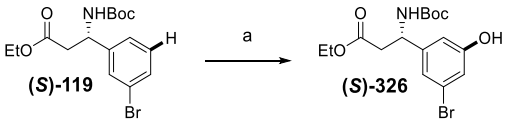

Scheme 48. Borylation and further functionalisation of the enantiopure substrate **(*S*)-119**, demonstrating that no racemisation occurs during the key borylation step. *Reagents and conditions*: a) i) B_2Pin_2, $[Ir(OMe)(cod)]_2$ (2.5 mol%), dtbpy (5 mol%), TBME, 80 °C, Ar, 3 h, μW; ii) Oxone®, acetone, rt, 45 min, e.e. 97%, 33%.

It was ultimately decided that the iridium catalysed borylation reaction would be performed at this earlier stage of the synthetic procedure, on the *N*-Boc β-3-aryl-amino ester substrate, and not on the late-stage tetrahydronaphthyridine containing substrate, due to the reduced chemoselectivity that would likely be experienced were the aromatic naphthyridine motif present. This would also avoid the separation of multiple regioisomers after the Chan-Lam amination at a stage where such separations are known to be particularly problematic.[130]

Consequently, a series of iridium catalysed borylations, followed by immediate Chan-Lam amination was designed for the pre functionalised *N*-Boc β-3-aryl amino esters **250** and **337**. The 2,2-difluoroethoxy ether containing inhibitors were derived from a pre-functionalised, commercially available 3,5-disubstituted benzaldehyde (**406**) and thus did not require iridium catalysed borylation at any stage of their preparation, simply Chan-Lam amination.

3.3 Application of developed methodology towards the synthesis of 3,5-disubstituted integrin inhibitors

Each of the pre-functionalised intermediates **250**, **(*S*)-313** and **341** were prepared using the established Reformatsky route for the generation of the requisite (*S*)-amino stereocentre.

The preparation of the intermediates **250**, **(*S*)-313** and **341** is described in Scheme 49.

Work performed by the author

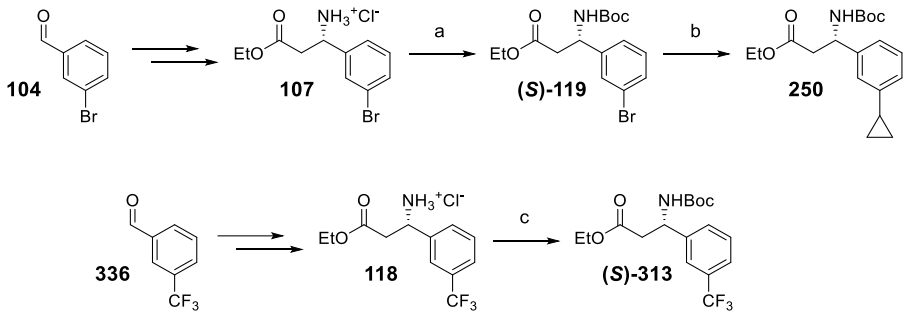

Work performed by Jay Tromans

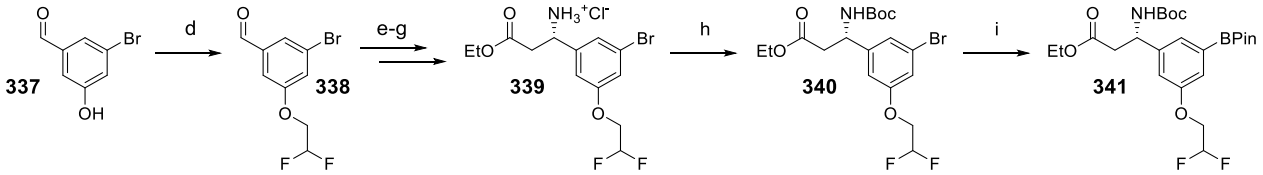

Scheme 49. The preparation of the three enantiopure, β-3-aryl-amino ester intermediates **250**, **(S)-313**, and **341**; the 2,2-difluoroethoxy ether **341** and all requisite intermediates **338**-**340** were prepared independently by a UoN MSci student (Jay Tromans).[6] *Reagents and conditions*: a) di-*tert*-butyl dicarbonate, Et_3N, THF, N_2, 0 °C to rt, 65 h, 94%; b) **252**, K_2CO_3, XPhos Pd G2 (3 mol%), CPME:water (10:1), N_2, 100 °C, 73%; c) di-*tert*-butyl dicarbonate, Et_3N, THF, N_2, 0 °C to rt, 16 h, quant.; d) 2,2-difluoroethyltrifluoromethane sulfonate, K_2CO_3, DMF, 70 °C, 2 h, 90%; e) (*R*)-*tert*-butyl-sulfinamide, Ti(O*i*-Pr)$_4$, THF, rt, 18 h; f) i) zinc powder, TMSCl, ethyl bromoacetate, THF, reflux, N_2, 1 h; ii) ***sulfinimine***, 0 °C to rt, 18 h; g) 4M HCl in 1,4-dioxane, diethyl ether, rt, 30 min, 53% over 3 steps; h) di-*tert*-butyl dicarbonate, Et_3N, THF, 16 h, 62%; i) B_2Pin_2, KOAc, Pd(dppf).CH_2Cl_2 (10 mol%), 1,4-dioxane, Ar, 80 °C, 88 h, 72%;

The requisite sulfinimines were prepared *via* condensation of the parent benzaldehydes with (*R*)-*tert*-butanesulfinamide, then submitted to Reformatsky conditions to give the relevant sulfinamide product; these were immediately deprotected using 2M HCl in diethyl ether and subsequently *N*-Boc protected, yielding **(S)-313**, **341** and **(*S*)-119**. The cyclopropyl motif was installed using the Suzuki-Miyaura methodology previously described in Section 2.4.2 yielding **250** and the pinacol borane in **341** installed *via* a Miyaura borylation reaction.

As previously stated, compounds **291**, **292** and **296**-**299** were prepared by UoN MSci students and as such, only the preparation of compounds **288**-**290** and **293**-**295** is described in the following section (Scheme 50); compounds **291**, **292** and **296**-**299** were however prepared using this same methodology.

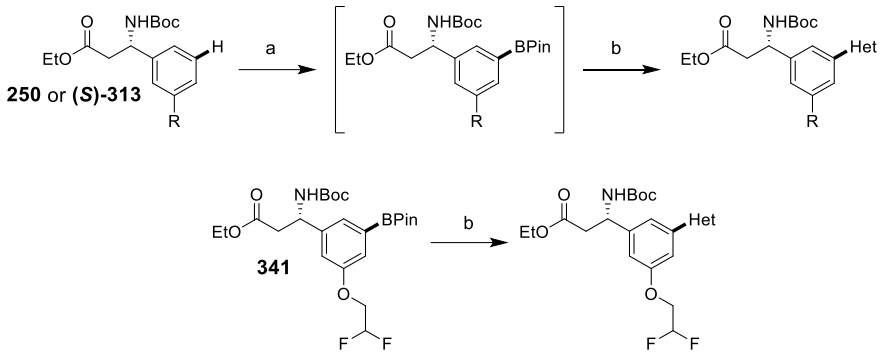

Scheme 50. The methodology used to prepare the requisite 3,5-disubstituted hybrid β-3-aryl-amino esters from the intermediates **250**, **(S)-313** and **341**, as depicted in Table 24; R is representative of either a cyclopropyl or a trifluoromethyl group. *Reagents and conditions*: a) B_2Pin_2, $[Ir(OMe)(cod)]_2$ (2.5 mol%), dtbpy (5 mol%), TBME, 80 °C, 3 h, μW; b) ***amine***, $B(OH)_3$, $Cu(OAc)_2$ (1.00 eq.), acetonitrile, 4 Å MS, 70 °C, 40 h.

The intermediates **(S)-313** and **250** were subjected to standard iridium borylation conditions as described in Section 3.2.1 and then submitted to Chan-Lam amination conditions with the relevant amines in a telescoped process to generate the compounds **414**-**417** depicted in Table 24 with yields ranging between 30-71%. As the 2,2-difluoroethoxy ether **409** already contained the requisite pinacol borane motif, compounds **418** and **419** were prepared simply *via* Chan-Lam amination in 95% and 61% yield, respectively.

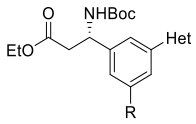

Compound no.	R	Het	Yield/%
342		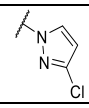	36
343		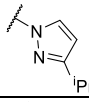	67
344		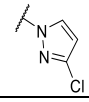	30
345		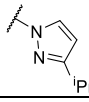	71
346	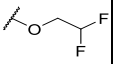	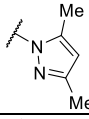	95
347	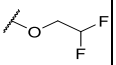	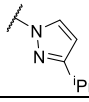	61

Table 24. The products and yields of reaction as they relate to the reactions depicted in Scheme 50; for compounds **342**-**345**, the yield is representative of the telescoped sequence combining the iridium catalysed borylation reaction with the Chan-Lam amination, whereas for **346** and **347**, the yields are representative solely of the Chan-Lam amination reaction.

To our surprise, no minor regioisomeric products were detected in any of the five Chan-Lam amination reactions detailed in Table 24 in which generation of regioisomers is possible; this is in direct contrast to the frequent generation of regioisomers observed in the Chan-Lam amination work described in Section 2.3 of this thesis. The reason for this is likely due to the increased steric hinderance experienced by the intermediate boronate species as a result of the additional *meta*-substituent. It is assumed that the regioisomeric outcome of the Chan-Lam amination is heavily influenced by the steric profile of the amine and its subsequent interaction with the aryl coupling partner, thus it would follow that a more hindered

boronate species would also affect the outcome somewhat; this hypothesis is visually depicted in Figure 49.[130]

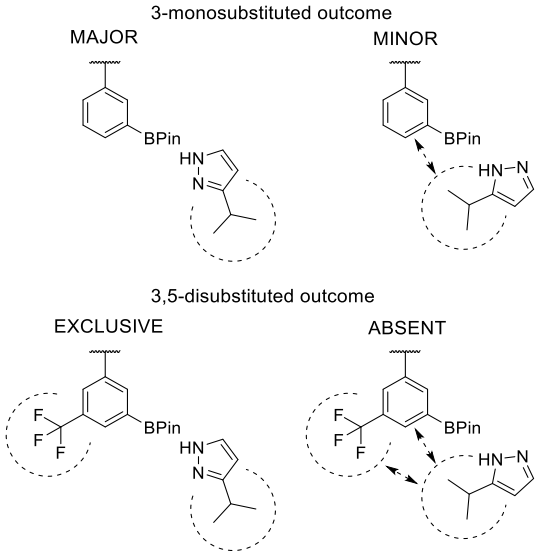

Figure 49. Visual depiction of the proposed effect imbued by steric interaction on the regioisomeric outcome of the Chan-Lam amination in both 3-monosubstituted and 3,5-disubstituted boronate species with 5-*iso*-propyl pyrazole through the N-H position. Dashed arrows indicate unfavourable steric interaction. Dotted curved lines indicate the arbitrary steric profile of a substituent to better describe the effect.

Compounds **342**-**347** were *N*-Boc deprotected with 2M HCl in diethyl ether and submitted to amide coupling conditions with the carboxylate **82** using HATU. The resulting intermediates were *N*-Boc deprotected using TFA and the esters saponified using 1M $LiOH_{(aq)}$, affording the integrin inhibitors **288**-**290** and **293**-**295** (Table 25).

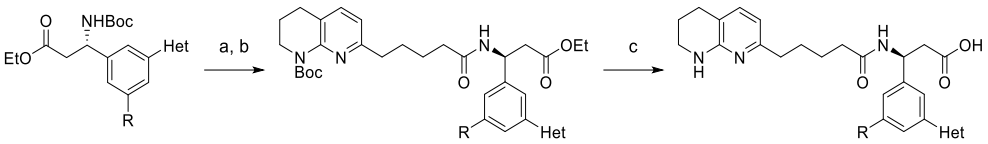

R	Het	a/b yield/%	c yield/%
	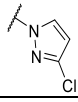	59 (**348**)	99 (**294**)
	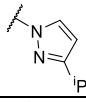	23 (**349**)	97 (**288**)
	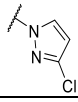	64 (**350**)	Quant. (**295**)
	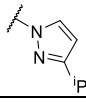	20 (**351**)	92 (**289**)
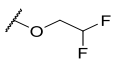	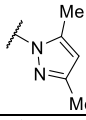	44 (**352**)	99 (**293**)
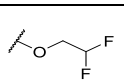	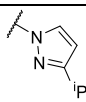	33 (**353**)	99 (**290**)

Table 25. Yields of each relevant reaction as related to the preparation of the integrin inhibitor analogues **288**-**290** and **293**-**295**; compound numbers for each relevant reaction product are given in parentheses. *Reagents and conditions*: a) 4M HCl in dioxane, rt, 40 min; b) **78**, HATU, *i*-Pr_2NEt, acetonitrile, 0 °C to rt, 16 h; c) i) TFA, CH_2Cl_2, rt, 7 h; ii) 1M $LiOH_{(aq)}$, THF, rt, 18 h.

Unfortunately, due to issues regarding the purification and subsequent separation of **354** and **(S)-313** (generated *via* protodeborylation of **(S)-314**), **354** was not successfully isolated and as such the inhibitor **297** is not included amongst the final tally of compounds presented in Table 26 (Scheme 51).

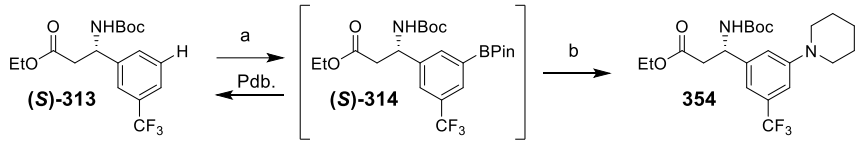

Scheme 51. Attempted preparation of the 3,5-disubstituted analogue **354** from the monosubstituted substrate **(S)-313**. Due to protodeborylation of the boronate species **(S)-314** during the Chan-Lam amination reaction and subsequent regeneration of **(S)-313**, **354** was not isolated in sufficient purity to allow for further reaction, due to the inseparable nature of **(S)-313** and **(S)-314** during column chromatography (Pdb. = protodeborylation). *Reagents and conditions*: a) B_2Pin_2, $[Ir(OMe)(cod)]_2$ (2.5 mol%), dtbpy (5 mol%), TBME, 80 °C, 3 h, μW; b) piperidine, $B(OH)_3$, $Cu(OAc)_2$ (1.00 eq.), acetonitrile, 4 Å MS, 70 °C, 40 h.

3.4 SAR relating to 3,5-disubstituted integrin inhibitors

3.4.1 Integrin assay data

The biochemical and physicochemical properties for compounds **288**-**296**, **298** and **299** are presented in Table 26. Each compound was subject to the same cell adhesion assays and other physical characteristic determinations as the 3-monosubstituted inhibitors presented in Chapter 2.

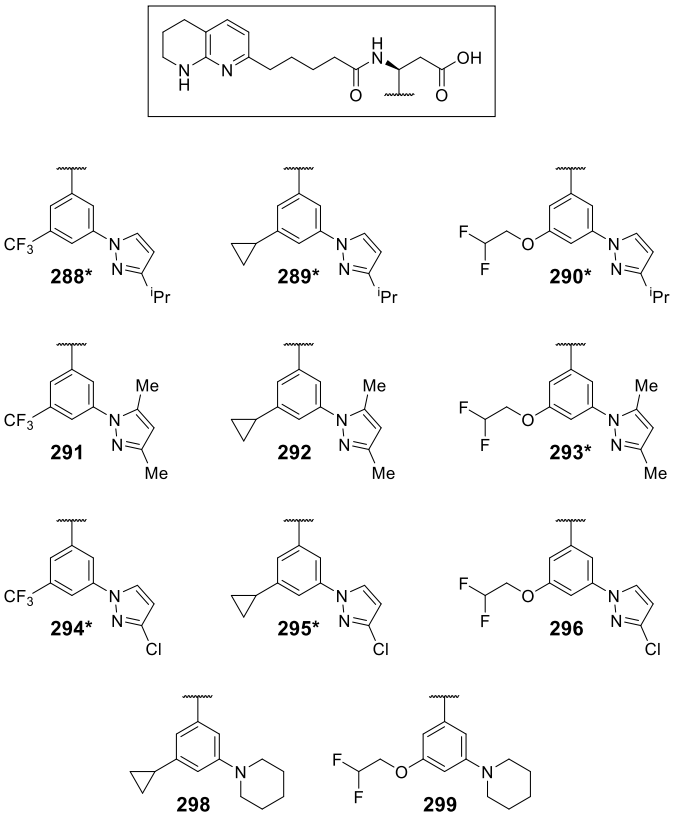

Compound no.	pIC$_{50}$ $\alpha_v\beta_6$	pIC$_{50}$ $\alpha_v\beta_3$	pIC$_{50}$ $\alpha_v\beta_5$	pIC$_{50}$ $\alpha_v\beta_8$	pIC$_{50}$ $\alpha_v\beta_1$	ChromLogD$_{7.4}$	HTP nm/s	MW
288	7.3	6.2	6.6	7.1	6.4	4.55	400	557
289	7.6	6.8	6.7	7.2	6.4	4.11	270	529
290	7.4	6.8	7.0	7.1	6.4	4.02	120	569
291	7.7	6.1	5.7	7.7	6.2	3.48	190	543
292	7.8	6.4	6.5	7.4	6.4	3.19	74	515
293	7.8	6.5	6.2	7.7	6.4	3.11	26	555
294	7.4	6.4	6.3	7.2	6.2	3.90	300	549
295	7.5	6.7	6.6	7.1	6.3	3.59	260	521
296	7.9	6.4	6.9	7.4	6.4	3.50	110	561
298	7.1	6.5	6.0	7.4	6.5	3.81	150	504
299	7.3	6.4	6.4	7.3	6.6	3.71	78	544

Table 26. Structures and relevant assay data for compounds **288**-**296**, **298** and **299**; the structures of compounds prepared by the author are marked with an asterisk (*).[3,6,10,12] Error in the cell adhesion assays = 0.3.

These compounds exhibit an average pIC$_{50}$ against $\alpha_v\beta_6$ of 7.5, similar to that exhibited by the *N*-linked aromatic heterocycle-substituted analogues described in Section 2.6.1, with an average selectivity for $\alpha_v\beta_6$ over $\alpha_v\beta_3$ and $\alpha_v\beta_5$ of 1.05 and 1.08, respectively (no correlation

in either case), compared to 0.42 and 0.72 for the *N*-linked aromatic heterocycle monosubstituted analogues. As expected, there is a correlation between these compounds in terms of potency between $\alpha_v\beta_3$ over $\alpha_v\beta_5$ (R^2 = 0.33), with no observable average selectivity for one over the another.

A graphical representation of the potency profiles for the 3,5-disubstituted compounds presented in Table 26 and their 3-monosubstituted parent compounds, is depicted in Figure 50.

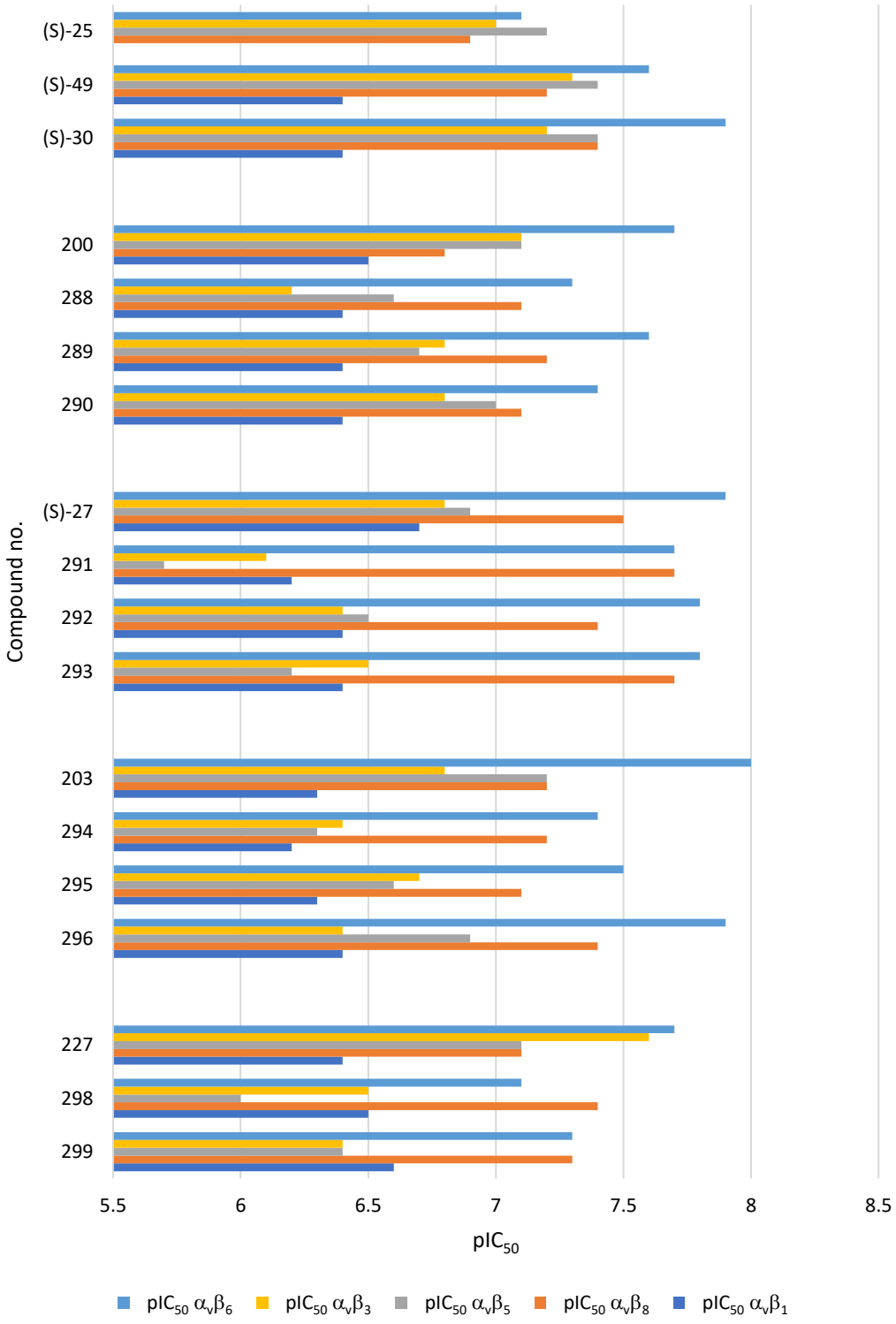

Figure 50. A plot of potency profiles for each of the 3,5-disubstituted integrin inhibitor analogues presented in Table 26 and their relevant parent 3-monosubstituted compounds.

Figure 50 demonstrates that in every case, 3,5-disubstitution results in a reduction of pIC_{50} against $\alpha_v\beta_3$ and $\alpha_v\beta_5$ compared to both parent *mono*-substituted analogues, ranging from within the error of the assay to greater than 10-fold; this correlates with our hypothesis discussed in Section 1.4 and 1.5.2.5 stating that 3,5-disubstitution typically facilitates at least a moderate improvement of selectivity for $\alpha_v\beta_6$ over $\alpha_v\beta_3$ and $\alpha_v\beta_5$.

The effect of 3,5-disubstitution on binding affinity within $\alpha_v\beta_6$ and $\alpha_v\beta_8$ is more complex. In every case, these 3,5-disubstituted analogues exhibit a reduction of pIC_{50} against $\alpha_v\beta_6$ compared to that exhibited by the relevant parent *N*-linked heterocycle monosubstituted parent analogue, ranging from within the error of the assay to 0.6 log units. This supports our hypothesis regarding 3,5-disubstituted analogues exhibiting a similar pIC_{50} against $\alpha_v\beta_6$ to that of the most efficacious parent monosubstituted compound, first discussed in Section 1.5.2.5. Likewise, the pIC_{50} against $\alpha_v\beta_8$ value corresponding to each of these 3,5-disubstituted analogues is within 0.4 log units and thus the error of the assay, of that exhibited by the parent *N*-linked heterocycle monosubstituted parent analogue and so it appears that 3,5-disubstitution does not affect binding affinity within the $\alpha_v\beta_6$ and $\alpha_v\beta_8$ integrins to a great degree.

Regarding the apparent lack of selectivity for $\alpha_v\beta_6$ over $\alpha_v\beta_8$ demonstrated by these compounds considering the greater than 10-fold selectivity exhibited by a number of the *N*-linked aromatic heterocycle monosubstituted analogues described in Chapter 2, it is important to note that the 3,5-dimethylpyrazole and 5-chloropyrazole monosubstituted compounds **(S)-27** and **203** do not exhibit more than a minor level of selectivity for $\alpha_v\beta_6$ over $\alpha_v\beta_8$. Thus, it is difficult to determine whether the lack of selectivity exhibited by their corresponding 3,5-disubstituted analogues is due to the already poor level of selectivity exhibited by **(S)-27** and **203** or whether it is in fact a result of 3,5-disubstitution. However, with the absence of any significant change of pIC_{50} against $\alpha_v\beta_8$ observed upon 3,5-

disubstitution, perhaps by utilising alternative *N*-linked aromatic heterocycles, we would be able to achieve improved selectivity for $\alpha_v\beta_6$ over $\alpha_v\beta_8$.

3.4.2 Additional pharmacokinetic data

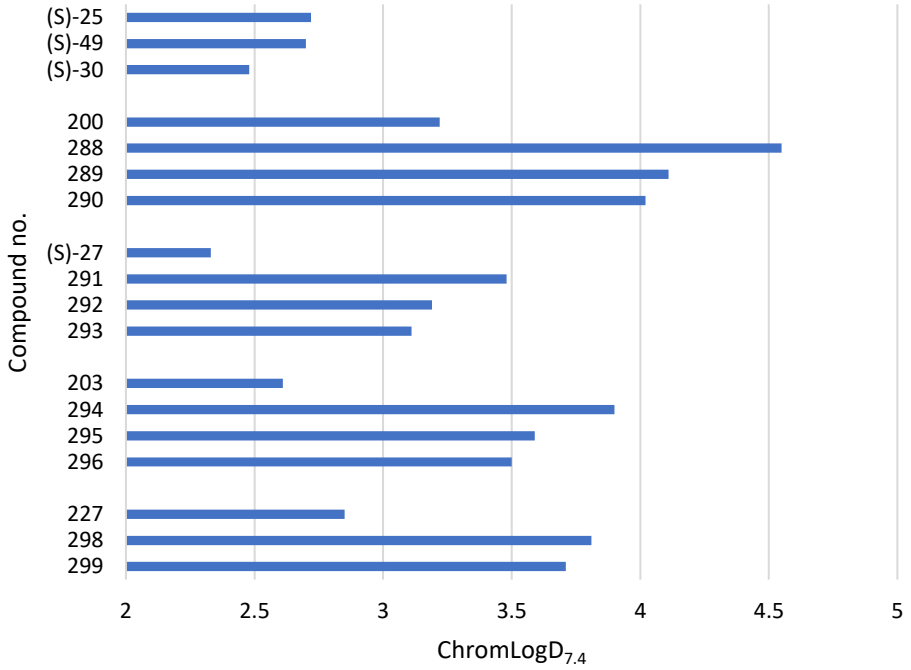

Figure 51. A plot of ChromLog$D_{7.4}$ for each of the 3,5-disubstituted integrin inhibitor analogues presented in Table 26 and their relevant parent 3-monosubstituted compounds (**(*S*)-25**, **(*S*)-49**, **(*S*)-30**, **(*S*)-27**, **200**, **203** and **227**).

As depicted in Figure 51, the lipophilicity of these compounds is significantly greater than that of their parent monosubstituted analogues; the 3,5-disusbtituted analogues appear to be more heavily influenced by the lipophilicity of the heterocyclic-parent compound, with the secondary substituent serving to provide a consistent increase of lipophilicity that does not seem to be proportional to the lipophilicity of its corresponding monosubstituted analogue.

As a result of this general increase of lipophilicity, the permeability characteristics of these analogues have been improved accordingly; only the 2,2-difluoroethoxy ether substituted analogue **293** exhibits less than moderate permeability, compared to 6 of the 7 *bis*-heterocycle substituted analogues described in Section 1.5.2.5 that exhibit poor permeability, with 5 analogues exhibiting the minimum possible permeability that can be measured by the assay.

The trifluoromethyl group appears to be one of the more efficacious substituents from the array of compounds described in Table 26 due to the consistent reduction of pIC_{50} against the $\alpha_v\beta_3$ and $\alpha_v\beta_5$ integrins observed in those 3,5-disubstituted inhibitors in which it is present compared to the parent heterocycle-substituted analogue; it must also be noted that inclusion of the trifluoromethyl moiety does appear to affect a very minor, if within the error of the assay, decrease of pIC_{50} against $\alpha_v\beta_6$. The compounds exhibiting the highest permeability and ChromLogD values from within each series (with the exception of the piperidine series) contain this trifluoromethyl motif and so it is possible that any reduction of pIC_{50} against $\alpha_v\beta_3$ or $\alpha_v\beta_5$ is driven by an unfavourable lipophilic interaction within the integrin binding pocket that is otherwise not experienced within $\alpha_v\beta_6$ or $\alpha_v\beta_8$.

Of the heterocycles included in this array, the 3,5-dimethyl pyrazole appears to be the most efficacious; Figure 50 demonstrates that its corresponding 3,5-disubstituted analogues generally exhibit the greatest levels of selectivity for $\alpha_v\beta_6$ over $\alpha_v\beta_3$ and $\alpha_v\beta_5$, whilst expressing amongst the highest potency values against $\alpha_v\beta_6$ of the 11 compounds depicted in Table 26 and within the UoN series as a whole. These analogues additionally express the lowest ChromLogD values of the 3,5-disubstituted analogues evaluated in this section; this gives us increased confidence that the high levels of selectivity and potency obtainable upon 3,5-disusbtitution are unlikely to be driven *via* lipophilic interactions as suggested above and

are indeed a result of unfavourable steric and electronic interactions within the target integrin binding sites.

The absence of any correlation between ChromLogD and selectivity for $\alpha_v\beta_6$ over $\alpha_v\beta_3$ as demonstrated by these 3,5-disusbtituted analogues and their parent monosubstituted compounds strengthens this conclusion further (Figure 52).

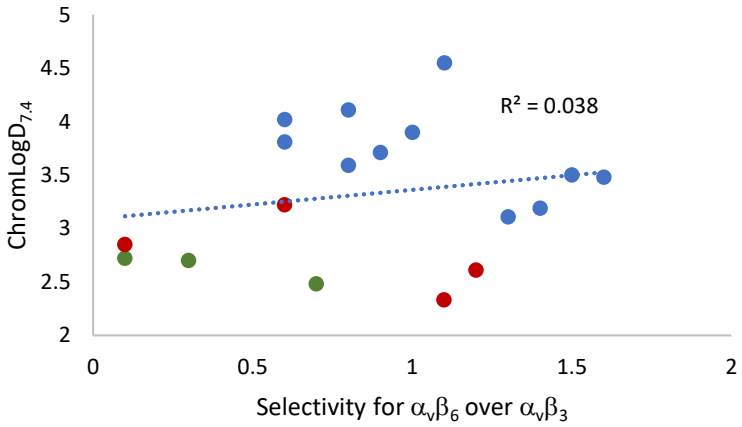

Figure 52. A plot of ChromLogD$_{7.4}$ against the selectivity for $\alpha_v\beta_6$ over $\alpha_v\beta_3$ corresponding to each of the 3,5-disubstituted integrin inhibitor analogues and their relevant parent 3-monosubstituted compounds (het. Parents in red, alkyl parents in green) presented in Table 26. 3,5-Disubstituted analogues are marked in blue, 3-heterocycle monosubstituted parent analogues in red and 3-alkyl monosubstituted analogues in green.

As discussed previously, there is an optimal range of ChromLogD for pharmacologically active compounds at pH 7.4 of approximately 1-3. A ChromLogD characteristic between these values is particularly important for potential orally active drug candidates where larger values may cause issues regarding solubility and high metabolic clearance.[87,88] Often in drug development, it is found that increasing lipophilicity directly correlates with a simultaneous increase or decrease of other physiochemical characteristics (e.g., lipophilicity driven toxicity, lipophilicity driven potency etc.); thus, utilising this correlation to improve a specific trait can

result in the most potent analogues exhibiting lipophilicity values significantly larger than is appropriate for drug-likeness. As a result, it is important to calculate the net effect of structural change to potency in the context of changing lipophilicity; lipophilic efficiency (LiPE) is a parameter that can ultimately be used to assess this effect, the calculation of which is shown in Equation 4:[146]

$$LiPE = pIC_{50} - LogD$$

Equation 4. Calculation of LiPE;[146] in the UoN project LogD is measured chromatographically and so ChromLogD is quoted.

As has been well established, within the UoN series, 3,5-disubstitution of the phenyl component is typically used as a tool to improve selectivity for the $\alpha_v\beta_6$ integrin against the $\alpha_v\beta_3$ integrin by inducing a reduction of pIC_{50} against $\alpha_v\beta_3$, typically without a simultaneous increase or decrease of pIC_{50} against $\alpha_v\beta_6$. As such, using the formula presented in Equation 4 would undoubtedly reveal that compounds **288-296, 298** and **299**, exhibit greatly reduced LiPE values compared to their parent monosubstituted compounds in terms of pIC_{50} against $\alpha_v\beta_6$; this would additionally prove to be the case regarding the LE and BEI of these 3,5-disusbtituted analogues. Therefore, a formula was devised to allow normalisation of selectivity for the $\alpha_v\beta_6$ integrin against the $\alpha_v\beta_3$ integrin relative to lipophilicity, allowing for a more accurate assessment of the overall effect of 3,5-disubstitution (Equation 5); we have named this parameter the lipophilicity to selectivity parameter (LSP).

$$LSP = LiPE + (pIC_{50}\ \alpha_v\beta_6 - pIC_{50}\ \alpha_v\beta_3)$$

Equation 5. Calculation of the LSP, used to compare the relative effect of changing lipophilicity to selectivity for the $\alpha_v\beta_6$ integrin against the $\alpha_v\beta_3$ integrin, where LiPE is calculated as shown in Equation 4, using the pIC_{50} against $\alpha_v\beta_6$ for each compound.

Thus, we can compare the relative effect of 3,5-disubstitution by comparing the LSP values of the compounds displayed in Table 26 with their parent monosubstituted compounds (Table 27).

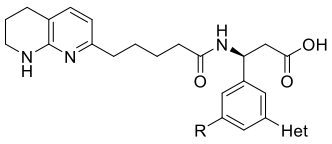

Compound no.	R	Het	pIC$_{50}$ $\alpha_v\beta_6$	ChromLogD$_{7.4}$	LiPE$_{7.4}$	pIC$_{50}$ $\alpha_v\beta_3$	LSP$_{7.4}$	BEI
(*S*)-25		H	7.1	2.72	4.38	7.0	4.48	15.8
(*S*)-49		H	7.6	2.70	4.90	7.3	5.20	18.1
(*S*)-30	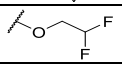	H	7.9	2.48	5.42	7.2	6.12	17.1
200	H	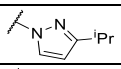	7.7	3.22	4.48	7.1	5.08	15.7
(*S*)-27	H	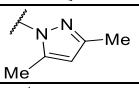	7.9	2.33	5.57	6.8	6.67	16.6
203	H	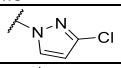	8.0	2.61	5.39	6.8	6.59	16.6
227	H		7.7	2.85	4.85	7.6	4.95	16.6
288		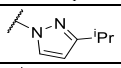	7.3	4.55	2.75	6.2	3.85	13.1
289		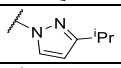	7.6	4.11	3.49	6.8	4.29	14.4
290	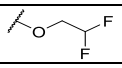	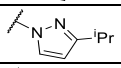	7.4	4.02	3.38	6.8	3.98	13.0
291		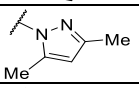	7.7	3.48	4.22	6.1	5.82	14.2
292		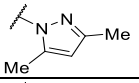	7.8	3.19	4.61	6.4	6.01	15.1
293	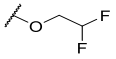	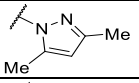	7.8	3.11	4.69	6.5	5.99	14.1
294		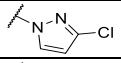	7.4	3.90	3.50	6.4	4.50	13.5
295		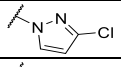	7.5	3.59	3.91	6.7	4.71	14.4
296	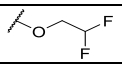	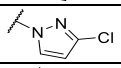	7.9	3.5	4.40	6.4	5.90	14.1
298			7.1	3.81	3.29	6.5	3.89	14.1
299	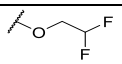		7.3	3.71	3.59	6.4	4.49	13.4

Table 27. The relative effect of 3,5-disubstitution in terms of lipophilicity vs selectivity for the UoN series of integrin inhibitors, quantified as LSP values; LiPE is calculated using pIC$_{50}$ against $\alpha_v\beta_6$. BEI ligand efficiency values are provided for comparison. Error in the cell adhesion assays = 0.3.

It must be noted that with a limited sample size and without further application of this metric to other drug development projects, we cannot define specific data values from Table 27 as

poor/moderate/good etc., and so these values can only be used to compare individual compounds with one another.

In every case, the 3,5 disubstituted analogues exhibit a LSP value less than that of their heterocyclic monosubstituted parent compound and, with the exception of the 3,5-dimethylpyrazole disubstituted compounds **291** and **292** and the 5-chloropyrazole disubstituted compound **294**, a LSP value less than that of their alkyl/ether-monosubstituted parent compound. This indicates an imbalance between increasing lipophilicity and improved selectivity for $\alpha_v\beta_6$ against $\alpha_v\beta_3$ upon 3,5-disusbtitution, as LiPE is reduced by a greater extent than selectivity is increased, ultimately demonstrating that 3,5-disubstitution is inferior to 3-monosubstitution in terms of LSP.

Thus, in the context of the UoN series, 3,5-disubstitution is only appropriate as a tool for improving selectivity for $\alpha_v\beta_6$ against $\alpha_v\beta_3$ where reasonable levels of ChromLogD are also exhibited by the resulting 3,5-disubstituted inhibitor.

Comparing LSP with BEI supports the observation that improved selectivity does not correlate with a simultaneously improved ligand efficiency; compounds **(*S*)-49** and **293** demonstrate this well, exhibiting a difference of 4 between their respective BEI values, favouring the non-selective inhibitor **(*S*)-49**, despite relatively comparable LSP values in favour of the selective inhibitor **293**.

3.4.3 Discussion of the most drug-like 3,5-disubstituted integrin inhibitor, analogue 291

Upon consideration of the data presented in Table 26 and Table 27, the 3,5-dimethylpyrazole containing analogues **291**-**293** emerge as the most drug-like compounds and thus, the strongest candidates for further development, of certainly the 3,5-disubstituted analogues presented in Table 26, but perhaps even within the UoN SAR as a whole; the 3-

trifluoromethyl-5-(3,5-dimethyl pyrazole) disubstituted analogue **291** is the best of these three analogues. The strength of the candidacy of **291** is due to excellent potency against $\alpha_v\beta_6$, almost 100-fold selectivity over both $\alpha_v\beta_3$ and $\alpha_v\beta_5$, 30-fold selectivity over $\alpha_v\beta_1$, combined with a lipophilicity value that is not particularly excessive compared to other 3,5-disusbtituted analogues and excellent permeability. The level of selectivity exhibited by **291** for $\alpha_v\beta_6$ over $\alpha_v\beta_5$ is particularly interesting considering how much greater this is in comparison to other analogues that exhibit similar levels of selectivity over the $\alpha_v\beta_3$ integrin (e.g., **293** and **296**). Comparison of key biological and physical data for **291** and its parent 3-monosubstituted compounds **(*S*)-25** and **(*S*)-27** is presented in Table 28; comparison of **291** with **(*S*)-25** is particularly interesting given the origins of **(*S*)-25** as the previous lead compound for the UoN series.

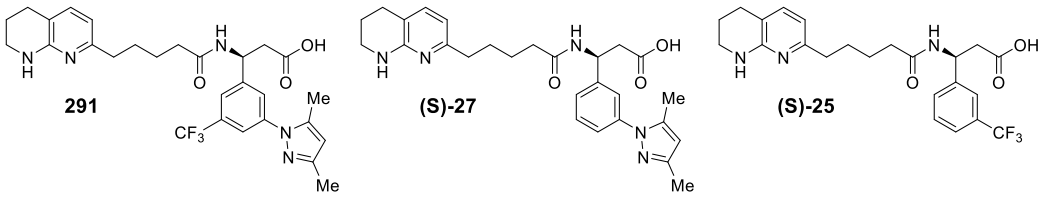

Compound no.	pIC_{50} $\alpha_v\beta_6$	pIC_{50} $\alpha_v\beta_3$	pIC_{50} $\alpha_v\beta_5$	pIC_{50} $\alpha_v\beta_8$	pIC_{50} $\alpha_v\beta_1$	$ChromLogD_{7.4}$	HTP nm/s	MW	$LSP_{7.4}$	BEI
291	7.7	6.1	5.7	7.7	6.2	3.48	190	543	5.82	14.2
(*S*)-27	7.9	6.8	6.9	7.5	6.7	2.33	19.5	475	6.67	16.6
(*S*)-25	7.1	7.0	7.2	6.9	-	2.72	100	449	4.48	15.8

Table 28. Comparison of cell adhesion assay data and other pharmacokinetic properties regarding the 3,5-disubstituted integrin inhibitor **291**, with its parent 3-monosubstituted compounds **(*S*)-25** and **(*S*)-27**. Error in the cell adhesion assays = 0.3.

The permeability of **291** is improved considerably compared to that of its monosubstituted parent compounds **(*S*)-25** and **(*S*)-27**; this demonstrates a major advantage of 3,5-disubstitution, in that analogues exhibiting selectivity for $\alpha_v\beta_6$ over $\alpha_v\beta_3$ but poor permeability can be made significantly more permeable, whilst potentially simultaneously improving selectivity, upon addition of a specific secondary *meta*-substituent.

The inhibitor **291** was subsequently docked into the $\alpha_v\beta_6$ and $\alpha_v\beta_3$ crystal structures (4UM9 and 1L5G, respectively) to generate binding poses to further rationalise the improved selectivity for $\alpha_v\beta_6$ over $\alpha_v\beta_3$ that is observed upon 3,5-disubstitution, compared to that of the 3-monosubstituted series (Figure 53).

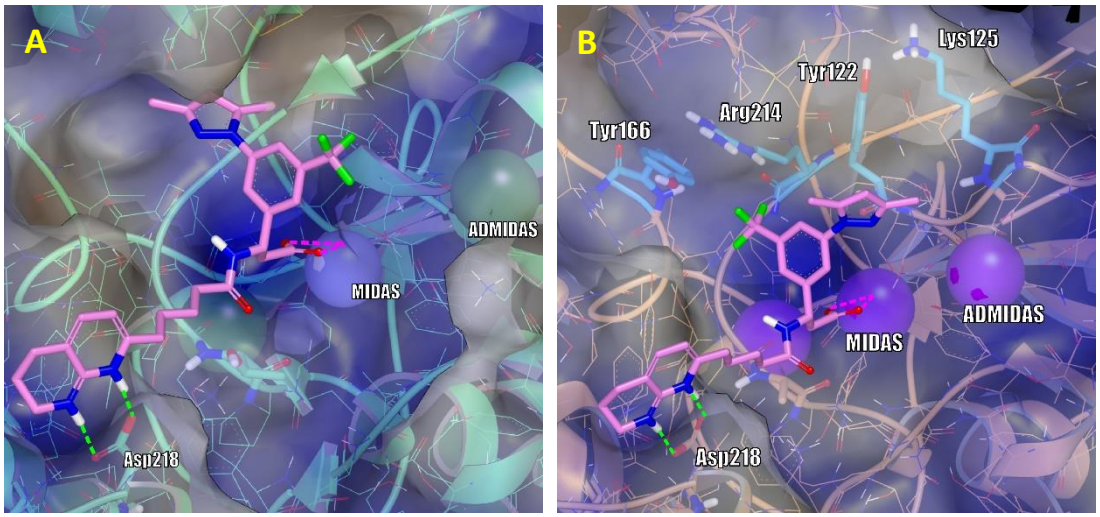

Figure 53. Modelled images of the 3-(3,5-dimethylpyrazole)-5-trifluoromethyl disubstituted integrin inhibitor **291** docked within the $\alpha_v\beta_6$ integrin (A) and the $\alpha_v\beta_3$ integrin (B); key residue interactions vital for the correct orientation of the molecule within the integrins are highlighted with green and pink dotted lines. The MIDAS, ADMIDAS and any other key residues within the binding sites are also highlighted. The proposed structure of the THN functionality as depicted is justified by Guest *et al*.[147] These molecular dockings and the subsequent generation of images were performed by Steven Oatley.

Figure 53A shows that the SDL in the $\alpha_v\beta_6$ binding site is relatively open and able to accommodate both the 3,5-dimethylpyrazole and the trifluoromethyl substituents; this agrees with our hypothesis first discussed in Section 1.4 (Figure 17). In contrast, in much the same way as depicted in Figure 41B, Figure 53B shows that the residues in the $\alpha_v\beta_3$ integrin SDL close off this pocket, preventing **291** from binding in the same conformation as seen with the $\alpha_v\beta_6$ integrin. As with **203** these residues limit the size of the pocket, forcing the

substituents into a more solvent exposed position, reducing the overall binding affinity. Additionally, in this more solvent exposed position, the ADMIDAS manganese ion in the crystal structure of $\alpha_v\beta_3$ may clash with the 3-methyl of the pyrazole motif, further reducing binding affinity. Whereas **203** and other similar 3-monosubstituted analogues are able to adjust their binding conformation to minimise the steric hinderance resulting from interaction between the $\alpha_v\beta_3$ binding surface and the 3-substituent, **291** and other similar 3,5-disubstituted analogues are far less effective at achieving this outcome, as by moving one substituent to a more favourable position, the secondary substituent is simply rotated back into the unfavourable position; thus to minimise interaction with the surface of the $\alpha_v\beta_3$ integrin binding site, the linker chain of the inhibitor must move from its preferred binding conformation in order to accommodate the aryl component of the molecule, which ultimately further reduces binding affinity beyond that of the 3-monosubstituted series.

Interestingly, despite the 3-trifluoromethyl-monosubstituted inhibitor **(*S*)-25** exhibiting the lowest LSP of all the monosubstituted parent compounds presented in Table 27, **291** exhibits one of the larger LSP values of the 3,5-disubstituted compounds, indicating perhaps that the moderately polar 3,5-dimethylpyrazole substituent offsets the effect of substituent combination that commonly results in significantly inflated ChromLogD values upon generation of 3,5-disusbtituted integrin inhibitors. This is supported further by the similar LSP values exhibited by the 3,5-dimethylpyrazole containing analogues **291**-**293**, despite the parent alkyl/ether monosubstituted compounds **(*S*)-25**, **(*S*)-49** and **(*S*)-30** exhibiting three significantly different LSP characteristics. This strengthens the role of the *N*-linked 3,5-dimethyl pyrazole as one of the better heterocyclic substituents in the UoN series.

Comparison of **291** with its parent heterocyclic-monosubstituted analogue **(*S*)-27** reveals that for an increase of 68 Da, selectivity for $\alpha_v\beta_6$ over $\alpha_v\beta_3$ and $\alpha_v\beta_5$ is improved five-fold and thirty-fold respectively (Table 28), however, pIC_{50} against $\alpha_v\beta_6$ is not increased. This

demonstrates well the disadvantage of 3,5-disubstitution within the UoN series in that such a structural modification results in the preparation of less ligand efficient analogues.

Discussion of both LSP and BEI indicates that whilst there are certainly considerations to be made regarding the overall effect of 3,5-disubstitution in terms of changing lipophilicity, molecular weight, efficiency metrics etc., 3,5-disubstitution of potent 3-monosubstituted inhibitors is often a favourable modification and can lead to the generation of particularly lead-like $\alpha_v\beta_6$ integrin inhibitors.

The level of average selectivity for $\alpha_v\beta_6$ over $\alpha_v\beta_3$ and $\alpha_v\beta_5$ exhibited by these analogues is not dissimilar to that exhibited by the *bis*-*C*-linked heterocycle-substituted analogues described in Section 1.5.2.5 and so, with an average pIC_{50} against $\alpha_v\beta_6$ of 7.5 and with the majority of the compounds depicted in Table 26 demonstrating good to excellent permeability, we have achieved our original objective of preparing potent, selective and importantly, more drug-like integrin inhibitors than those prepared previously within the UoN series.

3.5 Conclusions and discussion regarding all SAR developed in relation to the UoN series of integrin inhibitors

Table 29 shows the effect that each of the following substituents has on the core unsubstituted compound **15** relative to pIC_{50} against $\alpha_v\beta_6$ and pIC_{50} against $\alpha_v\beta_3$.

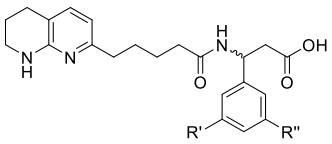

C. no.	R’	R’’	Chirality	pIC$_{50}$ $\alpha_v\beta_6$	pIC$_{50}$ $\alpha_v\beta_3$	pIC$_{50}$ $\alpha_v\beta_5$	pIC$_{50}$ $\alpha_v\beta_8$	pIC$_{50}$ $\alpha_v\beta_1$	ChromLogD$_{7.4}$	HTP nm/s
15	H	H	*(rac)*	5.7	7.0	7.1	6.1	-	1.56	32
25		H	*(rac)*	7.0	6.7	7.4	6.8	-	2.73	180
(*S*)-25		H	(*S*)	7.1	7.0	7.2	6.9	-	2.72	100
30	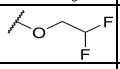	H	*(rac)*	7.5	7.1	7.0	6.7	6.2	2.60	49
27	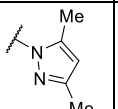	H	*(rac)*	7.3	5.9	6.4	7.2	6.3	2.27	29
203	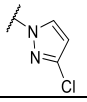	H	(*S*)	8.0	6.8	7.2	7.2	6.3	2.61	86
(*S*)-27	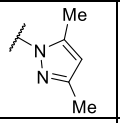	H	(*S*)	7.9	6.8	6.9	7.5	6.7	2.33	19.5
291	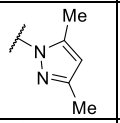		(*S*)	7.7	6.1	5.7	7.7	6.2	3.48	190
(*S*)-30	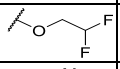	H	(*S*)	7.9	7.2	7.4	7.4	6.4	2.48	37
293	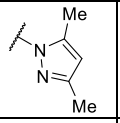	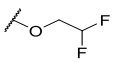	(*S*)	7.8	6.5	6.2	7.7	6.4	3.11	26
58	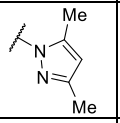	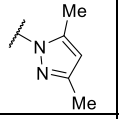	*(rac)*	7.4	5.2	5.5	7.0	5.4	3.07	26
46	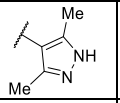	H	*(rac)*	6.8	7.0	7.0	7.2	6.5	1.74	<3
54	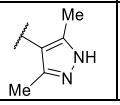	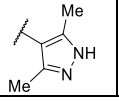	*(rac)*	6.8	5.2	5.0	-	6.4	1.42	<3

Table 29. Key integrin assay data and other pharmacokinetic characteristics of a selection of integrin inhibitors from the UoN SAR; C. no. = Compound number.[1,2,5,6,9,11,12,14,15] Error in the cell adhesion assays = 0.3.

As previously established, the core unsubstituted β-3-aryl-amino acid derived compound **15** is a moderately potent $\alpha_v\beta_3/\alpha_v\beta_5$ integrin inhibitor, exhibiting modest selectivity against the $\alpha_v\beta_6$ integrin. Whilst 3-monosubstitution has the potential to significantly increase the

exhibited pIC_{50} against $\alpha_v\beta_6$, this improvement is not conditional upon a simultaneous reduction of pIC_{50} against $\alpha_v\beta_3$, indicating no potency related mutual exclusivity between the two integrins (e.g., **30** *vs* **15**); in fact, it appears that pIC_{50} against $\alpha_v\beta_3$ is only decreased upon the introduction of a specific structural shape (e.g., **27** *vs* **30** *vs* **15**).

Whilst 3,5-disubstitution does not typically affect binding conformation within the $\alpha_v\beta_6$ and $\alpha_v\beta_8$ integrins to any significant degree, it has the potential to cause enormous disruption to binding conformation within $\alpha_v\beta_3$ and $\alpha_v\beta_5$, dramatically reducing their respective pIC_{50} values and ultimately augmenting the efficacy of substituents whose 3-monosubstituted analogues already exhibit moderate selectivity (**(*S*)-25** and **(*S*)-27** *vs* **291**). This strengthens further the argument presented in Section 1.4 suggesting there is a far more confined chemical space surrounding the phenyl motif of these integrin inhibitors within the SDL of the $\alpha_v\beta_3$ integrin binding pocket than within the $\alpha_v\beta_6$ integrin binding site. The modelling studies of the 3,5-disubstituted integrin inhibitor **291** docked in both the $\alpha_v\beta_6$ and $\alpha_v\beta_3$ integrins support this hypothesis further (Figure 53).

Upon inclusion of the 3,5-disubstituted integrin inhibitor analogues described in this Chapter, full analysis of the UoN SAR suggests that optimisation of the aryl component of these integrin inhibitors imbues a minimum and maximum threshold of pIC_{50} against $\alpha_v\beta_3$ and $\alpha_v\beta_6$ of ~6 and ~8, respectively, specifically in the context of (*S*)-enantiomers. The likely explanation for this phenomenon is that there is a limit to the steric disruption that can be caused in the region of the $\alpha_v\beta_3$ integrin binding site surrounding the phenyl component of these integrin inhibitors without also causing disruption to binding affinity within $\alpha_v\beta_6$, and conversely there is an upper limit to the improvement of binding affinity within the same region of the $\alpha_v\beta_6$ integrin that can be experienced upon optimisation of this component. This conclusion is supported by the observation that 3-monosubstituted inhibitors already exhibiting moderate levels of selectivity (e.g., **27**) do not experience a reduction of pIC_{50}

against $\alpha_v\beta_3$ of the same magnitude upon disubstitution as monosubstituted analogues exhibiting pan inhibition (**27** and **58** *vs* **46** and **54**). Similarly, 3-monosubstituted inhibitors exhibiting already high levels of pIC_{50} against $\alpha_v\beta_6$ are not augmented further by addition of another similarly efficacious substituent (e.g. **(*S*)-27** and **(*S*)-30** *vs* **293**).

As such, it would seem reasonable to recommend that further optimisation of these compounds as potent and selective $\alpha_v\beta_6$ integrin inhibitors must be focussed upon other areas of the core integrin inhibitor structure, be it through modification of the amide, the pentyl linker or even the naphthyridine. In terms of future work regarding additional optimisation of the phenyl component, it is likely that any potential improvement of potency or selectivity will come at the cost of a significant time investment and thus ultimately may not be worth the endeavour. Instead, the SAR presented in this thesis should be viewed as a suitable resource for the purposes of any who would wish to develop potent and selective β-3-aryl-amino acid derived $\alpha_v\beta_6$ integrin inhibitors.

3.6 Future work regarding the further development of potent and selective integrin inhibitors

As has been well established, high levels of selectivity for $\alpha_v\beta_6$ over each of the other α_v integrins is the ideal outcome of this project, however, as there is often moderate correlation between $\alpha_v\beta_6$ and $\alpha_v\beta_8$, this is challenging.

During evaluation of the UoN series SAR in Section 1.5, the analogues **47**, **56** and **63** were introduced (Table 30).

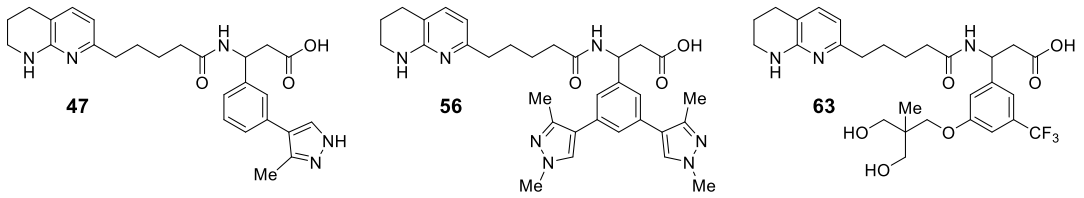

Compound no.	pIC$_{50}$ $\alpha_v\beta_6$	pIC$_{50}$ $\alpha_v\beta_3$	pIC$_{50}$ $\alpha_v\beta_5$	pIC$_{50}$ $\alpha_v\beta_8$	pIC$_{50}$ $\alpha_v\beta_1$
47	6.7	6.7	6.9	5.0	6.2
56	6.9	5.7	5.6	5.0	6.0
63	7.5	6.4	6.8	5.0	6.4

Table 30. Integrin assay data relating to the inhibitor analogues **47**, **56** and **63**. Error in the cell adhesion assays = 0.3

Amongst exhibiting moderate to good selectivity for $\alpha_v\beta_6$ over $\alpha_v\beta_3$ and $\alpha_v\beta_5$, these compounds demonstrate 100 and 300-fold selectivity for $\alpha_v\beta_6$ over $\alpha_v\beta_5$, significantly greater than any other analogue in the UoN series SAR. It was only during development of the *N*-linked aromatic heterocycle monosubstituted analogues described in Section 2.3 and 2.6.1 that consistent selectivity for $\alpha_v\beta_6$ over $\alpha_v\beta_8$ was obtained.

Thus, in one avenue of future research we would aim to elucidate the root cause of this selectivity, potentially *via* preparation of 3,5-disusbstituted analogues containing substituents whose monosubstituted parent compounds exhibit selectivity for $\alpha_v\beta_6$ over $\alpha_v\beta_8$.

If the assumption is made that optimisation of the phenyl component within the UoN series causes steric disruption to the extent of minimising binding affinity within the environment of the $\alpha_v\beta_3$ integrin binding site surrounding this moiety, it is thus logical to suggest that the RGD mimetic **355** itself exhibits some level of potency towards each integrin (Figure 54), as the most selective and drug-like $\alpha_v\beta_6$ integrin inhibitor **291** still exhibits a pIC$_{50}$ against $\alpha_v\beta_3$ of 6.1; this would be unsurprising, as the RGD tripeptide is naturally recognised as a suitable ligand by the α_v subset of integrins.

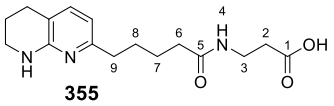

355

Figure 54. The RGD mimetic **355**; an analogue of the UoN series without the 3-aryl component.

As a result, we would likely focus upon modification of the central pentyl linker (positions 2-9 – Figure 54) in such a way as to reduce binding affinity within $\alpha_v\beta_3$ whilst also improving binding affinity within $\alpha_v\beta_6$.

The GSK series demonstrates that modification of the amide and central linker within these RGD mimetic integrin inhibitors can facilitate moderate improvements of pIC_{50} against $\alpha_v\beta_6$ whilst simultaneously decreasing pIC_{50} against $\alpha_v\beta_3$ (**(*S*)-27** *vs* **12**, Table 31): a near 3-fold increase and 10-fold reduction, respectively.

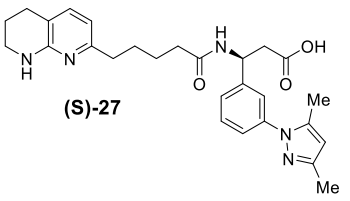

(S)-27

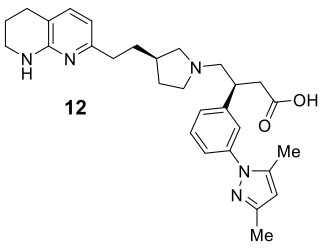

12

Compound no.	pIC_{50} $\alpha_v\beta_6$	pIC_{50} $\alpha_v\beta_3$	pIC_{50} $\alpha_v\beta_5$	pIC_{50} $\alpha_v\beta_8$
(*S*)-27	7.9	6.8	6.9	7.5
12	8.4	6.0	6.9	7.7

Table 31. Comparison of biological data between the UoN series analogue **(*S*)-27** and the GSK series analogue **12**, demonstrating the effect of replacing the central amide with the tertiary amine functionality. Error in the cell adhesion assays = 0.3.

As discussed in Section 2.5.1, the proposed reasoning for this observation is that the more basic tertiary amine will protonate more readily at pH 7.4 than the secondary amide and thus more frequently forms an advantageous hydrogen-bonding interaction with the proximal threonine residue Thr238, a residue that is not present in $\alpha_v\beta_3$. Additionally, replacing the

planar amide functionality with a tetrahedral tertiary amine, allows the amine in **12** to reside closer to the Thr238 target residue. Combination of these hypotheses with the data presented in Table 31 provides us with confidence that continuation and expansion of the scope of the *N*-alkylation work described in Section 2.5.1 may yield a similar result.

Further optimisation of the UoN Series could take inspiration from the series of guanidino-aryl integrin inhibitors reported by Ruminski and Griggs; this series will be referred to as the St Louis series (Figure 55).[144,145]

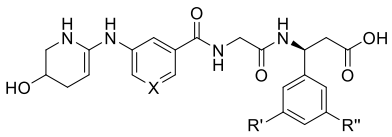

Figure 55. The primary structure within the series of integrin inhibitors reported by Ruminski and Griggs, where X = C-OH (**356**) or N (**357**).[144,145]

In this work, a series of potent, non-selective integrin inhibitors exhibiting excellent AUC values are reported; thus, to replicate this within our own series, further improving the moderate clearance exhibited by the 3-monosubstituted integrin inhibitor analogues described in Section 2.7, a hybrid between this series and the UoN series was designed. On application of the UoN series SAR relating to 3-monosubstituted and 3,5-disubstituted integrin inhibitors to this series, we found that the guanidine-aryl-amide moiety in **356** and **357** elicits a significant improvement of pIC_{50} against each of the α_v integrins at the cost of eliminating all permeability; the familiar reduction of pIC_{50} against $\alpha_v\beta_3$ was observed upon 3,5-disubstitution. To utilise this potential improvement of pIC_{50} against $\alpha_v\beta_6$ within our own optimised series of 3,5-disusbtituted integrin inhibitors, it would be of paramount importance to develop a solution to the observed elimination of permeability upon introduction of the guanidino-aryl-amide moiety.

In light of the recent patent disclosure by Pliant Therapeutics regarding a series of potent and selective dual $\alpha_v\beta_6/\alpha_v\beta_1$ integrin inhibitors, we would additionally explore the potential of β-2-aryl-amino acid derived analogues in an effort to determine the effect of modulating the position of the phenyl component of the UoN series of integrin inhibitors within the SDL of the α_v integrin binding pockets (Figure 56).[74]

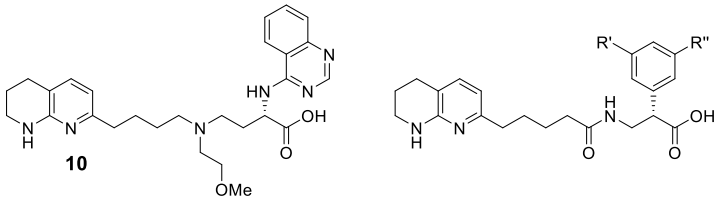

Figure 56. The assumed structure of the Pliant clinical candidate PLN-74809 (**10**) and the proposed structure of a β-2-aryl-amino acid derivative.[74]

Perhaps by moving this component closer to the carboxylic acid, the steric hinderance resulting from unfavourable interaction of the 3,5-aryl substituents within the SDL of the $\alpha_v\beta_3$ integrin binding site would be increased further (Figure 53, Section 3.4.3), ultimately reducing the pIC_{50} against $\alpha_v\beta_3$ beyond that which is already observed. Additionally, it is feasible that with a methylene functionality separating the amide from the 3,5-disubstituted phenyl moiety, the molecule would experience improved rotational and translational freedom, subsequently facilitating more optimal positioning of the compound within the $\alpha_v\beta_6$ integrin binding site.

These suggested structural changes would likely lead to the following synthetic projects: (1) further modification of the linker within the UoN series, (2) further hybridisation of the UoN series and the St Louis series and (3) preparation of a series of β-2-aryl-amino acid derived integrin inhibitors.

Continuation of the work described in Section 2.5.1 *via* modulation of the linker in the UoN series would initially result in the preparation of the following compounds (Figure 57):

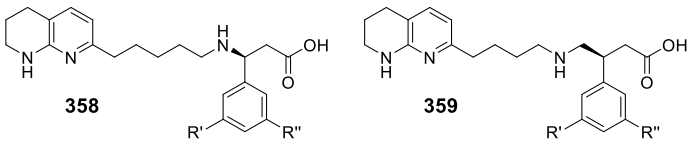

Figure 57. The target integrin inhibitor analogues that would be prepared in a continuation and expansion of the scope of the *N*-alkylation work described in Section 2.5.1 (**358** and **359**).

These compounds would meet the proposed requirement for a more basic nitrogen within the linker of the UoN series, whilst also indicating the effect of reducing planarity and thus, the rigidity of the molecule within the α_v integrin binding sites.

Preparation of **358** would likely be a relatively simple process: reduction of the acid **67**, followed by oxidation to the aldehyde **360**, before a final reductive amination with the requisite β-3-aryl-amino ester to give **358** (Scheme 52).

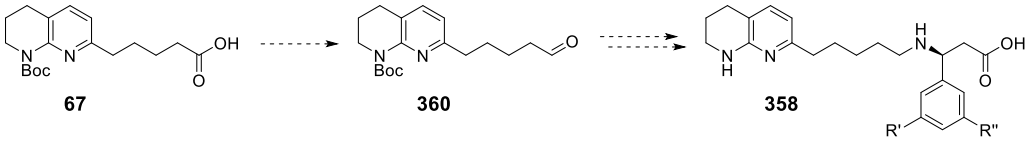

Scheme 52. Proposed preparation of **358** *via* generation of the aldehyde **360**, followed by reductive amination to form the desired secondary amine inhibitor analogue.

The inhibitor **359** may be derived from an intermediate similar to the medication baclofen (**361**, Figure 58).

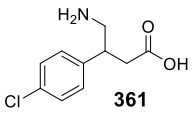

Figure 58. The commercially available medication baclofen (**361**).

One reported synthesis of (*S*)-baclofen hydrochloride (**366**) that could potentially be used to prepare similar γ-3-aryl-amino acids for our usage is depicted in Scheme 53.[148]

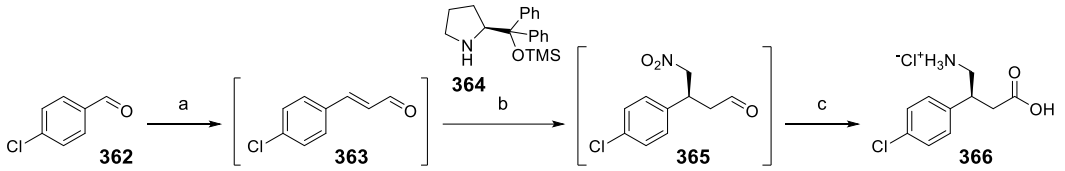

Scheme 53. Preparation of (S)-baclofen hydrochloride (**366**) from 4-chlorobenzaldehyde (**362**) as reported by Hayashi *et al*.[148] *Reagents and conditions*: a) i) acetaldehyde, DBU (20 mol%), THF, rt, 48 h; ii) b) nitromethane, **364** (4.00 mol%), HCO_2H (40 mol%), water, rt, 48 h; c) i) $NaClO_2$, $NaH_2PO_4.2H_2O$, 2-methyl-2-butene, *t*-BuOH/water (3:1), 3 h; ii) $Na_2HPO_3.5H_2O$, 1 h; iii) Raney Ni, H_2, methanol, rt, 48 h; iv) 2M $HCl_{(aq)}$, 31%.

In this work, a telescoped procedure is reported, beginning with aldol condensation of acetaldehyde with 4-chlorobenzaldehyde (**362**), followed by an asymmetric Michael reaction between **363** and nitromethane, catalysed using diphenylprolinol trimethyl silyl ether (**364**), before Pinnick oxidation and nitro reduction with sodium chlorite and Raney nickel furnished (*S*)-baclofen hydrochloride (**366**) on multi-gram scale. Use of benzaldehydes relevant to our requirements with this methodology would likely facilitate the generation of γ-3-aryl-amino acids suitable for further use in our efforts to prepare analogues of **359**.

Preparation of the requisite 'chain-shortened' THN aldehyde would simply be performed using the previously described Friedländer method, followed by the proposed reduction/oxidation depicted in Scheme 52; reductive amination of this aldehyde with the relevant γ-3-aryl-amino ester would then yield the desired compound **359** (Scheme 54).

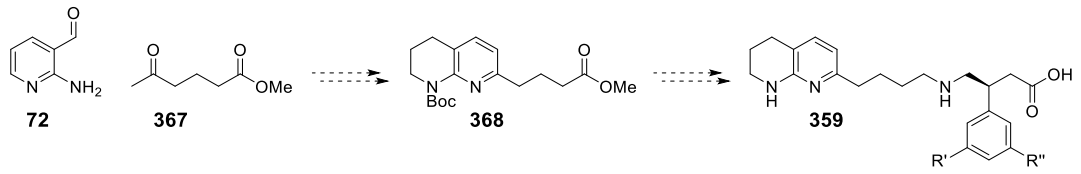

Scheme 54. Proposed preparation of the requisite 'chain-shortened' THN ester **368** *via* Friedländer reaction, followed by synthesis of the desired γ-3-aryl-amino acid derived inhibitor **359**.

Utilisation of structural features from the St Louis series would be slightly more complex due to the differences in length between the UoN and St Louis series, however, one can imagine that an analogue such as that depicted in Figure 59 would be prepared.

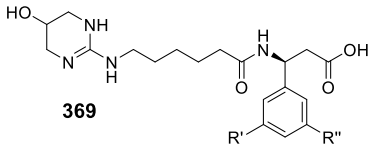

Figure 59. Potential integrin inhibitor analogues resulting from hybridisation of the UoN and St Louis series.

Inclusion of the pyridine/phenol functionality from the St Louis series likely reduces the permeability exhibited by the molecule and so the THN moiety would simply be replaced with the hydroxy-guanidine functionality; Scheme 55 depicts a possible method for the preparation of the hydroxy-guanidine containing fragment (**372**) that would be required for synthesis of analogues of **369**.

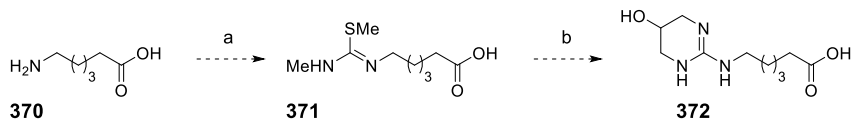

Scheme 55. Proposed generation of the hydroxy-guanidine fragment **372**. *Reagents and conditions*: a) i) methyl isothiocyanate, DMF, rt; ii) iodomethane; b) 1,3-diaminopropanol, DMF, reflux.

This methodology replicates that used in the preparation of the integrin inhibitors reported by Ruminski and Griggs;[144] the methane-thiol urea **371** is generated upon treatment of **370** with methyl isothiocyanate, followed by iodomethane, before generation of **372** *via* reaction of **371** with 1,3-diaminopropanol. The desired integrin inhibitor analogue would then simply be prepared upon amide coupling of **372** with the relevant β-3-aryl-amino ester, followed by ester saponification to give analogues of **369**.

Generation of β-2-aryl-amino acid derived integrin inhibitors would simply result in the preparation of a selection of 3,5-disubstituted analogues as depicted in Figure 60.

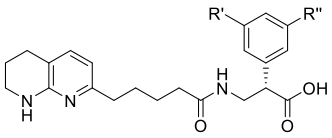

Figure 60. The likely structure of a series of β-2-aryl-amino acid derived integrin inhibitor analogues.

Methodology reported by Martin *et al*. facilitates the preparation of β-2-aryl-amino esters in good yield and with high enantioselectivity (Scheme 56).[149]

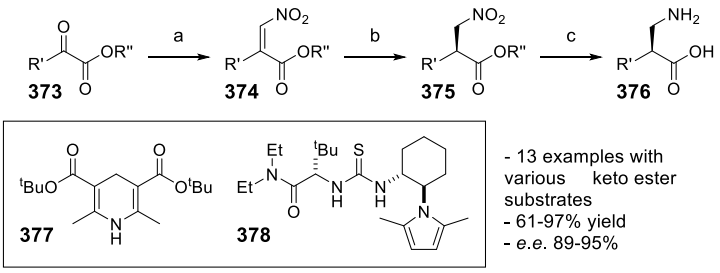

Scheme 56. Preparation of β-2-aryl-amino acids (**376**) from α-keto esters (**373**) as reported by Martin *et al*.[149] *Reagents and conditions*: a) i) nitromethane, Et_3N (20 mol%); ii) acetic anhydride, 71%; b) **377**, **378** (10 mol%), toluene, 0 °C to rt, 48 h, 91%; c) H_2, Pd/C, methanol, e.e. 94%, 81%.

In this work, the nitroacrylate intermediate (**374**) is prepared upon reaction of nitromethane with the relevant α-keto ester, subsequently followed by dehydration of the product with acetic anhydride. The requisite asymmetric conjugate reduction is performed using a catalytic amount of the thiourea **378**, with a stoichiometric quantity of the Hantzsch ester **377** as the transferhydrogenating reagent; Martin *et al*. report that the geometry of the nitroacrylate-olefin **374** determines the stereochemistry of the resulting nitroalkane product **375**, with (*E*) and (*Z*) isomers generating (*R*) and (*S*) enantiomers, respectively. Final reduction to the amine and generation of the carboxylic acid is performed under hydrogenating conditions with hydrogen and palladium on carbon, with aqueous HCl subsequently being used to cleave the ester where appropriate, giving analogues of **376**. A range of esters and 2-substituents, from unbranched alkanes to aromatics, are tolerated, with improved enantioselectivity being obtained upon use of bulkier ester moieties (e.g. -OBn). Application of this work to the UoN project would thus likely result in the successful preparation of 3,5-disubstituted analogues as depicted in Figure 60.

Upon completion of these works, it may prove prudent to combine the most favourable structural features, leading to the preparation of an additional series of hybridised integrin inhibitors.

Obviously, without any physicochemical data to support further target design, any proposed integrin inhibitors from this point are based somewhat on conjecture. However, if we deduce from the excellent potency and selectivity exhibited by the GSK series that a basic nitrogen at the 5-position of the central linker (Figure 54) is optimal for maximising binding affinity within the $\alpha_v\beta_6$ integrin binding site whilst minimising binding affinity in $\alpha_v\beta_3$, and that binding affinity within all integrins is improved by addition of the hydroxy-guanidine moiety present in the St Louis series, then it would not be unreasonable to suggest that compounds resembling **379**, as presented in Figure 61, would be prepared in due course.

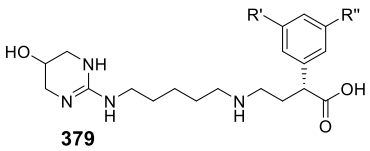

379

Figure 61. A potential target compound resulting from a hypothetical analysis of the first iteration of analogues deriving from this future work section.

Regardless of the level of success, all drug development projects will eventually be concluded, often before all possible target compounds can be prepared and tested. This project is no different and unfortunately the integrin screening assay facilities that we had access to through our collaborative effort with GSK were ended, resulting in an abrupt conclusion to this work.

In light of this development, we sought instead to focus on an alternative part of the drug development process, specifically the discovery, isolation and subsequent synthesis of natural product.

Chapter 4

Strategies towards the total synthesis of mescengricin

4.1 Mescengricin

In days past, and in contrast to the drug discovery process described in Chapters 2 and 3, the discovery, isolation and subsequent screening of naturally occurring compounds against a host of biological targets would be the major method. Once a potential use for a compound had been identified, the compound would be progressed to the 'hit-to-lead' stage, resembling a traditional drug discovery project in which a broad SAR is rapidly generated. However, for this stage to be initiated, the compound must first be synthesised under laboratory conditions, beginning from commercially available reagents; this is total organic synthesis.

This Chapter will see described a continuation of the attempted total synthesis of mescengricin (**5**, Figure 62).

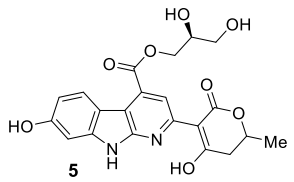

5

Figure 62. The structure of mescengricin (**5**) as reported by Seto *et al*.[150]

Mescengricin (**5**) was first isolated and reported by Seto *et al.* in 1997; isolated from bacteria within the *Streptomyces griseoflavus* 2853-SVS4, mescengricin (**5**) was found to decrease L-glutamate toxicity in chick primary mescencephalic neurons, with an EC_{50} value 6.0 nM.[150]

4.1.1 Medicinal implications and potential uses

L-Glutamate toxicity has been implicated in the progression and exacerbation of neurodegenerative diseases such as Huntington's disease and Alzheimer's disease.[151,152] L-Glutamate plays a pivotal role in normal bodily function and is a key agent in the *N*-methyl-D-aspartate (NMDA) receptor related process that oversees an influx of Ca^{2+} through the cell

membrane.[153] Excessive activation of these NMDA receptors can trigger a cascade of events resulting in significant increases in cellular calcium concentrations, ultimately resulting in neuronal cell death either by apoptosis or necrosis.[154,155]

4.1.2 Structural elucidation of mescengricin

Mescengricin (**5**) is comprised of three key structural moieties: a phenolic α-carboline, a glycerol derived ester and a hydroxymethyl dihydropyranone.

The stereochemistry of C-1 in the glycerol-derived motif was determined upon preparation of the acetonide **380**, followed by saponification to give the enantiopure (*R*)-(-)-2,2-dimethyl-1,3-dioxolane-4-methanol, also known as (*R*)-solketal **381**, the optical rotation of which was compared with that of the commercially available reagent (Scheme 57). The stereochemistry of C-2 within the lactone of **5** was unable to be determined at the time of reporting;[150] both C-1 and C-2 are classified as such by Seto *et al*.

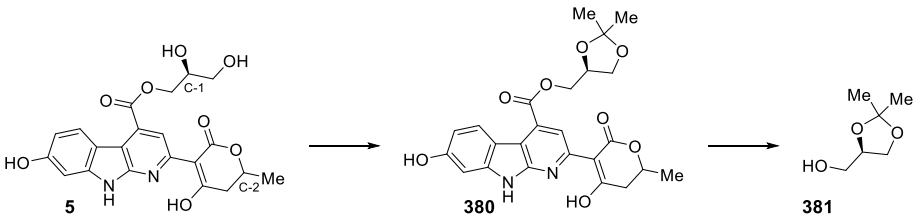

Scheme 57. The preparation of the acetonide (**380**) from **5** and subsequent saponification to give (*R*)-solketal (**381**), the absolute stereochemistry of which was determined upon comparison with commercially available reagents.[150]

4.1.3 Carbolines

α-Carboline (**382**) is a member of a group of four pyrido[x,y-b]indoles, collectively referred to as carbolines; the others being β-carboline (**383**), γ-carboline (**384**) and δ-carboline (**385**) (Figure 63).

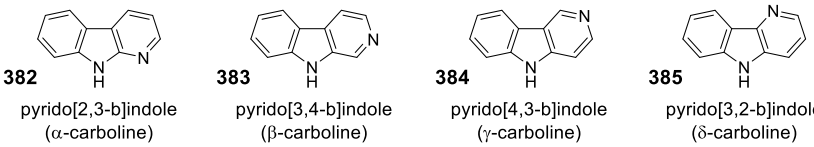

Figure 63. The four pyrido[x,y-b]indoles commonly referred to as carbolines.

These ring systems are found in a variety of naturally occurring compounds, of which a number have been found to exhibit biological activity, thus making them attractive targets for total synthesis and subsequent drug development projects.[156–158]

Of the carbolines, β-carboline occurs most prolifically in nature, due to being derived from the amino-acid L-tryptophan (**386**) *via* decarboxylation, followed by what is believed to be a Pictet-Spengler reaction to give the tetrahydro-carboline **388**, before oxidation to give the β-carboline **389** (Scheme 58).[159–163]

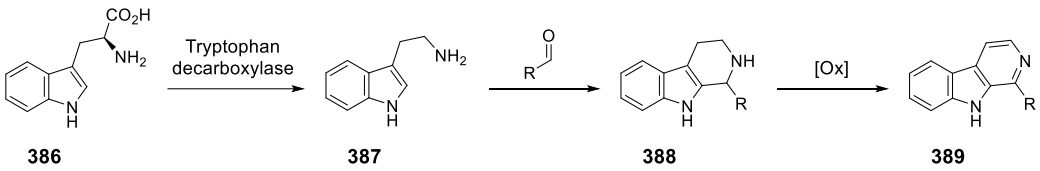

Scheme 58. The proposed biosynthetic pathway of β-carbolines from L-tryptophan (**386**).[159–163]

Molecules exhibiting the β-carboline feature have been isolated from various natural sources such as marine sponges, tunicates, plants and foods; examples include eudistomin A (**390**, part of a larger family of eudistomins) and manzamine A (**391**), isolated from a species of tunicate and marine sponge, respectively (Figure 64).[164,165]

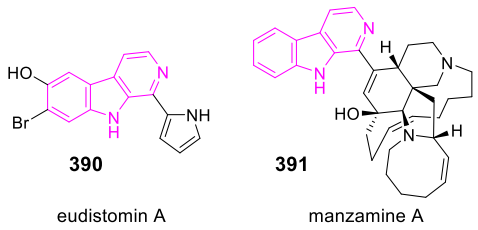

Figure 64. Two examples of naturally occurring β-carboline derived compounds: eudistomin A (**390**) and manzamine A (**391**); β-carboline functionalities are highlighted.

The eudistomins have been found to exhibit antiviral activity, inhibiting plaque formation by herpes simplex virus, type 1 (HSV-1) in CV-1 cells (monkey kidney tissue), whereas manzamine A (**391**) exhibits broad biological activity, specifically antibacterial, antimalarial, insecticidal, anti-inflammatory and anti-HIV.[164,165]

Whilst α, γ and δ-carbolines are more uncommon, a number of compounds exhibiting these structural groups have been isolated from natural sources, such as those presented in Figure 65.

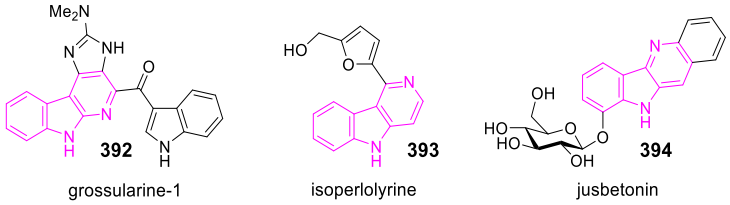

Figure 65. Examples of naturally occurring α, γ and δ-carboline derived compounds: grossularine-1 (**392**), isoperlolyrine (**393**) and jusbetonin (**394**); carboline functionalities are highlighted.

Little is known about the biological activity exhibited by naturally occurring γ-carbolines, primarily due to their rarity and thus the few examples of their isolation, however, synthetically derived γ-carbolines have exhibited such properties as monoamine oxidase (MAO) inhibition, antiviral and antimicrobial activity.[166] The δ-carboline derived species

jusbetonin (**394**), first synthesised by Jiang *et al.*, has shown moderate proliferation inhibitory activity against the MDA-231 breast cancer cell line, whilst the α-carboline derived species grossularine-1 (**392**), one of two α-carboline derived compounds isolated from the tunicate *Dendrodoa grossularia*, has been found to exhibit antitumour biological activity *via* cytotoxicity towards murine and human tumour cells.[167,168]

4.2 Retrosynthetic analysis of mescengricin and discussion of previously attempted syntheses

An outline retrosynthetic scheme for the preparation of mescengricin is presented in Scheme 59.

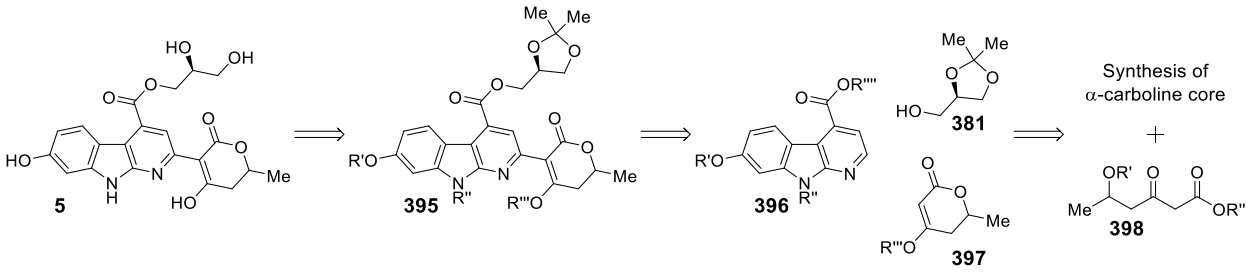

Scheme 59. A retrosynthetic analysis of mescengricin (**5**), depicting the three core structural fragments **381**, **396** and **397** as described in Section 4.1.2.

As discussed, mescengricin (**5**) is comprised of three main structural features; Scheme 59 suggests that the most likely path for the successful preparation of **5** involves the coupling of precursors of these groups to one another (**381**, **396** and **397**). The enantiopure acetonide (*R*)-solketal (**381**) is a commercially available reagent and so only preparation of the α-carboline core **396** and the lactone **397**, or appropriate precursors (**398**), would be required.

Whilst a relatively uncommon moiety in synthetic chemistry, there are a diverse range of methodologies available for the synthesis of α-carbolines; a thorough review of these methods are reported by Wadsworth *et al* (Scheme 60).[169]

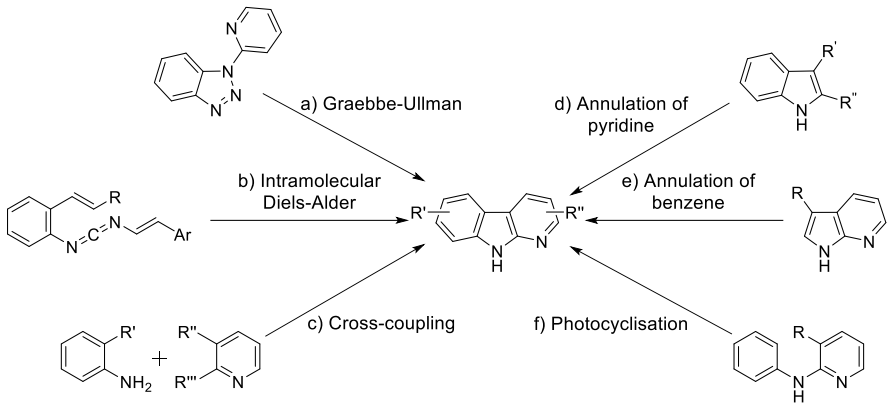

Scheme 60. A number of the available methods for the preparation of α-carbolines as reviewed by Wadsworth *et al*.[169]

During a postgraduate doctoral study by Wadsworth, the attempted synthesis of mescengricin was described.[170] Whilst the project was ultimately unsuccessful, a number of these methodologies were attempted in the specific context of preparing mescengricin precursor substrates, specifically, palladium catalysed cross-coupling reactions and photocyclisations to generate α-carbolines (Scheme 61).

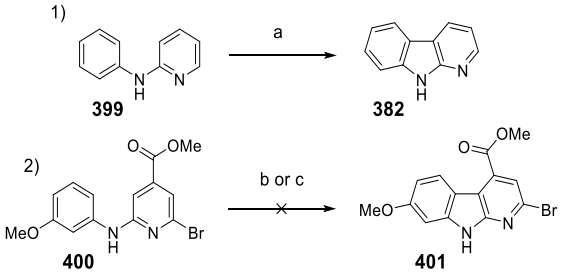

Scheme 61. Attempted cyclisation of 2-anilino-pyridine substrates *via* photochemical and palladium-catalysed methods, as reported by Wadsworth.[170] *Reagents and conditions*: a) h*v* (254-350 nm), cyclohexane, 12 h, 93%; b) h*v* (254-350 nm), cyclohexane, 12 h; c) $Pd(OAc)_2$, $Cu(OAc)_2$, *solvent*, *additive*, μW.

The failure of the cyclisation reactions depicted in Scheme 61 was proposed by Wadsworth to be a result of the presence of the carboxylate group in **400**. Thus, we felt that perhaps cyclisation of a 4-methyl pyridine substrate (**402**) to yield the 4-methyl carboline **403** would

be successful; this intermediate would subsequently require further functionalisation to give the desired 4-carboxylic acid **404** (Scheme 62).

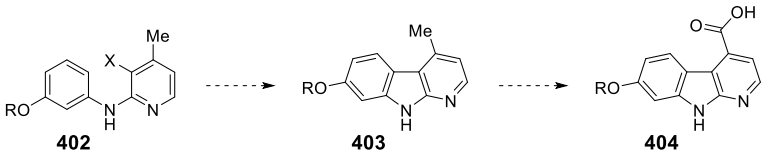

Scheme 62. The proposed solution to the cyclisation-related issues reported by Wadsworth with regards to generation of the 4-carboxylic acid α-carboline **404**: generation of the 4-methyl substrate **403** *via* palladium catalysis, followed by oxidation to give the acid **404**.

A methodology not described in Wadsworth's review and one that was identified as a suitable alternative to the synthesis of derivatives of **404** as described in Scheme 62 should the process be unsuccessful, is the 6π-electrocyclisation of indole-3-alkenyl oximes to form α-carbolines, reported by Markey *et al*. (Table 32).[171]

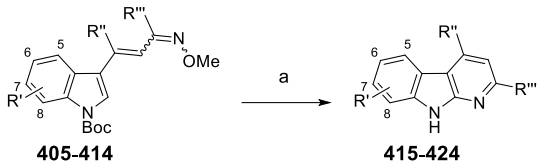

405-414 415-424

Oxime SM	R'	R''	R'''	α-carboline product	Yield/%
405	6-OMe	H	H	**415**	36
406	7-OMe	H	H	**416**	30
407	6-Cl	H	H	**417**	55
408	H	H	Me	**418**	90
409	7-OMe	H	Me	**419**	77
410	6-OMe	H	Me	**420**	41
411	H	CO_2Me	H	**421**	52
412	H	Me	H	**422**	62
413	H	Me	Me	**423**	65
414	H	CO_2Me	Me	**424**	51

Table 32. The yields of reaction for the 6π-electrocyclisation of the oxime substrates **405**-**414**, generating the α-carbolines **415**-**424**, as reported by Markey *et al.*[171] N.B. The numbering convention for the α-carboline products and precursors is depicted within the scheme shown above.[171,172] *Reagents and conditions*: a) 1,2-dichlorobenzene, 240 °C, μW, 3 h.

The required oxime precursors are prepared *via* Horner-Wadsworth-Emmons (HWE) reaction between the phosphonate oxime substrates **426** and the indoles **425** as depicted in Scheme 63.

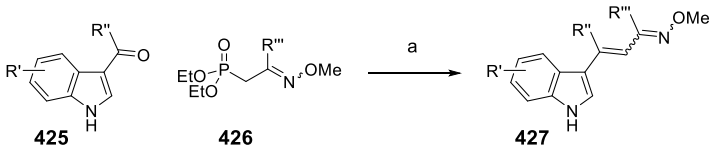

425 426 427

Scheme 63. HWE reaction between the carbonyl-indoles **425** and the phosphonate-oximes **426** to give the 6π-electrocyclisation precursor substrates **427**.[171,172] *Reagents and conditions*: a) i) **426**, ^{n}BuLi, THF, 0 °C, N_2, 1 h; ii) **425**, 0 °C to rt, 2-4 h.

The HWE reagent **426** is prepared *via* condensation of the carbonyl containing compounds **428** and **431** with *O*-methyl hydroxylamine (Scheme 64).

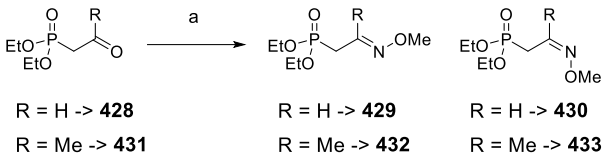

Scheme 64. Generation of the requisite oxime-HWE reagents from condensation of *O*-methyl hydroxylamine with the relevant phosphonate (**428** or **431**).[172] *Reagents and conditions*: a) $MeONH_2.HCl$, pyridine, CH_2Cl_2, rt; yield: R = H, 55% combined yield, 1:1.35 (**429**:**430**); R = Me, 91% combined yield, 1.4:1 (**432**:**433**)

There are four possible stereoisomeric outcomes for the HWE reaction and indeed Markey reports that for the reaction presented in Scheme 65 depicting the generation of the oxime **435** a ratio of 1:1:4.4 for the (*E*,*E*):(*E*,*Z*):(*Z*,*Z*) isomers, respectively is observed.[172]

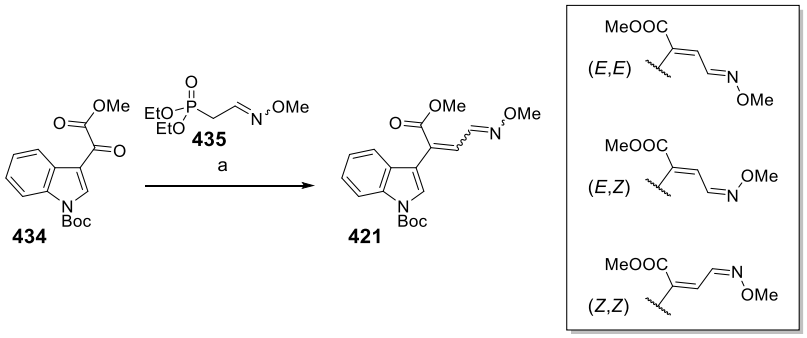

Scheme 65. Preparation of the oxime **421** in a 1:1:4.4 ratio of (E,E):(E,Z):(Z,Z) isomers respectively *via* HWE reaction between **434** and **435** as reported by Markey.[172] *Reagents and conditions*: a) i) **435**, ^{n}BuLi, THF, 0 °C, N_2, 1 h; ii) **434**, 0 °C to rt, 2-4 h, 50%

Separation of these stereoisomers is noted to be particularly challenging using traditional chromatographic techniques, however it is later reported that each stereoisomer successfully cyclises to give the desired α-carboline product; this is likely a result of oxime

isomerisation occurring due to the high temperatures required for the 6π-electrocylisation reaction.

Preparation of the glycerol ester **437** *via* transesterification has been reported previously and thus was not expected to require significant developmental effort (Scheme 66).[173]

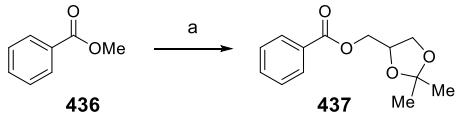

Scheme 66. Transesterification of methyl benzoate (**436**) with (*rac*)-solketal, using $Fe(acac)_3$, as reported by Weng *et al*.[173] *Reagents and conditions*: a) (*rac*)-solketal, Na_2CO_3 (5 mol%), $Fe(acac)_3$ (5 mol%), *n*-heptane, azeotropic reflux, 8 h, 93%.

Likewise, formation of the lactone moiety was not envisioned to be problematic as the preparation of such substrates are reported (Scheme 67).[174]

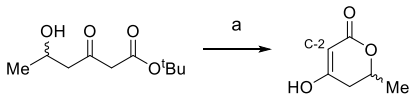

Scheme 67. Preparation of the enantiopure lactones **(*R*)-438** and **(*S*)-438** as reported by Drochner and Müller.[174] *Reagents and conditions*: a) TFA, CH_2Cl_2, rt, yield: **(*R*)-438** -> 78%, **(*S*)-438** -> 59%.

However, coupling from the position labelled C-2 of the lactone to the 2-pyridyl position of the α-carboline was predicted to be particularly challenging, as there did not appear to be many well-established methodologies for the functionalisation of the lactone in such a manner as would be appropriate for coupling to 'pyridine-like' substrates.

4.3 Strategies towards forming the 2-lactone moiety

Several methodologies were considered to achieve this modification: 1) procedures based upon the use of a pyridine *N*-oxide intermediate; 2) manipulation of a 2-methyl analogue; 3) coupling reactions using a pyridyl-halide substrate (Figure 66).

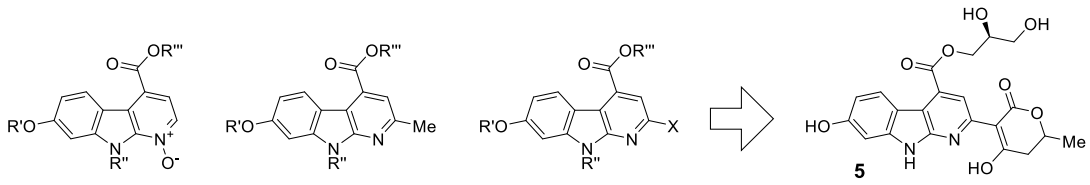

Figure 66. The three α-carboline substrates from which it is proposed that mescengricin (**5**) may be derived.

Londregan *et al*. report the development of methodology that facilitates the coupling of nucleophilic reagents with pyridine *N*-oxides using phosphonium coupling agents to generate 2-substituted pyridines in good yield.[175–177] These nucleophiles include a diverse range of amines, alcohols, thiols, silyl ketene acetals and enolisable substrates (Scheme 68).

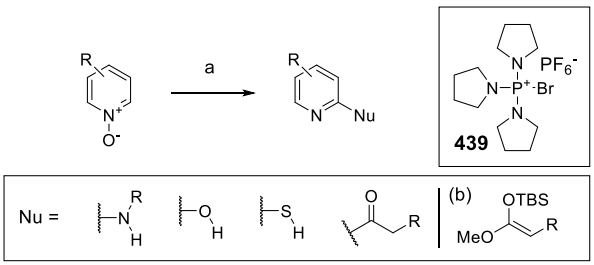

Scheme 68. Addition of nucleophiles to pyridine-*N*-oxides as reported by Londregan *et al*., generally facilitated by activation with PyBroP (**439**).[175–177] *Reagents and conditions*: a) ***nucleophile*** **(Nu)**, PyBroP, *i*-Pr_2NEt, CH_2Cl_2, rt. [b]THF used as solvent instead of CH_2Cl_2.

The mechanism for this reaction is predicted to be largely the same for each class of nucleophile: The *N*-oxide moiety reacts with the phosphonium reagent, further decreasing electron density at the 2-position of the pyridine ring, increasing electrophilicity and

subsequently facilitating nucleophilic attack at the 2-position, resulting in the elimination of the phosphine oxide **442** and generation of the 2-substituted pyridine (Scheme 69).

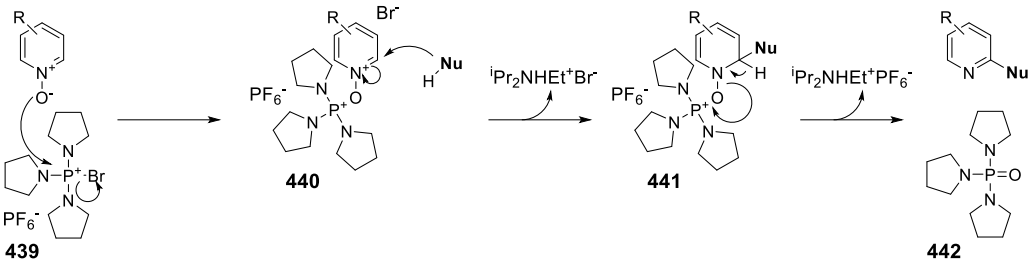

Scheme 69. Proposed mechanism of PyBroP facilitated 2-addition to pyridine-*N*-oxides, as proposed by Londregan *et al*.[175]

Whilst activation of pyridine *N*-oxide substrates with activating agents such as anhydrides often results in competitive addition at both the 2- and 4-position, Londregan *et al*. report that activation of the pyridine oxide substrate with the phosphonium salt PyBroP (**439**) in a basic mixture with *i*-Pr_2NEt results in no observable addition to the 4-position; it is thought that this regioselectivity is due to a charge association between **440** and the incoming nucleophile.[175]

Functionalisation of the 2-methyl substrate depicted in Figure 66 was envisioned to be achieved *via* halogenation of the methyl group to give the corresponding alkyl halide α-carboline product. Much of this methodology was based on work previously reported by Markey in her thesis detailing the attempted synthesis of mescengricin.[172]

In this work, the 2-methyl carboline **443** undergoes radical bromination to give **444** (Scheme 70).

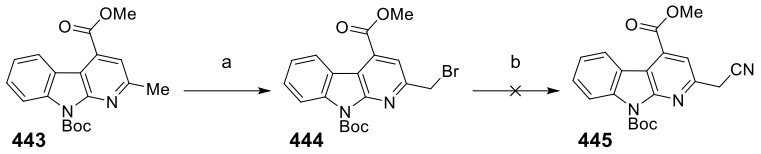

Scheme 70. The radical bromination of **443** and the attempted subsequent cyanation of **444** to give **445**, as reported by Markey.[172] *Reagents and conditions*: a) NBS, benzoyl peroxide, CCl_4, 70 °C, 16 h, 45%; b) NaCN, DMSO, rt.

However, subsequent cyanation of this intermediate was unsuccessful and so alternative methodologies based on use of the Wittig reagent **446** and formation of the organometallic reagent **447** were considered (Figure 67).

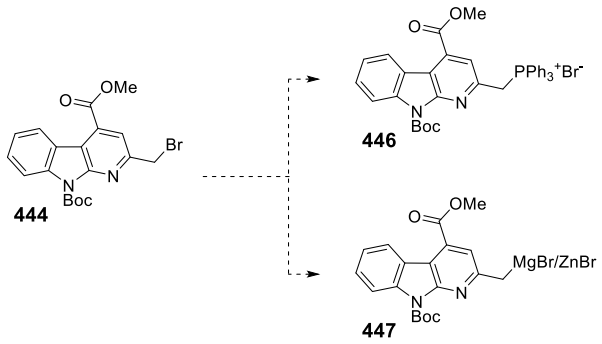

Figure 67. Proposed solutions in response to the failed cyanation of **444** include formation of the Wittig reagent **446** and some form of organometallic reagent **447**.

Alternatively, preparation of the 2-halo pyridine substrate depicted in Figure 66 would allow access to myriad methodologies developed in recent times that enables coupling of alkyl substrates to 2-halo pyridines *via* metal catalysis or simply *via* nucleophilic addition (Scheme 71).

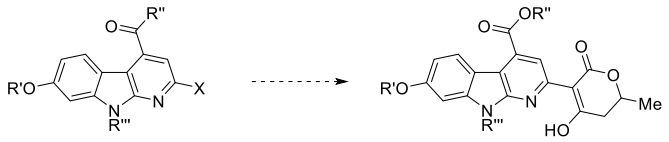

Scheme 71. Proposed coupling of the desired lactone moiety to the 2-halo α-carboline substrate the lactone substituted mescengricin precursor.

4.4 Results and discussion

4.4.1 Preparation of the α-carboline core *via* palladium catalysis

Before these methodologies could be attempted, the core α-carboline structure was required. Initial experimentation followed work reported Cuny *et al*., modified slightly to suit our own requirements, that facilitates the preparation of α-carbolines *via* palladium catalysis (Scheme 72).[178]

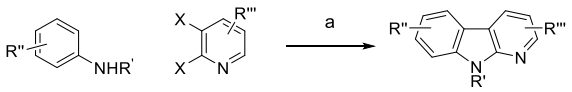

Scheme 72. The procedure for the one-pot synthesis of α-carbolines *via* palladium catalysed aryl-amination and intramolecular cyclisation as reported by Cuny *et al*.[178] *Reagents and conditions*: a) i) $Pd(OAc)_2$, PPh_3, NaO*t*-Bu, *ortho*-xylene, 120 °C, 3 h; ii) $Pd(OAc)_2$, $PCy_3.HBF_4$, DBU, *ortho*-xylene/DMAc, 145 °C, 16 h, **18 examples: 19-85%**.

Thus, the 4-methyl analogue **451** was prepared as follows: Buchwald-Hartwig reaction between the amino pyridine **449** and 3-iodobenzene (**448**) yielded the anilino-pyridine **450** in 90% yield, which was subsequently cyclised upon reaction with $Pd(OAc)_2$ and $PCy_3.HBF_4$ at 175 °C, giving the carboline **451** in poor yield (Scheme 73). Given that Wadsworth reports no observable cyclisation with their substrate **400**, as described previously in Scheme 61, this poor yield was unsurprising.[170]

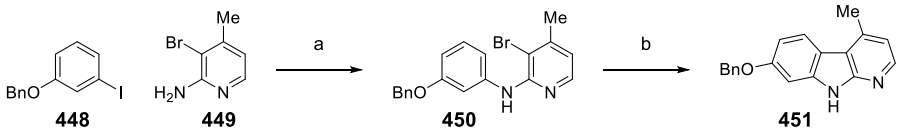

Scheme 73. Preparation of the 2-anilino-pyridine substrate **450** and subsequent cyclisation to give the α-carboline **451** *via* palladium catalysis. *Reagents and conditions*: a) NaO*t*-Bu, $Pd_2(dba)_3$ (4 mol%), Xantphos (8 mol%), *ortho*-xylene, 110 °C, N_2, 16 h, 90%; b) DBU, $Pd(OAc)_2$ (5 mol%), $PCy_3.HBF_4$ (1.00 eq.), *ortho*-xylene/DMAc (1:1), 145 °C, Ar, 16 h, 11%.

With **451** in hand, the oxidation of the 4-methyl position was attempted using a range of different methodologies; regrettably, in all cases no reaction was observed to have taken place (Scheme 74).

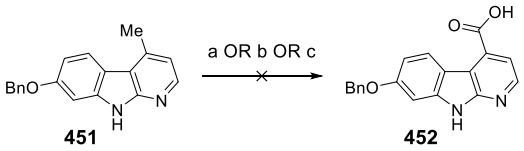

Scheme 74. The attempted oxidation of the 4-methyl α-carboline **451** to give the carboxylic acid **452**. *Reagents and conditions*: a) $KMnO_4$, water, reflux; b) Oxone®, acetone, water, rt; c) KO*t*-Bu, O_2, DMF/*t*-BuOH (3:2), rt.

As an alternative, it was thought that perhaps by using the bromination methodology utilised by Markey in the preparation of **444**, the 4-methyl position in **451** could be brominated, allowing further functionalisation to generate the desired carboxylate **452**. Unfortunately, this route and subsequently the '2-methyl functionalisation route' listed in Figure 66 was immediately rendered obsolete when it became clear that the bromination conditions used to form **444**, as reported by Markey, were not applicable to our own system (Scheme 75).[172]

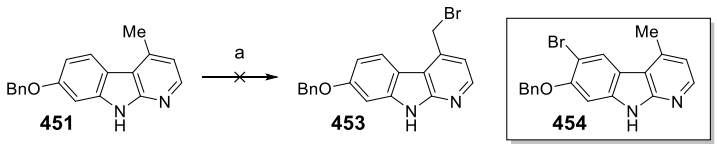

Scheme 75. Attempted bromination of the 4-methyl α-carboline **451** to give the alkyl bromide **453**; this methodology instead resulted in total consumption of **451** to give **454** *via* aryl bromination. *Reagents and conditions*: a) NBS, dibenzoyl peroxide, CCl_4, reflux.

Analysis of the reaction mixture of **451** with NBS and benzoyl peroxide by LCMS indicated that total consumption of **451** had taken place within 30 min, with subsequent formation of a single new product peak; the newly formed peak exhibited the mass of the desired product. However, upon NMR analysis of the unpurified reaction product, it became apparent that the benzene component of the carboline had been brominated, as the methyl CH_3 was observed whilst an aryl C-H was found to be absent, generating **454**; this outcome is presumably due to the increased electron density within the carboline structure resulting from the presence of the benzyloxy functionality.

This route was subsequently abandoned, and all remaining efforts were instead dedicated to utilisation of carboline intermediates generated *via* the 6π-electrocyclisation method reported by Markey *et al*.[171]

4.4.2 Preparation of the α-carboline core *via* 6π-electrocyclisation

The ester **457** was prepared in good yield *via* reaction of the commercially available benzyloxy indole **455** with oxalyl chloride to give the acid **456**, followed by subsequent esterification and *N*-Boc protection; initial attempts in which the reaction of the indole with oxalyl chloride was quenched with ethanol to generate **457** resulted in mixtures of **456** and **457**, and so for ease, the acid chloride intermediate was quenched with water to give the carboxylic acid **456** and then esterified separately to give the ethyl ester **457** (Scheme 76).

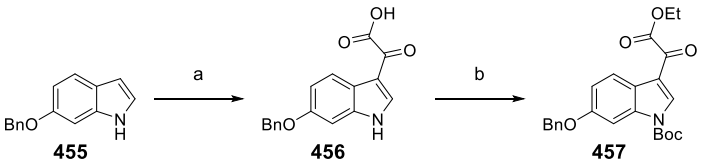

Scheme 76. Preparation of the *N*-Boc protected ethyl ester **457**. *Reagents and conditions*: a) $(COCl)_2$, diethyl ether, 0 °C to rt, N_2, 16 h; b) i) EDC.HCl, ethanol, DMAP, THF, 0 °C to rt, 16 h; ii) di-*tert*-butyl dicarbonate, rt, 16 h, 87% over two steps.

Installation of the desired α,β-unsaturated methyl-oxime functionality was achieved by a HWE reaction between **457** and the oxime **435** using sodium hydride as the required base; the preparation of both **435** and **459** is shown in Scheme 77**.**

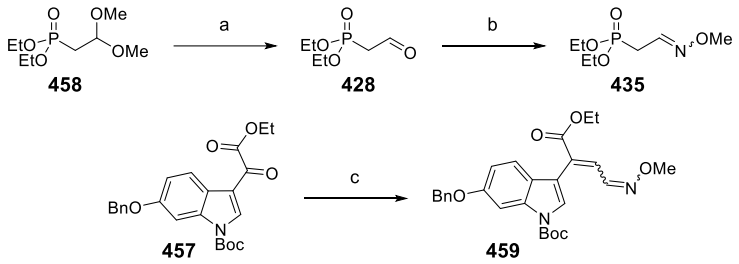

Scheme 77. Generation of the oxime **435** and subsequent HWE reaction with the ketone **457** to give the 6π-electrocyclisation precursor **459**. *Reagents and conditions*: a) 2M $HCl_{(aq)}$, rt, 16 h, 94%; b) $NH_2OMe.HCl$, sodium acetate, methanol/water (1:1), rt, 16 h, 91%; c) **435**, sodium hydride, THF, 0 °C to rt, N_2, 16 h, 81%.

As expected, NMR analysis of **435** and **459** after aqueous workup revealed a mixture of stereoisomers, but as previously discussed, the subsequent 6π-electrocyclisation reaction to generate the desired α-carboline does not require any one specific stereoisomer and so **435** and **459** were used without further purification.

Interestingly, the best yields for this HWE reaction were achieved using an almost counter intuitive reverse addition, in which the oxime **435** was added slowly to a solution of the ketone **457** and sodium hydride, rather than addition of the ketone **457** to a solution of the

preformed phosphonium ylide; in fact, preforming the ylide appeared to significantly reduce the yield of **459**. The reasoning for this is not particularly clear, perhaps it is due to reaction of the product **459** with the phosphonium ylide, or perhaps the ylide itself is unstable.

In the event, a consistent yield of ~80% of **459** was obtainable on relatively small scale (<200 mg); disappointingly, this reaction did not seem to proceed to the same extent on larger scale (>500 mg), despite repeated attempts varying reagent addition times and rates, reagent equivalents etc.

LCMS analysis of the HWE reaction indicated the formation of an intermediate that would break down in aqueous conditions to a species that ionises as the acid **461**. Over time, this intermediate converted to the product **459** and so it is likely that this intermediate is simply the intermediate common to HWE reactions (**460**), shown in Scheme 78. The rate of conversion of **460** to **459** appeared to stall after approximately 24 h, resulting in diminishing returns and thus a maximum yield of ~80% within a reasonable period of time.

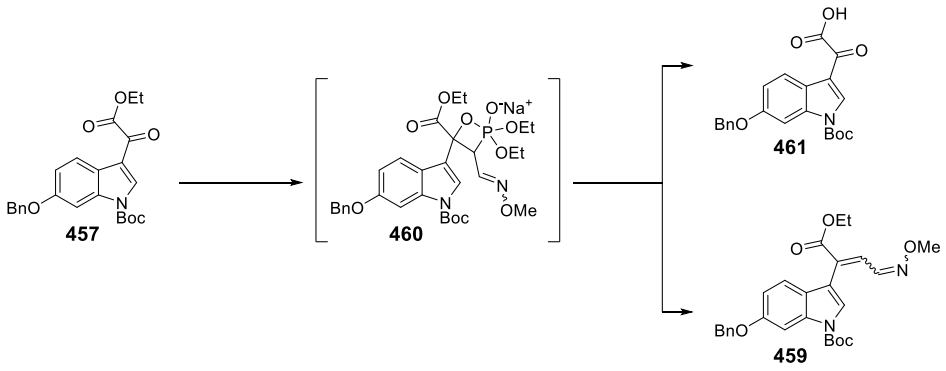

Scheme 78. Generation of the cyclic intermediate **460** from reaction of the phosphonium ylide with **457**, subsequently generating either the oxime **459** or a species that ionises as the acid **461** upon LCMS analysis.

Conversion of **459** to the α-carboline **462** was performed thermally *via* a 6π-electrocyclisation reaction. The reported methodology for this reaction indicates first the base-mediated removal of the *N*-Boc protecting group followed by the requirement for a

temperature of 240 °C under microwave irradiation in 1,2-dichlorobenzene to affect the desired cyclisation.[171] However, after malfunction of our microwave and consequently being required to use traditional heating methods, we found that both the *N*-Boc deprotection and cyclisation reactions proceeded almost quantitatively within 3 h in diphenyl ether at 150 °C without the use of microwave irradiation (Scheme 79); *N*-Boc protecting groups are often thermally labile and so it is unsurprising that such a temperature would result in this deprotection.[179–181]

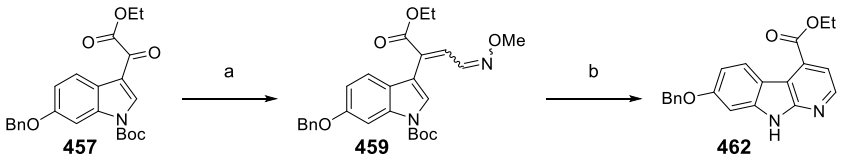

Scheme 79. Generation of the oxime **459** *via* HWE reaction between **457** and **435**, followed by 6π-electrocyclisation to give the α-carboline **462**. *Reagents and conditions*: a) **435**, sodium hydride, THF, 0 °C to rt, N_2, 16 h; b) diphenyl ether, 150 °C, 3 h, 71% over two steps.

Removal of the high boiling point solvent was achievable using column chromatography; however, the product **462** was found to streak on silica, likely due to the insolubility of **462** in cyclohexane, resulting in a reduction of yield. Alternatively, it was found that upon addition of a large quantity of cyclohexane to the reaction mixture, **462** precipitated and was thus isolated in high purity and with improved yield after filtration.

4.4.3 Preparation of the α-carboline *N*-oxide 465 and utilisation of phosphonium-mediated coupling

Whilst the preparation of 2-substituted pyridines from phosphonium-mediated coupling between pyridine *N*-oxides and enolisable substrates is reported in the literature, functionalisation of the ester **463** is not reported. Due to the commercial availability of the **463**, it was hoped that this species would behave as a suitable model substrate for the

optimisation of this reaction before attempting it with a far more precious α-carboline substrate. Thus, our initial efforts sought to determine whether this substrate would react in a similar manner, yielding the desired product **464** (Scheme 80).

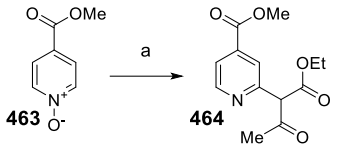

Scheme 80. Generation of the pyridyl 2-acetoacetate **464**, from phosphonium salt mediated coupling between ethyl acetoacetate and the commercially available *N*-oxide **463**. *Reagents and conditions*: a) ethyl acetoacetate, PyBroP, *i*-Pr_2NEt, THF, rt, 16 h, 38%.

Initial attempts revealed that the desired addition to generate **464** did take place, albeit with moderate yield and so to improve the likelihood of successful addition to the desired α-carboline substrate, a rudimentary reaction optimisation screen was performed, assessing the viability of a range of solvents, activating agents, bases, reaction temperatures and reaction protocols (Table 33); each reaction was assessed based on the conversion of **463** to **464** as measured by LCMS.

Entry	Activating agent	Base	Solvent	Temp./°C	Additional comments	**463** : **464**
1	PyBroP	*i*-Pr_2NEt	THF	45	-	1.75 : 1.00
2	PyBroP	*i*-Pr_2NEt	THF	rt	-	1.00 : 1.00
3	PyBroP	*i*-Pr_2NEt	THF	0	-	1.00 : 3.44
4	PyBroP	*i*-Pr_2NEt	THF	-20	-	1.00 : 2.80
5	PyBroP	*i*-Pr_2NEt	THF	rt	4 h addition of PyBroP soln in CH_2Cl_2 to RM	1.30 : 1.00
6	PyBroP	*i*-Pr_2NEt	THF	rt	4 h addition of PyBroP and **463** soln in CH_2Cl_2 to RM*	3.66 : 1.00
7	PyBroP	*i*-Pr_2NEt	THF	rt	5 min addition of PyBroP and **463** soln in CH_2Cl_2 to RM*	1.73 : 1.00
8	PyBroP	*i*-Pr_2NEt	CH_2Cl_2	rt	-	1.00 : 1.00
9	PyBroP	*i*-Pr_2NEt	Ethyl acetate	rt	-	1.35 : 1.00
10	PyBroP	*i*-Pr_2NEt	DMF	rt	-	No conversion
11	PyBroP	*i*-Pr_2NEt	PhMe	rt	-	1.00 : 4.00
12	PyBroP	*i*-Pr_2NEt	PhMe	0	-	1.00 : 4.00
13	PyBroP	*i*-Pr_2NEt	PhOMe	rt	-	1.39 : 1.00
14	PyBroP	*i*-Pr_2NEt	1,4-Dioxane	rt	-	1.29 : 1.00
15	PyBroP	*i*-Pr_2NEt	DME	rt	-	2.30 : 1.00
16	Ac_2O	*i*-Pr_2NEt	THF	rt	-	No conversion
17	TsCl	*i*-Pr_2NEt	THF	rt	-	No conversion
18	CBZCl	*i*-Pr_2NEt	THF	rt	-	No conversion
19	Di-*tert*-butyl dicarbonate	*i*-Pr_2NEt	THF	rt	-	No conversion
20	HATU	*i*-Pr_2NEt	THF	rt	-	No conversion
21	DIC	*i*-Pr_2NEt	THF	rt	-	No conversion
22	T3P	*i*-Pr_2NEt	THF	rt	-	No conversion
23	PyBroP	K_2CO_3	THF	rt	-	No conversion
24	PyBroP	Na_2CO_3	THF	rt	-	No conversion
25	PyBroP	Cs_2CO_3	THF	rt	-	No conversion
26	PyBroP	K_3PO_4	THF	rt	-	No conversion

Table 33. Reaction optimisation of the coupling between ethyl acetoacetate and the *N*-oxide **565** as depicted in Scheme 80; ratios between **463** and **464** were determined using LCMS analysis. RM = reaction mixture. *Reagents and conditions*: a) ethyl acetoacetate, ***activating***

agent, ***base***, ***solvent***, ***temperature***, 16 h. ***463**/PyBroP mixture stirred for 30 min before addition. A general procedure for this reaction screening is provided in the experimental section on page 514.

At rt, toluene was found to facilitate the highest levels of starting material conversion to **464** (Entry 11), whilst THF at 0 °C was found to facilitate a similar yield (Entry 3); raised temperatures appear to hinder the conversion of **463** to **464**. Interestingly, performing the reaction in toluene at 0 °C (Entry 12) provides no additional benefit to the reaction performed at rt (Entry 11); perhaps any stabilising interaction of the *N*-oxide/PyBroP complex by toluene is already maximised at rt, thus reducing the energy of the reaction system has no further effect. Somewhat unsurprisingly, we found that of the activating agents and bases trialled, PyBroP and Pr_2NEt were optimal. Entries 5-7 suggest that the active *N*-oxide/PyBroP complex degrades with time and should be formed *in situ* for optimal levels of starting material conversion to **464**.

Applying these alterations, the desired addition was attempted in order to generate **467** with the *N*-Boc protected carboline **466**, formed *via* oxidation of **463** using mCPBA to give **465**, followed by *N*-Boc protection using di-*tert*-butyl dicarbonate and DMAP (Scheme 81).

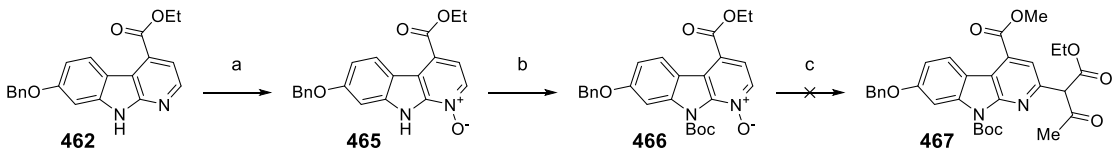

Scheme 81. Oxidation and subsequent *N*-Boc protection of **462** to give **466**, followed by the attempted generation of the 2-substituted carboline **467** *via* PyBroP mediated coupling with ethyl acetoacetate. *Reagents and conditions*: a) mCPBA (77% in water), ethyl acetate, 0 °C to rt, 16 h, 70%; b) di-*tert*-butyl dicarbonate, DMAP, 35 °C, 16 h, 70%; c) ethyl acetoacetate, PyBroP, *i*-Pr_2NEt, toluene, rt - Then again repeated using THF in place of toluene at 0 °C instead of rt with still no reaction observed.

Unfortunately, despite several attempts with varying reaction conditions, no reaction was observed to have taken place. This is perhaps a result of the increased electron density being directed into the pyridyl moiety by the indole-like nitrogen and benzyloxy functionality, reducing the electrophilicity of the 2-position, thus the electronic structure of **466**, and perhaps α-carbolines in general, is so dramatically different to that of a pyridine *N*-oxide, that this methodology is simply unfeasible.

In any case, this methodology was abandoned in favour of alternative synthetic routes.

4.4.4 Preparation of the 2-chloro substrate 474

The generation of 2-chloro pyridines from pyridine *N*-oxides has been reported many times in the literature, typically with use of phosphorous oxychloride (Scheme 82).[182–184]

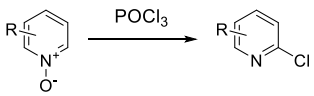

Scheme 82. Regioselective 2-chlorination of pyridine *N*-oxides with phosphorous oxychloride.

Use of these conditions with our own α-carboline substrate **465** did not generate the desired product in any significant yield as indicated by LCMS analysis, and so instead the chlorination of **465** was attempted using methodology reported by Ohshiro *et al*. (Scheme 83).[185]

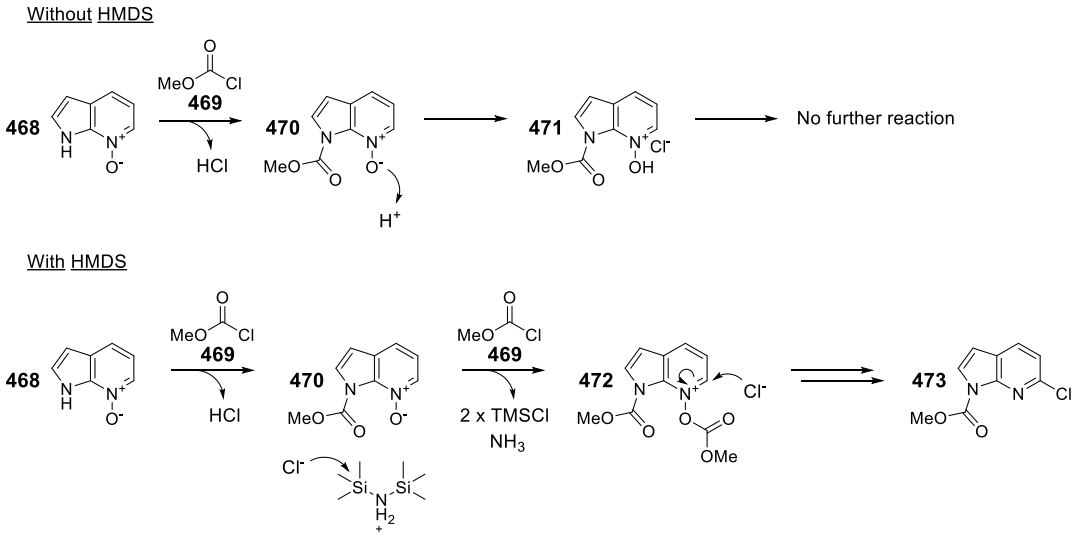

Scheme 83. The proposed effect of HMDS during the regioselective Reissert-Henze-type 2-chlorination of 1*H*-pyrrolo[2,3-*b*]pyridine (7-azaindole) as reported by Ohshiro *et al*.[185]

This methodology facilitates the 2-chlorination of 1*H*-pyrrolo[2,3-*b*]pyridine (7-azaindole) using its *N*-oxide **468** *via* a Reissert-Henze type reaction with methyl chloroformate. From a screen of organic and inorganic bases, Ohshiro *et al*. report that hexamethyldisilazane (HMDS) gives the best yield of 2-chlorinated material, the reason for which is hypothesised to be a result of the unique 'proton trapping' ability exhibited by HMDS.[185] In Reissert-Henze type reactions, unreacted starting material is often recovered as the hydrogen halide salt (**471**) and as such, trapping of the hydrogen halide resulting from acylation of the indole-like N-H or the *N*-oxide is considered to be an effective method for improving the yield of the reaction. Where bases such as Et_3N and DBU form ammonium salts upon contact with the hydrogen halide that can subsequently behave as proton donors, HMDS instead generates ammonia and TMSCl; the ammonia is presumably liberated from the reaction mixture as it forms, whilst TMSCl is free to behave as an additional chlorinating reagent.[185]

Examining these conditions on our own α-carboline substrate **465**, we found that best yields were obtained at an increased reaction temperature of 75 °C, with **474** generated in moderate yield (Scheme 84).

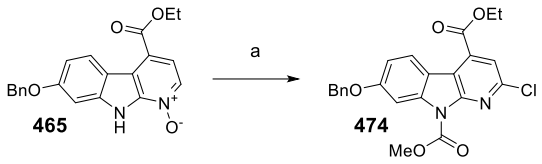

Scheme 84. 2-Chlorination of the *N*-oxide **465** using methyl chloroformate and HMDS, generating **474**. *Reagents and conditions*: a) methyl chloroformate, HMDS, THF, 75 °C, N_2, 16 h, 41%.

As expected, based on the mechanism depicted in Scheme 83, the indole-like nitrogen of **465** was *N*-methyl carbamate protected.

In a similar manner to the HWE reaction discussed previously, we found that this chlorination reaction proceeded *via* an intermediate that slowly converted to the product **474**. However, rather than stalling at the intermediate stage, it appeared that with time, instead of chlorinating to give **474**, a portion of the intermediate broke down to the pyridine **476** (Scheme 85); this by-product seemed to be the major product generated during the attempted chlorination reactions with phosphorous oxychloride.

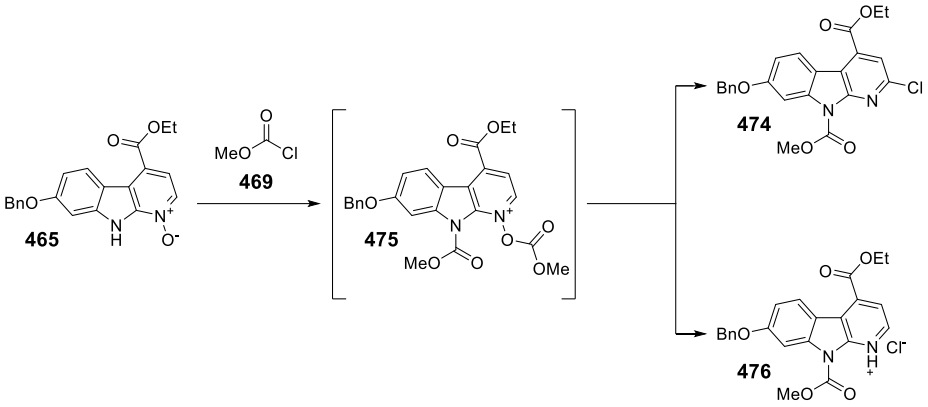

Scheme 85. The intermediate for this reaction (**475**) appears to either react with a chloride anion to give **474** or proceeds to break down to the hydrochloride salt **476**.

4.4.5 Preparation of the (*R*)-solketal derived ester 480

Installation of the acetonide motif was deemed to be appropriate at this stage, as transesterification after the lactone moiety had been introduced would likely cause chemoselectivity issues.

As discussed previously in Section 4.2, methodology reported by Weng *et al*. in which $Fe(acac)_3$ is used as a catalyst to facilitate the transesterification of methyl benzoate (**436**), was identified as suitable for application with **474** (Scheme 86); (*rac*)-solketal is specifically reported as a substrate in this work.[173]

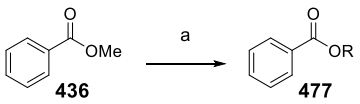

Scheme 86. The $Fe(acac)_3$ catalysed transesterification of methyl benzoate (**436**) as reported by Weng *et al*.[173] *Reagents and conditions*: ***alcohol***, Na_2CO_3 (5 mol%), $Fe(acac)_3$ (5 mol%), *n*-heptane, azeotropic reflux, 18-24 h, **12 examples: 83-98%**. The 12 examples refer to primary and secondary alcohols. Not included are four example of phenolic and tertiary alcohols that either do not react or give particularly poor yields (0-28%).

This methodology found that the transesterification proceeded best in non-polar solvents, specifically *n*-heptane, with fairly significant reductions in yield observed when using polar aprotic solvents (Table 34).

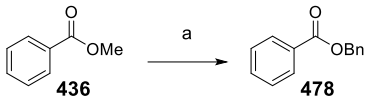

436 **478**

Solvent	Temp./°C	Yield/%
Xylene	80	28
PhMe	80	23
TBME	60	14
THF	70	0
DMF	80	0
n-hexane	70	12
c-hexane	80	42
n-heptane	80	56
n-heptane	100	99

Table 34. The effect of solvent and to an extent, temperature, on the transesterification of benzyl alcohol and methyl benzoate (**436**) to generate benzyl benzoate (**478**) as reported by Weng *et al*.[173] *Reagents and conditions*: $Fe(acac)_3$ (5 mol%), Na_2CO_3 (5 mol%), *solvent*, soxhlet extractor, 4 Å MS, 18-24 h.

As such, to avoid future chemoselectivity issues, the *N*-carbamate functionality was first removed *via* heating of **474** with *tert*-butylamine in methanol, generating the methyl ester **479**. It was found that **479** was entirely insoluble in cyclohexane, allowing purification of **479** *via* trituration, before finally being submitted to the transesterification conditions as described in Scheme 87.

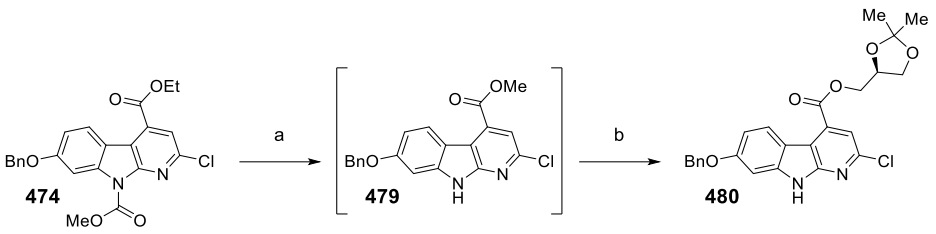

Scheme 87. Removal of the *N*-carbamate functionality followed by transesterification with (*R*)-solketal to give **480**. *Reagents and conditions*: a) *tert*-butylamine, methanol, reflux, 16 h; b) (*R*)-solketal, Na_2CO_3 (5 mol%), $Fe(acac)_3$ (5 mol%), toluene, 120 °C, 7 days, 27% over two steps.

The reaction was unsuccessful in *n*-heptane, likely due to the complete insolubility of **479** and so instead, toluene was used with **480** subsequently generated in poor yield after 7 days; the methyl ester **479** was found to be sparingly soluble in toluene which may help to explain the requirement for such a reaction time. Additionally, the yield of reaction when using toluene as a solvent is reported by Weng *et al.* to be 23% and so it is unsurprising that this reaction required such a significant time cost, whilst still only resulting in a poor yield of product.

With **480** in hand, a number of synthetic approaches were considered for the generation of the 2-lactone carboline structure present in mescengricin.

4.4.6 Coupling of the lactone functionality to 480

Ideally, the lactone fragment would be coupled to **480** in one step to give 584, leaving only simple deprotections to yield the target molecule mescengricin (**5**, Scheme 88); this would ultimately require functionalisation of the lactone fragment in some form to allow for this desired addition.

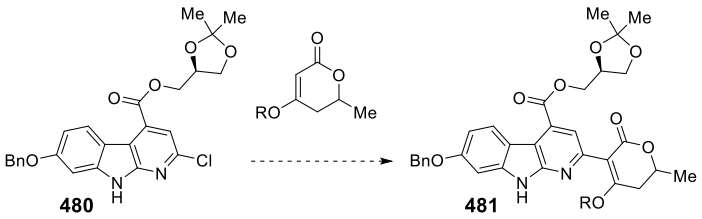

Scheme 88. The proposed coupling of the lactone fragment to the 2-chloro α-carboline substrate **480**.

Three separate methodologies were considered: 1) Heck-like coupling; 2) halogenation of the enol-lactone and 3) formation of an organometallic substrate.

Generation of a halo-lactone substrate was desired as a precursor for the formation of a boronate species, subsequently allowing for use of Suzuki-Miyaura coupling methodologies; preparation of a halo-lactone would additionally present an opportunity to investigate various cross-electrophile coupling methodologies (Scheme 89).

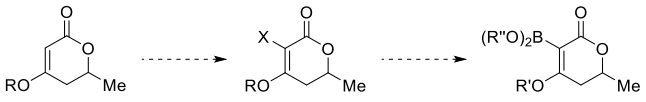

Scheme 89. Halogenation of the lactone to give the halo-lactone substrate, followed by generation of the boronate species; X = halo substituent.

An organometallic species would have similar applications to the halo-lactone in that it itself would be a suitable substrate for direct coupling to **480** but would also be a suitable intermediate for the formation of boronate or halo-substituted species (Scheme 90).

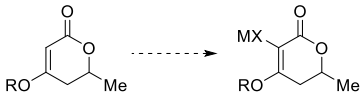

Scheme 90. The proposed generation of the organometallic lactone species resulting from direct metallation of the lactone.

For these synthetic strategies to be effective, the lactone **438** must be 'trapped' in its enol tautomeric form as not only would this maximise the efficacy of methodology targeting the α-position of the lactone, but it would also eliminate any deleterious effects resulting from the presence of the enol O-H moiety that would be possible if the lactone were freely able to tautomerise (Scheme 91).

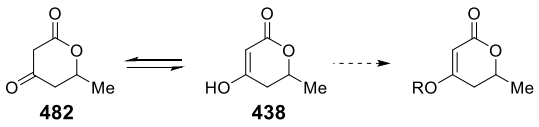

Scheme 91. The proposed 'trapping' of the lactone in its enol tautomeric form, prohibiting it from freely tautomerising.

Several approaches to achieve this outcome were considered: silylation, acetylation and methylation.

Of these methodologies, only methylation resulting from reaction of **438** with DBU and iodomethane in THF to give **483** generated the desired product (Scheme 92); attempts at silylation and acetylation reactions were unsuccessful. Isolation of the methyl enol ether **483** proved to be more difficult than was expected; literature detailing the synthesis of **483** states that purification was achieved *via* sublimation, with the compound exhibiting a melting point of 59-60 °C and so it was thus unsurprising that our attempted purification *via* column chromatography returned only 3% yield due to extended periods of time concentrating **483** *in vacuo*.[186]

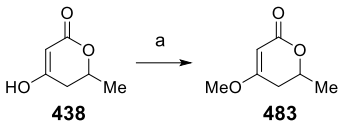

Scheme 92. Generation of methyl enol ether species **483**. *Reagents and conditions*: a) iodomethane, DBU, THF, rt, 16 h, used without purification.

Due to the limited quantity of **438** that was available, sublimation of **483** was not feasible due to the optimisation of this procedure that would no doubt be required and so a decision was made to simply use **483** directly as a crude reaction mixture. Thankfully, some modicum of purification was possible, as it was found that the DBU iodide salt formed during the reaction was insoluble in THF, allowing for its removal from the reaction mixture before further use of **483**.

Using this **483**-containing mixture, several methodologies with the aim of achieving a variety of functionalisations were attempted (Scheme 93).

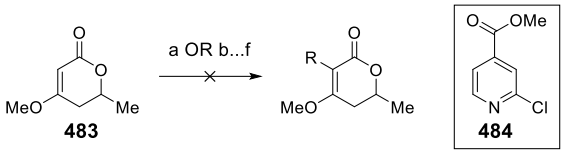

Scheme 93. Attempted functionalisation of the methyl ether lactone **483**. *Reagents and conditions*: a) ICl, AcOH, rt; b) I_2, pyridine, DMF, 0 °C, darkness; c) NIS, AcOH, THF, 50 °C, N_2; d) NBS, $CHCl_3$, 80 °C, N_2; e) B_2Pin_2, $[Ir(OMe)(cod)]_2$ (5 mol%), dtbpy (10 mol%), THF, 80 °C, Ar; f) **484**, Na_2CO_3, PivOH (30 mol%), $Pd(dba)_3$ (2 mol%), PPh_3 (4 mol%), NMP, 129 °C, Ar. R = I, I, Br, BPin and 2-substituted methyl isonicotinate for a-f, respectively.

Unfortunately, all attempted halogenations using ICl, NIS, NBS and elemental iodine were unsuccessful, with no detectable generation of the halo-lactone product. Similarly, both iridium catalysed borylation and palladium catalysed Heck coupling to **483** were unsuccessful with no detectable generation of product.

Finally, the attempted generation of the organometallic species **489** using the Turbo-Hauser base **486** and subsequent coupling to the 2-chloro pyridine **484** (a relatively cheap and commercially available substrate) was also unsuccessful.[187] This particular methodology attempted to closely mimic work reported by Knochel *et al.* in which 5-membered α,β-

unsaturated lactones (**485**) were coupled to a range of electrophiles at the α-position, using the previously mentioned Turbo-Hauser bases (**486**, Scheme 94).[187]

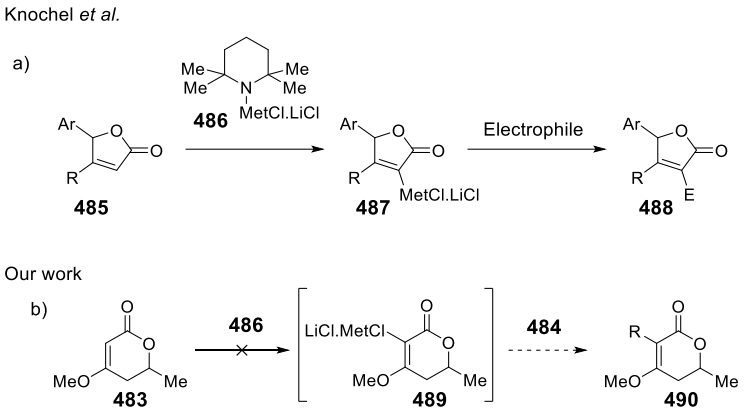

Scheme 94. a) Direct metalation of lactones (**485**) using TMPMetCl.LiCl (**486**) and subsequent addition to electrophiles as reported by Knochel *et al.*;[187] b) The proposed application of this work to fulfil our own requirements, by metalation of the lactone **483** and subsequent addition to the 2-chloropyridine **484**; Met = Zn or Mg.

Despite the failed generation of the organometallic species **489**, the significant volume of methodology surrounding the preparation of organometallic substrates from enol ethers and other such related species, in particular by Knochel *et al.*, leads us to believe that this is an avenue of research that may greatly benefit any future work focussed on the total synthesis of mescengricin.

4.4.6.1 Attempted preparation and subsequent functionalisation of a lactone precursor

With each attempted functionalisation of **483** failing, efforts were made to prepare a lactone precursor fragment that would be suitable for cross-coupling to the carboline core **480**; this fragment was determined to be the dioxinone **491** (Figure 68).

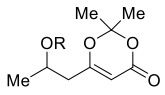

491

Figure 68. The dioxinone **491**, identified as a suitable lactone-precursor fragment for coupling to the α-carboline core **480**.

Whilst lacking the convenience of coupling the pre-formed lactone fragment (as depicted in Scheme 88), it was hypothesised that coupling an *O*-protected dioxinone species would allow for a single global deprotection/cyclisation step at the penultimate stage of the synthesis of mescengricin (**5**), ultimately compensating for the fact that the lactone moiety was not pre-formed upon coupling to **480** (Scheme 95).

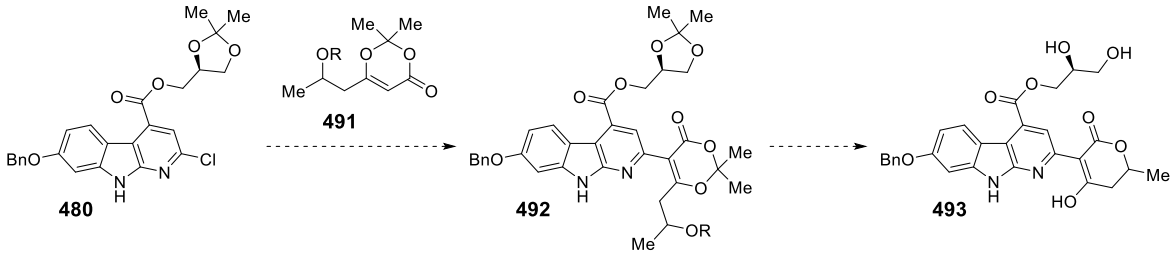

Scheme 95. The proposed coupling of the dioxinone **491** to **480**, followed by a global acid-catalysed deprotection and cyclisation to generate *O*-benzyl mescengricin (**493**).

The reported preparation of the dioxinone boronate species **497** from the iodo-substituted dioxinone **496**, itself a product of dioxinone formation and subsequent iodination from *tert*-butyl acetoacetate (**494**), led us to believe that a similar outcome could be achieved using the lactone precursor **498** (Scheme 96).[188,189]

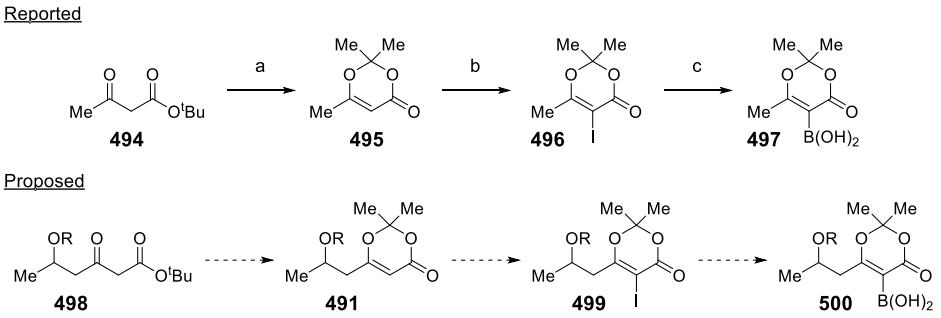

Scheme 96. The reported synthesis of the iodo species **496** from *tert*-butyl acetoacetate (**494**) as reported by Takahashi *et al.* and the subsequent preparation of the desired boronate species **497** as reported by Senanayake *et al*.[188,189] This methodology was proposed as a route to generate the ether boronate species **500**. *Reagents and conditions*: a) acetone, conc. H_2SO_4, acetic anhydride, 0 °C, 5 h, quant.; b) NIS, AcOH, rt, Ar, 8 h, dark, 86 %; c) i) *bis*[2-(*N*,*N*-dimethylaminoethyl)] ether, *i*-PrMgCl (2M in THF), THF, 15 °C, 20 min ii) **499**, rt, 10 min; iii) $B(OMe)_3$, 0 °C, 89%.

In this work, **494** is treated with conc. H_2SO_4, acetic anhydride and acetone to form the dioxinone **495**. The iodo species **496** is then formed upon reaction of **495** with NIS, which is in turn treated sequentially with *i*-PrMgCl and trimethyl borate to give the boronic acid **497**.

Thus, **503** was prepared *via* Claisen condensation between *tert*-butyl acetate and **502** (itself a product of silylation of **501** with TBSCl). The silyl ether **503** was subsequently treated with conc. H_2SO_4, acetic anhydride and acetone, following significant literature precedent, in an attempt to form the dioxinone **504** (Scheme 97).

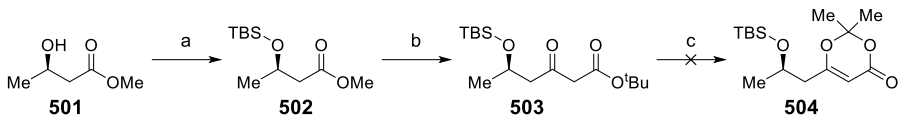

Scheme 97. Attempted preparation of the dioxinone **504** from the *O*-TBS protected keto-ester **503**, itself prepared *via* silylation and subsequent Claisen condensation from the hydroxyester **501**. *Reagents and conditions*: a) TMSCl, imidazole, CH_2Cl_2, 0 °C to rt, 16 h, 86%; b) i) *i*-Pr_2NH, ^{n}BuLi (2.5M in hexanes), THF, 0 °C, 45 min; ii) *tert*-butyl acetate, -78 °C, 1.5 h; iii) **501**, 16 h, 81%; c) conc. H_2SO_4, acetic anhydride, acetone, 0 °C, N_2.

Unfortunately, this reaction was largely unsuccessful, with only trace amounts of **504** being detected by LCMS. This is likely due to the *O*-silyl deprotection of **503** under acidic conditions and subsequent unchecked reaction of the hydroxyl moiety with both **503** and acetic anhydride.

As such, the benzyl ether **506** was prepared to improve the overall stability of the molecule in the dioxinone forming reaction. The ketoester **506** was prepared in much the same way as **503**, *via* Claisen condensation between *tert*-butyl acetate and **505** (Scheme 98); the generation of **505** is achieved upon *O*-benzylation of **501** with benzyl 2,2,2-trichloroacetimidate.

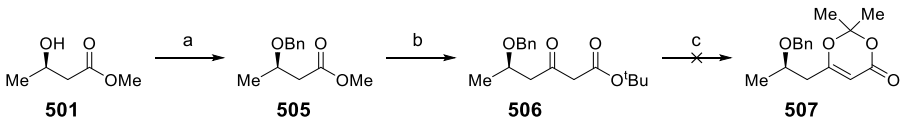

Scheme 98. Attempted preparation of the dioxinone **507** from the *O*-benzyl protected keto-ester **506**, itself prepared *via* benzylation and subsequent Claisen condensation from the hydroxy-ester **501**. *Reagents and conditions*: a) benzyl 2,2,2-trichloroacetimidate, TfOH, CH_2Cl_2/cyclohexane (1:2), 0 °C to rt, N_2, 16 h, 86%; b) i) *i*-Pr_2NH, ^{n}BuLi (2.5M in hexanes), THF, 0 °C, 45 min; ii) *tert*-butyl acetate, -78 °C, 1.5 h; iii) **505**, 64 h, 85%; c) conc. H_2SO_4, acetic anhydride, acetone, 0 °C, N_2.

Upon submitting **506** to the same dioxinone forming conditions as **503**, it became clear that **507** was not forming and upon TLC analysis, more than 8 separate entities were detected. This was perhaps a consequence of acid mediated *O*-debenzylation, an outcome that was not foreseen to have taken place to this extent, followed by a similar unchecked sequence of reactions as seen with **503**.

4.5 Discussion of future strategies towards the synthesis of mescengricin

Unfortunately, due to time constraints, no further experimental work was undertaken in the attempted solving of this synthetic challenge and so for the time being, the total synthesis of mescengricin remains unreported; there are however, several promising methodologies that, given more time, we would have utilised in our efforts.

Moving forward, we believe that isolation of **483** *via* sublimation on a large scale would be both necessary and vital for the full evaluation of the efficacy of methodology utilising Turbo-Hauser bases and other such similar reagents.

If after full evaluation of these methodologies it became clear that the desired structural transformation was not possible, there are alternative synthetic routes that may successfully lead to the preparation of mescengricin.

Markey reports successful reaction between the ketone-derived oxime **508** and the indole **434** to give **414**, ultimately allowing formation of the 2-methyl α-carboline **424** in good yield, and so it is proposed that the lactone-oxime fragment **514** be prepared to allow subsequent formation of the 6π-electrocyclisation precursor compound **515** *via* HWE reaction between **514** and **457** (Scheme 99).[172]

Reaction between 4-hydroxycoumarin (**509**) and acetyl chloride (**510**) is reported to proceed in good yield to give **511** and so initial attempts at the preparation of **513** would likely be performed using the previously described lactone **438** and the commercially available acid chloride **512**;[190] subsequent alkylation followed by condensation with *O*-methyl hydroxylamine hydrochloride would generate the required HWE reagent **514**.

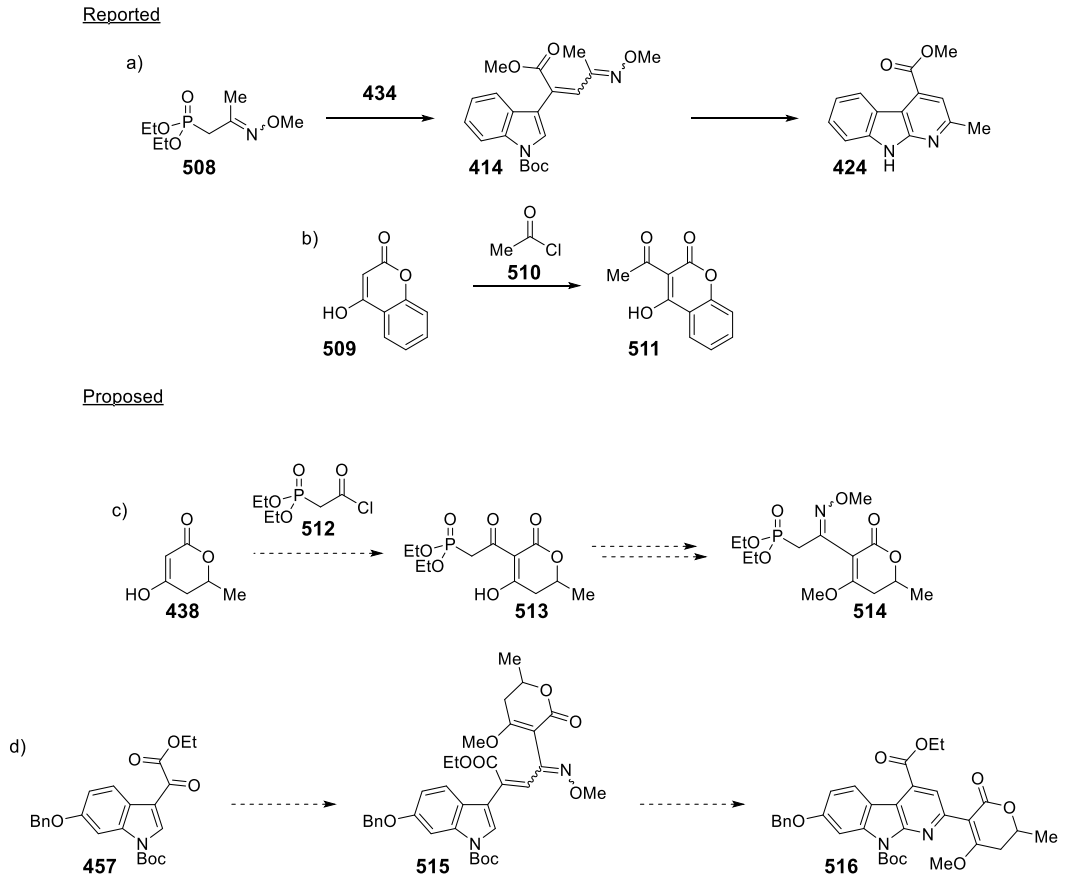

Scheme 99. a) The reported preparation of the 2-methyl carboline **424** from the ketone derived oxime **508**;[172] b) The reaction between 4-hydroxycoumarin (**509**) and acetyl chloride (**510**) to give the α-acetyl lactone **511**;[190] c) The proposed generation of the oxime **513** upon reaction of **438** with the acid chloride **512**, alkylation and subsequent condensation with *O*-methyl hydroxylamine hydrochloride to form the oxime **514**; d) HWE reaction of **514** with the ketone **457** to generate the 6π-electrocyclisation precursor **515** and ultimately the 2-lactone carboline substrate **516**.

Even if this approach were found to be successful, further difficulties stemming from various chemoselectivity issues such as during the subsequent transesterification step are likely to be experienced, and so whilst installation of the lactone at this early stage may be feasible, it may in fact be more appropriate for it to be introduced at a later stage, as originally intended.

Alternatively, the dioxinone fragment could be prepared from the commercially available dioxinone **495** *via* deprotonation with lithium hexamethyldisilazane and reaction with acetyl chloride to give **517**, followed by reduction with lithium aluminium hydride to give the racemic alcohol **518** (Scheme 100).

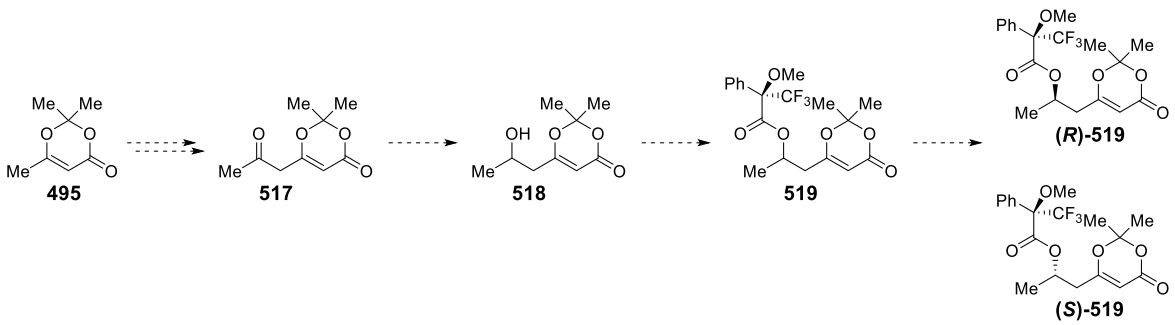

Scheme 100. The proposed synthetic route to generate a racemic mixture of the alcohol **518**, followed by derivatisation with Mosher's acid, allowing for separation of diastereomers and thus by extension, separation of (*R*) and (*S*) enantiomers of **519** (**(*R*)-519** and **(*S*)-519**, respectively).

Derivatisation of **518** with an enantiomerically pure reagent such as Mosher's acid, subsequently forming diastereomers, would allow separation of **(*R*)-519** and **(*S*)-519** using conventional purification methods.

Chemoselectivity issues may be encountered if after subsequent functionalisation, the dioxinone fragments were to be coupled to the carboline **480** before removal of the 'Mosher's acid' derived ester; hydrolysis of these esters is traditionally performed using

aqueous hydroxides, methodology that would be incompatible with the (*R*)-solketal-derived ester present on **480**. As such, it may be necessary to remove the Mosher's acid functionality after separation of the diastereomers **(*R*)-519** and **(*S*)-519**, subsequently protecting the newly formed alcohols with a group that will ultimately require *O*-deprotection conditions that would be tolerated by other functionalities within the molecule, such as silyl or benzyl ethers (Scheme 101).

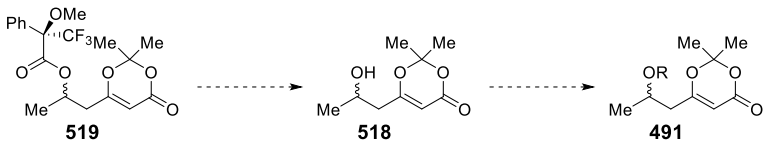

Scheme 101. Saponification of the 'Mosher's acid' derived ester to give **521** as an enantiopure substrate, followed by *O*-protection to give the dioxinone/ether substrate **491**.

With these protected dioxinone species in hand, the boronate species **(*R*)-522** and **(*S*)-522** may thus be prepared upon reaction of **(*R*)-520** and **(*S*)-520** with NIS to give **(*R*)-521** and **(*S*)-521**, and subsequent reaction with *i*-PrMgCl and trimethyl borate to give the desired products as initially proposed in Section 4.4.4.1 of this thesis (Scheme 102).

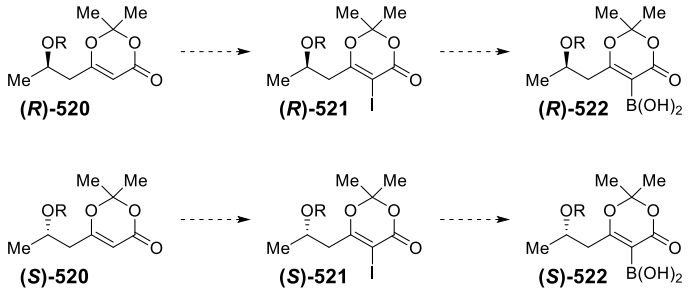

Scheme 102. Preparation of the boronate species **(*R*)-522** and **(*S*)-522** from the enantiopure dioxinones **(*R*)-520** and **(*R*)-520**.

These boronate species would then be coupled *via* Suzuki-Miyaura reaction to the chloro-species **480**, giving the mescengricin precursors **(*R*)-523** and **(*R*)-523** (Scheme 103).

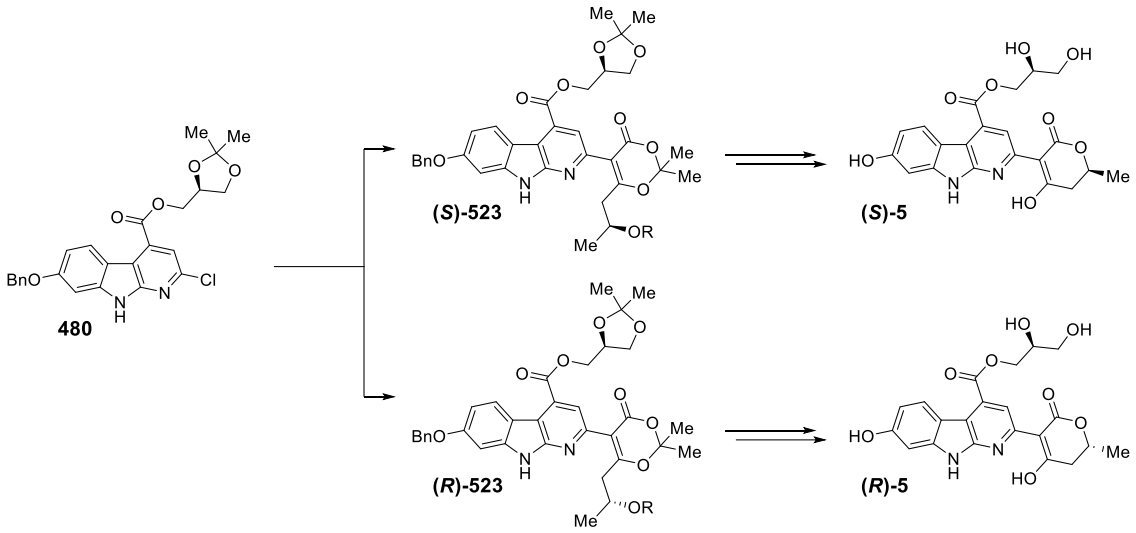

Scheme 103. The proposed coupling of **(*S*)-522** and **(*R*)-522** to the 2-chloro-carboline species **480**, followed by global deprotection/cyclisation and hydrogenation to give both (*S,S*) and (*S,R*) diastereomers of mescengricin (**(*S*)-5** and **(*R*)-5**, respectively).

Following global acid catalysed deprotection and cyclisation, and a final debenzylation reaction, both diastereomers of mescengricin, **(*S*)-5** and **(*R*)-5**, would be successfully prepared and isolated, allowing elucidation of the chirality of the C-2 position in the lactone moiety (Scheme 57), thus confirming the structure and completing the total synthesis of mescengricin more than two decades after its discovery.[150]

With the work described in this thesis and those authored by Markey and Wadsworth, there now exists a fairly substantial resource on which future researchers may base their work upon in the pursuit of this synthetic target, listing both methodologies in which there is little point pursuing and those from which success may be attained.[170,172]

Experimental section

5. Experimental

5.1 General experimental

General information All chemicals used were purchased from Sigma-Aldrich, Across Organics, Alfa Aesar, Enamine or Fluorochem. All reagents were used without further purification. Solvents were dried over 3 Å molecular sieves for 24 h before use. **Analytical thin-layer chromatography** was carried out on aluminium-backed plates coated with Merck Kieselgel 60 GF254 or Merck Kieselgel 60 NH2 F254S. TLC plates were visualised under UV light (254 or 365 nm) and/ or stained with the appropriate staining solution. The staining solution, basic aqueous potassium permanganate ($KMnO_4$), is reported when used. **NMR** analysis was performed on a Bruker 400 MHz spectrometer operating at 400 MHz for ^{1}H-NMR (δ_H) and 101 MHz for ^{13}C-NMR (δ_C). A 500 MHz Bruker spectrometer equipped with a cryoprobe, operating at 500 MHz for ^{1}H-NMR (δ_H) and 126 MHz for ^{13}C-NMR (δ_C) was also used for analysis of some examples. A 700 MHz Bruker spectrometer operating at 700 MHz for ^{1}H-NMR (δ_H) was used for analysis of all late-stage functionalised compounds. Samples were run in deuterated chloroform ($CDCl_3$), deuterated methanol (CD_3OD) or deuterated dimethyl sulfoxide (DMSO-d_6) as appropriate. Chemical shifts are quoted in parts per million (ppm), referenced to residual chloroform (7.26 ppm for ^{1}H NMR, 77.16 ppm for ^{13}C NMR), methanol (3.31 ppm for ^{1}H NMR, 49.00 ppm for ^{13}C NMR) and DMSO (2.50 ppm for ^{1}H NMR, 39.52 ppm for ^{13}C NMR) as internal standards and coupling constants (*J*) are quoted in Hz. Multiplicities are as follows: s-singlet, d-doublet, t-triplet, q-quartet, hept-heptet, dd-doublet of doublets, dt-doublet of triplets, dq-doublet of quartets, tt-triplet of triplets, tq-triplet of quartets, ddd-doublet of doublet of doublets, m-multiplet, bs-broad singlet or combinations thereof. Assignments of rotameric carbons are indicated with an asterisk where necessary e.g., (CH_2*). Carbon shifts assigned *via* HSQC are approximate due to the lack of a suitable

solvent reference point and the inherent inaccuracy associated with assigning NMR from HSQC spectra. **Infrared** (ν_{max}) analysis was carried out on a Bruker Alpha Platinum ATR single reflection diamond module spectrometer over the range of 4000–600 cm^{-1}. **Melting points** (MP) were determined using a Stuart SMP20 melting point apparatus and the values are expressed in degrees Celsius (°C). The parameters for the melting point analysis were set at 5 °C per minute ramp and melting point was determined manually. Melting points are uncorrected. **High resolution mass spectrometry** (HRMS) with accurate mass measurement to four decimal places was obtained for all new compounds described. Mass spectra were recorded on a Bruker MicroTOF 61 mass spectrometer using electrospray ionization (ESI). *m/z* values are reported in Daltons. **HPLC** for reaction monitoring used an Agilent 1200 system, with a standard gradient elution method: Waters XBridge 2.1x30 mm column, stationary phase C_{18} 3.5 µm, 0.8 mL/min flow rate, detection at 254 nm; elution with 5-95% acetonitrile/0.1% $NH_{3(aq)}$ over 4 minutes. Reaction monitoring and final purity values for all late-stage functionalised compounds was carried out on an Acquity UPLC CSH C18 column (2.1 mm × 50 mm i.d. 1.7 µm packing diameter) at 40 °C eluting with 10 mM NH_4HCO_3 in water adjusted to pH 10 with aqueous NH_3 (solvent A) and acetonitrile (solvent B), using the following elution gradient for the BEH column: 0.0-1.5 min 0−97% B, 1.5-1.9 min 97% B, and 1.9-2.0 min 97−0% B. **Chromatographic purifications** were performed on a Biotage SP4 with Puriflash 30 µm silica gel prepacked flash chromatography cartridges using an ethyl acetate/light petroleum or methanol/CH_2Cl_2 gradient elution system with manual fraction collection. UV detector wavelength was set at 254 nm. **Mass-directed auto purification** was performed using a CAT Mass Directed AutoPrep on a Xbridge C18 column (100 mm × 30 mm i.d. 5 µm packing diameter) at ambient temperature eluting with 10 mM NH_4HCO_3 in water adjusted to pH 10 with NH_3 and acetonitrile (solvent B), using an appropriate elution gradient over 10 min at a flow rate of 40 mL/min and detecting at 210−350 nm at room temperature. **Waters Oasis™** HLB cartridges were used for the removal of Li^+ to yield final compounds as

the free acid. **Chiral chromatography** (supercritical fluid chromatography (SFC)) to determine enantiomeric excess was undertaken at Reach Separations, Bio City, Nottingham, UK. Analyses to determine enantiomeric excess were performed using a Waters UPC SFC. Chromatography conditions: Method A: Lux A2 (4.6mm x 250mm, 5um) column, eluting with isocratic conditions: methanol/CO_2 (30:70, 0.2% v/v NH_3). Method B: Lux C4 5µm 4.6 x 250 mm column. Mobile phase 05:95 ethanol (+0.2% NH_3 v/v):CO_2. Flow rate 4 mL/min UV detection at 210-400nm. BPR 125 Bar. Column temperature 40 °C. Method C: Chiralpak IG 5µm 4.6 x 250 mm column. Mobile phase 15:85 ethanol (+0.2% NH_3 v/v):CO_2. Flow rate 4 mL/min UV detection at 210-400nm. BPR 125 Bar. Column temperature 40 °C. ***In vacuo*** refers to the use of a Vaccubrand CVC 3000 vacuum pump to remove solvent under reduced pressure on a Büchi Rotavapor R-3000 or Heidolph Vei-Vap Value G3 apparatus, with a water bath at 40 °C. **Microwave reactions** were carried out using a Biotage Initiator 2.0. **Miscellaneous:** Brine refers to aqueous saturated solution of sodium chloride.

5.2 Cell adhesion assay, ChromLogD measurement and HTP measurement protocols

The cell adhesion assay is prepared and performed as follows: The assay plates are coated with GST-LAP; a peptide that has an affinity for the integrin being screened against. The excess peptide is removed, before the cells are filled with a $MgCl_2$ containing media that is required for cell adhesion. The compound being screened is diluted to different concentrations in the $MgCl_2$ containing media and added to the assay plates. At this point the integrin cells are added to the media, diluted to the required concentration and then added to the assay plates before being incubated for 30 min. The assay plates are washed with a buffer solution, the cells detached using Triton X-100 and then shaken for five min before being read on an EnVision® plate reader and a 7-point dose response curve produced from which the IC_{50} and subsequently the pIC_{50} value of each integrin subtype is obtained;[83,191] a visual representation of this process is provided in Figure 69.

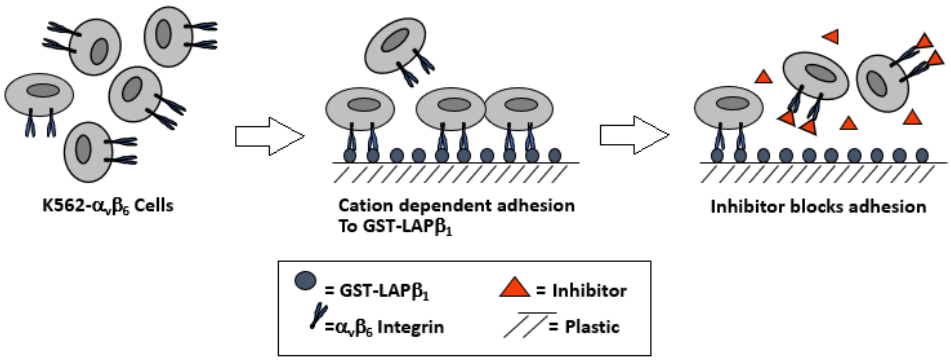

Figure 69. Visual depiction of the $\alpha_v\beta_6$ integrin assay used to determine the pharmacological characteristics of integrin inhibitors;[83,191] the assay is performed in the same way for each relevant integrin.

ChromLogD values were measured by GSK researchers using a protocol as described by Hill *et al*.[85]

HTP values were measured by GSK researchers using a protocol as described by Gubernator *et al*.[86]

5.3 Experimental data relating to the crystal structure depicted in Figure 322 (Section 2.2.2)

5.3.1 Crystal data and structure refinement

Empirical formula	$C_{17}H_{26}BrNO_3S$
Formula weight	404.36
Temperature/K	120(2)
Crystal system	monoclinic
Space group	$P2_1$
a/Å	12.78840(10)
b/Å	9.91640(10)
c/Å	31.2565(3)
α/°	90
β/°	90.0030(10)
γ/°	90
Volume/Å^3	3963.79(6)
Z	8
ρ_{calc}g/cm^3	1.355
μ/mm^{-1}	3.916
F(000)	1680.0
Crystal size/mm^3	0.172 × 0.078 × 0.046
Radiation	CuKα (λ = 1.54184)
2Θ range for data collection/°	7.468 to 154.018
Index ranges	-16 ≤ h ≤ 16, -12 ≤ k ≤ 11, -39 ≤ l ≤ 39
Reflections collected	75013
Independent reflections	15492 [R_{int} = 0.0334, R_{sigma} = 0.0254]
Data/restraints/parameters	15492/3413/1122
Goodness-of-fit on F^2	1.028
Final R indexes [I>=2σ (I)]	R_1 = 0.0269, wR_2 = 0.0679
Final R indexes [all data]	R_1 = 0.0275, wR_2 = 0.0684
Largest diff. peak/hole / e Å^{-3}	0.64/-0.46
Flack parameter	-0.012(5)

5.3.2 Experimental method

Suitable crystals of **106** for crystallographic analysis were obtained upon recrystallisation of **106** from *iso*-propyl alcohol.

SuperNova Duo Singular

The single crystal was selected and mounted using Fomblin® (YR-1800 perfluoropolyether oil) on a polymer-tipped MiTeGen MicroMountTM and cooled rapidly to 120 K in a stream of cold nitrogen using an Oxford Cryosystems open flow cryostat.[192] Single crystal X-ray diffraction data were collected on an SuperNova Duo diffractometer (Atlas CCD area detector, mirror-monochromated Cu-Kα radiation source; λ = 1.54184 Å; ω scans). Cell parameters were refined from the observed positions of all strong reflections and absorption corrections were applied using a Gaussian numerical method with beam profile correction (CrysAlisPro).[193] The structure was solved within Olex2 by dual space iterative methods (SHELXT) least squares refinement of the structure was carried using (SHELXL).[194–196] Structures were checked with checkCIF.[197] CCDC-1965462 contains the supplementary data for this compound. These data can be obtained free of charge from The Cambridge Crystallographic Data Centre *via* www.ccdc.cam.ac.uk/data_request/cif.

5.3.3 Refinement

The monoclinic crystal, solved in space group P2(1), has a beta angle close to 90° (90.003(1)); it was refined as a 2-component twin with law {1 0 0 0 -1 0 0 0 -1}. The batch scale factor for the two twin components refined to a value of 0.461(1) and the Flack parameter refined to a value of -0.012(5).

The structure has Z'=4; two residues of each handedness are present in the asymmetric unit. All four residues exhibit conformational disorder of the 3-bromophenyl moieties. All eight 3-

bromophenyl moieties are restrained to have similar (SAME) and planar (FLAT) geometries. The occupancies of all four pairs of moieties are refined and constrained to sum to unity giving values for the major components of 0.90(1), 0.82(1), 0.80(1) and 0.92(1).

Rigid bond (RIGU) and similarity restraints (SIMU) have been applied to the anisotropic displacement parameters of all atoms in the structure. The ADP's of bromine atoms Br1X and BR1Y (both minor disorder components) are restrained to have more isotropic character (ISOR).

All hydrogen atoms were observed in the electron density map. The hydrogen atom positions for the sulfinamide N-H groups are refined and restrained to have an N-H distance of 0.9 A. All other hydrogen atoms were geometrically placed and refined with a riding model.

5.4 HPLC analysis of (*S*)-119 and 119 as described in Section 2.2.2

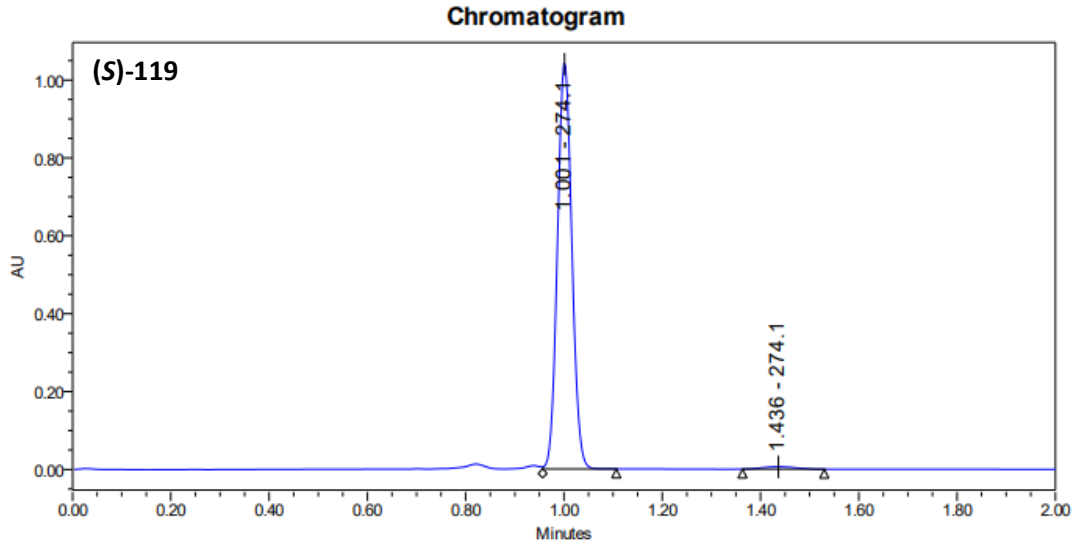

Peak Results

	Retention Time (min)	Area (µV*sec)	% Area	Width @ 50%
1	1.00	2118283	98.7	0.03168
2	1.44	27529	1.3	0.07355

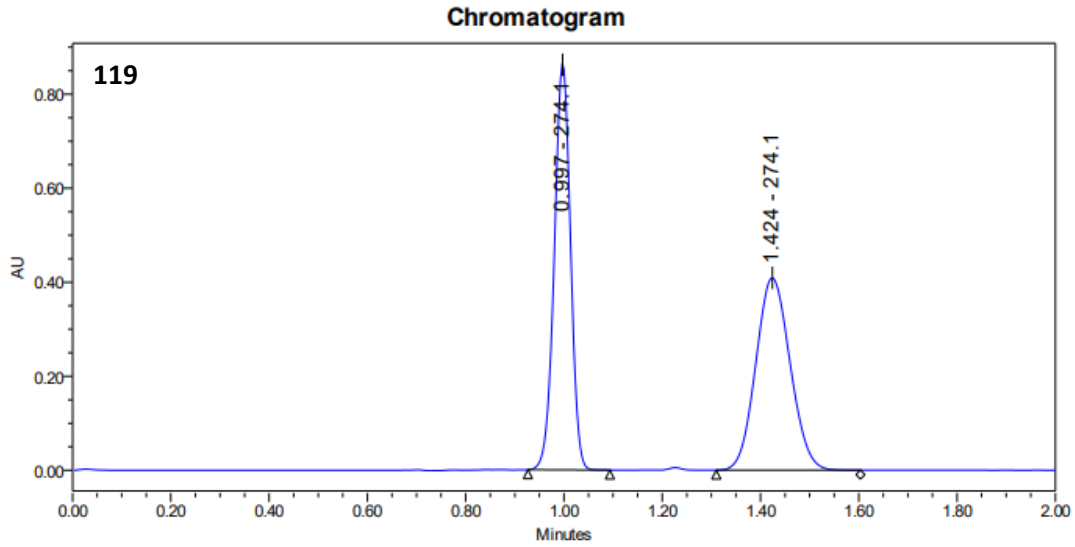

Peak Results

	Retention Time (min)	Area (µV*sec)	% Area	Width @ 50%
1	1.00	1979897	49.9	0.03545
2	1.42	1985051	50.1	0.07590

5.5 HPLC analysis of (*S*)-326 and 326 as described in Section 3.2.1

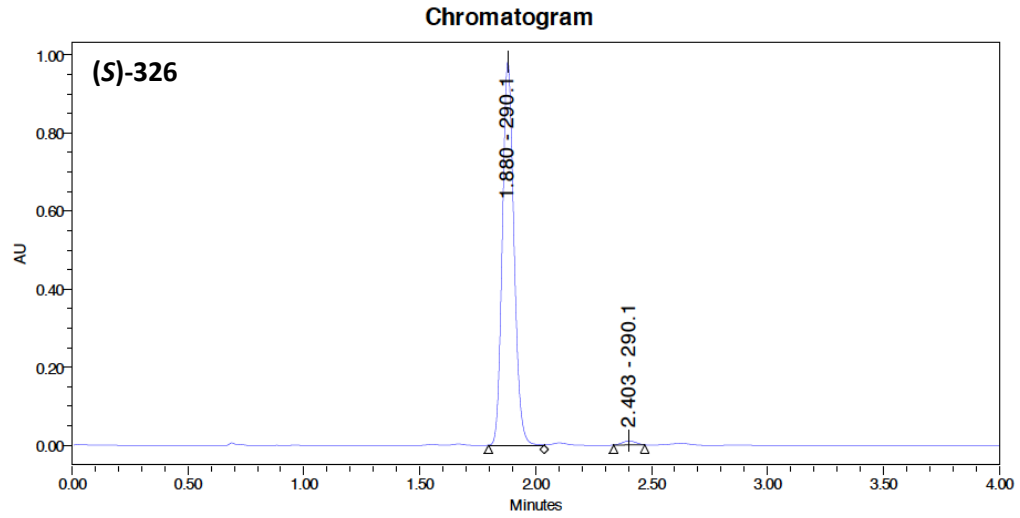

Peak Results

	Retention Time (min)	Area (μV*sec)	% Area	Width @ 50%
1	1.88	3416337	98.8	0.05334
2	2.40	39808	1.2	0.06562

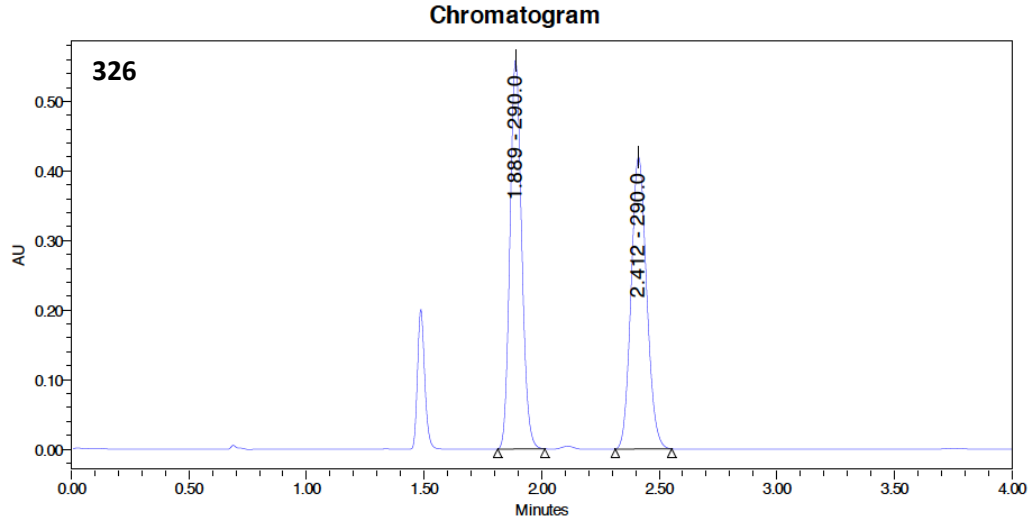

Peak Results

	Retention Time (min)	Area (μV*sec)	% Area	Width @ 50%
1	1.89	1927834	50.0	0.05307
2	2.41	1930947	50.0	0.07127

5.6 Experimental method relating to all molecular modelling

Docking was undertaken using OpenEye Scientific's toolkit, with conformers generated using OMEGA then docked using FRED.[198,199] A conformer library is generated by rotating bonds and individual conformers scored energetically using a modified version of the MMFF94s forcefield, with electrostatic and van der Waals terms removed. Conformers higher in energy than 20 kcal mol^{-1} from the lowest energy conformer are removed, as are conformers within 0.25 Å RMSD of any other. This set of conformers is then ready to be docked. Receptors were generated from the $\alpha_v\beta_3$ and $\alpha_v\beta_6$ crystal structures 1L5G and 4UM9, respectively, from the Protein Databank. A grid with points spaced 0.5 Å apart is set in the receptor binding site and conformers placed at each individual point and scored using chemguass3. Compounds that do not satisfy a set of restraints are immediately excluded, namely a bidentate hydrogen bond with Asp218 and a metal chelate interaction with the MIDAS Mn^{2+}/Mg^{2+} ion. Poses that satisfy these undergo a secondary optimisation step. Here the conformer is translated and rotated through a half step, generating 3^6 (729) additional poses that are scored using the enhanced chemgauss4 scoring function. Chemgauss4 models directionality in hydrogen bond and chelate interactions.

As pertaining to Figure 41: the scores (arbitrary units) for the monosubstituted compound **203**, docked in $\alpha_v\beta_6$ and $\alpha_v\beta_3$, were -15.9 and -14.5, respectively.

As pertaining to Figure 53: the scores (arbitrary units) for the 3,5-disubstituted compound **291**, docked in $\alpha_v\beta_6$ and $\alpha_v\beta_3$, were -15.8 and -11.3, respectively.

5.7 Experimental details and copies of ^{1}H and ^{13}C NMR spectra

Lithium 5-(8-(*tert*-butoxycarbonyl)-5,6,7,8-tetrahydro-1,8-naphthyridin-2-yl)pentanoate (**82**)

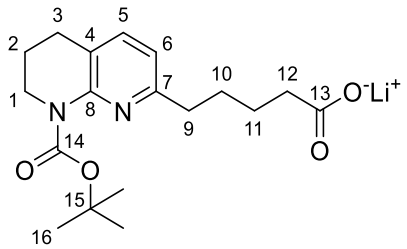

To a stirred solution of **81** (1.00 g, 2.87 mmol) in THF/water (7.50 mL, 4:1) was added lithium hydroxide monohydrate (241 mg, 5.74 mmol). The reaction mixture was stirred at rt for 4 h and the solvent removed *in vacuo* to give the title compound as a pale yellow solid (1.13 g, 3.32 mmol). The crude product was not purified further; **HRMS** *m/z* (ESI^+) calc. for $C_{18}H_{27}N_2O_4$ $[M+H]^+$ requires 335.1965, found 335.1972; $\boldsymbol{R_f}$ 0.70, 10% methanol/CH_2Cl_2, UV active; δ_H (400 MHz, DMSO) 7.37 (1H, d, *J* = 7.6 Hz, H-5), 6.85 (1H, d, *J* = 7.6 Hz, H-6), 3.65 – 3.56 (2H, m, H-1), 2.67 (2H, t, *J* = 6.6 Hz, H-3), 2.57 (2H, t, *J* = 7.6 Hz, H-9), 1.91 (2H, t, *J* = 7.5 Hz, H-12), 1.85 – 1.72 (2H, m, H-2), 1.66 – 1.55 (2H, m, H-10), 1.51 – 1.37 (11H, m, H-11 and H-16); δ_C (101 MHz, DMSO) 177.4 (CO), 157.8 (C), 153.7 (CO), 150.5 (C), 137.1 (ArH), 121.3 (C), 118.0 (ArH), 79.7 (C), 44.3 (CH_2), 38.2 (CH_2), 37.3 (CH_2), 29.5 (CH_2), 28.0 (CH_3), 26.2 (CH_2), 25.4 (CH_2), 22.9 (CH_2); ν_{max} (FT-ATR/cm^{-1}) 3299, 1692, 1570, 1148, 1031.

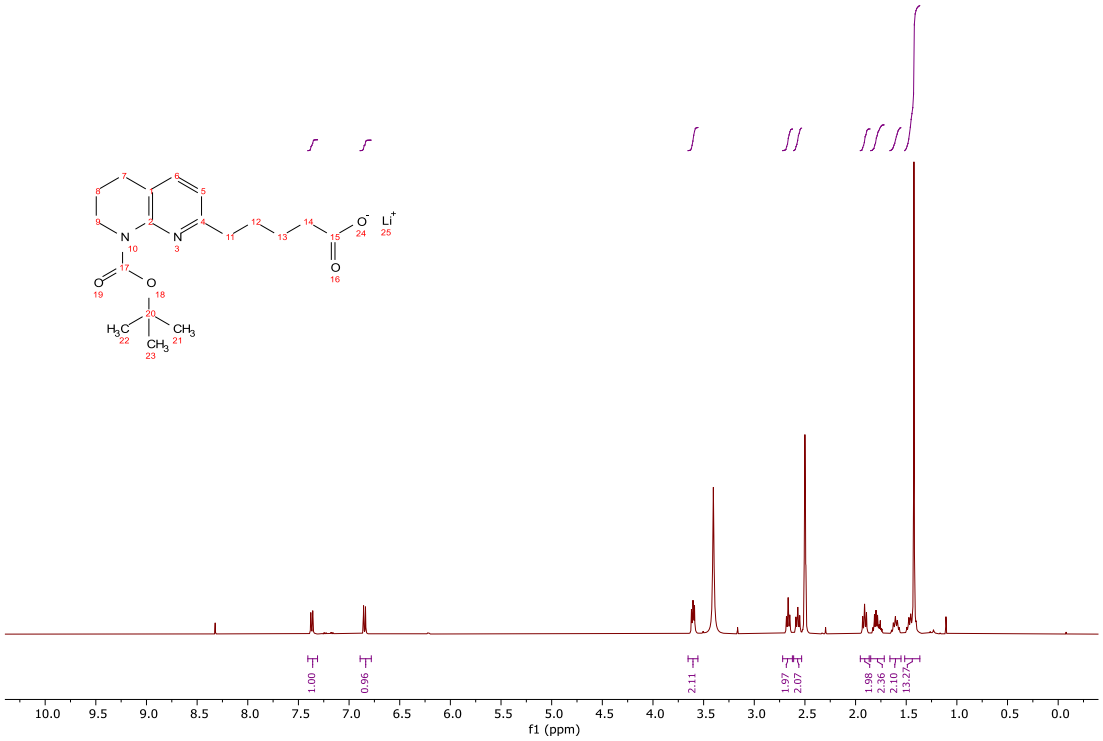
1.00
0.96
2.11
1.97
2.07
1.98
2.36
2.10
13.27
10.0 9.5 9.0 8.5 8.0 7.5 7.0 6.5 6.0 5.5 5.0 4.5 4.0 3.5 3.0 2.5 2.0 1.5 1.0 0.5 0.0
f1 (ppm)

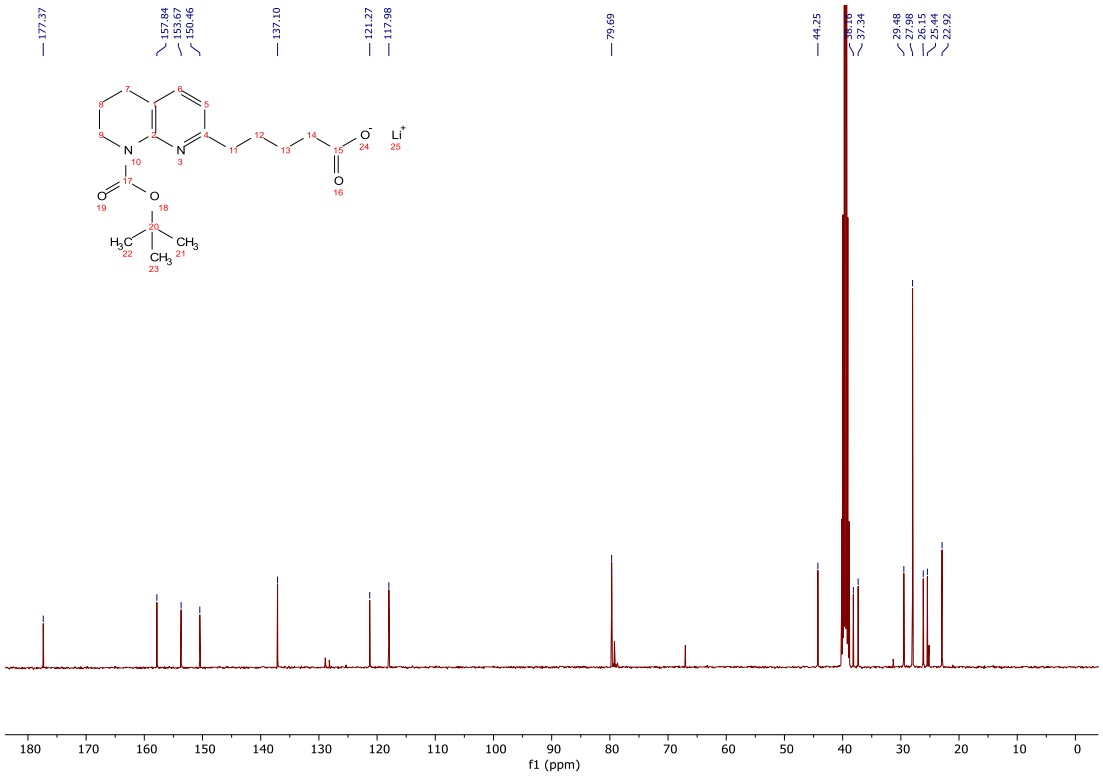
177.37
157.84
155.67
150.46
137.10
121.27
117.98
79.69
44.25
38.16
37.34
29.48
27.98
26.15
25.44
22.92
180 170 160 150 140 130 120 110 100 90 80 70 60 50 40 30 20 10 0
f1 (ppm)

(*R,E*)-*N*-(3-bromobenzylidene)-2-methylpropane-2-sulfinamide (**105**)

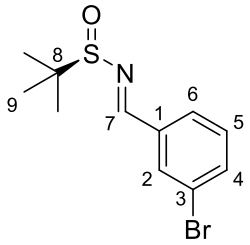

To a stirred solution of (*R*)-*tert*-butanesulfinamide (16.4 g, 135 mmol) in anhydrous THF (200 mL) was added 3-bromobenzaldehyde (**104**, 15.8 mL, 135 mmol). The mixture was stirred at rt for 5 min and Ti(O*i*-Pr)$_4$ (80.0 mL, 270 mmol) was added. The reaction mixture was stirred at rt for 18 h. The reaction mixture was concentrated *in vacuo*, dissolved in ethyl acetate (100 mL), poured into brine (200 mL) and filtered through Celite®. The layers were separated, and the organic layer washed with sat. $NaHCO_{3(aq)}$ (2 x 100 mL) and brine (2 x 100 mL). The aqueous was extracted with ethyl acetate (2 x 100 mL) and the organics combined. The organics were dried ($MgSO_4$) and concentrated *in vacuo* to afford a yellow oil (34.5 g). The crude product was not purified further; **HRMS** *m/z* (ESI$^+$) calc. for $C_{11}H_{15}BrNOS$ $[M+H]^+$ requires 288.0052, found 288.0052; $\boldsymbol{R_f}$ 0.26, 10% ethyl acetate/light petroleum, UV active; δ_H (400 MHz, $CDCl_3$) 8.52 (1H, s, H-7), 8.02 (1H, dd, *J* = 1.8, 1.8 Hz, H-2), 7.74 (1H, ddd, *J* = 7.7, 1.3, 1.3 Hz, H-6), 7.64 (1H, ddd, *J* = 8.0, 2.0, 1.1 Hz, H-4), 7.36 (1H, dd, *J* = 7.8, 7.8 Hz, H-5), 1.27 (9H, s, H-9); δ_C (101 MHz, $CDCl_3$) 161.5 (CH), 136.0 (C), 135.4 (ArH), 131.7 (ArH), 130.6 (ArH), 128.5 (ArH), 123.3 (C), 58.2 (C), 22.8 (CH_3); ν_{max} (FT-ATR/cm^{-1}) 2978, 1598, 1561, 1205, 1081, 786, 681, 584.

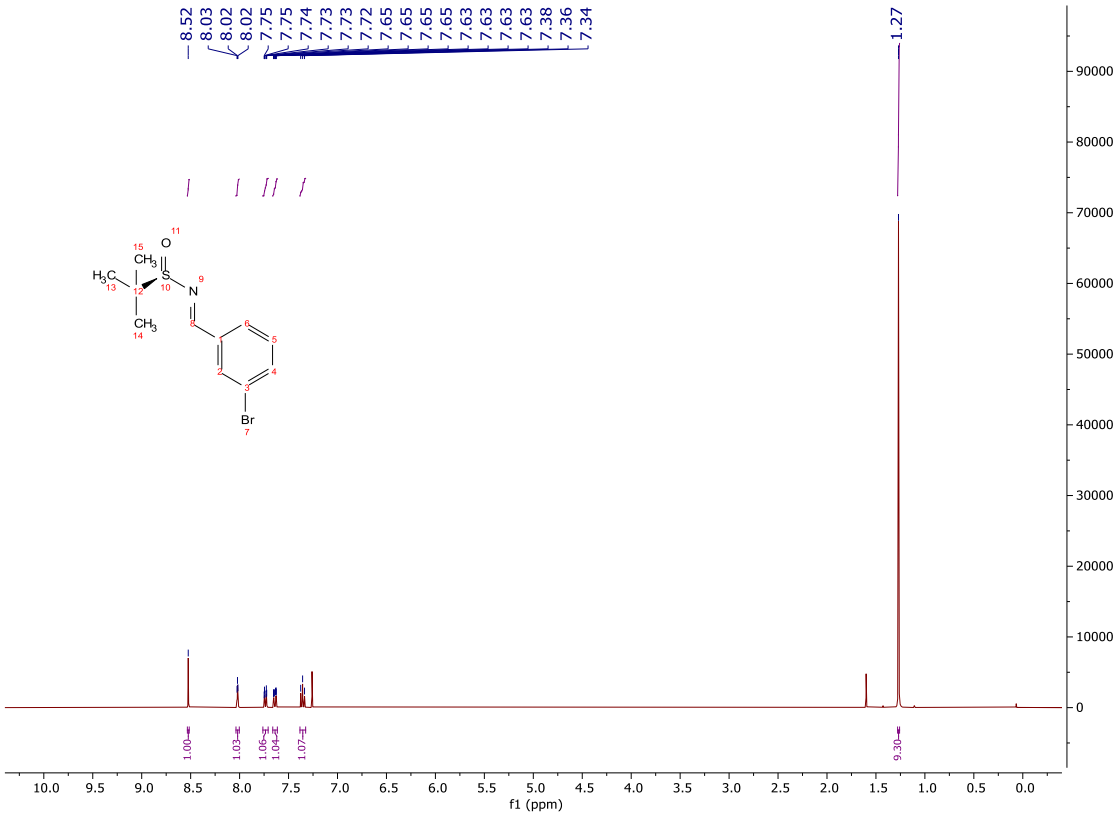
8.52
8.03
8.02
8.02
7.75
7.75
7.74
7.73
7.73
7.72
7.65
7.65
7.65
7.63
7.63
7.63
7.38
7.36
7.34
1.27
1.00
1.03
1.06
1.04
1.07
9.30
f1 (ppm)

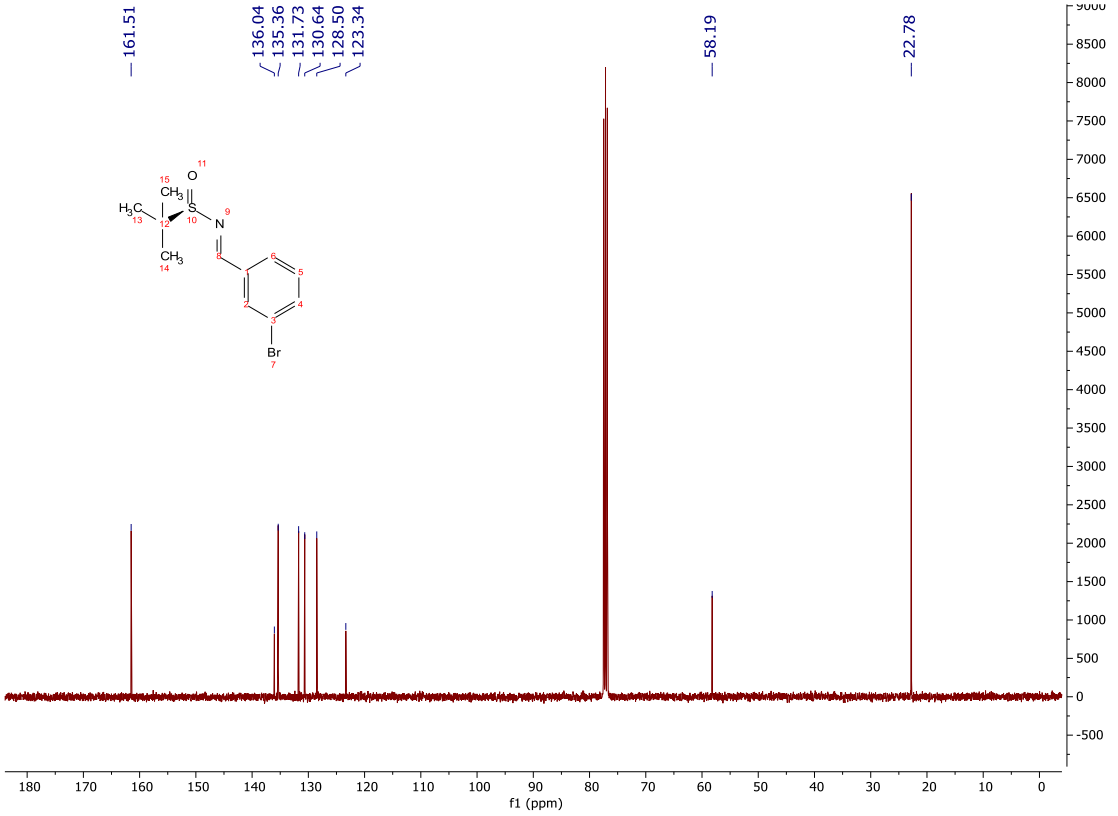
161.51
136.04
135.36
131.73
130.64
128.50
123.34
58.19
22.78
f1 (ppm)

Ethyl (*S*)-3-(3-bromophenyl)-3-(((*R*)-*tert*-butylsulfinyl)amino)propanoate (**106**)

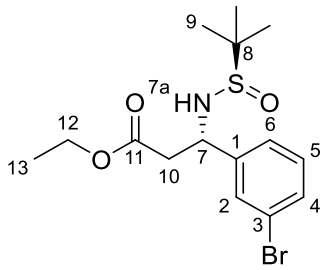

To a stirred suspension of zinc powder (21.0 g, 322 mmol) in anhydrous THF (80.0 mL) under a nitrogen atmosphere was added TMSCl (8.18 mL, 64.4 mmol). The suspension was heated under reflux for 5 min. Ethyl bromoacetate (28.3 mL, 257 mmol) was added dropwise over 20 min and the solution stirred under reflux for 1 h. The reaction mixture was cooled to 0 °C and a solution of **105** (18.5 g, 64.4 mmol) in anhydrous THF (50.0 mL) was added and stirred for 18 h. 10% Citric $acid_{(aq)}$ (200 mL) was added, and the mixture stirred for 10 min. The reaction mixture was filtered through Celite® and concentrated *in vacuo*. Ethyl acetate (200 mL) was added, and the layers separated. The organic was washed with sat. $NaHCO_{3(aq)}$ (2 x 200 mL), brine (100 mL), dried ($MgSO_4$) and concentrated *in vacuo* to afford a yellow oil (24.1 g). The crude product was not purified further; **HRMS** *m/z* (ESI^+) calc. for $C_{15}H_{23}BrNO_3S$ $[M+H]^+$ requires 376.0577, found 376.0578; $\boldsymbol{R_f}$ 0.20, 40% ethyl acetate/light petroleum, UV active; δ_H (400 MHz, $CDCl_3$) 7.49 (1H, dd, *J* = 1.9, 1.9 Hz, H-2), 7.42 (1H, ddd, *J* = 7.7, 2.0, 1.2 Hz, H-6), 7.29 – 7.25 (1H, m, H-4), 7.21 (1H, dd, *J* = 7.7, 7.7 Hz, H-5), 4.77 – 4.69 (2H, m, H-7 and H-7a), 4.13 (2H, q, *J* = 7.1 Hz, H-12), 2.90 – 2.76 (2H, m, H-10), 1.25 – 1.20 (12H, m, H-9 and H-13); δ_C (101 MHz, $CDCl_3$) 171.2 (CO), 143.2 (C), 131.2 (ArH), 130.5 (ArH), 130.4 (ArH), 126.1 (ArH), 122.8 (C), 61.3 (CH_2), 56.0 (C), 55.1 (CH), 42.3 (CH_2), 22.8 (CH_3), 14.2 (CH_3); ν_{max} (FT-ATR/cm^{-1}) 3218, 2980, 1735, 1378, 1168, 1045, 788, 698.

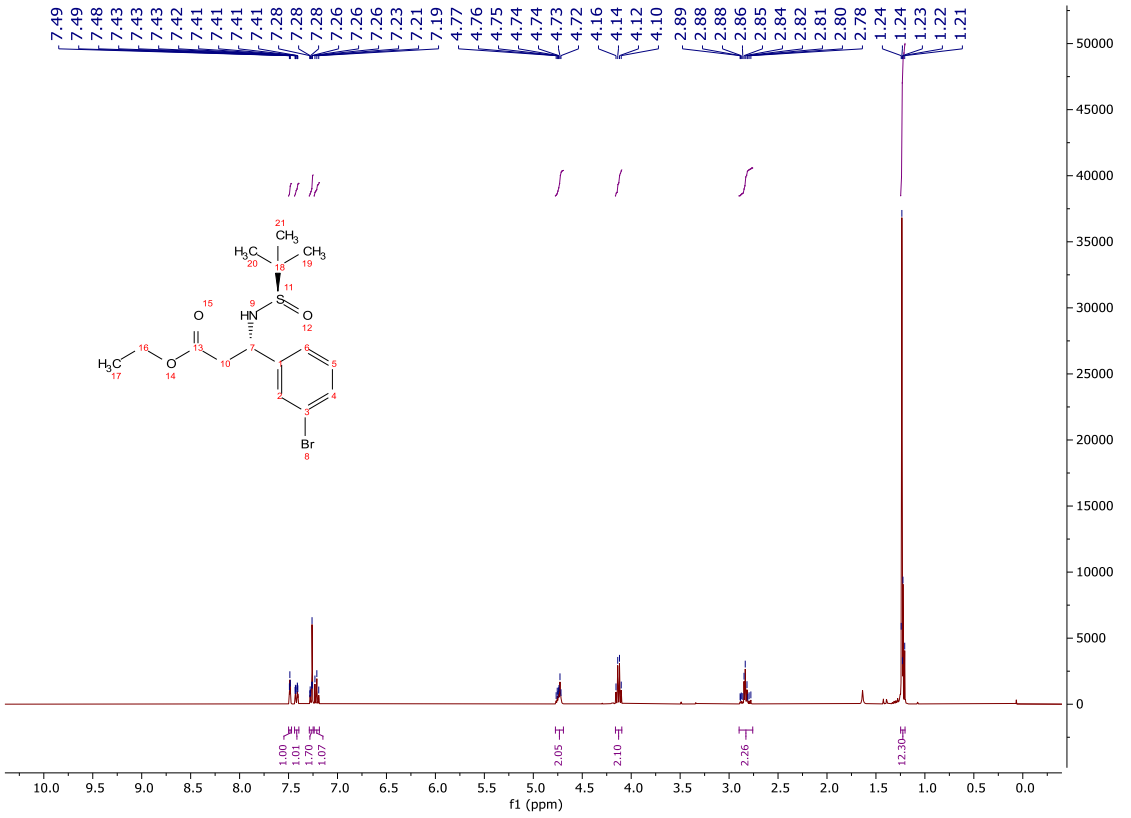
7.49
7.49
7.48
7.43
7.43
7.43
7.42
7.41
7.41
7.41
7.41
7.28
7.28
7.28
7.26
7.26
7.26
7.23
7.21
7.19
4.77
4.76
4.75
4.74
4.74
4.73
4.72
4.16
4.14
4.12
4.10
2.89
2.88
2.88
2.86
2.85
2.84
2.82
2.81
2.80
2.78
1.24
1.24
1.23
1.22
1.21
1.00
1.01
1.70
1.07
2.05
2.10
2.26
12.30
f1 (ppm)

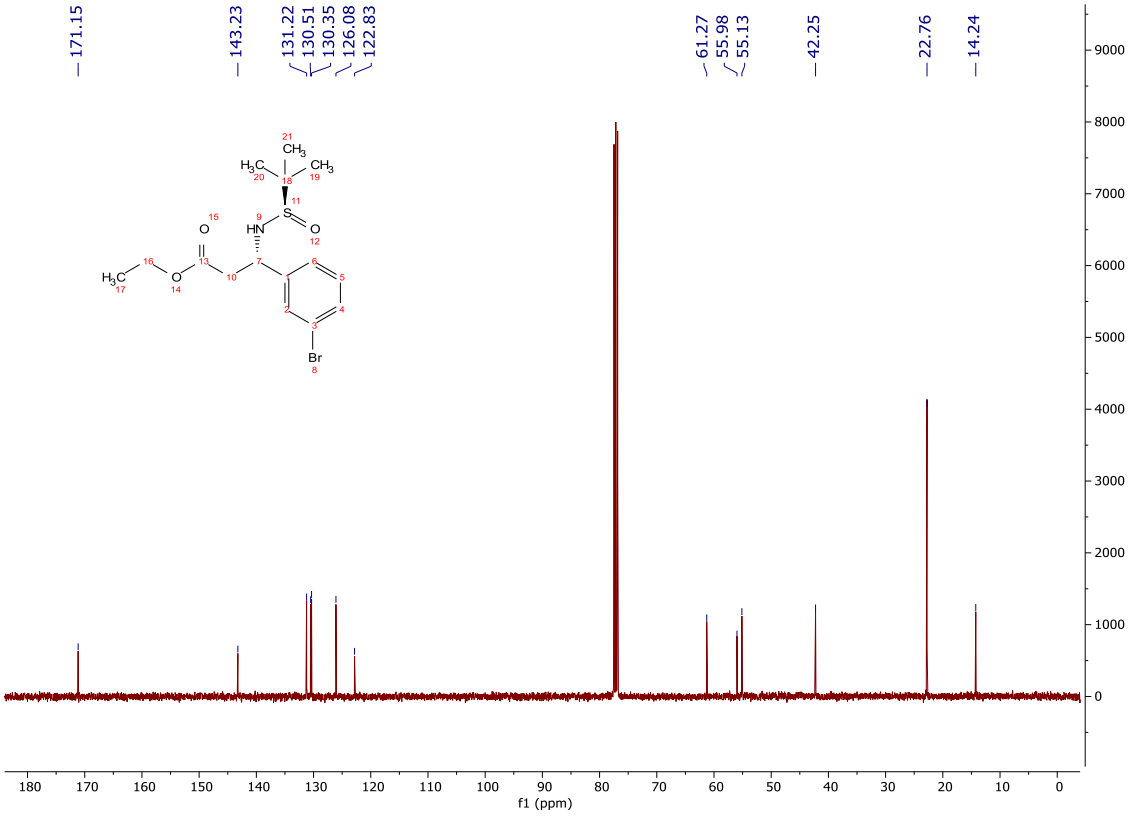
171.15
143.23
131.22
130.51
130.35
126.08
122.83
61.27
55.98
55.13
42.25
22.76
14.24
f1 (ppm)

Ethyl (*S*)-3-amino-3-(3-bromophenyl)propanoate hydrochloride (**107**)

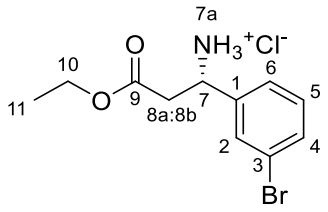

To a stirred solution of **106** (24.1 g, 64.4 mmol) in anhydrous diethyl ether (260 mL) at rt was added 4M HCl in dioxane (32.5 mL, 130 mmol). The reaction mixture was stirred for 20 min, filtered and the filter cake washed with diethyl ether to afford the title compound as a colourless powder (15.0 g, 48.7 mmol, 72% over three steps); **HRMS** *m/z* (ESI^+) calc. for $C_{11}H_{15}BrNO_2$ $[M+H]^+$ requires 272.0281, found 272.0280; $\boldsymbol{R_f}$ 0.24, 80% ethyl acetate/light petroleum, UV active; δ_H (400 MHz, DMSO-d_6) 8.81 (3H, bs, H-7a), 7.82 (1H, dd, *J* = 1.9, 1.9 Hz, H-2), 7.62 – 7.53 (2H, m, H-4 and H-6), 7.38 (1H, dd, *J* = 7.9, 7.9 Hz, H-5), 4.64 – 4.55 (1H, m, H-7), 4.07 – 3.93 (2H, m, H-10), 3.20 (1H, dd, *J* = 16.2, 5.7 Hz, H-8a), 3.07 – 2.97 (1H, m, H-8b), 1.08 (3H, t, *J* = 7.1 Hz, H-11); δ_C (101 MHz, DMSO-d_6) 168.9 (CO), 139.4 (C), 131.7 (ArH), 130.8 (ArH), 130.7 (ArH), 126.9 (ArH), 121.7 (C), 60.5 (CH_2), 50.3 (CH), 38.4 (CH_2), 13.9 (CH_3); **MP** 126-129 °C; ν_{max} (FT-ATR/cm^{-1}) 2865, 2626, 1736, 1519, 1250, 1025, 790, 697.

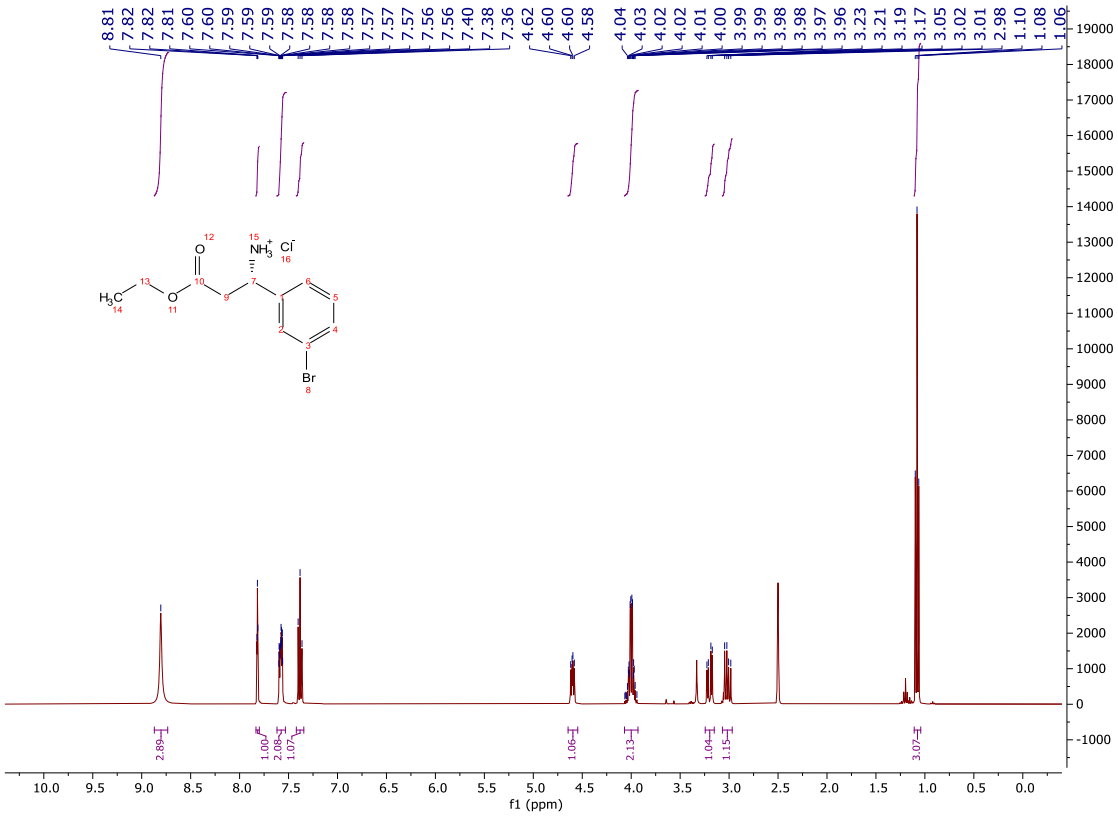
8.81 7.82 7.82 7.81 7.60 7.60 7.59 7.59 7.59 7.58 7.58 7.58 7.58 7.57 7.57 7.57 7.56 7.56 7.40 7.38 7.36 4.62 4.60 4.60 4.58 4.04 4.03 4.02 4.02 4.01 4.00 3.99 3.99 3.98 3.98 3.97 3.96 3.23 3.21 3.19 3.17 3.05 3.02 3.01 2.98 1.10 1.08 1.06
2.89 1.00 2.08 1.07 1.06 2.13 1.04 1.15 3.07
f1 (ppm)

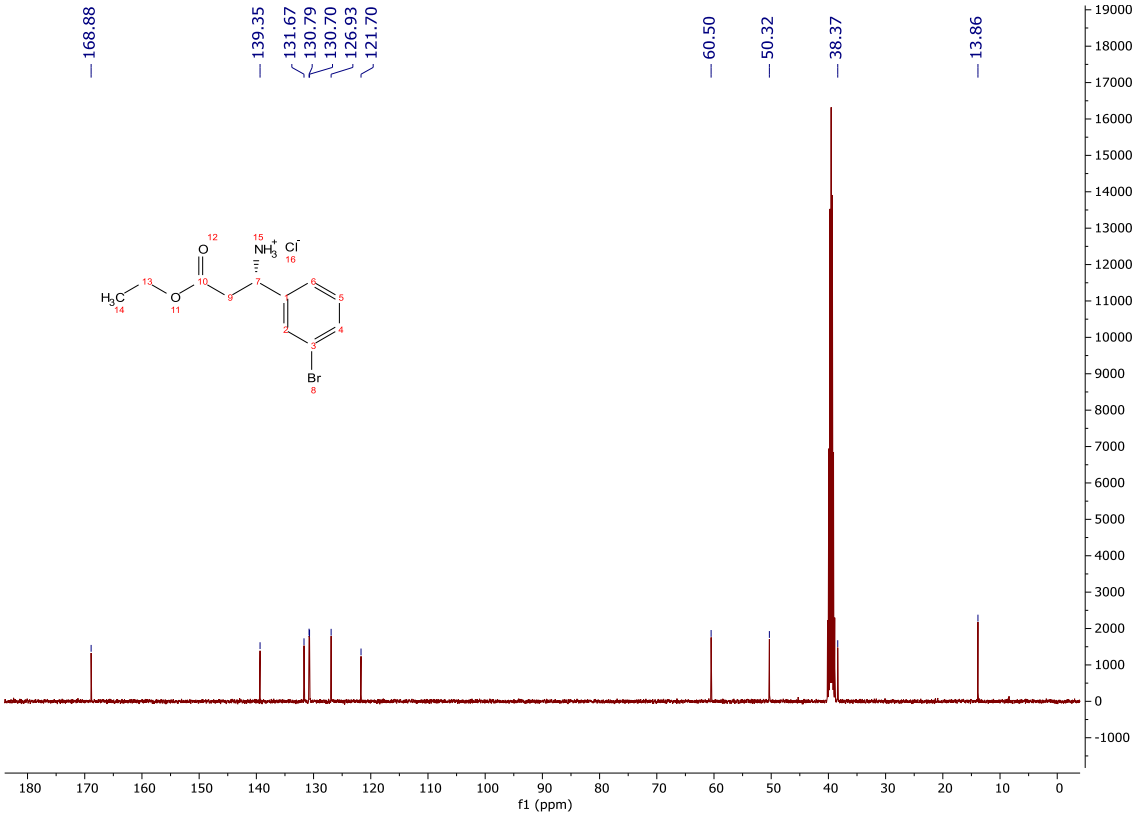
168.88 139.35 131.67 130.79 130.70 126.93 121.70 60.50 50.32 38.37 13.86
f1 (ppm)

tert-Butyl (*S*)-3-(3-bromophenyl)-3-(((*R*)-*tert*-butylsulfinyl)amino)propanoate (**109**)

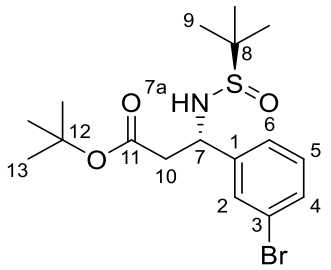

To a stirred suspension of zinc powder (20.0 g, 300 mmol) in anhydrous THF (175 mL) under a nitrogen atmosphere was added TMSCl (7.60 mL, 60.0 mmol). The suspension was heated under reflux for 5 min. *tert*-Butyl bromoacetate (25.0 mL, 170 mmol) was added dropwise over 20 min and the solution stirred under reflux for 1 h. The reaction mixture was cooled to 0 °C and a solution of **105** (17.3 g, 60.0 mmol) in anhydrous THF (75.0 mL) was added and stirred for 18 h. An aqueous solution of 10% Citric acid (200 mL) was added and the mixture stirred for 10 min. The reaction mixture was filtered through Celite® and concentrated *in vacuo*. Ethyl acetate (200 mL) was added, and the layers separated. The organic was washed with sat. $NaHCO_{3(aq)}$ (2 x 200 mL), brine (100 mL), dried ($MgSO_4$) and concentrated *in vacuo* to afford a yellow oil (27.7 g). The crude product was not purified further; **HRMS** *m/z* (ESI^+) calc. for $C_{17}H_{27}BrNO_3S$ $[M+H]^+$ requires 404.0890, found 404.0889; $\boldsymbol{R_f}$ 0.29, 40% ethyl acetate/light petroleum, UV active; δ_H (400 MHz, $CDCl_3$) 7.49 (1H, dd, *J* = 1.8, 1.8 Hz, H-2), 7.41 (1H, ddd, *J* = 7.7, 2.0, 1.2 Hz, H-6), 7.29 – 7.24 (1H, m, H-4), 7.20 (1H, dd, *J* = 7.7, 7.7 Hz, H-5), 4.74 – 4.68 (1H, m, H-7), 4.64 (1H, d, *J* = 4.1 Hz, H-7a), 2.77 – 2.73 (2H, m, H-10), 1.40 (9H, s, H-13), 1.23 (9H, s, H-9); δ_C (101 MHz, $CDCl_3$) 170.3 (CO), 143.4 (C), 131.1 (ArH), 130.6 (ArH), 130.3 (ArH), 126.2 (ArH), 122.7 (C), 82.1 (C), 55.9 (C), 55.3 (CH), 43.5 (CH_2), 28.1 (CH_3), 22.8 (CH_3); ν_{max} (FT-ATR/cm^{-1}) 3212, 2978, 1723, 1366, 1148, 1051, 788, 698.

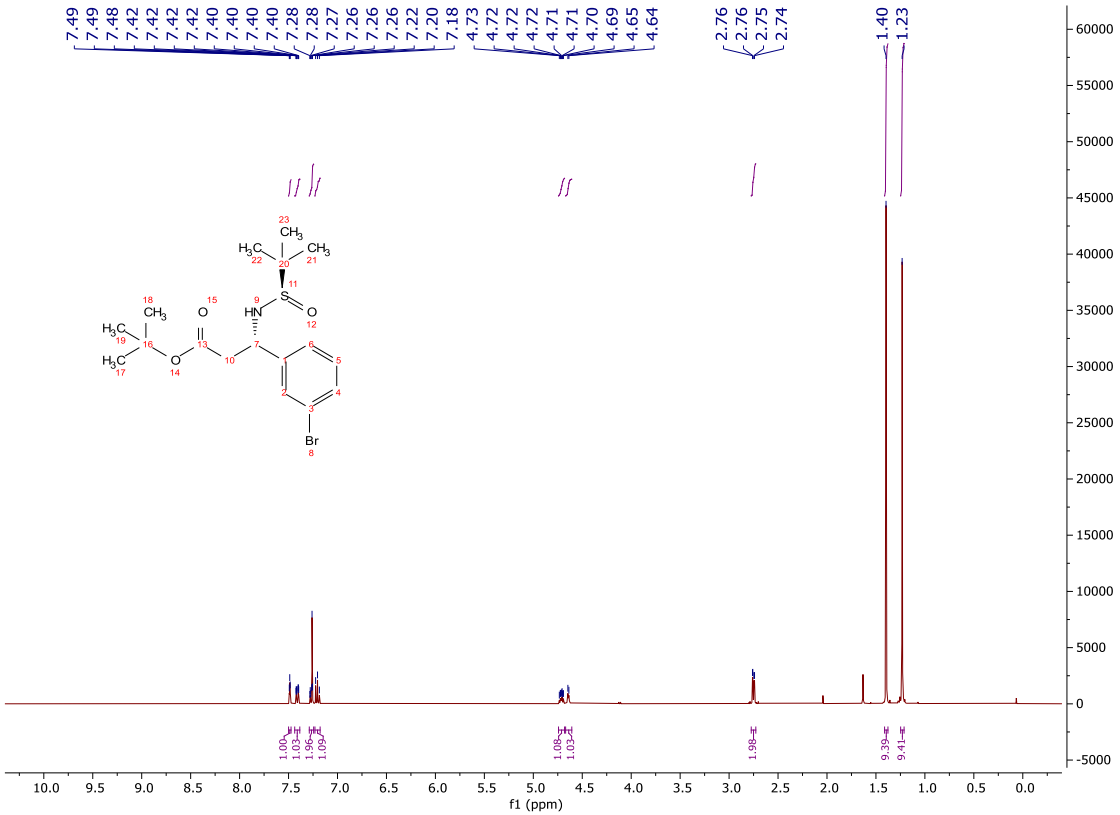
7.49
7.49
7.48
7.42
7.42
7.42
7.42
7.40
7.40
7.40
7.40
7.28
7.28
7.27
7.26
7.26
7.26
7.22
7.20
7.18
4.73
4.72
4.72
4.72
4.71
4.71
4.70
4.69
4.65
4.64
2.76
2.76
2.75
2.74
1.40
1.23
1.00
1.03
1.96
1.09
1.08
1.03
1.98
9.39
9.41
f1 (ppm)

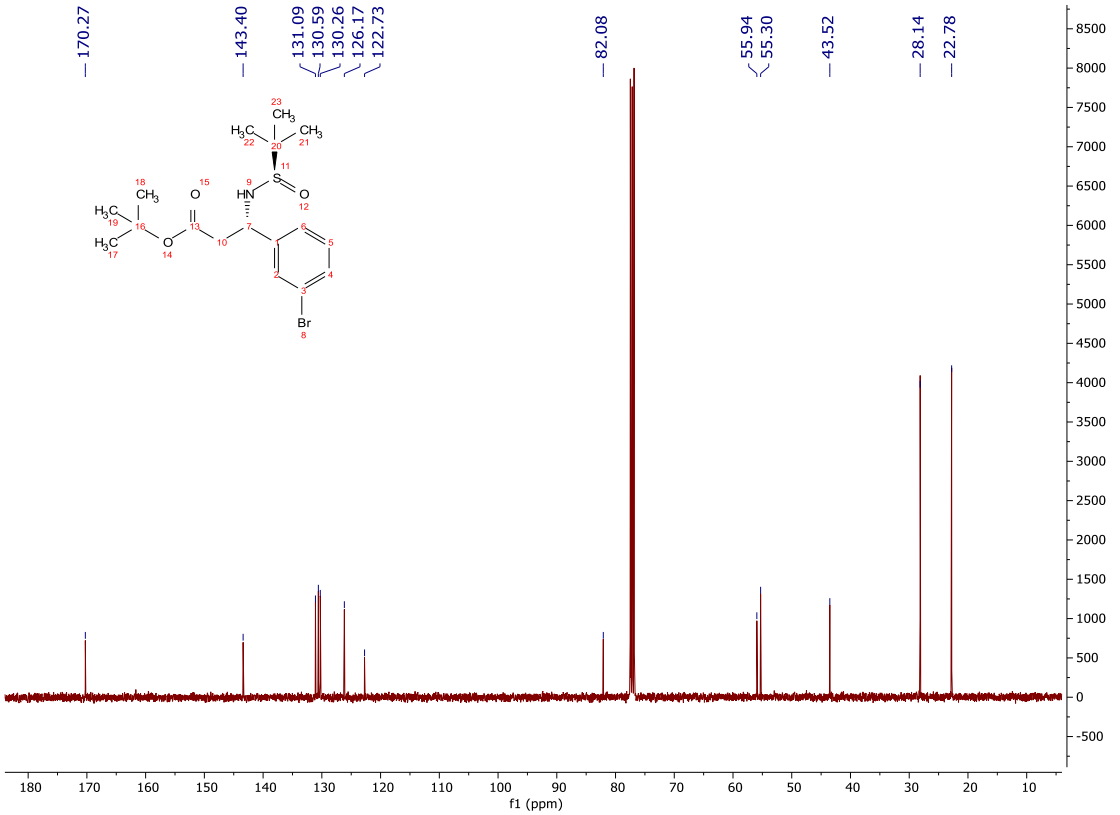
170.27
143.40
131.09
130.59
130.26
126.17
122.73
82.08
55.94
55.30
43.52
28.14
22.78
f1 (ppm)

tert-Butyl (*S*)-3-amino-3-(3-bromophenyl)propanoate hydrochloride (**110**)

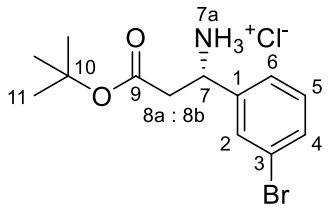

To a stirred solution of **109** (26.0 g, 64.5 mmol) in anhydrous diethyl ether (450 mL) at rt was added 4M HCl in dioxane (32.3 mL, 129 mmol). The reaction mixture was stirred for 20 min, filtered and the filter cake washed with diethyl ether to afford the title compound as a colourless powder (14.9 g, 44.5 mmol, 66% over three steps); **HRMS** *m/z* (ESI^+) calc. for $C_{13}H_{19}BrNO_2$ $[M+H]^+$ requires 300.0594, found 300.0586; $\boldsymbol{R_f}$ 0.35, 80% ethyl acetate/light petroleum, UV active; δ_H (400 MHz, DMSO-d_6) 8.81 (3H, bs, H-7a), 7.80 (1H, dd, *J* = 1.8, 1.8 Hz, H-2), 7.63 – 7.53 (2H, m, H-6 and H-4), 7.39 (1H, dd, *J* = 7.8, 7.8 Hz, H-5), 4.53 (1H, dd, *J* = 10.3, 5.2 Hz, H-7), 3.12 (1H, dd, *J* = 15.6, 5.2 Hz, H-8a), 2.89 (1H, dd, *J* = 15.6, 10.1 Hz, H-8b), 1.25 (9H, s, H-11); δ_C (101 MHz, DMSO-d_6) 168.0 (CO), 139.2 (C), 131.6 (ArH), 130.9 (ArH), 130.7 (ArH), 127.0 (ArH), 121.6 (C), 81.0 (C), 50.5 (CH), 39.5 (CH_2, assigned by HSQC), 27.5 (CH_3); **MP** 170-173 °C; ν_{max} (FT-ATR/cm^{-1}) 2977, 2870, 1733, 1519, 1372, 1160, 790, 699.

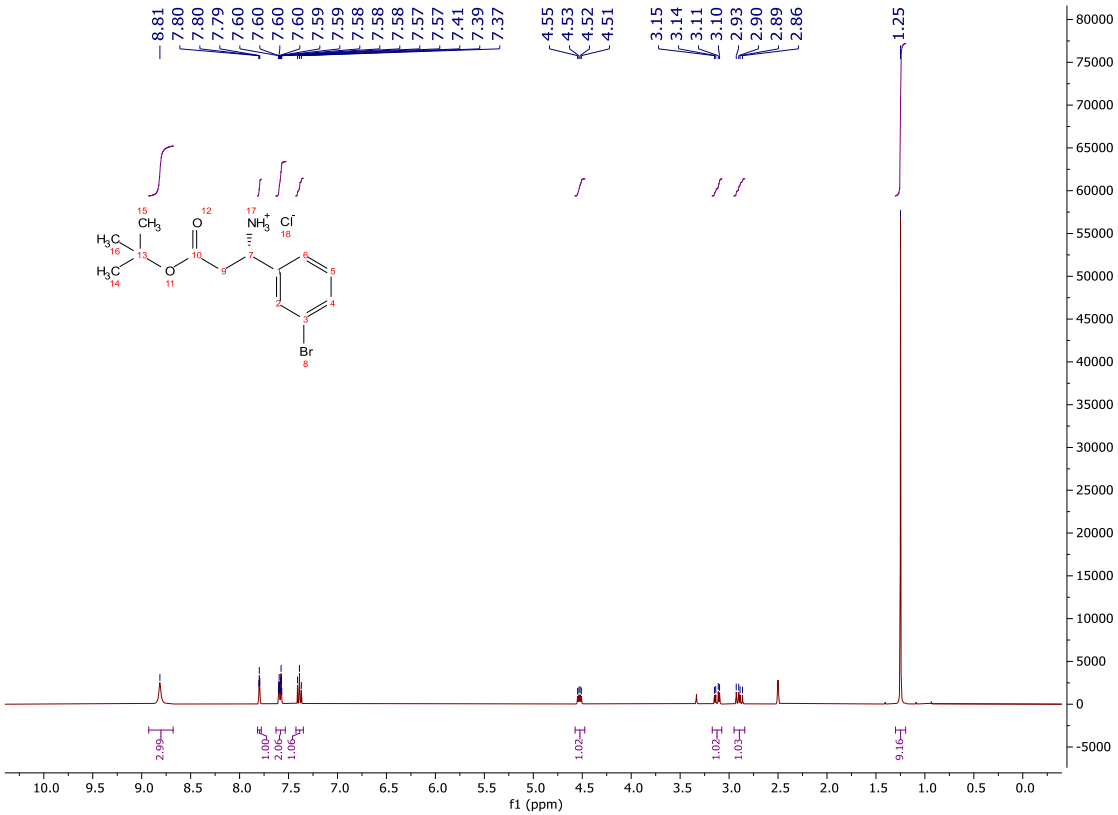
8.81
7.80
7.80
7.79
7.60
7.60
7.60
7.60
7.59
7.59
7.58
7.58
7.58
7.57
7.57
7.41
7.39
7.37
4.55
4.53
4.52
4.51
3.15
3.14
3.11
3.10
2.93
2.90
2.89
2.86
1.25
2.99
1.00
2.06
1.06
1.02
1.02
1.03
9.16
f1 (ppm)

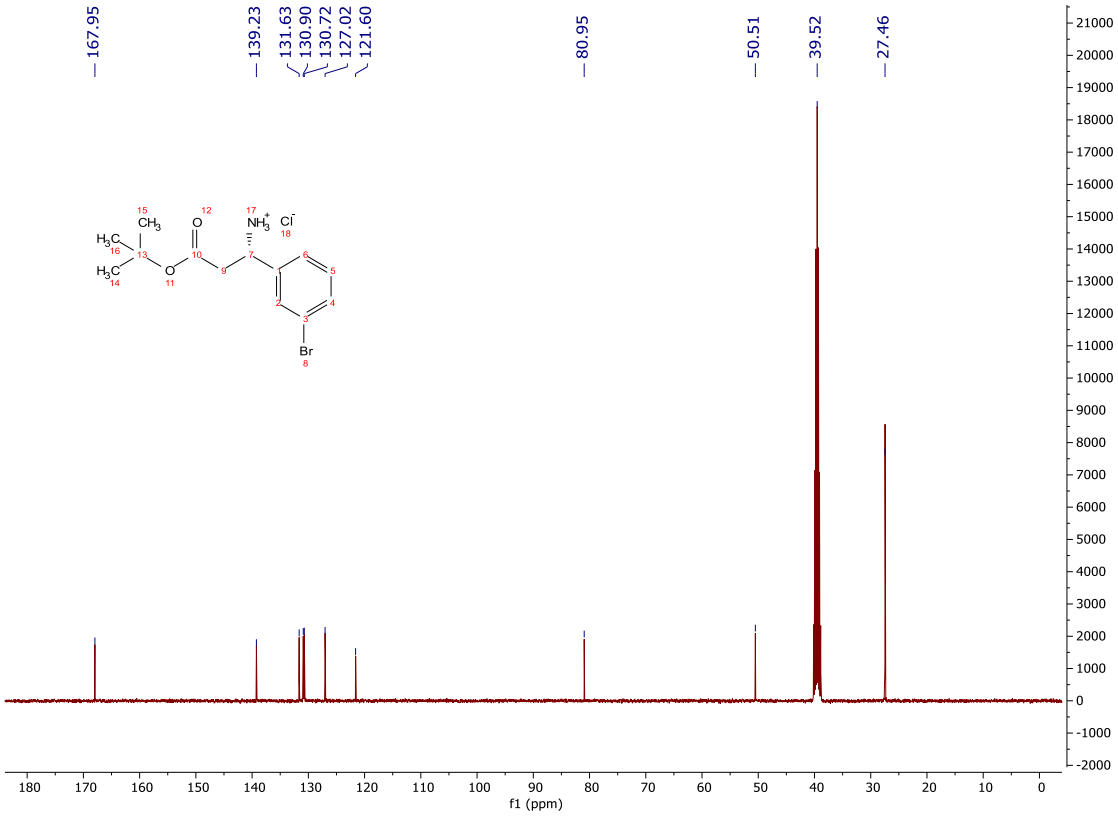
167.95
139.23
131.63
130.90
130.72
127.02
121.60
80.95
50.51
39.52
27.46
f1 (ppm)

(*E*)-*N*-(3-iodobenzylidene)-2-methylpropane-2-sulfinamide (**111**)

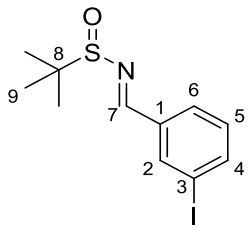

To a stirred solution of *tert*-butanesulfinamide (1.89 g, 15.6 mmol) in anhydrous THF (50.0 mL) at rt was added 3-iodobenzaldehyde (4.00 g, 17.2 mmol) and Ti(O*i*-Pr)$_4$ (9.23 mL, 31.2 mmol). The reaction mixture was stirred for 18 h, quenched with brine (50 mL) and filtered through Celite®. The mother liquors were washed with sat. $NaHCO_{3(aq)}$ (2 x 50 mL), brine (2 x 50 mL), dried ($MgSO_4$) and concentrated *in vacuo* to afford a yellow oil (6.07 g). The crude product was purified by column chromatography on silica gel, eluting with a gradient of ethyl acetate/light petroleum (5-50%) to afford the title compound as a yellow oil (4.54 g, 13.6 mmol, 87 %); **HRMS** *m/z* (ESI$^+$) calc. for $C_{11}H_{15}INOS$ $[M+H]^+$ requires 335.9914 found 335.9919; $\boldsymbol{R_f}$ 0.22, 10% ethyl acetate/light petroleum, UV active; δ_H (400 MHz, $CDCl_3$) 8.49 (1H, s, H-7), 8.21 (1H, dd, *J* = 1.7, 1.7 Hz, H-2), 7.84 (1H, ddd, *J* = 7.9, 1.8, 1.1 Hz, H-4), 7.77 (1H, ddd, *J* = 7.7, 1.4, 1.4 Hz, H-6), 7.22 (1H, dd, *J* = 7.8, 7.8 Hz, H-5), 1.27 (9H, s, H-9); δ_C (100 MHz, $CDCl_3$) 161.3 (CH), 141.1 (ArH), 137.6 (ArH), 135.9 (C), 130.6 (ArH), 128.9 (ArH), 94.7 (C), 58.1 (C), 22.7 (CH_3); $\boldsymbol{\nu_{max}}$ (FT-ATR/cm^{-1}) 2923, 1596, 1558, 1456, 1362, 1206, 1082, 993, 785, 732, 682.

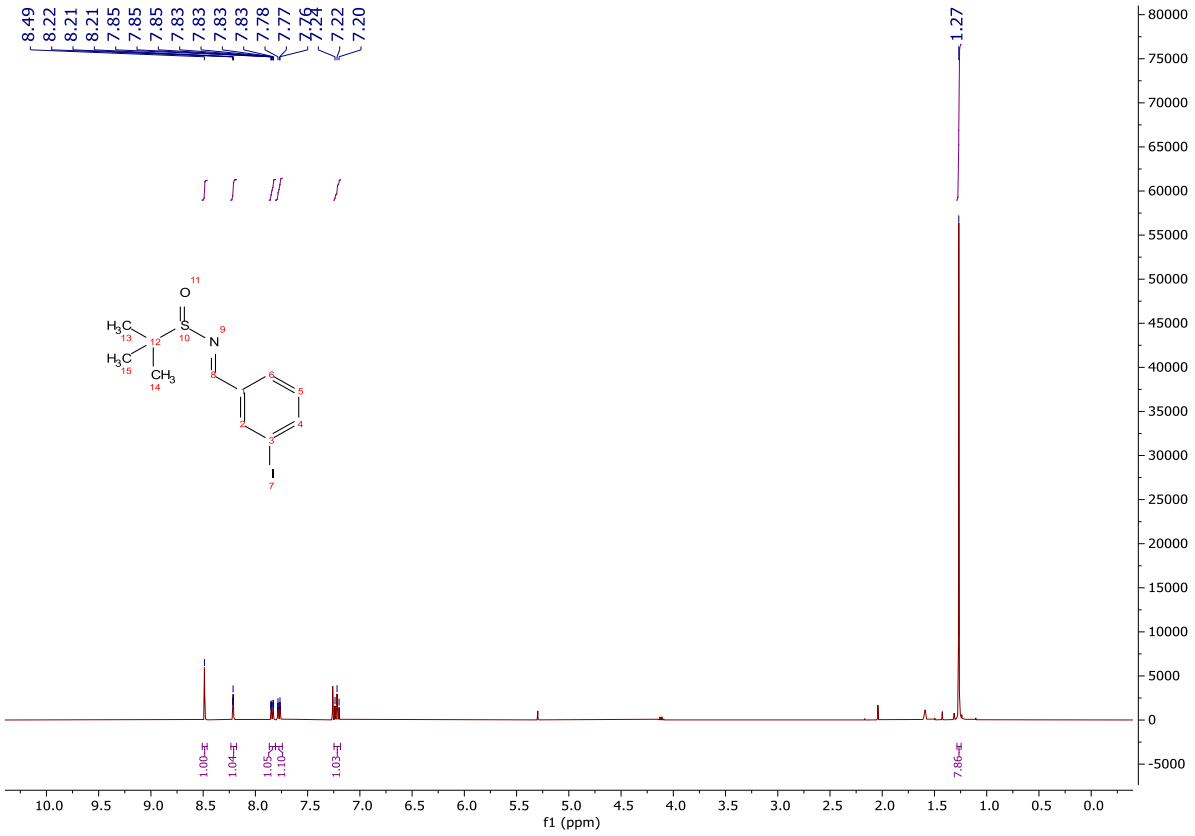
8.49
8.22
8.21
8.21
7.85
7.85
7.85
7.83
7.83
7.83
7.83
7.78
7.77
7.24
7.22
7.20
1.27
1.00
1.04
1.05
1.10
1.03
7.86
f1 (ppm)

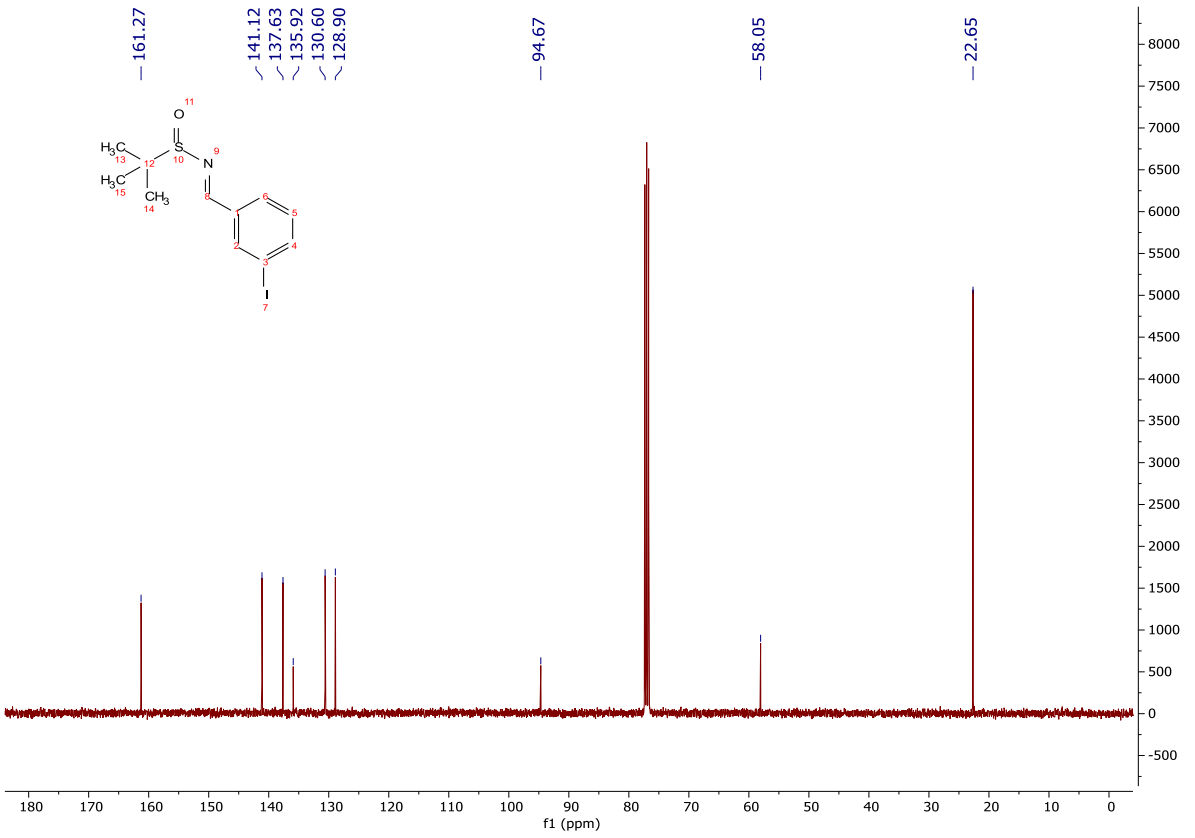
161.27
141.12
137.63
135.92
130.60
128.90
94.67
58.05
22.65
f1 (ppm)

tert-Butyl 3-((*tert*-butylsulfinyl)amino)-3-(3-iodophenyl)propanoate (**112**)

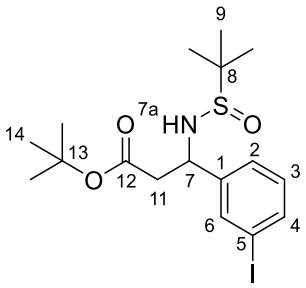

To a stirred suspension of zinc powder (12.0 g, 185 mmol) in anhydrous THF (50 mL) under a nitrogen atmosphere was added TMSCl (1.39 mL, 11.0 mmol). The suspension was stirred for 30 min and then heated under reflux at 85 °C. *tert*-Butyl bromoacetate (7.03 mL, 47.6 mmol) was added dropwise over 20 min and the solution stirred at 85 °C for 1 h. The reaction mixture was cooled to 0 °C and a solution of **111** (4.50 g, 13.4 mmol) in anhydrous THF (50.0 mL) was added and stirred for 18 h. The reaction was quenched with brine (100 mL) and filtered through Celite®. The mother liquors were washed with sat. $NaHCO_{3(aq)}$ (2 x 50 mL), brine (2 x 50 mL), dried ($MgSO_4$) and concentrated *in vacuo* to afford a yellow oil (5.62 g). The crude product was purified by column chromatography on silica gel, eluting with a gradient of ethyl acetate/light petroleum (0-60%) to afford the title compound as a yellow oil (4.85 g, 10.7 mmol, 80%); **HRMS** *m/z* (ESI^+) calc. for $C_{17}H_{27}INO_3S$ $[M+H]^+$ requires 452.0751, found 452.0797; $\boldsymbol{R_f}$ 0.33, 40% ethyl acetate/light petroleum, UV active; δ_H (400 MHz, $CDCl_3$) 7.69 (1H, dd, *J* = 1.8, 1.8 Hz, H-6), 7.61 (1H, ddd, *J* = 7.8, 1.8, 1.1 Hz, H-4), 7.30 (1H, ddd, *J* = 7.7, 1.4, 1.4 Hz, H-2), 7.07 (1H, dd, *J* = 7.8, 7.8 Hz, H-3), 4.72 – 4.65 (1H, m, H-7), 4.64 – 4.60 (1H, m, H-7a), 2.79 – 2.68 (2H, m, H-11), 1.40 (9H, s, H-14), 1.23 (9H, s, H-9); δ_C (101 MHz, $CDCl_3$) 170.1 (C), 143.3 (C), 136.9 (ArH), 136.4 (ArH), 130.3 (ArH), 126.7 (ArH), 94.3 (C), 82.0 (C), 55.8 (C), 55.0 (CH), 43.4 (CH_2), 28.0 (CH_3), 22.6 (CH_3); ν_{max} (FT-ATR/cm^{-1}) 3197, 2971, 1730, 1570, 1471, 1363, 1146, 1037, 957, 806.

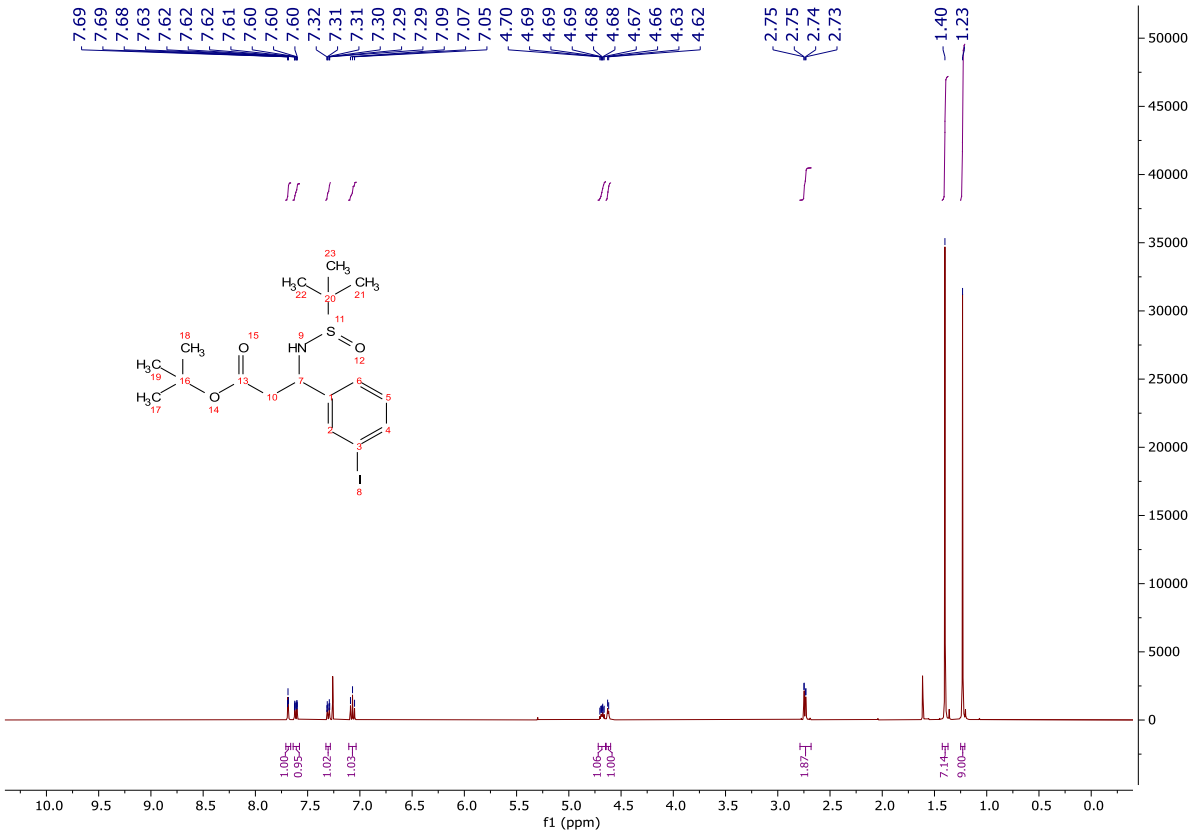
7.69
7.69
7.68
7.63
7.62
7.62
7.62
7.61
7.60
7.60
7.60
7.32
7.31
7.31
7.30
7.29
7.29
7.09
7.07
7.05
4.70
4.69
4.69
4.69
4.68
4.68
4.67
4.66
4.63
4.62
2.75
2.75
2.74
2.73
1.40
1.23
1.00
0.95
1.02
1.03
1.06
1.00
1.87
7.14
9.00
f1 (ppm)

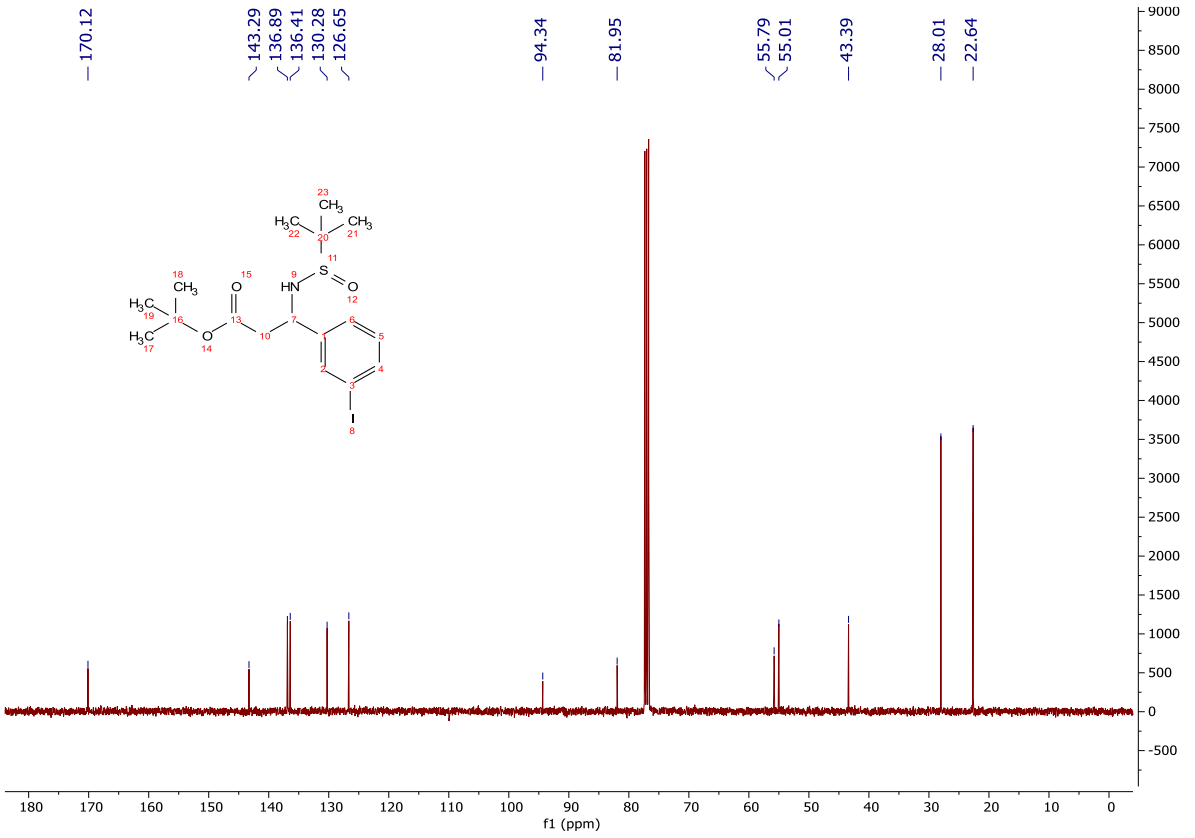
170.12
143.29
136.89
136.41
130.28
126.65
94.34
81.95
55.79
55.01
43.39
28.01
22.64
f1 (ppm)

tert-Butyl 3-amino-3-(3-iodophenyl)propanoate (**113**)

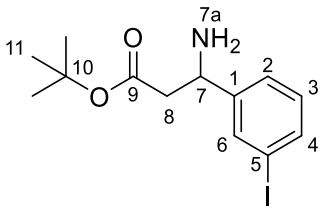

To a stirred solution of **112** (4.50 g, 9.98 mmol) in anhydrous diethyl ether (120 mL) under a nitrogen atmosphere at rt was added 4M HCl in dioxane (5.00 mL, 20.0 mmol). A colourless precipitate formed, and the reaction mixture was stirred for 2 h. The solvent was removed *in vacuo* to afford a colourless solid. The residue was dissolved in aqueous 2M $HCl_{(aq)}$ (50.0 mL) and washed with diethyl ether (2 x 50 mL). The aqueous phase was basified with sat. $Na_2CO_{3(aq)}$ and extracted with ethyl acetate (2 x 50 mL). The organics were combined, dried ($MgSO_4$) and the solvent removed *in vacuo* to afford the title compound as a clear oil (3.39 g, 9.78 mmol, 98%); **HRMS** *m/z* (ESI^+) calc. for $C_{13}H_{19}INO_2$ $[M+H]^+$ requires 348.0455, found 348.0448; $\boldsymbol{R_f}$ 0.13, 40% ethyl acetate/light petroleum, UV active; δ_H (400 MHz, $CDCl_3$) 7.73 (1H, dd, *J* = 1.8, 1.8 Hz, H-6), 7.58 (1H, ddd, *J* = 7.8, 1.8, 1.0 Hz, H-4), 7.35 – 7.30 (1H, m, H-2), 7.06 (1H, dd, *J* = 7.8, 7.8 Hz, H-3), 4.31 (1H, t, *J* = 6.8 Hz, H-7), 2.55 (2H, d, *J* = 6.8 Hz, H-8), 1.41 (9H, s, H-11); δ_C (101 MHz, $CDCl_3$) 171.1 (CO), 147.2 (C), 136.5 (ArH), 135.7 (ArH), 130.4 (ArH), 125.8 (ArH), 94.6 (C), 81.1 (C), 52.4 (CH), 45.3 (CH_2), 28.2 (CH_3); ν_{max} (FT-ATR/cm^{-1}) 2976, 1718, 1564, 1366, 1312, 1210, 1146, 1064, 994, 842, 783, 695.

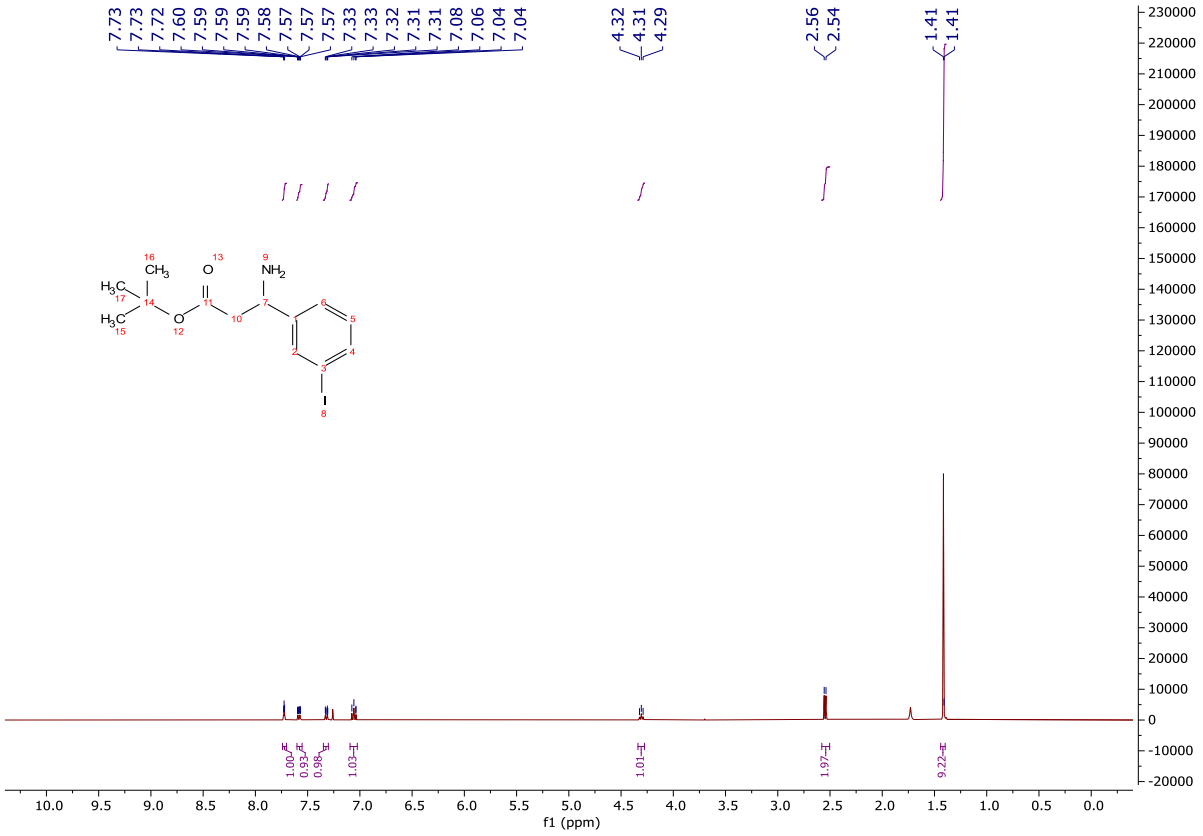
7.73
7.73
7.72
7.60
7.59
7.59
7.59
7.58
7.57
7.57
7.57
7.33
7.33
7.32
7.31
7.31
7.08
7.06
7.04
7.04
4.32
4.31
4.29
2.56
2.54
1.41
1.41
1.00
0.93
0.98
1.03
1.01
1.97
9.22
f1 (ppm)

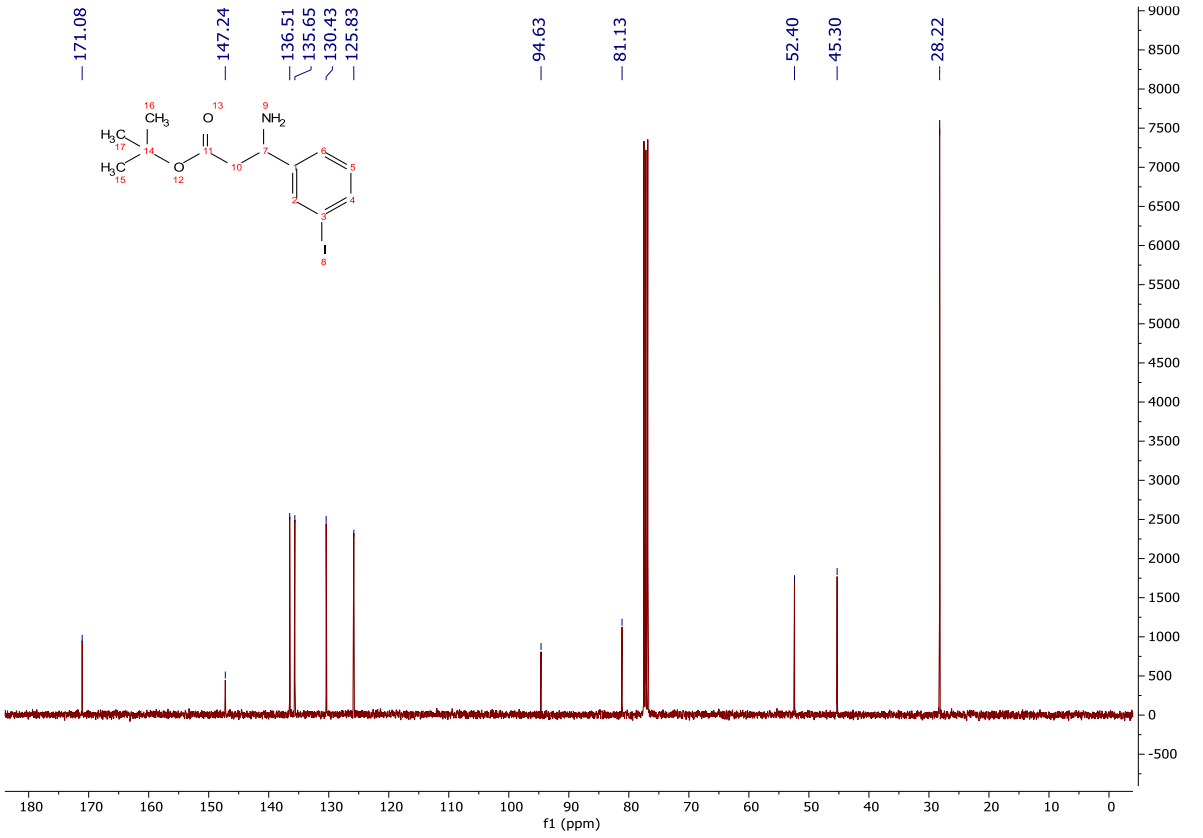
171.08
147.24
136.51
135.65
130.43
125.83
94.63
81.13
52.40
45.30
28.22
f1 (ppm)

(*E*)-2-methyl-*N*-(3-(trifluoromethyl)benzylidene)propane-2-sulfinamide (**114**)

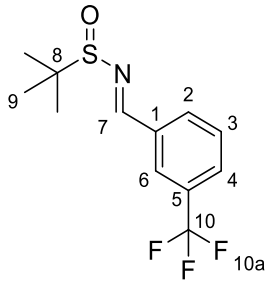

To a stirred solution of *tert*-butanesulfinamide (4.19 g, 34.6 mmol) in anhydrous THF (115 mL) was added 3-(trifluoromethyl)benzaldehyde) (5.10 mL, 38.1 mmol) and $Ti(OEt)_4$ (20.5 mL, 69.2 mmol). The reaction mixture was stirred at rt for 18 h, quenched with brine (100 mL) and filtered through Celite®. The mother liquors were washed with sat. $NaHCO_{3(aq)}$ (2 x 50 mL) and brine (2 x 50 mL), dried ($MgSO_4$) and concentrated *in vacuo* to afford the title compound as a colourless, amorphous solid (8.26 g, 29.7 mmol, 86%). No further purification was required; **HRMS** *m/z* (ESI^+) calc. for $C_{12}H_{15}F_3NOS$ $[M+H]^+$ requires 278.0821, found 278.0813; $\boldsymbol{R_f}$ 0.37, 40% ethyl acetate/light petroleum, UV active; δ_H (400 MHz, $CDCl_3$) 8.63 (1H, s, H-7), 8.12 (1H, d, *J* = 2.0 Hz, H-6), 8.04 – 7.99 (1H, m, H-2), 7.81 – 7.74 (1H, m, H-4), 7.62 (1H, t, *J* = 7.8 Hz, H-3), 1.28 (9H, s, H-9); δ_C (100 MHz, $CDCl_3$) 161.6 (CH), 134.8 (C), 132.8 (ArH), 131.8 (C, q, *J* = 32.8 Hz), 129.7 (ArH), 128.9 (ArH, q, *J* = 3.7 Hz), 125.8 (ArH, q, *J* = 3.7 Hz), 123.8 (CF_3, q, *J* = 272.7 Hz), 58.3 (C), 22.8 (CH_3); δ_F (376 MHz, $CDCl_3$) -62.9 (F-10a); **MP** 52-55 °C; ν_{max} (FT-ATR/cm^{-1}) 2965, 1605, 1584, 1350, 1326, 1204, 1160, 1120, 1079, 693.

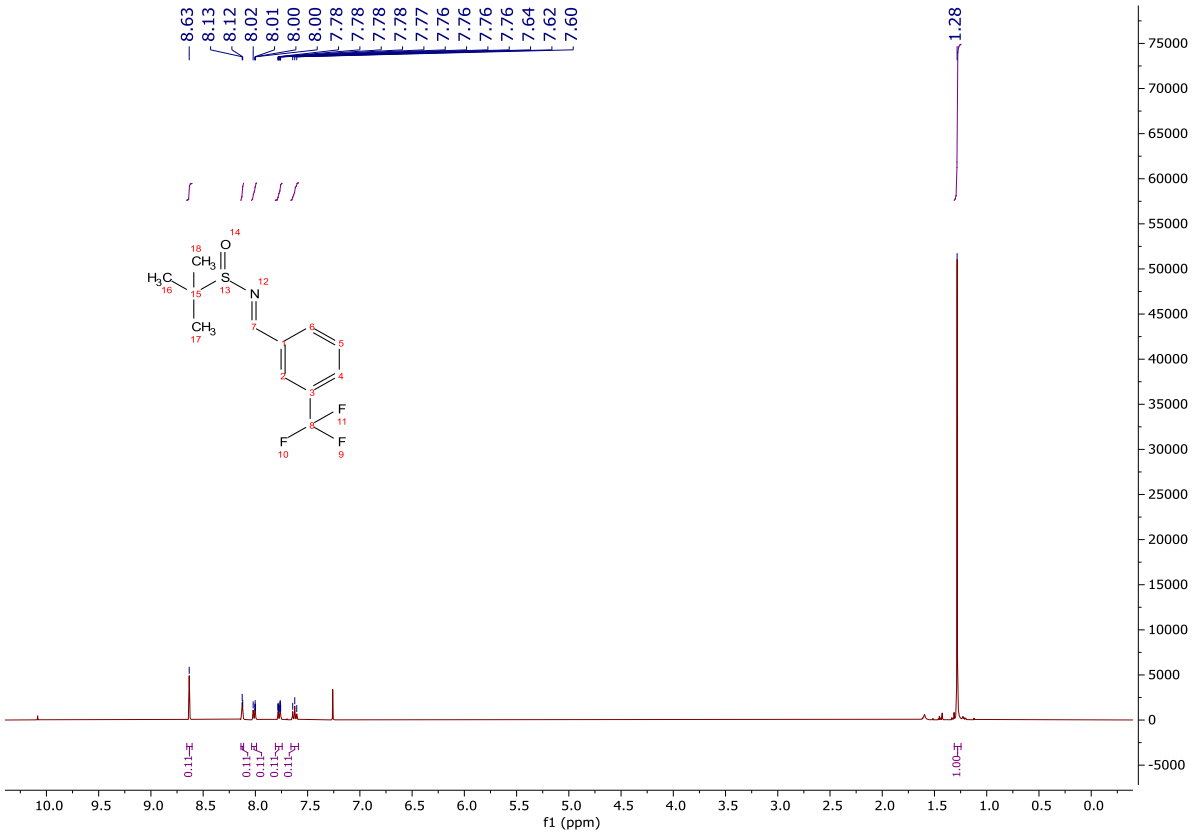
8.63
8.13
8.12
8.02
8.01
8.00
8.00
7.78
7.78
7.78
7.78
7.77
7.76
7.76
7.76
7.76
7.64
7.62
7.60
1.28
f1 (ppm)

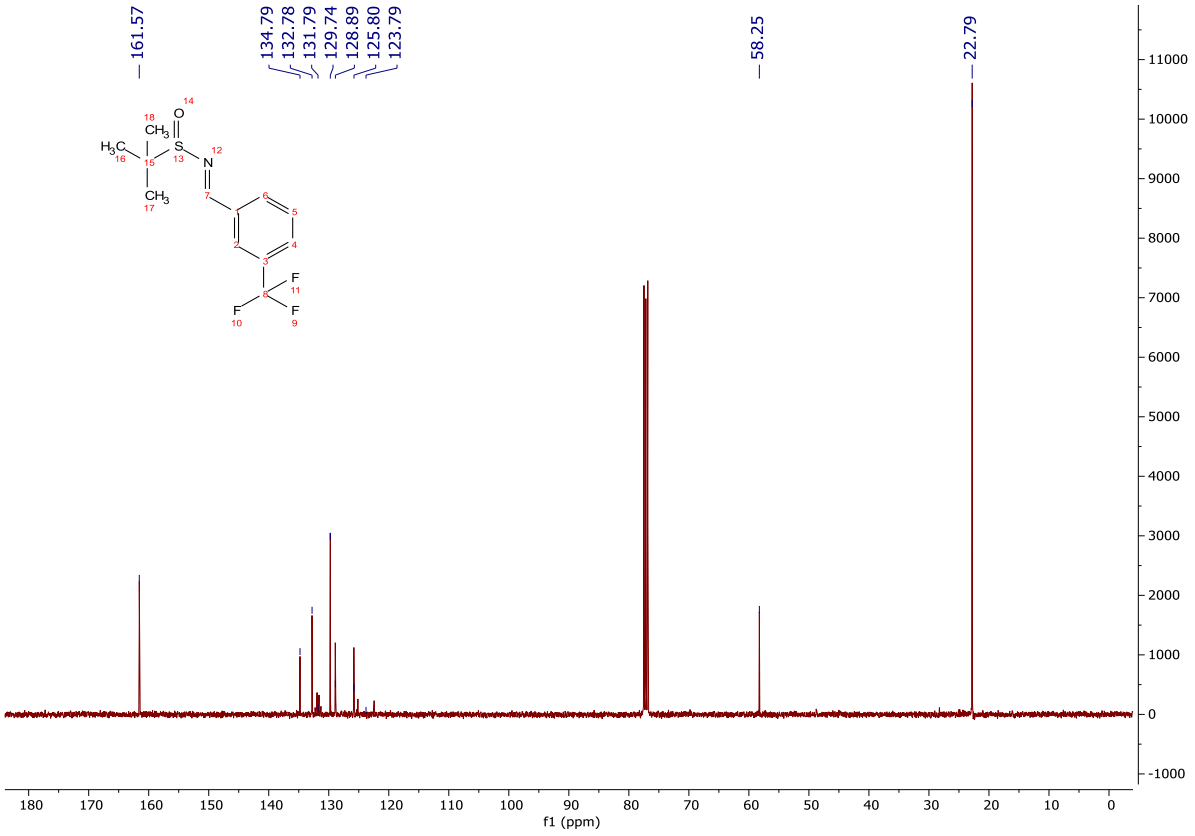
161.57
134.79
132.78
131.79
129.74
128.89
125.80
123.79
58.25
22.79
f1 (ppm)

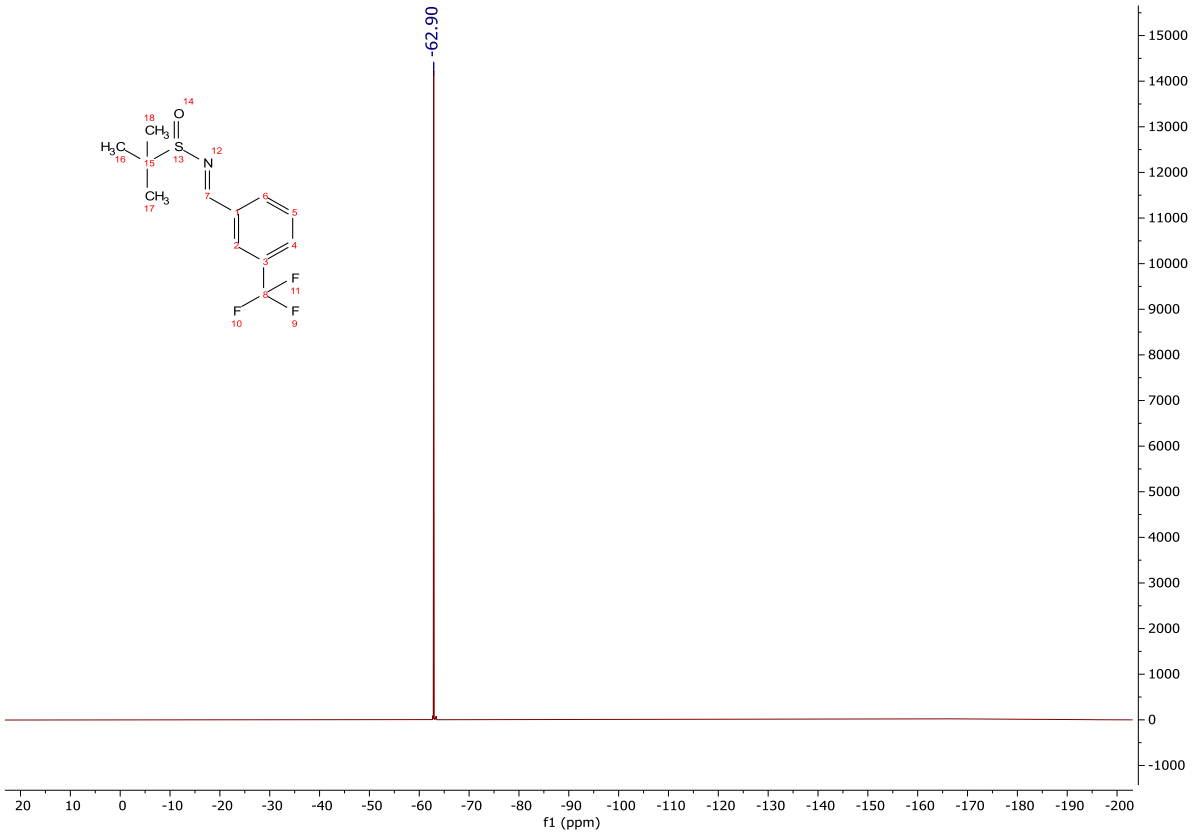
-62.90
15000
14000
13000
12000
11000
10000
9000
8000
7000
6000
5000
4000
3000
2000
1000
0
-1000
20 10 0 -10 -20 -30 -40 -50 -60 -70 -80 -90 -100 -110 -120 -130 -140 -150 -160 -170 -180 -190 -200
f1 (ppm)

tert-Butyl 3-((*tert*-butylsulfinyl)amino)-3-(3-(trifluoromethyl)phenyl)propanoate (**115**)

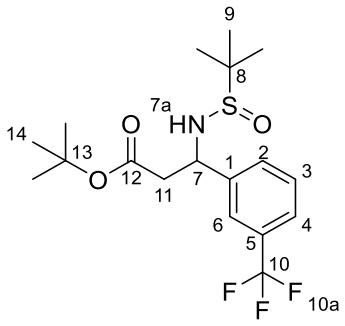

To a stirred suspension of zinc powder (12.0 g, 185 mmol) in anhydrous THF (50.0 mL) under a nitrogen atmosphere was added TMSCl (1.40 mL, 11.0 mmol). The suspension was stirred for 30 min and then heated under reflux at 85 °C. *tert*-Butyl bromoacetate (7.20 mL, 48.8 mmol) was added dropwise over 20 min and the suspension stirred at 85 °C for 1 h. The reaction mixture was cooled to 0^0C and a solution of **114** (3.39 g, 12.2 mmol) in anhydrous THF (20.0 mL) was added and stirred for 50 h. The reaction was quenched with brine (100 mL) and the reaction mixture was filtered through Celite®. The mother liquors were washed with sat. $NaHCO_{3(aq)}$ (3 x 40 mL), brine (3 x 40 mL), dried ($MgSO_4$) and concentrated *in vacuo* to afford a yellow oil (4.23 g). The crude product was purified by column chromatography on silica gel, eluting with a gradient of ethyl acetate/light petroleum (0-100%) to afford the title compound as a colourless, amorphous solid (3.61 g, 9.16 mmol, 75 %); **HRMS** *m/z* (ESI^+) calc. for $C_{18}H_{27}F_3NO_3S$ $[M+H]^+$ requires 394.1658, found 394.1657; $\boldsymbol{R_f}$ 0.59, 60% ethyl acetate/light petroleum, UV active; δ_H (400 MHz, $CDCl_3$) 7.61 (1H, m, H-6), 7.57 – 7.51 (2H, m, H-2 and H-4), 7.49 – 7.43 (1H, m, H-3), 4.82 (1H, td, *J* = 6.2, 4.0 Hz, H-7), 4.70 (1H, d, *J* = 4.0 Hz, H-7a), 2.79 (2H, dd, *J* = 6.3, 1.5 Hz, H-11), 1.39 (9H, s, H-14), 1.24 (9H, s, H-9); δ_C (100 MHz, $CDCl_3$) 170.0 (CO), 142.0 (C), 130.9 (C, q, *J* = 32.2 Hz), 130.8 (ArH), 129.0 (ArH), 124.7 (ArH, q, *J* = 3.7 Hz), 124.1 (ArH, q, *J* = 3.7 Hz), 82.0 (C), 55.9 (C), 55.3 (CH), 43.3 (CH_2), 28.0 (CH_3), 22.6 (CH_3); δ_F (376 MHz, $CDCl_3$) -62.7 (F-10a); ν_{max} (FT-ATR/cm^{-1}) 3191, 2984, 1708, 1327, 1161, 1116, 1048, 960, 808, 705.

N.B. One quaternary carbon is not observed: C-10.

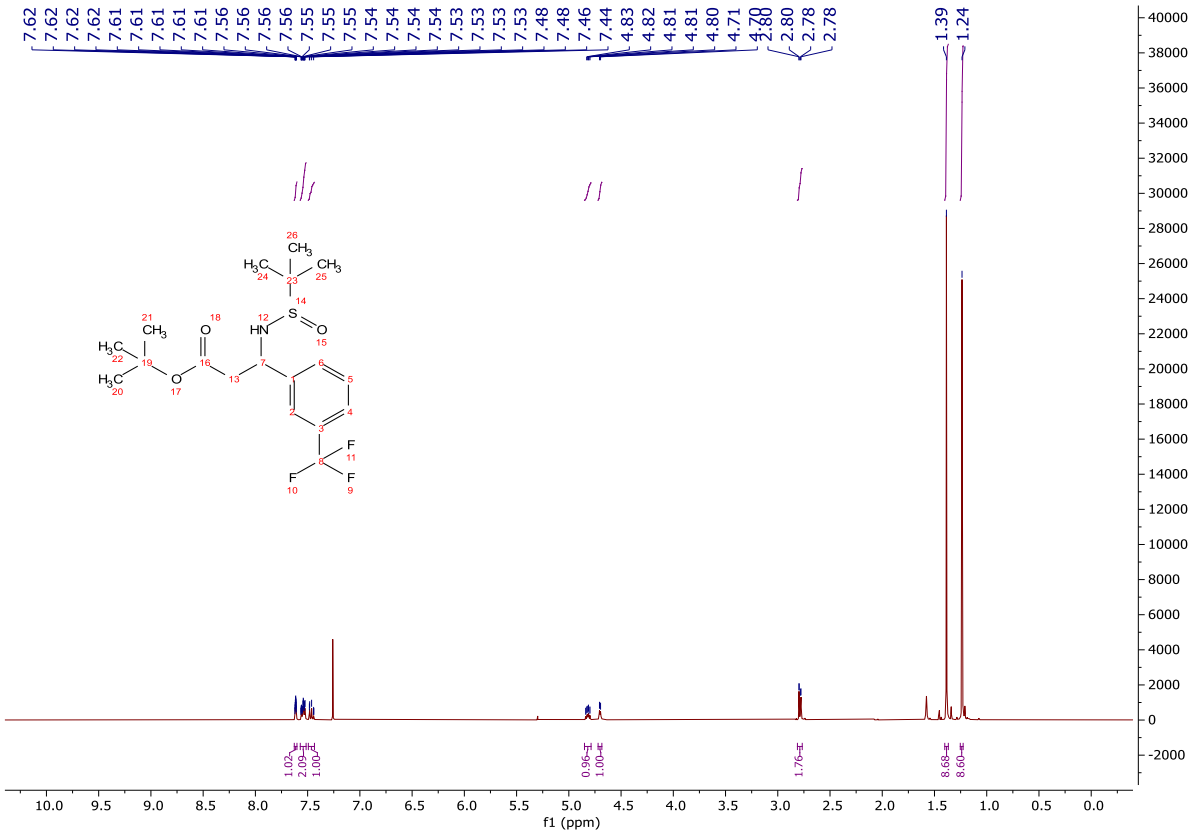
7.62
7.62
7.62
7.61
7.61
7.61
7.61
7.56
7.56
7.56
7.55
7.55
7.55
7.54
7.54
7.54
7.54
7.53
7.53
7.53
7.48
7.48
7.46
7.44
4.83
4.82
4.81
4.81
4.80
4.71
4.70
2.80
2.78
2.78
1.39
1.24
1.02
2.09
1.00
0.96
1.00
1.76
8.68
8.60
f1 (ppm)

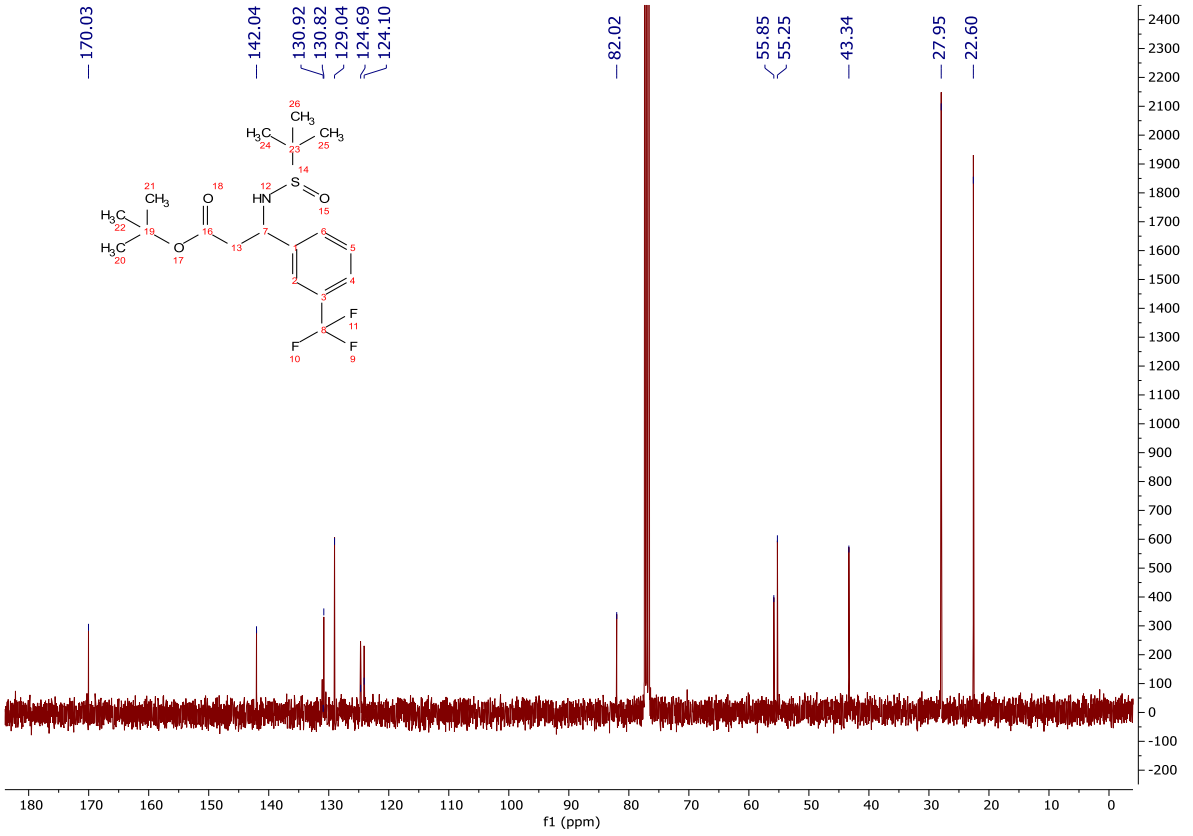
170.03
142.04
130.92
130.82
129.04
124.69
124.10
82.02
55.85
55.25
43.34
27.95
22.60
f1 (ppm)

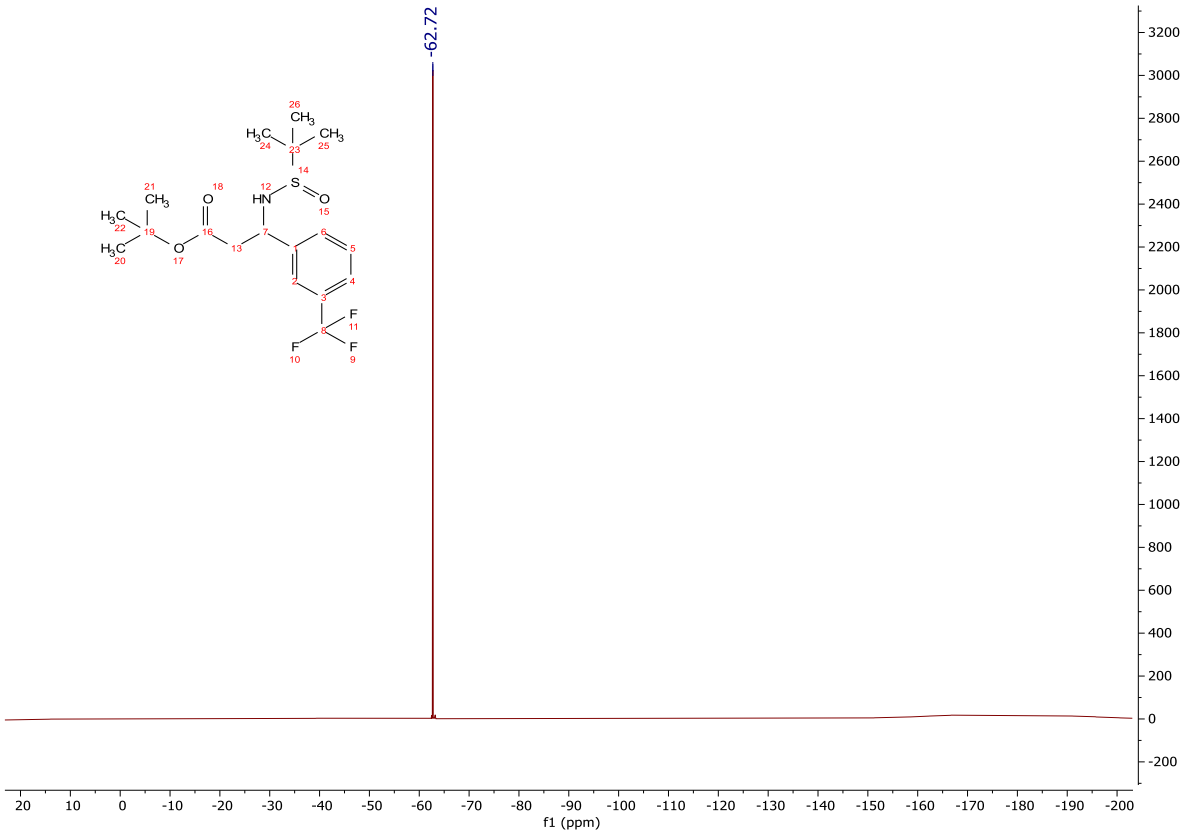
-62.72
f1 (ppm)

tert-Butyl 3-amino-3-(3-(trifluoromethyl)phenyl)propanoate hydrochloride (**116**)

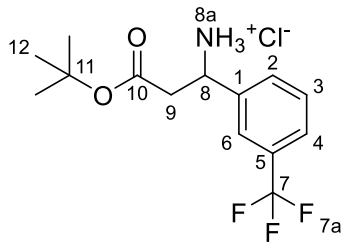

To a stirred solution of **115** (3.60 g, 9.16 mmol) in anhydrous diethyl ether (92.0 mL) under a nitrogen atmosphere at rt was added 4M HCl in dioxane (4.60 mL, 18.3 mmol). A colourless precipitate formed, and the reaction mixture was stirred for 2 h. The solvent was removed *in vacuo* to afford a colourless solid. The residue was triturated with diethyl ether and collected to afford the title compound as a colourless solid (2.96 g, 9.11 mmol, 99%); **HRMS** *m/z* (ESI^+) calc. for $C_{14}H_{19}F_3NO_2$ $[M+H]^+$ requires 290.1362, found 290.1383; $\boldsymbol{R_f}$ 0.54, 2% methanol/CH_2Cl_2, UV active; δ_H (400 MHz, DMSO-d_6) 8.76 (2H, m, H-8a), 7.96 – 7.85 (2H, m, H-6 and H-4), 7.77 (1H, d, *J* = 7.9 Hz, H-2), 7.68 (1H, t, *J* = 7.7 Hz, H-3), 4.73 – 4.63 (1H, m, H-8), 3.21 – 2.88 (2H, m, H-9), 1.22 (9H, s, H-12); δ_C (101 MHz, DMSO-d_6) 168.0 (CO), 138.0 (C), 132.1 (ArH), 129.8 (ArH), 129.2 (C, q, *J* = 32.2 Hz), 125.6 (ArH), 125.0 (ArH), 124.0 (CF_3, q, *J* = 272.1 Hz), 81.0 (C), 50.6 (CH), 39.5 (CH_2, assigned by HSQC), 27.4 (CH_3); δ_F (376 MHz, DMSO-d_6) -61.2 (F-7a); ν_{max} (FT-ATR/cm^{-1}) 3367, 1737, 1373, 1236, 1044.

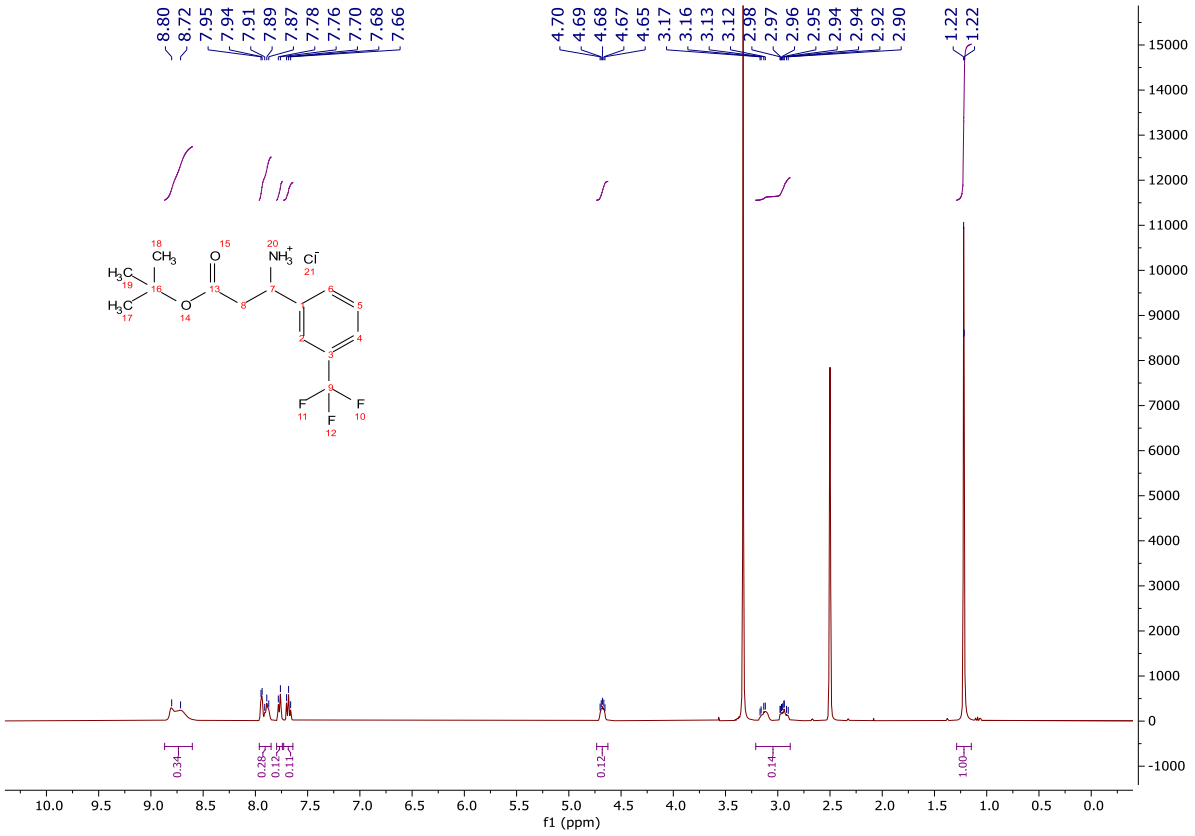
8.80
8.72
7.95
7.94
7.91
7.89
7.87
7.78
7.76
7.70
7.68
7.66
4.70
4.69
4.68
4.67
4.65
3.17
3.16
3.13
3.12
2.98
2.97
2.96
2.95
2.94
2.94
2.92
2.90
1.22
1.22
0.34
0.28
0.12
0.11
0.12
0.14
1.00
f1 (ppm)

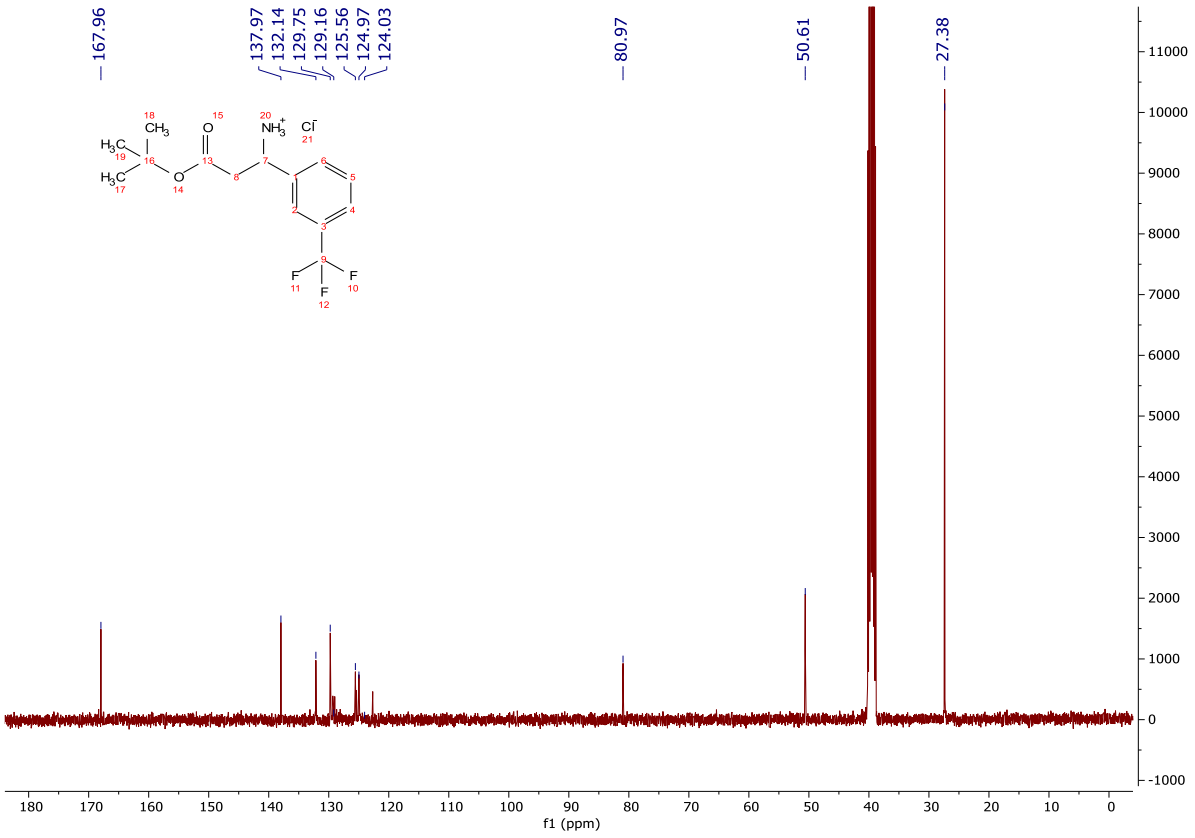
167.96
137.97
132.14
129.75
129.16
125.56
124.97
124.03
80.97
50.61
27.38
f1 (ppm)


-61.16
23000
22000
21000
20000
19000
18000
17000
16000
15000
14000
13000
12000
11000
10000
9000
8000
7000
6000
5000
4000
3000
2000
1000
0
-1000
-2000
20 10 0 -10 -20 -30 -40 -50 -60 -70 -80 -90 -100 -110 -120 -130 -140 -150 -160 -170 -180 -190 -200
f1 (ppm)

Ethyl (*S*)-3-amino-3-(3-(trifluoromethyl)phenyl)propanoate hydrochloride (**118**)

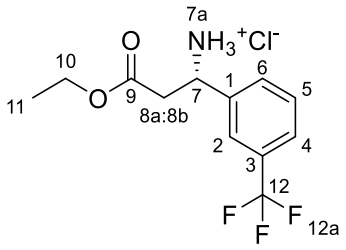

To a stirred solution of (*R*)-*tert*-butanesulfinamide (7.66 g, 63.3 mmol) in anhydrous THF (115 mL) was added 3-(trifluoromethyl)benzaldehyde (7.69 mL, 57.5 mmol). The mixture was stirred at rt for 5 min and Ti(O*i*-Pr)$_4$ (34.0 mL, 115 mmol) was added. The reaction mixture was stirred at rt for 18 h. The reaction mixture was concentrated *in vacuo*, dissolved in ethyl acetate (150 mL), poured into brine (150 mL) and filtered through Celite®. The layers were separated, and the organic layer washed with sat. $NaHCO_{3(aq)}$ (2 x 50 mL) and brine (2 x 50 mL). The organics were dried (Na_2SO_4) and concentrated *in vacuo* to afford the sulfinimine **(*R*)-114** as a yellow oil that solidified on standing to a colourless solid; the crude product was not purified further. To a stirred suspension of zinc powder (18.3 g, 282 mmol) in anhydrous THF (60.0 mL) under a nitrogen atmosphere was added TMSCl (7.15 mL, 56.3 mmol). The suspension was heated under reflux for 5 min. Ethyl bromoacetate (18.7 mL, 169 mmol) was added dropwise over 20 min and the solution stirred under reflux for 1 h. The reaction mixture was cooled to 0 °C and a solution of **(*R*)-114** in anhydrous THF (50.0 mL) was added and stirred for 18 h. 10% Citric acid$_{(aq)}$ (200 mL) was added, and the mixture stirred for 10 min. The reaction mixture was filtered through Celite® and concentrated *in vacuo*. Ethyl acetate (150 mL) was added, and the layers separated. The organic was washed with sat. $NaHCO_{3(aq)}$ (2 x 150 mL), brine (150 mL), dried ($MgSO_4$) and concentrated *in vacuo* to afford the sulfinamide **117** as a yellow oil; the crude product was not purified further. To a stirred solution of **117** in anhydrous diethyl ether (180 mL) at rt was added 4M HCl in dioxane (23.0 mL, 90.2 mmol). The reaction mixture was stirred for 20 min, filtered and the filter cake washed with diethyl ether to afford the title compound as a colourless powder (11.2 g, 37.7

mmol, 66% over three steps); **HRMS** *m/z* (ESI^+) calc. for $C_{12}H_{15}F_3NO_2$ $[M+H]^+$ requires 262.1049, found 262.1050; $\boldsymbol{R_f}$ 0.51, 5% methanol/CH_2Cl_2, UV active; δ_H (400 MHz, DMSO-d_6) 8.93 (3H, bs, H-7a), 8.03 – 7.96 (1H, m, H-2), 7.96 – 7.87 (1H, m, H-4), 7.78 – 7.71 (1H, m, H-6), 7.66 (1H, dd, *J* = 7.8, 7.8 Hz, H-5), 4.73 (1H, dd, *J* = 9.3, 5.6 Hz, H-7), 4.04 – 3.91 (2H, m, H-10), 3.26 (1H, dd, *J* = 16.2, 5.6 Hz, H-8a), 3.08 (1H, dd, *J* = 16.2, 9.3 Hz, H-8b), 1.05 (3H, t, *J* = 7.1 Hz, H-11); δ_C (101 MHz, DMSO-d_6) 168.9 (CO), 138.1 (C), 132.1 (ArH), 129.7 (ArH), 129.2 (C, q, *J* = 32.0 Hz), 125.6 (ArH, q, *J* = 3.8 Hz), 124.9 (ArH, q, *J* = 3.8 Hz), 124.0 (CF_3, q, *J* = 272.0 Hz), 60.5 (CH_2), 50.5 (CH), 38.4 (CH_2), 13.8 (CH_3); δ_F (376 MHz, DMSO-d_6) -61.1 (F-12a); **MP** 137-139 °C; ν_{max} (FT-ATR/cm^{-1}) 2856, 1742, 1599, 1518, 1454, 1394, 1324, 1255, 1192, 1165, 1120, 1077, 1028, 812, 706.

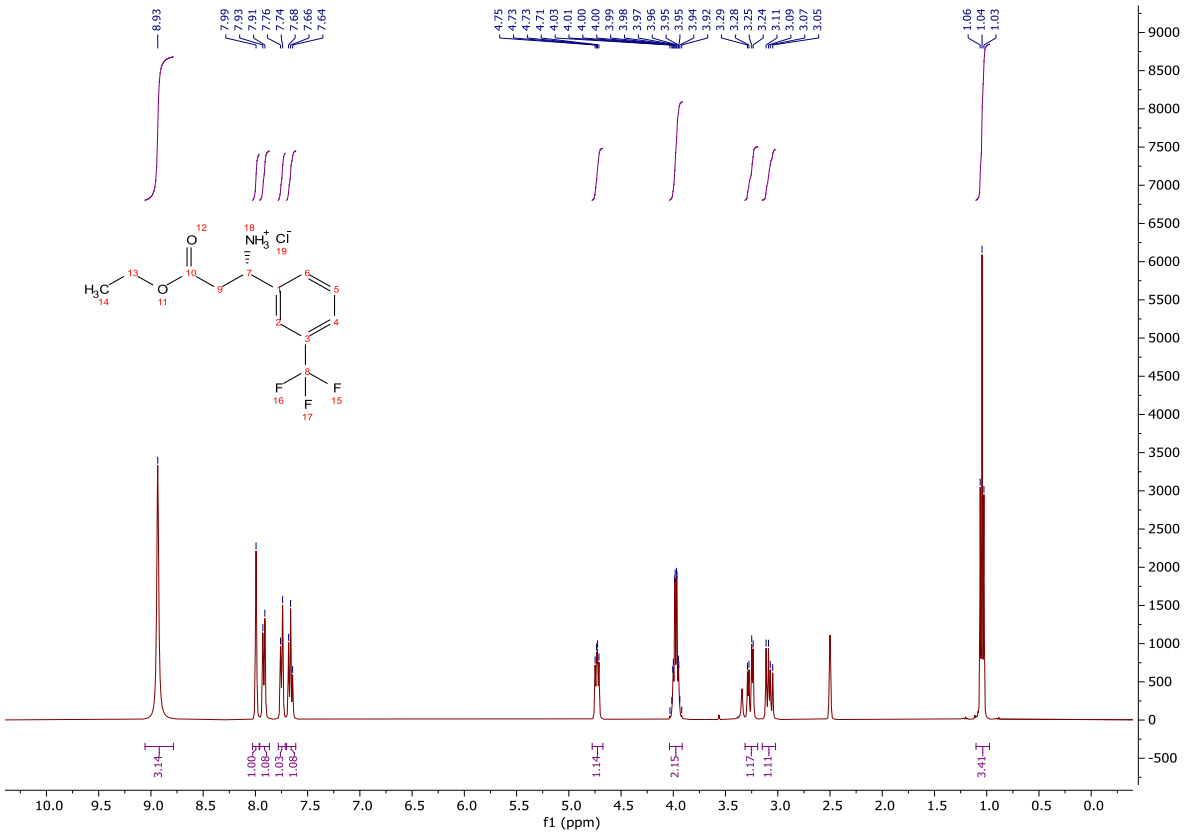
8.93
7.99
7.93
7.91
7.76
7.74
7.68
7.66
7.64
4.75
4.73
4.73
4.71
4.03
4.01
4.00
4.00
3.99
3.98
3.97
3.96
3.95
3.95
3.94
3.92
3.29
3.28
3.25
3.24
3.11
3.09
3.07
3.05
1.06
1.04
1.03
3.14
1.00
1.08
1.03
1.08
1.14
2.15
1.17
1.11
3.41
f1 (ppm)

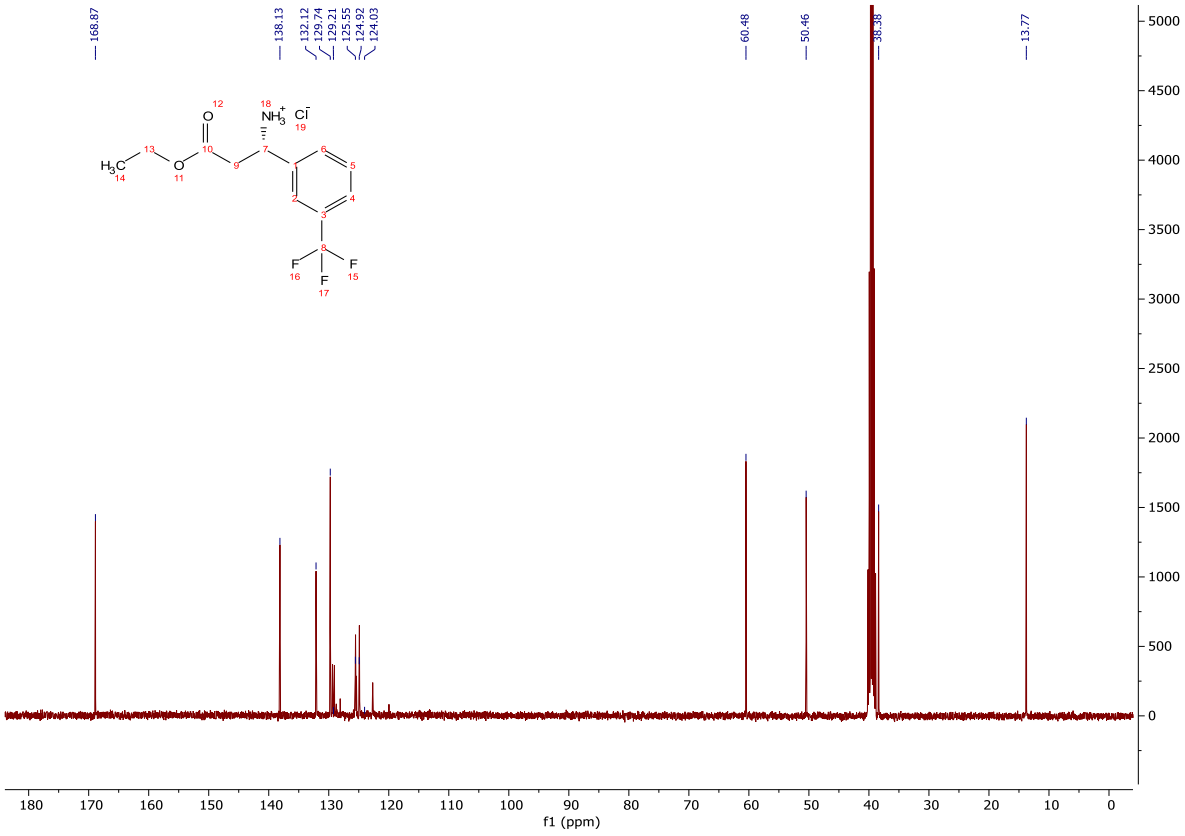
168.87
138.13
132.12
129.74
129.21
125.55
124.92
124.03
60.48
50.46
39.38
13.77
f1 (ppm)


-61.12
9000
8500
8000
7500
7000
6500
6000
5500
5000
4500
4000
3500
3000
2500
2000
1500
1000
500
0
-500
20 10 0 -10 -20 -30 -40 -50 -60 -70 -80 -90 -100 -110 -120 -130 -140 -150 -160 -170 -180 -190 -200
f1 (ppm)

Ethyl (*S*)-3-(3-bromophenyl)-3-((*tert*-butoxycarbonyl)amino)propanoate (**(*S*)-119**)

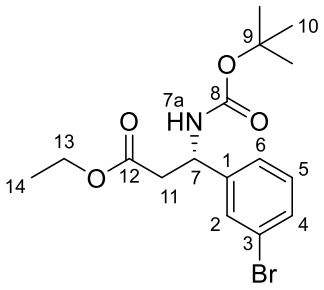

To a stirred solution of **107** (15.0 g, 48.9 mmol) in THF (200 mL) at 0 °C was added Et_3N (20.5 mL, 147 mmol). A solution of di-*tert*-butyl dicarbonate (14.6 mL, 63.6 mmol) in THF (20 mL) was added and the reaction mixture stirred for 65 h. The reaction mixture was concentrated *in vacuo* and the crude material dissolved in ethyl acetate (150 mL) and sat. $NaHCO_{3(aq)}$ (150 mL). The layers were separated and the organic washed with 10% citric $acid_{(aq)}$ (150 mL), water (150 mL), brine (150 mL), dried ($MgSO_4$) and concentrated *in vacuo* to afford a yellow oil. The crude product was recrystallised from light petroleum, affording the title compound as a colourless solid (17.1 g, 46.1 mmol, 94%); **HRMS** *m/z* (ESI^+) calc. for $C_{16}H_{23}BrNO_4$ $[M+H]^+$ requires 372.0805, found 372.0803; $\boldsymbol{R_f}$ 0.21, 10% ethyl acetate/light petroleum, UV active; δ_H (400 MHz, $CDCl_3$) 7.45 – 7.42 (1H, m, H-2), 7.38 (1H, ddd, *J* = 7.4, 1.7, 1.7 Hz, H-6), 7.25 – 7.16 (2H, m, H-3 and H-4), 5.65 – 5.42 (1H, m, H-7a), 5.14 – 4.94 (1H, m, H-7), 4.08 (2H, q, *J* = 7.1 Hz, H-13), 2.91 – 2.68 (2H, m, H-11), 1.42 (9H, s, H-10), 1.18 (3H, t, *J* = 7.1 Hz, H-14); δ_C (101 MHz, $CDCl_3$) 170.8 (CO), 155.1 (CO), 143.9 (C), 130.7 (ArH), 130.3 (ArH), 129.5 (ArH), 125.0 (ArH), 122.8 (C), 80.1 (C), 61.0 (CH_2), 50.9 (CH), 40.9 (CH_2), 28.5 (CH_3), 14.2 (CH_3); **MP** 65-69 °C; ν_{max} (FT-ATR/cm^{-1}) 3369, 2980, 1725, 1685, 1518, 1286, 1165, 1006, 697, 608.

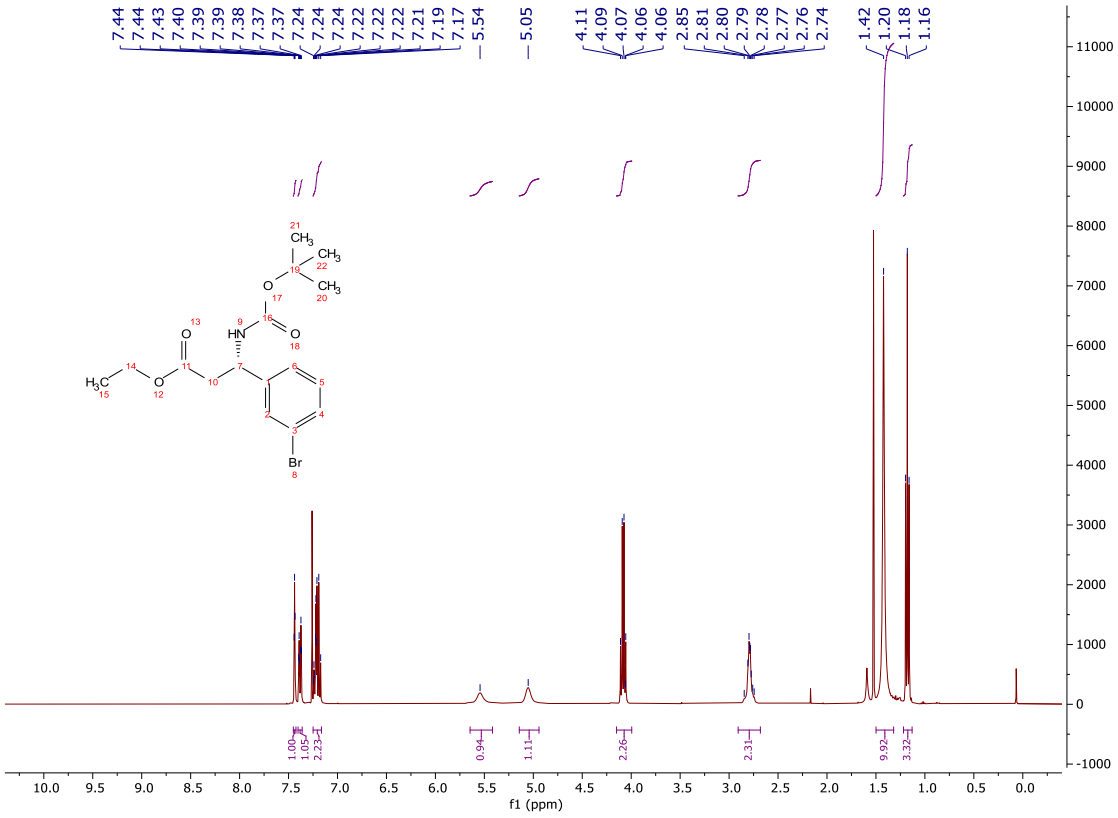
7.44
7.44
7.43
7.40
7.39
7.39
7.38
7.37
7.37
7.24
7.24
7.24
7.22
7.22
7.22
7.21
7.19
7.17
5.54
5.05
4.11
4.09
4.07
4.06
4.06
2.85
2.81
2.80
2.79
2.78
2.77
2.76
2.74
1.42
1.20
1.18
1.16
f1 (ppm)

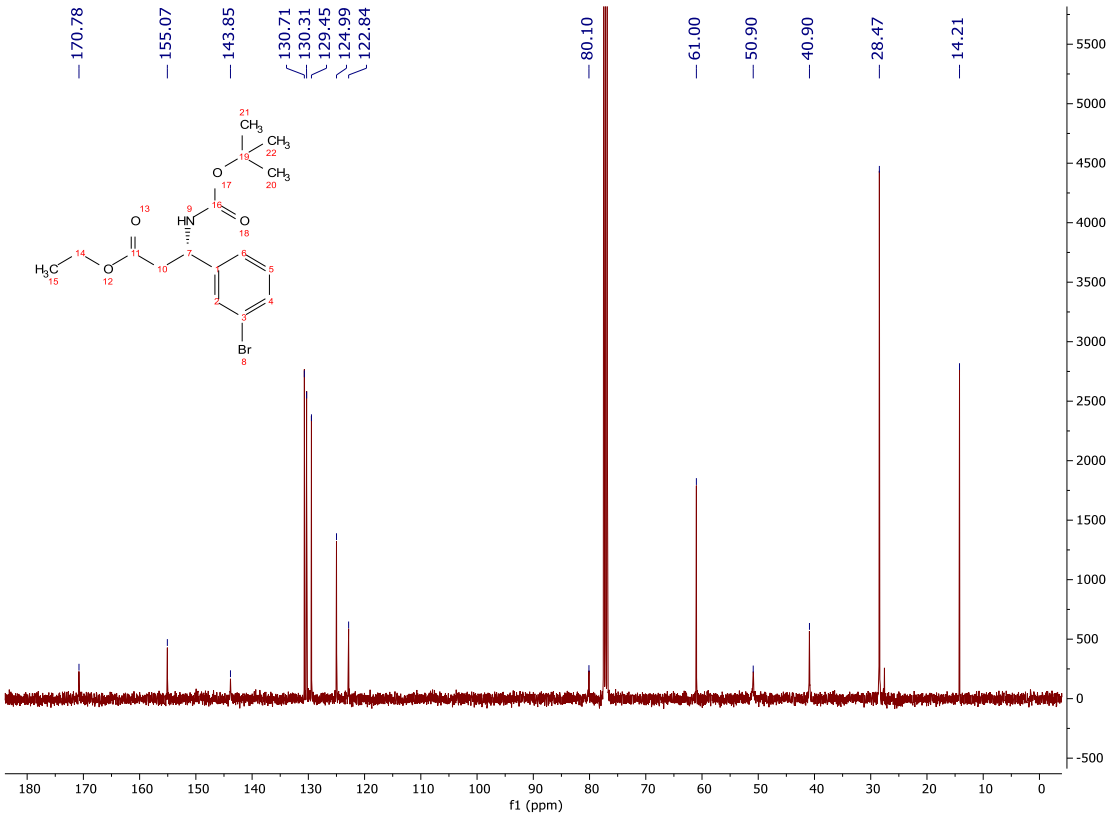
170.78
155.07
143.85
130.71
130.31
129.45
124.99
122.84
80.10
61.00
50.90
40.90
28.47
14.21
f1 (ppm)

tert-Butyl (*S*)-7-(5-((1-(3-bromophenyl)-3-(*tert*-butoxy)-3-oxopropyl)amino)-5-oxopentyl)-3,4-dihydro-1,8-naphthyridine-1(2*H*)-carboxylate (**191**)

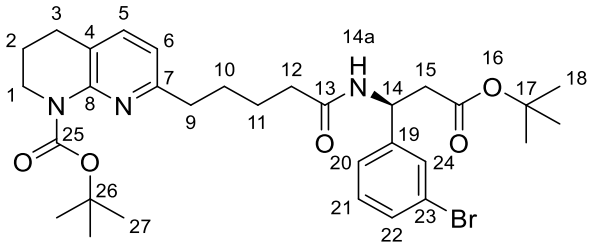

To a stirred solution of **110** (10.0 g, 29.9 mmol) and **82** (10.2 g, 29.9 mmol) in acetonitrile (150 mL) at 0 °C was added T3P (50% in ethyl acetate, 17.8 mL, 59.8 mmol) and *i*-Pr_2NEt (21.0 mL, 120 mmol). The reaction mixture was stirred at rt for 18 h and concentrated *in vacuo*. The crude product was dissolved in ethyl acetate (100 mL) and washed with sat. $NaHCO_{3(aq)}$ (50 mL), sat. $NH_4Cl_{(aq)}$ (100 mL), sat. $NaHCO_{3(aq)}$ (50 mL) and brine (50 mL). The organic layer was dried ($MgSO_4$) and concentrated *in vacuo* to afford a brown oil. The crude product was purified by column chromatography on silica gel, eluting with ethyl acetate to give the title compound as a yellow oil (15.7 g, 25.5 mmol, 85%); **HRMS** *m/z* (ESI^+) calc. for $C_{31}H_{43}BrN_3O_5$ $[M+H]^+$ requires 616.2381, found 616.2376; $\boldsymbol{R_f}$ 0.39, 60% ethyl acetate/light petroleum, UV active; δ_H (400 MHz, $CDCl_3$) 7.40 (1H, dd, *J* = 1.9, 1.9 Hz, H-24), 7.36 (1H, ddd, *J* = 7.6, 1.6, 1.6 Hz, H-20), 7.29 – 7.25 (1H, m, H-5), 7.22-7.19 (1H, m, H-22), 7.16 (1H, dd, *J* = 7.7, 7.7 Hz, H-21), 6.83 – 6.76 (2H, m, H-6 and H-14a), 5.33 (1H, dt, *J* = 8.4, 5.9 Hz, H-14), 3.78 – 3.70 (2H, m, H-1), 2.78 – 2.63 (6H, m, H-3, H-9 and H-15), 2.27 (2H, t, *J* = 7.2 Hz, H-12), 1.95 – 1.86 (2H, m, H-2), 1.82 – 1.67 (4H, m, H-10 and H-11), 1.50 (9H, s, H-18), 1.33 (9H, s, H-27); δ_C (101 MHz, $CDCl_3$) 172.4 (CO), 170.5 (CO), 158.2 (C), 154.2 (CO), 151.2 (C), 143.5 (C), 137.4 (ArH), 130.6 (ArH), 130.2 (ArH), 129.6 (ArH), 125.3 (ArH), 122.7 (C), 122.0 (C), 118.4 (ArH), 81.8 (C), 80.9 (C), 49.2 (C), 45.0 (CH_2), 41.1 (CH_2), 37.6 (CH_2), 36.6 (CH_2), 29.2 (CH_2), 28.6 (CH_3), 28.1 (CH_3), 26.4 (CH_2), 25.4 (CH_2), 23.5 (CH_2); ν_{max} (FT-ATR/cm^{-1}) 3300, 2976, 1692, 1465, 1365, 1252, 1146, 697.

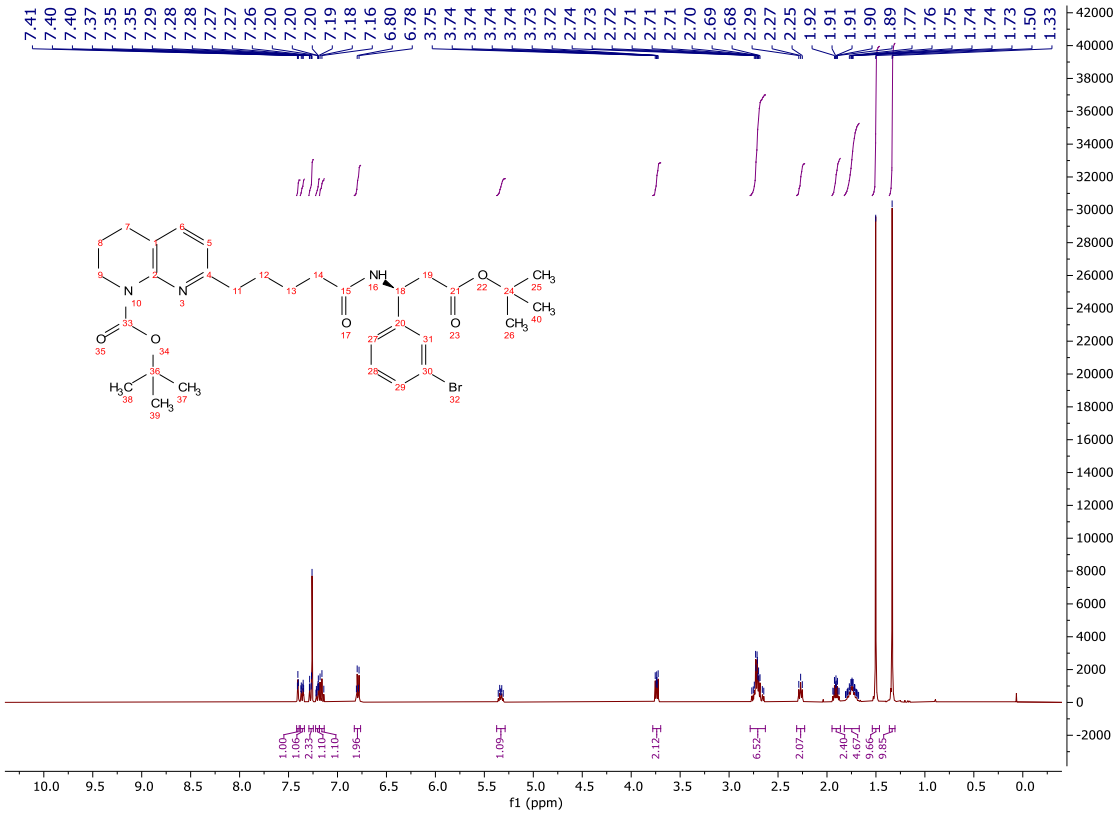
7.41 7.40 7.40 7.37 7.35 7.35 7.29 7.28 7.28 7.27 7.27 7.26 7.20 7.20 7.20 7.19 7.18 7.16 6.80 6.78 3.75 3.74 3.74 3.74 3.74 3.73 3.72 2.74 2.73 2.72 2.71 2.71 2.71 2.70 2.69 2.68 2.29 2.27 2.25 1.92 1.91 1.91 1.90 1.89 1.77 1.76 1.75 1.74 1.74 1.73 1.50 1.33
1.00 1.06 2.33 1.10 1.10 1.96 1.09 2.12 6.52 2.07 2.40 4.67 9.66 9.85
f1 (ppm)

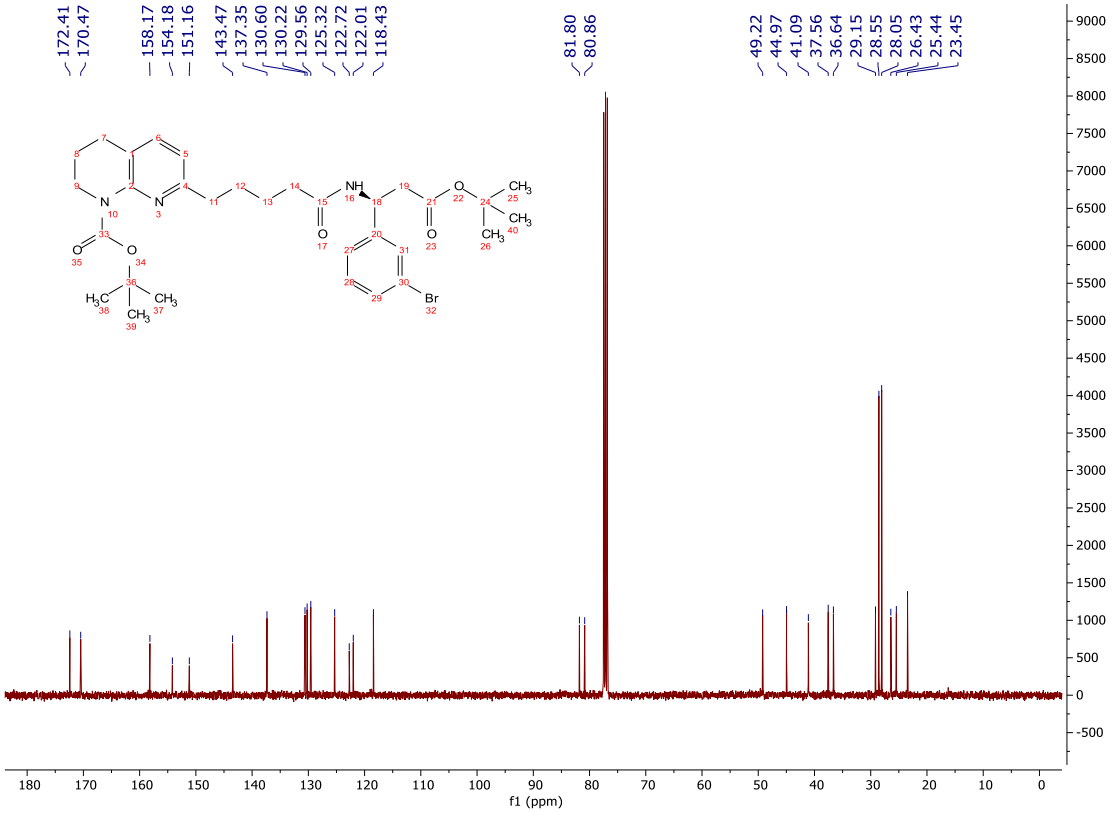
172.41 170.47 158.17 154.18 151.16 143.47 137.35 130.60 130.22 129.56 125.32 122.72 122.01 118.43 81.80 80.86 49.22 44.97 41.09 37.56 36.64 29.15 28.55 28.05 26.43 25.44 23.45
f1 (ppm)

tert-Butyl (*S*)-7-(5-((3-(*tert*-butoxy)-3-oxo-1-(3-(4,4,5,5-tetramethyl-1,3,2-dioxaborolan-2-yl)phenyl)propyl)amino)-5-oxopentyl)-3,4-dihydro-1,8-naphthyridine-1(2*H*)-carboxylate (**192**)

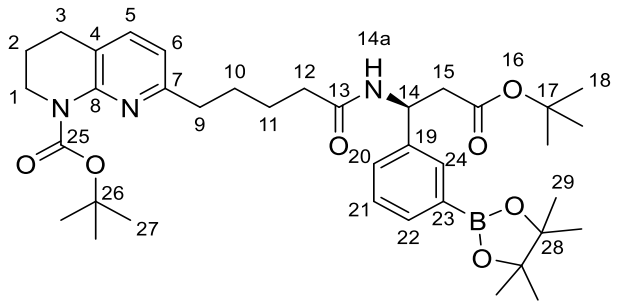

A mixture of **191** (6.24 g, 10.1 mmol), B_2Pin_2 (3.85 g, 15.2 mmol), KOAc (2.98 g, 30.4 mmol) and $Pd(dppf)Cl_2.CH_2Cl_2$ (826 mg, 1.01 mmol) in 1,4-dioxane (27.0 mL) was stirred under a nitrogen atmosphere at 80 °C for 16 h. The reaction mixture was concentrated *in vacuo* and the crude product dissolved in ethyl acetate (50 mL). The organic was filtered through Celite®, washed with sat. $NaHCO_{3(aq)}$ (2 x 50 mL), brine (2 x 50 mL), dried ($MgSO_4$) and concentrated *in vacuo* to afford a dark brown oil. The crude product was purified by column chromatography on silica gel, eluting with a gradient of ethyl acetate/light petroleum (0-100%) to afford the title compound as a dark yellow oil (6.69 g, 5.64 mmol, 56%); **HRMS** *m/z* (ESI^+) calc. for $C_{37}H_{55}BN_3O_7$ $[M+H]^+$ requires 664.4128, found 664.4131; $\boldsymbol{R_f}$ 0.34, 60% ethyl acetate/light petroleum, UV active; δ_H (400 MHz, $CDCl_3$) 7.72 – 7.64 (2H, m, H-22 and H-24), 7.38 (1H, ddd, *J* = 7.8, 1.8, 1.8 Hz, H-20), 7.32 – 7.23 (2H, m, H-21 and H-5), 6.77 (1H, d, *J* = 7.6 Hz, H-6), 6.63 (1H, d, *J* = 8.5 Hz, H-14a), 5.38 (1H, ddd, *J* = 8.5, 6.2, 6.2 Hz, H-14), 3.77 – 3.68 (2H, m, H-1), 2.84 – 2.63 (6H, m, H-3, H-9 and H-15), 2.24 (2H, t, *J* = 7.2 Hz, H-12), 1.94 – 1.83 (2H, m, H-2), 1.81 – 1.63 (4H, m, H-10 and H-11), 1.49 (9H, s, H-18), 1.36 – 1.28 (21H, m, H-27 and H-29); δ_C (126 MHz, $CDCl_3$) 172.1 (CO), 170.4 (CO), 158.0 (C), 154.0 (CO), 150.9 (C), 140.1 (C), 137.2 (ArH), 133.8 (ArH), 132.5 (ArH), 129.6 (ArH), 129.1 (C), 127.9 (ArH), 121.8 (C), 118.3 (ArH), 83.7 (C), 81.2 (C), 80.6 (C), 49.7 (CH), 44.7 (CH_2), 41.3 (CH_2), 37.4 (CH_2), 36.5 (CH_2),

29.0 (CH_2), 28.3 (CH_3), 27.8 (CH_3), 26.2 (CH_2), 25.3 (CH_2), 24.8 (CH_3), 23.2 (CH_2); ν_{max} (FT-ATR/cm^{-1}) 3309, 2976, 1694, 1538, 1465, 1357, 1142, 709.

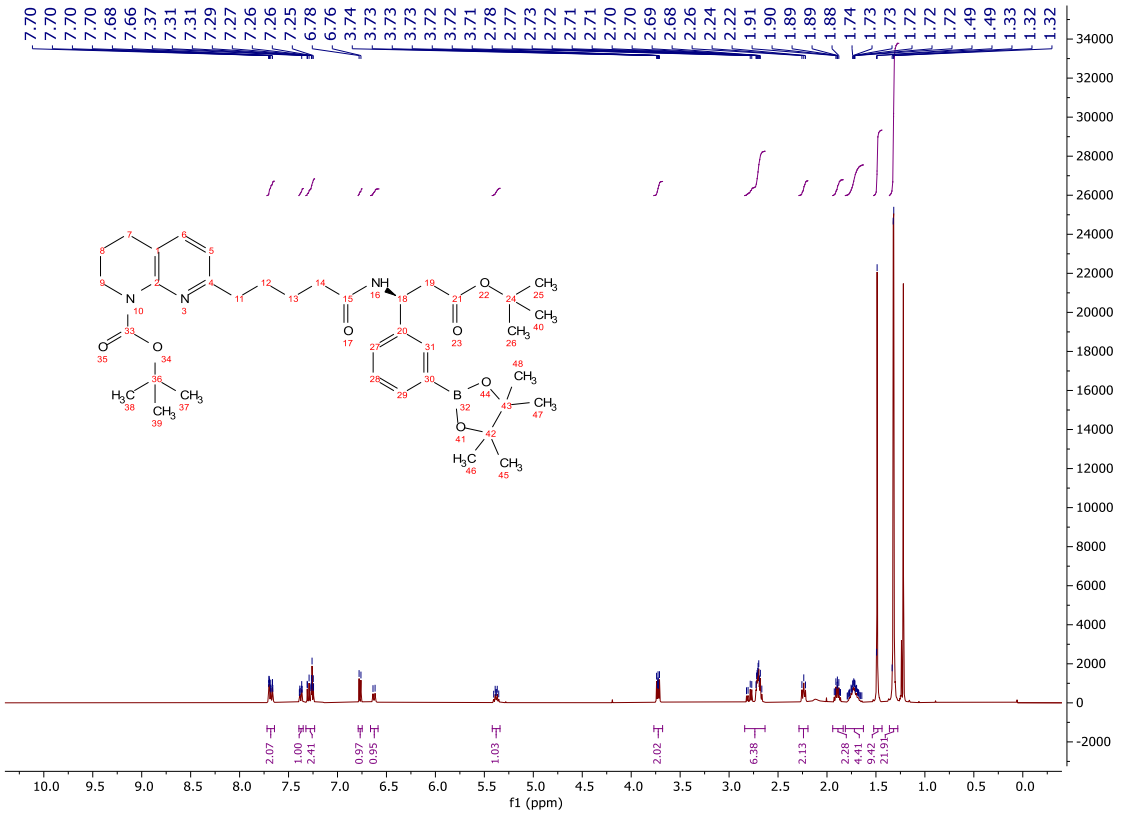
7.70 7.70 7.70 7.68 7.66 7.37 7.31 7.31 7.29 7.27 7.26 7.26 7.25 6.78 6.76 3.74 3.73 3.73 3.73 3.72 3.72 3.71 2.78 2.77 2.73 2.72 2.71 2.71 2.70 2.70 2.69 2.68 2.26 2.24 2.22 1.91 1.90 1.89 1.89 1.88 1.74 1.73 1.73 1.72 1.72 1.72 1.49 1.49 1.33 1.32 1.32
2.07 1.00 2.41 0.97 0.95 1.03 2.02 6.38 2.13 2.28 4.41 9.42 21.91
f1 (ppm)

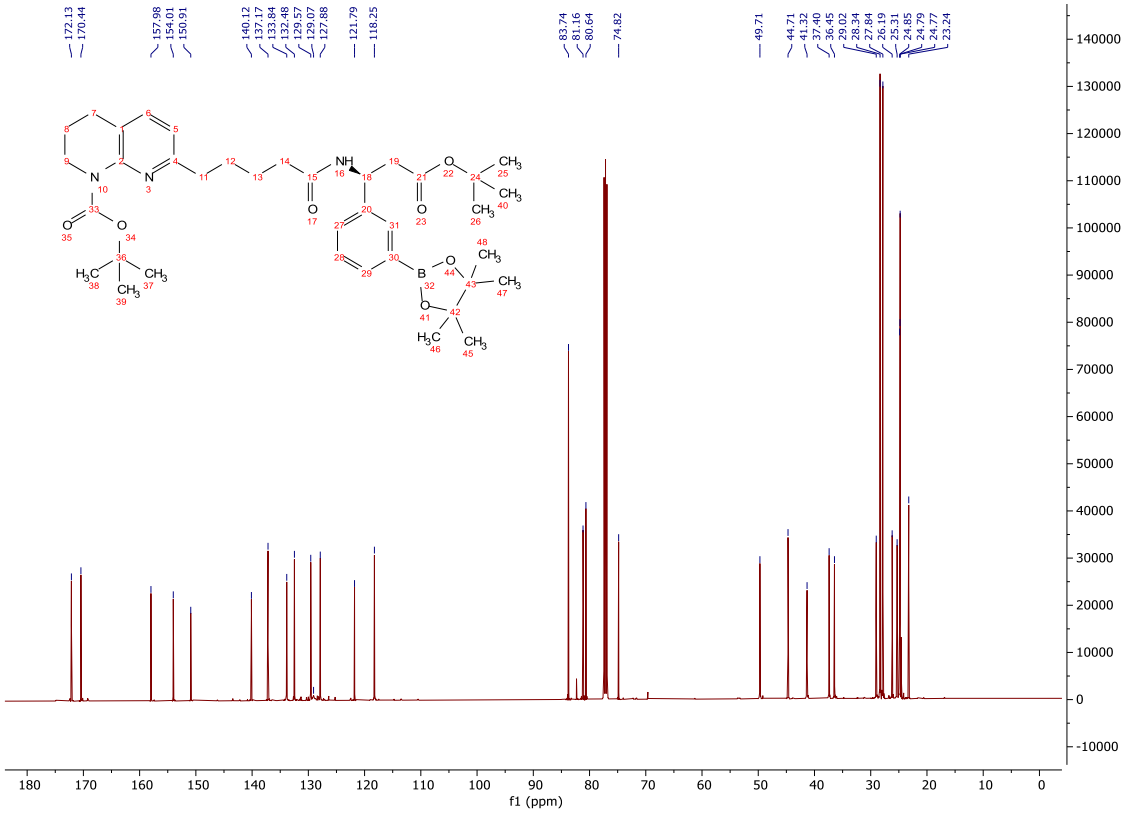
172.13 170.44 157.98 154.01 150.91 140.12 137.17 133.84 132.48 129.57 129.07 127.88 121.79 118.25 83.74 81.16 80.64 74.82 49.71 44.71 41.32 37.40 36.45 29.02 28.34 27.84 26.19 25.31 24.85 24.79 24.77 23.24
f1 (ppm)

High throughput array experimental details and copies of ^{1}H spectra

General preparation A of 3-phenyl-3-(5-(5,6,7,8-tetrahydro-1,8-napthyridin-2-yl)pentanamido)propanoic acid derivatives

192 (100 mg, 0.150 mmol), ***amine*** (0.375 mmol), $Cu(OAc)_2$ (27 mg, 0.150 mmol), $B(OH)_3$ (19 mg, 0.300 mmol), 4 Å M.S. (150 mg) in acetonitrile (0.500 mL) was stirred at 80 °C for 40 h. The crude reaction mixture was filtered through a 2 g isolute silica column, eluting with ethyl acetate/ethanol (3:1, 20 mL). The solvent was removed using Radleys blowdown apparatus and the crude product was then dissolved in CH_2Cl_2 (0.500 mL) before TFA (0.500 mL) was added and the reaction mixture stirred at rt for 4 h. The solvent and TFA was removed using Radleys blowdown apparatus. The crude product was dissolved in DMSO (2.00 mL) and purified by CAT Mass Directed AutoPrep on Xbridge column using Acetonitrile/Water with an ammonium carbonate modifier. The solvent was removed under a stream of nitrogen to give the required product.

General preparation B of 3-phenyl-3-(5-(5,6,7,8-tetrahydro-1,8-napthyridin-2-yl)pentanamido)propanoic acid derivatives

To a stirred solution of ***amine*** (0.375 mmol) in acetonitrile (0.250 mL) was added potassium carbonate (0.375 mmol). The mixture was stirred for 5 min at rt after which time, **192** (100 mg, 0.150 mmol) as a solution in acetonitrile (0.250 mL), $Cu(OAc)_2$ (27 mg, 0.150 mmol), $B(OH)_3$ (19 mg, 0.300 mmol) and 4 Å M.S. (150 mg) were added. The reaction mixture was stirred at 80 °C for 40 h. The crude reaction mixture was filtered through a 2 g isolute silica column, eluting with ethyl acetate/ethanol (3:1, 20 mL). The solvent was removed using Radleys blowdown apparatus and the crude product was then dissolved in CH_2Cl_2 (0.500 mL) before TFA (0.500 mL) was added and the reaction mixture stirred at rt for 4 h. The solvent and TFA was removed using Radleys blowdown apparatus. The crude product was dissolved in DMSO (2.00 mL) and purified by CAT Mass Directed AutoPrep on Xbridge column using

Acetonitrile/Water with an ammonium carbonate modifier. The solvent was removed under a stream of nitrogen to give the required product.

Where relevant, initial yield values refer to major regioisomers (indicated by given structure) and yields given in brackets refer to minor regioisomers. Major regioisomer structures were confirmed by 2D NMR techniques.

The following compounds (**(*S*)-27, (*S*)-39, (*S*)-40, 193**-**236**) were synthesised using general preparation A. General preparation B was used in the attempted synthesis of compounds that used the hydrochloride salt of the amine nucleophile (Figure 33); no products were successfully isolated using general preparation B.

(*S*)-3-(3-(1*H*-Pyrazol-1-yl)phenyl)-3-(5-(5,6,7,8-tetrahydro-1,8-naphthyridin-2-yl)pentanamido)propanoic acid (**(*S*)-40**)

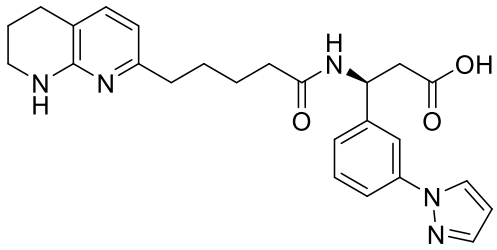

Mass 5.6 mg; Yield 7%; LCMS 90% purity; 0.55 min; *m/z* $[M+H]^+$ 448.34; Clear, colourless oil.

δ_H (700 MHz, DMSO-d_6) 8.46 (d, *J* = 8.2 Hz, 1H), 8.42 (d, *J* = 2.5 Hz, 1H), 7.79 (dd, *J* = 1.9. 1.9 Hz, 1H), 7.73 (d, *J* = 1.7 Hz, 1H), 7.68 – 7.64 (m, 1H), 7.39 (dd, *J* = 7.9, 7.9 Hz, 1H), 7.22 (d, *J* = 7.9 Hz, 1H), 7.05 – 6.99 (m, 1H), 6.53 (t, *J* = 2.1 Hz, 1H), 6.43 (bs, 1H), 6.24 – 6.20 (m, 1H), 5.24 – 5.19 (m, 1H), 3.23 (t, *J* = 5.6 Hz, 2H), 2.68 – 2.56 (m, 4H), 2.44 – 2.36 (m, 2H), 2.17 – 2.04 (m, 2H), 1.77 – 1.71 (m, 2H), 1.55 – 1.44 (m, 4H).

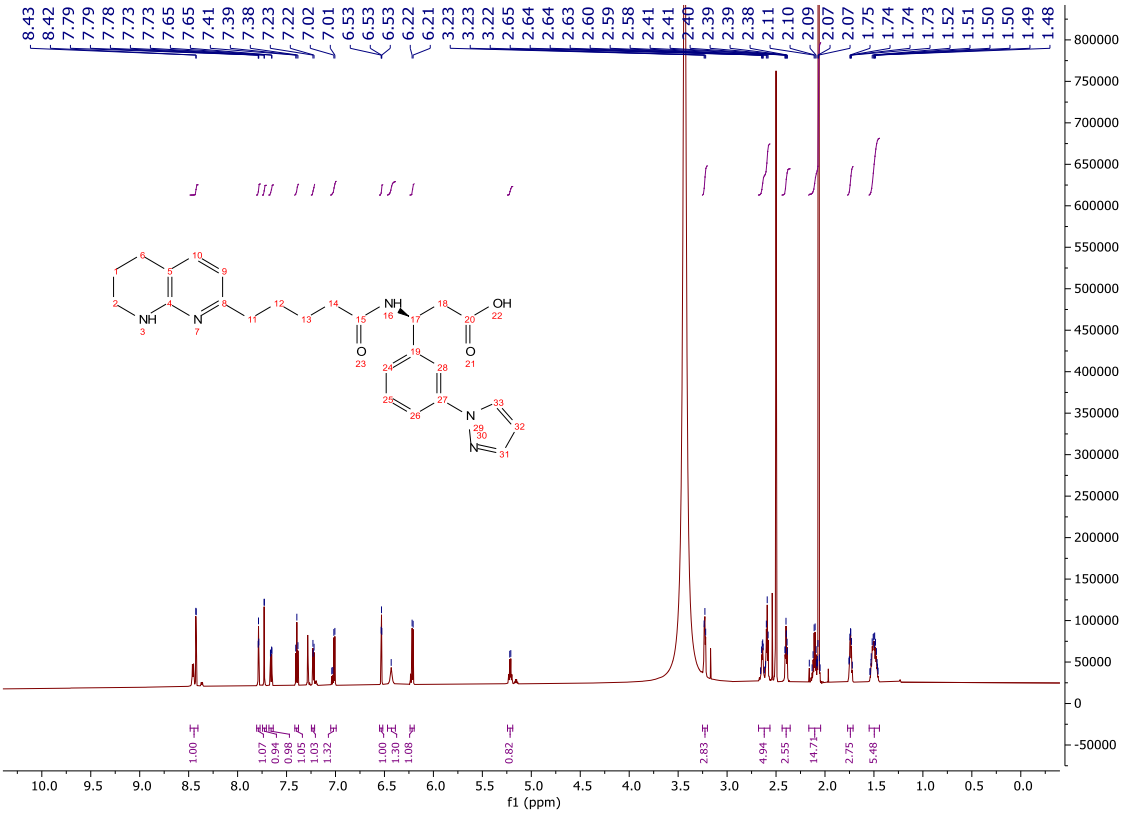

(*S*)-3-(3-(3-Methyl-1*H*-pyrazol-1-yl)phenyl)-3-(5-(5,6,7,8-tetrahydro-1,8-naphthyridin-2-yl)pentanamido)propanoic acid (**193**)

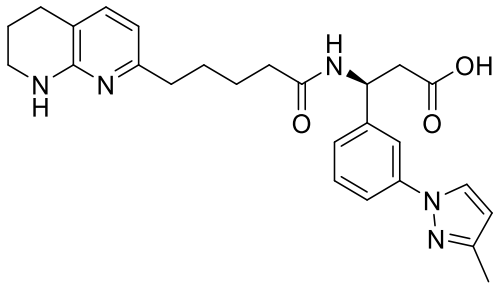

Mass 7.0 mg; Yield 10%; LCMS 98% purity; 1.97 min; *m/z* $[M+H]^+$ 462.2; Colourless solid.

δ_H (400 MHz, DMSO-d_6) 8.48 (d, *J* = 8.2 Hz, 1H), 8.30 (d, *J* = 2.4 Hz, 1H), 7.73 (dd, *J* = 2.0, 2.0 Hz, 1H), 7.59 (ddd, *J* = 8.1, 2.3, 1.0 Hz, 1H), 7.35 (dd, *J* = 7.9, 7.9 Hz, 1H), 7.17 (ddd, *J* = 7.7, 1.2, 1.2 Hz, 1H), 7.00 (d, *J* = 7.3 Hz, 1H), 6.45 (bs, 1H), 6.31 (d, *J* = 2.4 Hz, 1H), 6.20 (d, *J* = 7.2 Hz, 1H), 5.26 – 5.11 (m, 1H), 3.27 – 3.17 (m, 2H), 2.71 – 2.55 (m, 4H), 2.44 – 2.35 (m, 2H), 2.26 (s, 3H), 2.19 – 2.02 (m, 2H), 1.78 – 1.69 (m, 2H), 1.58 – 1.41 (m, 4H).

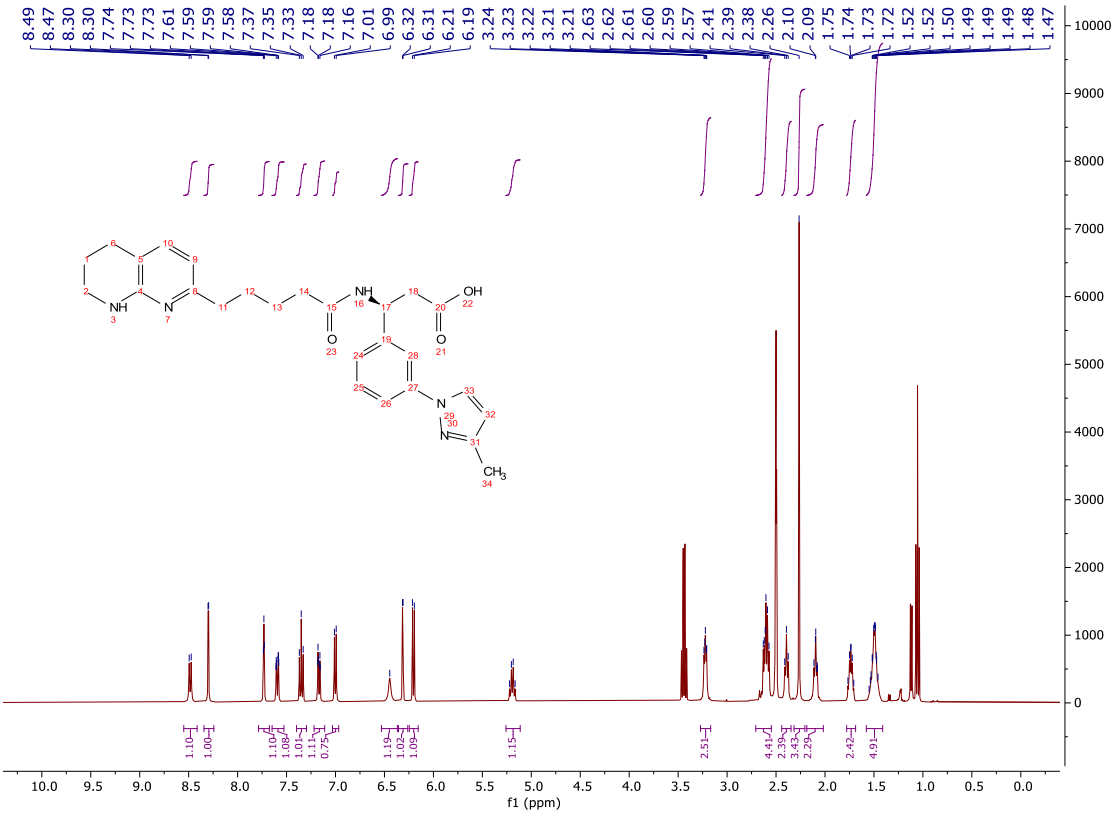

(*S*)-3-(3-(5-Methyl-1*H*-pyrazol-1-yl)phenyl)-3-(5-(5,6,7,8-tetrahydro-1,8-naphthyridin-2-yl)pentanamido)propanoic acid (**194**)

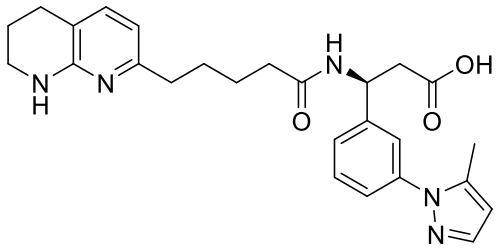

Mass 3.0 mg; Yield 4%; LCMS 95% purity; 1.93 min; *m/z* $[M+H]^+$ 462.2; Colourless solid.

δ_H (400 MHz, DMSO-d_6) 8.55 (d, *J* = 8.2 Hz, 1H), 7.54 (d, *J* = 1.7 Hz, 1H), 7.45 – 7.39 (m, 2H), 7.37 – 7.29 (m, 2H), 7.02 (d, *J* = 7.2 Hz, 1H), 6.45 (bs, 1H), 6.28 – 6.24 (m, 1H), 6.21 (d, *J* = 7.3 Hz, 1H), 5.25 – 5.16 (m, 1H), 3.26 – 3.18 (m, 2H), 2.63 – 2.56 (m, 4H), 2.42 – 2.35 (m, 2H), 2.30 (s, 3H), 2.16 – 2.02 (m, 2H), 1.78 – 1.70 (m, 2H), 1.56 – 1.41 (m, 4H).

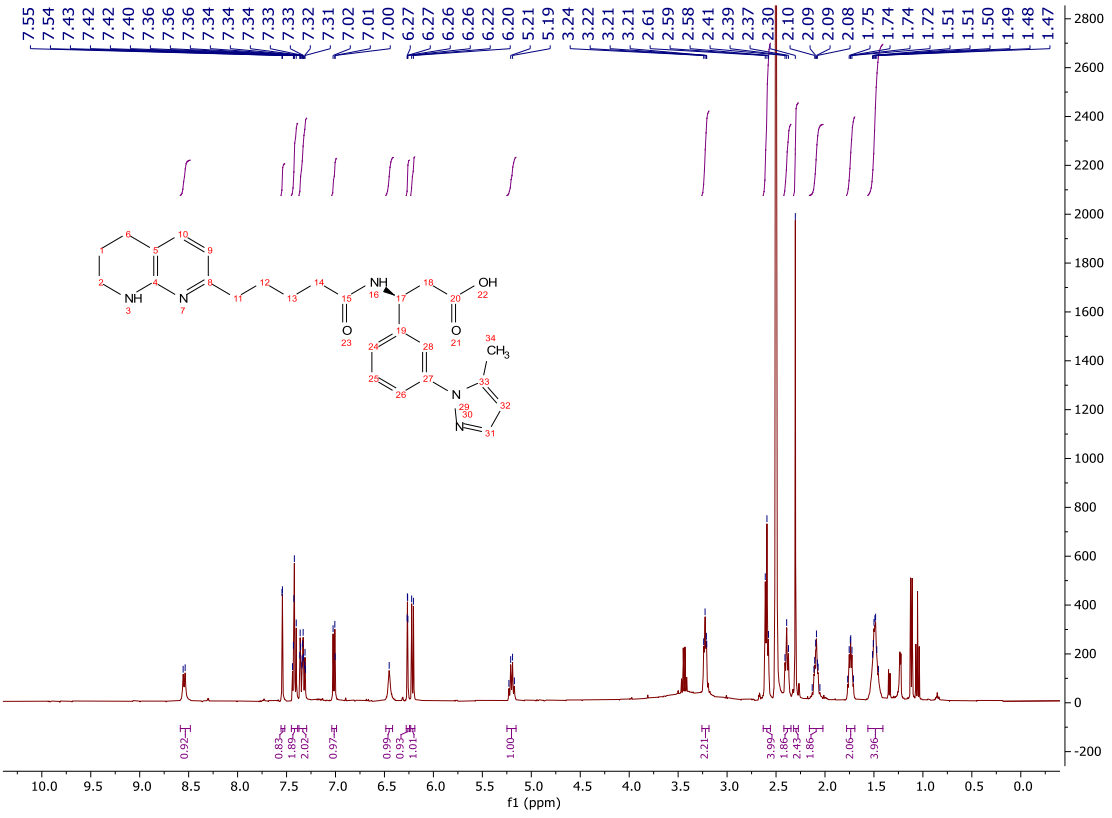

(*S*)-3-(3-(3,4-Dimethyl-1*H*-pyrazol-1-yl)phenyl)-3-(5-(5,6,7,8-tetrahydro-1,8-naphthyridin-2-yl)pentanamido)propanoic acid (**195**)

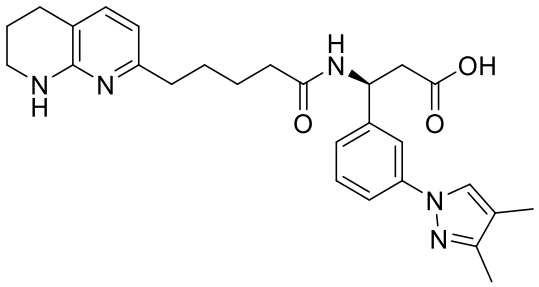

Mass 11.0 mg; Yield 15%; LCMS 99% purity; 2.03 min; *m/z* $[M+H]^+$ 476.2; Colourless solid.

δ_H (400 MHz, DMSO-d_6) 8.48 (d, *J* = 8.2 Hz, 1H), 8.10 (s, 1H), 7.71 – 7.63 (m, 1H), 7.57 – 7.48 (m, 1H), 7.32 (dd, *J* = 7.9, 7.9 Hz, 1H), 7.16 – 7.08 (m, 1H), 7.00 (d, *J* = 7.3 Hz, 1H), 6.43 (bs, 1H), 6.20 (d, *J* = 7.3 Hz, 1H), 5.23 – 5.12 (m, 1H), 3.27 – 3.15 (m, 2H), 2.70 – 2.54 (m, 4H), 2.44 – 2.34 (m, 2H), 2.18 (s, 3H), 2.14 – 2.05 (m, 2H), 2.01 (s, 3H), 1.78 – 1.68 (m, 2H), 1.60 – 1.38 (m, 4H).

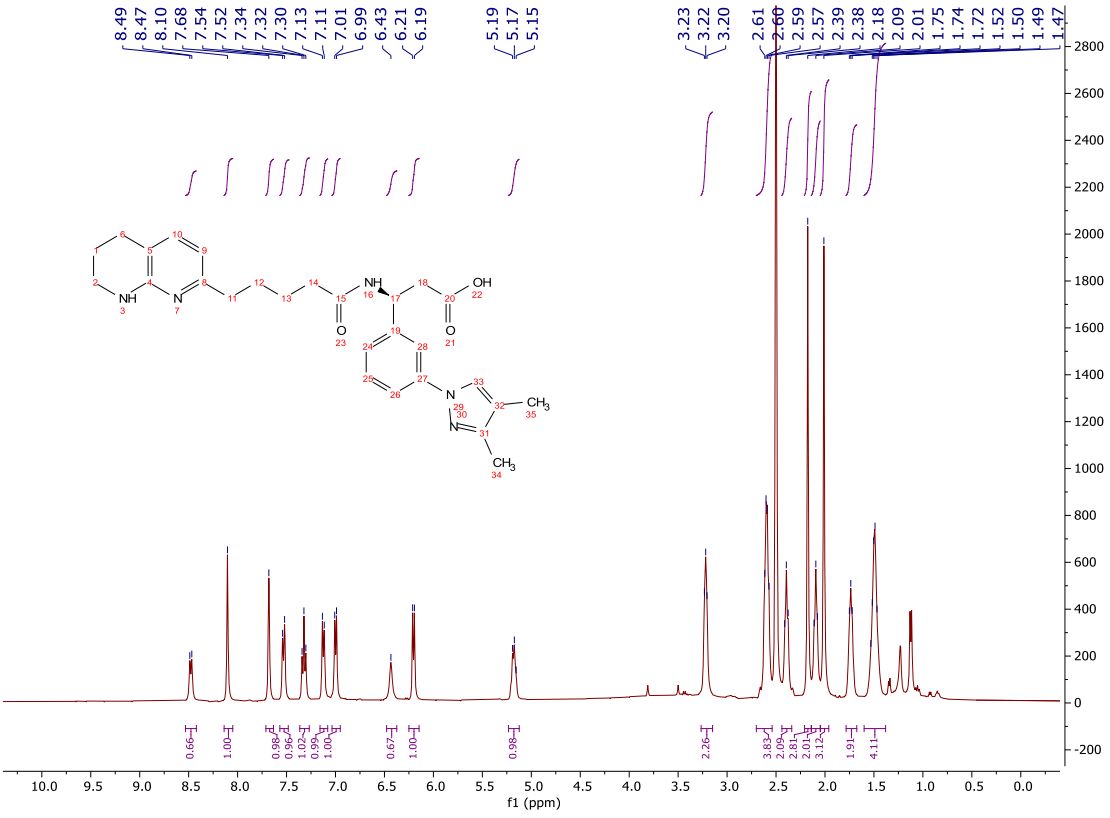

(*S*)-3-(3-(4,5-Dimethyl-1*H*-pyrazol-1-yl)phenyl)-3-(5-(5,6,7,8-tetrahydro-1,8-napthyridin-2-yl)pentanamido)propanoic acid (**196**)

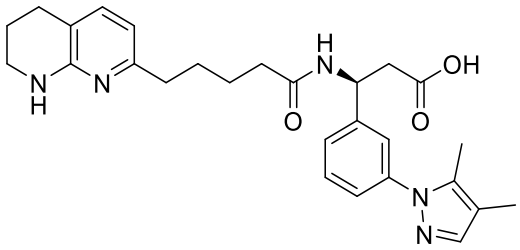

Mass 5.0 mg; Yield 7%; LCMS 98% purity; 2.02 min; *m/z* $[M+H]^+$ 476.2; Colourless solid.

δ_H (400 MHz, DMSO-d_6) 8.53 (d, *J* = 8.2 Hz, 1H), 7.45 – 7.35 (m, 3H), 7.34 – 7.27 (m, 2H), 7.04 – 6.98 (m, 1H), 6.45 (bs, 1H), 6.23 – 6.18 (m, 1H), 5.26 – 5.14 (m, 1H), 3.27 – 3.16 (m, 2H), 2.64 – 2.54 (m, 4H), 2.42 – 2.35 (m, 2H), 2.22 – 2.16 (m, 3H), 2.13 – 2.04 (m, 2H), 2.00 (s, 3H), 1.78 – 1.69 (m, 2H), 1.56 – 1.40 (m, 4H).

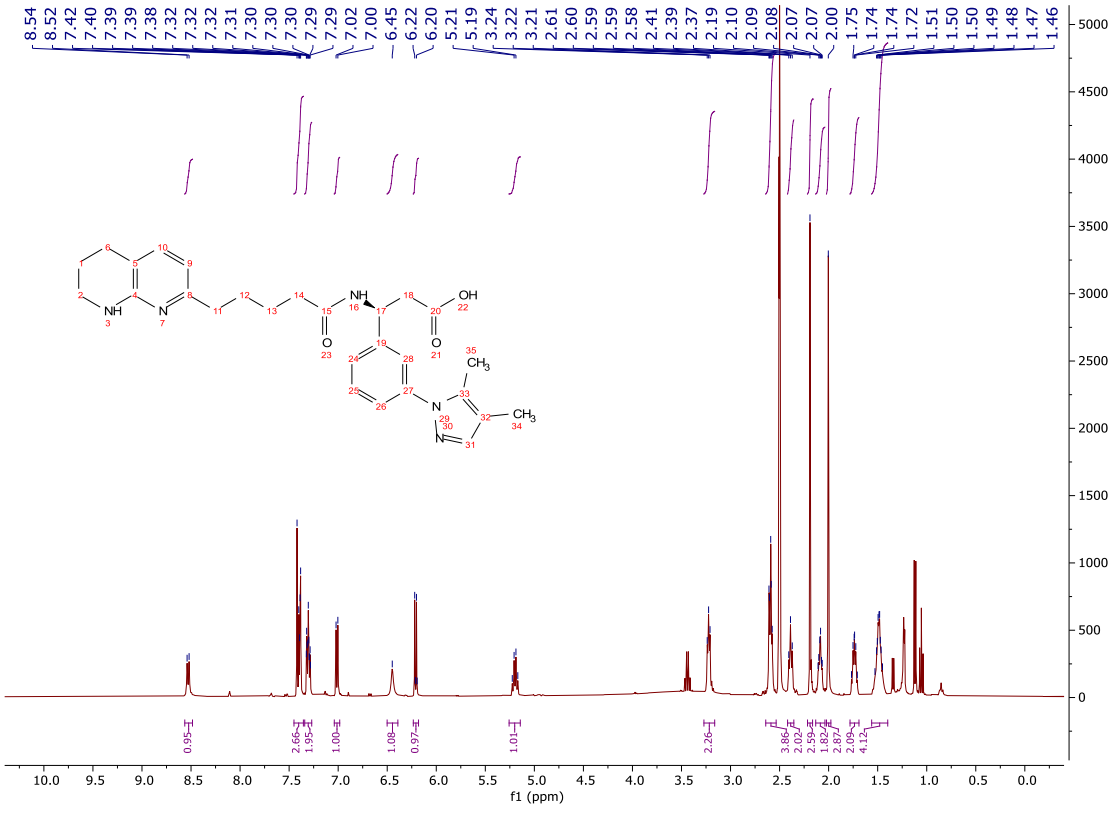

(*S*)-3-(3-(3,5-Dimethyl-1*H*-pyrazol-1-yl)phenyl)-3-(5-(5,6,7,8-tetrahydro-1,8-naphthyridin-2-yl)pentanamido)propanoic acid (**(*S*)-27**)

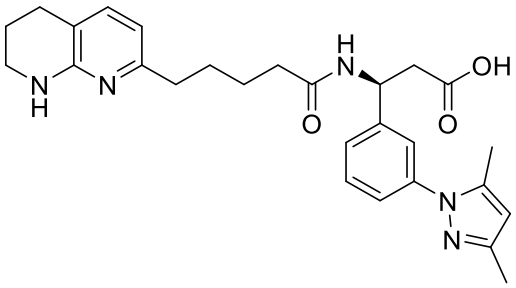

Mass 15.3 mg; Yield 21%; LCMS 100% purity; 0.61 min; *m/z* $[M+H]^+$ 476.48; Translucent, colourless oil.

δ_H (700 MHz, DMSO-d_6) 8.41 (d, *J* = 8.2 Hz, 1H), 7.40 (dd, *J* = 7.8, 7.8 Hz, 1H), 7.38 (dd, *J* = 2.0, 2.0 Hz, 1H), 7.33 – 7.30 (m, 1H), 7.30 – 7.27 (m, 1H), 7.05 (d, *J* = 7.3 Hz, 1H), 6.56 (bs, 1H), 6.23 (d, *J* = 7.2 Hz, 1H), 6.05 (s, 1H), 5.21 (q, *J* = 7.8 Hz, 1H), 3.23 (t, *J* = 5.6 Hz, 2H), 2.68 – 2.61 (m, 2H), 2.59 (t, *J* = 6.3 Hz, 2H), 2.44 – 2.35 (m, 2H), 2.24 (s, 3H), 2.16 (s, 3H), 2.15 – 2.03 (m, 2H), 1.76 – 1.71 (m, 2H), 1.53 – 1.43 (m, 4H).

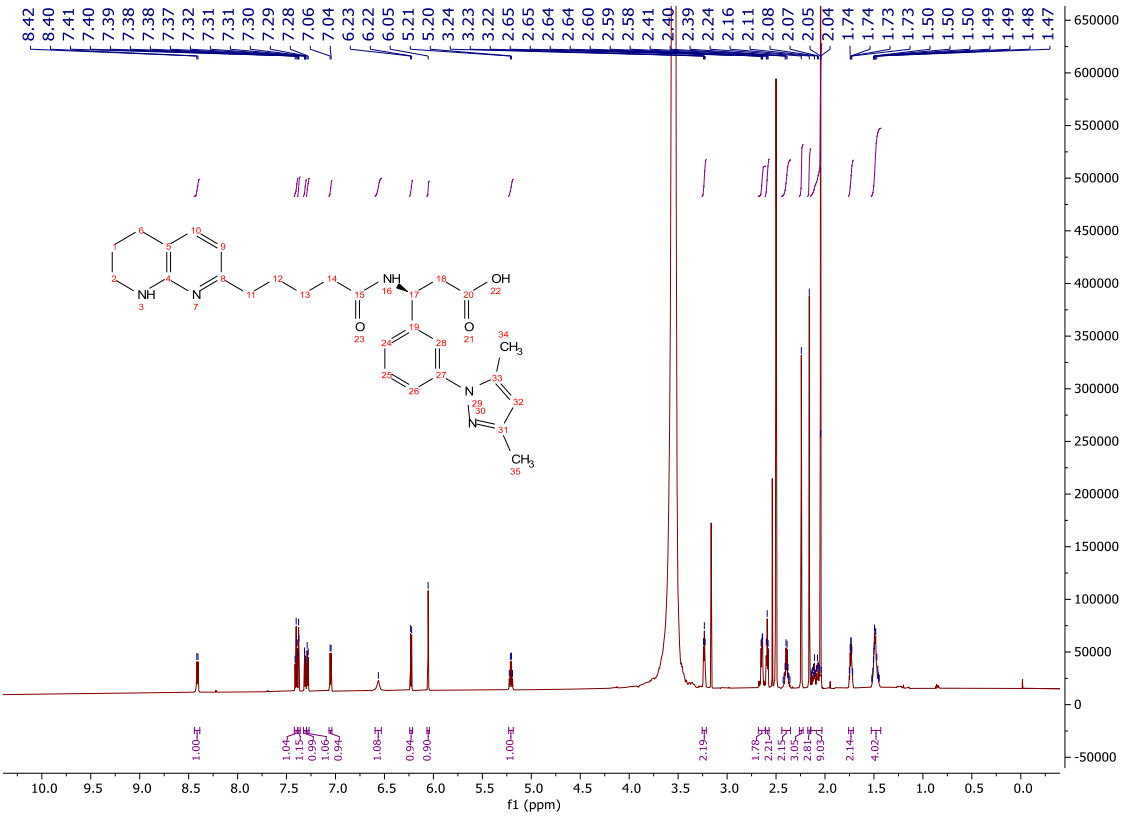

(*S*)-3-(5-(5,6,7,8-Tetrahydro-1,8-naphthyridin-2-yl)pentanamido)-3-(3-(3,4,5-trimethyl-1*H*-pyrazol-1-yl)phenyl)propanoic acid (**197**)

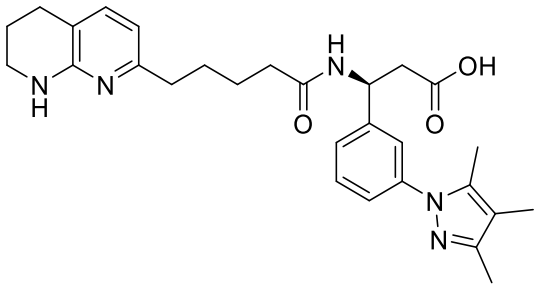

Mass 29.2 mg; Yield 40%; LCMS 100% purity; 0.77 min; *m/z* $[M+H]^+$ 490.48; Clear, yellow oil. δ_H (700 MHz, DMSO-d_6) 8.42 – 8.32 (m, 1H), 7.43 – 7.33 (m, 2H), 7.31 – 7.22 (m, 2H), 7.07 – 6.99 (m, 1H), 6.49 (bs, 1H), 6.22 (bs, 1H), 5.22 (bs, 1H), 3.27 – 3.20 (m, 2H), 2.72 – 2.56 (m, 4H), 2.54 (s, 3H), 2.40 (bs, 2H), 2.18 (s, 3H), 2.15 – 2.04 (m, 2H), 1.92 (s, 3H), 1.77 – 1.71 (m, 2H), 1.59 – 1.42 (m, 4H).

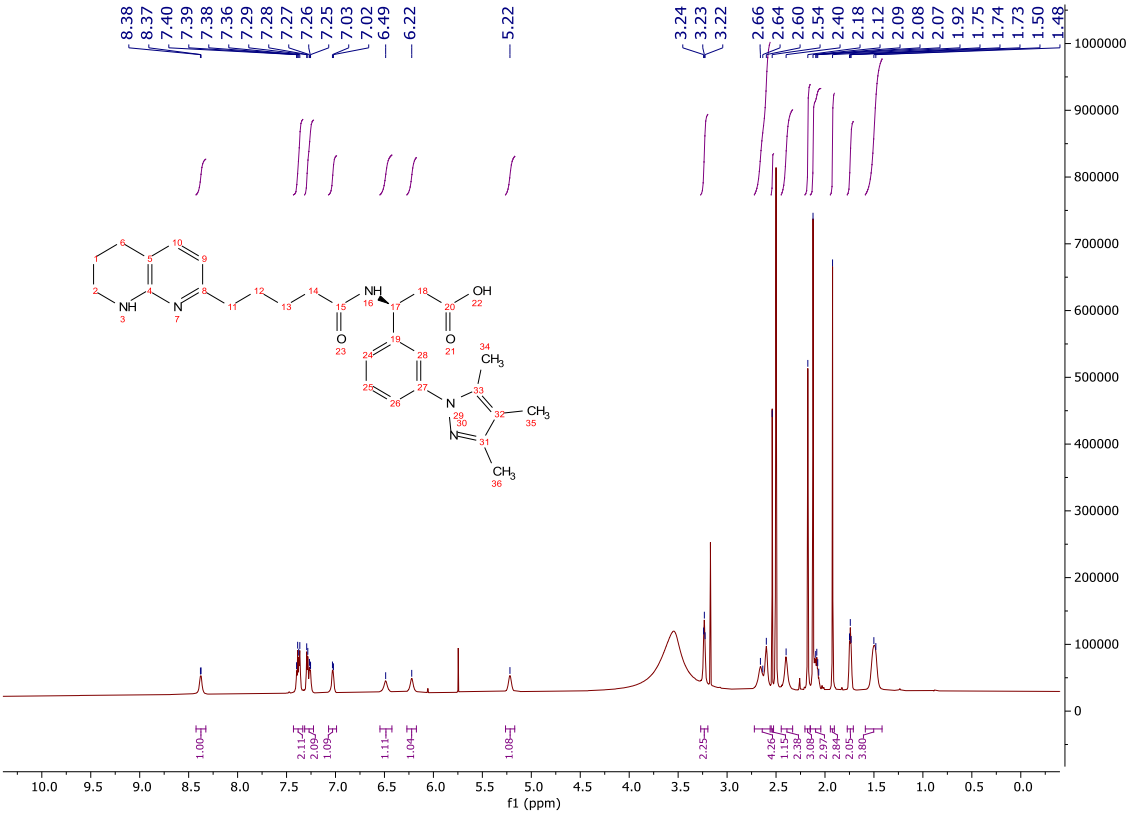

(*S*)-3-(3-(3-Ethyl-1*H*-pyrazol-1-yl)phenyl)-3-(5-(5,6,7,8-tetrahydro-1,8-naphthyridin-2-yl)pentanamido)propanoic acid (**198**)

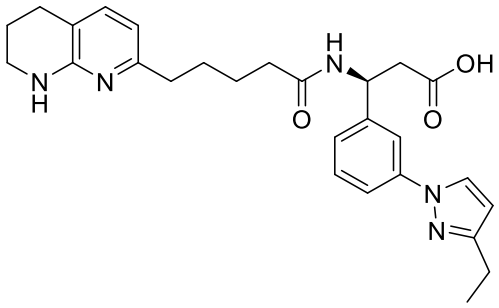

Mass 12.4 mg; Yield 17%; LCMS 96% (4%) purity; 0.65 min and 0.62 min; *m/z* $[M+H]^+$ 476.40 and 476.40; Colourless solid.

δ_H (700 MHz, DMSO-d_6) 8.44 (bs, 1H), 8.34 – 8.24 (m, 1H), 7.72 (bs, 1H), 7.59 (d, *J* = 8.0 Hz, 1H), 7.36 (dd, *J* = 7.7, 7.7 Hz, 1H), 7.22 – 7.14 (m, 1H), 7.07 – 6.97 (m, 1H), 6.51 – 6.30 (m, 2H), 6.21 (bs, 1H), 5.20 (bs, 1H), 3.30 – 3.15 (m, 2H), 2.73 – 2.45 (m, 6H), 2.44 – 2.34 (m, 2H), 2.19 – 1.94 (m, 2H), 1.79 – 1.69 (m, 2H), 1.58 – 1.42 (m, 4H), 1.22 (t, *J* = 7.6 Hz, 3H).

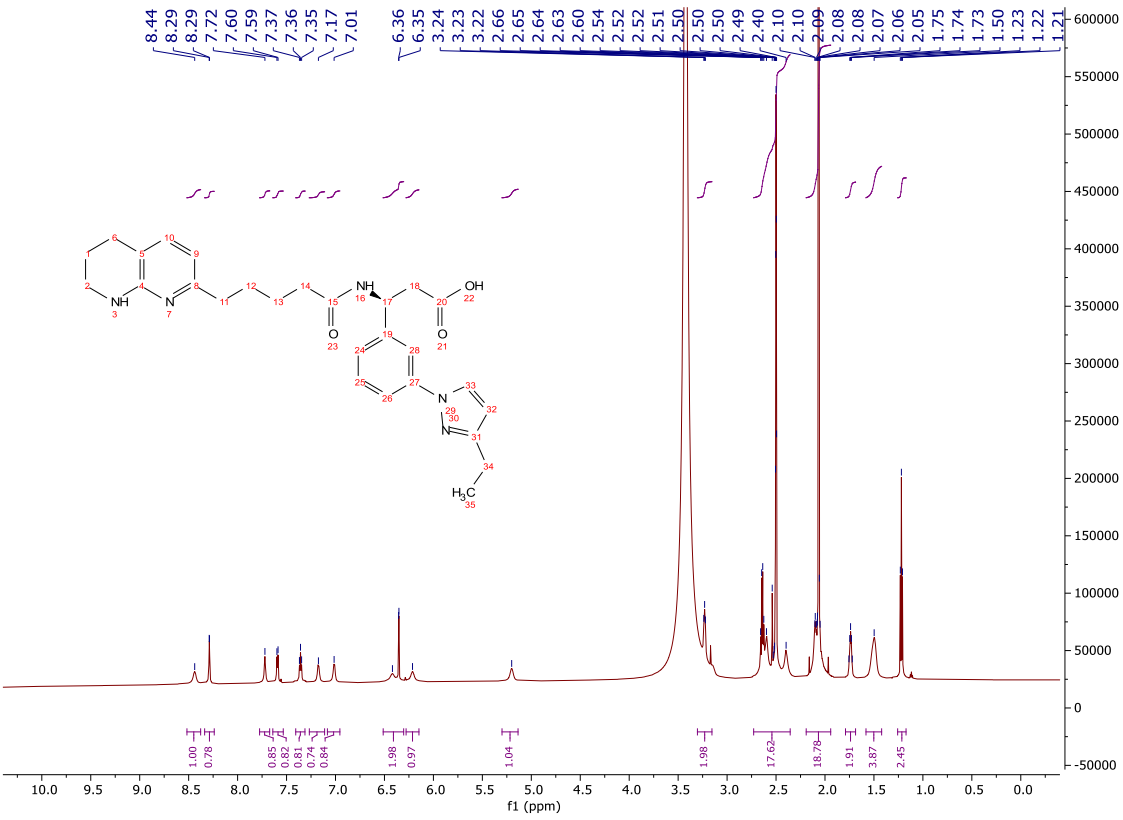

(*S*)-3-(3-(4-Ethyl-1*H*-pyrazol-1-yl)phenyl)-3-(5-(5,6,7,8-tetrahydro-1,8-naphthyridin-2-yl)pentanamido)propanoic acid (**199**)

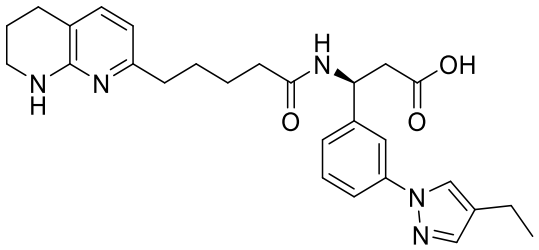

Mass 2.7 mg; Yield 4%; LCMS 100% purity; 0.66 min; *m/z* $[M+H]^+$ 476.45; Crystalline, colourless solid.

δ_H (700 MHz, DMSO-d_6) 8.46 (bs, 1H), 8.26 (s, 1H), 7.75 (bs, 1H), 7.68 – 7.53 (m, 2H), 7.37 (dd, *J* = 8.0, 8.0 Hz, 1H), 7.23 – 7.10 (m, 1H), 7.02 (d, *J* = 7.2 Hz, 1H), 6.64 (bs, 1H), 6.27 – 6.12 (m, 1H), 5.28 – 5.11 (m, 1H), 3.27 – 3.18 (m, 2H), 2.74 – 2.46 (m, 6H), 2.43 – 2.34 (m, 2H), 2.16 – 2.01 (m, 2H), 1.78 – 1.69 (m, 2H), 1.57 – 1.39 (m, 4H), 1.19 (t, *J* = 7.6 Hz, 3H).

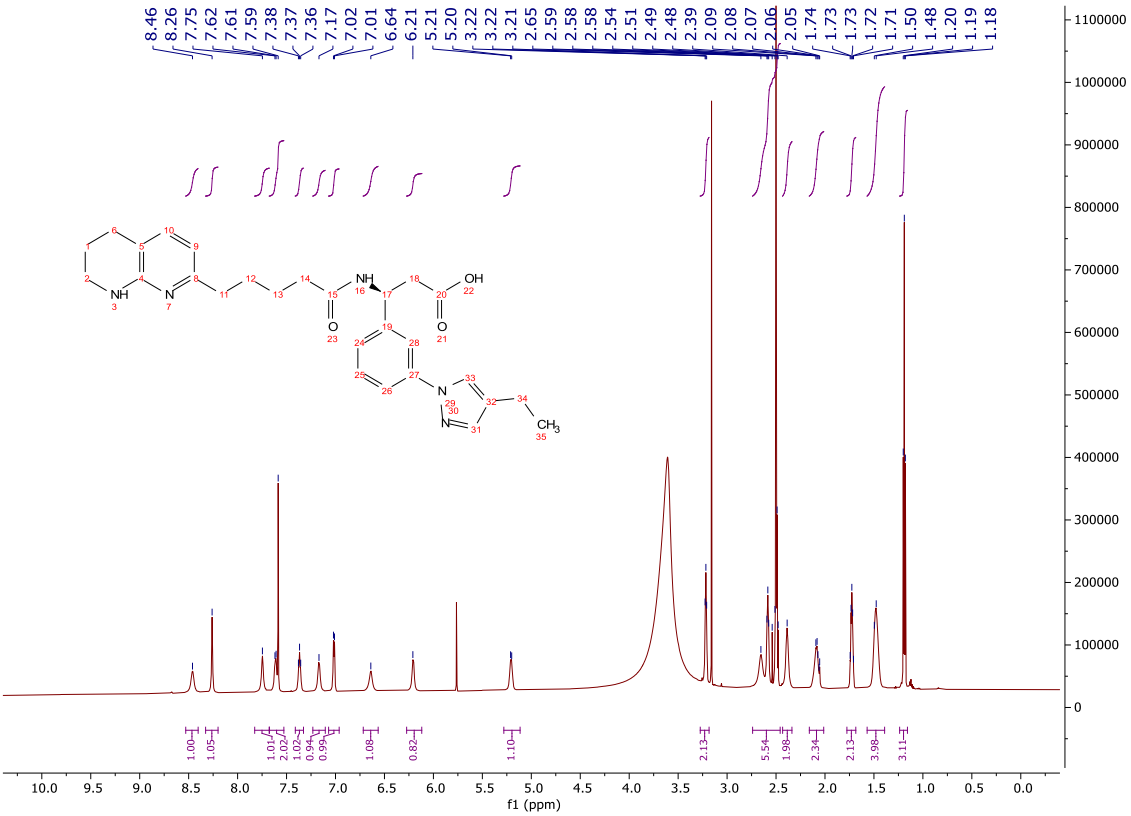

(*S*)-3-(3-(3-Isopropyl-1*H*-pyrazol-1-yl)phenyl)-3-(5-(5,6,7,8-tetrahydro-1,8-naphthyridin-2-yl)pentanamido)propanoic acid (**200**)

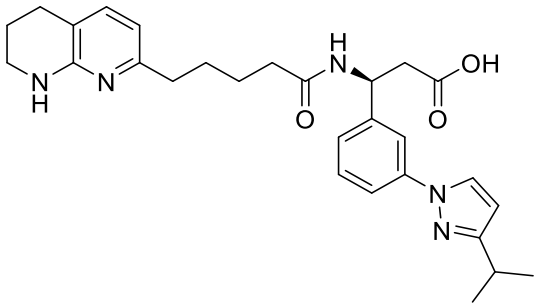

Mass 29.7 mg; Yield 37%; LCMS 91% (7%) purity; 0.71 min and 0.66 min; *m/z* $[M+H]^+$ 490.49 and 490.45; Clear, colourless oil.

δ_H (700 MHz, DMSO-d_6) 8.45 (bs, 1H), 8.32 (bs, 1H), 7.72 (bs, 1H), 7.66 – 7.56 (m, 1H), 7.37 (dd, *J* = 7.6, 7.6 Hz, 1H), 7.17 (bs, 1H), 7.02 (bs, 1H), 6.62 (s, 1H), 6.39 (s, 1H), 6.21 (s, 1H), 5.20 (bs, 1H), 3.22 (bs, 2H), 2.97 (hept, *J* = 6.3 Hz, 1H), 2.76 – 2.30 (m, 6H), 2.20 – 2.01 (m, 2H), 1.77 – 1.68 (m, 2H), 1.49 (bs, 4H), 1.30 – 1.13 (m, 6H).

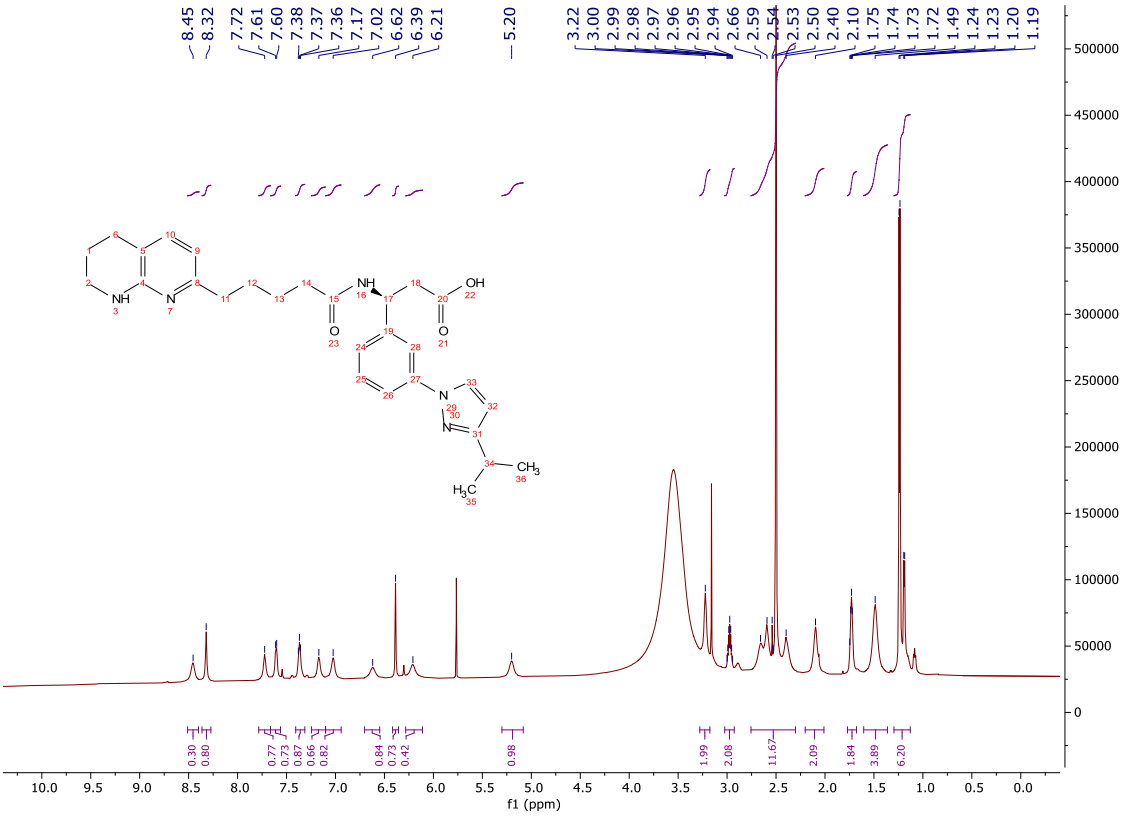

(*S*)-3-(3-(4-Isopropyl-1*H*-pyrazol-1-yl)phenyl)-3-(5-(5,6,7,8-tetrahydro-1,8-naphthyridin-2-yl)pentanamido)propanoic acid (**201**)

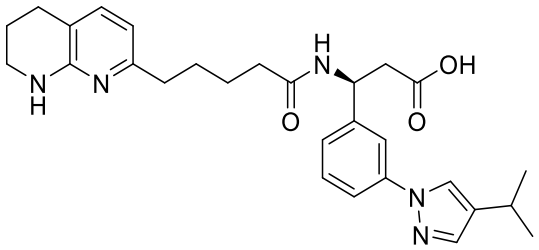

Mass 32.9 mg; Yield 44%; LCMS 98% purity; 0.81 min; *m/z* $[M+H]^+$ 490.46; Crystalline, colourless solid.

δ_H (700 MHz, DMSO-d_6) 8.35 (bs, 1H), 8.22 (s, 1H), 7.74 (bs, 1H), 7.68 – 7.54 (m, 2H), 7.36 (s, 1H), 7.17 (bs, 1H), 7.01 (d, *J* = 7.2 Hz, 1H), 6.45 (bs, 1H), 6.29 – 6.12 (m, 1H), 5.25 (bs, 1H), 3.25 – 3.20 (m, 2H), 2.86 (hept, *J* = 6.8 Hz, 1H), 2.77 – 2.55 (m, 4H), 2.45 – 2.33 (m, 2H), 2.17 – 2.01 (m, 2H), 1.79 – 1.70 (m, 2H), 1.57 – 1.40 (m, 4H), 1.23 (d, *J* = 6.9 Hz, 6H).

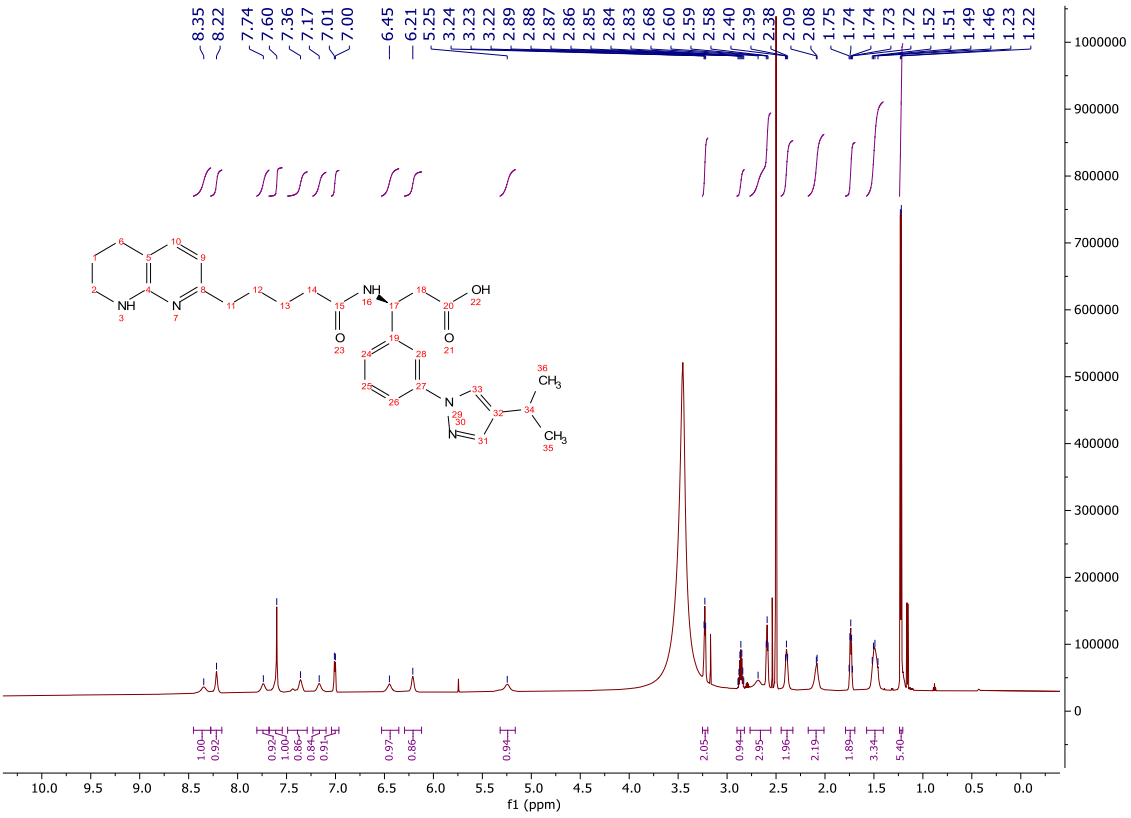

(*S*)-3-(3-(4-Propyl-1*H*-pyrazol-1-yl)phenyl)-3-(5-(5,6,7,8-tetrahydro-1,8-naphthyridin-2-yl)pentanamido)propanoic acid (**202**)

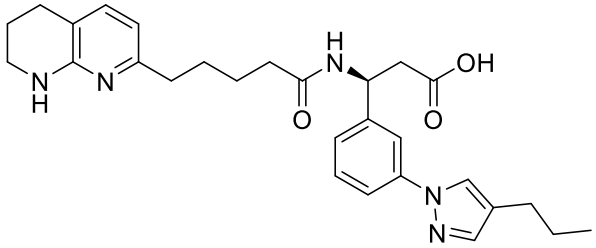

Mass 25.0 mg; Yield 31%; LCMS 97% purity; 0.82 min; *m/z* $[M+H]^+$ 490.47; Clear, colourless oil.

δ_H (700 MHz, DMSO-d_6) 8.37 (d, *J* = 8.3 Hz, 1H), 8.23 (s, 1H), 7.75 (bs, 1H), 7.65 – 7.59 (m, 1H), 7.56 (s, 1H), 7.42 – 7.34 (m, 1H), 7.22 – 7.15 (m, 1H), 7.01 (d, *J* = 7.2 Hz, 1H), 6.47 (bs, 1H), 6.21 (d, *J* = 7.2 Hz, 1H), 5.27 – 5.18 (m, 1H), 3.23 (t, *J* = 5.6 Hz, 2H), 2.72 – 2.63 (m, 2H), 2.59 (t, *J* = 6.3 Hz, 2H), 2.46 (t, *J* = 7.5 Hz, 2H), 2.43 – 2.36 (m, 2H), 2.15 – 2.06 (m, 2H), 1.77 – 1.72 (m, 2H), 1.63 – 1.56 (m, 2H), 1.54 – 1.45 (m, 4H), 0.93 (t, *J* = 7.3 Hz, 3H).

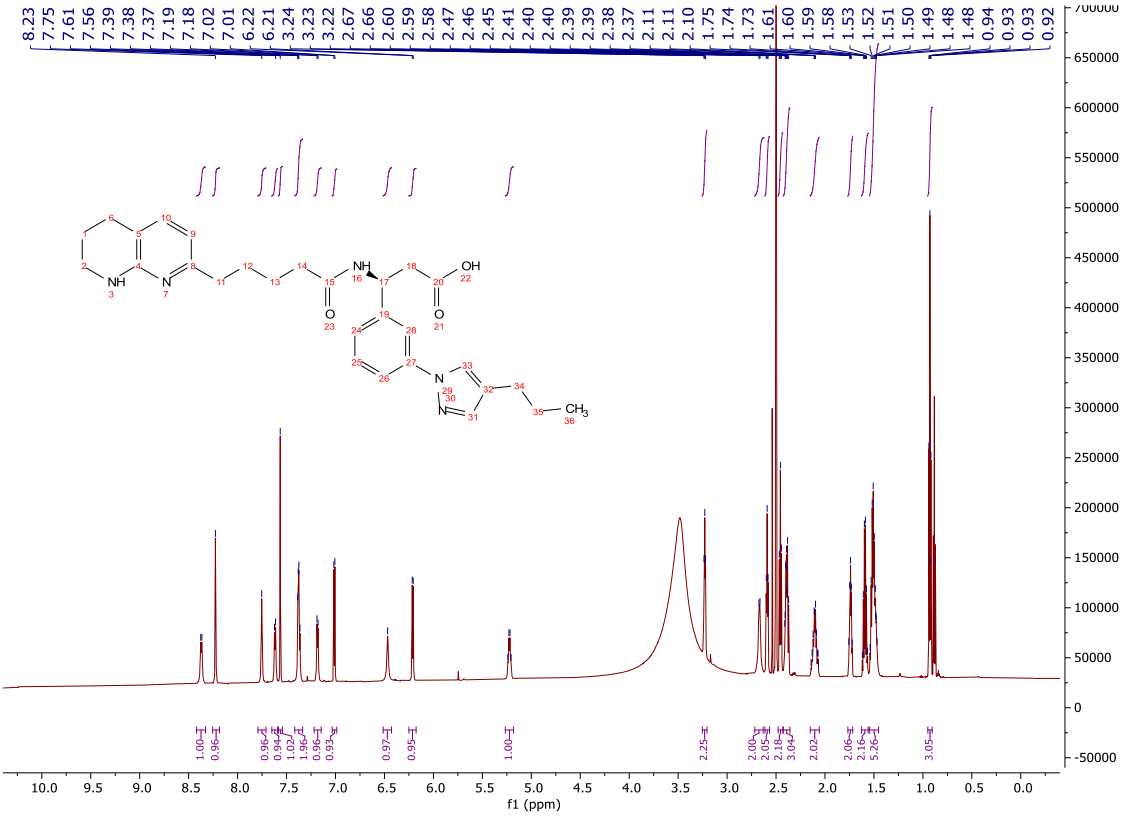

(*S*)-3-(3-(3-Chloro-1*H*-pyrazol-1-yl)phenyl)-3-(5-(5,6,7,8-tetrahydro-1,8-naphthyridin-2-yl)pentanamido)propanoic acid (**203**)

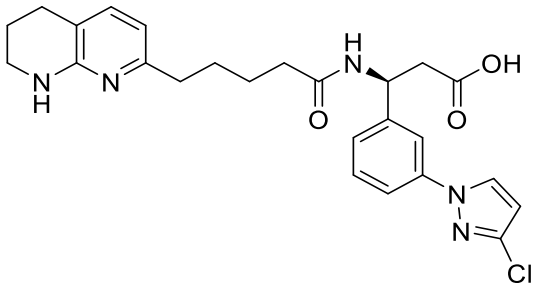

Mass 10.0 mg; Yield 13%; LCMS 92% (8%) purity; 0.64 min and 0.61 min; *m/z* $[M+H]^+$ 482.31 and 482.29; Colourless solid.

δ_H (700 MHz, DMSO-d_6) 8.55 – 8.49 (m, 1H), 8.45 (bs, 1H), 7.74 (bs, 1H), 7.62 (d, *J* = 8.0 Hz, 1H), 7.41 (dd, *J* = 7.7, 7.7 Hz, 1H), 7.30 – 7.22 (m, 1H), 7.07 – 6.99 (m, 1H), 6.63 (d, *J* = 2.2 Hz, 1H), 6.45 (bs, 1H), 6.21 (bs, 1H), 5.21 (bs, 1H), 3.26 – 3.20 (m, 2H), 2.73 – 2.55 (m, 4H), 2.46 – 2.34 (m, 2H), 2.15 – 2.03 (m, 2H), 1.77 – 1.70 (m, 2H), 1.50 (bs, 4H).

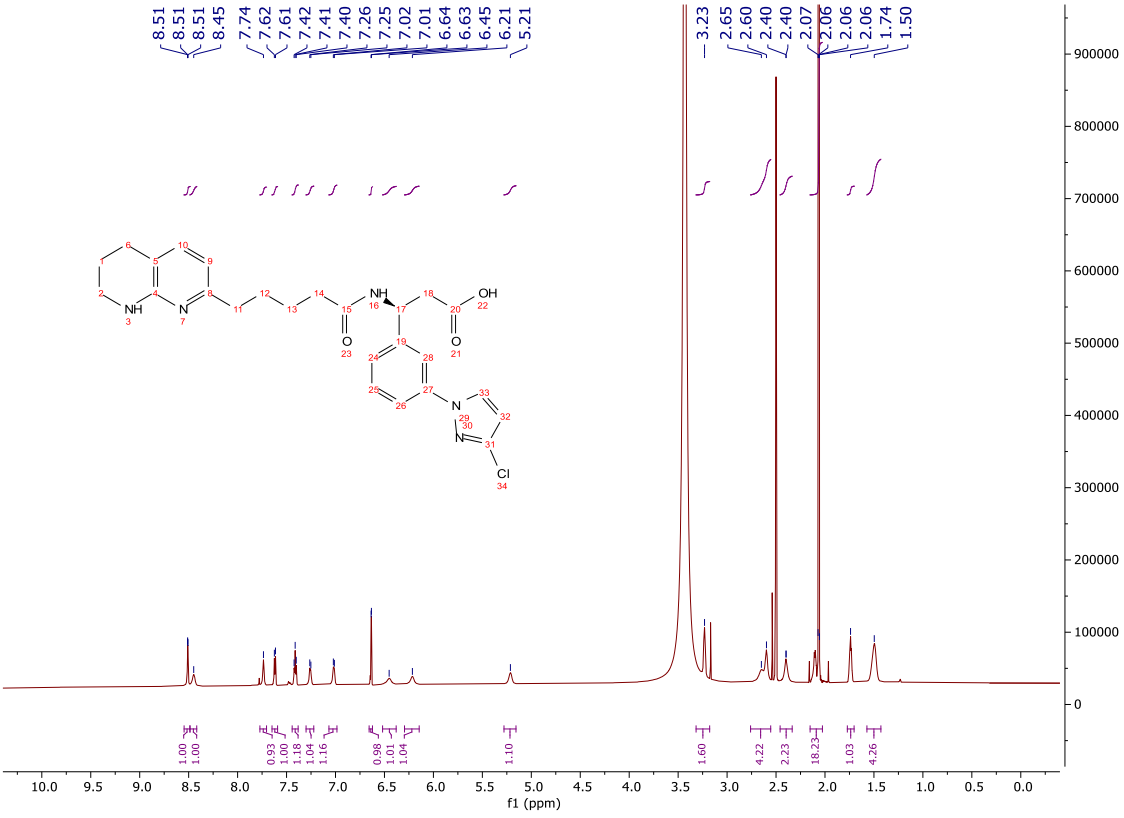

(*S*)-3-(3-(3-Fluoro-1*H*-pyrazol-1-yl)phenyl)-3-(5-(5,6,7,8-tetrahydro-1,8-naphthyridin-2-yl)pentanamido)propanoic acid (**205**)

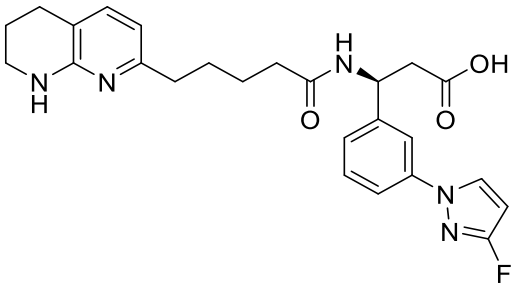

Mass 3.0 mg; Yield 4%; LCMS 99% purity; 0.58 min; *m/z* $[M+H]^+$ 466.38; Crystalline, colourless solid.

δ_H (700 MHz, DMSO-d_6) 8.50 – 8.43 (m, 2H), 7.70 (s, 1H), 7.60 (dd, *J* = 8.1, 2.2 Hz, 1H), 7.41 (t, *J* = 7.9 Hz, 1H), 7.22 (d, *J* = 7.7 Hz, 1H), 7.02 (d, *J* = 7.2 Hz, 1H), 6.64 (s, 1H), 6.34 (dd, *J* = 5.9, 2.6 Hz, 1H), 6.23 – 6.19 (m, 1H), 5.23 – 5.17 (m, 1H), 3.24 – 3.20 (m, 2H), 2.64 (d, *J* = 7.5 Hz, 2H), 2.61 – 2.56 (m, 2H), 2.42 – 2.35 (m, 2H), 2.15 – 2.04 (m, 2H), 1.76 – 1.70 (m, 2H), 1.53 – 1.43 (m, 4H).

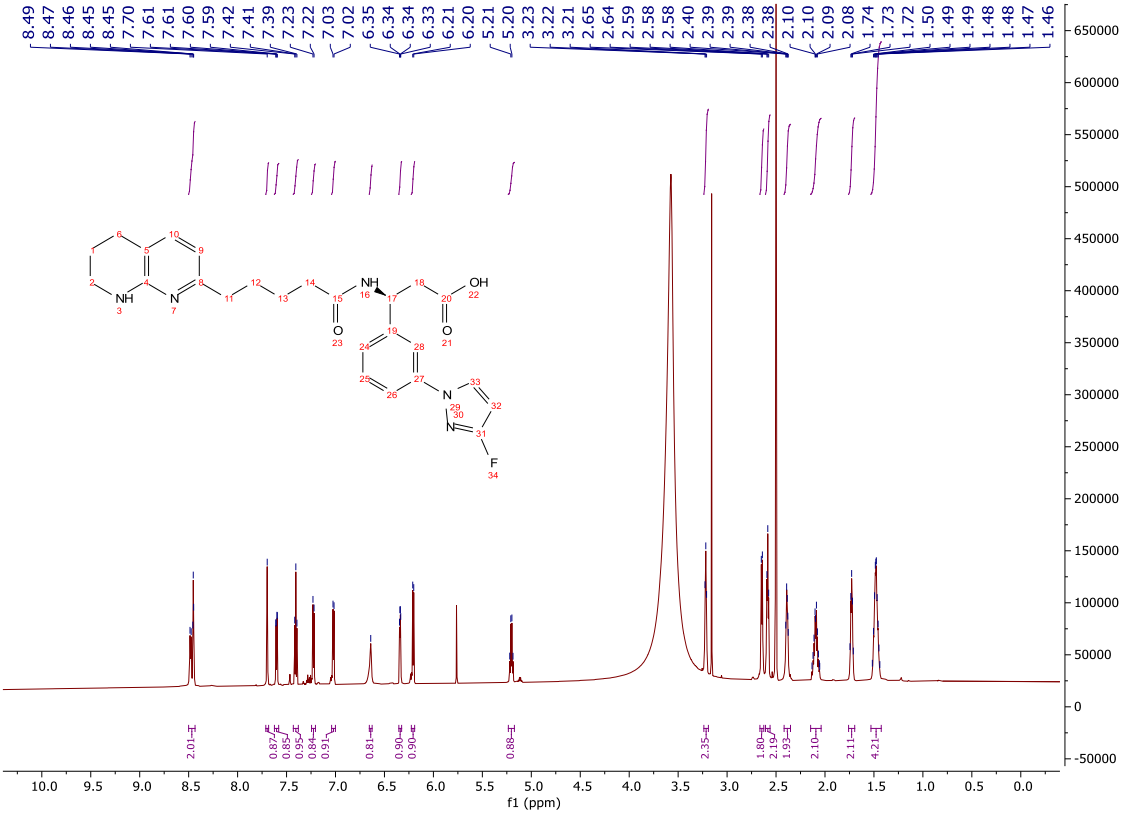

(*S*)-3-(3-(5-Fluoro-1*H*-pyrazol-1-yl)phenyl)-3-(5-(5,6,7,8-tetrahydro-1,8-naphthyridin-2-yl)pentanamido)propanoic acid (**206**)

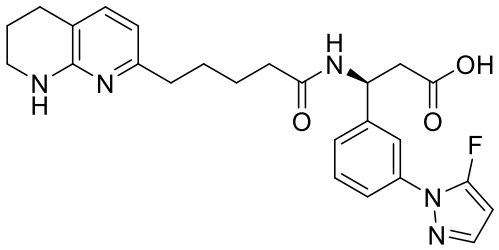

Mass 9.1 mg; Yield 13%; LCMS 100% purity; 0.61 min; *m/z* $[M+H]^+$ 466.40; Crystalline, colourless solid.

δ_H (700 MHz, DMSO-d_6) 8.60 – 8.50 (m, 1H), 7.72 – 7.63 (m, 1H), 7.61 – 7.53 (m, 1H), 7.52 – 7.41 (m, 2H), 7.39 – 7.29 (m, 1H), 7.08 – 6.99 (m, 1H), 6.65 (bs, 1H), 6.30 – 6.18 (m, 2H), 5.26 – 5.16 (m, 1H), 3.27 – 3.18 (m, 2H), 2.69 – 2.55 (m, 4H), 2.44 – 2.33 (m, 2H), 2.14 – 2.02 (m, 2H), 1.78 – 1.68 (m, 2H), 1.54 – 1.39 (m, 4H).

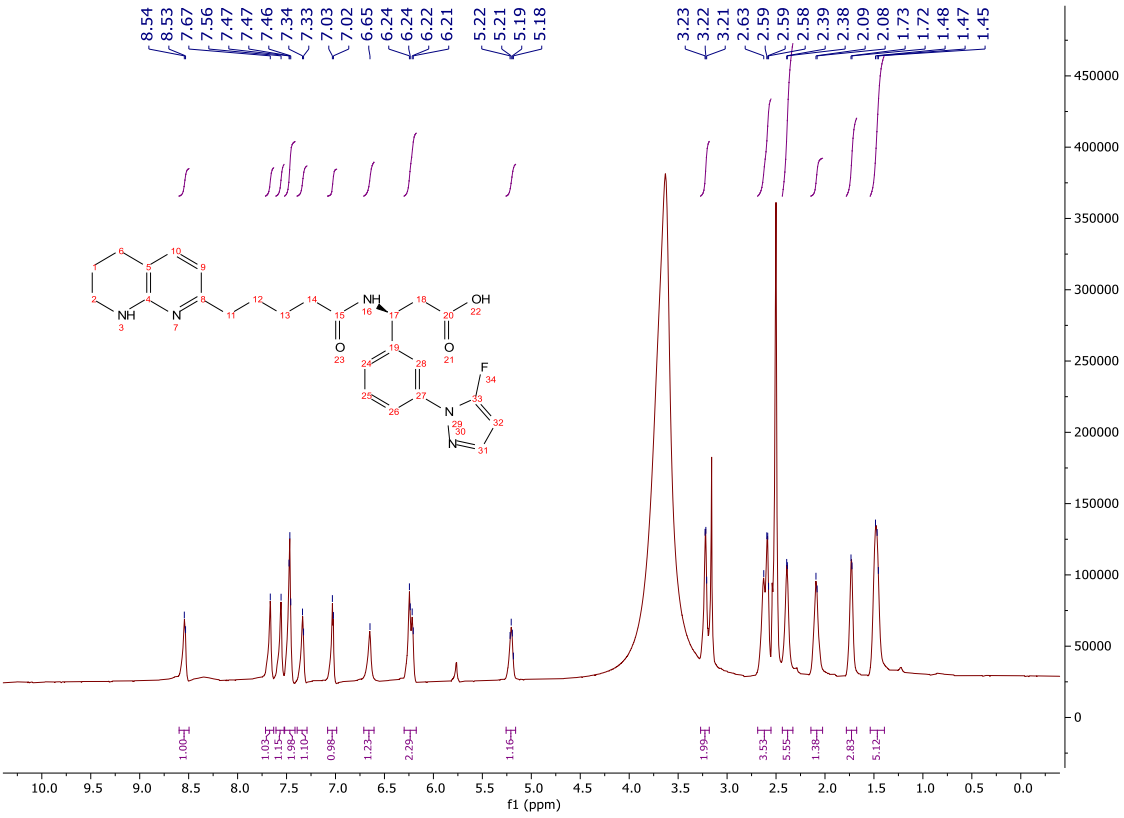

(*S*)-3-(3-(4-Fluoro-1*H*-pyrazol-1-yl)phenyl)-3-(5-(5,6,7,8-tetrahydro-1,8-naphthyridin-2-yl)pentanamido)propanoic acid (**207**)

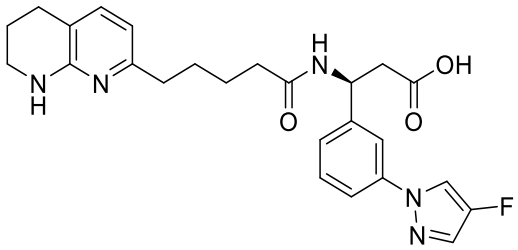

Mass 3.0 mg; Yield 4%; LCMS 85% purity; 0.60 min; *m/z* $[M+H]^+$ 466.41; Crystalline, colourless solid.

δ_H (700 MHz, DMSO-d_6) 8.68 (d, *J* = 4.4 Hz, 1H), 8.55 – 8.47 (m, 1H), 7.83 (d, *J* = 4.1 Hz, 1H), 7.75 (bs, 1H), 7.62 – 7.59 (m, 1H), 7.40 (dd, *J* = 7.8, 7.8 Hz, 1H), 7.26 – 7.20 (m, 1H), 7.05 – 6.99 (m, 1H), 6.59 (bs, 1H), 6.24 – 6.17 (m, 1H), 5.24 – 5.17 (m, 1H), 3.24 – 3.19 (m, 2H), 2.67 – 2.55 (m, 4H), 2.42 – 2.35 (m, 2H), 2.15 – 2.02 (m, 2H), 1.76 – 1.70 (m, 2H), 1.53 – 1.42 (m, 4H).

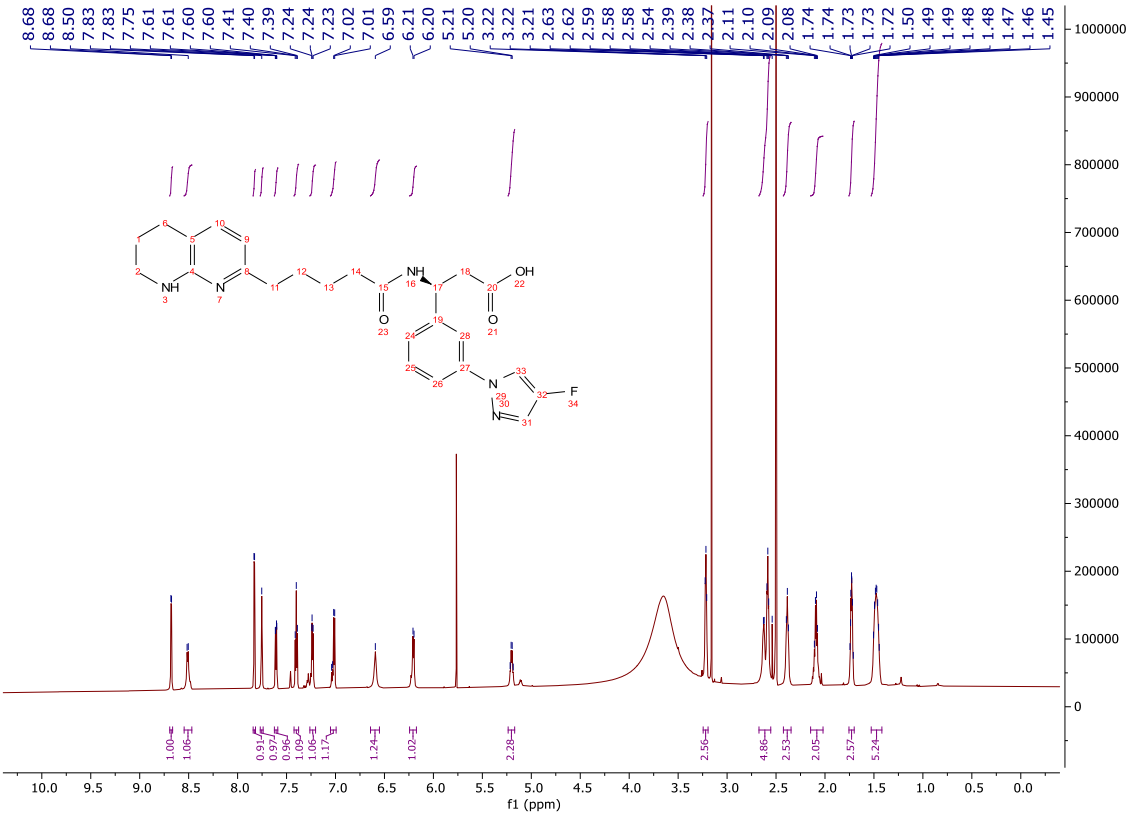

(*S*)-3-(3-(3-(Difluoromethyl)-1*H*-pyrazol-1-yl)phenyl)-3-(5-(5,6,7,8-tetrahydro-1,8-naphthyridin-2-yl)pentanamido)propanoic acid (**208**)

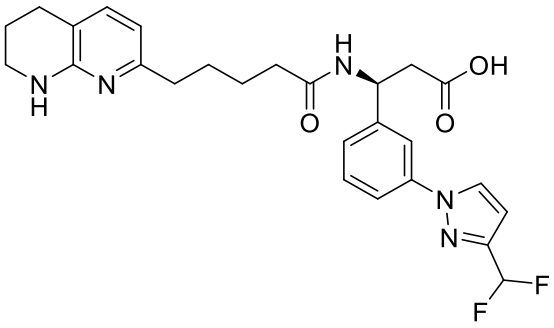

Mass 2.9 mg; Yield 4%; LCMS 100% purity; 0.76 min; *m/z* $[M+H]^+$ 498.39; Crystalline, colourless solid.

δ_H (700 MHz, DMSO-d_6) 8.57 (bs, 1H), 8.38 (bs, 1H), 7.84 – 7.74 (m, 1H), 7.72 – 7.64 (m, 1H), 7.50 – 7.40 (m, 1H), 7.35 – 7.23 (m, 1H), 7.21 – 6.96 (m, 1H), 6.83 – 6.78 (m, 1H), 6.51 (bs, 1H), 6.23 (bs, 1H), 5.23 (bs, 1H), 3.24 (bs, 2H), 2.83 – 2.55 (m, 4H), 2.48 – 2.33 (m, 2H), 2.21 – 2.04 (m, 2H), 1.78 – 1.70 (m, 2H), 1.64 – 1.40 (m, 4H).

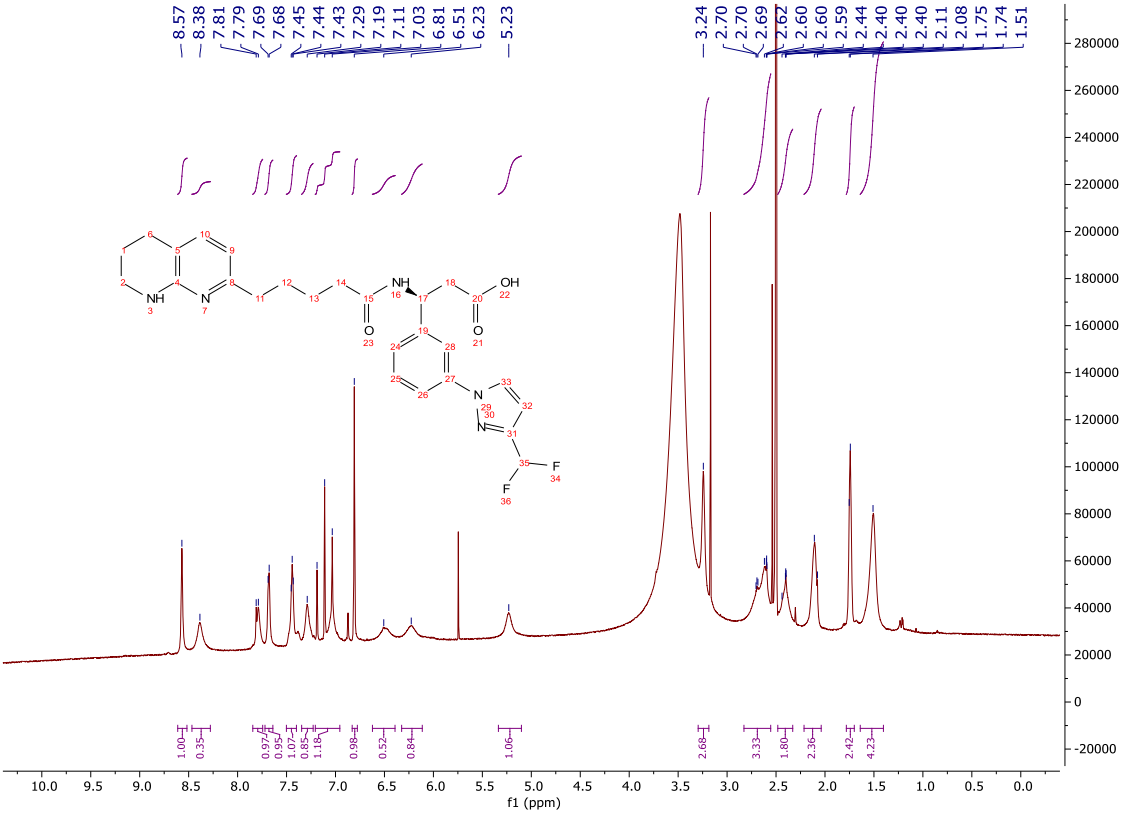

(*S*)-3-(3-(3-(Hydroxymethyl)-1*H*-pyrazol-1-yl)phenyl)-3-(5-(5,6,7,8-tetrahydro-1,8-naphthyridin-2-yl)pentanamido)propanoic acid (**209**)

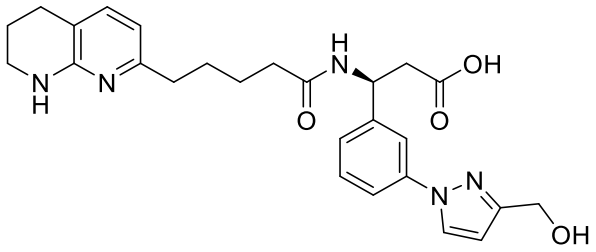

Mass 5.9 mg Yield 7% LCMS 99%* purity; 0.49 min and 0.48 min; *m/z* $[M+H]^+$ 478.43 and 478.43; Crystalline, colourless solid.

*1:1 mixture of regioisomers by NMR (labelled as A and B). Pyrazole signals are unable to be attributed to either A or B and are thus labelled as pyrazole 1 and 2 to distinguish between them.

δ_H (700 MHz, DMSO-d_6) 8.56 – 8.49 (m, 2H, A and B), 8.40 – 8.36 (m, 1H, pyrazole 1), 7.76 – 7.73 (m, 1H, A), 7.64 – 7.60 (m, 2H, A and pyrazole 2), 7.57 – 7.53 (m, 1H, B), 7.49 – 7.45 (m, 1H, B), 7.41 (dd, *J* = 7.8, 7.8 Hz, 1H, B), 7.37 (dd, *J* = 7.8, 7.8 Hz, 1H, A), 7.33 – 7.29 (m, 1H, B), 7.21 – 7.17 (m, 1H, A), 7.04 – 6.99 (m, 2H, A and B), 6.60 – 6.52 (m, 2H, A and B), 6.49 – 6.44 (m, 2H, pyrazole 1 and 2), 6.23 – 6.18 (m, 2H, A and B), 5.23 – 5.16 (m, 2H, A and B), 4.52 – 4.45 (m, 4H, A and B), 3.24 – 3.19 (m, 4H, A and B), 2.66 – 2.55 (m, 8H, A and B), 2.43 – 2.34 (m, 4H, A and B), 2.14 – 2.04 (m, 4H, A and B), 1.76 – 1.69 (m, 4H, A and B), 1.53 – 1.41 (m, 8H, A and B).

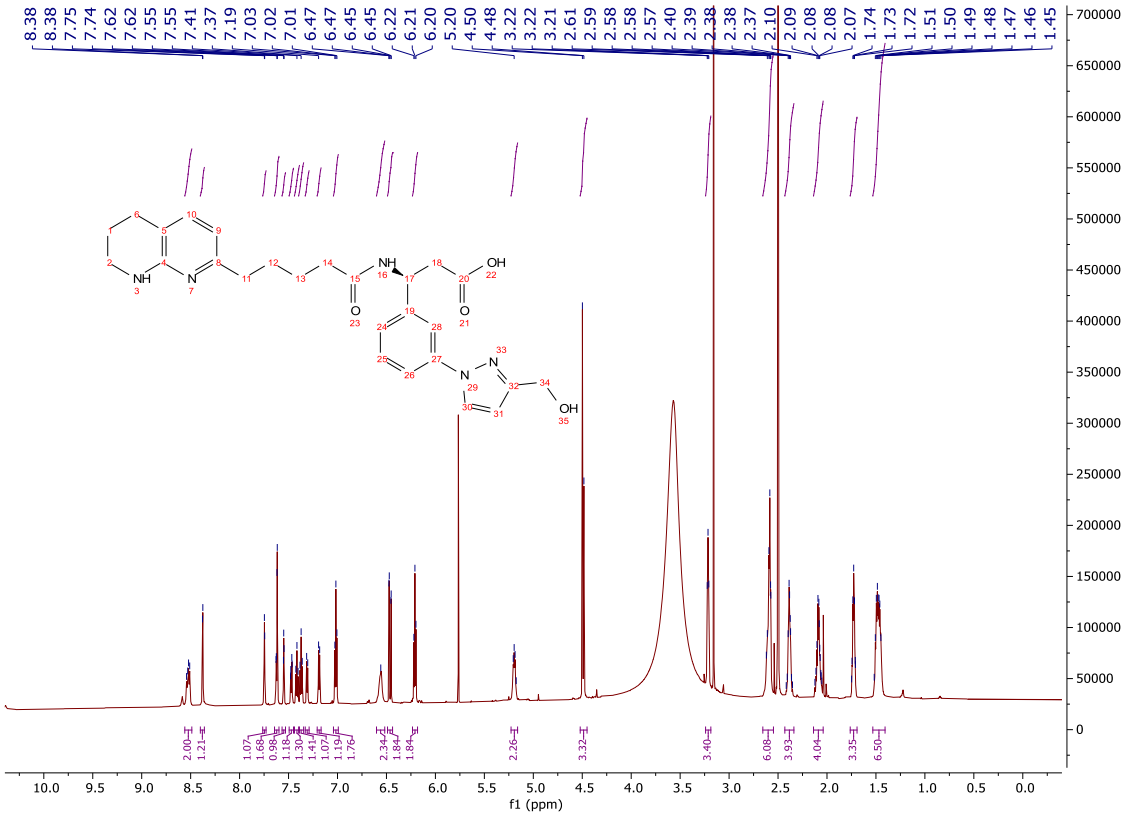
8.38 8.38 7.75 7.74 7.62 7.62 7.55 7.55 7.41 7.37 7.19 7.03 7.02 7.01 6.47 6.47 6.45 6.45 6.22 6.21 6.20 5.20 4.50 4.48 3.22 3.22 3.21 2.61 2.59 2.58 2.58 2.57 2.40 2.39 2.38 2.38 2.37 2.10 2.09 2.08 2.08 2.07 1.74 1.73 1.72 1.51 1.50 1.49 1.48 1.47 1.46 1.45
700000 650000 600000 550000 500000 450000 400000 350000 300000 250000 200000 150000 100000 50000 0
2.00 1.21 1.07 1.68 0.98 1.18 1.30 1.41 1.07 1.19 1.76 2.34 1.84 1.84 2.26 3.32 3.40 6.08 3.93 4.04 3.35 6.50
10.0 9.5 9.0 8.5 8.0 7.5 7.0 6.5 6.0 5.5 5.0 4.5 4.0 3.5 3.0 2.5 2.0 1.5 1.0 0.5 0.0
f1 (ppm)

(*S*)-3-(3-(4-(Hydroxymethyl)-1*H*-pyrazol-1-yl)phenyl)-3-(5-(5,6,7,8-tetrahydro-1,8-naphthyridin-2-yl)pentanamido)propanoic acid (**210**)

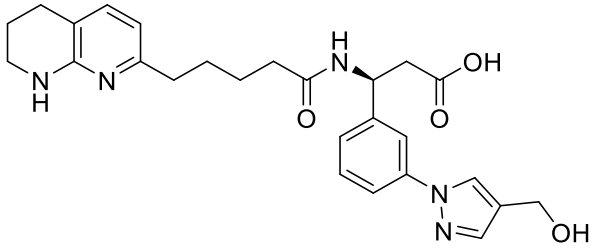

Mass 3.8 mg; Yield 5%; LCMS 98% purity; 0.48 min; *m/z* $[M+H]^+$ 478.43; Crystalline, colourless solid.

δ_H (700 MHz, DMSO-d_6) 8.49 (d, *J* = 8.2 Hz, 1H), 8.35 (s, 1H), 7.77 (dd, *J* = 1.9, 1.9 Hz, 1H), 7.66 (s, 1H), 7.65 – 7.61 (m, 1H), 7.38 (dd, *J* = 7.9, 7.9 Hz, 1H), 7.22 – 7.17 (m, 1H), 7.02 (d, *J* = 7.2 Hz, 1H), 6.60 (bs, 1H), 6.21 (d, *J* = 7.2 Hz, 1H), 5.23 – 5.17 (m, 1H), 4.43 (s, 2H), 3.25 – 3.18 (m, 2H), 2.68 – 2.55 (m, 4H), 2.43 – 2.35 (m, 2H), 2.15 – 2.04 (m, 2H), 1.76 – 1.70 (m, 2H), 1.54 – 1.42 (m, 4H).

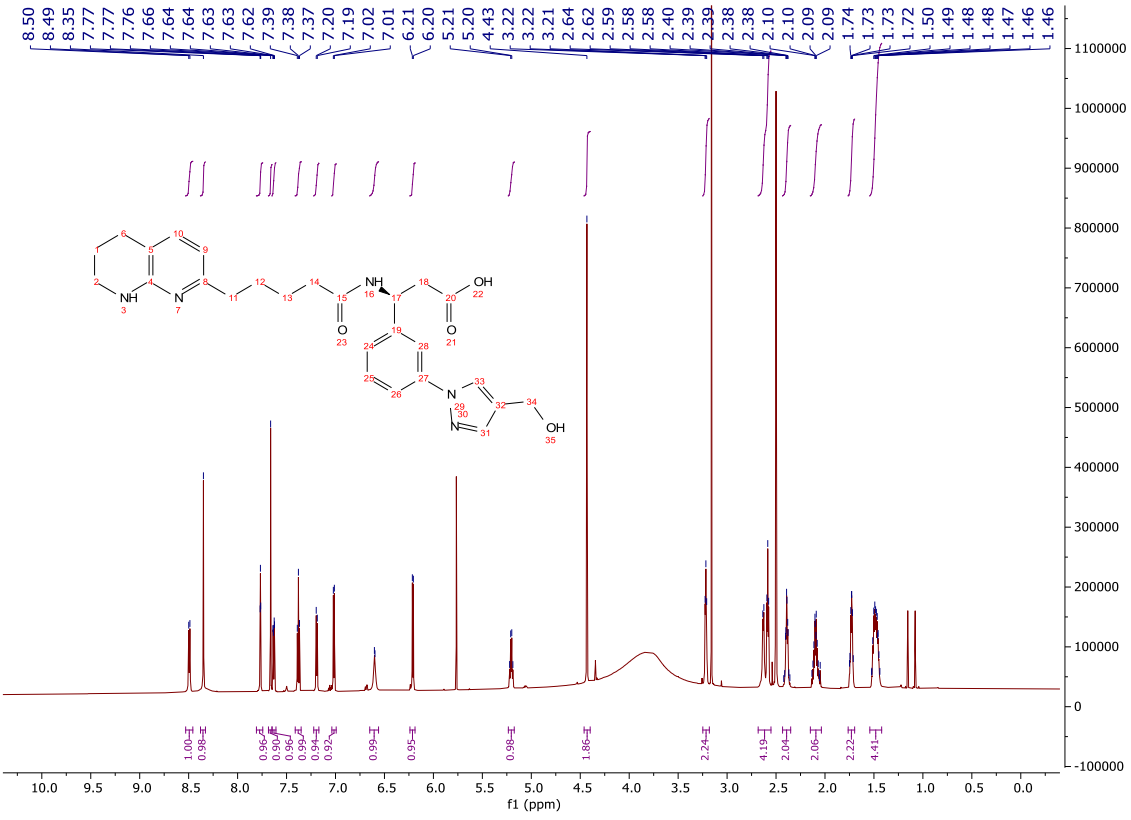

(*S*)-3-(3-(1*H*-Imidazol-1-yl)phenyl)-3-(5-(5,6,7,8-tetrahydro-1,8-naphthyridin-2-yl)pentanamido)propanoic acid (**(*S*)-39**)

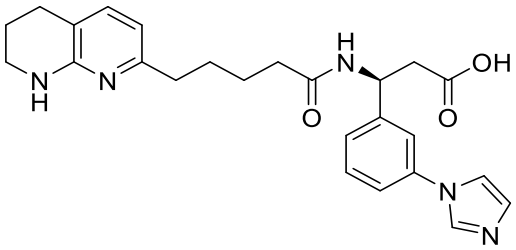

Mass 4.2 mg; Yield 6%; LCMS 97% purity; 0.35 min; *m/z* $[M+H]^+$ 448.36; Colourless solid.

δ_H (700 MHz, DMSO-d_6) 8.42 (d, *J* = 8.2 Hz, 1H), 8.20 (bs, 1H), 7.68 (bs, 1H), 7.56 (dd, *J* = 1.9, 1.9 Hz, 1H), 7.48 (ddd, *J* = 8.0, 2.3, 1.0 Hz, 1H), 7.42 (dd, *J* = 7.8, 7.8 Hz, 1H), 7.31 – 7.26 (m, 1H), 7.11 (bs, 1H), 7.02 (d, *J* = 7.2 Hz, 1H), 6.44 (bs, 1H), 6.22 (d, *J* = 7.3 Hz, 1H), 5.26 – 5.19 (m, 1H), 3.23 (t, *J* = 5.6 Hz, 2H), 2.66 – 2.62 (m, 2H), 2.59 (t, *J* = 6.3 Hz, 2H), 2.45 – 2.36 (m, 2H), 2.14 – 2.09 (m, 2H), 1.76 – 1.71 (m, 2H), 1.55 – 1.45 (m, 4H).

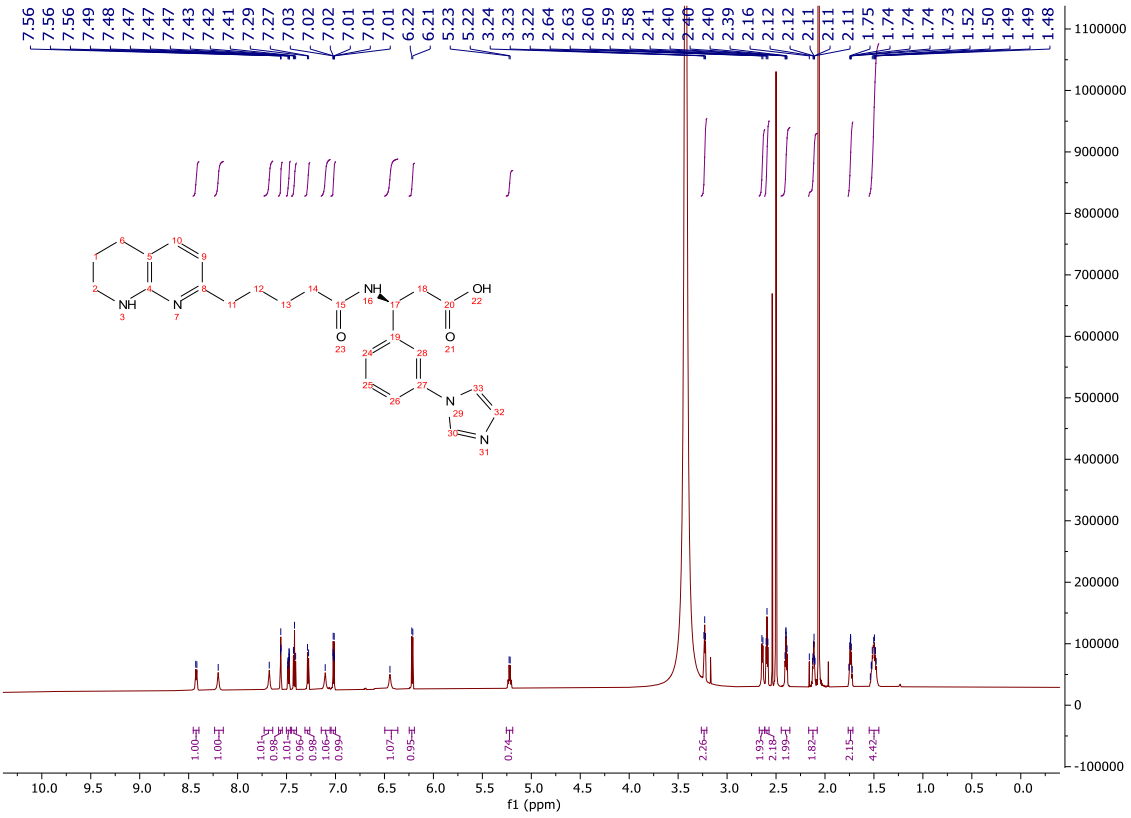

(*S*)-3-(3-(2-Methyl-1*H*-imidazol-1-yl)phenyl)-3-(5-(5,6,7,8-tetrahydro-1,8-naphthyridin-2-yl)pentanamido)propanoic acid (**211**)

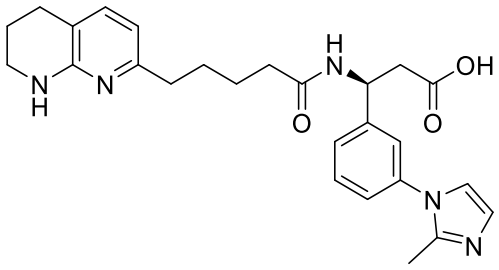

Mass 14.8 mg; Yield 21%; LCMS 99% purity; 0.35 min; *m/z* $[M+H]^+$ 462.43; Crystalline, colourless solid.

δ_H (700 MHz, DMSO-d_6) 8.43 (d, *J* = 8.2 Hz, 1H), 7.45 (dd, *J* = 7.8, 7.8 Hz, 1H), 7.36 (d, *J* = 7.9 Hz, 1H), 7.32 (d, *J* = 2.1 Hz, 1H), 7.30 – 7.25 (m, 1H), 7.22 (d, *J* = 1.4 Hz, 1H), 7.05 (d, *J* = 7.1 Hz, 1H), 6.89 (d, *J* = 1.3 Hz, 1H), 6.54 (bs, 1H), 6.23 (d, *J* = 7.3 Hz, 1H), 5.21 (q, *J* = 7.6 Hz, 1H), 3.23 (t, *J* = 5.6 Hz, 2H), 2.63 (d, *J* = 7.3 Hz, 2H), 2.59 (t, *J* = 6.3 Hz, 2H), 2.42 – 2.35 (m, 2H), 2.24 (s, 3H), 2.15 – 2.07 (m, 2H), 1.76 – 1.70 (m, 2H), 1.53 – 1.42 (m, 4H).

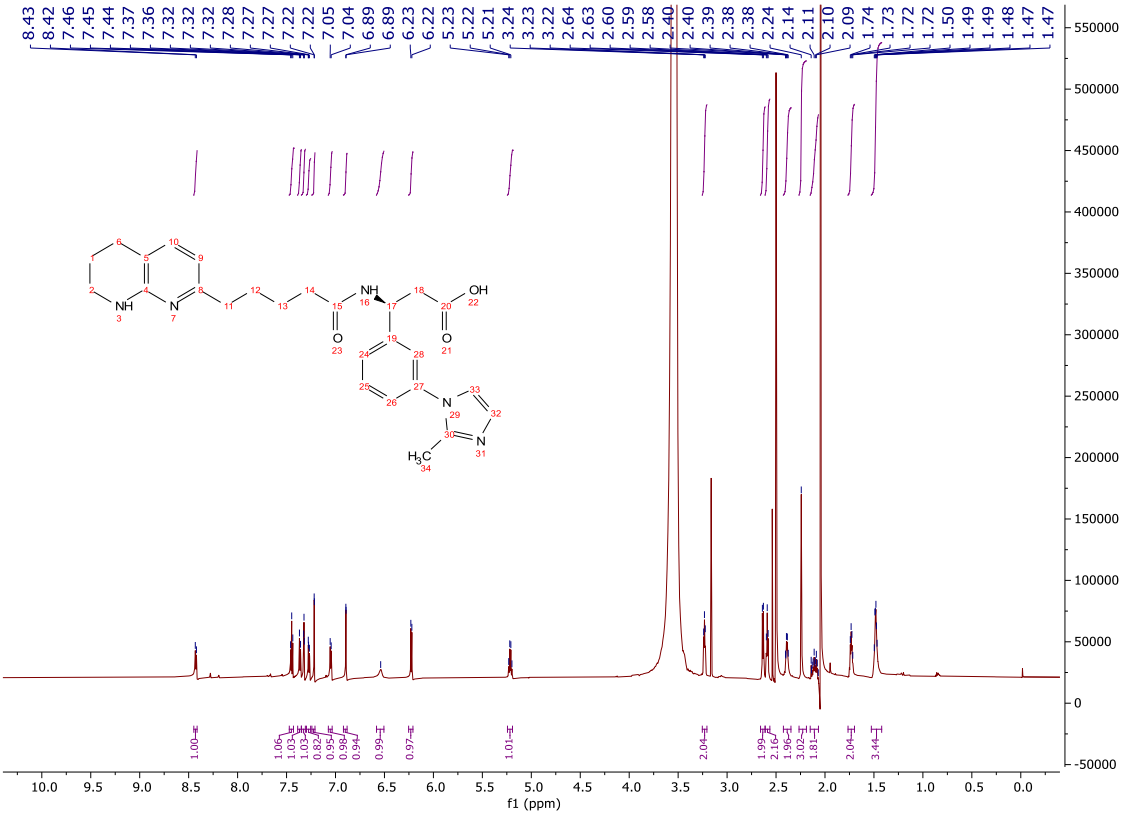

(*S*)-3-(3-(2,4-Dimethyl-1*H*-imidazol-1-yl)phenyl)-3-(5-(5,6,7,8-tetrahydro-1,8-naphthyridin-2-yl)pentanamido)propanoic acid (**212**)

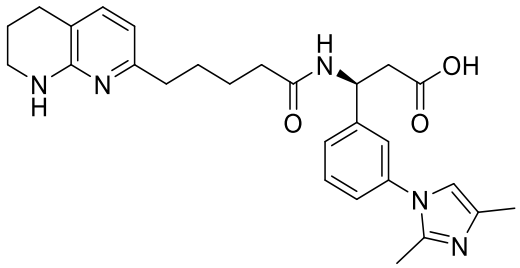

Mass 10.2 mg; Yield 14%; LCMS 99% purity; 0.37 min; *m/z* $[M+H]^+$ 476.49; Crystalline, colourless solid.

δ_H (400 MHz, DMSO-d_6) 8.42 (d, *J* = 8.2 Hz, 1H), 7.84 (bs, 1H), 7.57 – 7.33 (m, 4H), 7.28 – 7.21 (m, 1H), 7.20 – 7.11 (m, 1H), 6.46 (d, *J* = 7.3 Hz, 1H), 5.29 – 5.19 (m, 1H), 3.40 – 3.31 (m, 2H), 2.75 – 2.65 (m, 4H), 2.59 – 2.52 (m, 2H), 2.39 (s, 3H), 2.26 – 2.21 (m, 3H), 2.17 – 2.09 (m, 2H), 1.85 – 1.74 (m, 2H), 1.60 – 1.42 (m, 4H).

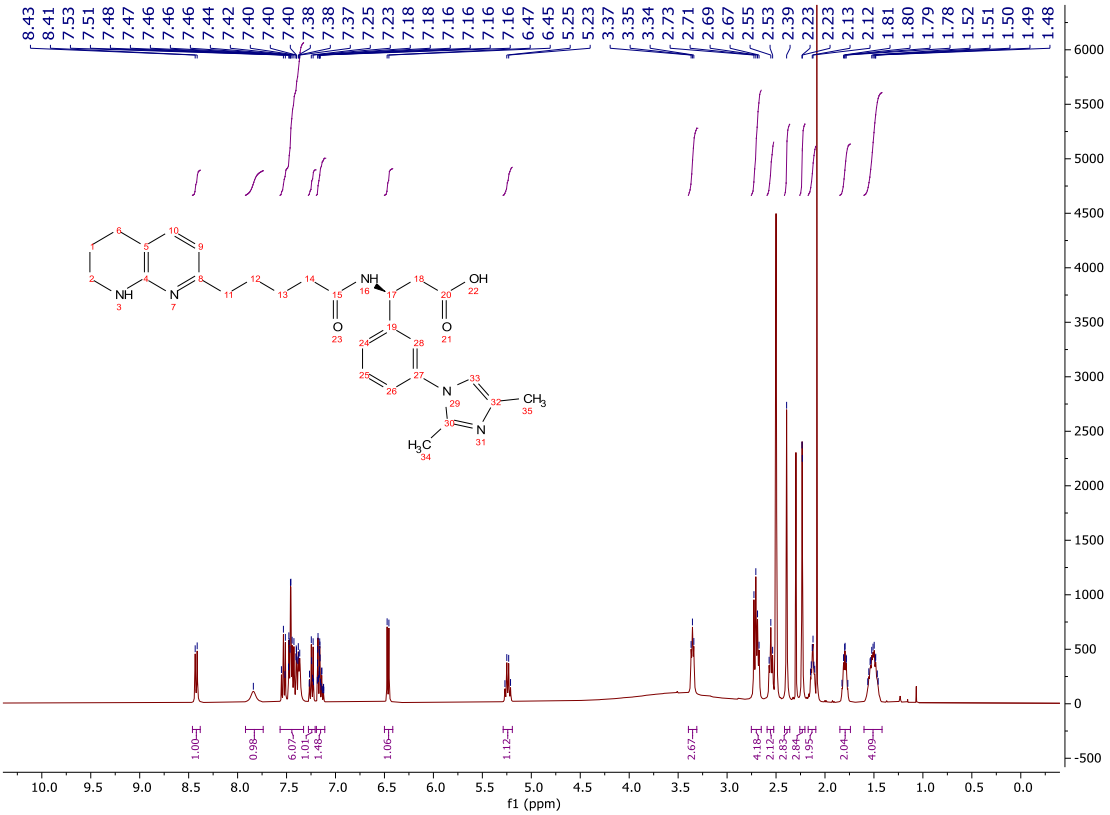

(*S*)-3-(3-(2-Ethyl-1*H*-imidazol-1-yl)phenyl)-3-(5-(5,6,7,8-tetrahydro-1,8-naphthyridin-2-yl)pentanamido)propanoic acid (**213**)

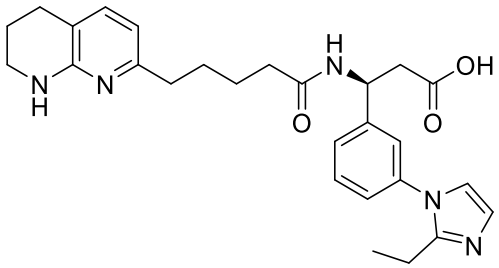

Mass 7.0 mg; Yield 10%; LCMS 100% purity; 0.37 min; *m/z* $[M+H]^+$ 476.46; Clear, yellow oil.

δ_H (700 MHz, DMSO-d_6) 8.45 – 8.38 (m, 1H), 7.44 (dd, *J* = 7.7, 7.7 Hz, 1H), 7.40 – 7.34 (m, 1H), 7.34 – 7.17 (m, 3H), 7.02 (d, *J* = 7.2 Hz, 1H), 6.93 (s, 1H), 6.45 (bs, 1H), 6.27 – 6.15 (m, 1H), 5.28 – 5.14 (m, 1H), 3.26 – 3.20 (m, 2H), 2.73 – 2.48 (m, 6H), 2.44 – 2.33 (m, 2H), 2.15 – 2.04 (m, 2H), 1.77 – 1.70 (m, 2H), 1.57 – 1.40 (m, 4H), 1.16 – 1.05 (m, 3H).

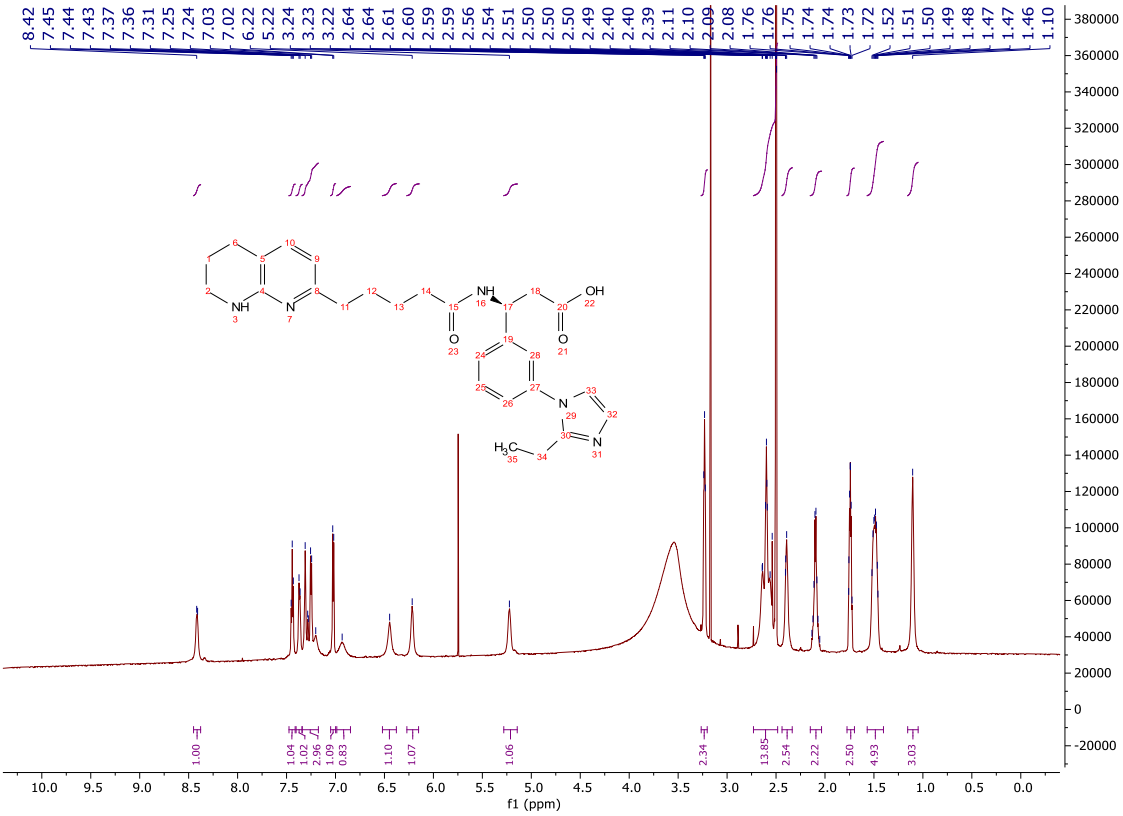

(*S*)-3-(3-(4-Ethyl-1*H*-imidazol-1-yl)phenyl)-3-(5-(5,6,7,8-tetrahydro-1,8-naphthyridin-2-yl)pentanamido)propanoic acid (**214**)

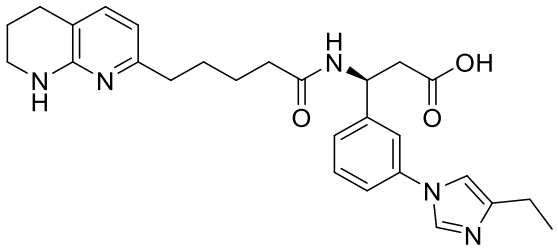

Mass 23.1 mg; Yield 30%; LCMS 92% purity; 0.39 min; *m/z* $[M-H]^-$ 474.42; Crystalline, colourless solid.

δ_H (700 MHz, DMSO-d_6) 8.48 – 8.37 (m, 1H), 8.12 (bs, 1H), 7.54 (bs, 1H), 7.51 – 7.35 (m, 2H), 7.31 – 7.26 (m, 1H), 7.26 – 7.18 (m, 1H), 7.08 – 7.00 (m, 1H), 6.71 – 6.58 (m, 1H), 6.27 – 6.14 (m, 1H), 5.27 – 5.18 (m, 1H), 3.26 – 3.18 (m, 2H), 2.75 – 2.44 (m, 6H), 2.44 – 2.32 (m, 2H), 2.16 – 2.04 (m, 2H), 1.77 – 1.69 (m, 2H), 1.54 – 1.42 (m, 4H), 1.19 (t, *J* = 7.3 Hz, 3H).

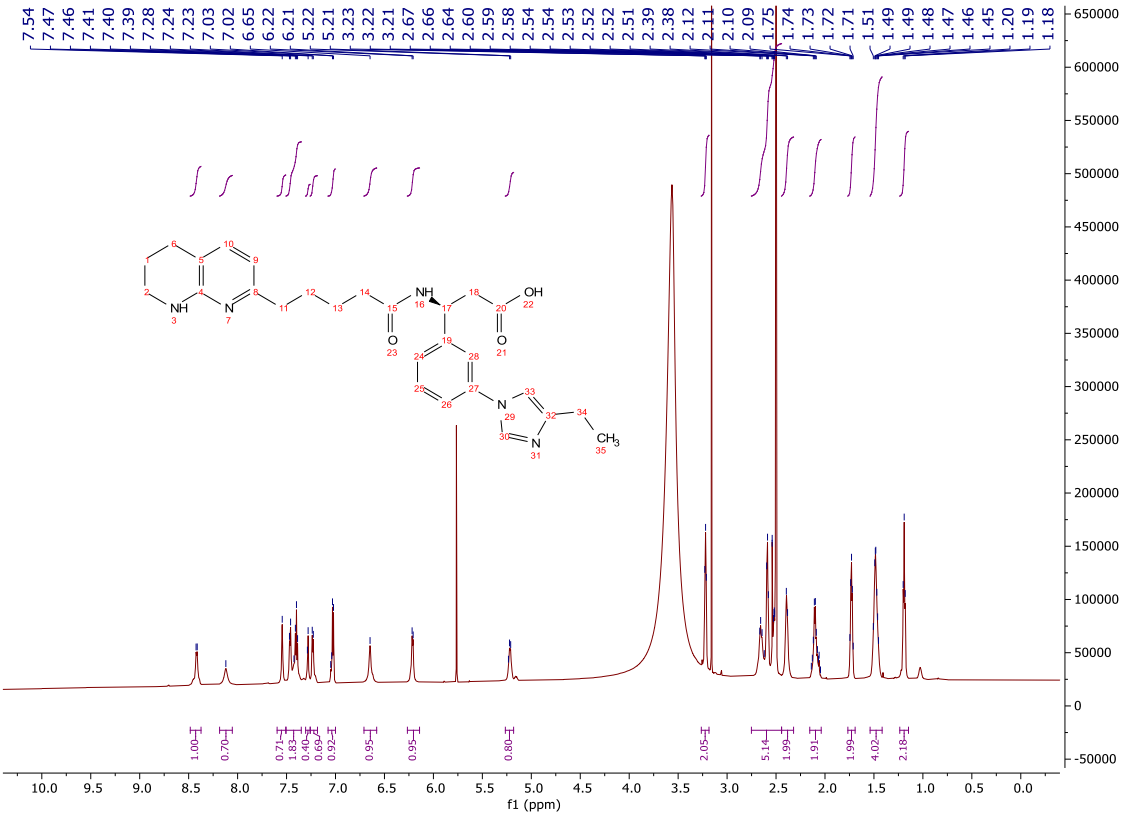

(*S*)-3-(3-(2-Isopropyl-1*H*-imidazol-1-yl)phenyl)-3-(5-(5,6,7,8-tetrahydro-1,8-naphthyridin-2-yl)pentanamido)propanoic acid (**215**)

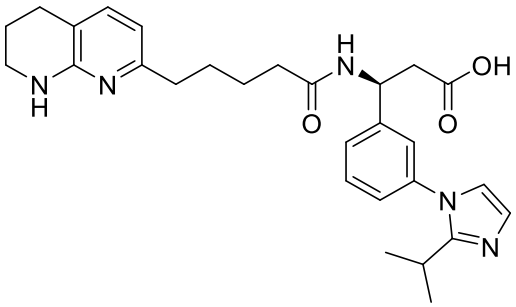

Mass 3.6 mg; Yield 4%; LCMS 92% purity; 0.39 min; *m/z* $[M-H]^-$ 488.46; Colourless solid.

δ_H (700 MHz, DMSO-d_6) 8.55 (d, *J* = 8.6 Hz, 1H), 7.43 (dd, *J* = 7.7, 7.7 Hz, 1H), 7.41 – 7.35 (m, 1H), 7.30 – 7.26 (m, 1H), 7.25 – 7.21 (m, 1H), 7.13 (d, *J* = 1.3 Hz, 1H), 7.06 – 6.99 (m, 1H), 6.93 – 6.88 (m, 1H), 6.52 (bs, 1H), 6.24 – 6.17 (m, 1H), 5.24 – 5.16 (m, 1H), 3.25 – 3.19 (m, 2H), 2.89 (hept, *J* = 6.8 Hz, 1H), 2.62 – 2.54 (m, 4H), 2.41 – 2.33 (m, 2H), 2.13 – 2.04 (m, 2H), 1.76 – 1.70 (m, 2H), 1.52 – 1.41 (m, 4H), 1.10 – 1.07 (m, 6H).

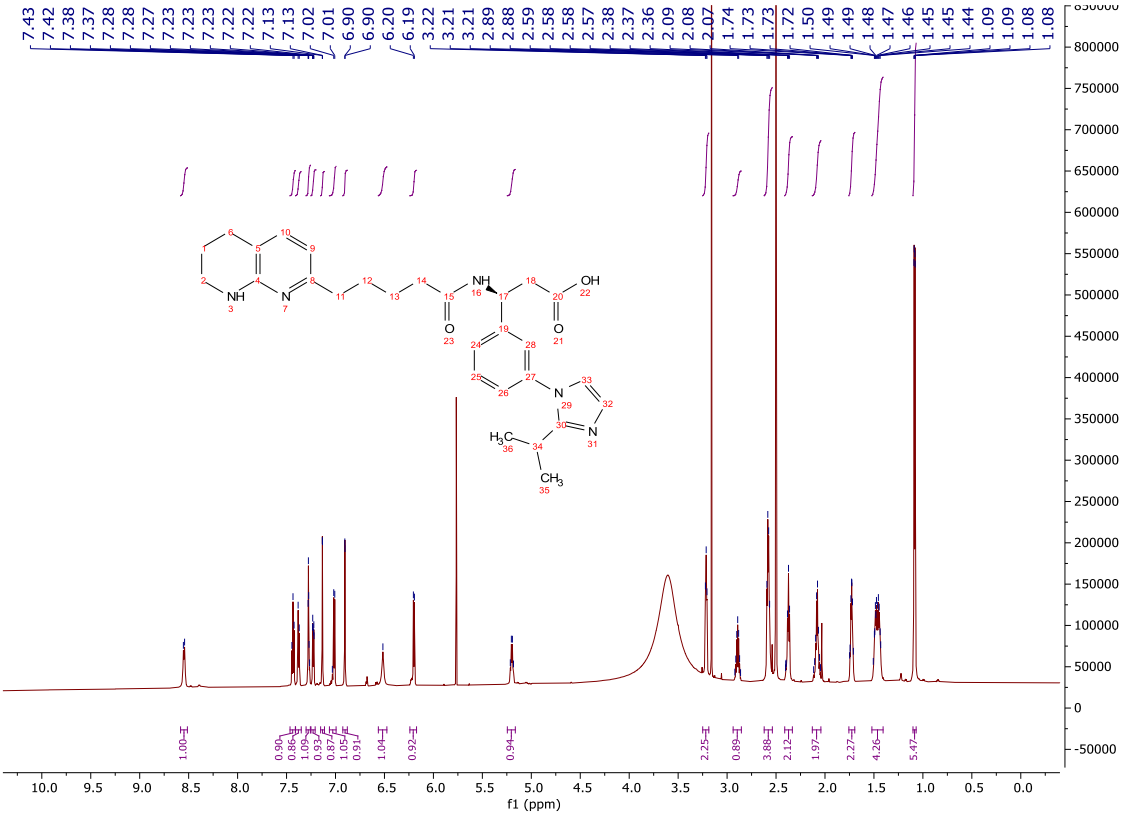

(*S*)-3-(3-(4-Isopropyl-1*H*-imidazol-1-yl)phenyl)-3-(5-(5,6,7,8-tetrahydro-1,8-naphthyridin-2-yl)pentanamido)propanoic acid (**216**)

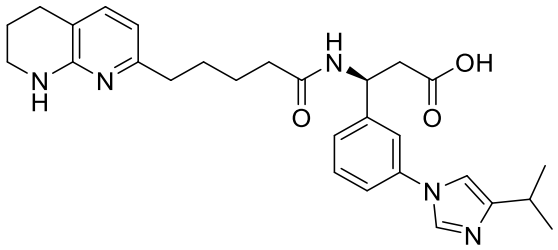

Mass 25.4 mg; Yield 35%; LCMS 100% purity; 0.73 min; *m/z* $[M+H]^+$ 490.52; Crystalline, colourless solid.

δ_H (700 MHz, DMSO-d_6) 8.33 (bs, 1H), 8.12 (bs, 1H), 7.61 – 7.33 (m, 4H), 7.24 (bs, 1H), 7.03 (bs, 1H), 6.49 (bs, 1H), 6.23 (bs, 1H), 5.23 (bs, 1H), 3.24 (bs, 2H), 2.91 – 2.55 (m, 5H), 2.48 – 2.31 (m, 2H), 2.18 – 2.04 (m, 2H), 1.78 – 1.70 (m, 2H), 1.62 – 1.43 (m, 4H), 1.30 – 1.17 (m, 6H).

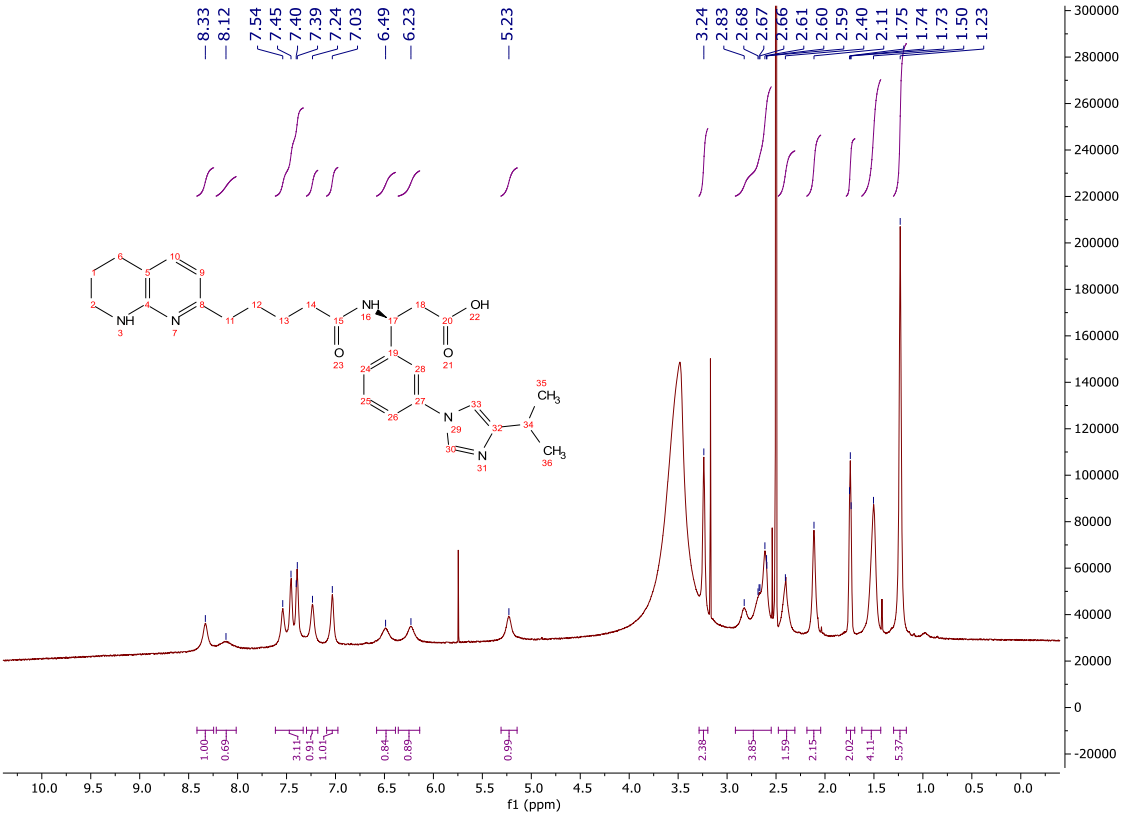

(*S*)-3-(3-(2-Propyl-1*H*-imidazol-1-yl)phenyl)-3-(5-(5,6,7,8-tetrahydro-1,8-naphthyridin-2-yl)pentanamido)propanoic acid (**217**)

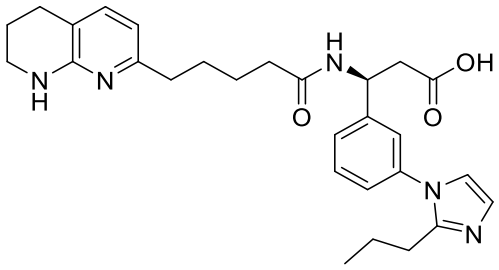

Mass 8.2 mg; Yield 10%; LCMS 97% purity; 0.69 min; *m/z* $[M+H]^+$ 490.45; Crystalline, colourless solid.

δ_H (700 MHz, DMSO-d_6) 8.42 (bs, 1H), 7.44 (dd, *J* = 7.7, 7.7 Hz, 1H), 7.40 – 7.33 (m, 1H), 7.30 (bs, 1H), 7.26 – 7.15 (m, 2H), 7.02 (d, *J* = 7.2 Hz, 1H), 6.93 (bs, 1H), 6.44 (bs, 1H), 6.26 – 6.16 (m, 1H), 5.27 – 5.17 (m, 1H), 3.26 – 3.20 (m, 2H), 2.72 – 2.48 (m, 6H), 2.45 – 2.33 (m, 2H), 2.15 – 2.04 (m, 2H), 1.77 – 1.71 (m, 2H), 1.62 – 1.43 (m, 6H), 0.80 (t, *J* = 7.1 Hz, 3H).

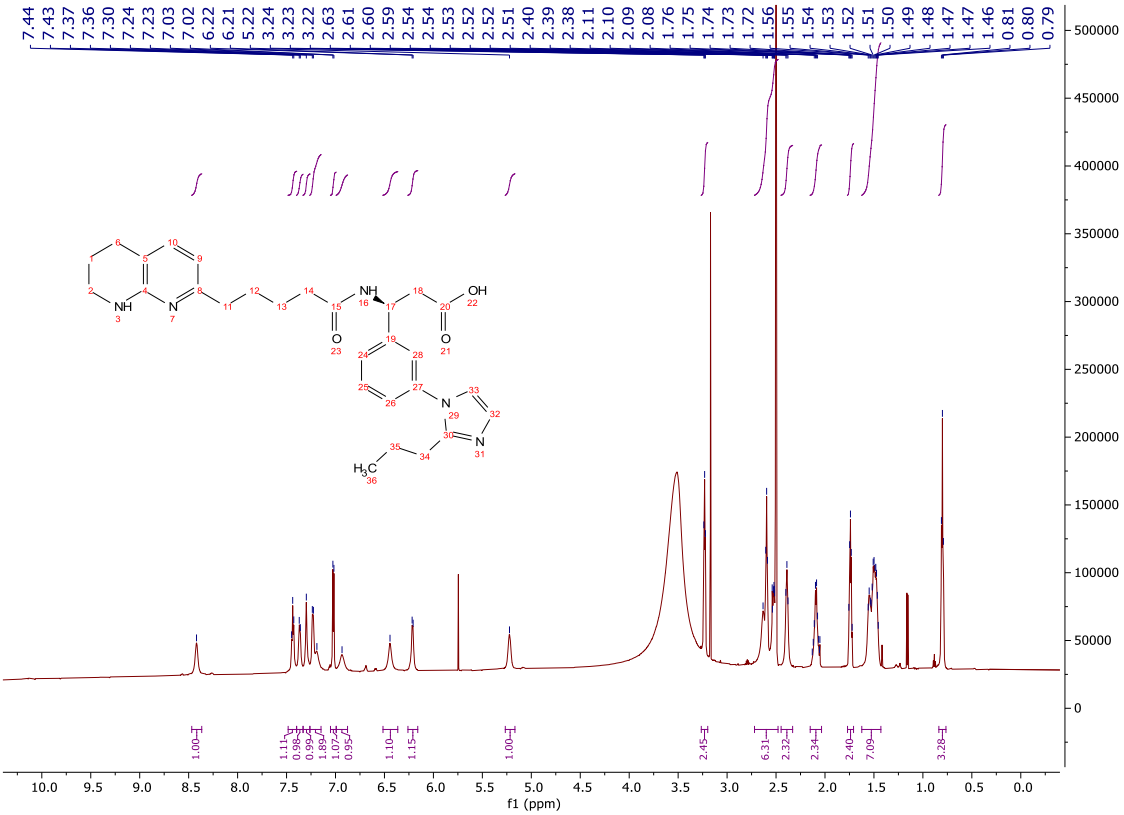

(*S*)-3-(3-(4-Chloro-1*H*-imidazol-1-yl)phenyl)-3-(5-(5,6,7,8-tetrahydro-1,8-naphthyridin-2-yl)pentanamido)propanoic acid (**219**)

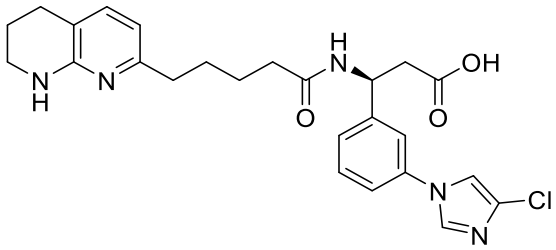

Mass 13.0 mg; Yield 15%; LCMS 81% (19%) purity; 0.56 min and 0.50 min; *m/z* $[M-H]^-$ 480.25 and 480.30; Pale yellow solid.

δ_H (700 MHz, DMSO-d_6) 8.40 (d, *J* = 8.2 Hz, 1H), 8.20 (d, *J* = 1.6 Hz, 1H), 7.85 (d, *J* = 1.6 Hz, 1H), 7.58 (dd, *J* = 1.9, 1.9 Hz, 1H), 7.51 – 7.47 (m, 1H), 7.46 – 7.41 (m, 1H), 7.34 – 7.29 (m, 1H), 7.04 – 7.00 (m, 1H), 6.45 (bs, 1H), 6.24 – 6.19 (m, 1H), 5.26 – 5.19 (m, 1H), 3.23 (t, *J* = 5.6 Hz, 2H), 2.68 – 2.57 (m, 4H), 2.42 – 2.37 (m, 2H), 2.17 – 2.06 (m, 2H), 1.77 – 1.71 (m, 2H), 1.54 – 1.45 (m, 4H).

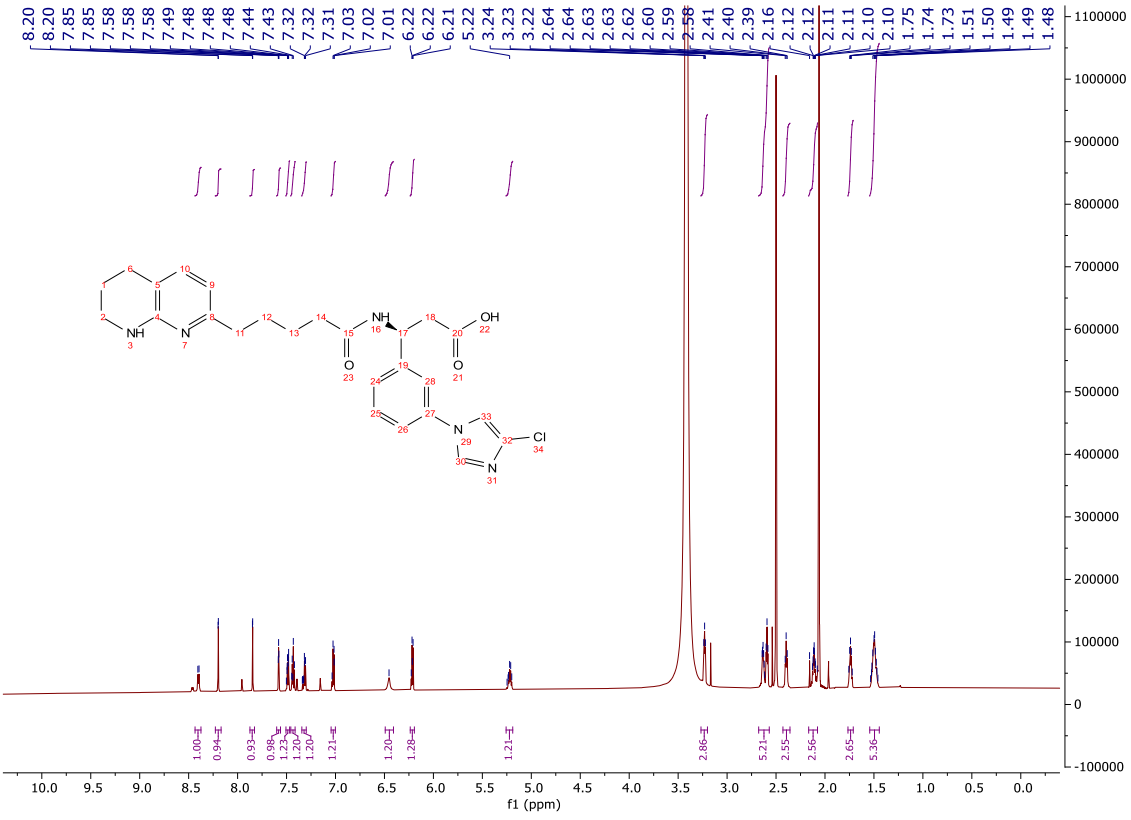

(*S*)-3-(3-(4-Fluoro-1*H*-imidazol-1-yl)phenyl)-3-(5-(5,6,7,8-tetrahydro-1,8-naphthyridin-2-yl)pentanamido)propanoic acid (**220**)

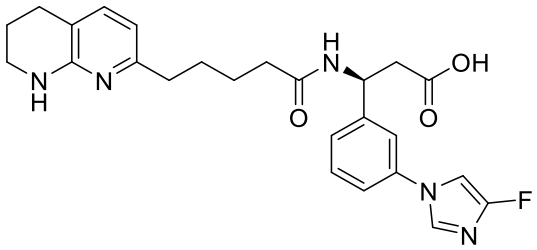

Mass 7.4 mg; Yield 11%; LCMS 100% purity; 0.68 min; *m/z* $[M+H]^+$ 466.34; Crystalline, colourless solid.

δ_H (700 MHz, DMSO-d_6) 8.43 – 8.34 (m, 1H), 7.96 (s, 1H), 7.57 (bs, 1H), 7.51 – 7.39 (m, 3H), 7.34 – 7.26 (m, 1H), 7.02 (d, *J* = 7.2 Hz, 1H), 6.45 (bs, 1H), 6.22 (bs, 1H), 5.29 – 5.17 (m, 1H), 3.26 – 3.19 (m, 2H), 2.74 – 2.54 (m, 4H), 2.47 – 2.33 (m, 2H), 2.17 – 2.07 (m, 2H), 1.78 – 1.69 (m, 2H), 1.57 – 1.43 (m, 4H).

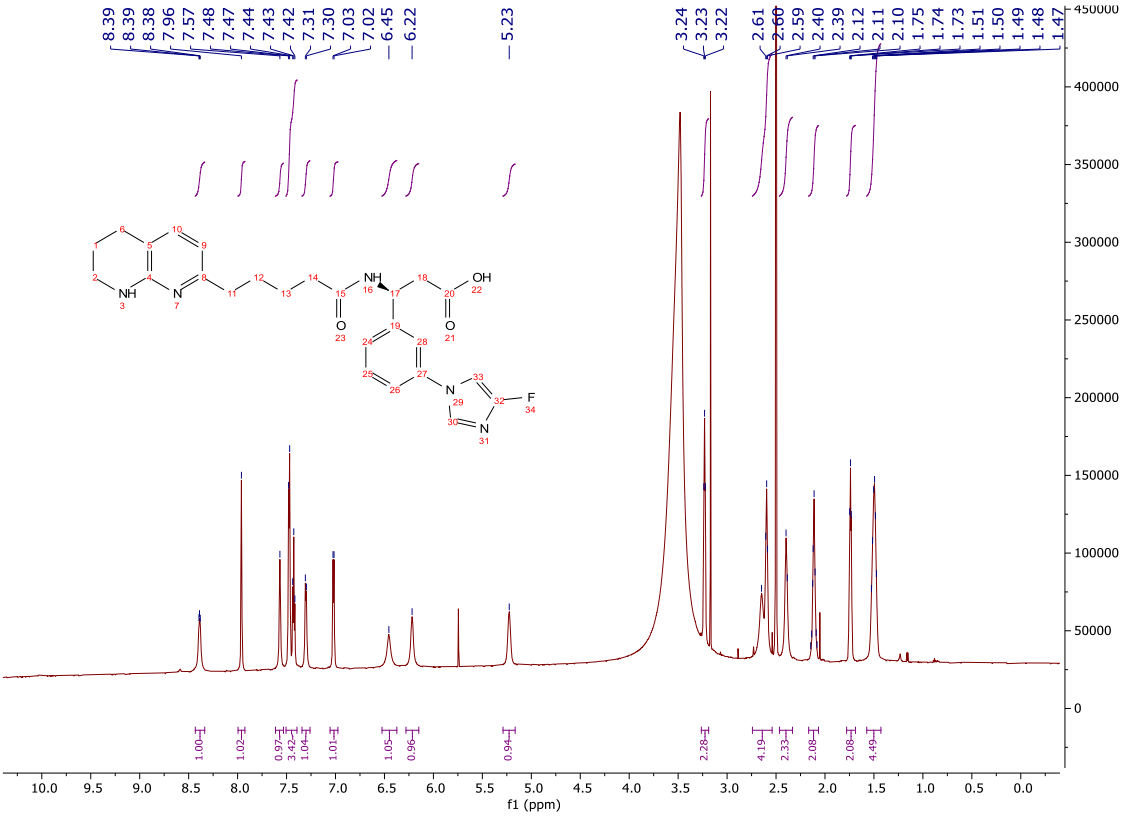

(*S*)-3-(3-(4-(Difluoromethyl)-1*H*-imidazol-1-yl)phenyl)-3-(5-(5,6,7,8-tetrahydro-1,8-naphthyridin-2-yl)pentanamido)propanoic acid (**221**)

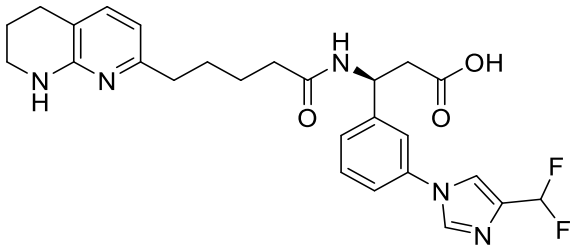

Mass 9.0 mg; Yield 12%; LCMS 97% purity; 0.55 min; *m/z* $[M+H]^+$ 498.43; Crystalline, colourless solid.

δ_H (700 MHz, DMSO-d_6) 8.45 (d, *J* = 8.2 Hz, 1H), 8.37 – 8.35 (m, 1H), 8.12 – 8.09 (m, 1H), 7.64 (dd, *J* = 1.9, 1.9 Hz, 1H), 7.54 (ddd, *J* = 8.0, 2.2, 2.2 Hz, 1H), 7.45 (dd, *J* = 7.9, 7.9 Hz, 1H), 7.33 – 7.30 (m, 1H), 7.08 – 6.88 (m, 2H), 6.62 (bs, 1H), 6.21 (d, *J* = 7.2 Hz, 1H), 5.23 (ddd, *J* = 8.4, 8.4, 6.1 Hz, 1H), 3.24 – 3.20 (m, 2H), 2.72 – 2.56 (m, 4H), 2.42 – 2.35 (m, 2H), 2.17 – 2.06 (m, 2H), 1.76 – 1.70 (m, 2H), 1.53 – 1.42 (m, 4H).

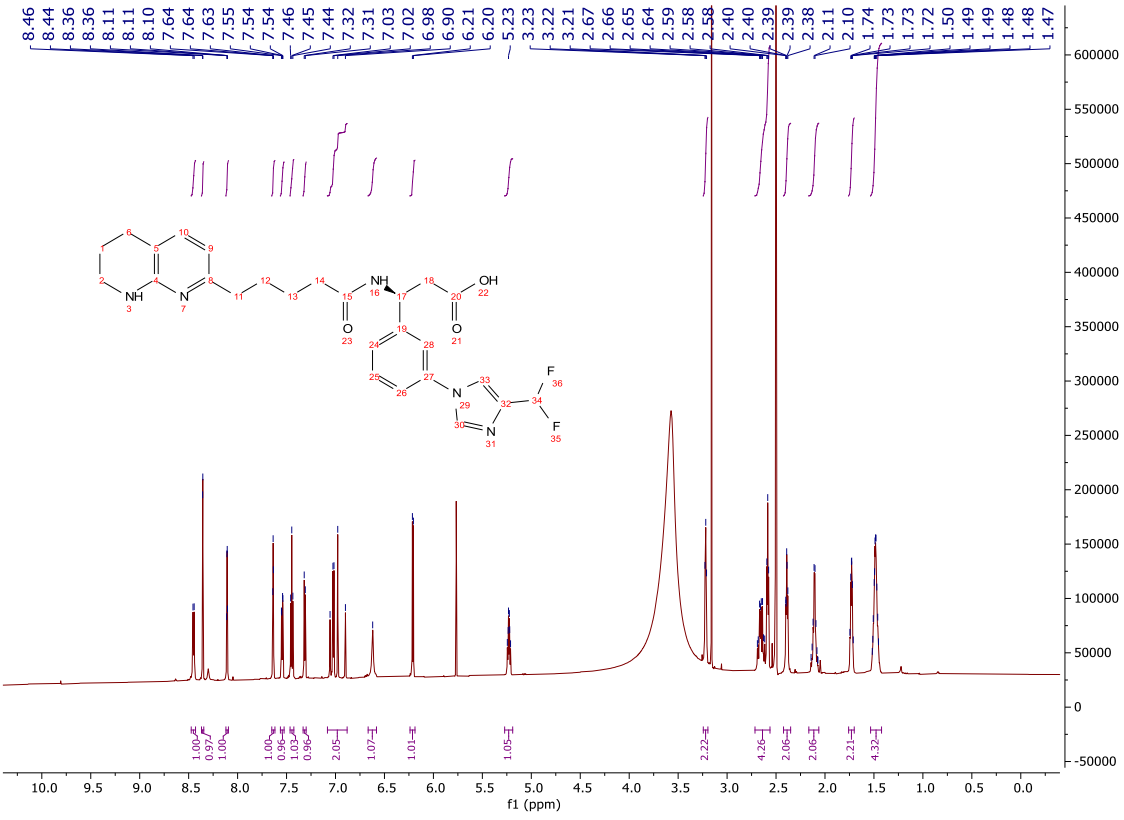

(*S*)-3-(3-(3,5-Dimethyl-1*H*-1,2,4-triazol-1-yl)phenyl)-3-(5-(5,6,7,8-tetrahydro-1,8-naphthyridin-2-yl)pentanamido)propanoic acid (**223**)

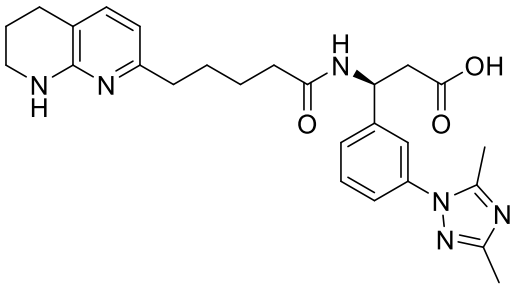

Mass 15.9 mg; Yield 22%; LCMS 100% purity; 0.63 min; *m/z* $[M+H]^+$ 477.43; Crystalline, colourless solid.

δ_H (700 MHz, DMSO-d_6) 8.46 (d, *J* = 8.0 Hz, 1H), 7.48 – 7.42 (m, 2H), 7.40 – 7.34 (m, 2H), 7.02 (d, *J* = 7.2 Hz, 1H), 6.43 (bs, 1H), 6.21 (d, *J* = 7.2 Hz, 1H), 5.26 – 5.17 (m, 1H), 3.26 – 3.19 (m, 2H), 2.69 – 2.55 (m, 4H), 2.44 – 2.34 (m, 5H), 2.26 (s, 3H), 2.14 – 2.06 (m, 2H), 1.77 – 1.71 (m, 2H), 1.55 – 1.43 (m, 4H).

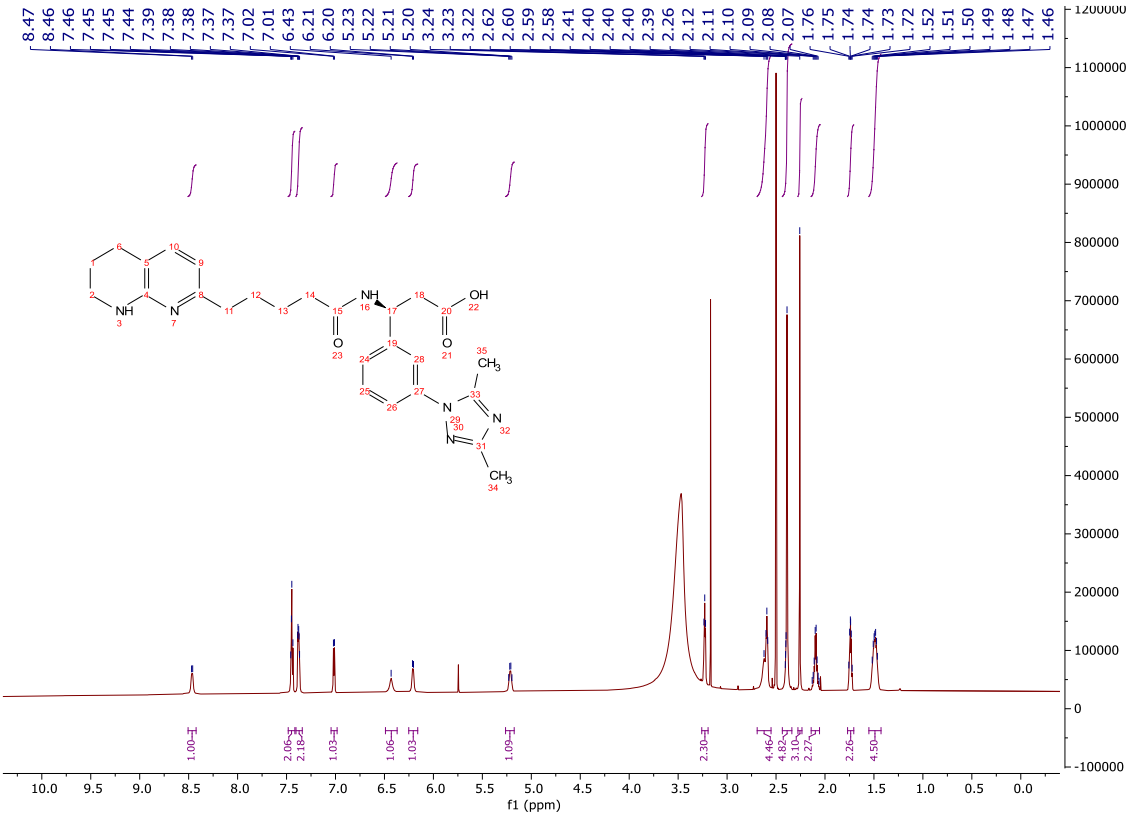

(*S*)-3-(3-(3-Ethyl-1*H*-1,2,4-triazol-1-yl)phenyl)-3-(5-(5,6,7,8-tetrahydro-1,8-naphthyridin-2-yl)pentanamido)propanoic acid (**224**)

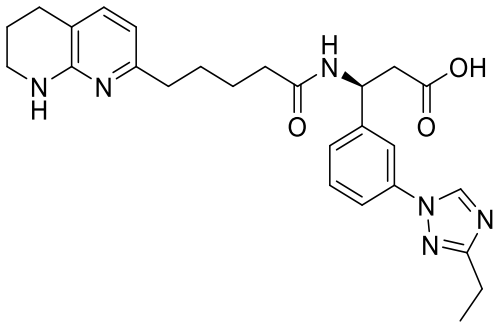

Mass 4.7 mg; Yield 6%; LCMS 71% (16%) purity; 0.55 min and 0.51 min; *m/z* $[M+H]^+$ 477.44 and 477.47; Crystalline, colourless solid.

δ_H (700 MHz, DMSO-d_6) 9.12 (s, 1H), 8.58 – 8.53 (m, 1H), 7.76 – 7.72 (m, 1H), 7.66 – 7.62 (m, 1H), 7.45 – 7.40 (m, 1H), 7.31 – 7.24 (m, 1H), 7.02 – 6.99 (m, 1H), 6.55 (s, 1H), 6.21 – 6.17 (m, 1H), 5.23 – 5.16 (m, 1H), 3.24 – 3.19 (m, 2H), 2.73 – 2.68 (m, 2H), 2.64 – 2.55 (m, 4H), 2.42 – 2.34 (m, 2H), 2.13 – 2.05 (m, 2H), 1.76 – 1.69 (m, 2H), 1.52 – 1.41 (m, 4H), 1.25 (t, *J* = 7.6 Hz, 3H).

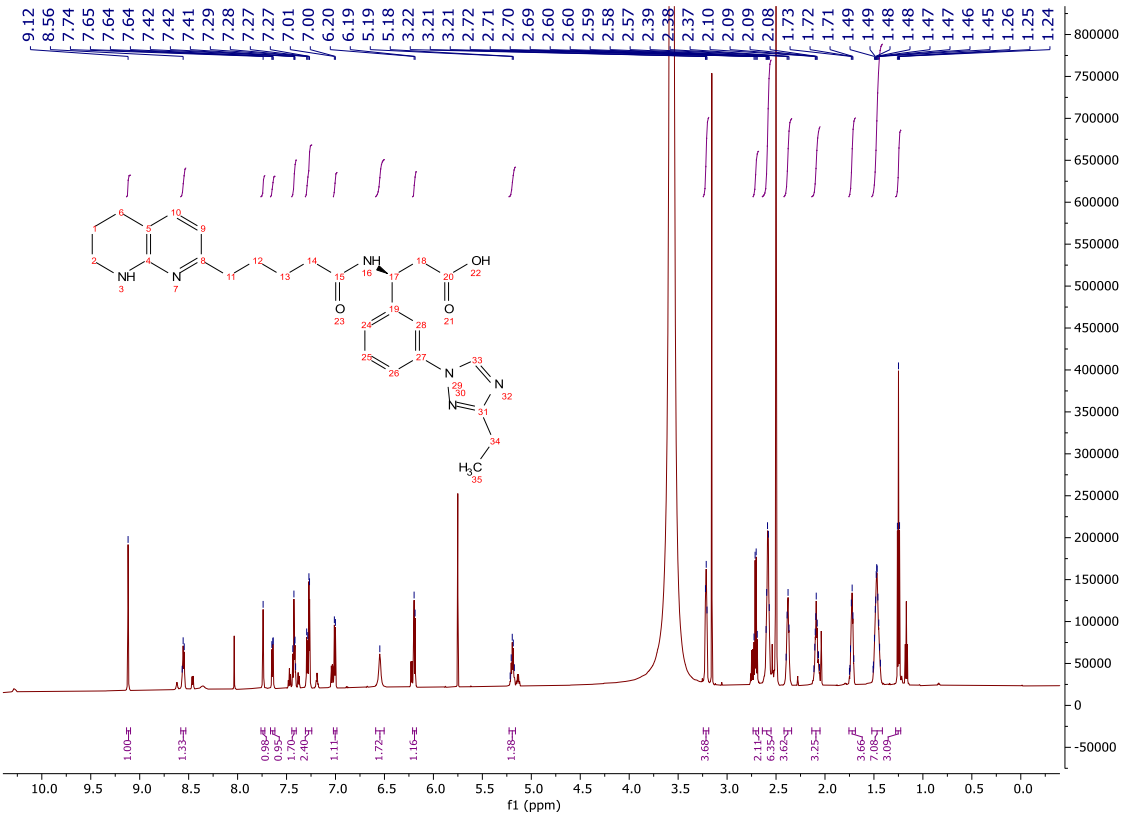

(*S*)-3-(3-(3-Isopropyl-1*H*-1,2,4-triazol-1-yl)phenyl)-3-(5-(5,6,7,8-tetrahydro-1,8-naphthyridin-2-yl)pentanamido)propanoic acid (**225**)

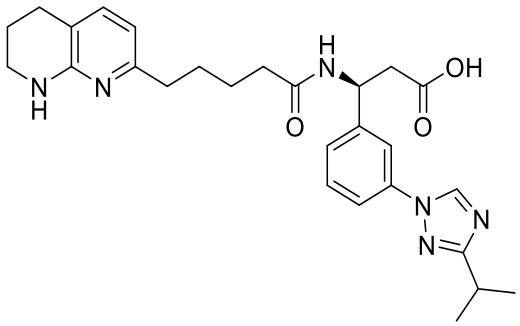

Mass 12.9 mg; Yield 15%; LCMS 84% (16%) purity; 0.60 min and 0.54 min; *m/z* $[M+H]^+$ 491.49 and 491.50; Off-white solid.

δ_H (700 MHz, DMSO-d_6) 9.12 (s, 1H), 8.51 (d, *J* = 8.1 Hz, 1H), 7.75 (dd, *J* = 1.9, 1.9 Hz, 1H), 7.69 – 7.64 (m, 1H), 7.44 (dd, *J* = 7.9, 7.9 Hz, 1H), 7.32 – 7.26 (m, 1H), 7.06 – 6.99 (m, 1H), 6.62 (bs, 1H), 6.25 – 6.17 (m, 1H), 5.25 – 5.18 (m, 1H), 3.25 – 3.19 (m, 2H), 3.09 – 3.01 (m, 1H), 2.65 (d, *J* = 7.4 Hz, 2H), 2.61 – 2.56 (m, 2H), 2.44 – 2.34 (m, 2H), 2.14 – 2.04 (m, 2H), 1.77 – 1.70 (m, 2H), 1.53 – 1.42 (m, 4H), 1.28 (d, *J* = 6.9 Hz, 6H).

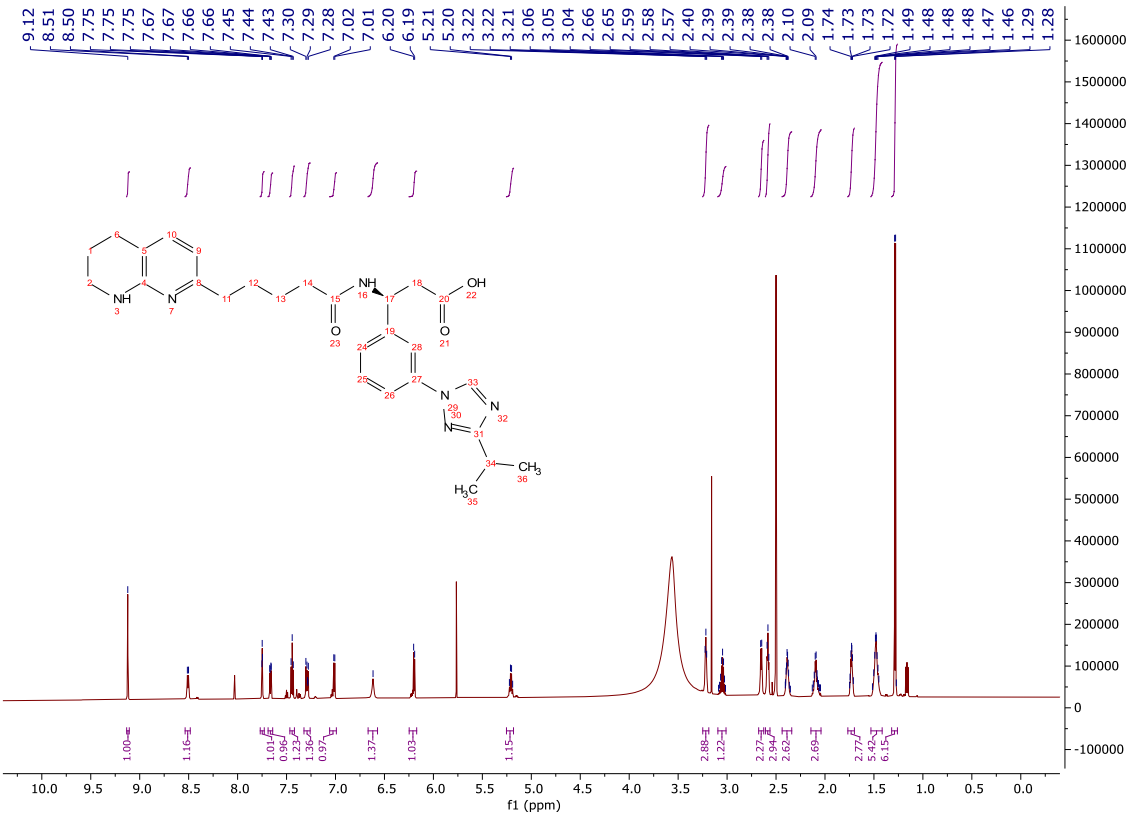

(*S*)-3-(3-(Piperidin-1-yl)phenyl)-3-(5-(5,6,7,8-tetrahydro-1,8-naphthyridin-2-yl)pentanamido)propanoic acid (**227**)

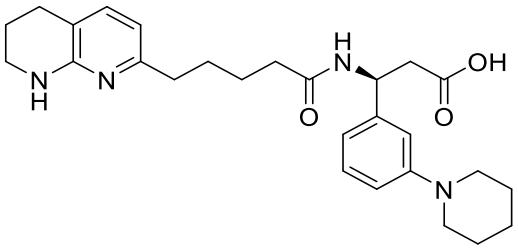

Mass 10.5 mg; Yield 15%; LCMS 99% purity; 0.42 min; *m/z* $[M+H]^+$ 465.47; Yellow oil.

δ_H (700 MHz, DMSO-d_6) 8.26 (d, *J* = 8.4 Hz, 1H), 7.09 (dd, *J* = 7.9, 7.9 Hz, 1H), 7.05 (d, *J* = 7.1 Hz, 1H), 6.84 (dd, *J* = 2.0, 2.0 Hz, 1H), 6.77 – 6.73 (m, 1H), 6.66 (d, *J* = 7.6 Hz, 1H), 6.46 (bs, 1H), 6.23 (d, *J* = 7.2 Hz, 1H), 5.13 – 5.07 (m, 1H), 3.23 (t, *J* = 5.6 Hz, 2H), 3.10 – 3.03 (m, 4H), 2.61 – 2.54 (m, 4H), 2.43 – 2.36 (m, 2H), 2.15 – 2.06 (m, 2H), 1.76 – 1.71 (m, 2H), 1.59 – 1.54 (m, 4H), 1.53 – 1.44 (m, 6H).

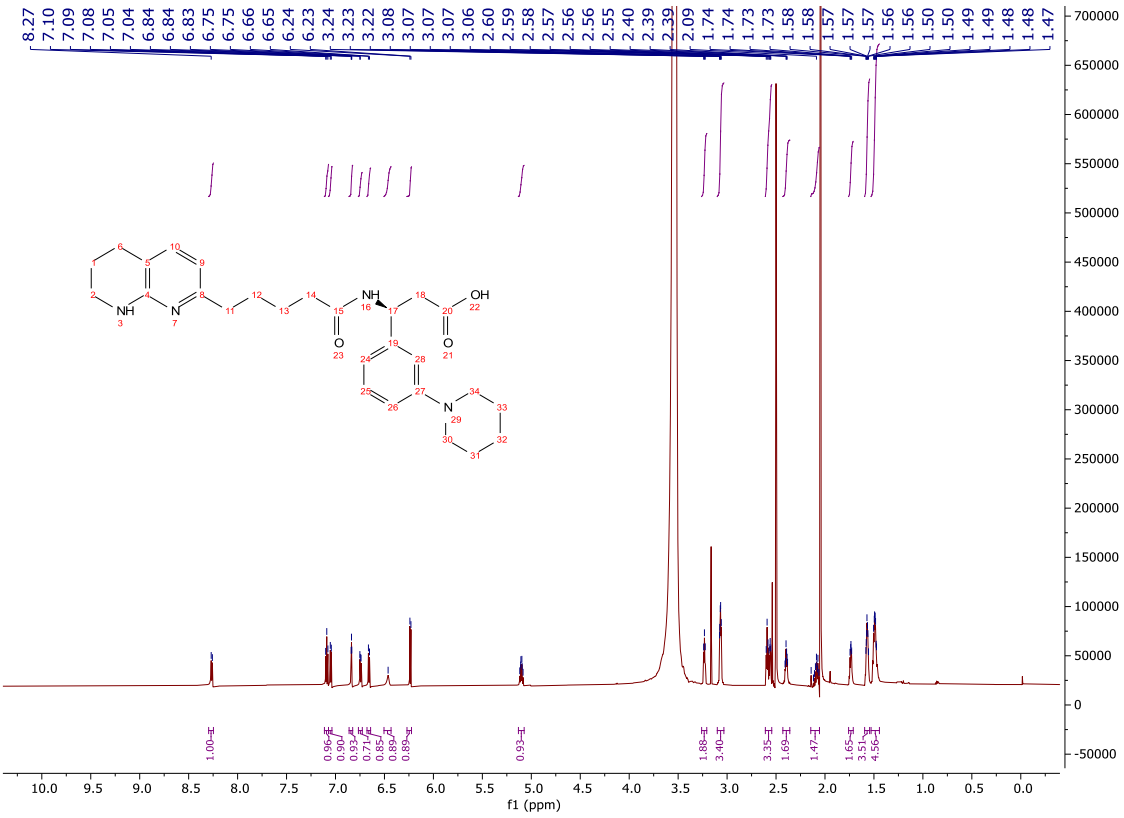

(*S*)-3-(3-(Piperazin-1-yl)phenyl)-3-(5-(5,6,7,8-tetrahydro-1,8-naphthyridin-2-yl)pentanamido)propanoic acid (**228**)

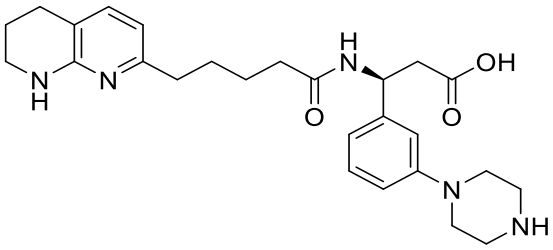

Mass 17.7 mg; Yield 22%; LCMS 86% purity; 0.35 min; *m/z* $[M+H]^+$ 466.40; Off-white solid.

δ_H (700 MHz, DMSO-d_6) 8.35 – 8.28 (m, 1H), 7.10 (dd, *J* = 7.9, 7.9 Hz, 1H), 7.05 – 7.01 (m, 1H), 6.88 – 6.83 (m, 1H), 6.76 – 6.72 (m, 1H), 6.72 – 6.67 (m, 1H), 6.40 (bs, 1H), 6.25 – 6.20 (m, 1H), 5.14 – 5.07 (m, 1H), 3.25 – 3.21 (m, 2H), 3.03 (bs, 4H), 2.84 (bs, 4H), 2.60 (t, *J* = 6.3 Hz, 2H), 2.58 – 2.48 (m, 2H), 2.43 – 2.36 (m, 2H), 2.13 – 2.03 (m, 2H), 1.77 – 1.71 (m, 2H), 1.55 – 1.44 (m, 4H).

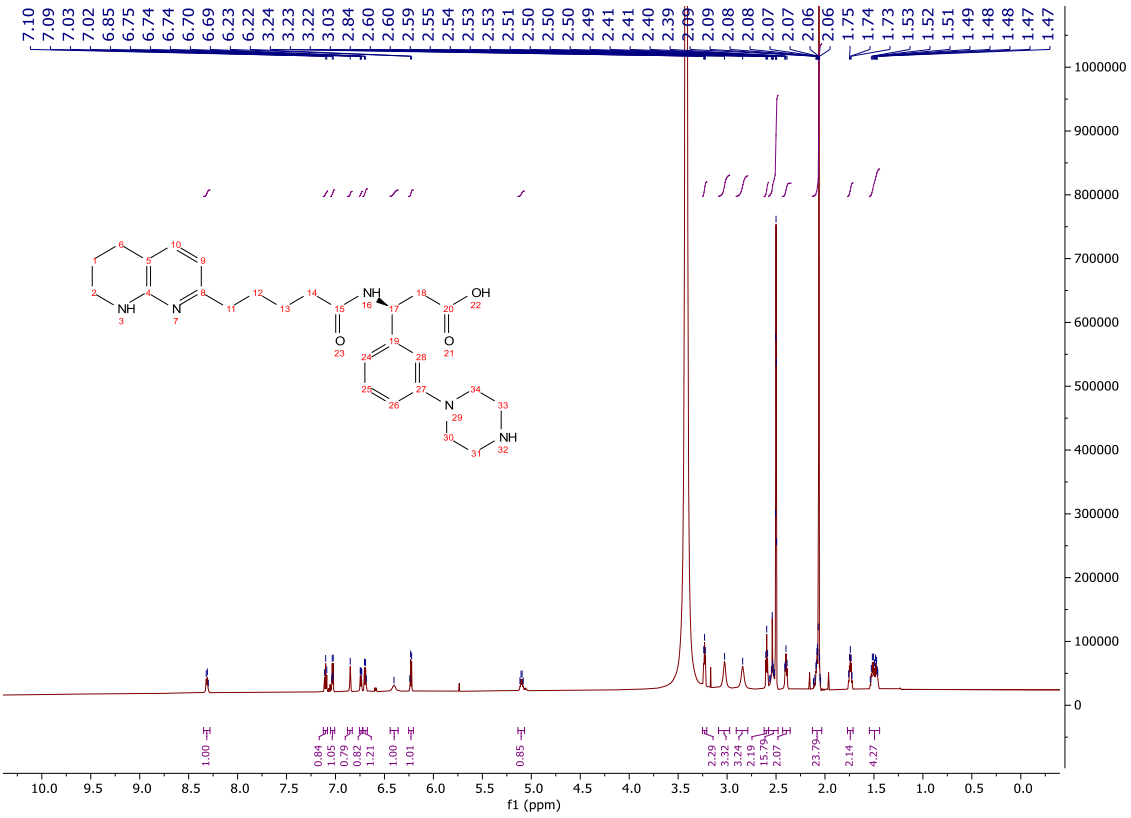

(3*S*)-3-(3-(2,6-Dimethylmorpholino)phenyl)-3-(5-(5,6,7,8-tetrahydro-1,8-naphthyridin-2-yl)pentanamido)propanoic acid (**231**)

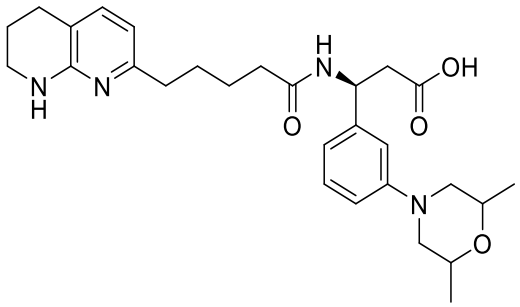

Mass 21.2 mg; Yield 29%; LCMS 100% purity; 0.61 min; *m/z* $[M+H]^+$ 495.48; Yellow oil.

δ_H (700 MHz, DMSO-d_6) 8.32 (d, *J* = 8.5 Hz, 1H), 7.12 (dd, *J* = 7.9, 7.9 Hz, 1H), 7.03 (d, *J* = 7.3 Hz, 1H), 6.87 (dd, *J* = 1.9, 1.9 Hz, 1H), 6.81 – 6.76 (m, 1H), 6.73 – 6.69 (m, 1H), 6.56 (bs, 1H), 6.22 (d, *J* = 7.2 Hz, 1H), 5.14 – 5.08 (m, 1H), 3.69 – 3.63 (m, 1H), 3.56 – 3.52 (m, 1H), 3.24 – 3.20 (m, 2H), 2.61 – 2.55 (m, 4H), 2.43 – 2.36 (m, 2H), 2.20 (td, *J* = 11.1, 4.7 Hz, 4H), 2.13 – 2.02 (m, 2H), 1.77 – 1.69 (m, 2H), 1.53 – 1.42 (m, 4H), 1.14 (dd, *J* = 6.2, 2.2 Hz, 6H).

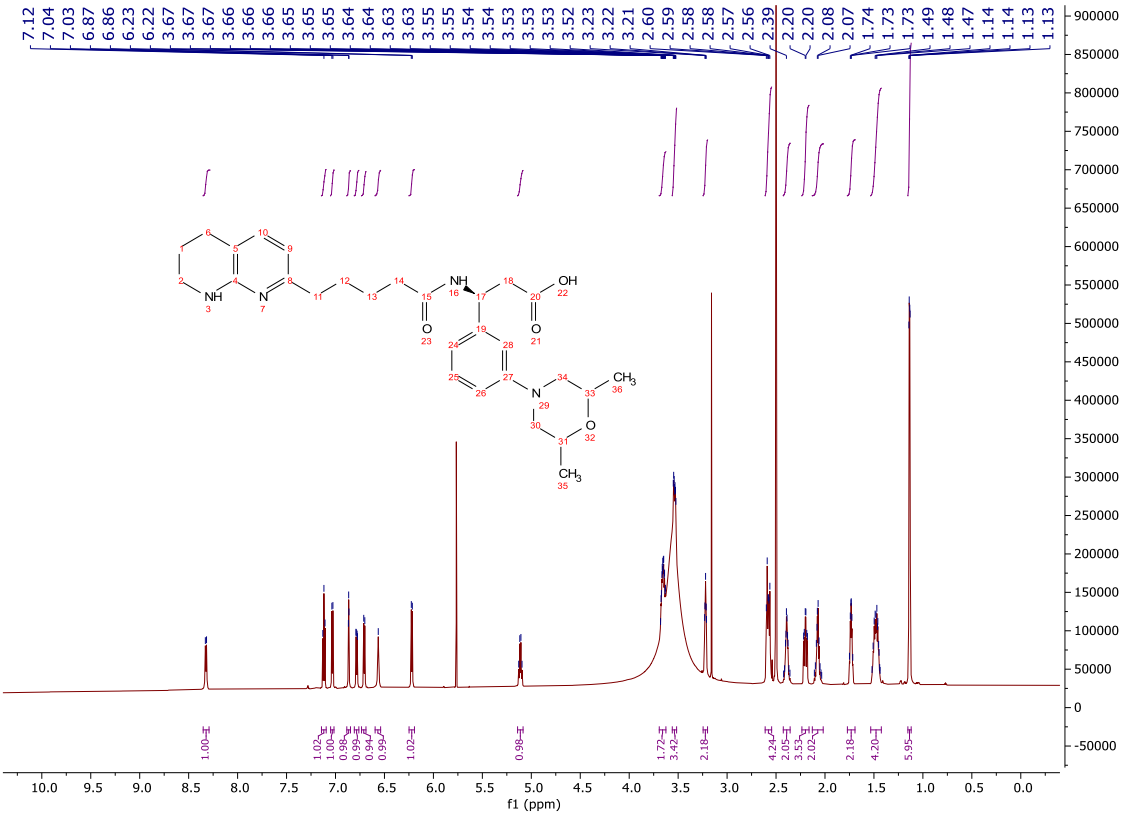

(*S*)-3-(3-(1,4-Oxazepan-4-yl)phenyl)-3-(5-(5,6,7,8-tetrahydro-1,8-naphthyridin-2-yl)pentanamido)propanoic acid (**233**)

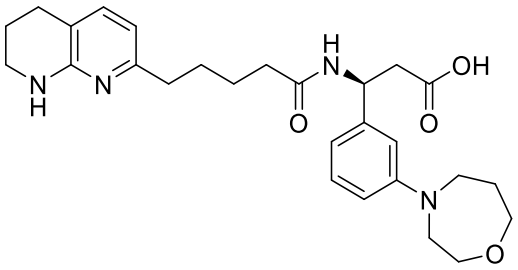

Mass 4.2 mg; Yield 5%; LCMS 86% purity; 0.56 min; *m/z* $[M+H]^+$ 481.38; Off-white solid.

δ_H (700 MHz, DMSO-d_6) 8.34 (d, *J* = 8.4 Hz, 1H), 7.07 – 6.99 (m, 2H), 6.66 (dd, *J* = 2.0, 2.0 Hz, 1H), 6.58 – 6.53 (m, 1H), 6.53 – 6.50 (m, 1H), 6.35 (bs, 1H), 6.22 (d, *J* = 7.3 Hz, 1H), 5.11 – 5.05 (m, 1H), 3.68 (t, *J* = 5.0 Hz, 2H), 3.57 – 3.47 (m, 6H), 3.25 – 3.20 (m, 2H), 2.59 (t, *J* = 6.2 Hz, 2H), 2.56 – 2.48 (m, 2H), 2.42 – 2.37 (m, 2H), 2.08 (t, *J* = 7.2 Hz, 2H), 1.86 (p, *J* = 5.9 Hz, 2H), 1.75 (p, 2H), 1.56 – 1.44 (m, 4H).

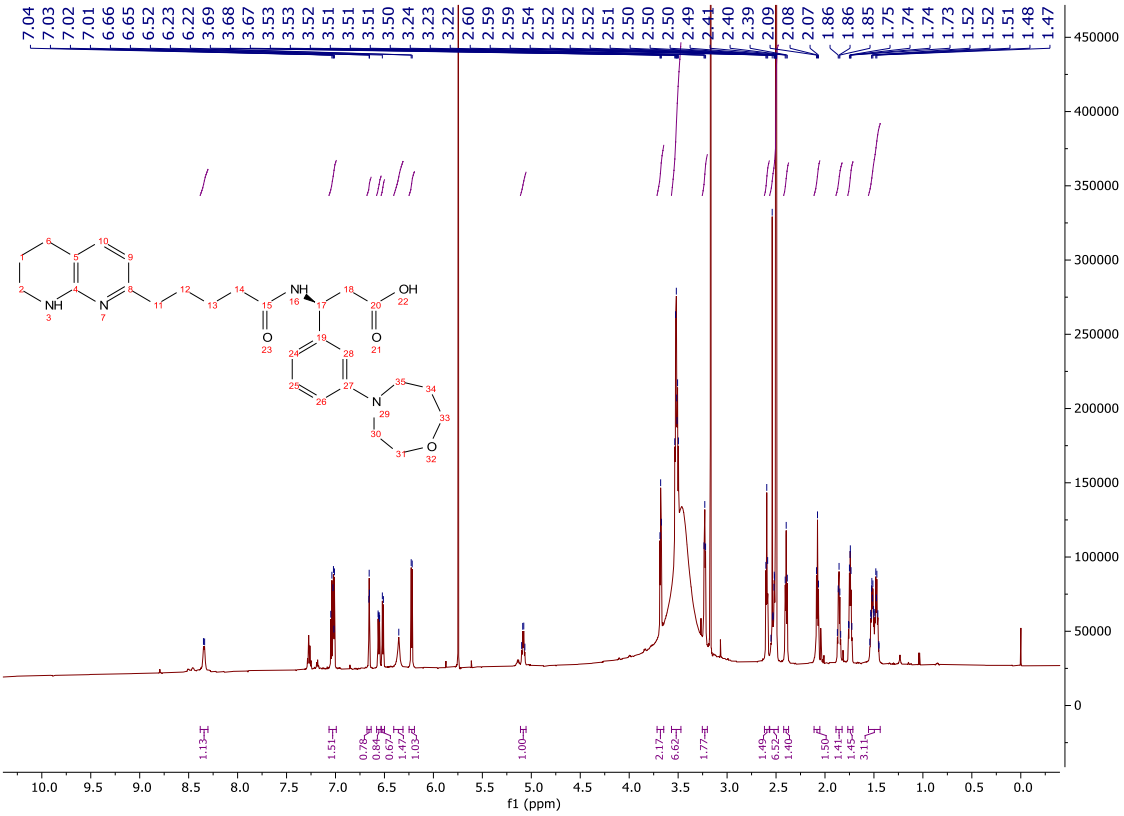

(*S*)-3-(3-(Pyrrolidin-1-yl)phenyl)-3-(5-(5,6,7,8-tetrahydro-1,8-naphthyridin-2-yl)pentanamido)propanoic acid (**234**)

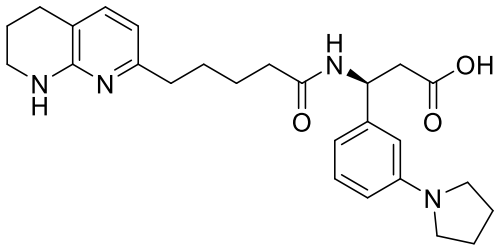

Mass 3.5 mg; Yield 4%; LCMS 87% purity; 0.62 min; *m/z* $[M+H]^+$ 451.45; Off-white solid.

δ_H (700 MHz, DMSO-d_6) 8.28 (d, *J* = 8.4 Hz, 1H), 7.07 – 7.00 (m, 2H), 6.50 (d, *J* = 7.5 Hz, 1H), 6.46 – 6.39 (m, 2H), 6.37 – 6.34 (m, 1H), 6.23 (d, *J* = 7.3 Hz, 1H), 5.11 – 5.06 (m, 1H), 3.23 (t, *J* = 5.6 Hz, 2H), 3.18 – 3.11 (m, 4H), 2.61 – 2.51 (m, 4H), 2.43 – 2.36 (m, 2H), 2.15 – 2.00 (m, 2H), 1.94 – 1.87 (m, 4H), 1.77 – 1.70 (m, 2H), 1.54 – 1.45 (m, 4H).

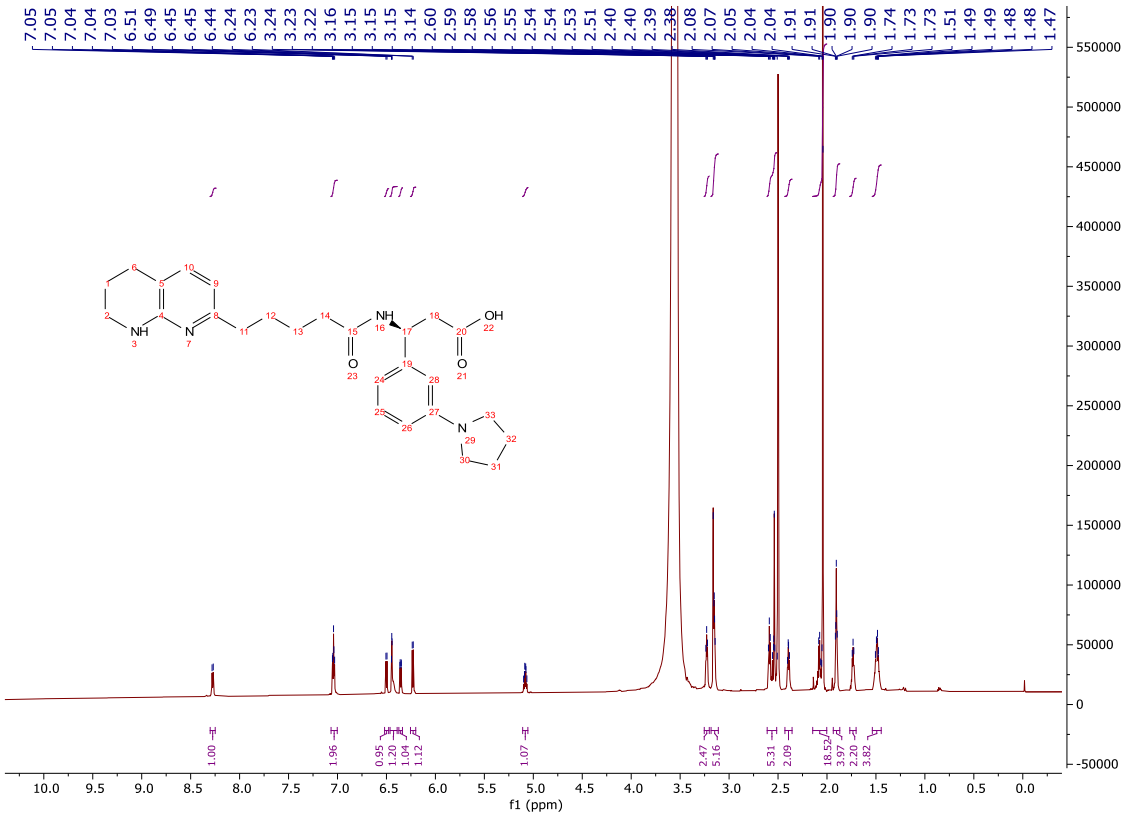

(*S*)-3-(3-(3,3-*Bis*(hydroxymethyl)azetidin-1-yl)phenyl)-3-(5-(5,6,7,8-tetrahydro-1,8-naphthyridin-2-yl)pentanamido)propanoic acid (**236**)

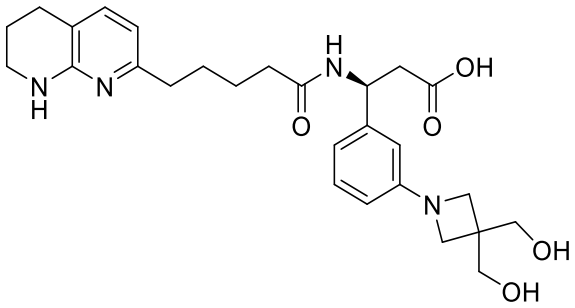

Mass 14.0 mg; Yield 16%; LCMS 85% purity; 0.46 min; *m/z* $[M+H]^+$ 497.43; Yellow oil.

δ_H (700 MHz, DMSO-d_6) 8.27 – 8.22 (m, 1H), 7.08 – 7.01 (m, 1H), 6.56 (d, *J* = 7.6 Hz, 1H), 6.46 – 6.39 (m, 2H), 6.31 (dd, *J* = 1.9, 1.9 Hz, 1H), 6.26 – 6.21 (m, 2H), 5.11 – 5.06 (m, 1H), 3.55 (s, 4H), 3.51 – 3.47 (m, 4H), 3.23 (t, *J* = 5.6 Hz, 2H), 2.62 – 2.51 (m, 4H), 2.45 – 2.37 (m, 2H), 2.17 – 2.02 (m, 2H), 1.77 – 1.71 (m, 2H), 1.56 – 1.44 (m, 4H).

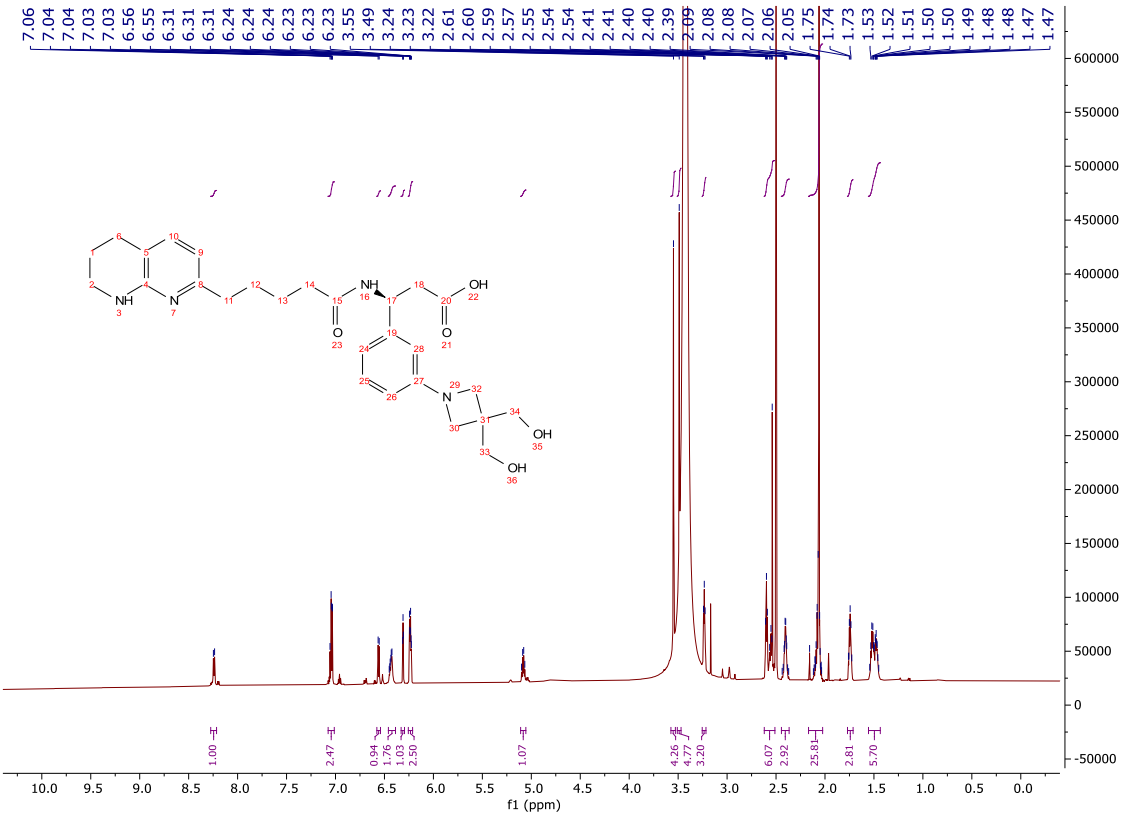

tert-Butyl 7-(5-((1-(3-bromophenyl)-3-ethoxy-3-oxopropyl)amino)-5-oxopentyl)-3,4-dihydro-1,8-naphthyridine-1(2*H*)-carboxylate (**239**)

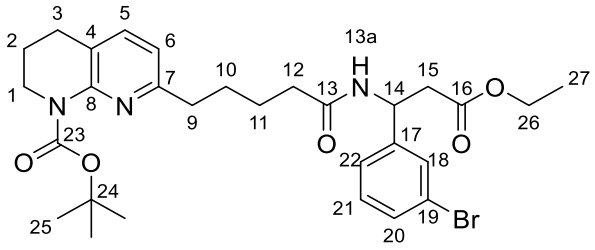

To a stirred solution of **82** (4.00 g, 11.8 mmol) in acetonitrile (60 mL) was added **238** (3.82 g, 14.1 mmol, purchased from commercial sources). The reaction mixture was cooled to 0 °C. *i*-Pr_2NEt (8.20 mL, 47.0 mmol) and T3P (50% in ethyl acetate, 7.00 mL, 23.5 mmol) were added over 5 min. The reaction mixture was stirred for 19 h. The reaction mixture was diluted with ethyl acetate (50 mL), quenched with sat. $NaHCO_{3(aq)}$ (50 mL), and the organic phase washed with sat. $NaHCO_{3(aq)}$ (2 x 25 mL), brine (2 x 25 mL), dried ($MgSO_4$) and concentrated *in vacuo* giving an orange oil (7.40 g). The crude product was purified by column chromatography on silica gel, eluting with a gradient of methanol/CH_2Cl_2 (2-5%) to afford the title compound as an amorphous, brown solid (5.70 g, 9.69 mmol, 82%); **HRMS** *m/z* (ESI^+) calc. for $C_{29}H_{39}BrN_3O_5$ $[M+H]^+$ requires 588.2068, found 588.2064; $\boldsymbol{R_f}$ 0.75, 10% methanol/CH_2Cl_2, UV active; δ_H (400 MHz, $CDCl_3$) 7.40 (1H, dd, *J* = 1.9, 1.9 Hz, H-18), 7.37 (1H, ddd, *J* = 7.5, 1.7, 1.7 Hz, H-20), 7.28 (1H, d, *J* = 7.6 Hz, H-5), 7.25 – 7.17 (1H, m, H-22), 7.17 (1H, dd, *J* = 7.6, 7.6 Hz, H-21), 6.79 (1H, d, *J* = 7.6 Hz, H-6), 6.73 (1H, d, *J* = 8.4 Hz, H-13a), 5.38 (1H, dt, *J* = 8.4, 5.9 Hz, H-14), 4.10 – 4.03 (2H, m, H-26), 3.79 – 3.68 (2H, m, H-1), 2.90 – 2.67 (6H, m, H-3, H-9 and H-15), 2.34 – 2.23 (2H, m, H-12), 1.96 – 1.86 (2H, m, H-2), 1.82 – 1.68 (4H, m, H-10 and H-11), 1.50 (9H, s, H-25), 1.17 (3H, t, *J* = 7.1 Hz, H-27); δ_C (100 MHz, $CDCl_3$) 173.5 (CO), 171.1 (CO), 158.2 (C), 154.2 (CO), 151.2 (C), 143.4 (C), 137.4 (ArH), 130.7 (ArH), 130.3 (ArH), 129.5 (ArH), 125.2 (ArH), 122.8 (C), 122.0 (C), 118.4 (ArH), 80.9 (C), 61.1 (CH_2), 49.1 (CH), 45.0 (CH_2), 40.0 (CH_2), 37.6 (CH_2), 36.6 (CH_2), 29.1 (CH_2), 28.6 (CH_3), 26.4 (CH_2), 25.4 (CH_2), 23.5 (CH_2), 14.2 (CH_3); ν_{max} (FT-ATR/cm^{-1}) 3303, 2934, 1732, 1690, 1647, 1568, 1465, 1366, 1250, 1148, 784, 696.

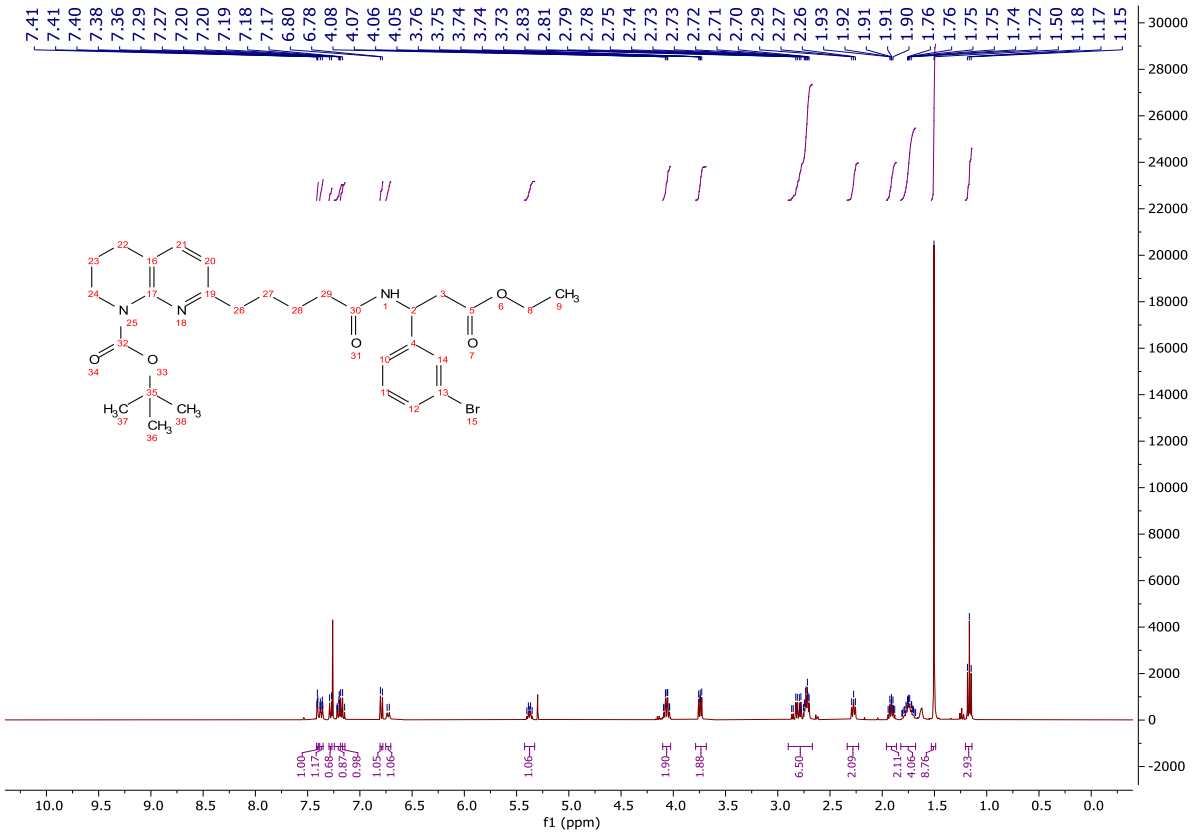
7.41 7.41 7.40 7.38 7.36 7.29 7.27 7.20 7.20 7.19 7.18 7.17 6.80 6.78 4.08 4.07 4.06 4.05 3.76 3.75 3.74 3.74 3.73 2.83 2.81 2.79 2.78 2.75 2.74 2.73 2.73 2.72 2.71 2.70 2.29 2.27 2.26 1.93 1.92 1.91 1.91 1.90 1.76 1.76 1.75 1.75 1.74 1.72 1.50 1.18 1.17 1.15
1.00 1.17 0.68 0.87 0.98 1.05 1.06 1.06 1.90 1.88 6.50 2.09 2.11 4.06 8.76 2.93
f1 (ppm)

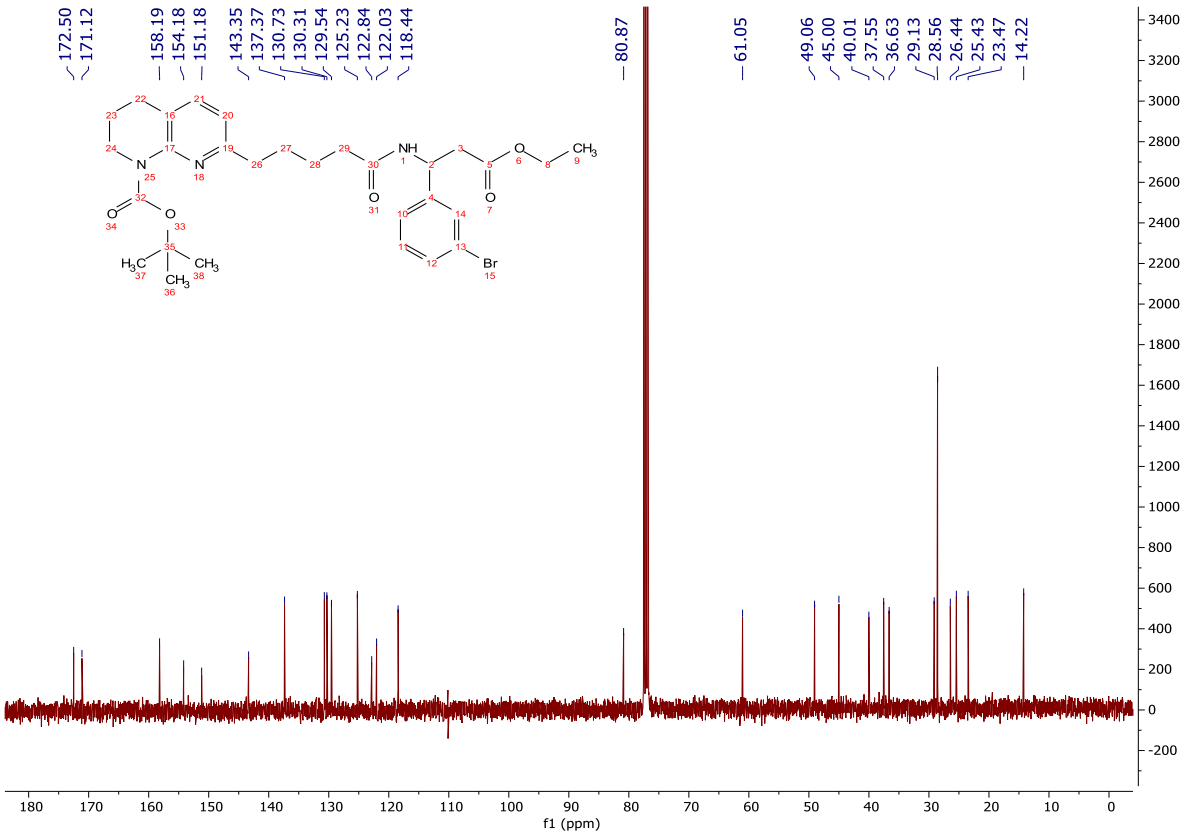
172.50 171.12 158.19 154.18 151.18 143.35 137.37 130.73 130.31 129.54 125.23 122.84 122.03 118.44 80.87 61.05 49.06 45.00 40.01 37.55 36.63 29.13 28.56 26.44 25.43 23.47 14.22
f1 (ppm)

tert-Butyl 7-(5-((3-ethoxy-3-oxo-1-(3-(prop-1-en-2-yl)phenyl)propyl)amino)-5-oxopentyl)-3,4-dihydro-1,8-naphthyridine-1(2*H*)-carboxylate (**241**)

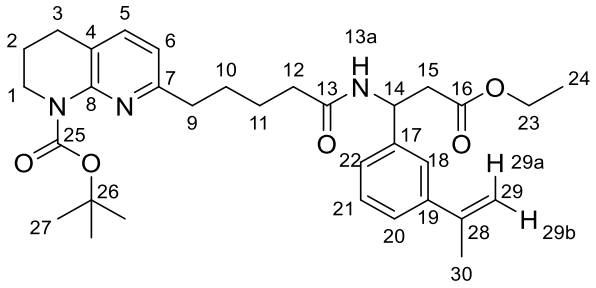

Under a nitrogen atmosphere, a solution of **239** (500 mg, 0.850 mmol), isopropenyl boronic pinacol ester (0.240 mL, 1.28 mmol), K_2CO_3 (352 mg, 2.55 mmol) and $Pd(dppf)Cl_2.CH_2Cl_2$ (72 mg, 0.088 mmol) in 1,4-dioxane (3.00 mL) was stirred at 75 °C for 16 h. The reaction mixture was cooled to rt, diluted with ethyl acetate (5.00 mL), filtered through Celite® and the organic phase washed with water (2 x 20.0 mL) and brine (2 x 20.0 mL), dried ($MgSO_4$) and concentrated *in vacuo* to give an orange/brown oil (693 mg). The crude product was purified by column chromatography on silica gel, eluting with a gradient of ethyl acetate/light petroleum (70-100%) to afford the title compound as a brown oil (376 mg, 0.684 mmol, 80%); **HRMS** *m/z* (ESI^+) calc. for $C_{32}H_{44}N_3O_5$ $[M+H]^+$ requires 550.3275, found 550.3278; $\boldsymbol{R_f}$ 0.10, 50% ethyl acetate/light petroleum, UV active; δ_H (400 MHz, DMSO-d_6) 8.40 – 8.27 (1H, m, H-13a), 7.45 – 7.07 (5H, m, H-5, H-18, H-20, H-21 and H-22), 6.86 – 6.79 (1H, m, H-6), 5.41 – 5.37 (1H, m, H-29a), 5.28 – 5.15 (1H, m, H-14), 5.12 – 5.05 (1H, m, H-29b), 4.05 – 3.94 (2H, m, H-23), 3.61 (2H, t, *J* = 6.0 Hz, H-1), 2.76 – 2.63 (4H, m, H-3 and H-15), 2.58 (2H, t, *J* = 7.5 Hz, H-9), 2.15 – 2.06 (5H, m, H-12 and H-30), 1.86 – 1.75 (2H, m, H-2), 1.66 – 1.36 (13H, m, H-10, H-11 and H-27), 1.13 – 1.03 (3H, m, H-24); δ_C (101 MHz, DMSO-d_6) 171.2 (CO), 170.1 (CO), 157.3 (C), 153.6 (C), 150.5 (C), 142.5 (C), 140.4 (C), 137.1 (ArH), 128.3 (ArH), 126.4 (C), 125.7 (ArH), 124.0 (ArH), 123.4 (ArH), 121.4 (C), 118.0 (ArH), 112.6 (CH_2), 79.7 (C), 59.9 (CH_2), 49.4 (CH), 44.3 (CH_2), 41.0 (CH_2), 36.9 (CH_2), 35.3 (CH_2), 28.6 (CH_2), 28.0 (CH_3), 25.4 (CH_2), 25.0 (CH_2),

22.9 (CH_2), 21.5 (CH_3), 14.0 (CH_3); ν_{max} (FT-ATR/cm^{-1}) 3296, 2931, 1732, 1692, 1647, 1541, 1464, 1367, 1253, 1150, 1027, 701.

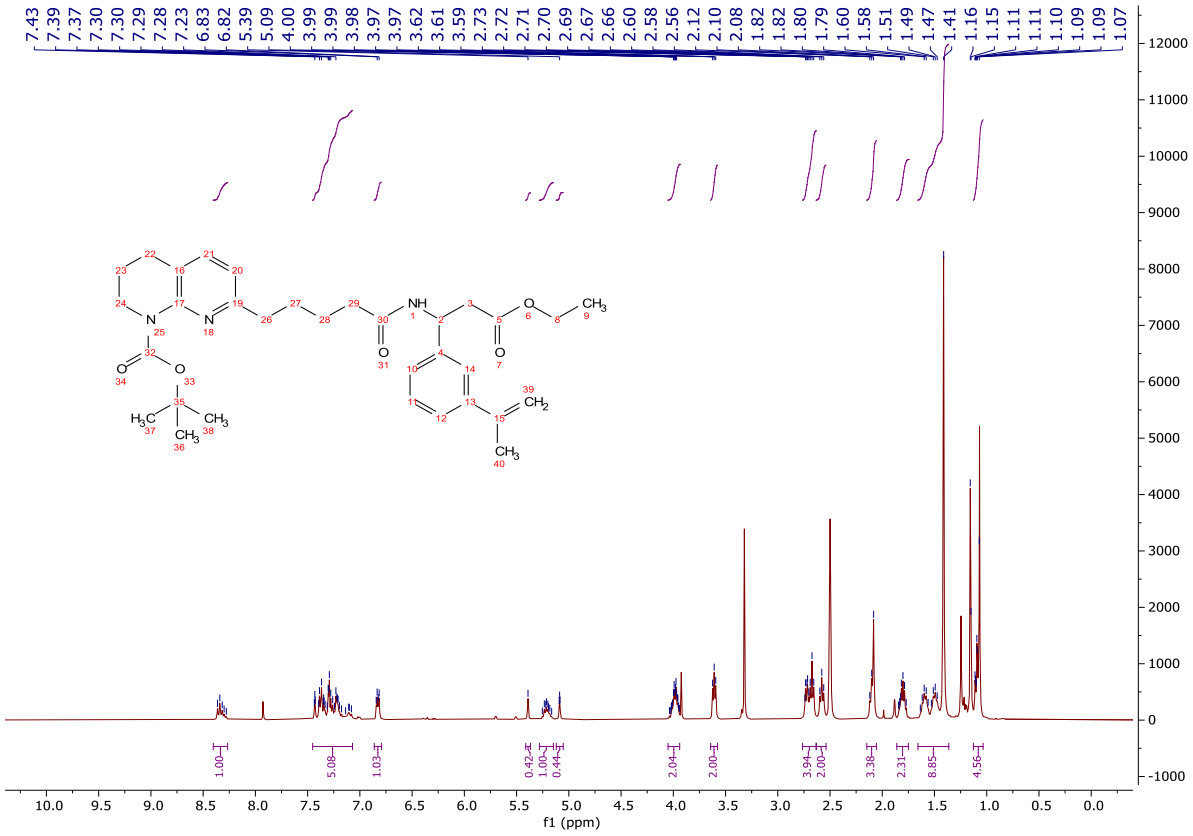
7.43 7.39 7.37 7.30 7.30 7.29 7.28 7.23 6.83 6.82 5.39 5.09 4.00 3.99 3.99 3.98 3.97 3.97 3.62 3.61 3.59 2.73 2.72 2.71 2.70 2.69 2.67 2.66 2.60 2.58 2.56 2.12 2.10 2.08 1.82 1.82 1.80 1.79 1.60 1.58 1.51 1.49 1.47 1.41 1.16 1.15 1.11 1.11 1.10 1.09 1.09 1.07
1.00 5.08 1.03 0.42 1.00 0.44 2.04 2.00 3.94 2.00 3.38 2.31 8.85 4.56
f1 (ppm)

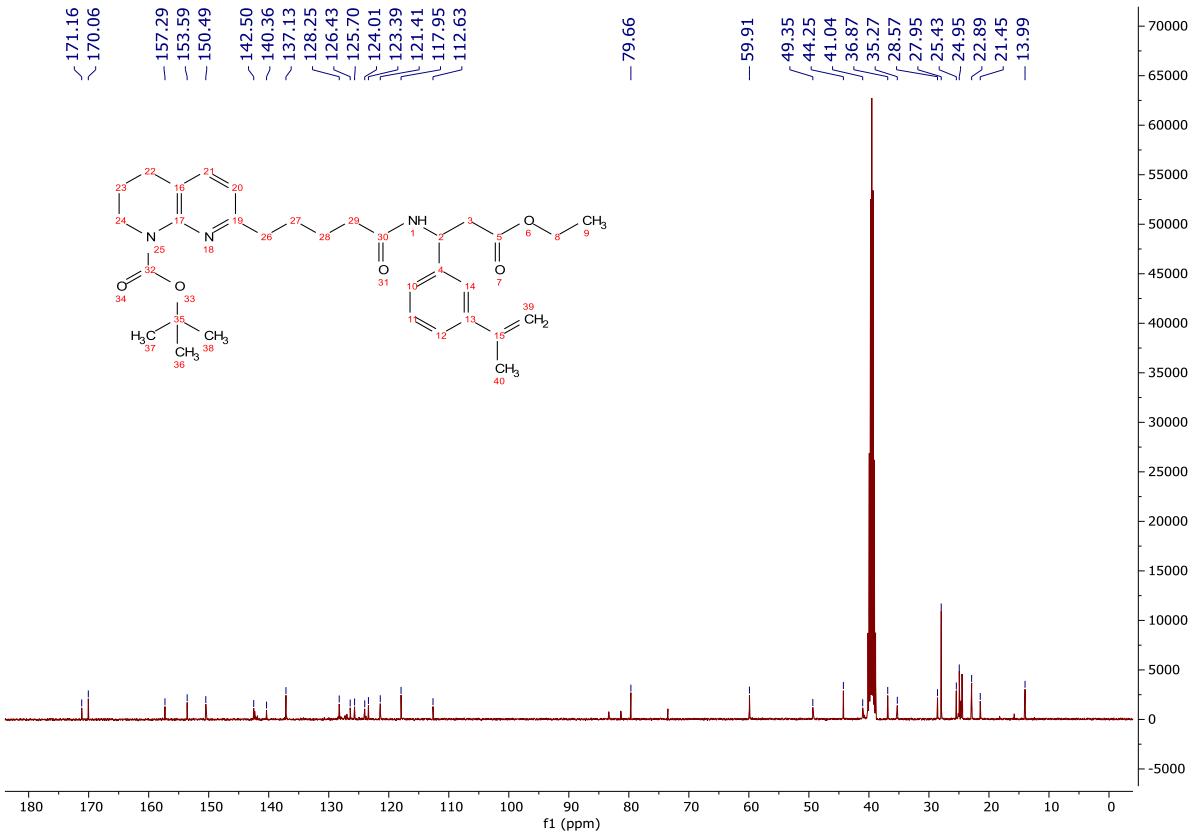
171.16 170.06 157.29 153.59 150.49 142.50 140.36 137.13 128.25 126.43 125.70 124.01 123.39 121.41 117.95 112.63 79.66 59.91 49.35 44.25 41.04 36.87 35.27 28.57 27.95 25.43 24.95 22.89 21.45 13.99
f1 (ppm)

tert-Butyl 7-(5-((1-(3-cyclopropylphenyl)-3-ethoxy-3-oxopropyl)amino)-5-oxopentyl)-3,4-dihydro-1,8-naphthyridine-1(2*H*)-carboxylate (**242**)

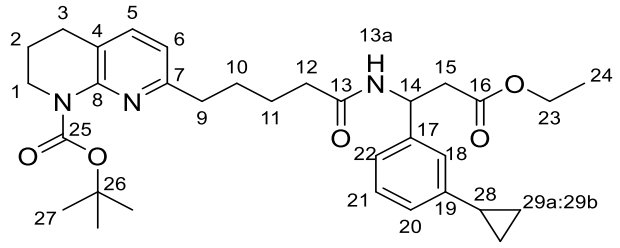

Under a nitrogen atmosphere, a suspension of **239** (508 mg, 0.860 mmol), cyclopropyl boronic ester (0.230 mL, 1.24 mmol), K_2CO_3 (352 mg, 2.55 mmol) and $Pd(dppf)Cl_2.CH_2Cl_2$ (124 mg, 0.170 mmol) in 1,4-dioxane (3.00 mL) was stirred at 80 °C for 16 h. The reaction mixture was cooled to rt, filtered through Celite® and the mother liquors washed with sat. $NaHCO_{3(aq)}$ (2 x 20.0 mL) and brine (2 x 40.0 mL). The organic was dried ($MgSO_4$) and concentrated *in vacuo* to give a dark green/brown oil (580 mg). The crude product was purified by column chromatography on amino propyl silica gel, eluting with a gradient of ethyl acetate/light petroleum (60-100%) to afford the title compound as a green/brown oil (186 mg, 0.338 mmol, 40%); **HRMS** *m/z* (ESI^+) calc. for $C_{32}H_{44}N_3O_5$ $[M+H]^+$ requires 550.3275, found 550.3278; $\boldsymbol{R_f}$ 0.32, 70% ethyl acetate/light petroleum, UV active; δ_H (400 MHz, $CDCl_3$) 7.30 – 7.28 (1H, m, H-5), 7.18 (1H, dd, *J* = 7.6, 7.6 Hz, H-21), 7.07 – 7.02 (1H, m, H-22), 7.01 – 6.98 (1H, m, H-18), 6.94 – 6.90 (1H, m, H-20), 6.79 (1H, d, *J* = 7.6 Hz, H-6), 6.53 (1H, d, *J* = 8.4 Hz, H-13a), 5.42 – 5.35 (1H, m, H-14), 4.09 – 4.02 (2H, m, H-23), 3.77 – 3.72 (2H, m, H-1), 2.93 – 2.68 (6H, m, H-3, H-9 and H-15), 2.28 – 2.22 (2H, m, H-12), 1.96 – 1.81 (3H, m, H-2 and H-28), 1.80 – 1.68 (4H, m, H-10 and H-11), 1.50 (9H, s, H-27), 1.19 – 1.14 (3H, m, H-24), 0.97 – 0.90 (2H, m, H-29a), 0.69 – 0.63 (2H, m, H-29b); $\boldsymbol{\nu_{max}}$ (FT-ATR/cm^{-1}) 3296, 2925, 1734, 1693, 1540, 1366, 1253, 1159, 1027, 704.

N.B. No ^{13}C NMR spectra available.

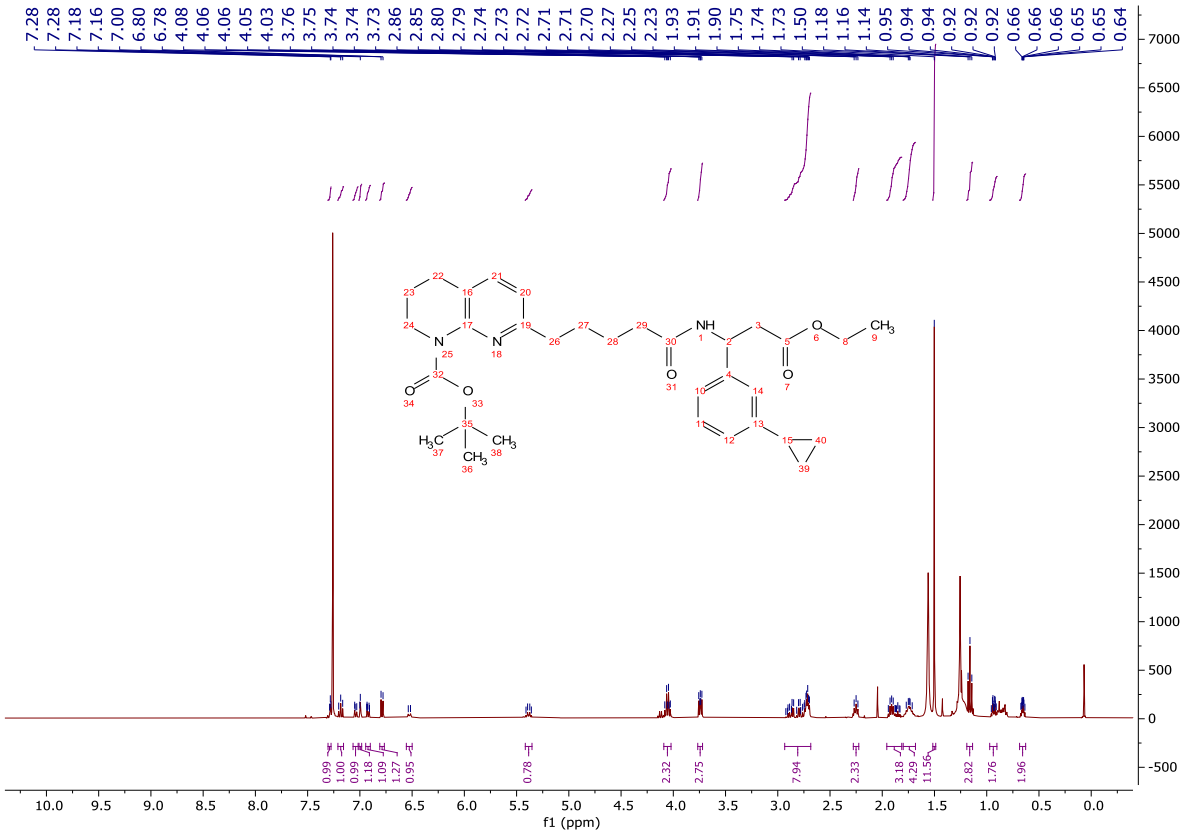
7.28 7.28 7.18 7.16 7.00 6.80 6.78 4.08 4.06 4.06 4.05 4.03 3.76 3.75 3.74 3.74 3.73 2.86 2.85 2.80 2.79 2.74 2.73 2.72 2.71 2.71 2.70 2.27 2.25 2.23 1.93 1.91 1.90 1.75 1.74 1.73 1.50 1.18 1.16 1.14 0.95 0.94 0.94 0.92 0.92 0.92 0.66 0.66 0.66 0.65 0.65 0.64
NH
CH3
H3C
CH3
0.99 1.00 0.99 1.18 1.09 1.27 0.95 0.78 2.32 2.75 7.94 2.33 3.18 4.29 11.56 2.82 1.76 1.96
f1 (ppm)

Ethyl 3-(isopropylphenyl)-3-(5-(5,6,7,8-tetrahydro-1,8-naphthyridin-2-yl)pentanamido)propanoate (**243**)

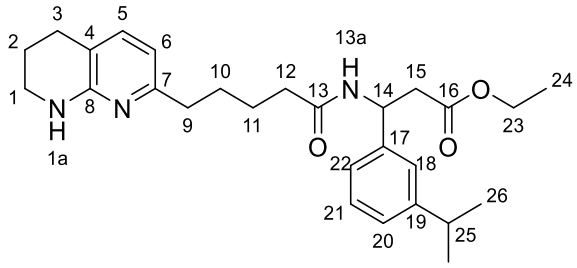

In a nitrogen atmosphere, a suspension of **241** (318 mg, 0.580 mmol), iron powder (325 mesh, 49 mg, 0.870 mmol) and Pd/C (10 wt%, 32 mg, 0.015 mmol) in water (1.07 mL) was stirred at 100 °C for 25 h. The reaction mixture was cooled to rt, diluted with ethyl acetate (5.00 mL), filtered through Celite® and the mother liquors washed successively with sat. $NaHCO_{3(aq)}$ (30.0 mL) and brine (30.0 mL). The organic was dried ($MgSO_4$) and concentrated *in vacuo* to give an orange/brown oil (206 mg). The crude product was purified by column chromatography on amino propyl silica gel, eluting with a gradient of ethyl acetate/light petroleum (10-100%) to afford the title compound as a clear oil (31 mg, 0.069 mmol, 12%); **HRMS** *m/z* (ESI^+) calc. for $C_{27}H_{38}N_3O_3$ $[M+H]^+$ requires 452.2908, found 452.2907; $\boldsymbol{R_f}$ 0.56, 100% ethyl acetate, UV active; δ_H (400 MHz, $CDCl_3$) 7.24 – 7.20 (1H, m, H-21), 7.13 – 7.03 (4H, m, H-5, H-18, H-20 and H-22), 6.60 – 6.53 (1H, m, H-6), 6.32 (1H, d, *J* = 7.3 Hz, H-13a), 5.46 – 5.38 (1H, m, H-14), 4.09 – 4.02 (2H, m, H-23), 3.42 – 3.36 (2H, m, H-1), 2.94 – 2.76 (3H, m, H-15 and H-25), 2.68 (2H, t, *J* = 6.4 Hz, H-3), 2.58 – 2.52 (2H, m, H-9), 2.27 – 2.22 (2H, m, H-12), 1.93 – 1.85 (2H, m, H-2), 1.73 – 1.60 (4H, m, H-10 and H-11), 1.31 – 1.19 (6H, m, H-26), 1.15 (3H, t, *J* = 7.1 Hz, H-24); δ_C (100 MHz, $CDCl_3$) 172.4 (CO), 171.5 (CO), 160.8 (C), 152.4 (C), 149.4 (C), 143.1 (ArH), 137.0 (C), 128.7 (ArH), 125.7 (ArH), 124.8 (ArH), 123.8 (ArH), 123.6 (C), 111.4 (ArH), 60.9 (CH_2), 49.7 (CH), 41.7 (CH_2), 40.3 (CH_2), 37.2 (CH_2), 36.8 (CH_2), 34.3 (CH), 29.4 (CH_2), 26.5 (CH_2), 25.5 (CH_2), 24.1 (CH), 21.6 (CH_2), 14.2 (CH_3); ν_{max} (FT-ATR/cm^{-1}) 3270, 2925, 1734, 1645, 1600, 1537, 1462, 1370, 1275, 1180, 1117, 797, 706.

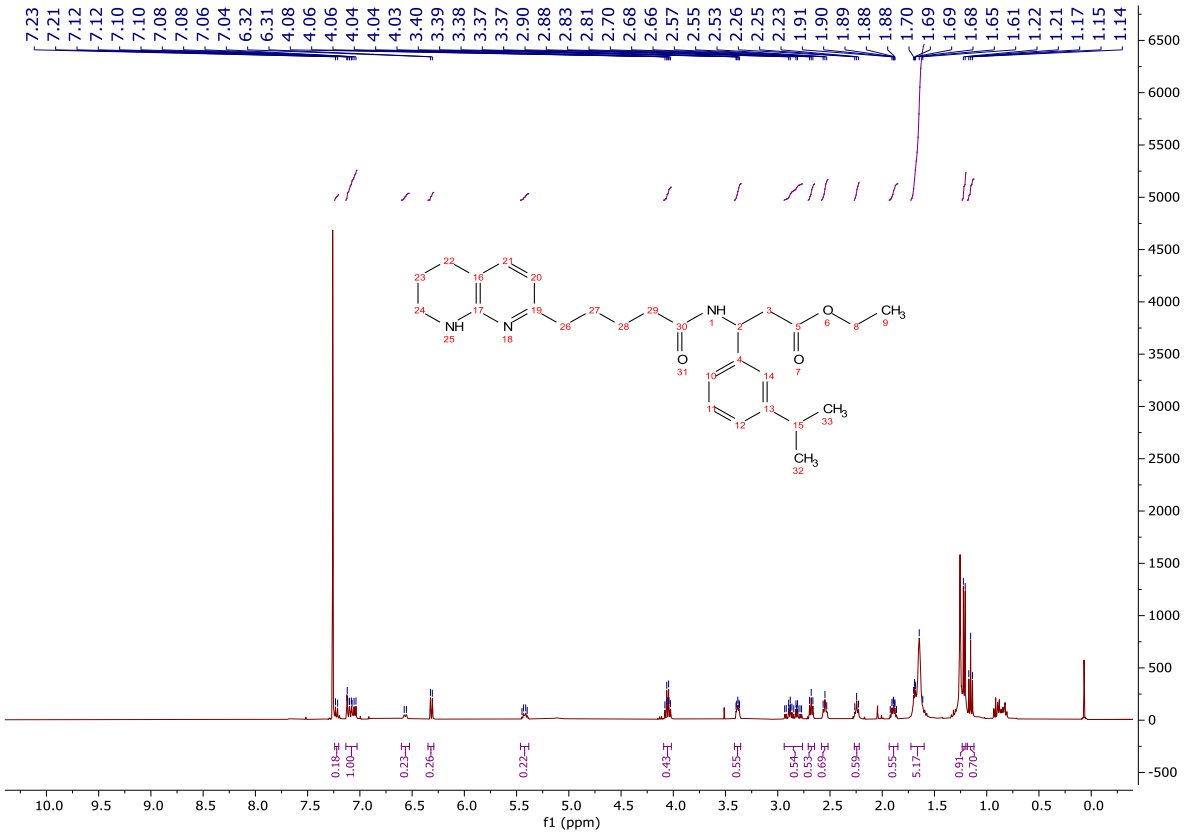
7.23 7.21 7.12 7.12 7.10 7.10 7.08 7.08 7.06 7.04 6.32 6.31 4.08 4.06 4.06 4.04 4.04 4.03 3.40 3.39 3.38 3.37 3.37 2.90 2.88 2.83 2.81 2.70 2.68 2.66 2.57 2.55 2.53 2.26 2.25 2.23 1.91 1.90 1.89 1.88 1.88 1.70 1.69 1.69 1.68 1.65 1.61 1.22 1.21 1.17 1.15 1.14
0.18 1.00 0.23 0.26 0.22 0.43 0.55 0.54 0.53 0.69 0.59 0.55 5.17 0.91 0.70
f1 (ppm)

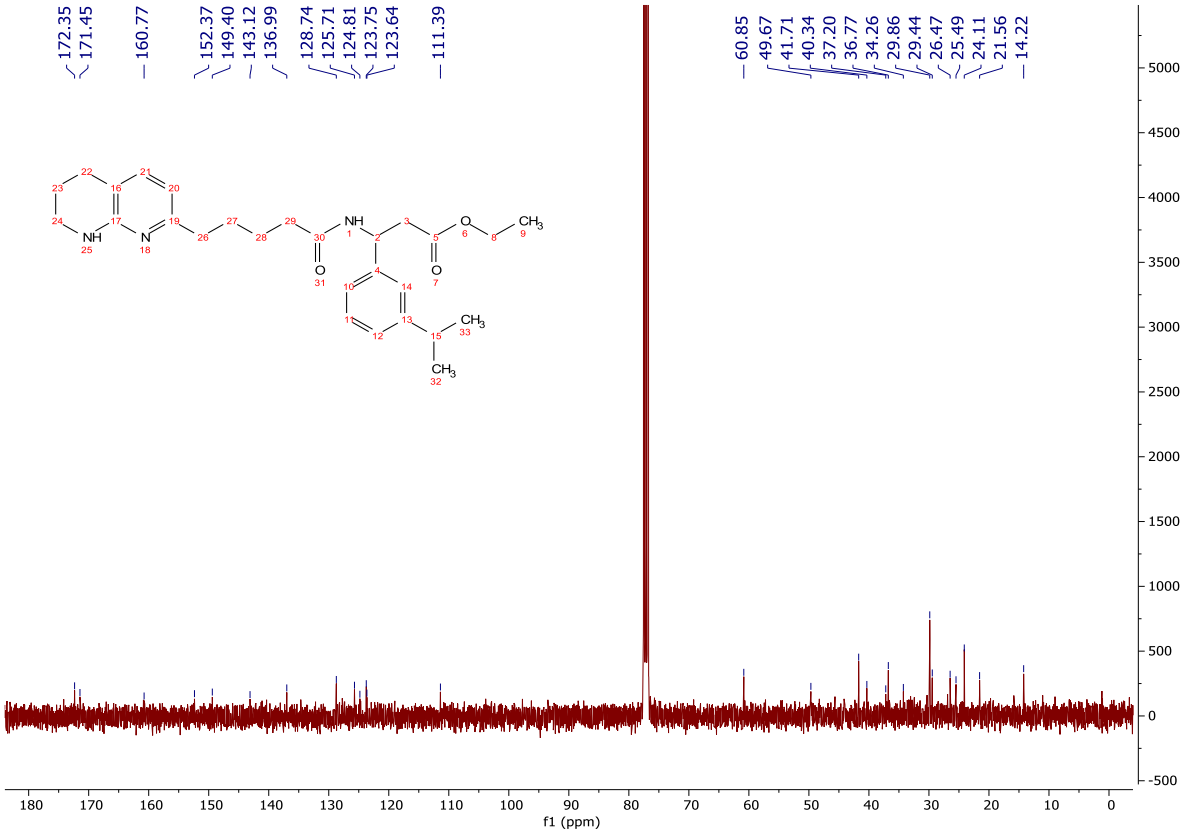
172.35 171.45 160.77 152.37 149.40 143.12 136.99 128.74 125.71 124.81 123.75 123.64 111.39
60.85 49.67 41.71 40.34 37.20 36.77 34.26 29.86 29.44 26.47 25.49 24.11 21.56 14.22
f1 (ppm)

3-(3-isopropylphenyl)-3-(-5-(5,6,7,8-tetrahydro-1,8-naphthyridin-2-yl)pentanamido)propanoic acid (**50**)

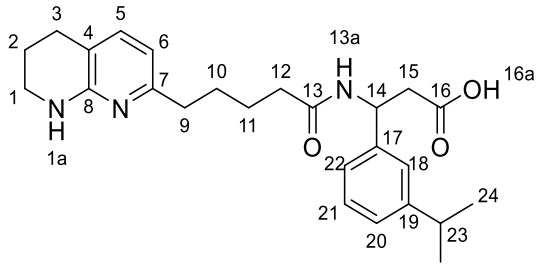

To a stirred solution of **243** (31 mg, 0.069 mmol) in THF (7.00 mL) at rt was added 1M $LiOH_{(aq)}$ (0.070 mL, 0.070 mmol) and stirred for 16 h. The reaction mixture was concentrated *in vacuo* to afford a light brown slurry. The crude product was purified on a Waters OASIS® HLB cartridge, eluting with a gradient of methanol/water (0-100%) to afford the title compound as a clear oil (20 mg, 0.047 mmol, 68%); **HRMS** *m/z* (ESI^+) calc. for $C_{25}H_{34}N_3O_3$ $[M+H]^+$ requires 424.2595, found 425.2623; $\boldsymbol{R_f}$ 0.34, 2% methanol/CH_2Cl_2, UV active; δ_H (400 MHz, MeOD) 7.42 (1H, d, *J* = 7.3 Hz, H-5), 7.25 – 7.02 (4H, m, H-18, H-20, H-21 and H-22), 6.47 (1H, d, *J* = 7.3 Hz, H-6), 5.42 – 5.33 (1H, m, H-14), 3.45 (2H, t, *J* = 5.7 Hz, H-1), 2.87 (1H, hept, *J* = 6.9 Hz, H-23), 2.80 – 2.53 (6H, m, H-3, H-9 and H-15), 2.41 – 2.16 (2H, m, H-12), 1.96 – 1.87 (2H, m, H-2), 1.83 – 1.56 (4H, m, H-10 and H-11), 1.23 (6H, d, *J* = 6.9 Hz, H-24); δ_C (100 MHz, MeOD) 180.2 (CO), 174.7 (CO), 154.1 (C), 151.3 (C), 150.3 (C), 144.2 (C), 141.6 (ArH), 129.5 (ArH), 126.0 (ArH), 125.4 (ArH), 124.8 (ArH), 119.5 (C), 111.3 (ArH), 52.9 (CH), 45.7 (CH_2), 41.8 (CH_2), 36.2 (CH_2), 35.5 (CH), 34.1 (CH_2), 29.5 (CH_2), 26.6 (CH_2), 26.2 (CH_2), 24.5 (CH_3), 20.9 (CH_2); ν_{max} (FT-ATR/cm^{-1}) 3274, 2927, 1648, 1549, 1462, 1397, 1321, 708.

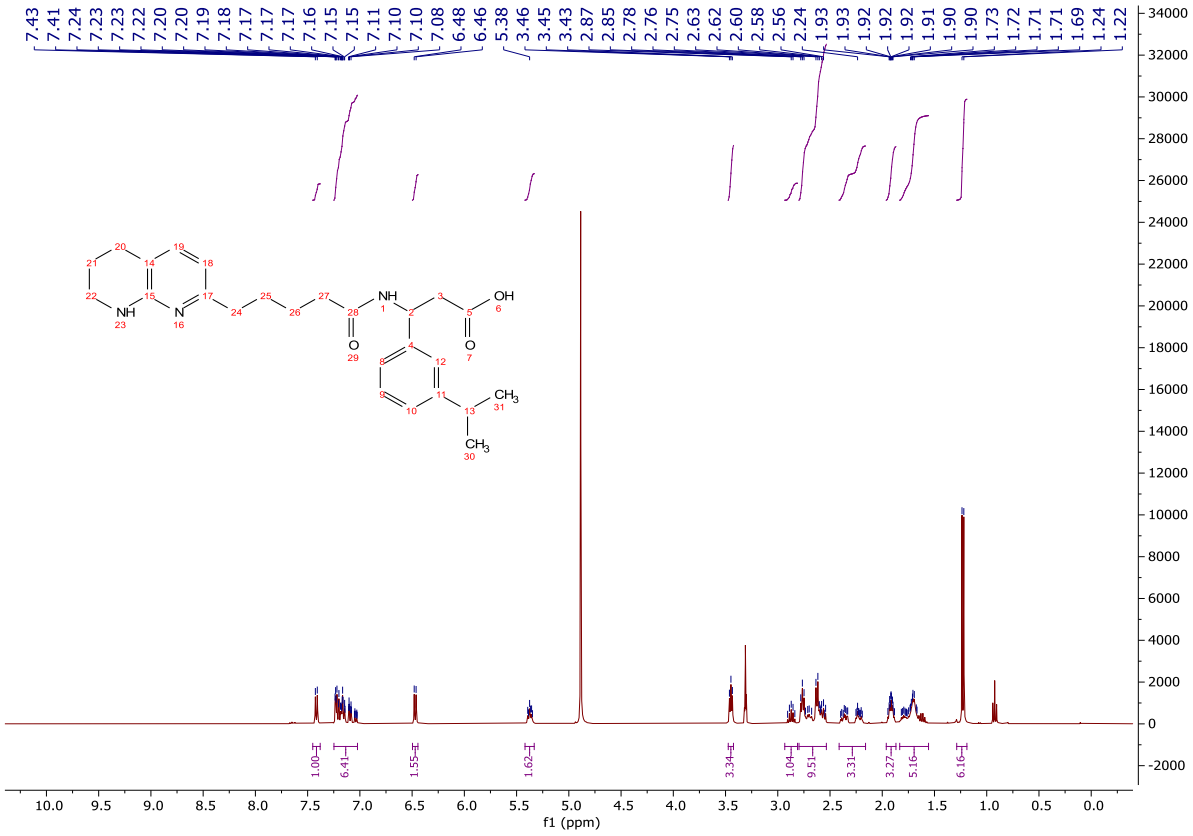
7.43 7.41 7.24 7.23 7.23 7.22 7.20 7.20 7.19 7.18 7.17 7.17 7.17 7.16 7.15 7.15 7.11 7.10 7.10 7.08 6.48 6.46 5.38 3.46 3.45 3.43 2.87 2.85 2.78 2.76 2.75 2.63 2.62 2.60 2.58 2.56 2.24 1.93 1.93 1.92 1.92 1.92 1.91 1.90 1.90 1.73 1.72 1.71 1.71 1.69 1.24 1.22
NH
OH
O
CH3
1.00 6.41 1.55 1.62 3.34 1.04 9.51 3.31 3.27 5.16 6.16
f1 (ppm)

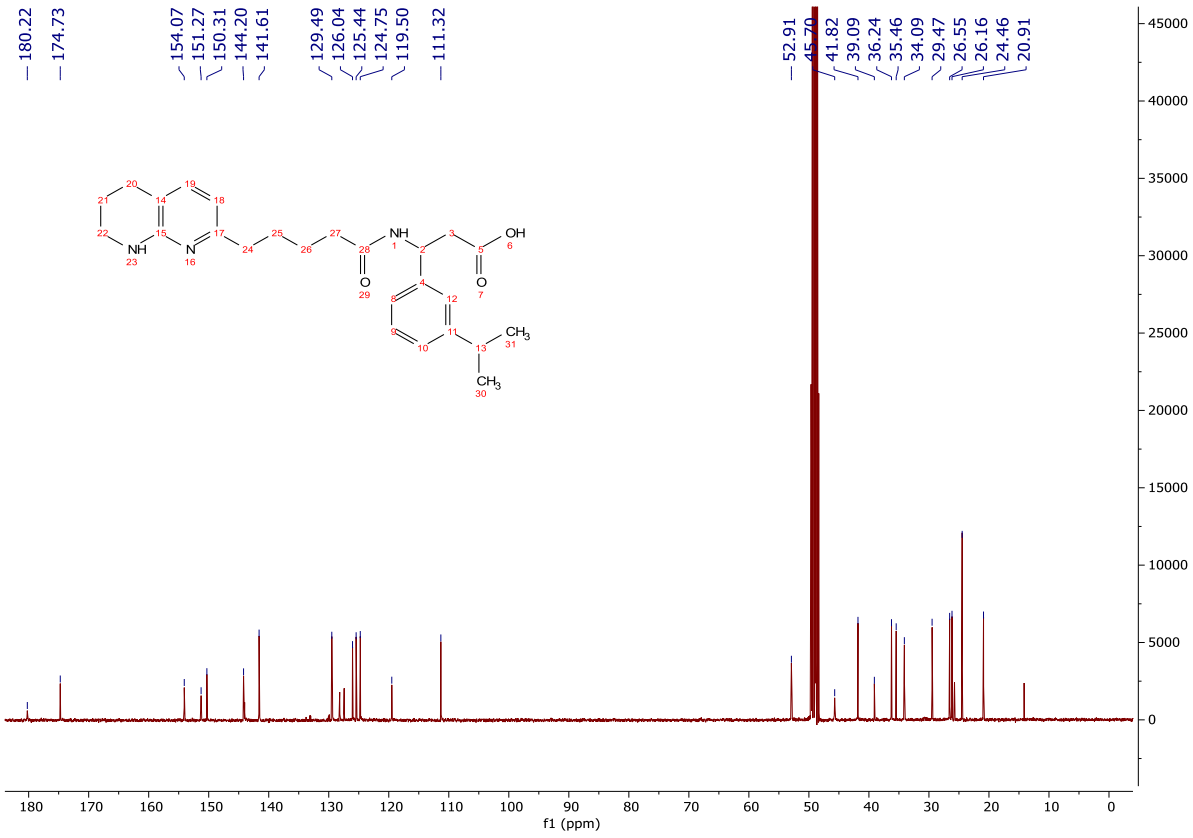
180.22 174.73 154.07 151.27 150.31 144.20 141.61 129.49 126.04 125.44 124.75 119.50 111.32 52.91 45.70 41.82 39.09 36.24 35.46 34.09 29.47 26.55 26.16 24.46 20.91
NH
OH
O
CH3
f1 (ppm)

Ethyl 3-(3-cyclopropylphenyl)-3-(-5-(5,6,7,8-tetrahydro-1,8-naphthyridin-2-yl)pentanamido)propanoate) (**244**)

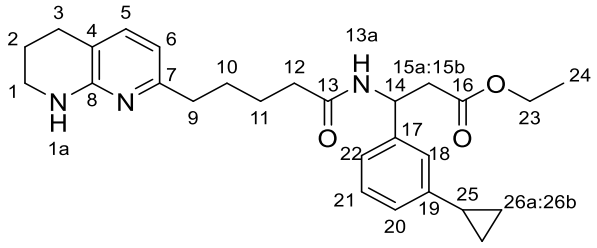

To a stirred solution of **242** (186 mg, 0.339 mmol) at rt in CH_2Cl_2 (20.0 mL) was added TFA (7.00 mL). The reaction was quenched after 21 h with addition of sat. $NaHCO_{3(aq)}$ (20.0 mL). The organic phase was washed with sat. $NaHCO_{3(aq)}$ (2 x 10.0 mL), dried ($MgSO_4$) and concentrated *in vacuo* to afford a brown/yellow oil (158 mg). The crude product was purified by column chromatography on amino propyl silica gel, eluting with a gradient of ethyl acetate/light petroleum (10-100%) to afford the title compound as a green/brown oil (31 mg, 0.069 mmol, 20%); **HRMS** *m/z* (ESI^+) calc. for $C_{27}H_{36}N_3O_3$ $[M+H]^+$ requires 450.2751, found 450.2737; δ_H (400 MHz, $CDCl_3$) 7.19 (1H, dd, *J* = 7.6, 7.6 Hz, H-21), 7.07 – 7.01 (2H, m, H-5 and H-22), 7.00 (1H, dd, *J* = 2.0, 2.0 Hz, H-18), 6.92 (1H, ddd, *J* = 7.8, 1.4, 1.4 Hz, H-20), 6.49 (1H, d, *J* = 8.5 Hz, H-13a), 6.32 (1H, d, *J* = 7.3 Hz, H-6), 5.39 (1H, dt, *J* = 8.4, 6.1 Hz, H-14), 4.09 – 4.02 (2H, m, H-23), 3.41 – 3.35 (2H, m, H-1), 2.89 (H, dd, *J* = 15.5, 6.1 Hz, H-15a), 2.79 (1H, dd, *J* = 15.5, 6.0 Hz, H-15b), 2.68 (2H, t, *J* = 6.3 Hz, H-3), 2.57 – 2.52 (2H, m, H-9), 2.27 – 2.20 (2H, m, H-12), 1.93 – 1.81 (3H, m, H-2 and H-25), 1.74 – 1.58 (4H, m, H-10 and H-11), 1.19 – 1.14 (3H, m, H-24), 0.97 – 0.90 (2H, m, H-26a), 0.69 – 0.63 (2H, m, H-26b); δ_C (100 MHz, $CDCl_3$) 172.3 (CO), 171.4 (CO), 158.1 (C), 155.8 (C), 144.6 (C), 140.8 (C), 136.8 (ArH), 128.7 (ArH), 124.8 (ArH), 124.3 (ArH), 123.4 (ArH), 113.3 (C), 111.6 (ArH), 60.9 (CH_2), 49.6 (CH), 41.8 (CH_2), 40.2 (CH_2), 37.6 (CH_2), 36.8 (CH_2), 29.5 (CH_2), 26.5 (CH_2), 25.6 (CH_2), 21.7 (CH_2), 15.6 (CH), 14.2 (CH_3), 9.4 (CH_2); ν_{max} (FT-ATR/cm^{-1}) 3334, 1636, 1415, 1202, 1147, 590.

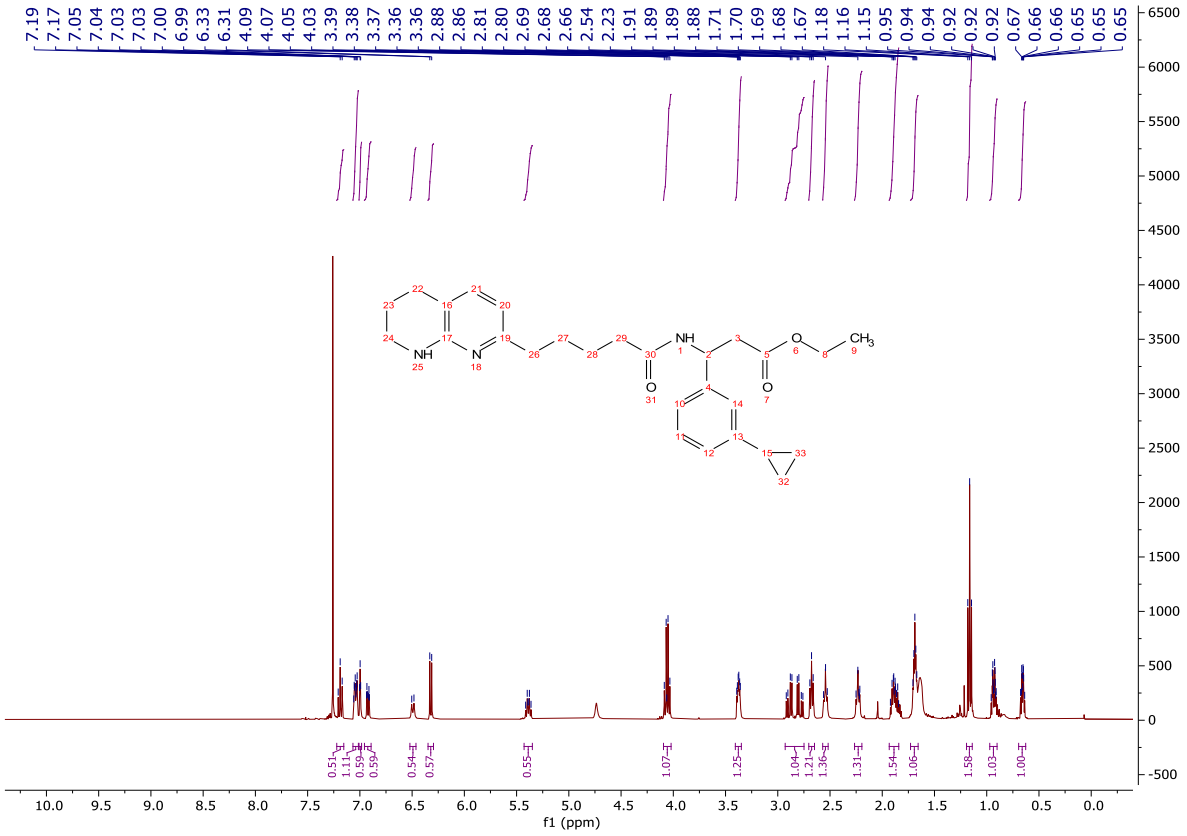
7.19 7.17 7.05 7.04 7.03 7.03 7.00 6.99 6.33 6.31 4.09 4.07 4.05 4.03 3.39 3.38 3.37 3.36 3.36 2.88 2.86 2.81 2.80 2.69 2.68 2.66 2.54 2.23 1.91 1.89 1.89 1.88 1.71 1.70 1.69 1.68 1.67 1.18 1.16 1.15 0.95 0.94 0.94 0.92 0.92 0.92 0.67 0.66 0.66 0.65 0.65 0.65
0.51 1.11 0.59 0.59 0.54 0.57 0.55 1.07 1.25 1.04 1.21 1.36 1.31 1.54 1.06 1.58 1.03 1.00
f1 (ppm)

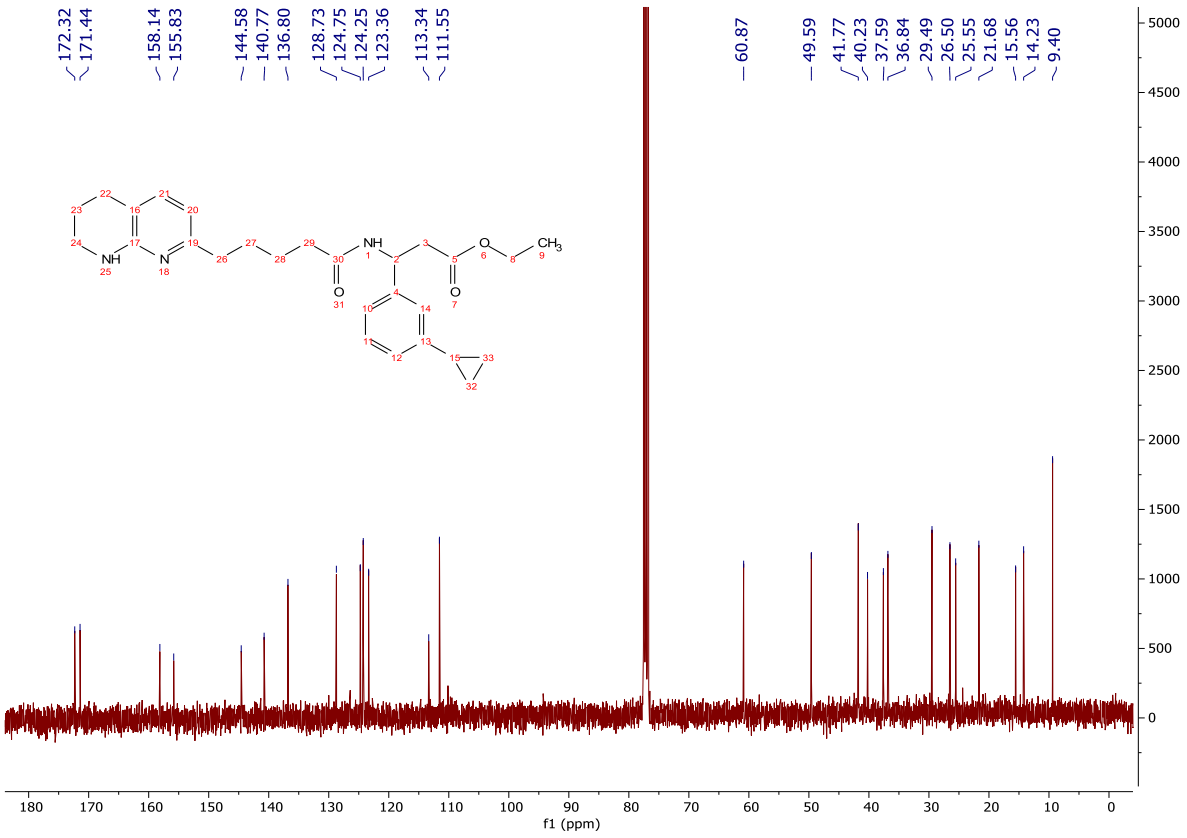
172.32 171.44 158.14 155.83 144.58 140.77 136.80 128.73 124.75 124.25 123.36 113.34 111.55 60.87 49.59 41.77 40.23 37.59 36.84 29.49 26.50 25.55 21.68 15.56 14.23 9.40
f1 (ppm)

3-(3-cyclopropylphenyl)-3-(-5-(5,6,7,8-tetrahydro-1,8-naphthyridin-2-yl)pentanamido)propanoic acid (**49**)

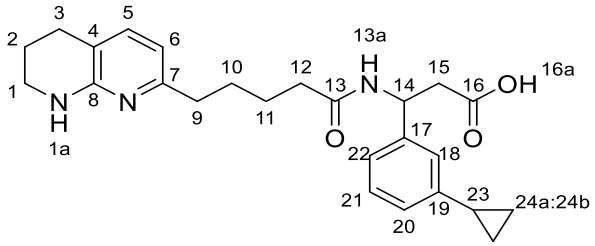

To a stirred solution of **244** (31 mg, 0.069 mmol) in THF (7.00 mL) at rt was added 1M $LiOH_{(aq)}$ (0.070 mL, 0.070 mmol). The reaction mixture was stirred for 16 h and concentrated *in vacuo* to afford a colourless solid. The crude product was purified on a Waters OASIS® HLB cartridge, eluting with a gradient of methanol/water (0-100%) to afford the title compound as a clear oil (17 mg, 0.040 mmol, 58%); **HRMS** *m/z* (ESI^+) calc. for $C_{25}H_{32}N_3O_3$ $[M+H]^+$ requires 422.2438, found 422.2441; $\boldsymbol{R_f}$ 0.40, 6% methanol/CH_2Cl_2, UV active; δ_H (400 MHz, MeOD) 7.42 (1H, d, *J* = 7.3 Hz, H-5), 7.17 (1H, dd, *J* = 7.6, 7.6 Hz, H-21), 7.11 (1H, ddd, *J* = 7.7, 1.5, 1.5 Hz, H-22), 7.07 (1H, dd, *J* = 1.8, 1.8 Hz, H-18), 6.92 (1H, ddd, *J* = 7.5, 1.5, 1.5 Hz, H-20), 6.47 (1H, d, *J* = 7.3 Hz, H-6), 5.34 (1H, t, *J* = 7.5 Hz, H-14), 3.45 (2H, t, *J* = 5.6 Hz, H-1), 2.81 – 2.54 (6H, m, H-3, H-9 and H-15), 2.41 – 2.17 (2H, m, H-12), 1.98 – 1.84 (3H, m, H-2 and H-23), 1.83 – 1.64 (4H, m, H-10 and H-11), 0.96 – 0.90 (2H, m, H-24a), 0.68 – 0.63 (2H, m, H-24b); δ_C (100 MHz, MeOD) 180.2 (CO), 174.7 (CO), 154.0 (C), 151.1 (C), 145.6 (C), 144.1 (C), 141.7 (ArH), 129.4 (ArH), 125.2 (ArH), 124.6 (ArH), 124.3 (ArH), 119.6 (C), 111.3 (ArH), 52.9 (CH), 45.6 (CH_2), 41.8 (CH_2), 36.2 (CH_2), 34.0 (CH_2), 29.5 (CH_2), 26.5 (CH_2), 26.1 (CH_2), 20.9 (CH_2), 16.2 (CH), 9.6 (CH_2); $\boldsymbol{\nu_{max}}$ (FT-ATR/cm^{-1}) 3263, 2928, 1644, 1539, 1392, 1287, 1113, 792, 703.

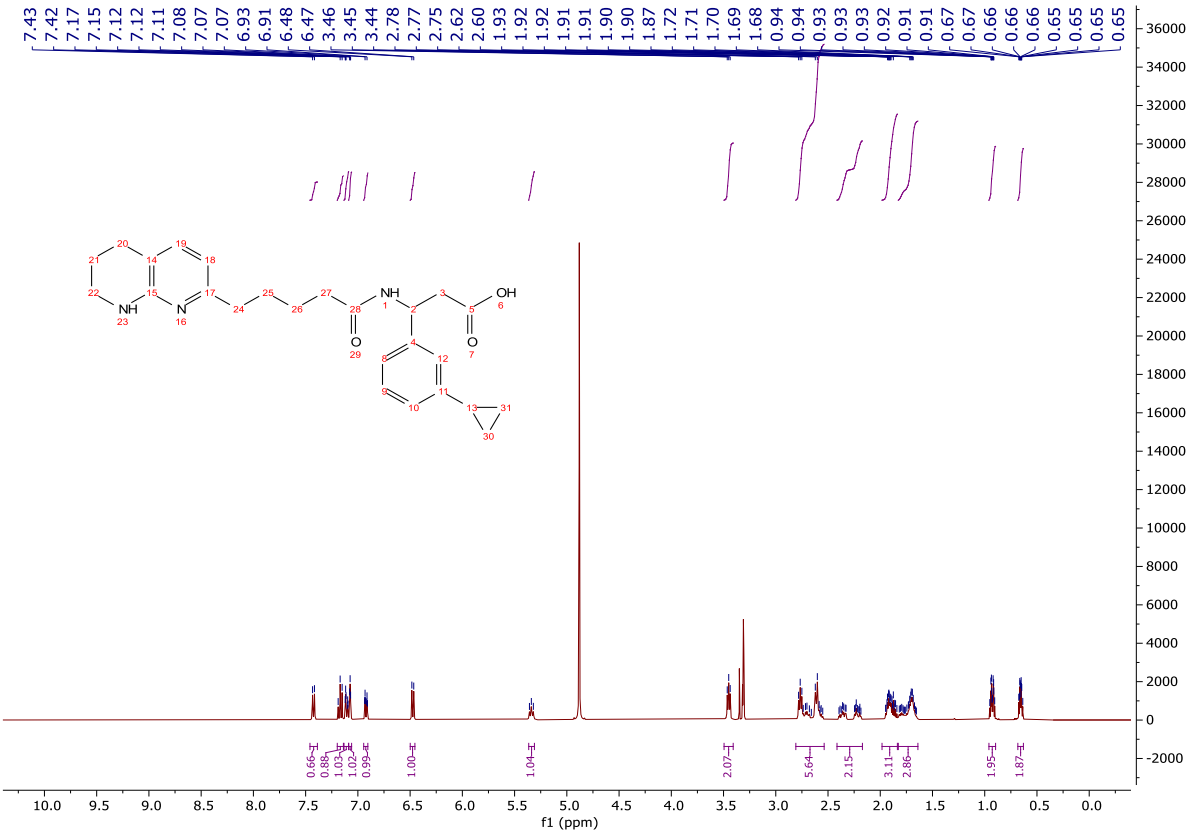
7.43 7.42 7.17 7.15 7.12 7.12 7.11 7.08 7.07 7.07 6.93 6.91 6.48 6.47 3.46 3.45 3.44 2.78 2.77 2.75 2.62 2.60 1.93 1.92 1.92 1.91 1.91 1.90 1.90 1.87 1.72 1.71 1.70 1.69 1.68 0.94 0.94 0.93 0.93 0.93 0.92 0.91 0.91 0.67 0.67 0.66 0.66 0.66 0.65 0.65 0.65
NH
N
OH
O
0.66 0.88 1.03 1.02 0.99 1.00 1.04 2.07 5.64 2.15 3.11 2.86 1.95 1.87
f1 (ppm)

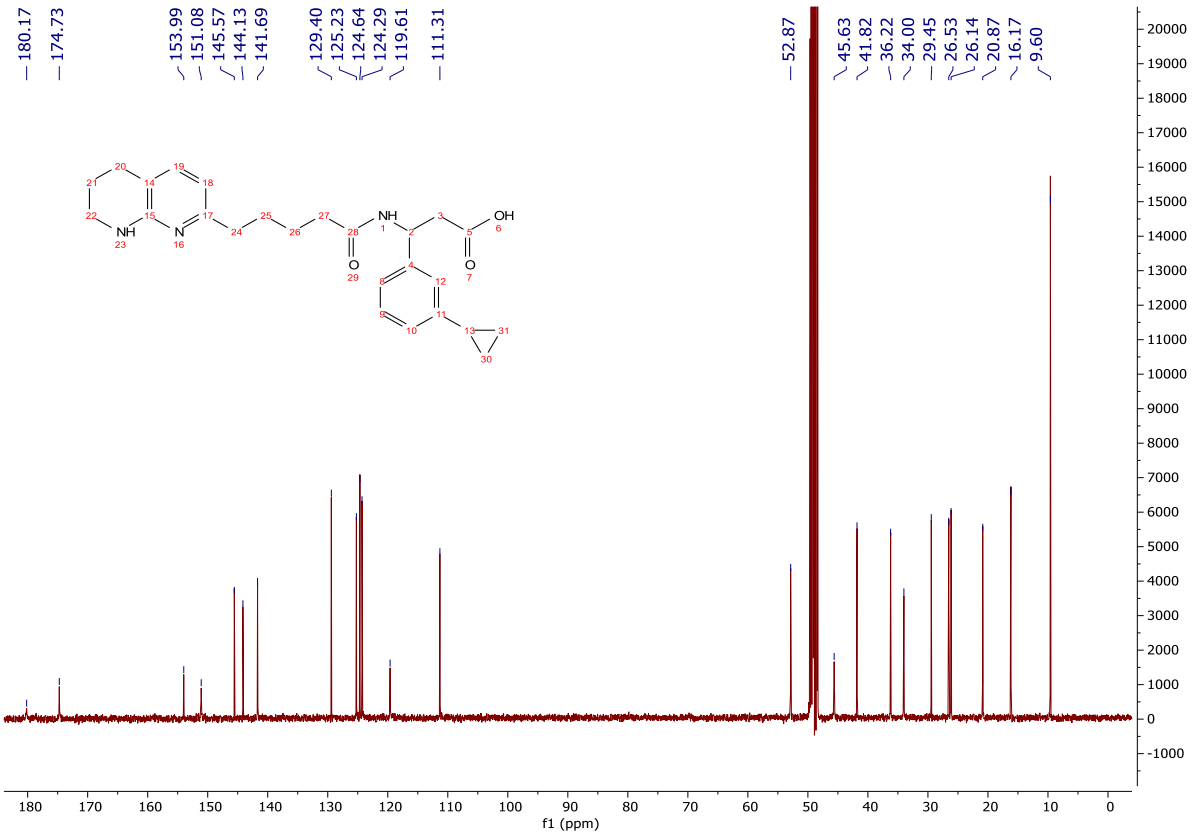
180.17 174.73 153.99 151.08 145.57 144.13 141.69 129.40 125.23 124.64 124.29 119.61 111.31 52.87 45.63 41.82 36.22 34.00 29.45 26.53 26.14 20.87 16.17 9.60
NH
N
OH
O
f1 (ppm)

tert-Butyl 7-(5-((3-*tert*-butoxy)-1-(3-iodophenyl)-3-oxophenyl)-3-oxopropyl)amino)-5-oxopentyl)-3,4-dihydro-1,8-naphthyridine-1(2*H*)-carboxylate (**245**)

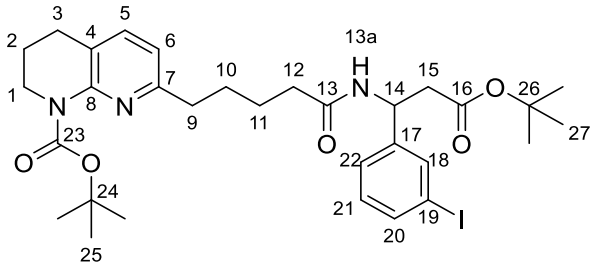

To a stirred solution of **113** (1.19 g, 3.42 mmol) and **82** (0.970 g, 2.85 mmol) in acetonitrile (15.0 mL) at 0 °C was added T3P (50% in ethyl acetate, 1.69 mL, 5.70 mmol) and *i*-Pr_2NEt (1.98 mL, 11.4 mmol). The reaction mixture was stirred for 16 h, ethyl acetate (20.0 mL) and sat. $NaHCO_{3(aq)}$ (20.0 mL) were added, the organic phase separated, then washed with sat. $NaHCO_{3(aq)}$ (2 x 20.0 mL), brine (2 x 20.0 mL), dried ($MgSO_4$) and concentrated *in vacuo* giving a yellow oil (2.02 g). The crude product was purified by column chromatography on silica gel, eluting with a gradient of ethyl acetate/light petroleum (10-80%) to afford the title compound as a clear oil (1.60 g, 2.41 mmol, 85%); **HRMS** *m/z* (ESI^+) calc. for $C_{31}H_{43}IN_3O_5$ $[M+H]^+$ requires 664.2242, found 664.2214; $\boldsymbol{R_f}$ 0.26, 80% ethyl acetate/light petroleum, UV active; δ_H (400 MHz, $CDCl_3$) 7.63 – 7.53 (2H, m, H-18 and H-20), 7.36 – 7.20 (2H, m, H-5 and H-22), 7.08 – 6.99 (1H, m, H-21), 6.83 – 6.74 (2H, m, H-6 and H-13a), 5.35 – 5.26 (1H, m, H-14), 3.78 – 3.69 (2H, m, H-1), 2.78 – 2.62 (6H, m, H-3, H-9 and H-15), 2.27 (2H, t, *J* = 7.2 Hz, H-12), 1.96 – 1.86 (2H, m, H-2), 1.82 – 1.61 (4H, m, H-10 and H-11), 1.51 (9H, s, H-27), 1.34 (9H, s, H-25); δ_C (101 MHz, $CDCl_3$) 172.4 (CO), 170.5 (CO), 158.2 (C), 154.2 (CO), 151.2 (C), 143.5 (C), 137.4 (ArH), 136.6 (ArH), 135.5 (ArH), 130.4 (ArH), 126.0 (ArH), 122.0 (C), 118.5 (ArH), 94.6 (C), 81.8 (C), 80.9 (C), 49.1 (CH), 45.0 (CH_2), 41.1 (CH_2), 37.6 (CH_2), 36.7 (CH_2), 29.2 (CH_2), 28.6 (CH_2), 28.1 (CH_3), 26.4 (CH_2), 25.5 (CH_2), 23.5 (CH_2); ν_{max} (FT-ATR/cm^{-1}) 3305, 2931, 1724, 1691, 1647, 1567, 1466, 1365, 1252, 1146, 844, 785, 697.

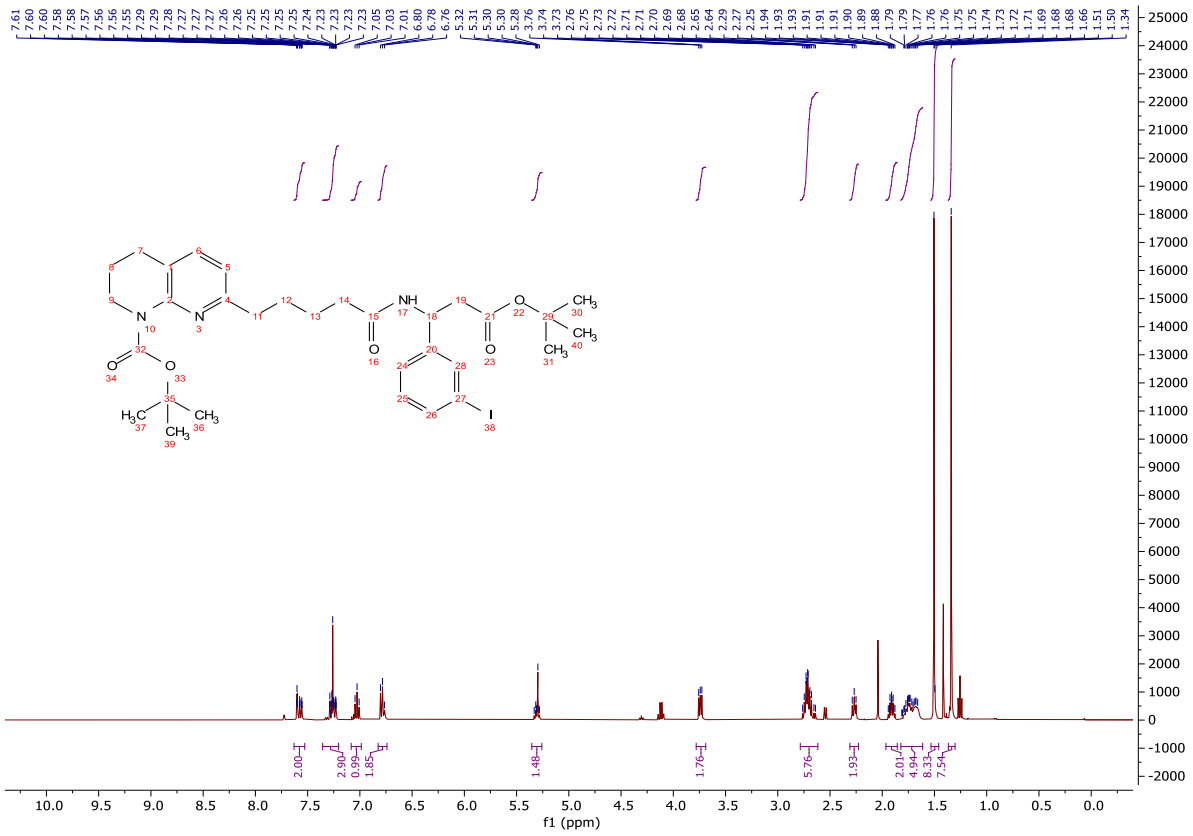
f1 (ppm)

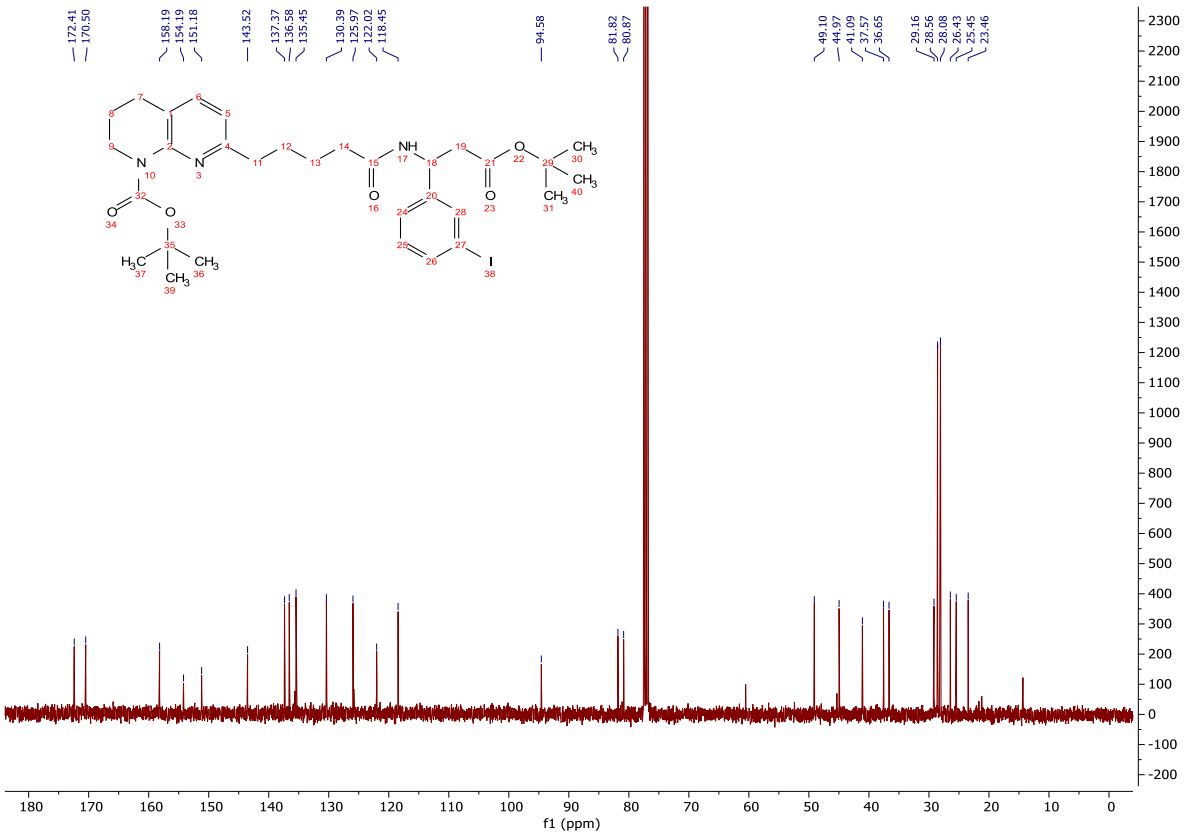
f1 (ppm)

Potassium cyclopropyltrifluoroborate (**252**)

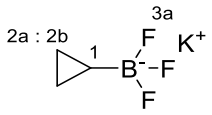

To a suspension of cyclopropyl boronic acid (**249**, 400 mg, 4.65 mmol) in acetonitrile (18.6 mL) was added a solution of KF (1.08 g, 18.6 mmol) in water (1.86 mL). The mixture was stirred at rt until full dissolution, then a solution of L-(+)-tartaric acid (1.43 g, 9.53 mmol) in THF (6.96 mL) was added slowly over 1 min. The reaction mixture was stirred vigorously for 10 min, then filtered and the filter cake washed with acetonitrile (3 x 20.0 mL). The filtrate was concentrated *in vacuo* to afford the title compound as a white solid (536 mg, 3.62 mmol, 78%). The crude product was used without further purification; δ_H (400 MHz, DMSO) -0.03 – -0.27 (4H, m, H-2a and H-2b), -0.77 – -0.90 (1H, m, H-1); δ_C (101 MHz, DMSO) 0.8 (CH_2, q, *J* = 2.4 Hz); δ_F (376 MHz, DMSO) -140.8 (F-3a). Data are consistent with the literature.[126]

N.B. C-1 is not observed.

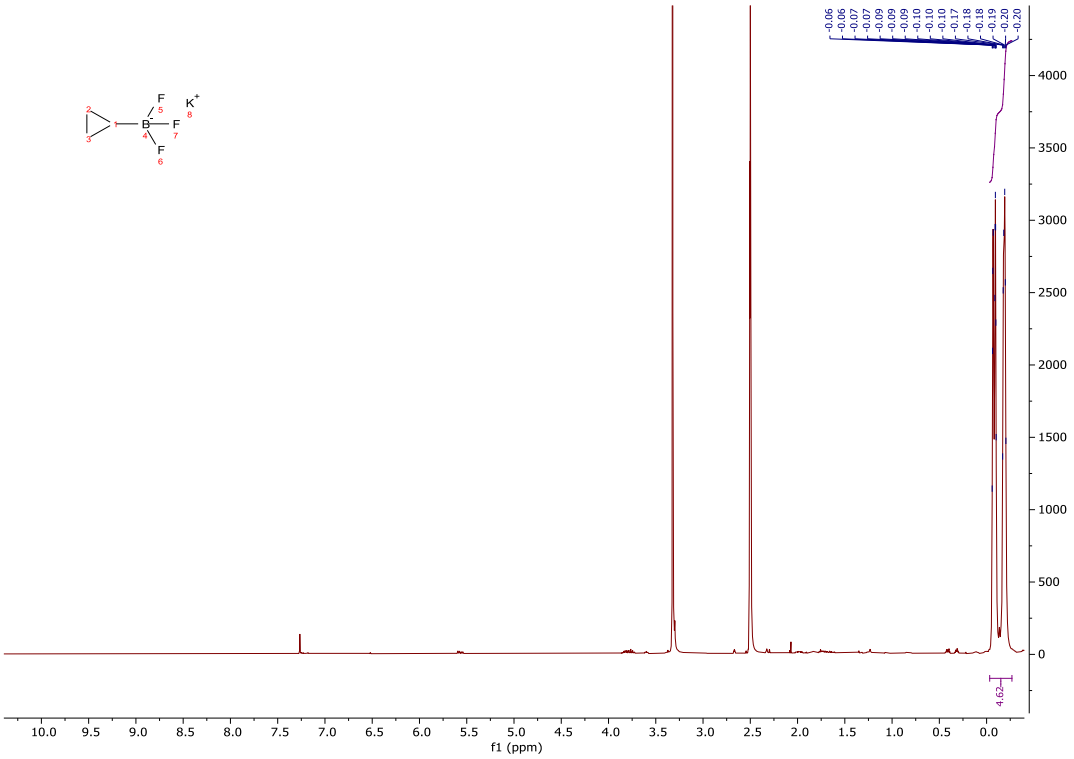
F
K+
B
F
F
-0.06
-0.06
-0.07
-0.07
-0.09
-0.09
-0.09
-0.10
-0.10
-0.10
-0.17
-0.18
-0.18
-0.19
-0.20
-0.20
4.62
f1 (ppm)

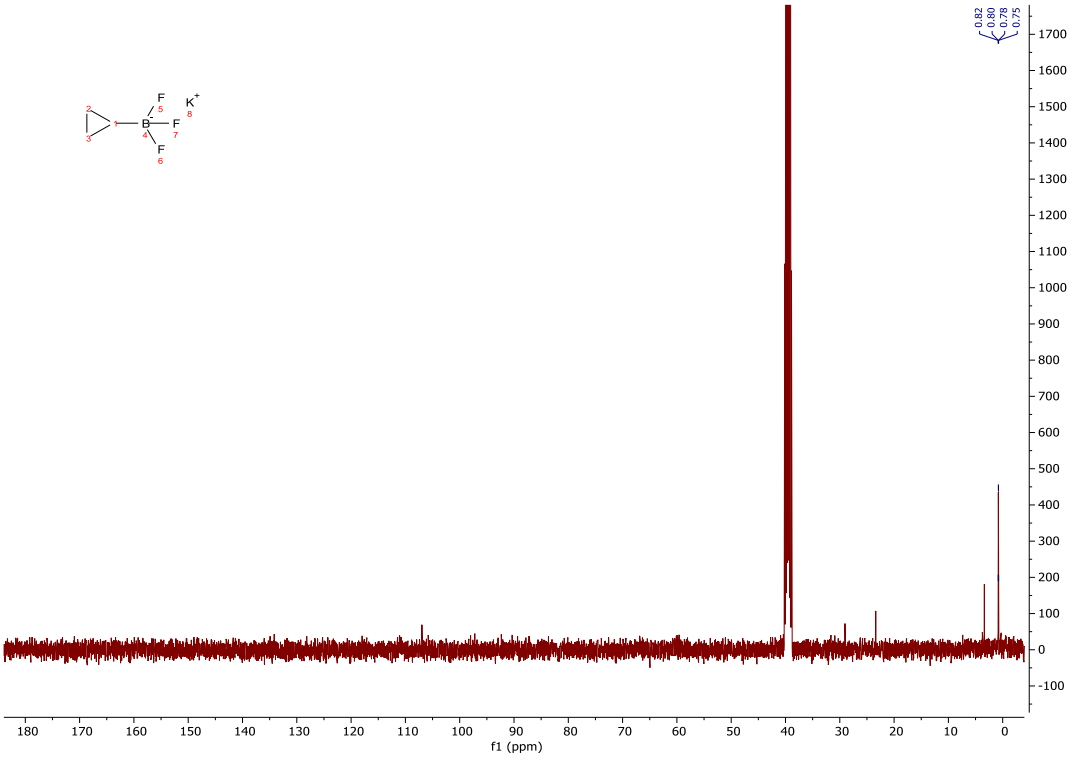
F
K+
B
F
F
0.82
0.80
0.78
0.75
f1 (ppm)

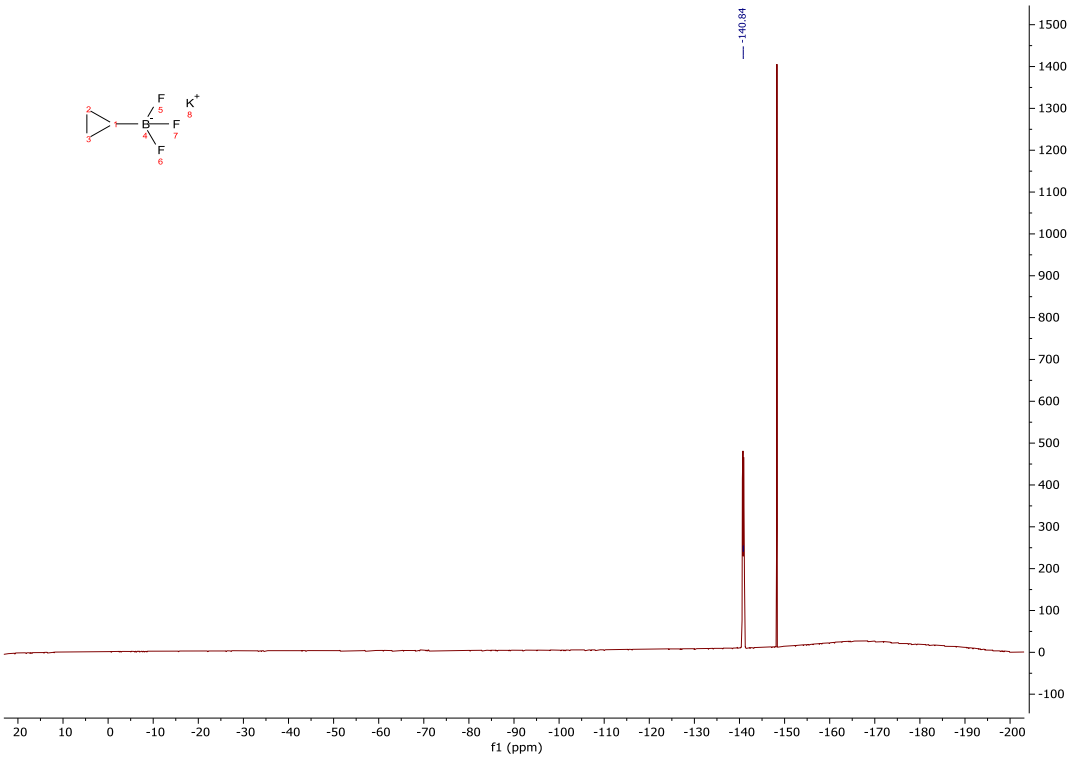
-140.84
F
5
K+
8
2
B
4
F
7
3
F
6
1500
1400
1300
1200
1100
1000
900
800
700
600
500
400
300
200
100
0
-100
20
10
0
-10
-20
-30
-40
-50
-60
-70
-80
-90
-100
-110
-120
-130
-140
-150
-160
-170
-180
-190
-200
f1 (ppm)

tert-Butyl (*S*)-3-(3-bromophenyl)-3-((*tert*-butoxycarbonyl)amino)propanoate (**253**)

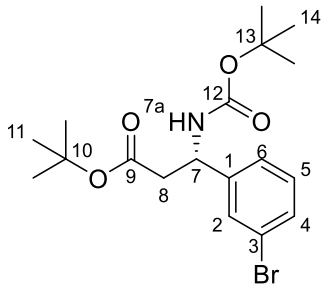

To a stirred solution of **110** (5.00 g, 14.9 mmol) in THF (60.0 mL) at 0 °C was added Et_3N (6.22 mL, 44.7 mmol). A solution of di-*tert*-butyl dicarbonate (4.45 mL, 19.4 mmol) in THF (10.0 mL) was added and the reaction mixture stirred for 16 h. The reaction mixture was concentrated *in vacuo* and the crude material dissolved in ethyl acetate (100 mL) and sat. $NaHCO_{3(aq)}$ (100 mL). The layers were separated and the organic washed with 10% citric $acid_{(aq)}$ (100 mL), water (100 mL), brine (100 mL), dried ($MgSO_4$) and concentrated *in vacuo* to afford a yellow oil. The crude product was recrystallised from light petroleum, affording the title compound as a clear, colourless oil (5.78 g, 14.5 mmol, 97%); **HRMS** *m/z* (ESI^+) calc. for $C_{18}H_{27}BrNO_4$ $[M+H]^+$ requires 400.1118, found 400.1117; $\boldsymbol{R_f}$ 0.27, 10% ethyl acetate/light petroleum, UV active; δ_H (400 MHz, $CDCl_3$) δ 7.44 (1H, dd, *J* = 1.8, 1.8 Hz, H-2), 7.38 (1H, ddd, *J* = 7.4, 1.7, 1,7 Hz, H-4), 7.25 – 7.16 (2H, m, H-5 and H-6), 5.57 (1H, bs, H-7a), 5.01 (1H, bs, H-7), 2.77 – 2.61 (2H, m, H-8), 1.42 (9H, s, H-14), 1.35 (9H, s, H-11); δ_C (101 MHz, $CDCl_3$) 170.1 (CO), 155.1 (CO), 144.0 (C), 130.6 (ArH), 130.3 (ArH), 129.5 (ArH), 125.1 (ArH), 122.8 (C), 81.7 (C), 80.0 (C), 51.1 (CH), 42.1 (CH_2), 28.5 (CH_3), 28.1 (CH_3); ν_{max} (FT-ATR/cm^{-1}) 3341, 2977, 1707, 1503, 1366, 1292, 1246, 1152, 1048, 843, 782, 696.

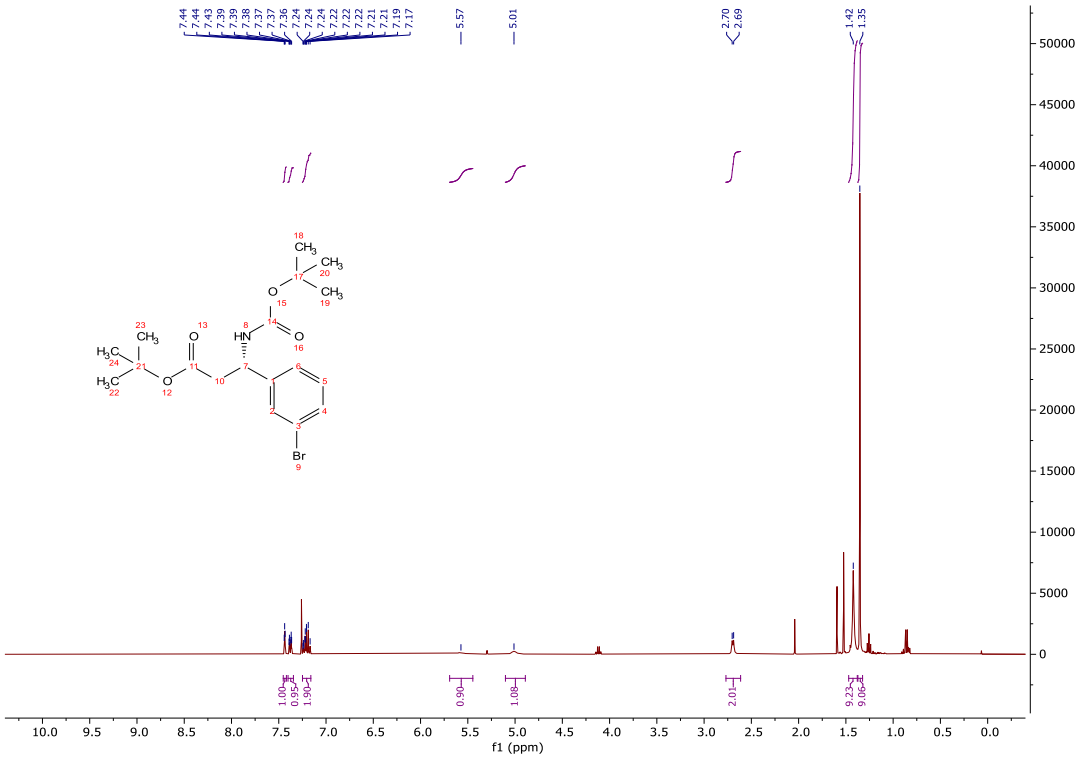
7.44
7.44
7.43
7.39
7.39
7.38
7.37
7.37
7.36
7.24
7.24
7.24
7.22
7.22
7.21
7.21
7.19
7.17
5.57
5.01
2.70
2.69
1.42
1.35
1.00
0.95
1.90
0.90
1.08
2.01
9.23
9.06
f1 (ppm)

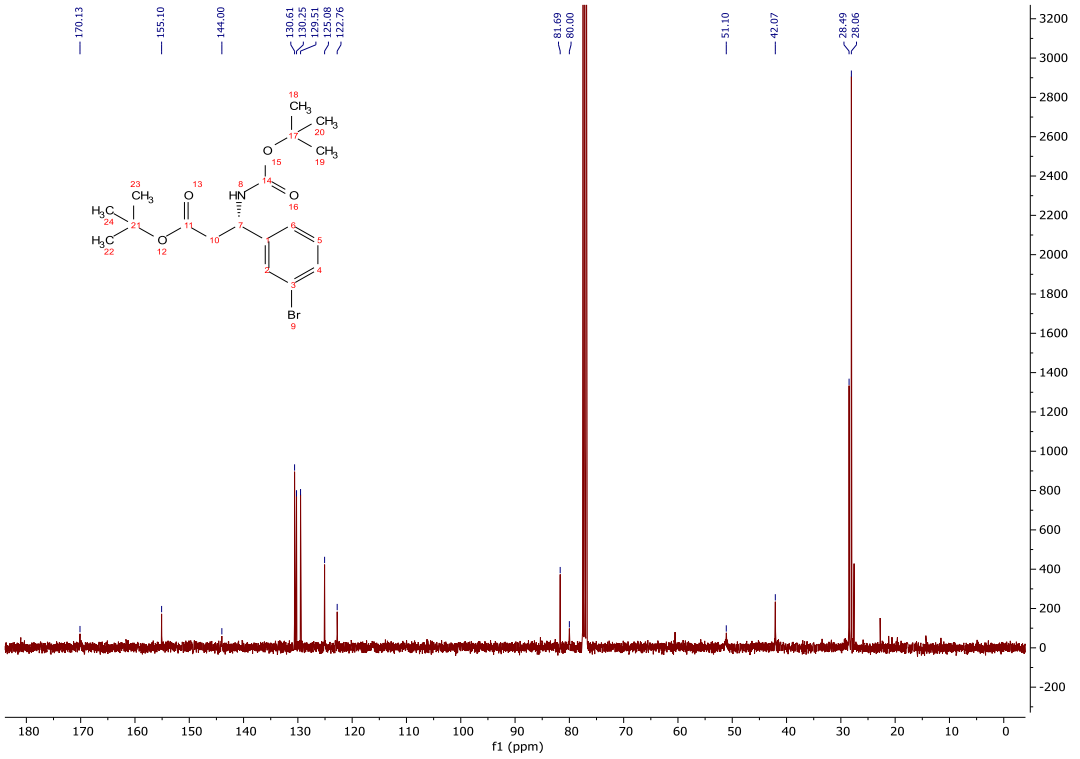
170.13
155.10
144.00
130.61
130.25
129.51
125.08
122.76
81.69
80.00
51.10
42.07
28.49
28.06
f1 (ppm)

tert-Butyl (*S*)-3-((*tert*-butoxycarbonyl)amino)-3-(3-cyclopropylphenyl)propanoate) (**254**)

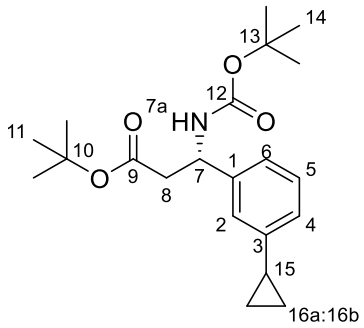

A microwave vial was charged with **252** (3.72 g, 25.1 mmol), XPhos Pd G2 (296 mg, 0.376 mmol) and K_2CO_3 (5.20 g, 37.6 mmol). The vial was sealed and purged with argon, and a solution of **253** (5.00 g, 12.5 mmol) in 10:1 CPME/water (50.0 mL) was added. The reaction mixture was degassed and then heated at 100 ^oC for 24 h. The reaction mixture was cooled to room temperature, diluted with water (50.0 mL) and the aqueous layer extracted with CH_2Cl_2 (3 x 50.0 mL). The combined organics were dried (Na_2SO_4) and concentrated *in vacuo* to give a yellow oil. The crude product was purified *via* column chromatography on silica gel, eluting with a gradient of ethyl acetate/light petroleum (0-10%) to give the title compound as a pale, yellow oil (3.50 g, 9.70 mmol, 78%); **HRMS** *m/z* (ESI^+) calc. for $C_{21}H_{32}NO_4$ $[M+H]^+$ requires 362.2326, found 362.2325; $\boldsymbol{R_f}$ 0.34, 10% ethyl acetate/light petroleum, UV active; δ_H (400 MHz, $CDCl_3$) 7.23 – 7.16 (1H, m, H-5), 7.06 (1H, ddd, *J* = 7.8, 1.6, 1.6 Hz, H-6), 7.00 (1H, dd, *J* = 1.9, 1.9 Hz, H-2), 6.93 (1H, ddd, *J* = 7.6, 1.5, 1.5 Hz, H-4), 5.40 (1H, bs, H-7a), 5.01 (1H, bs, H-7), 2.80 – 2.62 (2H, m, H-8), 1.87 (1H, tt, *J* = 8.4, 5.1 Hz, H-15), 1.42 (9H, s, H-11), 1.34 (9H, s, H-14), 0.97 – 0.86 (2H, m, H-16a), 0.70 – 0.64 (2H, m, H-16b); δ_C (101 MHz, $CDCl_3$) 170.4 (CO), 155.2 (CO), 144.4 (C), 128.6 (ArH), 124.7 (ArH), 124.0 (ArH), 123.4 (ArH), 81.2 (C), 79.7 (C), 51.6 (CH), 42.4 (CH_2), 28.5 (CH_3), 28.1 (CH_3), 15.6 (CH), 9.3 (CH_2); ν_{max} (FT-ATR/cm^{-1}) 3344, 2977, 1706, 1608, 1493, 1366, 1288, 1245, 1152, 1045, 779, 703.

N.B. One aryl quaternary carbon is not observed.

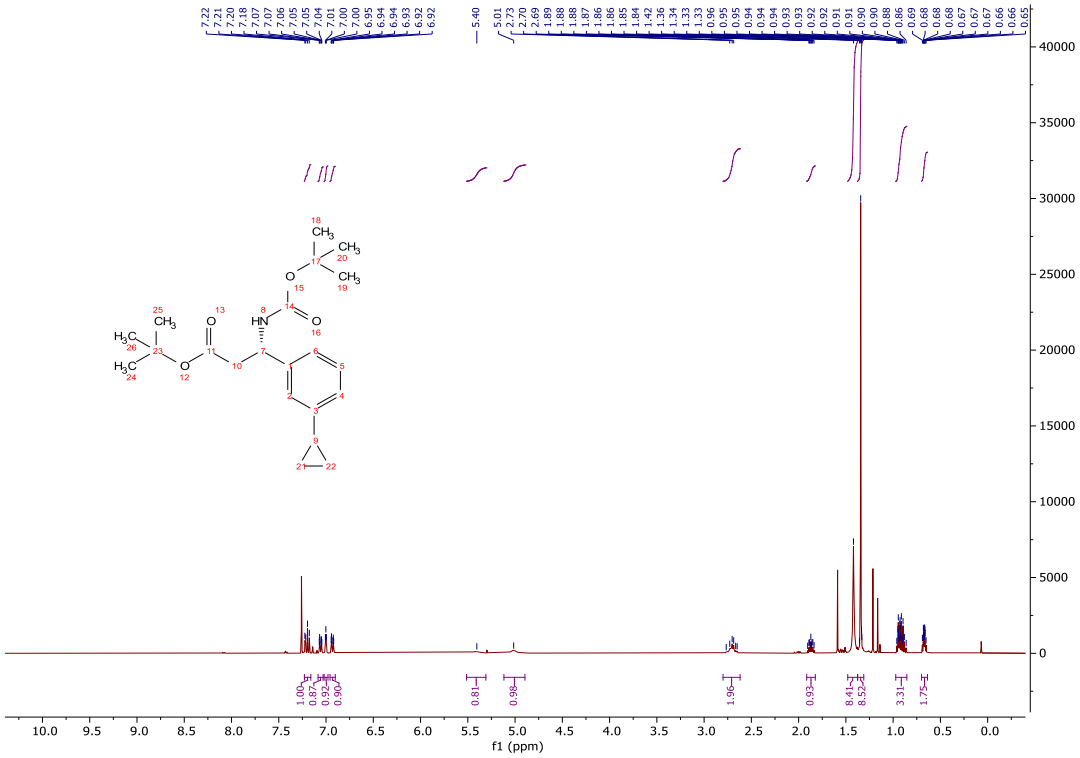
7.22 7.21 7.20 7.18 7.07 7.07 7.06 7.05 7.05 7.04 7.01 7.00 7.00 6.95 6.94 6.94 6.93 6.92 6.92
5.40
5.01 2.73 2.70 2.69 1.89 1.88 1.88 1.87 1.86 1.86 1.85 1.84 1.42 1.36 1.34 1.33 1.33 0.96 0.95 0.95 0.94 0.94 0.94 0.93 0.93 0.92 0.92 0.91 0.91 0.90 0.90 0.88 0.86 0.69 0.68 0.68 0.68 0.67 0.67 0.67 0.66 0.66 0.65
1.00 0.87 0.92 0.90 0.81 0.98 1.96 0.93 8.41 8.52 3.31 1.75
f1 (ppm)

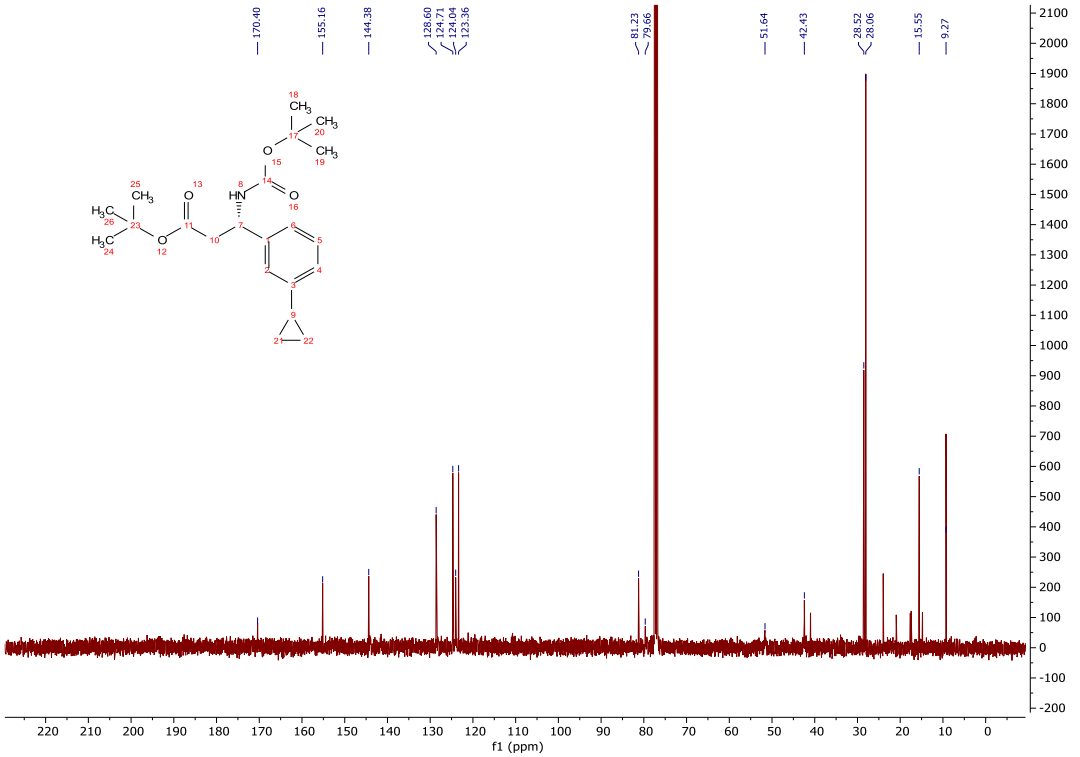
170.40 155.16 144.38 128.60 124.71 124.04 123.36 81.23 79.66 51.64 42.43 28.52 28.06 15.55 9.27
f1 (ppm)

Ethyl (*S*)-3-((*tert*-butoxycarbonyl)amino)-3-(3-cyclopropylphenyl)propanoate) (**250**)

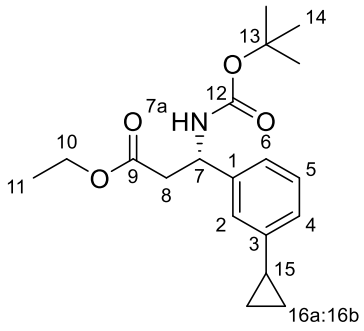

A large microwave vial was charged with **252** (8.00 g, 54.0 mmol), XPhos Pd G2 (628 mg, 0.800 mmol) and K_2CO_3 (11.2 g, 80.8 mmol). The vial was sealed and purged with argon before a solution of **(*S*)-119** (10.0 g, 26.9 mmol) in CPME/water (100 mL, 10:1) was added. The reaction mixture was degassed and then heated at 100 °C for 24 h. The reaction mixture was cooled to room temperature, diluted with water (100 mL) and the aqueous layer extracted with CH_2Cl_2 (3 x 100 mL). The combined organics were dried (Na_2SO_4) and concentrated *in vacuo* to give a yellow oil. The crude product was purified *via* column chromatography on silica gel, eluting with a gradient of ethyl acetate/light petroleum (0-20%) to give the title compound as as an oil that solidified on standing (6.50 g, 19.5 mmol, 73%); **HRMS** *m/z* (ESI^+) calc. for $C_{19}H_{28}NO_4$ $[M+H]^+$ requires 334.2013, found 334.2012; $\boldsymbol{R_f}$ 0.38, 10% ethyl acetate/light petroleum, UV active; δ_H (400 MHz, $CDCl_3$) 7.20 (1H, dd, *J* = 7.6, 7.6 Hz, H-5), 7.06 (1H, ddd, *J* = 7.8, 1.5, 1.5 Hz, H-6), 7.00 (1H, dd, *J* = 1.95, 1.95 Hz, H-2), 6.93 (1H, ddd, *J* = 7.6, 1.5, 1.5 Hz, H-4), 5.40 (1H, bs, H-7a), 5.05 (1H, bs, H-7), 4.16 – 4.01 (2H, m, H-10), 2.93 – 2.69 (2H, m, H-8), 1.87 (1H, tt, *J* = 8.4, 5.1 Hz, H-15), 1.42 (9H, s, H-14), 1.17 (3H, t, *J* = 7.1 Hz, H-11), 0.99 – 0.89 (2H, m, H-16a), 0.72 – 0.62 (2H, m, H-16b); δ_C (101 MHz, $CDCl_3$) 171.1 (CO), 155.2 (CO), 144.5 (C), 141.3 (C), 128.7 (ArH), 124.8 (ArH), 124.0 (ArH), 123.3 (ArH), 79.8 (C), 60.8 (CH_2), 51.5 (CH), 41.3 (CH_2), 28.5 (CH_3), 15.6 (CH), 14.2 (CH_3), 9.4 (CH_2); **MP** 58-61 °C; ν_{max} (FT-ATR/cm^{-1}) 3375, 2984, 1731, 1687, 1612, 1517, 1445, 1367, 1292, 1236, 1153, 1032, 1013, 851, 703, 614.

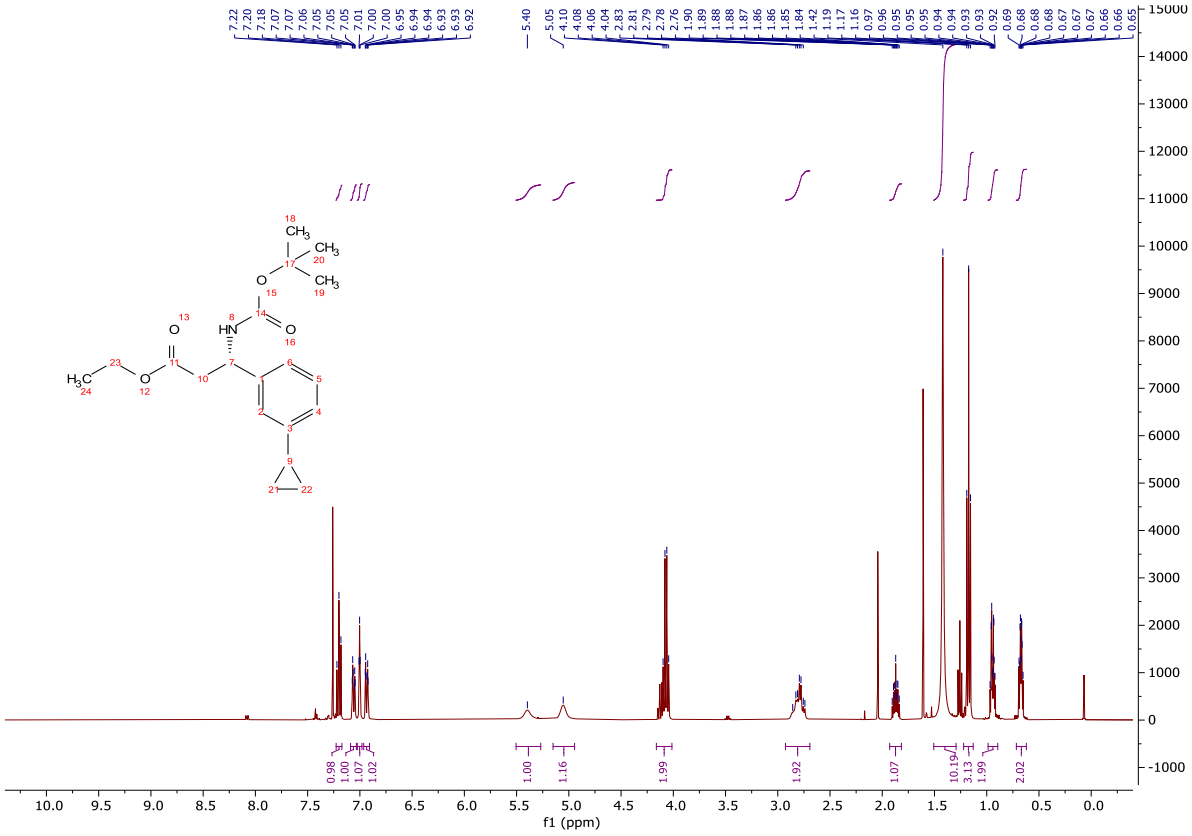
7.22 7.20 7.18 7.07 7.07 7.06 7.05 7.05 7.01 7.00 7.00 6.95 6.94 6.94 6.93 6.93 6.92
5.40 5.05 4.10 4.08 4.06 4.04 2.83 2.81 2.79 2.78 2.76 1.90 1.89 1.88 1.88 1.87 1.86 1.86 1.85 1.84 1.42 1.19 1.17 1.16 0.97 0.96 0.95 0.95 0.95 0.94 0.94 0.93 0.93 0.92 0.69 0.68 0.68 0.68 0.67 0.67 0.67 0.66 0.66 0.65
0.98 1.00 1.07 1.02 1.00 1.16 1.99 1.92 1.07 10.19 3.13 1.99 2.02
f1 (ppm)

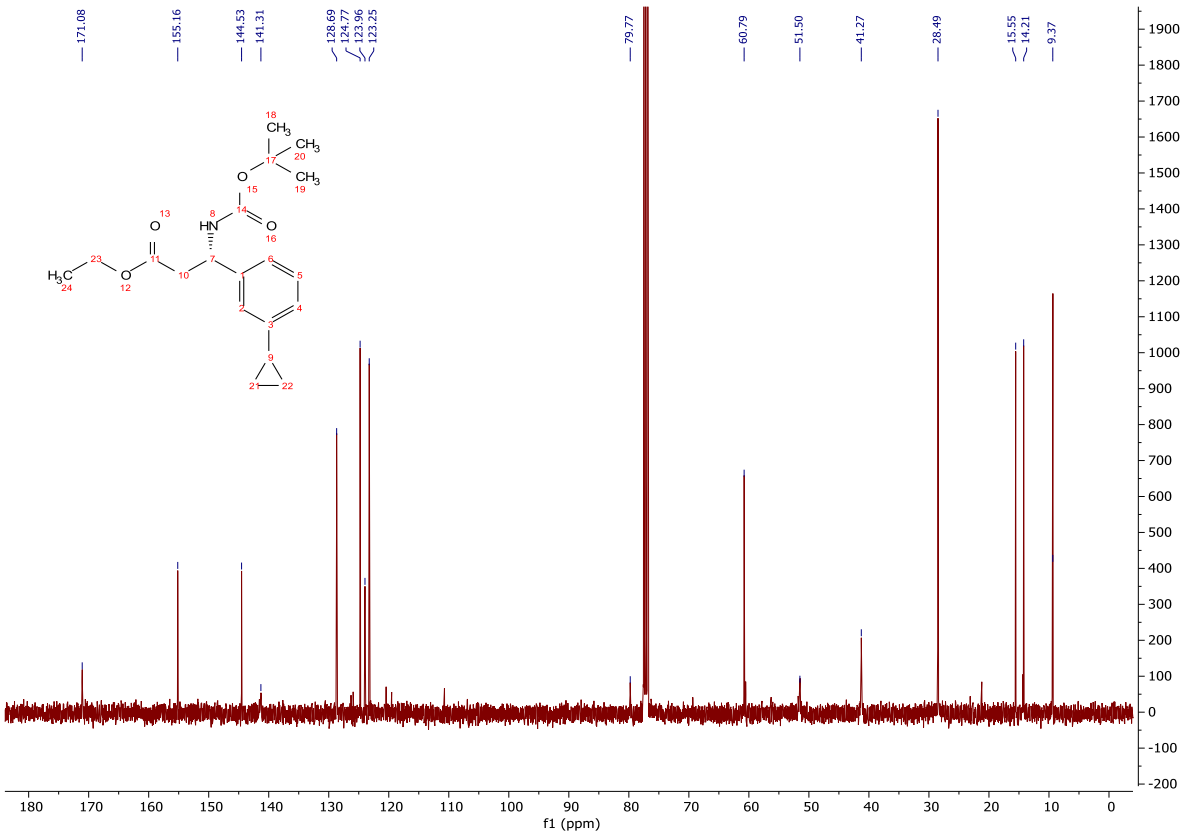
171.08 155.16 144.53 141.31 128.69 124.77 123.96 123.25 79.77 60.79 51.50 41.27 28.49 15.55 14.21 9.37
f1 (ppm)

tert-Butyl 7-(5-((3-isopropoxy-3-oxo-1-(3-(trifluoromethyl)phenyl)propyl)amino)-5-oxopentyl)-3,4-dihydro-1,8-naphthyridine-1(2*H*)-carboxylate (**258**)

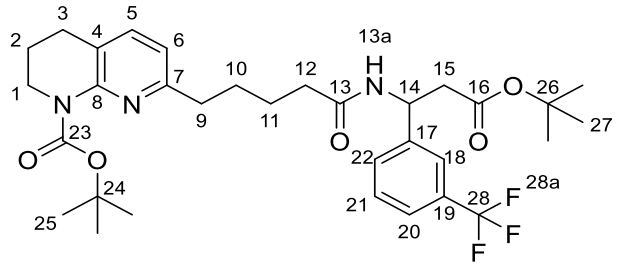

To a stirred solution of **82** (629 mg, 1.85 mmol) and **116** (600 mg, 1.85 mmol) in acetonitrile (8.00 mL) at 0 °C was added T3P (50% in ethyl acetate, 0.920 mL, 3.08 mmol) and *i*-Pr_2NEt (1.07 mL, 6.16 mmol). The reaction mixture was stirred for 16 h. Ethyl acetate (10.0 mL) and sat. $NaHCO_{3(aq)}$ (10.0 mL) were added, the organic phase was separated, washed with sat. $NaHCO_{3(aq)}$ (2 x 10.0 mL), brine (2 x 10.0 mL), dried ($MgSO_4$) and concentrated *in vacuo* giving a yellow oil (1.02 g). The crude product was purified by column chromatography on silica gel, eluting with a gradient of ethyl acetate/light petroleum (0-80%) to afford the title compound as a clear oil (862 mg, 1.42 mmol, 77%); **HRMS** *m/z* (ESI^+) calc. for $C_{32}H_{43}F_3N_3O_5$ $[M+H]^+$ requires 606.3149, found 606.3151; $\boldsymbol{R_f}$ 0.48, 80% ethyl acetate/light petroleum, UV active; δ_H (400 MHz, $CDCl_3$) 7.53 – 7.45 (3H, m, H-18, H-20 and H-22), 7.41 (1H, t, *J* = 7.6 Hz, H-21), 7.30 – 7.26 (1H, m, H-5), 6.95 – 6.90 (1H, m, H-13a), 6.79 (1H, d, *J* = 7.6 Hz, H-6), 5.42 (1H, m, H-14), 3.76 – 3.72 (2H, m, H-1), 2.82 – 2.68 (6H, m, H-3, H-9 and H-15), 2.29 (2H, t, *J* = 7.2 Hz, H-12), 1.95 – 1.87 (2H, m, H-2), 1.75 (4H, m, H-10 and H-11), 1.50 (9H, s, H-27), 1.31 (9H, s, H-25); δ_C (100 MHz, $CDCl_3$) 172.4 (CO), 170.3 (CO), 158.0 (C), 154.0 (CO), 151.0 (C), 142.1 (C), 137.2 (ArH), 130.8 (C, q, *J* = 32.2 Hz), 130.1 (ArH), 129.0 (ArH), 125.4 (CF_3), 124.3 (ArH, q, *J* = 3.7 Hz), 123.0 (ArH, q, *J* = 3.7 Hz), 121.9 (C), 118.3 (ArH), 81.7 (C), 80.7 (C), 49.2 (CH), 44.9 (CH_2), 40.9 (CH_2), 37.4 (CH_2), 36.5 (CH_2), 29.0 (CH_2), 28.4 (CH_3), 27.9 (CH_3), 26.3 (CH_2), 25.3 (CH_2), 23.3 (CH_2); δ_F (376 MHz, $CDCl_3$) -62.6 (F-28a); ν_{max} (FT-ATR/cm^{-1}) 1658, 1601, 1367, 1327, 1150, 1125, 1074, 907, 728.

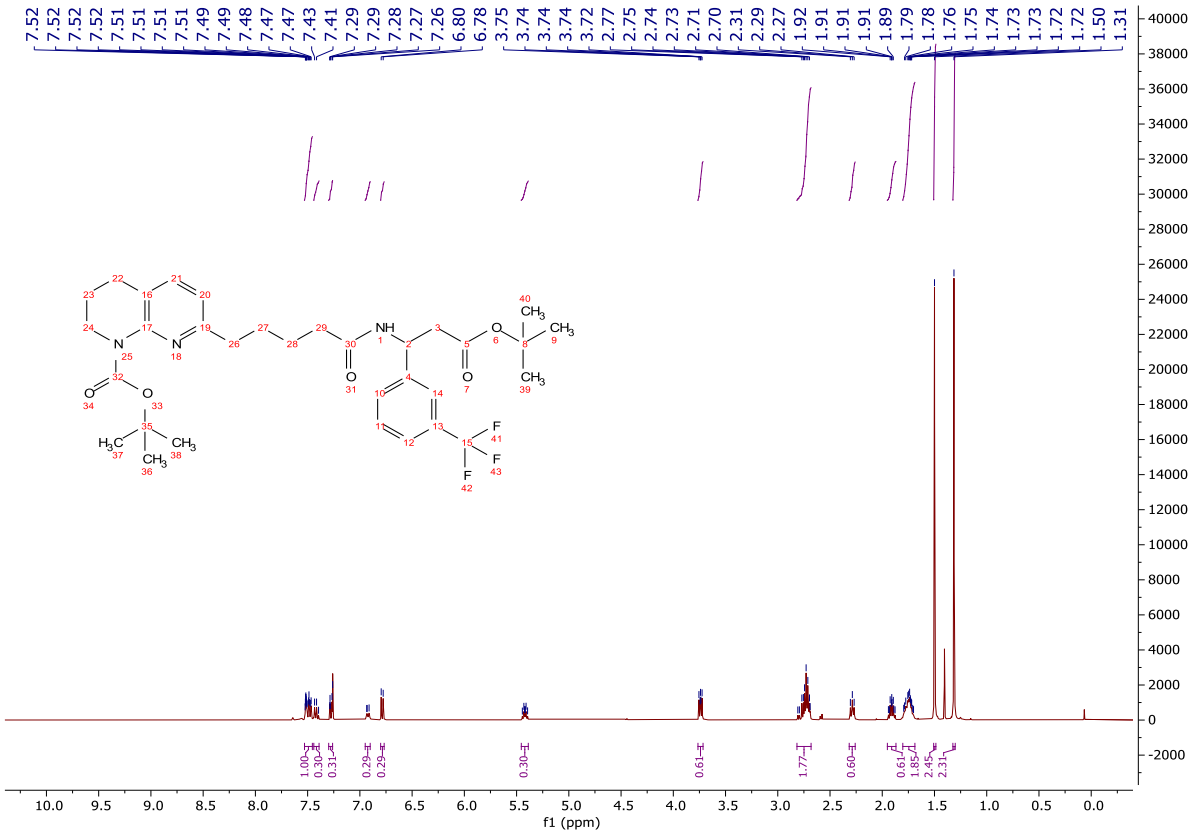
7.52 7.52 7.52 7.52 7.51 7.51 7.51 7.51 7.49 7.49 7.48 7.47 7.47 7.43 7.41 7.29 7.29 7.28 7.27 7.26 6.80 6.78 3.75 3.74 3.74 3.74 3.72 2.77 2.75 2.74 2.73 2.71 2.70 2.31 2.29 2.27 1.92 1.91 1.91 1.91 1.89 1.79 1.78 1.76 1.75 1.74 1.73 1.73 1.72 1.72 1.50 1.31
1.00 0.39 0.31 0.29 0.29 0.30 0.61 1.77 0.60 0.61 1.85 2.45 2.31
f1 (ppm)

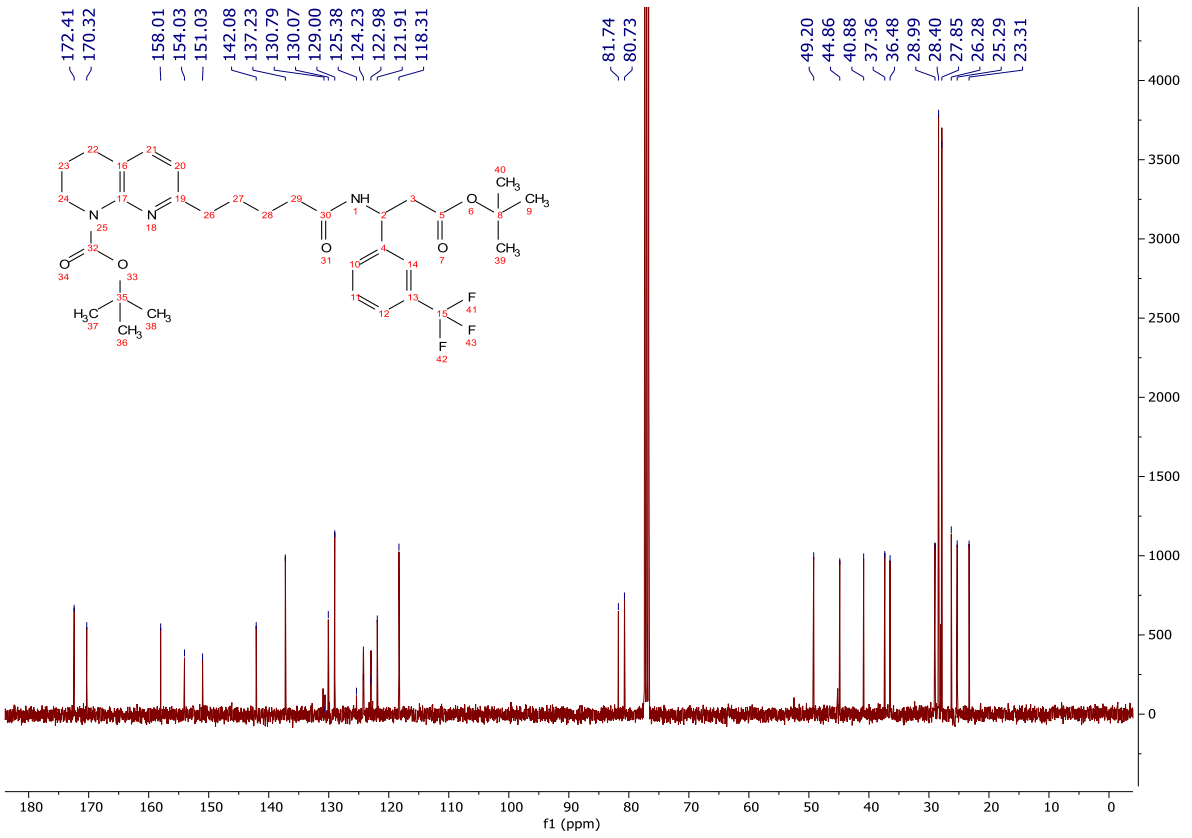
172.41 170.32 158.01 154.03 151.03 142.08 137.23 130.79 130.07 129.00 125.38 124.23 122.98 121.91 118.31 81.74 80.73 49.20 44.86 40.88 37.36 36.48 28.99 28.40 27.85 26.28 25.29 23.31
f1 (ppm)

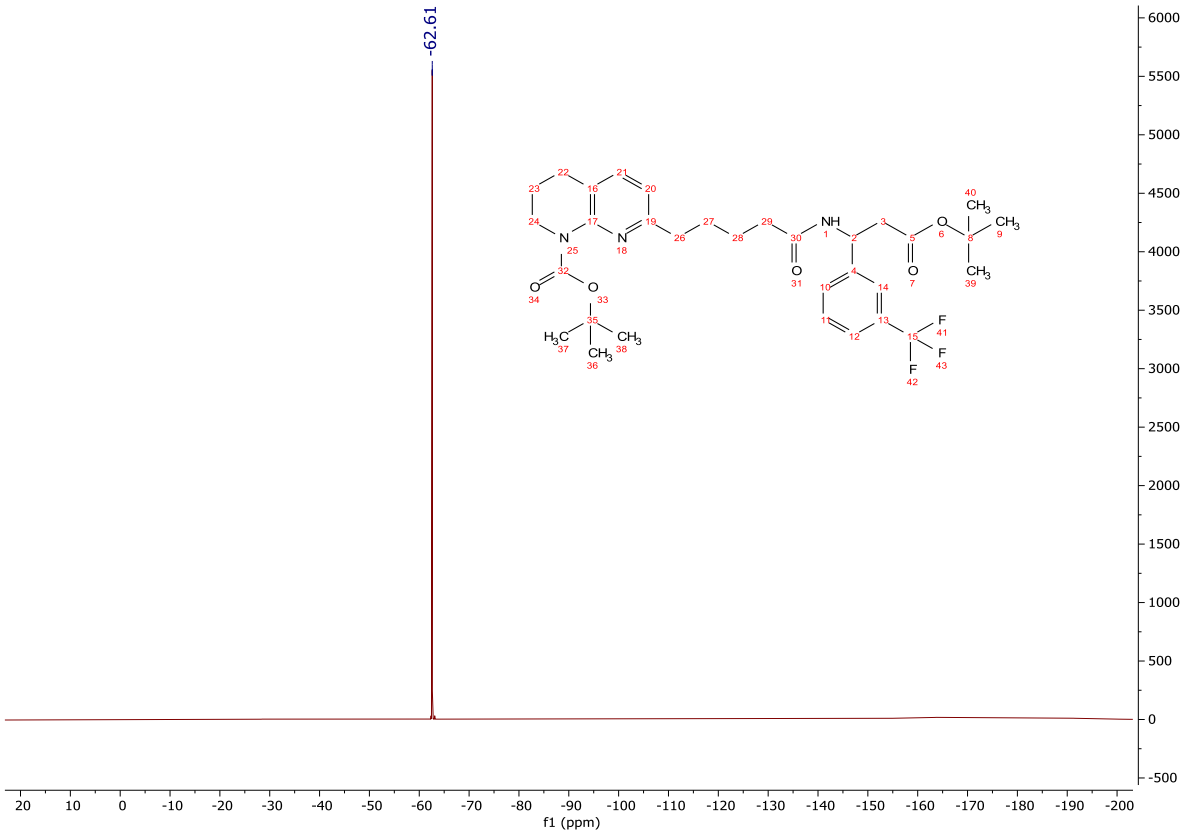
-62.61
6000
5500
5000
4500
4000
3500
3000
2500
2000
1500
1000
500
0
-500
20
10
0
-10
-20
-30
-40
-50
-60
-70
-80
-90
-100
-110
-120
-130
-140
-150
-160
-170
-180
-190
-200
f1 (ppm)

tert-Butyl 7-(5-((3-(*tert*-butoxy)-3-oxo-1-(3-(trifluoromethyl)phenyl)propyl)(methyl)amino)-5-oxopentyl)-3,4-dihydro-1,8-naphthyridine-1(2*H*)-carboxylate (**259**)

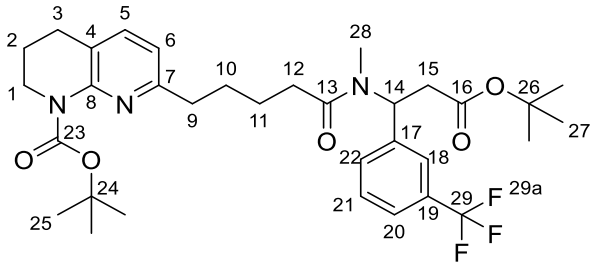

To a stirred solution of **258** (250 mg, 0.410 mmol) in anhydrous DMF (4.00 mL) at 0 °C was added NaH (60% solid in mineral oil, 16 mg, 0.410 mmol). The reaction mixture was stirred for 1 h. Iodomethane (0.130 mL, 2.05 mmol) was added, and the reaction mixture stirred for 16 h. Ethyl acetate (10.0 mL) and water (10.0 mL) were added, the organic phase was separated, washed with water (2 x 20.0 mL), sat. $NaHCO_{3(aq)}$ (2 x 20.0 mL) and brine (2 x 20.0 mL), dried ($MgSO_4$) and concentrated *in vacuo* giving a yellow oil (225 mg). The crude product was purified by column chromatography on silica gel, eluting with a gradient of ethyl acetate/light petroleum (0-80%) to afford the title compound as a clear oil (83 mg, 0.134 mmol, 33%); **HRMS** *m/z* (ESI^+) calc. for $C_{33}H_{45}F_3N_3O_5$ $[M+H]^+$ requires 620.3306, found 620.3302; $\boldsymbol{R_f}$ 0.37, 50% ethyl acetate/light petroleum, UV active; δ_H (400 MHz, $CDCl_3$) 7.60 – 7.34 (4H, m, H-18, H-20, H-21 and H-22), 7.30 – 7.19 (1H, m, H-5), 6.81 (1H, d, *J* = 7.6 Hz, H-6), 6.34 (1H, t, *J* = 8.1 Hz, H-14 Rotamer A), 5.58 – 5.47 (1H, m, H-14 Rotamer B), 3.77 – 3.68 (2H, m, H-1), 3.08 – 2.61 (11H, m, H-3, H-9, H-12 Rotamer A, H-15 and H-28), 2.57 – 2.45 (2H, m, H-12 Rotamer B), 2.43 – 2.28 (2H, m, H-12 Rotamer C), 1.96 – 1.86 (2H, m, H-2), 1.86 – 1.61 (4H, m, H-10 and H-11), 1.55 – 1.30 (18H, m, H-25 and H-27); δ_C (101 MHz, $CDCl_3$) 173.4 (CO*), 173.3 (CO), 169.6 (CO*), 169.6 (CO), 158.2 (C), 154.2 (CO), 151.2 (C), 140.4 (C), 140.0 (C*), 137.3 (ArH), 137.3 (ArH*), 131.2 (ArH), 131.0 (C, q, *J* = 32.3 Hz), 130.1 (ArH*), 129.7 (ArH*), 129.2 (ArH), 125.0 (ArH*), 124.6 (ArH, q, *J* = 3.8 Hz), 124.1 (CF_3, q, *J* = 272.6 Hz), 124.0 (ArH, q, *J* = 3.8 Hz), 123.1 (ArH*), 122.0 (C), 121.9 (C*), 118.4 (ArH), 82.1 (C*), 81.4 (C), 80.8 (C), 56.2 (CH*), 52.3 (CH), 44.9 (CH_2), 44.8 (CH_2*), 38.7 (CH_2*), 37.9 (CH_2*), 37.8 (CH_2), 37.0

(CH_2), 33.9 (CH_2), 33.2 (CH_2*), 30.4 (CH_3), 29.4 (CH_2), 28.5 (CH_3), 28.1 (CH_3*), 28.0 (CH_3), 26.4 (CH_2), 25.1 (CH_2*), 24.9 (CH_2), 23.4 (CH_2); δ_F (376 MHz, DMSO-d_6) -61.0 (F-29a); ν_{max} (FT-ATR/cm^{-1}) 1728, 1694, 1330, 1126.

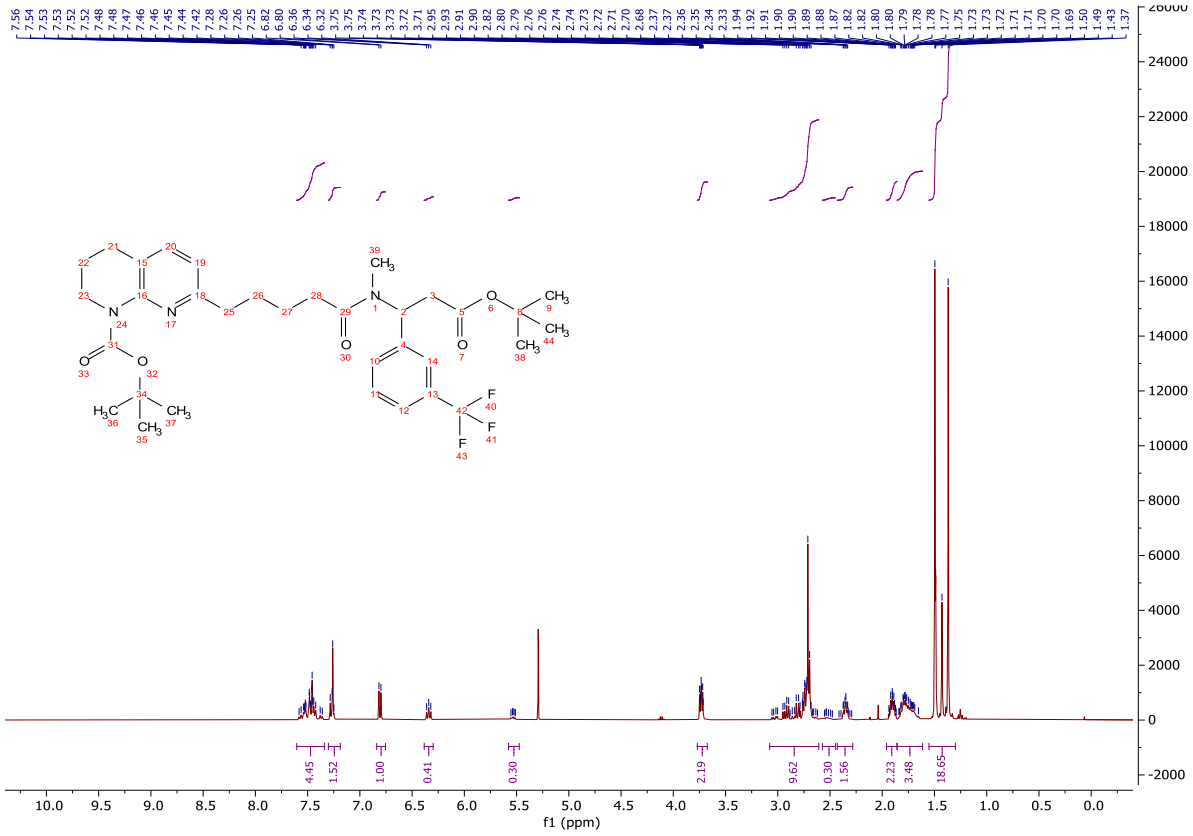
f1 (ppm)

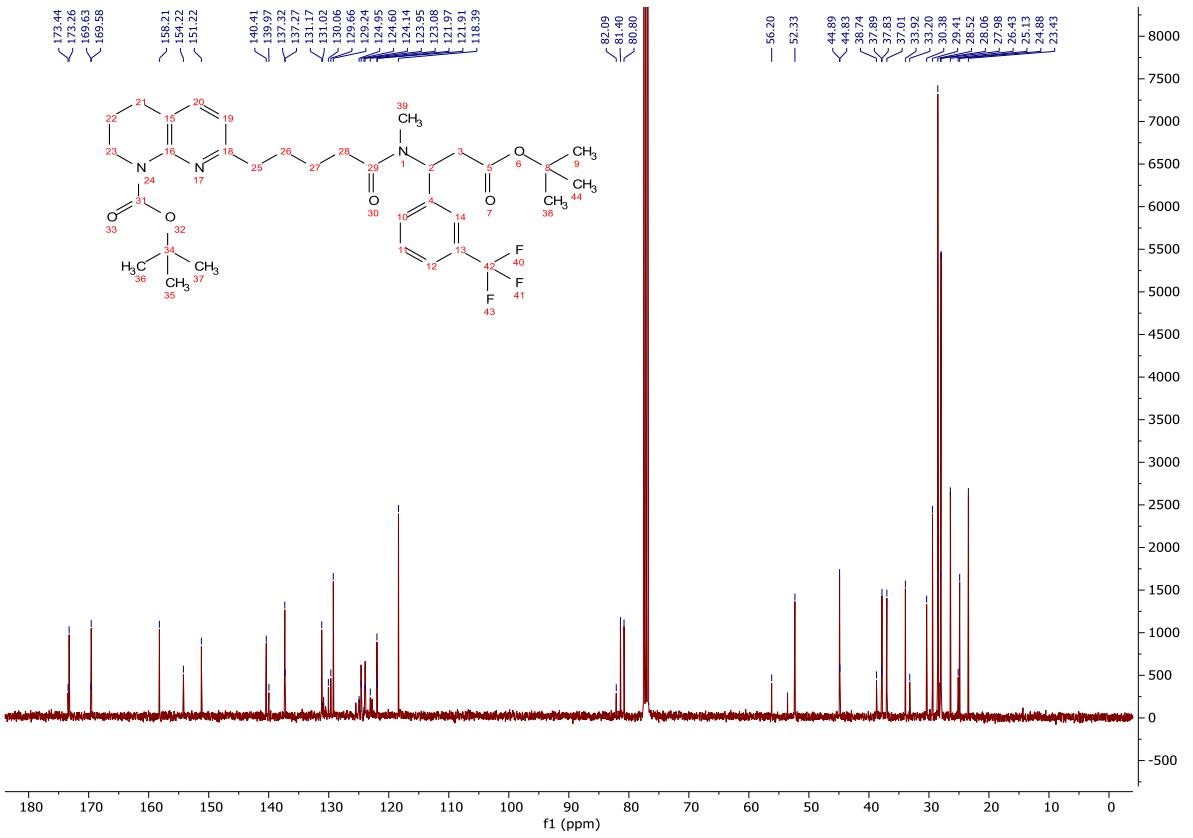
f1 (ppm)

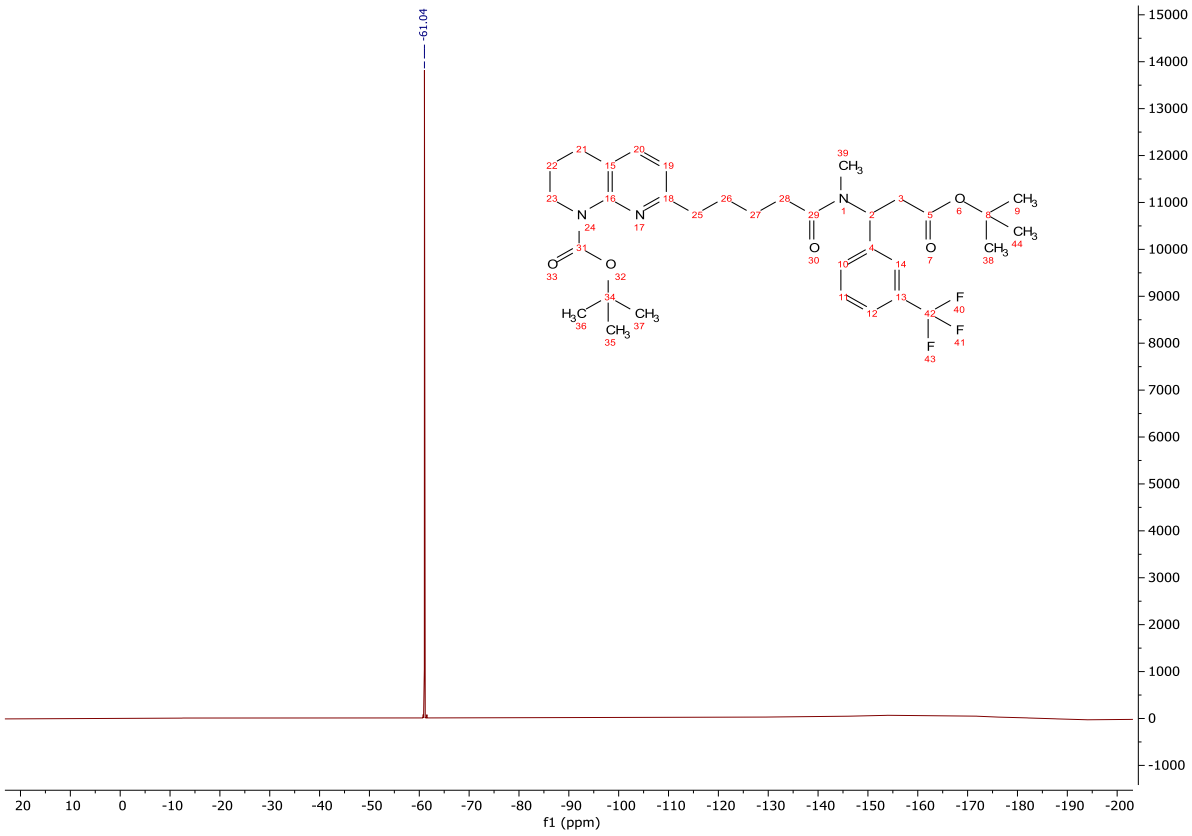
-61.04
15000
14000
13000
12000
11000
10000
9000
8000
7000
6000
5000
4000
3000
2000
1000
0
-1000
20 10 0 -10 -20 -30 -40 -50 -60 -70 -80 -90 -100 -110 -120 -130 -140 -150 -160 -170 -180 -190 -200
f1 (ppm)

3-(N-Methyl-5-(5,6,7,8-tetrahydro-1,8-naphthyridin-2-yl)pentanamido)-3-(3-(trifluoromethyl)phenyl)propanoic acid (**255**)

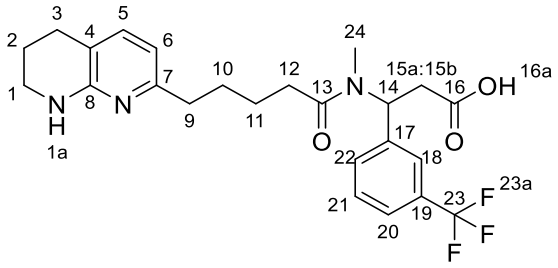

To a stirred solution of **259** (53 mg, 0.086 mmol) in CH_2Cl_2 (6.00 mL) at rt was added TFA (6.00 mL). The reaction mixture was stirred for 17 h, concentrated *in vacuo* and purified on a Waters OASIS® HLB cartridge to afford the title compound as a clear oil (38 mg, 0.082 mmol, 95%); **HRMS** *m/z* (ESI^+) calc. for $C_{24}H_{29}F_3N_3O_3$ $[M+H]^+$ requires 464.2156, found 464.2169; $\boldsymbol{R_f}$ 0.43, 2% methanol/CH_2Cl_2, UV active; δ_H (400 MHz, MeOD) 7.67 – 7.51 (4H, m, H-18, H-20, H-21 and H-22), 7.48 – 7.37 (1H, m, H-5), 6.53 – 6.44 (1H, m, H-6), 6.37 (1H, dd, *J* = 12.3, 3.8 Hz, H-14 Rotamer A), 5.92 – 5.84 (1H, m, H-14 Rotamer B), 3.81 – 3.68 (2H, m, H-12 Rotamer A), 3.50 – 3.38 (2H, m, H-1), 3.06 (1H, dd, *J* = 14.9, 3.8 Hz, H-15a Rotamer A), 3.01 – 2.85 (5H, m, H-15b Rotamer A, H-15a Rotamer B, H-24 Rotamer A), 2.85 – 2.52 (9H, m, H-3, H-9 Rotamer A, H-15b Rotamer B and H-24 Rotamer B), 2.43 – 2.27 (4H, m, H-9 Rotamer B and H-12 Rotamer B), 2.11 – 1.50 (8H, m, H-2, H-10 Rotamer A, H-11 and H-12 Rotamer C, 1.48 – 1.34 (2H, m, H-10 Rotamer B); δ_C (101 MHz, MeOD) 179.7 (CO), 176.1 (CO*), 175.8 (CO), 153.9 (C*), 153.8 (C), 151.1 (C), 150.8 (C*), 142.9 (ArH*), 142.2 (C*), 142.0 (ArH), 141.9 (C), 132.1 (C), 132.1 (ArH, q, *J* = 32.3 Hz), 130.8 (ArH), 130.5 (ArH*), 125.6 (ArH, q, *J* = 3.8 Hz), 125.55 (CF_3, q, *J* = 271.4 Hz), 125.3 (ArH*, q, *J* = 3.8 Hz), 125.0 (ArH*, q, *J* = 3.8 Hz), 124.6 (ArH, q, *J* = 3.8 Hz), 119.9 (C*), 119.7 (C), 111.2 (ArH*), 111.0 (ArH), 58.3 (CH), 54.8 (CH*), 41.7 (CH_2), 41.6 (CH_2*), 39.9 (CH_2), 38.5 (CH_2*), 33.3 (CH_2), 32.9 (CH_2*), 32.0 (CH_2*), 30.7 (CH_3), 30.6 (CH_2), 30.3 (CH_2), 29.4 (CH_2*), 28.4 (CH_3*), 26.5 (CH_2*), 26.4 (CH_2), 25.1 (CH_2*), 23.9 (CH_2), 20.80 (CH_2*), 20.77 (CH_2); δ_F (376 MHz, MeOD) -64.1 (F-23a); ν_{max} (FT-ATR/cm^{-1}) 3333, 1631, 1329, 1121.

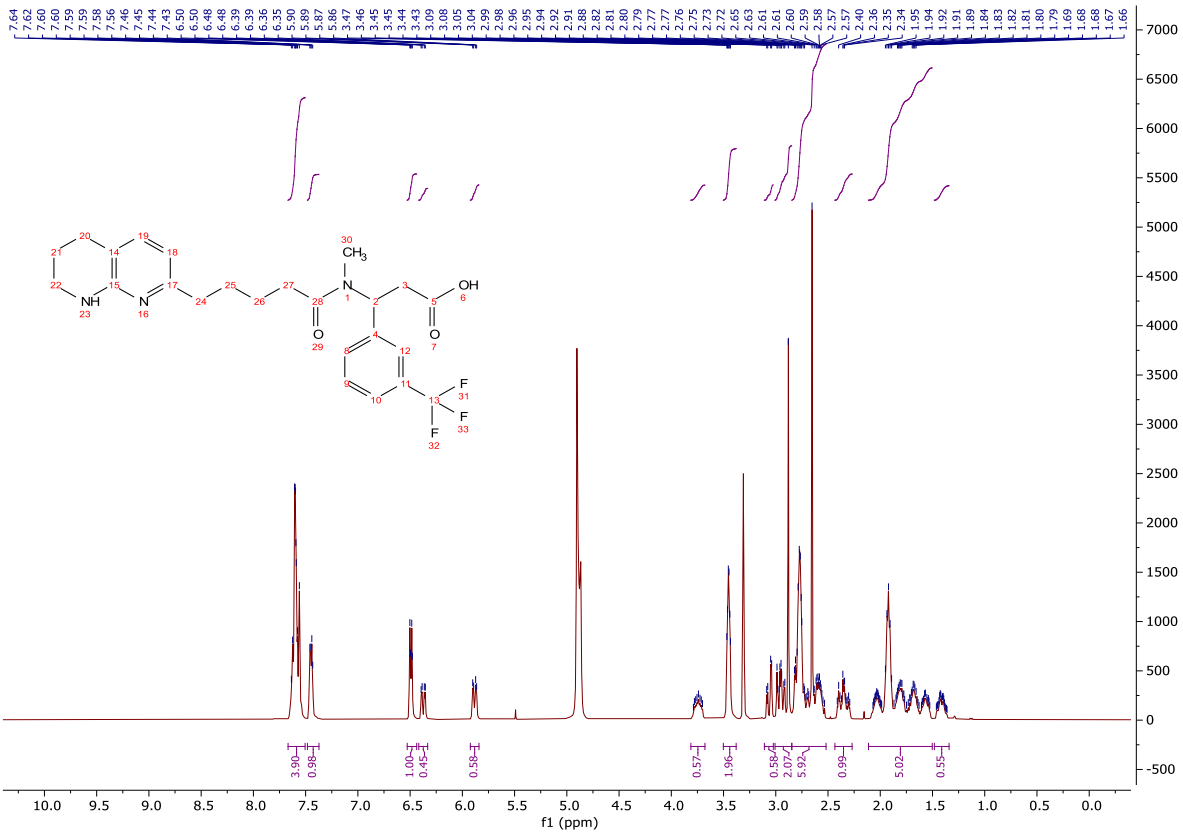
f1 (ppm)

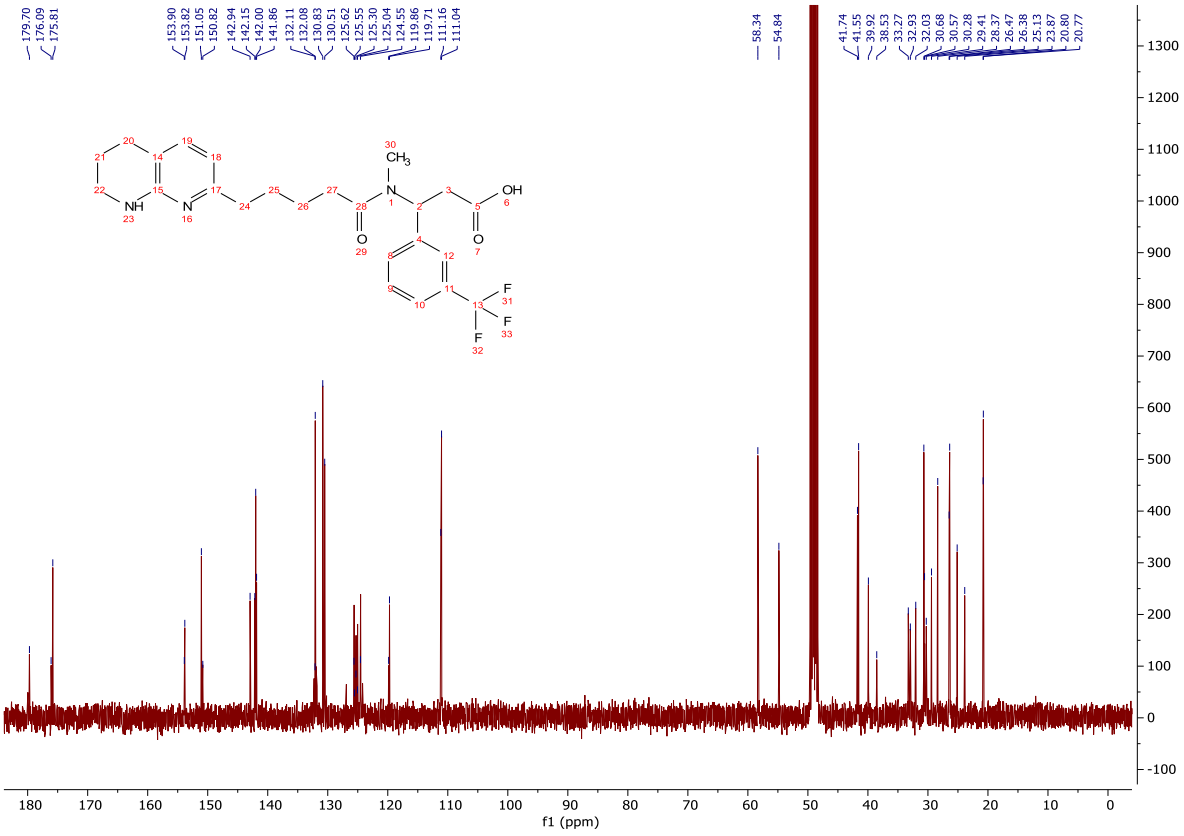
f1 (ppm)

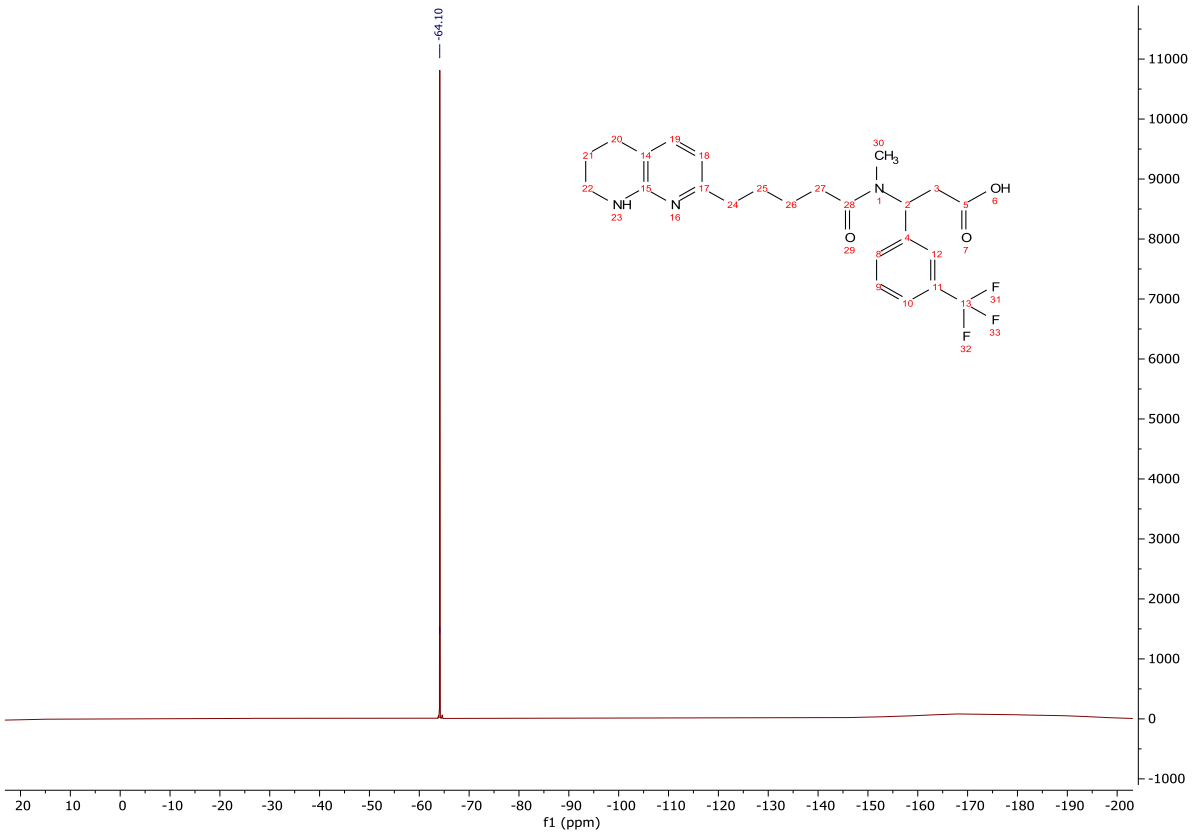
-64.10
11000
10000
9000
8000
7000
6000
5000
4000
3000
2000
1000
0
-1000
20 10 0 -10 -20 -30 -40 -50 -60 -70 -80 -90 -100 -110 -120 -130 -140 -150 -160 -170 -180 -190 -200
f1 (ppm)
CH3
OH
NH
N
O
F
F
F

tert-Butyl 3-((2-nitrophenyl)sulfonamido)-3-(3-(trifluoromethyl)phenyl)propanoate (**266**)

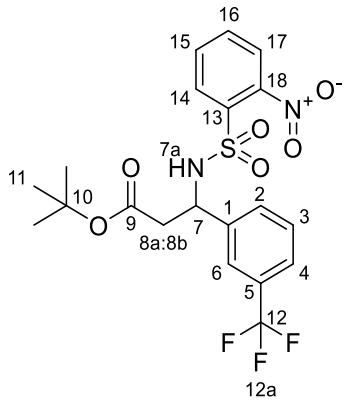

A solution of **116** (2.86 g, 9.90 mmol) in CH_2Cl_2 (100 mL) was cooled to 0 °C. 2-nitrobenzenesulfonyl chloride (2.42 g, 10.9 mmol) was added portion wise. *i*-Pr_2NEt (5.20 mL, 29.7 mmol) was added dropwise over 5 min and the reaction solution stirred for 16 h. The organic reaction solution was washed successively with sat. $NH_4Cl_{(aq)}$ (2 x 50.0 mL), sat. $NaHCO_{3(aq)}$ (2 x 50.0 mL), brine (2 x 50.0 mL), dried ($MgSO_4$) and concentrated *in vacuo* to afford the title compound as a yellow oil (4.42 g, 9.31 mmol, 94%). The crude product was not purified further; **HRMS** *m/z* (ESI^+) calc. for $C_{20}H_{21}F_3N_2NaO_6S$ $[M+Na]^+$ requires 497.0965, found 497.0961; $\boldsymbol{R_f}$ 0.59, 30% ethyl acetate/light petroleum, UV active; δ_H (400 MHz, $CDCl_3$) 7.73 (1H, dd, *J* = 8.0, 1.3 Hz, H-17), 7.62 (1H, dd, *J* = 7.9, 1.4 Hz, H-14), 7.54 (1H, ddd, *J* = 7.8, 7.8, 1.4 Hz, H-15), 7.44 – 7.31 (4H, m, H-2, H-4, H-6 and H-16), 7.30 – 7.23 (1H, m, H-3), 6.84 (1H, d, *J* = 9.0 Hz, H-7a), 5.03 (1H, dt, *J* = 9.1, 6.0 Hz, H-7), 2.84 (1H, dd, *J* = 15.8, 5.9 Hz, H-8a), 2.77 (1H, dd, *J* = 15.8, 6.1 Hz, H-8b), 1.35 (9H, s, H-11); δ_C (101 MHz, $CDCl_3$) 169.2 (CO), 147.5 (C), 140.1 (C), 134.4 (C), 133.4 (ArH), 132.5 (ArH), 130.9 (C, q, *J* = 32.3 Hz), 130.6 (ArH), 130.3 (ArH), 129.2 (ArH), 125.2 (ArH), 124.8 (ArH, q, *J* = 3.8 Hz), 123.7 (CF_3, q, *J* = 272.6 Hz), 123.6 (ArH, q, *J* = 3.8 Hz), 82.6 (C), 55.4 (CH), 42.5 (CH_2), 28.0 (CH_3); δ_F (376 MHz, $CDCl_3$) -62.8 (F-12a); ν_{max} (FT-ATR/cm^{-1}) 1708, 1534, 1366, 1356, 1314, 1125, 569.

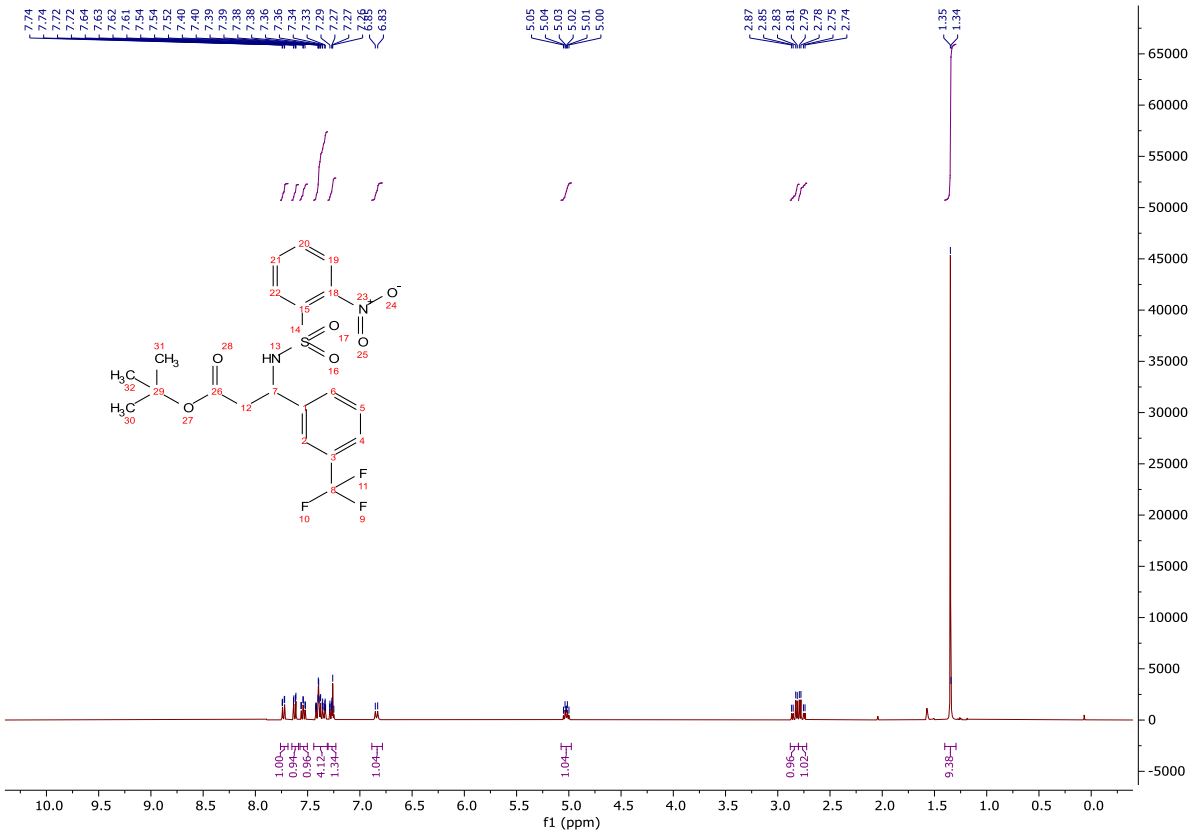
7.74
7.74
7.72
7.72
7.64
7.63
7.62
7.61
7.54
7.54
7.52
7.40
7.40
7.39
7.39
7.38
7.38
7.36
7.36
7.34
7.33
7.29
7.27
6.85
6.83
5.05
5.04
5.03
5.02
5.01
5.00
2.87
2.85
2.83
2.81
2.79
2.78
2.75
2.74
1.35
1.34
1.00
0.94
0.96
4.12
1.34
1.04
1.04
0.96
1.02
9.38
f1 (ppm)

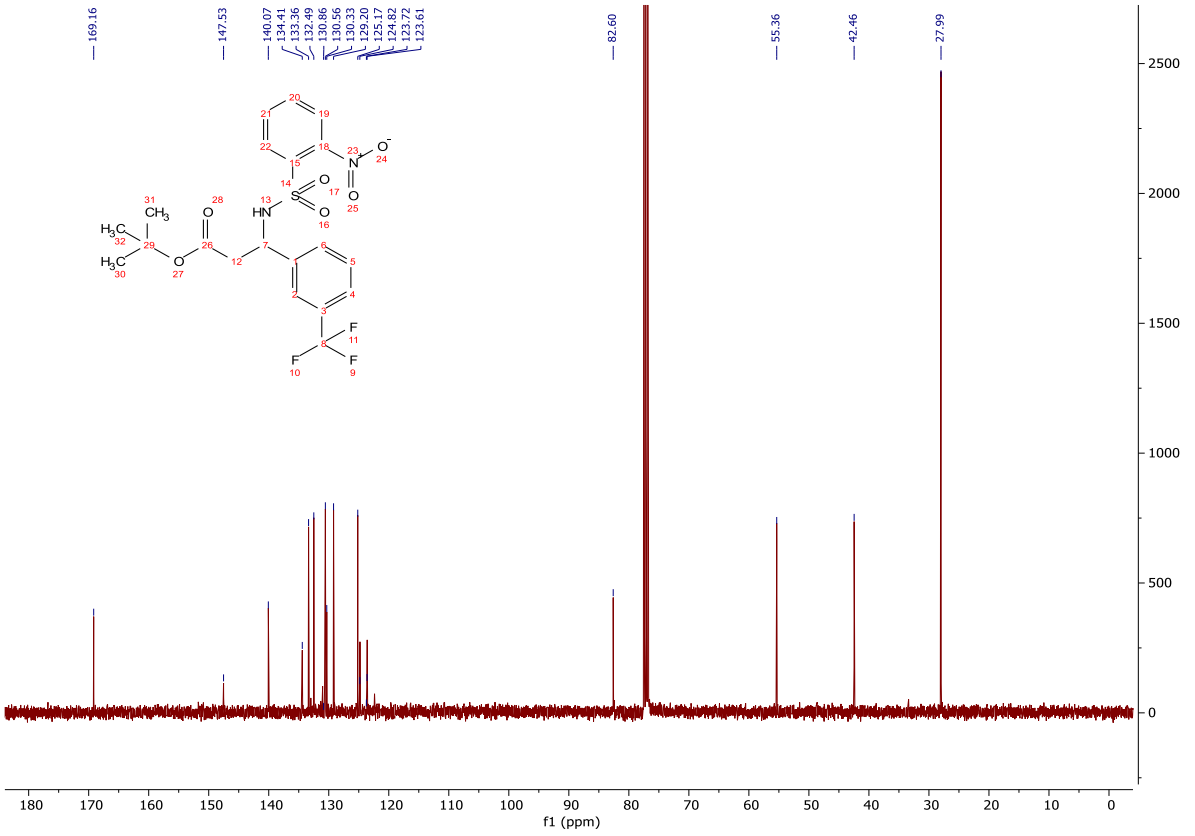
169.16
147.53
140.07
134.41
133.36
132.49
130.86
130.56
130.33
129.20
125.17
124.82
123.72
123.61
82.60
55.36
42.46
27.99
f1 (ppm)

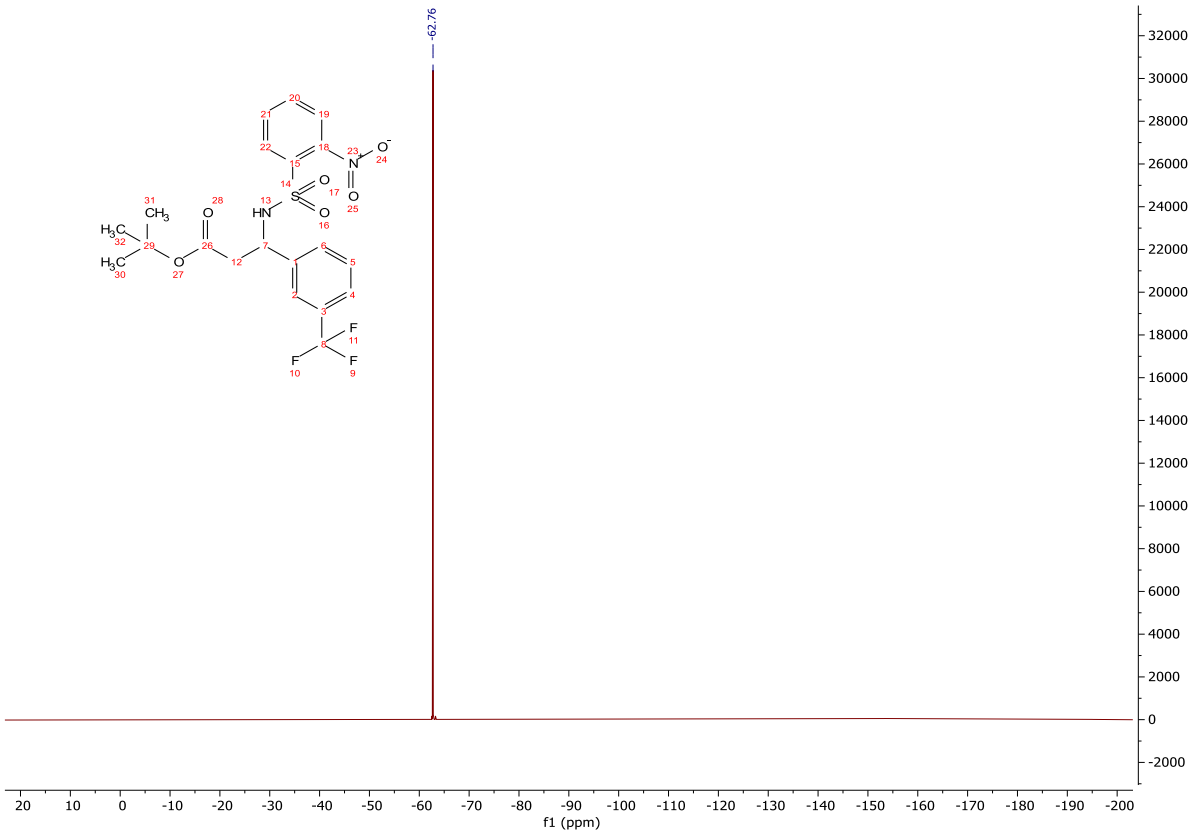
-62.76
32000
30000
28000
26000
24000
22000
20000
18000
16000
14000
12000
10000
8000
6000
4000
2000
0
-2000
20 10 0 -10 -20 -30 -40 -50 -60 -70 -80 -90 -100 -110 -120 -130 -140 -150 -160 -170 -180 -190 -200
f1 (ppm)

tert-Butyl 3-((2-nitrophenyl)sulfonamido)-3-(3-(trifluoromethyl)phenyl)propanoate (**267**)

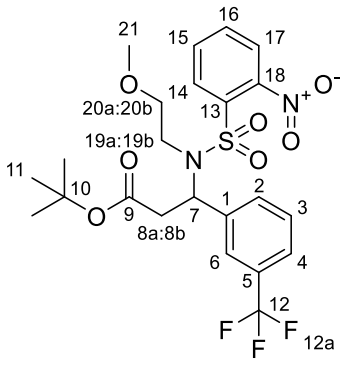

To a stirred solution of **266** (500 mg, 1.05 mmol), triphenylphosphine (370 mg, 1.37 mmol) and DEAD (0.630 mL, 1.37 mmol) in toluene (7.00 mL) at 0 °C was added 2-methoxy ethanol (0.130 mL, 1.58 mmol). The reaction mixture was heated at 60 °C and stirred for 1 h. The reaction mixture was cooled to rt, diluted with ethyl acetate (10.0 mL), washed with sat. $NaHCO_{3(aq)}$ (2 x 10.0 mL) and brine (2 x 10.0 mL), dried ($MgSO_4$) and concentrated *in vacuo* to afford an orange oil. The crude product was purified by column chromatography on silica gel, eluting with a gradient of ethyl acetate/light petroleum (0-30%) to afford the title compound as a yellow oil (448 mg, 0.842 mmol, 80%); **HRMS** *m/z* (ESI^+) calc. for $C_{23}H_{27}F_3N_2NaO_7S$ $[M+Na]^+$ requires 555.1383, found 555.1387; $\boldsymbol{R_f}$ 0.39, 30% ethyl acetate/light petroleum, UV active; $\boldsymbol{\delta_H}$ (400 MHz, $CDCl_3$) 8.01 – 7.96 (1H, m, H-17), 7.74 – 7.67 (1H, m, H-14), 7.66 – 7.59 (2H, m, H-15 and H-16), 7.53 – 7.46 (2H, m, H-2 and H-4), 7.41 (1H, dd, *J* = 7.8, 7.8 Hz, H-3), 7.37 – 7.34 (1H, m, H-6), 5.48 (1H, dd, *J* = 11.0, 4.4 Hz, H-7), 3.55 – 3.35 (2H, m, H-19a and H-20a), 3.33 – 3.17 (6H, m, H-8a, H-19b, H-20b and H-21), 2.96 (1H, dd, *J* = 16.1, 4.4 Hz, H-8b), 1.36 – 1.22 (9H, m, H-11); $\boldsymbol{\delta_C}$ (101 MHz, $CDCl_3$) 169.3 (CO), 148.1 (C), 138.4 (C), 133.9 (ArH), 133.6 (C), 131.8 (ArH), 131.7 (ArH), 131.4 (ArH), 131.0 (C, q, *J* = 32.3 Hz), 129.2 (ArH), 125.2 (ArH, q, *J* = 3.8 Hz), 125.0 (ArH, q, *J* = 3.8 Hz), 124.3 (ArH), 122.6 (CF_3), 81.7 (C), 72.1 (CH_2), 58.7 (CH_3), 57.5 (CH), 45.8 (CH_2), 38.8 (CH_2), 27.9 (CH_3); $\boldsymbol{\delta_F}$ (376 MHz, $CDCl_3$) -62.75 (F-12a); $\boldsymbol{\nu_{max}}$ (FT-ATR/cm^{-1}) 1725, 1544, 1369, 1329, 1159, 1122, 582.

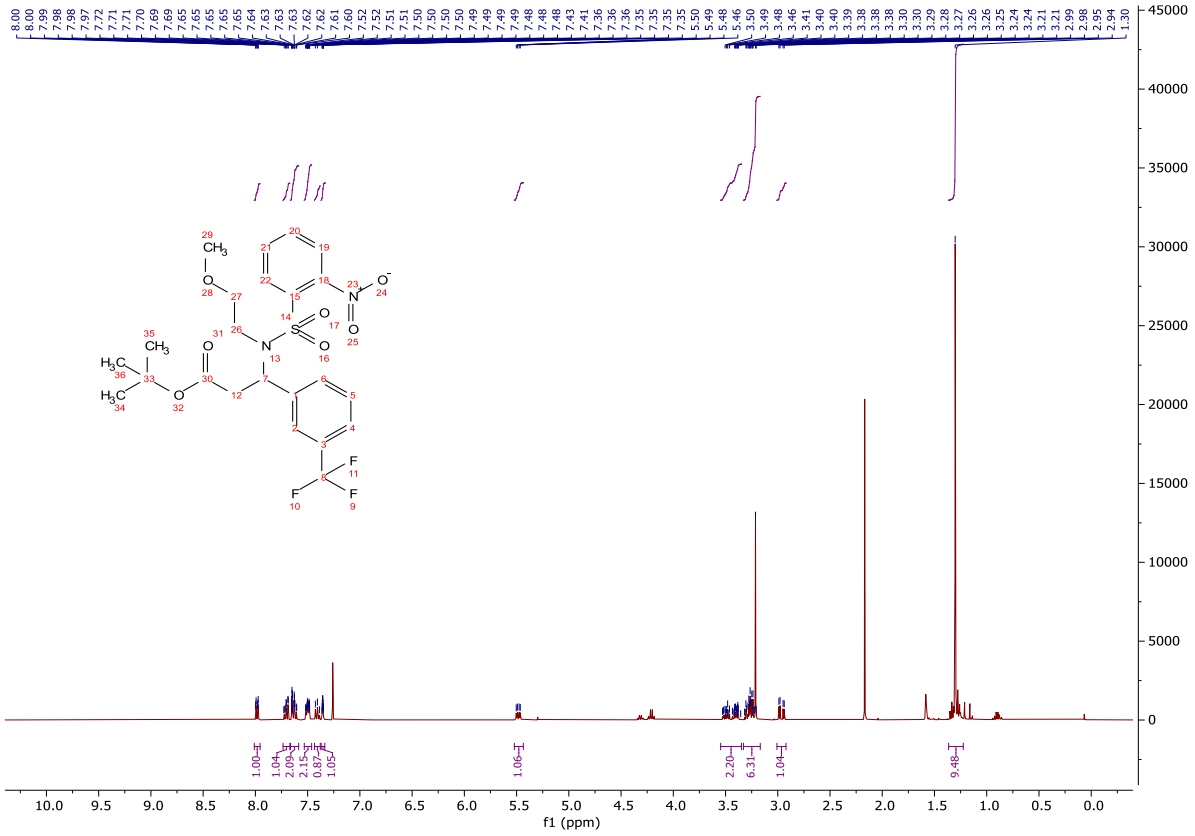
f1 (ppm)

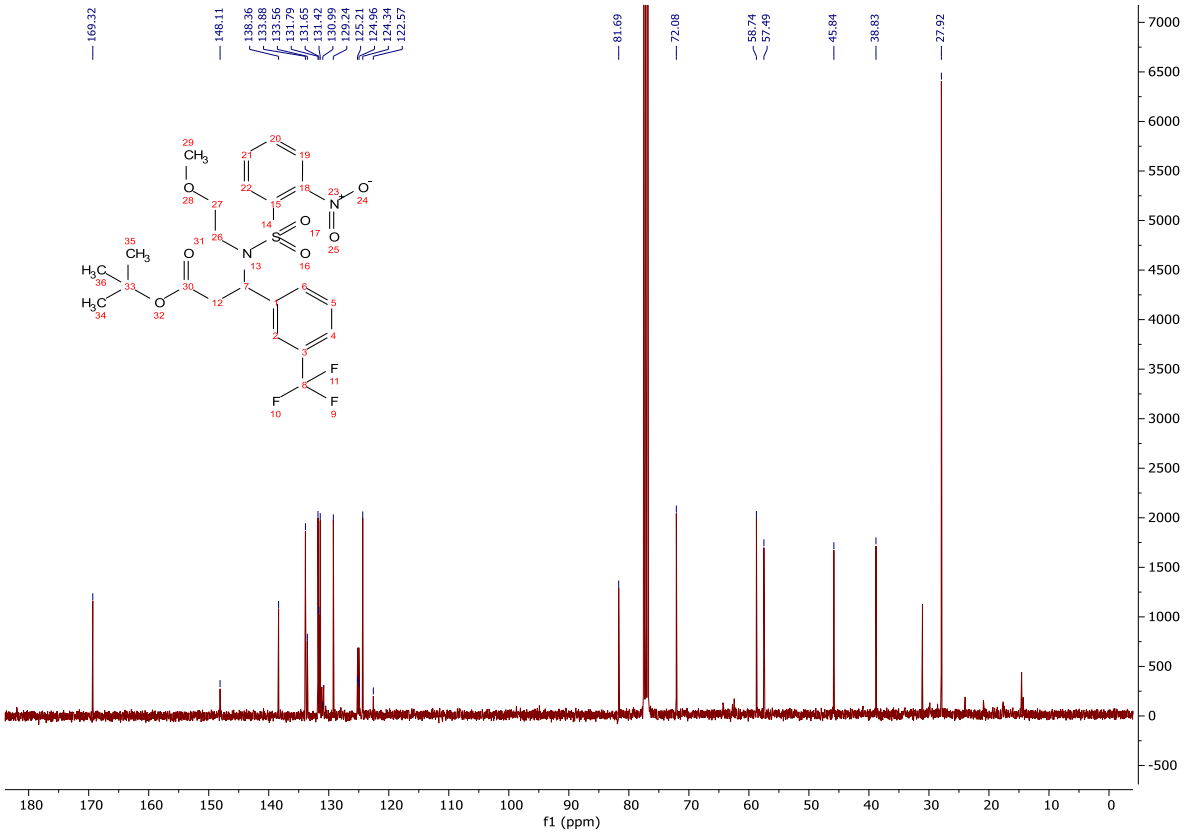
f1 (ppm)


-62.75
5000
4500
4000
3500
3000
2500
2000
1500
1000
500
0
20 10 0 -10 -20 -30 -40 -50 -60 -70 -80 -90 -100 -110 -120 -130 -140 -150 -160 -170 -180 -190 -200
f1 (ppm)

tert-Butyl 3-((*N*-(2-((*tert*-butyldimethylsilyl)oxy)ethyl)-2-nitrophenyl)sulfonamido)-3-(3-(trifluoromethyl)phenyl)propanoate (**270**)

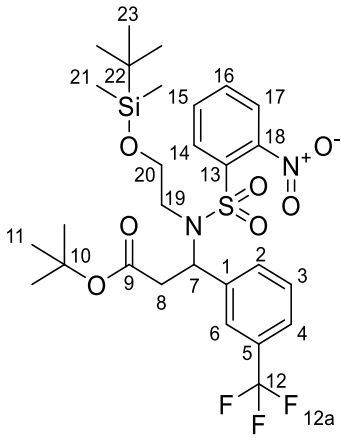

To a stirred solution of **266** (500 mg, 1.05 mmol), triphenylphosphine (370 mg, 1.37 mmol) and DEAD (0.630 mL, 1.37 mmol) in toluene (7.00 mL) at 0 °C was added 2-((*tert*-butyldimethylsilyl)oxy)-ethanol (280 mg, 1.58 mmol). The reaction mixture was heated at 60 °C and stirred for 1 h. The reaction mixture was cooled to rt, diluted with ethyl acetate (10.0 mL), washed with sat. $NaHCO_{3(aq)}$ (2 x 10.0 mL) and brine (2 x 10.0 mL), dried ($MgSO_4$) and concentrated *in vacuo* to afford an orange oil. The crude product was purified by column chromatography on silica gel, eluting with a gradient of ethyl acetate/light petroleum (0-20%) to afford the title compound as a colourless solid (378 mg, 0.598 mmol, 57%); **HRMS** *m/z* (ESI^+) calc. for $C_{28}H_{39}F_3N_2NaO_7SSi$ $[M+Na]^+$ requires 655.2092, found 655.2063; $\boldsymbol{R_f}$ 0.37, 20% ethyl acetate/light petroleum, UV active; δ_H (400 MHz, $CDCl_3$) 8.04 – 7.97 (1H, m, H-17), 7.74 – 7.68 (1H, m, H-14), 7.67 – 7.60 (2H, m, H-15 and H-16), 7.53 – 7.36 (4H, m, H-2, H-3 and H-4), 7.36 – 7.30 (1H, m, H-6), 5.44 (1H, dd, *J* = 11.4, 4.2 Hz, H-7), 3.74 – 3.61 (1H, m, H-20a), 3.49 – 3.28 (6H, m, H-8a, H-19a and H-20b), 3.23 – 3.11 (1H, m, H-19b), 3.01 – 2.92 (1H, m, H-8b), 1.32 – 1.23 (9H, m, H-11), 0.89 – 0.84 (9H, m, H-23), 0.03 – -0.02 (6H, m, H-21); δ_C (101 MHz, $CDCl_3$) 169.3 (CO), 148.1 (C), 138.4 (C), 133.9 (ArH), 133.6 (C), 131.8 (ArH), 131.7 (ArH), 131.4 (ArH), 131.1 (C, q, *J* = 32.7 Hz), 129.3 (ArH), 125.3 (ArH, q, *J* = 3.8 Hz), 124.8 (ArH, q, *J* = 3.8 Hz), 124.4 (ArH), 81.6 (C), 63.0 (CH_2), 57.3 (CH), 48.3 (CH_2), 39.0 (CH_2), 27.9 (CH_3), 26.0

(CH_3), 18.4 (C), -5.4 (CH_3); δ_F (376 MHz, $CDCl_3$) -62.7 (F-12a); **MP** 90-93 °C; ν_{max} (FT-ATR/cm^{-1}) 2953, 1714, 1546, 1365, 1331, 1252, 1162, 1130, 1095, 957, 832, 775, 586.

N.B. One quaternary carbon is not observed: C-12.

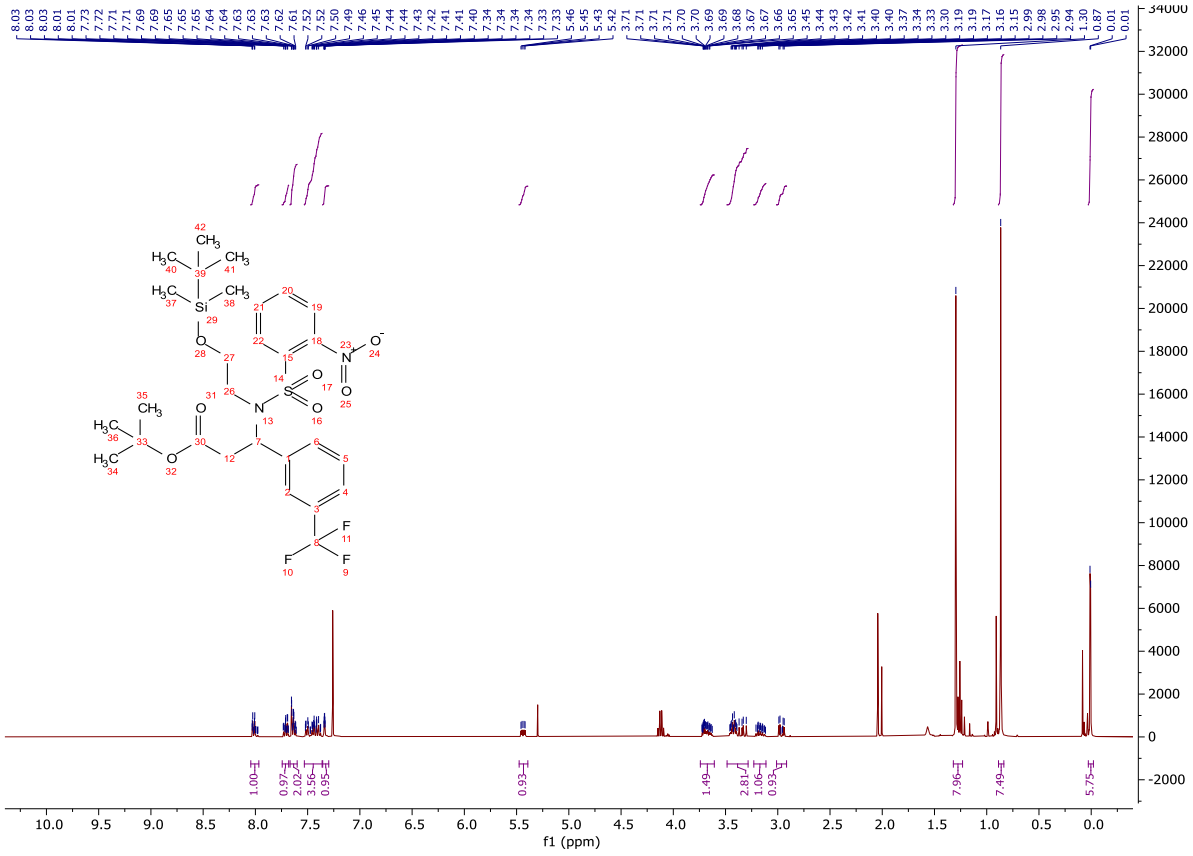
f1 (ppm)

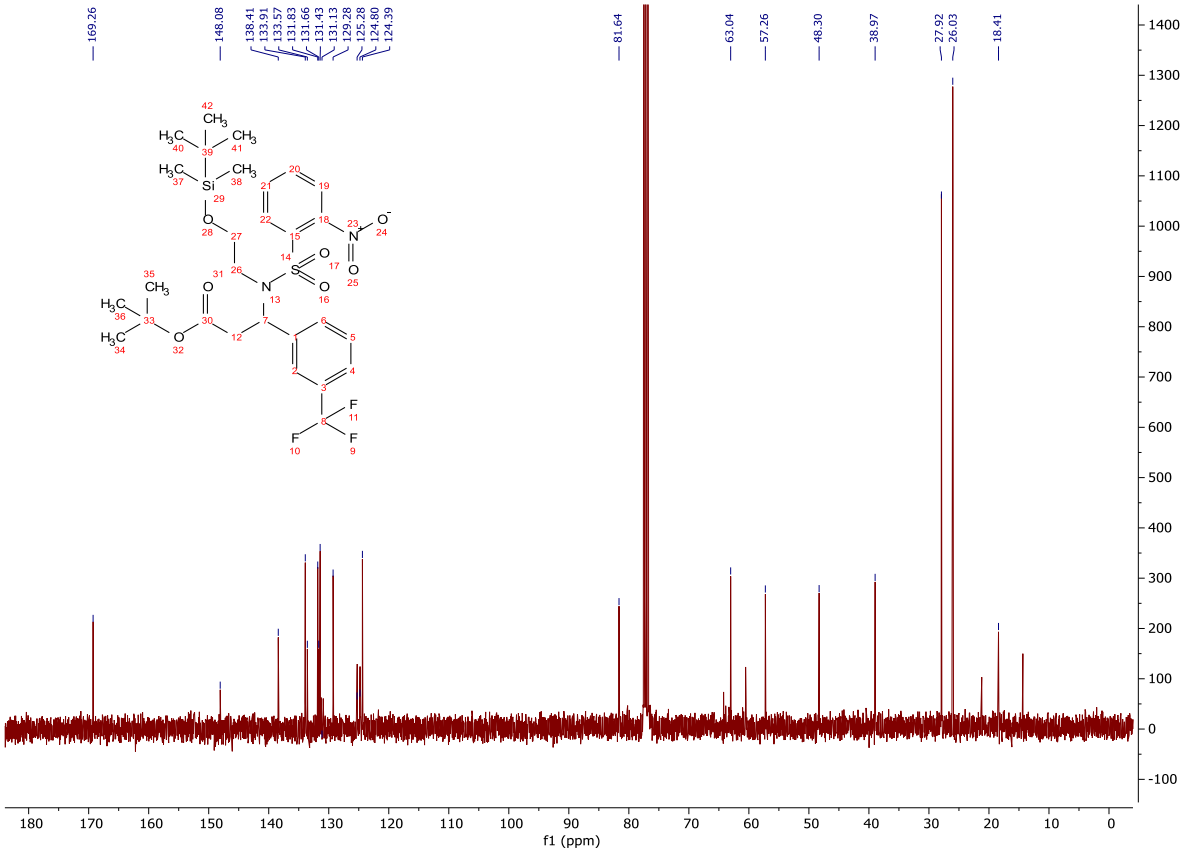
f1 (ppm)

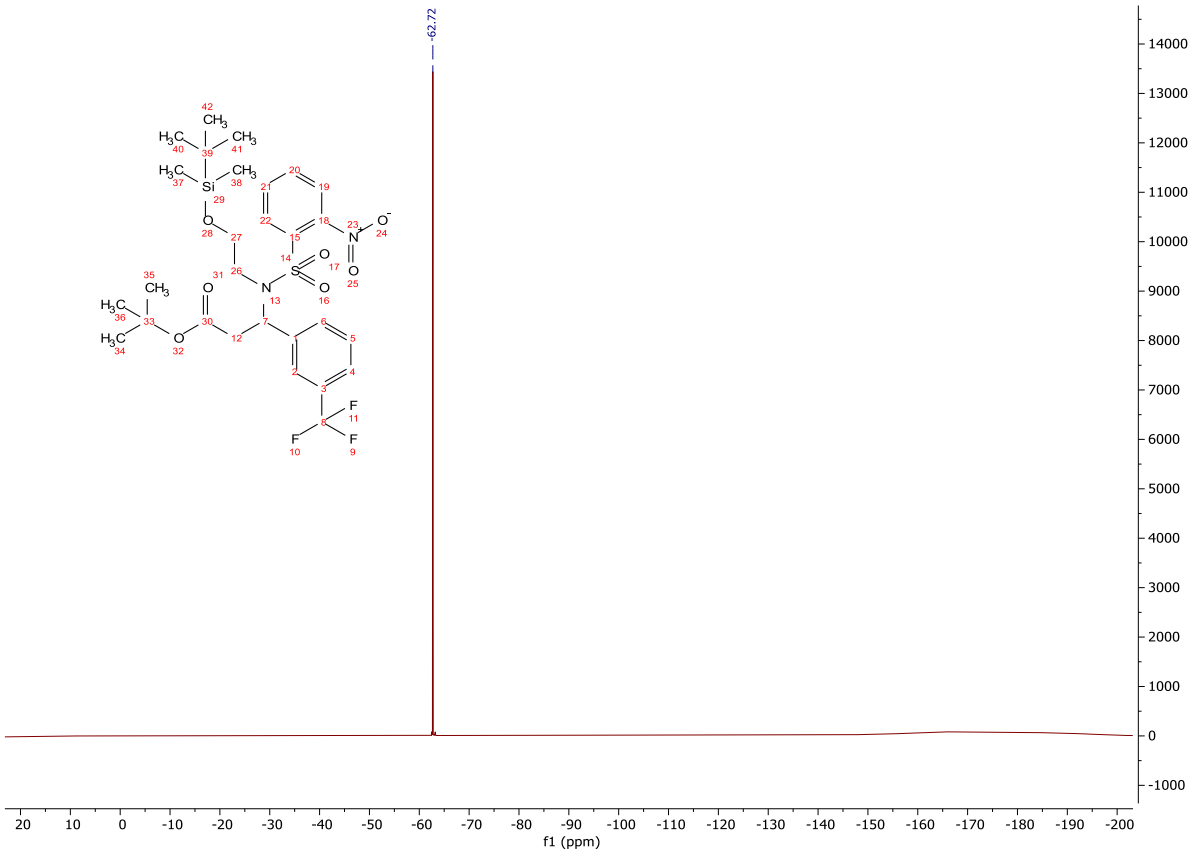
-62.72
14000
13000
12000
11000
10000
9000
8000
7000
6000
5000
4000
3000
2000
1000
0
-1000
20 10 0 -10 -20 -30 -40 -50 -60 -70 -80 -90 -100 -110 -120 -130 -140 -150 -160 -170 -180 -190 -200
f1 (ppm)

tert-Butyl 3-((2-methoxyethyl)amino-3-(3-(trifluoromethyl)phenyl)propanoate (**271**)

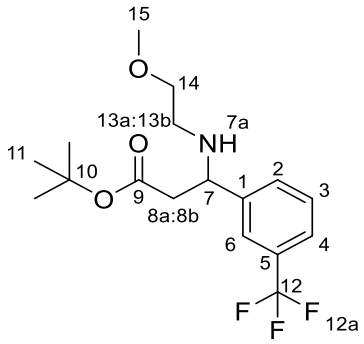

A mixture of **267** (440 mg, 0.827 mmol) and K_2CO_3 (342 mg, 2.48 mmol) in acetonitrile (8.50 mL) was stirred under a nitrogen atmosphere at rt. Thiophenol (0.260 mL, 2.48 mmol) was added and the reaction mixture stirred for 16 h. The reaction mixture was concentrated *in vacuo*, diluted with ethyl acetate (20.0 mL), washed with water (20.0 mL) and brine (20.0 mL), dried (Na_2SO_4) and concentrated *in vacuo* to afford an orange oil. The crude product was purified by column chromatography on silica gel, eluting with a gradient of ethyl acetate/light petroleum (0-50%) to afford the title compound as a colourless oil (230 mg, 0.663 mmol, 80%); **HRMS** *m/z* (ESI^+) calc. for $C_{17}H_{25}F_3NO_3$ $[M+H]^+$ requires 348.1781, found 348.1799; $\boldsymbol{R_f}$ 0.46, 50% ethyl acetate/light petroleum, UV active; δ_H (400 MHz, $CDCl_3$) 7.64 – 7.58 (1H, m, H-6), 7.58 – 7.48 (2H, m, H-2 and H-4), 7.43 (1H, dd, *J* = 7.6, 7.6 Hz, H-3), 4.13 – 4.05 (1H, m, H-7), 3.51 – 3.37 (2H, m, H-14), 3.32 (3H, s, H-15), 2.70 – 2.59 (2H, m, H-8a and H-13a), 2.57 – 2.46 (2H, m, H-8b and H-13b), 1.36 (9H, s, H-11); δ_C (101 MHz, $CDCl_3$) 170.6 (CO), 144.1 (C), 130.9 (C, q, *J* = 32.3 Hz), 130.8 (ArH), 129.1 (ArH), 124.4 (2 x ArH), 124.3 (CF_3, q, *J* = 272.2 Hz), 81.1 (C), 72.0 (CH_2), 59.9 (CH), 58.8 (CH_3), 47.2 (CH_2), 44.4 (CH_2), 28.1 (CH_3); δ_F (376 MHz, $CDCl_3$) -62.5 (F-12a); ν_{max} (FT-ATR/cm^{-1}) 2979, 2893, 1724, 1449, 1368, 1326, 1256, 1120, 805, 704, 658.

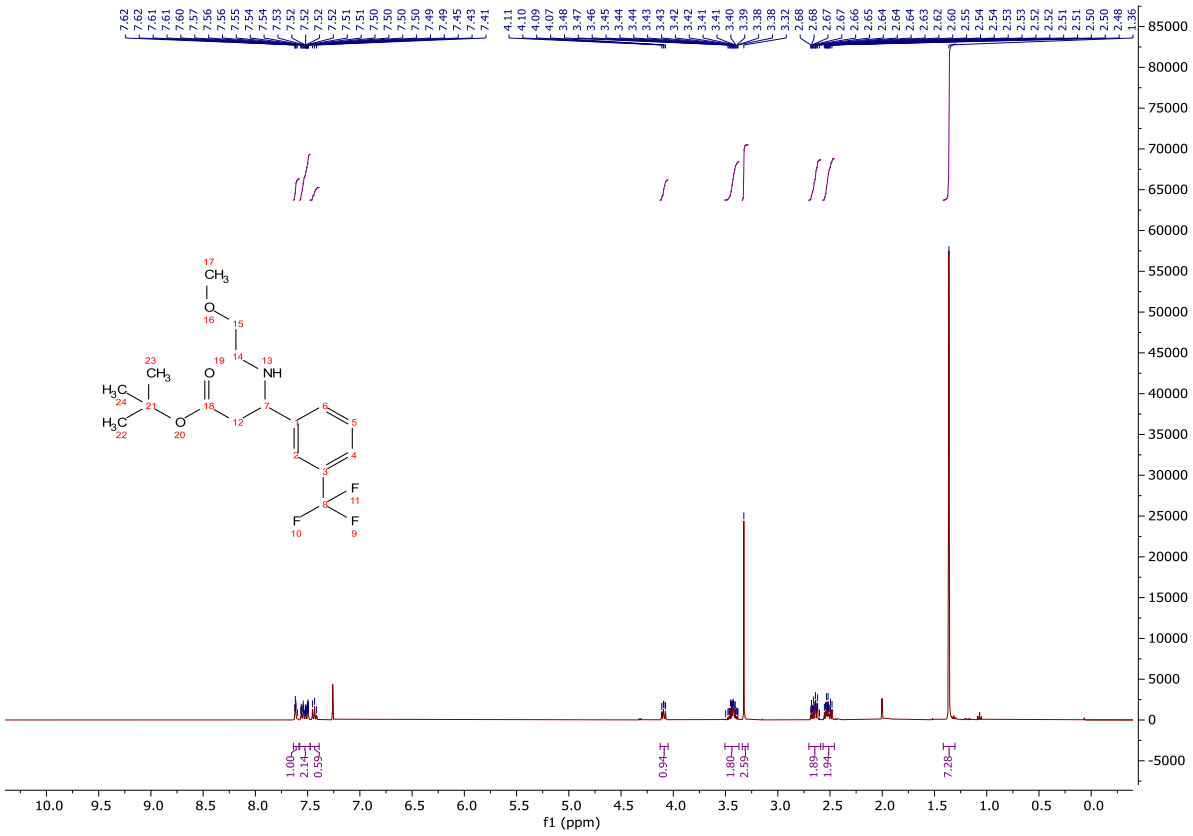
f1 (ppm)

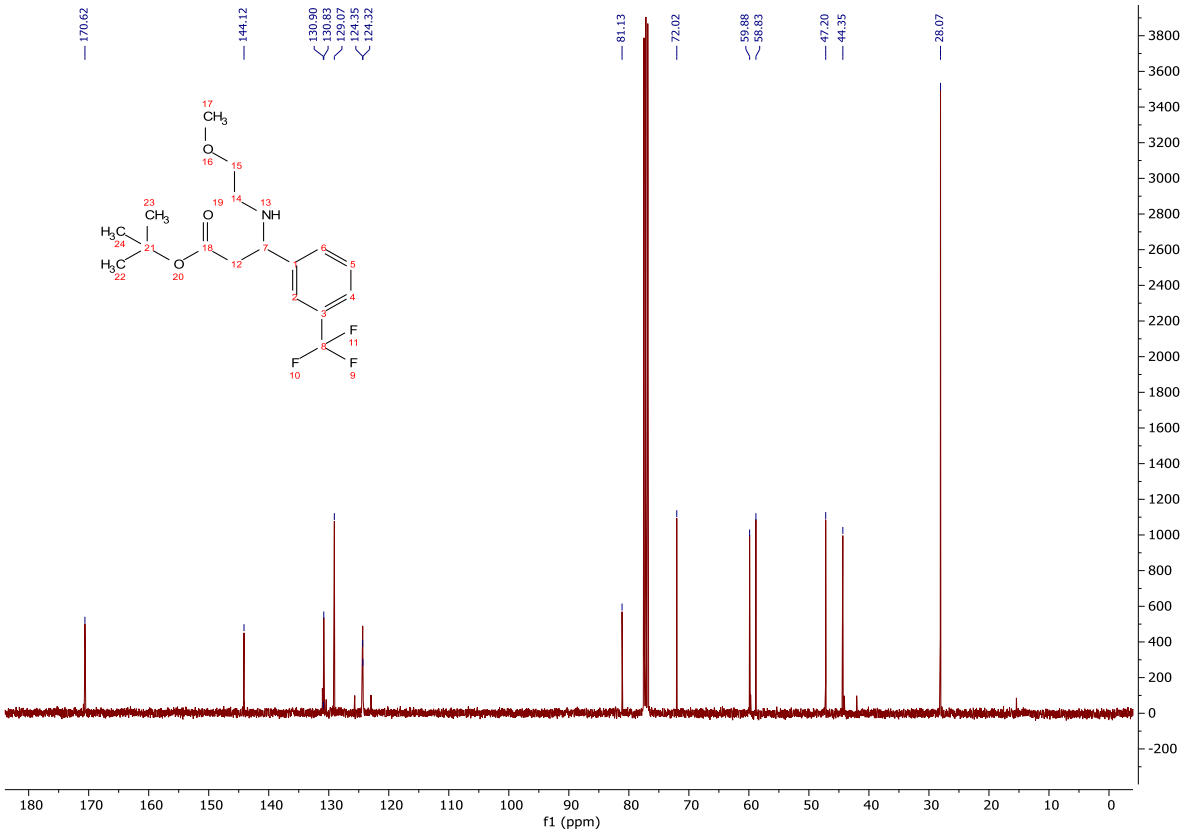
f1 (ppm)

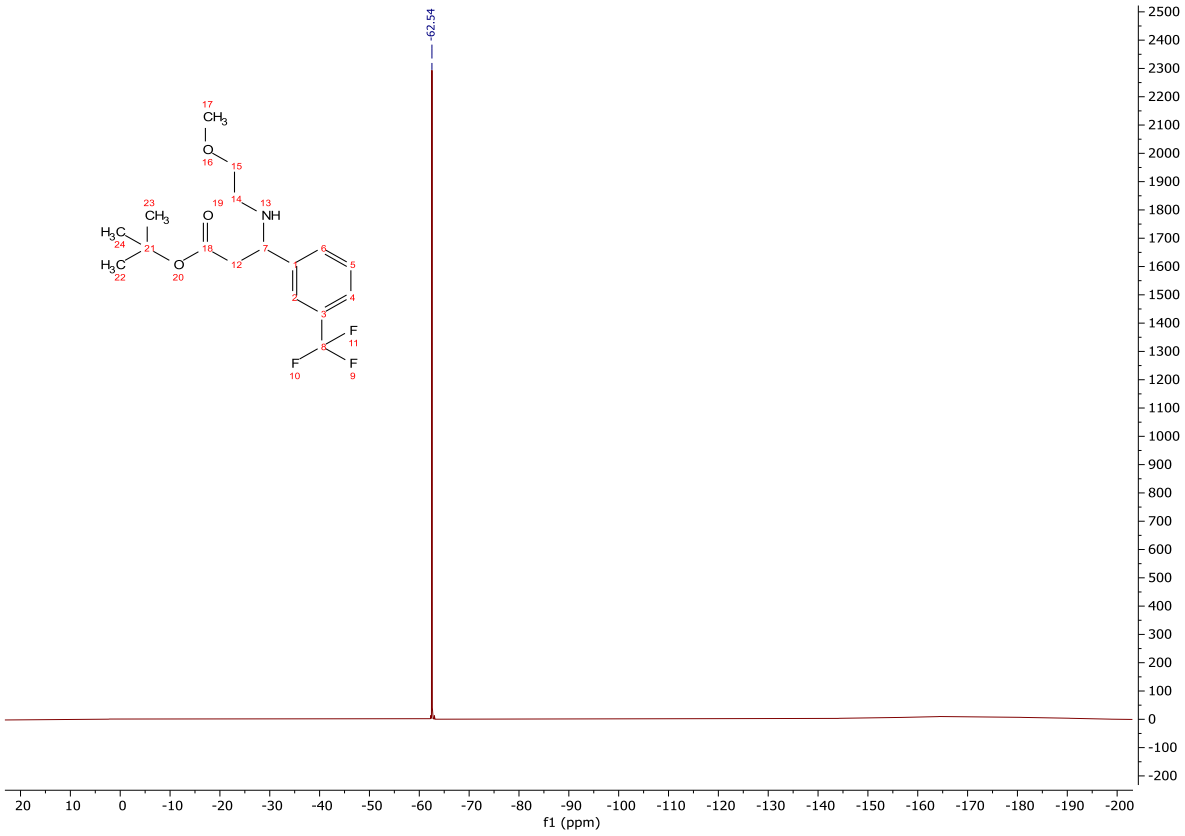
-62.54
2500
2400
2300
2200
2100
2000
1900
1800
1700
1600
1500
1400
1300
1200
1100
1000
900
800
700
600
500
400
300
200
100
0
-100
-200
20 10 0 -10 -20 -30 -40 -50 -60 -70 -80 -90 -100 -110 -120 -130 -140 -150 -160 -170 -180 -190 -200
f1 (ppm)

tert-Butyl 7-(5-((3-(*tert*-butoxy)-3-oxo-1-(3-(trifluoromethyl)phenyl)propyl)(2-methoxyethyl)amino)-5-oxopentyl)-3,4-dihydro-1,8-naphthyridine-1(2*H*)-carboxylate (**273**)

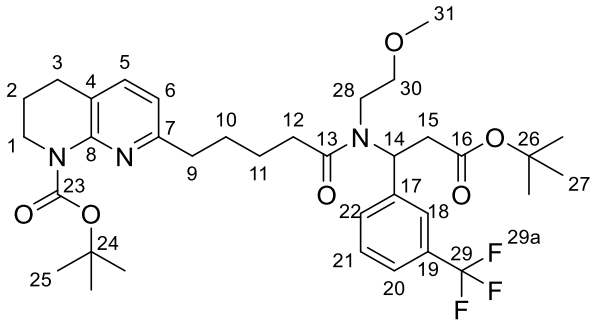

A mixture of **271** (165 mg, 0.476 mmol), **82** (194 mg, 0.571 mmol), HATU (593 mg, 1.56 mmol) in DMF (3.00 mL) was stirred under a nitrogen atmosphere at 0 °C. *i*-Pr_2NEt (0.721 mL, 4.15 mmol) was added, and the reaction mixture stirred for 96 h. The reaction mixture was diluted with ethyl acetate (10.0 mL), washed with water (30.0 mL), sat. $NaHCO_{3(aq)}$ (2 x 20.0 mL) and brine (2 x 20.0 mL), dried ($MgSO_4$) and concentrated *in vacuo* giving a brown oil (800 mg). The crude product was purified by column chromatography on silica gel, eluting with a gradient of ethyl acetate/light petroleum (20-50%) to afford the title compound as a clear oil (85 mg, 0.128 mmol, 27%); **HRMS** *m/z* (ESI^+) calc. for $C_{35}H_{49}F_3N_3O_6$ $[M+H]^+$ requires 664.3568, found 664.3555; $\boldsymbol{R_f}$ 0.41, 50% ethyl acetate/light petroleum, UV active; δ_H (400 MHz, $CDCl_3$) 7.61 – 7.35 (4H, m, H-18, H-20, H-21 and H-22), 7.31 – 7.21 (1H, m, H-5), 6.85 – 6.76 (1H, m, H-6), 6.06 (1H, t, *J* = 7.9 Hz, H-14 Rotamer A), 5.83 (1H, t, *J* = 7.7 Hz, H-14 Rotamer B), 5.59 – 5.48 (1H, m, H-14 Rotamer C), 3.74 (2H, t, *J* = 6.0 Hz, H-1), 3.58 – 2.81 (9H, m, H-15, H-28, H-30 and H-31), 2.80 – 2.63 (6H, m, H-2, H-9, H-12 Rotamer A), 2.61 – 2.49 (2H, m, H-12 Rotamer B), 2.47 – 2.28 (2H, m, H-12 Rotamer C), 1.97 – 1.86 (2H, m, H-2), 1.86 – 1.63 (4H, m, H-10 and H-11), 1.50 (9H, s, H-25), 1.43 (9H, s, H-27 Rotamer A), 1.39 – 1.32 (9H, m, H-27 Rotamer B); δ_C (101 MHz, $CDCl_3$) 173.8 (CO), 173.3 (CO*), 170.2 (CO), 169.9 (CO*), 169.8 (CO*), 158.2 (C), 154.2 (CO), 151.2 (C), 141.1 (C), 140.4 (C*), 137.3 (ArH), 131.1 (ArH), 130.8 (C, q, *J* = 32.3 Hz), 130.4 (ArH), 129.5 (ArH*), 129.1 (ArH*), 129.0 (ArH), 124.9 (ArH*), 124.3 (ArH), 124.2 (CF_3, q, *J* = 272.9 Hz), 123.6 (ArH*), 122.0 (C), 118.4 (ArH), 81.8 (C*), 81.2 (C), 80.9 (C), 71.3

(CH_2), 70.3 (CH_2*), 58.9 (CH_3), 58.8 (CH_3*), 56.3 (CH*), 55.1 (CH), 53.8 (CH*), 46.1 (CH_2), 44.9 (CH_2), 43.7 (CH_2*), 40.0 (CH_2*), 39.0 (CH_2*), 38.0 (CH_2), 37.9 (CH_2), 33.8 (CH_2), 33.6 (CH_2*), 33.5 (CH_2*), 29.4 (CH_2), 28.5 (CH_3), 28.1 (CH_3*), 28.0 (CH_3), 26.4 (CH_2), 25.2 (CH_2), 25.1 (CH_2*), 23.4 (CH_2); δ_F (376 MHz, $CDCl_3$) -62.55 (F-29a); ν_{max} (FT-ATR/cm^{-1}) 2932, 1725, 1692, 1646, 1463, 1414, 1366, 1327, 1147, 1119, 1076, 846, 807 703.

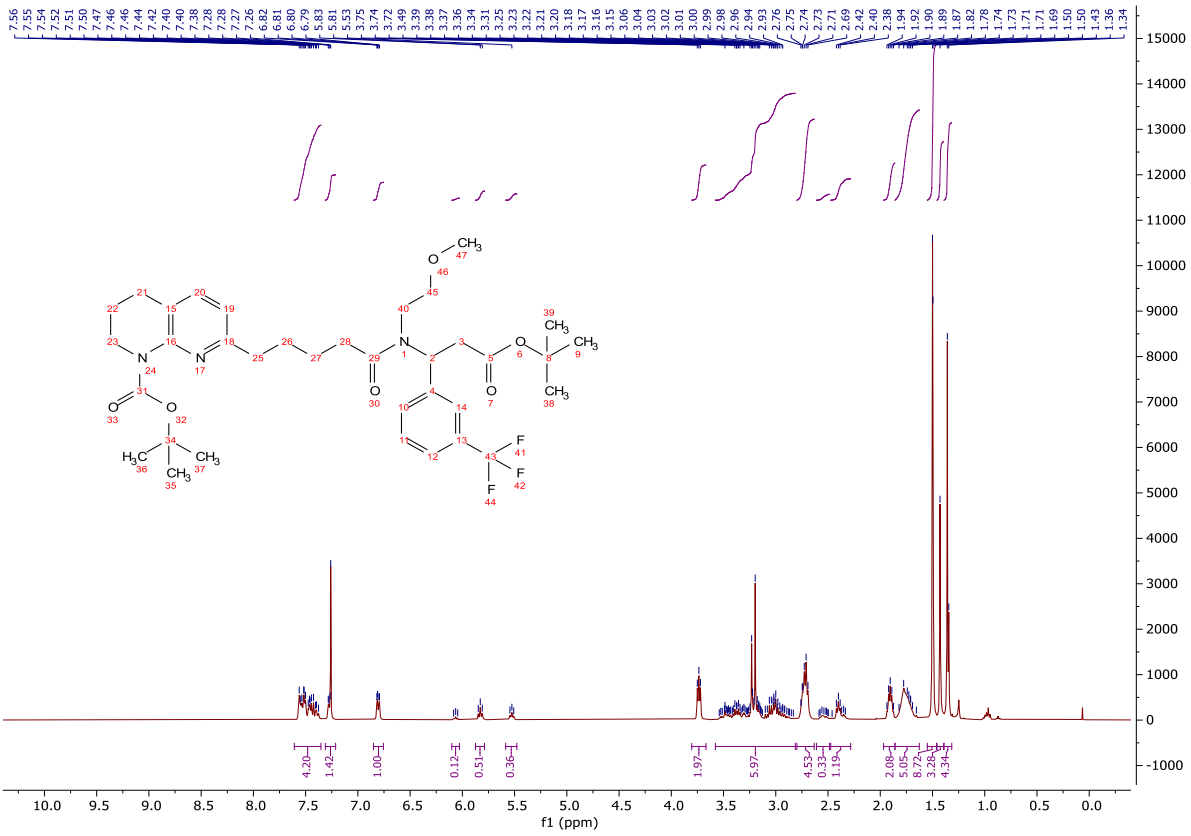
f1 (ppm)

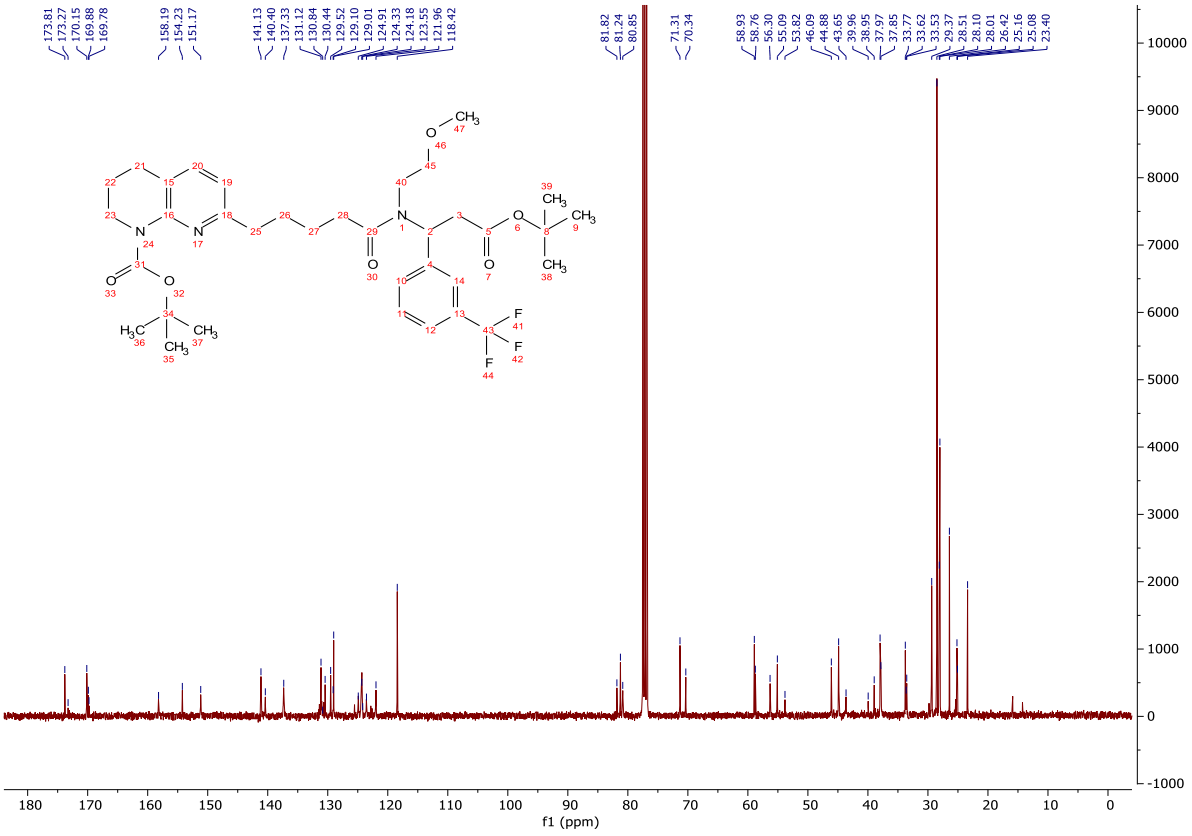
f1 (ppm)

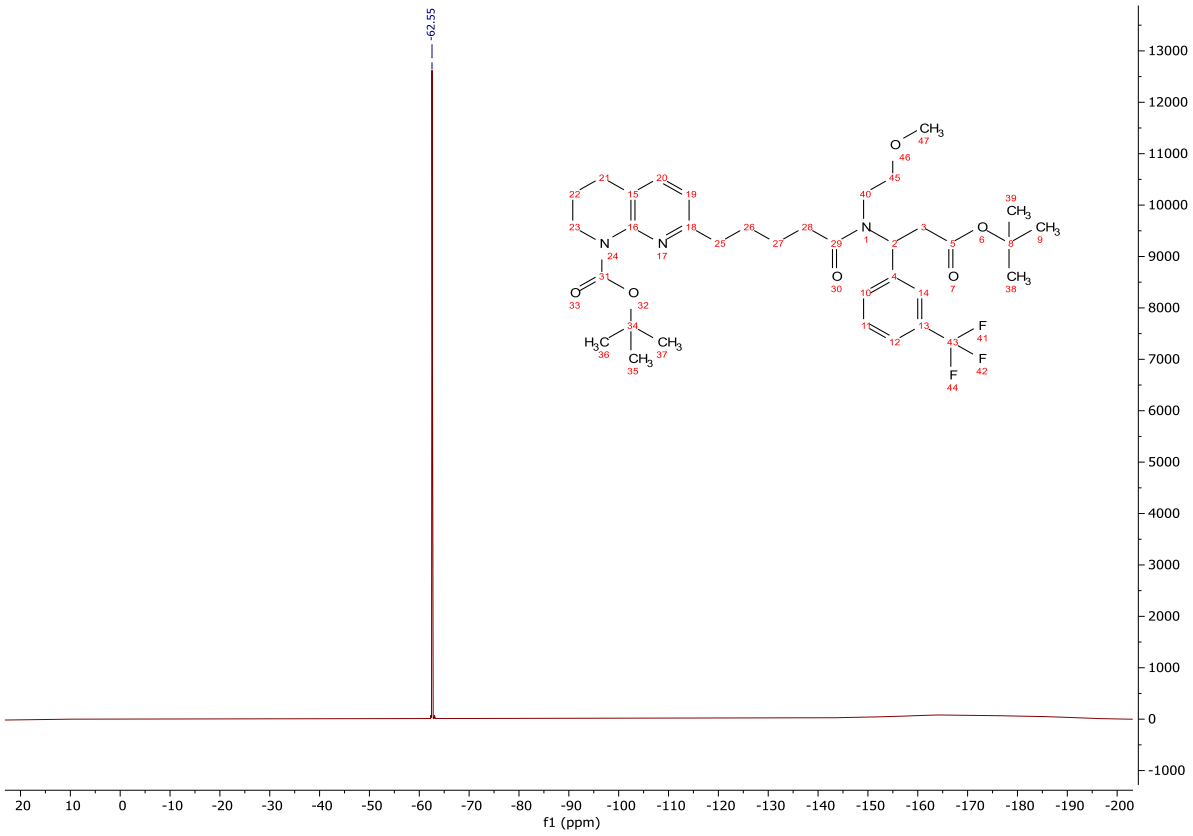
-62.55
13000
12000
11000
10000
9000
8000
7000
6000
5000
4000
3000
2000
1000
0
-1000
20 10 0 -10 -20 -30 -40 -50 -60 -70 -80 -90 -100 -110 -120 -130 -140 -150 -160 -170 -180 -190 -200
f1 (ppm)

3-(*N*-(2-Methoxyethyl)-5-(5,6,7,8-tetrahydro-1,8-napthyridin-2-yl)pentanamido)-3-(3-(trifluoromethyl)phenyl)propanoic acid (**256**)

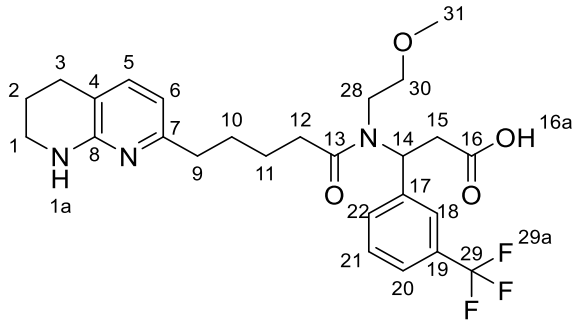

To a stirred solution of **273** (85 mg, 0.128 mmol) in CH_2Cl_2 (25.0 mL) at rt was added TFA (2.50 mL). The reaction mixture was stirred for 17 h, concentrated *in vacuo* and purified on a Waters OASIS® HLB cartridge to afford the title compound as a clear oil (65 mg, 0.128 mmol, quant.); **HRMS** *m/z* (ESI^+) calc. for $C_{26}H_{33}F_3N_3O_4$ $[M+H]^+$ requires 508.2418, found 508.2415; $\boldsymbol{R_f}$ 0.43, 5% methanol/CH_2Cl_2, UV active; δ_H (400 MHz, DMSO-d_6) 7.72 – 7.51 (4H, m, H-18, H-20, H-21 and H-22), 7.24 – 7.17 (1H, m, H-5 Rotamer A), 7.07 – 6.99 (1H, m, H-5 Rotamer B), 6.46 (1H, bs, H-1a), 6.40 – 6.31 (1H, m, H-6 Rotamer A), 6.28 – 6.20 (1H, m, H-6 Rotamer B), 5.68 – 5.57 (1H, m, H-14), 3.55 – 3.34 (2H, m, H-28), 3.33 – 2.81 (9H, m, H-1, H-15, H-30 and H-31), 2.69 – 2.26 (6H, m, H-3, H-9 and H-12), 1.86 – 1.32 (6H, m, H-2, H-10 and H-11); δ_C (126 MHz, MeOD) 179.5 (CO*), 179.3 (CO), 179.0 (CO*), 176.6 (CO*), 176.1 (CO), 175.3 (CO*), 168.2 (Ar*), 160.5 (Ar*), 156.4 (Ar*), 154.2 (Ar*), 153.8 (C), 153.7 (C*), 151.6 (Ar*), 150.9 (C), 150.7 (C*), 143.7 (C*), 143.2 (Ar*), 142.7 (Ar*), 142.5 (C), 142.0 (ArH), 141.9 (ArH*), 139.2 (ArH*), 139.0 (ArH*), 137.7 (C*), 132.5 (ArH), 132.4 (C*), 132.2 (ArH*), 132.0 (ArH*), 131.9 (ArH*), 131.7 (C, q, *J* = 32.0 Hz), 130.8 (ArH), 130.2 (ArH*), 125.7 (ArH, q, *J* = 3.8 Hz), 125.5 (CF_3, q, *J* = 271.7 Hz), 125.4 (ArH*, q, *J* = 3.8 Hz), 125.0 (ArH, q, *J* = 3.8 Hz), 119.8 (C*), 119.7 (C), 118.8 (ArH*), 111.3 (ArH*), 111.0 (ArH), 72.0 (CH_2*), 70.8 (CH_2), 58.9 (CH_3*), 58.8 (CH_3), 58.3 (CH), 56.8 (CH*), 54.8 (CH_2*), 46.8 (CH_2*), 43.3 (CH_2), 41.8 (CH_2*), 41.5 (CH_2), 39.9 (CH_2), 39.2 (CH_2*), 33.52 (CH_2), 33.50 (CH_2*), 32.3 (CH_2), 30.8 (CH_2*), 30.6 (CH_2), 29.2 (CH_2*), 26.5 (CH_2*), 26.4 (CH_2), 25.6 (CH_2*), 24.1 (CH_2), 20.7 (CH_2); δ_F (376 MHz, DMSO-d_6) -61.0 (F-29a);

ν_{max} (FT-ATR/cm^{-1}) 2925, 1676, 1629, 1565, 1446, 1392, 1326, 1284, 1160, 1074, 920, 729, 658.

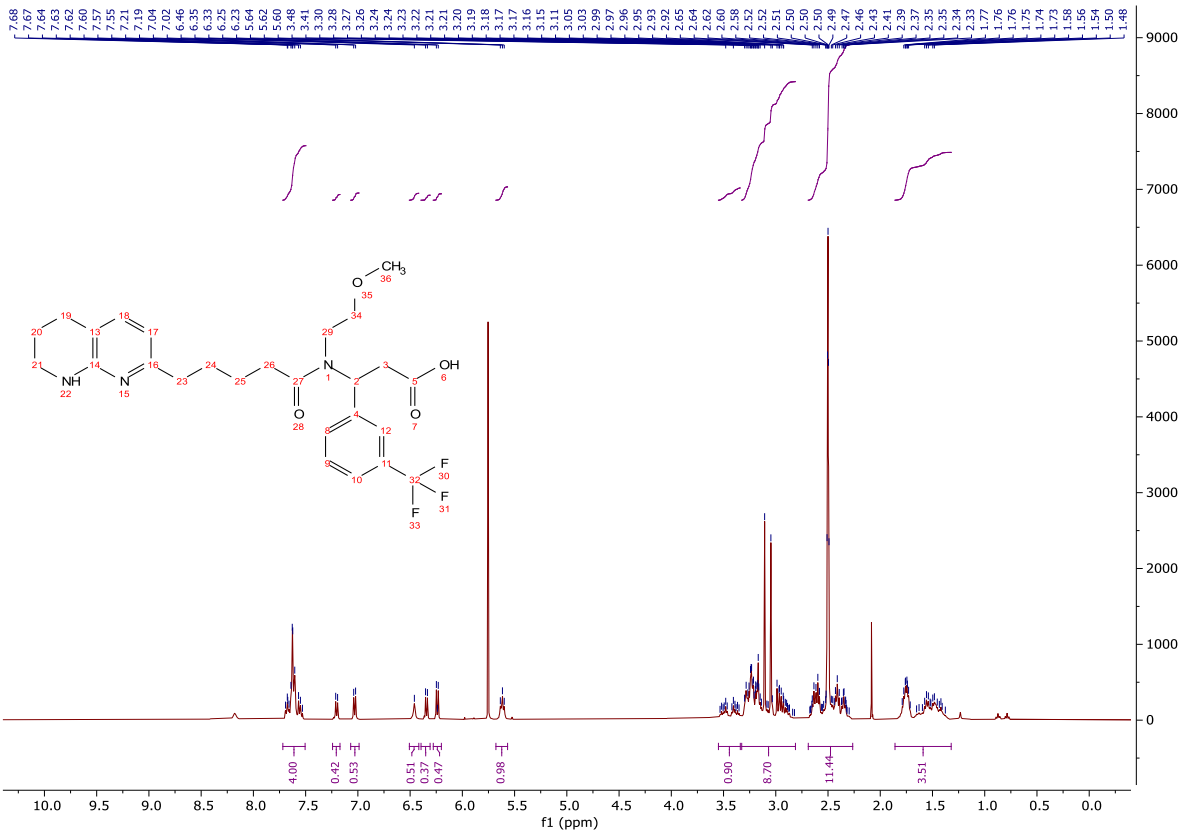
f1 (ppm)

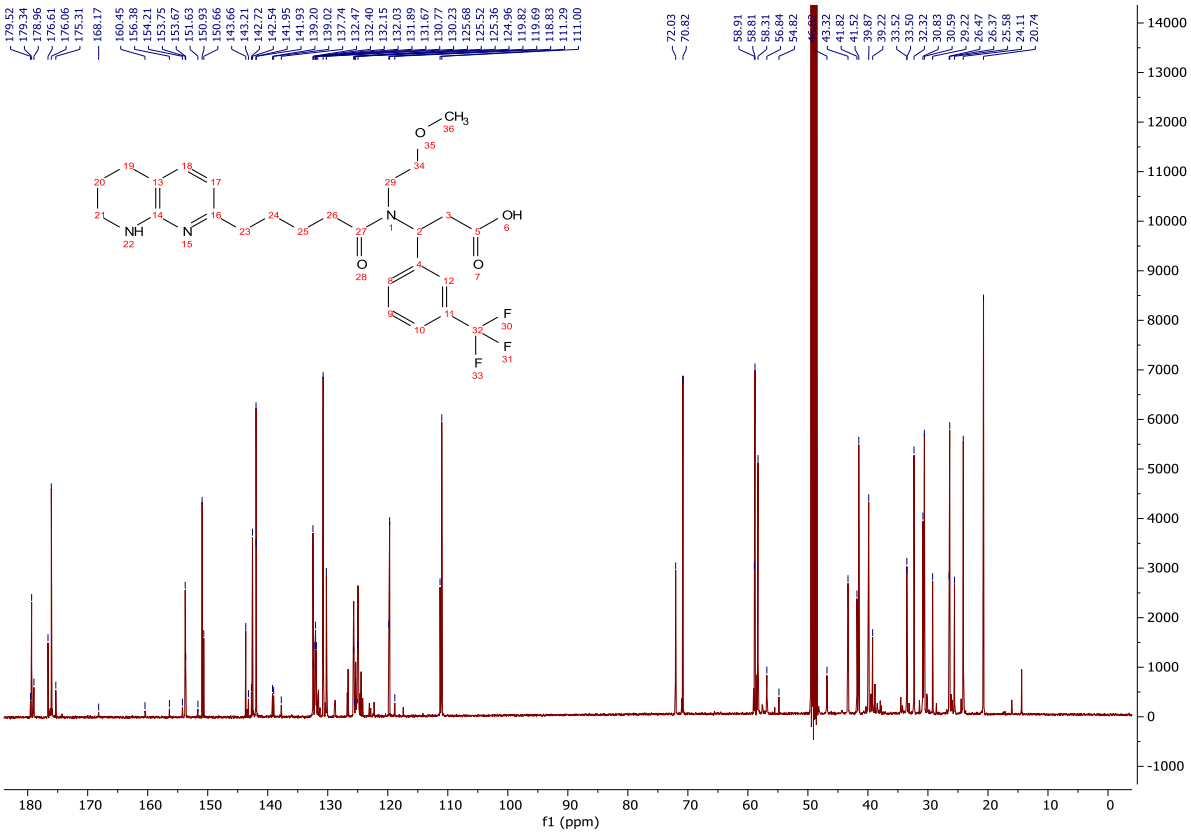
f1 (ppm)

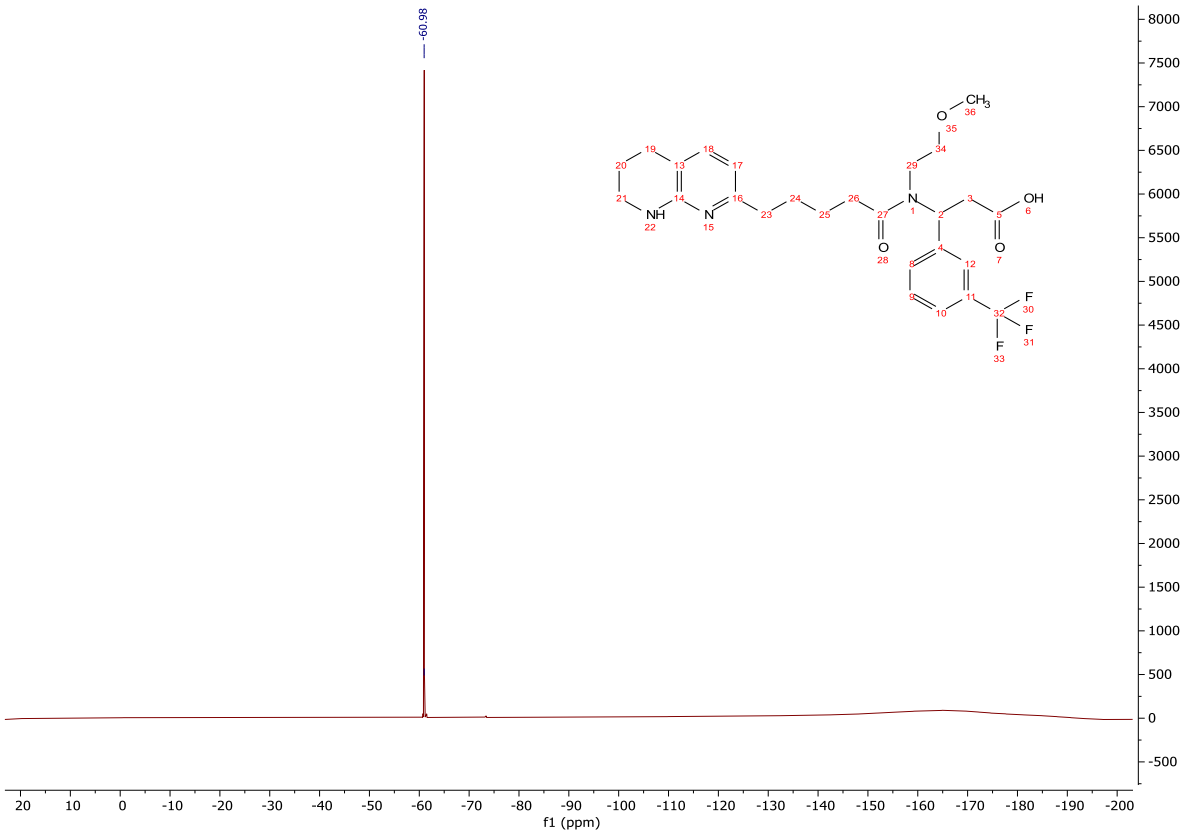
-60.98
f1 (ppm)

tert-Butyl 3-((2-((*tert*-butyldimethylsilyl)oxy)ethyl)amino)-3-(3-(trifluoromethyl)phenyl)propanoate (**272**)

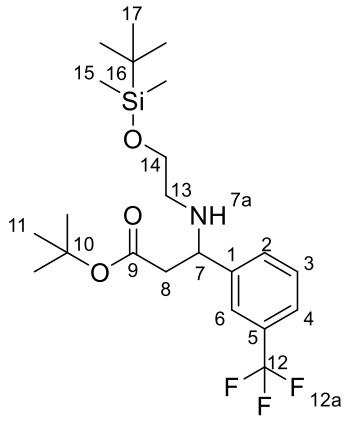

A mixture of **270** (368 mg, 0.581 mmol) and K_2CO_3 (240 mg, 1.74 mmol) in acetonitrile (6.00 mL) was stirred under a nitrogen atmosphere at rt. Thiophenol (0.180 mL, 1.74 mmol) was added and the reaction mixture stirred for 16 h. The reaction mixture was concentrated *in vacuo*, diluted with ethyl acetate (20.0 mL), washed with water (20.0 mL) and brine (20.0 mL), dried (Na_2SO_4) and concentrated *in vacuo* to afford a yellow oil. The crude product was purified by column chromatography on silica gel, eluting with a gradient of ethyl acetate/light petroleum (0-50%) to afford the title compound as a colourless oil (234 mg, 0.523 mmol, 90%); **HRMS** *m/z* (ESI$^+$) calc. for $C_{22}H_{37}F_3NO_3Si$ $[M+H]^+$ requires 448.2489, found 448.2484; $\boldsymbol{R_f}$ 0.70, 20% ethyl acetate/light petroleum, UV active; $\boldsymbol{\delta_H}$ (400 MHz, $CDCl_3$) 7.61 (1H, dd, *J* = 2.0, 2.0 Hz, H-6), 7.57 – 7.47 (2H, m, H-2 and H-4), 7.46 – 7.38 (1H, m, H-3), 4.14 – 4.06 (1H, m, H-7), 3.70 – 3.59 (2H, m, H-14), 2.78 – 2.38 (4H, m, H-8 and H-13), 1.35 (9H, s, H-11), 0.95 – 0.83 (9H, m, H-17), 0.07 – -0.01 (6H, m, H-15); $\boldsymbol{\delta_C}$ (101 MHz, $CDCl_3$) 170.6 (CO), 144.2 (C), 130.9 (C, q, *J* = 32.0 Hz), 130.85 (ArH), 129.0 (ArH), 124.33 (CF_3, q, *J* = 272.2 Hz), 124.31 (2 x ArH), 81.0 (C), 62.6 (CH_2), 59.6 (CH), 49.7 (CH_2), 44.3 (CH_2), 28.1 (CH_3), 26.1 (CH_3), 18.5 (C), -5.2 (CH_3); $\boldsymbol{\delta_F}$ (376 MHz, $CDCl_3$) -62.5 (F-12a); $\boldsymbol{\nu_{max}}$ (FT-ATR/cm^{-1}) 2930, 2857, 1727, 1464, 1368, 1326, 1254, 1125, 953, 834, 776, 704.

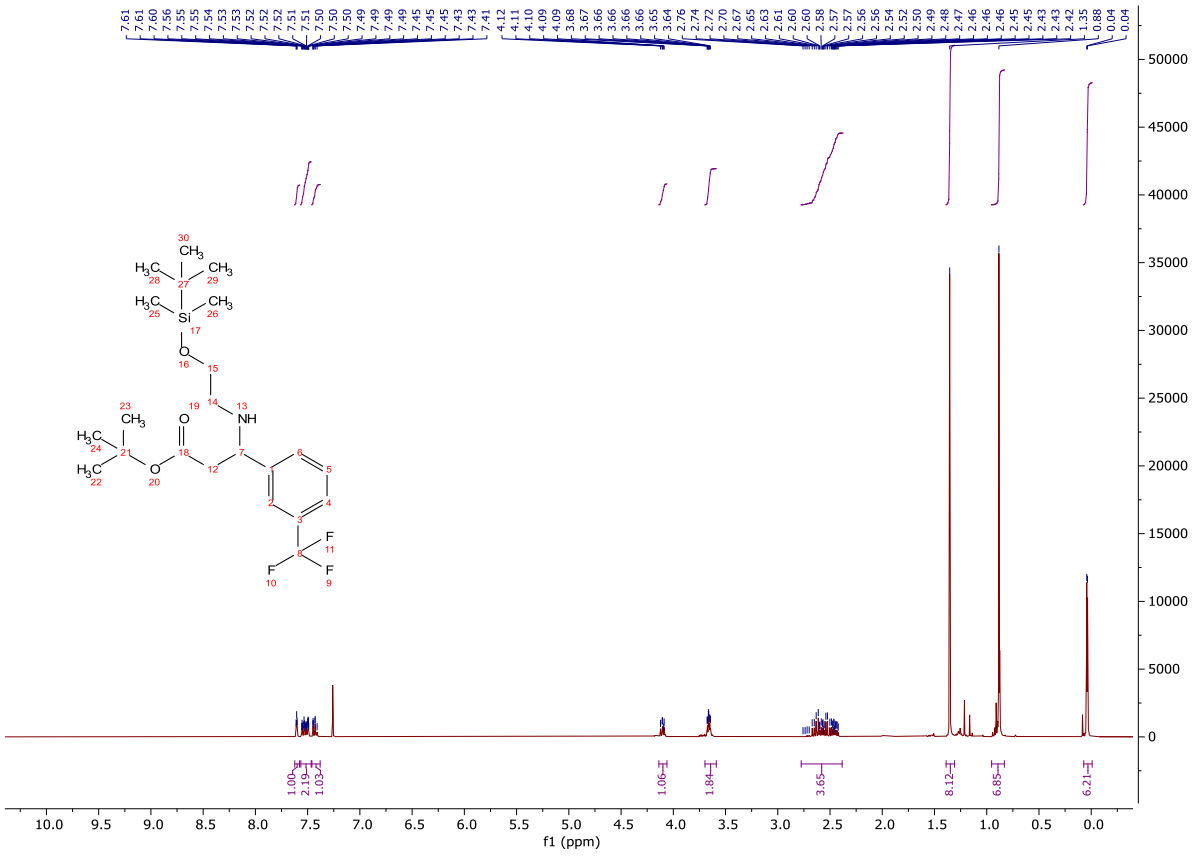
7.61 7.61 7.60 7.56 7.55 7.54 7.53 7.52 7.52 7.52 7.51 7.51 7.50 7.50 7.50 7.49 7.49 7.49 7.49 7.45 7.45 7.43 7.43 7.41
4.12 4.11 4.10 4.09 4.09 3.68 3.67 3.66 3.66 3.66 3.65 3.64 2.76 2.74 2.72 2.70 2.67 2.65 2.63 2.61 2.60 2.60 2.58 2.57 2.57 2.56 2.56 2.54 2.52 2.50 2.49 2.48 2.47 2.46 2.46 2.45 2.45 2.43 2.43 2.42 1.35 0.88 0.04 0.04
1.00 2.19 1.03 1.06 1.84 3.65 8.12 6.85 6.21
f1 (ppm)

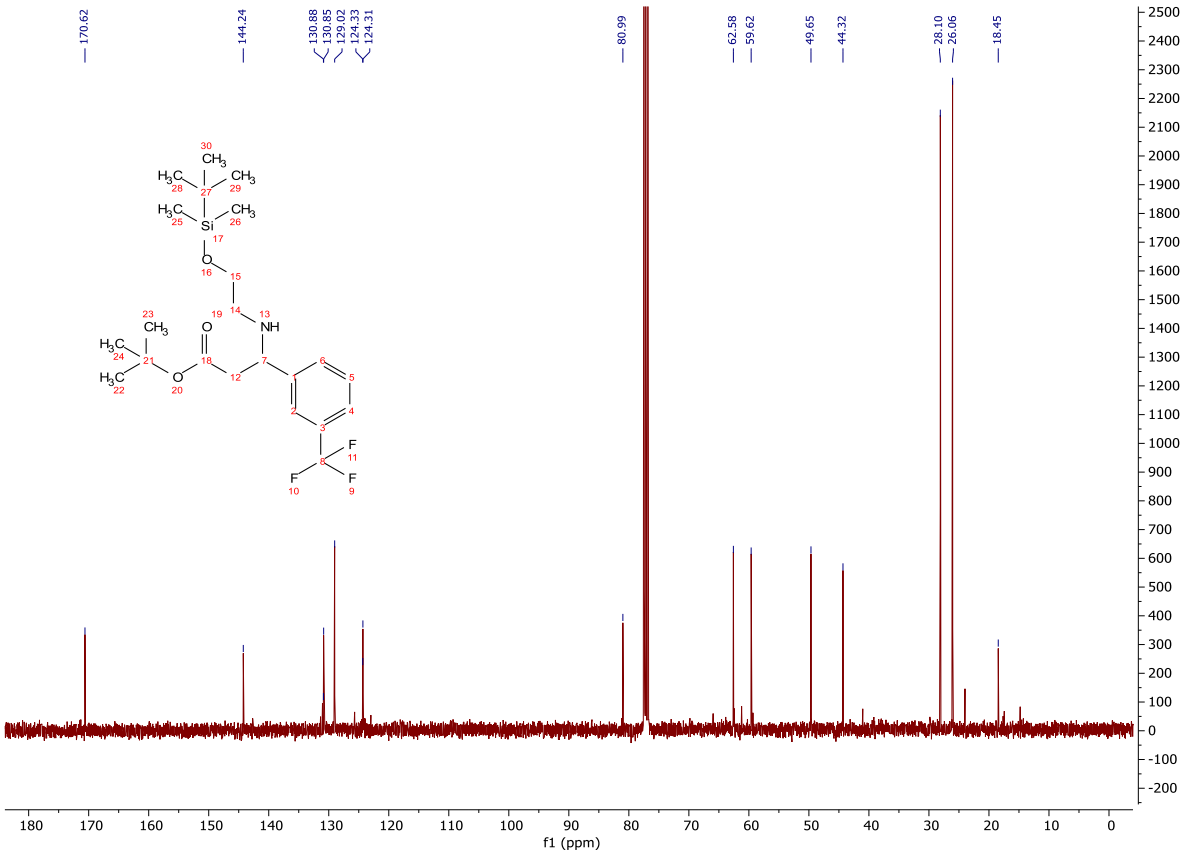
170.62 144.24 130.88 130.85 129.02 124.33 124.31 80.99 62.58 59.62 49.65 44.32 28.10 26.06 18.45
f1 (ppm)

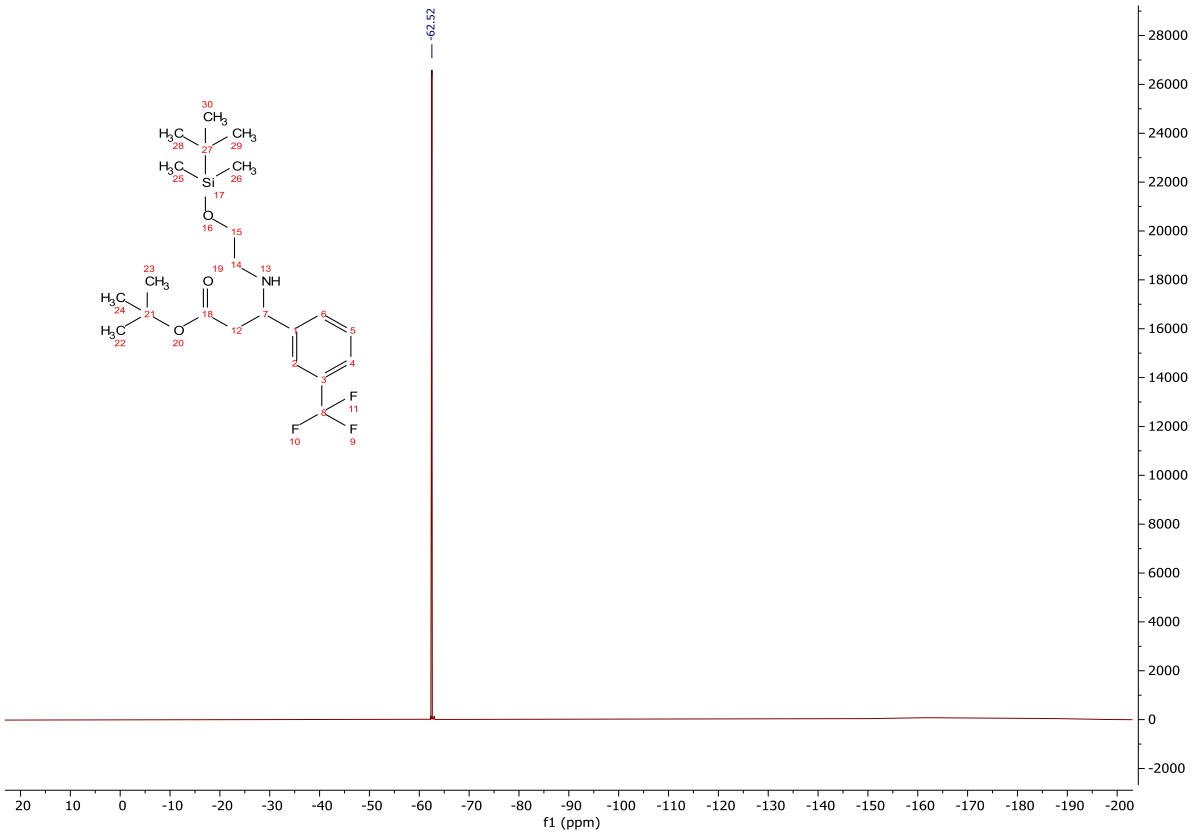
-62.52
28000
26000
24000
22000
20000
18000
16000
14000
12000
10000
8000
6000
4000
2000
0
-2000
20 10 0 -10 -20 -30 -40 -50 -60 -70 -80 -90 -100 -110 -120 -130 -140 -150 -160 -170 -180 -190 -200
f1 (ppm)

tert-Butyl 7-(5-((3-(*tert*-butoxy)-3-oxo-1-(3-(trifluoromethyl)phenyl)propyl)(2-((*tert*-butyldimethylsilyl)oxy)ethoxy)amino)-5-oxopentyl)-3,4-dihydro-1,8-naphthyridine-1(2*H*)-carboxylate (**274**)

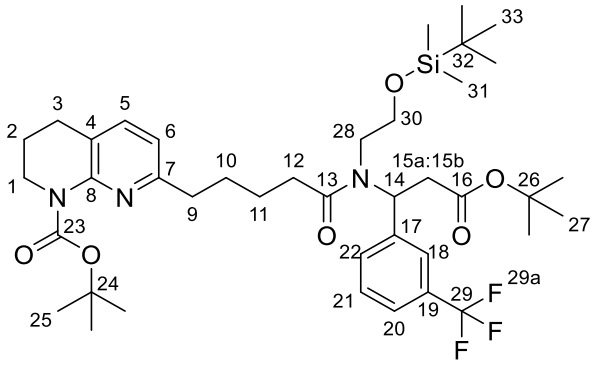

A mixture of **272** (220 mg, 0.492 mmol), **82** (184 mg, 0.541 mmol), HATU (562 mg, 1.48 mmol) in DMF (2.50 mL) was stirred under a nitrogen atmosphere at 0 °C. *i*-Pr_2NEt (0.685 mL, 3.94 mmol) was added, and the reaction mixture stirred for 18 h. The reaction mixture was diluted with ethyl acetate (10.0 mL), washed with water (30.0 mL), sat. $NaHCO_{3(aq)}$ (2 x 20.0 mL) and brine (2 x 20.0 mL), dried ($MgSO_4$) and concentrated *in vacuo* giving a brown oil (800 mg). The crude product was purified by column chromatography on silica gel, eluting with a gradient of ethyl acetate/light petroleum (0-50%) to afford the title compound as a clear, colourless oil (110 mg, 0.144 mmol, 29%); **HRMS** *m/z* (ESI^+) calc. for $C_{40}H_{61}F_3N_3O_6Si$ $[M+H]^+$ requires 764.4276, found 764.4246; $\boldsymbol{R_f}$ 0.66, 50% ethyl acetate/light petroleum, UV active; δ_H (400 MHz, $CDCl_3$) 7.62 – 7.33 (4H, m, H-18, H-20, H-21 and H-22), 7.31 – 7.17 (1H, m, H-5), 6.84 – 6.73 (1H, m, H-6), 5.91 – 5.80 (1H, m, H-14 Rotamer A), 5.55 – 5.46 (1H, m, H-14 Rotamer B), 3.81 – 3.63 (4H, m, H-1 and H-30 Rotamer A), 3.53 – 3.40 (4H, m, H-28 Rotamer A and H-30 Rotamer B), 3.37 – 3.24 (4H, m, H-28 Rotamer B and H-30 Rotamer C), 3.09 (1H, dd, *J* = 15.8, 8.2 Hz, H-15a), 3.01 – 2.83 (3H, m, H-15b and H-28 Rotamer C), 2.80 – 2.60 (6H, m, H-3, H-9 and H-12 Rotamer A), 2.58 – 2.47 (2H, m, H-12 Rotamer B), 2.47 – 2.36 (2H, m, H-12 Rotamer C), 1.96 – 1.85 (2H, m, H-2), 1.85 – 1.67 (4H, m, H-10 and H-11), 1.54 – 1.46 (9H, m, H-25), 1.42 (9H, s, H-27 Rotamer A), 1.35 (9H, s, H-27 Rotamer B), 0.94 – 0.73 (9H, m,

H-33), 0.02 – -0.11 (6H, m, H-31); δ_C (101 MHz, $CDCl_3$) 173.8 (CO), 173.6 (CO*), 170.0 (CO), 169.9 (CO*), 158.2 (C), 154.3 (CO), 151.2 (C), 141.1 (C), 140.5 (C*), 137.3 (ArH), 131.4 (ArH), 131.1 (ArH*), 130.3 (C), 129.6 (ArH*), 129.1 (ArH), 124.8 (ArH*), 124.6 (CF_3), 124.5 (ArH), 124.3 (ArH), 122.0 (C), 118.4 (ArH), 81.9 (C*), 81.3 (C), 80.8 (C), 61.8 (CH_2), 60.8 (CH_2*), 56.3 (CH*), 54.9 (CH), 48.3 (CH_2), 46.3 (CH_2*), 46.0 (CH_2*), 44.9 (CH_2), 39.5 (CH_2*), 38.1 (CH_2*), 38.0 (CH_2), 37.9 (CH_2), 33.9 (CH_2), 33.6 (CH_2*), 29.5 (CH_2), 28.5 (CH_3), 28.1 (CH_3*), 28.0 (CH_3), 26.5 (CH_2), 26.1 (CH_3*), 25.9 (CH_3), 25.3 (CH_2), 25.2 (CH_2*), 23.4 (CH_2), 18.4 (C*), 18.3 (C), -5.3 (CH_3*), -5.4 (CH_3); δ_F (376 MHz, $CDCl_3$) -62.55 (F-29a); ν_{max} (FT-ATR/cm^{-1}) 2931, 2858, 1727, 1693, 1650, 1571, 1464, 1366, 1328, 1253, 1124, 836, 777, 703, 661.

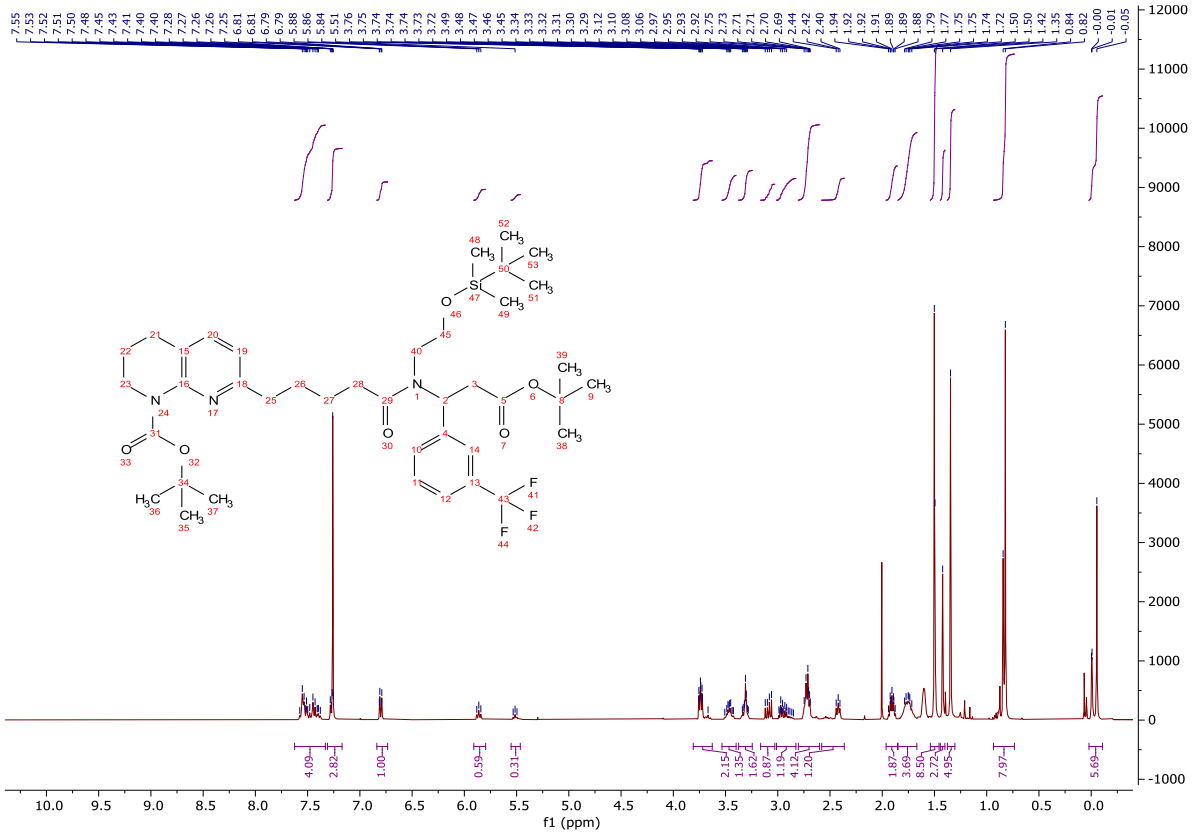
f1 (ppm)

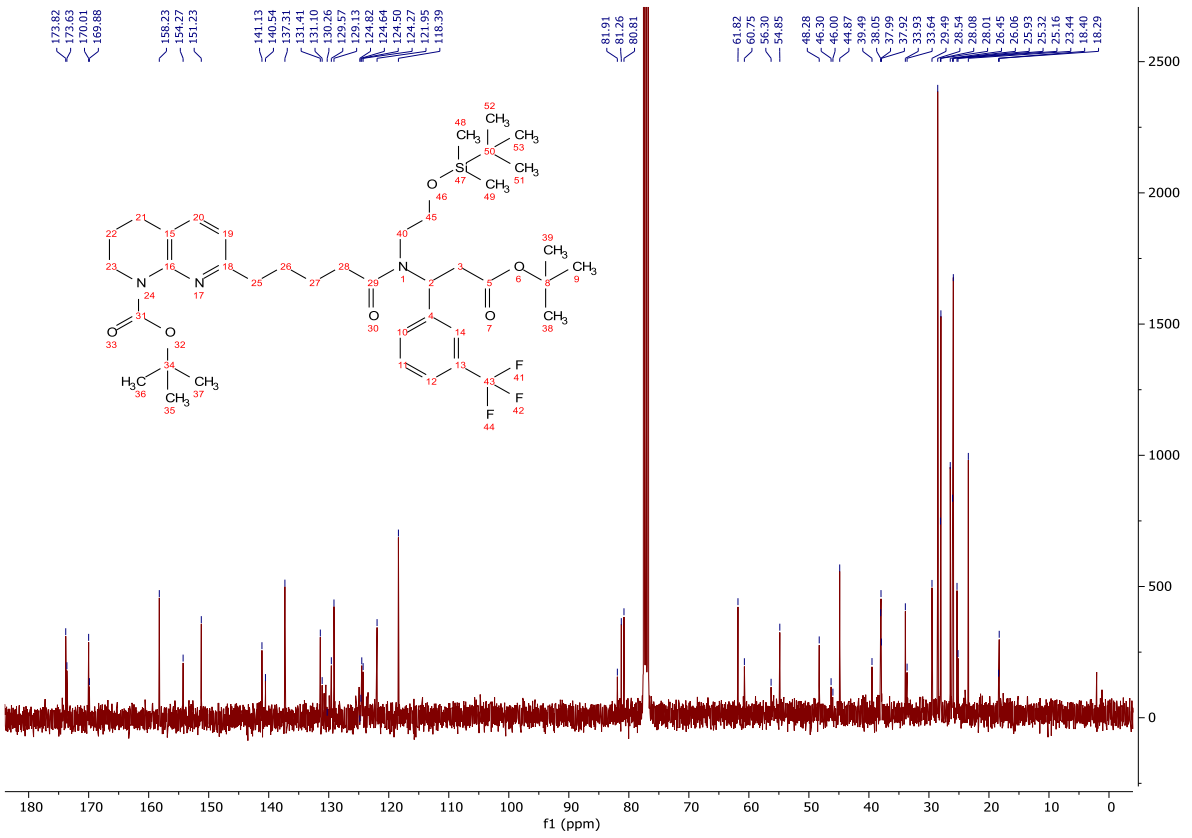
f1 (ppm)

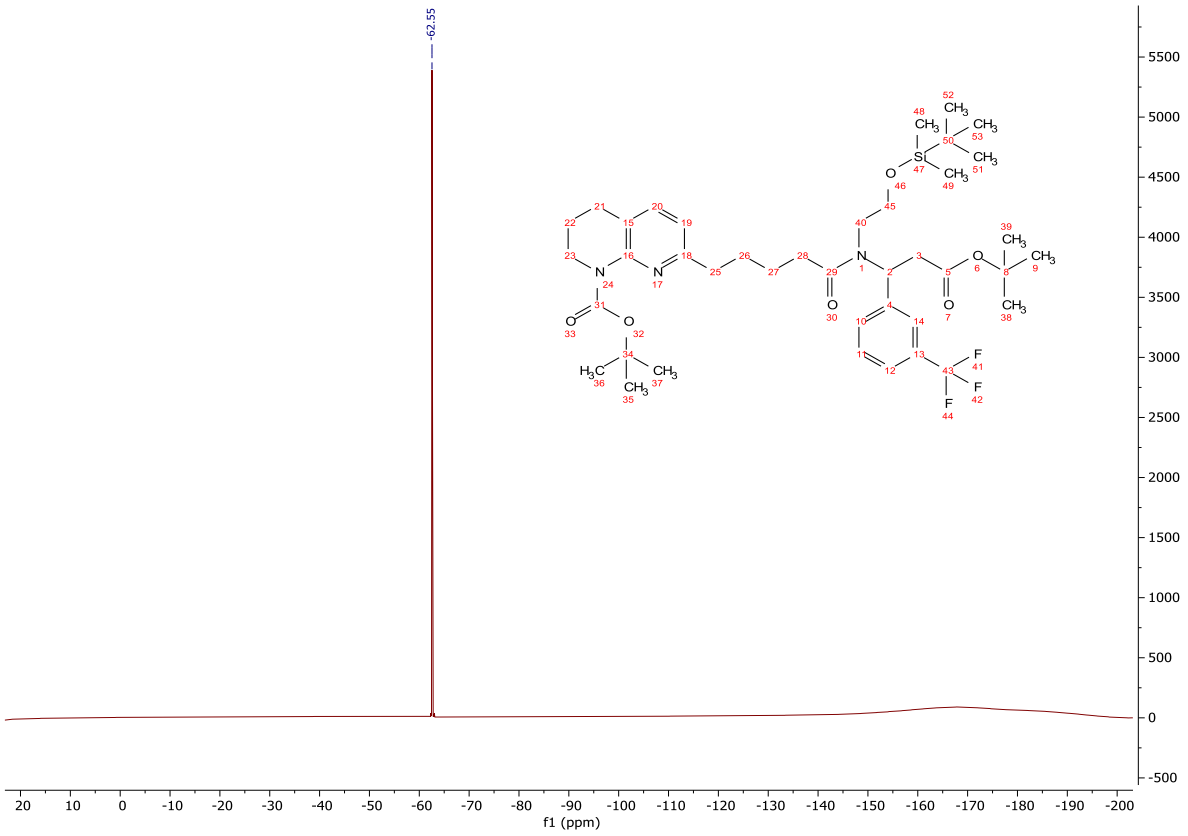
-62.55
5500
5000
4500
4000
3500
3000
2500
2000
1500
1000
500
0
-500
20 10 0 -10 -20 -30 -40 -50 -60 -70 -80 -90 -100 -110 -120 -130 -140 -150 -160 -170 -180 -190 -200
f1 (ppm)

3-(*N*-(2-Hydroxyethyl)-5-(5,6,7,8-tetrahydro-1,8-napthyridin-2-yl)pentanamido)-3-(3-(trifluoromethyl)phenyl)propanoic acid (**257**)

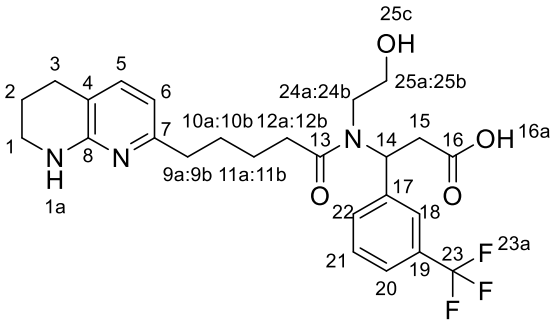

To a stirred solution of **374** (85 mg, 0.131 mmol) in CH_2Cl_2 (25.0 mL) at rt was added TFA (2.50 mL). The reaction mixture was stirred for 17 h, concentrated *in vacuo* and purified on a Waters OASIS® HLB cartridge to afford the title compound as a clear, colourless oil (64 mg, 0.130 mmol, 99%); **HRMS** *m/z* (ESI^+) calc. for $C_{25}H_{31}F_3N_3O_4$ $[M+H]^+$ requires 494.2261, found 494.2261; $\boldsymbol{R_f}$ 0.24, 5% methanol/CH_2Cl_2, UV active; δ_H (400 MHz, $CDCl_3$) 10.46 (1H, bs, H-1a), 7.58 – 7.38 (4H, m, H-18, H-20, H-21 and H-22), 7.29 – 7.21 (2H, m, H-5 and ArH Rotamer), 7.19 – 7.12 (1H, m, ArH Rotamer), 6.33 – 6.24 (1H, m, H-6), 5.92 – 5.81 (1H, m, H-14), 3.88 – 3.70 (2H, m, H-12a and H-25a), 3.65 – 3.53 (2H, m, H-24a and H-25b), 3.52 – 3.39 (2H, m, H-1), 3.10 – 2.98 (2H, m, H-15), 2.86 (1H, ddd, *J* = 13.3, 9.5, 6.2 Hz, H-9a), 2.80 – 2.64 (3H, m, H-3 and H-24b), 2.54 (1H, ddd, *J* = 13.3, 9.2, 6.0 Hz, H-9b), 2.39 – 2.25 (1H, m, H-12b), 2.07 – 1.77 (4H, m, H-2, H-10a and H-11a), 1.68 – 1.56 (1H, m, H-11b), 1.54 – 1.41 (1H, m, H-10b); δ_C (101 MHz, $CDCl_3$) 179.5 (CO), 174.7 (CO), 153.2 (C), 150.4 (C), 140.9 (C), 140.1 (ArH), 131.3 (C, q, *J* = 32.6 Hz), 130.6 (ArH), 129.4 (ArH), 129.2 (ArH*), 128.4 (ArH*), 124.8 (ArH, q, *J* = 3.8 Hz), 124.1 (CF_3, q, *J* = 272.9 Hz), 123.8 (ArH, q, *J* = 3.8 Hz), 118.1 (C), 109.4 (ArH), 62.4 (CH_2), 57.3 (CH), 48.3 (CH_2), 40.8 (CH_2), 40.4 (CH_2), 31.1 (CH_2), 29.8 (CH_2), 29.5 (CH_2), 25.8 (CH_2), 22.7 (CH_2), 19.7 (CH_2); δ_F (376 MHz, $CDCl_3$) -62.6 (F-23a); ν_{max} (FT-ATR/cm^{-1}) 3242, 2917, 1672, 1629, 1560,1444, 1412, 1389, 1374, 1287, 1203, 1162, 1006, 901, 807, 730, 604.

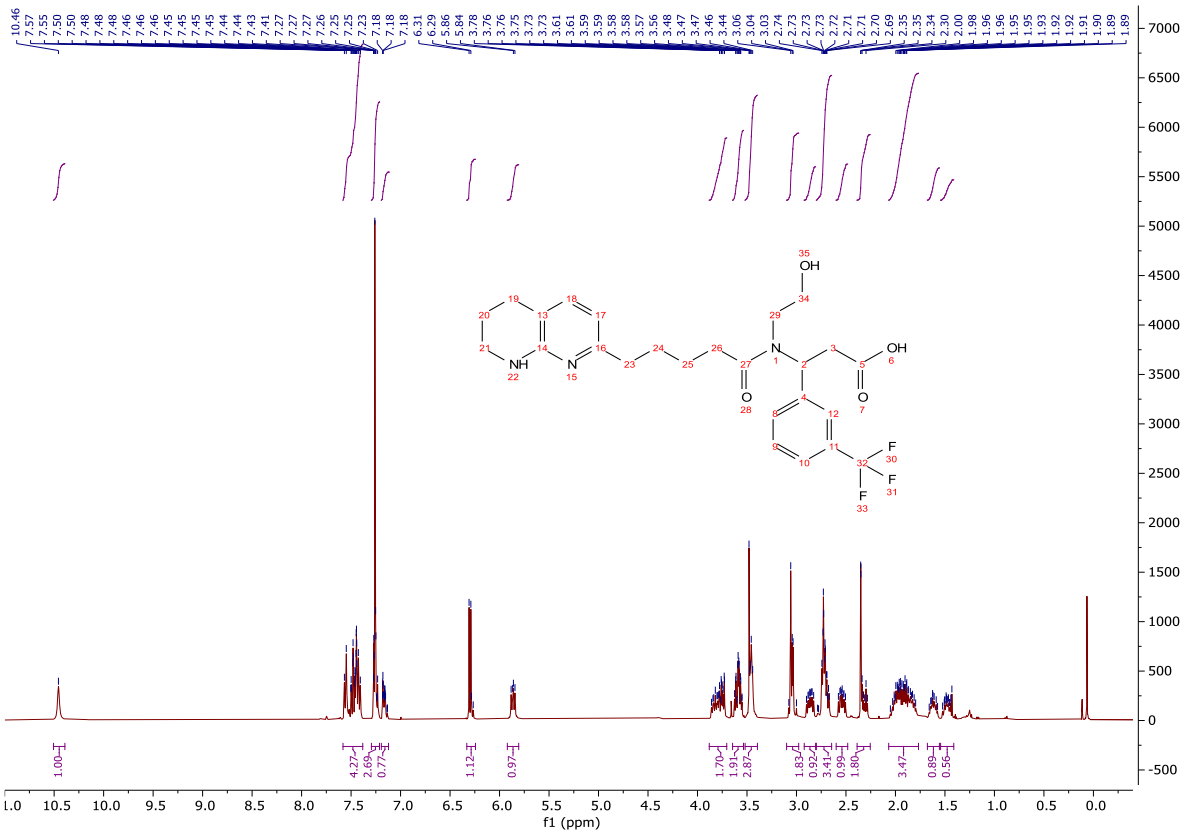
f1 (ppm)

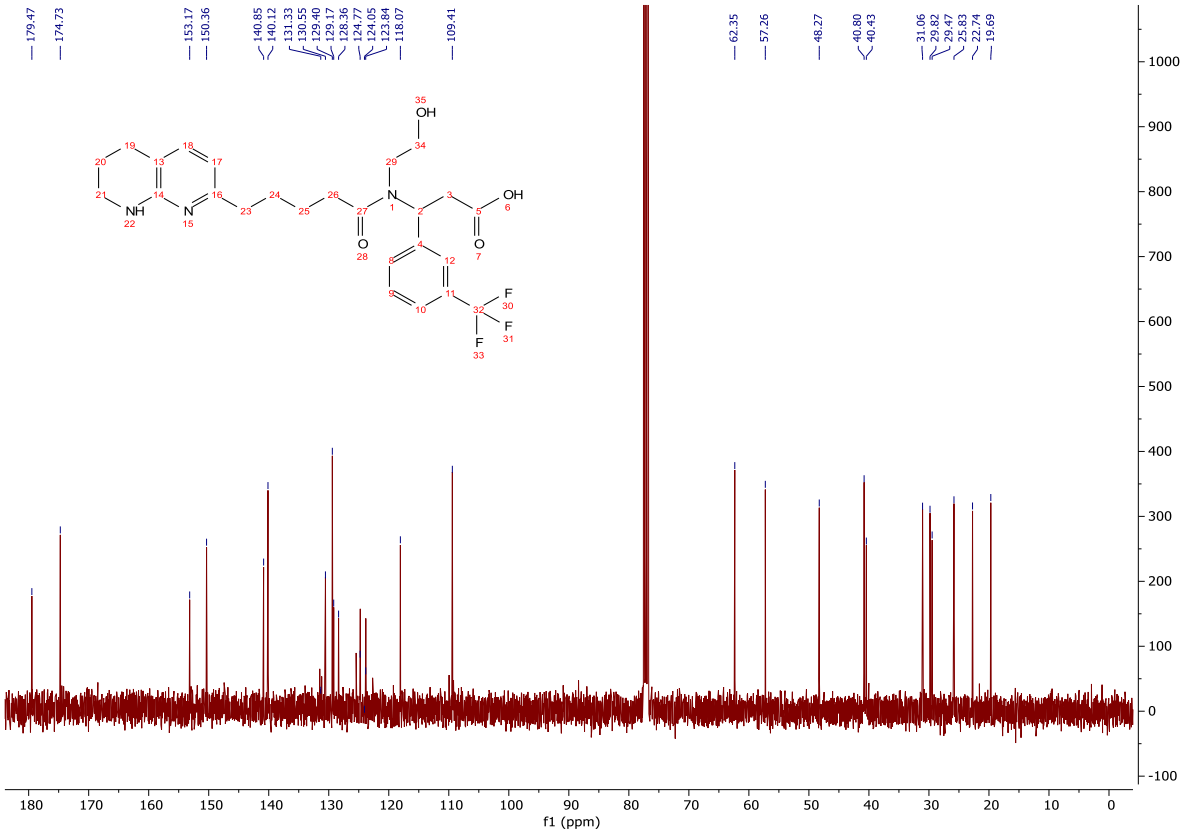
f1 (ppm)

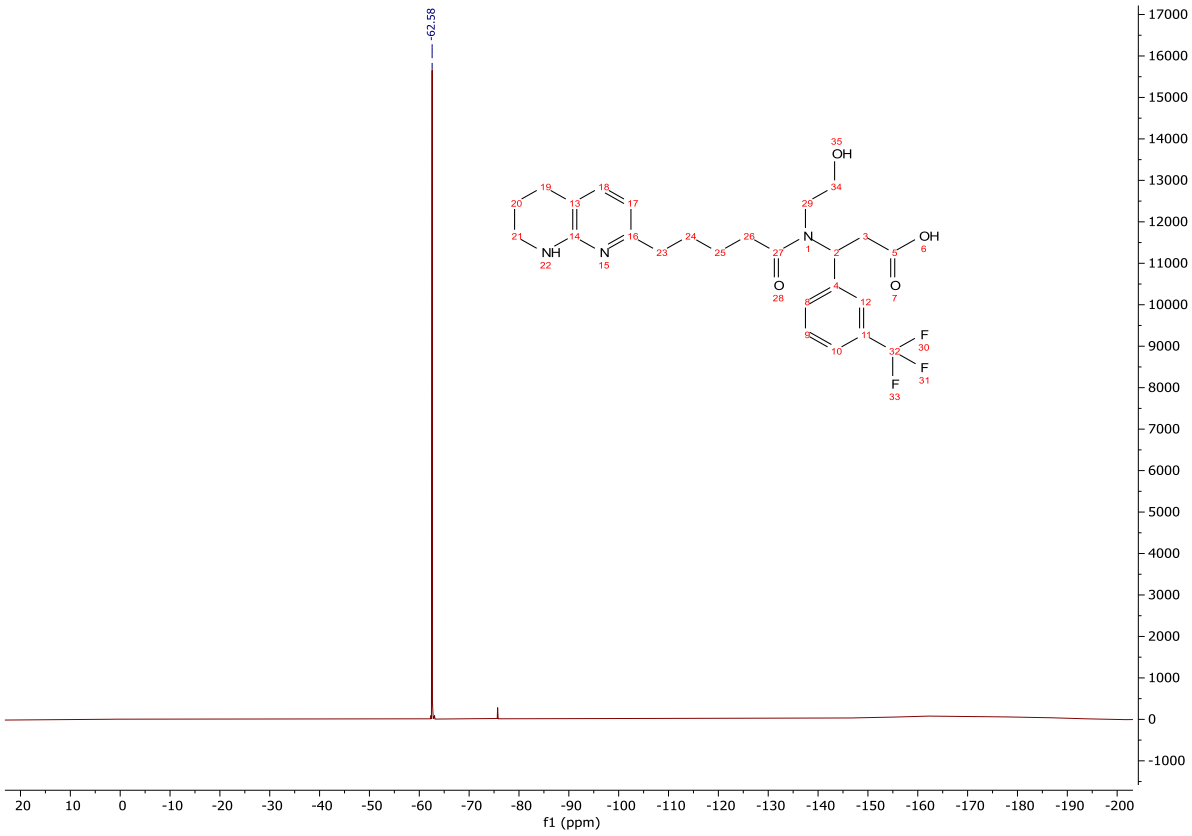
-62.58
f1 (ppm)

Ethyl (*S*)-3-((*tert*-butoxycarbonyl)amino)-3-(3-(4,4,5,5-tetramethyl-1,3,2-dioxaborolan-2-yl)phenyl)propanoate (**275**)

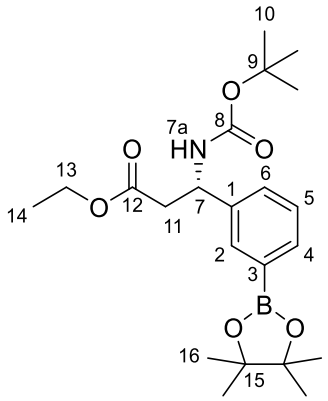

A mixture of **(*S*)-119** (2.71 g, 7.30 mmol), B_2Pin_2 (2.79 g, 11.0 mmol), KOAc (2.15 g, 21.9 mmol) and $Pd(dppf)Cl_2.CH_2Cl_2$ (596 mg, 0.730 mmol) in 1,4-dioxane (19.0 mL) was stirred under a nitrogen atmosphere at 80 °C for 16 h. The reaction mixture was concentrated *in vacuo* and the crude product dissolved in ethyl acetate (100 mL). The organic was filtered through Celite®, washed with sat. $NaHCO_{3(aq)}$ (2 x 100 mL), brine (2 x 100 mL), dried ($MgSO_4$) and concentrated *in vacuo* to afford a dark brown oil. The crude product was purified by column chromatography on silica gel, eluting with a gradient of ethyl acetate/light petroleum (0-50%) to afford the title compound as a colourless oil (1.98 g, 4.73 mmol, 65%); **HRMS** *m/z* (ESI^+) calc. for $C_{22}H_{35}BNO_6$ $[M+H]^+$ requires 420.2552, found 420.2555; $\boldsymbol{R_f}$ 0.30, 10% ethyl acetate/light petroleum, UV active; δ_H (400 MHz, $CDCl_3$) 7.73 – 7.66 (2H, m, H-2 and H-4), 7.40 (1H, ddd, *J* = 7.7, 1.7 Hz, H-6), 7.33 (1H, ddd, *J* = 7.8, 7.1, 0.7 Hz, H-5), 5.41 (1H, bs, H-7a), 5.10 (1H, bs, H-7), 4.07 (2H, q, *J* = 7.1 Hz, H-13), 2.93 – 2.71 (2H, m, H-11), 1.41 (9H, s, H-10), 1.34 (12H, s, H-16), 1.18 (3H, t, *J* = 7.1 Hz, H-14); δ_C (126 MHz, $CDCl_3$) 170.9 (CO), 155.1 (CO), 140.6 (C), 134.0 (ArH), 132.4 (ArH), 129.3 (ArH), 128.0 (ArH), 127.7 (C), 83.9 (C), 79.6 (C), 60.7 (CH_2), 51.5 (CH), 41.3 (CH_2), 28.4 (CH_3), 24.9 (CH_3), 14.1 (CH_3); ν_{max} (FT-ATR/cm^{-1}) 3349, 2978, 1713, 1501, 1365, 1245, 1161, 1020, 793, 708.

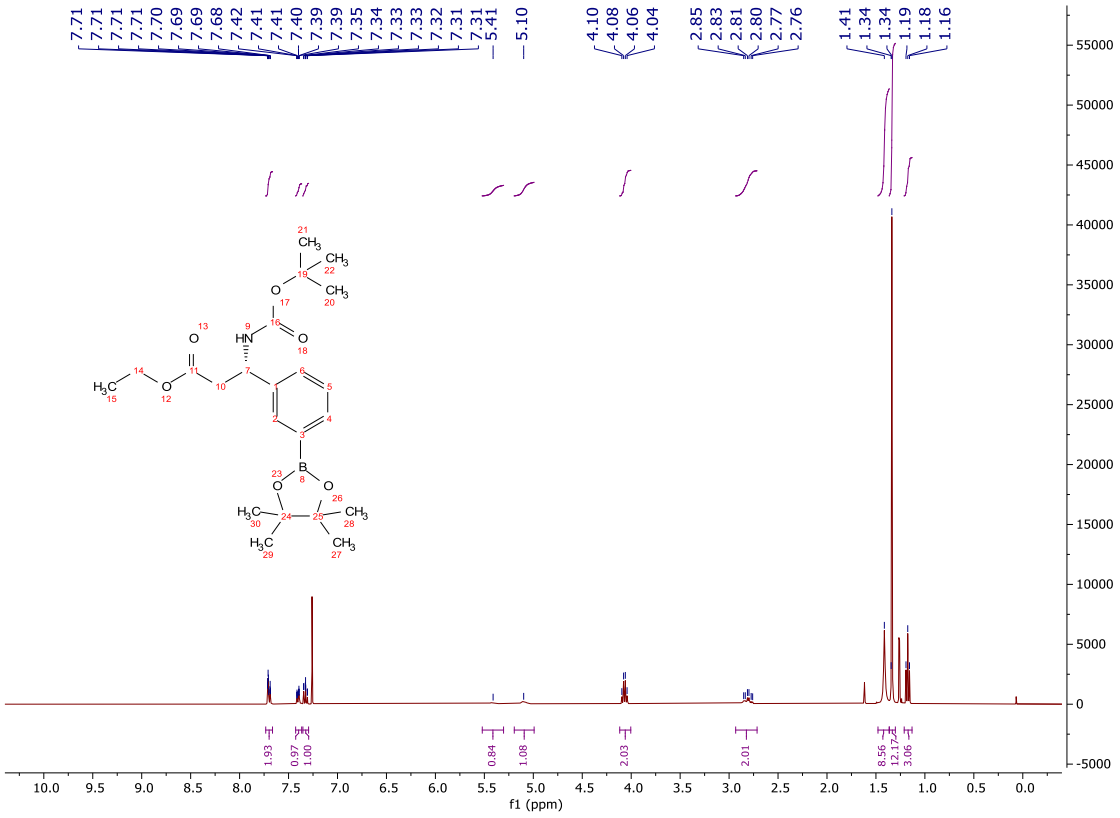
7.71
7.71
7.71
7.71
7.70
7.69
7.69
7.68
7.42
7.41
7.41
7.40
7.39
7.39
7.35
7.34
7.33
7.33
7.32
7.31
7.31
5.41
5.10
4.10
4.08
4.06
4.04
2.85
2.83
2.81
2.80
2.77
2.76
1.41
1.34
1.34
1.19
1.18
1.16
1.93
0.97
1.00
0.84
1.08
2.03
2.01
8.56
12.17
3.06
f1 (ppm)

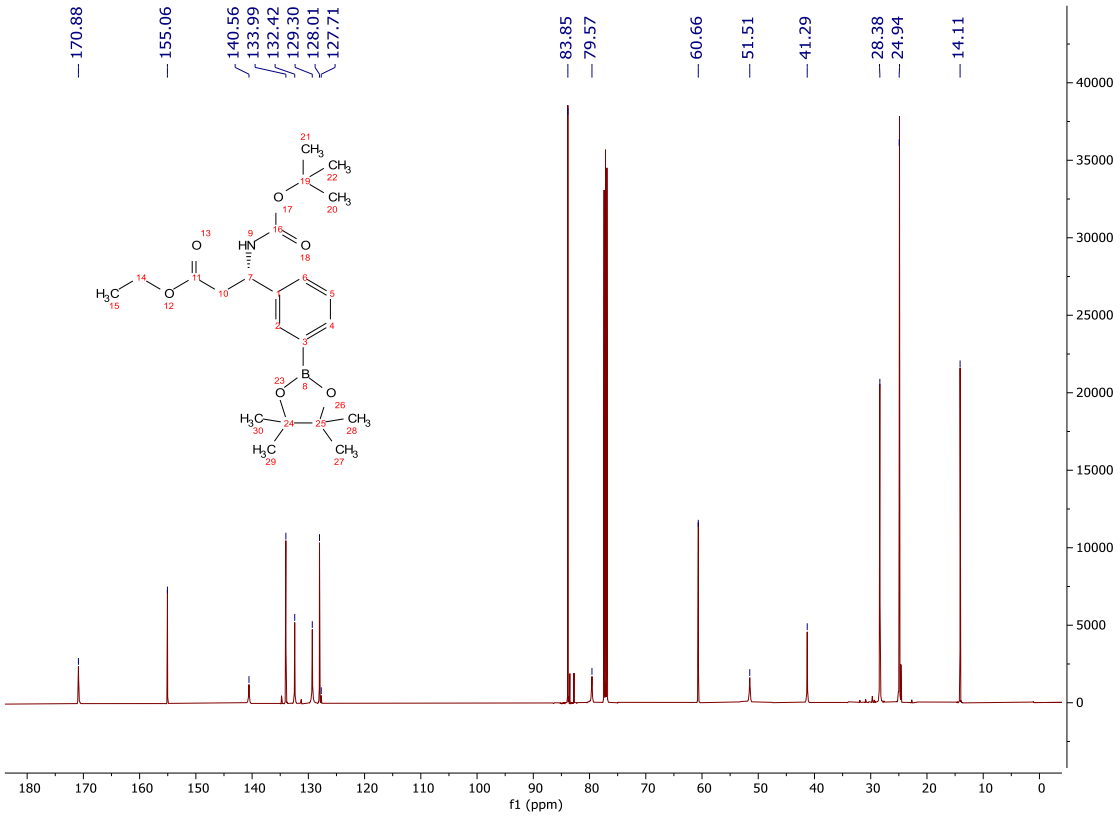
170.88
155.06
140.56
133.99
132.42
129.30
128.01
127.71
83.85
79.57
60.66
51.51
41.29
28.38
24.94
14.11
f1 (ppm)

Ethyl (*S*)-3-((*tert*-butoxycarbonyl)amino)-3-(3-(3-chloro-1*H*-pyrazol-1-yl)phenyl)propanoate (**276**)

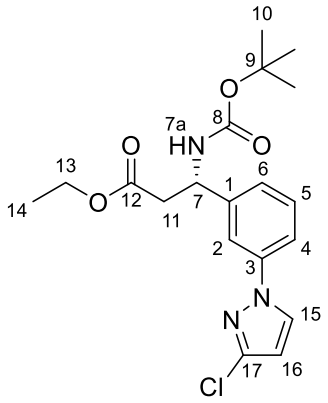

A mixture of **275** (400 mg, 0.955 mmol), 5-chloro-1*H*-pyrazole (246 mg, 2.39 mmol), $B(OH)_3$ (118 mg, 1.91 mmol), $Cu(OAc)_2$ (170 mg, 0.955 mmol) and 3 Å molecular sieves (300 mg) in acetonitrile (3.00 mL) was stirred at 70 °C for 18 h. The reaction mixture was cooled to rt, diluted with ethyl acetate (50.0 mL), filtered through Celite® and washed with sat. $NaHCO_{3(aq)}$ (30.0 mL). The layers were separated and the aqueous extracted with ethyl acetate (2 x 20.0 mL). The organics were combined and washed with sat. $NaHCO_{3(aq)}$ (30.0 mL), water (30.0 mL) and brine (30.0 mL). The organic was dried ($MgSO_4$) and concentrated *in vacuo* giving a dark brown oil. The crude product was purified by column chromatography on silica gel, eluting with a gradient of ethyl acetate/light petroleum (0-25%) to afford the title compound as a yellow oil (189 mg, 0.481 mmol, 50%); **HRMS** *m/z* (ESI^+) calc. for $C_{19}H_{25}ClN_3O_4$ $[M+H]^+$ requires 394.1528, found 394.1530; $\boldsymbol{R_f}$ 0.38, 20% ethyl acetate/light petroleum, UV active; δ_H (400 MHz, $CDCl_3$) 7.84 (1H, d, *J* = 2.5 Hz, H-15), 7.62 (1H, dd, *J* = 2.0, 2.0 Hz, H-2), 7.51 (1H, ddd, *J* = 8.2, 2.3, 1.1 Hz, H-4), 7.39 (1H, dd, *J* = 7.9, 7.9 Hz, H-5), 7.28 – 7.21 (1H, m, H-6), 6.40 – 6.35 (1H, m, H-16), 5.61 (1H, bs, H-7a), 5.13 (1H, s, H-7), 4.08 (2H, q, *J* = 7.1 Hz, H-13), 2.93 – 2.74 (2H, m, H-11), 1.42 (9H, s, H-10), 1.17 (3H, t, *J* = 7.1 Hz, H-14); δ_C (101 MHz, $CDCl_3$) 170.8 (CO), 155.2 (CO), 143.5 (C), 141.8 (C), 139.9 (C), 129.9 (ArH), 128.7 (ArH), 124.8 (ArH), 117.9 (ArH), 117.0 (ArH), 107.4 (ArH), 80.1 (C), 61.0 (CH_2), 51.3 (CH), 41.0 (CH_2), 28.5 (CH_3), 14.2 (CH_3); ν_{max} (FT-ATR/cm^{-1}) 3232, 2978, 1689, 1610, 1510, 1367, 1161, 1045, 753.

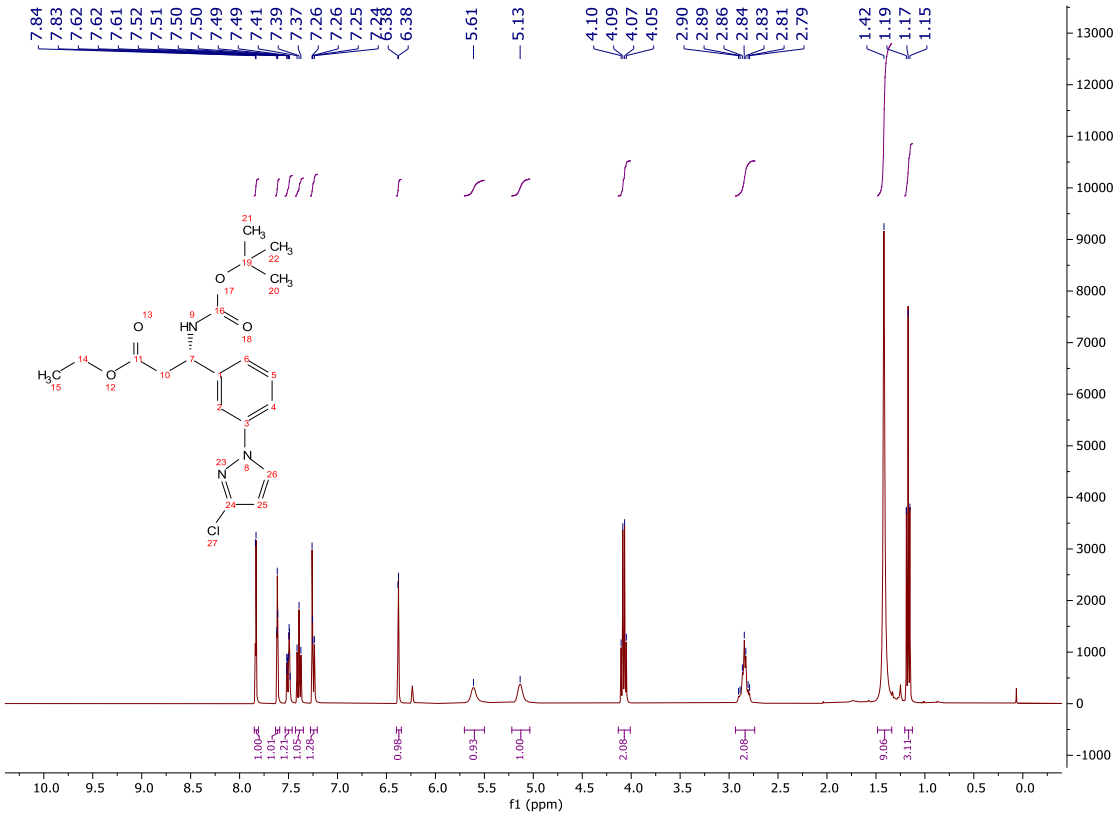
7.84
7.83
7.62
7.62
7.61
7.52
7.51
7.50
7.50
7.49
7.49
7.41
7.39
7.37
7.26
7.26
7.25
7.24
6.38
6.38
5.61
5.13
4.10
4.09
4.07
4.05
2.90
2.89
2.86
2.84
2.83
2.81
2.79
1.42
1.19
1.17
1.15
1.00
1.01
1.21
1.05
1.28
0.98
0.93
1.00
2.08
2.08
9.06
3.11
f1 (ppm)

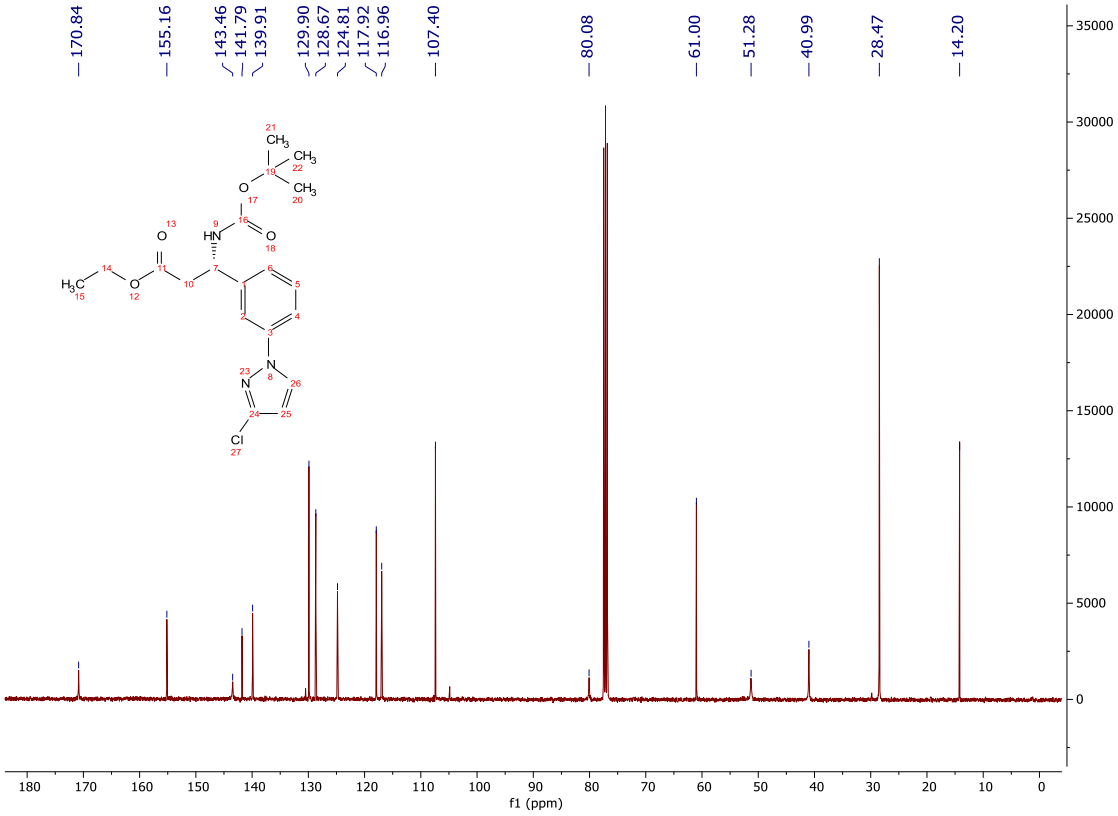
170.84
155.16
143.46
141.79
139.91
129.90
128.67
124.81
117.92
116.96
107.40
80.08
61.00
51.28
40.99
28.47
14.20
f1 (ppm)

Ethyl (*S*)-3-((*tert*-butoxycarbonyl)amino)-3-(3-(3-isopropyl-1*H*-pyrazol-1-yl)phenyl)propanoate (**277**)

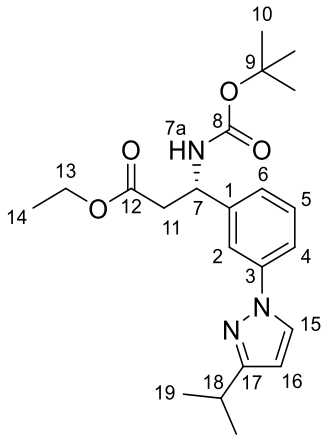

A mixture of **275** (400 mg, 0.955 mmol), 5-isopropyl-1*H*-pyrazole (263 mg, 2.39 mmol), $B(OH)_3$ (118 mg, 1.91 mmol), $Cu(OAc)_2$ (170 mg, 0.955 mmol) and 3 Å molecular sieves (300 mg) in acetonitrile (3.00 mL) was stirred at 70 °C for 18 h. The reaction mixture was cooled to rt, diluted with ethyl acetate (50.0 mL), filtered through Celite® and washed with sat. $NaHCO_{3(aq)}$ (30.0 mL). The layers were separated and the aqueous extracted with ethyl acetate (2 x 20.0 mL). The organics were combined and washed with sat. $NaHCO_{3(aq)}$ (30.0 mL), water (30.0 mL) and brine (30.0 mL). The organic was dried ($MgSO_4$) and concentrated *in vacuo* giving a dark brown oil. The crude product was purified by column chromatography on silica gel, eluting with a gradient of ethyl acetate/light petroleum (0-25%) to afford the title compound as a colourless oil (213 mg, 0.531 mmol, 56%); **HRMS** *m/z* (ESI^+) calc. for $C_{22}H_{32}N_3O_4$ $[M+H]^+$ requires 402.2387, found 402.2384; $\boldsymbol{R_f}$ 0.45, 20% ethyl acetate/light petroleum, UV active; δ_H (400 MHz, $CDCl_3$) 7.78 (1H, d, *J* = 2.5 Hz, H-15), 7.61 (1H, dd, *J* = 2.0, 2.0 Hz, H-2), 7.51 (1H, ddd, *J* = 8.2, 2.3, 1.0 Hz, H-4), 7.34 (1H, dd, *J* = 7.9, 7.9 Hz, H-5), 7.16 (1H, ddd, *J* = 7.6, 0.9, 0.9 Hz, H-6), 6.25 (1H, d, *J* = 2.5 Hz, H-16), 5.60 (1H, bs, H-7a), 5.13 (1H, bs, H-7), 4.06 (2H, q, *J* = 7.2 Hz, H-13), 3.06 (1H, hept, *J* = 6.9 Hz, H-18), 2.95 – 2.71 (2H, m, H-11), 1.40 (9H, s, H-10), 1.29 (6H, d, *J* = 7.0 Hz, H-19), 1.15 (3H, t, *J* = 7.2 Hz, H-14); δ_C (101 MHz, $CDCl_3$) 170.8 (CO), 161.1 (C), 155.1 (CO), 143.0 (C), 140.6 (C), 129.6 (ArH), 127.2 (ArH), 123.6

(ArH), 117.9 (ArH), 116.9 (ArH), 104.6 (ArH), 79.8 (C), 60.8 (CH_2), 51.3 (CH), 41.0 (CH_2), 28.4 (CH_3), 28.1 (CH), 22.9 (CH_3), 22.9 (CH_3), 14.1 (CH_3); ν_{max} (FT-ATR/cm^{-1}) 3359, 2967, 1705, 1595, 1495, 1366, 1161, 1043, 755.

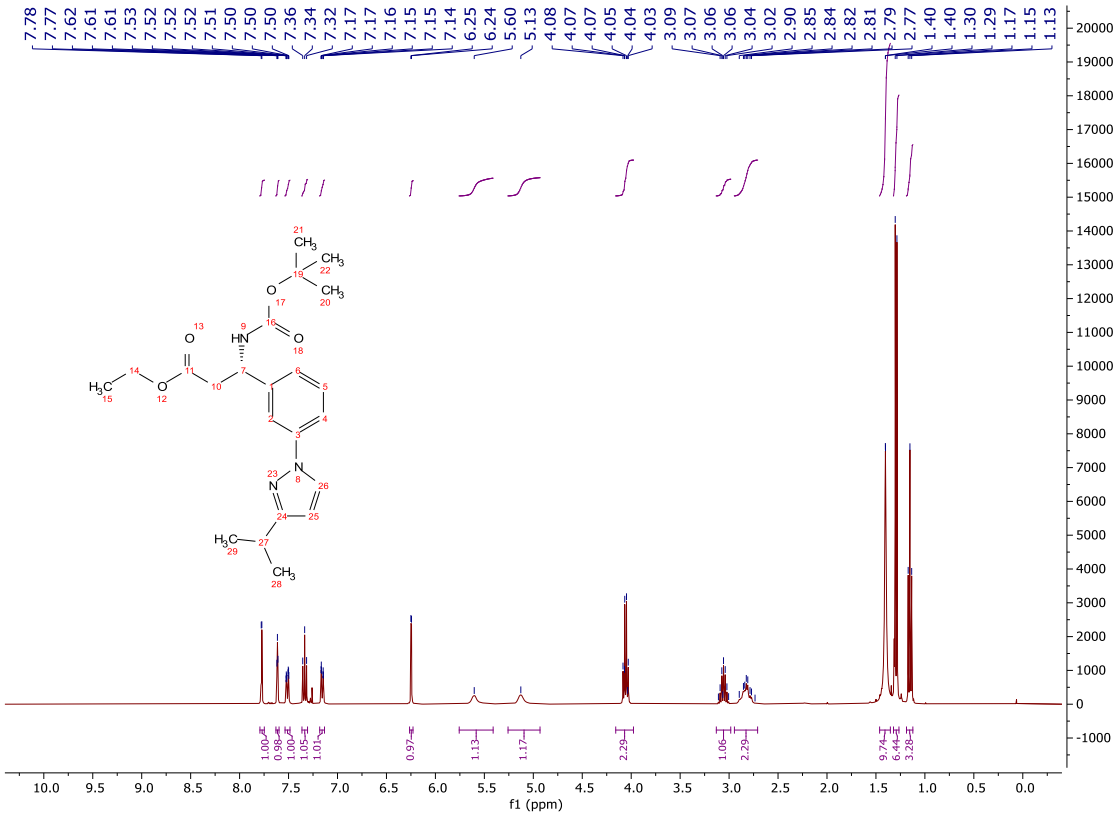
7.78 7.77 7.62 7.61 7.61 7.53 7.52 7.52 7.52 7.51 7.50 7.50 7.50 7.36 7.34 7.32 7.17 7.17 7.16 7.15 7.15 7.14 6.25 6.24 5.60 5.13 4.08 4.07 4.07 4.05 4.04 4.03 3.09 3.07 3.06 3.06 3.04 3.02 2.90 2.85 2.84 2.82 2.81 2.79 2.77 1.40 1.40 1.30 1.29 1.17 1.15 1.13
1.00 0.98 1.00 1.05 1.01 0.97 1.13 1.17 2.29 1.06 2.29 9.74 6.44 3.28
f1 (ppm)

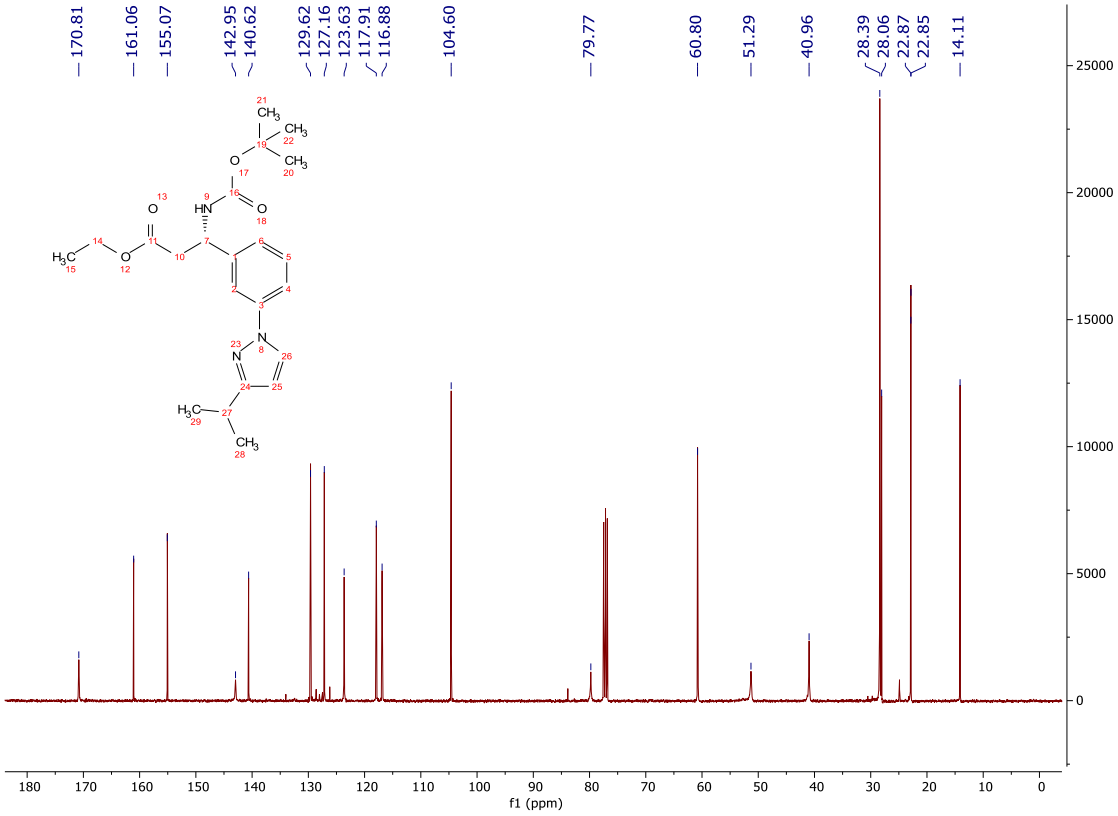
170.81 161.06 155.07 142.95 140.62 129.62 127.16 123.63 117.91 116.88 104.60 79.77 60.80 51.29 40.96 28.39 28.06 22.87 22.85 14.11
f1 (ppm)

Ethyl (*S*)-3-((*tert*-butoxycarbonyl)amino)-3-(3-(piperidin-1-yl)phenyl)propanoate (**278**)

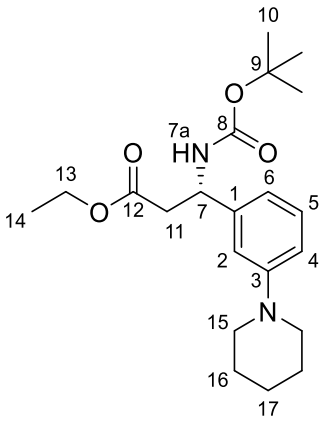

A mixture of **275** (400 mg, 0.955 mmol), piperidine (0.240 mL, 2.39 mmol), $B(OH)_3$ (118 mg, 1.91 mmol), $Cu(OAc)_2$ (170 mg, 0.955 mmol) and 3 Å molecular sieves (300 mg) in acetonitrile (3.00 mL) was stirred at 70 °C for 18 h. The reaction mixture was cooled to rt, diluted with ethyl acetate (50.0 mL), filtered through Celite® and washed with sat. $NaHCO_{3(aq)}$ (30.0 mL). The layers were separated and the aqueous extracted with ethyl acetate (2 x 20.0 mL). The organics were combined and washed with sat. $NaHCO_{3(aq)}$ (30.0 mL), water (30.0 mL) and brine (30.0 mL). The organic was dried ($MgSO_4$) and concentrated *in vacuo* giving a dark brown oil. The crude product was purified by column chromatography on silica gel, eluting with a gradient of ethyl acetate/light petroleum (0-25%) to afford the title compound as a yellow oil (160 mg, 0.426 mmol, 45%); **HRMS** *m/z* (ESI^+) calc. for $C_{21}H_{33}N_2O_4$ $[M+H]^+$ requires 377.2435, found 377.2427; $\boldsymbol{R_f}$ 0.46, 20% ethyl acetate/light petroleum, UV active; δ_H (400 MHz, $CDCl_3$) 7.19 (1H, dd, *J* = 7.9, 7.9 Hz, H-5), 6.87 – 6.84 (1H, m, H-2), 6.82 (1H, ddd, *J* = 8.2, 2.5, 0.9 Hz, H-4), 6.73 (1H, ddd, *J* = 7.5, 1.1, 1.1 Hz, H-6), 5.43 – 5.23 (1H, m, H-7a), 5.15 – 4.92 (1H, m, H-7), 4.07 (2H, q, *J* = 7.1 Hz, H-13), 3.14 (4H, t, H-15), 2.91-2.70 (2H, m, H-11), 1.75 – 1.64 (4H, m, H-16), 1.62 – 1.52 (2H, m, H-17), 1.42 (9H, s, H-10), 1.18 (3H, t, *J* = 7.1 Hz, H-14); δ_C (101 MHz, $CDCl_3$) 171.0 (CO), 155.0 (CO), 152.5 (C), 142.0 (C), 129.3 (ArH), 116.7 (ArH), 115.5 (ArH), 114.5 (ArH), 79.5 (C), 60.6 (CH_2), 51.7 (CH), 50.6 (CH_2), 41.2 (CH_2), 28.4 (CH_3), 25.8 (CH_2), 24.3 (CH_2), 14.1 (CH_3); ν_{max} (FT-ATR/cm^{-1}) 3355, 1932, 1702, 1493, 1241, 1162, 1023, 731.

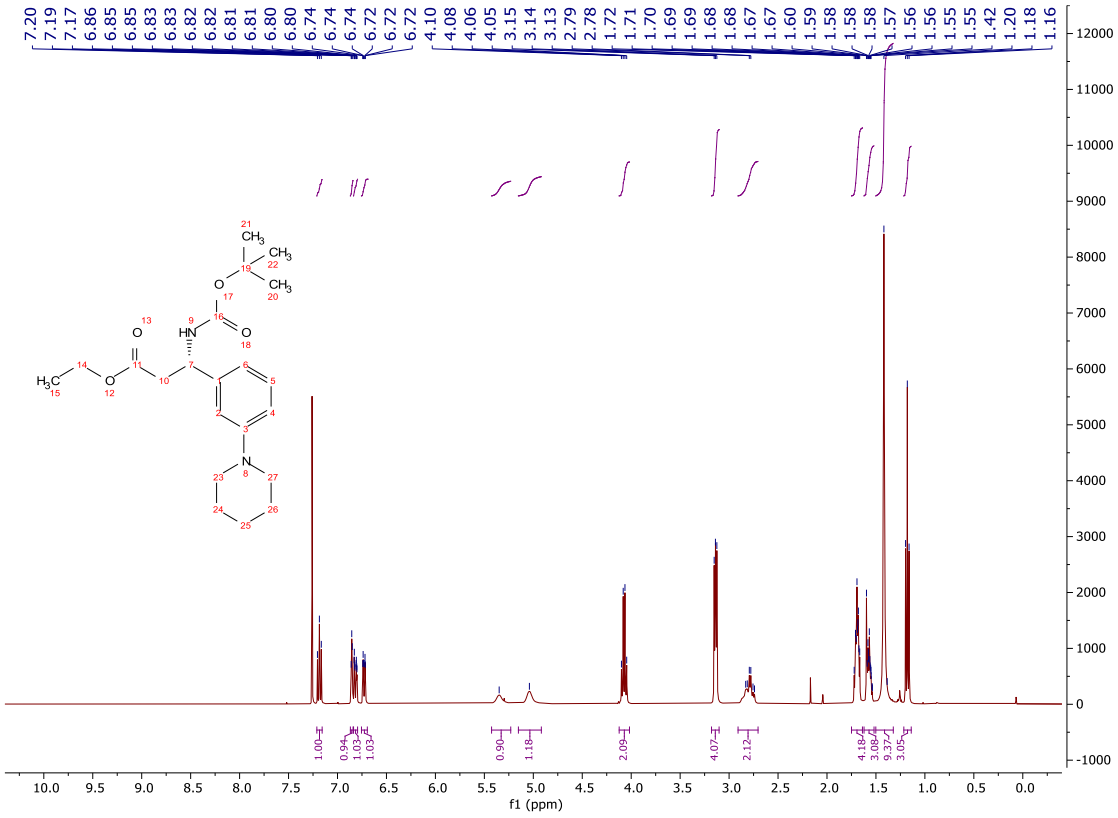
7.20 7.19 7.17 6.86 6.85 6.85 6.83 6.83 6.82 6.82 6.81 6.81 6.80 6.80 6.74 6.74 6.74 6.72 6.72 6.72 4.10 4.08 4.06 4.05 3.15 3.14 3.13 2.79 2.78 1.72 1.71 1.70 1.69 1.69 1.68 1.68 1.67 1.67 1.60 1.59 1.58 1.58 1.58 1.57 1.56 1.56 1.55 1.55 1.42 1.20 1.18 1.16
1.00 0.94 1.03 1.03 0.90 1.18 2.09 4.07 2.12 4.18 3.08 9.37 3.05
f1 (ppm)

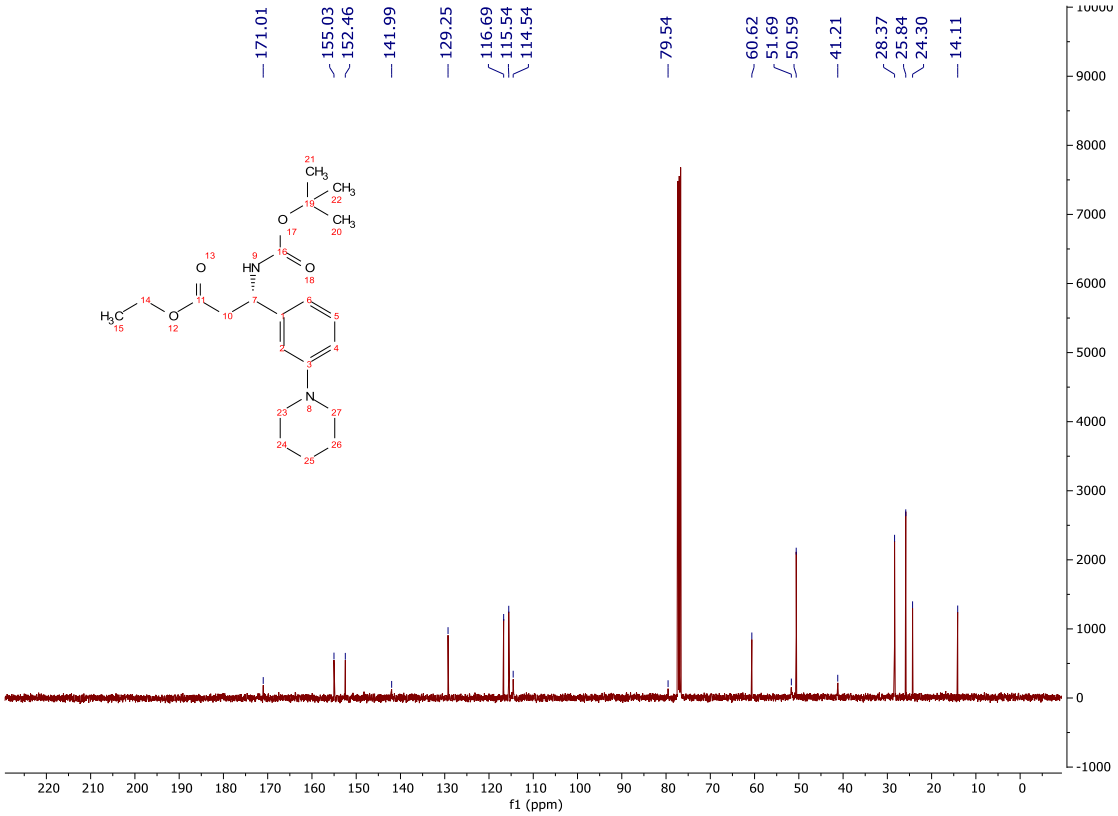
171.01 155.03 152.46 141.99 129.25 116.69 115.54 114.54 79.54 60.62 51.69 50.59 41.21 28.37 25.84 24.30 14.11
f1 (ppm)

tert-Butyl (*S*)-7-(5-((1-(3-(3-chloro-1*H*-pyrazol-1-yl)phenyl)-3-ethoxy-3-oxopropyl)amino)-5-oxopentyl)-3,4-dihydro-1,8-naphthyridine-1(2*H*)-carboxylate (**279**)

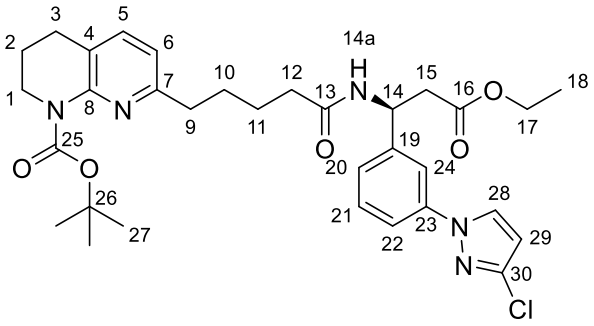

To a stirred solution of **276** (189 mg, 0.481 mmol) in diethyl ether (1.50 mL) at rt was added 4M HCl in dioxane (2.41 mL). The reaction mixture was stirred for 3 h and concentrated *in vacuo*. The crude product was dissolved in acetonitrile (2.50 mL) and **82** (164 mg, 0.481 mmol) was added and the mixture cooled to 0 °C. T3P (50% in ethyl acetate, 0.580 mL, 0.962 mmol) and *i*-Pr_2NEt (0.420 mL, 2.41 mmol) were added, and the reaction mixture stirred for 16 h. The reaction mixture was concentrated *in vacuo*, dissolved in ethyl acetate (10.0 mL) and washed with sat. $NaHCO_{3(aq)}$ (10.0 mL), sat. $NH_4Cl_{(aq)}$ (10.0 mL), sat. $NaHCO_{3(aq)}$ (10.0 mL) and brine (10.0 mL). The organic was dried ($MgSO_4$) and concentrated *in vacuo* giving a dark brown oil. The crude product was purified by column chromatography on silica gel, eluting with a gradient of ethyl acetate/light petroleum (50-100%) to afford the title compound as a yellow oil (104 mg, 0.171 mmol, 36%); **HRMS** *m/z* (ESI^+) calc. for $C_{32}H_{41}ClN_5O_5$ $[M+H]^+$ requires 610.2791, found 610.2791; $\boldsymbol{R_f}$ 0.30, 80% ethyl acetate/light petroleum, UV active; δ_H (400 MHz, $CDCl_3$) 7.82 (1H, d, *J* = 2.5 Hz, H-28), 7.60 (1H, dd, *J* = 2.0, 2.0 Hz, H-24), 7.53 – 7.47 (1H, m, H-22), 7.37 (1H, dd, *J* = 7.9, 7.9 Hz, H-21), 7.29 – 7.20 (2H, m, H-5 and H-20), 6.81 – 6.73 (2H, m, H-6 and H-14a), 6.36 (1H, d, *J* = 2.5 Hz, H-29), 5.45 (1H, ddd, *J* = 8.4, 6.1, 6.1 Hz, H-14), 4.06 (2H, q, *J* = 7.1 Hz, H-17), 3.77 – 3.69 (2H, m, H-1), 2.94 – 2.77 (2H, m, H-15), 2.77 – 2.65 (4H, m, H-3 and H-9), 2.27 (2H, t, *J* = 7.1 Hz, H-12), 1.95 – 1.85 (2H, m, H-2), 1.85 – 1.67 (4H, m, H-10 and H-11), 1.49 (9H, s, H-27), 1.16 (3H, t, *J* = 7.1 Hz, H-18); δ_C (101 MHz, $CDCl_3$) 172.6 (CO), 171.1 (CO), 158.2 (C), 154.2 (CO), 151.2 (C), 143.0 (C), 141.8 (C), 139.9 (C), 137.4 (ArH),

129.9 (ArH), 128.7 (ArH), 125.0 (ArH), 122.0 (C), 118.4 (ArH), 118.0 (ArH), 117.1 (ArH), 107.4 (ArH), 80.9 (C), 61.0 (CH_2), 49.5 (CH), 45.0 (CH_2), 40.1 (CH_2), 37.5 (CH_2), 36.6 (CH_2), 29.1 (CH_2), 28.5 (CH_3), 26.4 (CH_2), 25.4 (CH_2), 23.4 (CH_2), 14.2 (CH_3); ν_{max} (FT-ATR/cm^{-1}) 3297, 2930, 1690, 1596, 1511, 1366, 1147, 1046, 750.

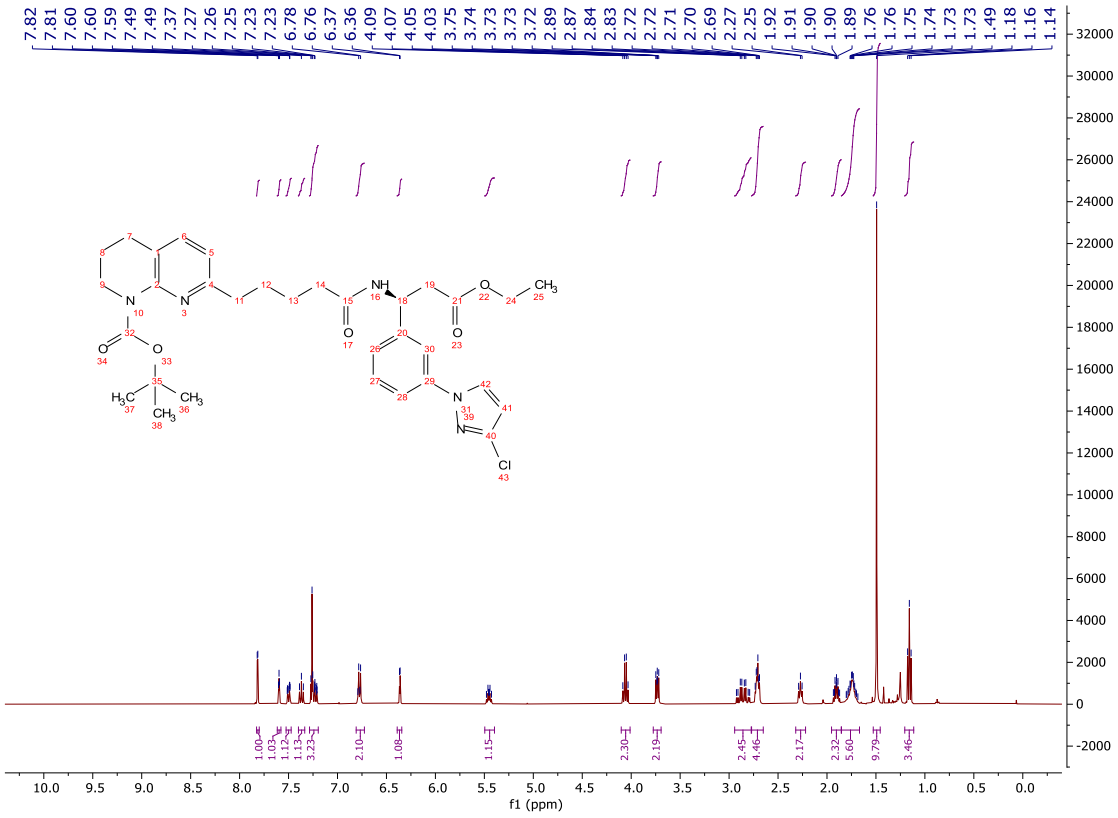
7.82 7.81 7.60 7.60 7.59 7.49 7.49 7.37 7.27 7.26 7.25 7.23 7.23 6.78 6.76 6.37 6.36 4.09 4.07 4.05 4.03 3.75 3.74 3.73 3.73 3.72 2.89 2.87 2.84 2.83 2.72 2.72 2.71 2.70 2.69 2.27 2.25 1.92 1.91 1.90 1.90 1.89 1.76 1.76 1.75 1.74 1.73 1.49 1.18 1.16 1.14
1.00 1.03 1.12 1.13 3.23 2.10 1.08 1.15 2.30 2.19 2.45 4.46 2.17 2.32 5.60 9.79 3.46
f1 (ppm)

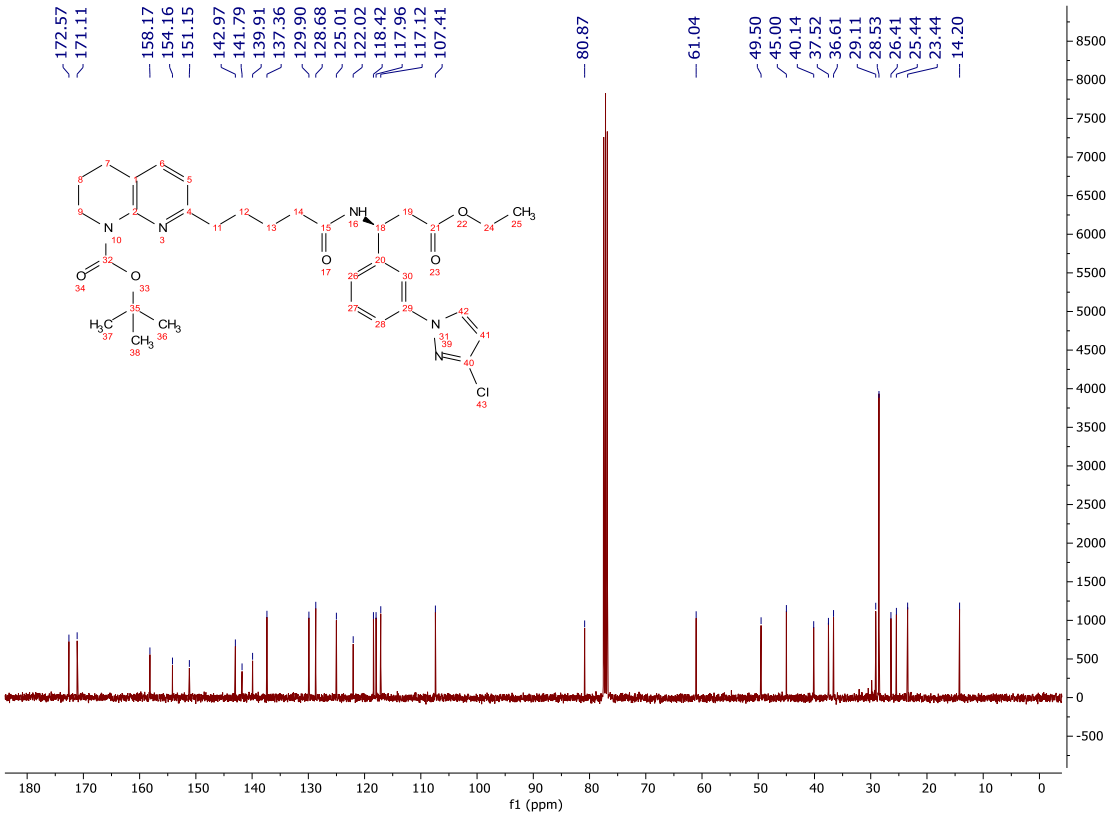
172.57 171.11 158.17 154.16 151.15 142.97 141.79 139.91 137.36 129.90 128.68 125.01 122.02 118.42 117.96 117.12 107.41 80.87 61.04 49.50 45.00 40.14 37.52 36.61 29.11 28.53 26.41 25.44 23.44 14.20
f1 (ppm)

tert-Butyl (*S*)-7-(5-((3-ethoxy-1-(3-(3-isopropyl-1*H*-pyrazol-1-yl)phenyl)-3-oxopropyl)amino)-5-oxopentyl)-3,4-dihydro-1,8-naphthyridine-1(2*H*)-carboxylate (**280**)

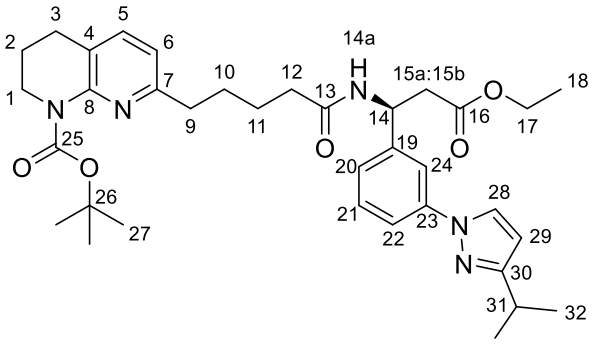

To a stirred solution of **277** (210 mg, 0.524 mmol) in diethyl ether (1.50 mL) at rt was added 4M HCl in dioxane (2.62 mL). The reaction mixture was stirred for 3 h and concentrated *in vacuo*. The crude product was dissolved in acetonitrile (2.60 mL) and **82** (178 mg, 0.524 mmol) was added and the mixture cooled to 0 °C. T3P (50% in ethyl acetate, 0.624 mL, 1.05 mmol) and *i*-Pr_2NEt (0.455 mL, 2.62 mmol) were added, and the reaction mixture stirred for 16 h. The reaction mixture was concentrated *in vacuo*, dissolved in ethyl acetate (10.0 mL) and washed with sat. $NaHCO_{3(aq)}$ (10.0 mL), sat. $NH_4Cl_{(aq)}$ (10.0 mL), sat. $NaHCO_{3(aq)}$ (10.0 mL) and brine (10.0 mL). The organic was dried ($MgSO_4$) and concentrated *in vacuo* giving a dark brown oil. The crude product was purified by column chromatography on silica gel, eluting with a gradient of ethyl acetate/light petroleum (50-100%) to afford the title compound as a clear, yellow oil (132 mg, 0.214 mmol, 41%); **HRMS** *m/z* (ESI^+) calc. for $C_{35}H_{48}N_5O_5$ $[M+H]^+$ requires 618.3650, found 618.3652; $\boldsymbol{R_f}$ 0.42, 2.5% methanol/CH_2Cl_2, UV active; $\boldsymbol{\delta_H}$ (400 MHz, $CDCl_3$) 7.78 (1H, d, *J* = 2.4 Hz, H-28), 7.61 (1H, dd, *J* = 2.0, 2.0 Hz, H-24), 7.52 (1H, ddd, *J* = 8.1, 2.2, 1.0 Hz, H-22), 7.35 (1H, dd, *J* = 7.9, 7.9 Hz, H-21), 7.28 – 7.24 (1H, m, H-5), 7.16 (1H, ddd, *J* = 7.7, 0.9, 0.9 Hz, H-20), 6.78 (1H, d, *J* = 7.6 Hz, H-6), 6.68 (1H, d, *J* = 8.4 Hz, H-14a), 6.26 (1H, d, *J* = 2.5 Hz, H-29), 5.47 (1H, ddd, *J* = 8.5, 6.1, 6.1 Hz, H-14), 4.06 (2H, q, *J* = 7.1 Hz, H-17), 3.77 – 3.69 (2H, m, H-1), 3.07 (1H, hept, *J* = 7.0 Hz, H-31), 2.96 – 2.87 (1H, m, H-15a), 2.83 (1H, dd, *J* = 15.6, 6.1 Hz, H-15b), 2.76 – 2.66 (4H, m, H-3 and H-9), 2.27 (2H, t, *J* = 7.1 Hz, H-12), 1.94 – 1.86 (2H, m, H-2), 1.82-1.62 (4H, m, H-10 and H-11), 1.50 (9H, s, H-27), 1.31 (6H,

d, *J* = 6.9 Hz, H-32), 1.16 (3H, t, *J* = 7.1 Hz, H-18); δ_C (101 MHz, $CDCl_3$) 172.5 (CO), 171.2 (CO), 161.2 (C), 158.2 (C), 154.2 (CO), 151.2 (C), 142.5 (C), 140.7 (C), 137.4 (ArH), 129.8 (ArH), 127.3 (ArH), 123.9 (ArH), 122.0 (C), 118.4 (ArH), 118.1 (ArH), 117.2 (ArH), 104.7 (ArH), 80.9 (C), 61.0 (CH_2), 49.6 (CH), 45.0 (CH_2), 40.2 (CH_2), 37.6 (CH_2), 36.7 (CH_2), 29.2 (CH_2), 28.5 (CH_3), 28.2 (CH), 26.4 (CH_2), 25.5 (CH_2), 23.5 (CH_2), 23.0 (CH_3), 23.0 (CH_3), 14.2 (CH_3); ν_{max} (FT-ATR/cm^{-1}) 3308, 2961, 1692, 1530, 1366, 1148, 1044, 753.

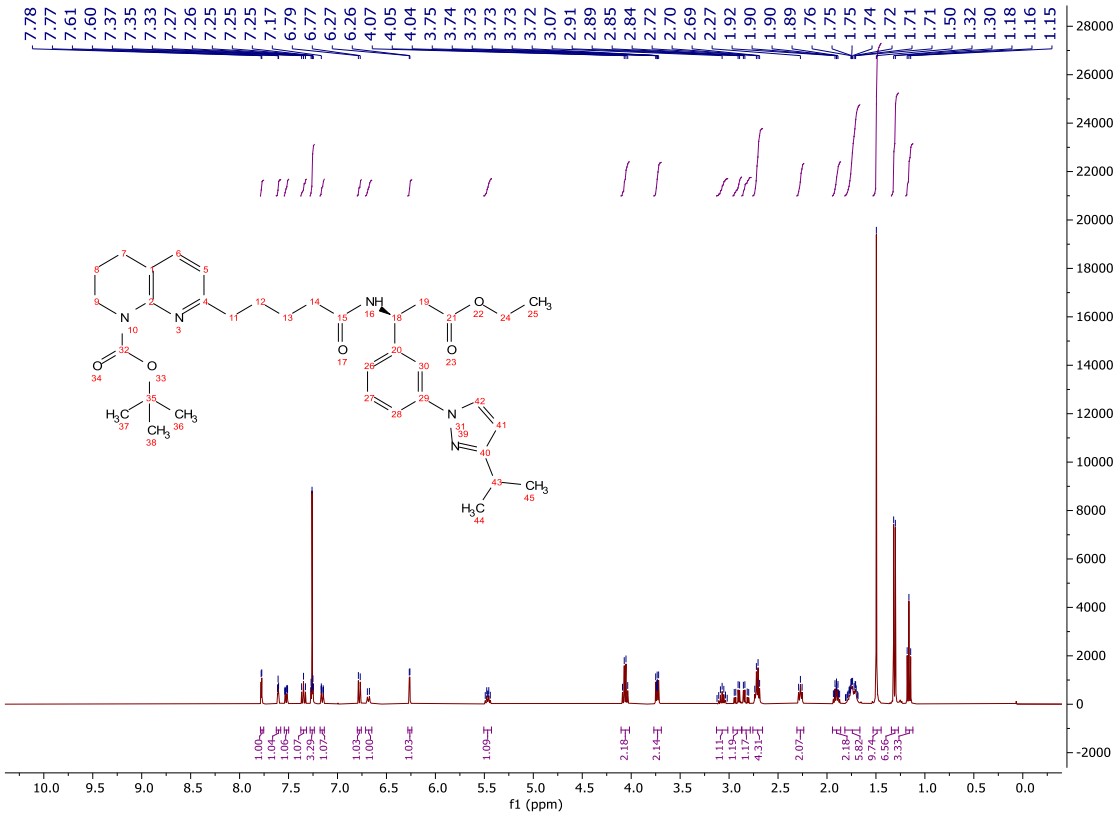
7.78 7.77 7.61 7.60 7.37 7.35 7.33 7.27 7.26 7.25 7.25 7.25 7.17 6.79 6.77 6.27 6.26 4.07 4.05 4.04 3.75 3.74 3.73 3.73 3.73 3.72 3.07 2.91 2.89 2.85 2.84 2.72 2.70 2.69 2.27 1.92 1.90 1.90 1.89 1.76 1.75 1.75 1.74 1.72 1.71 1.71 1.50 1.32 1.30 1.18 1.16 1.15
1.00 1.04 1.06 1.07 3.29 1.07 1.03 1.00 1.03 1.09 2.18 2.14 1.11 1.19 1.17 4.31 2.07 2.18 5.82 9.74 6.56 3.33
f1 (ppm)

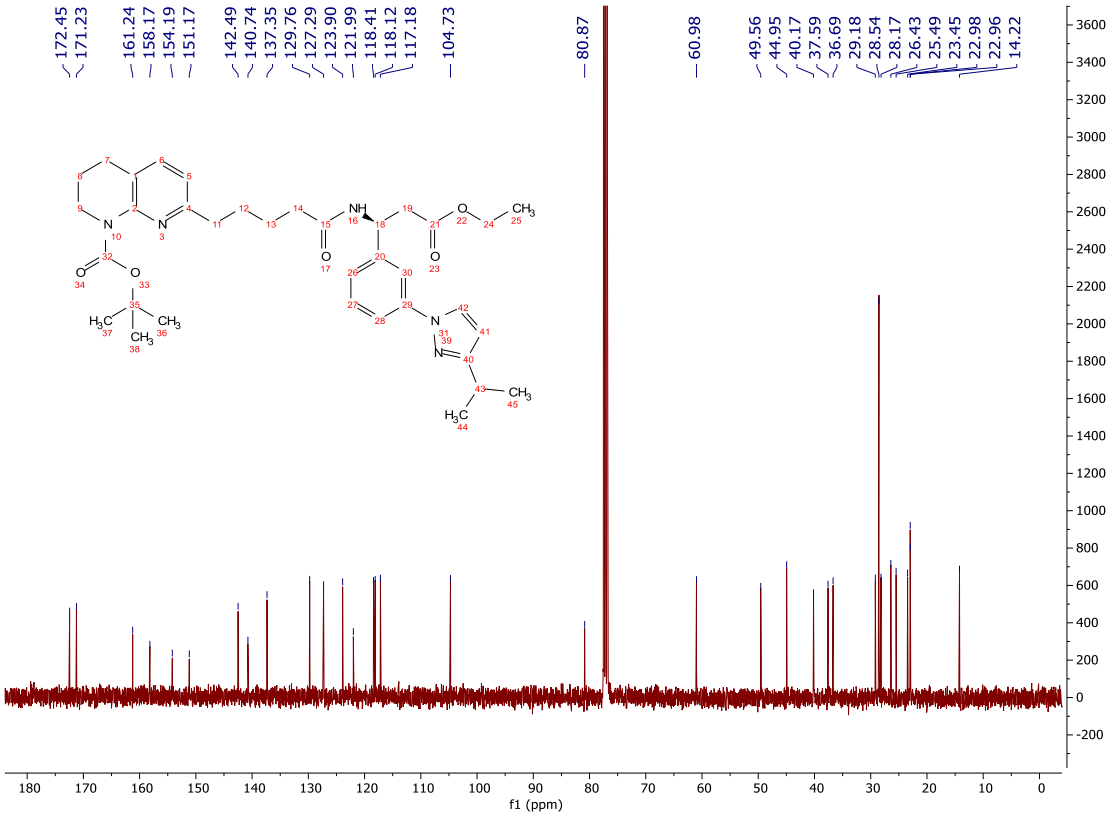
172.45 171.23 161.24 158.17 154.19 151.17 142.49 140.74 137.35 129.76 127.29 123.90 121.99 118.41 118.12 117.18 104.73 80.87 60.98 49.56 44.95 40.17 37.59 36.69 29.18 28.54 28.17 26.43 25.49 23.45 22.98 22.96 14.22
f1 (ppm)

tert-Butyl (*S*)-7-(5-((3-ethoxy-3-oxo-1-(3-(piperidin-1-yl)phenyl)propyl)amino)-5-oxopentyl)-3,4-dihydro-1,8-naphthyridine-1(2*H*)-carboxylate (**281**)

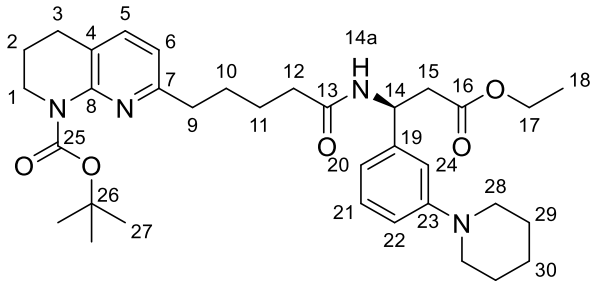

To a stirred solution of **278** (160 mg, 0.426 mmol) in diethyl ether (1.25 mL) at rt was added 4M HCl in dioxane (2.13 mL, 8.52 mmol). The reaction mixture was stirred for 3 h and concentrated *in vacuo*. The crude product was dissolved in acetonitrile (2.20 mL) and **82** (145 mg, 0.426 mmol) was added and the mixture cooled to 0 °C. T3P (50% in ethyl acetate, 0.500 mL, 0.852 mmol) and *i*-Pr_2NEt (0.370 mL, 2.13 mmol) were added, and the reaction mixture stirred for 16 h. The reaction mixture was concentrated *in vacuo*, dissolved in ethyl acetate (10.0 mL) and washed with sat. $NaHCO_{3(aq)}$ (10.0 mL), sat. $NH_4Cl_{(aq)}$ (10.0 mL), sat. $NaHCO_{3(aq)}$ (10.0 mL) and brine (10.0 mL). The organic was dried ($MgSO_4$) and concentrated *in vacuo* giving a dark brown oil. The crude product was purified by column chromatography on silica gel, eluting with a gradient of ethyl acetate/light petroleum (50-100%) to afford the title compound as a yellow oil (111 mg, 0.188 mmol, 44%); **HRMS** *m/z* (ESI^+) calc. for $C_{34}H_{49}N_4O_5$ $[M+H]^+$ requires 593.3697, found 593.3696; $\boldsymbol{R_f}$ 0.30, 80% ethyl acetate/light petroleum, UV active; δ_H (400 MHz, $CDCl_3$) 7.29 – 7.24 (1H, m, H-5), 7.17 (1H, dd, *J* = 7.9, 7.9 Hz, H-21), 6.86 – 6.76 (3H, m, H-6, H-22 and H-24), 6.71 (1H, ddd, *J* = 7.5, 0.9, 0.9 Hz, H-20), 6.45 (1H, d, *J* = 8.5 Hz, H-14a), 5.41 – 5.32 (1H, m, H-14), 4.05 (2H, q, *J* = 7.1 Hz, H-17), 3.76 – 3.71 (2H, m, H-1), 3.12 (4H, t, *J* = 5.3 Hz, H-28), 2.92 – 2.66 (6H, m, H-3, H-9 and H-15), 2.23 (2H, t, *J* = 7.2 Hz, H-12), 1.95 – 1.86 (2H, m, H-2), 1.81 – 1.63 (8H, m, H-10, H-11 and H-29), 1.61 – 1.46 (11H, m, H-27 and H-30), 1.16 (3H, t, *J* = 7.1 Hz, H-18); δ_C (101 MHz, $CDCl_3$) 172.1 (CO), 171.3 (CO), 158.0 (C), 154.1 (CO), 152.5 (C), 151.1 (C), 141.5 (C), 137.2 (ArH), 129.3 (ArH), 121.8 (C), 118.2

(ArH), 116.7 (ArH), 115.6 (ArH), 114.8 (ArH), 80.7 (C), 60.7 (CH_2), 50.5 (CH_2), 49.8 (CH), 44.8 (CH_2), 40.2 (CH_2), 37.5 (CH_2), 36.7 (CH_2), 29.1 (CH_2), 28.4 (CH), 26.3 (CH_2), 25.8 (CH_2), 25.4 (CH_2), 24.3 (CH_2), 23.3 (CH_2), 14.1 (CH_3); ν_{max} (FT-ATR/cm^{-1}) 3302, 2931, 1692, 1464, 1243, 1147, 1026, 701.

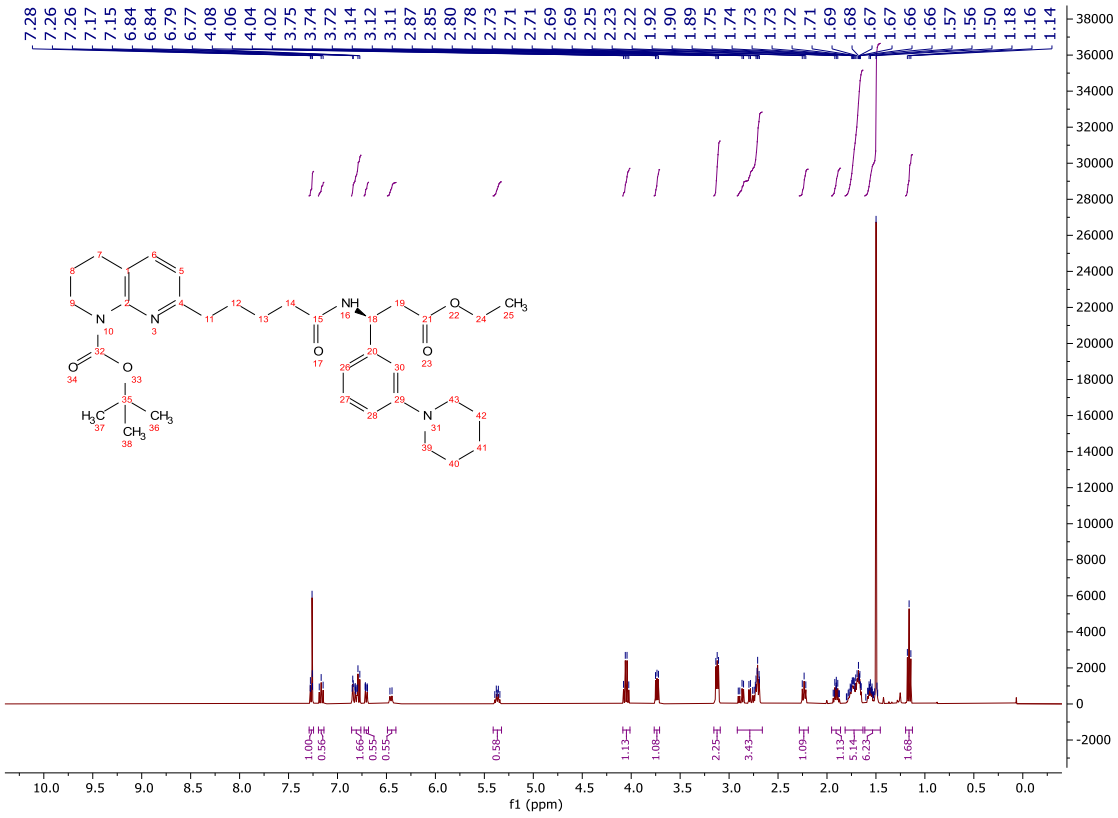
7.28 7.26 7.26 7.17 7.15 6.84 6.84 6.79 6.77 4.08 4.06 4.04 4.02 3.75 3.74 3.72 3.14 3.12 3.11 2.87 2.85 2.80 2.78 2.73 2.71 2.71 2.69 2.69 2.25 2.23 2.22 1.92 1.90 1.89 1.75 1.74 1.73 1.73 1.72 1.71 1.69 1.68 1.67 1.67 1.66 1.66 1.57 1.56 1.50 1.18 1.16 1.14
1.00 0.56 1.66 0.55 0.55 0.58 1.13 1.08 2.25 3.43 1.09 1.13 5.14 6.23 1.68
f1 (ppm)

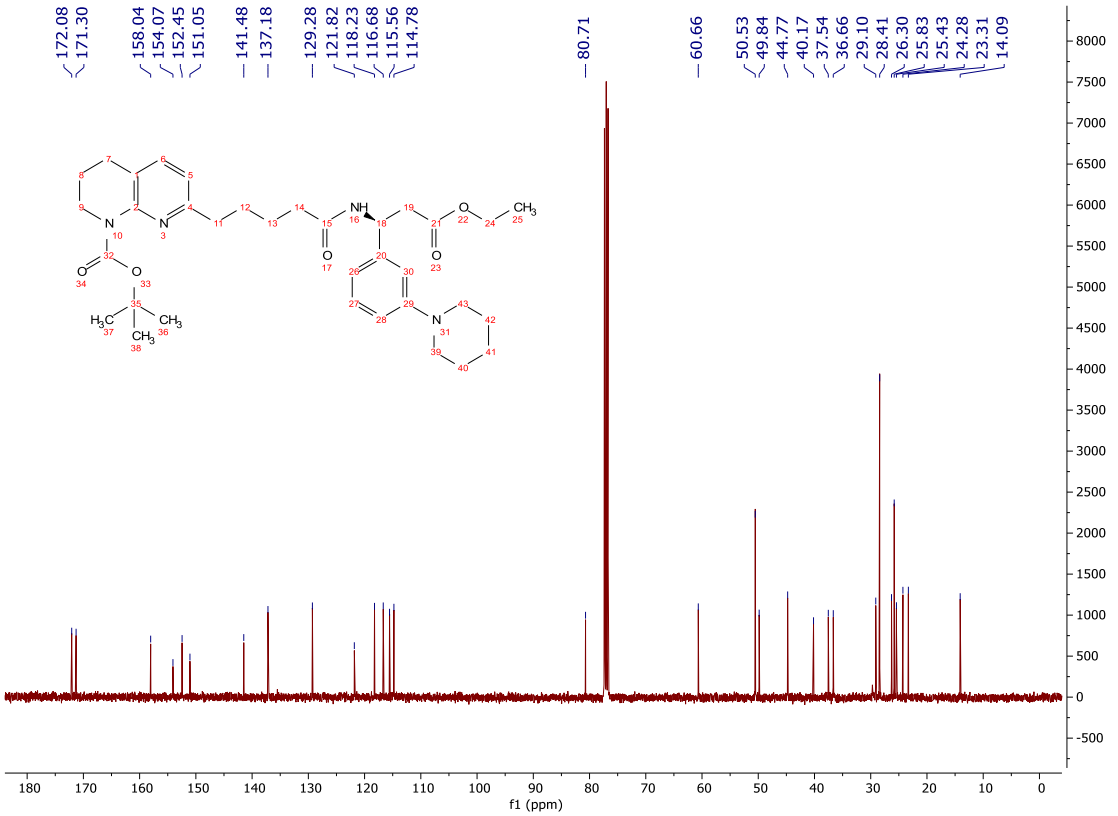
172.08 171.30 158.04 154.07 152.45 151.05 141.48 137.18 129.28 121.82 118.23 116.68 115.56 114.78 80.71 60.66 50.53 49.84 44.77 40.17 37.54 36.66 29.10 28.41 26.30 25.83 25.43 24.28 23.31 14.09
f1 (ppm)

(*S*)-3-(3-(3-Chloro-1*H*-pyrazol-1-yl)phenyl)-3-(5-(5,6,7,8-tetrahydro-1,8-naphthyridin-2-yl)pentanamido)propanoic acid (**203**)

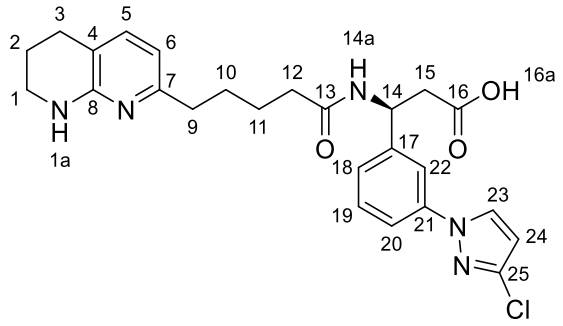

To a solution of **279** (104 mg, 0.171 mmol) in CH_2Cl_2 (5.00 mL) was added TFA (5.00 mL). The reaction mixture was stirred at rt for 7 h. The reaction mixture was concentrated *in vacuo*, dissolved in THF (15.0 mL) and 1M $LiOH_{(aq)}$ (3.00 mL, 3.00 mmol) was added. The reaction mixture was stirred at rt for 18 h and concentrated *in vacuo*. The crude product was purified using Waters OASIS® HLB resin, eluting with a gradient of methanol/water (0-100%) to afford the title compound as an off-white amorphous powder (78 mg, 0.162 mmol, 95%); **HRMS** *m/z* (ESI^+) calc. for $C_{25}H_{29}ClN_5O_3$ $[M+H]^+$ requires 482.1953, found 482.1954; $\boldsymbol{R_f}$ 0.27, 4% methanol/CH_2Cl_2, UV active; δ_H (400 MHz, DMSO-d_6) 8.94 (1H, d, *J* = 7.8 Hz, H-14a), 8.48 (1H, d, *J* = 2.6 Hz, H-23), 7.70 (1H, dd, *J* = 1.9, 1.9 Hz, H-22), 7.56 (1H, ddd, *J* = 8.0, 2.2, 2.2 Hz, H-20), 7.35 (1H, dd, *J* = 7.8, 7.8 Hz, H-19), 7.28 – 7.21 (1H, m, H-18), 6.98 (1H, d, *J* = 7.3 Hz, H-5), 6.62 (1H, d, *J* = 2.6 Hz, H-24), 6.28 (1H, s, H-1a), 6.19 (1H, d, *J* = 7.2 Hz, H-6), 5.15 – 5.04 (1H, m, H-14), 3.25 – 3.17 (2H, m, H-1), 2.58 (2H, t, *J* = 6.3 Hz, H-3), 2.43 – 2.32 (4H, m, H-9 and H-15), 2.17 – 2.04 (2H, m, H-12), 1.78 – 1.67 (2H, m, H-2), 1.59 – 1.42 (4H, m, H-10 and H-11); δ_C (101 MHz, DMSO-d_6) 173.0 (CO), 171.0 (CO), 157.4 (C), 155.8 (C), 146.8 (C), 140.0 (C), 138.8 (C), 135.9 (ArH), 130.3 (ArH), 129.0 (ArH), 125.0 (ArH), 116.6 (ArH), 116.1 (ArH), 112.1 (C), 109.9 (ArH), 107.1 (ArH), 50.4 (CH), 44.3 (CH_2), 40.7 (CH_2), 36.9 (CH_2), 35.6 (CH_2), 28.9 (CH_2), 26.0 (CH_2), 25.1 (CH_2), 21.1 (CH_2); **MP** Degrades >170 °C; $\boldsymbol{\nu_{max}}$ (FT-ATR/cm^{-1}) 3392, 2946, 1635, 1591, 1513, 1407, 1361, 1049, 756.

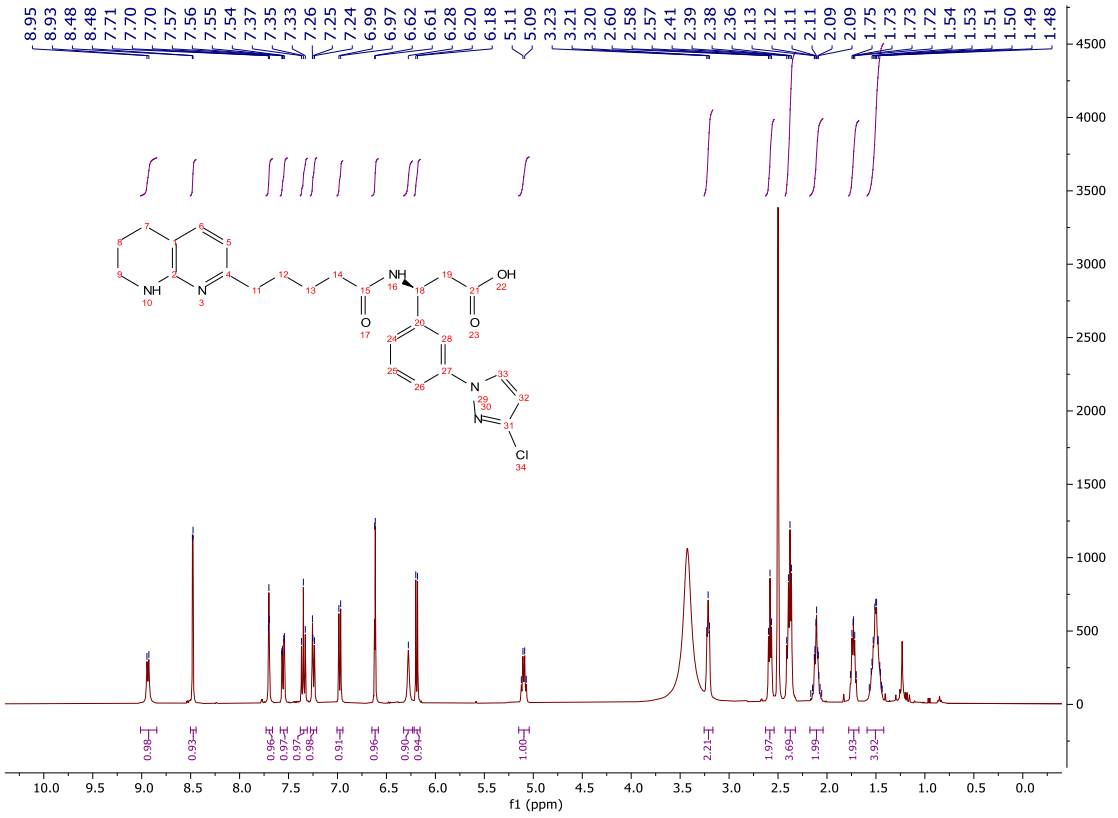
8.95
8.93
8.48
8.48
7.71
7.70
7.70
7.57
7.56
7.55
7.54
7.37
7.35
7.33
7.26
7.25
7.24
6.99
6.97
6.62
6.61
6.28
6.20
6.18
5.11
5.09
3.23
3.21
3.20
2.60
2.58
2.57
2.41
2.39
2.38
2.36
2.13
2.12
2.11
2.11
2.09
2.09
1.75
1.73
1.73
1.72
1.54
1.53
1.51
1.50
1.49
1.48
NH
N
NH
OH
O
O
Cl
0.98
0.93
0.96
0.97
0.97
0.98
0.91
0.96
0.90
0.94
1.00
2.21
1.97
3.69
1.99
1.93
3.92
f1 (ppm)

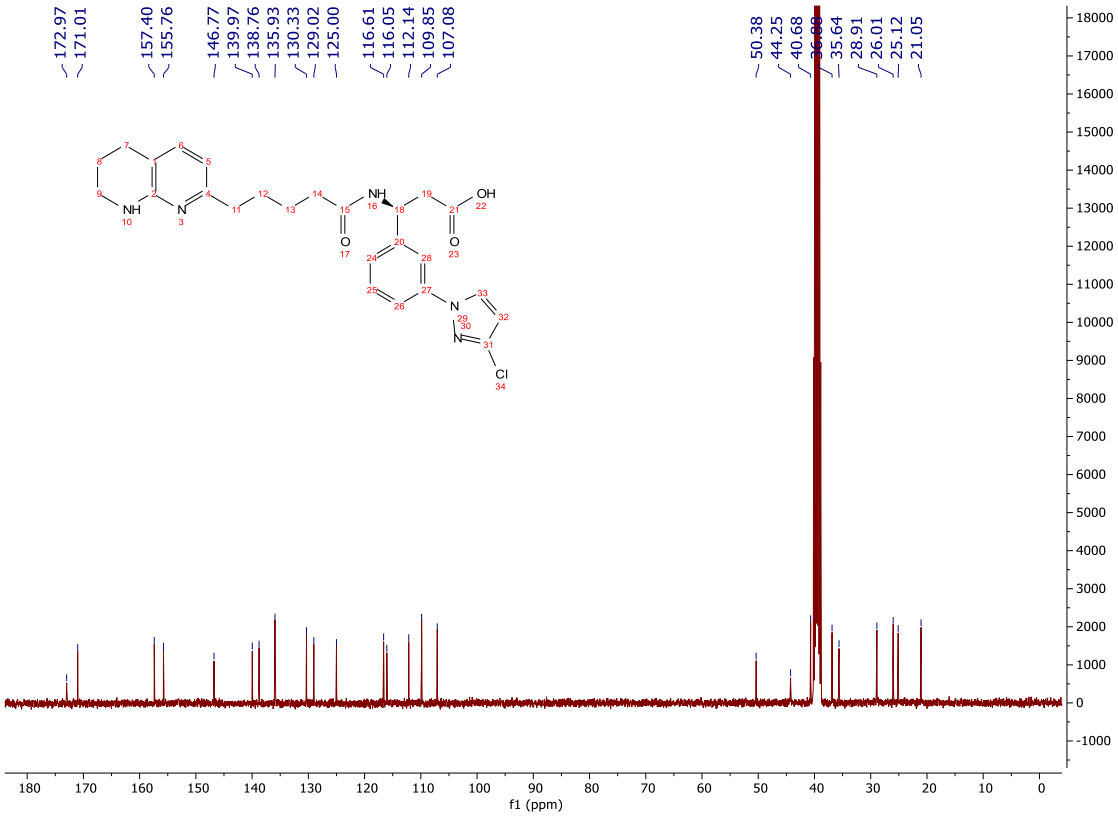
172.97
171.01
157.40
155.76
146.77
139.97
138.76
135.93
130.33
129.02
125.00
116.61
116.05
112.14
109.85
107.08
50.38
44.25
40.68
36.08
35.64
28.91
26.01
25.12
21.05
NH
N
NH
OH
O
O
Cl
f1 (ppm)

(*S*)-3-(3-(3-Isopropyl-1*H*-pyrazol-1-yl)phenyl)-3-(5-(5,6,7,8-tetrahydro-1,8-naphthyridin-2-yl)pentanamido)propanoic acid (**200**)

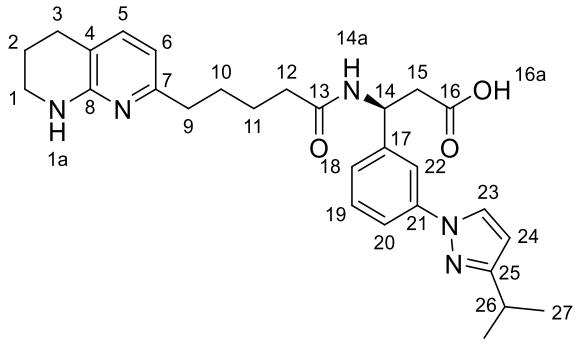

To a solution of **280** (132 mg, 0.214 mmol) in CH_2Cl_2 (5.00 mL) was added TFA (5.00 mL). The reaction mixture was stirred at rt for 7 h. The reaction mixture was concentrated *in vacuo*, dissolved in THF (15.0 mL) and 1M $LiOH_{(aq)}$ (3.00 mL, 3.00 mmol) was added. The reaction mixture was stirred at rt for 18 h and concentrated *in vacuo*. The crude product was purified using Waters OASIS® HLB resin, eluting with a gradient of methanol/water (0-100%) to afford the title compound as a colourless solid (102 mg, 0.209 mmol, 97%); **HRMS** *m/z* (ESI^+) calc. for $C_{28}H_{36}N_5O_3$ $[M+H]^+$ requires 490.2813, found 490.2813; $\boldsymbol{R_f}$ 0.27, 4% methanol/CH_2Cl_2, UV active; δ_H (400 MHz, DMSO-d_6) 8.41 (1H, d, *J* = 8.1 Hz, H-14a), 8.30 (1H, d, *J* = 2.5 Hz, H-23), 7.73 (1H, dd, *J* = 1.9, 1.9 Hz, H-22), 7.61 (1H, ddd, *J* = 8.1, 2.2, 0.9 Hz, H-20), 7.37 (1H, dd, *J* = 7.9, 7.9 Hz, H-19), 7.21 – 7.15 (1H, m, H-18), 7.01 (1H, d, *J* = 7.0 Hz, H-5), 6.49 (1H, s, H-1a), 6.38 (1H, d, *J* = 2.4 Hz, H-24), 6.21 (1H, d, *J* = 7.3 Hz, H-6), 5.27 – 5.17 (1H, m, H-14), 3.27 – 3.17 (2H, m, H-1), 2.98 (1H, hept, *J* = 7.0 Hz, H-26), 2.73 – 2.54 (2H, m, H-3 and H-15), 2.45 – 2.34 (2H, m, H-9), 2.16 – 2.03 (2H, m, H-12), 1.79 – 1.68 (2H, m, H-2), 1.57 – 1.42 (4H, m, H-10 and H-11), 1.25 (6H, d, *J* = 6.9 Hz, H-27); δ_C (101 MHz, DMSO-d_6) 172.2 (CO), 171.3 (CO), 159.8 (C), 156.9 (C), 155.5 (C), 144.6 (C), 139.7 (C), 136.2 (ArH), 129.3 (ArH), 128.0 (ArH), 123.7 (ArH), 116.4 (ArH), 116.3 (ArH), 112.5 (C), 109.9 (ArH), 104.8 (ArH), 49.6 (CH), 41.4 (CH_2), 40.6 (CH_2), 36.5 (CH_2), 35.3 (CH_2), 28.8 (CH_2), 27.4 (CH), 25.9 (CH_2), 25.1 (CH_2), 22.6 (CH_3), 22.6 (CH_3), 20.9 (CH_2); **MP** 94-98 °C; ν_{max} (FT-ATR/cm^{-1}) 3251. 2929, 1643, 1528, 1387, 1319, 1047, 701.

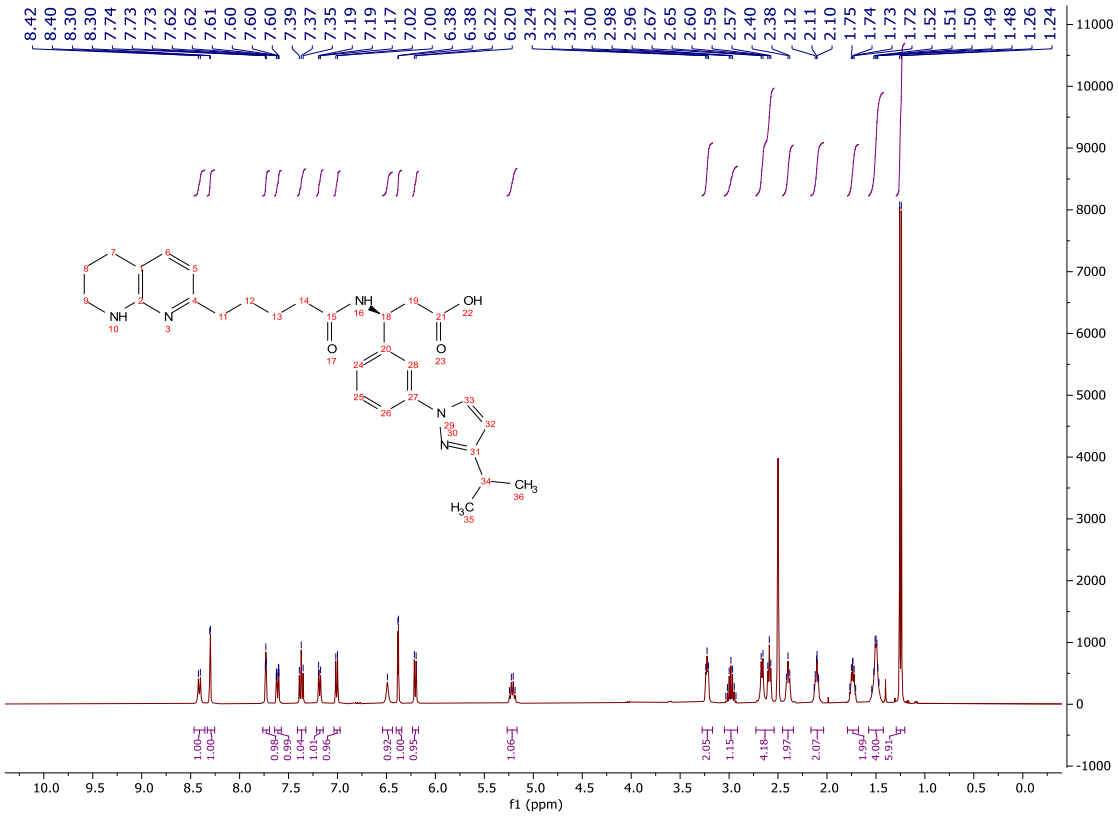
8.42 8.40 8.30 8.30 7.74 7.73 7.73 7.62 7.62 7.61 7.60 7.60 7.60 7.60 7.39 7.37 7.35 7.19 7.19 7.17 7.02 7.00 6.38 6.38 6.22 6.20 3.24 3.22 3.21 3.00 2.98 2.96 2.67 2.65 2.60 2.59 2.57 2.40 2.38 2.12 2.11 2.10 1.75 1.74 1.73 1.72 1.52 1.51 1.50 1.49 1.48 1.26 1.24
1.00 1.00 0.98 0.99 1.04 1.01 0.96 0.92 1.00 0.95 1.06 2.05 1.15 4.18 1.97 2.07 1.99 4.00 5.91
f1 (ppm)

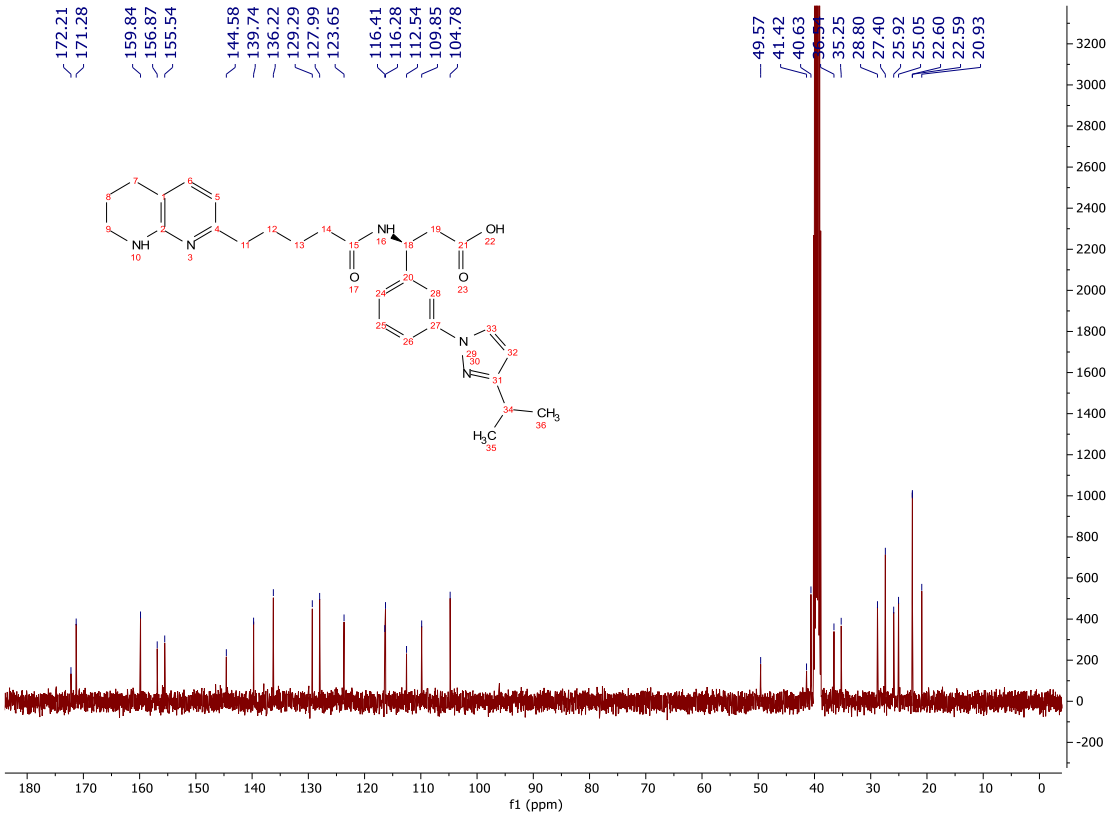
172.21 171.28 159.84 156.87 155.54 144.58 139.74 136.22 129.29 127.99 123.65 116.41 116.28 112.54 109.85 104.78 49.57 41.42 40.63 36.54 35.25 28.80 27.40 25.92 25.05 22.60 22.59 20.93
f1 (ppm)

(*S*)-3-(3-(Piperidin-1-yl)phenyl)-3-(5-(5,6,7,8-tetrahydro-1,8-naphthyridin-2-yl)pentanamido)propanoic acid (**227**)

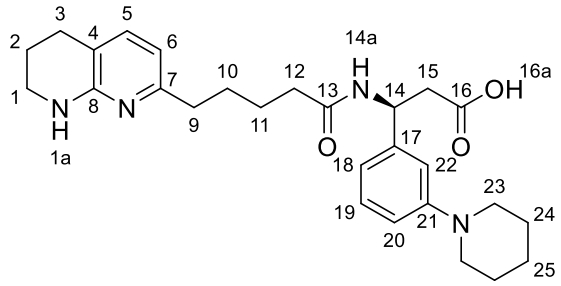

To a solution of **281** (111 mg, 0.188 mmol) in CH_2Cl_2 (5.00 mL) was added TFA (5.00 mL). The reaction mixture was stirred at rt for 7 h. The reaction mixture was concentrated *in vacuo*, dissolved in THF (15.0 mL) and 1M $LiOH_{(aq)}$ (3.00 mL, 3.00 mmol) was added. The reaction mixture was stirred at rt for 18 h and concentrated *in vacuo*. The crude product was purified using Waters OASIS® HLB resin, eluting with a gradient of methanol/water (0-100%) to afford the title compound as a free flowing pink powder (87 mg, 0.188 mmol, quant.); **HRMS** *m/z* (ESI^+) calc. for $C_{27}H_{37}N_4O_3$ $[M+H]^+$ requires 465.2860, found 465.2864; $\boldsymbol{R_f}$ 0.27, 4% methanol/CH_2Cl_2, UV active; δ_H (400 MHz, DMSO-d_6) 8.80 – 8.51 (1H, m, H-14a), 7.12 – 6.92 (2H, m, H-5 and H-19), 6.88 – 6.78 (1H, m, H-22), 6.74 – 6.61 (2H, m, H-18 and H-20), 6.29 (1H, s, H-1a), 6.21 (1H, d, *J* = 7.2 Hz, H-6), 5.10 – 4.97 (1H, m, H-14), 3.29 – 3.15 (2H, m, H-1), 3.12 – 2.95 (4H, m, H-23), 2.59 (2H, t, *J* = 6.3 Hz, H-3), 2.44 – 2.26 (4H, m, H-9 and H-15), 2.19 – 1.99 (2H, m, H-12), 1.81 – 1.67 (2H, m, H-2), 1.65 – 1.38 (10H, m, H-10, H-11, H-24 and H-25); δ_C (101 MHz, DMSO-d_6) 173.7 (CO), 170.9 (CO), 157.4 (C), 155.8 (C), 151.5 (C), 145.2 (C), 135.9 (ArH), 128.3 (ArH), 116.9 (ArH), 114.2 (ArH), 113.8 (ArH), 112.2 (C), 109.9 (ArH), 50.5 (CH), 49.8 (CH_2), 44.2 (CH_2), 40.7 (CH_2), 37.0 (CH_2), 35.6 (CH_2), 28.9 (CH_2), 26.0 (CH_2), 25.3 (CH_2), 25.2 (CH_2), 23.9 (CH_2), 21.1 (CH_2); **MP** Degrades >117 °C; ν_{max} (FT-ATR/cm^{-1}) 3260, 2929, 1643, 1582, 1386, 1242, 1118, 700.

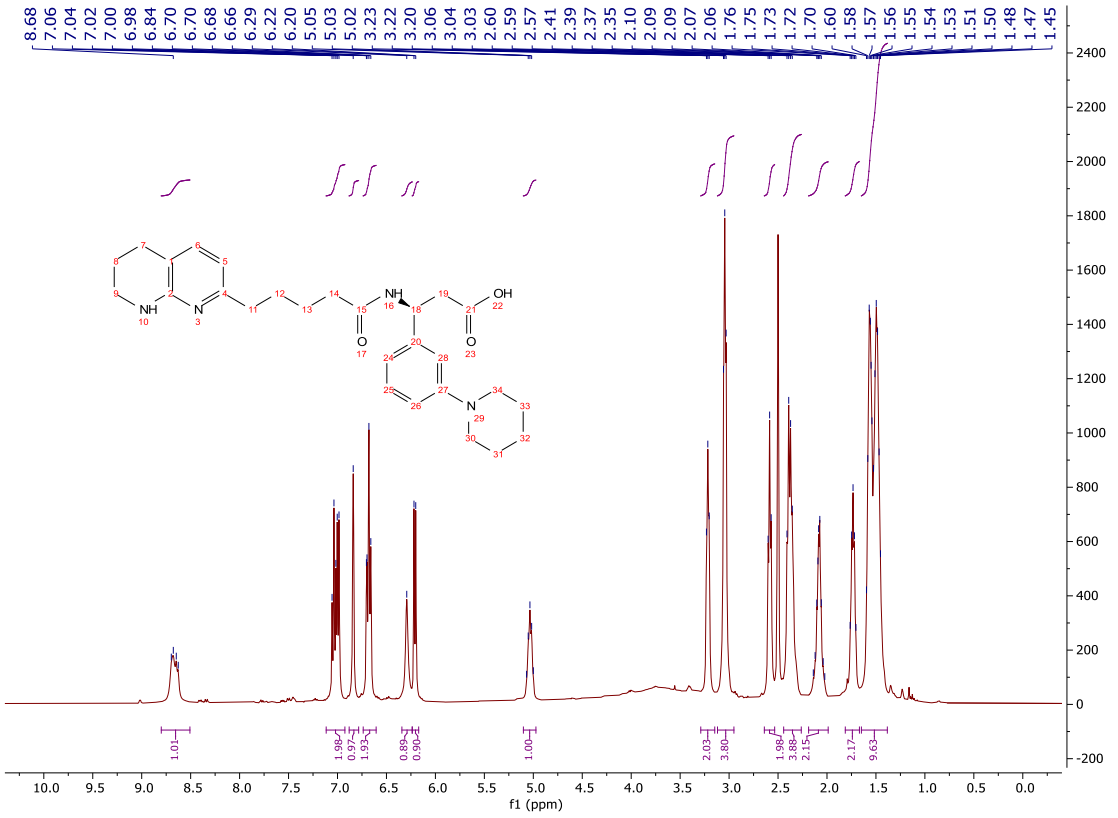
8.68 7.06 7.04 7.02 7.00 6.98 6.84 6.70 6.70 6.68 6.66 6.29 6.22 6.20 5.05 5.03 5.02 3.23 3.22 3.20 3.06 3.04 3.03 2.60 2.59 2.57 2.41 2.39 2.37 2.35 2.10 2.09 2.09 2.07 2.06 1.76 1.75 1.73 1.72 1.70 1.60 1.58 1.57 1.56 1.55 1.54 1.53 1.51 1.50 1.48 1.47 1.45
NH
N
O
OH
1.01 1.98 0.97 1.93 0.89 0.90 1.00 2.03 3.80 1.98 3.88 2.15 2.17 9.63
f1 (ppm)

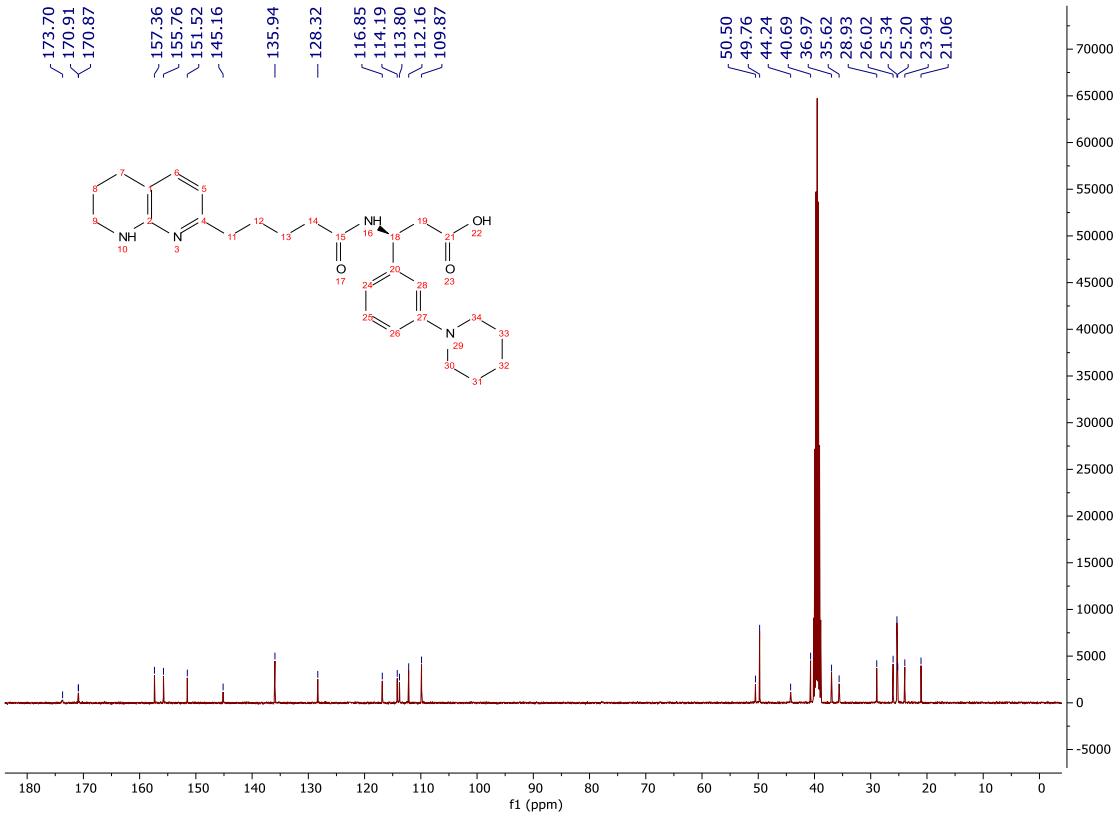
173.70 170.91 170.87 157.36 155.76 151.52 145.16 135.94 128.32 116.85 114.19 113.80 112.16 109.87 50.50 49.76 44.24 40.69 36.97 35.62 28.93 26.02 25.34 25.20 23.94 21.06
NH
N
O
OH
f1 (ppm)

Ethyl 3-((*tert*-butoxycarbonyl)amino)-3-(3-cyanophenyl)propanoate (**311**)

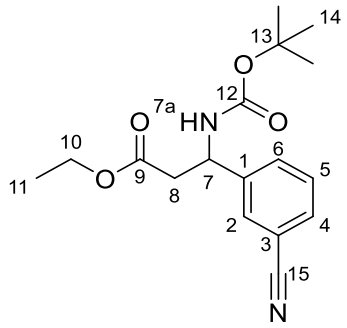

A suspension of formyl benzonitrile (5.00 g, 38.2 mmol), malonic acid (3.97 g, 38.2 mmol) and ammonium acetate (5.88 g, 76.4 mmol) in ethanol (100 mL) was stirred at reflux for 16 h. The reaction mixture was cooled to rt and filtered. The filter cake was washed with ethanol and diethyl ether to give a colourless solid (4.45 g) that was used without further purification. To a solution of the crude product (1.00 g) in 1,4-dioxane/water (1:1, 80.0 mL) was added potassium carbonate (7.26 g, 52.6 mmol). Di-*tert*-butyl dicarbonate (1.21 mL, 5.26 mmol) was added and the reaction mixture stirred for 16 h. The organic solvent was removed *in vacuo* and the resulting suspension acidified to pH 2 with 2M $HCl_{(aq)}$. The aqueous layer was extracted with ethyl acetate (100 mL), the organic was dried (Na_2SO_4) and concentrated *in vacuo* to give a colourless solid (1.38 g) that was used without further purification. To a solution of the crude product (500 mg) in THF (4.50 mL) at 0 °C was added CDI (279 mg, 1.72 mmol). The reaction mixture was stirred for 45 min, ethanol (0.100 mL, 1.72 mmol) was added, and the reaction stirred for 7 days. The reaction mixture was concentrated *in vacuo* and the crude product dissolved in ethyl acetate (50.0 mL). The organic was washed with sat. $NaHCO_{3(aq)}$ (2 x 25.0 mL), dried (Na_2SO_4) and concentrated *in vacuo* to give a brown oil. The crude product was purified *via* column chromatography on silica gel eluting with a gradient of ethyl acetate/light petroleum (0-80%) to give the title compound as a colourless, crystalline solid (260 mg, 0.817 mmol); **HRMS** *m/z* (ESI^+) calc. for $C_{17}H_{23}N_2O_4$ $[M+H]^+$ requires 319.1652, found 319.1659; $\boldsymbol{R_f}$ 0.33, 15% ethyl acetate/light petroleum, UV active; δ_H (400 MHz, $CDCl_3$) 7.62 – 7.58 (1H, m, H-2), 7.58 – 7.52 (2H, m, H-4 and H-6), 7.48 – 7.40 (1H, m, H-

5), 5.68 (1H, bs, H-7a), 5.10 (1H, bs, H-7), 4.08 (2H, q, *J* = 7.2 Hz, H-10), 2.82 (2H, d, *J* = 5.9 Hz, H-8), 1.42 (9H, s, H-14), 1.18 (3H, t, *J* = 7.1 Hz, H-11); δ_C (101 MHz, $CDCl_3$) 170.6 (CO), 155.2 (CO), 143.2 (C), 131.3 (ArH), 130.9 (ArH), 129.9 (ArH), 129.6 (ArH), 118.8 (CN), 112.9 (C), 80.4 (C), 61.2 (CH_2), 50.7 (CH), 40.5 (CH_2), 28.5 (CH_3), 14.2 (CH_3); **MP** 110-112 °C; ν_{max} (FT-ATR/cm^{-1}) 3357, 2979, 2231, 1713, 1503, 1367, 1244, 1160, 1020, 755.

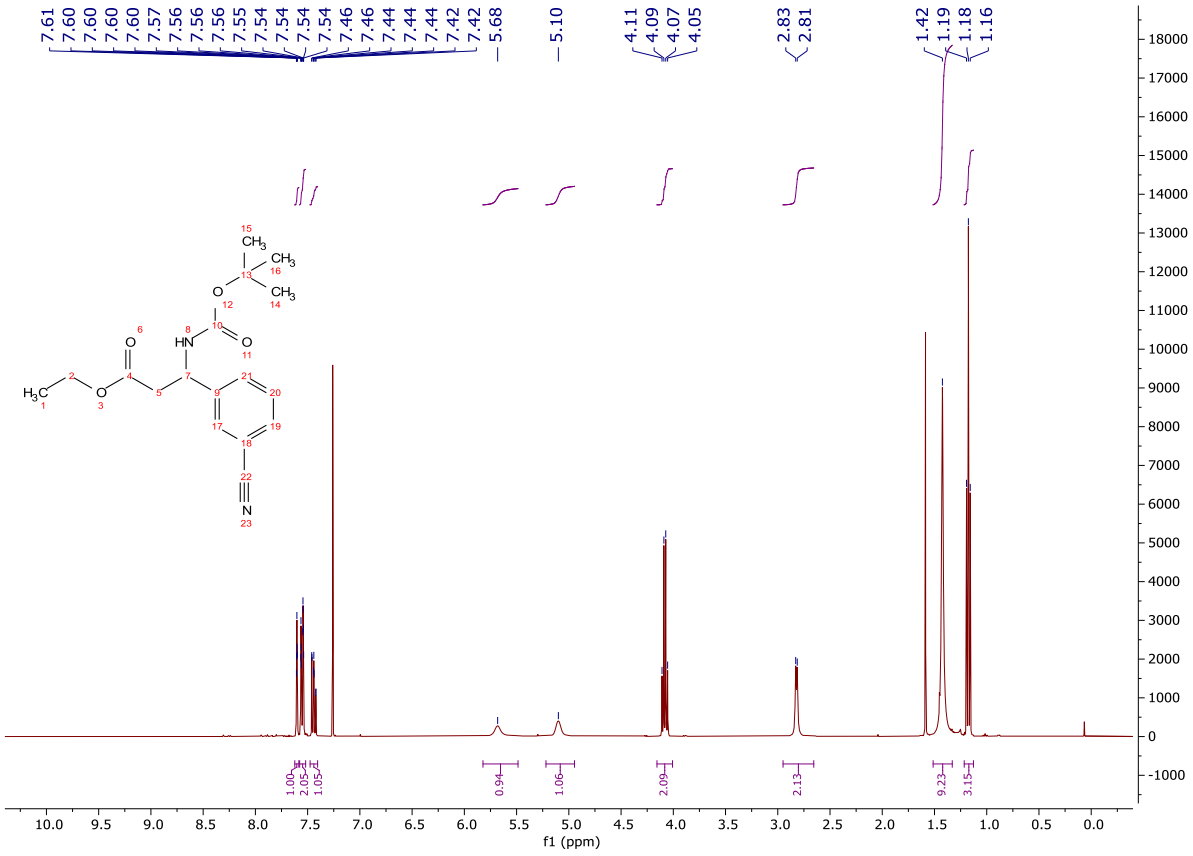
7.61
7.60
7.60
7.60
7.60
7.57
7.56
7.56
7.56
7.55
7.54
7.54
7.54
7.54
7.46
7.46
7.44
7.44
7.44
7.42
7.42
5.68
5.10
4.11
4.09
4.07
4.05
2.83
2.81
1.42
1.19
1.18
1.16
1.00
2.05
1.05
0.94
1.06
2.09
2.13
9.23
3.15
f1 (ppm)

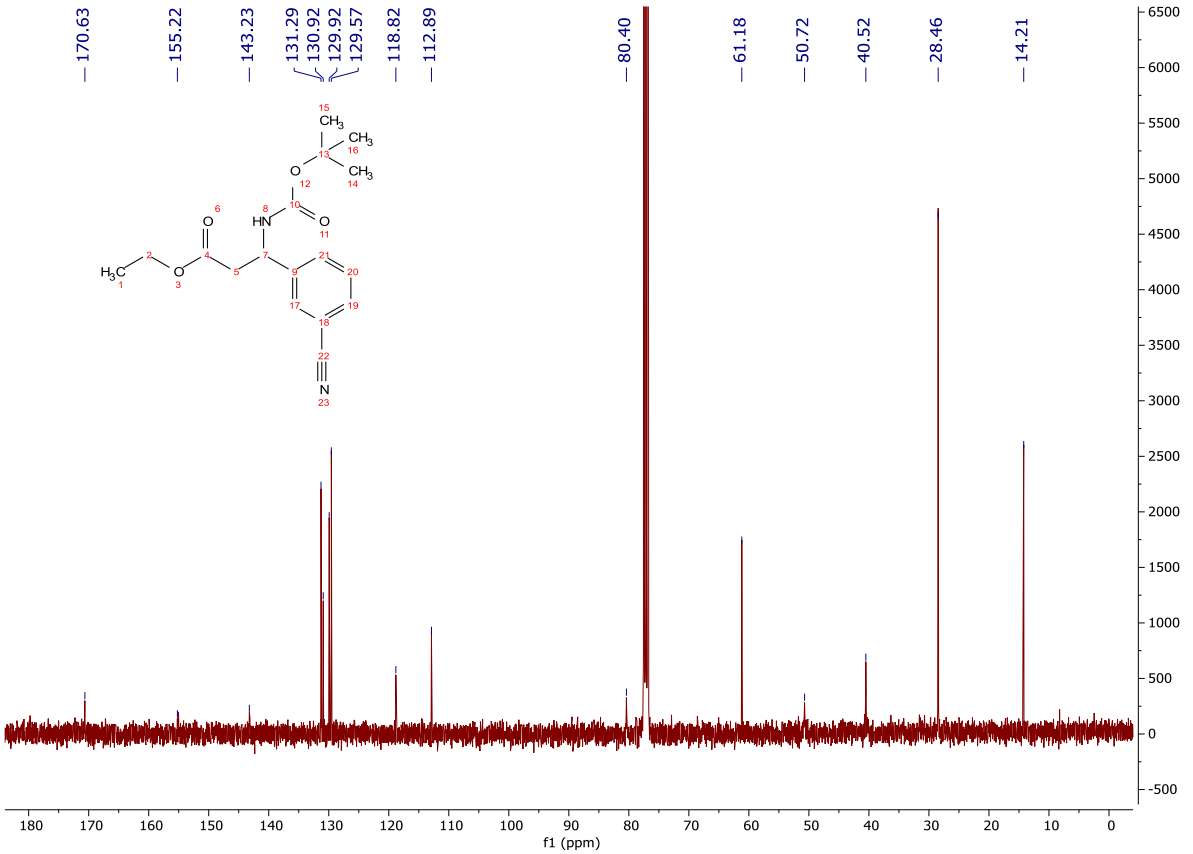
170.63
155.22
143.23
131.29
130.92
129.92
129.57
118.82
112.89
80.40
61.18
50.72
40.52
28.46
14.21
f1 (ppm)

Ethyl 3-((*tert*-butoxycarbonyl)amino)-3-(3-cyano-5-(4,4,5,5-tetramethyl-1,3,2-dioxaborolan-2-yl)phenyl)propanoate (**312**)

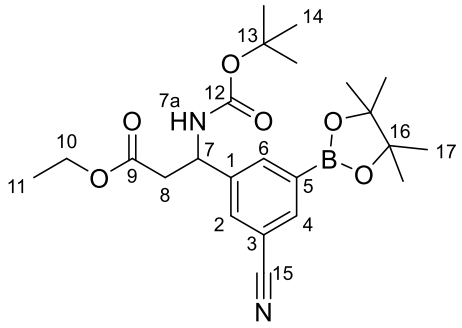

An oven dried microwave vial was charged with a solution of **311** (250 mg, 0.786 mmol) in TBME (3.00 mL), dtbpy (21 mg, 0.079 mmol), B_2Pin_2 (240 mg, 0.943 mmol) and $[Ir(OMe)(cod)]_2$ (26 mg, 0.039 mmol). The vial was sealed and degassed with Ar. The reaction mixture was stirred at 80 °C for 3 h with microwave irradiation. The mixture was cooled to rt, diluted with ethyl acetate (50.0 mL) and washed with 10 % $CuSO_{4(aq)}$ (2 x 50.0 mL). The organic was dried ($MgSO_4$), concentrated *in vacuo*, dissolved in diethyl ether (15.0 mL), filtered through Celite® and concentrated *in vacuo* to give an orange oil. The crude product was purified *via* column chromatography on silica gel eluting with a gradient of ethyl acetate/light petroleum (0-30%) to afford the title compound as a clear, colourless oil (240 mg, 0.540 mmol, 69%); **HRMS** *m/z* (ESI^+) calc. for $C_{23}H_{34}BN_2O_6$ $[M+H]^+$ requires 445.2504, found 445.2501; $\boldsymbol{R_f}$ 0.11, 10% ethyl acetate/light petroleum, UV active; δ_H (400 MHz, $CDCl_3$) 8.00 – 7.95 (1H, m, H-2), 7.93 – 7.89 (1H, m, H-6), 7.69 – 7.65 (1H, m, H-4), 5.64 (1H, bs, H-7a), 5.09 (1H, bs, H-7), 4.14 – 4.03 (2H, m, H-10), 2.81 (2H, d, *J* = 6.1 Hz, H-8), 1.42 (9H, s, H-14), 1.34 (12H, s, H-17), 1.19 (3H, t, *J* = 7.2 Hz, H-11); δ_C (101 MHz, $CDCl_3$) 170.5 (CO), 155.0 (CO), 142.4 (C), 137.4 (ArH), 136.7 (ArH), 132.2 (ArH), 130.9 (C), 118.7 (CN), 112.3 (C), 84.5 (C), 80.1 (C), 61.0 (CH_2), 50.8 (CH), 40.6 (CH_2), 28.3 (CH_3), 24.9 (CH_3), 14.1 (CH_3); ν_{max} (FT-ATR/cm^{-1}) 3363, 2979, 2231, 1715, 1513, 1368, 1141, 1020, 848, 705.

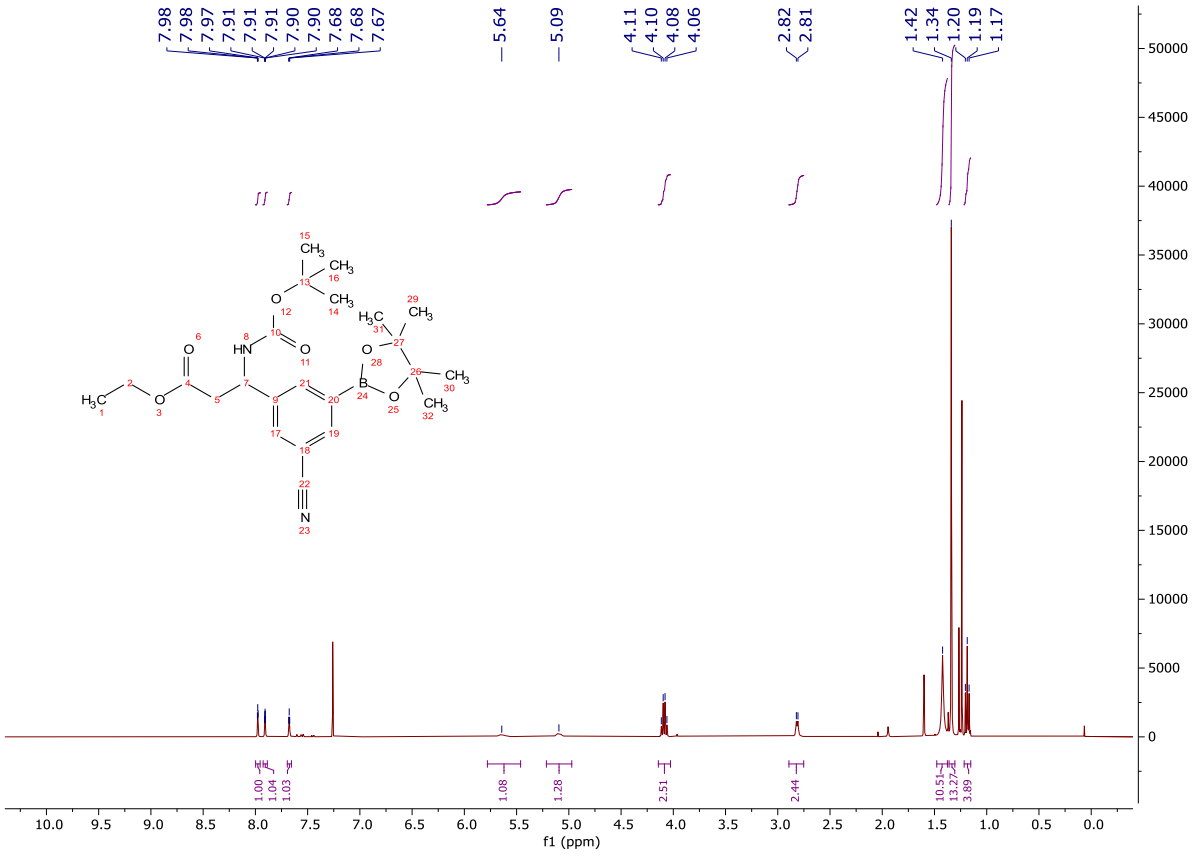
7.98
7.98
7.97
7.91
7.91
7.91
7.90
7.90
7.68
7.68
7.67
5.64
5.09
4.11
4.10
4.08
4.06
2.82
2.81
1.42
1.34
1.20
1.19
1.17
1.00
1.04
1.03
1.08
1.28
2.51
2.44
10.51
13.27
3.89
f1 (ppm)

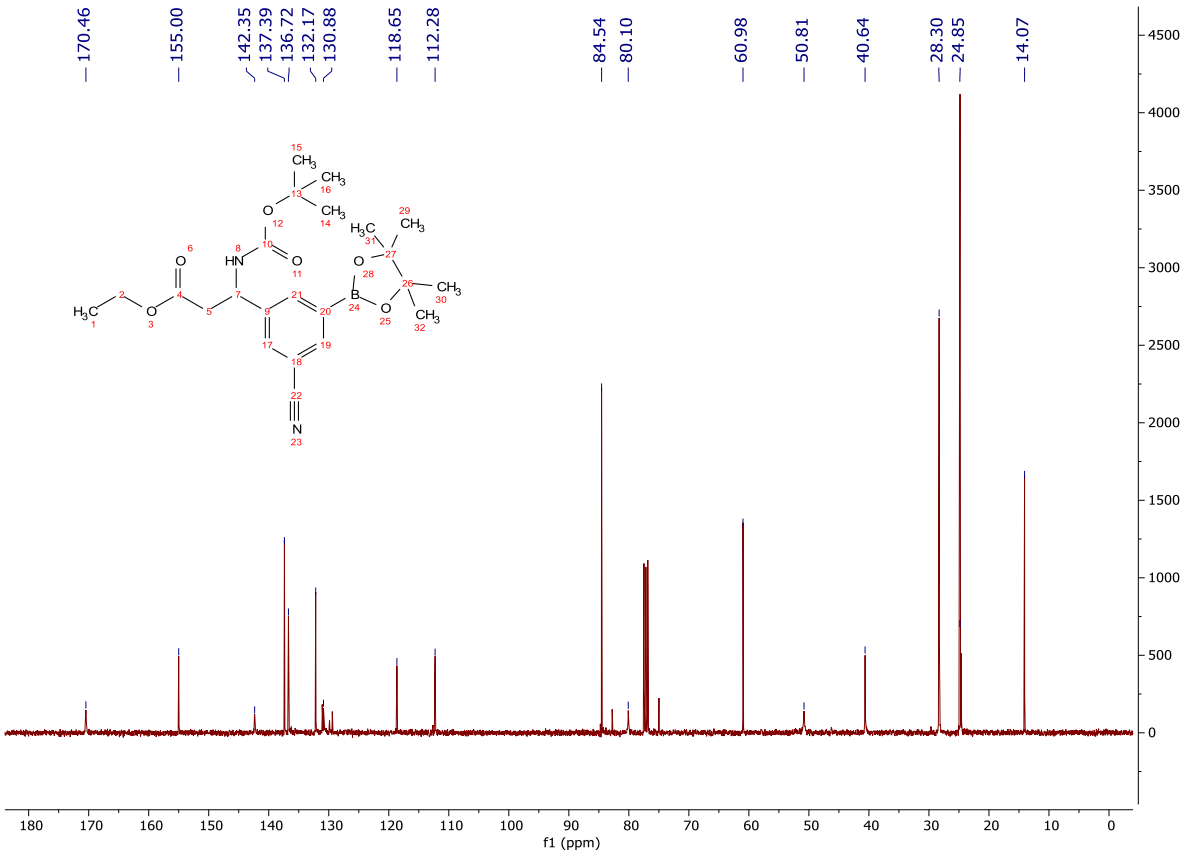
170.46
155.00
142.35
137.39
136.72
132.17
130.88
118.65
112.28
84.54
80.10
60.98
50.81
40.64
28.30
24.85
14.07
f1 (ppm)

Ethyl (*S*)-3-((*tert*-butoxycarbonyl)amino)-3-(3-(*tert*-butyl)phenyl)propanoate (**315**)

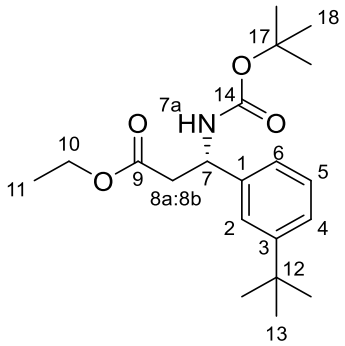

To a stirred solution of (*R*)-*tert*-butanesulfinamide (1.65 g, 24.7 mmol) in anhydrous THF (25.0 mL) was added 3-(*tert*-butyl)benzaldehyde (2.00 g, 12.4 mmol). The mixture was stirred at rt for 5 min and Ti(O*i*-Pr)$_4$ (7.31 mL, 24.7 mmol) was added. The reaction mixture was stirred at rt for 18 h. The reaction mixture was concentrated *in vacuo*, dissolved in ethyl acetate (50.0 mL), poured into brine (100 mL) and filtered through Celite®. The layers were separated, and the organic layer washed with sat. $NaHCO_{3(aq)}$ (2 x 50.0 mL) and brine (2 x 50.0 mL). The aqueous was extracted with ethyl acetate (2 x 50.0 mL) and the organics combined. The organics were dried ($MgSO_4$) and concentrated *in vacuo* to afford a yellow oil (2.71 g). The crude product was not purified further; To a stirred suspension of zinc powder (1.23 g, 18.9 mmol) in anhydrous THF (6.00 mL) under a nitrogen atmosphere was added TMSCl (0.470 mL, 3.77 mmol). The suspension was heated under reflux for 5 min. Ethyl bromoacetate (1.25 mL, 11.3 mmol) was added dropwise over 20 min and the solution stirred under reflux for 1 h. The reaction mixture was cooled to 0 °C and a solution of the crude sulfinimine (1.00 g, 3.77 mmol) in anhydrous THF (6.00 mL) was added and stirred for 18 h. An aqueous solution of 10% Citric acid (25.0 mL) was added and the mixture stirred for 10 min. The reaction mixture was filtered through Celite® and concentrated *in vacuo*. Ethyl acetate (25.0 mL) was added, and the layers separated. The organic was washed with sat. $NaHCO_{3(aq)}$ (2 x 25.0 mL), brine (25.0 mL), dried ($MgSO_4$) and concentrated *in vacuo* to afford a yellow oil. The crude product was purified by column chromatography on silica gel, eluting with a gradient of ethyl acetate/light petroleum (0-30%) to afford a clear, colourless oil (870 mg, 2.46 mmol). To a

stirred solution of the sulfinamide (770 mg, 2.18 mmol) in anhydrous diethyl ether (9.00 mL) at rt was added 4M HCl in dioxane (1.10 mL, 4.36 mmol). The reaction mixture was stirred for 20 min, filtered and the filter cake washed with diethyl ether to afford a colourless oil that solidified on standing (900 mg). To a stirred solution of the crude oil (900 mg) in THF (10.0 mL) at 0 °C was added Et_3N (0.910 mL, 6.54 mmol). A solution of di-*tert*-butyl dicarbonate (0.650 mL, 2.83 mmol) in THF (2.00 mL) was added and the reaction mixture stirred for 16 h. The reaction mixture was concentrated *in vacuo* and the crude material dissolved in ethyl acetate (50.0 mL) and sat. $NaHCO_{3(aq)}$ (50.0 mL). The layers were separated and the organic washed with 10% citric acid (50.0 mL), water (50.0 mL), brine (50.0 mL), dried ($MgSO_4$) and concentrated *in vacuo* to afford a yellow oil. The crude product was purified by column chromatography on silica gel, eluting with a gradient of ethyl acetate/light petroleum (0-10%) to afford the title compound as a clear, colourless oil (700 mg, 2.00 mmol); **HRMS** *m/z* (ESI^+) calc. for $C_{20}H_{32}NO_4$ $[M+H]^+$ requires 350.2326, found 350.2333; $\boldsymbol{R_f}$ 0.47, 15 % ethyl acetate/light petroleum, UV active; δ_H (400 MHz, $CDCl_3$) 7.32 – 7.23 (3H, m, H-2, H-4 and H-5), 7.12 – 7.07 (1H, m, H-6), 5.40 (1H, bs, H-7a), 5.10 (1H, bs, H-7), 4.04 (2H, q, *J* = 7.0 Hz, H-10), 2.94 – 2.72 (2H, m, H-8), 1.42 (9H, s, H-18), 1.30 (9H, s, H-13), 1.17 (3H, t, *J* = 7.2 Hz, H-11); δ_C (101 MHz, $CDCl_3$) 171.1 (CO), 155.2 (CO), 151.6 (C), 140.9 (C), 128.5 (ArH), 124.6 (ArH), 123.4 (ArH), 123.2 (ArH), 79.8 (C), 60.8 (CH_2), 51.7 (CH), 41.4 (CH_2), 34.9 (C), 31.5 (CH_3), 28.5 (CH_3), 14.2 (CH_3); ν_{max} (FT-ATR/cm^{-1}) 3361, 2965, 1714, 1492, 1366, 1243, 1163, 1020, 707.

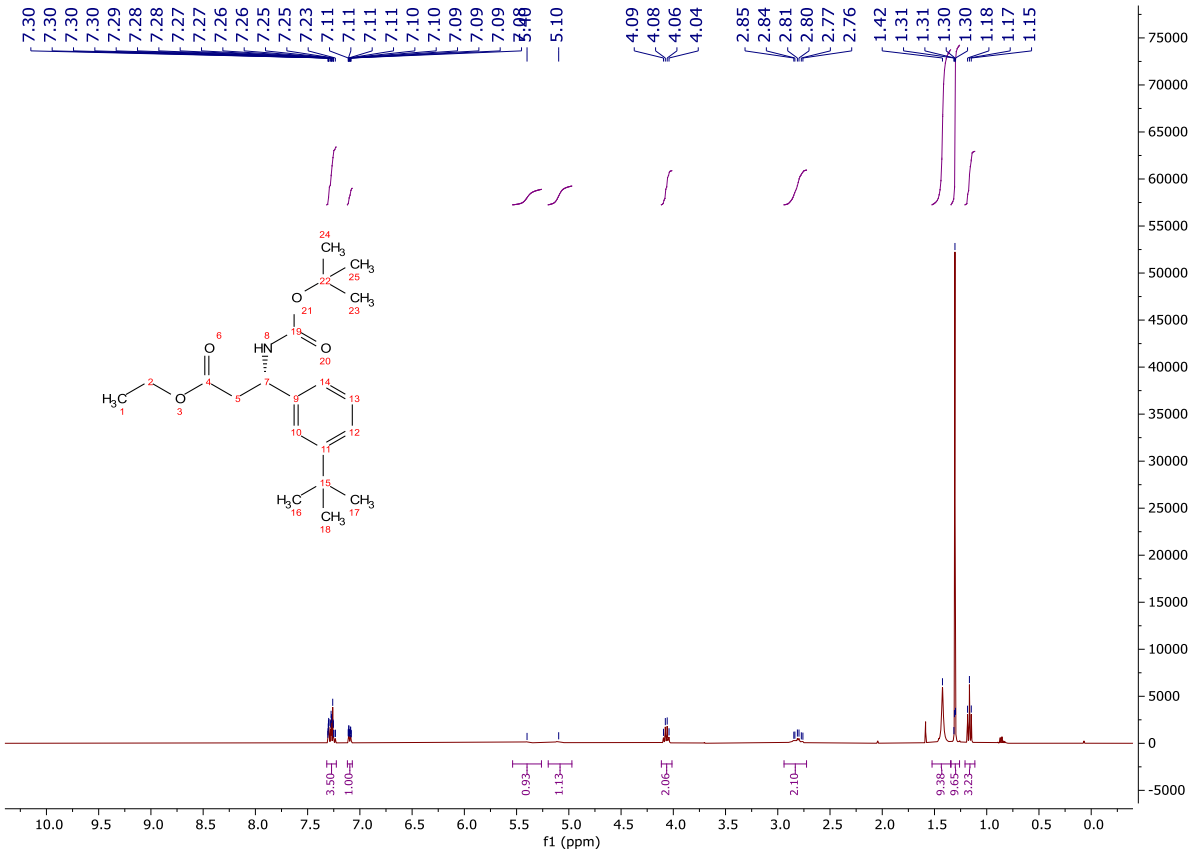
7.30
7.30
7.30
7.29
7.28
7.28
7.27
7.27
7.26
7.26
7.25
7.25
7.23
7.11
7.11
7.11
7.11
7.10
7.10
7.09
7.09
7.09
5.48
5.10
4.09
4.08
4.06
4.04
2.85
2.84
2.81
2.80
2.77
2.76
1.42
1.31
1.31
1.30
1.30
1.18
1.17
1.15
3.50
1.00
0.93
1.13
2.06
2.10
9.38
9.65
3.23
f1 (ppm)

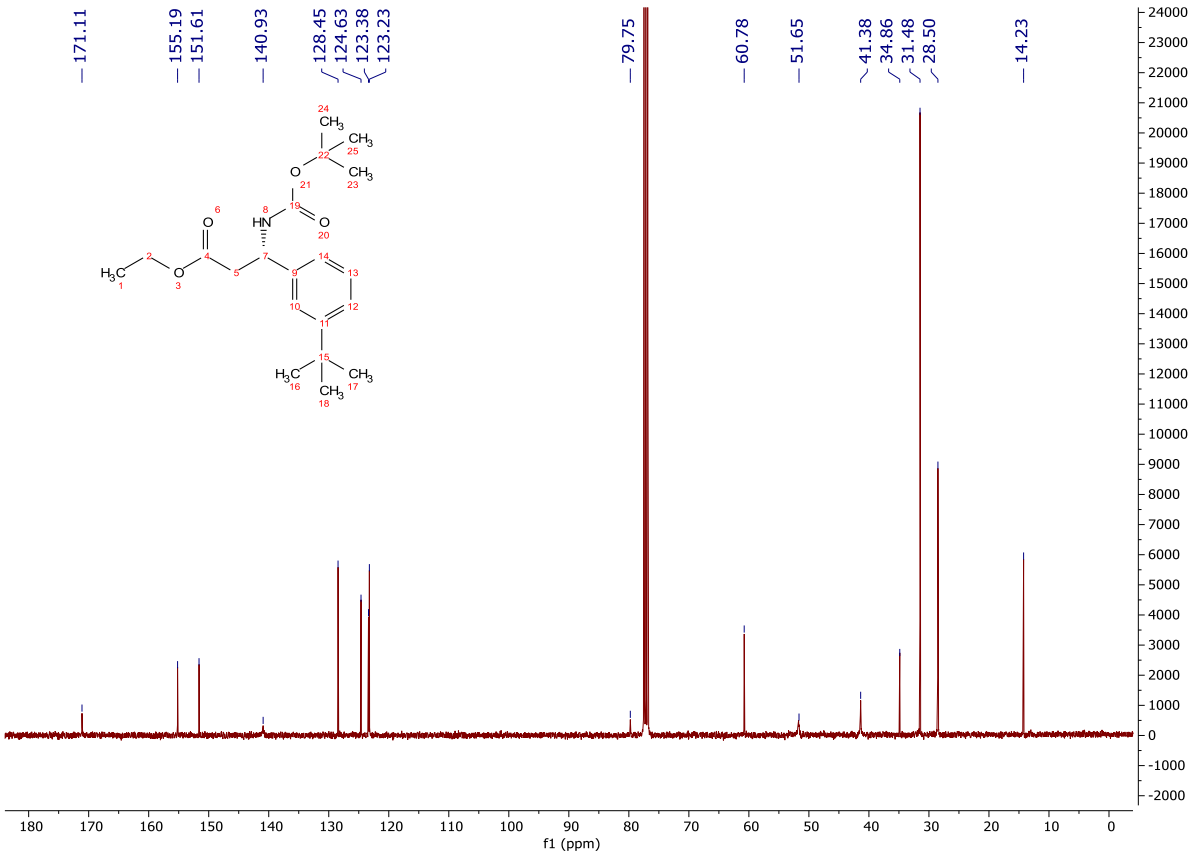
171.11
155.19
151.61
140.93
128.45
124.63
123.38
123.23
79.75
60.78
51.65
41.38
34.86
31.48
28.50
14.23
f1 (ppm)

Ethyl (*S*)-3-((*tert*-butoxycarbonyl)amino)-3-(3-(*tert*-butyl)-5-(4,4,5,5-tetramethyl-1,3,2-dioxaborolan-2-yl)phenyl)propanoate (**316**)

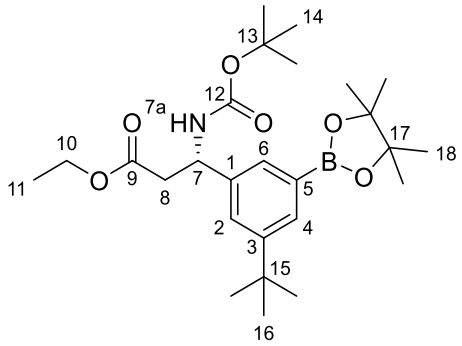

An oven dried microwave vial was charged with a solution of **315** (200 mg, 0.573 mmol) in TBME (3.00 mL), dtbpy (15 mg, 0.057 mmol), B_2Pin_2 (175 mg, 0.688 mmol) and $[Ir(OMe)(cod)]_2$ (19 mg, 0.029 mmol). The vial was sealed and degassed with Ar. The reaction mixture was stirred at 80 °C for 3 h with microwave irradiation. The mixture was cooled to rt, diluted with ethyl acetate (50.0 mL) and washed with 10 % $CuSO_{4(aq)}$ (2 x 50.0 mL). The organic was dried (Na_2SO_4), concentrated *in vacuo*, dissolved in diethyl ether (15.0 mL), filtered through Celite® and concentrated *in vacuo* to give an orange oil. The crude product was purified *via* column chromatography on silica gel eluting with a gradient of ethyl acetate/light petroleum (0-15%) to afford the title compound as a clear, colourless oil (150 mg, 0.316 mmol, 55%); **HRMS** *m/z* (ESI^+) calc. for $C_{26}H_{43}BNO_6$ $[M+H]^+$ requires 476.3178, found 476.3181; $\boldsymbol{R_f}$ 0.37, 10% ethyl acetate/light petroleum, UV active; δ_H (400 MHz, $CDCl_3$) 7.72 (1H, dd, *J* = 2.0, 1.0 Hz, H-4), 7.55 – 7.51 (1H, m, H-2), 7.44 – 7.39 (1H, m, H-6), 5.35 (1H, bs, H-7a), 5.10 (1H, bs, H-7), 4.07 (2H, q, *J* = 7.1 Hz, H-10), 2.94 – 2.73 (2H, m, H-8), 1.42 (9H, bs, H-14), 1.36 – 1.29 (21H, m, H-16 and H-18), 1.18 (3H, t, *J* = 7.2 Hz, H-11); δ_C (101 MHz, $CDCl_3$) 171.0 (CO), 155.2 (CO), 150.8 (C), 140.3 (C), 130.9 (ArH), 129.6 (ArH), 126.8 (ArH), 83.9 (C), 79.7 (C), 60.8 (CH_2), 52.0 (CH), 41.6 (CH_2), 34.9 (C), 31.5 (CH_3), 28.5 (CH_3), 25.0 (CH_3), 14.3 (CH_3); **MP** 51-52 °C; ν_{max} (FT-ATR/cm^{-1}) 3356, 2975, 1714, 1498, 1367, 1262, 1143, 1021, 851, 715.

N.B. One aryl quaternary carbon is not observed: C-5.

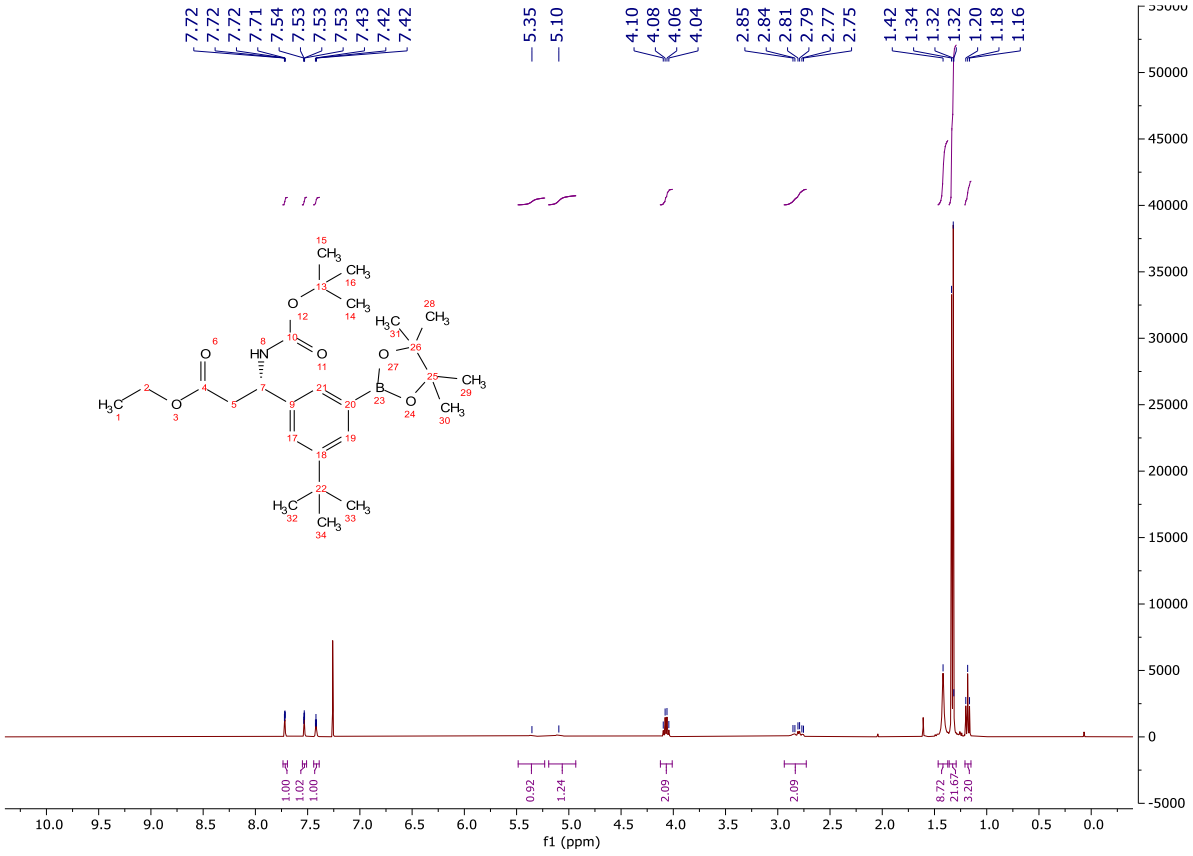
7.72
7.72
7.72
7.71
7.54
7.53
7.53
7.53
7.43
7.42
7.42
5.35
5.10
4.10
4.08
4.06
4.04
2.85
2.84
2.81
2.79
2.77
2.75
1.42
1.34
1.32
1.32
1.20
1.18
1.16
1.00
1.02
1.00
0.92
1.24
2.09
2.09
8.72
21.67
3.20
f1 (ppm)

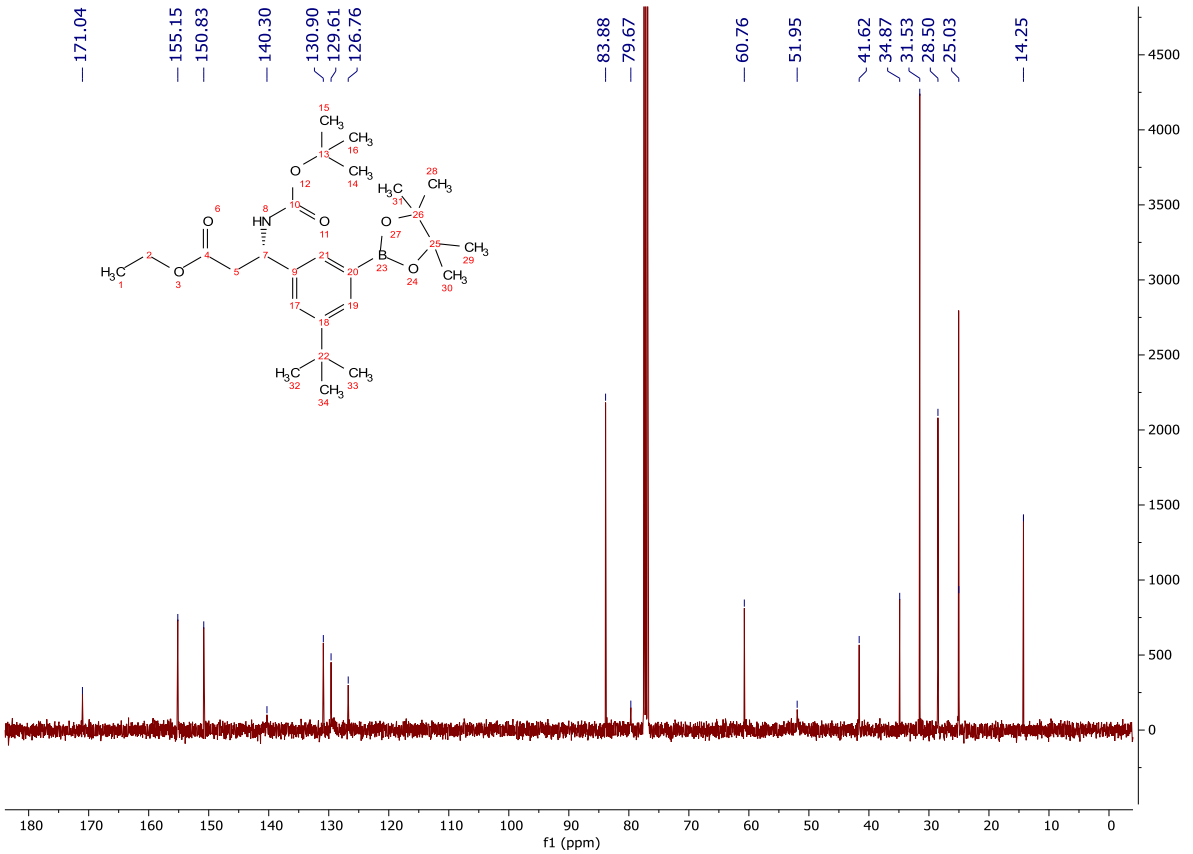
171.04
155.15
150.83
140.30
130.90
129.61
126.76
83.88
79.67
60.76
51.95
41.62
34.87
31.53
28.50
25.03
14.25
f1 (ppm)

tert-Butyl (*S*)-3-((*tert*-butoxycarbonyl)amino)-3-(3-cycloproypl-5-(4,4,5,5-tetramethyl-1,3,2-dioxaborolan-2-yl)phenyl)propanoate (**317**)

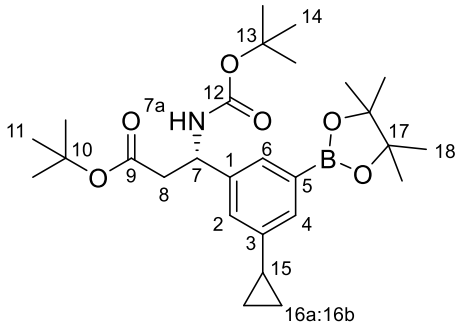

An oven dried microwave vial was charged with a solution of **254** (1.00 g, 2.78 mmol) in TBME (10.0 mL), dtbpy (74 mg, 0.278 mmol), B_2Pin_2 (848 mg, 3.34 mmol) and $[Ir(OMe)(cod)]_2$ (92 mg, 0.139 mmol). The vial was sealed and degassed with Ar. The reaction mixture was stirred at 80 °C for 3 h with microwave irradiation. The mixture was cooled to rt, diluted with ethyl acetate (100 mL) and washed with 10 % $CuSO_{4(aq)}$ (2 x 100 mL). The organic was dried ($MgSO_4$), concentrated *in vacuo*, dissolved in diethyl ether (15.0 mL), filtered through Celite® and concentrated *in vacuo* to give an orange oil. The crude product was purified *via* column chromatography on silica gel eluting with a gradient of ethyl acetate/light petroleum (0-10%) to afford the title compound as a clear, colourless oil (523 mg, 1.07 mmol, 38%); **HRMS** *m/z* (ESI^+) calc. for $C_{27}H_{43}BNO_6$ $[M+H]^+$ requires 488.3178, found 488.3183; $\boldsymbol{R_f}$ 0.21, 10 % ethyl acetate/light petroleum, UV active; δ_H (400 MHz, $CDCl_3$) 7.51 – 7.47 (1H, m, H-2), 7.42 – 7.38 (1H, m, H-4), 7.12 – 7.08 (1H, m, H-6), 5.41 (1H, bs, H-7a), 5.02 (1H, bs, H-7), 2.81 – 2.60 (2H, m, H-8), 1.93 – 1.84 (1H, m, H-15), 1.41 (9H, bs, H-11), 1.37 – 1.29 (21H, m, H-14 and H-18), 0.95 – 0.85 (2H, m, H-16a), 0.73 – 0.67 (2H, m, H-16b); δ_C (101 MHz, $CDCl_3$) 170.4 (CO), 155.2 (CO), 143.6 (C), 131.4 (ArH), 129.7 (ArH), 127.2 (ArH), 83.9 (C), 81.2 (C), 51.8 (CH), 42.6 (CH_2), 28.5 (CH_3), 28.1 (CH_3), 25.0 (CH_2), 15.5 (CH), 9.1 (CH_2); ν_{max} (FT-ATR/cm^{-1}) 3366, 2978, 1713, 1499, 1367, 1243, 1162, 1020, 862, 712.

N.B. Two aryl quaternary carbons are not observed: C-3 and C-5.

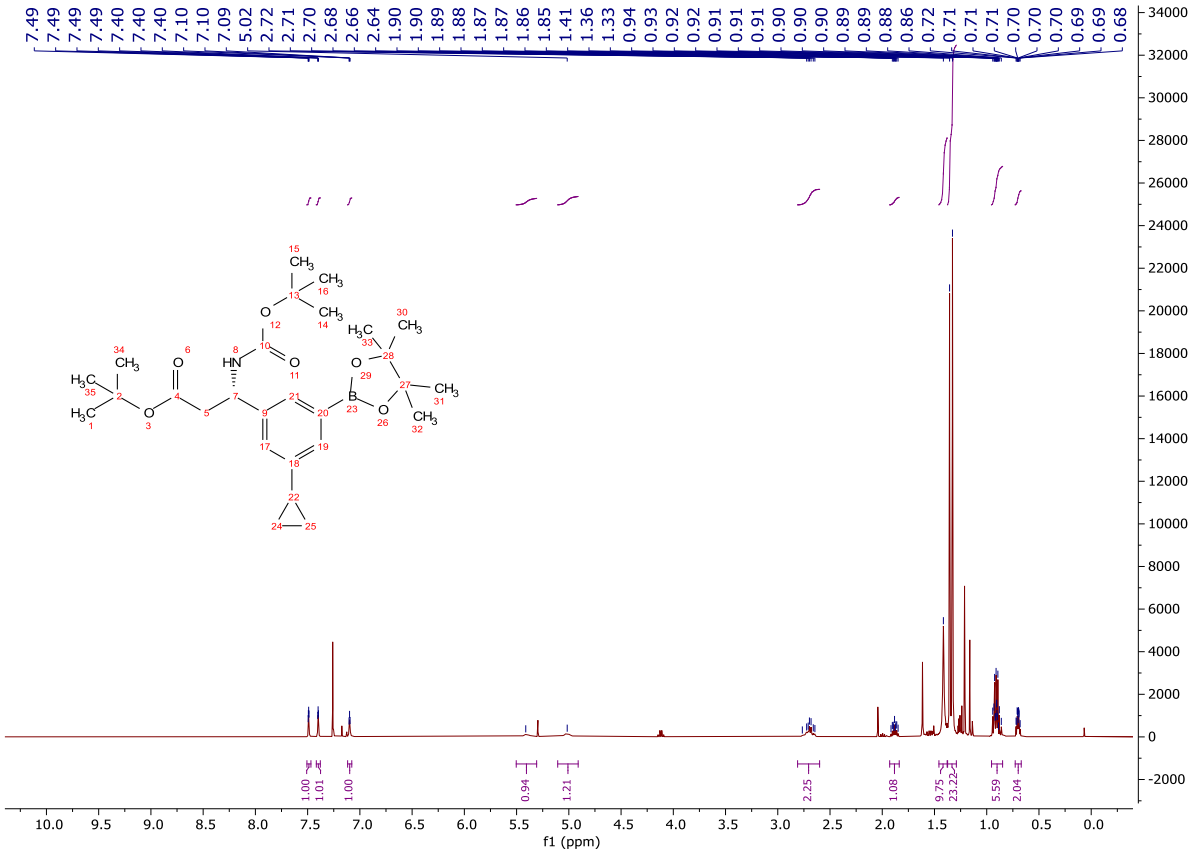
7.49 7.49 7.49 7.40 7.40 7.40 7.10 7.10 7.09 5.02 2.72 2.71 2.70 2.68 2.66 2.64 1.90 1.90 1.89 1.88 1.87 1.87 1.86 1.85 1.41 1.36 1.33 0.94 0.93 0.92 0.92 0.91 0.91 0.91 0.90 0.90 0.90 0.89 0.89 0.88 0.86 0.72 0.71 0.71 0.71 0.70 0.70 0.70 0.69 0.69 0.68
1.00 1.01 1.00 0.94 1.21 2.25 1.08 9.75 23.22 5.59 2.04
f1 (ppm)

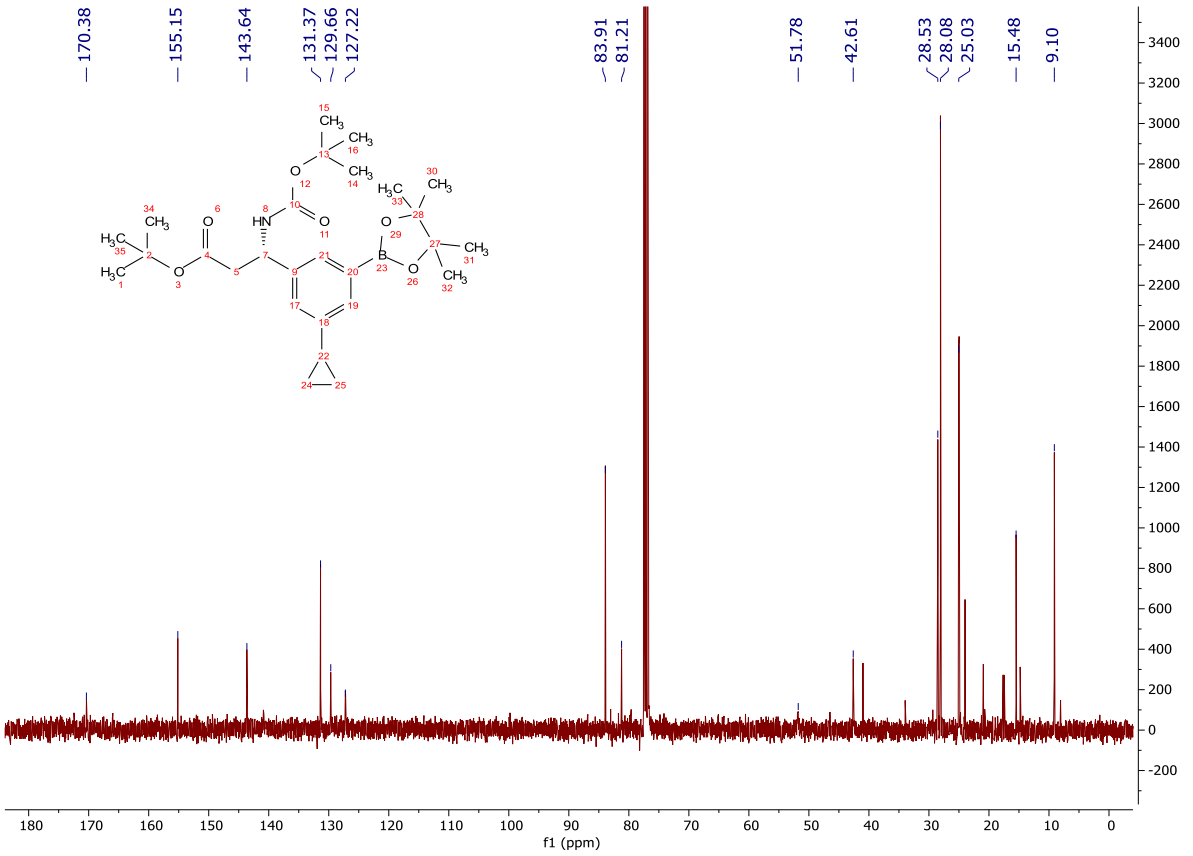
170.38 155.15 143.64 131.37 129.66 127.22 83.91 81.21 51.78 42.61 28.53 28.08 25.03 15.48 9.10
f1 (ppm)

Ethyl 3-((*tert*-butoxycarbonyl)amino)-3-(thiophen-2-yl)propanoate (**320**)

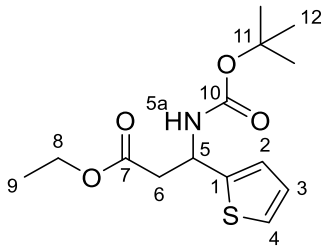

To a solution of 3-ethoxy-3-oxo-1-(thiophen-2-yl)propan-1-aminium chloride (500 mg, 2.13 mmol) in THF (8.50 mL) was added Et_3N (0.890 mL, 6.39 mmol). The reaction mixture was cooled to 0 °C and a solution of di-*tert*-butyl dicarbonate (604 mg, 2.77 mmol) in THF (4.00 mL) was added dropwise. The reaction mixture was warmed to room temperature and stirred for 16 h. The reaction mixture was concentrated *in vacuo*, the residue diluted with ethyl acetate (50.0 mL) and sat. $NaHCO_{3(aq)}$, then the organic layer washed successively with 10 % citric acid (25.0 mL), water (25.0 mL) and brine (25.0 mL). The organic layer was dried ($MgSO_4$) and concentrated *in vacuo* to give a clear colourless oil that solidified upon standing. The crude product was purified *via* column chromatography on silica gel, eluting with a gradient of ethyl acetate/light petroleum (0-10%) to give the title compound as a clear colourless oil that solidified upon standing (408 mg, 1.36 mmol, 64%); **HRMS** *m/z* (ESI^+) calc. for $C_{14}H_{22}NO_4S$ $[M+H]^+$ requires 300.1264, found 300.1266; $\boldsymbol{R_f}$ 0.35, 10% ethyl acetate/light petroleum, UV active; δ_H (400 MHz, $CDCl_3$) 7.21 – 7.16 (1H, m, H-4), 6.95 – 6.90 (2H, m, H-2 and H-3), 5.64 – 5.22 (2H, m, H-5 and H-5a), 4.12 (2H, q, *J* = 7.1 Hz, H-8), 3.00 – 2.82 (2H, m, H-6), 1.45 (9H, s, H-12), 1.21 (3H, t, *J* = 7.2 Hz, H-9); δ_C (101 MHz, $CDCl_3$) 170.8 (CO), 155.0 (CO), 145.4 (C), 127.0 (ArH), 124.6 (ArH), 124.1 (ArH), 80.1 (C), 61.0 (CH_2), 47.5 (CH), 41.2 (CH_2), 28.5 (CH_3), 14.2 (CH_3); **MP** 71-74 °C; ν_{max} (FT-ATR/cm^{-1}) 3329, 2983, 1732, 1685, 1513, 1252, 1158, 1048, 695.

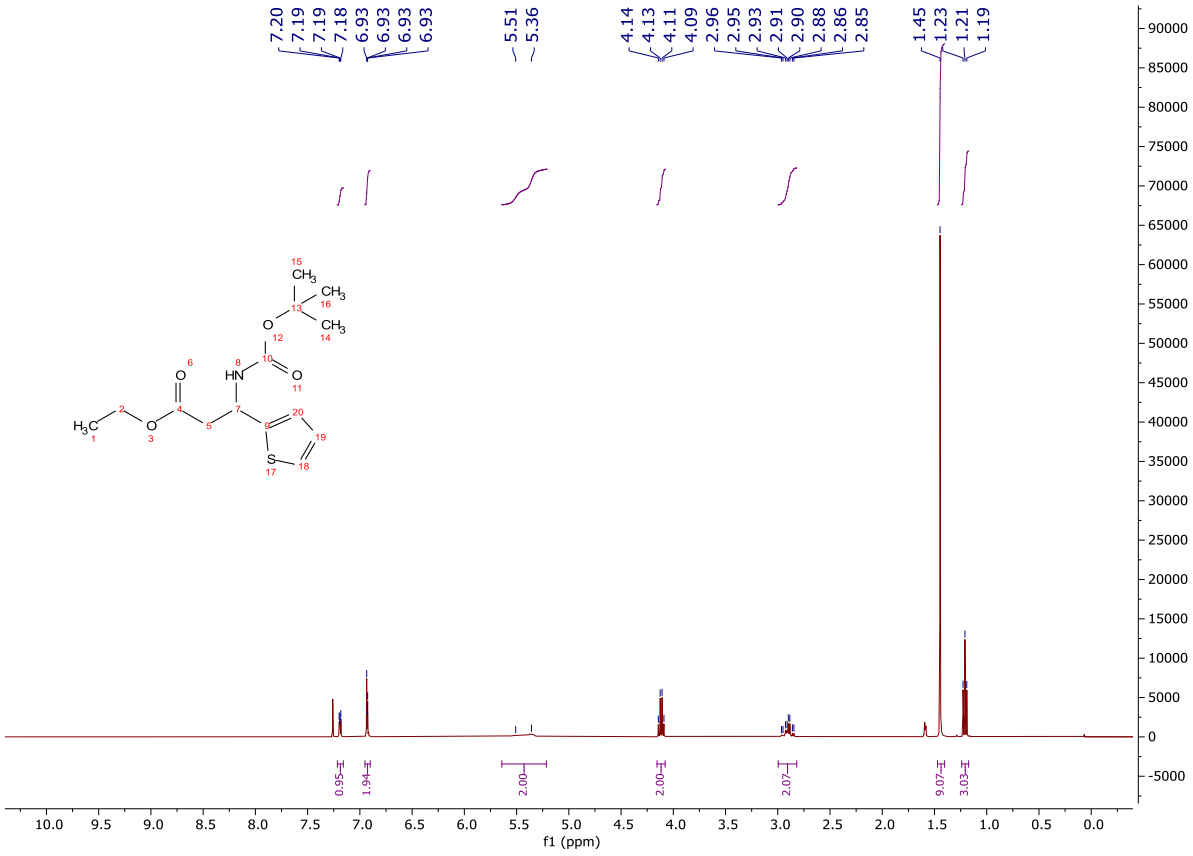
7.20
7.19
7.19
7.18
6.93
6.93
6.93
6.93
5.51
5.36
4.14
4.13
4.11
4.09
2.96
2.95
2.93
2.91
2.90
2.88
2.86
2.85
1.45
1.23
1.21
1.19
0.95
1.94
2.00
2.00
2.07
9.07
3.03
f1 (ppm)

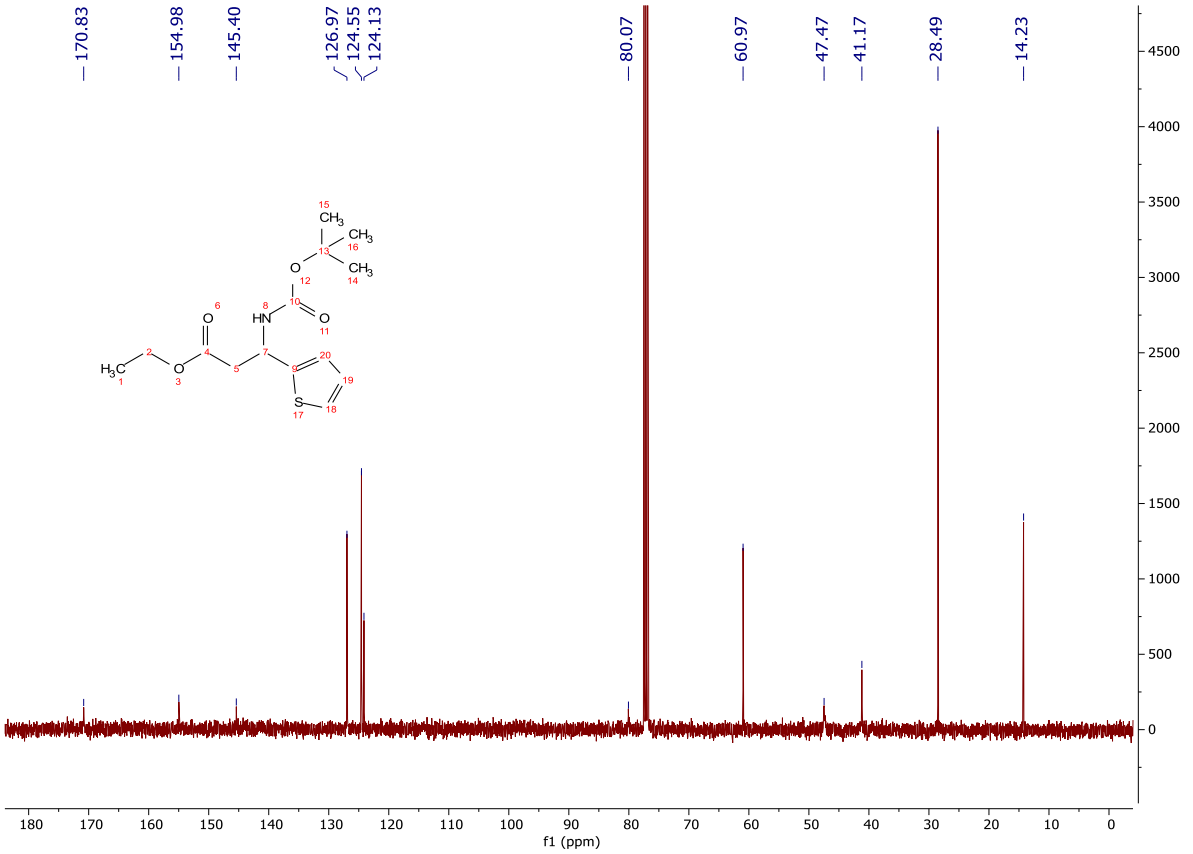
170.83
154.98
145.40
126.97
124.55
124.13
80.07
60.97
47.47
41.17
28.49
14.23
f1 (ppm)

Ethyl 3-((*tert*-butoxycarbonyl)amino)-3-(5-(4,4,5,5-tetramethyl-1,3,2-dioxaborolan-2-yl)thiophen-2-yl)propanoate (**321**)

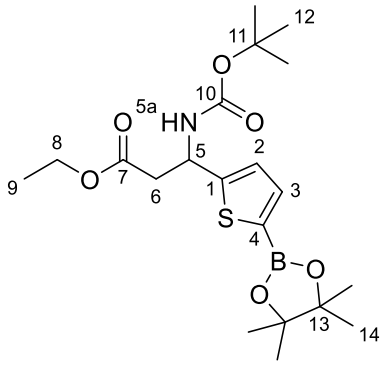

An oven dried microwave vial was charged with a solution of **320** (161 mg, 0.540 mmol) in TBME (1.00 mL), dtbpy (7 mg, 0.026 mmol), B_2Pin_2 (164 mg, 0.650 mmol) and $[Ir(OMe)(cod)]_2$ (9 mg, 0.014 mmol). The vial was sealed and degassed with Ar. The reaction mixture was stirred at room temperature for 16 h. The reaction mixture was diluted with ethyl acetate (25.0 mL) and washed with 10 % $CuSO_{4(aq)}$ (2 x 15.0 mL). The organic layer was dried ($MgSO_4$) and concentrated *in vacuo*. The crude product was dissolved in diethyl ether (15.0 mL), filtered through Celite® and concentrated *in vacuo*. The crude product was purified *via* column chromatography on silica gel, eluting with a gradient of ethyl acetate/light petroleum (10-20%) to afford the title compound as a clear, colourless oil (73 mg, 0.171 mmol, 31%); **HRMS** *m/z* (ESI^+) calc. for $C_{20}H_{33}BNO_6S$ $[M+H]^+$ requires 426.2116, found 426.2117; $\boldsymbol{R_f}$ 0.24, 15% ethyl acetate/light petroleum, UV active; δ_H (400 MHz, $CDCl_3$) 7.46 (1H, d, *J* = 3.5 Hz, H-3), 7.00 (1H, dd, *J* = 3.5, 0.9 Hz, H-2), 5.54 (1H, bs, H-5a), 5.39 (1H, bs, H-5), 4.15 – 4.06 (2H, m, H-8), 2.97 – 2.83 (2H, m, H-6), 1.44 (9H, s, H-12), 1.32 (12H, s, H-14), 1.23 – 1.18 (2H, m, H-9); δ_C (101 MHz, $CDCl_3$) 170.7 (CO), 154.9 (CO), 152.9 (C), 138.3 (C), 137.5 (ArH), 125.7 (ArH), 84.3 (C), 80.1 (C), 61.0 (CH_2), 47.6 (CH), 41.2 (CH_2), 28.5 (CH_3), 24.9 (CH_3), 14.2 (CH_3); ν_{max} (FT-ATR/cm^{-1}) 3351, 2978, 1693, 1472, 1331, 1141, 1016, 852, 665.

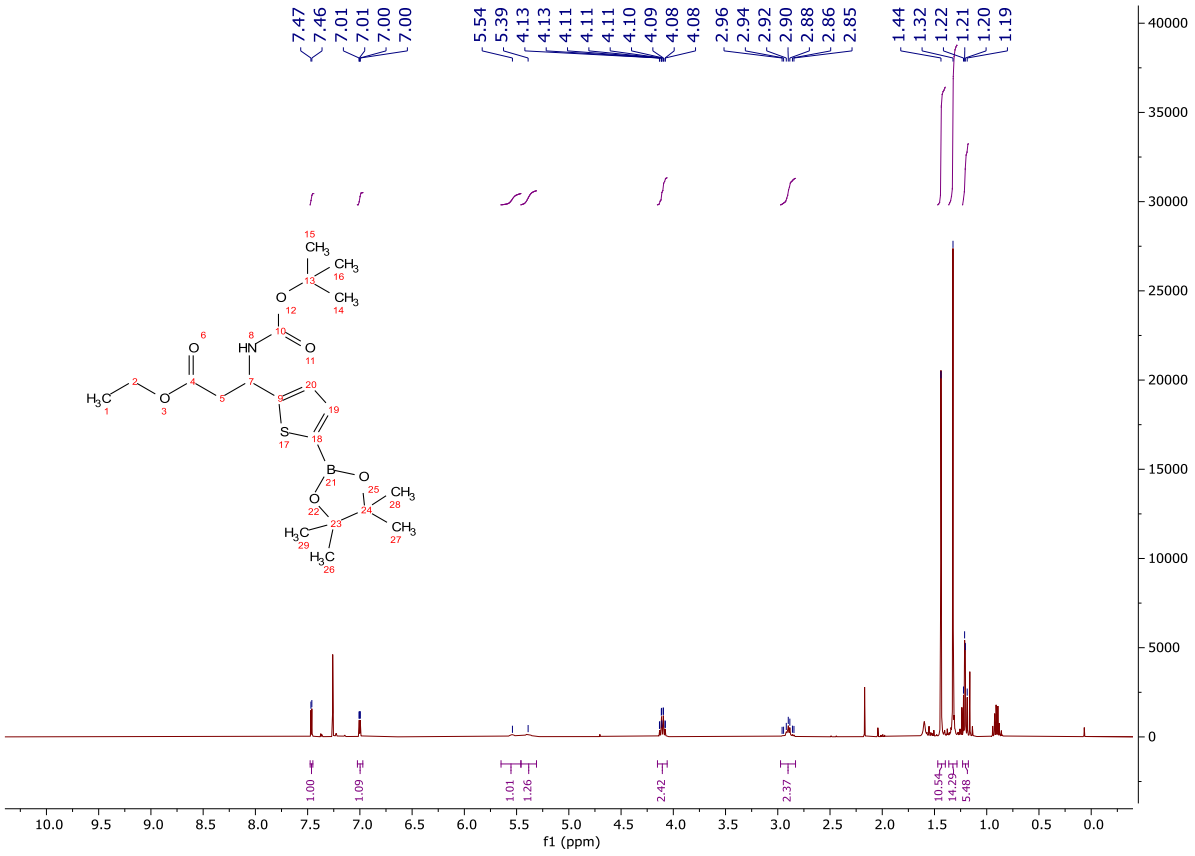
7.47
7.46
7.01
7.01
7.00
7.00
5.54
5.39
4.13
4.11
4.11
4.11
4.10
4.09
4.08
4.08
2.96
2.94
2.92
2.90
2.88
2.86
2.85
1.44
1.32
1.22
1.21
1.20
1.19
1.00
1.09
1.01
1.26
2.42
2.37
10.54
14.29
5.48
f1 (ppm)

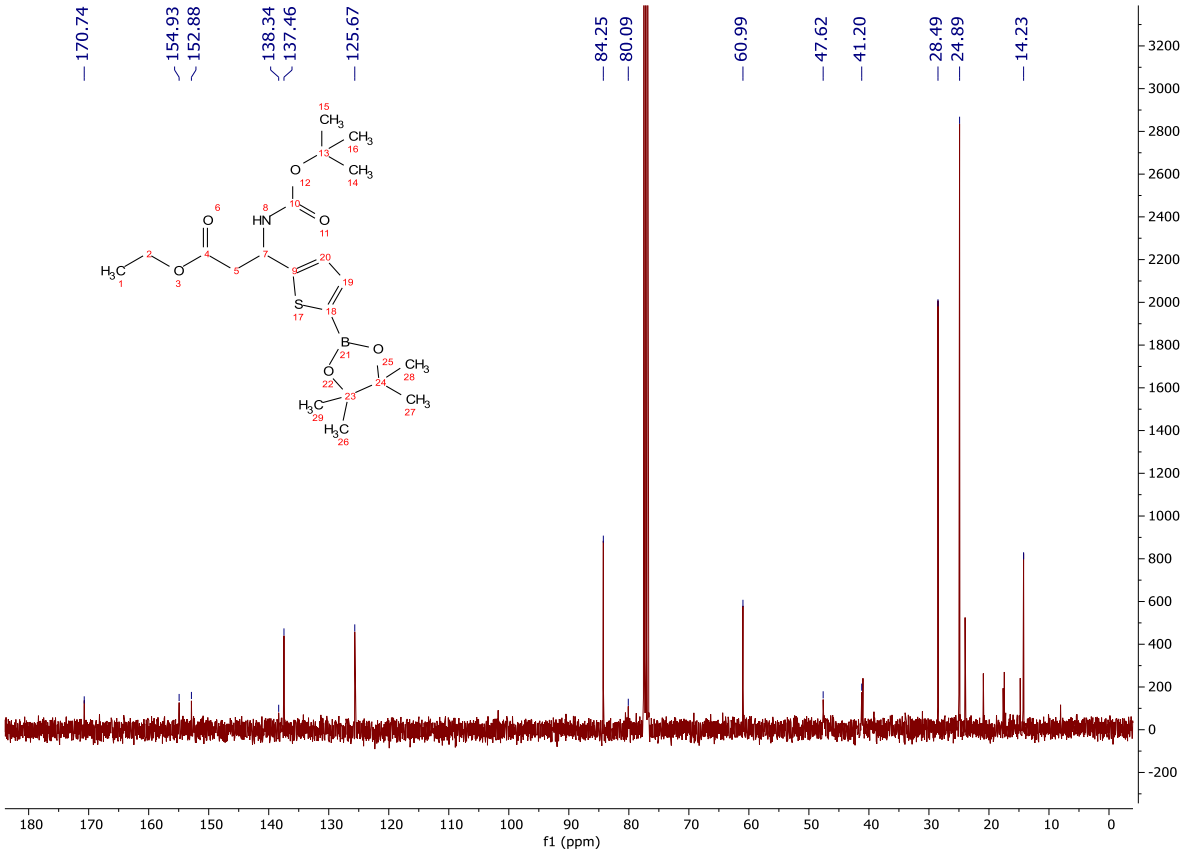
170.74
154.93
152.88
138.34
137.46
125.67
84.25
80.09
60.99
47.62
41.20
28.49
24.89
14.23
f1 (ppm)

Ethyl (*S*)-3-amino-3-(3-bromo-5-(*tert*-butyl)phenyl)propanoate hydrochloride (**323**)

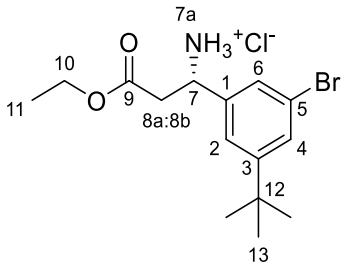

To a solution of **315** (140 mg, 0.295 mmol) in methanol (6.00 mL) was added a solution of $CuBr_2$ (197 mg, 0.885 mmol) in water (3.00 mL) at rt. The reaction mixture was stirred at 70 °C for 16 h. The reaction mixture was concentrated *in vacuo*, diluted with ethyl acetate (40.0 mL) and washed with water (2 x 20.0 mL) and brine (30.0 mL), dried (Na_2SO_4) and concentrated *in vacuo* to give a blue oil. To a solution of the crude product in diethyl ether (2.00 mL) was added 4M HCl in dioxane (3.00 mL). The reaction mixture was stirred for 16 h at rt. The reaction mixture was concentrated *in vacuo* and triturated with light petroleum to give the title compound as a colourless solid (38 mg, 0.116 mmol, 39%); **HRMS** *m/z* (ESI^+) calc. for $C_{15}H_{23}BrNO_2$ $[M+H]^+$ requires 328.0907, found 328.0197; $\boldsymbol{R_f}$ 0.50, 60 % ethyl acetate/light petroleum, UV active; δ_H (400 MHz, $CDCl_3$) 8.90 (3H, bs, H-7a), 7.64 – 7.38 (3H, m, H-2, H-4 and H-6), 4.73 (1H, bs, H-7), 4.05 (2H, q, *J* = 7.0 Hz, H-10), 3.24 (1H, d, *J* = 15.8 Hz, H-8a), 2.98 (1H, d, *J* = 15.4 Hz, H-8b), 1.27 (9H, s, H-13), 1.15 (3H, t, *J* = 6.9 Hz, H-11); δ_C (101 MHz, $CDCl_3$) 169.3 (CO), 154.7 (C), 137.2 (C), 129.8 (ArH), 128.0 (ArH), 123.9 (ArH), 122.9 (C), 61.5 (CH_2), 52.2 (CH), 39.0 (CH_2), 35.3 (C), 31.3 (CH_3), 14.2 (CH_3); **MP** 144-147 °C; ν_{max} (FT-ATR/cm^{-1}) 2963, 2869, 1740, 1569, 1377, 1185, 1027, 868, 702.

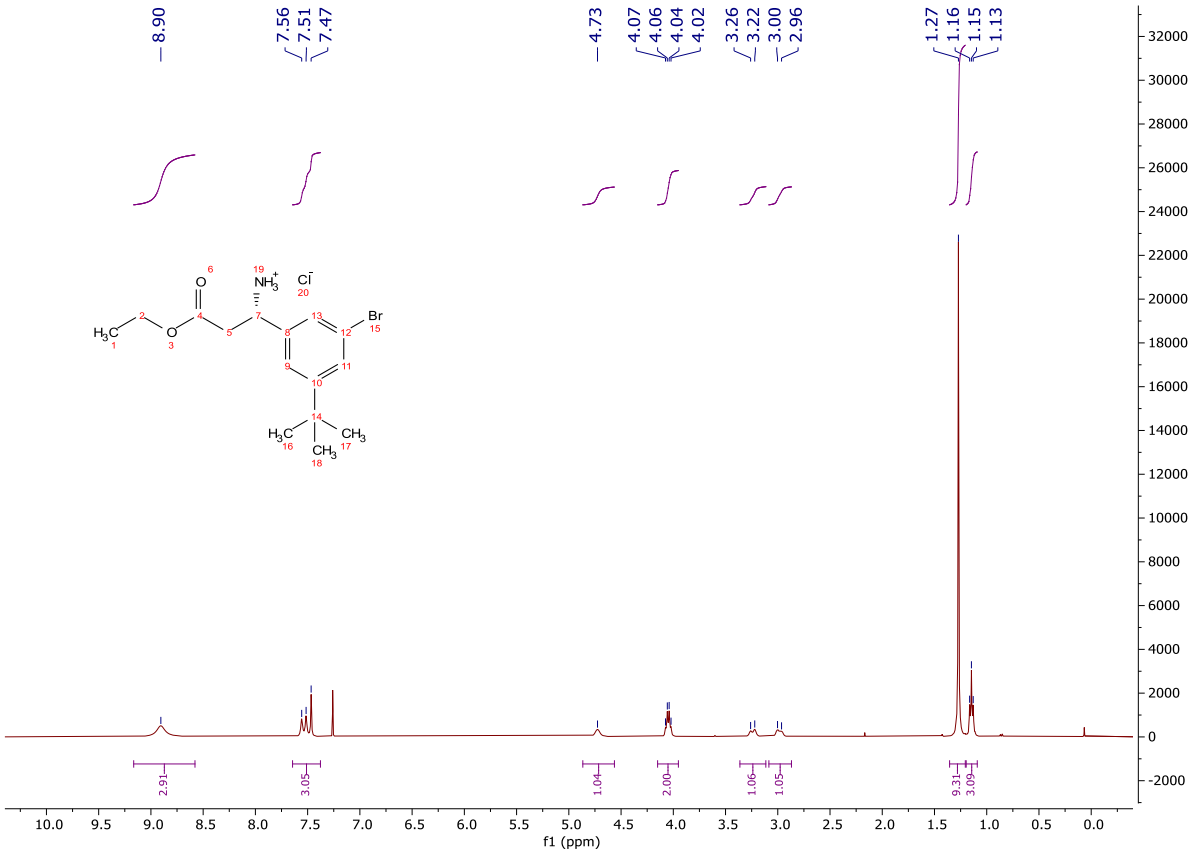
8.90
7.56
7.51
7.47
4.73
4.07
4.06
4.04
4.02
3.26
3.22
3.00
2.96
1.27
1.16
1.15
1.13
2.91
3.05
1.04
2.00
1.06
1.05
9.31
3.09
f1 (ppm)

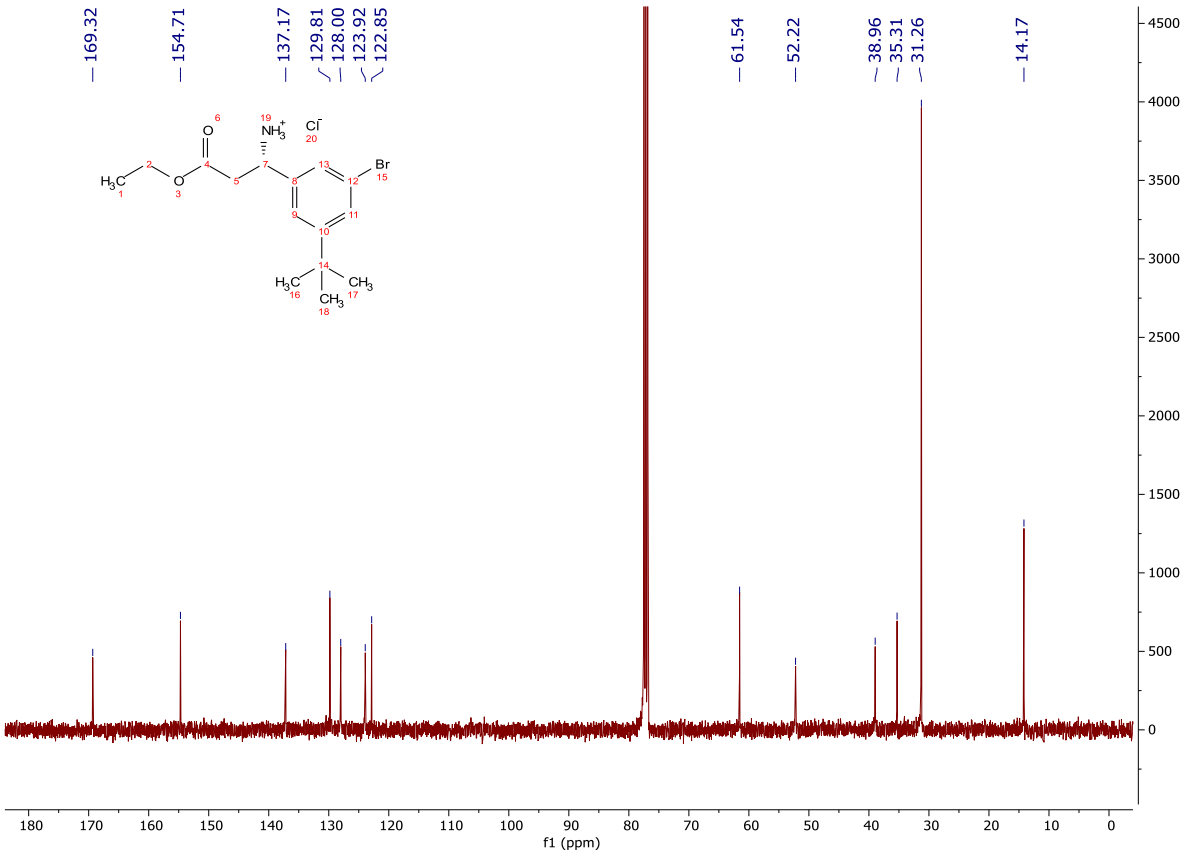
169.32
154.71
137.17
129.81
128.00
123.92
122.85
61.54
52.22
38.96
35.31
31.26
14.17
f1 (ppm)

Ethyl 3-(3-bromo-5-(3,5-dimethyl-1*H*-pyrazol-1-yl)phenyl)-3-((*tert*-butoxycarbonyl)amino)propanoate (**324**)

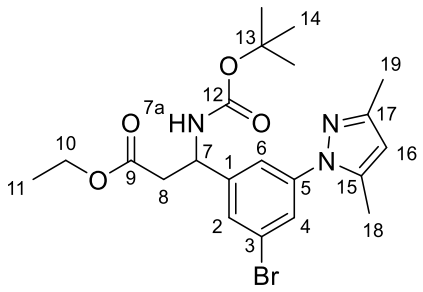

An oven dried microwave vial was charged with a solution of **119** (500 mg, 1.35 mmol) in TBME (5.00 mL), dtbpy (36 mg, 0.135 mmol), B_2Pin_2 (411 mg, 1.62 mmol) and $[Ir(OMe)(cod)]_2$ (45 mg, 0.068 mmol). The vial was sealed and degassed with Ar. The reaction mixture was stirred at 80 °C for 3 h with microwave irradiation. The mixture was cooled to rt, diluted with ethyl acetate (50.0 mL) and washed with 10 % $CuSO_{4(aq)}$ (2 x 50.0 mL). The organic was dried ($MgSO_4$), concentrated *in vacuo*, dissolved in diethyl ether (15.0 mL), filtered through Celite® and concentrated *in vacuo* to give an orange oil. A mixture of the crude product, 3,5-dimethyl pyrazole (324 mg, 3.38 mmol), $B(OH)_3$ (167 mg, 2.70 mmol), $Cu(OAc)_2$ (246 mg, 1.35 mg) and 4 Å molecular sieves (500 mg) in acetonitrile (4.00 mL) was stirred at 70 °C for 16 h. The crude reaction mixture was cooled to rt, diluted with ethyl acetate (50.0 mL) and sat. $NaHCO_{3(aq)}$ (60.0 mL). The aqueous was extracted with ethyl acetate (2 x 20.0 mL), the organics combined and washed with sat. $NaHCO_{3(aq)}$ (30.0 mL), water (30.0 mL) and brine (30.0 mL). The organic was dried $MgSO_4$ and concentrated *in vacuo* to give a brown oil. The crude product was purified *via* column chromatography on silica gel, eluting with a gradient of ethyl acetate/light petroleum (0-20%) to give the title compound as a clear yellow oil that solidified on standing (465 mg, 1.00 mmol, 74%); **HRMS** *m/z* (ESI^+) calc. for $C_{21}H_{29}BrN_3O_4$ $[M+H]^+$ requires 466.1336, found 466.1334; $\boldsymbol{R_f}$ 0.12, 10 % ethyl acetate/light petroleum, UV active; δ_H (400 MHz, $CDCl_3$) 7.53 (1H, dd, *J* = 1.9, 1.9 Hz, H-2), 7.41 (1H, dd, *J* = 1.7, 0.6 Hz, H-4), 7.34 – 7.31 (1H, m, H-6), 5.99 (1H, s, H-16), 5.62 (1H, bs, H-7a), 5.09 (1H, bs, H-7), 4.13 – 4.04 (2H, m, H-10), 2.90 – 2.74 (2H, m, H-8), 2.32 – 2.26 (6H, m, H-18 and H-19), 1.42 (9H, s, H-14), 1.22

– 1.16 (3H, m, H-11); δ_C (101 MHz, $CDCl_3$) 170.7 (CO), 155.0 (CO), 149.7 (C), 144.5 (C), 141.3 (C), 139.7 (C), 128.1 (ArH), 126.7 (ArH), 122.8 (C), 121.0 (ArH), 107.8 (ArH), 80.2 (C), 61.1 (CH_2), 50.7 (CH), 40.6 (CH_2), 28.5 (CH_3), 14.2 (CH_3), 13.6 (CH_3), 12.7 (CH_3); **MP** 124-127 °C; ν_{max} (FT-ATR/cm^{-1}) 3342, 2978, 1712, 1449, 1365, 1245, 1161, 1023, 864, 785.

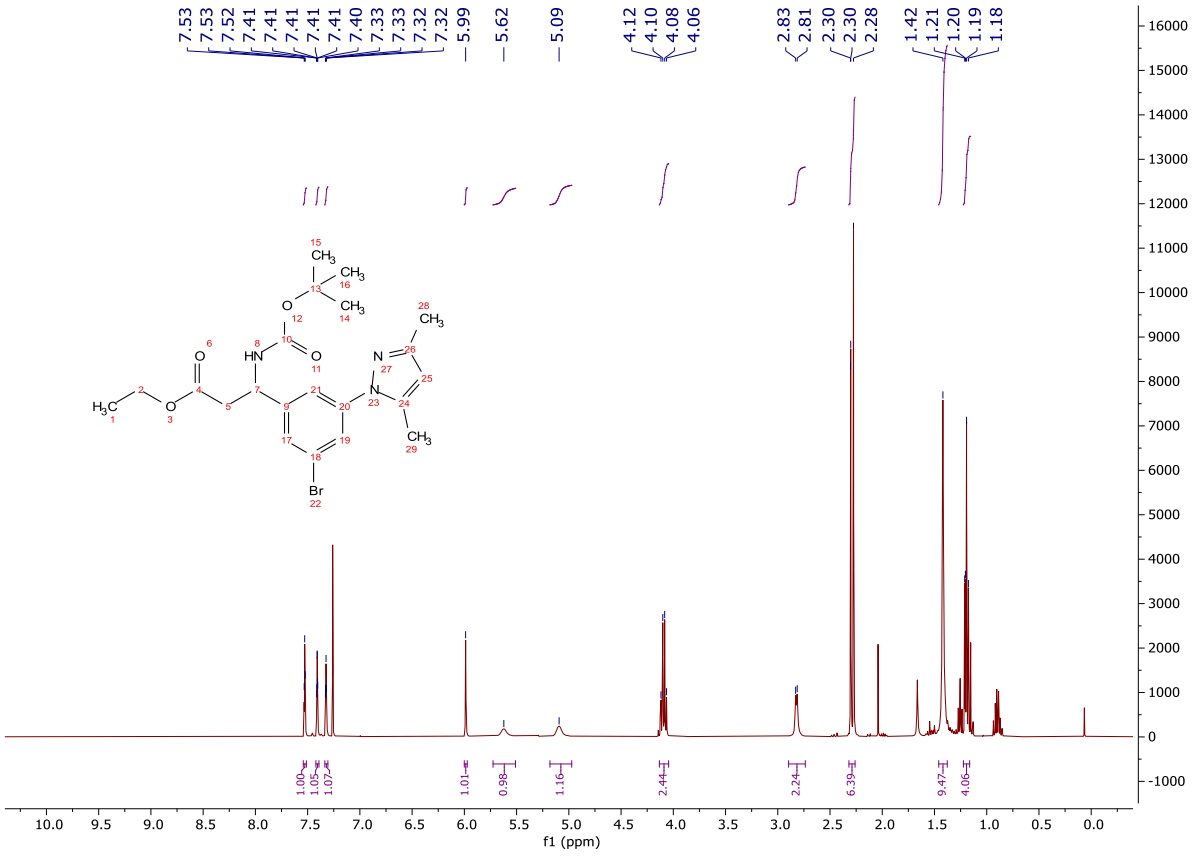
7.53
7.53
7.52
7.41
7.41
7.41
7.41
7.40
7.33
7.33
7.32
7.32
5.99
5.62
5.09
4.12
4.10
4.08
4.06
2.83
2.81
2.30
2.30
2.28
1.42
1.21
1.20
1.19
1.18
1.00
1.05
1.07
1.01
0.98
1.16
2.44
2.24
6.39
9.47
4.06
f1 (ppm)

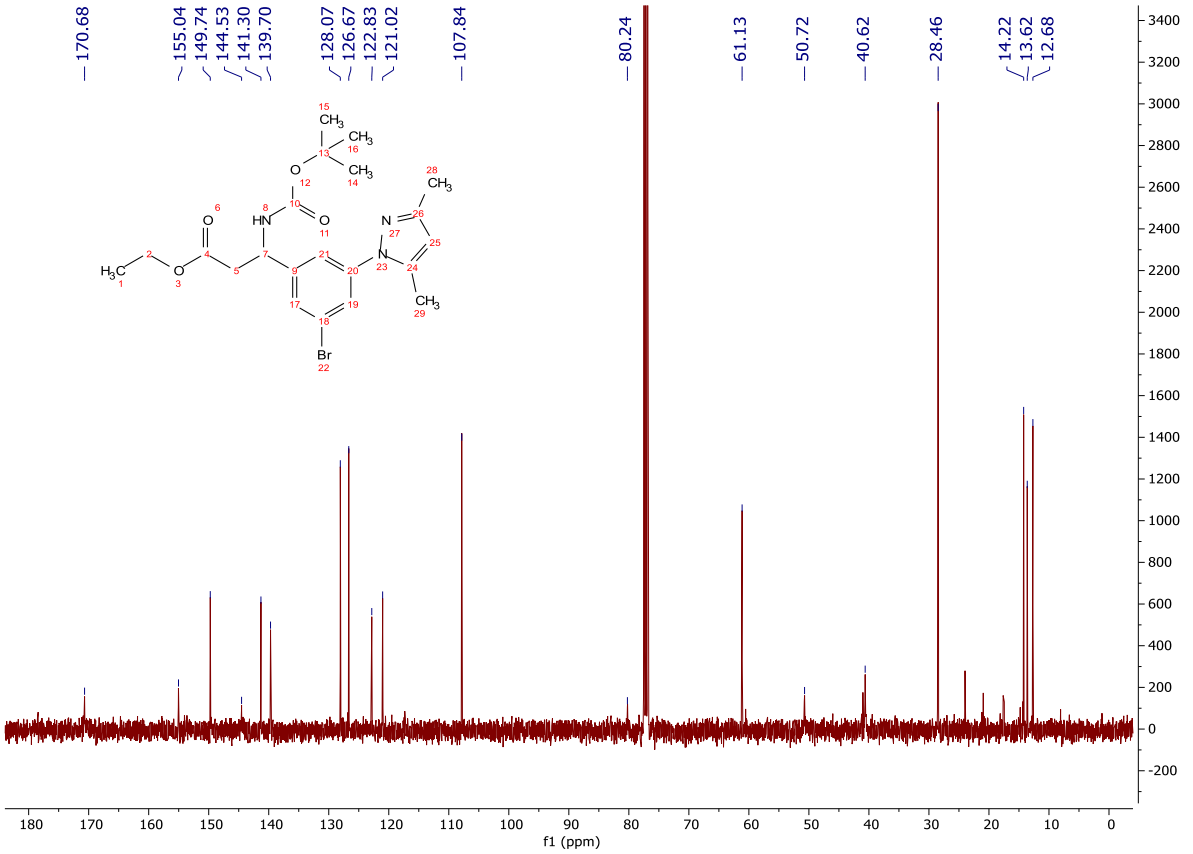
170.68
155.04
149.74
144.53
141.30
139.70
128.07
126.67
122.83
121.02
107.84
80.24
61.13
50.72
40.62
28.46
14.22
13.62
12.68
f1 (ppm)

Ethyl 3-(3-bromo-5-hydroxyphenyl)-3-((*tert*-butoxycarbonyl)amino)propanoate (**326**)

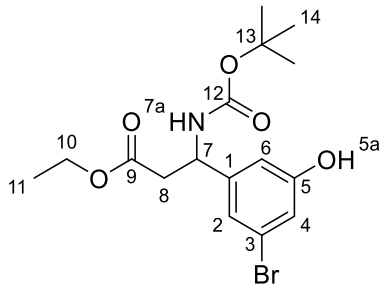

To a solution of **119** (133 mg, 0.268 mmol) in acetone (1.50 mL) was added a solution of Oxone® (540 mg, 1.76 mmol) in water (1.50 mL). The reaction mixture was vigorously stirred at rt for 45 min and subsequently quenched by slow addition of sat. $NaHCO_{3(aq)}$ (20.0 mL). The mixture was diluted further with sat. $NaHCO_{3(aq)}$ (30.0 mL) and CH_2Cl_2 (30.0 mL). The aqueous was extracted with CH_2Cl_2 (2 x 30.0 mL), the organics combined and dried ($MgSO_4$) and concentrated *in vacuo* to give a yellow oil. The crude product was purified *via* column chromatography on silica gel eluting with a gradient of diethyl ether/CH_2Cl_2 (0-20%) to afford the title compound as a clear, colourless oil (52 mg, 0.134 mmol, 50%); **HRMS** *m/z* (ESI^+) calc. for $C_{16}H_{23}BrNO_5$ $[M+H]^+$ requires 388.0754, found 388.0749; $\boldsymbol{R_f}$ 0.21, 5% diethyl ether/CH_2Cl_2, UV active; δ_H (400 MHz, DMSO-d_6) 9.88 (1H, s, H-5a), 7.48 (1H, d, *J* = 8.7 Hz, H-7a), 6.91 (1H, dd, *J* = 1.7, 1.7 Hz, H-2), 6.80 (1H, dd, *J* = 2.0, 2.0 Hz, H-4), 6.69 (1H, dd, *J* = 1.9, 1.9 Hz, H-6), 4.79 (1H, m, H-7), 4.09 – 3.95 (2H, m, H-10), 2.73 – 2.57 (2H, m, H-8), 1.35 (9H, s, H-14), 1.13 (3H, t, *J* = 7.1 Hz, H-11); δ_C (101 MHz, DMSO-d_6) 170.0 (CO), 158.4 (C), 154.6 (CO), 146.4 (C), 121.6 (C), 119.7 (ArH), 116.7 (ArH), 112.9 (ArH), 78.0 (C), 60.0 (CH_2), 50.7 (CH), 40.9 (CH_2), 28.2 (CH_3), 14.0 (CH_3); ν_{max} (FT-ATR/cm^{-1}) 3252, 2978, 1704, 1522, 1366, 1282, 1141, 1023, 848.

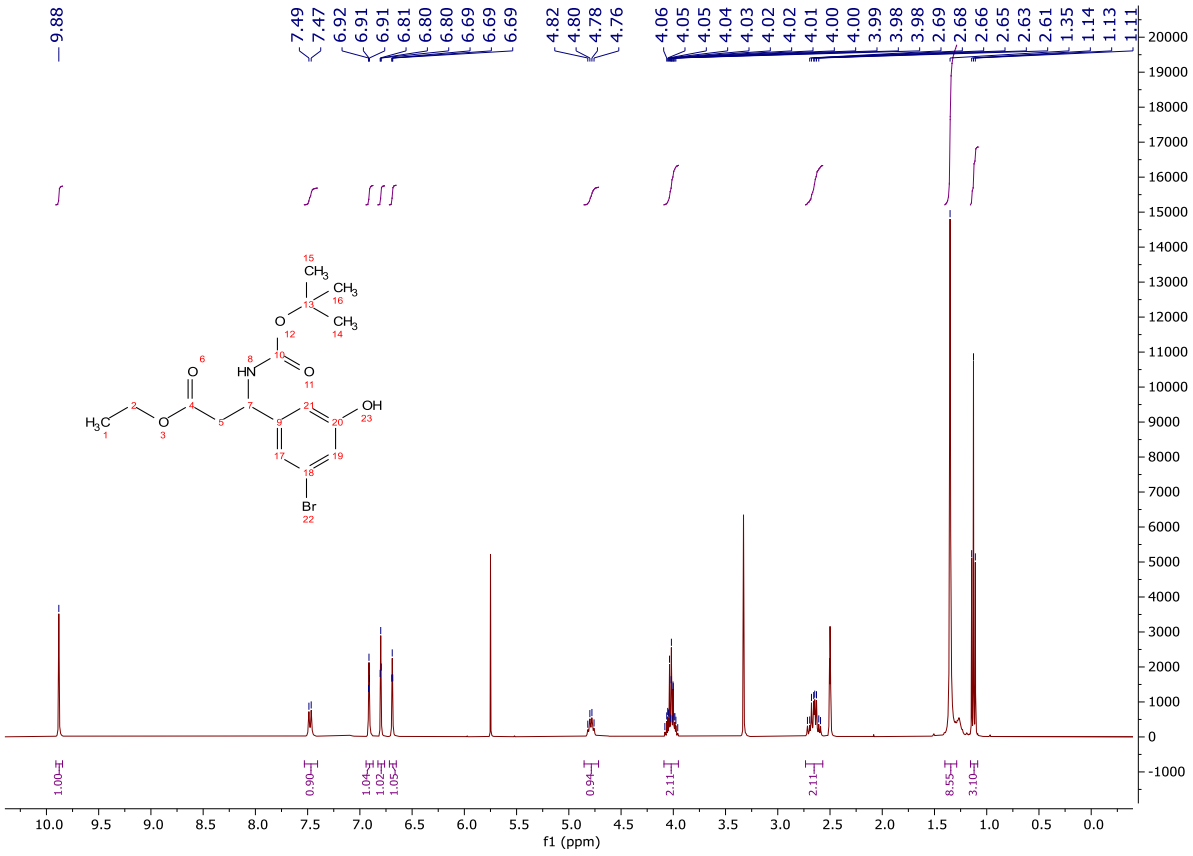
9.88
7.49
7.47
6.92
6.91
6.91
6.81
6.80
6.80
6.69
6.69
6.69
4.82
4.80
4.78
4.76
4.06
4.05
4.05
4.04
4.03
4.02
4.02
4.01
4.00
4.00
3.99
3.98
3.98
2.69
2.68
2.66
2.65
2.63
2.61
1.35
1.14
1.13
1.11
1.00
0.90
1.04
1.02
1.05
0.94
2.11
2.11
8.55
3.10
f1 (ppm)

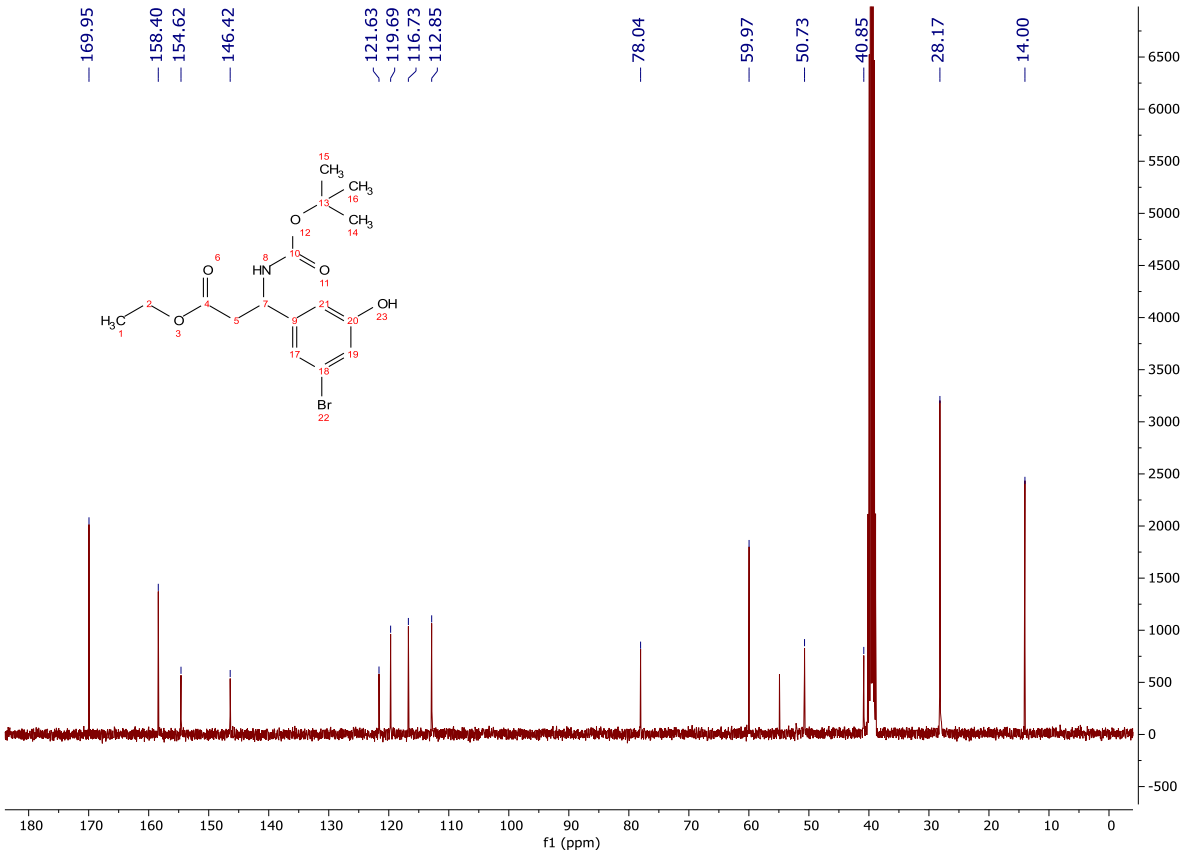
169.95
158.40
154.62
146.42
121.63
119.69
116.73
112.85
78.04
59.97
50.73
40.85
28.17
14.00
f1 (ppm)

Ethyl 3-(3-bromo-5-phenoxyphenyl)-3-((*tert*-butoxycarbonyl)amino)propanoate (**331**)

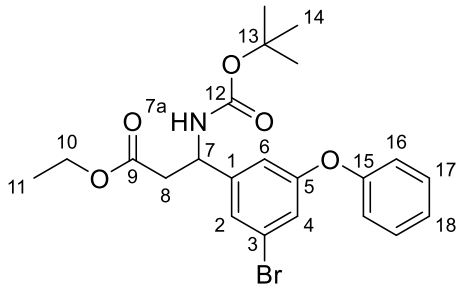

An oven dried microwave vial was charged with a solution of **119** (500 mg, 1.35 mmol) in TBME (5.00 mL), dtbpy (36 mg, 0.135 mmol), B_2Pin_2 (411 mg, 1.62 mmol) and $[Ir(OMe)(cod)]_2$ (45 mg, 0.068 mmol). The vial was sealed and degassed with Ar. The reaction mixture was stirred at 80 °C for 3 h with microwave irradiation. The mixture was cooled to rt, diluted with ethyl acetate (50.0 mL) and washed with 10 % $CuSO_{4(aq)}$ (2 x 50.0 mL). The organic was dried ($MgSO_4$), concentrated *in vacuo*, dissolved in diethyl ether (15.0 mL), filtered through Celite® and concentrated *in vacuo* to give an orange oil. A mixture of the crude product, phenol (381 mg, 4.05 mmol), $B(OH)_3$ (167 mg, 2.70 mmol), $Cu(OAc)_2$ (246 mg, 1.35 mmol) and 4 Å molecular sieves (500 mg) in acetonitrile (4.00 mL) was stirred at 70 °C for 16 h. The crude reaction mixture was cooled to rt, diluted with ethyl acetate (50.0 mL) and sat. $NaHCO_{3(aq)}$ (60.0 mL). The aqueous was extracted with ethyl acetate (2 x 20.0 mL), the organics combined and washed with sat. $NaHCO_{3(aq)}$ (30.0 mL), water (30.0 mL) and brine (30.0 mL). The organic was dried $MgSO_4$ and concentrated *in vacuo* to give a brown oil. The crude product was purified *via* column chromatography on silica gel, eluting with a gradient of ethyl acetate/light petroleum (0-20%) to give the title compound as a clear yellow oil (222 mg, 0.479 mmol, 36%); **HRMS** *m/z* (ESI^+) calc. for $C_{22}H_{27}BrNO_5$ $[M+H]^+$ requires 464.1067, found 464.1061; $\boldsymbol{R_f}$ 0.32, 10 % ethyl acetate/light petroleum, UV active; δ_H (400 MHz, $CDCl_3$) 7.40 – 7.32 (2H, m, H-17), 7.18 – 7.12 (2H, m, H-2 and H-18), 7.03 – 6.95 (3H, m, H-4 and H-16), 6.91 – 6.85 (1H, m, H-6), 5.54 (1H, bs, H-7a), 5.02 (1H, bs, H-7), 4.09 (2H, q, *J* = 7.1 Hz, H-10), 2.83 – 2.69 (2H, m, H-8), 1.42 (9H, s, H-14), 1.20 (3H, t, *J* = 7.1 Hz, H-11); δ_C (101 MHz, $CDCl_3$) 170.7 (CO), 158.6 (C), 156.2 (CO), 155.0 (C), 145.3 (C), 130.1 (ArH), 124.3 (ArH), 124.0 (ArH), 123.2

(C), 120.5 (ArH), 119.6 (ArH), 115.2 (ArH), 80.2 (C), 61.1 (CH_2), 50.8 (CH), 40.8 (CH_2), 28.5 (CH_3), 14.2 (CH_3); **MP** 125-127 °C; ν_{max} (FT-ATR/cm^{-1}) 3376, 2978, 1686, 1521, 1366, 1248, 1161, 1024, 778, 693.

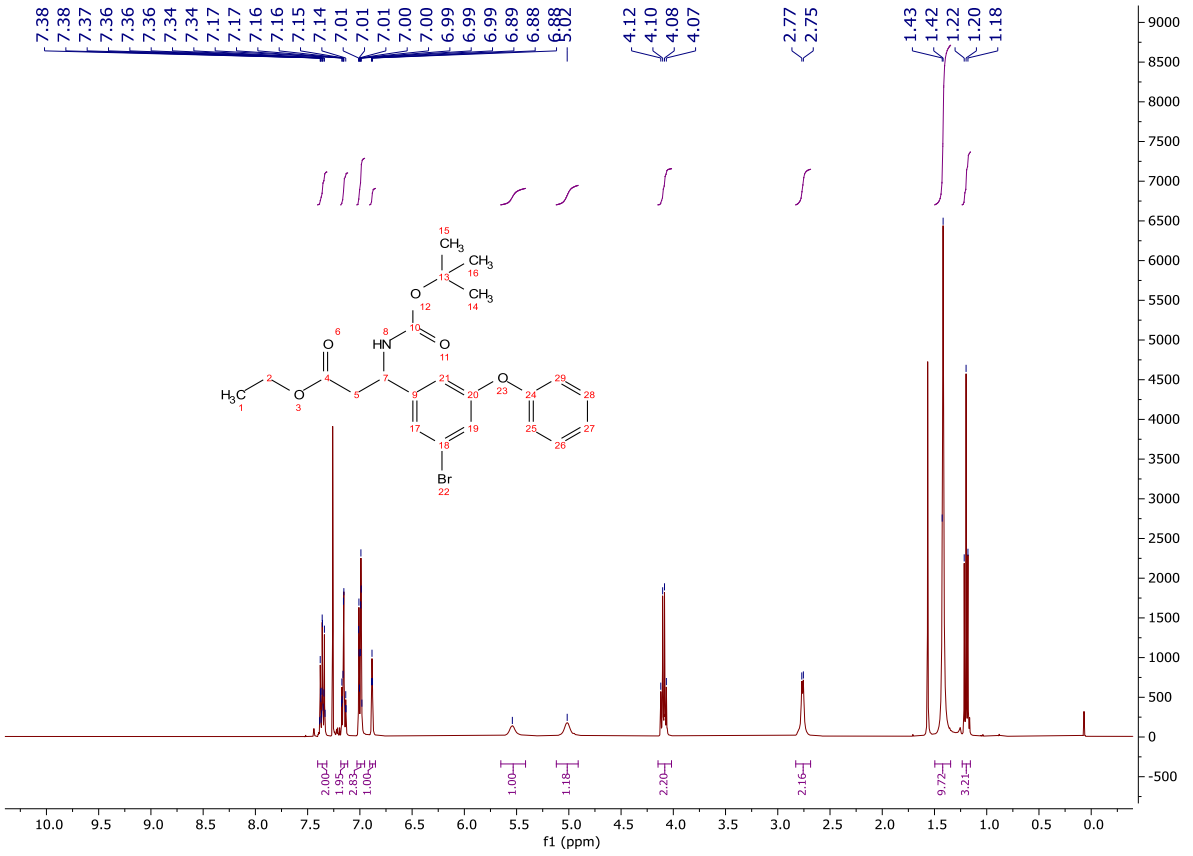
7.38
7.38
7.37
7.36
7.36
7.36
7.34
7.34
7.17
7.17
7.16
7.16
7.15
7.14
7.01
7.01
7.01
7.00
7.00
6.99
6.99
6.89
6.88
6.88
5.02
4.12
4.10
4.08
4.07
2.77
2.75
1.43
1.42
1.22
1.20
1.18
f1 (ppm)

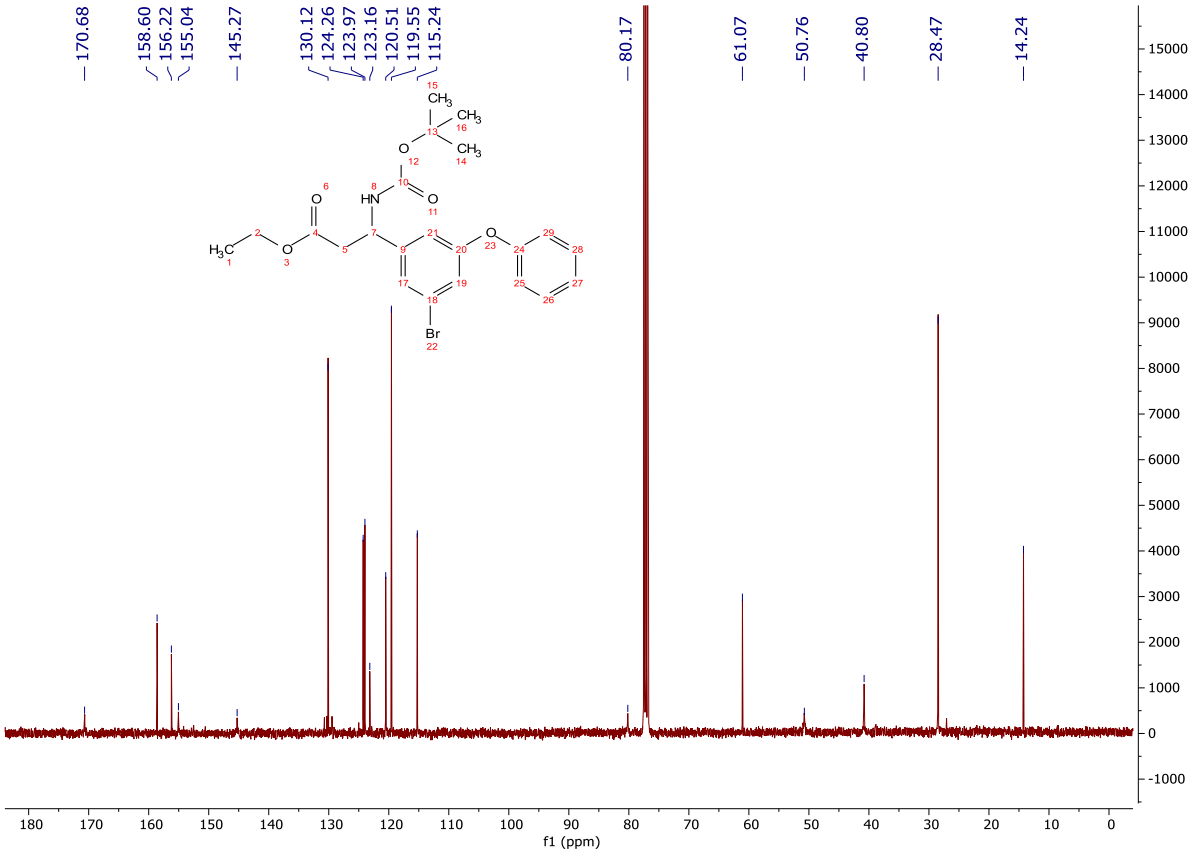
170.68
158.60
156.22
155.04
145.27
130.12
124.26
123.97
123.16
120.51
119.55
115.24
80.17
61.07
50.76
40.80
28.47
14.24
f1 (ppm)

Ethyl 3-((*tert*-butoxycarbonyl)amino)-3-(3-phenoxy-5-(trifluoromethyl)phenyl)propanoate (**332**)

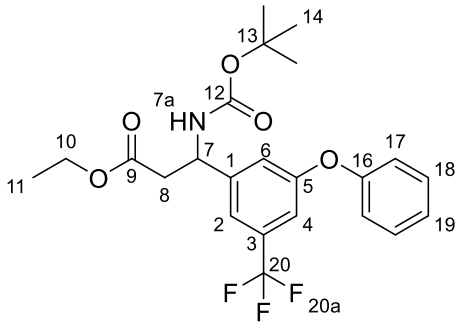

An oven dried microwave vial was charged with a solution of **313** (185 mg, 0.513 mmol) in TBME (2.50 mL), dtbpy (14 mg, 0.051 mmol), B_2Pin_2 (156 mg, 0.616 mmol) and $[Ir(OMe)(cod)]_2$ (17 mg, 0.026 mmol). The vial was sealed and degassed with Ar. The reaction mixture was stirred at 80 °C for 3 h with microwave irradiation. The mixture was cooled to rt, diluted with ethyl acetate (25.0 mL) and washed with 10 % $CuSO_{4(aq)}$ (2 x 25.0 mL). The organic was dried ($MgSO_4$), concentrated *in vacuo*, dissolved in diethyl ether (15.0 mL), filtered through Celite® and concentrated *in vacuo* to give an orange oil. A mixture of the crude product, phenol (145 mg, 1.54 mmol), $B(OH)_3$ (64 mg, 1.03 mmol), $Cu(OAc)_2$ (93 mg, 0.513 mmol) and 4 Å molecular sieves (250 mg) in acetonitrile (1.50 mL) was stirred at 70 °C for 16 h. The crude reaction mixture was cooled to rt, diluted with ethyl acetate (20.0 mL) and sat. $NaHCO_{3(aq)}$ (20.0 mL). The aqueous was extracted with ethyl acetate (2 x 20.0 mL), the organics combined and washed with sat. $NaHCO_{3(aq)}$ (20.0 mL), water (20.0 mL) and brine (10.0 mL). The organic was dried $MgSO_4$ and concentrated *in vacuo* to give a brown oil. The crude product was purified *via* column chromatography on silica gel, eluting with a gradient of ethyl acetate/light petroleum (0-10%) to give the title compound as a colourless solid (78 mg, 0.172 mmol, 34%); **HRMS** *m/z* (ESI^+) calc. for $C_{23}H_{27}F_3NO_5$ $[M+H]^+$ requires 454.1836, found 454.1837; R_f 0.33, 10 % ethyl acetate/light petroleum, UV active; δ_H (400 MHz, $CDCl_3$) 7.42 – 7.34 (2H, m, H-18), 7.28 – 7.24 (1H, m, H-2), 7.21 – 7.14 (1H, m, H-19), 7.14 – 7.07 (2H, m, H-4 and H-6), 7.04 – 6.98 (2H, m, H-17), 5.62 (1H, bs, H-7a), 5.09 (1H, bs, H-7), 4.08 (2H,

q, *J* = 7.1 Hz, H-10), 2.86 – 2.71 (2H, m, H-8), 1.41 (9H, s, H-14), 1.18 (3H, t, *J* = 7.2 Hz, H-11); δ_C (101 MHz, $CDCl_3$) 170.7 (CO), 158.3 (C), 156.1 (C), 155.1 (CO), 144.9 (C), 132.5 (C, q, *J* = 32.7 Hz), 130.2 (ArH), 124.5 (ArH), 123.7 (CF_3, q, *J* = 272.5 Hz), 119.6 (ArH), 119.5 (ArH), 117.4 (ArH, q, *J* = 3.7 Hz), 114.2 (ArH, q, *J* = 3.7 Hz), 80.3 (C), 61.1 (CH_2), 50.9 (CH), 40.7 (CH_2), 28.4 (CH_3), 14.2 (CH_3); δ_F (376 MHz, $CDCl_3$) -62.7; **MP** 125-127 °C; ν_{max} (FT-ATR/cm^{-1}) 3381, 2979, 1725, 1687, 1521, 1342, 1237, 1120, 694.

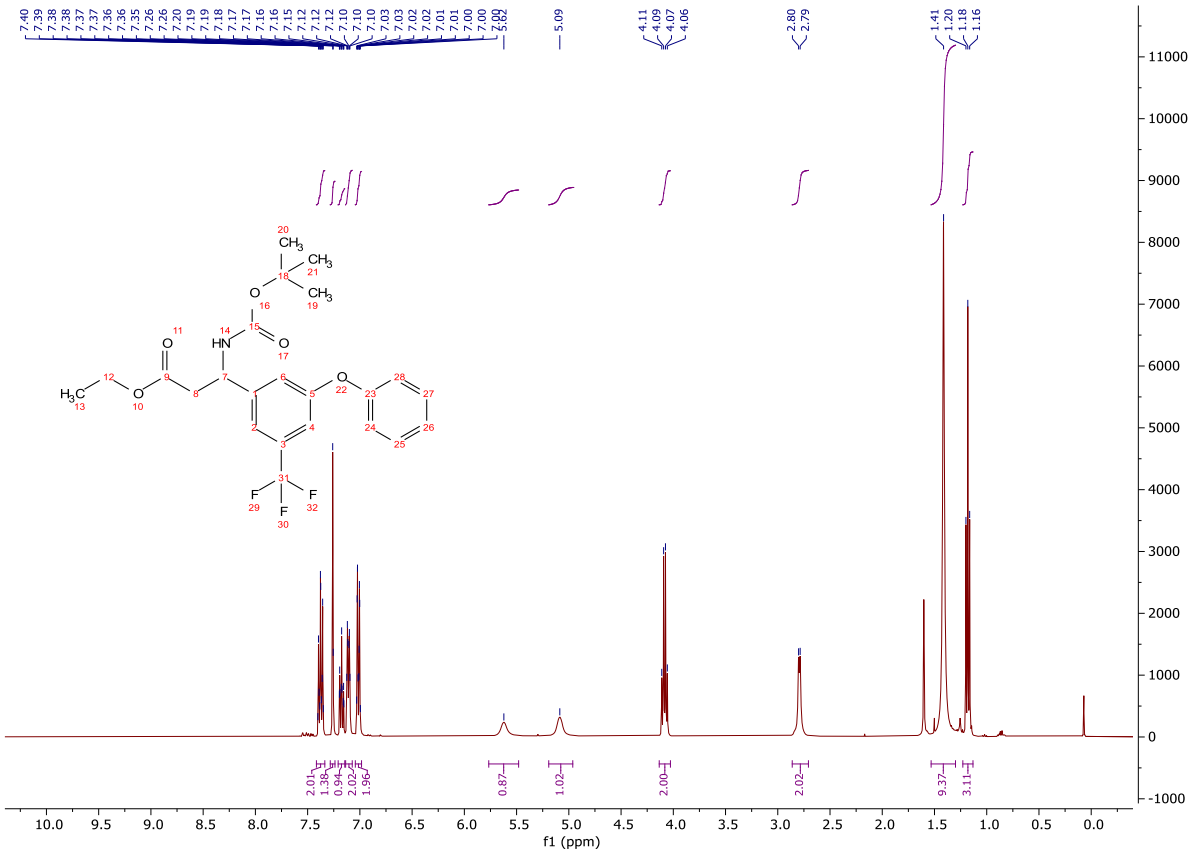
7.40 7.39 7.38 7.38 7.37 7.37 7.36 7.36 7.35 7.26 7.26 7.20 7.19 7.19 7.18 7.17 7.17 7.16 7.16 7.15 7.12 7.12 7.12 7.10 7.10 7.10 7.03 7.03 7.02 7.02 7.01 7.01 7.00 7.00 7.00 5.82
5.09
4.11 4.09 4.07 4.06
2.80 2.79
1.41 1.20 1.18 1.16
2.01 1.38 0.94 2.02 1.96 0.87 1.02 2.00 2.02 9.37 3.11
f1 (ppm)

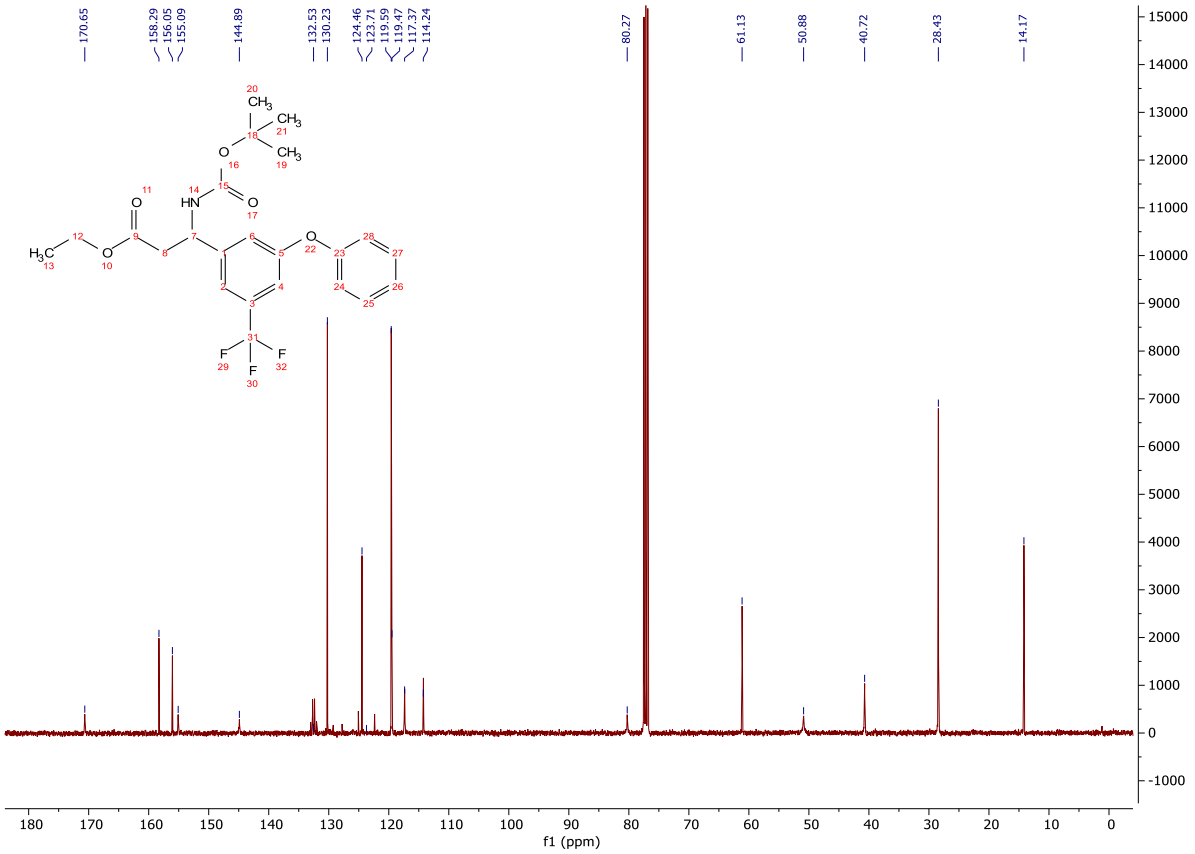
170.65 158.29 156.05 155.09 144.89 132.53 130.23 124.46 123.71 119.59 119.47 117.37 114.24 80.27 61.13 50.88 40.72 28.43 14.17
f1 (ppm)


-62.69
11000
10000
9000
8000
7000
6000
5000
4000
3000
2000
1000
0
-1000
20 10 0 -10 -20 -30 -40 -50 -60 -70 -80 -90 -100 -110 -120 -130 -140 -150 -160 -170 -180 -190 -200
f1 (ppm)

Ethyl (*S*)-3-(3-bromo-5-(*tert*-butyl)phenyl)-3-(2-((*tert*-butoxycarbonyl)amino)acetamindo)propanoate (**333**)

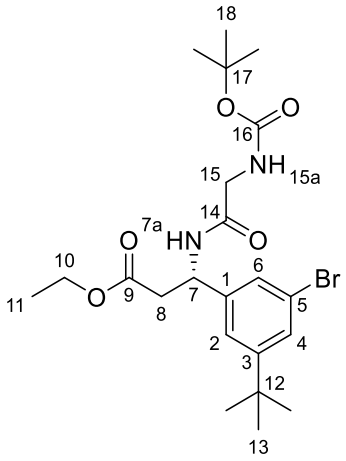

A solution of **323** (35 mg, 0.096 mmol), *N*-Boc-glycine (17 mg, 0.096 mmol) and HATU (334 mg, 0.288 mmol) in acetonitrile (1.00 mL) was stirred at 0 °C for 15 min. *i*-Pr_2NEt (0.083 mL, 0.480 mmol) was added and the reaction stirred for 16 h. The reaction mixture was concentrated *in vacuo* and dissolved in ethyl acetate (10.0 mL). The organic was washed with sat. $NH_4Cl_{(aq)}$ (10.0 mL), sat. $NaHCO_{3(aq)}$ (10.0 mL) and brine (10.0 mL), dried (Na_2SO_4) and concentrated *in vacuo* to give a brown oil. The crude product was purified *via* column chromatography on silica gel eluting with a gradient of ethyl acetate/light petroleum (0-35%) to give the title compound as a clear colourless oil (23 mg, 0.048 mmol, 50%); **HRMS** *m/z* (ESI^+) calc. for $C_{22}H_{34}BrN_2O_5$ $[M+H]^+$ requires 485.1646, found 485.1643; $\boldsymbol{R_f}$ 0.20, 25% ethyl acetate/light petroleum, UV active; $\boldsymbol{\delta_H}$ (400 MHz, $CDCl_3$) 7.41 – 7.29 (2H, m, H-4 and H-7a), 7.25 – 7.19 (2H, m, H-2 and H-6), 5.37 (1H, dt, *J* = 8.5, 5.9 Hz, H-7), 5.20 (1H, s, H-15a), 4.07 (2H, q, *J* = 7.1 Hz, H-10), 3.80 (2H, d, *J* = 5.8 Hz, H-15), 2.90 – 2.73 (2H, m, H-8), 1.44 (9H, s, H-17), 1.27 (9H, s, H-13), 1.17 (3H, t, *J* = 7.1 Hz, H-11); $\boldsymbol{\delta_C}$ (101 MHz, $CDCl_3$) 170.9 (CO), 169.0 (CO), 154.0 (CO), 142.3 (C), 128.2 (ArH), 126.4 (ArH), 122.8 (C), 122.5 (ArH), 80.4 (C), 61.1 (CH_2), 49.5 (CH), 44.7 (CH_2), 40.3 (CH_2), 35.1 (C), 31.3 (CH_3), 28.4 (CH_3), 14.2 (CH_3); $\boldsymbol{\nu_{max}}$ (FT-ATR/cm^{-1}) 3308, 3066, 1716, 1661, 1516, 1366, 1246, 1163, 1026, 864.

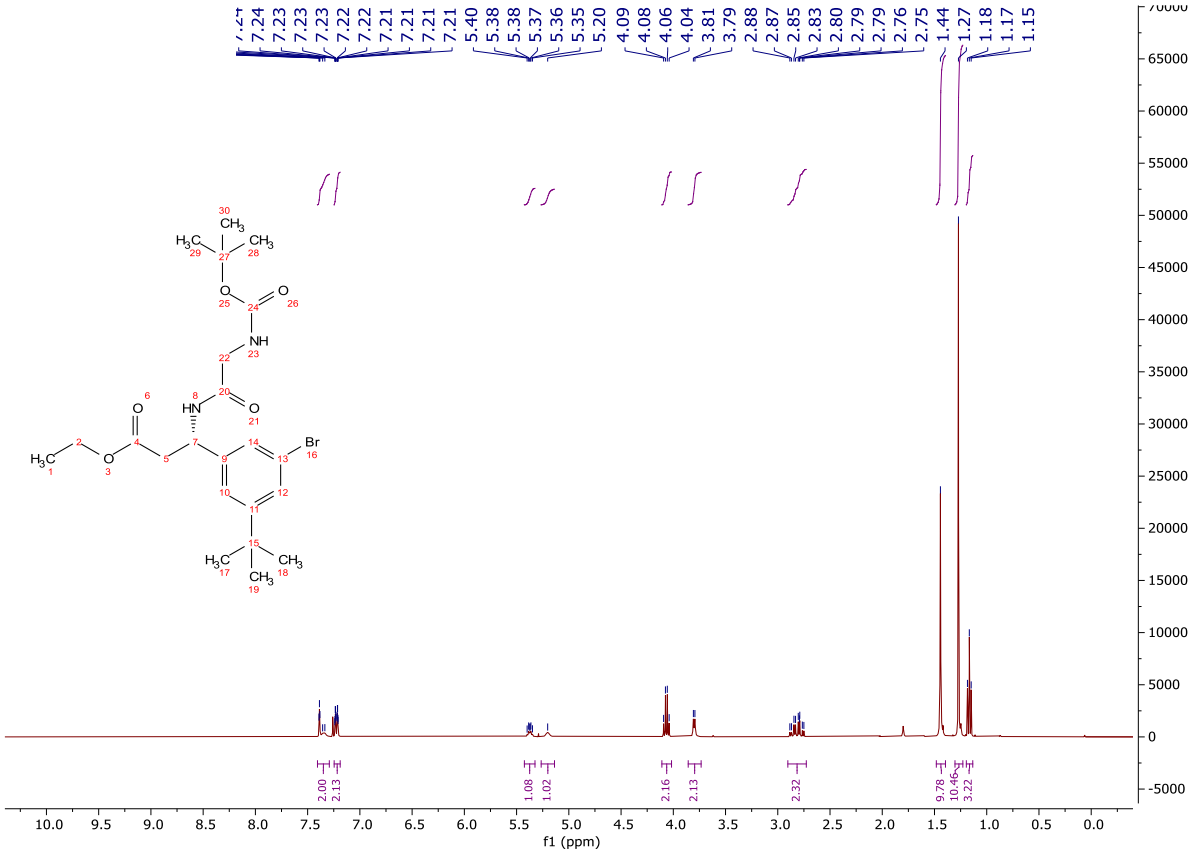
7.24
7.23
7.23
7.23
7.22
7.22
7.21
7.21
7.21
5.40
5.38
5.38
5.37
5.36
5.35
5.20
4.09
4.08
4.06
4.04
3.81
3.79
2.88
2.87
2.85
2.83
2.80
2.79
2.79
2.76
2.75
1.44
1.27
1.18
1.17
1.15
2.00
2.13
1.08
1.02
2.16
2.13
2.32
9.78
10.46
3.22
f1 (ppm)

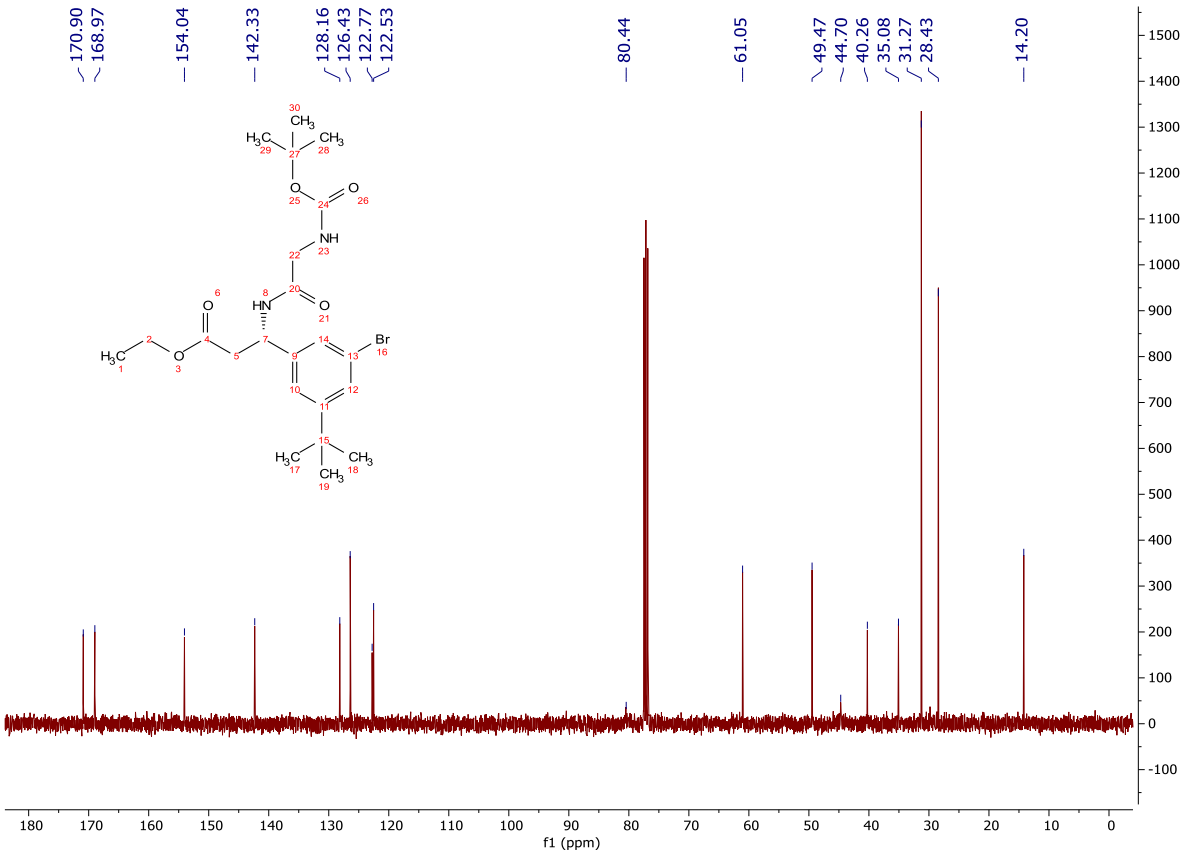
170.90
168.97
154.04
142.33
128.16
126.43
122.77
122.53
80.44
61.05
49.47
44.70
40.26
35.08
31.27
28.43
14.20
f1 (ppm)

3-Guanidinobenzoic acid (**334**)

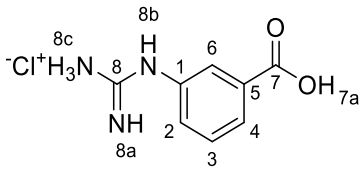

To a solution of 3,5-Dimethyl-1-pyrazolylformaminidium nitrate (1.00 g, 4.98 mmol) and diisopropylamine (0.700 mL, 4.98 mmol) in 1,4-dioxane (3.30 mL) and water (1.70 mL) was added 3-amino benzoic acid (455 mg, 3.32 mmol). The reaction mixture was heated under reflux for 2.5 h, cooled to room temperature and subsequently stirred for 16 h. The reaction mixture was filtered, and the filter cake washed successively with 1,4-dioxane and water to yield a beige solid. A slurry of the solid in water (5.00 mL) was acidified with conc. $HCl_{(aq)}$ until a homogenous solution was obtained. The mixture was concentrated *in vacuo*, then triturated with diethyl ether to afford the title compound as a pale purple solid (363 mg, 1.69 mmol 51%). The crude product was used without further purification; **HRMS** *m/z* (ESI^+) calc. for $C_8H_{10}N_3O_2$ $[M+H]^+$ requires 180.0768, found 180.0771; δ_H (400 MHz, DMSO) 13.18 (1H, bs, H-7a), 10.24 (1H, s, H-8b), 7.83 (1H, ddd, *J* = 7.7, 1.5, 1.5 Hz, H-4), 7.75 (1H, dd, *J* = 1.9, 1.9 Hz, H-6), 7.72 – 7.60 (4H, m, H-8a and H-8c), 7.56 (1H, dd, *J* = 7.8, 7.8 Hz, H-3), 7.51 – 7.45 (1H, m, H-2); δ_C (101 MHz, DMSO) 166.6 (CO), 156.1 (C), 135.8 (C), 132.2 (C), 130.0 (ArH), 128.5 (ArH), 126.9 (ArH), 124.8 (ArH).

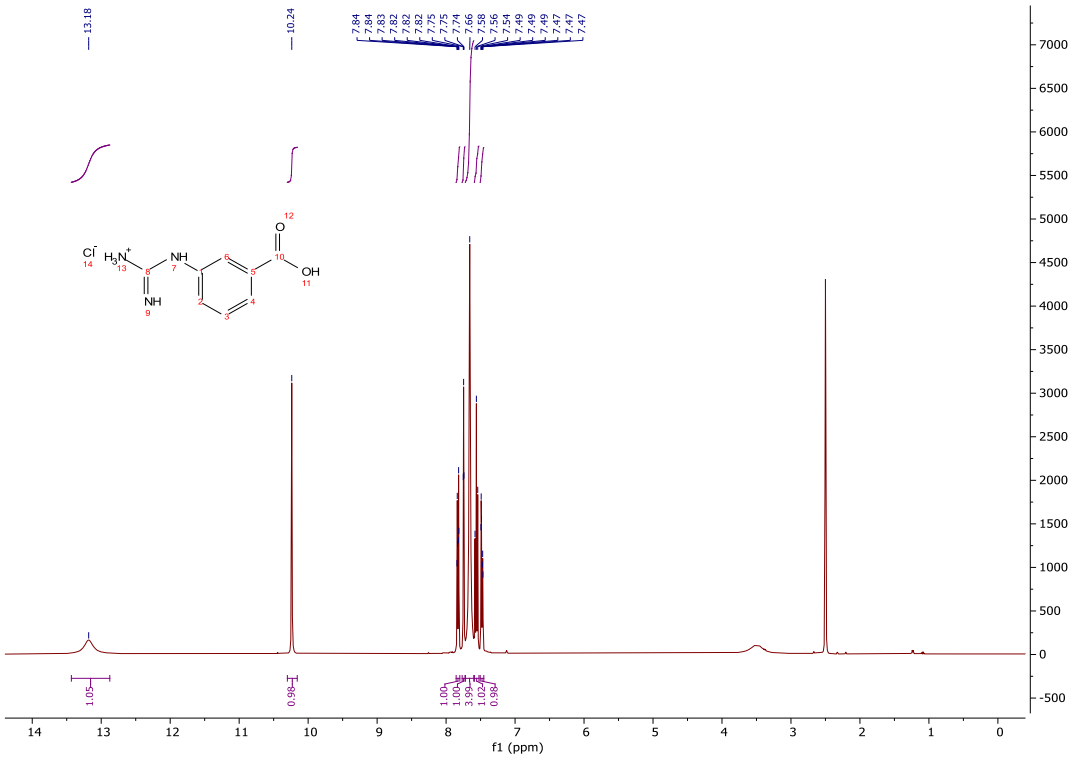
13.18
10.24
7.84
7.84
7.83
7.82
7.82
7.82
7.75
7.75
7.74
7.66
7.58
7.56
7.54
7.49
7.49
7.49
7.47
7.47
7.47
1.05
0.98
1.00
1.00
3.99
1.02
0.98
f1 (ppm)

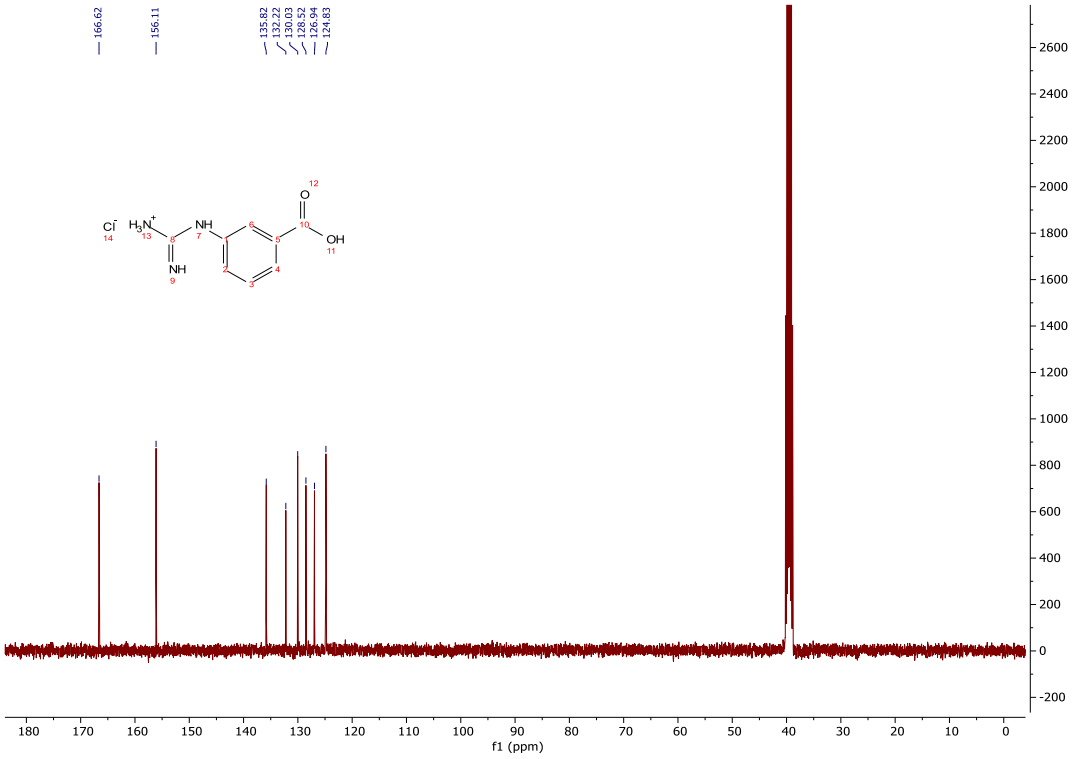
166.62
156.11
135.82
132.22
130.03
126.52
126.94
124.83
f1 (ppm)

(*S*)-3-(3-bromo-5-(*tert*-butyl)phenyl)-3-(2-(3-guanidinobenzamido)acetamido)propanoic acid (**335**)

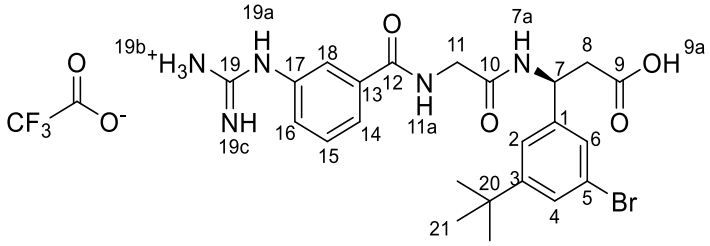

A solution of **333** (22 mg, 0.045 mmol) in 4M HCl in 1,4-dioxane (1.00 mL) was stirred at rt for 5 h. The reaction mixture was concentrated *in vacuo*, the residue dissolved in CH_2Cl_2 (0.200 mL) and DMF (0.200 mL), and HOBt (1.00 mg, 0.009 mmol) and **334** (10 mg, 0.045 mmol) added. The reaction mixture was stirred at rt for 5 min and DIC (0.010 mL, 0.060 mmol) was added. The reaction mixture was stirred for 64 h and concentrated *in vacuo* to give a crystalline solid. The crude solid was dissolved in THF (5.00 mL), 1M $LiOH_{(aq)}$ (0.230 mL, 0.230 mmol) was added, and the reaction mixture stirred for 64 h. The reaction mixture was concentrated *in vacuo*, the crude product dissolved in DMSO (20.0 mg/mL) and then purified by HPLC, eluting with a gradient of water (0.1% v/v TFA)/acetonitrile (15-100%), affording the title compound as a colourless solid (12 mg, 0.023 mmol, 52%). Spectroscopic analysis agrees with previously reported literature; **HRMS** *m/z* (ESI^+) calc. for $C_{23}H_{29}BrN_5O_4$ $[M+H]^+$ requires 518.1397, found 518.1403; δ_H (400 MHz, DMSO-d_6) 12.34 (1H, s, H-9a), 9.93 (1H, s, H-19c OR 19a), 8.80 (1H, t, *J* = 5.9 Hz, H-11a), 8.54 (1H, d, *J* = 8.3 Hz, H-7a), 7.78 (1H, ddd, *J* = 7.8, 1.3, 1.3 Hz, H-14), 7.72 (1H, dd, *J* = 1.9 Hz, H-4), 7.62 – 7.48 (4H, m, H-15 and 19b), 7.41 – 7.30 (4H, m, H-2, H-6, H-16 and H-18), 7.28 – 6.98 (1H, m, H-19c OR 19a), 5.19 (1H, q, *J* = 7.5 Hz, H-7), 3.90 (2H, d, *J* = 5.9 Hz, H-11), 2.71 (2H, d, *J* = 7.3 Hz, H-8), 1.26 (9H, s, H-21); δ_C (126 MHz, DMSO-d_6) 171.6 (CO), 168.1 (CO), 165.7 (CO), 155.8 (C), 153.5 (C), 144.8 (C), 135.6 (C), 135.5 (C), 129.7 (ArH), 127.3 (ArH), 126.7 (ArH), 126.4 (ArH), 125.2 (ArH), 123.5 (ArH), 122.8 (ArH), 121.6 (C), 49.3 (CH), 42.5 (CH_2), 40.8 (CH_2), 34.7 (C), 30.9 (CH_3); **MP** Degrades >115 °C.

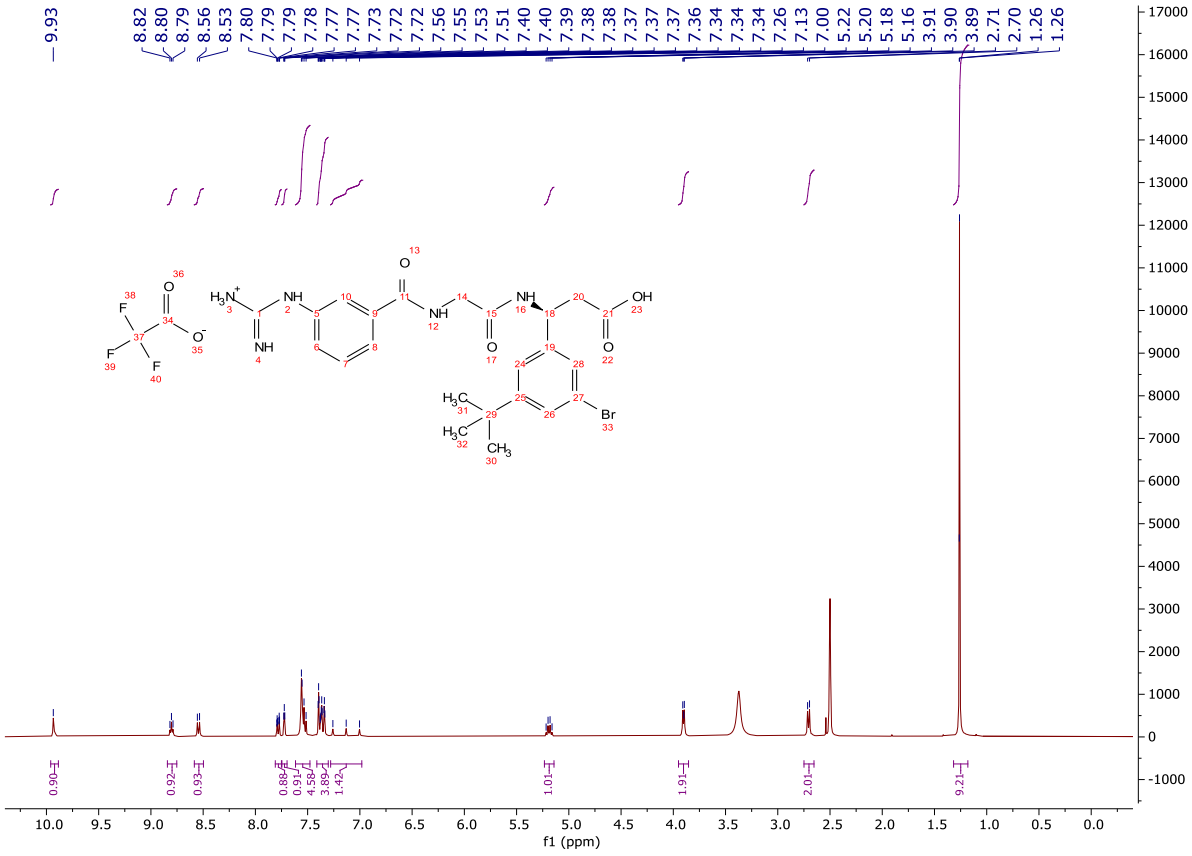
9.93
8.82
8.80
8.79
8.56
8.53
7.80
7.79
7.79
7.78
7.77
7.77
7.73
7.72
7.72
7.56
7.55
7.53
7.51
7.40
7.40
7.39
7.38
7.38
7.37
7.37
7.37
7.36
7.34
7.34
7.34
7.26
7.13
7.00
5.22
5.20
5.18
5.16
3.91
3.90
3.89
2.71
2.70
1.26
1.26
0.90
0.92
0.93
0.88
0.91
4.58
3.89
1.42
1.01
1.91
2.01
9.21
f1 (ppm)

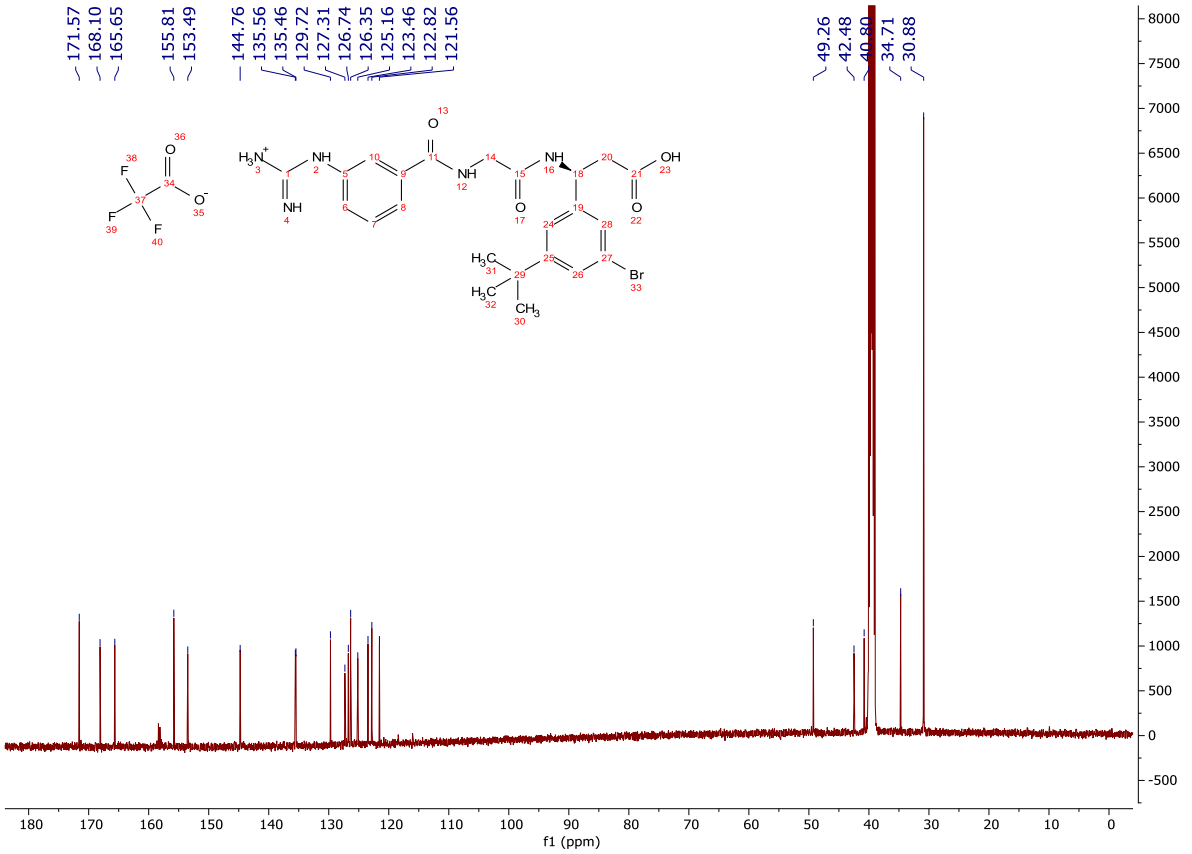
171.57
168.10
165.65
155.81
153.49
144.76
135.56
135.46
129.72
127.31
126.74
126.35
125.16
123.46
122.82
121.56
49.26
42.48
40.80
34.71
30.88
f1 (ppm)

Ethyl 3-(3-bromo-5-(4,4,5,5-tetramethyl-1,3,2-dioxaborolan-2-yl)phenyl)-3-((tertbutoxycarbonyl)amino)propanoate (**310**)

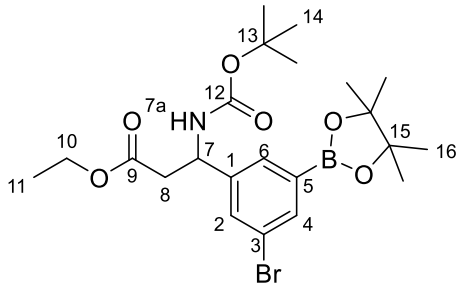

An oven dried microwave vial was charged with a solution of **119** (2.00 g, 5.40 mmol) in TBME (7.50 mL), dtbpy (72 mg, 0.270 mmol), B_2Pin_2 (2.41 g, 9.50 mmol), $[Ir(OMe)(cod)]_2$ (106 mg, 0.160 mmol). The vial was sealed and degassed with Ar. The reaction mixture was stirred at 80 °C for 3 h with microwave irradiation. The mixture was cooled to rt, diluted with ethyl acetate (200 mL) and washed with 10 % $CuSO_{4(aq)}$ (2 x 100 mL). The organic was dried ($MgSO_4$), concentrated *in vacuo*, dissolved in diethyl ether (150 mL), filtered through Celite® and concentrated *in vacuo* to give an orange oil. The crude product was purified *via* column chromatography on silica gel eluting with a gradient of diethyl ether/CH_2Cl_2 (0-20%) to afford the title compound as a clear, colourless oil (2.31 g, 4.60 mmol, 86%); **HRMS** *m/z* (ESI^+) calc. for $C_{22}H_{34}BBrNO_6$ $[M+H]^+$ requires 498.1657, found 498.1655; $\boldsymbol{R_f}$ 0.32, 20% ethyl acetate/light petroleum, $KMnO_4$ active; δ_H (400 MHz, $CDCl_3$) 7.84 – 7.79 (1H, m, H-4), 7.64 – 7.59 (1H, m, H-2), 7.53 (1H, dd, *J* = 2.0, 2.0 Hz, H-6), 5.49 (1H, bs, H-7a), 5.05 (1H, bs, H-7), 4.17 – 4.03 (2H, m, H-10), 2.89 – 2.72 (1H, m, H-8), 1.42 (9H, s, H-14), 1.33 (12H, s, H-16), 1.23 – 1.15 (3H, m, H-11); δ_C (101 MHz, $CDCl_3$) 170.7 (CO), 155.1 (CO), 143.2 (C), 136.7 (ArH), 132.2 (ArH), 131.0 (ArH), 122.8 (C), 84.4 (C), 61.0 (CH_2), 51.1 (CH), 41.1 (CH_2), 28.5 (CH_3), 25.0 (CH_3), 14.2 (CH_3); ν_{max} (FT-ATR/cm^{-1}) 3328, 2938, 1707, 1527, 1350, 1295, 1246, 1142.

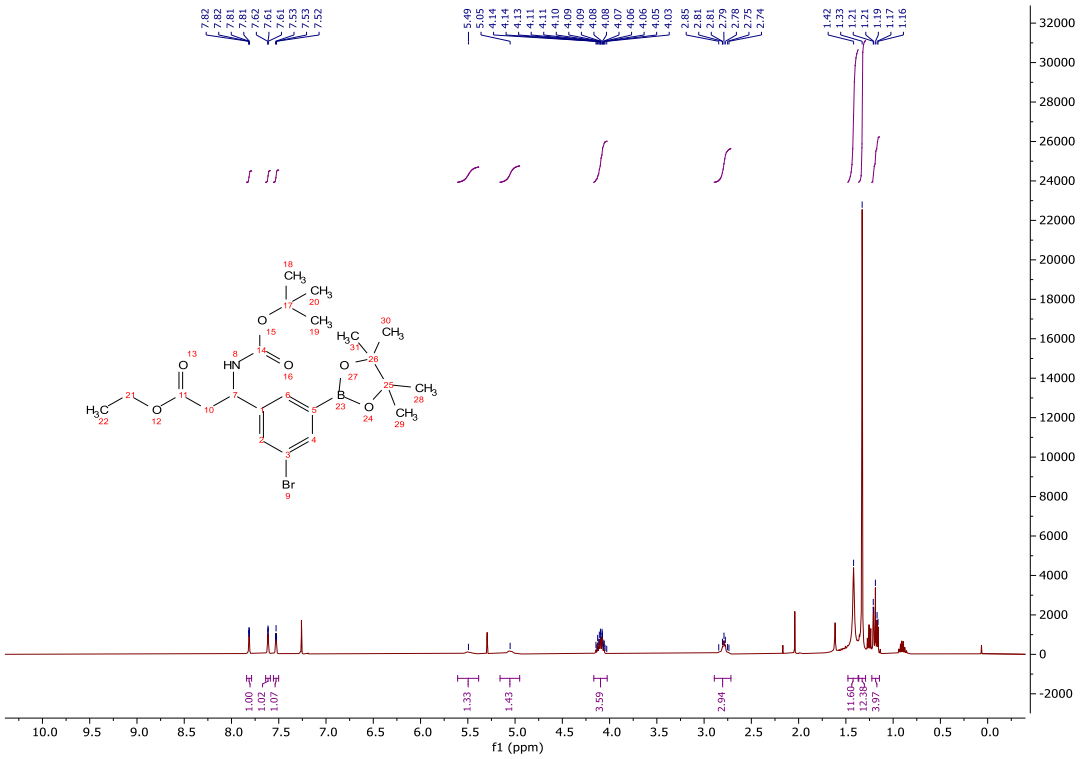
7.82
7.82
7.81
7.81
7.62
7.61
7.61
7.53
7.53
7.52
5.49
5.05
4.14
4.14
4.13
4.11
4.11
4.10
4.09
4.09
4.08
4.08
4.07
4.06
4.06
4.05
4.03
2.85
2.81
2.81
2.79
2.78
2.75
2.74
1.42
1.33
1.21
1.21
1.19
1.17
1.16
1.00
1.07
1.07
1.33
1.43
3.59
2.94
11.60
12.98
3.97
f1 (ppm)

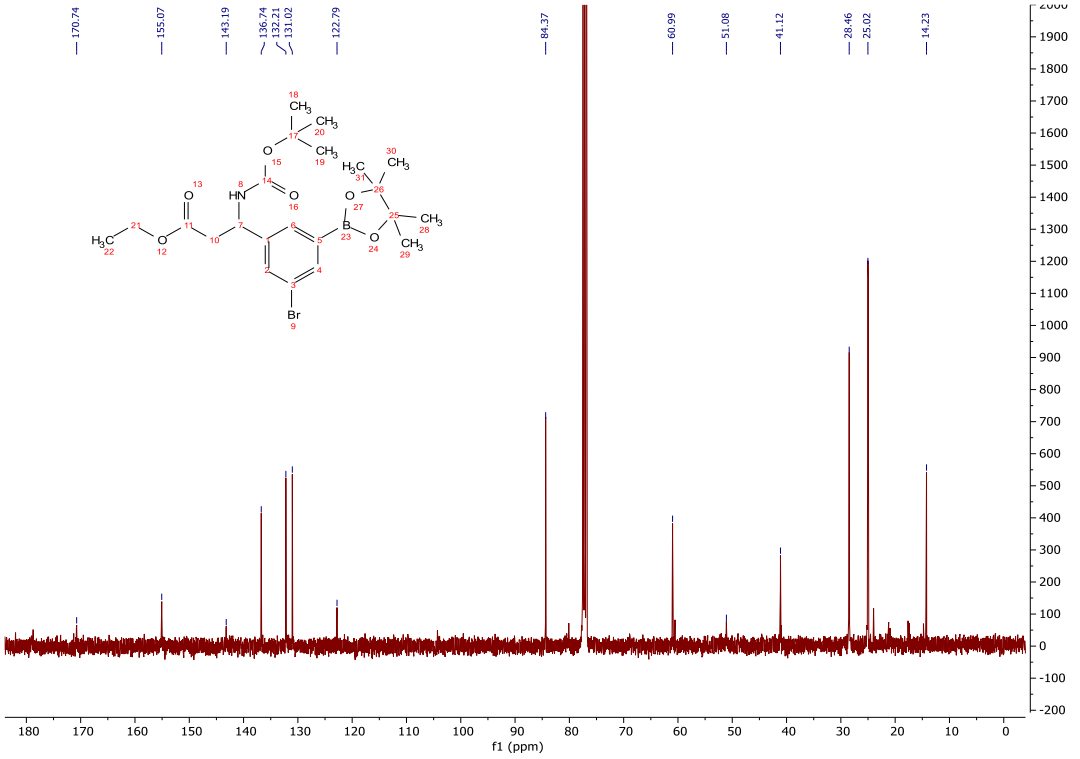
170.74
155.07
143.19
136.74
133.21
131.02
122.79
84.37
60.99
51.08
41.12
28.46
25.02
14.23
f1 (ppm)

Ethyl (*S*)-3-(3-bromo-5-hydroxyphenyl)-3-((*tert*-butoxycarbonyl)amino)propanoate (**(*S*)-326**)

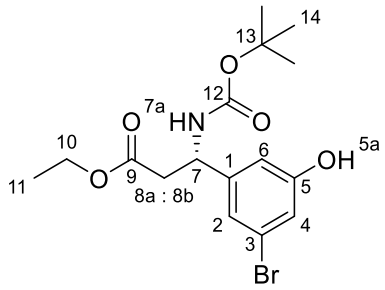

An oven dried microwave vial was charged with a solution of **(*S*)-119** (373 mg, 1.01 mmol) in TBME (2.00 mL), dtbpy (14 mg, 0.051 mmol), B_2Pin_2 (307 mg, 1.21 mmol) and $[Ir(OMe)(cod)]_2$ (17 mg, 0.025 mmol). The vial was sealed and degassed with Ar. The reaction mixture was stirred at 80 °C for 3 h with microwave irradiation. The mixture was cooled to rt, diluted with ethyl acetate (25.0 mL) and washed with 10 % $CuSO_{4(aq)}$ (2 x 15.0 mL). The organic was dried ($MgSO_4$), concentrated *in vacuo*, dissolved in diethyl ether (15.0 mL), filtered through Celite® and concentrated *in vacuo* to give an orange oil. To a solution of the crude product in acetone (5.00 mL) was added a solution of Oxone® (2.04 g, 6.64 mmol) in water (6.50 mL). The reaction mixture was vigorously stirred at rt for 45 min and subsequently quenched by slow addition of sat. $NaHCO_{3(aq)}$ (40.0 mL). The mixture was diluted further with sat. $NaHCO_{3(aq)}$ (20.0 mL) and CH_2Cl_2 (2 x 30.0 mL). The aqueous was extracted with CH_2Cl_2 (2 x 30.0 mL), the organics combined and dried ($MgSO_4$) and concentrated *in vacuo* to give a yellow oil. The crude product was purified *via* column chromatography on silica gel eluting with a gradient of diethyl ether/CH_2Cl_2 (0-20%) to afford the title compound as a clear, colourless oil (130 mg, 0.336 mmol, 33%); **HRMS** *m/z* (ESI^+) calc. for $C_{16}H_{23}BrNO_5$ $[M+H]^+$ requires 388.0754, found 388.0763; $\boldsymbol{R_f}$ 0.20, 20 % ethyl acetate/light petroleum, UV active; δ_H (400 MHz, DMSO-d_6) 9.88 (1H, s, H-5a), 7.48 (1H, d, *J* = 8.8 Hz, H-7a), 6.91 (1H, dd, *J* = 1.7, 1.7 Hz, H-2), 6.80 (1H, dd, *J* = 2.0, 2.0 Hz, H-4), 6.69 (1H, dd, *J* = 1.8, 1.8 Hz, H-6), 4.84 – 4.72 (1H, m, H-7), 4.09 – 3.94 (2H, m, H-10), 2.74 – 2.56 (2H, m, H-8a and H-8b), 1.35 (9H, s, H-14), 1.13 (3H, t, *J* = 7.1 Hz, H-11); δ_C (101 MHz, DMSO-d_6) 170.0 (CO), 158.4 (C), 154.6 (CO), 146.4 (C), 121.6 (C), 119.7

(ArH), 116.7 (ArH), 112.8 (ArH), 78.1 (C), 60.0 (CH_2), 50.7 (CH), 40.9 (CH_2), 28.2 (CH_3), 14.0 (CH_3); ν_{max} (FT-ATR/cm^{-1}) 3336, 2979, 1681, 1506, 1367, 1277, 1156, 1020, 846, 694.

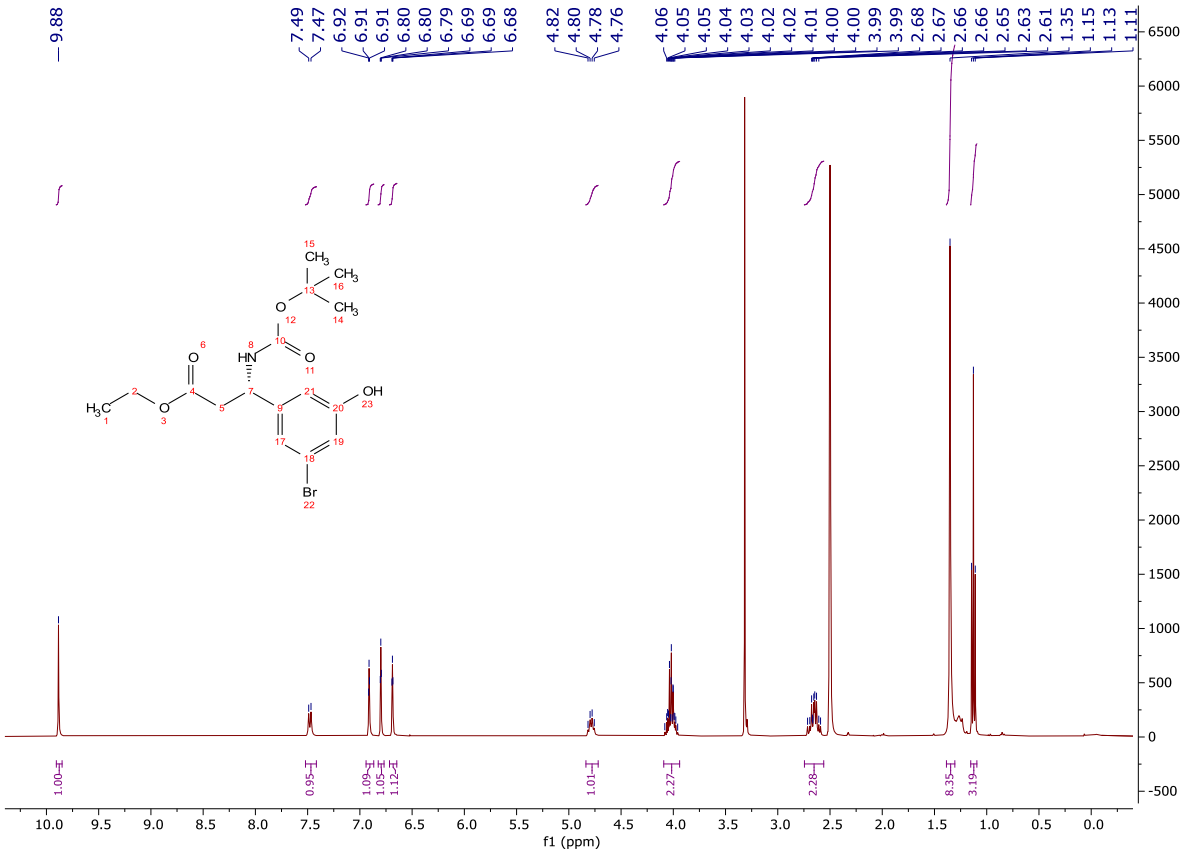
9.88
7.49
7.47
6.92
6.91
6.91
6.80
6.80
6.79
6.69
6.69
6.68
4.82
4.80
4.78
4.76
4.06
4.05
4.05
4.04
4.03
4.02
4.02
4.01
4.00
4.00
3.99
3.99
2.68
2.67
2.66
2.66
2.65
2.63
2.61
1.35
1.15
1.13
1.11
1.00
0.95
1.09
1.05
1.12
1.01
2.27
2.28
8.35
3.19
f1 (ppm)

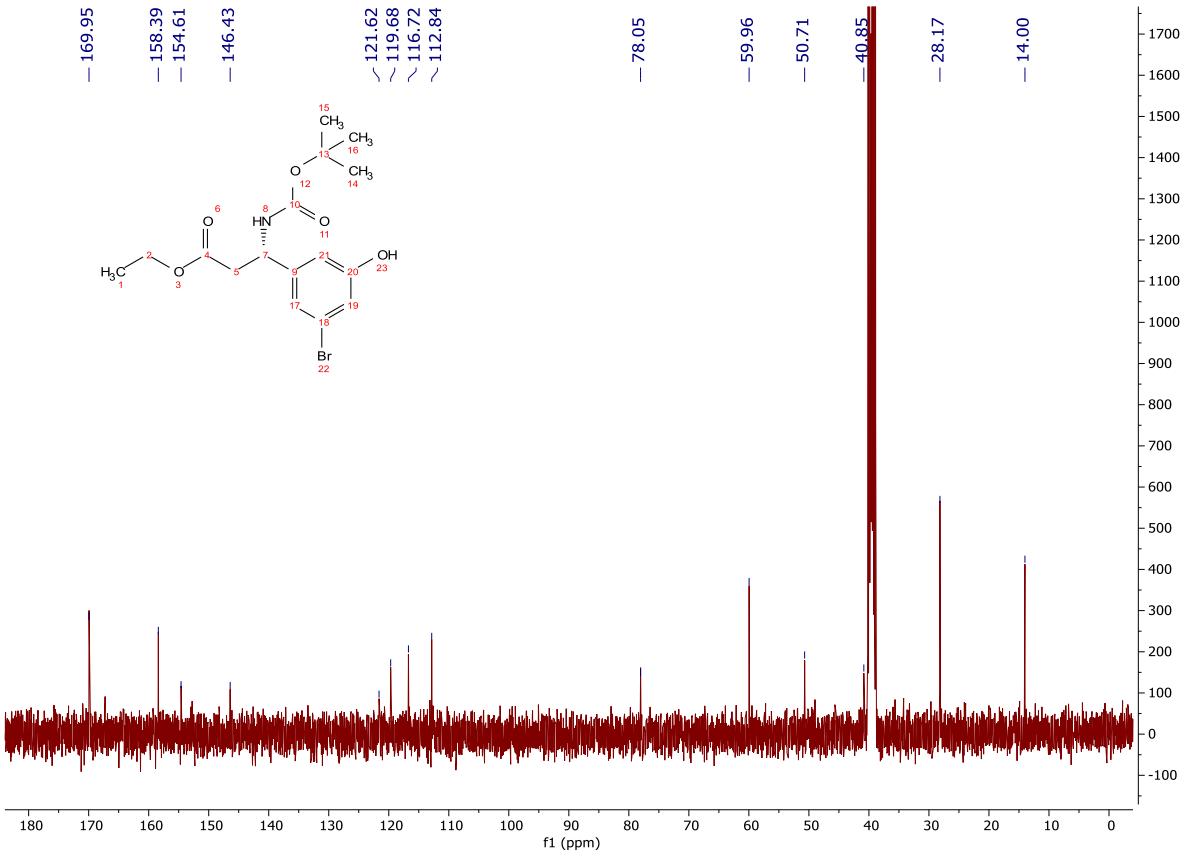
169.95
158.39
154.61
146.43
121.62
119.68
116.72
112.84
78.05
59.96
50.71
40.85
28.17
14.00
f1 (ppm)

Ethyl (*S*)-3-((*tert*-butoxycarbonyl)amino)-3-(3-(trifluoromethyl)phenyl)propanoate (**(*S*)-313**)

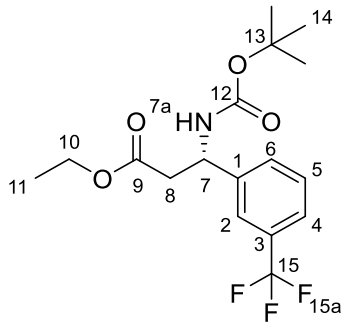

To a stirred solution of **118** (11.2 g, 37.7 mmol) in THF (130 mL) at 0 °C was added Et_3N (15.7 mL, 113 mmol). A solution of di-*tert*-butyl dicarbonate (11.2 mL, 49.0 mmol) in THF (20.0 mL) was added and the reaction mixture stirred for 65 h. The reaction mixture was concentrated *in vacuo* and the crude material dissolved in ethyl acetate (150 mL) and sat. $NaHCO_{3(aq)}$ (150 mL). The layers were separated and the organic washed with 10% citric $acid_{(aq)}$ (150 mL), water (150 mL), brine (150 mL), dried (Na_2SO_4) and concentrated *in vacuo* to afford a yellow oil. The crude product was purified *via* column chromatography on silica gel, eluting isocratically with ethyl acetate/light petroleum (20%) to give the title compound as a colourless, amorphous solid (13.9 g, 38.6 mmol, quant.*); **HRMS** *m/z* (ESI^+) calc. for $C_{17}H_{22}F_3NNaO_4$ $[M+Na]^+$ requires 384.1393, found 384.1389; $\boldsymbol{R_f}$ 0.55, 20 % ethyl acetate/light petroleum, UV active; δ_H (400 MHz, $CDCl_3$) 7.58 – 7.41 (4H, m, H-2, H-4, H-5 and H-6), 5.63 (1H, s, H-7a), 5.14 (1H, s, H-7), 4.07 (2H, q, *J* = 7.1 Hz, H-10), 2.91 – 2.75 (2H, m, H-8), 1.42 (9H, s, H-14), 1.16 (3H, t, *J* = 7.1 Hz, H-11); δ_C (101 MHz, $CDCl_3$) 170.7 (CO), 155.1 (CO), 142.7 (C), 130.9 (C, q, *J* = 32.2 Hz), 129.8 (ArH), 129.1 (ArH), 124.3 (ArH, q, *J* = 3.8 Hz), 124.1 (CF_3, q, *J* = 272.3 Hz), 123.0 (ArH), 80.0 (C), 60.9 (CH_2), 51.0 (CH), 40.8 (CH_2), 28.3 (CH_3), 14.0 (CH_3); δ_F (376 MHz, $CDCl_3$) -62.7 (F-15a); **MP** Becomes waxy at 45 °C, melts fully at 60 °C; ν_{max} (FT-ATR/cm^{-1}) 3371, 2982, 1723, 1681, 1525, 1450, 1328, 1248, 1159, 1113, 705.

*Excess di-*tert*-butyl dicarbonate remaining, hence the inflated product mmol value.

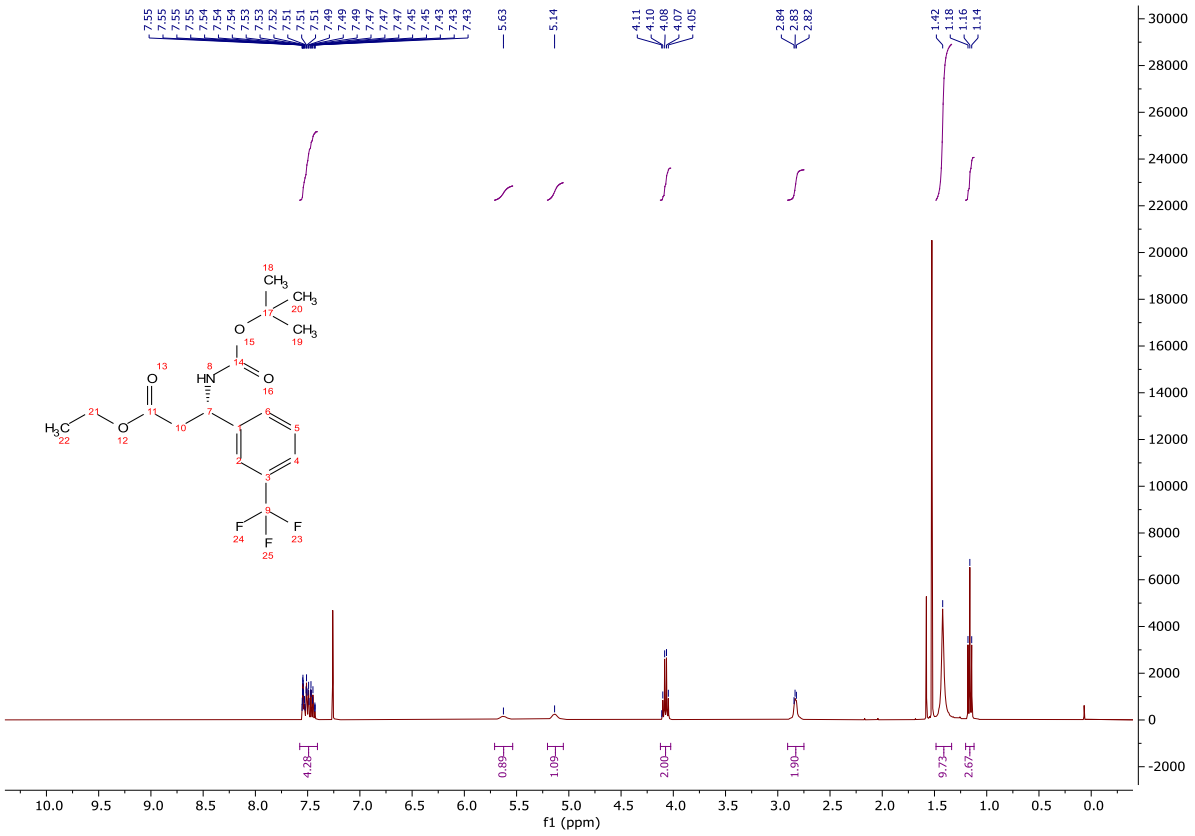
7.55 7.55 7.55 7.55 7.54 7.54 7.54 7.53 7.53 7.52 7.51 7.51 7.51 7.49 7.49 7.49 7.47 7.47 7.47 7.45 7.45 7.43 7.43 7.43
5.63
5.14
4.11 4.10 4.08 4.07 4.05
2.84 2.83 2.82
1.42 1.18 1.16 1.14
4.28
0.89
1.09
2.00
1.90
9.73
2.67
f1 (ppm)

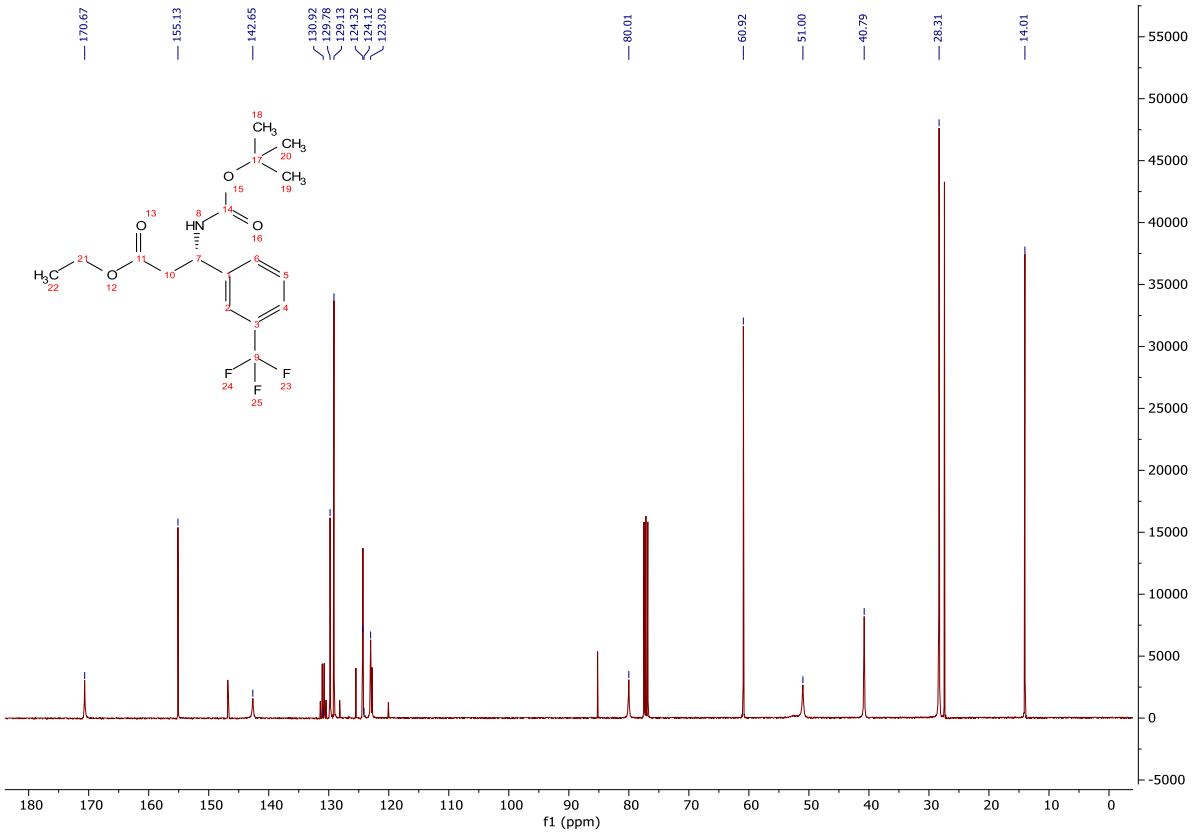
170.67
155.13
142.65
130.92 129.78 129.13 124.32 124.12 123.02
80.01
60.92
51.00
40.79
28.31
14.01
f1 (ppm)

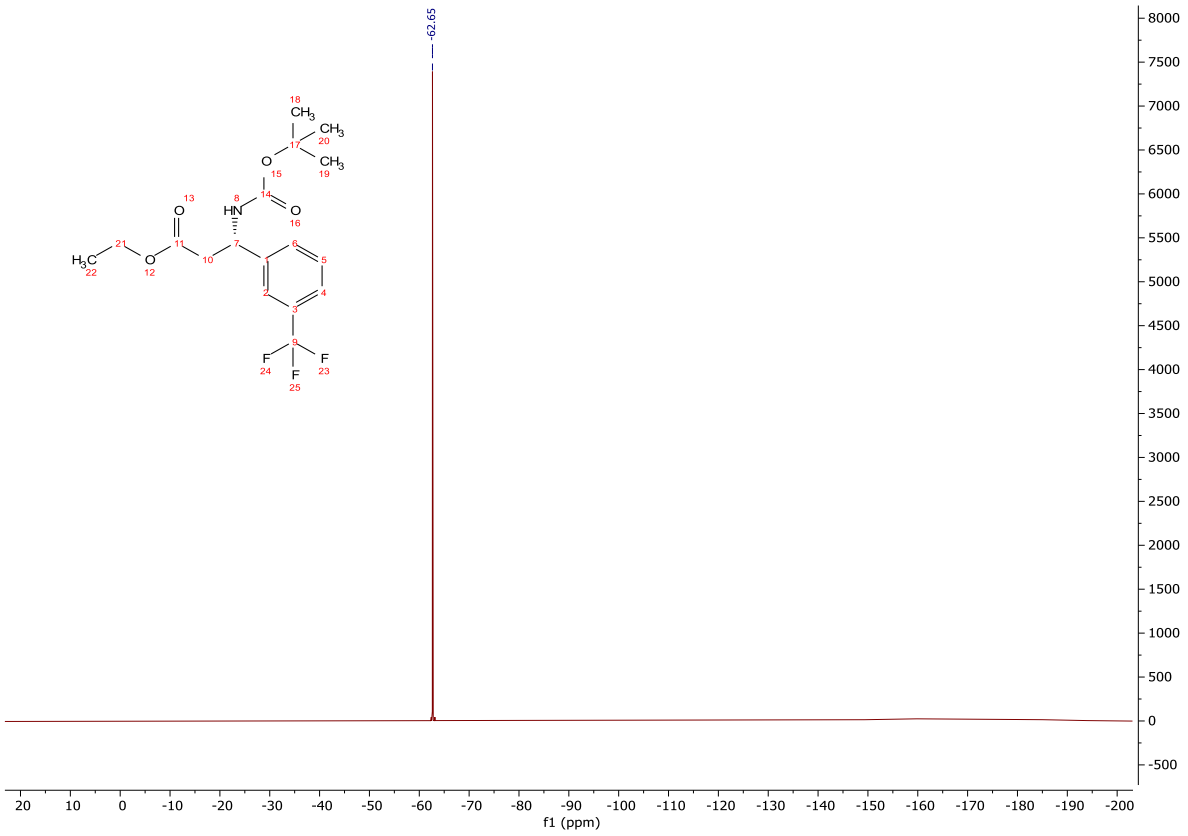
-62.65
8000
7500
7000
6500
6000
5500
5000
4500
4000
3500
3000
2500
2000
1500
1000
500
0
-500
20 10 0 -10 -20 -30 -40 -50 -60 -70 -80 -90 -100 -110 -120 -130 -140 -150 -160 -170 -180 -190 -200
f1 (ppm)

Ethyl (*S*)-3-((*tert*-butoxycarbonyl)amino)-3-(3-(3-chloro-1*H*-pyrazol-1-yl)-5-(trifluoromethyl)phenyl)propanoate (**342**)

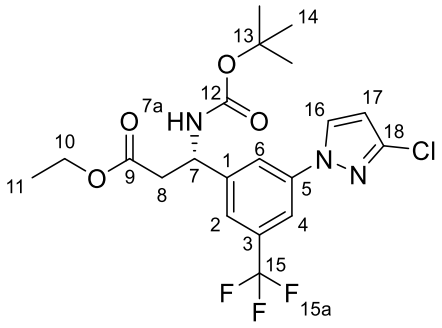

An oven dried microwave vial was charged with a solution of **(*S*)-313** (500 mg, 1.39 mmol) in TBME (5.00 mL), dtbpy (37 mg, 0.139 mmol), B_2Pin_2 (424 mg, 1.67 mmol) and $[Ir(OMe)(cod)]_2$ (46 mg, 0.070 mmol). The vial was sealed and degassed with Ar. The reaction mixture was stirred at 80 °C for 3 h with microwave irradiation. The mixture was cooled to rt, diluted with ethyl acetate (50.0 mL) and washed with 10 % $CuSO_{4(aq)}$ (2 x 50.0 mL). The organic was dried ($MgSO_4$), concentrated *in vacuo*, dissolved in diethyl ether (25.0 mL), filtered through Celite® and concentrated *in vacuo* to give an orange oil. A mixture of the crude product, 5-chloro-1*H*-pyrazole (355 mg, 3.48 mmol), $B(OH)_3$ (172 mg, 2.78 mmol), $Cu(OAc)_2$ (253 mg, 1.39 mmol) and 4 Å molecular sieves (300 mg) in acetonitrile (5.00 mL) was stirred at 70 °C for 16 h. The crude reaction mixture was cooled to rt, diluted with ethyl acetate (50.0 mL) and sat. $NaHCO_{3(aq)}$ (100 mL). The aqueous was extracted with ethyl acetate (2 x 50.0 mL), the organics combined and washed with sat. $NaHCO_{3(aq)}$ (50.0 mL), water (50.0 mL) and brine (50.0 mL). The organic was dried ($MgSO_4$) and concentrated *in vacuo* to give a brown oil. The crude product was purified *via* column chromatography on silica gel, eluting with a gradient of ethyl acetate/light petroleum (0-20%) to give the title compound as a colourless powder (230 mg, 0.499 mmol, 36%); **HRMS** *m/z* (ESI^+) calc. for $C_{20}H_{23}ClF_3N_3NaO_4$ $[M+Na]^+$ requires 484.1221, found 484.1219; $\boldsymbol{R_f}$ 0.45, 15 % ethyl acetate/light petroleum, UV active; δ_H (400 MHz, $CDCl_3$) 7.90 (1H, d, *J* = 2.6 Hz, H-16), 7.83 – 7.78 (2H, m, H-4 and H-6), 7.50 – 7.47 (1H, m, H-2), 6.43 (1H, d, *J* = 2.5 Hz, H-17), 5.72 (1H, s, H-7a), 5.17 (1H, s, H-7), 4.10 (2H, q, *J* = 7.1 Hz, H-10), 2.86

(2H, d, *J* = 6.0 Hz, H-8), 1.43 (9H, s, H-14), 1.18 (3H, t, *J* = 7.1 Hz, H-11); δ_C (126 MHz, $CDCl_3$) 170.6 (CO), 155.1 (CO), 145.0 (C), 142.7 (C), 140.2 (C), 132.6 (C, q, *J* = 33.0 Hz), 128.7 (ArH), 123.6 (CF_3, q, *J* = 272.6 Hz), 121.2 (ArH, q, *J* = 3.6 Hz), 119.9 (ArH), 114.8 (ArH), 108.3 (ArH), 80.5 (C), 61.3 (CH_2), 51.1 (CH), 40.6 (CH_2), 28.4 (CH_3), 14.2 (CH_3); δ_F (376 MHz, $CDCl_3$) -62.8 (F-15a); **MP** 167-170 °C; ν_{max} (FT-ATR/cm^{-1}) 3365, 2988, 1725, 1673, 1611, 1516, 1464, 1379, 1316, 1252, 1124, 757.

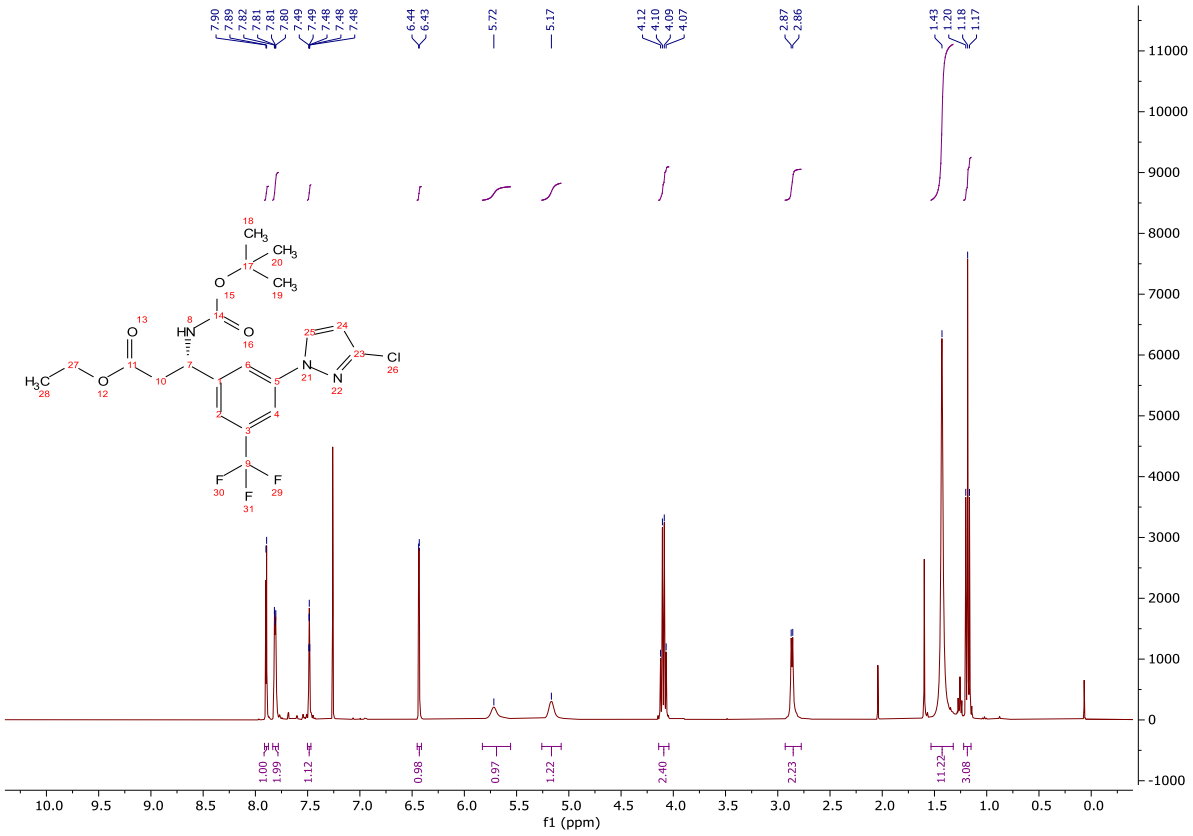
7.90
7.89
7.82
7.81
7.81
7.80
7.49
7.49
7.48
7.48
7.48
6.44
6.43
5.72
5.17
4.12
4.10
4.09
4.07
2.87
2.86
1.43
1.20
1.18
1.17
1.00
1.99
1.12
0.98
0.97
1.22
2.40
2.23
11.22
3.08
f1 (ppm)

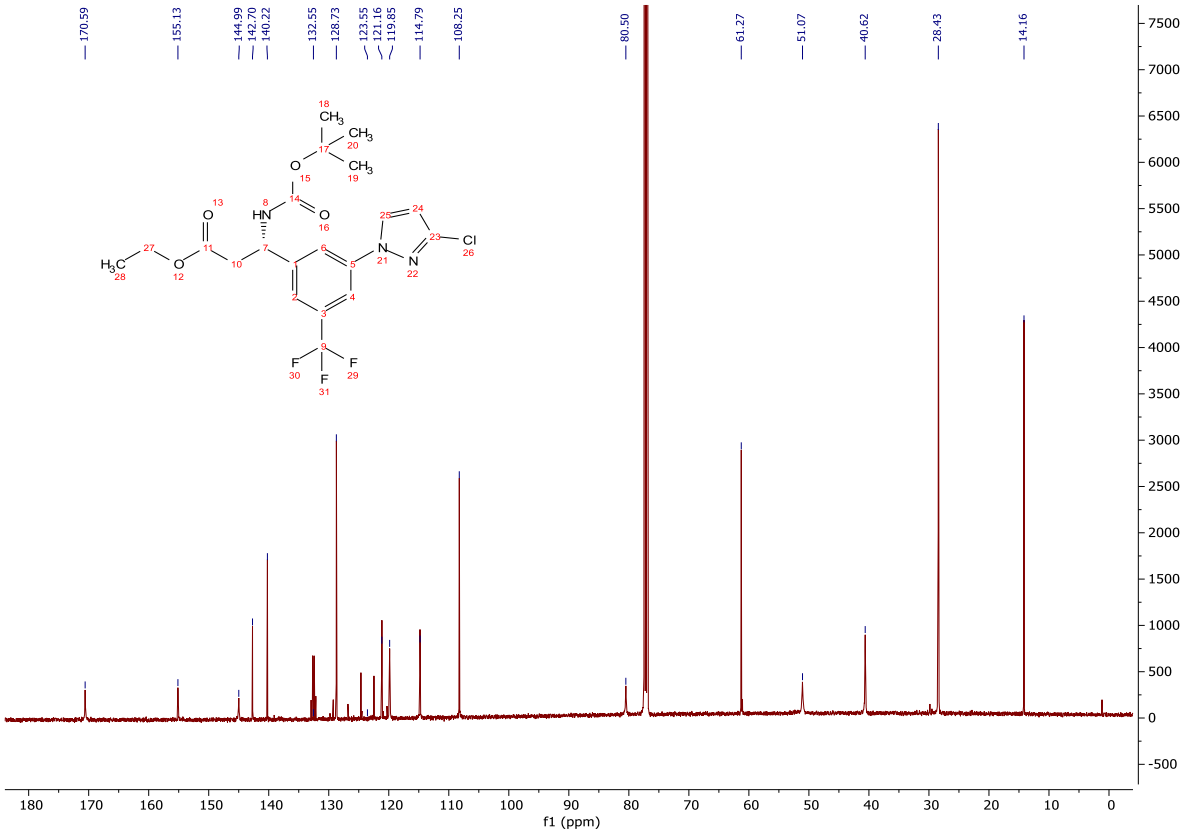
170.59
155.13
144.99
142.70
140.22
132.55
128.73
123.55
121.16
119.85
114.79
108.25
80.50
61.27
51.07
40.62
28.43
14.16
f1 (ppm)

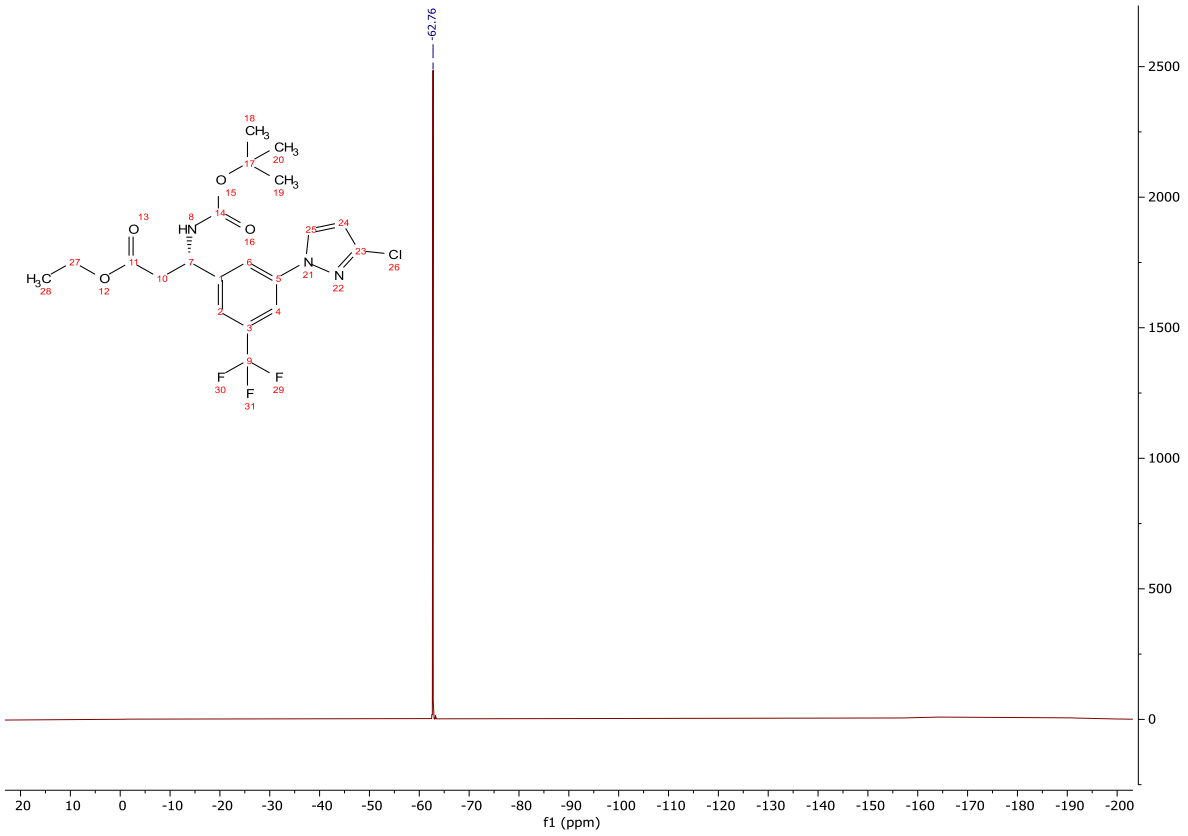
-62.76
2500
2000
1500
1000
500
0
20 10 0 -10 -20 -30 -40 -50 -60 -70 -80 -90 -100 -110 -120 -130 -140 -150 -160 -170 -180 -190 -200
f1 (ppm)

Ethyl (*S*)-3-((*tert*-butoxycarbonyl)amino)-3-(3-(3-isopropyl-1*H*-pyrazol-1-yl)-5-(trifluoromethyl)phenyl)propanoate (**343**)

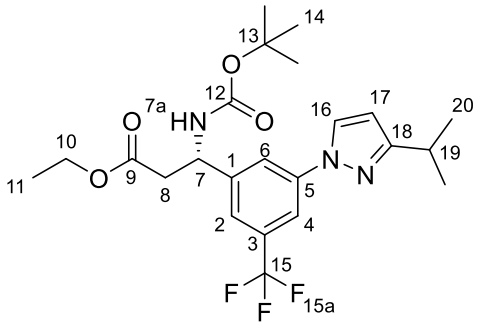

An oven dried microwave vial was charged with a solution of **(*S*)-313** (500 mg, 1.39 mmol) in TBME (5.00 mL), dtbpy (37 mg, 0.139 mmol), B_2Pin_2 (424 mg, 1.67 mmol) and $[Ir(OMe)(cod)]_2$ (46 mg, 0.070 mmol). The vial was sealed and degassed with Ar. The reaction mixture was stirred at 80 °C for 3 h with microwave irradiation. The mixture was cooled to rt, diluted with ethyl acetate (50.0 mL) and washed with 10 % $CuSO_{4(aq)}$ (2 x 50.0 mL). The organic was dried ($MgSO_4$), concentrated *in vacuo*, dissolved in diethyl ether (25.0 mL), filtered through Celite® and concentrated *in vacuo* to give an orange oil. A mixture of the crude product, 5-isopropyl-1*H*-pyrazole (345 mg, 3.48 mmol), $B(OH)_3$ (172 mg, 2.78 mmol), $Cu(OAc)_2$ (253 mg, 1.39 mmol) and 4 Å molecular sieves (300 mg) in acetonitrile (5.00 mL) was stirred at 70 °C for 16 h. The crude reaction mixture was cooled to rt, diluted with ethyl acetate (50.0 mL) and sat. $NaHCO_{3(aq)}$ (100 mL). The aqueous was extracted with ethyl acetate (2 x 50.0 mL), the organics combined and washed with sat. $NaHCO_{3(aq)}$ (50.0 mL), water (50.0 mL) and brine (50.0 mL). The organic was dried ($MgSO_4$) and concentrated *in vacuo* to give a brown oil. The crude product was purified *via* column chromatography on silica gel, eluting with a gradient of ethyl acetate/light petroleum (0-25%) to give the title compound as a colourless solid (437 mg, 0.932 mmol, 67%); **HRMS** *m/z* (ESI^+) calc. for $C_{23}H_{31}F_3N_3O_4$ $[M+H]^+$ requires 470.2261, found 470.2250; $\boldsymbol{R}_f$ 0.29, 15 % ethyl acetate/light petroleum, UV active; δ_H (400 MHz, $CDCl_3$) 7.87 – 7.77 (3H, m, H-4, H-6 and H-16), 7.43 – 7.37 (1H, m, H-2), 6.31 (1H, d, *J* = 2.5 Hz, H-17), 5.73 (1H, bs, H-7a), 5.17 (1H, bs, H-7), 4.09 (2H, q, *J* = 7.2 Hz, H-10), 3.07 (1H, hept, *J* = 6.9 Hz, H-

19), 2.93 – 2.74 (2H, m, H-8), 1.42 (9H, s, H-14), 1.31 (6H, d, *J* = 7.1 Hz, H-20), 1.17 (3H, t, *J* = 7.2 Hz, H-11); δ_C (101 MHz, $CDCl_3$) 170.7 (CO), 161.9 (C), 155.1 (CO), 144.5 (C), 141.1 (C), 132.2 (C, q, *J* = 32.8 Hz), 127.3 (ArH), 123.8 (CF_3, q, *J* = 272.7 Hz), 120.0 (ArH, q, *J* = 3.8 Hz), 119.8 (ArH), 114.7 (ArH), 105.6 (ArH), 80.3 (C), 61.1 (CH_2), 51.1 (CH), 40.7 (CH_2), 28.4 (CH_3), 28.2 (CH), 22.8 (CH_3), 14.1 (CH_3); δ_F (376 MHz, $CDCl_3$) -62.7 (F-15a); **MP** 117-120 °C; ν_{max} (FT-ATR/cm^{-1}) 3371, 2981, 1724, 1681, 1524, 1329, 1249, 1160, 1115, 1028, 705, 608.

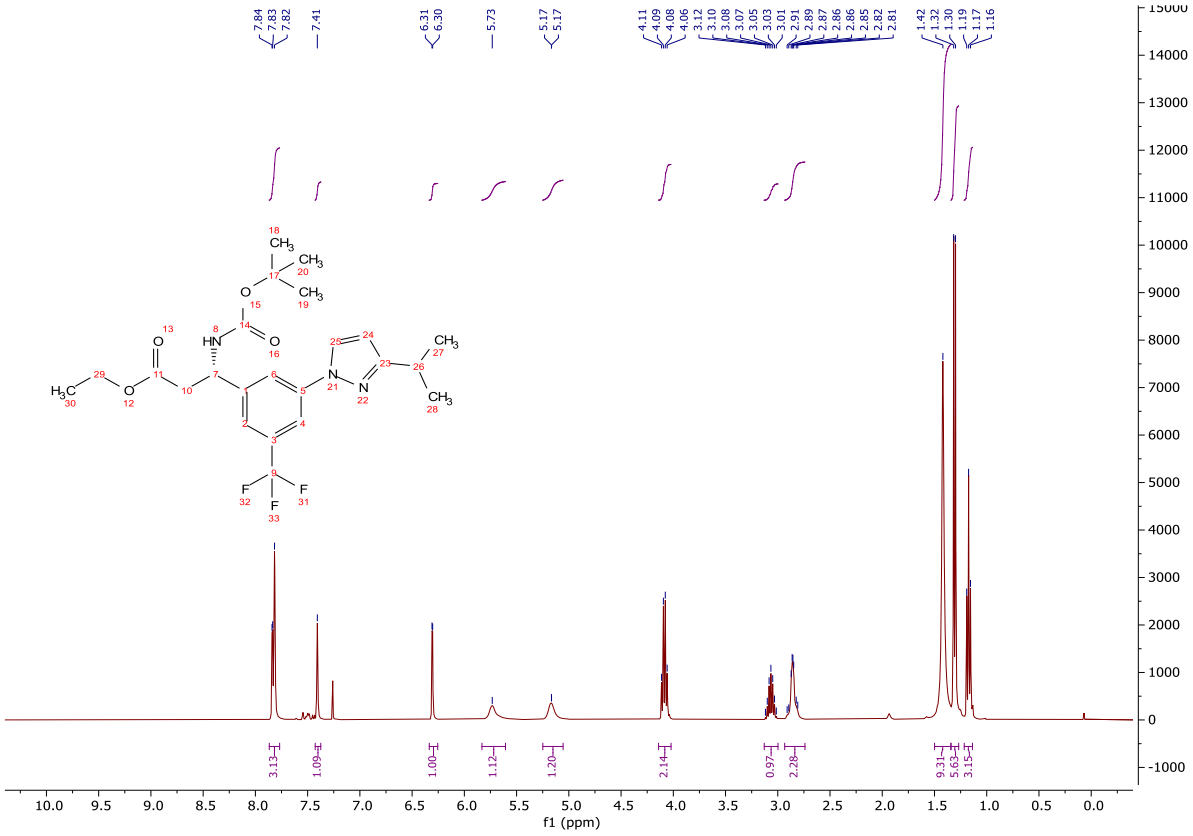
7.84
7.83
7.82
7.41
6.31
6.30
5.73
5.17
5.17
4.11
4.09
4.08
4.06
3.12
3.10
3.08
3.07
3.05
3.03
3.01
2.91
2.89
2.87
2.86
2.86
2.85
2.82
2.81
1.42
1.32
1.30
1.19
1.17
1.16
3.13
1.09
1.00
1.12
1.20
2.14
0.97
2.28
9.31
5.63
3.15
f1 (ppm)

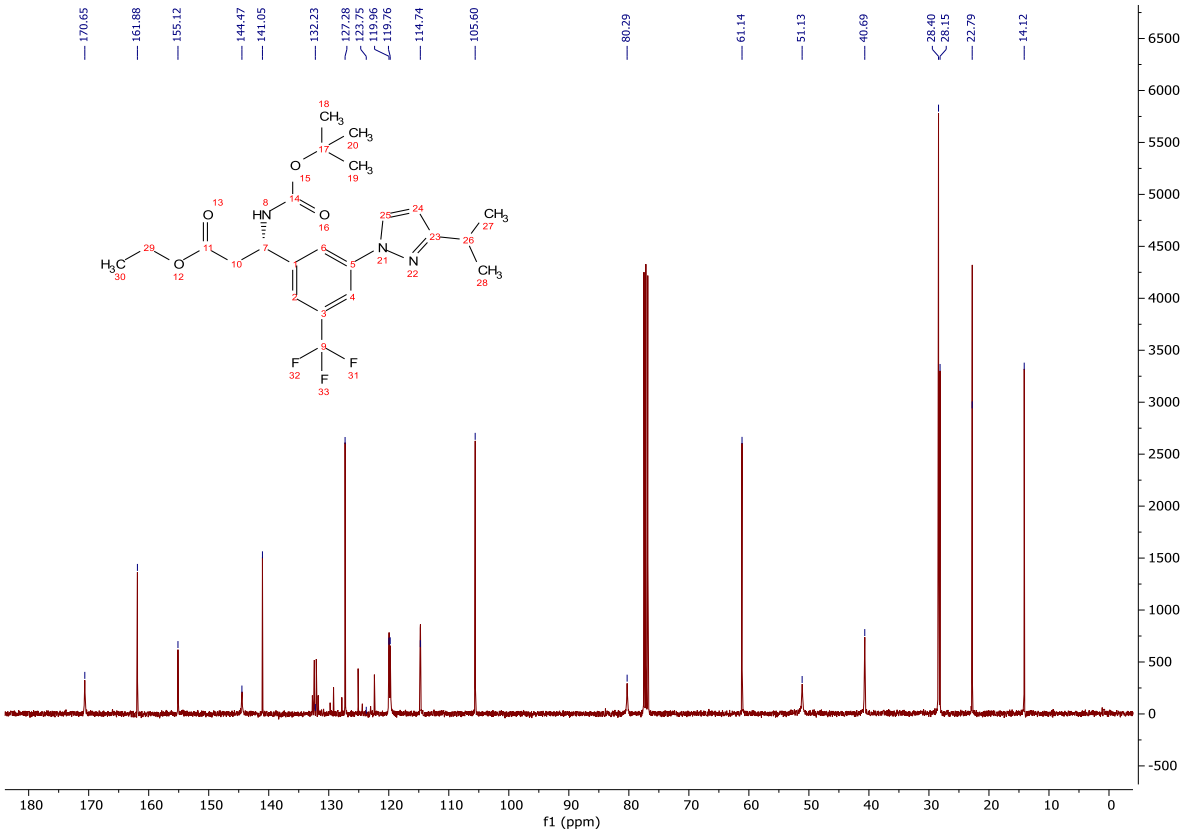
170.65
161.88
155.12
144.47
141.05
132.23
127.28
123.75
119.96
119.76
114.74
105.60
80.29
61.14
51.13
40.69
28.40
28.15
22.79
14.12
f1 (ppm)

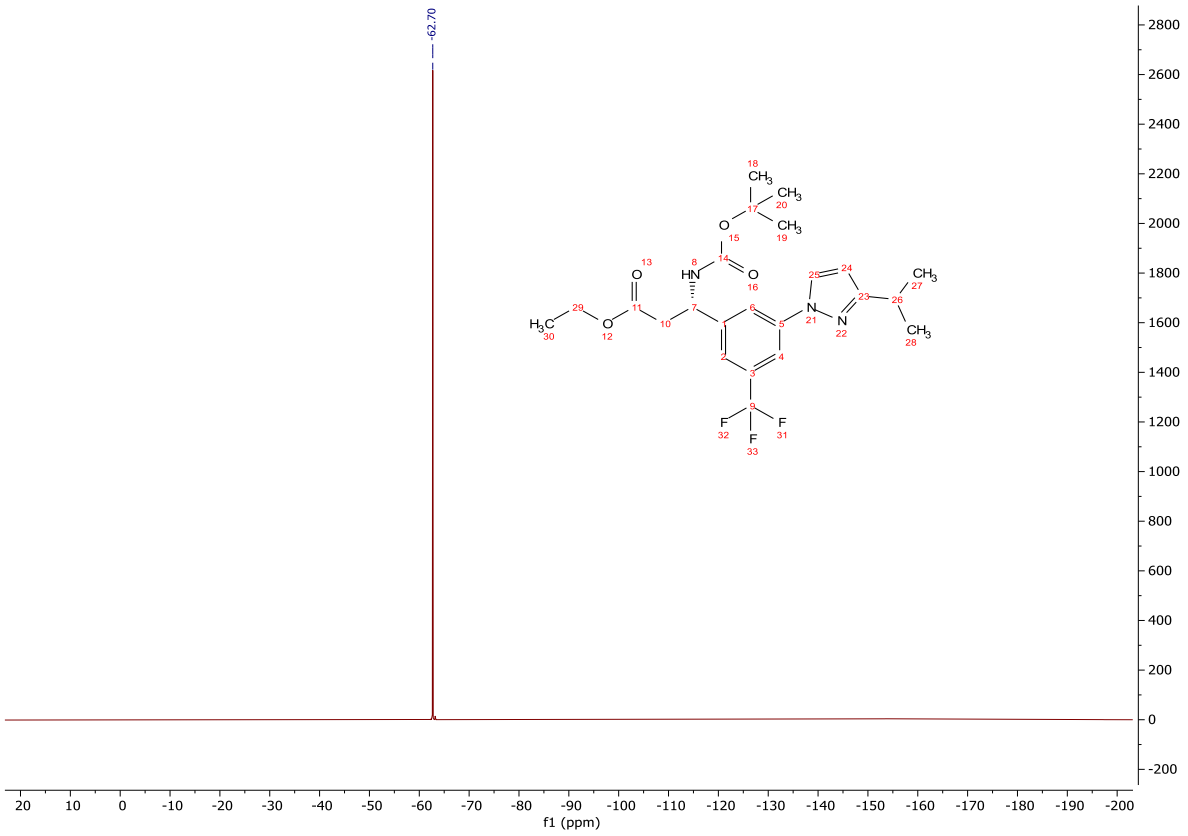
-62.70
2800
2600
2400
2200
2000
1800
1600
1400
1200
1000
800
600
400
200
0
-200
20 10 0 -10 -20 -30 -40 -50 -60 -70 -80 -90 -100 -110 -120 -130 -140 -150 -160 -170 -180 -190 -200
f1 (ppm)

Ethyl (*S*)-3-((*tert*-butoxycarbonyl)amino)-3-(3-(3-chloro-1*H*-pyrazol-1-yl)-5-cyclopropylphenyl)propanoate (**344**)

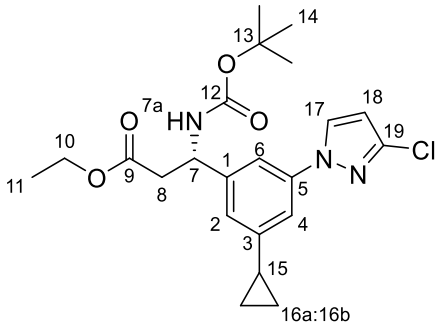

An oven dried microwave vial was charged with a solution of **250** (500 mg, 1.50 mmol) in TBME (5.00 mL), dtbpy (40 mg, 0.150 mmol), B_2Pin_2 (457 mg, 1.80 mmol) and $[Ir(OMe)(cod)]_2$ (50 mg, 0.075 mmol). The vial was sealed and degassed with Ar. The reaction mixture was stirred at 80 °C for 3 h with microwave irradiation. The mixture was cooled to rt, diluted with ethyl acetate (50.0 mL) and washed with 10 % $CuSO_{4(aq)}$ (2 x 50.0 mL). The organic was dried ($MgSO_4$), concentrated *in vacuo*, dissolved in diethyl ether (25.0 mL), filtered through Celite® and concentrated *in vacuo* to give an orange oil. A mixture of the crude product, 5-chloro-1*H*-pyrazole (383 mg, 3.75 mmol), $B(OH)_3$ (186 mg, 3.00 mmol), $Cu(OAc)_2$ (273 mg, 1.50 mmol) and 4 Å molecular sieves (300 mg) in acetonitrile (5.00 mL) was stirred at 70 °C for 16 h. The crude reaction mixture was cooled to rt, diluted with ethyl acetate (50.0 mL) and sat. $NaHCO_{3(aq)}$ (100 mL). The aqueous was extracted with ethyl acetate (2 x 50.0 mL), the organics combined and washed with sat. $NaHCO_{3(aq)}$ (50.0 mL), water (50.0 mL) and brine (50.0 mL). The organic was dried ($MgSO_4$) and concentrated *in vacuo* to give a brown oil. The crude product was purified *via* column chromatography on silica gel, eluting with a gradient of ethyl acetate/light petroleum (0-20%) to give the title compound as a colourless, amorphous solid (193 mg, 0.446 mmol, 30%); **HRMS** *m/z* (ESI^+) calc. for $C_{22}H_{28}ClN_3NaO_4$ $[M+Na]^+$ requires 456.1661, found 456.1660; $\boldsymbol{R}_f$ 0.24, 15 % ethyl acetate/light petroleum, UV active; δ_H (500 MHz, $CDCl_3$) 7.81 (1H, d, *J* = 2.5 Hz, H-17), 7.33 (1H, dd, *J* = 1.9, 1.9 Hz, H-4), 7.23 (1H, dd, *J* = 2.0, 2.0 Hz, H-6), 6.95 (1H, dd, *J* = 1.6, 1.6 Hz, H-2), 6.37 (1H, d, *J* = 2.4 Hz, H-18), 5.52 (1H, bs,

H-7a), 5.08 (1H, bs, H-7), 4.08 (2H, q, *J* = 7.1 Hz, H-10), 2.92 – 2.72 (2H, m, H-8), 1.98 – 1.83 (1H, m, H-15), 1.42 (9H, s, H-14), 1.18 (3H, t, *J* = 7.1 Hz, H-11), 1.04 – 0.96 (2H, m, H-16a), 0.78 – 0.67 (2H, m, H-16b); δ_C (126 MHz, $CDCl_3$) 170.9 (CO), 155.2 (CO), 146.6 (C), 143.2 (C), 141.6 (C), 140.1 (C), 128.7 (ArH), 122.5 (ArH), 115.6 (ArH), 114.0 (ArH), 107.2 (ArH), 83.9 (C), 61.0 (CH_2), 51.4 (CH), 41.1 (CH_2), 28.5 (CH_3), 15.8 (CH), 14.2 (CH_3), 9.6 (CH_2); **MP** Becomes waxy at 96 °C, fully melts at 108 °C; ν_{max} (FT-ATR/cm^{-1}) 3369, 2981, 1724, 1687, 1601, 1508, 1418, 1366, 1244, 1161, 1047, 885, 754, 654.

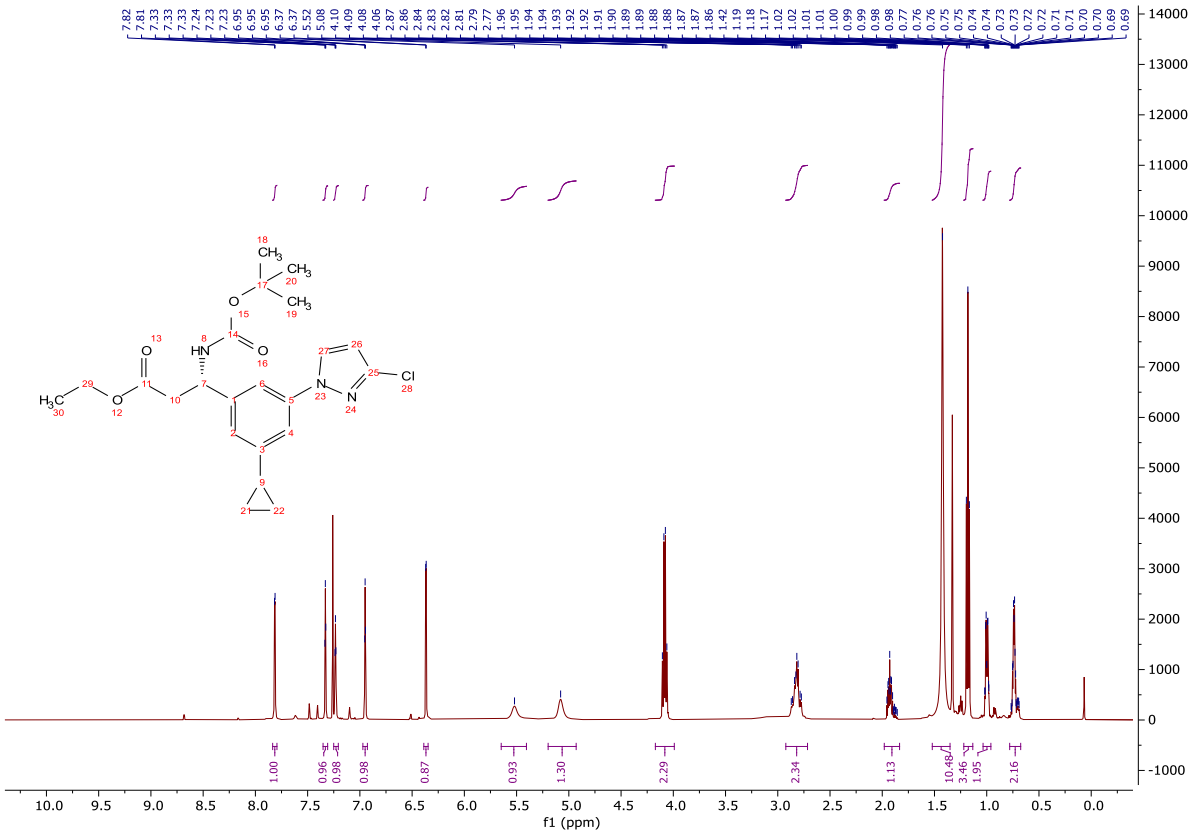
f1 (ppm)

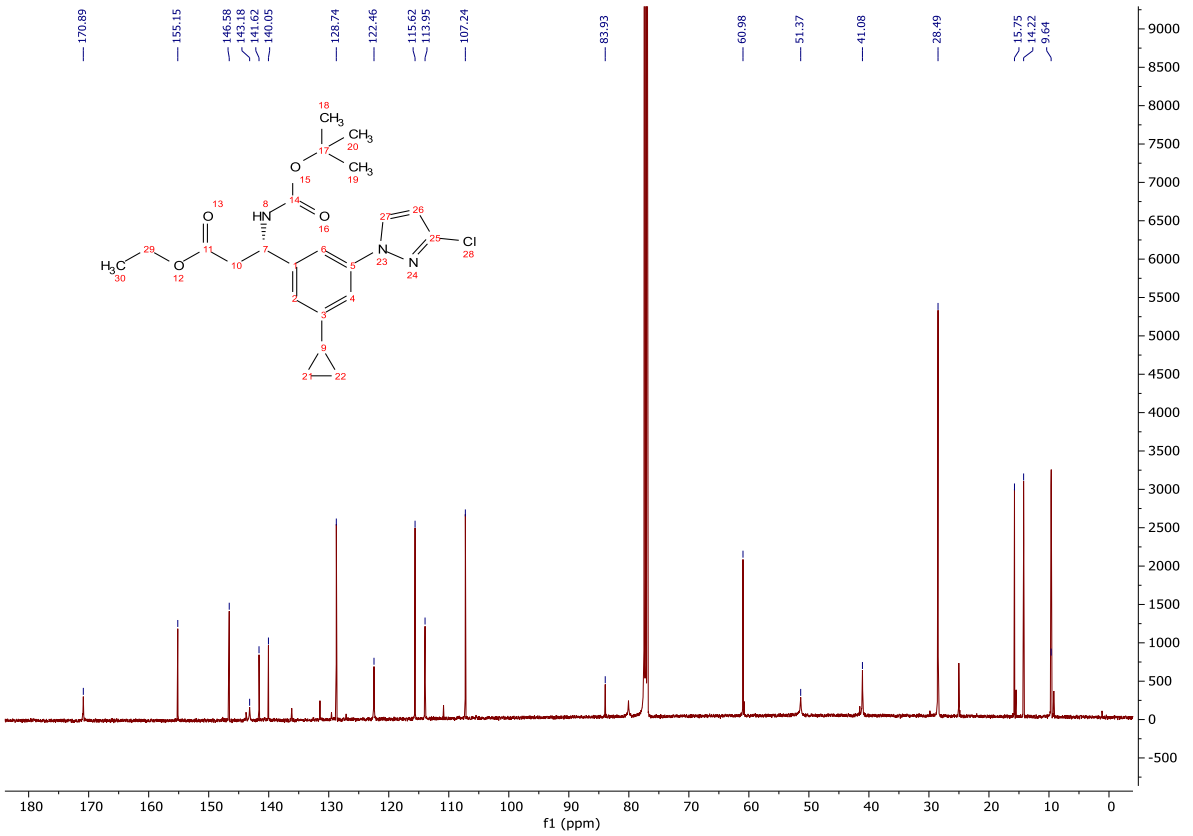
f1 (ppm)

Ethyl (*S*)-3-((*tert*-butoxycarbonyl)amino)-3-(3-cyclopropyl-5-(3-isopropyl-1*H*-pyrazol-1-yl)phenyl)propanoate (**345**)

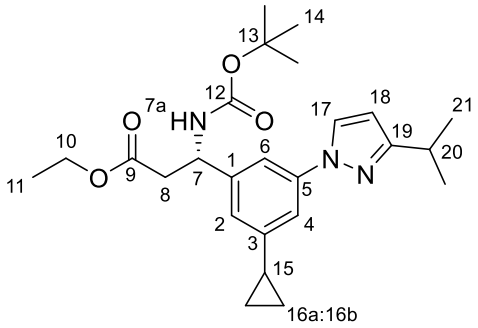

An oven dried microwave vial was charged with a solution of **250** (500 mg, 1.50 mmol) in TBME (5.00 mL), dtbpy (40 mg, 0.150 mmol), B_2Pin_2 (457 mg, 1.80 mmol) and $[Ir(OMe)(cod)]_2$ (50 mg, 0.075 mmol). The vial was sealed and degassed with Ar. The reaction mixture was stirred at 80 °C for 3 h with microwave irradiation. The mixture was cooled to rt, diluted with ethyl acetate (50.0 mL) and washed with 10 % $CuSO_{4(aq)}$ (2 x 50.0 mL). The organic was dried ($MgSO_4$), concentrated *in vacuo*, dissolved in diethyl ether (25.0 mL), filtered through Celite® and concentrated *in vacuo* to give an orange oil. A mixture of the crude product, 5-isopropyl-1*H*-pyrazole (413 mg, 3.75 mmol), $B(OH)_3$ (186 mg, 3.00 mmol), $Cu(OAc)_2$ (273 mg, 1.50 mmol) and 4 Å molecular sieves (300 mg) in acetonitrile (5.00 mL) was stirred at 70 °C for 16 h. The crude reaction mixture was cooled to rt, diluted with ethyl acetate (50.0 mL) and sat. $NaHCO_{3(aq)}$ (100 mL). The aqueous was extracted with ethyl acetate (2 x 50.0 mL), the organics combined and washed with sat. $NaHCO_{3(aq)}$ (50.0 mL), water (50.0 mL) and brine (50.0 mL). The organic was dried ($MgSO_4$) and concentrated *in vacuo* to give a brown oil. The crude product was purified *via* column chromatography on silica gel, eluting with a gradient of ethyl acetate/light petroleum (0-25%) to give the title compound as a colourless solid (470 mg, 1.07 mmol, 71%); **HRMS** *m/z* (ESI^+) calc. for $C_{25}H_{36}N_3O_4$ $[M+H]^+$ requires 442.2700, found 442.2700; $\boldsymbol{R_f}$ 0.48, 20 % ethyl acetate/light petroleum, UV active; δ_H (400 MHz, $CDCl_3$) 7.76 (1H, d, *J* = 2.5 Hz, H-17), 7.38 – 7.31 (1H, m, H-4), 7.28 – 7.20 (1H, m, H-6), 6.91 – 6.81 (1H, m, H-2), 6.25 (1H, d, *J* = 2.5 Hz, H-18), 5.52 (1H, bs, H-7a), 5.08 (1H, bs, H-7), 4.07 (2H, q, *J* =

7.1 Hz, H-10), 3.07 (1H, hept, *J* = 6.9 Hz, H-20), 2.95 – 2.69 (2H, m, H-8), 1.92 (1H, tt, *J* = 8.6, 4.3 Hz, H-15), 1.42 (9H, s, H-14), 1.30 (6H, d, *J* = 7.0 Hz, H-21), 1.17 (3H, t, *J* = 7.1 Hz, H-11), 1.01 – 0.90 (2H, m, H-16a), 0.78 – 0.67 (2H, m, H-16b); δ_C (101 MHz, $CDCl_3$) 170.9 (CO), 161.0 (C), 155.1 (CO), 146.1 (C), 142.8 (C), 140.7 (C), 127.3 (ArH), 121.3 (ArH), 115.8 (ArH), 114.1 (ArH), 104.4 (ArH), 79.8 (C), 60.8 (CH_2), 51.4 (CH), 41.1 (CH_2), 28.4 (CH_3), 28.1 (CH), 23.0 (CH_3), 15.7 (CH), 14.2 (CH_3), 9.4 (CH_2); **MP** 97-100 °C; ν_{max} (FT-ATR/cm^{-1}) 3370, 2962, 1726, 1685, 1602, 1517, 1367, 1292, 1235, 1154, 1013, 925, 859, 757, 700, 618.

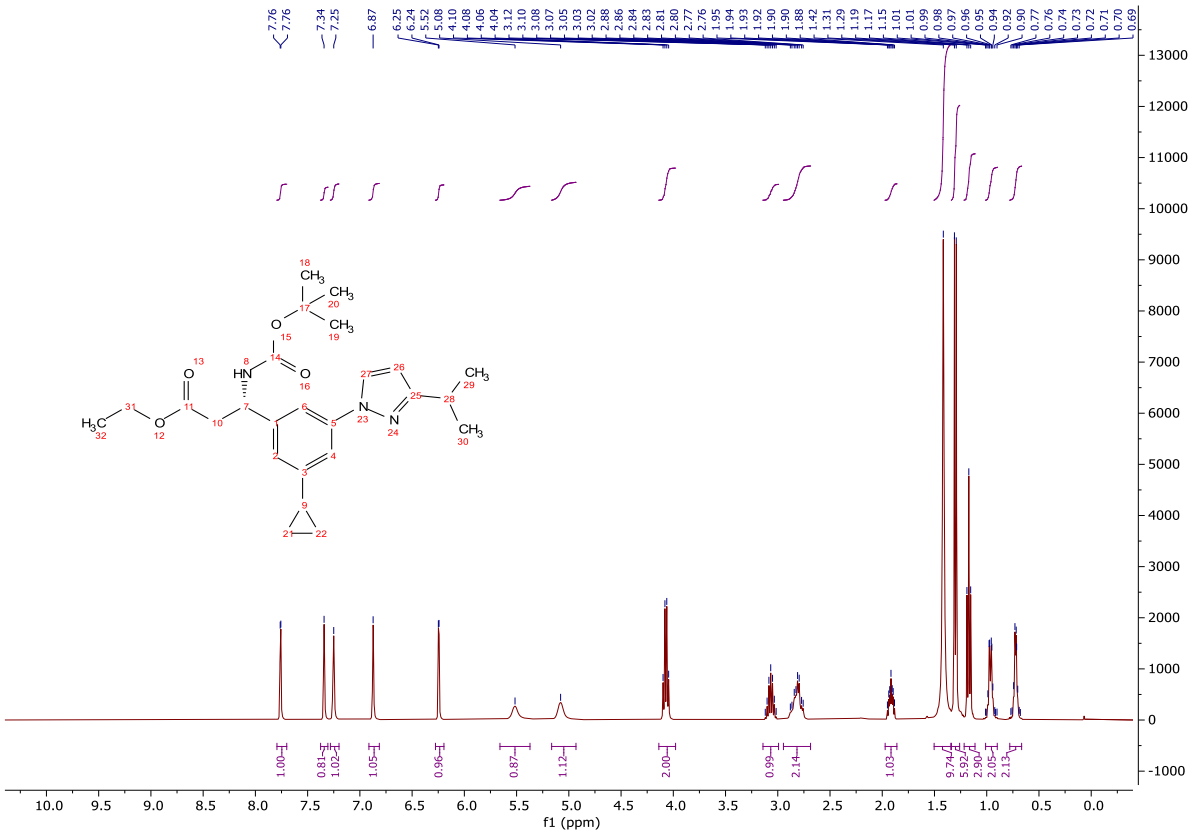
7.76
7.76
7.34
7.25
6.87
6.25
6.24
5.52
5.08
4.10
4.08
4.06
4.04
3.12
3.10
3.08
3.07
3.05
3.03
3.02
2.88
2.86
2.84
2.83
2.81
2.80
2.77
2.76
1.95
1.94
1.93
1.92
1.90
1.90
1.88
1.42
1.31
1.29
1.19
1.17
1.15
1.01
1.01
0.99
0.98
0.97
0.96
0.95
0.94
0.92
0.90
0.77
0.76
0.74
0.73
0.72
0.71
0.70
0.69
1.00
0.81
1.02
1.05
0.96
0.87
1.12
2.00
0.99
2.14
1.03
9.74
5.92
2.90
2.05
2.13
f1 (ppm)

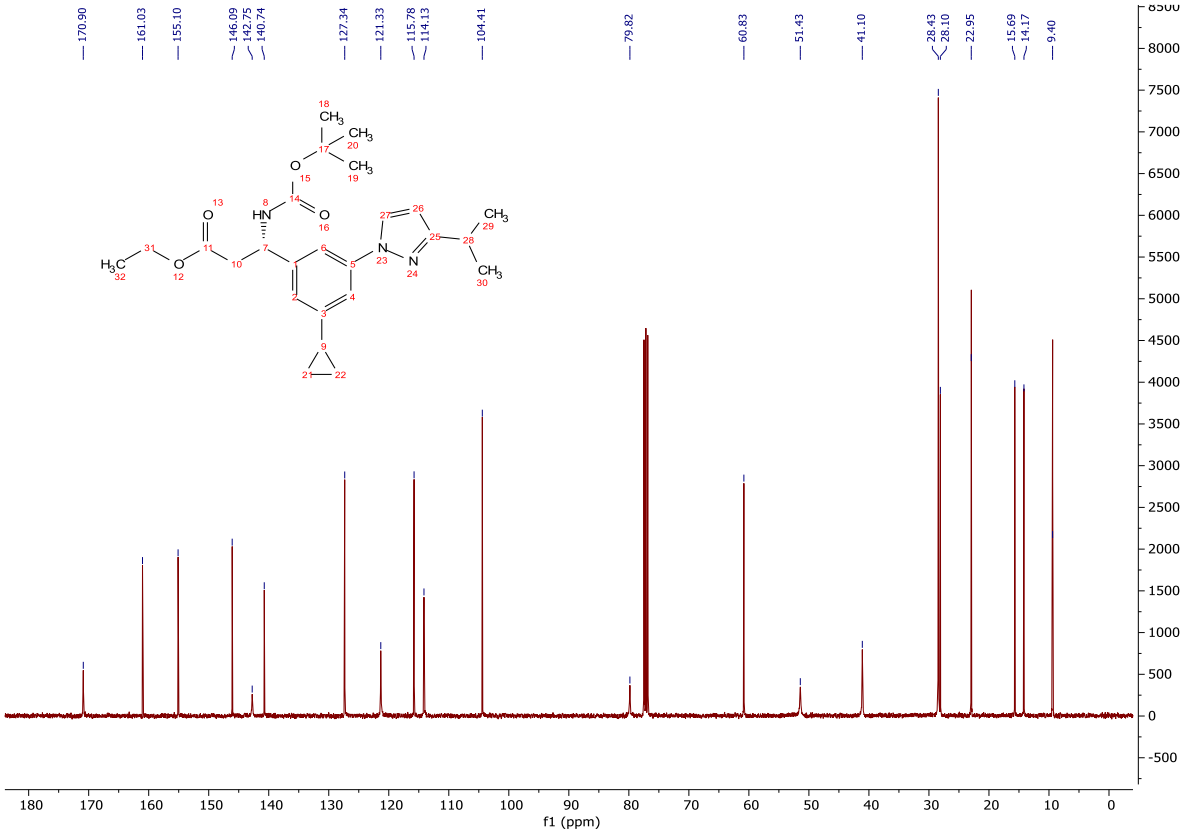
170.90
161.03
155.10
146.09
142.75
140.74
127.34
121.33
115.78
114.13
104.41
79.82
60.83
51.43
41.10
28.43
28.10
22.95
15.69
14.17
9.40
f1 (ppm)

Ethyl (*S*)-3-((*tert*-butoxycarbonyl)amino)-3-(3-(2,2-difluoroethoxy)-5-(3,5-dimethyl-1*H*-pyrazol-1-yl)phenyl)propanoate (**346**)

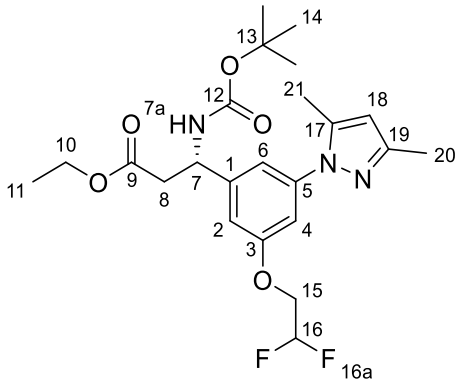

A mixture of **341** (135 mg, 0.271 mmol), 3,5-dimethyl pyrazole (65 mg, 0.678 mmol), $B(OH)_3$ (34 mg, 0.542 mmol), $Cu(OAc)_2$ (50 mg, 0.271 mmol) and 4 Å molecular sieves (200 mg) in acetonitrile (1.00 mL) was stirred at 70 °C for 16 h. The crude reaction mixture was cooled to rt, diluted with ethyl acetate (50.0 mL) and sat. $NaHCO_{3(aq)}$ (60.0 mL). The aqueous was extracted with ethyl acetate (2 x 20.0 mL), the organics combined and washed with sat. $NaHCO_{3(aq)}$ (30.0 mL), water (30.0 mL) and brine (30.0 mL). The organic was dried ($MgSO_4$) and concentrated *in vacuo* to give a brown oil. The crude product was purified *via* column chromatography on silica gel, eluting with a gradient of ethyl acetate/light petroleum (0-50%) to give the title compound as a clear, colourless oil (120 mg, 0.257 mmol, 95%); **HRMS** *m/z* (ESI^+) calc. for $C_{23}H_{32}F_2N_3O_5$ $[M+H]^+$ requires 468.2305, found 468.2298; $\boldsymbol{R_f}$ 0.23, 25 % ethyl acetate/light petroleum, UV active; δ_H (400 MHz, $CDCl_3$) 7.03 – 6.99 (1H, m, H-6), 6.92 (1H, dd, *J* = 2.1, 2.1 Hz, H-2), 6.89 – 6.85 (1H, m, H-4), 6.23 – 5.92 (2H, m, H-16 and H-18), 5.58 (1H, bs, H-7a), 5.09 (1H, bs, H-7), 4.20 (2H, td, *J* = 13.0, 4.1 Hz, H-15), 4.13 – 4.03 (2H, m, H-10), 2.90 – 2.76 (2H, m, H-8), 2.32 – 2.25 (6H, m, H-20 and H-21), 1.42 (9H, s, H14), 1.22 – 1.15 (3H, m, H-11); δ_C (101 MHz, $CDCl_3$) 170.9 (CO), 158.4 (C), 155.1 (CO), 149.4 (C), 144.2 (C), 141.4 (C), 139.7 (C), 115.8 (ArH), 113.6 (CHF_2, t, *J* = 241.1 Hz), 112.1 (ArH), 109.9 (ArH), 107.6 (ArH), 80.1 (C), 67.6 (CH_2, t, *J* = 29.7 Hz), 61.0 (CH_2), 51.0 (CH), 40.7 (CH_2), 28.5 (CH_3), 14.2

(CH_3), 13.6 (CH_3), 12.7 (CH_3); δ_F (376 MHz, $CDCl_3$) -125.3 (F-16a); ν_{max} (FT-ATR/cm^{-1}) 3355, 2977, 1726, 1686, 1601, 1515, 1450, 1367, 1286, 1247, 1161, 1129, 1064, 851, 782, 700, 585.

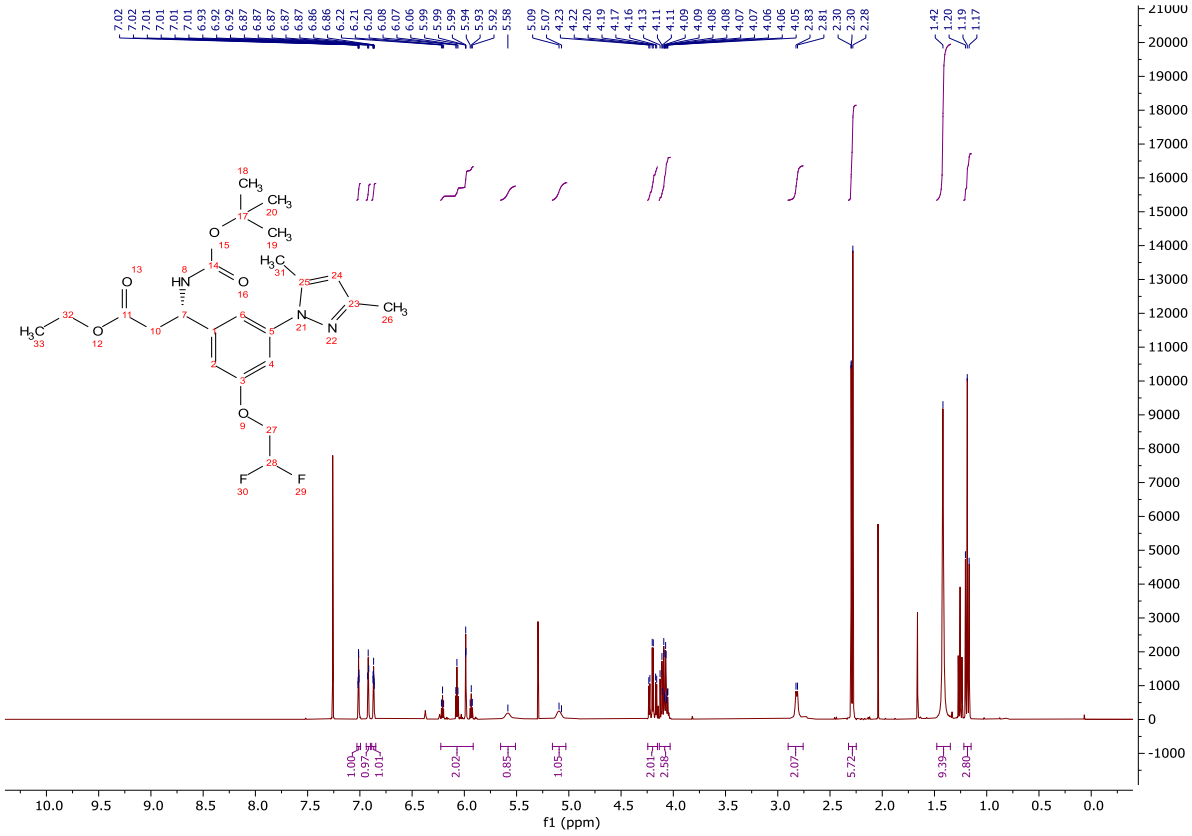
7.02 7.02 7.01 7.01 7.01 6.93 6.92 6.92 6.87 6.87 6.87 6.87 6.87 6.86 6.86 6.22 6.21 6.20 6.08 6.07 6.06 5.99 5.99 5.99 5.94 5.93 5.92 5.58
5.09 5.07 4.23 4.22 4.20 4.19 4.17 4.16 4.13 4.11 4.11 4.09 4.09 4.08 4.08 4.07 4.07 4.06 4.06 4.05 2.83 2.81 2.30 2.30 2.28
1.42 1.20 1.19 1.17
1.00 0.97 1.01 2.02 0.85 1.05 2.01 2.58 2.07 5.72 9.39 2.80
f1 (ppm)

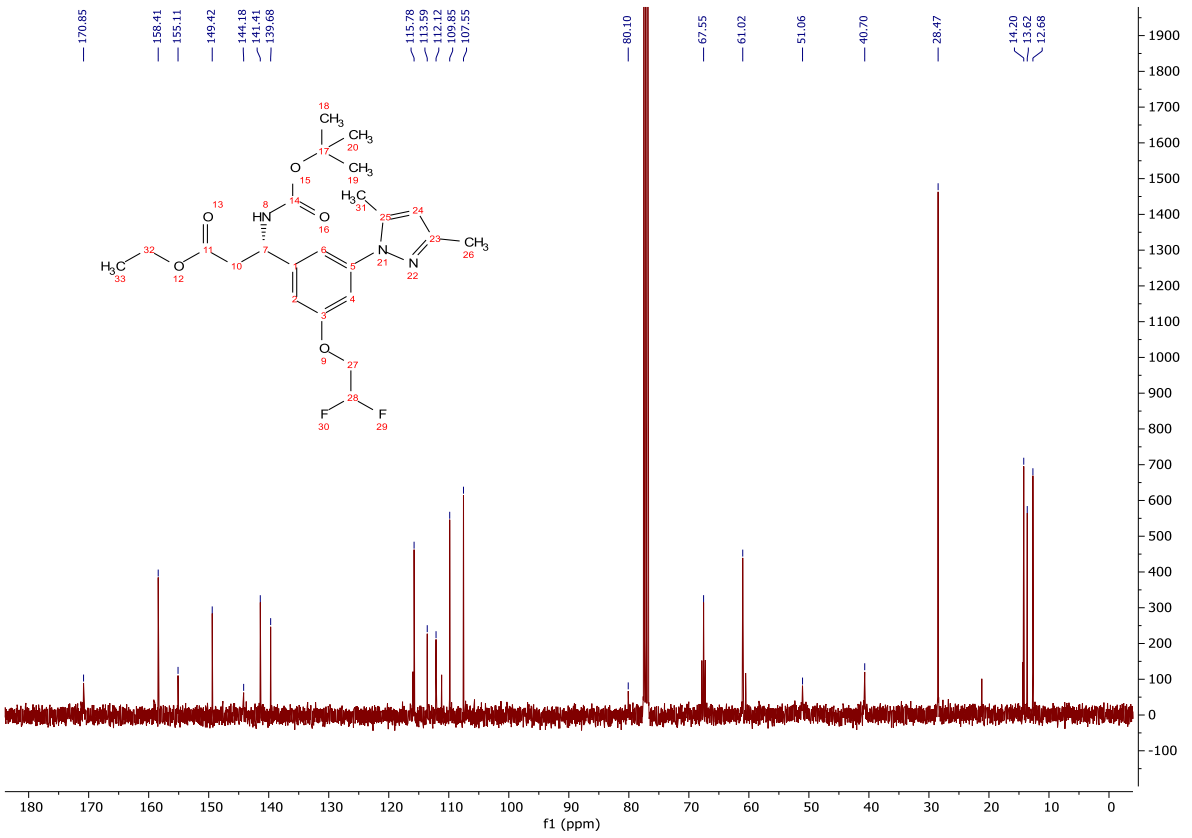
170.85 158.41 155.11 149.42 144.18 141.41 139.68 115.78 113.59 112.12 109.85 107.55 80.10 67.55 61.02 51.06 40.70 28.47 14.20 13.62 12.68
f1 (ppm)

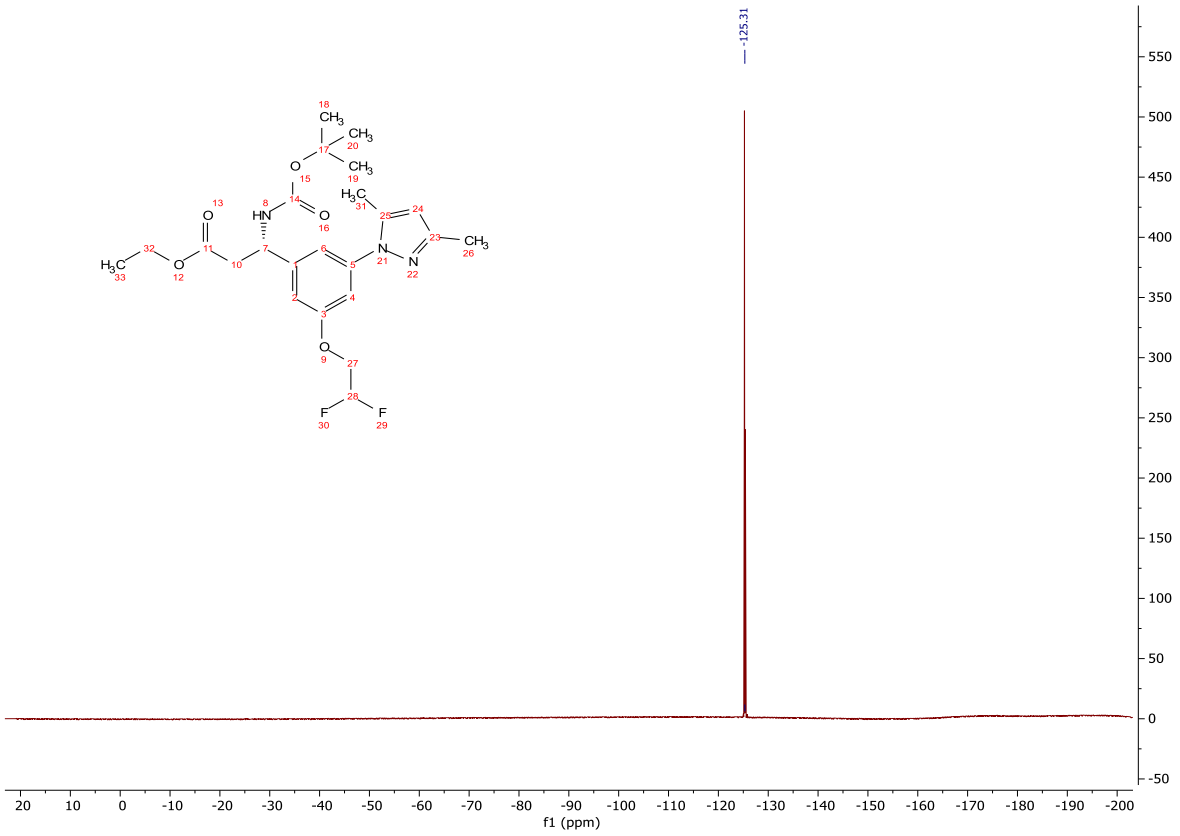
-125.31
550
500
450
400
350
300
250
200
150
100
50
0
-50
20 10 0 -10 -20 -30 -40 -50 -60 -70 -80 -90 -100 -110 -120 -130 -140 -150 -160 -170 -180 -190 -200
f1 (ppm)

Ethyl (*S*)-3-((*tert*-butoxycarbonyl)amino)-3-(3-(2,2-difluoroethoxy)-5-(3-isopropyl-1*H*-pyrazol-1-yl)phenyl)propanoate (**347**)

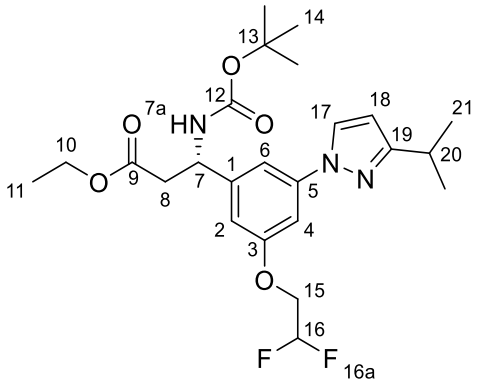

A mixture of **341** (135 mg, 0.271 mmol), 5-isopropyl pyrazole (75 mg, 0.678 mmol), $B(OH)_3$ (34 mg, 0.542 mmol), $Cu(OAc)_2$ (50 mg, 0.271 mg) and 4 Å molecular sieves (200 mg) in acetonitrile (1.00 mL) was stirred at 70 °C for 16 h. The crude reaction mixture was cooled to rt, diluted with ethyl acetate (50.0 mL) and sat. $NaHCO_{3(aq)}$ (60.0 mL). The aqueous was extracted with ethyl acetate (2 x 20.0 mL), the organics combined and washed with sat. $NaHCO_{3(aq)}$ (30.0 mL), water (30.0 mL) and brine (30.0 mL). The organic was dried ($MgSO_4$) and concentrated *in vacuo* to give a brown oil. The crude product was purified *via* column chromatography on silica gel, eluting with a gradient of ethyl acetate/light petroleum (0-30%) to give the title compound as a colourless solid (80 mg, 0.166 mmol, 61%); **HRMS** *m/z* (ESI^+) calc. for $C_{24}H_{34}F_2N_3O_5$ $[M+H]^+$ requires 482.2461, found 482.2453; $\boldsymbol{R_f}$ 0.22, 15 % ethyl acetate/light petroleum, UV active; δ_H (400 MHz, $CDCl_3$) 7.78 (1H, d, *J* = 2.5 Hz, H-17), 7.22 (1H, dd, *J* = 1.7, 1.7 Hz, H-4), 7.19 (1H, dd, *J* = 2.2, 2.2 Hz, H-6), 6.75 (1H, dd, *J* = 2.0, 2.0 Hz, H-2), 6.28 (1H, d, *J* = 2.5 Hz, H-18), 6.09 (1H, tt, *J* = 55.1, 4.1 Hz, H-16), 5.56 (1H, bs, H-7a), 5.09 (1H, bs, H-7), 4.24 (2H, td, *J* = 13.0, 4.1 Hz, H-15), 4.09 (2H, q, *J* = 7.1 Hz, H-10), 3.07 (1H, hept, *J* = 6.9 Hz, H-19), 2.93 – 2.74 (2H, m, H-8), 1.43 (9H, s, H-14), 1.31 (6H, d, *J* = 6.9 Hz, H-21), 1.19 (3H, t, *J* = 7.1 Hz, H-11); δ_C (101 MHz, $CDCl_3$) 171.0 (CO), 161.4 (C), 158.8 (C), 155.1 (CO), 144.7 (C), 141.9 (C), 127.4 (ArH), 113.6 (CHF_2, t, *J* = 241.1 Hz), 110.2 (ArH), 110.1 (ArH), 105.0 (ArH), 104.6 (ArH), 80.1 (C), 67.5 (CH_2, t, *J* = 29.6 Hz), 61.0 (CH_2), 51.3 (CH), 40.9 (CH_2), 28.5

(CH_3), 28.2 (CH), 22.9 (CH_3), 14.2 (CH_3); δ_F (376 MHz, $CDCl_3$) -125.3 (F-16a); **MP** 171-174 °C; ν_{max} (FT-ATR/cm^{-1}) 3371, 2965, 1726, 1679, 1606, 1524, 1452, 1368, 1297, 1239, 1203, 1130, 1070, 869, 759, 611.

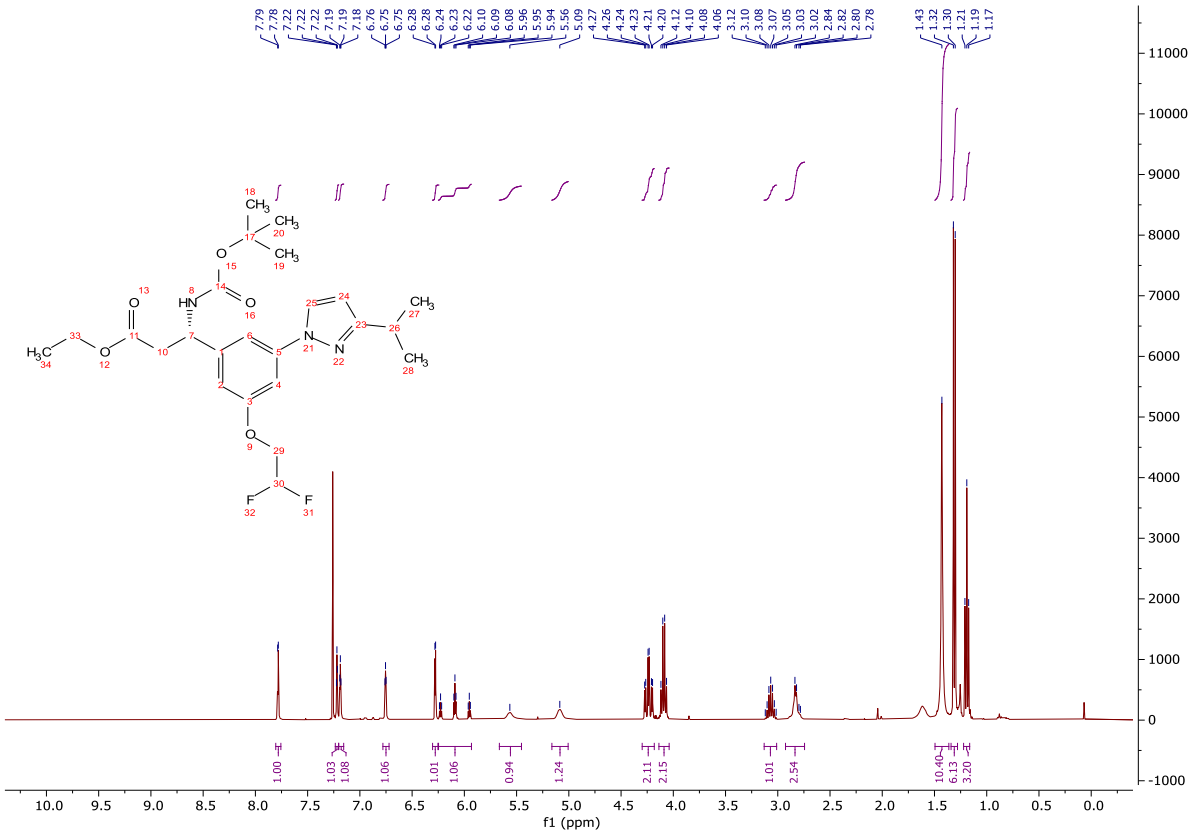
7.79 7.78 7.22 7.22 7.22 7.19 7.19 7.18 6.76 6.75 6.75 6.28 6.28 6.24 6.23 6.22 6.10 6.09 6.08 5.96 5.95 5.94 5.56 5.09 4.27 4.26 4.24 4.23 4.21 4.20 4.12 4.10 4.08 4.06 3.12 3.10 3.08 3.07 3.05 3.03 3.02 2.84 2.82 2.80 2.78
1.43 1.32 1.30 1.21 1.19 1.17
1.00 1.03 1.08 1.06 1.01 1.06 0.94 1.24 2.11 2.15 1.01 2.54 10.40 6.13 3.20
f1 (ppm)

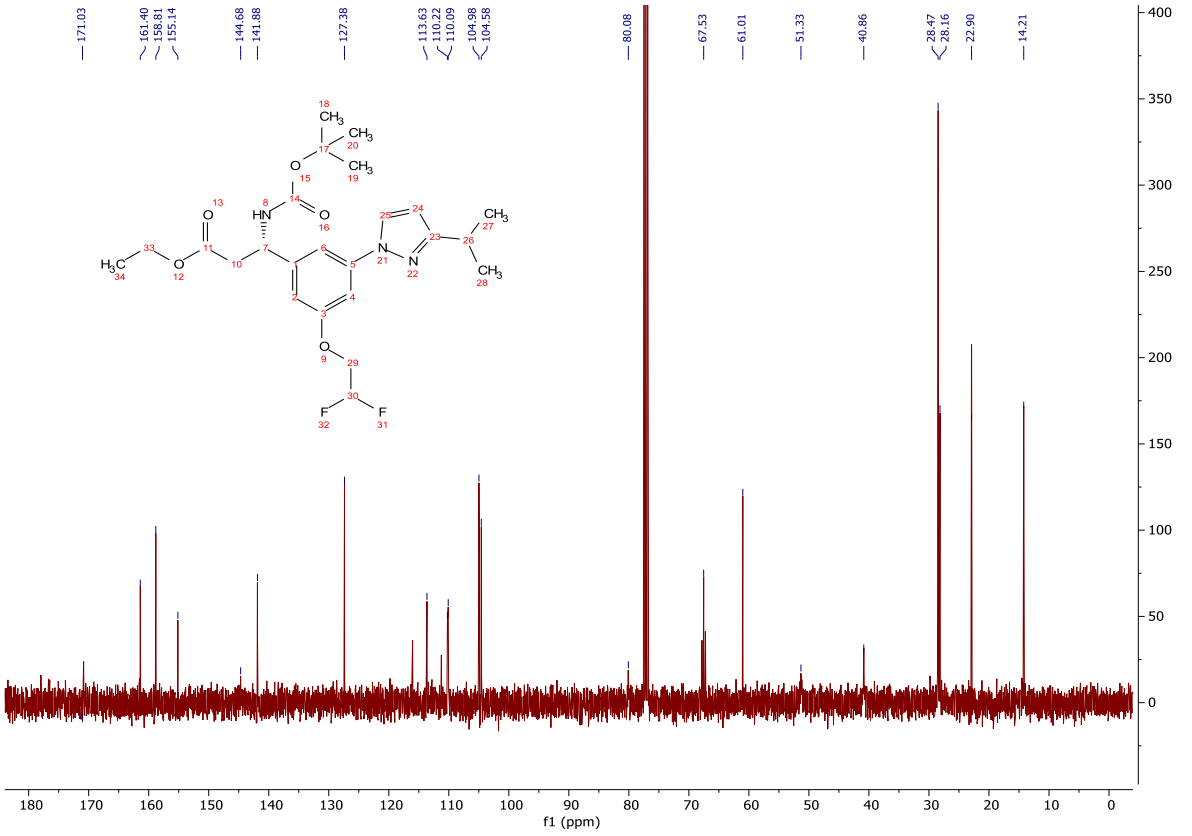
171.03 161.40 158.81 155.14 144.68 141.88 127.38 113.63 110.22 110.09 104.98 104.58 80.08 67.53 61.01 51.33 40.86 28.47 28.16 22.90 14.21
f1 (ppm)

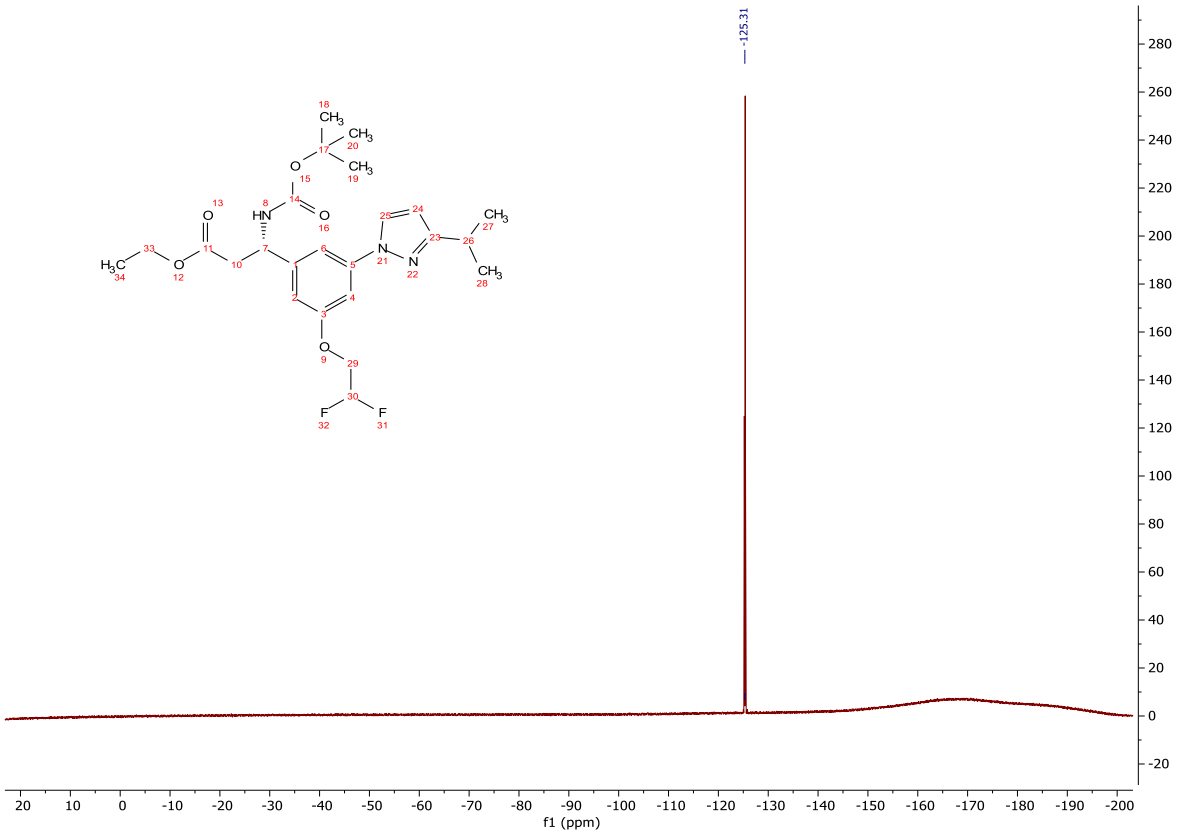
-125.31
f1 (ppm)

tert-Butyl (*S*)-7-(5-((1-(3-(3-chloro-1*H*-pyrazol-1-yl)-5-(trifluoromethyl)phenyl)-3-ethoxy-3-oxopropyl)amino)-5-oxopentyl)-3,4-dihydro-1,8-napthyridine-1(2*H*)-carboxylate (**348**)

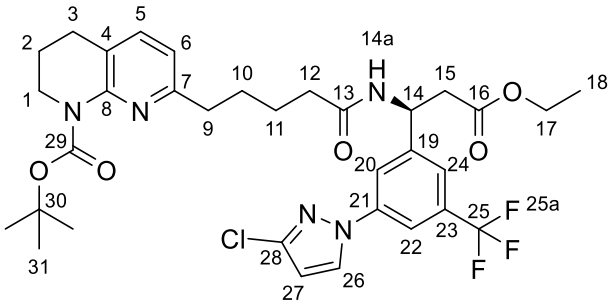

A solution of **342** (220 mg, 0.477 mmol) in 4M HCl in dioxane (5.00 mL, 20.0 mmol) was stirred at rt for 40 min and concentrated *in vacuo*. The crude product was dissolved in acetonitrile (2.00 mL) and **82** (162 mg, 0.477 mmol) was added and the mixture cooled to 0 °C. HATU (236 mg, 0.620 mmol) was added, and the reaction mixture stirred for 15 min. *i*-Pr_2NEt (0.250 mL, 1.43 mmol) was added and the reaction mixture stirred for 16 h. The reaction mixture was concentrated *in vacuo*, dissolved in ethyl acetate (40.0 mL) and washed with sat. $NaHCO_{3(aq)}$ (40.0 mL), sat. $NH_4Cl_{(aq)}$ (40.0 mL), sat. $NaHCO_{3(aq)}$ (40.0 mL) and brine (40.0 mL). The organic was dried (Na_2SO_4) and concentrated *in vacuo* giving a dark brown oil. The crude product was purified by column chromatography on silica gel, eluting with a gradient of ethyl acetate/light petroleum (40-100%) to afford the title compound as a clear, colourless oil (190 mg, 0.281 mmol, 59%); **HRMS** *m/z* (ESI^+) calc. for $C_{33}H_{40}ClF_3N_5O_5$ $[M+H]^+$ requires 678.2665, found 678.2659; $\boldsymbol{R_f}$ 0.56, 80% ethyl acetate/light petroleum, UV active; δ_H (400 MHz, $CDCl_3$) 7.88 (1H, d, *J* = 2.6 Hz, H-26), 7.82 – 7.78 (2H, m, H-20 and H-22), 7.46 – 7.43 (1H, m, H-24), 7.30 – 7.24 (1H, m, H-5), 7.03 – 6.96 (1H, m, H-14a), 6.78 (1H, d, *J* = 7.7 Hz, H-6), 6.41 (1H, d, *J* = 2.6 Hz, H-27), 5.48 (1H, dt, *J* = 8.2, 6.1 Hz, H-14), 4.12 – 4.03 (2H, m, H-17), 3.78 – 3.70 (2H, m, H-1), 2.93 – 2.79 (2H, m, H-15), 2.77 – 2.67 (4H, m, H-3 and H-9), 2.34 – 2.26 (2H, m, H-12), 1.96 – 1.86 (2H, m, H-2), 1.82 – 1.68 (4H, m, H-10 and H-11), 1.50 (9H, s, H-31), 1.21 – 1.13 (3H, m, H-18); δ_C (101 MHz, $CDCl_3$) 172.9 (CO), 170.9 (CO), 158.1 (C), 154.2 (CO), 151.1 (C), 144.5 (C), 142.5 (C), 140.2 (C), 137.5 (ArH), 128.8 (ArH), 122.1 (C), 121.5 (ArH), 120.1 (ArH), 118.5

(ArH), 114.8 (ArH), 108.2 (ArH), 61.3 (CH_2), 49.4 (CH_3), 45.1 (CH_2), 39.9 (CH_2), 37.3 (CH_2), 36.5 (CH_2), 29.0 (CH_2), 28.5 (CH_3), 26.4 (CH_2), 25.3 (CH_2), 23.4 (CH_2), 14.2 (CH_3); δ_F (376 MHz, $CDCl_3$) -62.7 (F-25a); ν_{max} (FT-ATR/cm^{-1}) 3296, 2932, 1732, 1651, 1514, 1464, 1376, 1161, 1125, 882, 751, 698.

N.B. C-25 and three aryl quaternary carbons are not observed.

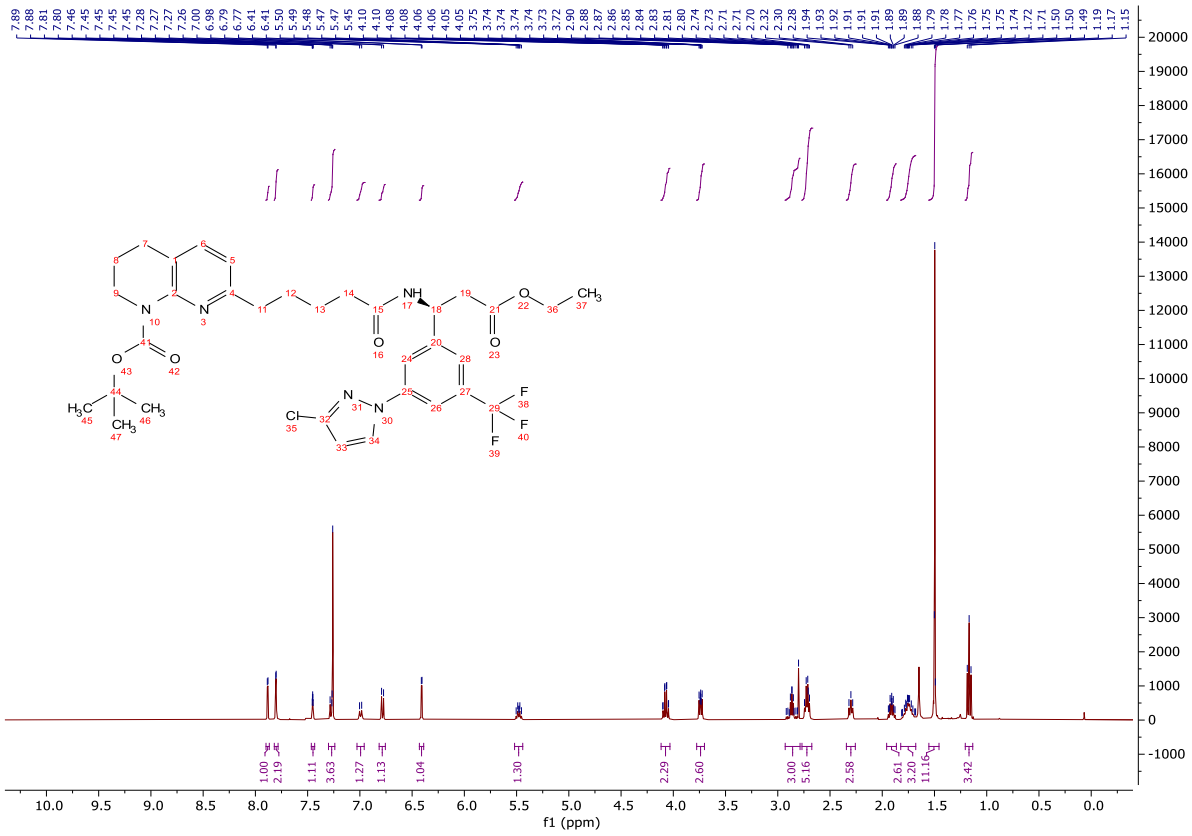
f1 (ppm)

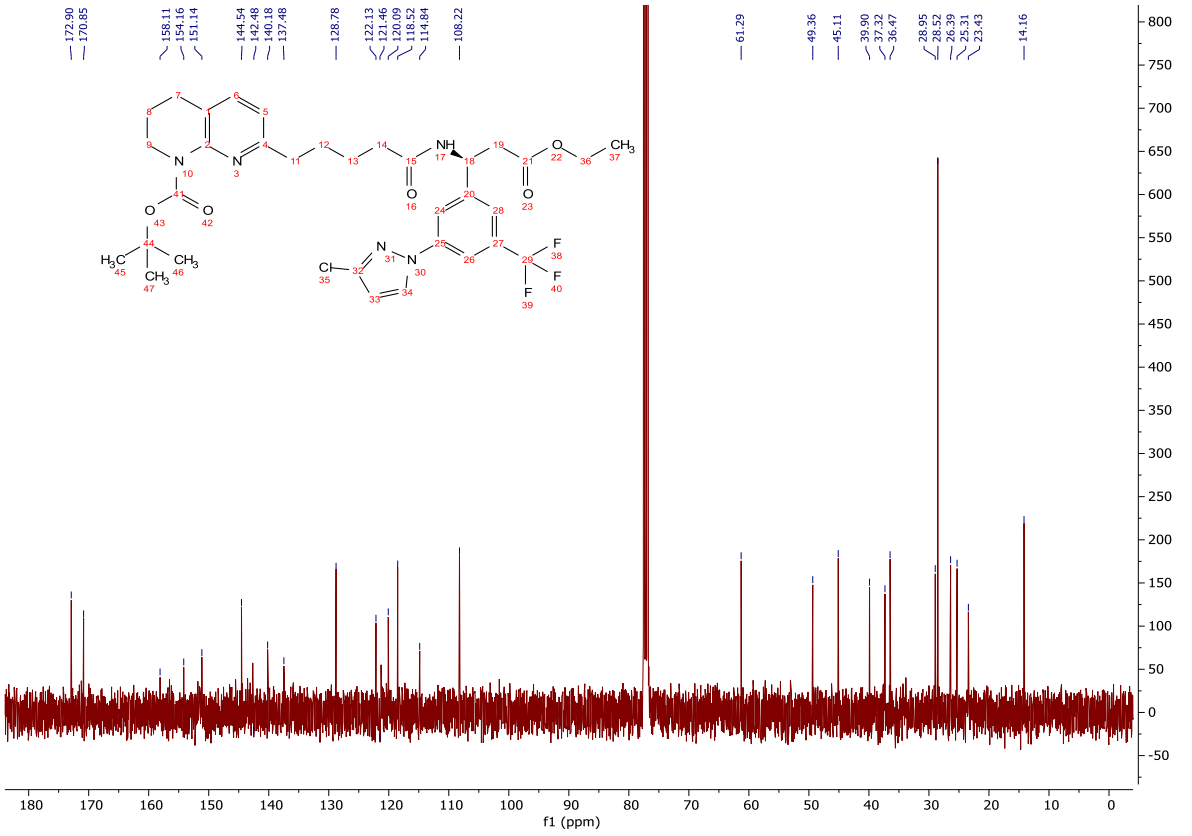
f1 (ppm)

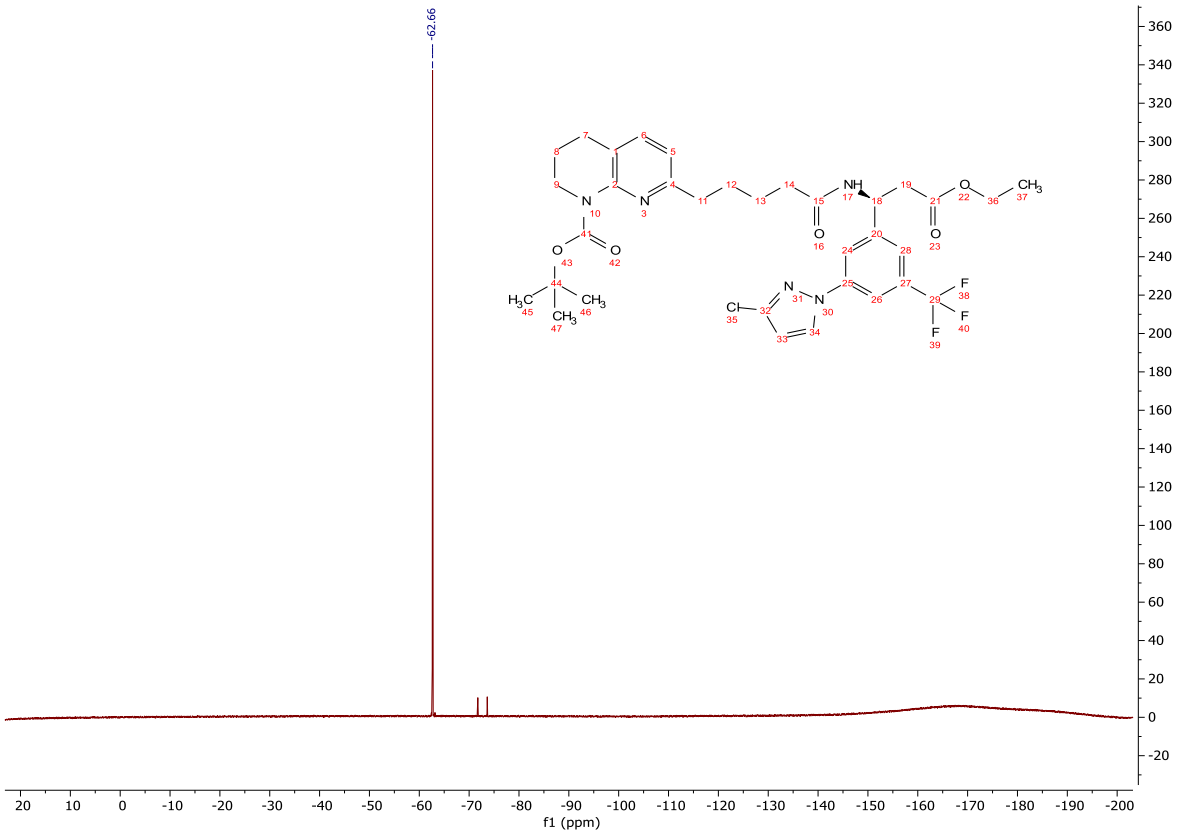
-62.66
360
340
320
300
280
260
240
220
200
180
160
140
120
100
80
60
40
20
0
-20
20 10 0 -10 -20 -30 -40 -50 -60 -70 -80 -90 -100 -110 -120 -130 -140 -150 -160 -170 -180 -190 -200
f1 (ppm)

(*S*)-3-(3-(3-chloro-1*H*-pyrazol-1-yl)-5-(trifluoromethyl)phenyl)-3-(5-(5,6,7,8-tetrahydro-1,8-napthyridin-2-yl)pentanamido)propanoic acid (**294**)

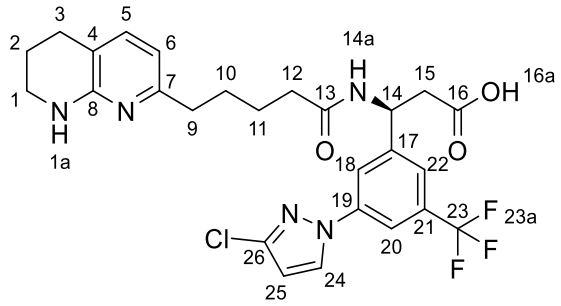

To a solution of **348** (180 mg, 0.266 mmol) in CH_2Cl_2 (2.50 mL) was added TFA (2.50 mL). The reaction mixture was stirred at rt for 7 h. The reaction mixture was concentrated *in vacuo*, dissolved in methanol (1.00 mL) and 1M $LiOH_{(aq)}$ (5.32 mL, 5.32 mmol) was added. The reaction mixture was stirred at rt for 18 h and concentrated *in vacuo*. The crude product was dissolved in a minimum volume of water and acidified to pH 5 with 2M $HCl_{(aq)}$. The precipitate was filtered and washed with water to afford the title compound as a colourless, amorphous powder (145 mg, 0.264 mmol, 99%); **HRMS** *m/z* (ESI^+) calc. for $C_{26}H_{28}ClF_3N_5O_3$ $[M+H]^+$ requires 550.1827, found 550.1829; $\boldsymbol{R_f}$ 0.36, 5% methanol/CH_2Cl_2, UV active; δ_H (400 MHz, MeOD) 8.39 (1H, d, *J* = 2.6 Hz, H-24), 8.07 – 8.01 (1H, m, H-18), 7.97 – 7.91 (1H, m, H-20), 7.65 – 7.58 (1H, m, H-22), 7.49 (1H, d, *J* = 7.4 Hz, H-5), 6.56 – 6.46 (2H, m, H-6 and H-25), 5.47 (1H, t, *J* = 7.5 Hz, H-14), 3.47 (2H, t, *J* = 5.7 Hz, H-1), 2.84 – 2.58 (6H, m, H-3, H-9 and H-15), 2.44 – 2.23 (2H, m, H-12), 1.99 – 1.87 (2H, m, H-2), 1.84 – 1.59 (4H, m, H-10 and H-11); δ_C (101 MHz, DMSO-d_6) 171.8 (CO), 171.6 (CO), 153.3 (C), 152.4 (C), 146.6 (C), 141.1 (C), 139.5 (C), 138.7 (ArH), 131.1 (ArH), 130.4 (C, q, *J* = 32.2 Hz), 123.7 (CF_3, q, *J* = 272.4 Hz), 121.1 (ArH, q, *J* = 3.8 Hz), 120.2 (ArH), 115.6 (C), 113.3 (ArH, q, *J* = 3.8 Hz), 109.9 (ArH), 108.0 (ArH), 49.3 (CH), 40.7 (CH_2), 40.6 (CH_2), 35.0 (CH_2), 34.0 (CH_2), 28.2 (CH_2), 25.4 (CH_2), 24.7 (CH_2), 19.9 (CH_2); δ_F (376 MHz, MeOD) -64.2 (F-23a), -76.9 (F-23a); **MP** Becomes waxy at 124 °C, fully melts at 150 °C; $\boldsymbol{\nu_{max}}$ (FT-ATR/cm^{-1}) 3289, 2925, 1645, 1515, 1487, 1377, 1239, 1169, 1054, 868, 762, 647.

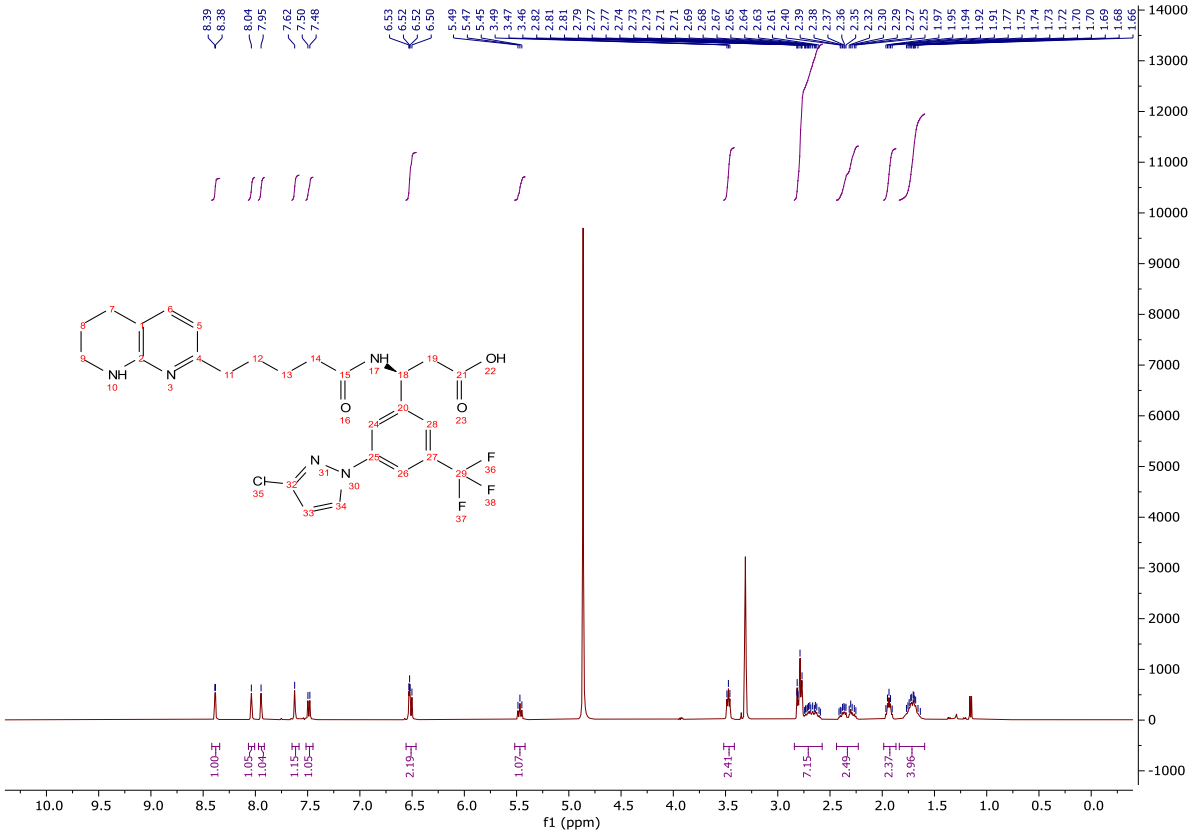
8.39
8.38
8.04
7.95
7.62
7.50
7.48
6.53
6.52
6.52
6.50
5.49
5.47
5.45
5.49
3.47
3.46
2.82
2.81
2.81
2.79
2.77
2.77
2.74
2.73
2.73
2.71
2.71
2.69
2.68
2.67
2.65
2.64
2.63
2.61
2.40
2.39
2.38
2.37
2.36
2.35
2.32
2.30
2.29
2.27
2.25
1.97
1.95
1.94
1.92
1.91
1.77
1.75
1.74
1.73
1.72
1.70
1.70
1.69
1.68
1.66
1.00
1.05
1.04
1.15
1.05
2.19
1.07
2.41
7.15
2.49
2.37
3.96
f1 (ppm)

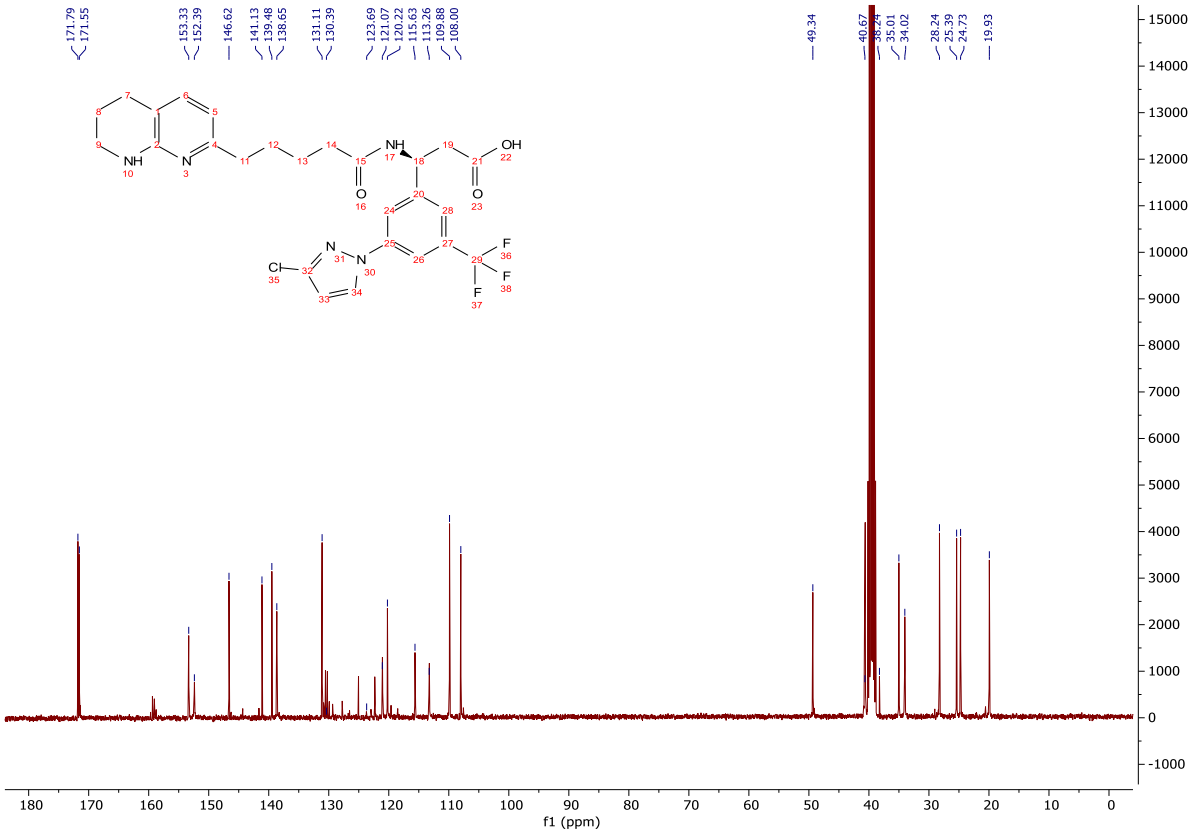
171.79
171.55
153.33
152.39
146.62
141.13
139.48
138.65
131.11
130.39
123.69
121.07
120.22
115.63
113.26
109.88
108.00
49.34
40.67
38.21
35.01
34.02
28.24
25.39
24.73
19.93
f1 (ppm)

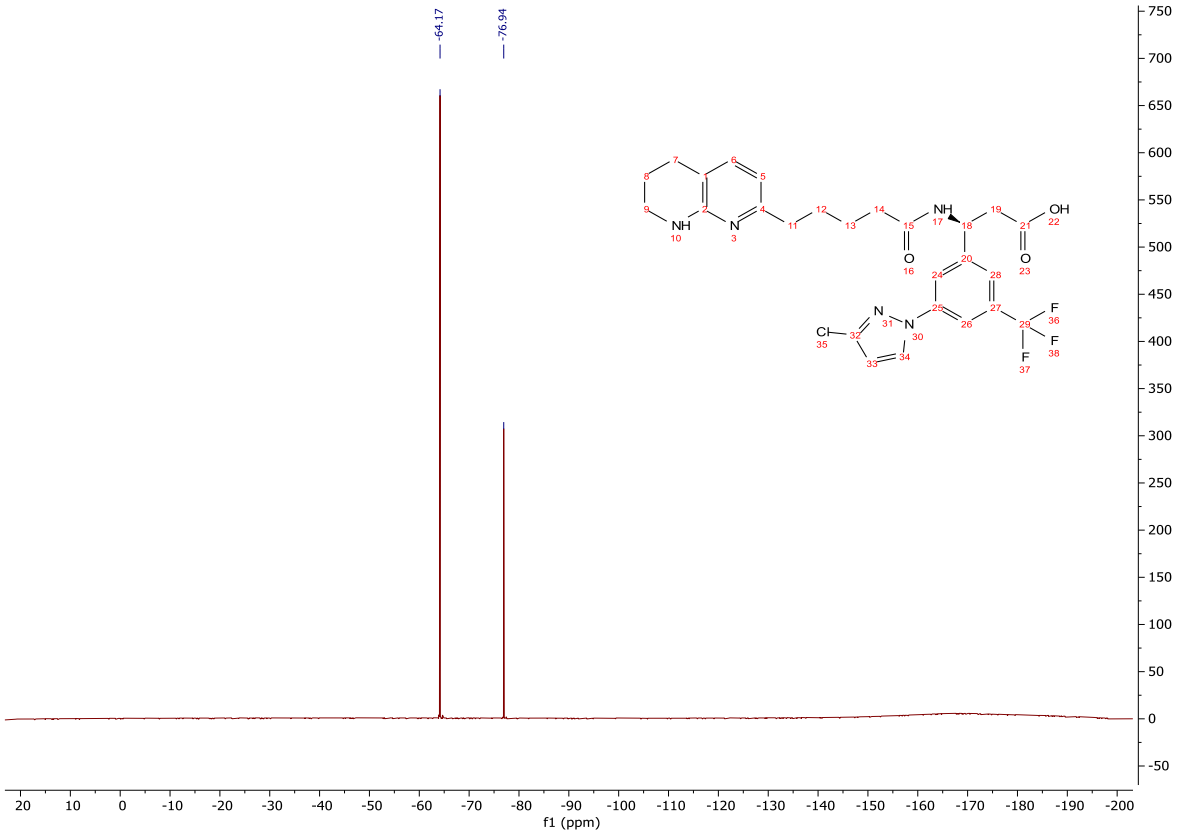
-64.17
-76.94
f1 (ppm)

tert-Butyl (*S*)-7-(5-((3-ethoxy-1-(3-(3-isopropyl-1*H*-pyrazol-1-yl)-5-(trifluoromethyl)phenyl)-3-oxopropyl)amino)-5-oxopentyl)-3,4-dihydro-1,8-napthyridine-1(2*H*)-carboxylate (**349**)

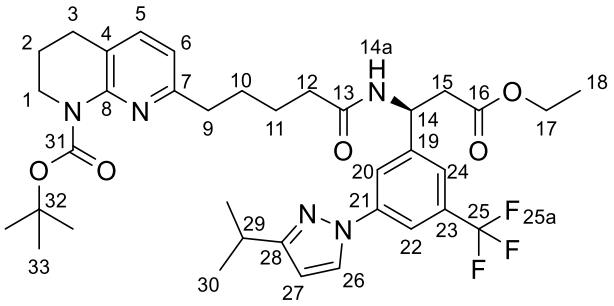

A solution of **343** (250 mg, 0.533 mmol) in 4M HCl in dioxane (5.00 mL, 20.0 mmol) was stirred at rt for 40 min and concentrated *in vacuo*. The crude product was dissolved in acetonitrile (2.00 mL) and **82** (181 mg, 0.533 mmol) was added and the mixture cooled to 0 °C. HATU (263 mg, 0.693 mmol) was added, and the reaction mixture stirred for 15 min. *i*-Pr_2NEt (0.280 mL, 1.60 mmol) was added and the reaction mixture stirred for 16 h. The reaction mixture was concentrated *in vacuo*, dissolved in ethyl acetate (40.0 mL) and washed with sat. $NaHCO_{3(aq)}$ (40.0 mL), sat. $NH_4Cl_{(aq)}$ (40.0 mL), sat. $NaHCO_{3(aq)}$ (40.0 mL) and brine (40.0 mL). The organic was dried (Na_2SO_4) and concentrated *in vacuo* giving a dark brown oil. The crude product was purified by column chromatography on silica gel, eluting with a gradient of ethyl acetate/light petroleum (40-100%) to afford the title compound as a clear, colourless oil (83 mg, 0.121 mmol, 23%); **HRMS** *m/z* (ESI^+) calc. for $C_{36}H_{47}F_3N_5O_5$ $[M+H]^+$ requires 686.3524, found 686.3551; $\boldsymbol{R_f}$ 0.52, 80% ethyl acetate/light petroleum, UV active; δ_H (400 MHz, $CDCl_3$) 7.86 – 7.75 (3H, m, H-20, H-22 and H-26), 7.37 (1H, dd, *J* = 1.7, 1.7 Hz, H-24), 7.29 – 7.22 (1H, m, H-5), 6.99 (1H, d, *J* = 8.2 Hz, H-14a), 6.76 (1H, d, *J* = 7.6 Hz, H-6), 6.28 (1H, d, *J* = 2.5 Hz, H-27), 5.48 (1H, dt, *J* = 8.2, 6.1 Hz, H-14), 4.06 (2H, q, *J* = 7.2 Hz, H-17), 3.77 – 3.68 (2H, m, H-1), 3.05 (1H, hept, *J* = 6.9 Hz, H-29), 2.84 (2H, ddd, *J* = 25.7, 15.7, 6.2 Hz H-15), 2.77 – 2.64 (4H, m, H-3 and H-9), 2.28 (2H, t, *J* = 7.2 Hz, H-12), 1.96 – 1.84 (2H, m, H-2), 1.81 – 1.66 (4H, m, H-10 and H-11), 1.49 (9H, s, H-33), 1.30 (6H, d, *J* = 7.0 Hz, H-30), 1.15 (3H, t, *J* = 7.2 Hz, H-18); δ_C (101 MHz, $CDCl_3$) 172.8 (CO), 170.9 (CO), 161.8 (C), 158.1 (C), 154.1 (CO), 151.1 (C), 144.0 (C),

141.0 (C), 137.4 (ArH), 132.2 (C, q, *J* = 32.8 Hz), 127.3 (ArH), 123.7 (CF_3, q, *J* = 272.8 Hz), 122.0 (C), 120.03 (ArH), 120.00 (ArH), 118.4 (ArH), 114.8 (ArH, q, *J* = 3.8 Hz), 105.6 (ArH), 80.8 (C), 61.2 (CH_2), 49.3 (CH), 45.0 (CH_2), 40.0 (CH_2), 37.4 (CH_2), 36.5 (CH_2), 29.0 (CH_2), 28.5 (CH_3), 28.1 (CH), 26.3 (CH_2), 25.3 (CH_2), 23.4 (CH_2), 22.8 (CH_3), 14.1 (CH_3); δ_F (376 MHz, $CDCl_3$) -62.65 (F-25a); ν_{max} (FT-ATR/cm^{-1}) 3301, 2963, 1734, 1692, 1650, 1533, 1464, 1366, 1330, 1252, 1160, 1124, 1046, 758, 699.

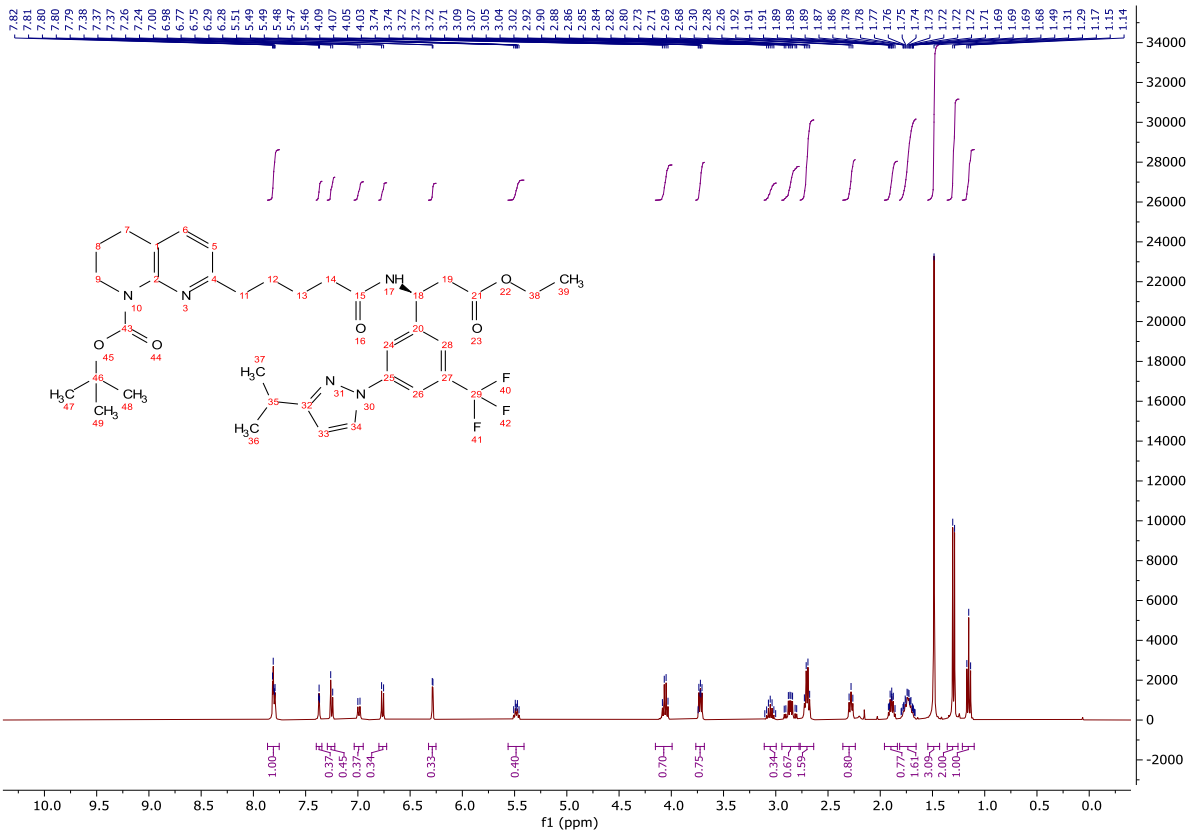
f1 (ppm)

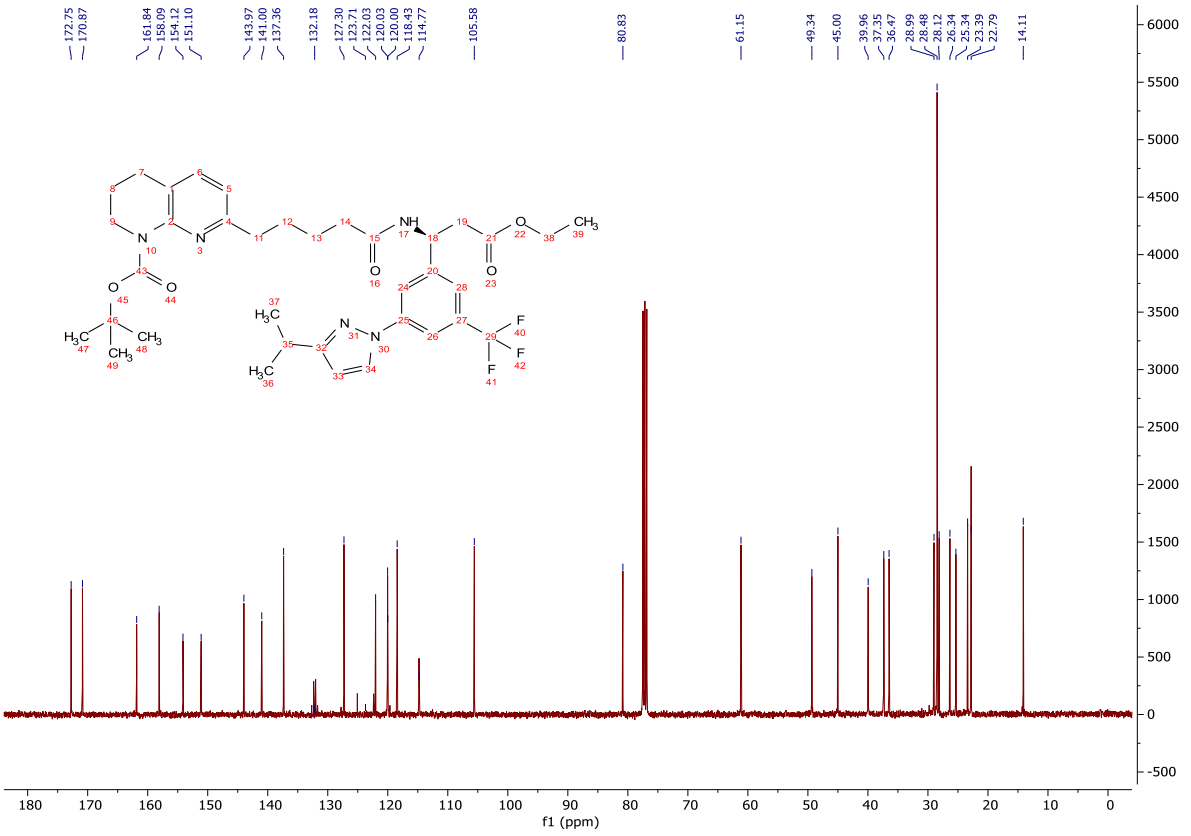
f1 (ppm)

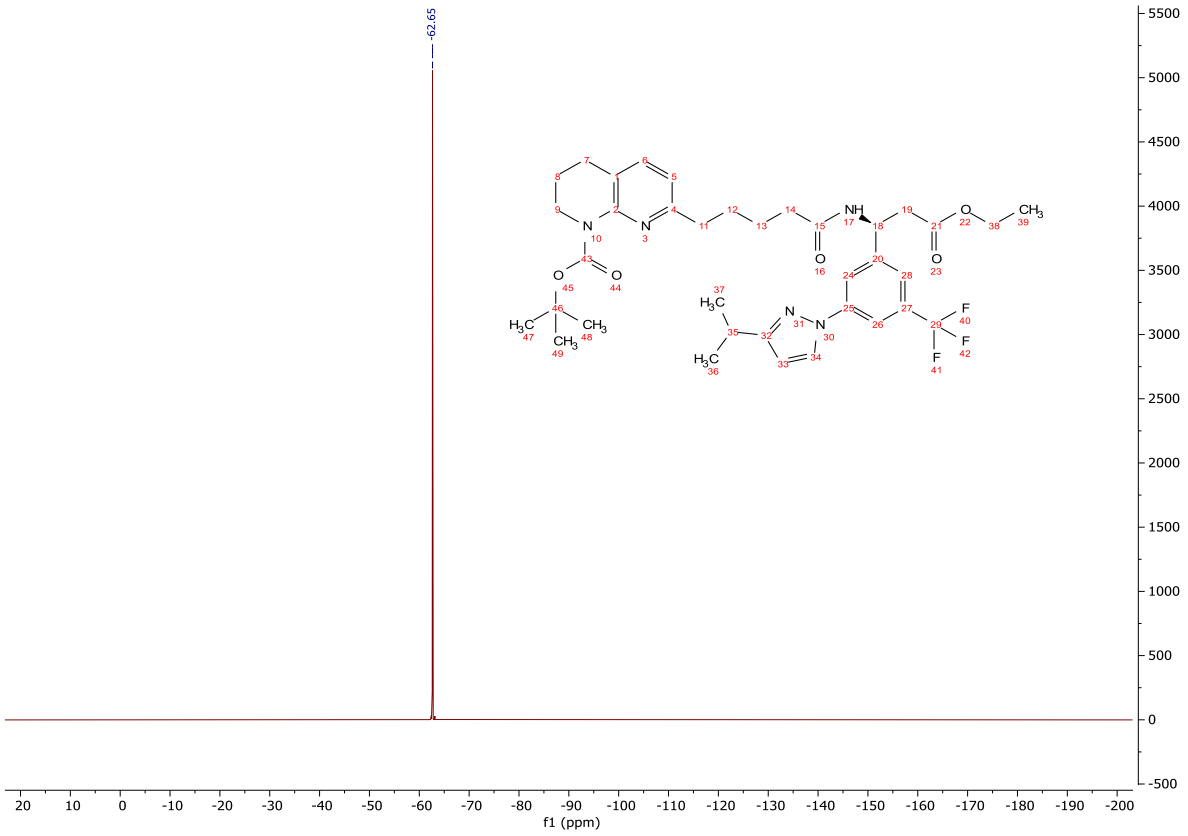
-62.65
5500
5000
4500
4000
3500
3000
2500
2000
1500
1000
500
0
-500
20 10 0 -10 -20 -30 -40 -50 -60 -70 -80 -90 -100 -110 -120 -130 -140 -150 -160 -170 -180 -190 -200
f1 (ppm)

(*S*)-3-(3-(Piperidin-1-yl)phenyl)-3-(5-(5,6,7,8-tetrahydro-1,8-naphthyridin-2-yl)pentanamido)propanoic acid (**288**)

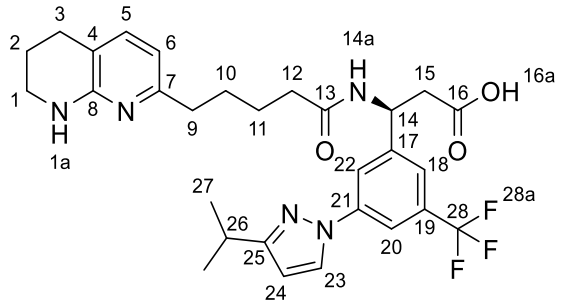

To a solution of **349** (73 mg, 0.107 mmol) in CH_2Cl_2 (2.50 mL) was added TFA (2.50 mL). The reaction mixture was stirred at rt for 7 h. The reaction mixture was concentrated *in vacuo*, dissolved in methanol (1.00 mL) and 1M $LiOH_{(aq)}$ (2.14 mL, 2.14 mmol) was added. The reaction mixture was stirred at rt for 18 h and concentrated *in vacuo*. The crude product was dissolved in a minimum volume of water and acidified to pH 5 with 2M $HCl_{(aq)}$. The precipitate was filtered and washed with water to afford the title compound as a colourless powder (58 mg, 0.104 mmol, 97%); **HRMS** *m/z* (ESI^+) calc. for $C_{29}H_{35}F_3N_5O_3$ $[M+H]^+$ requires 558.2687, found 558.2685; $\boldsymbol{R_f}$ 0.34, 5% methanol/CH_2Cl_2, UV active; δ_H (400 MHz, MeOD) 8.21 (1H, d, *J* = 2.6 Hz, H-23), 8.03 – 7.97 (1H, m, H-22), 7.95 – 7.89 (1H, m, H-20), 7.59 – 7.53 (1H, m, H-18), 7.48 (1H, d, *J* = 7.3 Hz, H-5), 6.50 (1H, d, *J* = 7.3 Hz, H-6), 6.41 (1H, d, *J* = 2.5 Hz, H-24), 5.47 (1H, t, *J* = 7.5 Hz, H-14), 3.46 (2H, t, *J* = 5.7 Hz, H-1), 3.05 (1H, hept, *J* = 7.1 Hz, H-26), 2.84 – 2.56 (6H, m, H-3, H-9 and H-15), 2.43 – 2.22 (2H, m, H-12), 1.98 – 1.87 (2H, m, H-2), 1.83 – 1.58 (4H, m, H-10 and H-11), 1.31 (6H, d, *J* = 7.0 Hz, H-27); δ_C (101 MHz, DMSO-d_6) 171.9 (CO), 171.5 (CO), 160.7 (C), 154.2 (C), 146.3 (C), 140.3 (C), 137.7 (ArH), 130.3 (C, q, *J* = 32.0 Hz), 128.7 (ArH), 123.8 (CF_3, q, *J* = 272.5 Hz), 119.9 (ArH), 119.7 (ArH, q, *J* = 3.7 Hz), 114.4 (C), 112.8 (ArH, q, *J* = 3.7 Hz), 109.9 (ArH), 105.7 (ArH), 49.4 (CH), 40.8 (CH_2), 40.6 (CH_2), 35.1 (CH_2), 35.0 (CH_2), 28.4 (CH_2), 27.4 (CH), 25.6 (CH_2), 24.8 (CH_2), 22.5 (CH_3), 20.3 (CH_2); δ_F (376 MHz, MeOD) -64.1 (F-28a), -76.9 (F-28a); **MP** Degrades >180 °C; ν_{max} (FT-ATR/cm^{-1}) 3320, 2926, 1645, 1610, 1534, 1488, 1400, 1335, 1256, 1165, 1056, 867, 753, 642.

N.B. One aryl quaternary carbon is not observed.

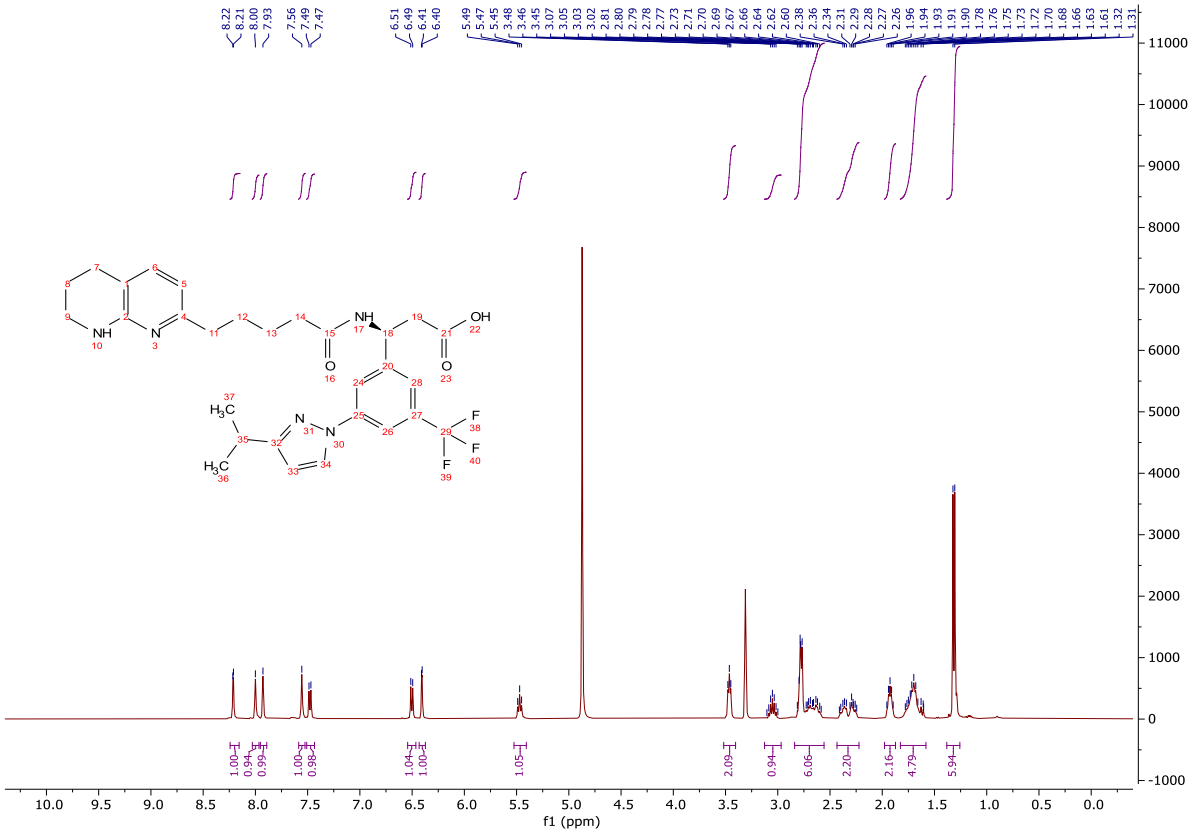
8.22
8.21
8.00
7.93
7.56
7.49
7.47
6.51
6.49
6.41
6.40
5.49
5.47
5.45
3.48
3.46
3.45
3.07
3.05
3.03
3.02
2.81
2.80
2.79
2.78
2.77
2.73
2.71
2.70
2.69
2.67
2.66
2.64
2.62
2.60
2.38
2.36
2.34
2.31
2.29
2.28
2.27
2.26
1.96
1.94
1.93
1.91
1.90
1.78
1.76
1.75
1.73
1.72
1.70
1.68
1.66
1.63
1.61
1.32
1.31
1.00
0.94
0.99
1.00
0.98
1.04
1.00
1.05
2.09
0.94
6.06
2.20
2.16
4.79
5.94
f1 (ppm)

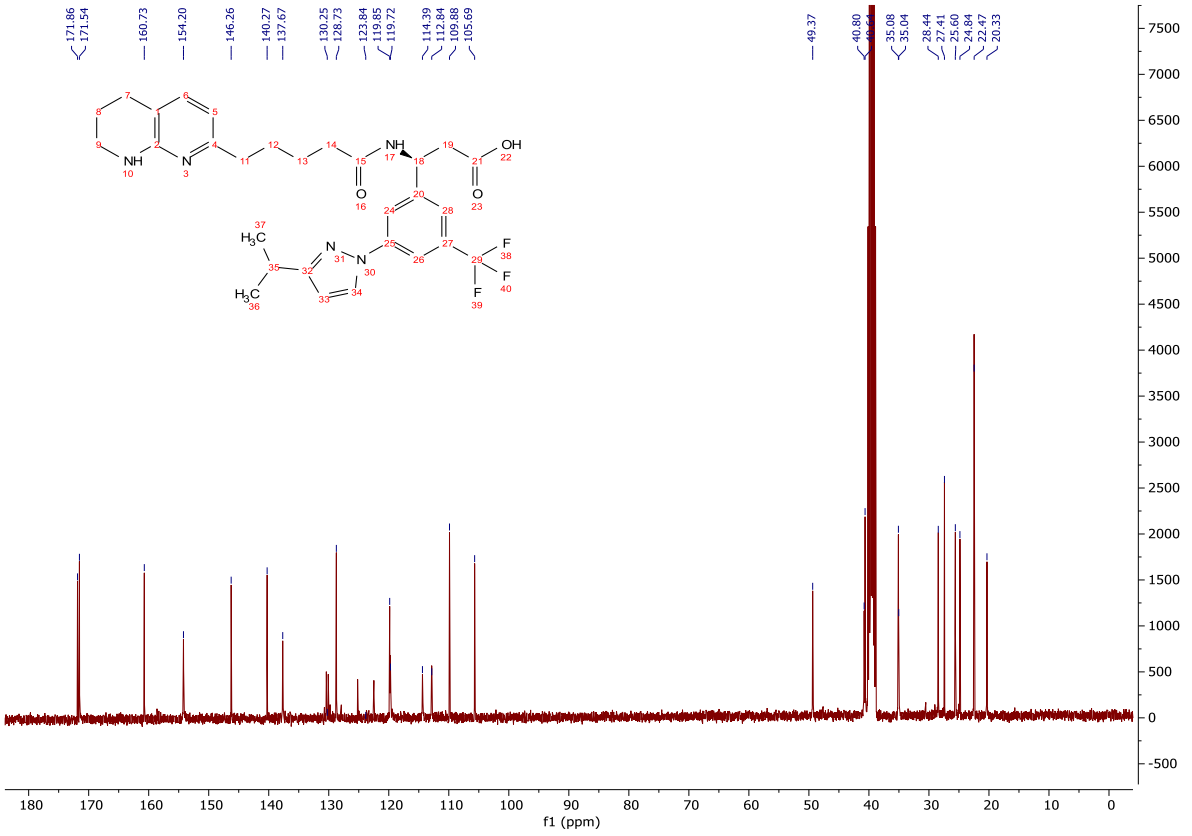
171.86
171.54
160.73
154.20
146.26
140.27
137.67
130.25
128.73
123.84
119.85
119.72
114.39
112.84
109.88
105.69
49.37
40.80
35.08
35.04
28.44
27.41
25.60
24.84
22.47
20.33
f1 (ppm)


-64.12
-76.93
f1 (ppm)

tert-Butyl (*S*)-7-(5-((1-(3-chloro-1*H*-pyrazol-1-yl)-5-cyclopropylphenyl)-3-ethoxy-3-oxopropyl)amino)-5-oxopentyl)-3,4-dihydro-1,8-napthyridine-1(2*H*)-carboxylate (**350**)

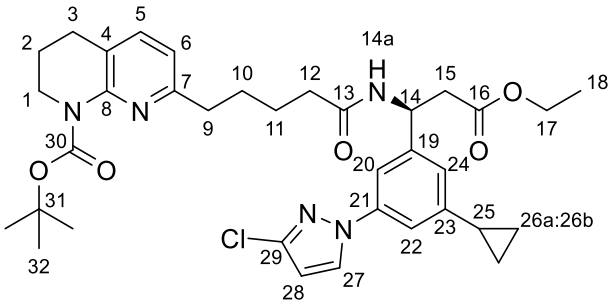

A solution of **344** (183 mg, 0.423 mmol) in 4M HCl in dioxane (5.00 mL, 20.0 mmol) was stirred at rt for 40 min and concentrated *in vacuo*. The crude product was dissolved in acetonitrile (2.00 mL) and **82** (144 mg, 0.423 mmol) was added and the mixture cooled to 0 °C. HATU (209 mg, 0.550 mmol) was added, and the reaction mixture stirred for 15 min. *i*-Pr_2NEt (0.220 mL, 1.27 mmol) was added and the reaction mixture stirred for 16 h. The reaction mixture was concentrated *in vacuo*, dissolved in ethyl acetate (40.0 mL) and washed with sat. $NaHCO_{3(aq)}$ (40.0 mL), sat. $NH_4Cl_{(aq)}$ (40.0 mL), sat. $NaHCO_{3(aq)}$ (40.0 mL) and brine (40.0 mL). The organic was dried (Na_2SO_4) and concentrated *in vacuo* giving a dark brown oil. The crude product was purified by column chromatography on silica gel, eluting with a gradient of ethyl acetate/light petroleum (40-100%) to afford the title compound as a clear, colourless oil (175 mg, 0.270 mmol, 64%); **HRMS** *m/z* (ESI^+) calc. for $C_{35}H_{45}ClN_5O_5$ $[M+H]^+$ requires 650.3104, found 650.3099; $\boldsymbol{R_f}$ 0.40, 80% ethyl acetate/light petroleum, UV active; δ_H (400 MHz, $CDCl_3$) 7.79 (1H, d, *J* = 2.5 Hz, H-27), 7.31 (1H, dd, *J* = 1.6, 1.6 Hz, H-22), 7.28 – 7.25 (1H, m, H-5), 7.21 (1H, dd, *J* = 1.8, 1.8 Hz, H-20), 6.94 (1H, dd, *J* = 1.6, 1.6 Hz, 1H), 6.78 (1H, d, *J* = 7.6 Hz, H-6), 6.71 (1H, d, *J* = 8.3 Hz, H-14a), 6.34 (1H, d, *J* = 2.5 Hz, H-28), 5.40 (1H, dt, *J* = 8.4, 6.2 Hz, H-14), 4.06 (2H, q, *J* = 7.3 Hz, H-17), 3.76 – 3.70 (2H, m, H-1), 2.91 – 2.76 (2H, m, H-15), 2.75 – 2.67 (4H, m, H-3 and H-9), 2.30 – 2.24 (2H, m, H-12), 1.95 – 1.86 (3H, m, H-2 and H-25), 1.82 – 1.66 (4H, m, H-10 and H-11), 1.49 (9H, s, H-32), 1.16 (3H, t, *J* = 7.1 Hz, H-18), 1.01 – 0.94 (2H, m, H-26a), 0.74 – 0.69 (2H, m, H-26b); δ_C (101 MHz, $CDCl_3$) 172.5 (CO), 171.2 (CO), 158.1 (C), 154.2 (CO),

151.2 (C), 146.6 (C), 142.7 (C), 141.6 (C), 140.0 (C), 137.4 (ArH), 128.8 (ArH), 122.8 (ArH), 122.0 (C), 118.4 (ArH), 115.6 (ArH), 114.1 (ArH), 107.2 (ArH), 80.9 (C), 61.0 (CH_2), 49.6 (CH), 45.0 (CH_2), 40.2 (CH_2), 37.5 (CH_2), 36.6 (CH_2), 29.1 (CH_2), 28.5 (CH_3), 26.4 (CH_2), 25.5 (CH_2), 23.4 (CH_2), 15.7 (CH_3), 14.2 (CH_3), 9.6 (CH_3); ν_{max} (FT-ATR/cm^{-1}) 3296, 2930, 1732, 1648, 1599, 1509, 1464, 1366, 1252, 1147, 1047, 853, 750, 701.

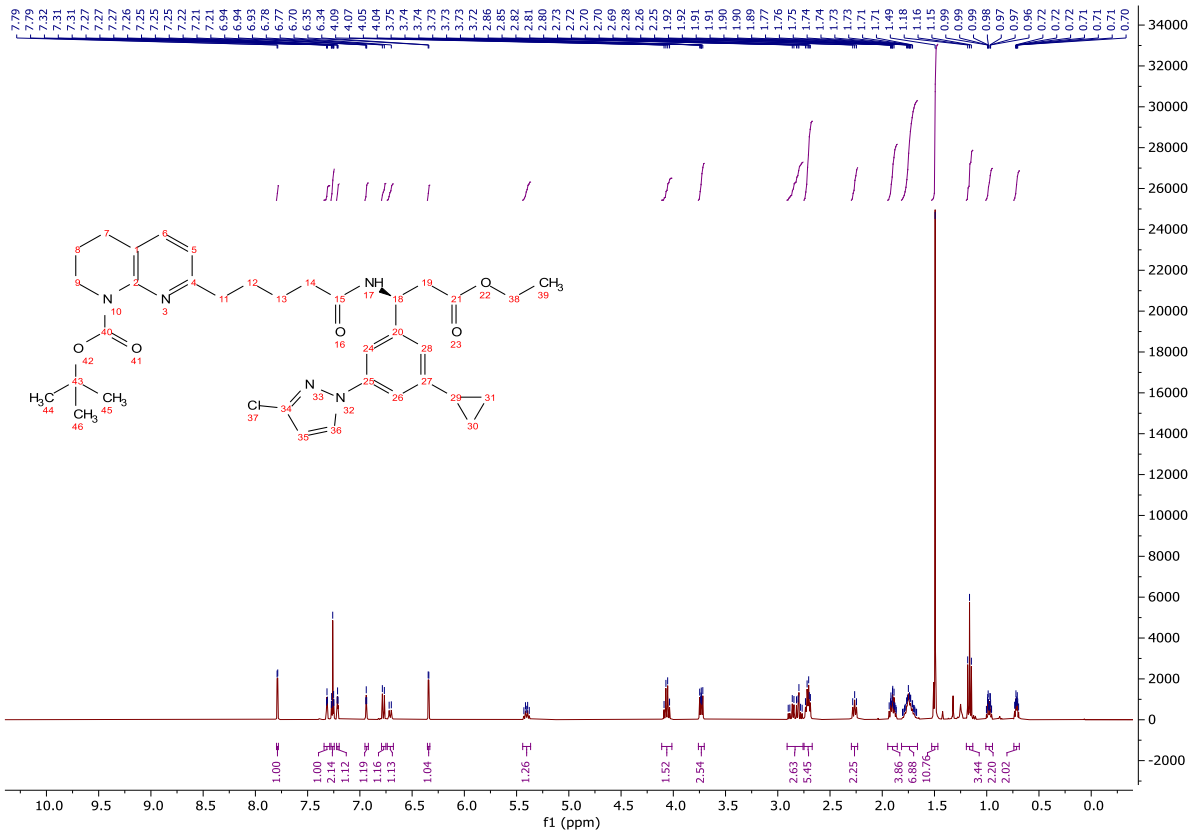
f1 (ppm)

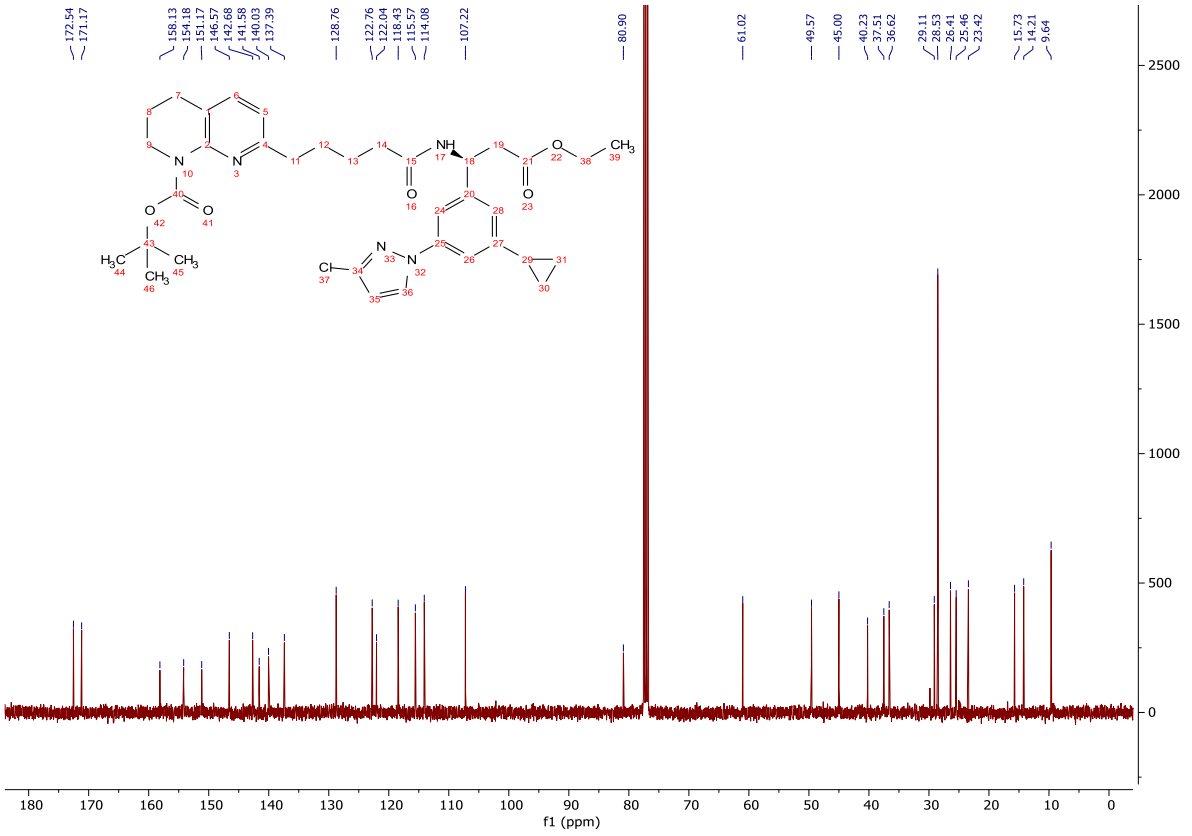
f1 (ppm)

(*S*)-3-(3-(3-chloro-1*H*-pyrazol-1-yl-1-yl)-5-cyclopropylphenyl)-3-(5-(5,6,7,8-tetrahydro-1,8-napthyridin-2-yl)pentanamido)propanoic acid (**295**)

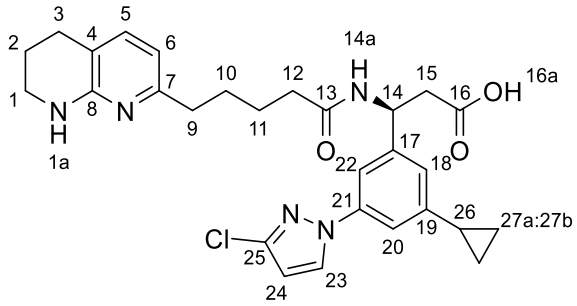

To a solution of **350** (165 mg, 0.250 mmol) in CH_2Cl_2 (2.50 mL) was added TFA (2.50 mL). The reaction mixture was stirred at rt for 7 h. The reaction mixture was concentrated *in vacuo*, dissolved in methanol (1.00 mL) and 1M $LiOH_{(aq)}$ (5.00 mL, 5.00 mmol) was added. The reaction mixture was stirred at rt for 18 h and concentrated *in vacuo*. The crude product was dissolved in a minimum volume of water and acidified to pH 5 with 2M $HCl_{(aq)}$. The precipitate was filtered and washed with water to afford the title compound as a colourless, amorphous powder (130 mg, 0.250 mmol, 100%); **HRMS** *m/z* (ESI^+) calc. for $C_{28}H_{33}ClN_5O_3$ $[M+H]^+$ requires 522.2266, found 522.2269; $\boldsymbol{R_f}$ 0.36, 5% methanol/CH_2Cl_2, UV active; δ_H (400 MHz, MeOD) 8.19 (1H, d, *J* = 2.6 Hz, H-23), 7.50 – 7.39 (2H, m, H-5 and H-20), 7.27 (1H, dd, *J* = 1.8, 1.8 Hz, H-22), 7.05 (1H, dd, *J* = 1.7, 1.7 Hz, H-18), 6.49 – 6.40 (2H, m, H-6 and H-24), 5.37 (1H, t, *J* = 7.5 Hz, H-14), 3.44 (2H, t, *J* = 5.7 Hz, H-1), 2.83 – 2.54 (6H, m, H-3, H-9 and H-15), 2.47 – 2.18 (2H, m, H-12), 2.00 – 1.83 (3H, m, H-2 and H-26), 1.79 – 1.56 (4H, m, H-10 and H-11), 1.03 – 0.96 (2H, m, H-27a), 0.78 – 0.71 (2H, m, H-27b); δ_C (101 MHz, MeOD) 176.8 (CO), 174.9 (CO), 163.4 (C), 153.1 (C), 149.8 (C), 147.9 (C), 145.5 (C), 142.4 (ArH), 141.1 (C), 130.9 (ArH), 123.5 (ArH), 120.2 (C), 115.7 (ArH), 115.1 (ArH), 111.4 (ArH), 108.0 (ArH), 52.1 (CH), 43.4 (CH_2), 42.0 (CH_2), 36.3 (CH_2), 33.3 (CH_2), 29.2 (CH_2), 26.4 (CH_2), 26.1 (CH_2), 20.6 (CH_2), 16.3 (CH), 10.1 (CH_2); **MP** Becomes waxy at 83 °C, fully melts at 120 °C; ν_{max} (FT-ATR/cm^{-1}) 3248, 3080, 2924, 1651, 1543, 1509, 1419, 1385, 1319, 1289, 1198, 1131, 1048, 862, 750, 647.

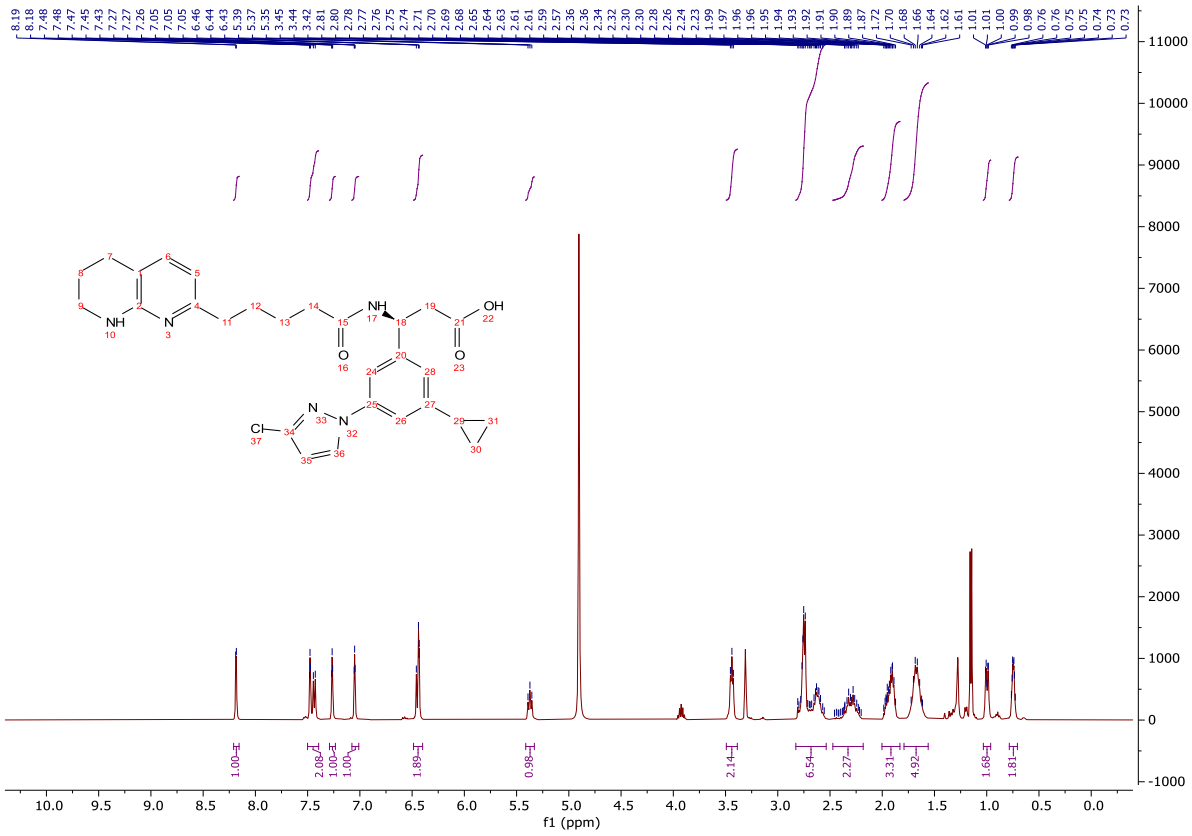
f1 (ppm)

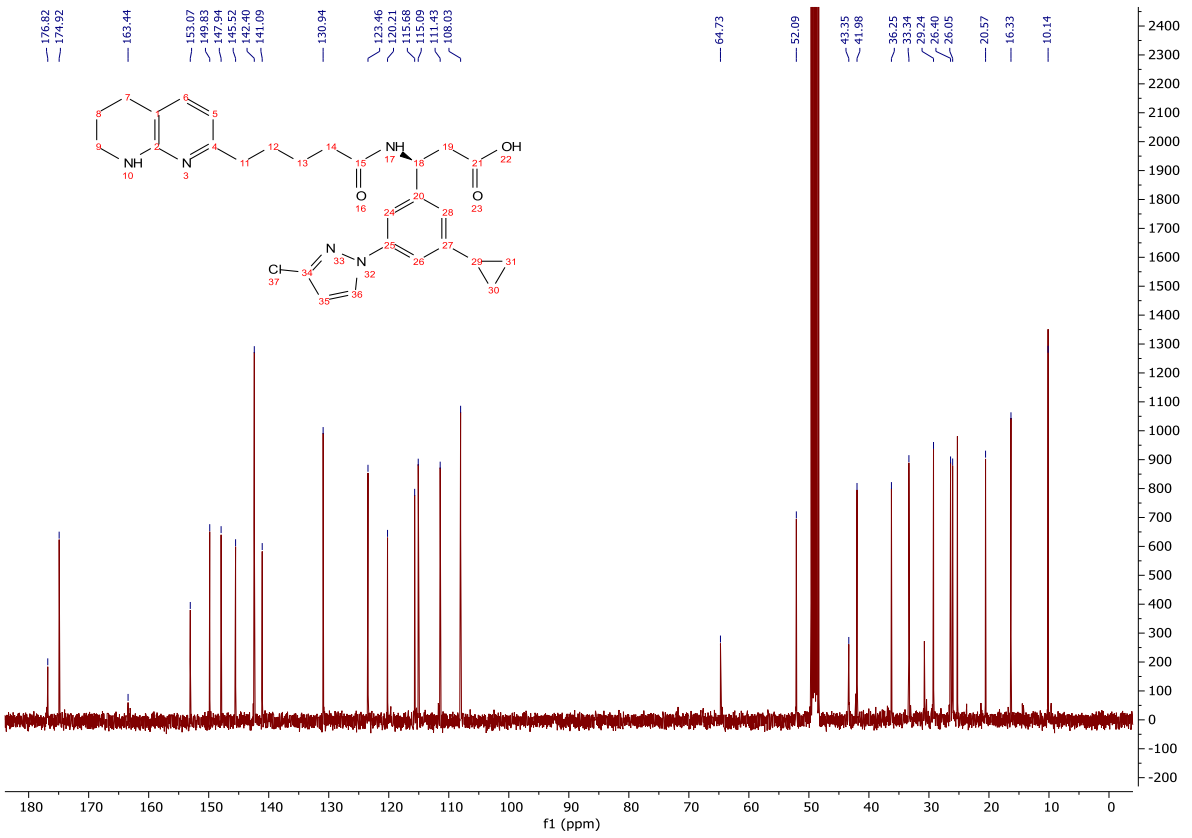
f1 (ppm)

tert-Butyl (*S*)-7-(5-((1-(3-cyclopropyl-5-(3-isopropyl-1*H*-pyrazol-1-yl)phenyl)-3-ethoxy-3-oxopropyl)amino)-5-oxopentyl)-3,4-dihydro-1,8-napthyridin-1(2*H*)-carboxylate (**351**)

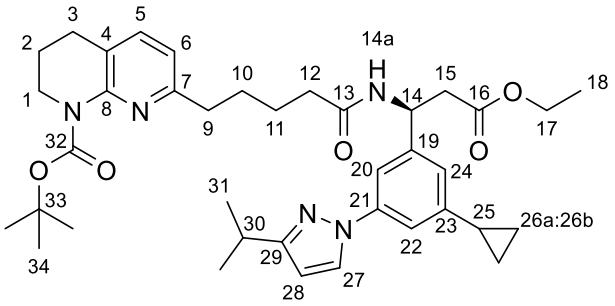

A solution of **345** (170 mg, 0.385 mmol) in 4M HCl in dioxane (5.00 mL, 20.0 mmol) was stirred at rt for 40 min and concentrated *in vacuo*. The crude product was dissolved in acetonitrile (2.00 mL) and **82** (131 mg, 0.385 mmol) was added and the mixture cooled to 0 °C. HATU (190 mg, 0.501 mmol) was added, and the reaction mixture stirred for 15 min. *i*-Pr_2NEt (0.200 mL, 1.16 mmol) was added and the reaction mixture stirred for 16 h. The reaction mixture was concentrated *in vacuo*, dissolved in ethyl acetate (40.0 mL) and washed with sat. $NaHCO_{3(aq)}$ (40.0 mL), sat. $NH_4Cl_{(aq)}$ (40.0 mL), sat. $NaHCO_{3(aq)}$ (40.0 mL) and brine (40.0 mL). The organic was dried (Na_2SO_4) and concentrated *in vacuo* giving a dark brown oil. The crude product was purified by column chromatography on silica gel, eluting with a gradient of ethyl acetate/light petroleum (40-100%) to afford the title compound as a clear, colourless oil (50 mg, 0.076 mmol, 20%); **HRMS** *m/z* (ESI^+) calc. for $C_{38}H_{52}N_5O_5$ $[M+H]^+$ requires 658.3963, found 658.3998; $\boldsymbol{R_f}$ 0.34, 80% ethyl acetate/light petroleum, UV active; δ_H (400 MHz, $CDCl_3$) 7.73 (1H, d, *J* = 2.5 Hz, H-27), 7.33 (1H, dd, *J* = 1.9, 1.9 Hz, H-22), 7.28 – 7.20 (2H, m, H-5 and H-20), 6.86 (1H, dd, *J* = 1.7, 1.7 Hz, H-24), 6.76 (1H, d, *J* = 7.7 Hz, H-6), 6.68 (1H, d, *J* = 8.4 Hz, H-14a), 6.23 (1H, d, *J* = 2.5 Hz, H-28), 5.45 – 5.33 (1H, m, H-14), 4.10 – 4.00 (2H, m, H-17), 3.76 – 3.67 (2H, m, H-1), 3.06 (1H, hept, *J* = 7.1 Hz, H-30), 2.93 – 2.62 (6H, m, H-3, H-9 and H-15), 2.29 – 2.20 (2H, m, H-12), 1.94 – 1.84 (3H, m, H-2 and H-25), 1.81 – 1.65 (4H, m, H-10 and H-11), 1.49 (9H, s, H-34), 1.29 (6H, d, *J* = 7.0 Hz, H-31), 1.20 – 1.11 (3H, m, H-18), 0.99 – 0.89 (2H, m, H-26a), 0.75 – 0.67 (2H, m, H-26b); δ_C (101 MHz, $CDCl_3$) 172.4 (CO), 171.2 (CO), 161.1 (C), 158.1 (C),

154.1 (CO), 151.1 (C), 146.1 (C), 142.2 (C), 140.8 (C), 137.3 (ArH), 127.4 (ArH), 121.9 (C), 121.6 (ArH), 118.4 (ArH), 115.8 (ArH), 114.3 (ArH), 104.4 (ArH), 80.8 (C), 60.9 (CH_2), 49.6 (CH), 44.9 (CH_2), 40.2 (CH_2), 37.5 (CH_2), 36.6 (CH_2), 29.1 (CH_2), 28.5 (CH_3), 28.1 (CH), 26.4 (CH_2), 25.5 (CH_2), 23.4 (CH_2), 23.0 (CH_3), 15.7 (CH), 14.2 (CH_3), 9.4 (CH_3); ν_{max} (FT-ATR/cm^{-1}) 3297, 2961, 1733, 1692, 1646, 1600, 1530, 1464, 1366, 1252, 1148, 1045, 855, 758, 702.

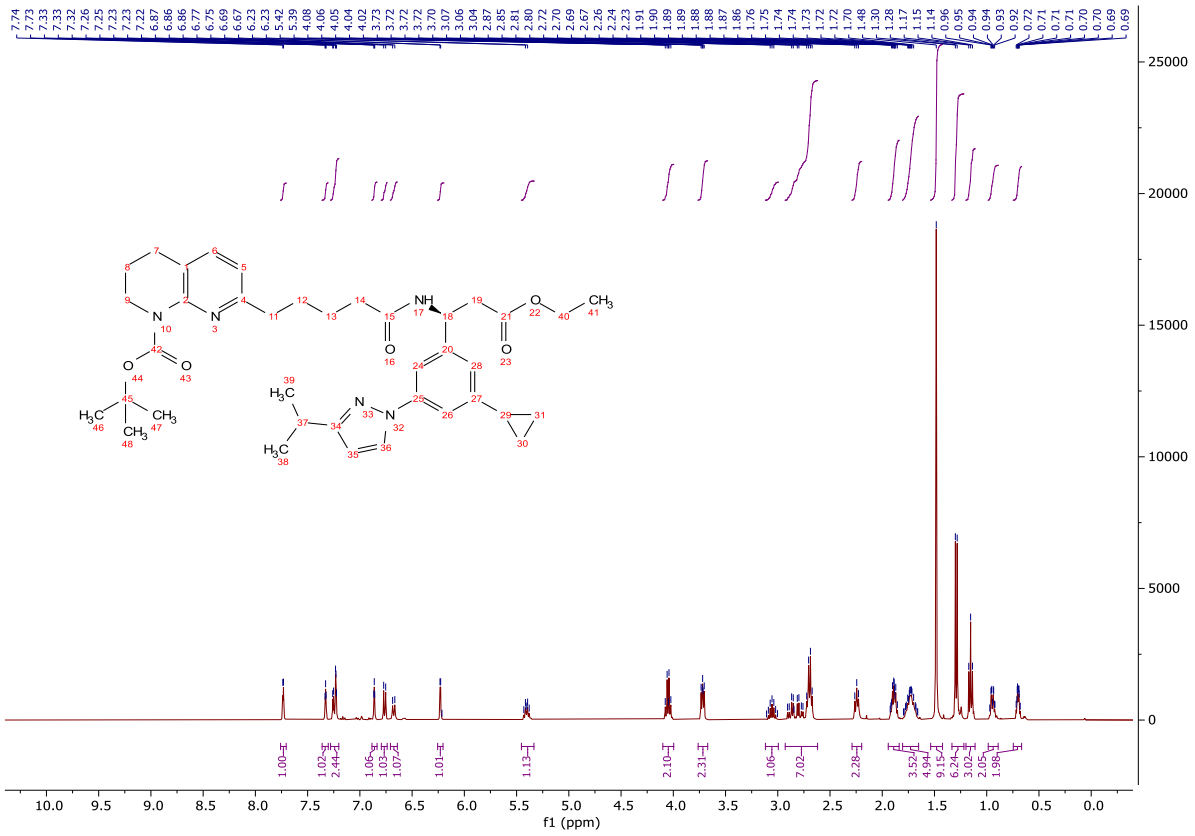
f1 (ppm)

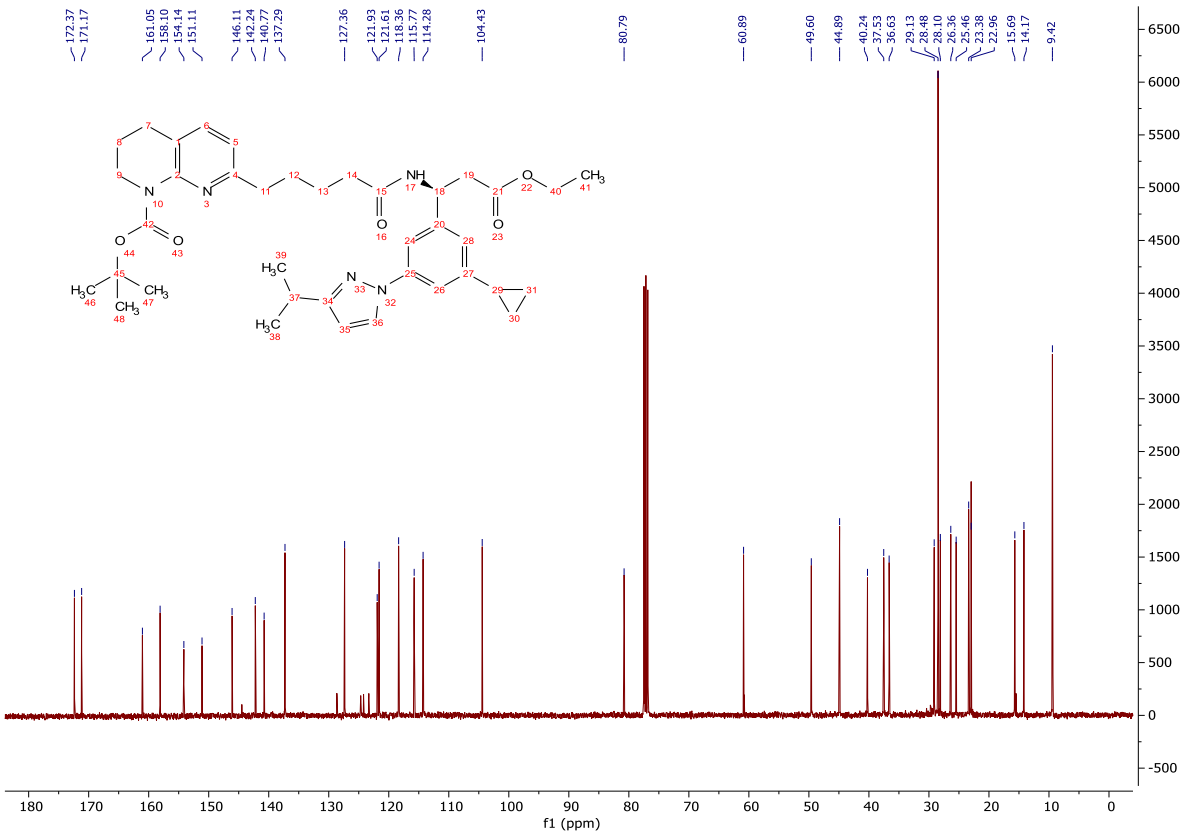
f1 (ppm)

(*S*)-3-(3-cyclopropyl-5-(3-isopropyl-1*H*-pyrazol-1-yl)phenyl)-3-(5-(5,6,7,8-tetrahydro-1,8-napthyridin-2-yl)pentanamido)propanoic acid (**289**)

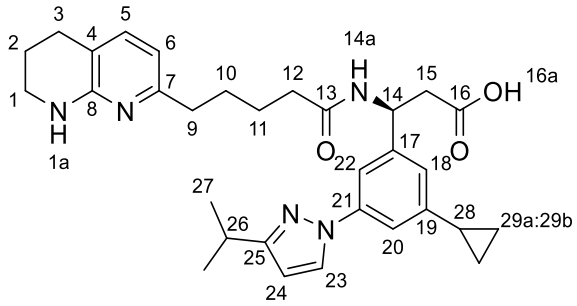

To a solution of **351** (41 mg, 0.062 mmol) in CH_2Cl_2 (2.50 mL) was added TFA (2.50 mL). The reaction mixture was stirred at rt for 7 h. The reaction mixture was concentrated *in vacuo*, dissolved in methanol (1.00 mL) and 1M $LiOH_{(aq)}$ (1.24 mL, 1.24 mmol) was added. The reaction mixture was stirred at rt for 18 h and concentrated *in vacuo*. The crude product was dissolved in a minimum volume of water and acidified to pH 5 with 2M $HCl_{(aq)}$. The precipitate was filtered and washed with water to afford the title compound as a colourless powder (30 mg, 0.057 mmol, 92%); **HRMS** *m/z* (ESI^+) calc. for $C_{31}H_{40}N_5O_3$ $[M+H]^+$ requires 530.3126, found 530.3132; $\boldsymbol{R_f}$ 0.34, 5% methanol/CH_2Cl_2, UV active; δ_H (500 MHz, MeOD) 8.03 (1H, d, *J* = 2.5 Hz, H-23), 7.48 – 7.41 (2H, m, H-5 and H-22), 7.27 (1H, dd, *J* = 1.8, 1.8 Hz, H-20), 7.01 (1H, dd, *J* = 1.6, 1.6 Hz, H-18), 6.48 (1H, d, *J* = 7.4 Hz, H-6), 6.33 (1H, d, *J* = 2.5 Hz, H-24), 5.42 – 5.35 (1H, m, H-14), 3.45 (2H, t, *J* = 5.6 Hz, H-1), 3.03 (1H, hept, *J* = 7.0 Hz, H-26), 2.81 – 2.56 (6H, m, H-3, H-9 and H-15), 2.40 – 2.22 (2H, m, H-12), 2.00 – 1.83 (3H, m, H-2 and H-28), 1.81 – 1.58 (4H, m, H-10 and H-11), 1.30 (6H, d, *J* = 7.0 Hz, H-27), 1.02 – 0.97 (2H, m, H-29a), 0.79 – 0.72 (2H, m, H-29b); δ_C (126 MHz, MeOD) 177.5 (CO), 174.9 (CO), 162.4 (C), 153.2 (C), 150.0 (C), 147.7 (C), 145.4 (C), 142.3 (ArH), 141.7 (C), 129.6 (ArH), 122.7 (ArH), 120.2 (C), 116.2 (ArH), 115.4 (ArH), 111.5 (ArH), 105.4 (ArH), 52.3 (CH), 43.9 (CH_2), 42.0 (CH_2), 36.2 (CH_2), 33.4 (CH_2), 29.3 (CH_2), 29.2 (CH), 26.4 (CH_2), 26.0 (CH_2), 23.3 (CH_3), 20.6 (CH_2), 16.3 (CH), 10.0 (CH_2); **MP** 105-107 °C; ν_{max} (FT-ATR/cm^{-1}) 3258, 3060, 2927, 1650, 1599, 1528, 1373, 1290, 1198, 1133, 1045, 758, 654.

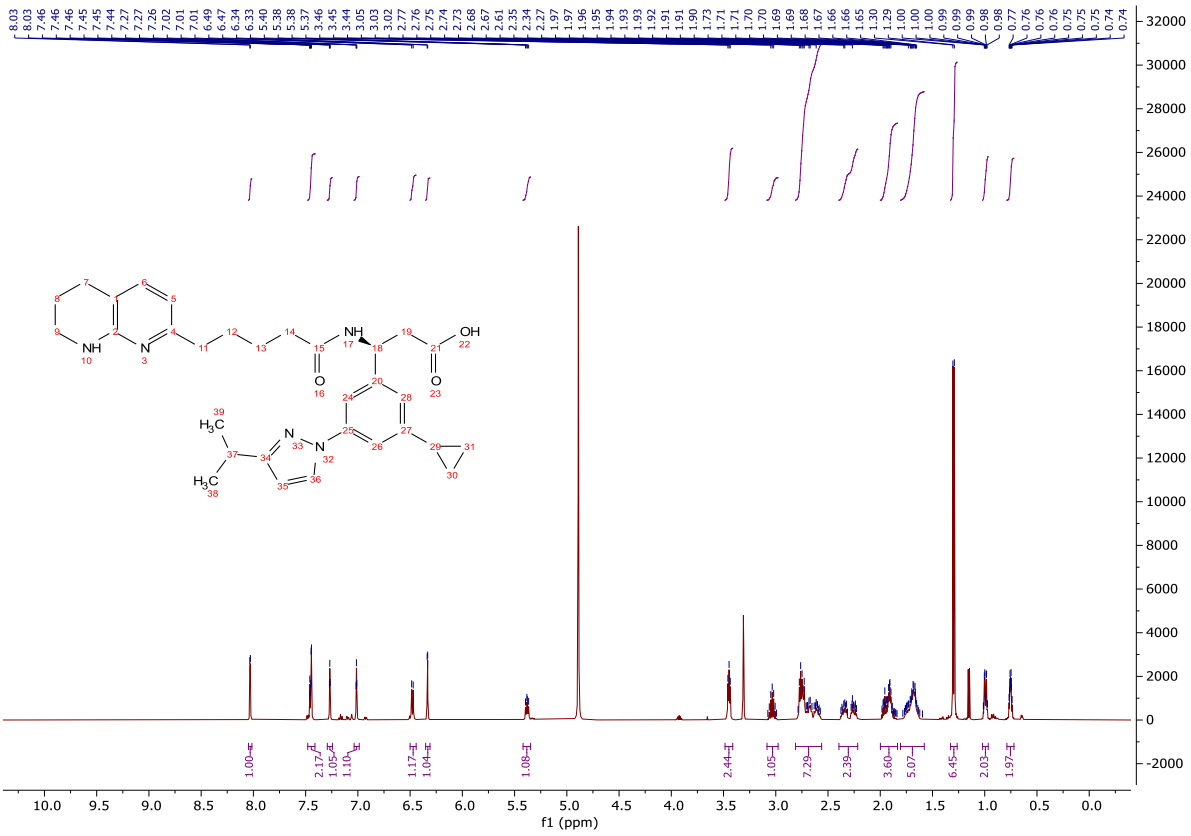
f1 (ppm)

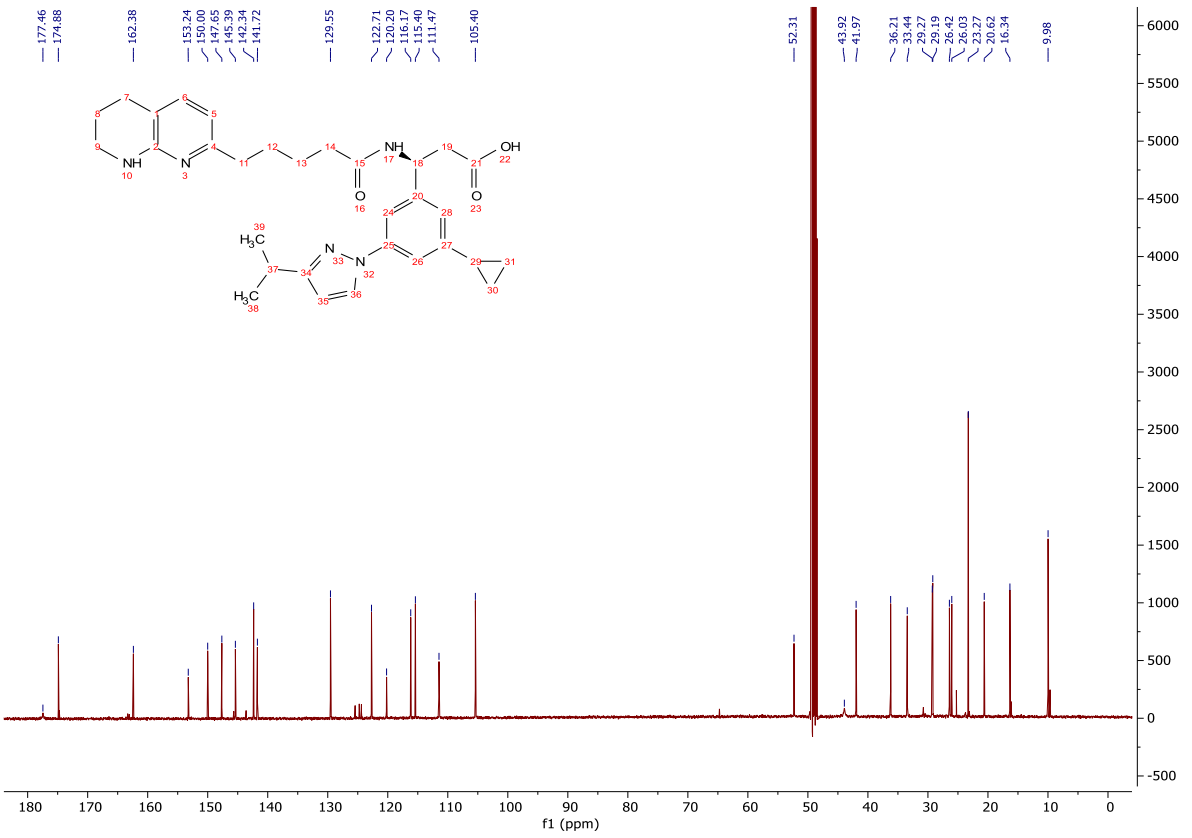
f1 (ppm)

tert-Butyl (*S*)-7-(5-((1-(3-(2,2-difluoroethoxy)-5-(3,5-dimethyl-1*H*-pyrazol-1-yl)phenyl)-3-ethoxy-3-oxopropyl)amino)-5-oxopentyl)-3,4-dihydro-1,8-napthyridine-1(2*H*)-carboxylate (**352**)

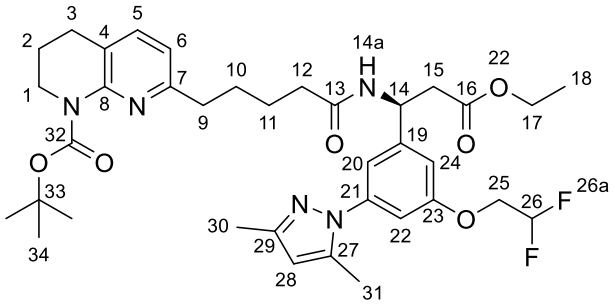

A solution of **346** (110 mg, 0.240 mmol) in 4M HCl in dioxane (5.00 mL, 20.0 mmol) was stirred at rt for 40 min and concentrated *in vacuo*. The crude product was dissolved in acetonitrile (1.00 mL) and **82** (82 mg, 0.240 mmol) was added and the mixture cooled to 0 °C. HATU (274 mg, 0.720 mmol) was added, and the reaction mixture stirred for 15 min. *i*-Pr_2NEt (0.210 mL, 1.20 mmol) was added and the reaction mixture stirred for 16 h. The reaction mixture was concentrated *in vacuo*, dissolved in ethyl acetate (10.0 mL) and washed with sat. $NaHCO_{3(aq)}$ (10.0 mL), sat. $NH_4Cl_{(aq)}$ (10.0 mL), sat. $NaHCO_{3(aq)}$ (10.0 mL) and brine (10.0 mL). The organic was dried ($MgSO_4$) and concentrated *in vacuo* giving a dark brown oil. The crude product was purified by column chromatography on silica gel, eluting with a gradient of ethyl acetate/light petroleum (0-100%) to afford the title compound as a yellow oil (72 mg, 0.105 mmol, 44%); **HRMS** *m/z* (ESI^+) calc. for $C_{36}H_{48}F_2N_5O_6$ $[M+H]^+$ requires 684.3567, found 684.3553; $\boldsymbol{R_f}$ 0.19, 80% ethyl acetate/light petroleum, UV active; δ_H (400 MHz, $CDCl_3$) 7.30 – 7.24 (1H, m, H-5), 6.99 (1H, dd, *J* = 1.6, 1.6 Hz, H-20), 6.90 (1H, dd, *J* = 2.0, 2.0 Hz, H-24), 6.85 (1H, dd, *J* = 2.0, 2.0 Hz, H-22), 6.81 – 6.70 (2H, m, H-6 and 14a), 6.22 – 5.89 (2H, m, H-26 and H-28), 5.41 (1H, dt, *J* = 8.4, 6.1 Hz, H-14), 4.24 – 4.01 (4H, m, H-17 and H-25), 3.77 – 3.69 (2H, m, H-1), 2.92 – 2.76 (2H, m, H-15), 2.74 – 2.65 (4H, m, H-3 and H-9), 2.31 – 2.22 (8H, m, H-12, H-30 and H-31), 1.95 – 1.85 (2H, m, H-2), 1.82 – 1.64 (4H, m, H-10 and H-11), 1.52 – 1.45 (9H, m, H-34), 1.20 – 1.14 (3H, m, H-18); δ_C (101 MHz, $CDCl_3$) 172.6 (CO), 171.1 (CO), 158.4 (C), 158.1 (C),

154.2 (CO), 151.1 (C), 149.4 (C), 143.7 (C), 141.4 (C), 139.6 (C), 137.4 (ArH), 122.1 (C), 118.4 (ArH), 116.0 (ArH), 113.6 (CHF_2, t, *J* = 241.1 Hz), 112.2 (ArH), 109.8 (ArH), 107.5 (ArH), 80.9 (C), 67.5 (CH_2, t, *J* = 29.5 Hz), 61.0 (CH_2), 49.3 (CH), 45.0 (CH_2), 39.9 (CH_2), 37.5 (CH_2), 36.5 (CH_2), 29.1 (CH_2), 28.5 (CH_3), 26.4 (CH_2), 25.4 (CH_2), 23.4 (CH_2), 14.2 (CH_3), 13.6 (CH_3), 12.6 (CH_3); δ_F (376 MHz, $CDCl_3$) -125.3 (F-26a); ν_{max} (FT-ATR/cm^{-1}) 3300, 2928, 1732, 1689, 1651, 1600, 1557, 1464, 1366, 1148, 1075, 845, 776, 697, 456.

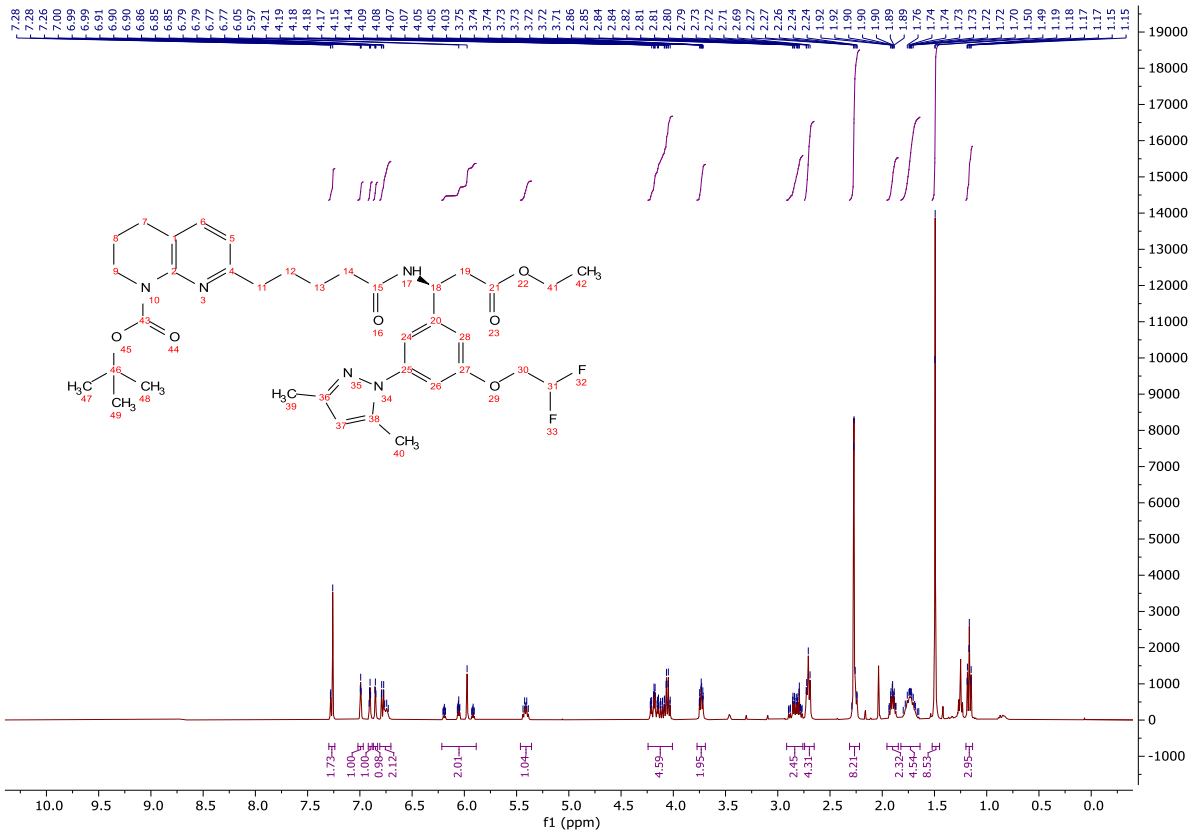
f1 (ppm)

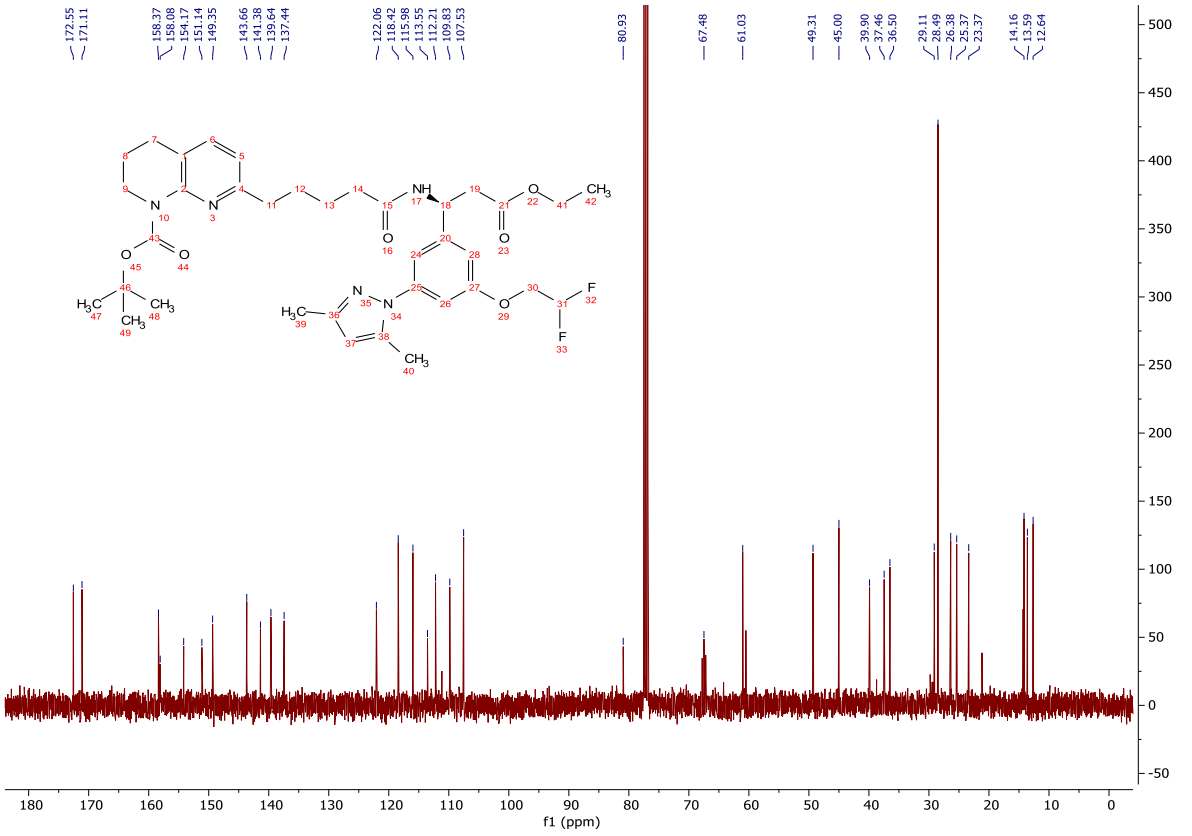
f1 (ppm)

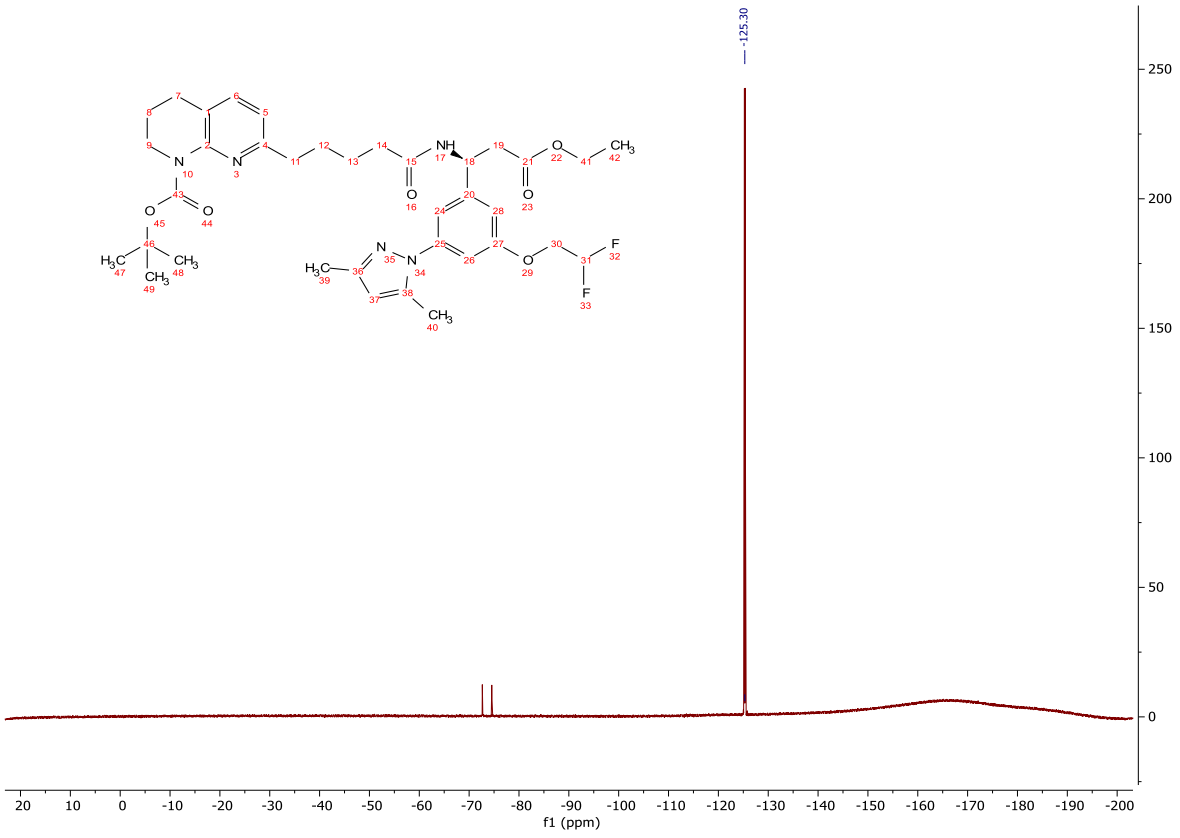
-125.30
250
200
150
100
50
0
20
10
0
-10
-20
-30
-40
-50
-60
-70
-80
-90
-100
-110
-120
-130
-140
-150
-160
-170
-180
-190
-200
f1 (ppm)

(*S*)-3-(3-(2,2-difluoroethoxy)-5-(3,5-dimethyl-1*H*-pyrazol-1-yl)phenyl)-3-(5-(5,6,7,8-tetrahydro-1,8-napthyridin-2-yl)pentanamido)propanoic acid (**293**)

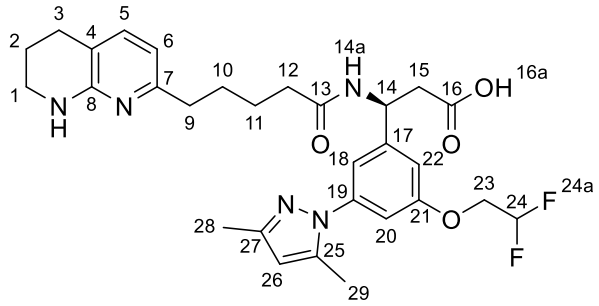

To a solution of **352** (70 mg, 0.100 mmol) in CH_2Cl_2 (2.50 mL) was added TFA (2.50 mL). The reaction mixture was stirred at rt for 7 h. The reaction mixture was concentrated *in vacuo*, dissolved in methanol (1.00 mL) and 1M $LiOH_{(aq)}$ (0.500 mL, 0.500 mmol) was added. The reaction mixture was stirred at rt for 18 h and concentrated *in vacuo*. The crude product was dissolved in a minimum volume of water and acidified to pH 5 with 2M $HCl_{(aq)}$. The precipitate was filtered and washed with water to afford the title compound as a colourless powder (55 mg, 0.099 mmol, 99%); **HRMS** *m/z* (ESI^+) calc. for $C_{29}H_{36}F_2N_5O_4$ $[M+H]^+$ requires 556.2730, found 556.2723; $\boldsymbol{R_f}$ 0.41, 5% methanol/CH_2Cl_2, UV active; δ_H (400 MHz, MeOD) 7.45 (1H, d, *J* = 7.3 Hz, H-5), 7.10 – 7.03 (2H, m, 18 and H-22H), 6.94 (1H, dd, *J* = 2.1, 2.1 Hz, H-20), 6.49 (1H, d, *J* = 7.3 Hz, H-6), 6.35 – 6.03 (2H, m, H-24 and H-26), 5.41 (1H, dd, *J* = 10.1, 4.8 Hz, H-14), 4.30 (2H, td, *J* = 13.8, 3.8 Hz, H-23), 3.50 – 3.42 (2H, m, H-1), 2.83 – 2.54 (6H, m, H-3, H-9 and H-15), 2.43 – 2.18 (8H, m, H-12, H-28 and H-29), 1.98 – 1.87 (2H, m, H-2), 1.87 – 1.64 (4H, m, H-10 and H-11); δ_C (126 MHz, DMSO-d_6) 172.2 (CO), 171.4 (CO), 157.8 (C), 156.7 (C), 155.5 (C), 147.9 (C), 145.5 (C), 140.6 (C), 139.3 (C), 136.4 (ArH), 115.2 (ArH), 114.1 (CHF_2, t, *J* = 239.2 Hz), 112.8 (C), 111.8 (ArH), 109.9 (ArH), 108.4 (ArH), 107.4 (ArH), 66.6 (CH_2, t, *J* = 26.7 Hz), 49.3 (CH), 41.3 (CH_2), 40.7 (CH_2), 36.4 (CH_2), 35.3 (CH_2), 28.8 (CH_2), 25.9 (CH_2), 25.0 (CH_2), 20.9 (CH_2), 13.3 (CH_3), 12.2 (CH_3); δ_F (376 MHz, MeOD) -127.6 (F-24a); **MP** 125-128 °C; ν_{max} (FT-ATR/cm^{-1}) 3320, 2927, 1649, 1602, 1531, 1454, 1382, 1251, 1164, 1081, 987, 853, 736, 656.

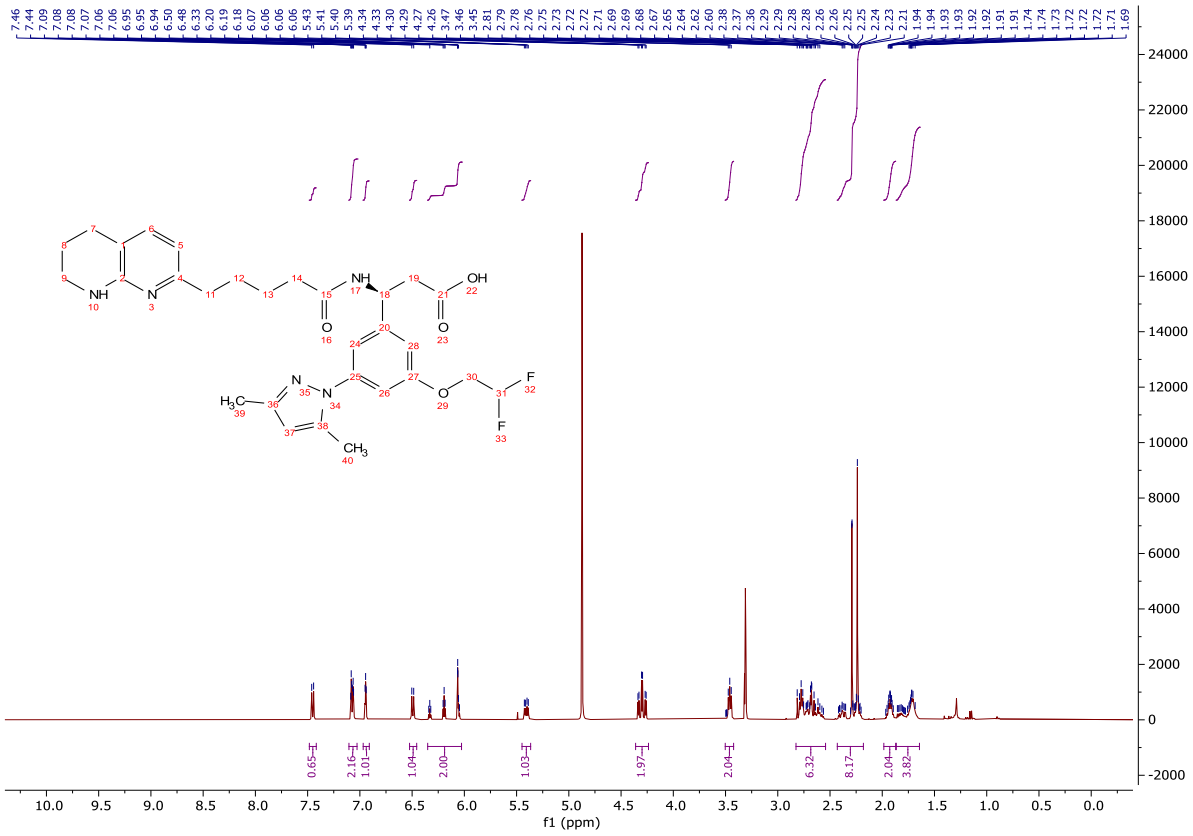
f1 (ppm)

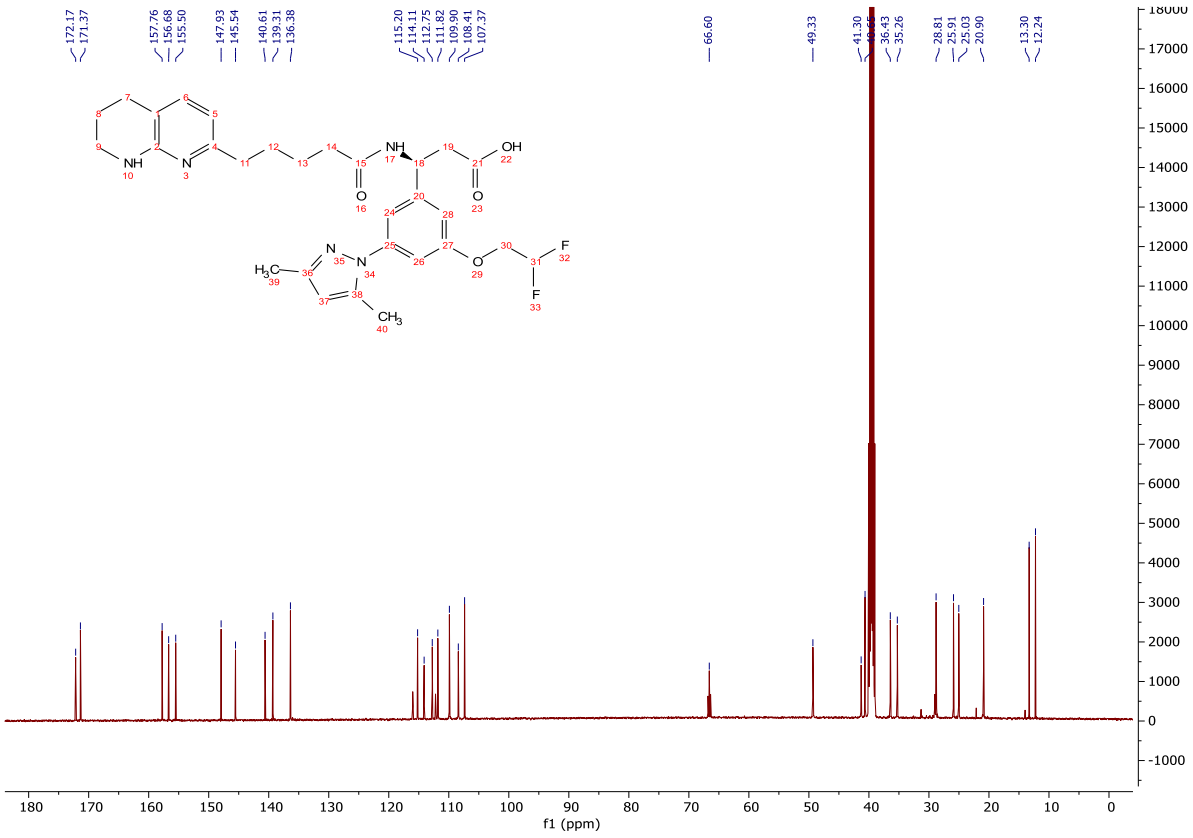
f1 (ppm)

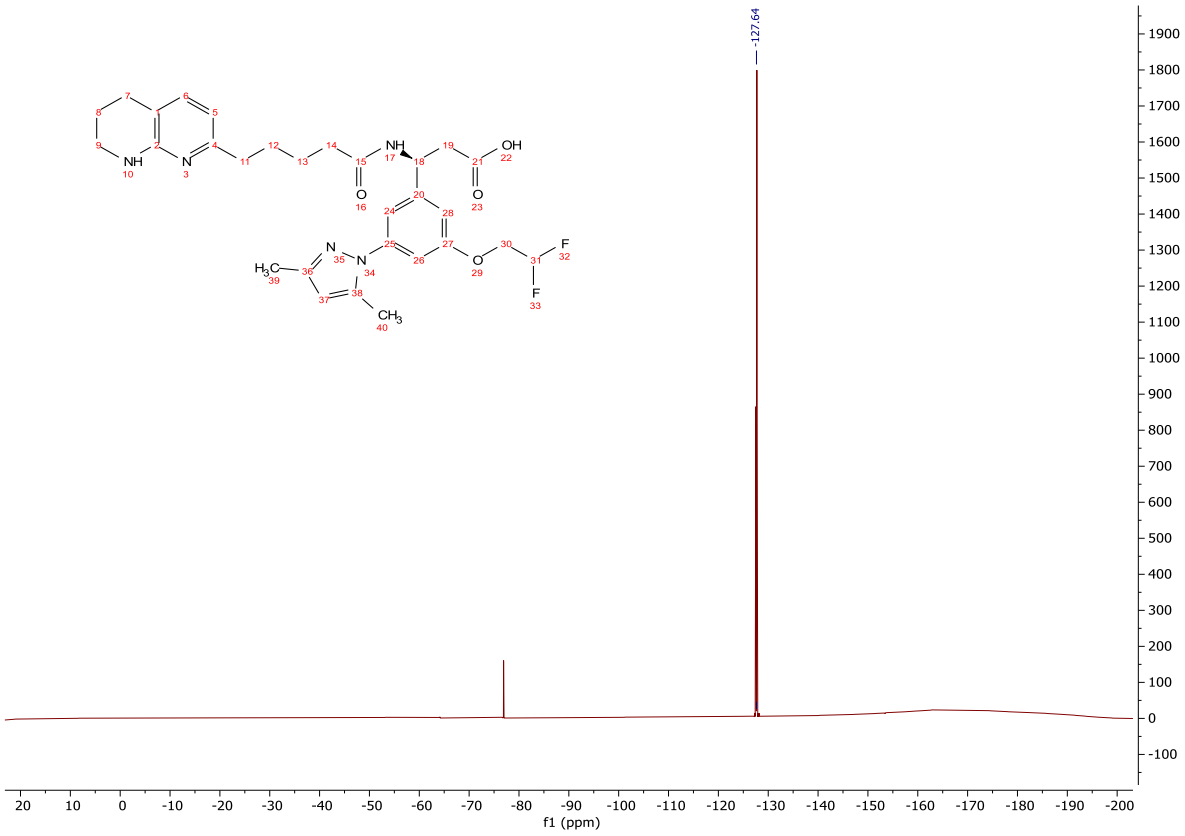
-127.64
1900
1800
1700
1600
1500
1400
1300
1200
1100
1000
900
800
700
600
500
400
300
200
100
0
-100
20 10 0 -10 -20 -30 -40 -50 -60 -70 -80 -90 -100 -110 -120 -130 -140 -150 -160 -170 -180 -190 -200
f1 (ppm)

tert-Butyl (*S*)-7-(5-((1-(3-(2,2-difluoroethoxy)-5-(3-isopropyl-1*H*-pyrazol-1-yl)phenyl)-3-ethoxy-3-oxopropyl)amino)-5-oxopentyl)-3,4-dihydro-1,8-napthyridine-1(2*H*)-carboxylate (**353**)

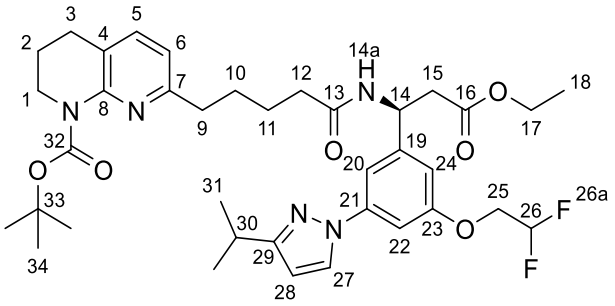

A solution of **347** (42 mg, 0.087 mmol) in 4M HCl in dioxane (5.00 mL, 20.0 mmol) was stirred at rt for 40 min and concentrated *in vacuo*. The crude product was dissolved in acetonitrile (1.00 mL) and **82** (30 mg, 0.087 mmol) was added and the mixture cooled to 0 °C. HATU (99 mg, 0.261 mmol) was added, and the reaction mixture stirred for 15 min. *i*-Pr_2NEt (0.080 mL, 0.440 mmol) was added and the reaction mixture stirred for 16 h. The reaction mixture was concentrated *in vacuo*, dissolved in ethyl acetate (10.0 mL) and washed with sat. $NaHCO_{3(aq)}$ (10.0 mL), sat. $NH_4Cl_{(aq)}$ (10.0 mL), sat. $NaHCO_{3(aq)}$ (10.0 mL) and brine (10.0 mL). The organic was dried ($MgSO_4$) and concentrated *in vacuo* giving a dark brown oil. The crude product was purified by column chromatography on silica gel, eluting with a gradient of ethyl acetate/light petroleum (0-100%) to afford the title compound as a clear, colourless oil (18 mg, 0.029 mmol, 33%); **HRMS** *m/z* (ESI^+) calc. for $C_{37}H_{50}F_2N_5O_6$ $[M+H]^+$ requires 698.3724, found 698.3712; $\boldsymbol{R_f}$ 0.32, 80% ethyl acetate/light petroleum, UV active; δ_H (400 MHz, $CDCl_3$) 7.76 (1H, d, *J* = 2.5 Hz, H-27), 7.30 – 7.23 (1H, m, H-5), 7.20 (1H, dd, *J* = 1.7, 1.7 Hz, H-20), 7.17 (1H, dd, *J* = 2.1, 2.1 Hz, H-24), 6.82 – 6.69 (3H, m, H-6, H-14a and H-22), 6.26 (1H, d, *J* = 2.5 Hz, H-28), 6.07 (1H, tt, *J* = 55.0, 4.1 Hz, H-26), 5.41 (1H, dt, *J* = 8.4, 6.1 Hz, H-14), 4.21 (2H, td, *J* = 13.1, 4.1 Hz, H-25), 4.07 (2H, q, *J* = 7.1 Hz, H-17), 3.77 – 3.70 (2H, m, H-1), 3.12 – 3.00 (1H, m, H-30), 2.93 – 2.77 (2H, m, H-15), 2.76 – 2.67 (4H, m, H-3 and H-9), 2.32 – 2.24 (2H, m, H-12), 1.96 – 1.85 (2H, m, H-2), 1.83 – 1.64 (4H, m, H-10 and H-11), 1.50 (9H, s, H-34), 1.30 (6H, d, *J*

= 6.9 Hz, H-31), 1.17 (3H, t, *J* = 7.1 Hz, H-18); δ_C (101 MHz, $CDCl_3$) 172.6 (CO), 171.2 (CO), 161.4 (C), 158.8 (C), 154.2 (CO), 151.2 (C), 144.1 (C), 141.9 (C), 137.5 (ArH), 127.4 (ArH), 122.1 (C), 118.5 (ArH), 113.6 (CHF_2), 110.5 (ArH), 110.3 (ArH), 105.0 (ArH), 104.6 (ArH), 81.0 (C), 67.5 (CH_2, assigned by HSQC), 61.1 (CH_2), 49.5 (CH), 45.0 (CH_2), 40.1 (CH_2), 37.5 (CH_2), 36.6 (CH_2), 29.1 (CH_2), 28.5 (CH_3), 28.2 (CH), 26.4 (CH_2), 25.4 (CH_2), 23.4 (CH_2), 22.9 (CH_3), 14.2 (CH_3); δ_F (376 MHz, $CDCl_3$) -125.3 (F-26a); ν_{max} (FT-ATR/cm^{-1}) 3312, 2926, 1732, 1690, 1651, 1600, 1531, 1463, 1367, 1252, 1149, 1076, 845, 696, 457.

N.B. One aryl quaternary carbon is not observed.

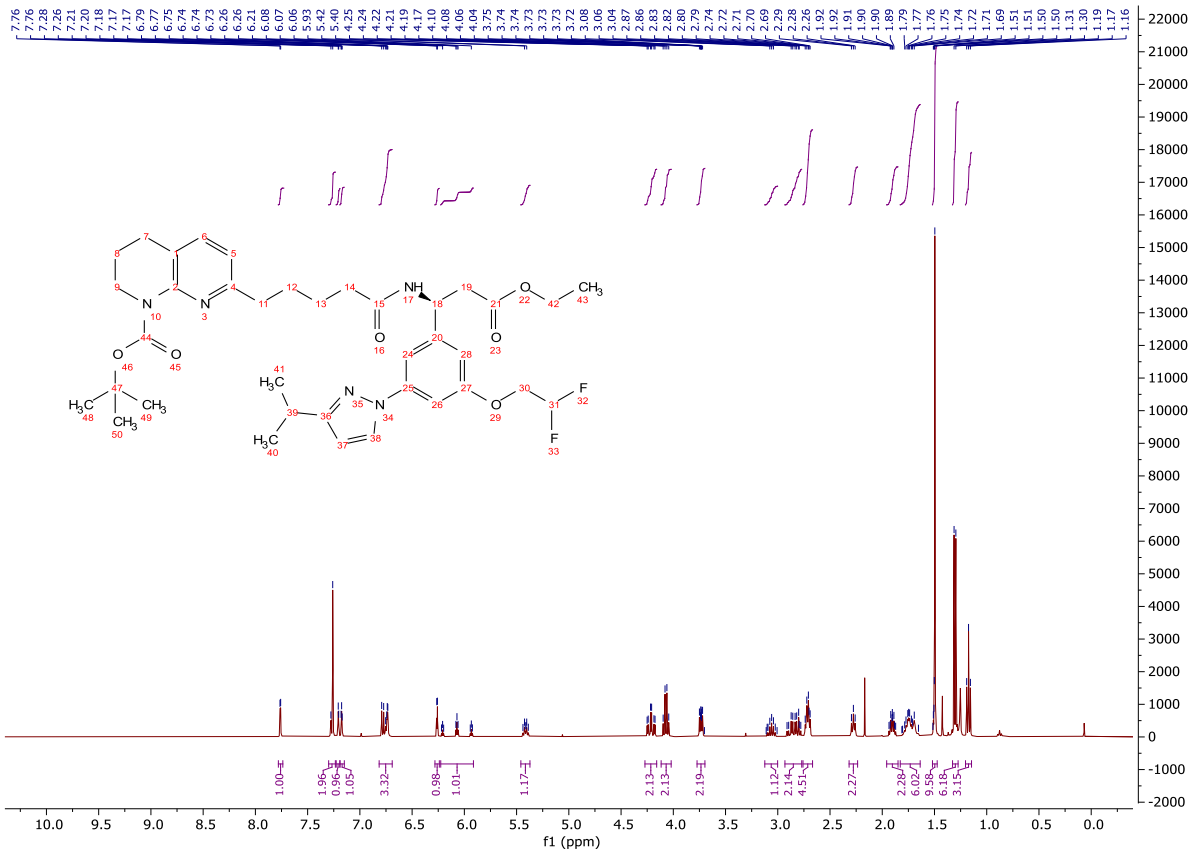
f1 (ppm)

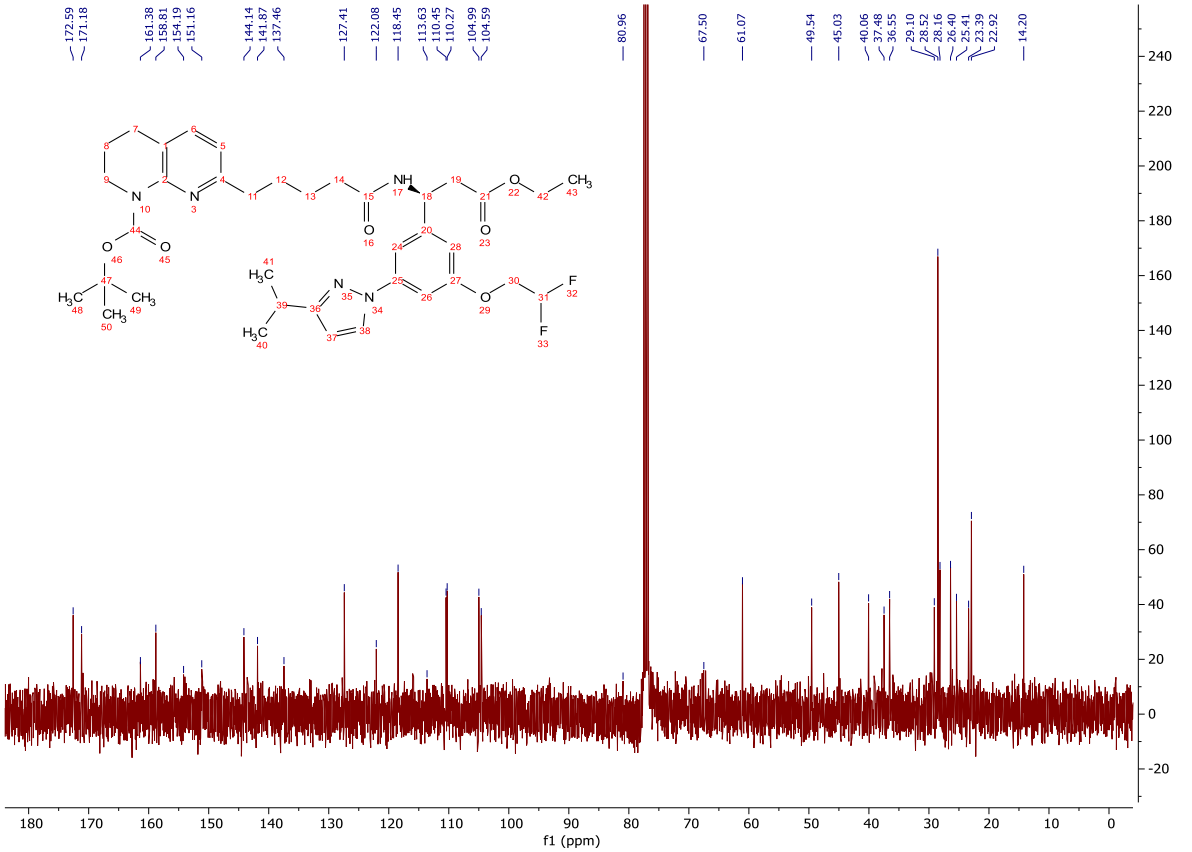
f1 (ppm)

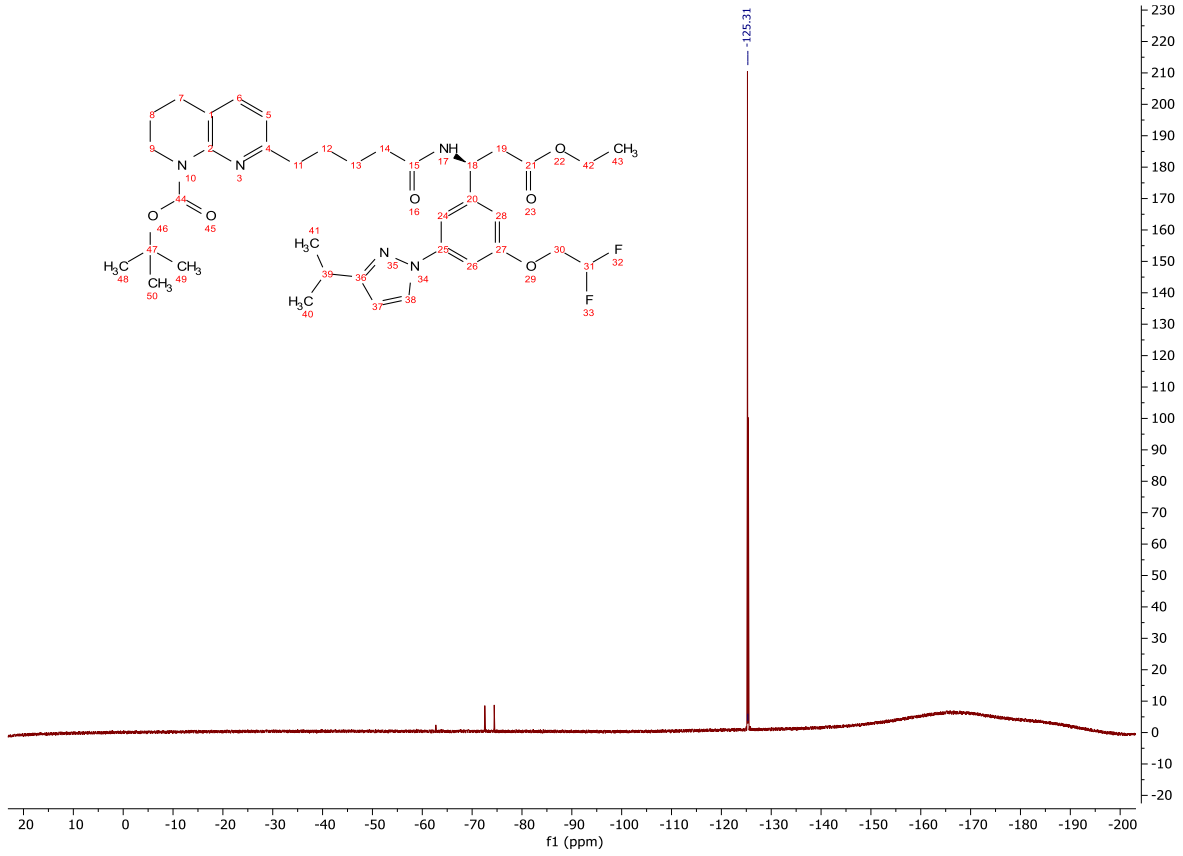
-125.31
f1 (ppm)

(*S*)-3-(3-(2,2-difluoroethoxy)-5-(3-isopropyl-1*H*-pyrazol-1-yl)phenyl)-3-(5-(5,6,7,8-tetrahydro-1,8-napthyridin-2-yl)pentanamido)propanoic acid (**290**)

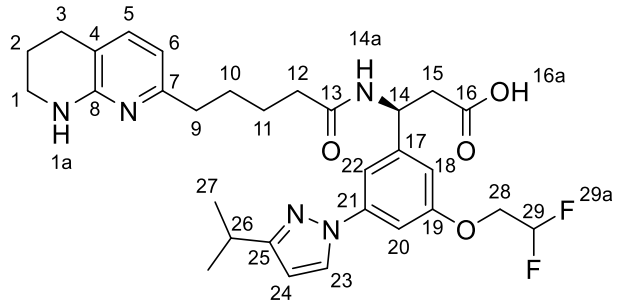

To a solution of **353** (20 mg, 0.029 mmol) in CH_2Cl_2 (2.50 mL) was added TFA (2.50 mL). The reaction mixture was stirred at rt for 7 h. The reaction mixture was concentrated *in vacuo*, dissolved in methanol (1.00 mL) and 1M $LiOH_{(aq)}$ (0.145 mL, 0.145 mmol) was added. The reaction mixture was stirred at rt for 18 h and concentrated *in vacuo*. The crude product was dissolved in a minimum volume of water and acidified to pH 5 with 2M $HCl_{(aq)}$. The precipitate was filtered and washed with water to afford the title compound as a colourless powder (16 mg, 0.029 mmol, 99%); **HRMS** *m/z* (ESI^+) calc. for $C_{30}H_{38}F_2N_5O_4$ $[M+H]^+$ requires 570.2886, found 570.2875; $\boldsymbol{R_f}$ 0.34, 5% methanol/CH_2Cl_2, UV active; δ_H (400 MHz, MeOD) 8.09 (1H, d, *J* = 2.5 Hz, H-23), 7.47 (1H, d, *J* = 7.3 Hz, H-5), 7.36 (1H, dd, *J* = 2.0 Hz, H-22), 7.23 (1H, dd, *J* = 2.2 Hz, H-18), 6.92 (1H, dd, *J* = 2.0 Hz H-20), 6.50 (1H, d, *J* = 7.3 Hz, H-6), 6.38 – 6.04 (2H, m, H-24 and H-29), 5.39 (1H, t, *J* = 7.4 Hz, H-14), 4.31 (2H, td, *J* = 13.7, 3.8 Hz, H-28), 3.47 (2H, t, *J* = 5.7 Hz, H-1), 3.04 (1H, hept, *J* = 6.9 Hz, H-26), 2.85 – 2.56 (6H, m, H-3, H-9 and H-15), 2.44 – 2.18 (2H, m, H-12), 2.00 – 1.87 (2H, m, H-2), 1.86 – 1.63 (4H, m, H-10 and H-11), 1.36 – 1.25 (6H, m, H-27); δ_C (126 MHz, <u>DMSO-d_6</u>) δ 172.0 (CO), 171.3 (CO); δ_C (101 MHz, <u>MeOD</u>) 175.0 (CO), 162.6 (C), 160.4 (C), 153.5 (C), 150.2 (C), 147.4 (C), 142.8 (C), 142.3 (ArH), 129.6 (ArH), 120.2 (C), 115.3 (CHF_2, t, *J* = 239.2 Hz), 111.6 (ArH), 111.4 (ArH), 111.3 (ArH), 105.7 (ArH), 105.3 (ArH), 68.5 (CH_2, t, *J* = 28.6 Hz), 52.6 (CH), 44.4 (CH_2), 41.9 (CH_2), 36.2 (CH_2), 33.6 (CH_2), 30.8 (CH_2), 29.3 (CH_2), 29.2 (CH), 26.4 (CH_2), 26.0 (CH_2), 23.2 (CH_3), 20.7 (CH_2); δ_F (376 MHz,

MeOD) -76.9 (F-29a), -127.6 (F-29a); **MP** Degrades >200 °C; ν_{max} (FT-ATR/cm^{-1}) 3308, 2926, 2646, 1597, 1530, 1489, 1453, 1394, 1286, 1199, 1132, 1073, 847, 764, 548.

N.B. C-13 and C-16 are observed in DMSO, but two aryl quaternary carbons are not. In MeOD, all quaternary carbons are observed, but one carbonyl carbon is not.

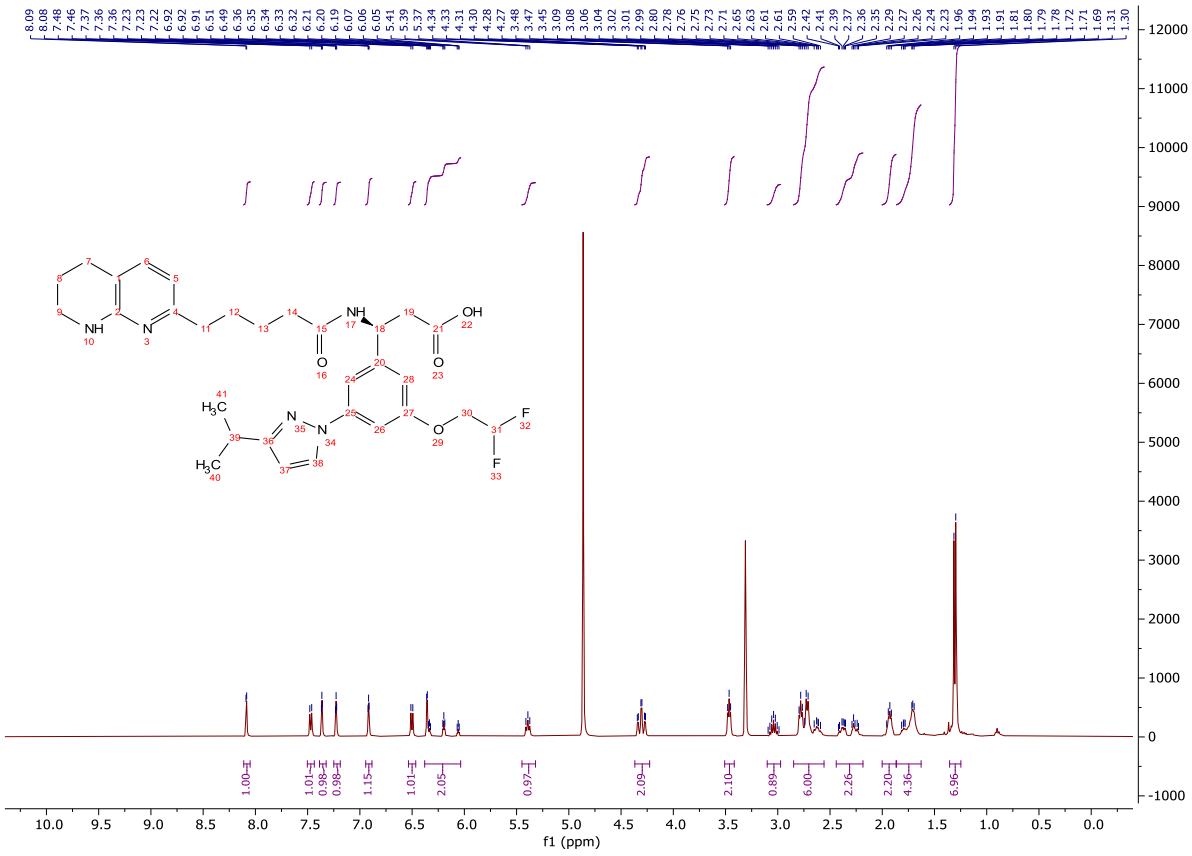
f1 (ppm)

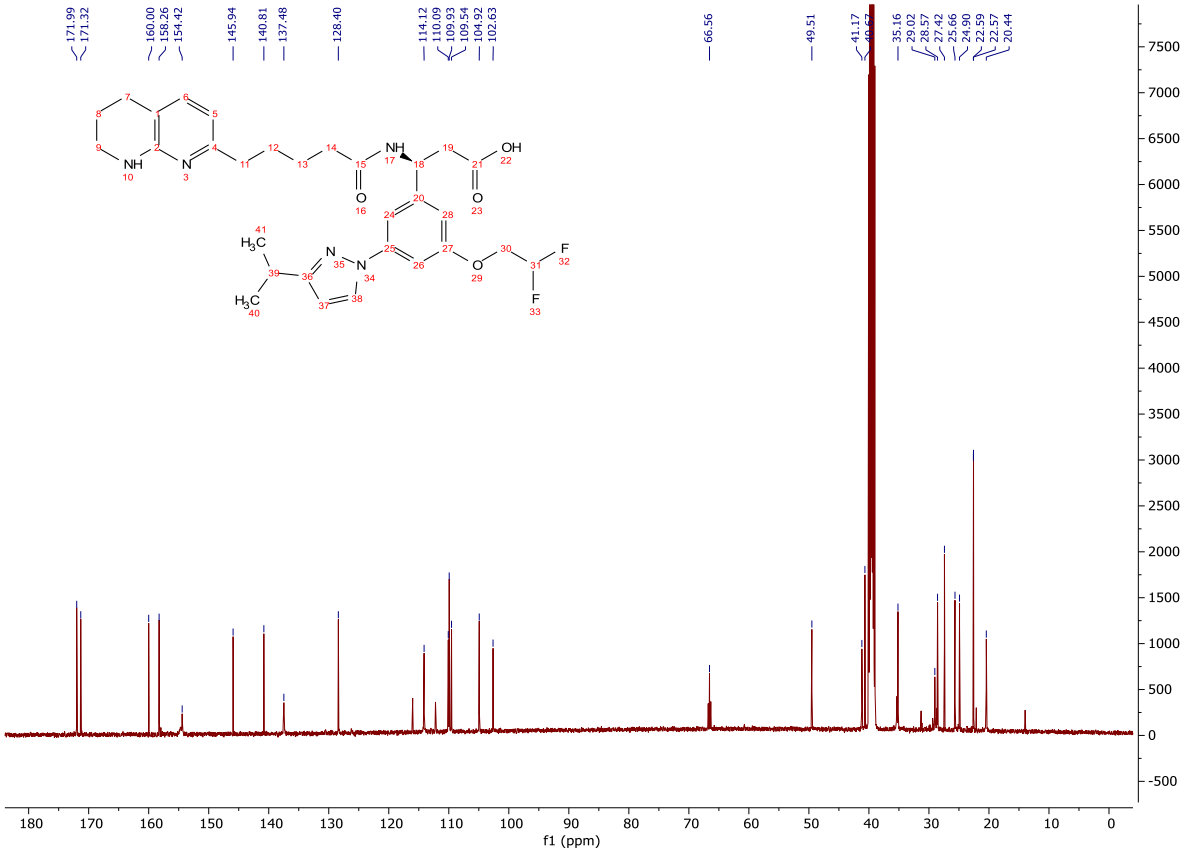
f1 (ppm)

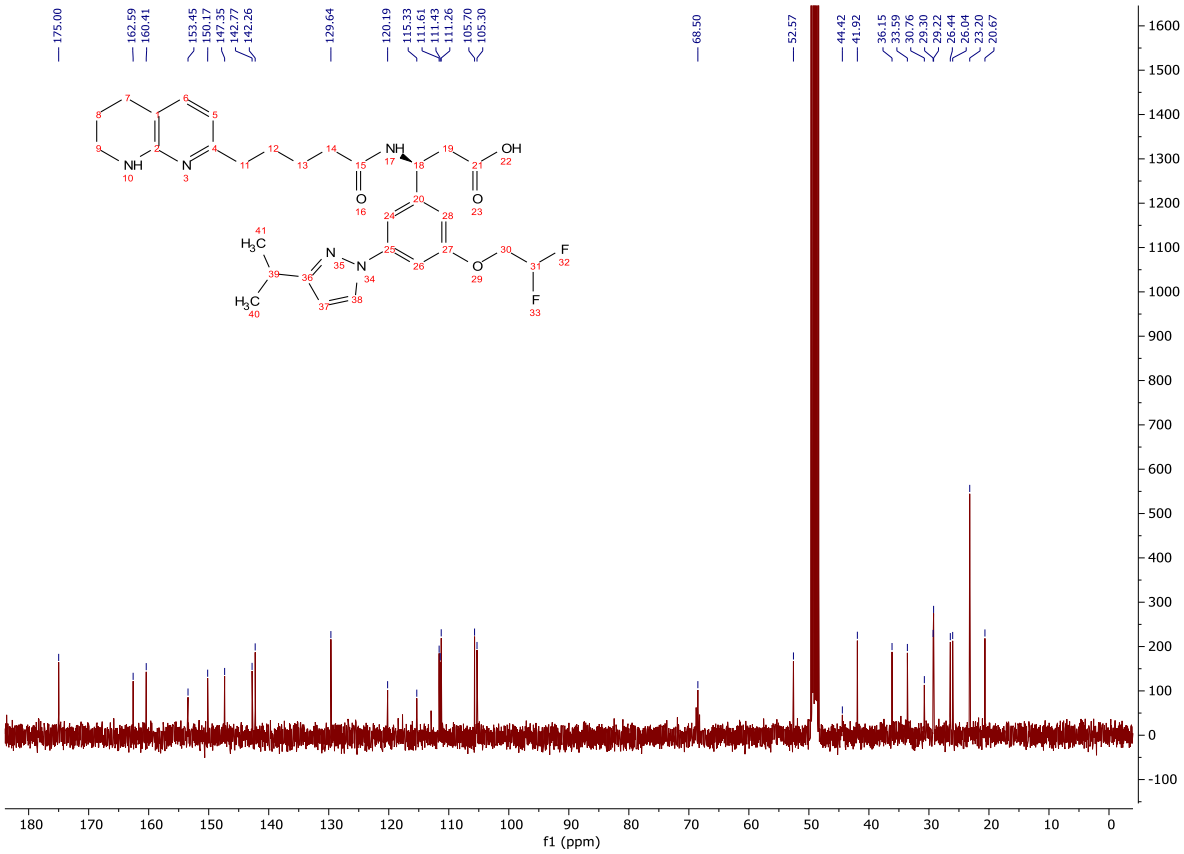
175.00
162.59
160.41
153.45
150.17
147.35
142.77
142.26
129.64
120.19
115.33
111.61
111.43
111.26
105.70
105.30
68.50
52.57
44.42
41.92
36.15
33.59
30.76
29.30
29.22
26.44
26.04
23.20
20.67
f1 (ppm)

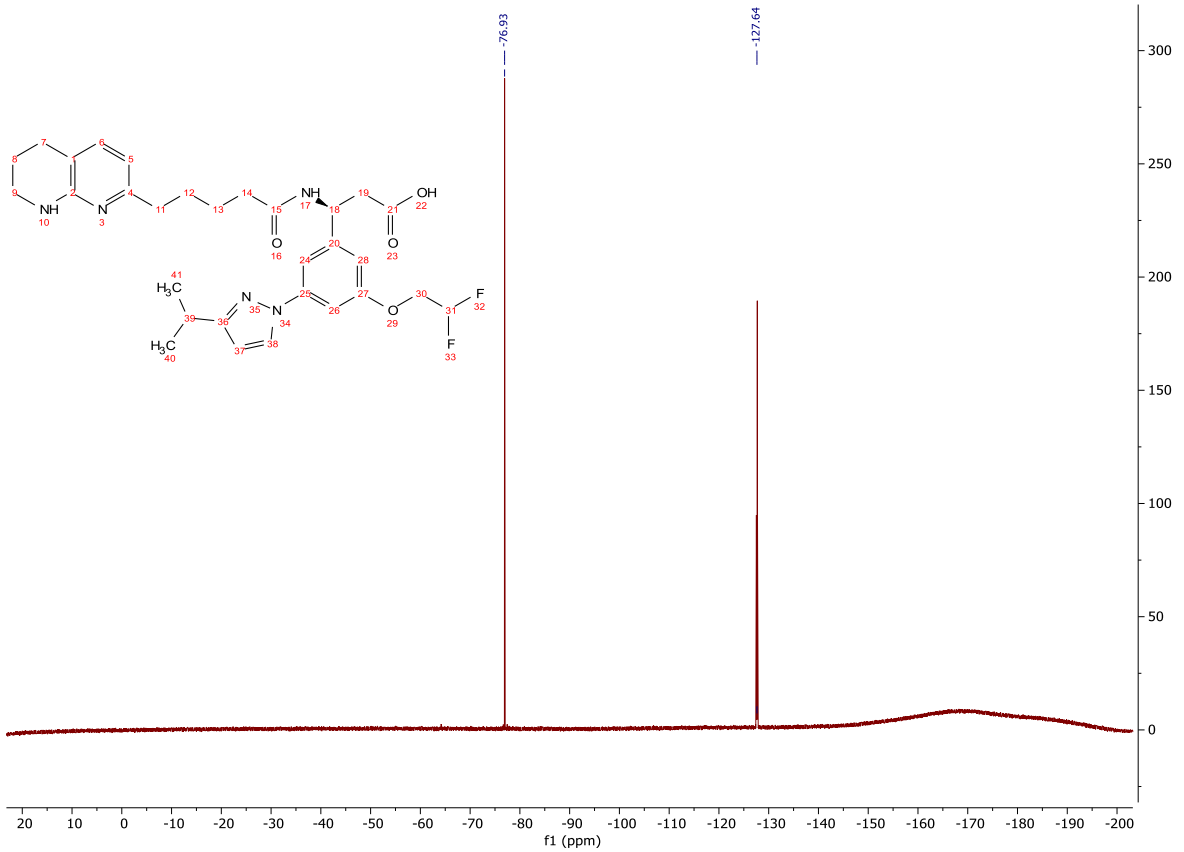
-76.93
-127.64
f1 (ppm)

N-(3-(Benzyloxy)phenyl)-3-bromo-4-methylpyridin-2-amine (**450**)

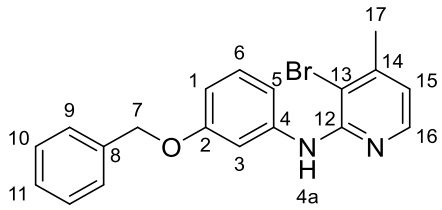

A suspension of 2-amino-3-bromo-4-picoline (**449**, 500 mg, 2.69 mmol), 1-(benzyloxy)-3-iodobenzene (**448**, 1.00 g, 3.23 mmol), Pd_2dba_3 (99 mg, 0.108 mmol), xantphos (124 mg, 0.215 mmol) and sodium *tert*-butoxide (516 mg, 5.38 mmol) in *ortho*-xylene (13.0 mL) under a nitrogen atmosphere was heated at 110 °C for 16 h. The reaction mixture was cooled to rt, filtered through Celite®, washing the filter cake with ethyl acetate, then concentrated *in vacuo*. The crude product was purified *via* column chromatography on silica gel, eluting with a gradient of ethyl acetate/light petroleum (0-20%) to give the title compound as a yellow oil (893 mg, 2.43 mmol, 90%); **HRMS** *m/z* (ESI^+) calc. for $C_{19}H_{18}BrN_2O$ $[M+H]^+$ requires 369.0597, found 369.0593; $\mathbf{R_f}$ 0.30, 5% ethyl acetate/cyclohexane, UV active; δ_H (400 MHz, $CDCl_3$) 8.01 (1H, d, *J* = 4.9 Hz, H-16), 7.51 (1H, dd, *J* = 2.3, 2.3 Hz, H-3), 7.49 – 7.44 (2H, m, H-9), 7.42 – 7.36 (2H, m, H-10), 7.35 – 7.30 (1H, m, H-11), 7.27 – 7.20 (1H, m, H-6), 7.14 (1H, bs, H-4a), 7.10 (1H, ddd, *J* = 8.1, 2.1, 0.9 Hz, H-5), 6.70 – 6.61 (2H, m, H-1 and H-15), 5.09 (2H, s, H-7), 2.39 (3H, s, H-17)*; δ_C (101 MHz, $CDCl_3$) 159.6 (C), 152.1 (C), 147.8 (C), 145.5 (ArH), 141.5 (C), 137.3 (C), 129.7 (ArH), 128.7 (ArH), 128.0 (ArH), 127.7 (ArH), 117.5 (ArH), 112.7 (ArH), 109.0 (ArH), 106.8 (ArH), 70.1 (CH_2), 23.4 (CH_3); ν_{max} (FT-ATR/cm^{-1}) 3417, 1601,1525, 1449, 1372, 1266, 1157, 1023, 870, 813, 756, 738, 681, 514.

*Confirmed as CH_3 by HSQC NMR

N.B. One aryl quaternary carbon is not observed.

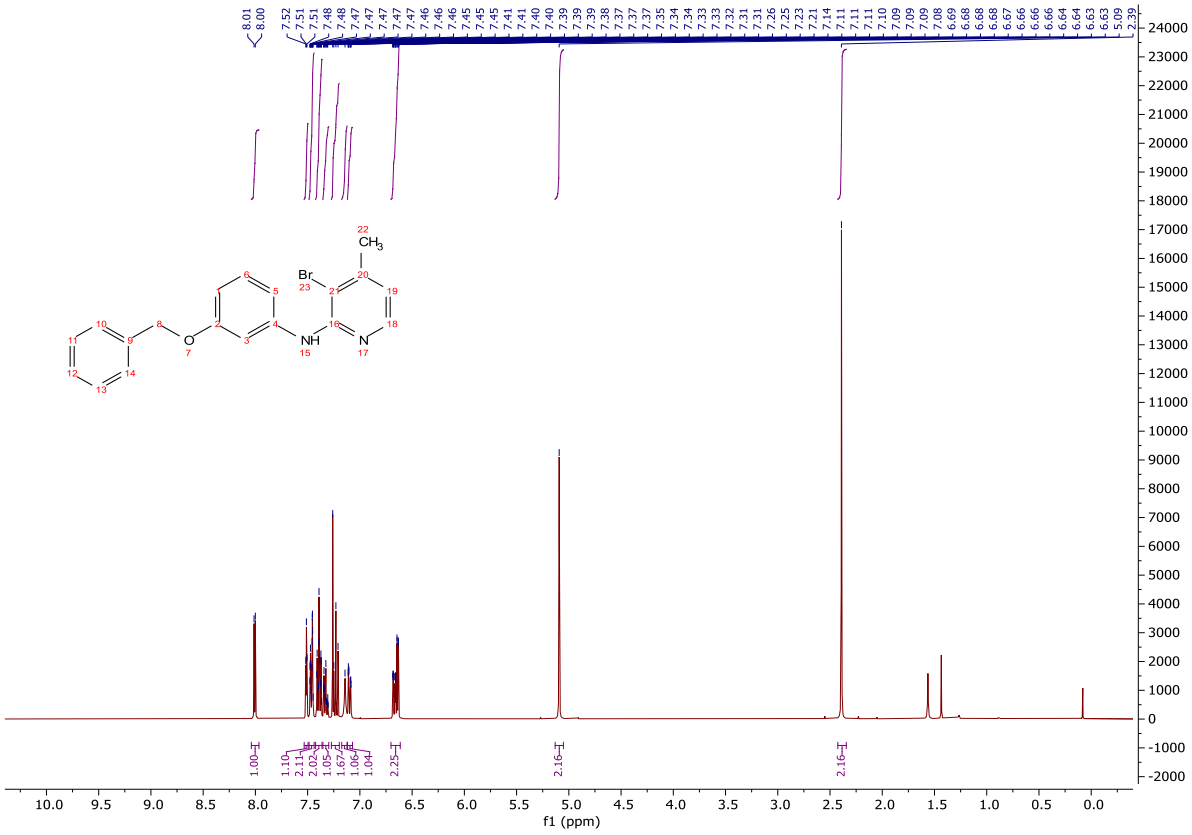
8.01
8.00
7.52
7.51
7.51
7.48
7.48
7.47
7.47
7.47
7.47
7.47
7.46
7.46
7.46
7.45
7.45
7.45
7.41
7.41
7.40
7.40
7.39
7.39
7.39
7.38
7.37
7.37
7.35
7.34
7.34
7.33
7.33
7.32
7.31
7.31
7.26
7.25
7.23
7.21
7.14
7.11
7.11
7.10
7.09
7.09
7.09
7.08
6.69
6.68
6.68
6.68
6.67
6.66
6.66
6.66
6.64
6.64
6.63
6.63
5.09
2.39
1.00
1.10
2.11
2.02
1.05
1.67
1.06
1.04
2.25
2.16
2.16
f1 (ppm)

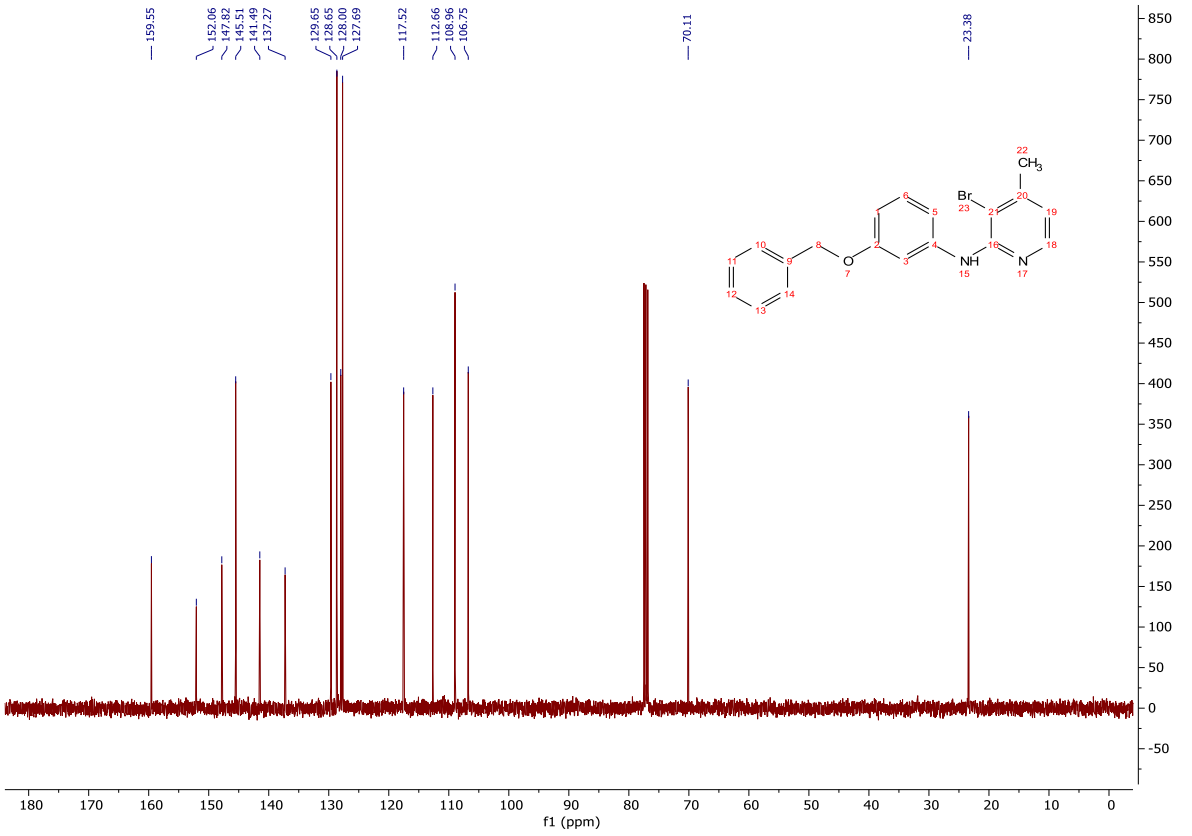
159.55
152.06
147.82
145.51
141.49
137.27
129.65
128.65
128.00
127.69
117.52
112.66
108.96
106.75
70.11
23.38
f1 (ppm)

7-(Benzyloxy)-4-methyl-9*H*-pyrido[2,3-*b*]indole (**451**)

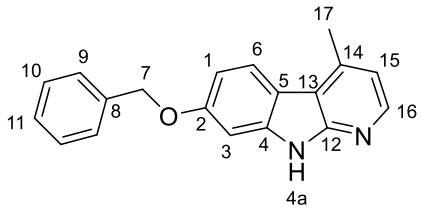

A suspension of **450** (58 mg, 0.158 mmol), $Pd(OAc)_2$ (2 mg, 0.008 mmol), $PCy_3.HBF_4$ (6 mg, 0.158 mmol) and DBU (0.050 mL, 0.316 mmol) in dimethylacetamide/*ortho*-xylene (1:1, 1.00 mL) under an argon atmosphere was heated at 145 °C for 16 h. The reaction mixture was cooled to rt, filtered through Celite® and concentrated *in vacuo*. The gum was diluted with ethyl acetate (10.0 mL) and washed with sat. $NaHCO_{3(aq)}$ (2 x 10.0 mL), brine (10.0 mL), dried (Na_2SO_4) and concentrated *in vacuo*. The crude product was purified *via* column chromatography on silica gel, eluting with a gradient of ethyl acetate/light petroleum (0-100%) to give the title compound as a beige powder (5 mg, 0.017 mmol, 11%); **HRMS** *m/z* (ESI^+) calc. for $C_{19}H_{17}N_2O$ $[M+H]^+$ requires 289.1335, found 289.1341; $\mathbf{R_f}$ 0.33, 40% ethyl acetate/cyclohexane, UV active; δ_H (500 MHz, DMSO-d_6) 11.64 (1H, s, H-4a), 8.17 (1H d, *J* = 4.9 Hz, H-16), 7.98 (1H, d, *J* = 8.6 Hz, H-6), 7.53 – 7.47 (2H, m, H-9), 7.45 – 7.38 (2H, m, H-10), 7.37 – 7.31 (1H, m, H-11), 7.06 (1H, d, *J* = 2.3 Hz, H-3), 6.98 – 6.95 (1H, m, H-15), 6.93 (1H, dd, *J* = 8.6, 2.3 Hz, H-1), 5.21 (2H, s, H-7), 2.75 (3H, s, H-17); δ_C (Assigned by HSQC, DMSO-d_6) 143.9 (ArH), 127.9 (ArH), 127.6 (ArH), 127.3 (ArH), 123.4 (ArH), 116.5 (ArH), 108.7 (ArH), 95.6 (ArH), 69.2 (CH_2), 19.0 (CH_3).

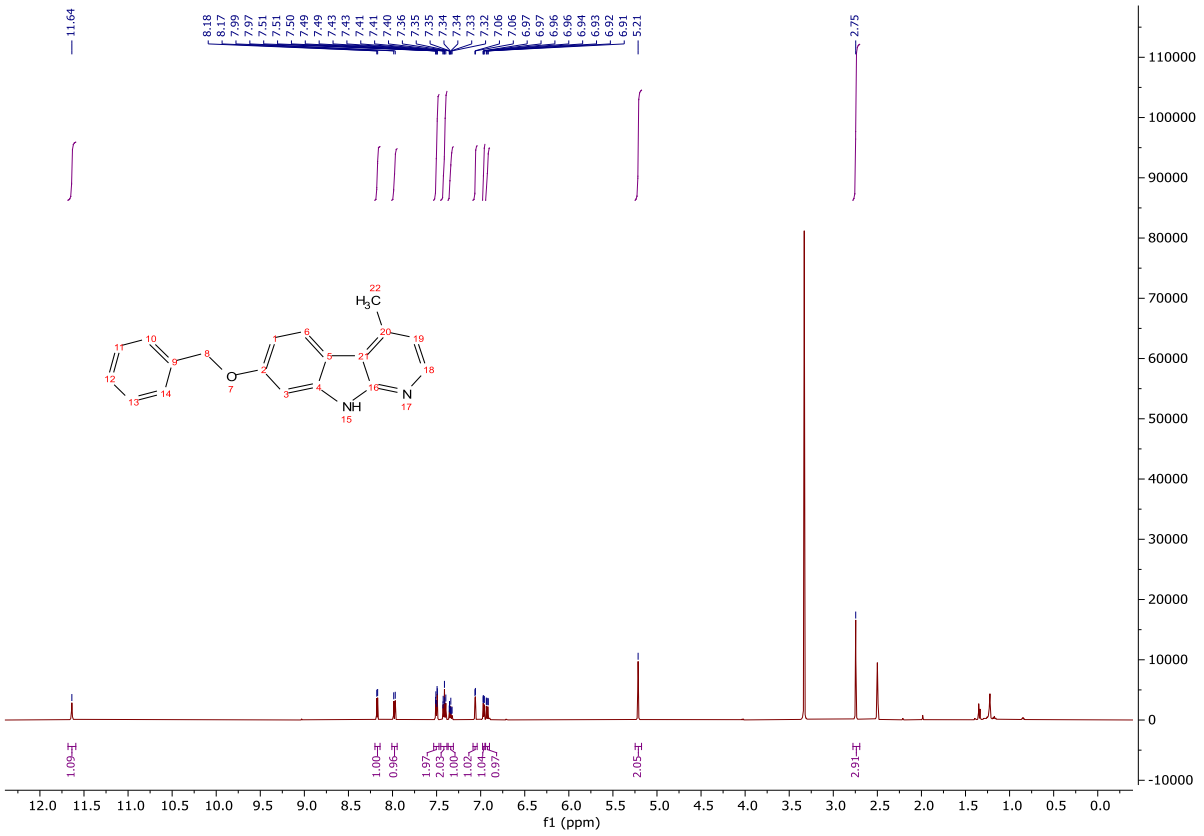
11.64
8.18
8.17
7.99
7.97
7.51
7.51
7.50
7.49
7.49
7.43
7.43
7.41
7.41
7.40
7.36
7.35
7.35
7.34
7.34
7.33
7.32
7.06
7.06
6.97
6.97
6.96
6.96
6.94
6.93
6.92
6.91
5.21
2.75
1.09
1.00
0.96
1.97
2.03
1.00
1.02
1.04
0.97
2.05
2.91
f1 (ppm)

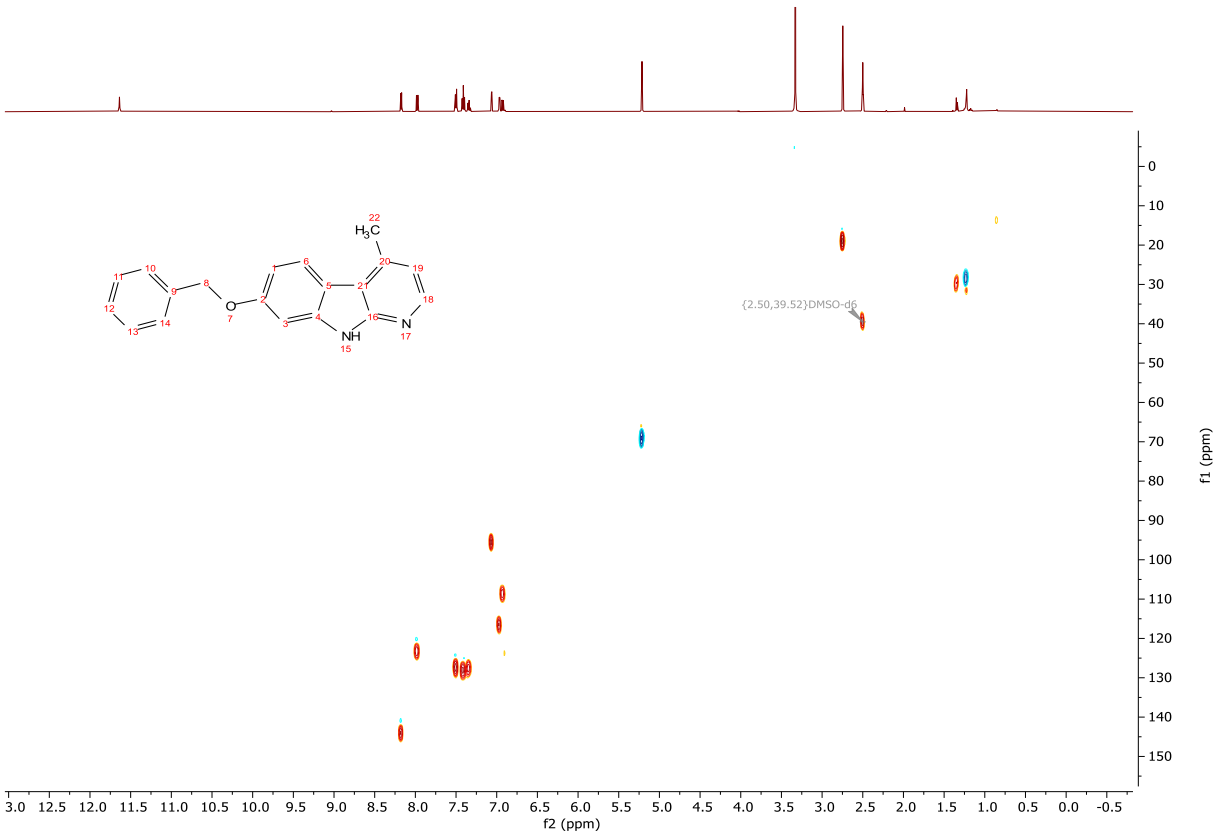
{2.50,39.52}DMSO-d6
f1 (ppm)
f2 (ppm)

tert-Butyl 6-(benzyloxy)-3-(2-ethoxy-2-oxoacetyl)-1*H*-indole-1-carboxylate (**457**)

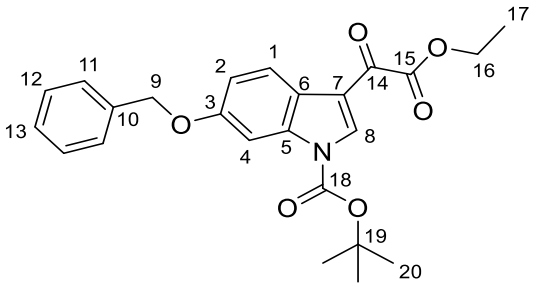

To a suspension of 6-benzyloxyindole (**455**, 10.0 g, 44.8 mmol) in anhydrous diethyl ether (150 mL) at 0 °C under a nitrogen atmosphere was added oxalyl chloride (3.80 mL, 44.8 mmol) dropwise. The reaction mixture was stirred for 16 h, water (10.0 mL) was added, and the mixture stirred for 5 min. The mixture was concentrated *in vacuo*, affording a brown solid. The crude acid was dissolved in THF (210 mL) and stirred at 0 °C. EDC.HCl (12.2 g, 63.3 mmol) and ethanol (4.92 mL, 84.4 mmol) were added, and the reaction mixture stirred for 5 min, after which time DMAP (515 mg, 4.22 mmol) was added. The reaction mixture was stirred for 16 h. The solvent was removed *in vacuo* and the resulting solid was then dissolved in THF/DMF (4:1, 250 mL). Di-*tert*-butyl dicarbonate (9.66 g, 44.3 mmol) was added and the reaction mixture was stirred for 16 h. The solvent was removed *in vacuo*, the gum was diluted with ethyl acetate (250 mL) and the organic washed with water (250 mL), 10% $LiCl_{(aq)}$ (250 mL), sat. $NaHCO_{3(aq)}$ (250 mL) and brine (250 mL), dried (Na_2SO_4) and concentrated *in vacuo*. The crude product was purified *via* column chromatography on silica gel, eluting with a gradient of ethyl acetate/light petroleum (0-25%) to give the title compound as an off-white solid (16.5 g, 39.0 mmol, 87%); **HRMS** *m/z* (ESI^+) calc. for $C_{24}H_{25}NNaO_6$ $[M+Na]^+$ requires 446.1574, found 446.1568; $\mathbf{R_f}$ 0.38, 20% ethyl acetate/cyclohexane, UV active; δ_H (400 MHz, $CDCl_3$) 8.67 (1H, s, H-8), 8.26 (1H, d, *J* = 8.7 Hz, H-1), 7.84 (1H, d, *J* = 2.4 Hz, H-4), 7.50 – 7.44 (2H, m, H-11), 7.43 – 7.37 (2H, m, H-12), 7.36 – 7.31 (1H, m, H-13), 7.09 (1H, dd, *J* = 8.7, 2.4 Hz, H-2), 5.14 (2H, s, H-9), 4.44 (2H, q, *J* = 7.2 Hz, H-16), 1.70 (9H, s, H-20), 1.45 (3H, t, *J* = 7.2 Hz, H-17); δ_C (101 MHz, $CDCl_3$) 179.3 (CO), 162.1 (CO), 158.1 (C), 148.9 (CO), 136.9 (C), 136.6 (C), 136.2 (ArH), 128.7 (ArH), 128.2 (ArH), 127.7 (ArH), 123.3 (ArH), 121.4 (C), 116.5 (C), 114.7

(ArH), 100.6 (ArH), 85.9 (C), 70.5 (CH_2), 62.5 (CH_2), 28.2 (CH_3), 14.2 (CH_3); **MP** 105-107 °C; ν_{max} (FT-ATR/cm^{-1}) 2985, 1746, 1658, 1535, 1491, 1365, 1279, 1221, 1137, 1100, 1023, 951, 817, 734.

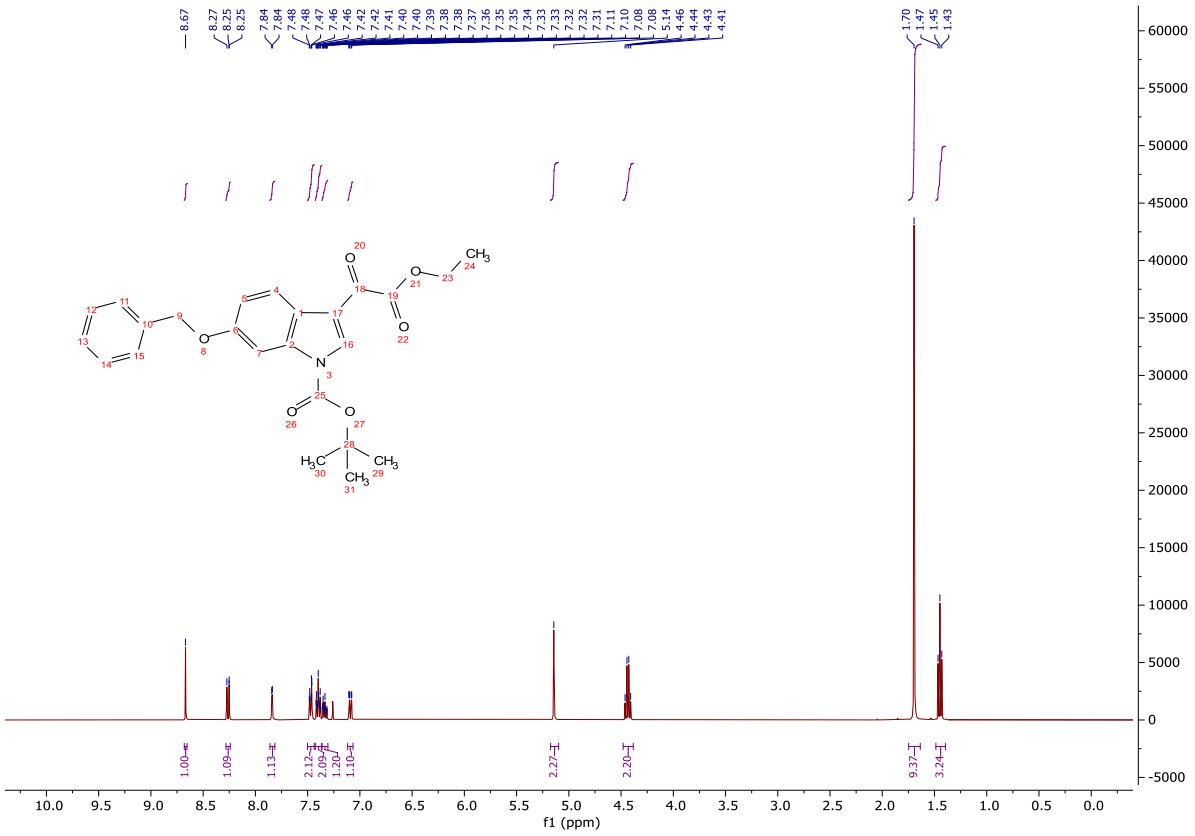
8.67
8.27
8.25
8.25
7.84
7.84
7.48
7.48
7.47
7.46
7.46
7.42
7.42
7.41
7.40
7.40
7.39
7.38
7.38
7.37
7.36
7.35
7.35
7.34
7.33
7.33
7.32
7.32
7.31
7.11
7.10
7.08
7.08
5.14
4.46
4.44
4.43
4.41
1.70
1.47
1.45
1.43
1.00
1.09
1.13
2.12
2.09
1.20
1.10
2.27
2.20
9.37
3.24
f1 (ppm)

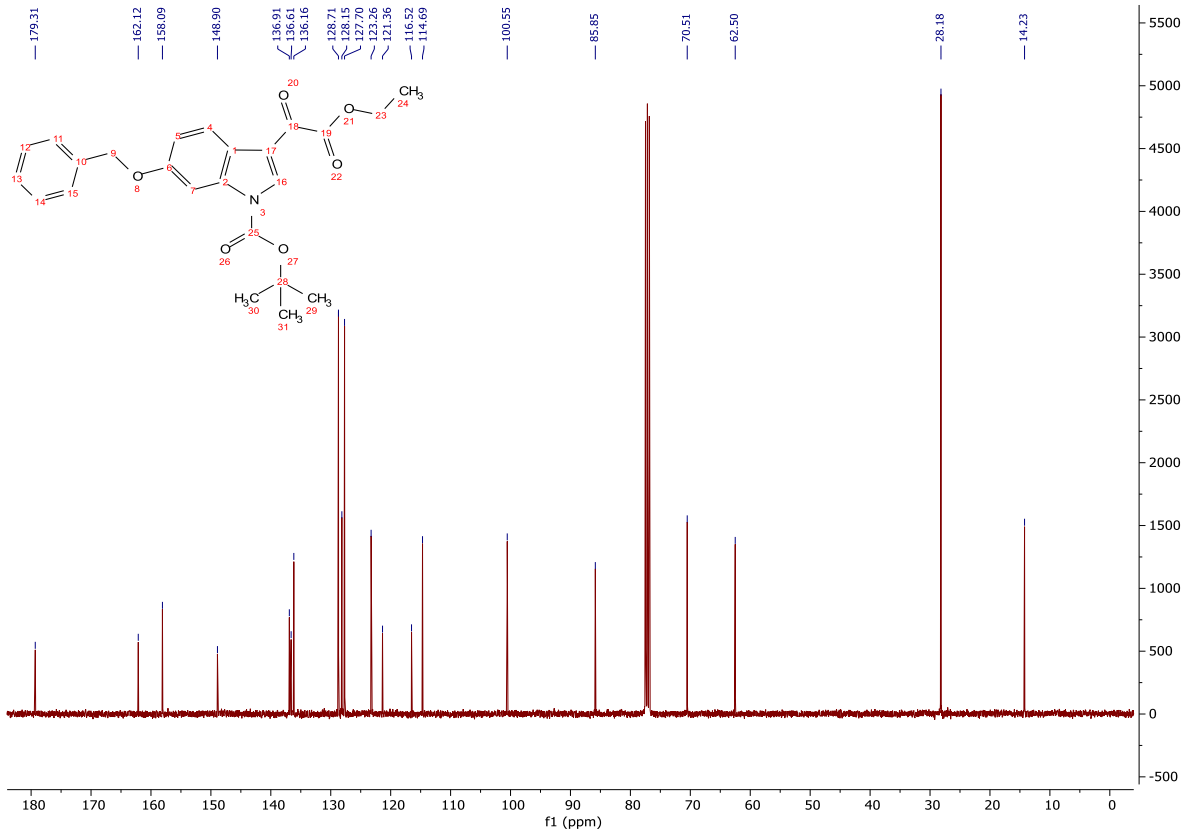
179.31
162.12
158.09
148.90
136.91
136.61
136.16
128.71
128.15
127.70
123.26
121.36
116.52
114.69
100.55
85.85
70.51
62.50
28.18
14.23
f1 (ppm)

Diethyl (2-oxoethyl)phosphonate (**428**)

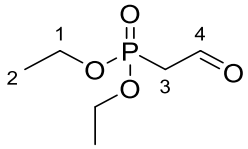

A solution of diethyl (2-ethoxy-2-methoxyethyl)phosphonate (**458**, 10.0 mL, 41.4 mmol) in 2M $HCl_{(aq)}$ (125 mL) was stirred at rt for 16 h. The reaction mixture was extracted with CH_2Cl_2 (6 x 50.0 mL), the organics were combined, dried (Na_2SO_4) and concentrated *in vacuo* to afford the title compound as a clear, colourless oil (7.04 g, 39.1 mmol, 94%); **HRMS** *m/z* (ESI^+) calc. for $C_6H_{13}NaO_4P$ $[M+Na]^+$ requires 203.0444, found 203.0441; δ_H (400 MHz, $CDCl_3$) 9.66 (1H, td, *J* = 3.2, 1.0 Hz, H-4), 4.24 – 4.10 (4H, m, H-1), 3.07 (2H, dd, *J* = 21.9, 3.3 Hz, H-3), 1.39 – 1.30 (6H, m, H-2); δ_C (Assigned by HSQC, $CDCl_3$) 62.6 (CH_2), 43.5 (CH_2), 16.4 (CH_3); δ_P (162 MHz, $CDCl_3$) 18.88. Data are consistent with the literature.[171]

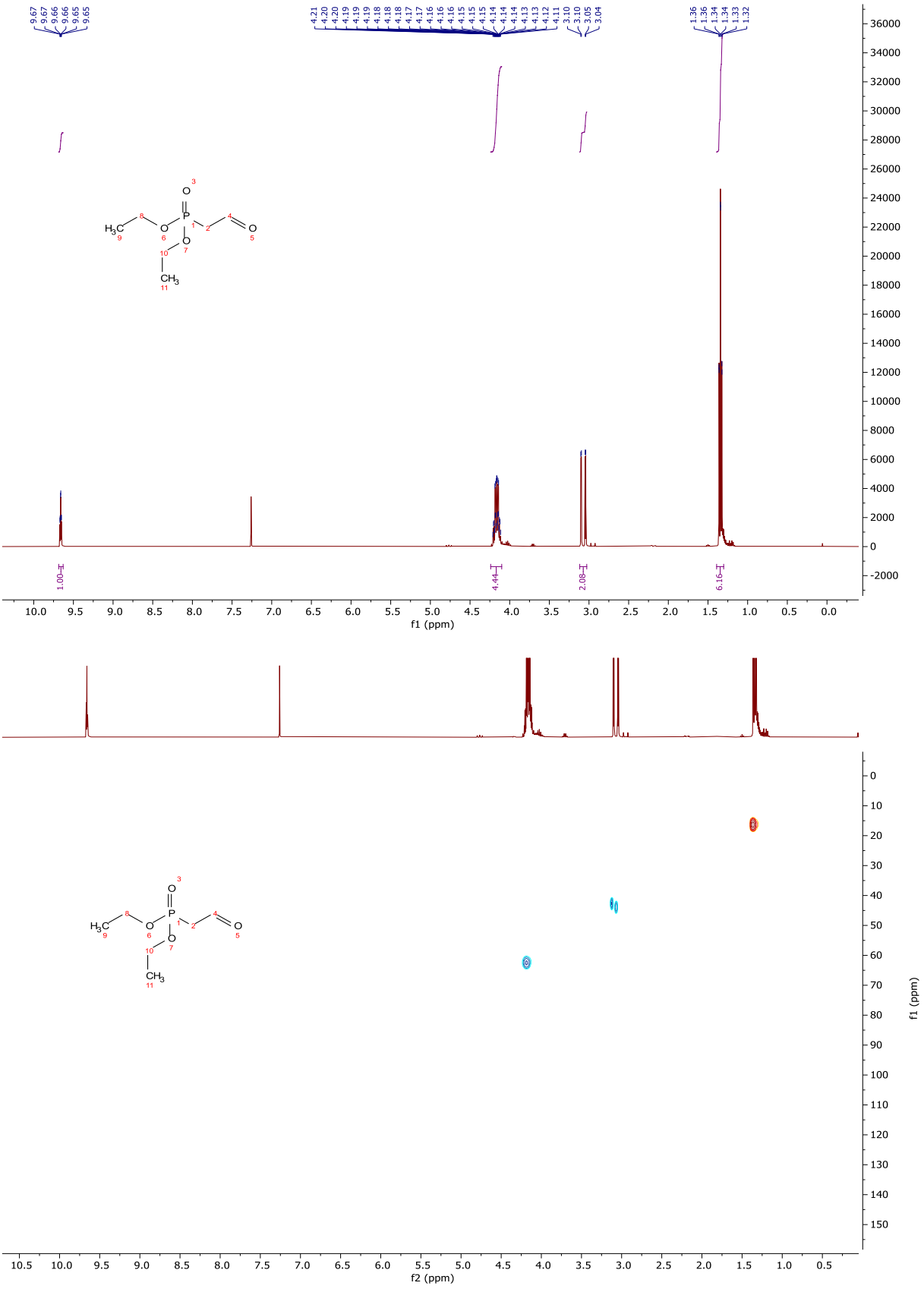
9.67 9.67 9.66 9.66 9.65 9.65
4.21 4.20 4.20 4.19 4.19 4.19 4.18 4.18 4.18 4.17 4.17 4.16 4.16 4.16 4.15 4.15 4.15 4.14 4.14 4.14 4.13 4.13 4.12 4.11 3.10 3.10 3.05 3.04
1.36 1.36 1.34 1.34 1.33 1.32
1.00
4.44
2.08
6.16
f1 (ppm)
f2 (ppm)
f1 (ppm)

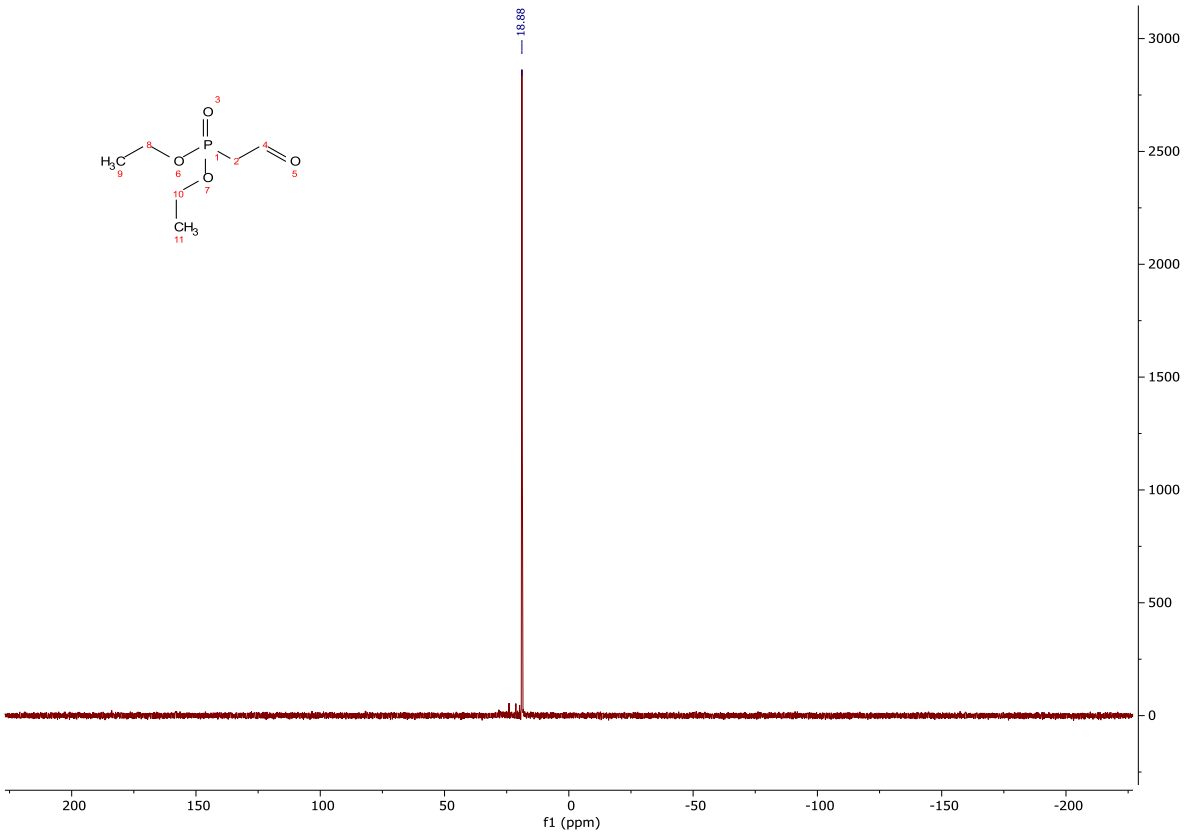
18.88
3000
2500
2000
1500
1000
500
0
200
150
100
50
0
-50
-100
-150
-200
f1 (ppm)

Diethyl (2-(methoxyimino)ethyl)phosphonate (**435**)

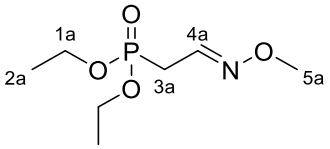

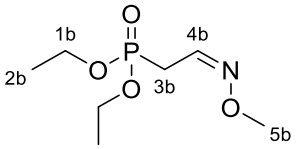

A solution of **428** (7.44 g, 41.3 mmol), methoxyamine hydrochloride (13.9 g, 165 mmol) and sodium acetate (23.7 g, 289 mmol) in methanol/water (1:1, 270 mL) was stirred at rt for 16 h. The organic solvent was removed *in vacuo* and the aqueous extracted with ethyl acetate (6 x 50.0 mL). The organics were combined, washed with sat. $Na_2CO_{3(aq)}$ (2 x 50.0 mL), 1M $HCl_{(aq)}$ (2 x 50.0 mL), brine (2 x 50.0 mL), dried (Na_2SO_4) and concentrated *in vacuo* to afford the title compound as a clear colourless oil (7.83 g, 37.5 mmol, 91%); **HRMS** *m/z* (ESI^+) calc. for $C_7H_{17}NO_4P$ $[M+H]^+$ requires 210.0890, found 210.0889; δ_H (400 MHz, $CDCl_3$) 7.35 (1H, td, *J* = 6.6, 4.7 Hz, H-4a), 6.74 (1H, td, *J* = 6.2, 5.0 Hz, H-4b), 4.21 – 4.04 (8H, m, H-1a and H-1b), 3.90 (3H, s, H-5b), 3.84 (3H, s, H-5a), 2.97 (2H, dd, *J* = 21.9, 6.2 Hz, H-3b), 2.76 (2H, dd, *J* = 21.7, 6.6 Hz, H-3a), 1.40 – 1.25 (12H, m, H-2a and H-2b); δ_C (Assigned by HSQC, $CDCl_3$) 142.1 (CH), 140.5 (CH), 62.1 (CH_2), 62.0 (CH_3), 61.6 (CH_3), 28.3 (CH_2), 24.4 (CH_2), 16.4 (CH_3); δ_P (162 MHz, $CDCl_3$) 23.40. Data are consistent with the literature.[171]

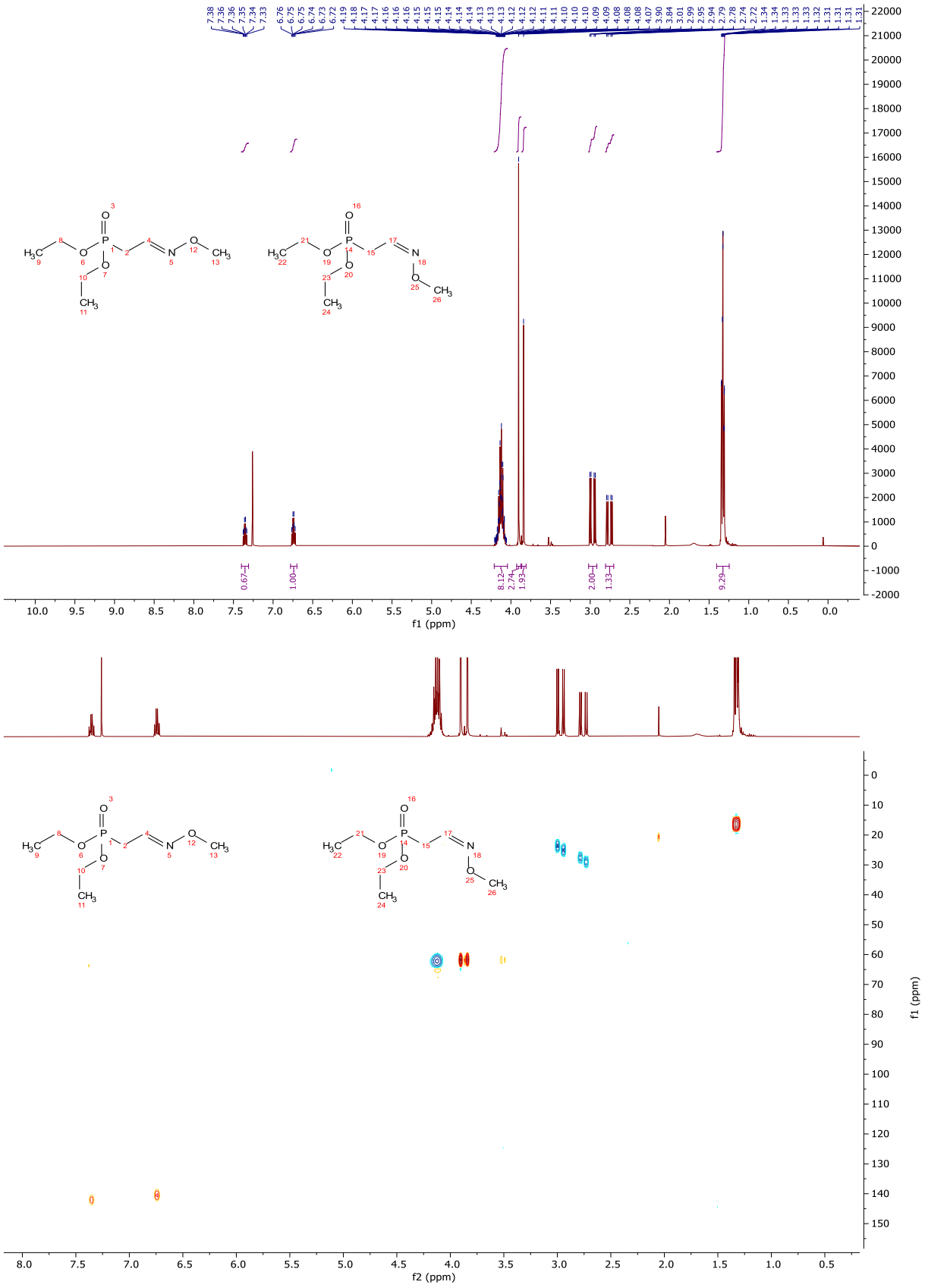
f1 (ppm)
f2 (ppm)

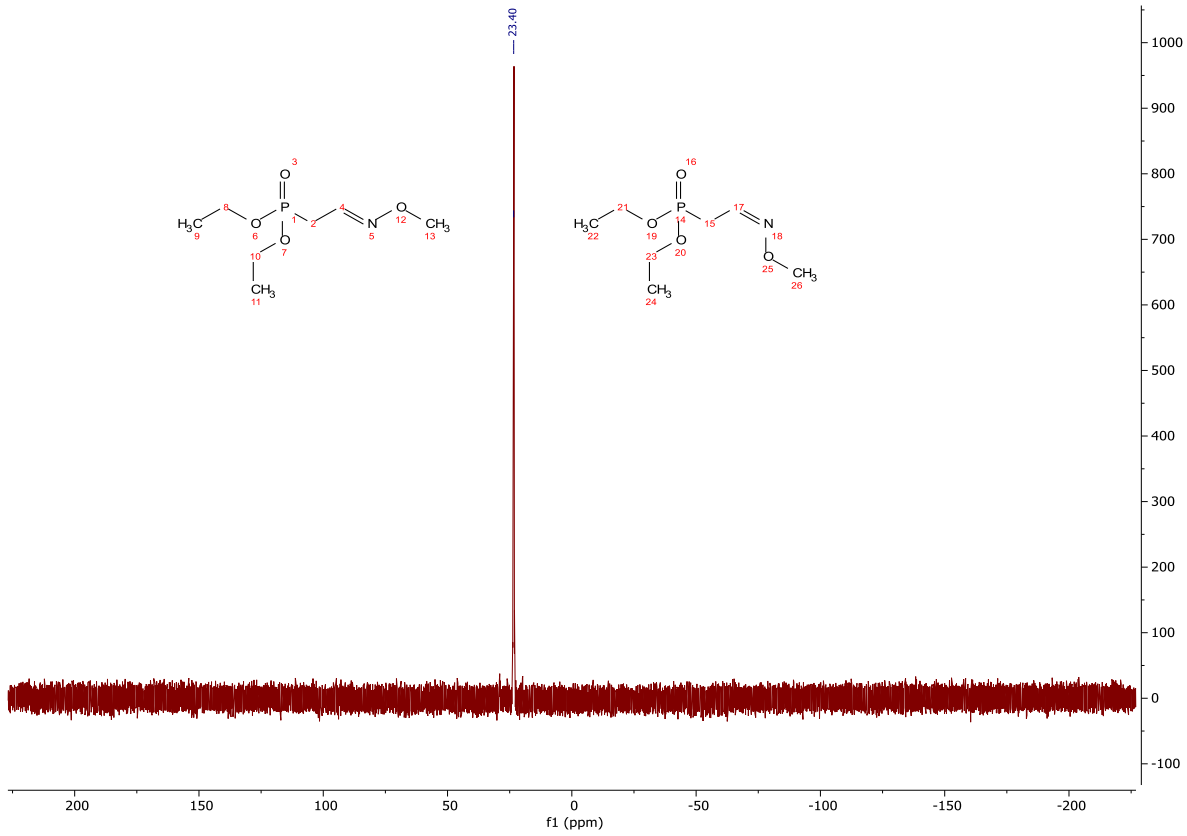
23.40
1000
900
800
700
600
500
400
300
200
100
0
-100
200
150
100
50
0
-50
-100
-150
-200
f1 (ppm)

Ethyl 7-(benzyloxy)-9*H*-pyrido[2,3-*b*]indole-4-carboxylate (**462**)

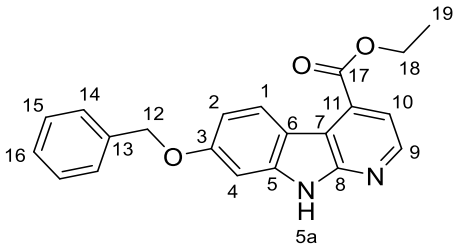

The following reaction protocol was performed simultaneously in ten separate microwave vials. To a solution of **457** (100 mg, 0.236 mmol) in THF (0.590 mL) at 0 °C under an argon atmosphere was added sodium hydride (60% in mineral oil, 10 mg, 0.260 mmol), followed by a solution of **435** (54 mg, 0.260 mmol) in THF (0.150 mL). The reaction mixture was stirred for 16 h and ethanol (0.200 mL) was added. The contents of the ten vials were combined and the mixture concentrated *in vacuo*. The resulting gum was diluted with ethyl acetate (100 mL), washed with sat. $NaHCO_{3(aq)}$ (2 x 100 mL), brine (100 mL), dried (Na_2SO_4) and concentrated *in vacuo* to give the crude oxime **459** as a dark orange oil. A solution of **459** in diphenyl ether (3.00 mL) in an open-topped, large microwave vial at 180 °C for 3 h. The reaction mixture was cooled rt, diluted with diethyl ether (50.0 mL) and filtered. The filtrate was concentrated *in vacuo*, and the resulting gum triturated in cyclohexane, affording the title compound as an orange solid (582 mg, 1.68 mmol, 71% over 2 steps); **HRMS** *m/z* (ESI^+) calc. for $C_{21}H_{19}N_2O_3$ $[M+H]^+$ requires 347.1390, found 347.1393; $\mathbf{R_f}$ 0.33, 40% ethyl acetate/cyclohexane, UV active; δ_H (400 MHz, $CDCl_3$) 10.18 (1H, s, H-5a), 8.78 (1H, d, *J* = 9.0 Hz, H-1), 8.44 (1H, d, *J* = 5.2 Hz, H-9), 7.71 (1H, d, *J* = 5.2 Hz, H-10), 7.50 (2H, d, *J* = 7.5 Hz, H-14), 7.45 – 7.31 (3H, m, H-15 and H-16), 7.06 – 6.95 (2H, m, H-2 and H-4), 5.21 (2H, s, H-12), 4.56 (2H, q, *J* = 7.1 Hz, H-18), 1.51 (3H, t, *J* = 7.1 Hz, H-19); δ_C (101 MHz, $CDCl_3$) 166.7 (CO), 159.7 (C), 153.5 (C), 143.3 (ArH), 141.4 (C), 136.9 (C), 131.2 (C), 128.8 (ArH), 128.2 (ArH), 127.9 (ArH), 127.7 (ArH), 119.0 (C), 116.1 (ArH), 114.1 (C), 110.2 (ArH), 95.8 (ArH), 70.5 (CH_2), 61.8 (CH_2), 14.5 (CH_3); ν_{max} (FT-ATR/cm^{-1}) 2922, 2853, 1722, 1619, 1421, 1380, 1248, 1171, 1124, 1099, 1012, 828, 745, 697.

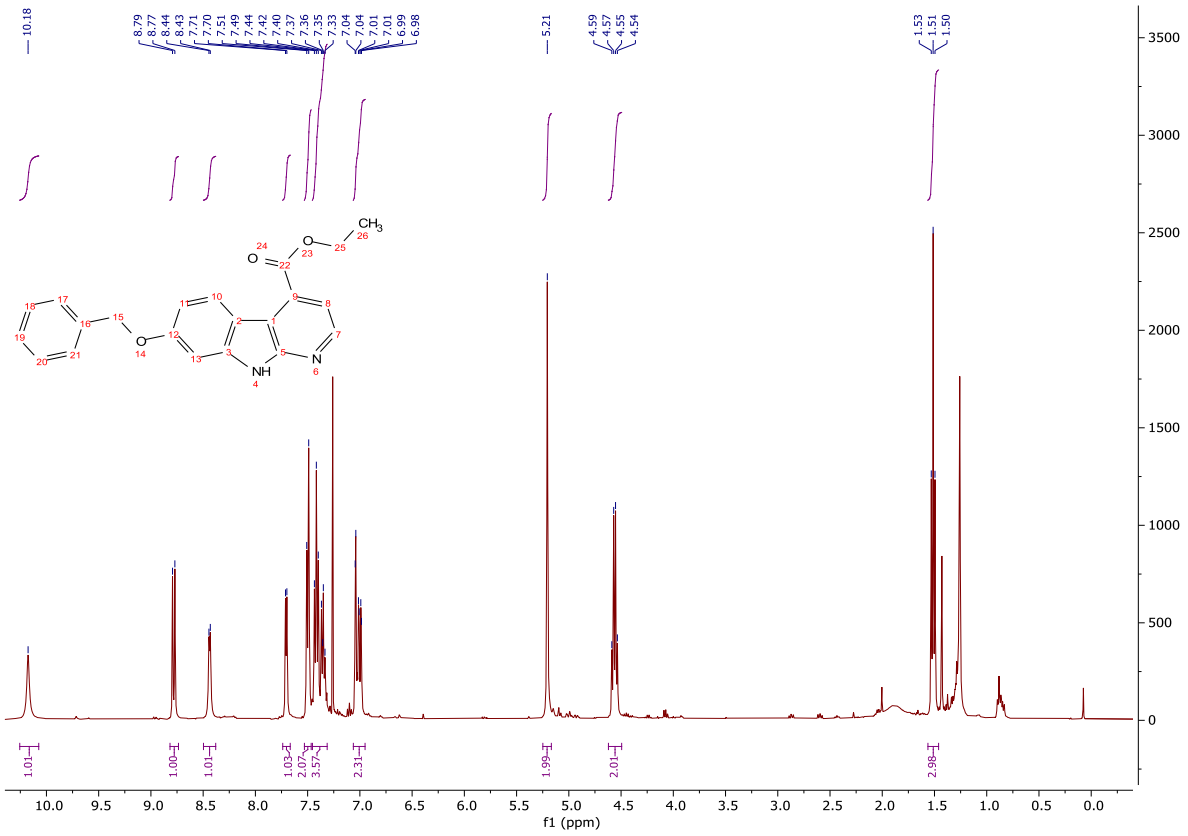
10.18
8.79
8.77
8.44
8.43
7.71
7.70
7.51
7.49
7.44
7.42
7.40
7.37
7.36
7.35
7.33
7.04
7.04
7.01
7.01
6.99
6.98
5.21
4.59
4.57
4.55
4.54
1.53
1.51
1.50
1.01
1.00
1.01
1.03
2.07
3.57
2.31
1.99
2.01
2.98
f1 (ppm)

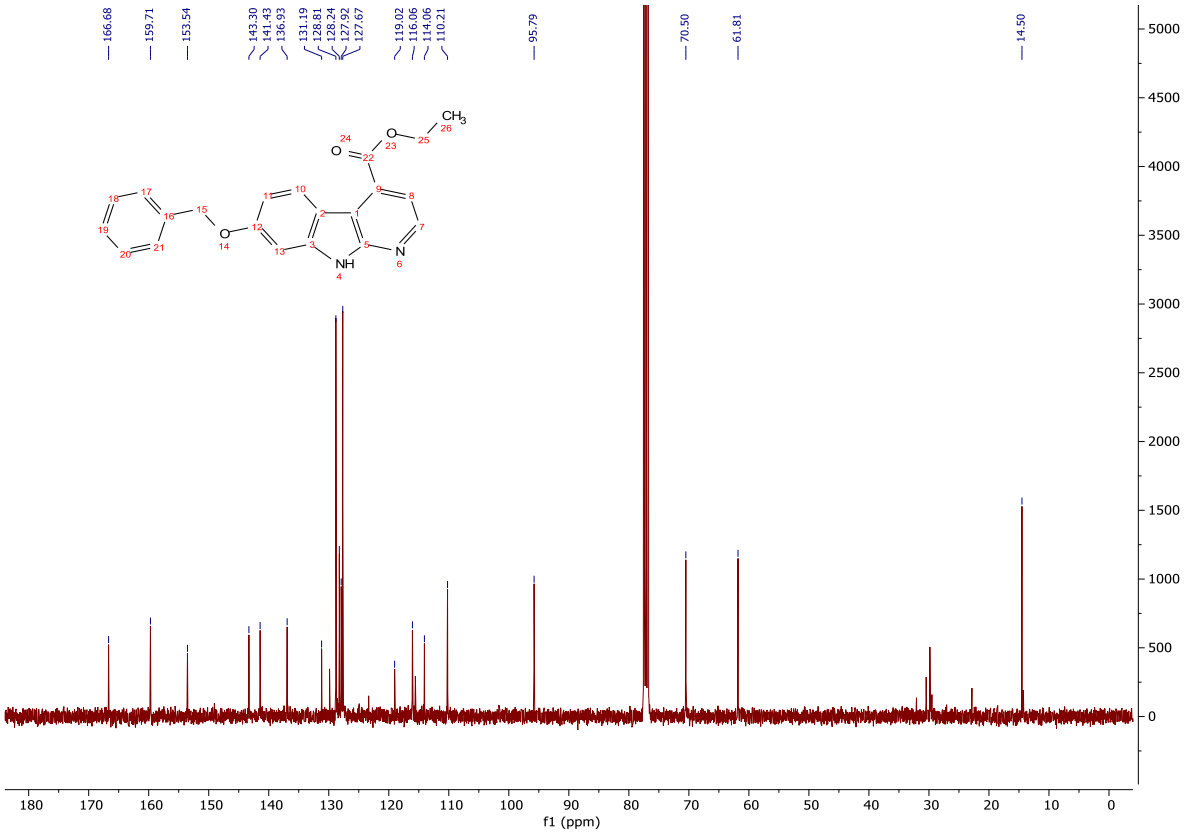
166.68
159.71
153.54
143.30
141.43
136.93
131.19
128.81
128.24
127.92
127.67
119.02
116.06
114.06
110.21
95.79
70.50
61.81
14.50
f1 (ppm)

2-(1-Ethoxy-1,3-dioxobutan-2-yl)-4-(methoxycarbonyl)pyridine 1-oxide (**464**)

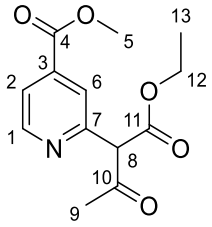

To a solution of **463** (252 mg, 1.65 mmol), ethyl acetoacetate (0.630 mL, 4.95 mmol) and *i*-Pr_2NEt (1.08 mL, 6.19 mmol) in anhydrous THF (6.50 mL) was added PyBroP (1.00 g, 2.15 mmol). The reaction mixture was stirred at rt for 16 h and concentrated *in vacuo*. The reaction mixture was filtered through Celite®, washing the filter cake with THF (2 x 10.0 mL), the filtrate was dried (Na_2SO_4) and concentrated *in vacuo*. The crude product was purified *via* column chromatography on silica gel, eluting with a gradient of ethyl acetate/light petroleum (0-25%) to give the title compound as an orange solid (164 mg, 0.619 mmol, 38%); **HRMS** *m/z* (ESI^+) calc. for $C_{10}H_{10}NO_5$ $[M^*+H]^+$ requires 224.0553, found 224.0916 (*M = Diacid); δ_H (400 MHz, $CDCl_3$) 13.25 – 13.22 (1H, m, OH taut.), 8.81 – 8.66 (1H, m, ArH taut.), 8.56 – 8.48 (1H, m, H-6), 8.15 – 8.07 (1H, m, H-1), 8.04 – 7.95 (1H, m, ArH taut.), 7.88 – 7.71 (2H, m, 2 x ArH taut.), 7.51 – 7.44 (1H, m, H-2), 5.08 (1H, s, H-8), 4.46 – 4.11 (4H, m, H-12 and H-12 taut.), 3.99 – 3.94 (6H, m, H-5 and H-5 taut.), 3.92 (3H, s, H-5 taut.), 3.89 (3H, s, H-5 taut.), 2.43 (3H, s, H-9), 2.34 (3H, s, H-9 taut.), 2.30 (3H, s, H-9 taut.), 1.93 – 1.87 (3H, m, CH_3 taut.), 1.40 (3H, t, *J* = 7.1 Hz, H-13), 1.35 – 1.14 (3H, m, H-13 taut); δ_C (101 MHz, $CDCl_3$) 185.5 (CO), 165.2 (CO), 157.3 (C), 150.8 (ArH taut.), 150.5 (ArH taut.), 139.5 (ArH), 139.1 (C), 138.4 (C taut.), 126.1 (ArH taut.), 125.0 (ArH taut.), 123.6 (ArH taut.), 122.4 (ArH taut.), 122.2 (ArH), 121.0 (ArH taut.), 116.3 (ArH), 67.8 (CH), 62.2 (CH_2 taut.), 61.1 (CH_2 taut.), 60.4 (CH_2), 53.1 (CH_3), 53.0 (CH_3 taut.), 52.9 (CH_3 taut.), 29.7 (CH_3 taut.), 26.4 (CH_3), 20.0 (CH_3 taut.), 14.5 (CH_3), 14.2 (CH_3 taut.).

N.B. C-10 is not observed.

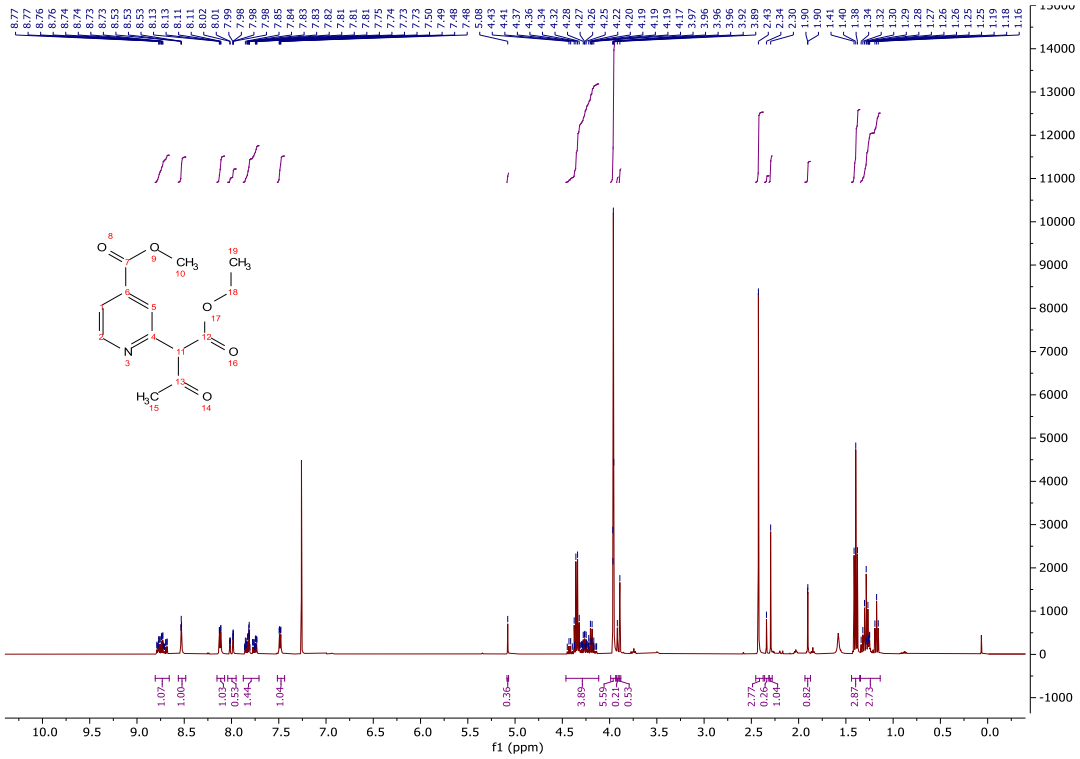
f1 (ppm)

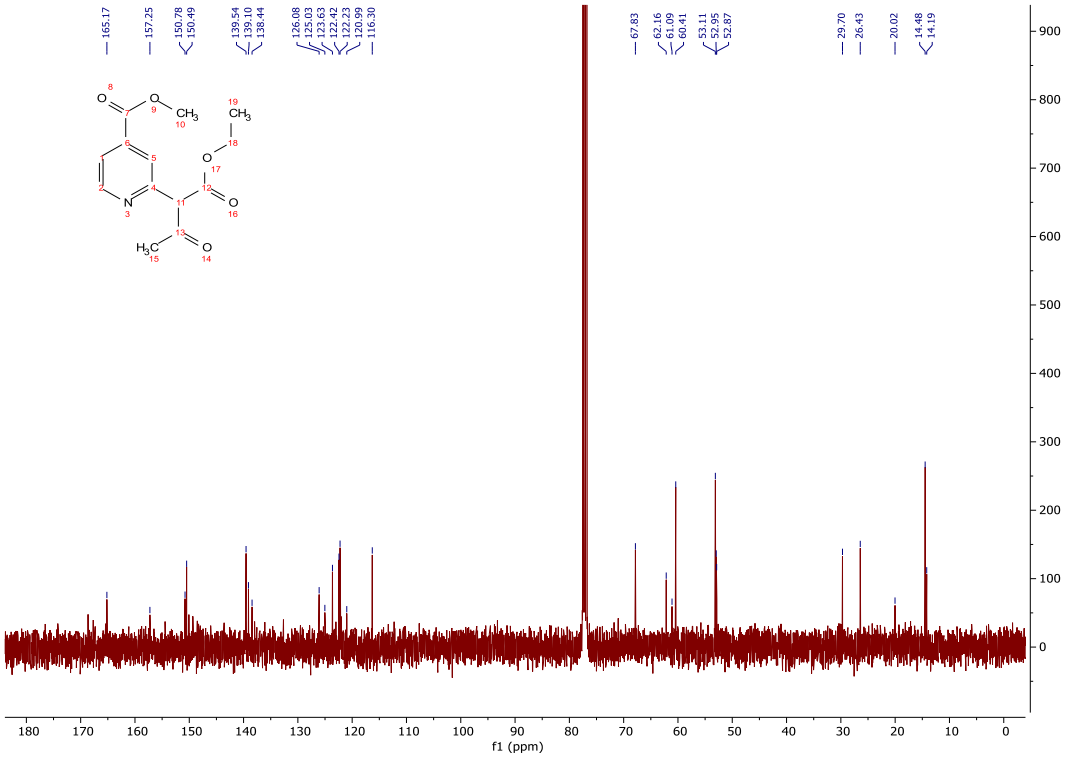
f1 (ppm)

General experimental procedure for the reaction optimisation screening described on page 188 for the synthesis of **464**

A suspension of **463** (1.00 eq.), ethyl acetoacetate (3.00 eq.), **activating agent** (1.30 eq.) and **base** (3.75 eq.) in **solvent** (0.25 M) was stirred at **temperature** for 16 h. The crude reaction mixture was submitted to LCMS analysis and the resulting ratio between **463** and **464** recorded.

7-(Benzyloxy)-4-(ethoxycarbonyl)-9*H*-pyrido[2,3-*b*]indole 1-oxide (**465**)

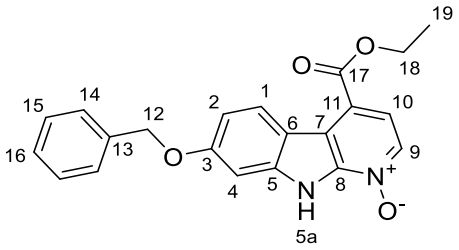

To a solution of **462** (400 mg, 1.16 mmol) in ethyl acetate (6.00 mL) at 0 °C was added *m*CPBA (77% in water, 260 mg, 1.16 mmol) portionwise. The reaction mixture was stirred for 16h, then sodium sulfite (139 mg, 1.10 mmol) was added and the reaction mixture stirred for 10 min. The reaction mixture was basified to pH 9 with conc. $NH_{3(aq)}$ and stirred for 1 h. The reaction mixture was filtered, the solid collected and partitioned between CH_2Cl_2 (25.0 mL) and water (25.0 mL). The organic was dried (Na_2SO_4) and concentrated *in vacuo*, affording the title compound as a colourless, crystalline solid (295 mg, 0.815 mmol, 70%); **HRMS** *m/z* (ESI^+) calc. for $C_{21}H_{18}N_2NaO_4$ $[M+Na]^+$ requires 385.1159, found 385.1162; $\mathbf{R_f}$ 0.14, 100% ethyl acetate/cyclohexane, UV active; δ_H (400 MHz, $CDCl_3$) 12.54 – 12.04 (1H, m, H-5a), 8.83 (1H, d, *J* = 9.0 Hz, H-1), 8.29 (1H, d, *J* = 6.8 Hz, H-9), 7.75 (1H, d, *J* = 6.6 Hz, H-10), 7.51 – 7.45 (2H, m, H-14), 7.45 – 7.31 (3H, m, H-15 and H-16), 7.24 – 7.18 (1H, m, H-4), 7.04 – 6.96 (1H, m, H-2), 5.20 (2H, s, H-12), 4.53 (2H, q, *J* = 7.1 Hz, H-18), 1.49 (3H, t, *J* = 7.1 Hz, H-19); δ_C (101 MHz, $CDCl_3$) 165.1 (CO), 160.6 (C), 143.6 (C), 141.6 (C), 136.7 (C), 132.2 (ArH), 128.8 (ArH), 128.4 (ArH), 128.3 (ArH), 127.7 (ArH), 123.3 (C), 120.3 (C), 117.4 (ArH), 114.7 (C), 111.7 (ArH), 96.6 (ArH), 70.5 (CH_2), 61.9 (CH_2), 14.5 (CH_3); **MP** Degrades >222 °C; ν_{max} (FT-ATR/cm^{-1}) 2702, 1721, 1608, 1440, 1323, 1251, 1200, 1165, 1135, 1083, 1006, 830, 756, 710.

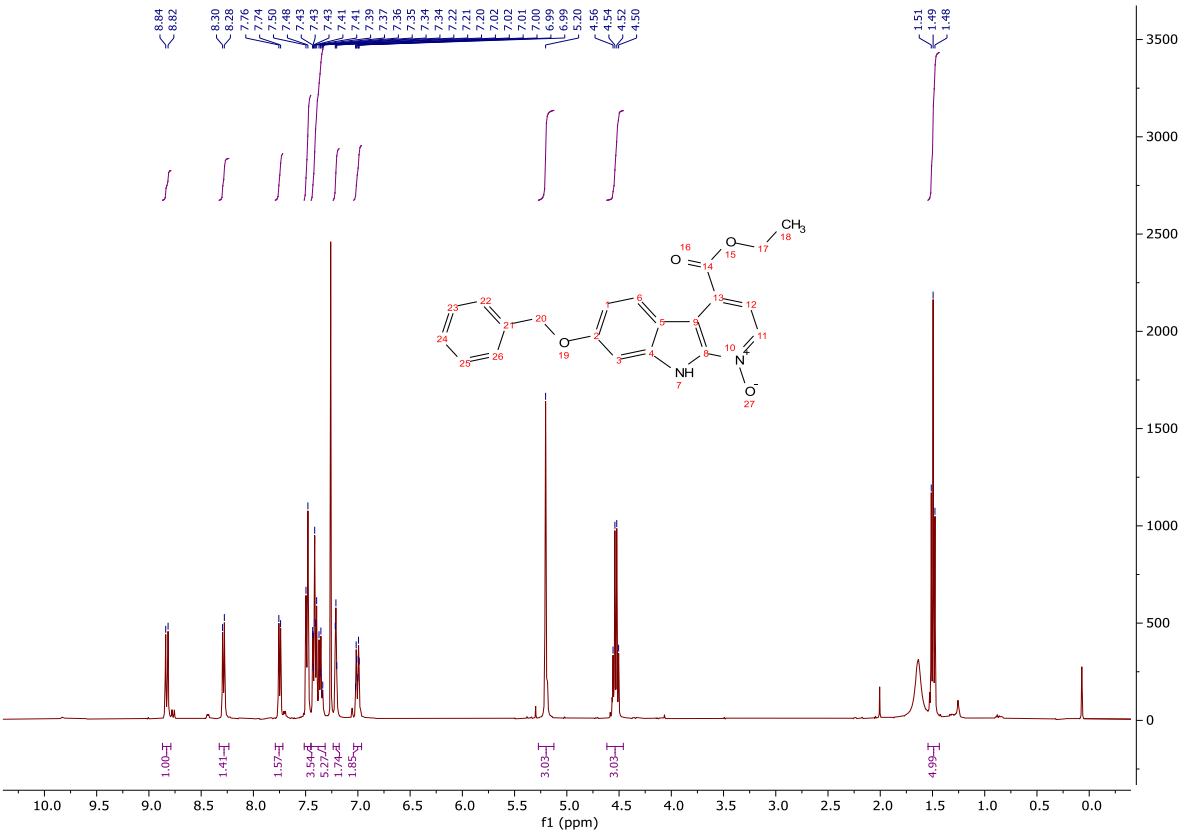
8.84
8.82
8.30
8.28
7.76
7.74
7.50
7.48
7.43
7.43
7.41
7.41
7.39
7.37
7.36
7.35
7.34
7.34
7.22
7.21
7.20
7.02
7.02
7.01
7.00
6.99
6.99
5.20
4.56
4.54
4.52
4.50
1.51
1.49
1.48
1.00
1.41
1.57
3.54
5.27
1.74
1.85
3.03
3.03
4.99
f1 (ppm)

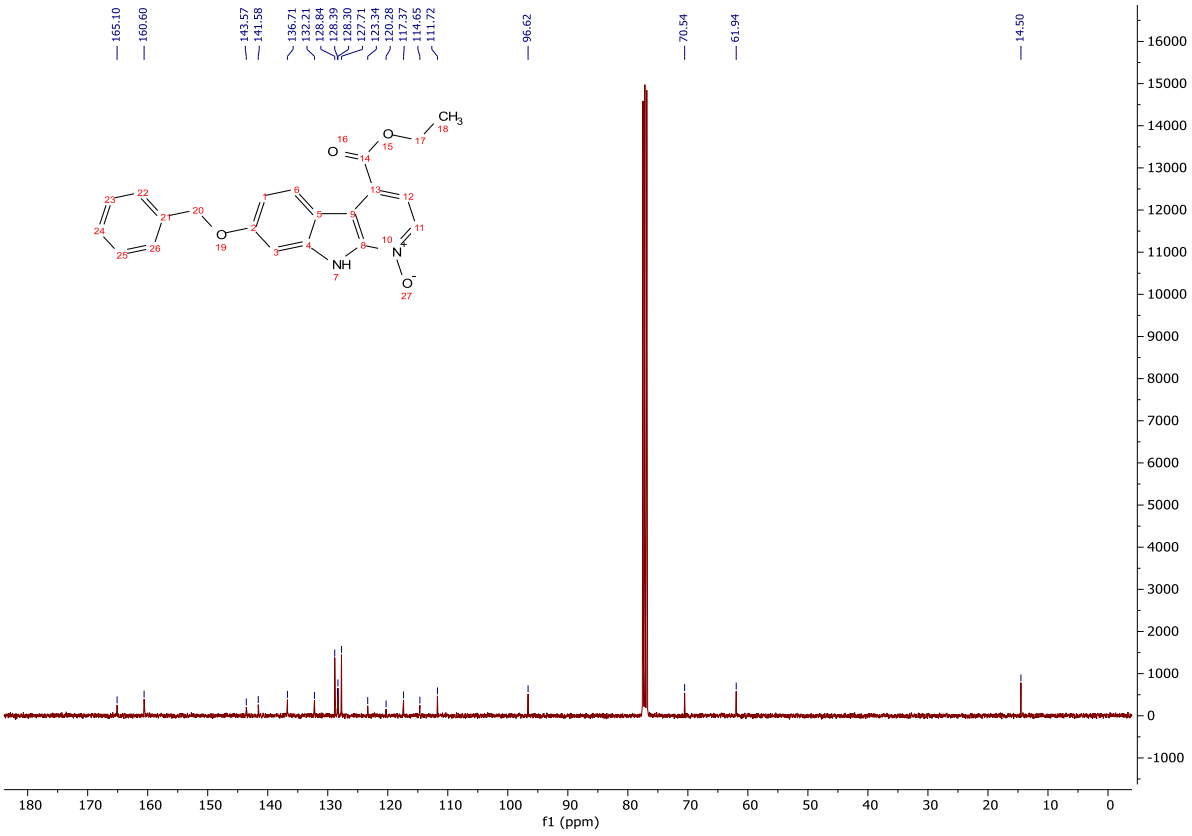
165.10
160.60
143.57
141.58
136.71
132.21
128.84
128.39
128.30
127.71
123.34
120.28
117.37
114.65
111.72
96.62
70.54
61.94
14.50
f1 (ppm)

7-(Benzyloxy)-9-(*tert*-butoxycarbonyl)-4-(ethoxycarbonyl)-9*H*-pyrido[2,3-*b*]indole 1-oxide (**466**)

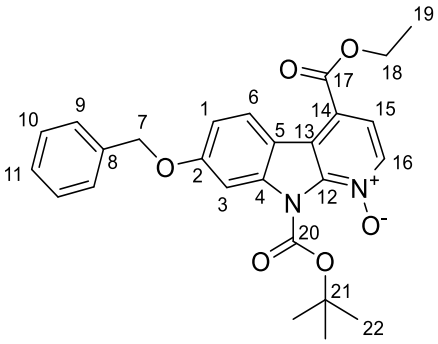

A mixture of **465** (50 mg, 0.138 mmol), di-*tert*-butyl dicarbonate (150 mg, 0.690 mmol) and DMAP (5 mg, 0.040 mmol) was heated at 35 °C for 16 h. The reaction mixture was cooled to rt and triturated with cold diethyl ether (3 x 5.00 mL) to afford the title compound as a yellow solid (45 mg, 0.097 mmol, 70%); **HRMS** *m/z* (ESI$^+$) calc. for $C_{26}H_{27}N_2O_6$ $[M+H]^+$ requires 463.1864, found 463.1868; $\mathbf{R_f}$ 0.30, 40% ethyl acetate/cyclohexane, UV active; $\delta_\mathbf{H}$ (500 MHz, DMSO-d_6) 8.78 (1H, d, *J* = 9.0 Hz, H-6), 8.41 (1H, d, *J* = 6.8 Hz, H-16), 7.85 (1H, d, *J* = 6.8 Hz, H-15), 7.53 – 7.47 (2H, m, H-9), 7.44 – 7.38 (2H, m, H-10), 7.38 – 7.32 (1H, m, H-11), 7.27 (1H, d, *J* = 2.4 Hz, H-3), 7.20 (1H, dd, *J* = 9.1, 2.4 Hz, H-1), 5.29 (2H, s, H-7), 4.53 – 4.43 (2H, m, H-18), 1.56 (9H, s, H-22), 1.44 – 1.37 (3H, m, H-19); $\delta_\mathbf{C}$ (126 MHz, DMSO-d_6) 164.2 (CO), 160.2 (C), 147.7 (CO), 141.6 (C), 140.4 (C), 136.4 (C), 134.7 (ArH), 128.5 (ArH), 128.1 (ArH), 128.0 (ArH), 127.7 (ArH), 121.5 (C), 121.4 (ArH), 120.1 (C), 114.2 (C), 113.0 (ArH), 96.4 (ArH), 85.7 (C), 69.8 (CH_2), 61.7 (CH_2), 27.2 (CH_3), 14.1 (CH_3); **MP** Degrade >145 °C; ν_{max} (FT-ATR/cm^{-1}) 2983, 1749, 1619, 1424, 1366, 1295, 1251, 1183, 1142, 1073, 1026, 839, 777.

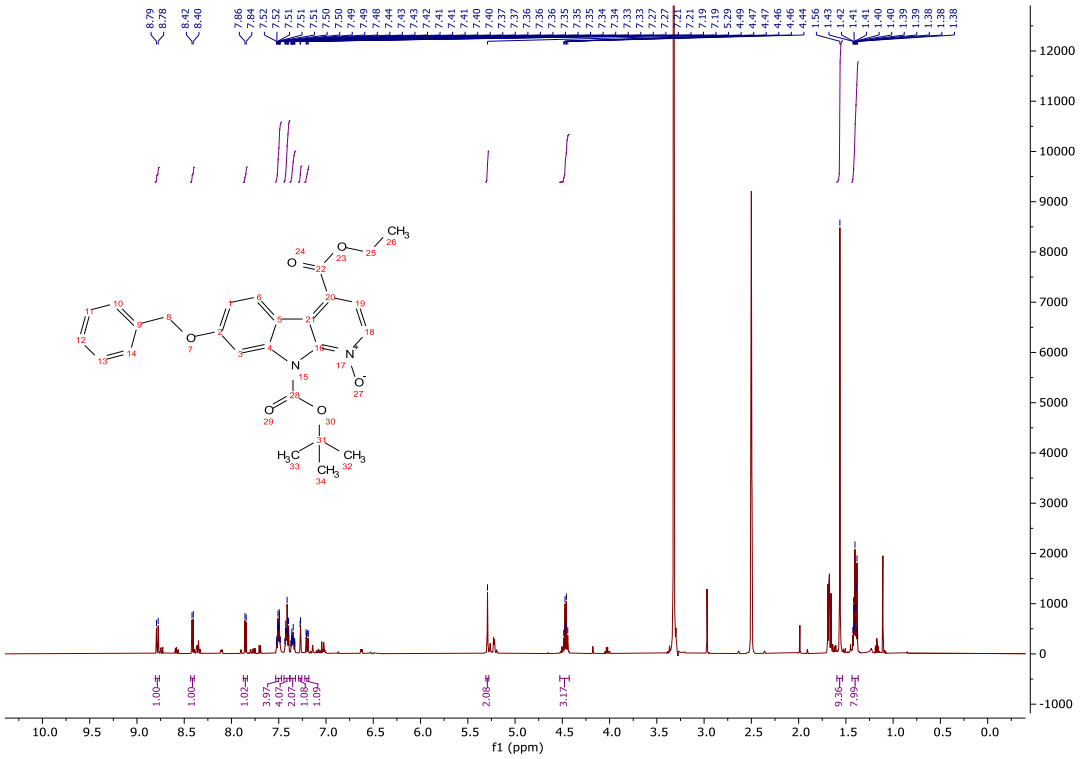
8.79
8.78
8.42
8.40
7.86
7.84
7.52
7.52
7.51
7.51
7.51
7.50
7.50
7.49
7.49
7.48
7.44
7.43
7.43
7.42
7.41
7.41
7.41
7.40
7.40
7.37
7.37
7.36
7.36
7.35
7.35
7.35
7.34
7.34
7.33
7.23
7.22
7.27
7.21
7.21
7.19
7.19
5.29
4.49
4.47
4.47
4.46
4.46
4.44
1.56
1.43
1.42
1.41
1.41
1.40
1.40
1.39
1.39
1.38
1.38
1.38
1.00
1.00
1.02
3.97
4.07
2.07
1.08
1.09
2.08
3.17
9.36
7.99
f1 (ppm)

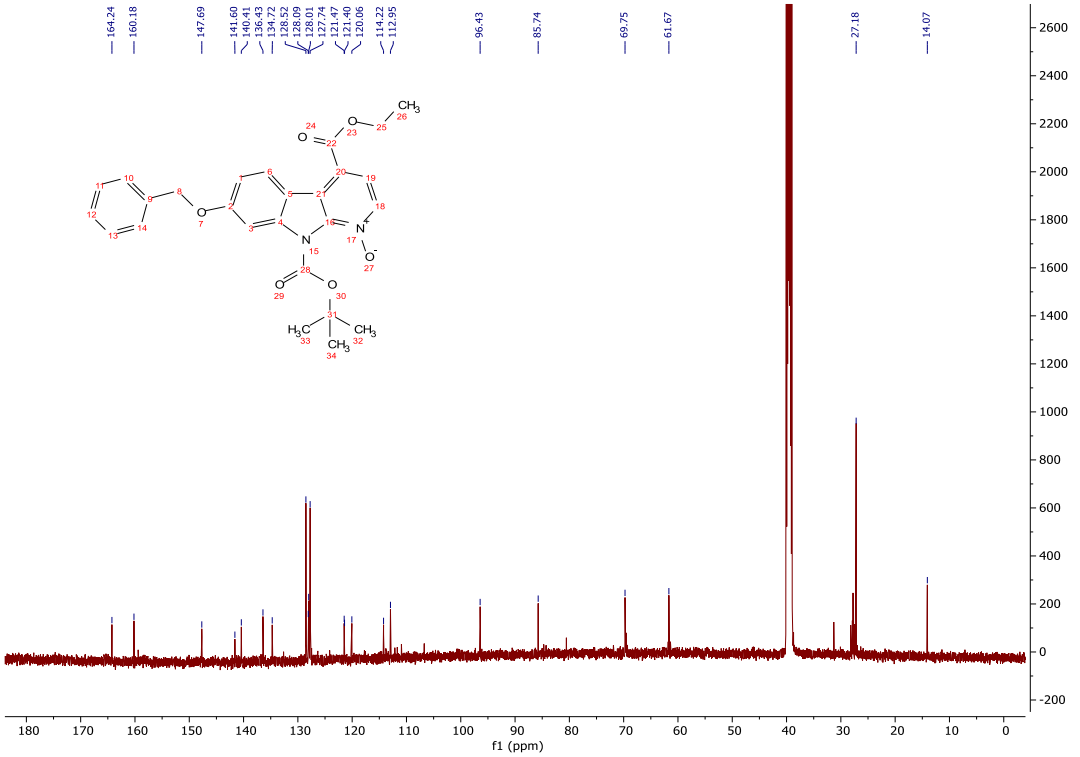
164.24
160.18
147.69
141.60
140.41
136.43
134.72
128.52
128.09
128.01
127.74
121.47
121.40
120.06
114.22
112.95
96.43
85.74
69.75
61.67
27.18
14.07
f1 (ppm)

4-Ethyl 9-methyl 7-(benzyloxy)-2-chloro-9*H*-pyrido[2,3-*b*]indole-4,9-dicarboxylate (**474**)

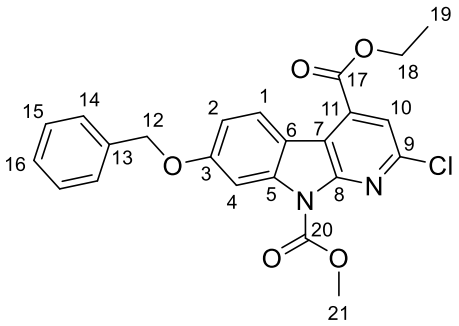

To a suspension of **465** (285 mg, 0.787 mmol) in anhydrous THF (4.00 mL) was added HMDS (0.165 mL, 0.787 mmol) and methyl chloroformate (0.530 mL, 1.97 mmol). The reaction vessel was fitted with a reflux condenser and the reaction mixture heated to 75 °C and stirred for 16 h. Sat. $Na_2CO_{3(aq)}$ (5.00 mL) was added, and the mixture stirred for 5 min, then the organic solvent removed *in vacuo*. Ethyl acetate (25.0 mL) and sat. $Na_2CO_{3(aq)}$ (25.0 mL) were added, and the layers separated. The organic layer was washed with brine, dried (Na_2SO_4) and concentrated *in vacuo*. The crude product was purified *via* column chromatography on silica gel, eluting with a gradient of ethyl acetate/light petroleum (0-30%) to give the title compound as a colourless solid (140 mg, 0.320 mmol, 41%); **HRMS** *m/z* (ESI^+) calc. for $C_{23}H_{20}ClN_2O_5$ $[M+H]^+$ requires 439.1055, found 439.1051; $\mathbf{R_f}$ 0.44, 20% ethyl acetate/cyclohexane, UV active; δ_H (500 MHz, $CDCl_3$) 8.66 (1H, d, *J* = 9.0 Hz, H-1), 8.07 (1H, d, *J* = 2.4 Hz, H-4), 7.79 (1H, s, H-10), 7.52 – 7.48 (2H, m, H-14), 7.45 – 7.39 (2H, m, H-15), 7.38 – 7.32 (1H, m, H-16), 7.07 (1H, dd, *J* = 9.0, 2.5 Hz, 2H), 5.21 (2H, s, H-12), 4.53 (2H, q, *J* = 7.1 Hz, H-18), 4.17 (3H, s, H-21), 1.49 (3H, t, *J* = 7.2 Hz, H-19); δ_C (126 MHz, $CDCl_3$) 165.1 (CO), 160.3 (C), 151.8 (CO), 151.1 (C), 146.2 (C), 140.3 (C), 136.6 (C), 133.6 (C), 128.8 (ArH), 128.3 (ArH), 127.8 (ArH), 126.9 (ArH), 119.7 (ArH), 116.6 (C), 114.5 (C), 113.1 (ArH), 100.9 (ArH), 70.5 (CH_2), 62.4 (CH_2), 54.5 (CH_3), 14.4 (CH_3); **MP** 195-197 °C; ν_{max} (FT-ATR/cm^{-1}) 2922, 1726, 1604, 1562, 1434, 1376, 1201, 1225, 1179, 1117, 1078, 1013, 839, 749.

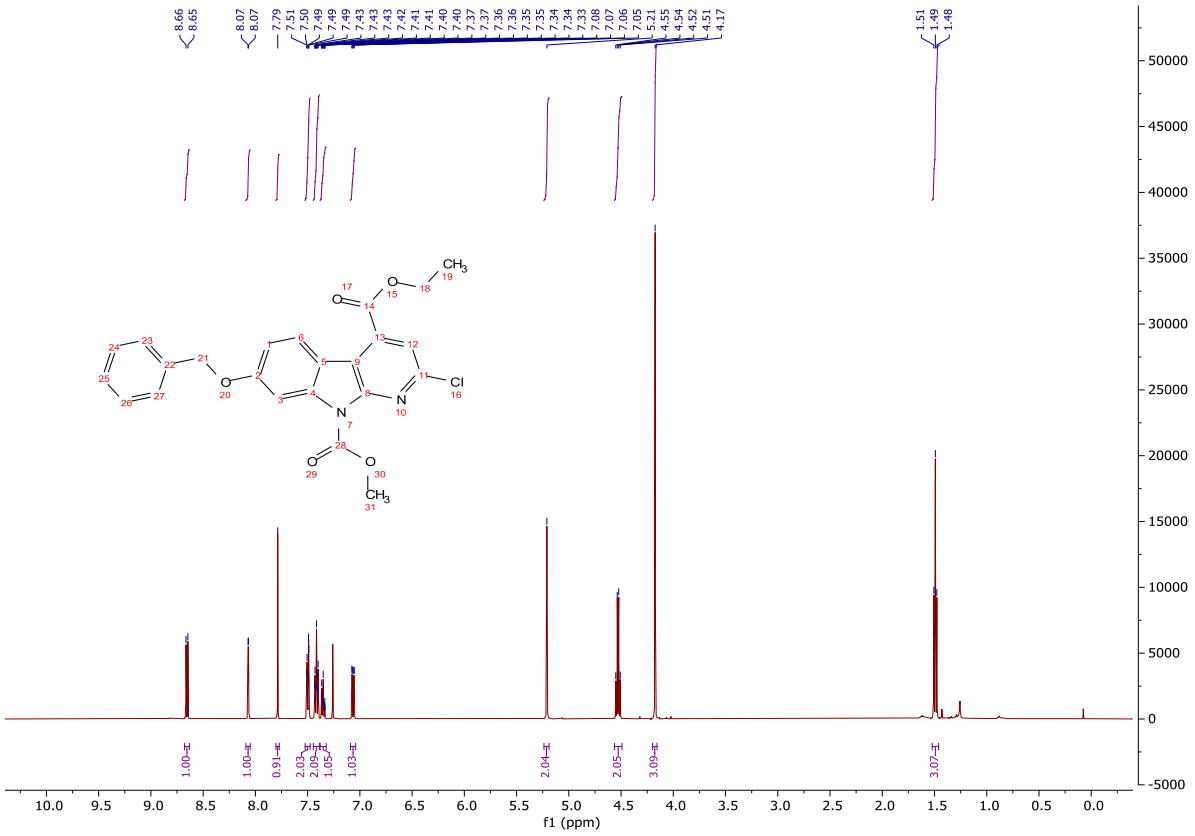
8.66
8.65
8.07
8.07
7.79
7.51
7.50
7.49
7.49
7.49
7.43
7.43
7.42
7.41
7.41
7.40
7.40
7.37
7.37
7.36
7.36
7.35
7.35
7.34
7.34
7.33
7.08
7.07
7.06
7.05
5.21
4.55
4.54
4.52
4.51
4.17
1.51
1.49
1.48
1.00
1.00
0.91
2.03
2.09
1.05
1.03
2.04
2.05
3.09
3.07
f1 (ppm)

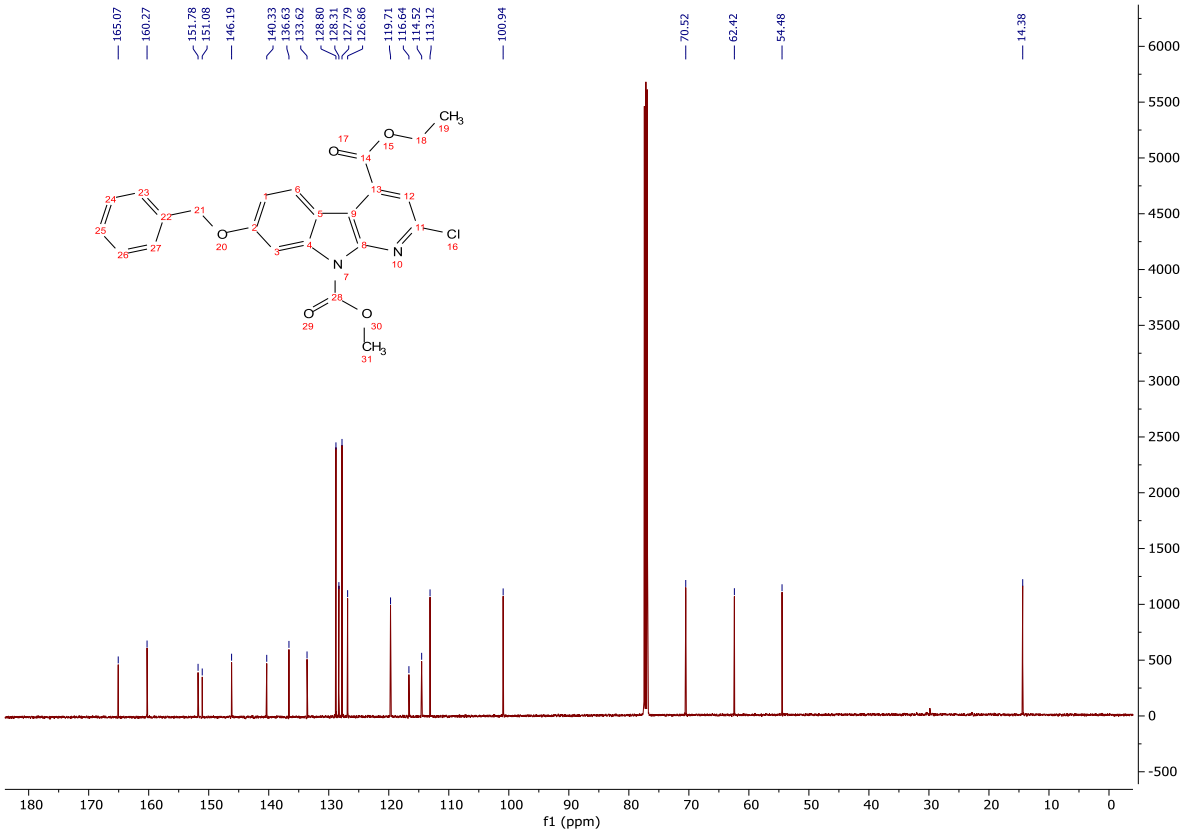
165.07
160.27
151.78
151.08
146.19
140.33
136.63
133.62
128.80
128.31
127.79
126.86
119.71
116.64
114.52
113.12
100.94
70.52
62.42
54.48
14.38
f1 (ppm)

(*S*)-2,2-Dimethyl-1,3-dioxolan-4-yl)methyl 7-(benzyloxy)-2-chloro-9*H*-pyrido[2,3-*b*]indole-4-carboxylate (**480**)

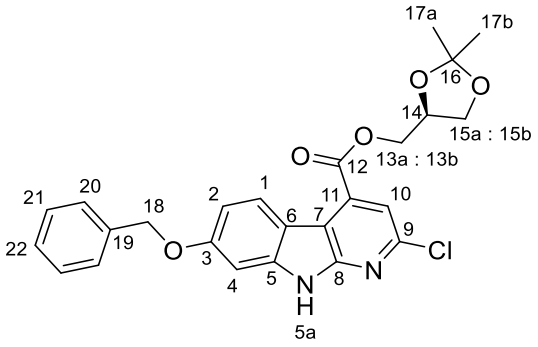

A solution of **474** (157 mg, 0.359 mmol) in *tert*-butylamine (1.13 mL, 10.8 mmol) and methanol (4.00 mL) was heated under reflux for 16 h. The reaction mixture was cooled to rt and concentrated *in vacuo*. The resulting gum was triturated with cold diethyl ether (3 x 10.0 mL), affording the methyl ester **479** as a beige solid. In a large, open-topped microwave vial, a suspension of **479**, (*R*)-(-)-2,2-dimethyl-1,3-dioxolane-4-methanol (0.045 mL, 0.359 mmol), $Fe(acac)_3$ (6.00 mg, 0.018 mmol), and sodium carbonate (2.00 mg, 0.018 mmol) in anhydrous toluene (1.80 mL) was heated at 120 °C for 7 days; the solvent was replaced periodically throughout the day upon evaporation and overnight the reaction temperature was reduced to 90 °C. The reaction mixture was cooled to rt, triturated with ether and the resulting organic layer concentrated *in vacuo*. The crude product was purified *via* column chromatography on silica gel, eluting with a gradient of ethyl acetate/light petroleum (0-30%) to give the title compound as a yellow solid (45 mg, 0.097 mmol, 27%); **HRMS** *m/z* (ESI^+) calc. for $C_{25}H_{23}ClN_2NaO_5$ $[M+Na]^+$ requires 489.1188, found 489.1193; $\mathbf{R_f}$ 0.55, 25% ethyl acetate/cyclohexane, UV active; δ_H (500 MHz, $CDCl_3$) 10.55 (1H, s, H-5a), 8.71 (1H, d, *J* = 9.0 Hz, H-1), 7.68 (1H, s, H-10), 7.52 – 7.45 (2H, m, H-20), 7.44-7.38 (2H, m, H-21), 7.38 – 7.32 (1H, m, H-22), 7.17 (1H, d, *J* = 2.4 Hz, H-4), 6.98 (1H, dd, *J* = 9.0, 2.3 Hz, H-2), 5.18 (2H, s, H-18), 4.59 – 4.52 (2H, m, H-13a and H-14), 4.52 – 4.46 (1H, m, H-13b), 4.20 (1H, dd, *J* = 8.5, 6.0 Hz, H-15a), 3.91 (1H, dd, *J* = 8.6, 5.4 Hz, H-15b), 1.50 (3H, s, H-17a), 1.42 (3H, s, H-17b); δ_C (126 MHz, $CDCl_3$) 165.2 (CO), 159.9 (C), 152.9 (C), 144.8 (C), 141.6 (C), 136.8 (C), 132.1 (C),

128.8 (ArH), 128.3 (ArH), 127.7 (ArH), 127.6 (ArH), 115.8 (ArH), 114.7 (C), 113.3 (C), 111.1 (ArH), 110.3 (C), 96.0 (ArH), 73.6 (CH), 70.4 (CH_2), 66.5 (CH_2), 66.2 (CH_2), 27.0 (CH_3), 25.5 (CH_3); **MP** 171-174 °C; ν_{max} (FT-ATR/cm^{-1}) 3162, 2925, 1729, 1621, 1514, 1414, 1370, 1255, 1174, 1133, 1015, 820, 752, 696.

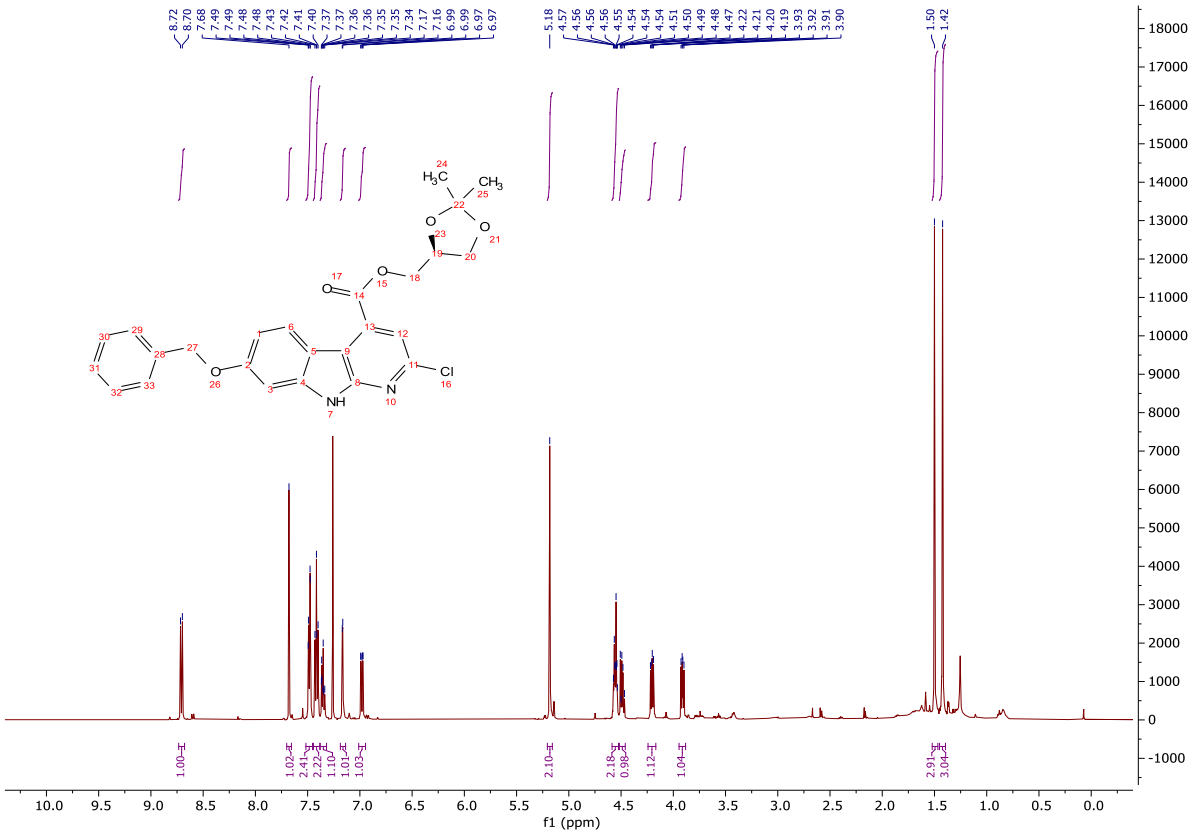
8.72
8.70
7.68
7.49
7.49
7.49
7.48
7.48
7.43
7.42
7.41
7.40
7.37
7.37
7.36
7.36
7.35
7.35
7.34
7.17
7.16
6.99
6.99
6.97
6.97
5.18
4.57
4.56
4.56
4.56
4.55
4.54
4.54
4.54
4.51
4.50
4.49
4.48
4.47
4.22
4.21
4.20
4.19
3.93
3.92
3.91
3.90
1.50
1.42
1.00
1.02
2.41
2.22
2.10
1.01
1.03
2.10
2.18
0.98
1.12
1.04
2.91
3.04
f1 (ppm)

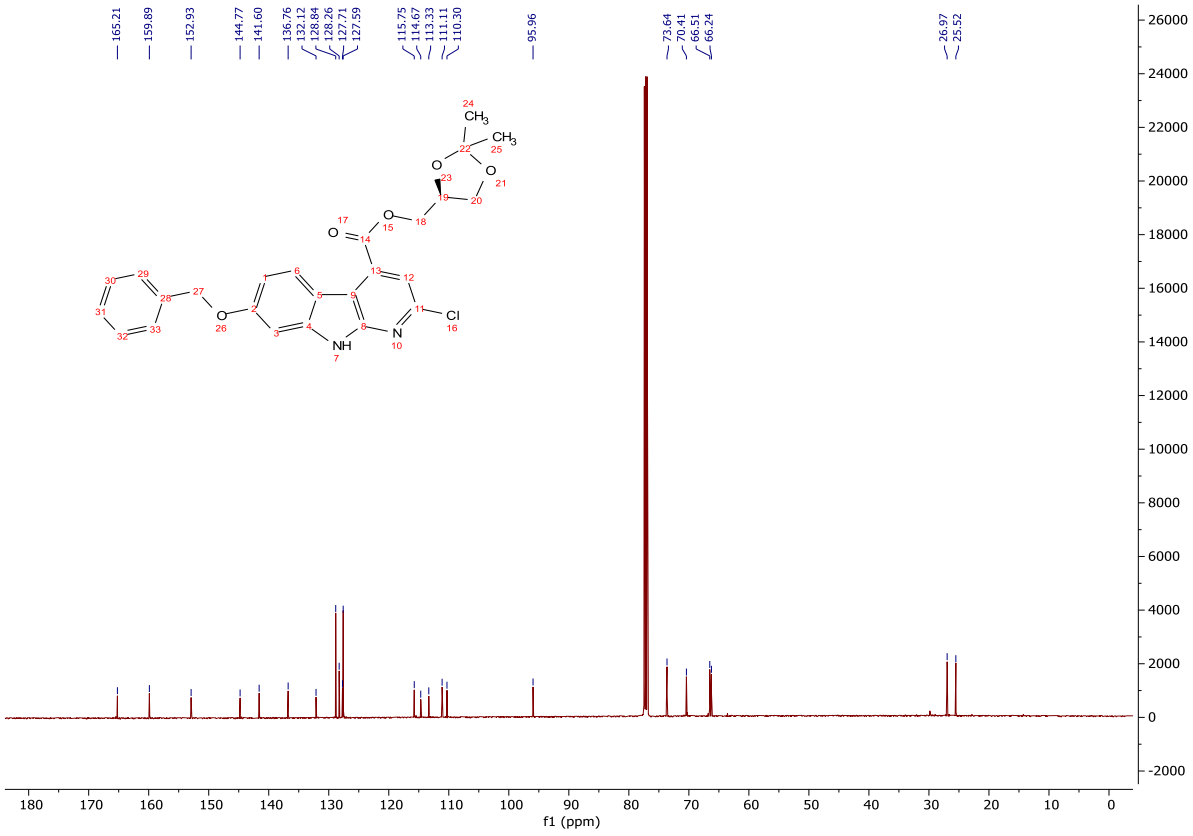
165.21
159.89
152.93
144.77
141.60
136.76
132.12
128.84
128.26
127.71
127.59
115.75
114.67
113.33
111.11
110.30
95.96
73.64
70.41
66.51
66.24
26.97
25.52
f1 (ppm)

4-Methoxy-6-methyl-5,6-dihydro-2*H*-pyran-2-one (**483**)

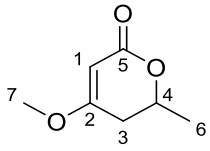

To a stirred solution of 4-hydroxy-6-methyl-5,6-dihydro-2*H*-pyran-2-one (**438**, 128 mg, 1.00 mmol) in THF (5.00 mL) was added iodomethane (0.187 mL, 3.00 mmol) and DBU (0.447 mL, 3.00 mmol). The reaction mixture was stirred at rt for 3 h, then filtered, washing the filter cake with cold THF (2 x 5.00 mL), before concentrating the filtrate *in vacuo* to give a yellow oil. The crude product was used without further purification; **HRMS** *m/z* (ESI^+) calc. for $C_7H_{10}NaO_3$ $[M+Na]^+$ requires 165.0522, found 165.0530; δ_H (400 MHz, $CDCl_3$) 5.19 – 5.07 (1H, m, H-1), 4.60 – 4.44 (1H, m, H-4), 3.74 (3H, s, H-7), 2.52 – 2.26 (2H, m, H-3), 1.43 (3H, d, *J* = 6.3 Hz, H-6); δ_C (101 MHz, $CDCl_3$) 172.9 (C), 167.6 (CO), 90.4 (CH), 72.4 (CH), 56.1 (CH_3), 34.7 (CH_2), 20.7 (CH_3).

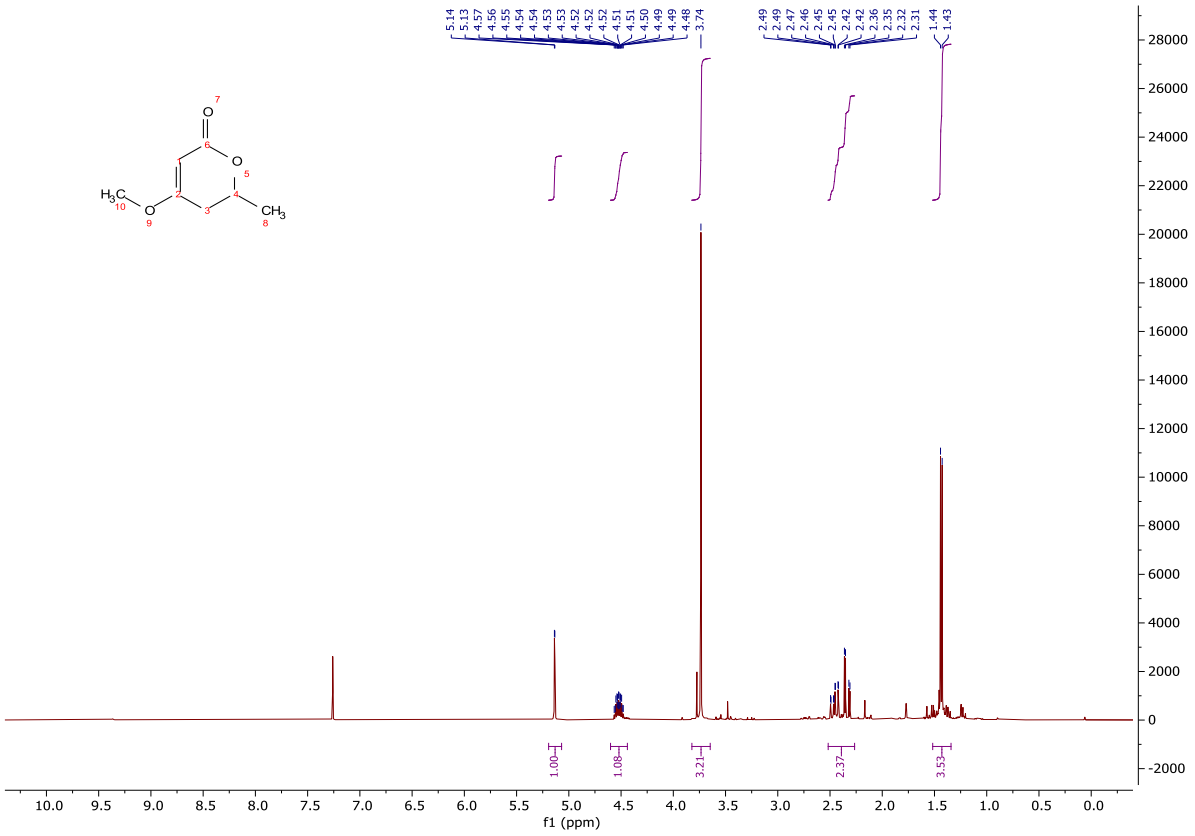
5.14
5.13
4.57
4.56
4.55
4.54
4.54
4.53
4.53
4.52
4.52
4.52
4.51
4.51
4.50
4.49
4.49
4.48
3.74
2.49
2.49
2.47
2.46
2.45
2.45
2.42
2.42
2.36
2.35
2.32
2.31
1.44
1.43
1.00
1.08
3.21
2.37
3.53
f1 (ppm)

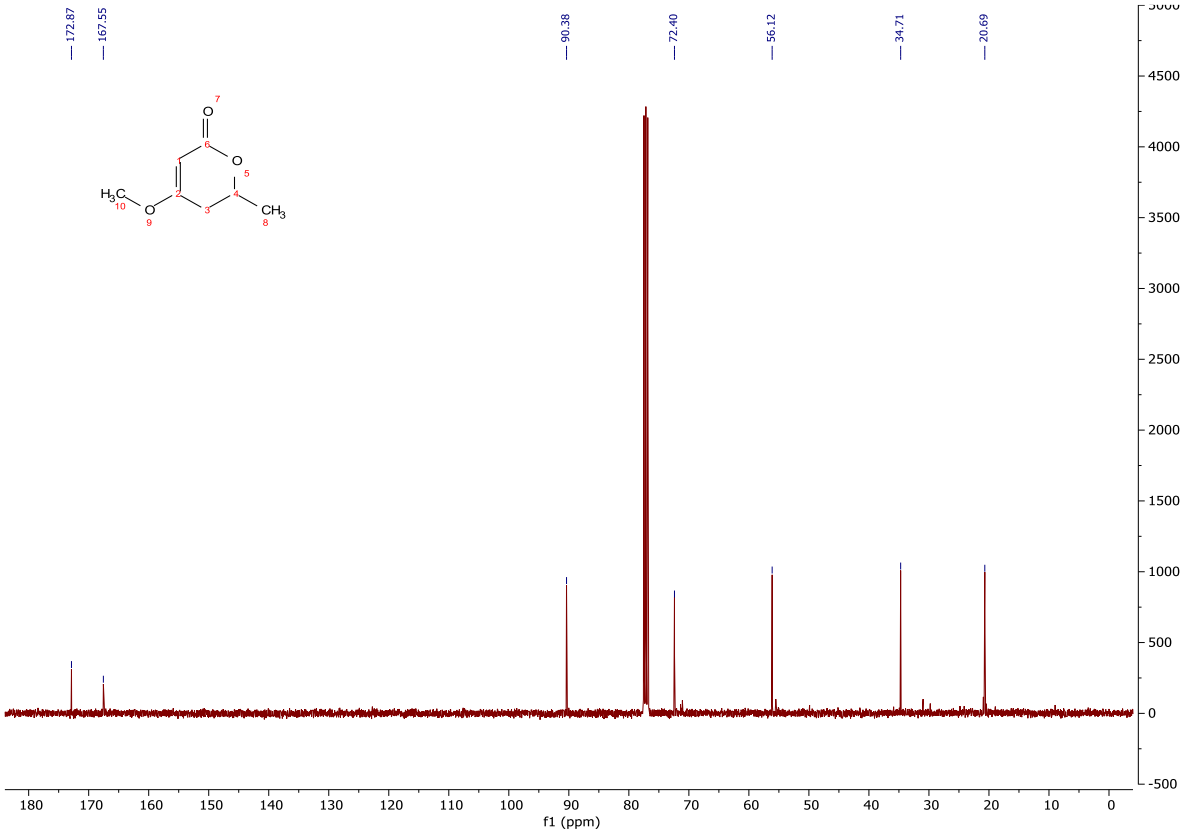
172.87
167.55
90.38
72.40
56.12
34.71
20.69
f1 (ppm)

Methyl (*R*)-3-((*tert*-butyldimethylsilyl)oxy)butanoate (**502**)

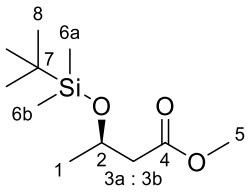

To a solution of (*R*)-methyl-3-hydroxybutanoate (**501**, 3.31 mL, 29.6 mmol) in CH_2Cl_2 (130 mL) at 0 °C was added TMSCl (8.94 g, 59.2 mmol). Imidiazole (8.00 g, 119 mmol) was added portionwise and the reaction mixture was stirred for 16 h. The reaction mixture was washed with sat. $NH_4Cl_{(aq)}$ (2 x 50.0 mL), sat. $NaHCO_{3(aq)}$ (2 x 50.0 mL) and brine (2 x 50.0 mL), dried (Na_2SO_4) and concentrated *in vacuo*. The crude product was purified *via* column chromatography on silica gel, eluting with a gradient of ethyl acetate/light petroleum (0-10%) to give the title compound as a clear, colourless oil (5.93 g, 25.6 mmol, 86%); **HRMS** *m/z* (ESI^+) calc. for $C_{11}H_{25}O_3Si$ $[M+H]^+$ requires 233.1567, found 233.0740; δ_H (400 MHz, $CDCl_3$) 4.33 – 4.21 (1H, m, H-2), 3.66 (3H, s, H-5), 2.48 (1H, dd, *J* = 14.5, 7.7 Hz, H-3a), 2.37 (1H, dd, *J* = 14.5, 5.3 Hz, H-3b), 1.19 (3H, d, *J* = 6.1 Hz, H-1), 0.86 (9H, s, H-8), 0.05 (6H, m, H-6a and H-6b); δ_C (101 MHz, $CDCl_3$) 172.2 (CO), 66.0 (CH), 51.6 (CH_3), 44.9 (CH_2), 25.9 (CH_3), 24.1 (CH_3), 18.1 (C), -4.4 (CH_3), -4.9 (CH_3).

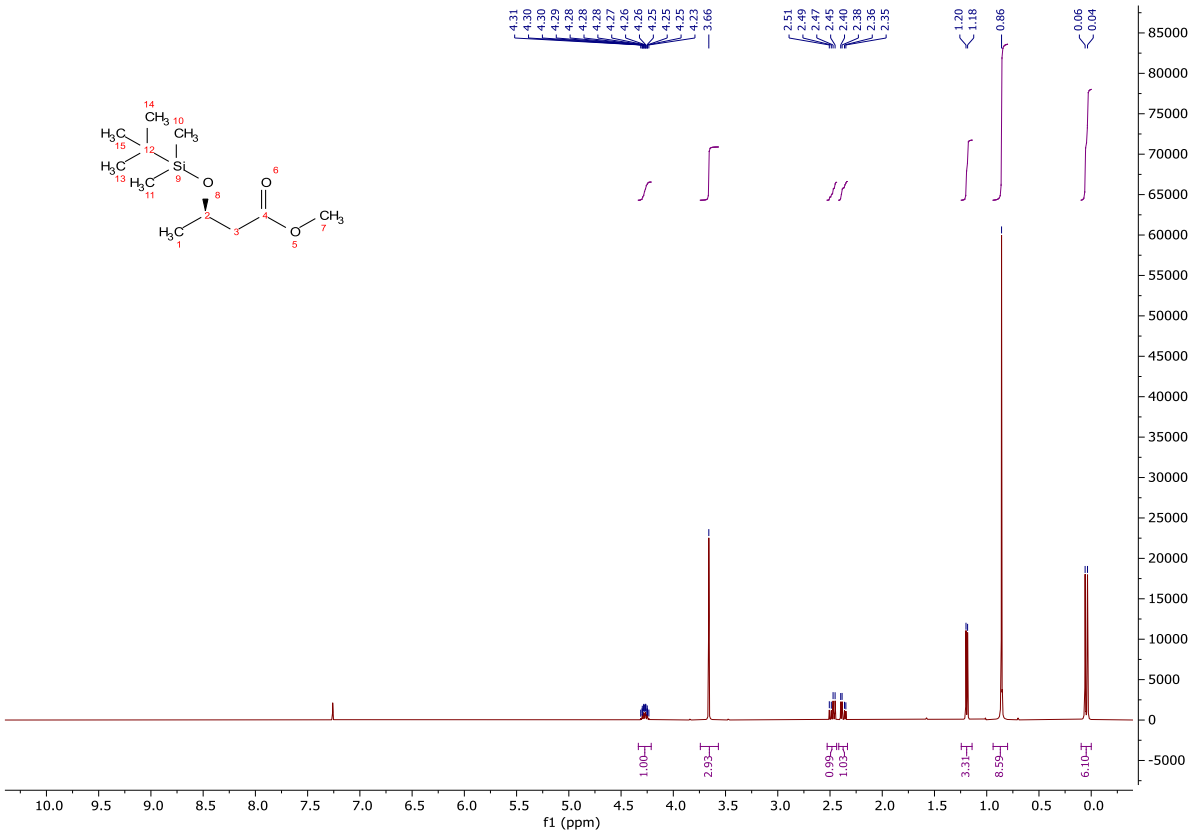
4.31
4.30
4.30
4.29
4.28
4.28
4.28
4.27
4.26
4.26
4.25
4.25
4.25
4.23
3.66
2.51
2.49
2.47
2.45
2.40
2.38
2.36
2.35
1.20
1.18
0.86
0.06
0.04
1.00
2.93
0.99
1.03
3.31
8.59
6.10
f1 (ppm)

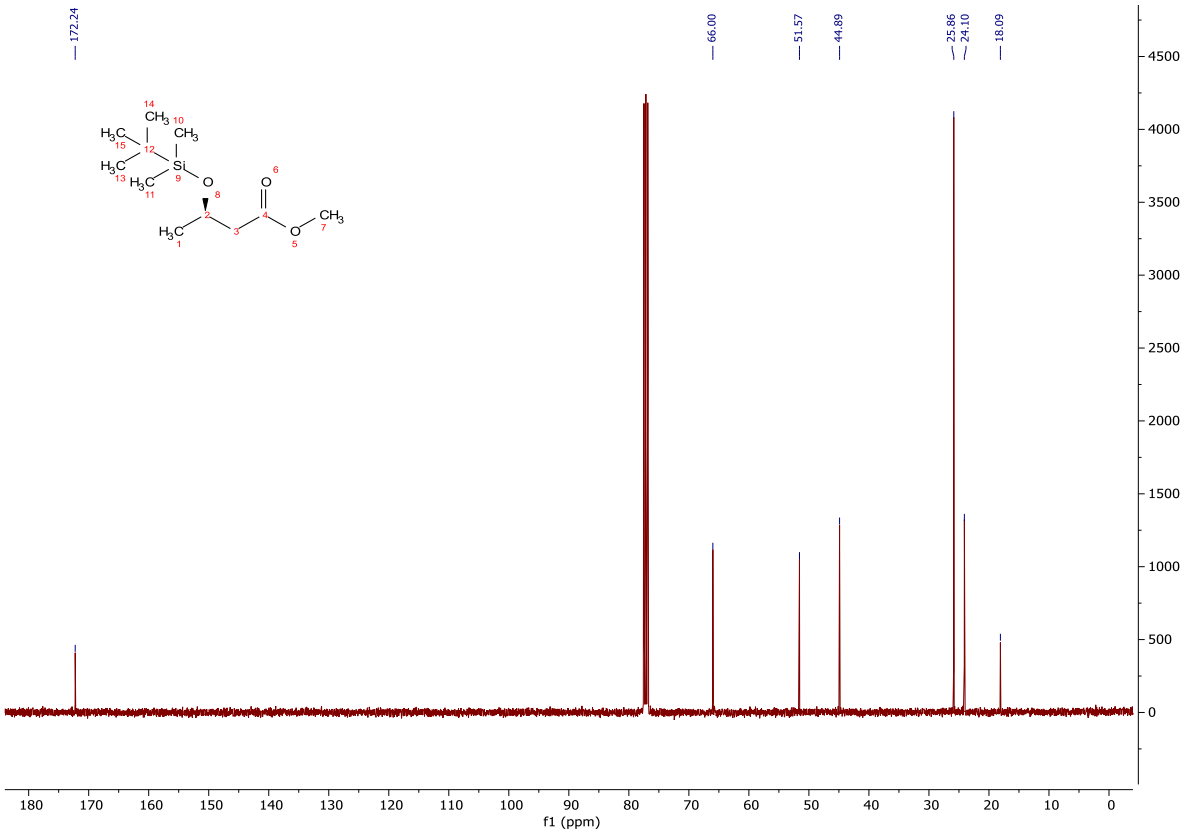
172.24
66.00
51.57
44.89
25.86
24.10
18.09
f1 (ppm)

tert-Butyl (*R*)-5-((*tert*-butyldimethylsilyl)oxy)-3-oxohexanoate (**503**)

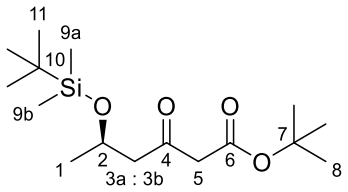

To a solution of *i*-Pr_2NH (4.34 mL, 31.0 mmol) in THF (50.0 mL) at 0 °C under an argon atmosphere was slowly added ^{n}BuLi (2.5M in hexanes, 12.1 mL, 30.2 mmol). The reaction mixture was stirred for 45 min, then cooled to -78 °C. *tert*-Butyl acetate (4.62 mL, 34.5 mmol) was added, and the reaction mixture stirred for 1.5 h. A solution of **502** (2.00 g, 8.62 mmol) in THF (25.0 mL) was added slowly and the reaction mixture stirred for 16 h. Sat. $NH_4Cl_{(aq)}$ (25.0 mL) was added, the mixture was stirred for 15 min and then the organic solvent removed *in vacuo*. The aqueous layer was extracted with ethyl acetate (2 x 50.0 mL) and the organic washed with sat. $NaHCO_{3(aq)}$ (2 x 50.0 mL), brine (2 x 50.0 mL), dried (Na_2SO_4) and concentrated *in vacuo*. The crude product was purified *via* column chromatography on silica gel, eluting with a gradient of ethyl acetate/light petroleum (0-10%) to give the title compound as a yellow oil (2.20 g, 6.96 mmol, 81%); **HRMS** *m/z* (ESI$^+$) calc. for $C_{16}H_{32}NaO_4Si$ $[M+Na]^+$ requires 339.1962, found 339.1960; $\mathbf{R_f}$ 0.48, 5% ethyl acetate/cyclohexane, UV active; δ_H (400 MHz, $CDCl_3$) 12.14 (1H, s, O<u>H</u> taut.), 4.89 (1H, s, C=C<u>H</u> taut.), 4.33 – 4.08 (1H, m, H-2), 3.35 (2H, s, H-5), 2.74 – 2.46 (4H, m, H-3a, H-3b and H-5 C<u>H</u>$_2$ taut.), 2.27 – 2.12 (1H, m, H-3a C<u>H</u>$_2$ taut.), 1.90 – 1.67 (1H, m, H-3b C<u>H</u>$_2$ taut.), 1.51 – 1.38 (9H, m, H-8), 1.20 – 1.11 (3H, m, H-1), 0.91 – 0.77 (9H, m, H-11), 0.13 – -0.05 (6H, m, H-9a and 9b); δ_C (101 MHz, $CDCl_3$) 202.4 (CO), 175.1 (<u>C</u>O/<u>C</u>OH taut), 172.7 (<u>C</u>O/<u>C</u>OH taut), 171.1 (<u>C</u>O/<u>C</u>OH taut), 171.0 (<u>C</u>O/<u>C</u>OH taut), 166.5 (CO), 92.8 (C=<u>C</u>H taut), 81.9 (C), 80.8 (C taut.), 80.7 (C taut.), 71.8 (C taut.), 66.9 (CH taut.), 66.2 (CH taut.), 65.6 (CH), 52.4 (CH_2), 52.2 (CH_2), 47.3 (CH_2 taut.), 45.8 (CH_2 taut.), 45.0 (CH_2 taut.), 44.8 (CH_2 taut.), 28.4 (C), 28.3 (CH_3 taut.), 28.2 (CH_3 taut.), 28.1 (CH_3), 25.9 (CH_3), 24.1 (CH_3), -4.4 (CH_3), -4.9 (CH_3); ν_{max} (FT-ATR/cm^{-1}) 2930, 1717, 1648, 1368, 1320, 1250, 1145, 1077, 1001, 833, 775.

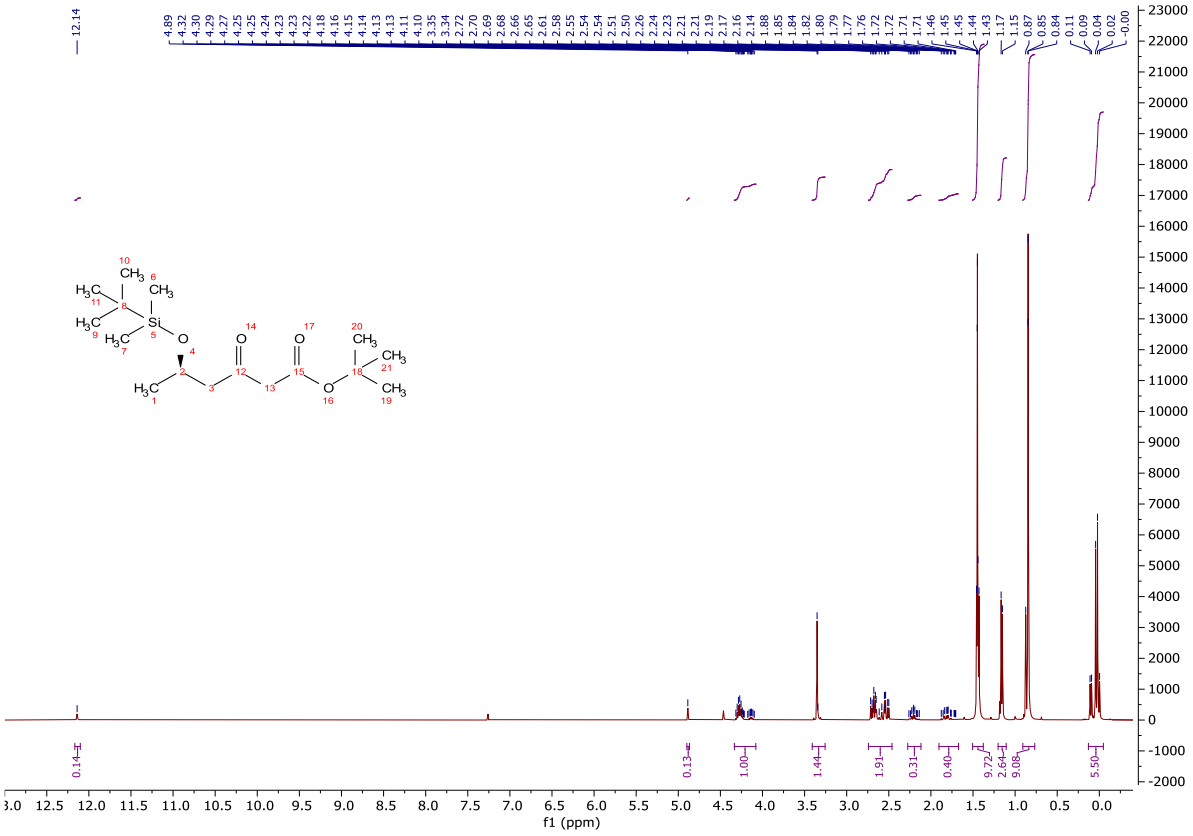
12.14
4.89
4.32
4.30
4.29
4.27
4.25
4.25
4.24
4.23
4.23
4.22
4.18
4.16
4.15
4.14
4.13
4.13
4.11
4.10
3.35
3.34
2.72
2.70
2.69
2.68
2.66
2.65
2.61
2.58
2.55
2.54
2.54
2.51
2.50
2.26
2.24
2.23
2.21
2.21
2.19
2.17
2.16
2.14
1.88
1.85
1.84
1.82
1.80
1.79
1.77
1.76
1.72
1.72
1.71
1.71
1.46
1.45
1.45
1.44
1.43
1.17
1.15
0.87
0.85
0.84
0.11
0.09
0.04
0.02
-0.00
0.14
0.13
1.00
1.44
1.91
0.31
0.40
9.72
2.64
9.08
5.50
f1 (ppm)

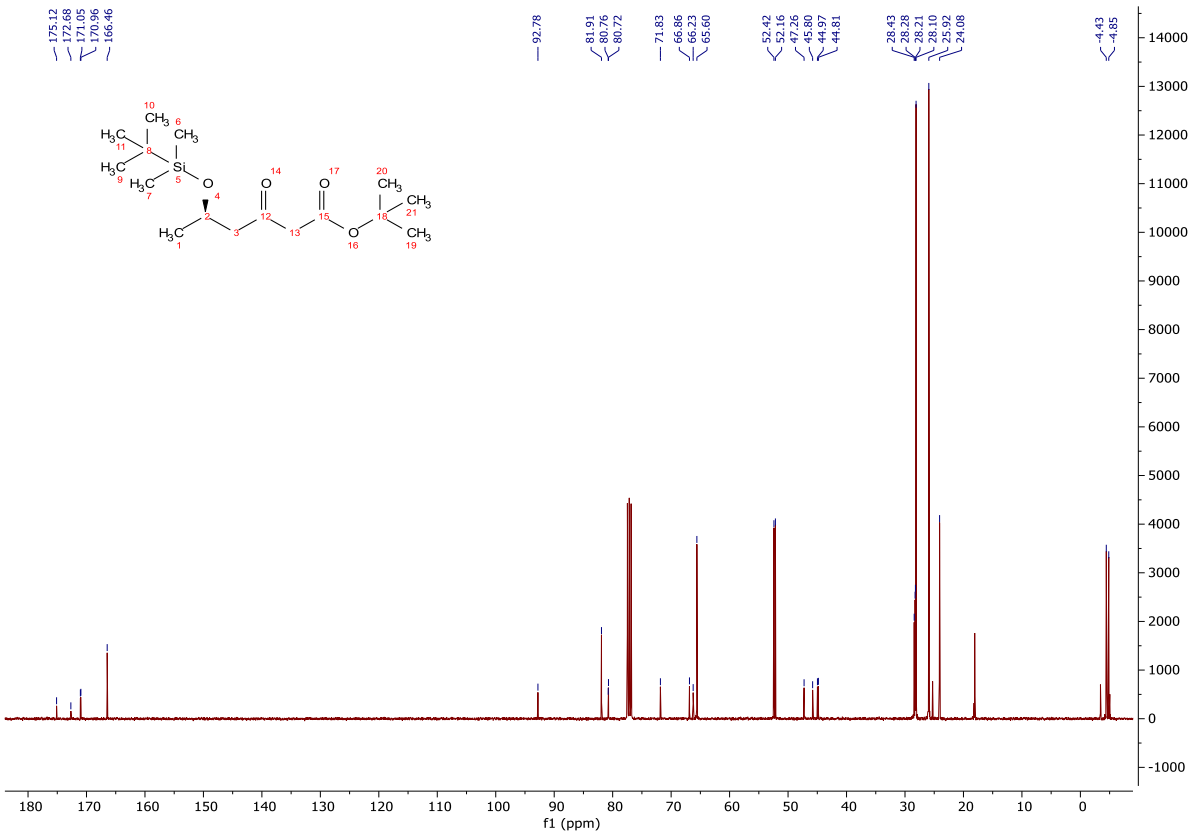
175.12
172.68
171.05
170.96
166.46
92.78
81.91
80.76
80.72
71.83
66.86
66.23
65.60
52.42
52.16
47.26
45.80
44.97
44.81
28.43
28.28
28.21
28.10
25.92
24.08
-4.43
-4.85
f1 (ppm)

Methyl (*R*)-3-(benzyloxy)butanoate (**505**)

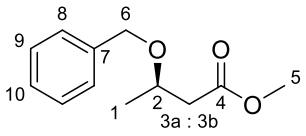

A solution of (*R*)-methyl-3-hydroxybutanoate (**501**, 3.31 mL, 29.6 mmol) and benzyl 2,2,2-trichloroacetimidate (11.0 mL, 59.2 mmol) in CH_2Cl_2/cyclohexane (1:2, 300 mL) was stirred at 0 °C under a nitrogen atmosphere. Triflic acid (0.260 mL, 2.96 mmol) was added dropwise, and the reaction mixture stirred for 16 h. Sat. $Na_2CO_{3(aq)}$ (200 mL) was added, and the mixture stirred for 15 min. The layers were separated and the aqueous was extracted with CH_2Cl_2 (2 x 100 mL). The organics were combined, dried ($MgSO_4$) and concentrated *in vacuo*. The crude product was purified *via* column chromatography on silica gel, eluting with a gradient of ethyl acetate/light petroleum (0-20%) to give the title compound as a clear, yellow oil (5.31 g, 25.5 mmol, 86%); **HRMS** *m/z* (ESI^+) calc. for $C_{12}H_{16}NaO_3$ $[M+Na]^+$ requires 231.0992, found 231.0991; δ_H (400 MHz, $CDCl_3$) 7.43 – 7.08 (5H, m, H-8, H-9 and H-10), 4.62 – 4.37 (2H, m, H-6), 4.16 – 3.87 (1H, m, H-2), 3.68 (3H, m, H-5), 2.66 (1H, m, H-3a), 2.45 (1H, m, H-3b), 1.31 – 1.19 (3H, m, H-1); δ_C (101 MHz, $CDCl_3$) 172.1 (CO), 138.6 (C), 129.1 (ArH), 128.5 (ArH), 127.8 (ArH), 72.0 (CH), 71.0 (CH_2), 51.7 (CH_3), 42.0 (CH_2), 20.0 (CH_3).

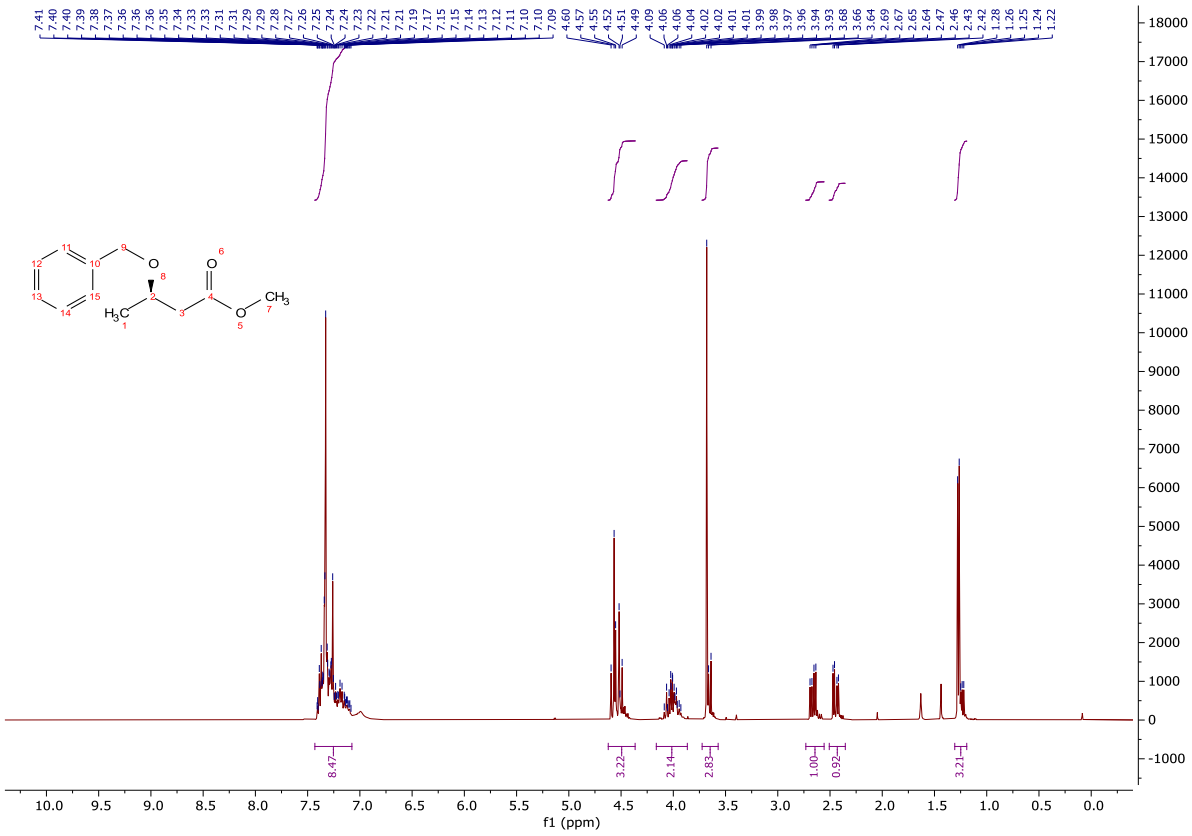
7.41 7.40 7.40 7.39 7.38 7.37 7.36 7.36 7.35 7.34 7.33 7.31 7.31 7.29 7.29 7.28 7.27 7.26 7.25 7.24 7.24 7.23 7.22 7.21 7.21 7.19 7.17 7.15 7.15 7.14 7.13 7.12 7.11 7.10 7.10 7.09 4.60 4.57 4.55 4.52 4.51 4.49 4.09 4.06 4.06 4.04 4.02 4.02 4.01 4.01 3.99 3.98 3.97 3.96 3.94 3.93 3.68 3.66 3.64 2.69 2.67 2.65 2.64 2.47 2.46 2.43 2.42 1.28 1.26 1.25 1.24 1.22
8.47 3.22 2.14 2.83 1.00 0.92 3.21
f1 (ppm)

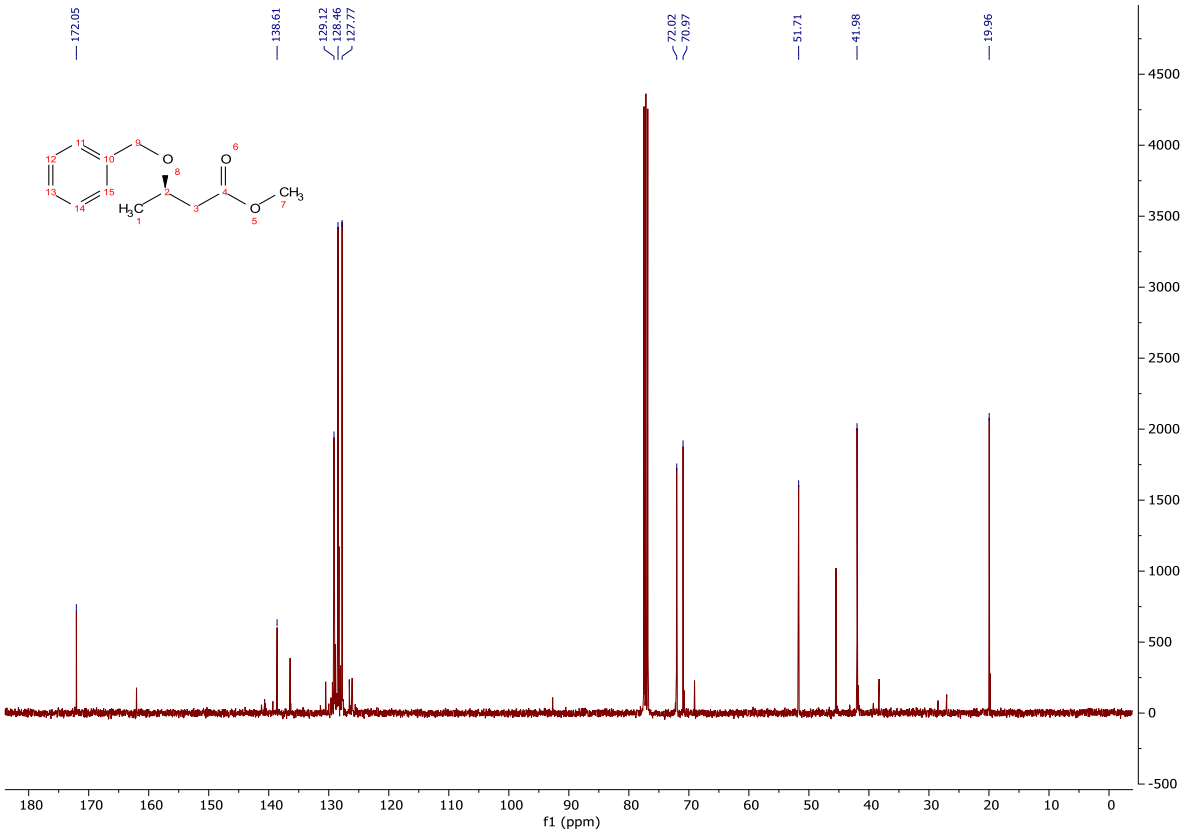
172.05 138.61 129.12 128.46 127.77 72.02 70.97 51.71 41.98 19.96
f1 (ppm)

tert-Butyl (*R*)-5-(benzyloxy)-3-oxohexanoate (**506**)

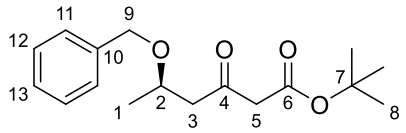

To a solution of *i*-Pr_2NH (4.34 mL, 31.0 mmol) in THF (50.0 mL) at 0 °C under an argon atmosphere was slowly added ^{n}BuLi (2.5M in hexanes, 12.0 mL, 30.1 mmol). The reaction mixture was stirred for 45 min, then cooled to -78 °C. *tert*-Butyl acetate (4.61 mL, 34.4 mmol) was added, and the reaction mixture stirred for 1.5 h. A solution of **505** (1.79 g, 8.61 mmol) in THF (25.0 mL) was added slowly and the reaction mixture stirred for 64 h. Sat. $NH_4Cl_{(aq)}$ (25 mL) was added, the mixture was stirred for 15 min and then the organic solvent removed *in vacuo*. The aqueous layer was extracted with ethyl acetate (2 x 50.0 mL) and the organic washed with sat. $NaHCO_{3(aq)}$ (2 x 50.0 mL), brine (2 x 50.0 mL), dried (Na_2SO_4) and concentrated *in vacuo*. The crude product was purified *via* column chromatography on silica gel, eluting with a gradient of ethyl acetate/light petroleum (0-15%) to give the title compound as a yellow oil (2.15 g, 7.36 mmol, 85%); **HRMS** *m/z* (ESI^+) calc. for $C_{17}H_{24}NaO_4$ $[M+Na]^+$ requires 315.1567, found 315.1566; $\mathbf{R_f}$ 0.46, 20% ethyl acetate/cyclohexane, UV active; δ_H (400 MHz, $CDCl_3$) 12.23 (1H, s, OH taut.), 7.41 – 6.98 (5H, m, H-11, H-12 and H-13), 4.96 (1H, s, C=CH taut.), 4.67 – 4.28 (2H, m, H-9), 4.12 – 3.84 (1H, m, H-2), 3.39 – 3.35 (2H, m, H-5), 2.95 – 2.45 (4H, m, H-3a, H-3b and H-5 CH_2 taut.), 2.07 – 1.96 (1H, m, H-3a CH_2 taut.), 1.89 – 1.77 (1H, m, H-3b CH_2 taut.), 1.54 – 1.37 (9H, m, H-8), 1.29 – 1.21 (3H, m, H-1); δ_C (101 MHz, $CDCl_3$) 202.1 (CO), 171.5 (CO/COH), 171.1 (CO/COH), 171.0 (CO/COH), 166.5 (CO), 138.5 (C), 138.3 (C taut.), 128.54 (ArH taut.), 128.49 (ArH), 128.1 (ArH), 127.84 (ArH), 127.78 (ArH taut.), 127.7 (ArH), 92.5 (C=CH taut.), 82.0 (C), 81.3 (C taut.), 80.9 (C taut.), 80.8 (C taut.), 72.4 (CH taut.), 71.7 (CH taut.), 71.6 (CH), 71.0 (CH_2), 70.3 (CH_2 taut.), 70.0 (CH_2 taut.), 51.7 (CH_2), 50.1 (CH_2), 46.2 (CH_2 taut.), 45.7 (CH_2 taut.), 45.0 (CH_2 taut.), 44.7 (CH_2 taut.), 28.3 (C taut.), 28.2 (C), 28.1 (C taut.), 20.3 (CH_3 taut.), 19.9 (CH_3); ν_{max} (FT-ATR/cm^{-1}) 3495, 2976, 1715, 1454, 1368, 1251, 1144, 956, 842, 735, 697, 460.

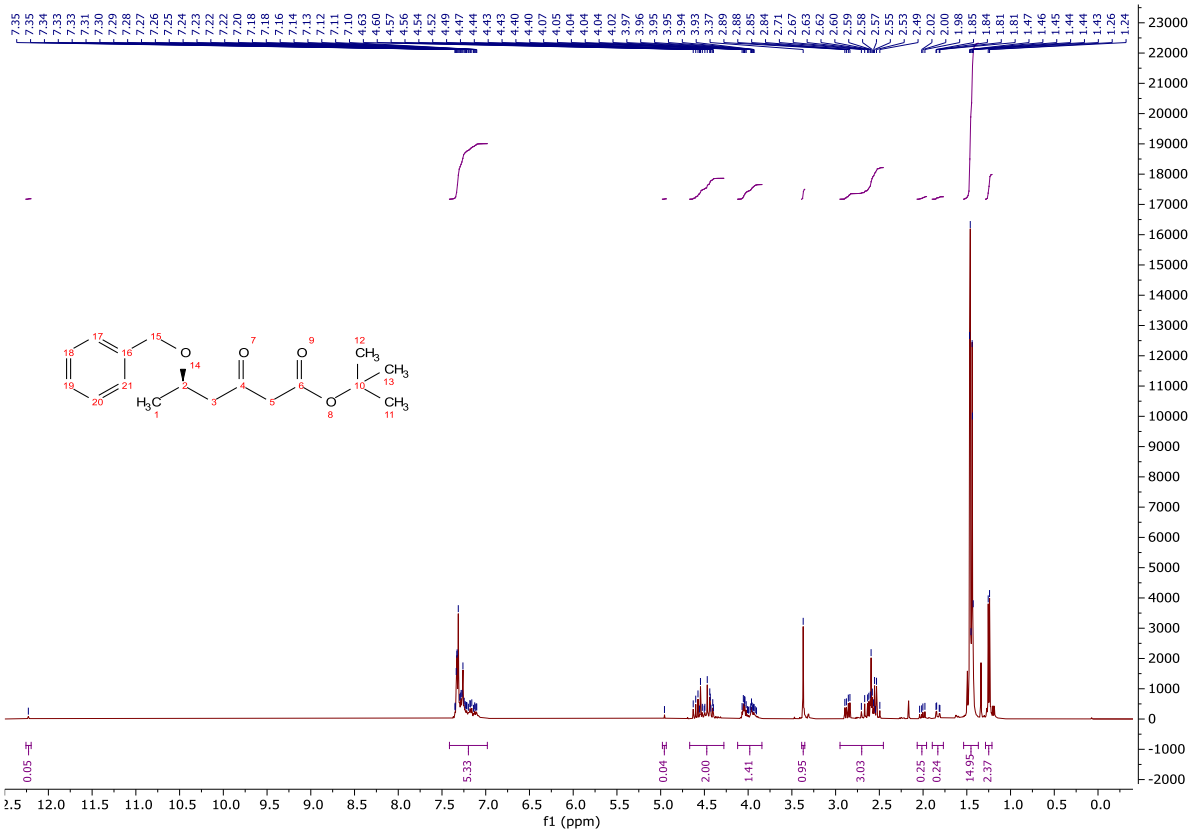
f1 (ppm)

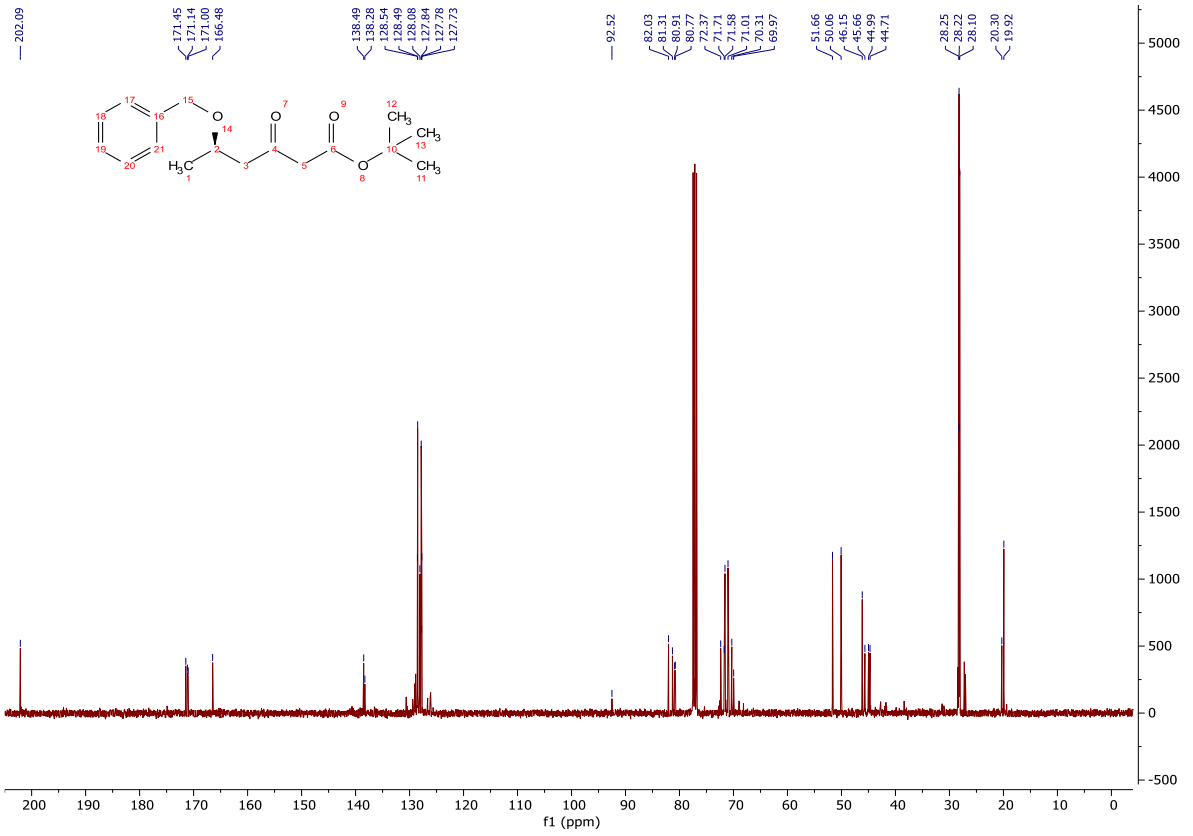
f1 (ppm)

References

[1] S. Armstrong, Integrin Antagonists for Idiopathic Pulmonary Fibrosis, University of Nottingham, **2017**.

[2] H. Bird, Integrin Antagonists for Idiopathic Pulmonary Fibrosis, University of Nottingham, **2018**.

[3] N. C. Rose, Integrin Antagonists for Idiopathic Pulmonary Fibrosis, University of Nottingham, **2019**.

[4] K. R. Saunders-Coombs, Integrin Antagonists for Idiopathic Pulmonary Fibrosis, University of Nottingham, **2018**.

[5] K. Simelis, Integrin Antagonists for Idiopathic Pulmonary Fibrosis, University of Nottingham, **2017**.

[6] J. S. Tromans, Integrin Antagonists for Idiopathic Pulmonary Fibrosis, University of Nottingham, **2019**.

[7] J. Waters, Integrin Antagonists for Idiopathic Pulmonary Fibrosis, University of Nottingham, **2018**.

[8] S. Bryers, Integrin Antagonists for Idiopathic Pulmonary Fibrosis, University of Nottingham, **2017**.

[9] E. J. P. Hogarth, Integrin Antagonists for Idiopathic Pulmonary Fibrosis, University of Nottingham, **2017**.

[10] T. C. Keenan, Integrin Antagonists for Idiopathic Pulmonary Fibrosis, University of Nottingham, **2019**.

[11] M.-L. MacKinnon, Integrin Antagonists for Idiopathic Pulmonary Fibrosis, University of Nottingham, **2018**.

[12] E. O. I. Makinde, Integrin Antagonists for Idiopathic Pulmonary Fibrosis, University of Nottingham, **2019**.

[13] C. Merrett, Integrin Antagonists for Idiopathic Pulmonary Fibrosis, University of Nottingham, **2018**.

[14] M. J. Millward, Integrin Antagonists for Idiopathic Pulmonary Fibrosis, University of Nottingham, **2017**.

[15] C. Pike, Integrin Antagonists for Idiopathic Pulmonary Fibrosis, University of Nottingham, **2017**.

[16] D. A. Dias, S. Urban, U. Roessner, *Metabolites* **2012**, *2*, 303–336.

[17] C. Veeresham, *J. Adv. Pharm. Technol. Res.* **2012**, *3*, 200–201.

[18] G. M. Cragg, D. J. Newman, *Pharm. Biol.* **2001**, *39*, 8–17.

[19] N. R. Farnsworth, O. Akerele, A. S. Bingel, D. D. Soejarto, Z. Guo, *Bull. World Health Organ.* **1985**, *63*, 965–981.

[20] G. M. Cragg, D. J. Newman, K. M. Snader, *J. Nat. Prod.* **1997**, *60*, 52–60.

[21] A. Batta, B. S. Kalra, R. Khirasaria, *J. Fam. Med. Prim. Care* **2020**, *9*, 105–114.

[22] H. Wiig, M. A. Swartz, *Physiol. Rev.* **2012**, *92*, 1005–1060.

[23] J. Scallan, V. H. Huxley, R. J. Korthuis, *Capillary Fluid Exchange: Regulation, Functions, and Pathology*, Morgan And Claypool Life Sciences, **2010**.

[24] P. C. Benias, R. G. Wells, B. Sackey-Aboagye, H. Klavan, J. Reidy, D. Buonocore, M. Miranda, S. Kornacki, M. Wayne, D. L. Carr-Locke, et al., *Sci. Rep.* **2018**, *8*, 1–8.

[25] J. Gribbin, R. B. Hubbard, I. Le Jeune, C. J. P. Smith, J. West, L. J. Tata, *Thorax* **2006**, *61*, 980–985.

[26] G. Raghu, D. Weycker, J. Edelsberg, W. Z. Bradford, G. Oster, *Am. J. Respir. Crit. Care Med.* **2006**, *174*, 810–816.

[27] V. Navaratnam, K. M. Fleming, J. West, C. J. P. Smith, R. G. Jenkins, A. Fogarty, R. B. Hubbard, *Thorax* **2011**, *66*, 462–467.

[28] A. Datta, C. J. Scotton, R. C. Chambers, *Br. J. Pharmacol.* **2011**, *163*, 141–172.

[29] G. Hughes, H. Toellner, H. Morris, C. Leonard, N. Chaudhuri, *J. Clin. Med.* **2016**, *5*, 78.

[30] G. Margaritopoulos, E. Vasarmidi, K. Antoniou, *Core Evid.* **2016**, *11*, 11–22.

[31] R. S. Williams, *Circulation* **2000**, *101*, 1227–1228.

[32] T. E. King, W. Z. Bradford, S. Castro-Bernardini, E. A. Fagan, I. Glaspole, M. K. Glassberg, E. Gorina, P. M. Hopkins, D. Kardatzke, L. Lancaster, et al., *N. Engl. J. Med.* **2014**, *370*, 2083–2092.

[33] L. Wollin, E. Wex, A. Pautsch, G. Schnapp, K. E. Hostettler, S. Stowasser, M. Kolb, *Eur. Respir. J.* **2015**, *45*, 1434–1445.

[34] G. Raghu, H. R. Collard, J. J. Egan, F. J. Martinez, J. Behr, K. K. Brown, T. V. Colby, J. F. Cordier, K. R. Flaherty, J. A. Lasky, et al., *Am. J. Respir. Crit. Care Med.* **2011**, *183*, 788–824.

[35] R. L. Hernandez, M. A. Perez, M. T. L. Carrasco, P. U. Gil, *Med. Sci.* **2018**, *6*, 68.

[36] B. Alberts, A. Johnson, J. Lewis, M. Raff, K. Roberts, P. Walter, *Integrins*, Garland Science, New York, **2002**.

[37] M. Barczyk, S. Carracedo, D. Gullberg, *Cell Tissue Res.* **2010**, *339*, 269–280.

[38] N. C. Henderson, D. Sheppard, *Biochim. Biophys. Acta* **2014**, *1832*, 891–896.

[39] P. Aluwihare, Z. Mu, Z. Zhao, D. Yu, P. H. Weinreb, G. S. Horan, S. M. Violette, J. S. Munger, *J. Cell Sci.* **2009**, *122*, 227–232.

[40] A. B. Roberts, M. B. Sporn, R. K. Assoian, J. M. Smith, N. S. Roche, L. M. Wakefield, U. I. Heine, L. A. Liotta, V. Falanga, J. H. Kehrl, *Proc. Natl. Acad. Sci. U. S. A.* **1986**, *83*, 4167–4171.

[41] J. Porte, G. Jenkins, *Pharmacol. Res. Perspect.* **2014**, *2*, e00030.

[42] A. Biernacka, M. Dobaczewski, N. G. Frangogiannis, *Growth Factors* **2011**, *29*, 196–202.

[43] D. Sheppard, *Eur. Respir. J.* **2008**, *17*, 157–162.

[44] N. C. Henderson, D. Sheppard, *Biochim. Biophys. Acta* **2012**, *1832*, 891–896.

[45] S. M. Weis, D. A. Cheresh, *Cold Spring Harb. Perspect. Med.* **2011**, *1*, 1–14.

[46] Z. Liu, F. Wang, X. Chen, *Drug Dev. Res.* **2008**, *69*, 329–339.

[47] A. McCurley, S. Alimperti, S. B. Campos-Bilderback, R. M. Sandoval, J. E. Calvino, T. L. Reynolds, C. Quigley, J. W. Mugford, W. J. Polacheck, I. G. Gomez, et al., *J. Am. Soc. Nephrol.* **2017**, *28*, 1741–1752.

[48] E. Dodagatta-Marri, H. Y. Ma, B. Liang, J. Li, D. S. Meyer, S. Y. Chen, K. H. Sun, X. Ren, B. Zivak, M. D. Rosenblum, et al., *Cell Rep.* **2021**, *36*, 109309.

[49] J. Zhu, K. Motejlek, D. Wang, K. Zang, A. Schmidt, L. F. Reichardt, *Development* **2002**, *129*, 2891–2903.

[50] M. A. Travis, B. Reizis, A. C. Melton, E. Masteller, Q. Tang, J. M. Proctor, Y. Wang, X. Bernstein, X. Huang, L. F. Reichardt, et al., *Nature* **2007**, *449*, 361–365.

[51] J. Li, Y. Qu, X. Li, D. Li, F. Zhao, M. Mao, D. Ferriero, D. Mu, *Neurotox. Res.* **2010**, *17*, 406–417.

[52] H. M. Sheldrake, L. H. Patterson, *J. Med. Chem.* **2014**, *57*, 6301–6315.

[53] J. Chen, J. S. Alexander, A. W. Orr, *Int. J. Cell Biol.* **2012**, *2012*, 1–12.

[54] G. S. Horan, S. Wood, V. Ona, D. J. Li, M. E. Lukashev, P. H. Weinreb, K. J. Simon, K. Hahm, N. E. Allaire, N. J. Rinaldi, et al., *Am. J. Respir. Crit. Care Med.* **2008**, *177*, 56–65.

[55] A. L. Tatler, G. Jenkins, *Proc. Am. Thorac. Soc.* **2012**, *9*, 130–136.

[56] G. S. Horan, S. Wood, V. Ona, J. L. Dan, M. E. Lukashev, P. H. Weinreb, K. J. Simon, K. Hahm, N. E. Allaire, N. J. Rinaldi, et al., *Am. J. Respir. Crit. Care Med.* **2008**, *177*, 56–65.

[57] G. Su, A. Atakilit, J. T. Li, N. Wu, M. Bhattacharya, J. Zhu, J. E. Shieh, E. Li, R. Chen, S. Sun, et al., *Am. J. Respir. Crit. Care Med.* **2012**, *185*, 58–66.

[58] S. Goswami, *Adv. Biol. Chem.* **2013**, *3*, 224–252.

[59] G. Köhler, C. Milstein, *Nature* **1975**, *256*, 495–497.

[60] M. Berger, V. Shankar, A. Vafai, *Am. J. Med. Sci.* **2002**, *324*, 14–30.

[61] M. S. Cohen, *N. Engl. J. Med.* **2021**, *384*, 289–291.

[62] N. S. Lipman, L. R. Jackson, L. J. Trudel, F. Weis-Garcia, *ILAR J.* **2005**, *46*, 258–268.

[63] A. Byron, J. D. Humphries, J. A. Askari, S. E. Craig, A. P. Mould, M. J. Humphries, *J. Cell Sci.* **2012**, *122*, 4009–4011.

[64] M. J. Humphries, *Biochem. Soc. Trans.* **2004**, *32*, 407–411.

[65] M. A. Schwartz, K. McRoberts, M. Coyner, K. L. Andarawewa, H. F. Frierson, J. M.

Sanders, S. Swenson, F. Markland, M. R. Conaway, D. Theodorescu, *Clin. Cancer Res.* **2008**, *14*, 6193–6197.

[66] A. Paul Mould, S. K. Akiyama, M. J. Humphries, *J. Biol. Chem.* **1996**, *271*, 20365–20374.

[67] P. H. Weinreb, K. J. Simon, P. Rayhorn, W. J. Yang, D. R. Leone, B. M. Dolinski, B. R. Pearse, Y. Yokota, H. Kawakatsu, A. Atakilit, et al., *J. Biol. Chem.* **2004**, *279*, 17875–17887.

[68] J. K. Arruda Macêdo, J. W. Fox, M. D. S. Castro, *Curr. Protein Pept. Sci.* **2015**, *16*, 532–548.

[69] I. Limam, A. Bazaa, N. Srairi-Abid, S. Taboubi, J. Jebali, R. Zouari-Kessentini, O. Kallech-Ziri, H. Mejdoub, A. Hammami, M. El Ayeb, et al., *Matrix Biol.* **2010**, *29*, 117–126.

[70] C. Mas-Moruno, F. Rechenmacher, H. Kessler, *Anticancer. Agents Med. Chem.* **2011**, *10*, 753–768.

[71] M. A. Dechantsreiter, E. Planker, B. Mathä, E. Lohof, G. Hölzemann, A. Jonczyk, S. L. Goodman, H. Kessler, *J. Med. Chem.* **1999**, *42*, 3033–3040.

[72] D. A. Reardon, L. B. Nabors, S. Roger, T. Mikkelsen, *Expert Opin. Investig. Drugs* **2008**, *17*, 1225–1235.

[73] M. Cully, *Nat. Rev. Drug Discov.* **2020**, *19*, 739–741.

[74] J. Cha, M. Decaris, C. Dong, T. Hom, L. Jiang, K. Leftheris, H. Li, D. J. Morgans Jr, M. Munoz, M. Reilly, et al., *Dosage Forms and Regimens for Amino Acid Compounds*, **2020**, WO2020210404A1.

[75] N. C. Henderson, T. D. Arnold, Y. Katamura, M. M. Giacomini, J. D. Rodriguez, J. H. McCarty, A. Pellicoro, E. Raschperger, C. Betsholtz, P. G. Ruminski, et al., *Nat. Med.* **2013**, *19*, 1617–1624.

[76] R. J. D. Hatley, S. J. F. Macdonald, R. J. Slack, J. Le, S. B. Ludbrook, P. T. Lukey, *Angew. Chem. Int. Ed. Engl.* **2018**, *57*, 2–26.

[77] G. Su, M. Hodnett, N. Wu, A. Atakilit, C. Kosinski, M. Codzich, X. Z. Huang, J. K. Kim, J. A. Frank, M. A. Matthay, et al., *Am. J. Respir. Cell Mol. Biol.* **2007**, *36*, 377–386.

[78] C. H. Maden, D. Fairman, M. Chalker, M. J. Costa, W. A. Fahy, N. Garman, P. T. Lukey, T. Mant, S. Parry, J. K. Simpson, et al., *Eur. J. Clin. Pharmacol.* **2018**, *74*, 701–709.

[79] P. J. Coleman, B. C. Askew, J. H. Hutchinson, D. B. Whitman, J. J. Perkins, G. D. Hartman, G. A. Rodan, C. T. Leu, T. Prueksaritanont, C. Fernandez-Metzler, et al., *Bioorg. Med. Chem. Lett.* **2002**, *12*, 2463–2465.

[80] X. Dong, N. E. Hudson, C. Lu, T. A. Springer, *Nat. Struct. Mol. Biol.* **2014**, *21*, 1091–1096.

[81] G. A. G. Sulyok, C. Gibson, S. L. Goodman, G. Hölzemann, M. Wiesner, H. Kessler, *J. Med. Chem.* **2001**, *44*, 1938–1950.

[82] J. Adams, E. C. Anderson, E. E. Blackham, Y. W. R. Chiu, T. Clarke, N. Eccles, L. A. Gill,

J. J. Haye, H. T. Haywood, C. R. Hoenig, et al., *ACS Med. Chem. Lett.* **2014**, *5*, 1207–1212.

[83] S. B. Ludbrook, S. T. Barry, C. J. Delves, C. M. T. Horgan, *Biochem. J.* **2003**, *369*, 311–318.

[84] A. P. Hill, R. J. Young, *Drug Discov. Today* **2010**, *15*, 648–655.

[85] R. J. Young, D. V. S. Green, C. N. Luscombe, A. P. Hill, *Drug Discov. Today* **2011**, *16*, 822–830.

[86] M. Kansy, F. Senner, K. Gubernator, *J. Med. Chem.* **1998**, *41*, 1007–1010.

[87] M. Chen, J. Borlak, W. Tong, *Hepatology* **2013**, *58*, 388–396.

[88] M. R. Naylor, A. M. Ly, M. J. Handford, D. P. Ramos, C. R. Pye, A. Furukawa, V. G. Klein, R. P. Noland, Q. Edmondson, A. C. Turmon, et al., *J. Med. Chem.* **2018**, *61*, 11169–11182.

[89] N. A. Anderson, B. J. Fallon, J. M. Pritchard, *Naphthyridine Derivatives Useful as Alpha-V-Beta-6 Integrin Antagonists*, **2014**, WO2014154725A1.

[90] N. A. Anderson, M. H. J. Campbell-Crawford, A. P. Hancock, J. M. Pritchard, J. M. Redmond, *Novel Compounds*, **2016**, WO2016046225A1.

[91] N. A. Anderson, I. B. Campbell, M. H. J. Campbell-Crawford, A. P. Hancock, S. Lemma, S. J. F. Macdonald, J. M. Pritchard, P. A. Procopiou, *Naphthyridine Derivatives as Alpha-V-Beta-6 Integrin Antagonists for the Treatment of E.G. Fibrotic Diseases*, **2016**, WO2016046230A1.

[92] P. A. Procopiou, N. A. Anderson, J. Barrett, T. N. Barrett, M. H. J. Crawford, B. J. Fallon, A. P. Hancock, J. Le, S. Lemma, R. P. Marshall, et al., *J. Med. Chem.* **2018**, *61*, 8417–8443.

[93] I. D. Kuntz, K. Chen, K. A. Sharp, P. A. Kollman, *Proc. Natl. Acad. Sci. U. S. A.* **1999**, *96*, 9997–10002.

[94] C. Abad-Zapatero, *Expert Opin. Drug Discov.* **2007**, *2*, 469–488.

[95] M. D. Shultz, *Bioorg. Med. Chem. Lett.* **2013**, *23*, 5980–5991.

[96] C. Abad-Zapatero, J. T. Metz, *Drug Discov. Today* **2005**, *10*, 464–469.

[97] E. Perola, *J. Med. Chem.* **2010**, *53*, 2986–2997.

[98] P. G. Dormer, K. K. Eng, R. N. Farr, G. R. Humphrey, J. C. McWilliams, P. J. Reider, J. W. Sager, R. P. Volante, *J. Org. Chem.* **2003**, *68*, 467–477.

[99] M. Bursavich, A. Gerasyuto, K. Hahn, B. Harrison, K. Konze, F.-Y. Lin, B. Lippa, A. Lugovskoy, B. Rogers, M. Svensson, et al., *Inhibitors of (Alpha-V)(Beta-6) Integrin*, **2018**, WO2018160522A1.

[100] W. M. Rodionow, E. A. Postovskaja, *J. Am. Chem. Soc.* **1929**, *51*, 841–847.

[101] W. M. Rodionow, *J. Am. Chem. Soc.* **1929**, *51*, 847–852.

[102] C. Y. K. Tan, D. F. Weaver, *Tetrahedron* **2002**, *58*, 7449–7461.

[103] G. Liu, D. A. Cogan, J. A. Ellman, *J. Am. Chem. Soc.* **1997**, *119*, 9913–9914.

[104] M. T. Robak, M. A. Herbage, J. A. Ellman, *Chem. Rev.* **2010**, *110*, 3600–3740.

[105] F. A. Davis, R. E. Reddy, J. M. Szewczyk, G. V. Reddy, P. S. Portonovo, H. Zhang, D. Fanelli, R. Thimma Reddy, P. Zhou, P. J. Carroll, *J. Org. Chem.* **1997**, *62*, 2555–2563.

[106] F. A. Davis, P. S. Portonovo, R. E. Reddy, Y. Chiu, *J. Org. Chem.* **1996**, *61*, 440–441.

[107] F. A. Davis, R. E. Reddy, J. M. Szewczyk, *J. Org. Chem.* **1995**, *60*, 7037–7039.

[108] D. D. Staas, K. L. Savage, C. F. Homnick, N. N. Tsou, R. G. Ball, *J. Org. Chem.* **2002**, *67*, 8276–8279.

[109] M. Mineno, Y. Sawai, K. Kanno, N. Sawada, H. Mizufune, *J. Org. Chem.* **2013**, *78*, 5843–5850.

[110] D. G. Brown, J. Boström, *J. Med. Chem.* **2016**, *59*, 4443–4458.

[111] T. Cernak, K. D. Dykstra, S. Tyagarajan, P. Vachal, S. W. Krska, *Chem. Soc. Rev.* **2016**, *45*, 546–576.

[112] A. R. D. Taylor, M. Maccoss, A. D. G. Lawson, *J. Med. Chem.* **2013**, *57*, 5845–5859.

[113] D. M. T. Chan, K. L. Monaco, R. P. Wang, M. P. Winters, *Tetrahedron Lett.* **1998**, *39*, 2933–2936.

[114] D. A. Evans, J. L. Katz, T. R. West, *Tetrahedron Lett.* **1998**, *39*, 2937–2940.

[115] P. Y. S. Lam, C. G. Clark, S. Saubern, J. Adams, M. P. Winters, D. M. T. Chan, A. Combs, *Tetrahedron Lett.* **1998**, *39*, 2941–2944.

[116] D. J. Cundy, S. A. Forsyth, *Tetrahedron Lett.* **1998**, *39*, 7979–7982.

[117] D. Ma, Q. Cai, H. Zhang, *Org. Lett.* **2003**, *5*, 2453–2455.

[118] S. M. Mennen, C. Alhambra, C. L. Allen, M. Barberis, S. Berritt, T. A. Brandt, A. D. Campbell, J. Castanon, A. H. Cherney, M. Christensen, et al., *Org. Process Res. Dev.* **2019**, *23*, 1213–1242.

[119] J. C. Vantourout, H. N. Miras, A. Isidro-Llobet, S. Sproules, A. J. B. Watson, *J. Am. Chem. Soc.* **2017**, *139*, 4769–4779.

[120] S. Ahmad, M. Yousaf, A. Mansha, N. Rasool, A. F. Zahoor, F. Hafeez, S. M. A. Rizvi, *Synth. Commun.* **2016**, *46*, 1397–1416.

[121] P. H. Dussault, T. K. Trullinger, F. Noor-e-Ain, *Org. Lett.* **2002**, *4*, 4591–4593.

[122] J. A. Bull, R. A. Croft, O. A. Davis, R. Doran, K. F. Morgan, *Chem. Rev.* **2016**, *116*, 12150–12233.

[123] R. D. Patil, Y. Sasson, *Asian J. Org. Chem.* **2015**, *4*, 1258–1261.

[124] A. Schnyder, A. Indolese, M. Studer, H. Blaser, *Angew. Chem. Int. Ed. Engl.* **2002**, *41*, 3668–3671.

[125] G. A. Molander, P. E. Gormisky, *J. Org. Chem.* **2008**, *73*, 7481–7485.

[126] A. J. J. Lennox, G. C. Lloyd-Jones, *Angew. Chem. Int. Ed.* **2012**, *51*, 9385–9388.

[127] E. Filali, G. C. Lloyd-Jones, D. A. Sale, *Synlett* **2009**, 205–208.

[128] W. Kurosawa, T. Kan, T. Fukuyama, *J. Am. Chem. Soc.* **2003**, *125*, 8112–8113.

[129] M. Matoba, T. Kajimoto, M. Node, *Synth. Commun.* **2008**, *38*, 1194–1200.

[130] H. Robinson, S. A. Oatley, J. E. Rowedder, P. Slade, S. J. F. Macdonald, S. P. Argent, J. D. Hirst, T. McInally, C. J. Moody, *Chem. Eur. J.* **2020**, *26*, 7678–7684.

[131] S. Luo, D. Pal, S. J. Shah, D. Kwatra, K. D. Paturi, A. K. Mitra, *Mol. Pharm.* **2010**, *7*, 412–420.

[132] C. A. Lipinski, F. Lombardo, B. W. Dominy, P. J. Feeney, *Adv. Drug Deliv. Rev.* **1997**, *23*, 3–25.

[133] M. D. Shultz, *J. Med. Chem.* **2019**, *62*, 1701–1714.

[134] T. Ishiyama, J. Takagi, K. Ishida, N. Miyaura, N. R. Anastasi, J. F. Hartwig, *J. Am. Chem. Soc.* **2002**, *124*, 390–391.

[135] R. E. Maleczka, F. Shi, D. Holmes, M. R. Smith, *J. Am. Chem. Soc.* **2003**, *125*, 7792–7793.

[136] C. Sandford, V. K. Aggarwal, *Chem. Commun.* **2017**, *53*, 5481–5494.

[137] J. W. B. Fyfe, A. J. B. Watson, *Chem* **2017**, *3*, 31–55.

[138] S. M. Nicolle, A. Nortcliffe, H. E. Bartrum, W. Lewis, C. J. Hayes, C. J. Moody, *Chem. Eur. J.* **2017**, *23*, 13623–13627.

[139] F. M. Meyer, S. Liras, A. Guzman-Perez, C. Perreault, J. Bian, K. James, *Org. Lett.* **2010**, *12*, 3870–3873.

[140] V. A. Kallepalli, F. Shi, S. Paul, E. N. Onyeozili, R. E. Maleczka, M. R. Smith, *J. Org. Chem.* **2009**, *74*, 9199–9201.

[141] S. M. Preshlock, B. Ghaffari, P. E. Maligres, S. W. Krska, R. E. Maleczka, M. R. Smith, *J. Am. Chem. Soc.* **2013**, *135*, 7572–7582.

[142] H. Robinson, J. Stillibrand, K. Simelis, S. J. Macdonald, A. Nortcliffe, *Org. Biomol. Chem.* **2020**, *18*, 6696–6701.

[143] T. Ishiyama, Y. Nobuta, J. F. Hartwig, N. Miyaura, *Chem. Commun.* **2003**, *3*, 2924–2925.

[144] D. W. Griggs, P. G. Ruminski, *Meta-Azacyclic Amino Benzoic Acid Derivatives as Pan Integrin Antagonists*, **2017**, WO2017117538A1.

[145] D. W. Griggs, P. G. Ruminski, *Beta Amino Acid Derivatives as Integrin Antagonists*, **2014**, WO2014015054A1.

[146] K. D. Freeman-Cook, R. L. Hoffman, T. W. Johnson, *Future Med. Chem.* **2013**, *5*, 113–115.

[147] E. E. Guest, S. A. Oatley, S. J. F. Macdonald, J. D. Hirst, *J. Chem. Inf. Model.* **2020**, *60*,

5487–5498.

[148] Y. Hayashi, D. Sakamoto, D. Okamura, *Org. Lett.* **2016**, *18*, 4–7.

[149] N. J. A. Martin, X. Cheng, B. List, *J. Am. Chem. Soc.* **2008**, *130*, 13862–13863.

[150] J. S. Kim, K. Shin-Ya, K. Furihata, Y. Hayakawa, H. Seto, *Tetrahedron Lett.* **1997**, *38*, 3431–3434.

[151] J. Lewerenz, P. Maher, *Front. Neurosci.* **2015**, *9*, 1–20.

[152] R. Wang, H. Reddy, *J. Alzheimer's Dis.* **2017**, *57*, 1041–1048.

[153] H. Furukawa, S. K. Singh, R. Mancusso, E. Gouaux, *Nature* **2005**, *438*, 185–192.

[154] N. R. Sims, E. Zaidan, *Int. J. Biochem. Cell Biol.* **1995**, *27*, 531–550.

[155] L. T. Ndountse, H. M. Chan, *Toxicol. Lett.* **2009**, *184*, 50–55.

[156] Q. Yan, E. Gin, M. G. Banwell, A. C. Willis, P. D. Carr, *J. Org. Chem.* **2017**, *82*, 4328–4335.

[157] T. Q. Hung, T. T. Dang, J. Janke, A. Villinger, P. Langer, *Org. Biomol. Chem.* **2015**, *13*, 1375–1386.

[158] O. B. Smirnova, T. V. Golovko, V. G. Granik, *Pharm. Chem. J.* **2011**, *44*, 654–678.

[159] M. Slaytor, I. J. McFarlane, *Phytochemistry* **1968**, *7*, 605–611.

[160] J. C. Thomas, D. C. Adams, C. Nessler, J. K. Brown, H. J. Bohnert, *Plant Physiol.* **1995**, *109*, 717–720.

[161] J. Liu, M. Nakagawa, K. Ogata, T. Hino, *Chem. Pharm. Bull.* **1991**, *39*, 1672–1676.

[162] J. J. Maresh, L. A. Giddings, A. Friedrich, E. A. Loris, S. Panjikar, B. L. Trout, J. Stöckigt, B. Peters, S. E. O'Connor, *J. Am. Chem. Soc.* **2008**, *130*, 710–723.

[163] J. Stöckigt, A. P. Antonchick, F. Wu, H. Waldmann, *Angew. Chem. Int. Ed.* **2011**, *50*, 8538–8564.

[164] K. L. Rinehart, J. Kobayashi, G. C. Harbour, J. Gilmore, M. Mascal, T. G. Holt, L. S. Shield, F. Lafargue, *J. Am. Chem. Soc.* **1987**, *109*, 3378–3387.

[165] T. Toma, Y. Kita, T. Fukuyama, *J. Am. Chem. Soc.* **2010**, *132*, 10233–10235.

[166] R. S. Alekseyev, A. V. Kurkin, M. A. Yurovskaya, *Chem. Heterocycl. Compd.* **2009**, *45*, 889–925.

[167] Z. Zhang, S. Wang, S. Wan, S. Ren, W. Li, T. Jiang, *Carbohydr. Res.* **2009**, *344*, 291–297.

[168] C. Moquin-Pattey, M. Guyot, *Tetrahedron* **1989**, *45*, 3445–3450.

[169] A. D. Wadsworth, B. J. Naysmith, M. A. Brimble, *Eur. J. Med. Chem.* **2015**, *97*, 816–29.

[170] A. Wadsworth, Synthetic Investigations towards the Total Synthesis of Neuroprotective Natural Products, PhD thesis, The University of Auckland (New

Zealand), **2014**.

[171] S. J. Markey, W. Lewis, C. J. Moody, *Org. Lett.* **2013**, *15*, 6306–6308.

[172] S. J. Markey, Synthetic Approaches towards the Synthesis of the α-Carboline Mescengricin, PhD thesis, The University of Nottingham (UK), **2014**.

[173] S. S. Weng, C. S. Ke, F. K. Chen, Y. F. Lyu, G. Y. Lin, *Tetrahedron* **2011**, *67*, 1640–1648.

[174] D. Drochner, M. Müller, *Eur. J. Org. Chem.* **2001**, 211–215.

[175] A. T. Londregan, S. Jennings, L. Wei, *Org. Lett.* **2010**, *12*, 4554–4557.

[176] A. T. Londregan, S. Jennings, L. Wei, *Org. Lett.* **2011**, *13*, 1840–1843.

[177] A. T. Londregan, K. Burford, E. L. Conn, K. D. Hesp, *Org. Lett.* **2014**, *16*, 3336–3339.

[178] J. K. Laha, P. Petrou, G. D. Cuny, *J. Org. Chem.* **2009**, *74*, 3152–3155.

[179] V. H. Rawal, R. J. Jones, M. P. Cava, *J. Org. Chem.* **1987**, *52*, 19–28.

[180] H. H. Wasserman, G. D. Berger, K. R. Cho, *Tetrahedron Lett.* **1982**, *23*, 465–468.

[181] R. Downham, F. W. Ng, L. E. Overman, *J. Org. Chem.* **1998**, *63*, 8096–8097.

[182] D. Wang, H. Jia, W. Wang, Z. Wang, *Tetrahedron Lett.* **2014**, *55*, 7130–7132.

[183] H. Zhang, F. Y. Kwong, Y. Tian, K. S. Chan, *J. Org. Chem.* **1998**, *63*, 6886–6890.

[184] X. H. Liu, H. F. Liu, X. Shen, B. A. Song, P. S. Bhadury, H. L. Zhu, J. X. Liu, X. B. Qi, *Bioorg. Med. Chem. Lett.* **2010**, *20*, 4163–4167.

[185] S. Minakata, M. Komatsu, Y. Ohshiro, *Synthesis* **1992**, 661–663.

[186] S. Nagumo, T. Toyonaga, T. Inoue, M. Nagai, *Chem. Pharm. Bull.* **1989**, *37*, 2621–2623.

[187] M. A. Ganiek, M. R. Becker, M. Ketels, P. Knochel, *Org. Lett.* **2016**, *18*, 828–831.

[188] S. Fuse, H. Yoshida, K. Oosumi, T. Takahashi, *Eur. J. Org. Chem.* **2014**, *2014*, 4854–4860.

[189] X. J. Wang, X. Sun, L. Zhang, Y. Xu, D. Krishnamurthy, C. H. Senanayake, *Org. Lett.* **2006**, *8*, 305–307.

[190] U. Rashid, F. Rahim, M. Taha, M. Arshad, H. Ullah, T. Mahmood, M. Ali, *Bioorg. Chem.* **2016**, *66*, 111–116.

[191] S. T. Barry, S. B. Ludbrook, E. Murrison, C. M. T. Horgan, *Biochem. Biophys. Res. Commun.* **2000**, *267*, 764–769.

[192] J. Cosier, A. M. Glazer, *J. Appl. Crystallogr.* **1986**, *19*, 105–107.

[193] R. O. Diffraction, **2018**.

[194] O. V. Dolomanov, L. J. Bourhis, R. J. Gildea, J. A. K. Howard, H. Puschmann, *J. Appl. Crystallogr.* **2009**, *42*, 339–341.

[195] G. M. Sheldrick, *Acta Crystallogr. A* **2015**, *A71*, 3–8.

[196] G. M. Sheldrick, *Acta Crystallogr. C* **2015**, *C71*, 3–8.

[197] "CheckCIF," can be found under http://checkcif.iucr.org, **n.d.**

[198] P. C. D. Hawkins, A. G. Skillman, G. L. Warren, B. A. Ellingson, M. T. Stahl, *J. Chem. Inf. Model.* **2010**, *50*, 572–584.

[199] M. McGann, *J. Chem. Inf. Model.* **2011**, *51*, 578–596.